

spatiotemporal cats
or, try herding 7 cats

[siminos/spatiotemp](#), rev. 8006: last edit by Predrag Cvitanović, 12/07/2021

Predrag Cvitanović, Han Liang, Sidney V. Williams,
Rana Jafari, Li Han, Adrien K. Saremi and Boris Gutkin

December 26, 2021

Contents

1 Cat map	11
1.1 Adler-Weiss partition of the Thom-Arnol'd cat map	11
1.2 Adler-Weiss partition of the Percival-Vivaldi cat map	13
1.3 Cat map: Hamiltonian formulation	19
1.3.1 Adler-Weiss partition of the cat map state space	19
1.3.2 Counting Hamiltonian cat map periodic orbits	20
1.3.3 An example: Fundamental parallelogram for period-2 cycle points	25
1.3.4 An example: period-4 orbits	25
1.3.5 Adler / Adler98	26
1.3.6 Percival and Vivaldi / PerViv	26
1.3.7 Isola / Isola90	27
1.3.8 Creagh / Creagh94	29
1.3.9 Keating / Keating91	29
1.4 Green's function for 1-dimensional lattice	30
1.5 Green's blog	34
1.6 Chebyshev series	37
1.6.1 Spectral methods	37
1.6.2 Discretizing with Chebyshev polynomials	38
1.7 Bernoulli map, beta transformation	40
1.8 Any piecewise linear map has "linear code"	54
1.9 Cat map blog	55
References	68
1.10 Examples	75
1.11 *	85
exercises	85
2 Temporal Hénon	93
2.1 Hénon blog	93
2.1.1 Temporal Hénon; anti-integrable limit	93
2.2 Hénon map symmetries	97
2.3 "Center of mass" puzzle	98
2.4 Symmetries of the symbol square	111
2.4.1 Symmetry lines	112

CONTENTS

References	112
2.5 *	120
exercises	120
3 LC21: A chaotic lattice field theory in one dimension	123
3.1 LC21: Introduction	123
3.2 Deterministic lattice field theory	127
3.2.1 Lattice Laplacian	129
3.2.2 1-dimensional lattice field theories	130
3.3 A fair coin toss	131
3.3.1 Bernoulli map	131
3.3.2 Temporal Bernoulli	132
3.3.3 Bernoulli as a continuous time dynamical system	133
3.4 A kicked rotor	134
3.4.1 Cat map	135
3.4.2 Temporal cat	135
3.4.3 Temporal cat as a continuous time dynamical system	136
3.5 A ϕ^3 field theory	138
3.6 A ϕ^4 field theory	139
3.6.1 Computing lattice states for nonlinear theories	140
3.6.2 Papers to refer to?	140
3.7 Reciprocal lattice	142
3.7.1 Reciprocal lattice state	144
3.7.2 Irreducible representations of the symmetry group	145
3.7.3 Fundamental domain	149
3.8 Orbit stability	151
3.8.1 Temporal Bernoulli, temporal cat	151
3.8.2 Nonlinear field theories	152
3.8.3 Fundamental fact	153
3.8.4 Orbit Jacobian matrix on reciprocal lattice	158
3.9 Stability of an orbit vs. its time-evolution stability	159
3.9.1 Hill determinant for a d -component lattice field	161
3.9.2 Hill determinant of a forward-in-time map	162
3.9.3 Hill determinant for a 2nd order difference equation	164
3.9.4 Hill determinant: fundamental parallelepiped evaluation	166
3.9.5 Hill determinant: time-evolution evaluation	166
3.9.6 Hill determinant: Reciprocal lattice evaluation	166
3.9.7 Remarks	167
3.10 Translations and reflections	169
3.10.1 Symmetries of 1-dimensional lattices, sublattices	169
3.10.2 Classes	170
3.10.3 Reflections	171
3.10.4 Symmetries of a system and of its solutions	173
3.10.5 What are ‘lattice states’? Orbits?	175
3.10.6 Symmetries of lattice states	177
3.11 Permutation representation	179

3.12	Periodic orbit theory	184
3.12.1	Periodic orbit theory	184
3.12.2	Topological zeta function	185
3.12.3	Counting temporal Bernoulli prime periodic orbits	186
3.12.4	Topological zeta function	187
3.13	Topological D_∞ -zeta function	188
3.13.1	Counting temporal cat lattice states	191
3.13.2	Counting lattice states	193
3.14	Summary	195
	References	196
4	Group theory	205
4.1	Temporal lattice systems	207
4.1.1	Temporal Bernoulli system	207
4.1.2	Temporal cat	208
4.1.3	Lattice states	209
4.1.4	Reflection-symmetric lattice states	209
4.2	Time reversal symmetry reduction	213
4.2.1	Laplacians (and time reversal?)	213
4.2.2	Time reversal blog	216
4.2.3	Poles of dynamical zeta functions	225
4.3	Time reversal literature	227
4.3.1	Grava <i>et al.</i> 2021 paper GKMM21	227
4.3.2	Baake <i>et al.</i> 2008 paper BaRoWe08	232
4.3.3	Baake <i>et al.</i> 1997 paper BaHePl97	237
4.3.4	Baake 2018 paper Baake18	238
4.3.5	Lamb and Roberts 1998 paper lamb98	238
4.3.6	Calogero 2007 paper BrCaDr07	239
4.3.7	Variational method, Dong 2020 paper DoLiLi20	240
4.3.8	Dong 2021 paper LDJL21	242
4.3.9	Letter from Ping Ao	244
4.4	A Lind zeta function for flip systems	245
4.4.1	Counting lattice states	247
4.5	Permutation representations	248
4.6	Reduction to the reciprocal lattice	254
4.7	Dynamical symmetry factorization	257
4.7.1	Dynamical symmetry blog	258
4.8	Symmetry factorization blog	262
4.9	Group theory and symmetries: a review	267
4.9.1	Regular representation	267
4.9.2	Irreducible representations	268
4.9.3	Projection operator	270
4.10	Examples	271
4.11	Discrete factorization of the dynamical zeta function	294
4.11.1	Factorization of C_3 and D_3	294
4.11.2	Factorization of C_n and D_n	297

CONTENTS

References	302
5 Spatiotemporal cat	309
5.1 Coupled map lattices	310
5.2 Helmholtz type equations	316
5.2.1 Poisson and Laplace's equations	316
5.2.2 Screened Poisson equation	316
5.2.3 Klein–Gordon equation	317
5.2.4 Spatiotemporal cat equation	318
5.2.5 Helmholtz blog	318
5.3 Green's function for 2-dimensional square lattice	322
5.4 Toeplitz tensors	323
5.5 Green's blog	324
5.6 Generating functions; temporal cat	337
5.6.1 Lagrangian formulation	340
5.6.2 Temporary: Cat map in the Lagrangian formulation	342
5.7 Lattice discretization of a field theory	345
5.7.1 Transfer matrix	347
5.7.2 Classical ϕ^3 lattice field theory	348
5.7.3 Classical ϕ^4 lattice field theory	348
5.8 Normalizing flows	353
5.9 Noise is your friend	359
5.9.1 Noisy Gábor	364
5.10 Kuramoto–Sivashinsky equation	366
5.11 Field theory blog	366
5.12 Lattice points enumeration	370
5.12.1 Complex plane	370
5.12.2 Integer lattice in d dimensions	371
5.12.3 Primitive parallelogram	384
5.12.4 Tensor eigenvalues	388
5.13 Difference equations	389
5.13.1 Time quasilattices	391
5.14 Generating functions	395
5.15 Resistor networks	401
5.16 Counting invariant 2-tori	417
5.17 Elastodynamic equilibria of 2D solids	419
5.18 Integer lattices literature	420
References	421
6 Zeta functions in 2D	437
References	449

7 Spatiotemporal stability	453
7.1 Temporal lattice	453
7.1.1 Second-order difference equation	455
7.1.2 Third-order difference equation	455
7.1.3 Hill's formula for a first-order system	457
7.1.4 Hill's formula for a second-order system	459
7.2 Spatiotemporal lattice	464
7.3 Noether's theorem	464
7.4 Stability blog	465
7.5 Hill's formula blog	468
7.6 Generating function literature	479
References	480
8 Hill's formula	485
8.1 An overview over "Hill's formulas"	485
8.2 Generating functions; action	485
8.3 Homoclinic and periodic orbit actions in chaotic systems	486
8.4 Hill's formula, Lagrangian setting	489
8.5 Spatiotemporal cat Hill's formula	491
8.6 Hill's formula for relative periodic orbits	495
8.7 Han's temporal cat Hill's formula	497
8.8 Han's spatiotemporal cat Hill's formula	498
8.8.1 Han's relative-periodic Hill's formula	499
8.9 Han's Hénon map Hill's formula	501
References	503
9 Chronotopic musings	505
9.1 Chronotopic literature	505
9.2 PolTor92b Towards a statistical mechanics of spatiotemporal chaos	509
9.3 PolTor92 Periodic orbits in coupled Hénon maps	513
9.4 PoToLe98 Lyapunov exponents from node-counting	514
9.5 PolPuc92 Invariant measure in coupled maps	515
9.6 PolTor09 Stable chaos	515
References	516
10 Article edits	518
10.1 Cats' GHJSC16blog	518
10.1.1 Cats/nonlin-v2/ GHJSC16 revisions	542
10.2 Kittens' CL18blog	545
10.2.1 Hill's formula: stability of an orbit vs. its time-evolution stability	575
10.3 Kittens' LC21blog	583
References	586

CONTENTS

11 Symbolic dynamics: a glossary	591
11.1 Symbolic dynamics, inserts	595
References	596
11.2 Enumeration of prime invariant 2-tori	597
11.2.1 Covering alphabet	597
11.2.2 Admissible prime invariant 2-tori	599
12 Statistical mechanics applications	604
12.1 Cat map	604
12.2 New example: Arnol'd cat map	604
References	608
13 Ising model in 2D	609
13.1 Ihara zeta functions	622
13.1.1 Heat equation	622
13.1.2 Heat kernel	622
13.1.3 Clair / Clair14	628
13.1.4 Ihara blog	631
13.1.5 Maillard	643
13.2 Gaussian model	648
13.3 Tight-binding Hamiltonians	650
13.4 Discrete Schrödinger equation	654
13.5 Harper's model	657
13.6 Frenkel-Kontorova model	660
13.7 Mean field theory for the Ising model	663
13.8 Clock model	664
13.9 X-Y model	667
References	668
14 Checkerboard	677
14.1 Checkerboard model	677
14.1.1 Checkerboard literature	678
References	679
15 Sidney's blog	680
15.1 2020 blog	680
15.2 2021 blog	710
15.3 Sidney exercises	753
References	757
16 Ibrahim's blog	759
16.1 Spring 2021 blog	760
References	761
17 Xuanqi's blog	762
17.1 Spring 2021 blog	763
References	763

CONTENTS

18 Han's blog	765
18.1 Rhomboid corner partition	767
18.2 Rhomboid center partition	785
18.2.1 Reduction to the reciprocal lattice	795
18.3 Time reversal	797
18.4 Reduction to the fundamental domain	802
18.5 Spatiotemporal cat partition	805
18.6 Running blog	814
18.6.1 Stability of a periodic point vs. stability of the orbit	866
18.6.2 2020-06-12 Han : Temporal cat derivation using determinant recursion	867
18.6.3 Lattices and periodicities	879
References	963
19 Frequencies of Cat Map Winding Numbers	967
19.1 Introduction	967
19.2 Numbers of periodic orbits	968
19.2.1 Keating's counting of periodic points	969
19.3 Relative frequencies of cat map words	969
19.3.1 Numerical computations	970
19.3.2 Entropy	971
19.4 Spatiotemporal cat	972
19.4.1 Frequencies of symbols	973
19.4.2 Frequency of blocks of length two	974
19.4.3 Frequencies of $[2 \times 2]$ spatiotemporal domains	976
19.5 Summary	976
References	977
20 Symbolic Dynamics for Coupled Cat Maps	978
20.1 Introduction	978
20.2 Arnol'd Cat Map	979
20.2.1 Periodic orbits - first approach	980
20.2.2 Periodic orbits - second approach	980
20.2.3 Symbolic dynamics for 1 particle	983
20.3 Coupled Cat Maps	985
20.3.1 Computation of symbols	985
20.3.2 Nature of our alphabet	987
20.3.3 Admissibility of sequences of more than 2 symbols	989
20.4 Future work...	992
References	992
21 Rana's blog	995
References	997

CONTENTS

22 Adrien's blog	998
22.1 Introduction	998
22.2 Arnol'd cat map	999
22.2.1 First approach	999
22.2.2 2nd approach	1000
22.2.3 Computing periodic orbits	1000
22.3 Coupled Cat Maps	1009
22.3.1 Periodic orbits	1009
22.3.2 Ergodic orbits	1010
22.4 Adrien's blog	1014
References	1017
23 Spatiotemporal cat, blogged	1019
References	1040
24 Pow Wows	1045
24.1 Pow wow 2020-12-08	1045
24.1.1 Hereby resolved:	1045
24.2 Pow wow 2020-12-28	1046
24.2.1 Hereby resolved:	1046
24.3 Pow wow 2021-01-08	1046
24.3.1 Hereby resolved:	1046
24.4 Pow wow 2021-03-22	1047
24.5 Pow wow 2021-04-02	1047
24.6 Pow wow 2021-04-09	1048
24.7 Pow wow 2021-04-27	1049
24.7.1 Hereby resolved:	1049
24.8 Pow wow 2021-05-04	1050
24.8.1 Hereby resolved:	1050
24.9 Pow wow 2021-05-07	1050
24.10 Pow wow 2021-05-14	1051
24.10.1 Hereby resolved:	1051
References	1051

CONTENTS

This cat has been skinned in more ways than any other cat in the history of cats.

— Professore Gatto Nero

This is a project of many movable parts, so here is a guide where to blog specific topics (or where to find them)

- sect. 1.5 1-dimensional / cat map lattice Green's functions
- sect. 1.9 cat map blog
- sect. 1.10 Examples: Cat map
- chapter 5 d -dimensional spatiotemporal cat
- sect. 5.4 d -dimensional / spatiotemporal cat Green's function
- sect. 4.6 Reduction to the reciprocal lattice
- chapter 8 Hill's formula
- sect. 8.2 1-dimensional action
- sect. 10.1 Herding five cats [1] edits
- chapter 11 Symbolic dynamics: a glossary
- chapter 13 2D Ising model; Ihara and multi-dimensional zetas
- chapter 14 Checkerboard
- chapter 15 Sidney's blog
- chapter 18 Han's blog - the most important blog
- chapter 21 Rana's blog
- chapter 22 Adrien's blog
- chapter 23 Spatiotemporal cat blog

Blog fearlessly: this is your own lab-book, a chronology of your learning and research that you might find invaluable years hence.

Chapter 1

Cat map

If space is infinite, we are in no particular point in space.
If time is infinite, we are in no particular point in time.

— *The Book of Sand*, by Jorge Luis Borges

What is a natural way to cover the torus, in such a way that the dynamics and the partition borders are correctly aligned? You are allowed to coordinatize the unit torus by any set of coordinates that covers the torus by a unit area. The origin is fixed under the action of \mathbf{A} , and straight lines map into the straight lines, so Adler and Weiss did the natural thing, and used parallelograms (following Bowen [22] we shall refer to such parallelograms as ‘rectangles’) with edges parallel to the two eigenvectors of \mathbf{A} . Adler and Weiss observed that the torus in the new eigen-coordinates is covered by two rectangles, labelled A and B in figure 1.1.¹

1.1 Adler-Weiss partition of the Thom-Arnol'd cat map

Figure 1.1 for the canonical Thom-Arnol'd cat map

remark ??

$$A = \begin{bmatrix} 2 & 1 \\ 1 & 1 \end{bmatrix}. \quad (1.1)$$

String people, [arXiv:1608.07845](#), find the identity

$$\begin{bmatrix} 2 & 1 \\ 1 & 1 \end{bmatrix} = \begin{bmatrix} 1 & 1 \\ 0 & 1 \end{bmatrix} \begin{bmatrix} 1 & 0 \\ 1 & 1 \end{bmatrix} = LL^\top \quad (1.2)$$

¹Predrag 2018-02-09: (1) motivate Manning multiples by doing the 1D circle map first. Maybe Robinson [86] does that.

(2) motivate spatiotemporal cat by recent Gutkin *et al.* many-body paper

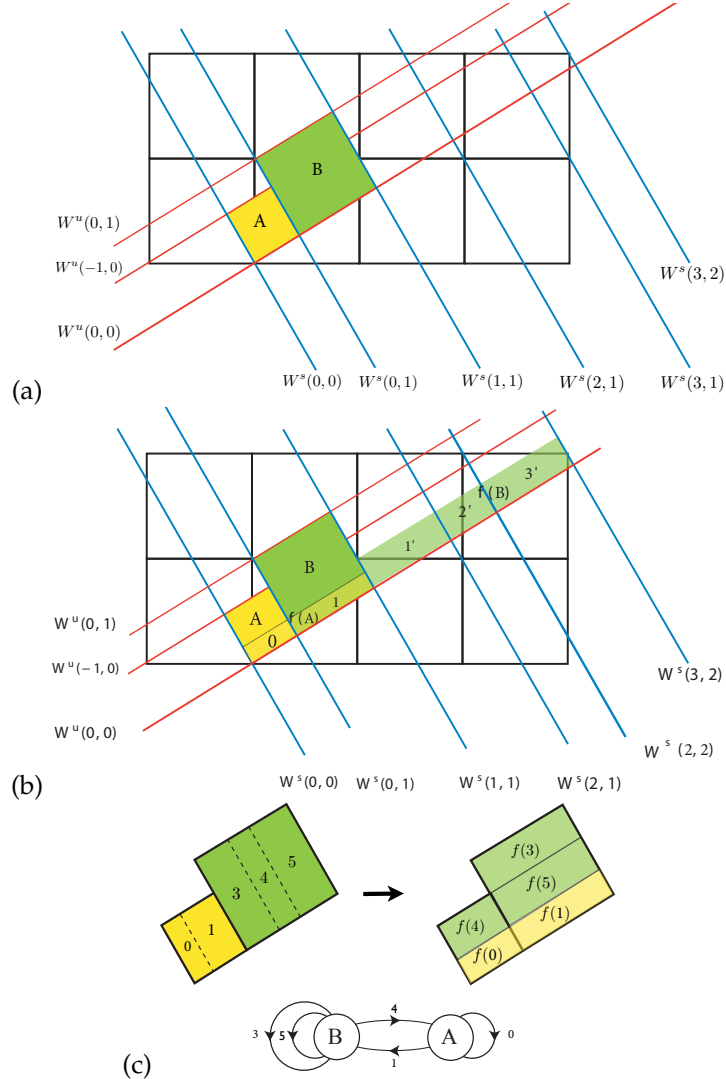


Figure 1.1: (a) Two-rectangle Adler-Weiss generating partition for the canonical Arnol'd cat map (1.1), with borders given by stable-unstable manifolds of the unfolded cat map lattice points near to the origin. (b) The first iterate of the partition. (c) The iterate pulled back into the generating partition, and the corresponding 5-letter transition graph. In (b) and (c) I have not bothered to re-label Crutchfield partition labels with our shift code. This is a “linear code,” in the sense that for each square one can count how many side-lengths are needed to pull the overhanging part of $f(x)$ back into the two defining squares. (Figure by Crutchfield [28])

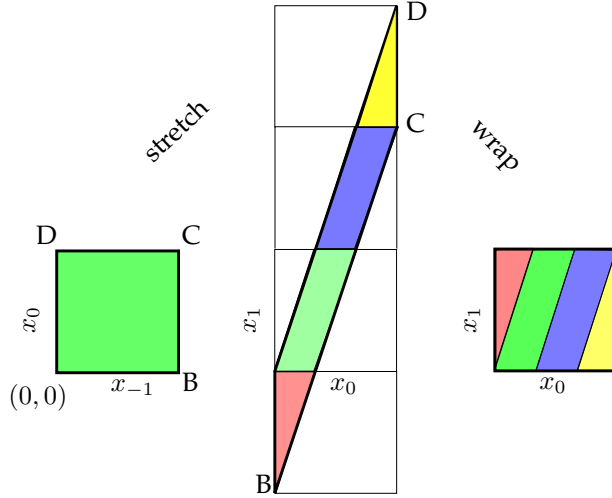


Figure 1.2: (Color online) The $s = 3$ Percival-Vivaldi cat map matrix (1.5) stretches the unit square into a parallelogram. Translations by m_0 from alphabet $\mathcal{A} = \{-1, 0, 1, 2\} = \{\text{red, green, blue, yellow}\}$ bring stray regions back onto the torus.

significant: “The map corresponds to successive kicks, forwards and backwards along the light cone [...]”

As another example, with $s = 4$, Manning [72] discusses a Markov partition for the cat map (also discussed by Anosov, Klimenko and Kolutsky [5])

$$A = \begin{bmatrix} 3 & 1 \\ 2 & 1 \end{bmatrix}. \quad (1.3)$$

In order to count all admissible walks, one associates with the transition graph such as the one in figure 1.1 (c) the *connectivity* matrix

$$C = \begin{bmatrix} 1 & 1 \\ 1 & 2 \end{bmatrix}, \quad (1.4)$$

where C_{ij} is the number of ways (number of links) of getting to i from j .

1.2 Adler-Weiss partition of the Percival-Vivaldi cat map

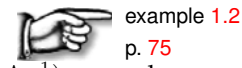
As illustrated in figure 1.2, the action of the cat map in the Percival-Vivaldi [80] “two-configuration representation” is given by the antisymmetric area preserving $[2 \times 2]$ matrix

$$\mathbf{A} = \begin{bmatrix} 0 & 1 \\ -1 & s \end{bmatrix} \quad (1.5)$$

For the Arnol'd value $s = 3$, in one time step the map stretches the unit square into a parallelogram, and than wraps it around the torus 3 times, as in figure 1.2. Visualise the phase space as a bagel, with x_0 axis a circle on the outside of the bagel. This circle is divided into three color segments, which map onto each other as you got in the x_1 axis direction. Now apply the inverse map - you get 3 strips intersecting the the above strips, for 9 rectangles in all: a full shift, i.e., a ternary Smale horseshoe. So on the torus there are only 3 strips - there is no distinction between the two outer letters $\mathcal{A}_1 = \{-1, 2\} = \{\text{red, yellow}\}$, it is the same third strip. The division into 2 triangles is an artifact of plotting the torus as a unit square. All complicated pruning of (the current draft of) Gutkin *et al.* [53] is a red herring, due to over-partitioning of the torus with a 4-letter alphabet.

This is stupid.

How do Adler-Weiss coordinates work out for the Arnol'd cat map in the Percival-Vivaldi representation (1.5) used here? First one needs to construct the eigen-coordinates.



For $s > 2$ the stability multipliers $(\Lambda^+, \Lambda^-) = (\Lambda, \Lambda^{-1})$ are real,

$$\Lambda^\pm = \frac{1}{2}(s \pm \sqrt{D}), \quad \Lambda = e^\lambda, \quad (1.6)$$

where

$$\begin{aligned} s &= \Lambda + \Lambda^{-1} = 2 \cosh(\lambda), \\ \sqrt{D} &= \Lambda - \Lambda^{-1} = 2 \sinh(\lambda) \end{aligned} \quad (1.7)$$

discriminant $D = s^2 - 4$, with a positive Lyapunov exponent $\lambda > 0$, and the right, left eigenvectors:

$$\begin{aligned} \{\mathbf{e}^{(+)}, \mathbf{e}^{(-)}\} &= \left\{ \begin{bmatrix} \Lambda^{-1} \\ 1 \end{bmatrix}, \begin{bmatrix} \Lambda \\ 1 \end{bmatrix} \right\} \\ \{\mathbf{e}_{(+)}, \mathbf{e}_{(-)}\} &= \{[-\Lambda^{-1}, 1], [\Lambda, -1]\}, \end{aligned} \quad (1.8)$$

(where the overall scale is arbitrary). As the matrix is not symmetric, the $\{\mathbf{e}^{(j)}\}$ do not form an orthogonal basis.

What does this do to the partition of figure 1.2? The origin is still the fixed point. For a state space point in the new, dynamically intrinsic right eigenvector Adler-Weiss coordinate basis x'

$$\begin{pmatrix} x'_{t-1} \\ x'_t \end{pmatrix} = \begin{pmatrix} -\Lambda x_t + x_{t-1} \\ -\Lambda^{-1} x_t + x_{t-1} \end{pmatrix}.$$

the abscissa (x_{t-1} direction) is not affected, but the ordinate (x_t direction) is flipped and stretched/shrunk by factor $-\Lambda, -\Lambda^{-1}$ respectively,

$$\begin{pmatrix} x'_t \\ x'_{t+1} \end{pmatrix} = \begin{bmatrix} \Lambda^{-1} & 0 \\ 0 & \Lambda \end{bmatrix} \begin{pmatrix} x'_{t-1} \\ x'_t \end{pmatrix} - \begin{pmatrix} 0 \\ m_t \end{pmatrix},$$

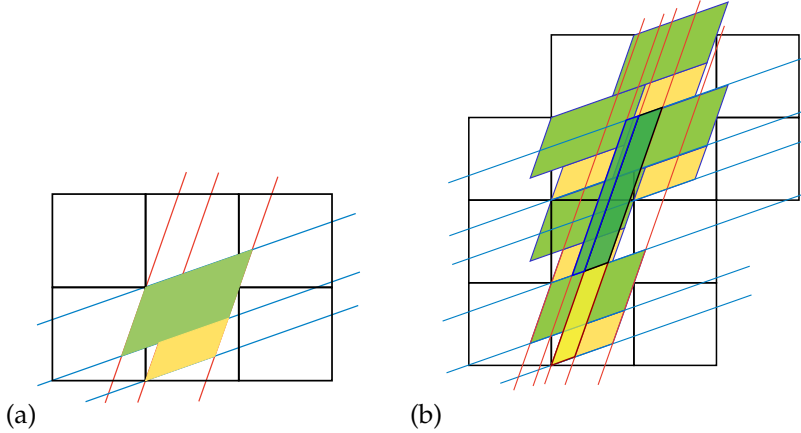


Figure 1.3: (a) An abandoned two-rectangle Adler-Weiss generating partition for the Percival-Vivaldi cat map (1.5), with borders given by cat map stable-unstable manifolds. (b) An abandoned attempt to identify the finite partition, since superseded by the partition of figure 1.6(b) and figure 1.9.

preserving the vertical strip nature of the partition of figure 1.2. In the Adler-Weiss right eigenbasis, \mathbf{A} acts by stretching the $e^{(+)}$ direction by Λ , and shrinking the $e^{(-)}$ direction by Λ^{-1} , without any rotation of either direction.

Thus the Adler-Weiss coordinates preserve the convenient feature of the Percival-Vivaldi cat map, figure 1.2: the torus ‘rewrapping’ translations remain all vertical, specified by a single integer.

The angles of stable / unstable manifolds are irrational respective to the lattice, and they never hit another vertex (and so they do not close onto themselves under quotienting of translations).

Note that from figure 1.4(a) to figure 1.4(b) we have used the continuous translation invariance to center the large tile A within the unit square. That makes the time reversal invariance more explicit. It might not be obvious that the two parallelograms of figure 1.3(a) tile the square lattice, but they do, as illustrated in figure 1.4(a). Such tilings are known as ‘Pythagorean’.

Given the stable/unstable eigenvectors, the natural eigen-coordinates are given. I had first constructed a 2-rectangle generating partition for the Percival-Vivaldi [80] two-configuration representation (1.5) - it is a squashed and rotated version of figure 1.1 (a) drawn in figure 1.3 (a). The point is, after a linear change of coordinates one has finite grammar Adler-Weiss symbolic dynamics, and the symbolic dynamics is a linear code in sense of Boris, but this time with all admissible sequences generated as walks on a transition graph isomorphic to the one in figure 1.1 (c).

remark 1.4

I actually like better the three-rectangle, time reversal symmetric generating partition of figure 1.5 and figure 1.6.

Thus we have constructed Percival-Vivaldi cat map coordinate transforma-

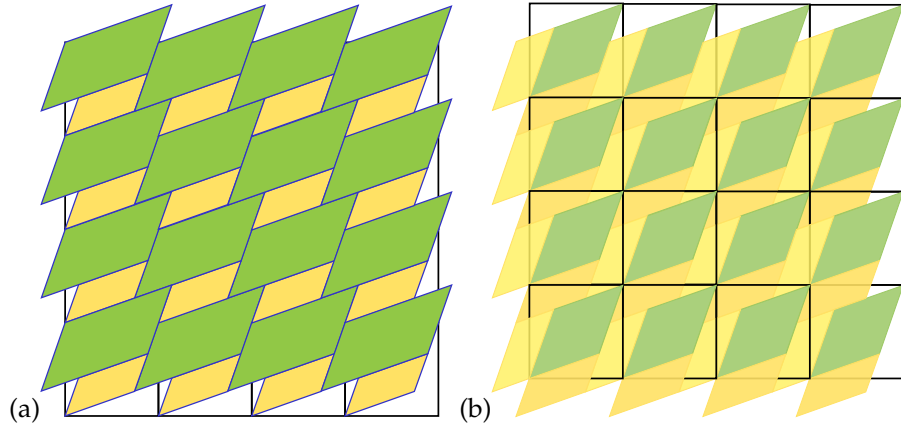


Figure 1.4: (a) [Abandoned] Tiling of the square lattice by the two-rectangle Adler-Weiss generating partition of figure 1.3(a) for the Percival-Vivaldi cat map (1.5). (b) Tiling of the square lattice by the three-rectangle, time reversal symmetric generating partition. Note that we have used the continuous translation invariance to center the large tile A within the unit square (continued in figure 1.5 (a)).

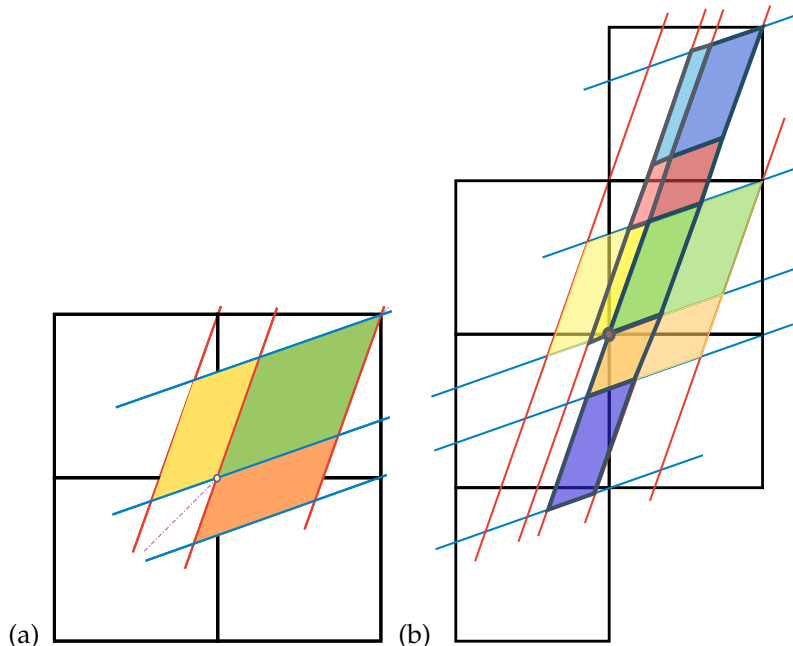


Figure 1.5: (a) The three-rectangle, time reversal symmetric generating partition for the Percival-Vivaldi cat map (1.5), with borders given by cat map stable-unstable manifolds. (b) The three-rectangle mapped one step forward in time.

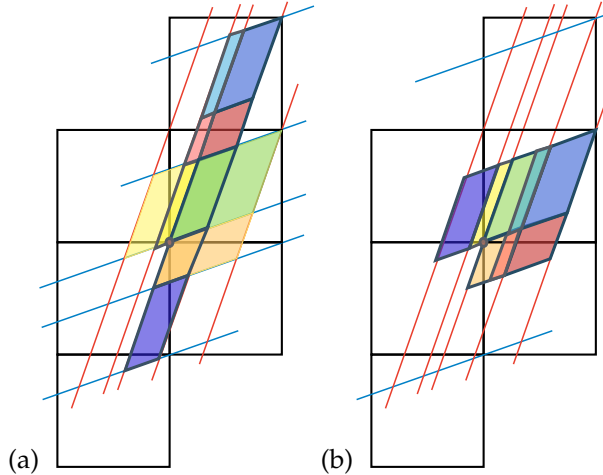


Figure 1.6: (a) The three-rectangle mapped one step forward in time. (b) The three-rectangle wrapped back onto the torus, along the unstable direction, yields 8-letter alphabet generating partition, with three-nodes transition graph. One could have kept the two-rectangle Adler-Weiss generating partition of figure 1.3 (a), in which case the alphabet is the standard 5 letters.

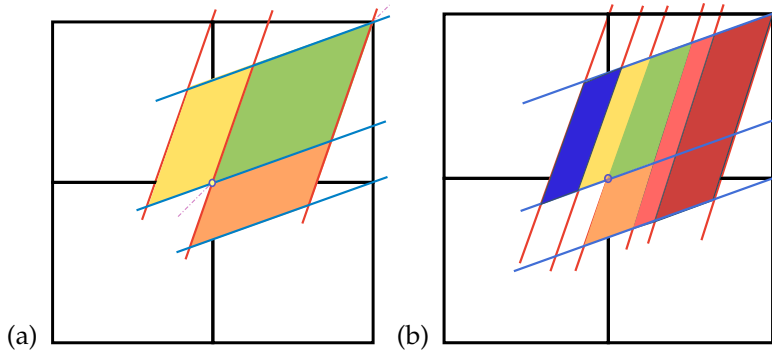


Figure 1.7: Figure 1.6 continued. (a) The three-rectangle, time reversal symmetric generating partition for the Percival-Vivaldi cat map (1.5), with borders given by cat map stable-unstable manifolds. (b) The three-rectangle subpartition, one step forward in time. A into three strips, B into three strips, B' into two strips, for a total of 8 forward links in the graph **continue with a sensible coloring of these regions**. Label the graph links by translations that bring these pieces back into the unit square. Under time reversal, interchange B and B' , get the same partition going backwards in time. Then make it Lagrangian, meaning the combined graph should have undirected links (?).

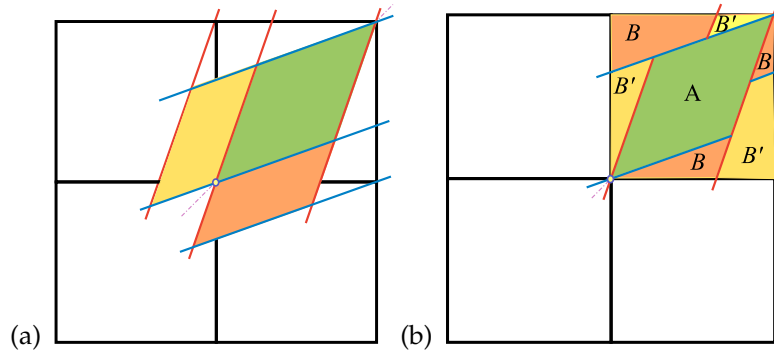


Figure 1.8: (a) The three-rectangle, time reversal symmetric generating partition for the Percival-Vivaldi cat map (1.5), with borders given by cat map stable-unstable manifolds. (b) The three-rectangle partition of the unit square (torus laid out). In this partition A already lies entirely within the unit square, while B and B' are wrapped around the torus, and only seem to consist of three pieces each, an artifact of the wrapping. The unit square borders have no physical meaning.

tion from the square to the intrinsic Adler-Weiss eigencoordinate basis. This is a LINEAR transformation. As this has been falling on deaf ears for last few years, let me say it again:

This is a **LINEAR** code,

as is every code in ChaosBook, as illustrated by the examples of sect. 1.8 that I worked out for feline pleasure some years back. Got that?

As Adler-Weiss partition is generating, there is noting for Dirichlet boundary conditions Green's functions to accomplish - all admissible symbol blocks are known. The problem is now *trivial*, in the Soviet sense (i.e., after a few years of work, I understand it).

What is wrong with the argument so far? I used Newtonian, evolution-in-time thinking to generate the $d = 1$ partition. That will not work in higher dimensions, so the above argument has to be recast in the Lagrangian form.

Be my guest - I'm going to bed:)

A few side, symmetry related remarks: we *must* quotient translation symmetries, do calculations in the elementary cell or, better still, the fundamental domain.

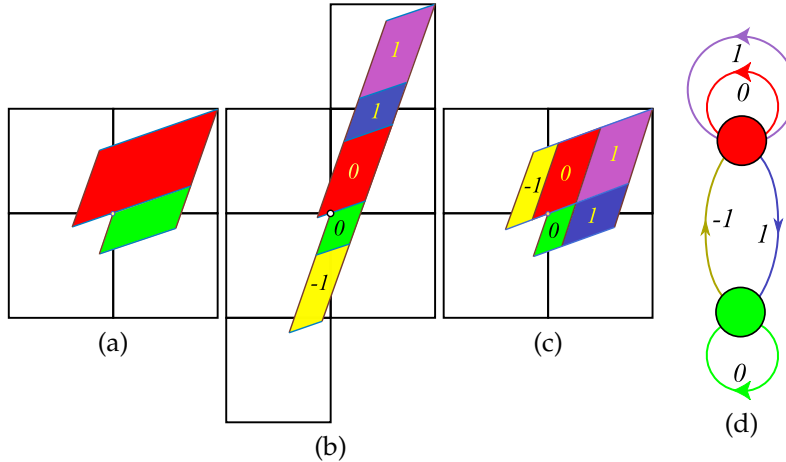


Figure 1.9: (Color online) (a) An Adler-Weiss generating partition of the unit torus for the $s = 3$ Percival-Vivaldi cat map (1.101), with rectangle \mathcal{M}_A (red) and \mathcal{M}_B (green) borders given by the cat map stable (blue) and unstable (dark red) manifolds, i.e., along the two eigenvectors corresponding to the eigenvalues (3.40). (b) Mapped one step forward in time, the rectangles are stretched along the unstable direction and shrunk along the stable direction. Sub-rectangles \mathcal{M}_j that have to be translated back into the partition are indicated by color and labeled by their lattice translation $m_j \in \mathcal{A} = \{\underline{1}, 0, 1\}$, which also doubles as the 3-letter alphabet \mathcal{A} . (c) The sub-rectangles \mathcal{M}_j translated back into the initial partition yield a generating partition, with the finite grammar given by the transition graph (d). The nodes refer to the rectangles A and B , and the five links correspond to the five sub-rectangles induced by one step forward-time dynamics. For details, see appendix 1.3 and ChaosBook [30].

1.3 Cat map: Hamiltonian formulation

²

1.3.1 Adler-Weiss partition of the cat map state space

Cat maps, also known as Thom-Anosov diffeomorphisms, or Thom-Anosov-Arnol'd-Sinai cat maps [6, 35, 102], have been extensively studied as the simplest examples of chaotic Hamiltonian systems.

Percival-Vivaldi cat map (1.101) is a discrete time non-autonomous Hamiltonian system, time-forced by ‘pulses’ m_t . The m_t translations reshuffle the state space, as in figure 1.9, thus partitioning it into regions \mathcal{M}_m , labeled with letters m of the $|\mathcal{A}|$ -letter alphabet \mathcal{A} , and associating a symbol sequence $\{m_t\}$

²Predrag 2019-12-12: Make sure no clip & paste from ref. [53]

to the dynamical trajectory $\{x_t\}$. As the relation (1.101) between the trajectory x_t and its symbolic dynamics encoding m_t is linear, Percival and Vivaldi refer to m_t as a ‘linear code’.

As explained in the companion paper [53], the deep problem with the Percival-Vivaldi code prescription is that it does not yield a generating partition; the borders (i.e., x_0, x_1 axes) of their unit-square partition $(x_{t-1}, x_t) \in (0, 1] \times (0, 1]$ do not map onto themselves, resulting in the infinity of, to us unknown, grammar rules for inadmissible symbol sequences.

This problem was resolved in 1967 by Adler and Weiss [2, 3, 6] who utilized the stable/unstable manifolds of the fixed point at the origin to cover a unit area torus by a two-rectangles generating partition; for the Percival-Vivaldi cat map (1.101), such partition [30] is drawn in figure 1.9. Following Bowen [22], one refers to parallelograms in figure 1.9 as ‘rectangles’; for details see Devaney [35], Robinson [86], or ChaosBook [30]. Siemaszko and Wojtkowski [91] refer to such partitions as the ‘Berg partitions’, and Creagh [27] studies their generalization to weakly nonlinear mappings. Symbolic dynamics on this partition is a subshift of finite type, with the 3-letter alphabet

$$\mathcal{A} = \{1, 0, 1\} \quad (1.9)$$

that indicates the translation needed to return the given sub-rectangle \mathcal{M}_j back into the two-rectangle partition $\mathcal{M} = \mathcal{M}_A \cup \mathcal{M}_B$.

While Percival and Vivaldi were well aware of Adler-Weiss partitions, they felt that their “coding is less efficient in requiring more symbols, but it has the advantage of linearity.” Our construction demonstrates that one can have both: an Adler-Weiss generating cat map partition, and a linear code. The only difference from the Percival-Vivaldi formulation [80] is that one trades the single unit-square cover of the torus of (1.101) for the dynamically intrinsic, two-rectangles cover of figure 1.9, but the effect is magic - now every infinite walk on the transition graph of figure 1.9(d) corresponds to a unique admissible orbit $\{x_t\}$, and the transition graph generates all admissible itineraries $\{m_t\}$.

To summarize: an explicit Adler-Weiss generating partition, such as figure 1.9, completely solves the Hamiltonian cat map problem, in the sense that it generates all admissible orbits. Rational and irrational initial states generate periodic and ergodic orbits, respectively [65, 81], with every state space orbit uniquely labeled by an admissible bi-infinite itinerary of symbols from alphabet \mathcal{A} .

1.3.2 Counting Hamiltonian cat map periodic orbits

The five sub-rectangles \mathcal{M}_j of the two-rectangle Adler-Weiss partition of figure 1.9 (c) motivate introduction of a 5-letter alphabet

$$\bar{\mathcal{A}} = \{1, 2, 3, 4, 5\} = \{A^0A, B^1A, A^1A, B^0B, A^1B\}, \quad (1.10)$$

see figure 1.10 (b), which encodes the links of the transition graph of figure 1.9 (d). The loop expansion of the determinant [29] of the transition graph T of fig-

ure 1.10 (b) is given by all non-intersecting walks on the graph

$$\det(1 - zT) = 1 - z(t_1 + t_3 + t_4) - z^2(t_{25} - (t_1 + t_3)t_4), \quad (1.11)$$

where t_p are traces over fundamental cycles, the three fixed points $t_1 = T_{A^0A}$, $t_3 = T_{A^1A}$, $t_4 = T_{B^0B}$, and the 2-cycle $t_{25} = T_{B^1A}T_{A^1B}$.

As the simplest application, consider counting all admissible cat map periodic orbits. This is accomplished by setting the non-vanishing links of the transition graph to $T_{ji} = 1$, resulting in the cat map topological zeta function [30, 61] (4.183), (13.74),

$$1/\zeta_{\text{top}}(z) = \frac{1 - 3z + z^2}{(1 - z)^2}, \quad (1.12)$$

where the numerator $(1 - z)^2$ corrects the overcounting of the fixed point at the origin due to assigning it to both \mathcal{M}_A (twice) and \mathcal{M}_B rectangles [71] (see figure 1.12 (a) for an example of such over-counting).

2CB

According to [ChaosBook count](#) [29], N_n , the number of *periodic points* of period n is given by the logarithmic derivative of the topological zeta function

$$\sum_{n=1} N_n z^n = -\frac{z}{1/\zeta_{\text{top}}} \frac{d}{dz}(1/\zeta_{\text{top}}). \quad (1.13)$$

Substituting the cat map topological zeta function (1.12) we obtain

$$\begin{aligned} \sum_{n=1} N_n z^n &= z + 5z^2 + 16z^3 + 45z^4 + 121z^5 + 320z^6 + 841z^7 \\ &\quad + 2205z^8 + 5776z^9 + 15125z^{10} + O(z^{11}) \end{aligned} \quad (1.14)$$

The number of *prime* cycles can be computed recursively

$$M_n = \frac{1}{n} \left(N_n - \sum_{d|n}^{d < n} d M_d \right), \quad (1.15)$$

(see [siminos/mathematica/CatMapTopZeta.nb](#)) or by the Möbius inversion formula

$$M_n = n^{-1} \sum_{d|n} \mu\left(\frac{n}{d}\right) N_d. \quad (1.16)$$

where the Möbius function $\mu(1) = 1$, $\mu(n) = 0$ if n has a squared factor, and $\mu(p_1 p_2 \dots p_k) = (-1)^k$ if all prime factors are different.³ Hence

$$\begin{aligned} \sum_{n=1} M_n z^n &= z + 2z^2 + 5z^3 + 10z^4 + 24z^5 + 50z^6 + 120z^7 \\ &\quad + 270z^8 + 640z^9 + 1500z^{10} \dots, \end{aligned} \quad (1.17)$$

in agreement with the Bird and Vivaldi [16] census. These counts are tabulated in table 4.1.

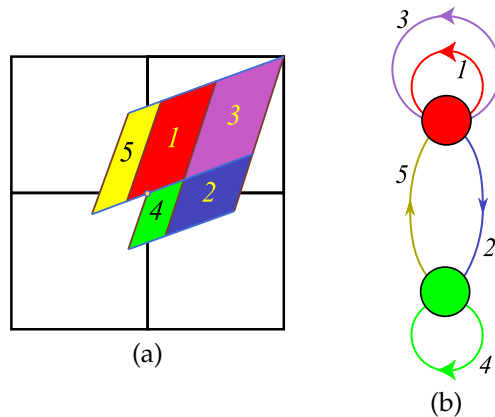


Figure 1.10: (Color online) (a) The sub-rectangles \mathcal{M}_j of figure 1.9(c). (b) Admissible orbits correspond to walks on the transition graph of figure 1.9(d), with rectangles \mathcal{M}_A (red) and \mathcal{M}_B (green) as nodes, and the links labeled by 5-letter alphabet (1.10), see the loop expansion (1.11).

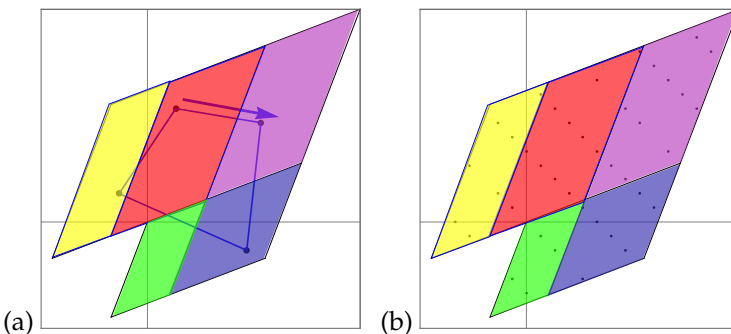


Figure 1.11: (a) An example of a 4-cycle: X_{0111} . (b) All period 4 orbits periodic points land in the partition of figure 1.10(a).

This derivation was based on the Adler-Weiss generating partition, a clever explicit visualization of the cat map dynamics, whose generalization to several coupled maps (let alone spatially infinite coupled cat maps lattice) is far from obvious: one would have to construct covers of high-dimensional parallelepipeds by sets of sub-volumes. However, as Keating [65] explains, no such explicit generating partition is needed to count cat map periodic orbits. Cat map (1.101) periodic points are the fixed points of

$$\begin{bmatrix} q_t \\ p_t \end{bmatrix} = \begin{bmatrix} q_{t+n} \\ p_{t+n} \end{bmatrix} = A^n \begin{bmatrix} q_t \\ p_t \end{bmatrix} \pmod{1},$$

so on the unwrapped phase space lattice, tiled by repeats of the unit square of the cat map torus,

$$(A^n - \mathbf{1}) \begin{bmatrix} q_t \\ p_t \end{bmatrix} = \begin{bmatrix} m_t^q \\ m_t^p \end{bmatrix}, \quad (m_t^q, m_t^p) \in \mathbb{Z}^2, \quad (1.18)$$

matrix $(A^n - \mathbf{1})$ stretches the unit square into what Keating calls the ‘fundamental parallelogram’ (an example is drawn in figure 1.12). The number of periodic points of period n is given by the area of this parallelogram

$$N_n = |\det(A^n - \mathbf{1})| = \Lambda^n + \Lambda^{-n} - 2, \quad (1.19)$$

where the Λ is the stability multiplier (3.40) of the Hamiltonian time evolution matrix A in (??).

Jaidee, Moss and Ward [62], *Time-changes preserving zeta functions*, say that a Lehmer–Pierce sequence [69, 82], with n th term $|\det(A^n - I)|$ for some integer matrix A , counts periodic points for an ergodic toral endomorphism if it is non-zero for all $n \geq 1$.

Substituting the numbers of periodic points N_n into the *topological* or *Artin-Mazur* zeta function [7, 29] we obtain (3.190), (4.183), (13.74)

$$\begin{aligned} 1/\zeta_{\text{top}}(z) &= \exp\left(-\sum_{n=1}^{\infty} \frac{z^n}{n} N_n\right) = \exp\left(-\sum_{n=1}^{\infty} \frac{z^n}{n} (\Lambda^n + \Lambda^{-n} - 2)\right) \\ &= \exp[\ln(1 - z\Lambda) + \ln(1 - z\Lambda^{-1}) - 2\ln(1 - z)] \\ &= \frac{(1 - z\Lambda)(1 - z\Lambda^{-1})}{(1 - z)^2} \\ &= \frac{1 - sz + z^2}{(1 - z)^2}, \end{aligned} \quad (1.20)$$

in agreement with Isola [61], as well as the Adler-Weiss generating partition topological zeta function (1.12). As explained in ChaosBook [29], topological zeta functions count *prime* orbits (1.70), i.e., the time invariant sets of periodic points, rather than the individual periodic points.

³Predrag 2020-01-18: did not know how to use MoebiusMu[]

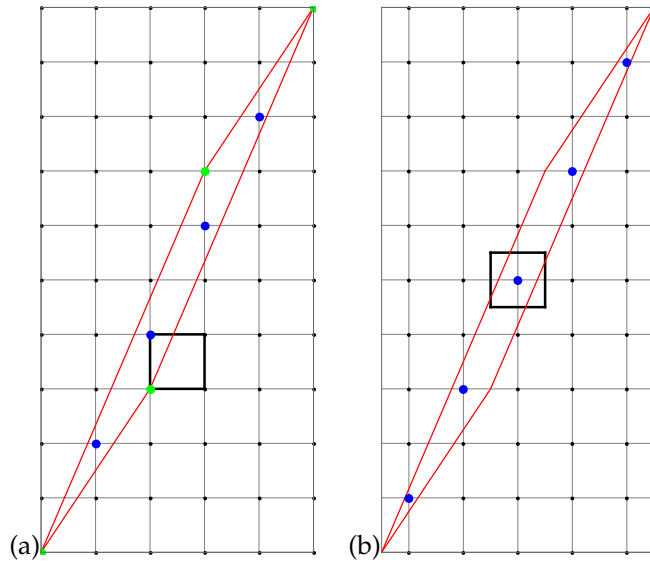


Figure 1.12: (Color online) (a) The corner-centered [black] unit square $(0, 1] \times (0, 1]$ is stretched by $(A^2 - 1)$ into the [red] fundamental parallelogram. By (1.18), each integer point within the fundamental parallelogram corresponds to a periodic point solution of period 2. The 4 internal integer points are marked by the blue dots. Note however that the 4 vertex integer points [green] are the same point mod 1, and thus have to be counted as 1 fixed point solution. (b) The face-centered [black] (Wigner-Seitz cell?) unit square $(-1/2, 1/2] \times (-1/2, 1/2]$ is stretched by $(A^2 - 1)$ into the [red] fundamental parallelogram. Now all 5 integer points [blue] are within the fundamental parallelogram, yielding again 5 periodic point solutions of period 2, but without any over-counting. Percival-Vivaldi cat map (1.101), $s = 3$.

1.3.3 An example: Fundamental parallelogram for period-2 cycle points

To visualize the fundamental parallelogram (1.18) counting of periodic solutions, consider Percival-Vivaldi $s = 3$ cat map (1.101) acting on states x_t within the unit square $(x_{t-1}, x_t) \in (0, 1] \times (0, 1]$, as in figure 1.12(a). In 2 time steps matrix $(A^2 - 1)$ stretches the unit square into the fundamental parallelogram, with integer points within the parallelogram corresponding to periodic points of period 2. Note however that the integer points on the vertices of the fundamental parallelogram over-count the number distinct solutions, as was already noted in the construction of the topological zeta function (1.12).

The $(x_{t-1}, x_t) = (0, 0)$ solution is a repeat of the fixed point solution for $n = 1$, so the total number of period-2 orbits is 2, as given in (1.70).

1.3.4 An example: period-4 orbits

As a hands-on example, let us count the $M_4 = 10$ admissible period 4 orbits, as stated in (1.70). The admissible blocks M_p can be read off as walks on either the 5-letter alphabet (1.10) graph, see figure 1.10(b), or the 3-letter alphabet (1.9) graph, see figure 1.9(d). They are, in 5-letter (top), and 3-letter (bottom) alphabets⁴

$$\begin{array}{ccccc} \overline{1113} & \overline{1125} & \overline{1245} & \overline{1253} & \overline{1325} \\ 0001 & 001\underline{1} & 010\underline{1} & 01\underline{11} & 011\underline{1} \\ \overline{1133} & \overline{3325} & \overline{3331} & \overline{3245} & \overline{4452} \\ 0011 & 111\underline{1} & 1110 & 110\underline{1} & 001\underline{1} \end{array} . \quad (1.21)$$

The corresponding periodic orbits X_p are computed using Green's function (??) (the inverse of the - of the $[4 \times 4]$ orbit Jacobian matrix (3.81), easiest to evaluate by discrete Fourier transforms, see appendix ??):

$$M_{0001} \Rightarrow X_{0001} = g \begin{bmatrix} 0 \\ 0 \\ 0 \\ 1 \end{bmatrix} = \frac{1}{15} \begin{bmatrix} 3 \\ 2 \\ 3 \\ 7 \end{bmatrix} .$$

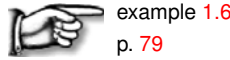
Likewise,⁵

⁴Predrag 2019-12-20: For covering symbolic dynamics, use/refer to ChaosBook.
Order (18.12) lexically.

⁵Predrag 2019-12-20: To Han: order lexically.

$$\begin{aligned}
 X_{0011}^\top &= \frac{1}{15} \begin{bmatrix} -1 & 1 & 4 & -4 \end{bmatrix}, & X_{0101}^\top &= \frac{1}{15} \begin{bmatrix} 0 & 5 & 0 & -5 \end{bmatrix} \\
 X_{0111}^\top &= \frac{1}{15} \begin{bmatrix} 4 & 6 & -1 & 6 \end{bmatrix}, & X_{0111}^\top &= \frac{1}{15} \begin{bmatrix} 2 & 8 & 7 & -2 \end{bmatrix} \\
 X_{0011}^\top &= \frac{1}{15} \begin{bmatrix} 5 & 5 & 10 & 10 \end{bmatrix}, & X_{1111}^\top &= \frac{1}{15} \begin{bmatrix} 9 & 11 & 9 & 1 \end{bmatrix} \\
 X_{1110}^\top &= \frac{1}{15} \begin{bmatrix} 12 & 13 & 12 & 8 \end{bmatrix}, & X_{1101}^\top &= \frac{1}{15} \begin{bmatrix} 7 & 8 & 2 & -2 \end{bmatrix} \\
 X_{0011}^\top &= \frac{1}{15} \begin{bmatrix} 1 & -1 & -4 & 4 \end{bmatrix}. & & (1.22)
 \end{aligned}$$

One can verify that for each of these 10 period 4 orbits the periodic points (x_t, x_{t+1}) visit the rectangles \mathcal{M}_A or \mathcal{M}_B of figure 1.9 (b) in the temporal order dictated by the transition graph, and thus they are all admissible cycles.⁶



1.3.5 Adler / Adler98

Predrag 2017-10-02 excerpts from or notes on
Adler [1] *Symbolic dynamics and Markov partitions*, ([click here](#)) an excellent overview of symbolic dynamics techniques.

$$A = \begin{pmatrix} a & b \\ c & d \end{pmatrix}, \quad (1.23)$$

where a, b, c, d and $\det A = 1$. The row vectors

$$\{\mathbf{e}_{(+)}, \mathbf{e}_{(-)}\} = \{[c, \Lambda - a], [c, \Lambda^{-1} - a]\} \quad (1.24)$$

are the left expanding / contracting eigenvectors. The matrix (1.23) is in general not symmetric, so $\{\mathbf{e}_{(j)}\}$ do not form an orthogonal basis. For matrix (1.5) the left eigenvectors are

$$\{\mathbf{e}_{(+)}, \mathbf{e}_{(-)}\} = \{[-1, \Lambda], [-1, \Lambda^{-1}]\}, \quad (1.25)$$

in agreement with (1.8). I prefer the right eigenvectors basis $\{\mathbf{e}^{(j)}\}$, as it lies in the first quadrant.

1.3.6 Percival and Vivaldi / PerViv

Predrag 2016-05-29 excerpts from or notes on
Percival and Vivaldi [80] *A linear code for the sawtooth and cat maps* ([click here](#))

“Completely chaotic systems are comparatively well understood, but they have been neglected as a starting point for the study of systems with divided phase space. It is the purpose of this and related papers to remedy this.”

⁶Predrag 2019-09-11: Add here the blog figure that has all points in the partition.

"When one starts with an integrable system, and perturbs it to introduce some chaos, new orbits and new classes of orbits keep on appearing by bifurcation processes, and they are very difficult to follow or to classify. It is better to start with a purely chaotic system and then reduce the chaos by *removing* orbits."⁷

"In this paper we present the symbolic dynamics of the sawtooth maps, and in the companion paper [81] *Arithmetical properties of strongly chaotic motions* the number theory for the periodic orbits of the automorphisms of the torus, including the cat maps."

"we start with the simplest systems that show the phenomena of interest-area preserving maps. The sawtooth maps are piecewise linear systems. They depend on a parameter K and for positive K they are completely chaotic. For positive *integer* K they are automorphisms of the torus, of which the simplest is the Arnol'd-Sinai cat map, with K = 1. We shall refer to all such toral automorphisms, with positive integer K, as cat maps. They are Anosov systems, continuous on the torus. On the other hand, when K is not an integer, the sawtooth map is discontinuous."

"Most of this paper is concerned with a 'linear code' for the symbolic dynamics of the sawtooth maps, including the cat maps. This code is chosen for its convenience in practice, and differs from the usual codes for the Arnol'd-Sinai cat."

"In section 3 a practical problem of stabilisation is considered, that provides a concrete model for the sawtooth and cat maps, and a natural introduction to the linear codes. An explicit linear transformation from the itinerary to the orbit is given."

⁸ Every Anosov diffeomorphism of the torus is topologically conjugate to a hyperbolic automorphism. These are represented by $[2 \times 2]$ matrices with integer entries (for continuity), unit determinant (for area preservation) and real eigenvalues (for hyperbolicity), and are known as cat maps.

In order to describe certain collective properties of cat map orbits Hannay and Berry [54] introduced a function closely related to the least common multiple of their periods.

1.3.7 Isola / Isola90

Predrag 2016-06-02 excerpts from or notes on

S. Isola [61] ζ -functions and distribution of periodic orbits of toral automorphisms

Bellissard's friend Isola gives counting formulas of the usual type - could easily be turned into examples/exercises for ChaosBook. But I am looking for symbolic dynamics - not even mentioned here.

We consider canonical automorphisms of the torus T^2 , i.e. maps of the form

$$T(x, y) = (ax + by, cx + dy) \quad \text{mod } 1,$$

⁷Predrag 2016-05-29: totally agree - they say it well

⁸Predrag 2016-06-02: verbatim from Keating [64]

which are implemented by the group of [2x2] matrices with integer entries, determinant 1, and eigenvalues (12.12).

To study the properties of this dense set of unstable periodic orbits, observe that the periodic orbits of T consist precisely of those points having rational coordinates $(p_l/q_l, p_1/q_2)$. If p_1, q_1 are coprime and g is the least common multiple of q_1 and q_2 , then the square lattice of size l/g is invariant under T .

In this direction, Percival and Vivaldi [16, 80, 81] have constructed a nice translation of the dynamical problem into the language of modular arithmetic, allowing a profound understanding of the structure of periodic orbits. Here, however, we follow another approach where a general expression for the N 's is derived through a simple iterative scheme. Consider the numbers

$$u_n = \frac{\Lambda^n - \Lambda^{-n}}{\sqrt{D}}. \quad (1.26)$$

The first two terms of the series are $u_0 = 0$, $u_1 = 1$ and each term after is given by

$$u_n = su_{n-1} - u_{n-2}. \quad (1.27)$$

[stuff to work out: Isola has nice figures that illustrate the partitions of the 2-torus]

For the number of periodic points he finds, for any integer $s > 2$

$$N_n = \Lambda^n + \Lambda^{-n} - 2, \quad (1.28)$$

in agreement with the numerics of ref. [78]. Walters [110] defines the topological entropy as

$$h = \lim_{n \rightarrow \infty} \frac{1}{n} \ln N_n, \quad (1.29)$$

This yields $h = \log \Lambda$, i.e., the Sinai theorem for the entropy of an automorphism [6, 94].

The topological zeta function for cat-map class of models is

$$\frac{1}{\zeta_{\text{top}}(z)} = \frac{(1 - \Lambda z)(1 - \Lambda^{-1}z)}{(1 - z)^2} = \frac{1 - sz + z^2}{(1 - z)^2}. \quad (1.30)$$

The denominator $(1 - z)^2$ takes care of the over-counting of the fixed point at the origin due to the 2-periodicity on the torus.⁹

He also gives the number of orbits of period n , which is as usual given in terms of the Moebius function $\mu(m)$,

$$P_n = \frac{1}{n} \sum_{m|n} \mu(m) N_{n/m}. \quad (1.31)$$

⁹Predrag 2016-06-02: I wonder whether the fact that this is quadratic in z has something to do with the time-reversibility, and the unsigned graph's Ihara zeta functions, see sect. 13.1 and (4.174).

1.3.8 Creagh / Creagh94

Predrag 2016-06-02 excerpts from or notes on
 Creagh [27], *Quantum zeta function for perturbed cat maps* ([click here](#)), who says:
 “ The behavior of semiclassical approximations to the spectra of perturbed quantum cat maps is examined as the perturbation parameter brings the corresponding classical system into the nonhyperbolic regime. The approximations are initially accurate but large errors are found to appear in the traces and in the coefficients of the characteristic polynomial after nonhyperbolic structures appear. Nevertheless, the eigenvalues obtained from them remain accurate up to large perturbations. ”

Thom-Arnol'd cat map

$$A = \begin{pmatrix} 1 & 1 \\ 1 & 2 \end{pmatrix}, \quad \det A = 1. \quad (1.32)$$

This system can be written as:

$$\begin{pmatrix} q_{t+1} \\ p_{t+1} \end{pmatrix} = A \begin{pmatrix} q_t \\ p_t \end{pmatrix} \mod 1 \quad (1.33)$$

It is possible to construct a symbolic coding with finite grammar, as described in Devaney [35]. Robinson [86] goes through the construction clearly, step by step. The coding is constructed for an antisymplectic map whose double iteration is (1.33) - orbits of the cat map are then coded by sequences whose length is even. A brief summary of the construction follows (see Devaney [35] for figures and details). The stable and unstable manifolds coming from the fixed point at $(q, p) = (0, 0)$ are used to divide the phase space into 3 rectangles R_1 , R_2 and R_3 . Under iteration of the antisymplectic map, R_1 is mapped into $R_2 \cup R_3$, R_2 into $R_1 \cup R_3$ and R_3 is mapped completely into R_2 . Therefore orbits of the antisymplectic map are coded by sequences of 3 symbols (1,2,3), where 1 must be followed by 2 or 3, 2 is followed by 1 or 3, and 3 must be followed by 2. The full cat map is coded by even sequences of symbols following the same grammar. We can alternatively code orbits of the full map with 5 symbols denoting the admissible pairs of the symbols above: $(a, b, c, d, e) = (12, 13, 21, 23, 32)$.

The integers that must be subtracted from the phase space coordinates following application of the linear map in (1.33) in order to take the point back into the unit torus are fixed for each pair of symbols. The equation defining a periodic orbit can be written out as an explicit affine equation and solved for each itinerary. In this way a complete list of primitive periodic orbits is obtained for the unperturbed map.

1.3.9 Keating / Keating91

Keating [65] *The cat maps: quantum mechanics and classical motion.*

the action of map on the vector (p, q) can be described as the motion in the phase space specified by the Hamiltonian [65]

$$H(p, q) = (k^2 - 4)^{-1/2} \sinh^{-1}[(k^2 - 4)^{-1/2}/2][m_{12}p^2 - m_{21}q^2 + (m_{11} - m_{22})pq]. \quad (1.34)$$

Here, (p, q) are taken modulo 1 at each observation (the integer part is ignored), and observations occur at integer points of time.

The paper has a nice discussion of (possible discrete symmetries of cat maps.

Keating and F. Mezzadri [66] *Pseudo-symmetries of Anosov maps and spectral statistics.*¹⁰

Earlier work: Rykken [89] constructed new types of Markov partitions. Snavely [98] studied the connectivity matrices of Markov partitions for hyperbolic automorphisms of T^2 . He found that for Berg partitions the connectivity matrices are conjugated to the dynamics. He also found a way to list all such matrices and hence to classify the shapes of Berg partitions. He relied on the result of Adler [1] that such partitions are indeed present for any toral automorphism. Manning [72] gave a powerful generalization of this to T^n .

Anosov, Klimenko and Kolutsky [5] give an introduction to Anosov diffeomorphisms, ways to represent their chaotic properties and some historical remarks on this subject: “As far as we know, the first example of such kind was pointed out by J. Hadamard about 1900. A couple of decades earlier H. Poincaré discovered the “homoclinic points” which now serve as the main “source” of “chaoticity”; however, Poincaré himself spoke only that the “phase portrait” (i.e., the qualitative picture of trajectories’ behaviour in the phase space) near such points is extremely complicated. A couple of decades after Hadamard, E. Borel encountered a much simpler example of the “chaoticity” where it is easy to understand the “moving strings” of this phenomenon. We shall begin with a description of his example. About 100 years later it remains the simplest manifestation of the fact that a dynamical system (which, by definition, is deterministic) can somehow resemble a stochastic process.”

1.4 Green’s function for 1-dimensional lattice

Cat map is a second order difference equation

$$x_{t+1} - s x_t + x_{t-1} = -m_t, \quad (1.35)$$

with the unique integer “winding number” m_t at every time step t ensuring that x_{t+1} lands in the unit interval. This is a 1-dimensional discrete screened Poisson equation of form

$$\mathcal{D}x = m, \quad (1.36)$$

¹⁰Predrag 2016-08-29: not useful for the deterministic case

where x_t are lattice states, and m_t are the ‘sources’. Since $\mathcal{D}_{tt'}$ is of a tridiagonal form, its inverse, or its Green’s discrete matrix g on infinite lattice satisfies

$$(\mathcal{D}g)_{t0} = \delta_{t0}, \quad t \in \mathbb{Z} \quad (1.37)$$

with a point source at $t = 0$. By time-translation invariance $g_{tt'} = g_{t-t',0}$, and by time-reversal invariance $g_{t',t} = g_{t,t'}$. In this simple, tridiagonal case, g can be evaluated explicitly [73, 80],

$$g_{tt'} = \frac{1}{\Lambda^{|t'-t|}} \frac{1}{\Lambda - \Lambda^{-1}}, \quad (1.38)$$

where, in the hyperbolic $s > 2$ case, the cat map “stretching” parameter s is related to the 1-time step cat map eigenvalues $\{\Lambda, \Lambda^{-1}\}$ by

$$s = \Lambda + \Lambda^{-1} = e^\lambda + e^{-\lambda} = 2 \cosh \lambda, \quad \lambda > 0. \quad (1.39)$$

While the “Laplacian” matrix \mathcal{D} is sparse, it is non-local (i.e., not diagonal), and its inverse is the full matrix g , whose key feature, however, is the prefactor $\Lambda^{-|t'-t|}$ which says that the magnitude of the matrix elements falls off exponentially with their distance from the diagonal. For this it is crucial that the \mathcal{D} eigenvalues (1.39) are hyperbolic. In the elliptic, $-2 < s < 2$ case, the sinh’s and cosh’s are replaced by sines and cosines, $s = 2 \cos \theta = \exp(i\theta) + \exp(-i\theta)$, and there is no such decay of the off-diagonal matrix elements.

For a finite-time lattice with n sites we can represent \mathcal{D} by a symmetric tridiagonal $[n \times n]$ Toeplitz matrix. The matrix

$$\mathcal{D}_n = \begin{pmatrix} s & -1 & 0 & 0 & \dots & 0 & 0 \\ -1 & s & -1 & 0 & \dots & 0 & 0 \\ 0 & -1 & s & -1 & \dots & 0 & 0 \\ \vdots & \vdots & \vdots & \vdots & \ddots & \vdots & \vdots \\ 0 & 0 & \dots & \dots & \dots & s & -1 \\ 0 & 0 & \dots & \dots & \dots & -1 & s \end{pmatrix} \quad (1.40)$$

satisfies *Dirichlet boundary conditions*, in the sense that the first and the last site do not have a left (right) neighbor to couple to. We distinguish it from the circulant matrix (1.47) by emphasising that $(\mathcal{D}_n)_{0,n-1} = (\mathcal{D}_n)_{n-1,0} = 0$. As the time-translation invariance is lost, the matrix elements of its inverse, the Green’s $[n \times n]$ matrix $g_{tt'}$, with a delta-function source term and the Dirichlet boundary conditions

$$\begin{aligned} (\mathcal{D}g)_{tt'} &= \delta_{tt'} \quad t, t' \in 0, 1, 2, \dots, n-1 \\ 0 &= g_{-1,t'} = g_{t,-1} = g_{nt'} = g_{tn} \end{aligned} \quad (1.41)$$

depend on the point source location t , and no formula for its matrix elements as simple as (1.38) is to be expected. In general, a finite matrix inverse is of the form

$$\mathcal{D}^{-1} = \frac{1}{\det \mathcal{D}} (\text{cofactor matrix of } \mathcal{D})^\top.$$

While the cofactor matrix might be complicated, the key here is, as in formula (1.38), that the prefactor $1/\det \mathcal{D}$ falls off exponentially, and for Toeplitz matrices can be computed recursively.

Associated with this simple tridiagonal matrix are the Chebyshev polynomials of the first and the second kind

$$T_n(s/2) = \cosh(n\lambda), \quad U_n(s/2) = \sinh(n+1)\lambda / \sinh(n\lambda),$$

generated by a three-term recursion relation (second-order difference equation [40]).

The identity

$$2T_n(s/2) = \Lambda^n + \Lambda^{-n} \quad (1.42)$$

follows from $s = \Lambda + \Lambda^{-1}$, see (1.6).

The inverse of the Dirichlet boundary conditions matrix \mathcal{D}_n (1.40) can be determined explicitly, in a number of different ways [59, 92, 97, 101]. Here we find it convenient to write the inverse of \mathcal{D}_n in the Chebyshev polynomial form [114]. The determinant of \mathcal{D}_n , i.e., the Jacobian of the linear transformation (1.36) is well known [48]

$$\det \mathcal{D}_n = U_n(s/2), \quad (1.43)$$

and the matrix elements of the Green's function in the Chebyshev polynomial form [59, 114] are explicitly

$$g_{ij} = \frac{1}{\det \mathcal{D}_n} \times \begin{cases} U_{i-1}(s/2) U_{n-j}(s/2) & \text{for } i \leq j \\ U_{j-1}(s/2) U_{n-i}(s/2) & \text{for } i > j. \end{cases}. \quad (1.44)$$

$\det \mathcal{D}_n$ is also known as the determinant of the *Dirichlet kernel* (see [wiki](#))

$$D_n(x) = \sum_{k=-n}^n e^{ikx} = 1 + 2 \sum_{k=1}^n \cos(kx) = \frac{\sin((n+1/2)x)}{\sin(x/2)}. \quad (1.45)$$

It follows from the recurrence relation $x_{i+1} = sx_i - x_{i-1}$, mod 1, that $U_n(s/2)$ Chebyshev polynomials have the generating function

$$\begin{aligned} \sum_{n=0}^{\infty} U_n(s/2) z^n &= \frac{1}{1 - sz + z^2} \\ &= 1 + sz + (s^2 - 1)z^2 + (s^3 - 2s)z^3 + \dots, \end{aligned} \quad (1.46)$$

with $U_n(s/2) \approx s^n \approx \Lambda^n$, and for a hyperbolic system the off-diagonal matrix elements $g_{tt'}$ are again falling off exponentially with their separation $|t' - t|$, as in (1.38), but this time only in an approximate sense.

¹¹ Alternatively, for finite time n we can represent \mathcal{D} by a symmetric tridiagonal $[n \times n]$ circulant matrix with *periodic boundary conditions*

$$\mathcal{D}_n = \begin{pmatrix} s & -1 & 0 & 0 & \dots & 0 & -1 \\ -1 & s & -1 & 0 & \dots & 0 & 0 \\ 0 & -1 & s & -1 & \dots & 0 & 0 \\ \vdots & \vdots & \vdots & \vdots & \ddots & \vdots & \vdots \\ 0 & 0 & \dots & \dots & \dots & s & -1 \\ -1 & 0 & \dots & \dots & \dots & -1 & s \end{pmatrix}. \quad (1.47)$$

In the periodic boundary conditions case the determinant (in contrast to the Dirichlet case (1.43)) is obtained by Fourier-transform diagonalization

$$\det \mathcal{D}_n = \prod_{j=0}^{n-1} \left[s - 2 \cos\left(\frac{2\pi j}{n}\right) \right] = 2 T_n(s/2) - 2, \quad (1.48)$$

see (1.42). ¹²

Now the discrete matrix Green's function $\mathbf{g}_{tt'}$ satisfies periodic boundary conditions

$$\begin{aligned} (\mathcal{D}\mathbf{g})_{t1} &= \delta_{t1}, & t = 1, 2, \dots, n \\ \mathbf{g}_{n+1,t'} &= \mathbf{g}_{1t'}, & \mathbf{g}_{t,n+1} = \mathbf{g}_{t1}. \end{aligned} \quad (1.49)$$

Note that the Green's matrix is strictly negative for both the periodic and Dirichlet boundary conditions.

Left over from Boris version: Consider the single cat map equation with a delta-function source term

$$(-\square + \mu^2)\mathbf{g}_t = \delta_{t,0}, \quad t \in \mathbb{Z}^1. \quad (1.50)$$

An alternative way to evaluate $g_{i,j}$ is to use Green's function g and take antiperiodic sum (similar method can be used for periodic and Neumann boundary conditions)

$$g_{i,j} = \sum_{n=-\infty}^{\infty} g_{i,j+2n(n+1)} - g_{i,-j+2n(n+1)}. \quad (1.51)$$

This approach has an advantage of being extendable to the \mathbb{Z}^2 case. After substituting g and taking the sum one obtains (1.44).

See also sect. 1.6 Chebyshev series.

¹¹Predrag 2017-09-20: Probably should do circulants first, then the complicated Dirichlet case next, in the spirit of starting out with the infinite lattice case (1.38).

¹²Han 2018-12-01: I still have to derive and recheck this formula!

1.5 Green's blog

2017-08-24,2017-09-09 Predrag This to all curious cats, but mostly likely only Boris might care: OK now I see why Chebyshevs...

2CB

Chebyshev expansions are used here because of the recurrence relations that they satisfy.

A *Toeplitz matrix*, T , is a matrix that is constant along each diagonal, i.e., $T_{jk} = t_{j-k}$. A *Hankel matrix*, H , is a matrix that is constant along each anti-diagonal, i.e., $H_{jk} = h_{j+k}$. There is also the *Laurent matrix* or *doubly infinite Toeplitz matrix*.

2CB

R. M. Gray (2009) [Toeplitz and Circulant Matrices: A Review](#) focuses on bounds of sums of eigenvalues - I see nothing here that is of immediate use to us, with maybe the exception of the discussion of the diagonalization of circulant matrices (discrete Fourier series).

A look at a Toeplitz matrix evokes time evolution of a periodic orbit symbolic block: it looks like successive time shifts stacked upon each other, every entry is doubly periodic on a torus of size $[n_p \times n_p]$. Does that have to do something with Chebyshev polynomials (rather than with the usual discrete Fourier series)? One uses Chebyshev polynomials of the first, second, third, and fourth kind, denoted by T_n, U_n, V_n, W_n , if, as an example, one looks at a pentadiagonal symmetric Toeplitz matrix, a generalization of the 3rd order spatial derivative.

Circulant matrices are discussed in Aitkenref. [4] (1939).

Maybe some of the literature cited here illuminates this:

2017-09-09 Predrag The eigenvalues and eigenvectors for the finite symmetric tridiagonal Toeplitz matrix might have been obtained by Streater [101] *A bound for the difference Laplacian*, but I do not see where in the article they are. They seem to also be given in Smith [97] *Numerical Solution of Partial Differential Equations: Finite Difference Methods*.

Hu and O'Connell [59] *Analytical inversion of symmetric tridiagonal matrices* " present an analytical formula for the inversion of symmetrical tridiagonal matrices. As an example, the formula is used to derive an exact analytical solution for the one-dimensional discrete screened Poisson equation (DPE) with Dirichlet boundary conditions. " The n eigenvalues and orthonormal n -dimensional eigenvectors of \mathcal{D} are ¹³

$$\begin{aligned}\gamma_k &= s + 2 \cosh \frac{k\pi}{n+1}, & k &= 1, 2, \dots, n \\ e_n^{(k)} &= \sqrt{\frac{2}{n+1}} \sinh \frac{k\pi}{n+1}\end{aligned}\tag{1.52}$$

¹³Predrag 2017-09-09: recheck!

(see, for example, refs. [59, 114]). This is a typical inverse propagator, see ChaosBook [9]

$$(\varphi_k^\dagger \cdot \Delta \cdot \varphi_{k'}) = \left(-2 \cos\left(\frac{2\pi}{N} k\right) + 2 \right) \delta_{kk'} \quad (1.53)$$

The inverse (the Green's function) $g\mathcal{D} = 1$ is [59]¹⁴

$$g_{jk} = \frac{\cosh(n+1-|k-j|)\lambda - \cosh(n+1-j-k)\lambda}{2 \sinh \lambda \sinh(n+1)\lambda} \quad (1.54)$$

The above paper is applied to physical problems in Hu and O'Connell [57] *Exact solution for the charge soliton in a one-dimensional array of small tunnel junctions*, and in Hu and O'Connell [58] *Exact solution of the electrostatic problem for a single electron multijunction trap*. The **erratum** is of no importance for us, unless the - sign errors affect us.

A cute fact is that they also state the solution for $s = 2$, which, unlike (1.54) has no exponentials - it's a power law.

Eigenvalues, eigenvectors and inverse for $[n \times n]$ matrix \mathcal{D} (1.40), $-2 < s < 2$,

$$\begin{aligned} \lambda_k &= -s + 2 \cos \frac{k\pi}{n+1} \\ e_k &= \sqrt{\frac{2}{n+1}} \left(\sin \frac{k\pi}{n+1}, \sin \frac{2k\pi}{n+1}, \dots, \sin \frac{nk\pi}{n+1} \right) \\ (\mathcal{D}^{-1})_{kn} &= \frac{2}{n+1} \sum_{m=1}^n \frac{\sin \frac{km\pi}{n+1} \sin \frac{n m \pi}{n+1}}{-s + 2 \cos \frac{k\pi}{n+1}} \end{aligned} \quad (1.55)$$

are computed in Meyer [74] *Matrix Analysis and Applied Linear Algebra*.

Yamani and Abdelmonem [114] *The analytic inversion of any finite symmetric tridiagonal matrix* rederive Hu and O'Connell [59], using the theory of orthogonal polynomials in order to write down explicit expressions for the polynomials of the first and second kind associated with a given infinite symmetric tridiagonal matrix H.

The matrix representation of many physical operators are tridiagonal, and some computational methods, are based on creating a basis that renders a given system Hamiltonian operator tridiagonal. The advantage lies in the connections between tridiagonal matrices and the orthogonal polynomials, continued fractions, and the quadrature approximation which can be used to invert the tridiagonal matrix by finding the matrix representation of the Green's functions.

The Green's function $G(z)$ associated with the matrix H is defined by the relation

$$(H - zI)G = I. \quad (1.56)$$

¹⁴Predrag 2017-09-09: It is shown in ref. [114] that is the same as the formula (1.44) Boris uses (without a source citation).

It is more convenient to calculate the inverse of the matrix $(H - zI)$ instead of the inverse of the matrix H . Note that in this formulation G is the *resolvent* of H .

Simons [92] *Analytical inversion of a particular type of banded matrix* re derives Hu and O'Connell [59] by a "a simpler and more direct approach". The structure of (1.56) is that of a homogeneous difference equation with constant coefficients and therefore one looks for a solution of the form

$$G_{pq} = A_q e^{p\lambda} + A_q e^{-p\lambda}, \quad (1.57)$$

with appropriate boundary conditions. This leads to the Hu and O'Connell formulas for the inverses of G .

How to invert a very regular banded Toeplitz matrix.

Yueh [115] *Explicit inverses of several tridiagonal matrices* has a bunch of fun tri-diagonal Toeplitz matrix inverses, full of integers - of no interest to us.

Dow [36] *Explicit inverses of Toeplitz and associated matrices*: " We discuss Toeplitz and associated matrices which have simple explicit expressions for their inverses. We first review existing results and generalize these where possible, including matrices with hyperbolic and trigonometric elements. In Section 4 we invert a tridiagonal Toeplitz matrix with modified corner elements. A bunch of fun tri-diagonal Toeplitz matrix inverses, full of integers - of no interest to us.

Noschese, Pasquini and Reichel [77] *Tridiagonal Toeplitz matrices: properties and novel applications* use the eigenvalues and eigenvectors of tridiagonal Toeplitz matrices to investigate the sensitivity of the spectrum. Of no interest to us.

Berlin and Kac [15] *The spherical model of a ferromagnet* use bloc-circulant matrices; see also

Davis [34] *Circulant Matrices*

2017-09-09 Predrag Gover [46] *The Eigenproblem of a Tridiagonal 2-Toeplitz Matrix* seems less useful: " The characteristic polynomial of a tridiagonal 2-Toeplitz matrix is shown to be closely connected to polynomials which satisfy the three point Chebyshev recurrence relationship. This is an extension of the well-known result for a tridiagonal Toeplitz matrix. When the order of the matrix is odd, the eigenvalues are found explicitly in terms of the Chebyshev zeros. The eigenvectors are found in terms of the polynomials satisfying the three point recurrence relationship. "

Gover [46] motivates his paper by reviewing a tridiagonal 1-Toeplitz, or Toeplitz matrix, referring to the original literature. Consider a tridiagonal $[\ell \times \ell]$ Toeplitz matrix with Dirichlet boundary conditions (1.40), with eigenvalues (1.52).

Kübra Duru and Bozkurt [67] *Integer powers of certain complex pentadiagonal 2-Toeplitz matrices*

Elouafi [41] *On a relationship between Chebyshev polynomials and Toeplitz determinants:* “Explicit formulas are given for the determinants of a band symmetric Toeplitz matrix T_n with bandwidth $2r + 1$. The formulas involve $r \times r$ determinants whose entries are the values of Chebyshev polynomials on the zeros of a certain r th degree q which is independent of n .”

2017-09-09 Predrag Felsner and Heldt *Lattice paths* seem to be all on graphs - I see no 2-dimensional lattice here.

Spectral asymptotics in one-dimensional periodic lattices with geometric interaction

1.6 Chebyshev series

Chebyshev series are Fourier (cosine) series in disguise.
— Jason Mireles-James

The canonical reference is Boyd [24] *Chebyshev and Fourier Spectral Methods* ([click here](#)). Perhaps check also:

Keaton J. Burns *Chebyshev Spectral Methods with applications to Astrophysical Fluid Dynamics*.

Philippe Grandclement [49] *Introduction to spectral methods* [arXiv:gr-qc/0609020](https://arxiv.org/abs/gr-qc/0609020).

1.6.1 Spectral methods

The basic idea of all numerical techniques is to approximate any function $u(x)$ by polynomials, $\hat{u} = \sum_{n=0}^N \hat{u}_n p_n(x)$ where the $p_n(x)$ are polynomial *trial functions*. Depending on the choice of trial functions, one has various classes of numerical techniques. For example, the *finite difference* schemes are obtained by choosing local polynomials of low degree. In *spectral methods* the $p_n(x)$ are global polynomials, typically Legendre or Chebyshev. Spectral methods can reach very good accuracy with only moderate computational resources; for C^∞ functions, the error decays exponentially, as one increases the degree of the approximation.

2CB

A function u can be described either by its value $u(x_i)$ at each collocation point x_i or by the coefficients \tilde{u}_i of the *interpolant* of u

$$[I_N u](x) = \sum_{n=0}^N \tilde{u}_n p_n(x). \quad (1.58)$$

The computation of \tilde{u} only requires evaluation of u at the $N + 1$ collocation points. The interpolant of u is the spectral approximate of u in terms of polynomials of degree N that coincide with u at each collocation point:

$$[I_n u](x_i) = u(x_i) \quad \forall i \leq N.$$

If the values at collocation points are known one is working in the *configuration space*, and in the *coefficient space* if u is given in terms of its coefficients.

Depending on the operation one has to perform, one choice of space is usually more suited than the other. The derivative of u can be evaluated in the coefficient space by approximating u' by the derivative of the interpolant,

$$u'(x) \approx [I_N u]'(x) = \sum_{n=0}^N \tilde{u}_n p'_n(x).$$

This requires only the knowledge of the coefficients of u and the derivatives of the basis polynomials. This approximate derivative is not the interpolant of u' , as the polynomials that represent $(I_N u)'$ do not coincide with u' at the collocation points.

1.6.2 Discretizing with Chebyshev polynomials

To use Chebyshev series as a basis, one shifts the problem to functions defined over $x \in [-1, 1]$, and expands them in Chebyshev polynomial of the first kind $T_k(x)$

$$\phi(x) = \phi_0 + 2 \sum_{n=1}^{\infty} \phi_n T_n(x), \quad (1.59)$$

where $T_k(z)$ are defined by 3-term recurrence (13.61).

Expanded as Chebyshev series, the product of functions

$$a(x) = a_0 + 2 \sum_{n=1}^{\infty} a_n T_n(x), \quad b(x) = b_0 + 2 \sum_{n=1}^{\infty} b_n T_n(x),$$

satisfies the Fourier-like convolution formula ¹⁵

$$(a \cdot b)(x) = (a * b)_0 + 2 \sum_{n=1}^{\infty} (a * b)_n T_n(x)$$

where

$$(a * b)_n = \sum_{k_1+k_2=n} a_{|k_1|} b_{|k_2|}, \quad k_1, k_2 \in \mathbb{Z}$$

Chebyshev polynomials are an analogue of the Fourier expansion for non periodic functions on an interval and, as the Chebyshev polynomials of the first kind [24] satisfy

$$T_n(\cos(x)) = \cos(nx), \quad (1.60)$$

they are Fourier series in disguise. Mapping (1.60) geometric interpretation: the n th Chebyshev polynomial is the projection onto a plane of the function $y = \cos(nx)$ drawn on a cylinder.

¹⁵Predrag 2020-06-07: I think of Fourier convolution formula as a statement of the translation invariance condition on matrices, not sure how to think about this.

For $x = 0$, $T_n(1) = 1$. For $x = 2\pi k/n$, $k = 0, 1, \dots, n - 1$, $\cos(2\pi k/n)$ is the k th root of equation

$$T_n(x) - 1 = 0.$$

This equation can be written as a product over the eigenvalues

$$T_n(x) - 1 = 2^{n-1} \prod_{k=0}^{n-1} [x - \cos(2\pi k/n)]. \quad (1.61)$$

Here the coefficient 2^{n-1} comes from matching the coefficient of x^n term in the definition of $T_n(x) = \dots + 2^{n-1}x^n$. For $x = s/2$, this is the orbit Jacobian matrix determinant formula

$$N_n = \prod_{k=0}^{n-1} [s - 2 \cos(2\pi k/n)] = 2T_n(s/2) - 2. \quad (1.62)$$

Three different types of partial differential equation solvers [49] are the *Tau-method*, the *collocation method* and the *Galerkin method*.

The basic idea of the Galerkin method is to expand the solution as a linear combinations of polynomials -the *Galerkin basis*- that fulfill the boundary conditions.

The Chebyshev polynomials T_n are an orthogonal set on $[-1, 1]$ for the measure $w = \frac{1}{\sqrt{1-x^2}}$,

$$\int_{-1}^1 \frac{T_n T_m}{\sqrt{1-x^2}} dx = \frac{\pi}{2} (1 + \delta_{0n}) \delta_{mn}. \quad (1.63)$$

2020-06-03 Jason Mireles-James talk, *Parameterization of unstable manifolds for delay differential equations*: Delay differential equations (DDEs) are important in physical applications where there is a time lag in communication between subsystems. They provide natural examples of infinite dimensional dynamical systems. He discusses Chebyshev spectral numerical methods for computing invariant manifolds for DDEs.

2020-06-03 Jean-Philippe Lessard talk, *Rigorous integration of infinite dimensional dynamical systems via Chebyshev series*: In this talk we introduce recent general methods to rigorously compute solutions of infinite dimensional Cauchy problems. The idea is to expand the solutions in time using Chebyshev series and use the contraction mapping theorem to construct a neighbourhood about an approximate solution which contains the exact solution of the Cauchy problem. We apply the methods to some semi-linear parabolic partial differential equations (PDEs) and delay differential equations (DDEs).

For my screen grabs from the 2 talks, ([click here](#)).

2020-06-03 Predrag We (John Gibson channelflow.org, etc.) use Chebyshev in the wall-normal directions in Navier-Stokes channel flow high-accuracy integrators, as the Laplacian is a banded matrix in the Chebyshev basis. But I do not like them, as they put all wiggles close to the walls, and lots of interesting turbulence is going on in the middle of the channel, around the middle of the $[-1, 1]$ interval.

Dear Abby, am I just being prejudiced for no good reason?

1.7 Bernoulli map, beta transformation

2021-01-04 Predrag discussed here:

[ChaosBook example 14.5 Bernoulli shift map state space partition](#)

[ChaosBook example 27.3 Lyapunov exponents for 1-dimensional maps.](#)

The (unnumbered) equation, the end of [ChaosBook section 28.5 Analyticity of spectral determinants](#).

[ChaosBook example 28.2 Bernoulli shift eigenfunctions](#).

[ChaosBook exercise 28.5 Bernoulli shift on L spaces](#).

[ChaosBook example 29.1 Return times for the Bernoulli map](#).

[ChaosBook appendix 28.5 Pruned Bernoulli shift](#).

See remark 1.1 *Bernoulli map*. remark 1.2 *Bernoulli shift*.

See discussion around (3.30).

See (5.225).

[wiki: Dyadic transformation](#) also known as the dyadic map, bit shift map, $2x \bmod 1$ map, Bernoulli map, doubling map, sawtooth map.

2020-01-27 Predrag Dropped: Much of ergodic theory can be illustrated by a Bernoulli map [23, 37]. One can explicitly construct a Perron-Frobenius operator, and compute its eigenvalues and its eigenvectors; construct the dynamical zeta function, and count lattice states and orbits [31].

(for d written out as a matrix, see (1.83))

2019-07-30 Predrag Since all coefficients in (3.49) are integers, the lattice states x_t are always rational. This allows for their exact evaluation by integer arithmetic.

2019-12-18 Predrag (dropped from CL18.tex)

Restrict the admissible field values x_t at time-lattice site t to the symmetric unit interval $x \in [-1/2, 1/2]$, with ??-letter alphabet

$$\mathcal{A} = \{\underline{4}, \underline{3}, \underline{2}, \underline{1}, 0, 1, 2, 3, 4\}. \quad (1.64)$$

It maps the unit interval onto itself, with fixed points $x_0 = 0, x_1 = 1$.

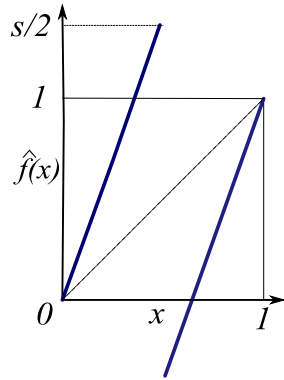


Figure 1.13: $\hat{f}(x)$, the full space sawtooth map (1.65), $s > 2$.

reduction $\hat{f}(x_t) \mapsto f(x_t)$

Recall how the subpartitions of figure 3.2 were used to obtain the total number of periodic points (3.28), as every subpartition contained one and only one periodic point.

The closely related *sawtooth map*, sketched in figure 1.13, with ‘stretching’ parameter $s > 2$,

$$\hat{x}_{t+1} = \hat{f}(\hat{x}_t) = \begin{cases} s\hat{x}_t, & \hat{x}_t \in [0, 1/2) \\ s\hat{x}_t + 1 - s, & \hat{x}_t \in (1/2, 1] \end{cases} \quad (1.65)$$

Since the relation between m_t symbol sequences and x_t states is linear, it is straightforward to go back and forth between a lattice state and its symbolic representation.

The n th preimages $b^{-(n-1)}(x)$ of the critical point $x_c = 1/2$ partition the state space into 2^n subintervals, each labeled by the first n binary digits of points $x = .m_1 m_2 m_3 \dots$ within the subinterval: figure 3.2 illustrates such 4-intervals state space partition $\{\mathcal{M}_{00}, \mathcal{M}_{01}, \mathcal{M}_{11}, \mathcal{M}_{10}\}$ for $n = 2$.

known as the *doubling map* if $s = 2$,

$$x_{t+1} = 2x_t \pmod{1}, \quad (1.66)$$

and *s-tupling map*, figure 1.18 (b), for integer stretching parameter $s \geq 3$,

The relation is linear, and a given block M , or ‘code’ in terms of alphabet (3.26), corresponds to a unique temporal lattice state X given by the lattice Green’s function

$$X = g M, \quad g = -\frac{d}{d-s} \mathbf{1}, \quad (1.67)$$

provided we specify the boundary conditions (bc’s) for the shift operator d .

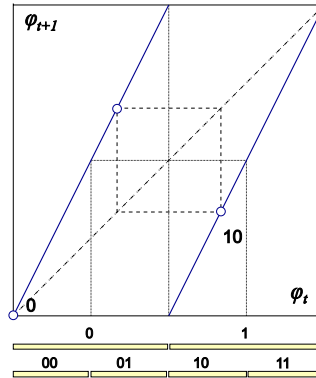


Figure 1.14: The Bernoulli map (1.65) for $s = 2$, together with the $\bar{0}$ fixed point, and the $\bar{0}\bar{1}$ 2-cycle. Preimages of the critical point $x_c = 1/2$ partition the unit interval into $\{\mathcal{M}_0, \mathcal{M}_1\}, \{\mathcal{M}_{00}, \mathcal{M}_{01}, \mathcal{M}_{10}, \mathcal{M}_{11}\}, \dots$, subintervals. As the map is a circle map, $x_5 = 1 = 0 = x_0 \pmod{1}$.

The power of the linear encoding of the temporal Bernoulli condition (3.30) is that the *integer-valued* symbols m_t from the finite alphabet (3.26) encode the *real-valued* lattice site states x_t .

For the piecewise linear map of figure 3.2 we can evaluate the dynamical zeta function in closed form. Each branch has the same value of the slope, and the map can be parameterized by the single parameter s . The larger s is, the stronger is the stretching action of the map.

The power of the code

$$\mathbf{M}^\top = (m_t, m_{t+1}, \dots, m_{t+k}) \quad (1.68)$$

for the temporal cat (3.49) is that one can use *integers* m_t to encode the *real-valued* lattice states x_t .

$$(\partial - (s-1)d^{-1})\mathbf{X} = -\mathbf{M}. \quad (1.69)$$

For the $s = 3$ cat map example at hand, they are

$$\{M_j\} = (M_1, M_2, M_3, M_4, M_5, \dots) = (1, 2, 5, 10, 24, \dots), \quad (1.70)$$

Visualizing the volume relation (5.203) for a general n -dimensional fundamental parallelepiped is not easy, but

As the temporal Bernoulli (3.31) is linear, eigenmodes of \mathcal{J} , shifted by \mathbf{M} as in (3.31) for each distinct lattice state, are also lattice states of temporal Bernoulli.

2020-01-17 Han The determinant of this \mathcal{J} from (3.31) is negative so we cannot use the determinant trace formula directly. A correct way is: first rewrite the \mathcal{J} as in (1.67)

$$\mathcal{J} = \mathbf{1} - sd^{-1} = -\frac{s}{d} \left(\mathbf{1} - \frac{d}{s} \right).$$

Note that $\det(d) = (-1)^{n-1}$. The determinant of \mathcal{J} is:

$$\det \mathcal{J} = \det \left(\frac{d}{s} - \mathbf{1} \right) s^n (-1)^{n-1} = -s^n \det \left(\mathbf{1} - \frac{d}{s} \right).$$

Then use the determinant-trace formula:

$$\ln \det \left(\mathbf{1} - \frac{d}{s} \right) = \text{tr} \ln \left(\mathbf{1} - d/s \right) = - \sum_{k=1}^{\infty} \frac{1}{k} \frac{\text{tr}(d^k)}{s^k},$$

and use $\text{tr } d^k = n\delta_{k,nr}$ if k is a multiple of n , 0 otherwise (follows from $d^n = \mathbf{1}$),

$$\ln \det \left(\mathbf{1} - \frac{d}{s} \right) = - \sum_{r=1}^{\infty} \frac{1}{r} \frac{1}{s^{nr}} = \ln(1 - s^{-n}),$$

and the determinant of \mathcal{J} is:

$$\det \mathcal{J} = -s^n \det \left(\mathbf{1} - \frac{d}{s} \right) = 1 - s^n,$$

which is negative. So for the temporal Bernoulli the count is:

$$N_n = |\det \mathcal{J}| = s^n - 1,$$

in agreement with the time-evolution count (3.28).

2020-01-25 Predrag: A Bernoulli map example. The action of orbit Jacobian matrix \mathcal{J} for the period-2 periodic points of the base-2 Bernoulli map, figure 3.2, which partitions the unit interval into 2 subintervals $\{\mathcal{M}_m\}$, is

$$\phi_{t+1} = 2\phi_t - m_{t+1}, \quad \phi_t \in \mathcal{M}_{m_t}, \quad (1.71)$$

where m_t takes values in the 2-letter alphabet

$$m \in \mathcal{A} = \{0, 1\}. \quad (1.72)$$

should suffice to convey the idea. In this case, the $[2 \times 2]$ orbit Jacobian matrix, the unit square basis vectors, and their images are

$$\begin{aligned} \mathcal{J} &= \begin{pmatrix} 1 & -2 \\ -2 & 1 \end{pmatrix}; \quad \mathbf{x}_B = \begin{pmatrix} 1 \\ 0 \end{pmatrix}, \quad \mathbf{x}_D = \begin{pmatrix} 0 \\ 1 \end{pmatrix} \\ \mathbf{x}_{B'} &= \mathcal{J} \mathbf{x}_B = \begin{pmatrix} 1 \\ -2 \end{pmatrix}, \quad \mathbf{x}_{D'} = \begin{pmatrix} -2 \\ 1 \end{pmatrix}, \end{aligned} \quad (1.73)$$

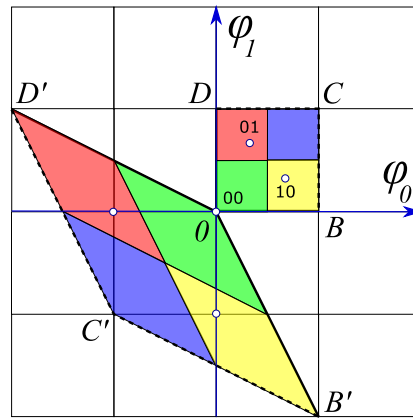


Figure 1.15: (2020-02-14 Predrag: his is “wrong”, now superseded with the updated figure in ref. [33]; 2020-09-11 the whole example seems misplaced here, move it to wherever it belongs) The base-2 Bernoulli map (1.71) period-2 points $X_p = (\phi_0, \phi_1)$ are $\bar{0} = (0, 0)$, $\bar{1} = (1, 1)$ fixed point repeats, and the 2-cycle $X_{01} = (1/3, 2/3)$, see figure 3.2. They all lie within the unit square $[0BCD]$, one within each $\mathcal{M}_{m_0 m_1}$ subregion, and are mapped by the $[2 \times 2]$ orbit Jacobian matrix \mathcal{J} into the parallelogram $[0B'C'D']$, whose area is 4 times the unit area. The images of periodic points X_p land on the integer lattice, and are sent back into the origin by integer translations M_p , in order to satisfy the fixed point condition $\mathcal{J}X_p + M_p = 0$.

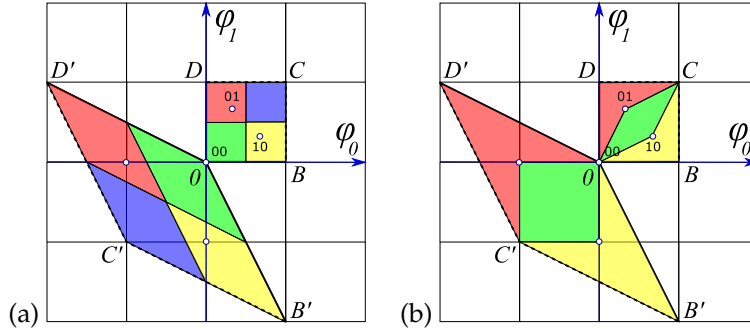


Figure 1.16: [OLD VERSION] The Bernoulli map (3.22) period-2 lattice states $X_M = (x_0, x_1)$ are the $\bar{0} = (0, 0)$ fixed point, and the 2-cycle $X_{01} = (1/3, 2/3)$, see figure 3.2. They all lie within the unit square $[0BCD]$, one within each $M_{m_0 m_1}$ subregion, and are mapped by the $[2 \times 2]$ orbit Jacobian matrix J (3.89) into the fundamental parallelepiped $[0B'C'D']$. The images of periodic points X_M land on the integer lattice, and are sent back into the origin by integer translations M , in order to satisfy the fixed point condition `refeq{tempFixPoint}`, $JX_M + M = 0$. Figure 3.2 suggests subdividing the fundamental parallelepiped into (a) 4 areas, but they are not unit areas. The theory of integer lattices dictates instead (b) covering the fundamental parallelepiped by 3 unit area rectangles, with all vertices on the integer lattice.

with the resulting fundamental parallelogram of area 4 shown in figure 3.7. The volume of the fundamental parallelogram lattice \mathcal{L} (5.179) is

$$\text{Det}(\mathcal{L}) = \text{Det}(X_{B'}|X_{D'}) = \text{Det}(J) \text{Det}(X_B|X_D) = -3, \quad (1.74)$$

where in this case the unit cell matrix $(X_B|X_D) = \mathbf{1}$.

The $[3 \times 3]$ orbit Jacobian matrix and the unit cube basis vectors are

$$-J = \begin{pmatrix} -1 & 0 & 2 \\ 2 & -1 & 0 \\ 0 & 2 & -1 \end{pmatrix}, \quad (X_B|X_C|X_D) = \begin{pmatrix} 1 & 0 & 0 \\ 0 & 1 & 0 \\ 0 & 0 & 1 \end{pmatrix}.$$

Clearly $\text{Det}(-J) = s^3 - 1$, and so on, reproducing the periodic states count for Bernoulli. No point of looking at $\text{Det}(-J)$, as that changes sign at every order - always evaluate $|\text{Det}(J)|$.

2020-02-16 Predrag Dropped from CL18 [33]:

The temporal Bernoulli lattice Green's function in the matrix form

$$g = \begin{pmatrix} 0 & \Lambda^{-1} & \Lambda^{-2} & \Lambda^{-3} & \Lambda^{-4} & \Lambda^{-5} & \dots \\ 0 & 0 & \Lambda^{-1} & \Lambda^{-2} & \Lambda^{-3} & \Lambda^{-4} & \dots \\ 0 & 0 & 0 & \Lambda^{-1} & \Lambda^{-2} & \Lambda^{-3} & \dots \\ 0 & 0 & 0 & 0 & \ddots & & \\ 0 & 0 & 0 & 0 & 0 & \Lambda^{-1} & \dots \\ 0 & 0 & 0 & 0 & 0 & 0 & \ddots \\ \vdots & \vdots & \vdots & \vdots & \vdots & \vdots & \ddots \end{pmatrix}, \quad (1.75)$$

for an infinite temporal Bernoulli lattice $t \in \mathbb{Z}$, where $\Lambda = s$ is the 1-time step stability multiplier for the Bernoulli system.

2020-02-18 Predrag Clipped here from *Ising.tex*, might be relevant to generalizing Bernoulli to 2-dimensional lattice, as a warm-up to spatiotemporal cat zeta functions:

Roettger [87], *Periodic points classify a family of Markov shifts*, writes:

Ledrappier introduced the following type of space of doubly indexed sequences over a finite abelian group G ,

$$X_G = \{(x_{s,t}) \in G^{\mathbb{Z}^2} \mid x_{s,t+1} = x_{s,t} + x_{s+1,t} \text{ for all } s, t \in \mathbb{Z}\}.$$

The group \mathbb{Z}^2 acts naturally on the space X_G via left and upward shifts.

2020-02-19 Predrag Suarez [103] *Difference equations and a principle of double induction*, ([click here](#)) studies this as a “partial difference equations,” that is, difference equations in two or more variables. He refers to many books on the subject. His example is a first order hyperbolic equation, with initial conditions on space and time axes, which describes some thermal properties,

$$f(r, m) = f(r, m - 1) + f(r - 1, m).$$

The goal is to calculate, step by step, all the values of the temperature $T(m,n)$, starting with the initial and boundary conditions. But then I do not get the rest of the papers. Perhaps best not to use much time on ‘spatiotemporal’ Bernoulli.

2020-03-28 Predrag The Bernoulli first-order difference equation

$$\phi_t - s\phi_{t-1} = -m_t, \quad \phi_t \in [0, 1], \quad (1.76)$$

characteristic equation (for $m_t=0$)

$$\Lambda - s = 0, \quad (1.77)$$

has one characteristic root $\{s\}$.

Comparing with (5.227) we see that we need to solve a first-order inhomogeneous difference equation with a constant forcing term ($s - 1$).

Weijie Chen does this pedagogically in his 2011 lecture notes ([click here](#)), sect. 1.2.1 *One Example*, where he considers

$$\phi_t - s\phi_{t-1} = M, \quad (1.78)$$

and finds the particular solution by taking $\phi_{p,n} = \phi_p$ for all n ,

$$\phi_p - s\phi_p = M \quad \rightarrow \quad \phi_p = -M/(s - 1).$$

Hence the solution is

$$\phi_n = \phi_{c,n} + \phi_{p,n} = c s^n - \frac{M}{s - 1}, \quad (1.79)$$

with c determined by the initial value $\phi_0 = c s^0 - M/(s - 1)$. Bernoulli starts with $\phi_0 = 0$, and according to (5.227), $M = (s - 1)$, so $c = 1$.

Weijie Chen also works out the particular solution when $s = 1$. He also 2CB remarks that in econometrics the shift operator d is called the *lag operator*.

Weijie Chen solves the temporal cat pedagogically in his lecture notes ([click here](#)), sect. 2 *Second-Order Difference Equation*.

Questions

- Why is it OK to take site-independent particular solution?
- $M/(s - 1)$ looks awkward, can one reformulate? so instead of M , have $M/(s - 1) \rightarrow 1$
- I am guessing that $M = (s - 1)$ in (1.78) something like the total number of 'letters' I can add to the count N_n at time n . Something like that.
- Similarly for $M = 2\mu^2$ forcing term in temporal cat second-order difference equation (5.239).
- This is still just a verification of my guess recurrence (5.227). Make this argument into a derivation.

2020-02-23 Predrag Just curious - what does the Bernoulli fundamental parallelepiped defined by the columns of $[3 \times 3]$ orbit Jacobian matrix

$$\mathcal{J} = \begin{pmatrix} 1 & -2 & 0 \\ 0 & 1 & -2 \\ -2 & 0 & 1 \end{pmatrix}, \quad N_3 = |\text{Det } \mathcal{J}| = 2^3 - 1, \quad (1.80)$$

look like in a 3-dimensional rendition? Hopefully it is not symmetric, like figure 3.8 (b).

2020-03-01 Predrag Wilf [112] *Generatingfunctionology* starts out in his sect. 1.1 *An easy 2-term recurrence*, with our Bernoulli periodic points count (5.225) and (5.236) as a trivial example of a two-term recurrence (first-order difference equation).

2020-12-21 Predrag Counting temporal Bernoulli lattice states removed from CL18.tex → Bernoulli.tex, replaced by refsects:Hill1stOrd

To evaluate the Hill determinant (5.203), observe that from (3.31) it follows that

$$\text{Det}(-\mathcal{J}) = \text{Det}(s/d) \text{Det}(\mathbf{1} - d/s),$$

where $|\text{Det}(s/d)| = s^n$. Expand $\ln \text{Det}(\mathbf{1} - d/s) = \text{Tr} \ln(\mathbf{1} - d/s)$ as a series in $1/s$,

$$\text{Tr} \ln \left(\mathbf{1} - \frac{d}{s} \right) = - \sum_{k=1}^{\infty} \frac{1}{k} \frac{\text{Tr}(d^k)}{s^k}. \quad (1.81)$$

It follows from $d^n = \mathbf{1}$ that $\text{Tr } d^k = n\delta_{k,n}$ is non-vanishing if k is a multiple of n , 0 otherwise:

$$\ln \text{Det}(\mathbf{1} - d/s) = - \sum_{r=1}^{\infty} \frac{1}{r} \frac{1}{s^{nr}} = \ln(1 - s^{-n}).$$

2020-12-09 Predrag Temporal Bernoulli

After n shifts, the lattice state X returns to the initial state, $d^n = \mathbf{1}$. This relation leads to the explicit expression for the orbit Jacobian matrix (1.67),

$$g = \frac{d}{s \mathbf{1} - d} = \frac{1}{\mathbf{1} - \frac{d}{s}} \frac{d}{s} = \sum_{k=1}^{\infty} \frac{d^k}{s^k} = \frac{s^n}{s^n - 1} \sum_{k=1}^n \frac{d^k}{s^k}. \quad (1.82)$$

From (1.67) it then follows that the last field in X is the field at lattice site n

$$x_n = \frac{s^n}{s^n - 1} \cdot m_1 m_2 m_3 \cdots m_n = \frac{1}{s-1} \frac{s^{n-1} m_1 + \cdots + s m_{n-1} + m_n}{s^{n-1} + \cdots + s + 1}, \quad (1.83)$$

and the rest are obtained by cyclic permutations of M .

For example, for $s = 2$, the lattice fields are (they are always rational-valued),

$$\begin{aligned} x_{m_1 m_2 \cdots m_n} &= \sum_{k=1}^n \frac{m_k}{2^k} \sum_{m=0}^{\infty} \frac{1}{2^{nm}} = \frac{2^n}{2^n - 1} \cdot m_1 m_2 \cdots m_n \\ &= \frac{1}{2^n - 1} \sum_{k=1}^n m_k 2^{n-k}, \end{aligned} \quad (1.84)$$

where $p = \overline{m_1 m_2 \cdots m_n}$ is an orbit of period n , with stability multiplier $\Lambda_p = 2^n$.

For a Bernoulli map, the rational x_0 are either periodic or land eventually on a periodic orbit (the base- s version of the familiar fact that the decimal expansion of a rational number is eventually periodic), while the orbit of a normal irrational x_0 is ergodic.

2020-12-09, 2020-12-11 Predrag Quotienting the temporal Bernoulli system

$$x_t - sx_{t-1} = -m_t, \quad x_t \in [0, 1], \quad (1.85)$$

by its *dynamical* $D_1 = \{e, \sigma\}$ symmetry

$$\sigma x_t = 1 - x_t, \quad \sigma m_t = (s - 1) - m_t, \quad \text{for all } t \in \mathbb{Z}, \quad (1.86)$$

where m_t takes values in the s -letter alphabet

$$m \in \mathcal{A} = \{0, 1, 2, \dots, s - 1\}. \quad (1.87)$$

Define the fundamental domain to be $\hat{x}_t \in [0, 1/2]$. We construct the Bernoulli fundamental domain lattice system, with ' $1/2$ ' unit hypercube $\hat{X} \in [0, 1/2]^n$, as in [ChaosBook Group \$D_1\$ and reduction to the fundamental domain](#), see figure 1.17 (b), and the fundamental domain symbolic dynamics $\hat{\mathcal{A}}$. The temporal lattice Bernoulli condition (1.85) is now two conditions (Bernoulli)/ D_1 . They are different for s even or odd:

$$\begin{aligned} \hat{x}_{t+1} - s\hat{x}_t &= -m_{t+1}, \quad \hat{x}_t \in \mathcal{M}_{m_t}, \quad s \text{ even} \\ \hat{x}_{t+1} + s\hat{x}_t &= 1 + m_{t+1}, \quad \hat{x}_t \in \mathcal{M}_{\sigma m_t} \\ \hat{\mathcal{A}} &= \{\{m\}, \{\sigma m\}\}, \quad \{m\} = \{0, 1, 2, \dots, s/2\}, \end{aligned} \quad (1.88)$$

$$\begin{aligned} \hat{x}_{t+1} - s\hat{x}_t &= , \quad s \text{ odd} \\ \hat{\mathcal{A}} &= \{\{m\}, (s-1)/2, \{\sigma m\}\}, \quad m \in \{0, 1, 2, \dots, (s-3)/2\}. \end{aligned} \quad (1.89)$$

As an example, case $s = 6$, $m_t \in \{0, 1, 2\}$ is worked out in figure 1.17 (c). (Plot also the fundamental domain map for odd values of s .)

In the matrix form (1.85), the orbit Jacobian matrix

$$\mathcal{J} X = -M, \quad \mathcal{J} = \mathbf{1} - sd^{-1}, \quad (1.90)$$

is independent of M . Not so for the symmetry reduced orbit Jacobian matrix $\hat{A}_{\hat{M}}$ in (1.88): it depends on \hat{M} , as its diagonal takes values $\pm s$. We need to prove that the Hill determinant $\text{Det } \hat{A}$ does not.

I had not noticed before that this parametrization converts Bernoulli into tent map, with full state space 2-cycles turned into negative slope fixed points.

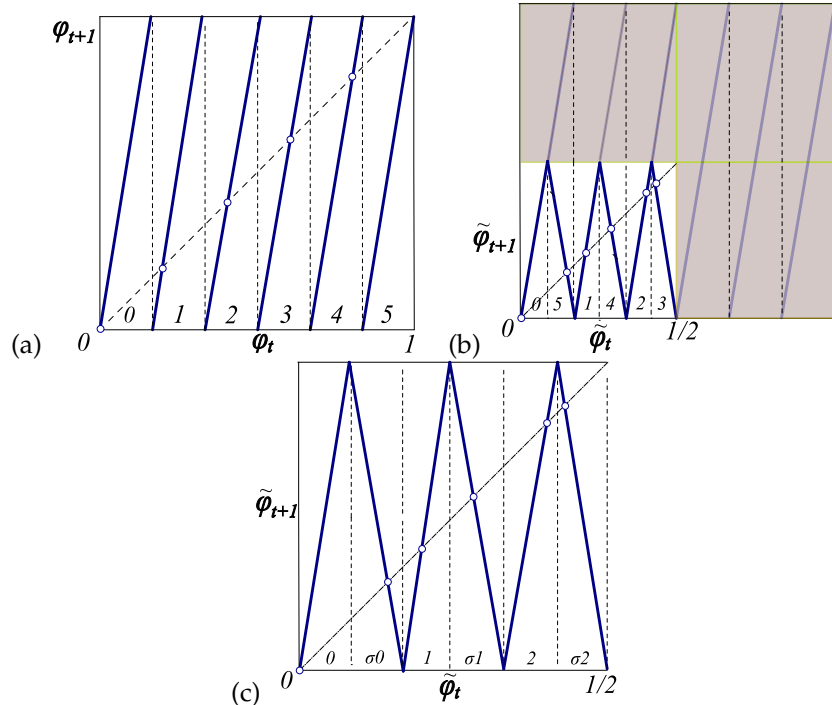


Figure 1.17: (a) The Bernoulli map f with the stretching parameter $s = 6$ partitions the unit interval into 6 subintervals $\{\mathcal{M}_m\}$, labeled by the 6-letter alphabet (1.87). As the map is a circle map, $x_5 = 1 = 0 = x_0 \pmod{1}$. (b) The Bernoulli map is quotiented by the dynamical $G = D_1 = \{e, \sigma\}$ symmetry to (c) the fundamental domain $\hat{x}_t \in [0, 1/2]$ map $\hat{f} = f/G$ partitions the half interval into the three $1/12$ subintervals $\{\mathcal{M}_0, \mathcal{M}_1, \mathcal{M}_2\}$, and their reflections, the three 3 subintervals $\{\mathcal{M}_{\sigma 0}, \mathcal{M}_{\sigma 1}, \mathcal{M}_{\sigma 2}\}$, labeled by a 6-letter reduced system's alphabet. Reduced space fixed points $\{\bar{\sigma}_0, \bar{\sigma}_1, \bar{\sigma}_2\}$ correspond to self-dual 2-cycles $\{\bar{05}, \bar{14}, \bar{23}\}$ in the full space. Fixed point $\bar{0}$ is in the border, and thus over-counted; $\bar{1}$ corresponds to $\{\bar{1}, \bar{4}\}$, and $\bar{2}$ corresponds to $\{\bar{2}, \bar{3}\}$.

By the inclusion-exclusion principle (18.278)

$$N_n = \hat{N}_n + \sigma\hat{N}_n - \hat{N}_n \cap (\sigma\hat{N}_n) = 2\hat{N}_n - \hat{N}_n \cap (\sigma\hat{N}_n). \quad (1.91)$$

Let's call the number of points in the shared boundary I . The $x = 0$ is in I for any n , if I am allowed to identify $x = 1 \rightarrow 0$, and that is the only point in the boundary. Presumably this leads to the denominator $(1 - z)$ in (1.92). I guess that the symmetric irrep of $D_1 = \{e, \sigma\}$ leads to $N_+ = s^n$ and the numerator $(1 - sz)$, while the antisymmetric irrep leads to $N_- = 0$, and a trivial factor 1 contribution to the numerator (1.92).

$$1/\zeta_{\text{top}}(z) = \frac{1 - sz}{1 - z}. \quad (1.92)$$

Temporal cat should be more interesting. Also any nonlinear s -branch map 'Bernoulli-like' lattice with a *dynamical* D_1 symmetry; then the weights t_p do not necessarily cancel for the antisymmetric irrep.

2018-12-27 Linas Vepstas *On the Beta Transformation* arXiv:1812.10593: The beta transformation is the iterated map (1.93). The $\beta = 2$ is known as the Bernoulli map, and is exactly solvable. The Bernoulli map provides a model for pure, unrestrained chaotic (ergodic) behavior: it is the full invariant shift on the Cantor space. The beta transformation defines a subshift: iterated on the unit interval, it singles out a subspace of the Cantor space, in such a way that it is invariant under the action of the left-shift operator. That is, lopping off one bit at a time gives back the same subspace. The beta transform seems to capture something basic about the multiplication of two real numbers: β and x . It offers a window into understanding the nature of multiplication. Iterating on multiplication, one would get exponentiation; although the mod 1 of the beta transform distorts this in interesting ways. The work presented here is a research diary: a pastiche of observations and some shallow insights. The eigenvalues of the transfer operator seem to lie on a circle of radius $1/\beta$ in the complex plane. Given that the transfer operator is purely real, the appearance of such a quasi-unitary spectrum seems surprising. The spectrum appears to be the limit of a dense set of quasi-cyclotomic polynomials, the positive real roots of which include the Golden and silver ratios, the Pisot numbers, the n-bonacci (tribonacci, tetranacci, etc.) numbers.

Beta transformation

$$T_\beta(x) = \beta x \mod 1, \quad 1 < \beta \leq 2 \quad (1.93)$$

was introduced by Alfréd Rényi [84] in 1957, and an invariant measure for it was given by Alexander Gelfond in 1959 and independently by Bill Parry [79] in 1960.

[Beta transformation literature review and references](#).

[A concise intro to beta-transformations?](#) has references.

2020-09-08 Predrag Bing Li *Some fractal problems in beta-expansions* ([video](#)) ([slides](#))

For greedy beta-expansions, we study some fractal sets of real numbers whose orbits under beta-transformation share some common properties. For example, the partial sum of the greedy beta-expansion converges with the same order, the orbit is not dense, the orbit is always far from that of another point etc. The usual tool is to approximate the beta-transformation dynamical system by Markov subsystems. We also discuss the similar problems for intermediate beta-expansions.

2021-01-05 Predrag Hofbauer and Keller [[56](#)] *Zeta-functions and transfer-operators for piecewise linear transformations* (1984) has no Bernoulli zeta. Not useful to us at this time.

2021-01-05 Predrag Takahashi [[104](#)] *Fredholm determinant of unimodal linear maps* has lots of detail and examples. I might have missed something, but Bernoulli zeta is not there, or anything we care about.

2021-01-04 Predrag Flatto, Lagarias and Poonen [[42](#)] *The zeta function of the beta transformation* (1994)

which should have the $\beta = 2$ Bernoulli zeta function as the trivial case.

2021-01-05 Han Notes from Flatto, Lagarias and Poonen [[42](#)] paper:

β -transformation map is:

$$f_\beta(x) = \beta x \pmod{1},$$

where $\beta > 1$, $x \in [0, 1]$. The symbolic dynamics of f_β is based on the fact that the graph of f_β consists of $\lfloor \beta \rfloor + 1$ monotone pieces which they call laps, which are assigned by the symbols $0, 1, \dots, \lfloor \beta \rfloor$. When $\beta \in \mathbb{Z}^+$, the piece $\lfloor \beta \rfloor$ consists of a single point, and the symbol $\lfloor \beta \rfloor$ only appears in the itinerary of 1. To each $x \in [1, 0]$ its itinerary is $I_\beta(x) = A_0 A_1 A_2 \dots$, where the symbol

$$A_n := A_n(x) = \lfloor \beta f_\beta^n(x) \rfloor.$$

In particular the itinerary of 1, $I_\beta(1) = A_0^* A_1^* A_2^* \dots$ encodes complete information about the behavior of f_β .

They introduced a power series with integer coefficients:

$$\phi_\beta(z) = A_0^* z + A_1^* z^2 + A_2^* z^3 + \dots = \sum_{n=0}^{\infty} A_n^* z^{n+1}.$$

This function is related to the iterates of 1 by:

$$\phi_\beta(z) = 1 + (\beta z - 1) \left(\sum_{n=0}^{\infty} f_\beta^n(1) z^n \right).$$

Then the zeta function is:

$$\zeta_\beta(z) = \frac{1}{1 - \phi_\beta(z)},$$

if β is not a simple β -number, and

$$\zeta_\beta(z) = \frac{1 - z^N}{1 - \phi_\beta(z)},$$

if β is a simple β -number, and N is minimal with $f_\beta^N(1) = 0$. Simple β -numbers are the β -numbers such that for some n , $f_\beta^n(1) = 0$. This formula gives the correct topological zeta function of temporal Bernoulli.

Associated with the β -transformation is the set X_β of all $I_\beta(x)$ for $0 \leq x < 1$. The β -shift S_β is a symbolic dynamical system obtained as the smallest closed (two-sided) subshift of $\{1, 2, \dots, \lfloor \beta \rfloor\}^\mathbb{Z}$ generated by all finite substrings of X_β . For simple β -numbers S_β is a subshift of finite type.

There is a zeta function associated to the β -shift S_β , which is studied by Takahashi [105], who showed that

$$\hat{\zeta}_\beta(z) = \frac{1}{1 - \phi_\beta(z)}.$$

This formula is closely related to $\zeta_\beta(z)$ but differs from it for simple β -numbers, in which case the closure operation defining S_β adds some extra periodic points.

2021-01-11 Predrag Seth Lloyd *et al.*. *Quantum algorithm for nonlinear differential equations* [arXiv:2011.06571](https://arxiv.org/abs/2011.06571):

[1] showed how to map the problem of solving a general linear differential equation to that of matrix inversion, which can then be performed using the quantum linear systems algorithm [12-13]. Consider a linear differential equation of the form,

$$\frac{dx}{dt} + Ax = b(t), \quad (6)$$

where as above $x, b \in \mathcal{C}^d$ and A is a $[d \times d]$ matrix.

2CB

Discretize the equation in time at intervals Δt , and take k to be the index for the discretized time, so that x_k and b_k are the values of x and b at time label k .

We wish to integrate equation (6) numerically starting from the initial state $x_0 \equiv b_0$. We obtain a series of equations of the form:

$$x_0 = b_0 \quad x_1 = x_0 - \Delta t A x_0 + \Delta t b_1 \quad \dots \quad x_{k+1} = x_k - \Delta t A x_k + \Delta t b_k \quad \dots \quad (7)$$

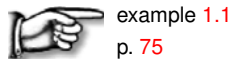
Here, we have used the Euler forward method for numerical integration, but it is straightforward to implement implicit methods such as Euler backward, Crank-Nicholson, Runge-Kutta, etc. [3]. Written in matrix form, these equations become

$$-\begin{pmatrix} -I & 0 & 0 & \dots & 0 & 0 \\ I - \Delta t A & -I & 0 & \dots & 0 & 0 \\ 0 & I - \Delta t A & -I & \dots & 0 & 0 \\ & & \dots & & & \\ 0 & 0 & 0 & \dots & -I & 0 \\ 0 & 0 & 0 & \dots & I - \Delta t A & -I \end{pmatrix} \begin{pmatrix} x_0 \\ x_1 \\ x_2 \\ \dots \\ x_{T-1} \\ x_T \end{pmatrix} = \begin{pmatrix} b_0 \\ \Delta t b_1 \\ \Delta t b_2 \\ \dots \\ \Delta t b_{T-1} \\ \Delta t b_T \end{pmatrix},$$

Commentary

Remark 1.1. Bernoulli map. The Bernoulli shift map (3.22) and the doubling map (1.66) are also known as the dyadic transformation, dyadic map, bit shift map, angle doubling map or sawtooth map (??). There are many fine books that discuss it in depth, for example Driebe [37]. See also remark 1.2.

Remark 1.2. Bernoulli shift. For a more in-depth discussion, consult chapter 3 of ref. [37]. The extension of Fredholm theory to the case of Bernoulli shift on $\mathbb{C}^{k+\alpha}$ (in which the Perron-Frobenius operator is *not* compact – technically it is only *quasi-compact*). That is, the essential spectral radius is strictly smaller than the spectral radius) has been given by Ruelle [88]: a concise and readable statement of the results is contained in ref. [11]. We see from (??) that for the Bernoulli shift the exponential decay rate of correlations coincides with the Lyapunov exponent: while such an identity holds for a number of systems, it is by no means a general result, and there exist explicit counterexamples. See also remark 1.1.



1.8 Any piecewise linear map has “linear code”

2CB

For reasons unbeknownst to me, it is below the dignity of any cat to work out any problem in ChaosBook, or in the online course, no matter how often I point out that it is easier to understand what we do for cat maps if you first work it out for 1-dimensional maps.

So I have to do these exercises myself - I’m forced to it, so Li Han can be motivated to re-derive his polynomials (as described in Bird and Vivaldi [16], see my notes of 2016-05-21, -12-12 below), rather than to fit them to Mathematica grammar rule counts for integer s .

Basically, I am baffled by why should “linear code” be such a big deal that it has to go into the title of our paper [53]. Every example of symbolic dynamics worked out in ChaosBook is a “linear code.” The strategy is always the same - find a topological conjugacy from your map to a piecewise linear map,

and then use the fact that any piecewise linear map has “linear code.” The pruning theory is always the same - kneading orbit separates admissible from the inadmissible, also in the infinite 1-dimensional discrete lattice case worked out in the *Diffusion* chapter in the ChaosBook, and the appendix (chapter 12 reproduced here) that no one wants to read either.

A tent map is a 1-dimensional example (a simpler one would be Bernoulli, and its sawtooth generalizations). The 2-dimensional examples are the Belykh map, example 1.13, and the Lozi map, example 1.14. Belykh map is of particular interest to us, as it is in form very close to the cat map. Both maps have the pruning front conjecture is proven for them, for a some sets of parameters.



1.9 Cat map blog

2CB

2016-05-18 Predrag I start with our 2011 *Notes for cat map* (former *appendStatMnotes.doc* in *dasbuch/book/notes*), to be eventually merged with *chapter/appendStatM.tex*.

2011-05-14 Jean-Luc Thiffeault I figured out that the grouping of periodic orbits is crucial, and moreover that there is something delicate with the fixed point of the cat map, which lies on the boundary of Markov boxes.

2011-05-14 Predrag For Anosov (linear Anosov?) - Arnol'd cat map - it should work like ton of rocks, but you have to note that because of the periodicity there is one fixed point, not two. If you screw up an early term in the series, then it converges very slowly. I think the Stephen Creagh [27] tested it on weakly nonlinearly perturbed cat map (weakly, so golden-mean grammar is working) and it converged super-exponentially (you know the grammar, flow has bounded hyperbolicity, so weight-truncated cycle expansions are not needed - they perform less well).

2011-05-14 Jean-Luc Thiffeault I know how to do it with the Markov partition now, and it works much better. Keep in mind this is a warmup problem: what I really have in mind (with my collaborator Erwan Lanneau [68]) is to compute periodic orbits for Teichmuller flow, where the periodic orbits themselves are actually now pseudo-Anosovs!

2011-05-16 Hans-Henrik Rugh The situation as I recall it is roughly as follows:

When you construct the symbolic dynamics you may start by picking one periodic orbit, typically the fixed point $p = f(p)$ (but the following depends on the choice). You then cut the torus into pieces following s/u -manifolds until you get a small collection of N rectangles.

$$R_1, \dots, R_N$$

Associated to this collection you have a transition matrix (for SINGLE rectangles). Now, you also need to construct a transition matrix for PAIRS of rectangles, e.g. $(R_1, R_2) \rightarrow (R_2, R_1)$ and then TRIPLES of rectangles ... $(R_1, R_2, R_3) \rightarrow (R_2, R_1, R_3)$, etc.... These k'th - order transitions comes from the fact that there is a fixed point/periodic cycle on the boundary of the Markov partition elements.

You get determinants $d_k(z)$ for each of these k'th-order transition matrices. NB : $(R_1, R_2) \rightarrow (R_2, R_1)$ is a periodic orbit of prime length 2 even if it represents a fixed point of f. I think (but is not sure?) that the weights in the determinant are calculated in the same way...

The final determinant is $d(z) = d_1(z)d_3(z)\dots/(d_2(z)d_4(z)\dots)$ if I am not mistaken. This is related to the so-called Manning trick [71] for counting real orbits related to

$$\det(1 - s) = 1 - \text{tr } s + \text{tr } s \wedge s - \dots$$

where s is a permutation. What is not obvious is that $d(z)$ is entire, but it is!

It's a kind of model problem anyway. In more realistic systems I suppose that one may run into the problem of having several orbits on boundaries.

One of the tricky points is to see how such an orbit in the 'higher' order zeta-functions/Fredholm-det.

As mentioned in e.g. $d_1(z)$ a 'physical' fixed point may appear zero times, or twice, or,...? In $d_2(z)$ a fixed point may actually appear as a period two orbit, so should be treated as such when looking for cancelling terms.

Great, if you have managed to make it work in practice. I don't think that one can call it a standard trick but one may perhaps get it implicitly from the paper of Ruelle [88]. But it is difficult to digest and even more difficult to convert into computable formulae.

2018-02-10 Predrag Manning [71] writes: " According to Bowen [22], a Markov partition is a finite cover of state space by closed subsets called *rectangles*. The rectangles are pairwise disjoint except possibly for the intersection of their boundaries. [...] At the boundaries of the rectangles, that is where they intersect, several periodic points individual rectangles may be mapped to the same periodic point in the full state space. "

" Counting the periodic points involves also certain auxiliary subshifts of finite type to remedy overcounting of points in the boundaries of the rectangles. "

2011-05-18 Jean-Luc Thiffeault emailed to Predrag pdf file *Notes on periodic orbit expansions for Teichmüller flow* (saved as *POexp.pdf* in *dasbuch/book/notes/*). which maybe figures out cat map symbolic dynamics. He writes:

" Updated notes: on page 4-5 I used the Markov boxes to compute the PO expansion. I used a trick to deal with the orbit on the boundary: include

several copies of the orbit, but divide by the correct factor. It makes the series very nicely convergent. I don't know if this is a standard trick but it seems to work well. "

2011-05-17 Predrag It is standard, it is in ChaosBook.org Chapter *Counting*, Sect *Counting cycles*. I introduced it in Roberto Artuso, Erik Aurell and Predrag Cvitanović [8], *Recycling of strange sets: II. applications*, see eq. (4) and Fig. 6, but Manning [71] did it in 1971 (if that's what he did), and Ruelle [88] at the same time, according to Hans Henrik. ChaosBook says: "Smale [96] conjectured rationality of the zeta functions for Axiom A diffeomorphisms, later proved by Guckenheimer [52] and Manning [71]," and ChaosBook cannot be wrong.

The rule of thumb is that all credit should go to old white male mathematicians whose names one knows how to spell.

The argument is something like this: the correct object, the Fredholm determinant, can be written as ratios of products of skew products (AKA determinants of different dimensions), each one being the not correct object, but historically the first thing written down (dynamical or Ruelle zeta function).

The ones on partition boundaries (what I currently call 'ridges') are of lower dimensions, either downstairs or upstairs in these ratios. They account for overcounting of the boundary fixed and periodic points.

ChaosBook does something of that when explaining the relation between Fredholm determinants and dynamical zeta functions, but is so far silent on explicit examples of the Manning multiples. That is why I would really like us to write up the cat map symbolic dynamics simply and elegantly. Jean-Luc is not the only person who has gotten lost here, anybody mathematician who thinks that Arnol'd is the simplest exercise to try sinks precisely at this spot (physicists train on unimodal maps and the 3-disk system, remaining blissfully ignorant of the Manning multiples)

Hans Henrik might have more elegant way of saying this. Vivianne still more elegant.

2012-03-01 Predrag I've been dreaming about this forever, see for example my post of [2012-03-01], pipes repository, *A letter to our experimental friends*:

" For large aspect systems I imagine we fit local templates whose 2-dimensional or 3-dimensional volume is concentrated on a region big enough to capture interaction of close-by structures, but small enough not to track weakly interacting ones.

In other words, cover 3-dimensional volume with a finite-size template that tracks a neighborhood for a finite time. It's OK to make it spatially periodic, as long as distance is measured in finite size spatiotemporal windows. That is what we already do when we use unstable periodic orbits - we use temporally-infinite periodic solution (that cannot be seen

in experiment) to identify a finite-time neighboring segment of a chaotic trajectory.

It has not been tried, so I might be wrong (again). ”

2016-05-04 Predrag I am not suggesting that we should study this, but it's something to maybe keep in mind: Slipantschuk, Bandtlow and Just [95], *Complete spectral data for analytic Anosov maps of the torus*, construct a family of analytic hyperbolic diffeomorphisms of the torus (of which Arnol'd cat map is a special case) for which the spectral properties of the associated transfer operator acting on a suitable Hilbert space can be computed explicitly. They introduce an example of an analytic hyperbolic diffeomorphism on the complex unit torus, of which the cat map is a special, linear case. the real representation of the map, Eq. (2) is area-preserving and thus provides an example of a chaotic Hamiltonian system. Unlike the situation for one-dimensional non-invertible maps, here is no distinction between Perron-Frobenius operators and Koopman operators as diffeomorphism is area-preserving.

Note that the eigenvalues of the evolution (transfer) operators come in doublets or quadruplets, presumably because of the discrete symmetries of the unit square.

Just looking at their Figs. 1 is inspirational.

The cat map can always be written as a composition of area preserving orientation reversing linear automorphisms. They define a two-parameter area-preserving family, Eq. (85), and show that measures for such maps, where the determinant of the Jacobian varies, may have fractal properties, see Fig. 2.

2016-05-16 PC Weirdly, Wolfram's Weisstein [111] is wrong: what he calls “[Lyapunov characteristic exponents](#)” for Arnol'd cat map are certainly not “exponents” but multipliers. Maybe you guys could alert him, ask him to fix it.

The eigenvectors are correct. They are the same for all periodic points and thus parallel: cat map is uniformly hyperbolic (the same stability exponents for all orbits), a nice example of the Anosov Axiom A system, with the stable and unstable manifolds transverse everywhere, at the same intersection angle.

2016-05-16 PC The boyscout version of ChaosBook Appendix N *Statistical mechanics applications*, Artuso's Sect. N.1 *Diffusion in sawtooth and cat maps* sure merits a read. The pruning rules are given there. Exercise e-Per-P-Cats gives the exact number of T -periodic points of the cat map.

2016-05-17 Predrag I have added for the time being chapter 12 *Statistical mechanics applications* from ChaosBook to this blog. Note that there are yet more references to read in the Commentary to the chapter 12.

2016-05-21 Predrag I had included Percival and Vivaldi [16, 80, 81] among the papers to read (search for 2016-05-16 PC; see remark 12.1). Percival and Vivaldi [81] *Arithmetical properties of strongly chaotic motions* is about cat maps. ChaosBook material included in sect. ?? might be based on that, but I do not remember now, I had last worked on that section in 1996 :)

Maybe working out exercise ?? to exercise ?? is the fastest way to make sure one understands this symbolic dynamics..

2016-05-17 Li Han Uploaded to siminos/mathematica two Mathematica notebooks. *CatMap - single cat map symbolic dynamics and statistics* counts the single cat map symbols and determines their statistics. It is interactive and one can modify the parameters and play with it. *CatMap - single cat map periodic orbits and topological zeta functions* verifies the number of periodic orbits and the topological zeta functions for a single cat map.

2016-05-21 Predrag Adrien and Rana wondered why are (22.2) and (22.3) the same equation. Have a look at the two forms of the [Hénon equation](#) in the ChaosBook Example 3.6. Or see (??) (eq. (2.2) in Percival and Vivaldi [80]). Does that help in understanding the relation? Once you do, write it up in your reports.

2016-06-01 Predrag As no one has written anything down, I am not sure what happened in the rest of the WebEx session, but my impression is that perhaps we should step a step back and first work through some more introductory material for cat-map dynamics to start making sense. Do not be discouraged - it is all very different in flavor from what one learns in most traditional physics courses (though once you learn the stuff, deep connections to statistical mechanics emerge). My recommendation is that Rana and Adrien work through [week 9](#), [week 10](#), and at least parts of [week 12](#) (skip Chap. 23. Cycle expansions).

Could one of you focus on understanding the cat-map ‘the linear code’ part of Percival and Vivaldi [80] - perhaps just complete sect. 1.3.6 started by me.

The other one could describe the ‘standard’ generating partition code allegedly given in Arnol’d and Avez [6] and in most of the references in remark 12.1, so we all understand what Boris means when he says that code is not good for a study of spatiotemporal chaos.

2016-07-01 Li Han :

code: *mathematica/Catmap - single cat map symbol diagram and symbol frequencies.nb*

Single cat map symbol diagram and symbol frequencies. Analytical results of 2-symbol frequencies, up to a gap of 5. Great thanks to the new geometry package in Mathematica 10.

2016-07-06 Li Han :

code: *mathematica/Catmap - single cat map symbol diagram and symbol frequencies v2.nb*

Modified the form of matrix A so that area calculation is easier;
Added sections for 3-7 symbol frequencies (joint probability).

Total pruning rules for consecutive n symbols of single Arnol'd cat map,
 $s = \text{tr}[A] = 3$, see table 1.1. Compare with Rana's table 19.2: the number
of inadmissible sequences that she found for $n_a = 7$ differs.

It would take 12 core*hours to run all (up to 6 symbols: 1 core*hour)

2016-07-10 Rana I agree with Li Han table 1.1 on the numbers of pruned blocks.

2016-07-20 Li Han :

code: *mathematica/Catmap - single cat map symbol diagram and symbol frequencies v3.nb*

Total pruning rules for consecutive n symbols of single Arnol'd cat map,
 $s = \text{tr}[A] = 3$ up to length 12, see table 1.1. Compare with Rana's ta-
ble 19.2: the number of inadmissible sequences that she found for $n_a = 7$
differs.

For $s = 3$ up to ...:

length 7: ≈ 1 Core*hour

length 10: ≈ 3 Core*days

length 12: $\approx 15 - 20$ Core*days

2016-08-01 Predrag : According to table 1.1, there is a single new pruning rule
for each prime-number period. Li Han lists it as 2, but by the reflection
symmetry there is only one. One should really quotient the symmetry,
and it is not just by removing overall factor 2 in the table: there are pruning
blocks that map into each other by the reflection symmetry, and there
are pruning blocks that are self-dual under reflection, giving one pruning
rule rather than two in the not-desymmetrized listing of this table.

- Is this surmise something proved by Dyson [39]? Or does Behrends [13, 14] explain it?
- Does this new rule have a simple geometric interpretation, in terms
of the inequalities? What is the code of the pruned block?

None of

0, 2, 22, 132, 684, 3164, 13894, 58912, 244678, 1002558, 4073528, 16460290
= 2(1, 11, 66, 342, 1582, 6947, 29456, 122339, 501279, 2036764, 8230145)

0, 2, 8, 2, 30, 2, 70, 16, 198, 2, 528, 2, ...

$$= 2(1, 4, 1, 15, 1, 35, 8, 99, 1, 264, 1, \dots)$$

sequences is in the [On-Line Encyclopedia](#) of Integer Sequences, which is bad news. It means that not only this is a number-theoretic problem that has to do with prime factorization (bad news) but in addition it is not one of the standard number-theoretic problems. Means this is an undoable problem, unlikely to have any simple explanation. Do not waste any more time on it.

2018-07-26 Li Han lhan629@gmail.com

Added to the repo my notes [han/catMapItineraries.pdf](#) on the cat map symbolic sequence, mostly about the empirical (polynomial) fit of the total and new pruning rules \tilde{N}_n , table II, which displays the “anomalous” behavior with periodicity of 6, i.e. at

$$n = 2 + 6m = 2, 8, 14, 20, \dots \quad m = 0, 1, 2, 3, \dots$$

At even lengths $n = 2\ell$ there are always 2 new pruning rules $\{-1, 0, 0, \Delta\Delta\Delta, 0, -1\}$ and (reflection symmetry related sequence) $\{s-1, s-2, s-2, \Delta\Delta\Delta, s-2, s-1\}$.

At $n = 2$ the anomalous new pruning rules are vanishing.

Still a mystery: why anomalies at 2, 8, 14, ...? and what will be further occurrences? Explicit formula?

Learning some new math theory in progress, mirror symmetry (here of elliptic curve?), topological recursion from random matrix theory, which might give clue to these numbers.

2018-07-29 Predrag My interpretation of table 1.1 is that the “anomalous” behavior happens when $n - 1$ is prime, is now confirmed by $n - 1 = 3, 5, 7, 11, \dots$ Li Han’s [catMapItineraries.pdf](#) table II, also for $n - 1 = 13, 17, 19$. Perhaps even higher, as the table is cut off at the right edge. I do not see what Li Han’s $n = 2 + 6m$ anomalies are...

2016-08-15 Predrag : I need this stupid Arnol’d cat map in [ChaosBook.org](#), because an example of a tractable Hamiltonian system is useful, and because so many people refer to it.

I say “stupid” because it is very seductive (as much of number theory is), and totally useless as physics. The moment one goes away from the piece-wise linear (and integer!) cat map to any physical nonlinear flow, all this symbol counting falls apart, and one needs cycle expansions ([ChaosBook.org/course1](#), the 2nd course) to describe the physics. I had wasted too much time on number theory in my life to be ever dragged into that again. You have to be very smart, as sooner or later you discover you are assuming the Riemann Hypothesis holds true :)

2016-10-15 Predrag Boris is thinking about temporal and spatial correlations in spatiotemporal cats. Here is some literature on the topic, just for cat maps:

Brini *et al.* [25] *Decay of correlations for the automorphism of the torus T^2*

García-Mata and Saraceno [43] *Spectral properties and classical decays in quantum open systems* (who study the Arnol'd cat map with a small sinusoidal perturbation write that Blank, Keller and Liverani [17] and Nonnenmacher [76] provide a rigorous theoretical underpinning to their calculations for quantum and classical maps on the torus.

Blank, Keller and Liverani [17] *Ruelle-Perron-Frobenius spectrum for Anosov maps* extend a number of results from one-dimensional dynamics based on spectral properties of the Ruelle–Perron–Frobenius transfer operator to Anosov diffeomorphisms on compact manifolds.

Nonnenmacher [76] studies classical and quantum maps on the torus phase space, in the presence of noise. We focus on the spectral properties of the noisy evolution operator, and prove that for any amount of noise, the quantum spectrum converges to the classical one in the semiclassical limit.

2016-11-11 Predrag For fun and games with the cat map, check out Hunt, and B. D. Todd [60, 107] *On the Arnol'd cat map and periodic boundary conditions for planar elongational flow*

2016-08-11 Predrag Read Gozzi [47] *Counting periodic trajectories via topological classical mechanics* ([click here](#)): “ We prove that the number of periodic trajectories of arbitrary period T on the flow tangent to periodic trajectories in phase space of the same period T , is equal to the Euler number of the underlying phase-space. This result holds for systems with compact phase-space and isolated periodic orbits. ”

Giulietti, Liverani and Pollicott [44] *Anosov flows and dynamical zeta functions* ([click here](#)): “ We study the Ruelle and Selberg zeta functions for an Anosov flow on a compact smooth manifold. We prove several results, the most remarkable being (a) for C^∞ flows the zeta function is meromorphic on the entire complex plane; (b) for contact flows satisfying a bunching condition, the zeta function has a pole at the topological entropy and is analytic in a strip to its left; (c) under the same hypotheses as in (b) we obtain sharp results on the number of periodic orbits. ” A good paper, deserving a deeper study.

A discussion of determinants of graphs - says that Levins [83] illuminated a connection between the characteristic polynomial and the feedback loops of a sparse matrix: D. Cates Wylie [113] *Linked by loops: Network structure and switch integration in complex dynamical systems*, [arXiv:0704.3640](#) (2007).

Wylie [113]: for the stability of control systems ref. [99] ([click here](#)).

n	N_n	\tilde{N}_{n-1}
2	2	0
3	22	2
4	132	$8 = 2 \cdot 2 \cdot 2$
5	684	2
6	3164	$30 = 2 \cdot 3 \cdot 5$
7	13894	2
8	58912	$70 = 2 \cdot 5 \cdot 7$
9	244678	$16 = 2 \cdot 2 \cdot 2 \cdot 2$
10	1002558	$198 = 2 \cdot 3 \cdot 3 \cdot 11$
11	4073528	2
12	16460290	$528 = 2 \cdot 2 \cdot 2 \cdot 2 \cdot 3 \cdot 11$
13	??	2
14	??	1326
15	??	124
16	??	3410
17	??	2
18	??	9264
19	??	2

Table 1.1: N_n is the total number of pruned blocks of length $n = n_a$ for the $s = 3$ Arnol'd cat map. \tilde{N}_n is the number of *new* pruned blocks of length n_a , with all length n_a blocks that contain shorter pruned blocks already eliminated. Note that (empirically) there is a single new pruning rule for each prime-number period (it is listed as 2 rules, but by the reflection symmetry there is only one). $n = 14$ to $n = 19$ added 2018-07-28.

2016-12-12 Predrag Percival and Vivaldi [80] write: “The linear code described here may be considered as a development of the code used by Bullett [26] for the piecewise linear tent map.” But Bullett mentions no tent map, I see nothing there... :) His piecewise linear standard map is the simplest possible area preserving piecewise linear twist homeomorphism of zero flux.

Beardon, Bullett and Rippon [12] *Periodic orbits of difference equations* might be of interest (but I have not found it online).

2016-12-12 Predrag Pondering Li Han's undisputable polynomial fits in s to the (new) pruned blocks \tilde{N}_n . Li Han now has a set of polynomials that counts the number of pruning rules $\tilde{N}_n(s)$ for small finite n , but any s . (table 1.1 lists them only for $s = 3$, but Li Han has new tables, not included in the blog as yet).

What's so unique about primes? I think that if cycle period $n - 1 = p$ is a prime, there is always one “most monotone $(p + 1)$ -cycle” such that cycle

points order themselves monotonically along the spatial coordinate q ,

$$q_{1/(p+1)} < q_{2/(p+1)} < \cdots < q_{p/(p+1)},$$

and one would have to show that this forces $1 < q_{p/(p+1)}$, so that one $(p + 1)$ -cycle is pruned, but all the rest are somehow protected and fall within the unit interval. Keating [64] is all about orbits, so maybe this is explained there - or if not there, maybe in Percival-Vivaldi [81]? Percival and Vivaldi [80] and Boris' Green's functions are polynomial functions of s , so maybe the answer is there already.

What about non-prime periods $n = p_1 p_2 \cdots p_m$? Perhaps one has to replace the cat map f by the commuting set of maps $f_{p_\ell} = f^{p_\ell}$, one for each prime, and argue about pruning rules for $f^n = f_{p_1} \circ f_{p_2} \circ \cdots \circ f_{p_m}$. Will be messy. But while cat map f is linear in s , f_p are polynomial in s , and that might lead to Li Han's polynomials for $\hat{N}_n(s)$.

2016-05-21, -12-12 Predrag I had included Bird and Vivaldi [16] *Periodic orbits of the sawtooth maps* among the papers to read, but the paper remained woefully unread. Now Li Han has no choice but to read it :)

They assert that for the Arnol'd cat map there are 11 440 548 orbits of period 20.

Percival and Vivaldi [80] refer to the discrete Laplacian as the "central difference operator."

The special case $s = 2$ corresponds to an unperturbed twist map, for which orbits represent uniform motions of a free rotor.

The one-parameter s family of sawtooth maps (of the 2-torus), within which reside infinitely many Anosov diffeomorphisms. Sawtooth maps are piecewise linear, and for this reason we are able to construct the parameter dependence of the sawtooth orbits explicitly in terms of rational functions with integer coefficients.

- (i) for integral s the sawtooth map reduces to a toral automorphism, and the structure of periodic orbits of such maps is known [81]. They are found to coincide with points having rational coordinates, and can be dealt with using arithmetical techniques, one can locate and count all periodic orbits.
- (ii) if an orbit is known for one value of s , it can be computed for any other value.

We represent orbits as doubly infinite sequences of integers (words), where the integers are drawn from a finite set (alphabet). An orbit is written in terms of the configuration coordinate x_t alone and is denoted by (x_t) . The word we denote by (m_t) . For $s > 2$ the code is an isomorphism. For a given s , the possible values of the m_t are bounded in magnitude by $|m_t| \leq \text{Int}(1 + s/2)$. The itinerary of a given orbit is independent of the

parameter. The orbit is recovered by Green's function (1.38):

$$q_t = \frac{1}{\sqrt{D}} \sum_{s \in \mathbb{N}} \frac{1}{\Lambda^{|t-s|}} b_s , \quad (1.94)$$

The leading eigenvalue of the cat map Jacobian matrix M is given by (1.6). For an n -cycle x_t are rational functions of Λ , given by the quotient of two reflexive polynomials (for example, $P_t(\Lambda) = \Lambda^n P_t(1/\Lambda)$),

$$\begin{aligned} x_t &= \Lambda P_t(\Lambda)/Q(\Lambda) \\ P_t(\Lambda) &= \sum_{\tau=1}^{n-1} \Lambda^{n-\tau} (\Lambda m_{t+\tau-1} + m_{t-\tau}) \\ Q(\Lambda) &= (\Lambda^2 - 1)(\Lambda^n - 1) \end{aligned} \quad (1.95)$$

Bird and Vivaldi [16] then discuss pruning, give formulas for the numbers of orbits for integer s , etc.. Most likely Li Han's polynomials are implicit in these formulas.

2016-12-15 Predrag to Roberto, **Going catty**: What is the main question? My Question of the Day is:

In ChaosBook Diffusion chapter we show that whenever the critical point of the 1D sawtooth map (the rightmost highest point) is pre-periodic, we have finite grammar and an analytic cycle expansion formula (essentially the topological zeta function, with the uniform expansion rate stuck into z^n) for the diffusion constant.

As far as I can tell, both you and Boris ignore the issues of the grammar, get some long-time limit estimate of the diffusion constant.

Usually in 2D there is a fractal set of critical points (AKA pruning front) - we had worked it out for the Lozi map and the Hénon map. If the strange set is a strange repeller, there we have infinitely many examples of finite grammars. But it never happens for non-repelling sets, like the cat map for integer trace s . There there is a new (only one!) pruning rule for each prime period set of cycles (ie, are we on the way to prove Riemann conjecture?) and a messy set of rules for non-prime periods (which can be described by a polynomial in s).

The Question: Is the cat map pruning front a fractal set? Is there a systematic set of formulas for the diffusion constant, one for each set of grammar rules? Is this implicit in papers of Vivaldi and/or Keating?

I'm attaching the list of table 1.1, generated by Li Han. He (and not only he) operates on a different astral plane, so getting him to commit his results to our blog or draft of the paper is harder than pulling teeth. He has the grammar rules count to length 17 and the polynomials in s , but that I have only seen on his laptop screen.

PS - I am throwing in for a good measure a tent map, sect. 1.8, to illustrate what these polynomials in the stretching rate (s for cat, Λ for tent) are.

Now, what was YOUR main question that is still blowing in the wind?

2016-12-12 Roberto Artuso The main question, as I thought of it in my work of many years ago [10] (see ChaosBook.org Appendix *Statistical mechanics applications*, included in this blog as chapter 12), was to understand the behavior of D as $K \rightarrow 0$, since it seems to get an extra factor $D \sim K^{2.5}$, while $D \sim K^2$ is the usual quasilinear result. The Percival-Vivaldi linear code seemed to me appealing since it selects allowed itineraries within a sort of rhombus in many dimensions, and the symbols are directly linked to transport, while usual Markov partitions for integer K are not. My thought was that non-integer K behavior could be linked to the number of lattice points within the "rhombus", and that the K correction (as well as oscillations with respect to quasilinear estimate), could be related to estimates of errors in volumes vs. number of lattice points (something like Dyson-Bleher [18–21] work for ellipses).

2017-09-29 Predrag Vaienti [108] *Ergodic properties of the discontinuous sawtooth map* might be worthy of a read.

2017-09-27 Predrag Vallejos and Saraceno [109] *The construction of a quantum Markov partition* (1999), present in Figure 6 the 5-rectangles Markov partition of the Arnol'd cat map of Adler-Weiss [3] *Similarity of automorphisms of the torus*. Work it out for our A' .

The three regions partition of the cat map is explained at length in Tabrizian's notes.

Chernov (see his Fig. 1) writes: "If the matrix A' is not symmetric, the stable and unstable lines for on the torus may not be orthogonal. Then, the atoms of Markov partitions are, geometrically, parallelograms rather than rectangles. In early works on Markov partitions [93], the term 'parallelogram' was used instead of 'rectangle'."

Check also Nonnenmacher notes, and the Sect. 5 of Huntsman's paper.

From **math stockexchange**: A reference would be the Handbook of dynamical systems by Hasselblatt and Katok [55], Volume 1, starting on page 324. The cat map example is on pages 327–328. Another good source is the original paper by Adler-Weiss [2] from 1967 and R. Bowen's paper on Axiom A from 1970. Constructing Markov partitions for higher dimensional tori is much more complicated, as the borders of their atoms are fractal and not differentiable, hence the nice rectangles only happen to exist in 2 dimensions.

The two and M regions partition of the cat map are drawn in Vorobets' lecture.

Here is a beautifully laid out problem set.

For a cat map, the SRB measure is just the Lebesgue measure, which also serves as a probability measure.

Bruin, in his Sect. 12 discussion of *Toral automorphisms*, asserts that Arnol'd didn't seem to like cats. So, never ever forget to blame the **cat**. Whatever you do, the cat will be **back**.

2018-02-11 Predrag Ignore the following cryptic remark about symbolic dynamics intrinsic to being in the stable / unstable manifolds coordinates: The symbolic dynamics is 2-dimensional: a partition can be $\{\text{left,right}\} = \{L, R\}$ with respect to the unstable eigendirection through the origin, and $\{\text{up,down}\} = \{U, D\}$ with respect to the stable eigendirection, so partitions are labeled by pairs of symbols (the canonical Arn 3-letter alphabet)

$$\{h_j, v_j\} \in \{RU, LU, RD\},$$

with $\{LD\}$ forbidden.

2012-01-15 Predrag Read Jézéquel [63] *Global trace formula for ultra-differentiable Anosov flows*: "[...] we prove that a trace formula that holds for Anosov flows in a certain class of regularity. The main ingredient of the proof is the construction of a family of anisotropic Hilbert spaces of generalized distributions on which the generator of the flow has discrete spectrum.

Commentary

Remark 1.3. Phase space. The cylinder phase is $[-1/2, 1/2) \times \mathbb{R}$: the map is originally defined in $[-1/2, 1/2]^2$, and is generalized over the cylinder by symmetry requirements.¹⁶

Remark 1.4. Pythagorean tiling or two squares tessellation is a tiling of a Euclidean plane by squares of two different sizes, in which each square touches four squares of the other size on its four sides (see [wikipedia.org/wiki/Pythagorean_tiling](https://en.wikipedia.org/wiki/Pythagorean_tiling)). This tiling has four-way rotational symmetry around each of its squares. When the ratio of the side lengths of the two squares is an irrational number such as the golden ratio, its cross-sections form aperiodic sequences with a Fibonacci-type recursive structure. It has a cyclic set of symmetries around the corresponding points, giving it **p4** symmetry: square lattice, point group C_4 , two rotation centres of order four (90°), and one rotation centre of order two (180°). It has no reflections or glide reflections. It is a chiral pattern, meaning that it is impossible to superpose it on top of its mirror image using only translations and rotations; a Pythagorean tiling is not symmetric under mirror reflections. Although a Pythagorean tiling is itself periodic (it has a square lattice of translational symmetries) its cross sections can be used to generate one-dimensional aperiodic sequences.

Remark 1.5. Symmetries of the symbol square. For a discussion of symmetry lines of example 2.6 see refs. [50, 51, 75, 85, 90]. It is an open question (see remark ??) as to

↓PRIVATE

how time reversal symmetry can be exploited for reduction of cycle expansions of chapter ???. For example, the fundamental domain symbolic dynamics for reflection symmetric systems is discussed in some detail in sect. 4.11, but how does one recode from time-reversal symmetric symbol sequences to desymmetrized 1/2 state space symbols? In discussion of example 2.5, we have followed refs. [38, 45, 100].¹⁷

↑PRIVATE

Remark 1.6. XXX.

References

- [1] R. L. Adler, “Symbolic dynamics and Markov partitions”, Bull. Amer. Math. Soc. **35**, 1–56 (1998).
- [2] R. L. Adler and B. Weiss, “Entropy, a complete metric invariant for automorphisms of the torus”, Proc. Natl. Acad. Sci. USA **57**, 1573–1576 (1967).
- [3] R. L. Adler and B. Weiss, *Similarity of automorphisms of the torus*, Vol. 98, Memoirs Amer. Math. Soc. (Amer. Math. Soc., Providence RI, 1970).
- [4] A. Aitken, *Determinants & Matrices* (Oliver & Boyd, Edinburgh, 1939).
- [5] D. V. Anosov, A. V. Klimenko, and G. Kolutsky, *On the hyperbolic automorphisms of the 2-torus and their Markov partitions*, 2008.
- [6] V. I. Arnol’d and A. Avez, *Ergodic Problems of Classical Mechanics* (Addison-Wesley, Redwood City, 1989).
- [7] M. Artin and B. Mazur, “On periodic points”, Ann. Math. **81**, 82–99 (1965).
- [8] R. Artuso, E. Aurell, and P. Cvitanović, “Recycling of strange sets: II. Applications”, Nonlinearity **3**, 361–386 (1990).
- [9] R. Artuso and P. Cvitanović, “Deterministic diffusion”, in *Chaos: Classical and Quantum*, edited by P. Cvitanović, R. Artuso, R. Mainieri, G. Tanner, and G. Vattay (Niels Bohr Inst., Copenhagen, 2019).
- [10] R. Artuso and R. Strepparava, “Reycling diffusion in sawtooth and cat maps”, Phys. Lett. A **236**, 469–475 (1997).
- [11] V. Baladi, Dynamical zeta functions, in *Real and Complex Dynamical Systems: Proceedings of the NATO ASI*, edited by B. Branner and P. Hjorth (1995), pp. 1–26.
- [12] A. F. Beardon, S. R. Bullett, and P. J. Rippon, “Periodic orbits of difference equations”, Proc. Roy. Soc. Edinburgh Sect. A **125**, 657–674 (1995).
- [13] E. Behrends, “The ghosts of the cat”, Ergod. Theor. Dynam. Syst. **18**, 321–330 (1998).

¹⁶Predrag 2016-08-03: missing eq. refeqtra-sym reference.

¹⁷Predrag 2021-04-03: Improve references; eventually return to ChaosBook *cycles.tex*.

- [14] E. Behrends and B. Fielder, “Periods of discretized linear Anosov maps”, *Ergod. Theor. Dynam. Syst.* **18**, 331–341 (1998).
- [15] T. H. Berlin and M. Kac, “The spherical model of a ferromagnet”, *Phys. Rev.* **86**, 821–835 (1952).
- [16] N. Bird and F. Vivaldi, “Periodic orbits of the sawtooth maps”, *Physica D* **30**, 164–176 (1988).
- [17] M. Blank, G. Keller, and C. Liverani, “Ruelle-Perron-Frobenius spectrum for Anosov maps”, *Nonlinearity* **15**, 1905–1973 (2002).
- [18] P. M. Bleher and F. J. Dyson, “Mean square limit for lattice points in a sphere”, *Acta Arith.* **68**, 383–393 (1994).
- [19] P. M. Bleher and F. J. Dyson, “Mean square value of exponential sums related to representation of integers as sum of two squares”, *Acta Arith.* **68**, 71–84 (1994).
- [20] P. M. Bleher and F. J. Dyson, “The variance of the error function in the shifted circle problem is a wild function of the shift”, *Commun. Math. Phys.* **160**, 493–505 (1994).
- [21] P. Bleher, “Trace formula for quantum integrable systems, lattice-point problem, and small divisors”, in *Emerging Applications of Number Theory*, edited by D. A. Hejhal, J. Friedman, M. C. Gutzwiller, and A. M. Odlyzko (Springer, 1999), pp. 1–38.
- [22] R. Bowen, “Markov partitions for Axiom A diffeomorphisms”, *Amer. J. Math.* **92**, 725–747 (1970).
- [23] A. Boyarsky and P. Góra, *Laws of Chaos: Invariant Measures and Dynamical Systems in One Dimension* (Birkhäuser, Boston, 1997).
- [24] J. P. Boyd, *Chebyshev and Fourier Spectral Methods*, 2nd ed. (Dover, New York, 2000).
- [25] F. Brini, S. Siboni, G. Turchetti, and S. Vaienti, “Decay of correlations for the automorphism of the torus T^2 ”, *Nonlinearity* **10**, 1257–1268 (1997).
- [26] S. Bullett, “Invariant circles for the piecewise linear standard map”, *Commun. Math. Phys.* **107**, 241–262 (1986).
- [27] S. C. Creagh, “Quantum zeta function for perturbed cat maps”, *Chaos* **5**, 477–493 (1995).
- [28] J. Crutchfield, *Roadmap for Natural Computation and Self-Organization*, tech. rep., Physics 256A course (U. California, Davis, 2017).
- [29] P. Cvitanović, “Counting”, in *Chaos: Classical and Quantum* (Niels Bohr Inst., Copenhagen, 2020).
- [30] P. Cvitanović, R. Artuso, R. Mainieri, G. Tanner, and G. Vattay, *Chaos: Classical and Quantum* (Niels Bohr Inst., Copenhagen, 2020).
- [31] P. Cvitanović, R. Artuso, R. Mainieri, G. Tanner, and G. Vattay, *Chaos: Classical and Quantum* (Niels Bohr Inst., Copenhagen, 2020).

- [32] P. Cvitanović, R. Artuso, L. Rondoni, and E. A. Spiegel, “Transporting densities”, in *Chaos: Classical and Quantum*, edited by P. Cvitanović, R. Artuso, R. Mainieri, G. Tanner, and G. Vattay (Niels Bohr Inst., Copenhagen, 2017).
- [33] P. Cvitanović and H. Liang, *Spatiotemporal cat: A chaotic field theory*, In preparation, 2021.
- [34] P. J. Davis, *Circulant matrices*, 2nd ed. (Amer. Math. Soc., New York, 1979).
- [35] R. L. Devaney, *An Introduction to Chaotic Dynamical systems*, 2nd ed. (Westview Press, Cambridge, Mass, 2008).
- [36] M. Dow, “Explicit inverses of Toeplitz and associated matrices”, *ANZIAM J.* **44**, E185–E215 (2003).
- [37] D. J. Driebe, *Fully Chaotic Maps and Broken Time Symmetry* (Springer, New York, 1999).
- [38] H. R. Dullin, J. D. Meiss, and D. G. Sterling, “Symbolic codes for rotational orbits”, *SIAM J. Appl. Dyn. Sys.* **4**, 515–562 (2005).
- [39] F. J. Dyson and H. Falk, “Period of a discrete cat mapping”, *Amer. Math. Monthly* **99**, 603–614 (1992).
- [40] S. Elaydi, *An Introduction to Difference Equations*, 3rd ed. (Springer, Berlin, 2005).
- [41] M. Elouafi, “On a relationship between Chebyshev polynomials and Toeplitz determinants”, *Appl. Math. Comput.* **229**, 27–33 (2014).
- [42] L. Flatto, J. C. Lagarias, and B. Poonen, “The zeta function of the beta transformation”, *Ergodic Theory Dynam. Systems* **14**, 237–266 (1994).
- [43] I. García-Mata and M. Saraceno, “Spectral properties and classical decays in quantum open systems”, *Phys. Rev. E* **69**, 056211 (2004).
- [44] P. Giulietti, C. Liverani, and M. Pollicott, “Anosov flows and dynamical zeta functions”, *Ann. Math.* **178**, 687–773 (2013).
- [45] A. Gómez and J. D. Meiss, “Reversible polynomial automorphisms of the plane: The involutory case”, *Phys. Lett. A* **312**, 49–58 (2003).
- [46] M. J. C. Gover, “The eigenproblem of a tridiagonal 2-Toeplitz matrix”, *Linear Algebra Appl.* **197**, 63–78 (1994).
- [47] E. Gozzi, “Counting periodic trajectories via topological classical mechanics”, *Chaos Solit. Fract.* **4**, 653–660 (1994).
- [48] I. S. Gradshteyn and I. M. Ryzhik, *Tables of Integrals, Series and Products*, 8th ed. (Elsevier LTD, Oxford, New York, 2014).
- [49] P. Grandclément, “Introduction to spectral methods”, *EAS Publications Series* **21**, 153–180 (2006).
- [50] J. M. Greene, “A method for determining a stochastic transition”, *J. Math. Phys.* **20**, 1183–1201 (1979).

- [51] J. M. Greene, R. S. MacKay, F. Vivaldi, and M. J. Feigenbaum, “Universal behaviour in families of area-preserving maps”, *Physica D* **3**, 468–486 (1981).
- [52] J. Guckenheimer, “On the bifurcation of maps of the interval”, *Inv. Math.* **39**, 165–178 (1977).
- [53] B. Gutkin, L. Han, R. Jafari, A. K. Saremi, and P. Cvitanović, “Linear encoding of the spatiotemporal cat map”, *Nonlinearity* **34**, 2800–2836 (2021).
- [54] J. H. Hannay and M. V. Berry, “Quantization of linear maps on a torus – Fresnel diffraction by a periodic grating”, *Physica D* **1**, 267–290 (1980).
- [55] B. Hasselblatt and A. Katok, *Handbook of Dynamical Systems* (Elsevier, New York, 2002).
- [56] F. Hofbauer and G. Keller, “Zeta-functions and transfer-operators for piecewise linear transformations”, *J. Reine Angew. Math. (Crelle)* **1984**, 100–113 (1984).
- [57] G. Y. Hu and R. F. O’Connell, “Exact solution for the charge soliton in a one-dimensional array of small tunnel junctions”, *Phys. Rev. B* **49**, 16773–16776 (1994).
- [58] G. Y. Hu and R. F. O’Connell, “Exact solution of the electrostatic problem for a single electron multijunction trap”, *Phys. Rev. Lett.* **74**, 1839–1842 (1995).
- [59] G. Y. Hu and R. F. O’Connell, “Analytical inversion of symmetric tridiagonal matrices”, *J. Phys. A* **29**, 1511 (1996).
- [60] T. A. Hunt and B. D. Todd, “On the Arnold cat map and periodic boundary conditions for planar elongational flow”, *Molec. Phys.* **101**, 3445–3454 (2003).
- [61] S. Isola, “ ζ -functions and distribution of periodic orbits of toral automorphisms”, *Europhys. Lett.* **11**, 517–522 (1990).
- [62] S. Jaidee, P. Moss, and T. Ward, “Time-changes preserving zeta functions”, *Proc. Amer. Math. Soc.* **147**, 4425–4438 (2019).
- [63] M. Jézéquel, “Global trace formula for ultra-differentiable Anosov flows”, *Comm. Math. Phys.* (2021).
- [64] J. P. Keating, “Asymptotic properties of the periodic orbits of the cat maps”, *Nonlinearity* **4**, 277 (1991).
- [65] J. P. Keating, “The cat maps: quantum mechanics and classical motion”, *Nonlinearity* **4**, 309–341 (1991).
- [66] J. P. Keating and F. Mezzadri, “Pseudo-symmetries of Anosov maps and spectral statistics”, *Nonlinearity* **13**, 747–775 (2000).
- [67] H. Kübra Duru and D. Bozkurt, *Integer powers of certain complex pentadiagonal 2-Toeplitz matrices*, 2017.

- [68] E. Lanneau and J.-L. Thiffeault, “On the minimum dilatation of pseudo-Anosov homeomorphisms on surfaces of small genus”, *Ann. Inst. Fourier* **61**, 105–144 (2011).
- [69] D. H. Lehmer, “Factorization of certain cyclotomic functions”, *Ann. of Math.* (2) **34**, 461–479 (1933).
- [70] D. Li and J. Xie, “Symbolic dynamics of Belykh-type maps”, *Appl. Math. Mech.* **37**, 671–682 (2016).
- [71] A. Manning, “Axiom A diffeomorphisms have rational zeta function”, *Bull. London Math. Soc.* **3**, 215–220 (1971).
- [72] A. Manning, “A Markov partition that reflects the geometry of a hyperbolic toral automorphism”, *Trans. Amer. Math. Soc.* **354**, 2849–2864 (2002).
- [73] B. D. Mestel and I. Percival, “Newton method for highly unstable orbits”, *Physica D* **24**, 172 (1987).
- [74] C. Meyer, *Matrix Analysis and Applied Linear Algebra* (SIAM, Philadelphia, 2000).
- [75] C. Mira, *Chaotic dynamics – From one dimensional endomorphism to two dimensional diffeomorphism* (World Scientific, Singapore, 1987).
- [76] S. Nonnenmacher, “Spectral properties of noisy classical and quantum propagators”, *Nonlinearity* **16**, 1685–1713 (2003).
- [77] S. Noschese, L. Pasquini, and L. Reichel, “Tridiagonal Toeplitz matrices: properties and novel applications”, *Numer. Linear Algebra Appl.* **20**, 302–326 (2013).
- [78] A. M. Ozorio de Almeida and J. H. Hannay, “Periodic orbits and a correlation function for the semiclassical density of states”, *J. Phys. A* **17**, 3429 (1984).
- [79] W. Parry, “On the β -expansions of real numbers”, *Acta Math. Acad. Sci. Hung.* **11**, 401–416 (1960).
- [80] I. Percival and F. Vivaldi, “A linear code for the sawtooth and cat maps”, *Physica D* **27**, 373–386 (1987).
- [81] I. Percival and F. Vivaldi, “Arithmetical properties of strongly chaotic motions”, *Physica D* **25**, 105–130 (1987).
- [82] T. A. Pierce, “The numerical factors of the arithmetic forms $\prod(1 \pm \alpha_i^m)$ ”, *Ann. of Math.* (2) **18**, 53–64 (1916).
- [83] C. Puccia and R. Levins, *Qualitative Modeling of Complex Systems: An Introduction to Loop Analysis and Time Averaging* (Harvard Univ. Press, 1985).
- [84] A. Rényi, “Representations for real numbers and their ergodic properties”, *Acta Math. Acad. Sci. Hung.* **8**, 477–493 (1957).
- [85] P. H. Richter, H.-J. Scholz, and A. Wittek, “A breathing chaos”, *Nonlinearity* **3**, 45–67 (1990).

- [86] R. C. Robinson, *An Introduction to Dynamical Systems: Continuous and Discrete* (Amer. Math. Soc., New York, 2012).
- [87] C. G. J. Roettger, “Periodic points classify a family of markov shifts”, *J. Number Theory* **113**, 69–83 (2005).
- [88] D. Ruelle, “An extension of the theory of Fredholm determinants”, *Inst. Hautes Études Sci. Publ. Math.* **72**, 175–193 (1990).
- [89] E. Rykken, “Markov partitions for hyperbolic toral automorphisms of T^2 ”, *Rocky Mountain J. Math.* **28**, 1103–1124 (1998).
- [90] S. J. Shenker and L. P. Kadanoff, “Critical behavior of a KAM surface: i. Empirical results”, *J. Stat. Phys.* **27**, 631–656 (1982).
- [91] A. Siemaszko and M. P. Wojtkowski, “Counting Berg partitions”, *Nonlinearity* **24**, 2383–2403 (2011).
- [92] S. Simons, “Analytical inversion of a particular type of banded matrix”, *J. Phys. A* **30**, 755 (1997).
- [93] Y. G. Sinai, “Construction of Markov partitions”, *Funct. Anal. Appl.* **2**, 245–253 (1968).
- [94] Y. G. Sinai, *Introduction to Ergodic Theory* (Princeton Univ. Press, Princeton, 1976).
- [95] J. Slipantschuk, O. F. Bandtlow, and W. Just, “Complete spectral data for analytic Anosov maps of the torus”, *Nonlinearity* **30**, 2667 (2017).
- [96] S. Smale, “Generalized Poincaré’s conjecture in dimensions greater than four”, *Ann. Math.* **74**, 199 (1961).
- [97] G. D. Smith, *Numerical Solution of Partial Differential Equations: Finite Difference Methods* (Clarendon Press, Oxford UK, 1985).
- [98] M. R. Snavely, “Markov partitions for the two-dimensional torus”, *Proc. Amer. Math. Soc.* **113**, 517–517 (1991).
- [99] E. D. Sontag, *Mathematical Control Theory: Deterministic Finite Dimensional Systems* (Springer, New York, 1998).
- [100] D. G. Sterling, H. R. Dullin, and J. D. Meiss, “Homoclinic bifurcations for the Hénon map”, *Physica D* **134**, 153–184 (1999).
- [101] R. F. Streater, “A bound for the difference Laplacian”, *Bull. London Math. Soc.* **11**, 354–357 (1979).
- [102] R. Sturman, J. M. Ottino, and S. Wiggins, *The Mathematical Foundations of Mixing* (Cambridge Univ. Press, 2006).
- [103] R. Suarez, “Difference equations and a principle of double induction”, *Math. Mag.* **62**, 334–339 (1989).
- [104] Y. Takahashi, “Fredholm determinant of unimodal linear maps”, *Scientific Papers Coll. Gen. Ed. Univ.Tokyo* **31**, 61–87 (1981).
- [105] Y. Takahashi, “Shift with orbit basis and realization of one-dimensional maps”, *Osaka J. Math.* **20**, 599–629 (1983).

- [106] T. Tél, “Fractal dimension of the strange attractor in a piecewise linear two-dimensional map”, *Phys. Lett. A* **97**, 219–223 (1983).
- [107] B. D. Todd, “Cats, maps and nanoflows: some recent developments in nonequilibrium nanofluidics”, *Molec. Simul.* **31**, 411–428 (2005).
- [108] S. Vaienti, “Ergodic properties of the discontinuous sawtooth map”, *J. Stat. Phys.* **67**, 251–269 (1992).
- [109] R. O. Vallejos and M. Saraceno, “The construction of a quantum Markov partition”, *J. Phys. A* **32**, 7273 (1999).
- [110] P. Walters, *An Introduction to Ergodic Theory* (Springer, New York, 1982).
- [111] E. W. Weisstein, [Arnold’s Cat Map](#), MathWorld—A Wolfram Web Resource.
- [112] H. S. Wilf, *Generatingfunctionology* (Academic Press, New York, 1994).
- [113] D. C. Wylie, “Linked by loops: Network structure and switch integration in complex dynamical systems”, *Physica A* **388**, 1946–1958 (2009).
- [114] H. A. Yamani and M. S. Abdelmonem, “The analytic inversion of any finite symmetric tridiagonal matrix”, *J. Phys. A* **30**, 2889 (1997).
- [115] W.-C. Yueh, “Explicit inverses of several tridiagonal matrices”, *Appl. Math. E-Notes* **6**, 74–83 (2006).

Example 1.1. Temporal Bernoulli shadowing.

As the temporal Bernoulli condition (3.31) is a linear relation, a given block M , or ‘code’ in terms of alphabet (3.26), corresponds to a unique temporal lattice state X given by the temporal lattice Green’s function

$$X_M = g M, \quad g = \frac{d/s}{\mathbb{1} - d/s}. \quad (1.96)$$

For an infinite lattice $t \in \mathbb{Z}$, this Green’s function can be expanded as a series in Λ^{-k} ,

$$g = \frac{d/\Lambda}{\mathbb{1} - d/\Lambda} = \sum_{k=1}^{\infty} \frac{d^k}{\Lambda^k}, \quad (1.97)$$

where $\Lambda = s$ is the 1-time step stability multiplier for the Bernoulli system. From (1.96) it follows that the influence of a source $m_{t'}$ back in the past, at site t' , falls off exponentially with the temporal lattice distance $t - t'$,

$$x_t = \sum_{t'=-\infty}^{t-1} g_{tt'} m_{t'}, \quad g_{tt'} = \frac{1}{\Lambda^{t-t'}}, \quad t > t', \quad 0 \text{ otherwise}. \quad (1.98)$$

That means that an ergodic lattice state segment of length n (or a periodic lattice state of a longer period) is shadowed by the periodic lattice state (3.29) with the same n -sites symbol block M , ¹⁸

$$x_t = \frac{1}{1 - 1/\Lambda^n} \left(\frac{m_1}{\Lambda} + \frac{m_2}{\Lambda^2} + \cdots + \frac{m_{n-1}}{\Lambda^{n-1}} + \frac{m_n}{\Lambda^n} \right), \quad (1.99)$$

with exponentially decreasing shadowing error of order $O(1/\Lambda^{n+1})$. The error is controlled by the (3.106) prefactor $1/|\text{Det } \mathcal{J}| = 1/|\det(\mathbb{1} - \mathbb{J}_M)|$, with the determinant arising from inverting the orbit Jacobian matrix \mathcal{J} to obtain the Green’s function (3.31).

This error estimate is deeper than what it might seem at the first glance. In fluid dynamics, pattern recognition, neuroscience and other high or ∞ -dimensional settings distances between ‘close solutions’ (let’s say pixel images of two faces in a face recognition code) are almost always measured using some arbitrary yardstick, let’s say a Euclidean L_2 norm, even though the state space that has no Euclidean symmetry. Not so in the periodic orbit theory: here $1/|\text{Det } \mathcal{J}|$ is the intrinsic, coordinatization and norm independent measure of the distance between similar spatiotemporal states.

[click to return: p. 54](#)

1.10 Examples

Example 1.2. Projection operator decomposition of the cat map: Let’s illustrate how the decomposition works for the Percival-Vivaldi [80] “two-configuration representation” of the Arnol’d cat map by the $[2 \times 2]$ matrix

$$\mathbf{A} = \begin{bmatrix} 0 & 1 \\ -1 & s \end{bmatrix}. \quad (1.100)$$

¹⁸Predrag 2020-02-16: Do I need to derive this?

To interpret m_n 's, consider the action of the this map (3.49) on a 2-dimensional state space point (x_{n-1}, x_n) ,

$$\begin{pmatrix} x_n \\ x_{n+1} \end{pmatrix} = \mathbf{A} \begin{pmatrix} x_{n-1} \\ x_n \end{pmatrix} - \begin{pmatrix} 0 \\ m_n \end{pmatrix}. \quad (1.101)$$

In Percival and Vivaldi [80] this representation of cat map is referred to as “the two-configuration representation”. As illustrated in figure 1.2, in one time step the area preserving map A' stretches the unit square into a parallelogram, and a point (x_0, x_1) within the initial unit square in general lands outside it, in another unit square m_n steps away. As they shepherd such stray points back into the unit torus, the integers m_n can be interpreted as “winding numbers” [65], or “stabilising impulses” [80]. The m_n translations reshuffle the state space, thus partitioning it into $|\mathcal{A}|$ regions \mathcal{M}_m , $m \in \mathcal{A}$.

Associated with each root Λ^i in (??) is the projection operator $P^i = \prod(\mathbf{A} - \Lambda^j \mathbf{1}) / (\Lambda^i - \Lambda^j)$, $j \neq i$,

$$P^+ = \frac{1}{\sqrt{D}}(\mathbf{A} - \Lambda^{-1} \mathbf{1}) = \frac{1}{\sqrt{D}} \begin{bmatrix} -\Lambda^{-1} & 1 \\ -1 & \Lambda \end{bmatrix} \quad (1.102)$$

$$P^- = -\frac{1}{\sqrt{D}}(\mathbf{A} - \Lambda \mathbf{1}) = \frac{1}{\sqrt{D}} \begin{bmatrix} \Lambda & -1 \\ 1 & -\Lambda^{-1} \end{bmatrix}. \quad (1.103)$$

Matrices P^\pm are orthonormal and complete. The dimension of the i th subspace is given by $d_i = \text{tr } P_i$; in case at hand both subspaces are 1-dimensional. From the characteristic equation it follows that P^\pm satisfy the eigenvalue equation $\mathbf{A} P^\pm = \Lambda^\pm P^\pm$, with every column a right eigenvector, and every row a left eigenvector. Picking –for example– the first row/column we get the right and the left eigenvectors:

$$\begin{aligned} \{\mathbf{e}^{(+)}, \mathbf{e}^{(-)}\} &= \left\{ \frac{1}{\sqrt{D}} \begin{bmatrix} -\Lambda^{-1} \\ -1 \end{bmatrix}, \frac{1}{\sqrt{D}} \begin{bmatrix} \Lambda \\ 1 \end{bmatrix} \right\} \\ \{\mathbf{e}_{(+)}, \mathbf{e}_{(-)}\} &= \left\{ \frac{1}{\sqrt{D}}[-\Lambda^{-1}, 1], \frac{1}{\sqrt{D}}[\Lambda, -1] \right\}, \end{aligned} \quad (1.104)$$

with overall scale arbitrary.¹⁹ The matrix is not symmetric, so $\{\mathbf{e}^{(j)}\}$ do not form an orthogonal basis. The left-right eigenvector dot products $\mathbf{e}_{(j)} \cdot \mathbf{e}^{(k)}$, however, are orthogonal,

$$\mathbf{e}_{(i)} \cdot \mathbf{e}^{(j)} = c_j \delta_{ij}.$$

What does this do to the partition figure 1.2? The origin is still the fixed point. A state space point in the new, dynamically intrinsic right eigenvector Adler-Weiss [3] coordinate basis is

$$\begin{aligned} \begin{pmatrix} x_{n-1} \\ x_n \end{pmatrix} &= (P^+ + P^-) \begin{pmatrix} x_{n-1} \\ x_n \end{pmatrix} \\ &= \frac{1}{\sqrt{D}} \begin{bmatrix} -\Lambda^{-1} & 1 \\ -1 & \Lambda \end{bmatrix} \begin{pmatrix} x_{n-1} \\ x_n \end{pmatrix} + \frac{1}{\sqrt{D}} \begin{bmatrix} \Lambda & -1 \\ 1 & -\Lambda^{-1} \end{bmatrix} \begin{pmatrix} x_{n-1} \\ x_n \end{pmatrix} \\ &= \frac{1}{\sqrt{D}} \begin{pmatrix} x_n - \Lambda^{-1} x_{n-1} \\ \Lambda x_n - x_{n-1} \end{pmatrix} + \frac{1}{\sqrt{D}} \begin{pmatrix} -x_n + \Lambda x_{n-1} \\ -\Lambda^{-1} x_n + x_{n-1} \end{pmatrix} \\ &= -(\Lambda x_n - x_{n-1}) \frac{1}{\sqrt{D}} \begin{bmatrix} -\Lambda^{-1} \\ -1 \end{bmatrix} + (-\Lambda^{-1} x_n + x_{n-1}) \frac{1}{\sqrt{D}} \begin{bmatrix} \Lambda \\ 1 \end{bmatrix} \end{aligned}$$

¹⁹Predrag 2017-10-02: compare with (1.24)

$$= (-\Lambda x_n + x_{n-1}) P^+ + (-\Lambda^{-1} x_n + x_{n-1}) P^-.$$

The abscissa (x_{n-1} direction) is not affected, but the ordinate (x_n direction) is flipped and stretched/shrunk by factor $-\Lambda$, $-\Lambda^{-1}$ respectively, preserving the vertical strip nature of the partition figure 1.2. In the Adler-Weiss right eigenbasis, \mathbf{A} acts by stretching the $e^{(+)}$ direction by Λ , and shrinking the $e^{(-)}$ direction by Λ^{-1} , without any rotation of either direction.

Example 1.3. A linear cat map code. Eqs. (7.54,7.55) are the discrete-time Hamilton's equations, which induce temporal evolution on the 2-torus (x_n, p_n) phase space. For the problem at hand, it pays to go from the Hamiltonian (x_n, p_n) phase space formulation to the Newtonian (or Lagrangian) (x_{n-1}, x_n) state space formulation [80], with p_n replaced by $p_n = (x_n - x_{n-1})/\Delta t$. Eq. (7.55) then takes the 3-term recurrence form (the discrete time Laplacian \square formula for the second order time derivative d^2/dt^2 , with the time step set to $\Delta t = 1$),

$$\square x_n \equiv x_{n+1} - 2x_n + x_{n-1} = P(x_n) \quad \text{mod } 1, \quad (1.105)$$

i.e., Newton's Second Law: "acceleration equals force." For a cat map, with force $P(x)$ linear in the displacement x , the Newton's equation of motion (1.105) takes form

$$(\square + 2 - s) x_n = -m_n, \quad (1.106)$$

with mod 1 enforced by m_n 's, integers from the alphabet

$$\mathcal{A} = \{1, 0, \dots, s-1\}, \quad (1.107)$$

necessary to keep x_n for all times t within the unit interval $[0, 1]$. The genesis of this alphabet is illustrated by figure 1.2. We have introduced here the symbol $|m_n|$ to denote m_n with the negative sign, i.e., ' $\underline{1}$ ' stands for symbol ' -1 '.

Example 1.4. Perron-Frobenius operator for the Arnol'd cat map. For a piecewise linear maps acting on a finite generating partition the Perron-Frobenius operator takes the finite, transfer matrix form (see ref. [32]).

$$\mathbf{L}_{ij} = \frac{|\mathcal{M}_i \cap f^{-1}(\mathcal{M}_j)|}{|\mathcal{M}_i|}, \quad \rho' = \rho \mathbf{L} \quad (1.108)$$

The two rectangles and five sub-rectangle areas $|\mathcal{M}_j|$ are given by inspection of figure 1.10(a):²⁰

$$\begin{aligned} |\mathcal{M}_A| &= \Lambda/(\Lambda + 1), & |\mathcal{M}_B| &= 1/(\Lambda + 1), \\ |\mathcal{M}_1| &= |\mathcal{M}_A|/\Lambda, & |\mathcal{M}_2| &= (\Lambda - 1)|\mathcal{M}_B|/\Lambda, & |\mathcal{M}_3| &= |\mathcal{M}_A|/\Lambda, \\ |\mathcal{M}_4| &= |\mathcal{M}_B|/\Lambda, & |\mathcal{M}_5| &= (\Lambda - 2)|\mathcal{M}_A|/\Lambda, \end{aligned} \quad (1.109)$$

where Λ and D are given in (??), and we are considering the $s = 3$ Arnol'd cat map case (the generalization to $s > 3$ is immediate). The areas are symplectic invariants, and thus the same in any choice of cat-map coordinates. As in the ChaosBook example exam:FP_eigs_Ulam (currently 19.1), the Adler-Weiss partitioned Percival-Vivaldi cat map is an expanding piecewise-linear map, so we can construct the associated transfer

²⁰Predrag 2018-02-16: to Han: PLEASE RECHECK

matrix explicitly, by weighing the links of transition graph figure 1.10(a) by the ratios of out-, in-rectangle areas $T_{kj} = |\mathcal{M}_{m_k}|/|\mathcal{M}_{m_j}|$:²¹

$$\begin{bmatrix} \phi'_1 \\ \phi'_2 \\ \phi'_3 \\ \phi'_4 \\ \phi'_5 \end{bmatrix} = \mathbf{T}\phi = \frac{1}{\Lambda} \begin{bmatrix} 1 & \Lambda - 2 & 1 & 0 & 0 \\ 0 & 0 & 0 & \Lambda - 1 & 1 \\ 1 & \Lambda - 2 & 1 & 0 & 0 \\ 0 & 0 & 0 & 1 & \Lambda - 1 \\ 1 & \Lambda - 1 & \frac{\Lambda - 2}{\Lambda - 1} & 0 & 0 \end{bmatrix} \begin{bmatrix} \phi_1 \\ \phi_2 \\ \phi_3 \\ \phi_4 \\ \phi_5 \end{bmatrix} \quad (1.110)$$

The probability for starting in initial state j is conserved, $\sum_k L_{kj} = 1$, as it should be. Such non-negative matrix whose columns conserve probability is called Markov, probability or stochastic matrix. Thanks to the same expansion everywhere, and a finite transition graph, the Fredholm determinant is the characteristic polynomial of the transfer matrix (currently ChaosBook Eq. (18.13)) defined by the transition graph of figure 1.1(c), expanded in non-intersecting loops $t_A = T_{A^0 A}, t'_A = T_{A^1 A}, t_B = T_{B^0 B}, t_{AB} = T_{A^1 B} T_{B^1 A}$:

$$\det(1-z\mathbf{T}) = 1 - z(t_A + t'_A + t_B) - z^2 t_{AB} + z^2(t_A + t'_A)t_B = 1 - 3\frac{z}{\Lambda} - (\Lambda - 3)\frac{z^2}{\Lambda}, \quad (1.111)$$

$$\det(1 - z\mathbf{T}) = 1 - 3\frac{z}{\Lambda} - (\Lambda - 3)\frac{z^2}{\Lambda}, \quad (1.112)$$

in agreement with (1.11). This counts the fixed point at the origin thrice (it lives in the invariant subspace spanned by stable and unstable manifolds, the border) so that has to be divided out.

Due to probability (unit area) conservation, \mathbf{T} has a unit eigenvalue $z = 1 = e^{s_0}$, with constant density eigenvector $\rho_0 = \rho_1$.

In the orbit-counting case one retrieves Isola's ζ -function [61] (3.190).

This simple explicit matrix representation of the Perron-Frobenius operator is a consequence of the piecewise linearity of the time-forward map, and the restriction of the densities ρ to the space of piecewise constant functions.

Example 1.5. Counting temporal cat lattice states.

The temporal cat equation (3.45) is a linear 2nd-order inhomogeneous difference equation (3-term recurrence relation) with constant coefficients that can be solved by standard methods [40] that parallel the theory of linear differential equations.²² Inserting a solution of form $x_t = \Lambda^t$ into the associated ($m_t=0$) homogenous 2nd-order difference equation

$$x_{t+1} - s x_t + x_{t-1} = 0 \quad (1.113)$$

yields the characteristic equation

$$\Lambda^2 - s\Lambda + 1 = 0, \quad (1.114)$$

which, for $|s| > 2$, has two real roots $\{\Lambda, \Lambda^{-1}\}$,

$$\Lambda = \frac{1}{2}(s + \sqrt{(s-2)(s+2)}), \quad (1.115)$$

²¹Predrag 2018-02-11: the matrix is NOT CORRECT yet, FIX!

²²Predrag 2020-06-10: Comparing with (5.239) we see that we need to solve a second-order inhomogeneous difference equation with a constant forcing term $2(s-2)$.

and the so-called complementary solution of form

$$x_{c,t} = a_1 \Lambda^t + a_{-1} \Lambda^{-t}. \quad (1.116)$$

A difference of any pair of solutions to the temporal cat inhomogenous equation (3.45) is a solution of the homogenous difference equation (1.113), so the general solution is a sum of the complementary solution (1.116) and a particular solution x_p ,

$$x_t = x_{c,t} + x_{p,t}. \quad (1.117)$$

Eq. (1.113) is time-reversal invariant, $x_t = x_{-t}$, so $a_1 = a_{-1} = a$. To determine the particular solution, assume that both the source $m_t = m$ and $x_{p,t} = x_p$ in (3.45) are site-independent,

$$x_p - s x_p + x_p = -m, \quad (1.118)$$

so $x_p = m/(s-2)$. Hence the solution is

$$x_t = x_{c,t} + x_{p,t} = a(\Lambda^t + \Lambda^{-t}) + m/(s-2), \quad (1.119)$$

with a_i determined by fields at two lattice sites,

$$x_0 = 2a + m/(s-2), \quad x_1 = a(\Lambda + \Lambda^{-1}) + m/(s-2), \quad .$$

Temporal cat starts with $N_0 = 0$, and according to (3.92), $N_1 = s-2$, so $a = 1$, $m = -2(s-2)$, and the number of temporal lattice states of period n is

$$N_n = \Lambda^n + \Lambda^{-n} - 2. \quad (1.120)$$

Example 1.6. Temporal cat shadowing.

As the relation between the symbol blocks M and the corresponding lattice states X_M is linear, for M an admissible symbol block, the corresponding lattice state X_M is given by the Green's function

$$X_M = g M, \quad g = \frac{1}{-d + s \mathbb{1} - d^{-1}}, \quad (1.121)$$

as in the Bernoulli case (??).

As in sect. ??, the Green's function (1.121) decays exponentially with the distance from the origin, a fact that is essential in establishing the 'shadowing' between lattice states sharing a common sub-block M . For an infinite temporal lattice $t \in \mathbb{Z}$, the lattice field at site t is determined by the sources $m_{t'}$ at all sites t' , by the Green's function $g_{tt'}$ for one-dimensional discretized heat equation [73, 80],

$$x_t = \sum_{t'=-\infty}^{\infty} g_{tt'} m_{t'}, \quad g_{tt'} = \frac{1}{\Lambda - \Lambda^{-1}} \frac{1}{\Lambda^{|t-t'|}}, \quad (1.122)$$

with Λ is the expanding stability multiplier defined in (3.40).

Suppose there is a non-vanishing point source $m_0 \neq 0$ only at the present, $t' = 0$ temporal lattice site. Its contribution to $x_t \sim \Lambda^{-|t|}$ decays exponentially with the distance from the origin. More generally, as in the Bernoulli case (1.99), if two lattice states X , X' share a common sub-block M of length n , they shadow each other with accuracy of order of $O(1/\Lambda^n)$.

[click to return: p. 26](#)

Example 1.7. Two-degrees of freedom Hamiltonian flows: ²³ For a 2-degrees of freedom Hamiltonian flow the energy conservation eliminates one phase-space variable, and restriction to a Poincaré section eliminates the marginal longitudinal eigenvalue $\Lambda = 1$, so a periodic orbit of 2-degrees of freedom hyperbolic Hamiltonian flow (or of a 1-degree of freedom hyperbolic Hamiltonian map) has one expanding transverse eigenvalue Λ , $|\Lambda| > 1$, and one contracting transverse eigenvalue $1/\Lambda$. The weight in (??) is expanded as follows:

$$\frac{1}{|\det(\mathbf{1} - M_p^r)|} = \frac{1}{|\Lambda|^r(1 - 1/\Lambda_p^r)^2} = \frac{1}{|\Lambda|^r} \sum_{k=0}^{\infty} \frac{k+1}{\Lambda_p^{kr}}. \quad (1.123)$$

The spectral determinant exponent can be resummed,

$$-\sum_{r=1}^{\infty} \frac{1}{r} \frac{e^{(\beta A_p - s T_p)r}}{|\det(\mathbf{1} - M_p^r)|} = \sum_{k=0}^{\infty} (k+1) \log \left(1 - \frac{e^{\beta A_p - s T_p}}{|\Lambda_p| \Lambda_p^k} \right),$$

and the spectral determinant for a 2-dimensional hyperbolic Hamiltonian flow rewritten as an infinite product over orbits

$$\det(s - \mathcal{A}) = \prod_p \prod_{k=0}^{\infty} \left(1 - t_p / \Lambda_p^k \right)^{k+1}. \quad (1.124)$$

²⁴

exercise ??

click to return: p. ??

Example 1.8. Dynamical zeta function in terms of determinants, 2-dimensional Hamiltonian maps: ²⁵ For 2-dimensional Hamiltonian flows the above identity yields ²⁶

$$\frac{1}{|\Lambda|} = \frac{1}{|\Lambda|(1 - 1/\Lambda)^2} (1 - 2/\Lambda + 1/\Lambda^2),$$

so

$$1/\zeta = \frac{\det(1 - z\mathcal{L}) \det(1 - z\mathcal{L}_{(2)})}{\det(1 - z\mathcal{L}_{(1)})^2}. \quad (1.125)$$

²⁷ This establishes that for nice 2-dimensional hyperbolic flows the dynamical zeta function is meromorphic. ²⁸

click to return: p. ??

Example 1.9. Dynamical zeta functions for 2-dimensional Hamiltonian flows: ²⁹ The relation (1.125) is not particularly useful for our purposes. Instead we insert the identity

$$1 = \frac{1}{(1 - 1/\Lambda)^2} - \frac{2}{\Lambda} \frac{1}{(1 - 1/\Lambda)^2} + \frac{1}{\Lambda^2} \frac{1}{(1 - 1/\Lambda)^2}$$

²³Predrag 2018-12-13: if edited, return to ChaosBook

²⁴Predrag 2015-03-09: state here also the d -dimensional result ala Gaspard

²⁵Predrag 2018-12-13: if edited, return to ChaosBook

²⁶Predrag 2015-03-09: define $\det(1 - z\mathcal{L}_{(2)})$

²⁷Predrag 2015-03-09: compare with $1/\zeta = \frac{F^2}{F_1 F_{-1}}$ of the preceeding section

²⁸Predrag 2015-03-09: write out Ruelle's alternating product for any dimensions

²⁹Predrag 2018-12-13: if edited, return to ChaosBook

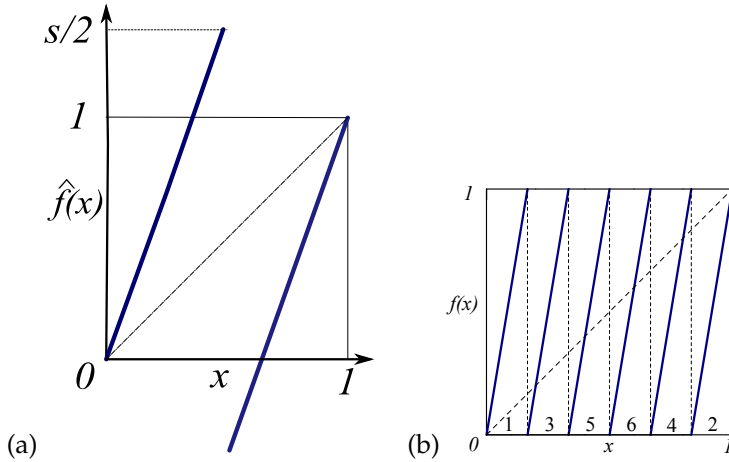


Figure 1.18: (a) $\hat{f}(\hat{x})$, the full space sawtooth map (??), $\Lambda > 2$. (b) $f(x)$, the sawtooth map restricted to the unit circle (3.25), $\Lambda = 6$.

³⁰ into the exponential representation (??) of $1/\zeta_k$, and obtain ³¹

$$\frac{1}{\zeta_k} = \frac{\det(1 - z\mathcal{L}_{(k)})\det(1 - z\mathcal{L}_{(k+2)})}{\det(1 - z\mathcal{L}_{(k+1)})^2}. \quad (1.126)$$

Even though we have no guarantee that $\det(1 - z\mathcal{L}_{(k)})$ are entire, we do know (by arguments explained in sect. ?!) ³² that the upper bound on the leading zeros of $\det(1 - z\mathcal{L}_{(k+1)})$ lies strictly below the leading zeros of $\det(1 - z\mathcal{L}_{(k)})$, and therefore we expect that for 2-dimensional Hamiltonian flows the dynamical zeta function $1/\zeta_k$ generically has a double leading pole coinciding with the leading zero of the $\det(1 - z\mathcal{L}_{(k+1)})$ spectral determinant. This might fail if the poles and leading eigenvalues come in wrong order, but we have not encountered such situations in our numerical investigations. This result can also be stated as follows: the theorem establishes that the spectral determinant (1.124) is entire, and also implies that the poles in $1/\zeta_k$ must have the right multiplicities to cancel in the $\det(1 - z\mathcal{L}) = \prod 1/\zeta_k^{k+1}$ product.

↓PRIVATE
↑PRIVATE

click to return: p. ??

Example 1.10. Linear code for a piecewise linear map. the piecewise linear map of figure 1.18

click to return: p. ??

Example 1.11. Tent map linear code. The simplest example of a piece-wise linear unimodal map with a binary (in general, pruned) symbolic dynamics is the tent map,

$$f(x) = \begin{cases} f_0(x) = \Lambda x & \text{if } x < 1/2 \\ f_1(x) = \Lambda(1-x) & \text{if } x > 1/2 \end{cases}, \quad (1.127)$$

with $1 < \Lambda < \infty$ and $x \in \mathcal{M} = [0, 1]$. (Everything would go through for a skew tent map with $\Lambda_0 \neq -\Lambda_1$, but there is no need here for that complication.) For this family of

³⁰Predrag 2015-03-09: seems the same as (1.125)?

³¹Predrag 2015-03-09: recheck, looks wrong

³²Predrag 2015-03-09: find the sect. referred to

unimodal maps the coarse (covering) partition of the unit interval $\mathcal{M} = \mathcal{M}_0 \cap C \cap \mathcal{M}_1$ is given by intervals $\mathcal{M}_0 = [0, 1/2)$, $\mathcal{M}_1 = (1/2, 1]$, and the critical point $C = 1/2$. Let's rewrite this as a linear first-order difference equation, in the manner of cat lovers enamoured of matters feline:

$$\frac{1}{\Lambda} x_{t+1} + (2m_t - 1)x_t = m_t, \quad \begin{cases} m_t = 0 & \text{if } x_t < 1/2 \\ m_t = 1 & \text{if } x_t > 1/2 \end{cases}. \quad (1.128)$$

That every such code is a ‘linear code’ is best understood by computing a periodic orbit for a specified itinerary.

The fixed point condition $f^n(x) = x$ for n -cycle $\overline{m_1 m_2 m_3 \cdots m_{n-1} m_n}$ is a linear relation between the finite alphabet $m_t \in \{0, 1\}$ code, and the $x_t \in \mathbb{R}$ orbit

$$\Delta(m)q(m) = m(m) \quad (1.129)$$

with orbit-dependent inverse propagator $\Delta(m) =$

$$\left(\begin{array}{cccccc} 2m_n - 1 & 0 & 0 & \dots & 0 & \Lambda^{-1} \\ \Lambda^{-1} & 2m_{n-1} - 1 & 0 & \dots & 0 & 0 \\ 0 & \Lambda^{-1} & 2m_{n-2} - 1 & \dots & 0 & 0 \\ \vdots & \vdots & \vdots & \ddots & \vdots & \vdots \\ 0 & 0 & 0 & \dots & 2m_2 - 1 & 0 \\ 0 & 0 & 0 & \dots & \Lambda^{-1} & 2m_1 - 1 \end{array} \right),$$

$$q(m) = \begin{pmatrix} x_n \\ x_{n-1} \\ x_{n-2} \\ \vdots \\ x_2 \\ x_1 \end{pmatrix}, \quad m(m) = \begin{pmatrix} m_n \\ m_{n-1} \\ m_{n-2} \\ \vdots \\ m_2 \\ m_1 \end{pmatrix},$$

and $m(m)$ is needed to fold the stretched orbit back into the unit interval. While the off-diagonal “1”s do generate cyclic shifts, the diagonal $\pm\Lambda$ terms are not shift invariant, so I do not believe this can be diagonalized by a discrete Fourier transform. I had worked it out for $\Lambda = 2$ in ChaosBook, but not sure if there are elegant tricks for arbitrary $\Lambda \neq 2$. For an orbit

$$q(m) = \Delta(m)^{-1}m(m) \quad (1.130)$$

to be admissible, no point should be to the right of the kneading value $x_\kappa = f(C)$. It follows from the kneading theory for unimodal maps (dike map with slope $\Lambda = 2$ being the canonical example) that if a periodic orbit exists for a given Λ , it exists for all larger Λ , and that all orbits exist for $\Lambda \geq 2$.

In other words, Λ is the “stretching parameter” for this problem, and the rational polynomial expressions in Λ for x_t correspond to Li Han’s polynomials for cat maps.

click to return: p. 55

Example 1.12. Periodic points of a tent map.

Exercise Check (1.130) for fixed point(s).

Exercise Check (1.130) for the 2-cycle $\overline{01}$.

$$\begin{aligned}\Delta(m) &= \begin{pmatrix} -\Lambda & 1 \\ 1 & \Lambda \end{pmatrix}, \quad m(m) = \Lambda \begin{pmatrix} 0 \\ 1 \end{pmatrix}. \\ \Delta^{-1} &= \frac{1}{\Lambda^2 + 1} \begin{pmatrix} -\Lambda & 1 \\ 1 & \Lambda \end{pmatrix}, \quad \det \Delta(m) = -(\Lambda^2 + 1) \\ \begin{pmatrix} x_{01} \\ x_{10} \end{pmatrix} &= \frac{\Lambda}{\Lambda^2 + 1} \begin{pmatrix} -\Lambda & 1 \\ 1 & \Lambda \end{pmatrix} \begin{pmatrix} 0 \\ 1 \end{pmatrix} = \frac{\Lambda}{\Lambda^2 + 1} \begin{pmatrix} 1 \\ \Lambda \end{pmatrix}.\end{aligned}$$

For the Ulam tent map this yields the correct periodic points $\{x_{01}, x_{10}\} = \{2/5, 4/5\}$. In the $\Lambda \rightarrow 1$ limit, this 2-cycle collapses into the critical point $C = 1/2$.

Exercise Check (1.130) for the two 3-cycles. For the Ulam tent map case, the periodic points are

$$\begin{aligned}\{\gamma_{001}, \gamma_{010}, \gamma_{100}\} &= \{2/9, 4/9, 8/9\} \\ \{\gamma_{011}, \gamma_{110}, \gamma_{101}\} &= \{2/7, 4/7, 6/7\}.\end{aligned}$$

Exercise Check (1.130) for $\Lambda = \text{golden mean}$. The $\overline{001} \rightarrow \overline{0C1}$ as $\Lambda \rightarrow \text{golden mean}$ from above. Do you get all admissible cycles? That is worked out in ChaosBook, but not in this formulation.

Exercise Is there a systematic solution to (1.130) for arbitrary n -cycle? The $\Lambda = 2$ case has the elegant solution described in ChaosBook; whatever polynomials you find, they should agree with that particular factorization. In other words, think of the sums (1.131) and (1.132) as the expansion of a real number in terms of the digits w_t in the nonintegral base Λ . As the symbolic dynamics of a cycle is independent of Λ , the Ulam tent map calculation, in the familiar base 2 clinches the arbitrary tent map case.

The rest of the section might even be right - has to factorize in agreement with my Ulam tent map computations. Please fix at your leisure, if I am wrong.

If the repeating string $m_1m_2\dots m_n$ contains an even number of '1's, the repeating string of well ordered symbols $w_1w_2\dots w_n$ is of the same length. The cycle-point x is a geometrical sum which we can rewrite as the odd-denominator fraction

$$\begin{aligned}x(\overline{m_1m_2\dots m_n}) &= \sum_{t=1}^n \frac{w_t}{\Lambda^t} + \frac{1}{\Lambda^{-n}} \sum_{t=1}^n \frac{w_t}{\Lambda^t} + \dots \\ &= \frac{1}{\Lambda^n - 1} \sum_{t=1}^n w_t \Lambda^{n-t} \tag{1.131}\end{aligned}$$

If the repeating string $m_1m_2\dots m_n$ contains an odd number of '1's, the string of well ordered symbols $w_1w_2\dots w_{2n}$ has to be of the double length before it repeats itself. The cycle-point x is a geometrical sum which we can rewrite as the odd-denominator fraction

$$\begin{aligned}x(\overline{m_1m_2\dots m_n}) &= \sum_{t=1}^{2n} \frac{w_t}{\Lambda^t} + \frac{1}{\Lambda^{-2n}} \sum_{t=1}^{2n} \frac{w_t}{\Lambda^t} + \dots \\ &= \frac{1}{(\Lambda^n - 1)(\Lambda^n + 1)} \sum_{t=1}^{2n} w_t \Lambda^{2n-t} \tag{1.132}\end{aligned}$$

click to return: p. 55

Example 1.13. Belykh map linear code. Li and Xie [70] Symbolic dynamics of Belykh-type maps: “The symbolic dynamics of a Belykh-type map (a two-dimensional discontinuous piecewise linear map) is investigated. The pruning front conjecture (the admissibility condition for symbol sequences) is proved under a hyperbolicity condition. Using this result, a symbolic dynamics model of the map is constructed according to its pruning front and primary pruned region.”

The Belykh map is a piecewise linear map given by

$$\begin{pmatrix} x_{n+1} \\ y_{n+1} \end{pmatrix} = \begin{pmatrix} \sigma_n - ax_n + by_n \\ x_n \end{pmatrix} = \begin{pmatrix} \sigma_n \\ 0 \end{pmatrix} + \begin{pmatrix} -a & b \\ 1 & 0 \end{pmatrix} \begin{pmatrix} x_n \\ y_n \end{pmatrix}.$$

where

$$\sigma_n = \begin{cases} 1 & \text{if } x_n \geq 0 \\ -1 & \text{if } x_n < 0 \end{cases}.$$

The two branches of the map are

$$f_{\pm} = \begin{cases} \pm 1 - ax + by \\ x \end{cases}.$$

In the 3-term recurrence formulation (the linear code), the map is an asymmetric tridiagonal Toeplitz matrix

$$x_{n+1} + ax_n - bx_{n-1} = \sigma_n,$$

or

$$\square x_n + (2+a)x_n - (1+b)x_{n-1} = \sigma_n. \quad (1.133)$$

For $b = -1$ (the Hamiltonian, time-reversible case) this is almost the cat map, with $a = -s$, except that the single sawtooth discontinuity is across $x = 0$, there is no mod 1 condition.

Li and Xie consider the $a, b > 0$ case. The strange attractor (for example, for $a = 1.5$ and $b = 0.3$) looks like a fractal set of parallel lines. They define the pruning front, the primary pruned region, plot them in the symbol plane, and prove the pruning front conjecture for this map. In the symbol plane there is a symmetry under rotation by π , but they do not seem to exploit that.

They call the past and the future itineraries of the tail and the head, and start the head with s_0 .

Tél [106] Fractal dimension of the strange attractor in a piecewise linear two-dimensional map computes the box-counting dimension of this map (which he does not call Belykh map).

Example 1.14. Lozi map linear code. The Lozi map

$$x_{n+1} = 1 - \sigma_n ax_n + bx_{n-1}.$$

written as a 3-term recurrence relation

$$x_{n+1} - 2x_n + x_{n-1} + (2 + \sigma_n a)x_n - (b + 1)x_{n-1} = 1. \quad (1.134)$$

That has the same nonlinear term $\sigma_n x_n$ as (1.128), so maybe we can figure out the pruning front as well, in this formulation.

click to return: p. 55

Exercises boy scout

1.1. **Cat map Green's function, infinite lattice.**

(a) Show that the eigenvalues of the cat map M are given by

$$\Lambda^\pm = \frac{1}{2}(s \pm \sqrt{D}), \quad \Lambda = e^\lambda, \quad (1.135)$$

where $\Lambda \equiv \Lambda^+$, $s = \Lambda + \Lambda^{-1}$, $\sqrt{D} = \Lambda - \Lambda^{-1}$, and the discriminant is $D = s^2 - 4$.

(b) Verify by substitution that the Green's function is given by

$$g_{nn'} = \frac{1}{\sqrt{D}} \frac{1}{\Lambda^{|n'-n|}}. \quad (1.136)$$

(c) Show that the orbit is then recovered by

$$x_n = \frac{1}{\sqrt{D}} \sum_{n' \in \mathbb{Z}} \Lambda^{-|n-n'|} m_{n'}. \quad (1.137)$$

1.2. **Cat map Green's function for a periodic orbit.** Show that the Green's function for a periodic orbit of period n_p is obtained by summing (1.136) over period n_p :

$$g_{nn'}^p = \sum_{j=-\infty}^{\infty} g_{n-n', j n_p} = \frac{1}{\sqrt{D}} \frac{\Lambda^{-|n-n'|} + \Lambda^{-n_p+|n-n'|}}{1 - \Lambda^{-n_p}}. \quad (1.138)$$

Verify this formula by explicit matrix inversion for a few periodic points of cycles p of periods $n_p = 1, 2, 3, 4, \dots$

1.3. **$d = 2$ cat map guess Green's function, infinite lattice.** Show by substitution that a $d = 2$ "Green's function" guess given by

$$g_{zz'} = \frac{1}{2} \frac{1}{\sqrt{D}} \frac{1}{\Lambda^{|\ell'-\ell|+|t'-t|}}, \quad (1.139)$$

(and similarly, in arbitrary dimension $d > 1$) does not satisfy the Green's function conditions

$$(\mathcal{D}g)_{zz'} = \delta_{zz'} = \delta_{ll'} \delta_{tt'}, \quad (1.140)$$

Here the eigenvalues of the cat map M are

$$\Lambda^\pm = \frac{1}{2}(s/2 \pm \sqrt{D}), \quad \Lambda = e^\lambda, \quad (1.141)$$

where $\Lambda \equiv \Lambda^+$, $s/2 = \Lambda + \Lambda^{-1}$, $\sqrt{D} = \Lambda - \Lambda^{-1}$, and the discriminant is $D = (s/2)^2 - 4$.

Hint: the check works just like for exercise 1.1.

1.4. **Periodic orbits of Arnol'd cat map.**

- (a) Describe precisely how you actually pick “random q_1 and q_2 ”
- (b) Explain what happens if q_1 and q_2 are rational
- (c) Can you get a periodic orbit if q_1 and q_2 are irrational?
- (d) What do you mean by period 0?
- (e) Does the Arnol'd cat map have periodic orbits of any period?
- (f) Derive analytically that $m_j \in \{-1, 0, 1, 2\}$ (you can continue the exposition that I started in sect. 1.3.6, if that helps). Does your result agree with Percival and Vivaldi [80]?
- 1.5. **The second iterate generating partition.** Figure 1.10 is very helpful in giving us a visual understanding of what a Hamiltonian cat map does, and how the generating partition comes about. Draw the corresponding Adler-Weiss generating partition for $s = 3$, the second, $n = 2$ iterate, to verify that the $n = 1$ determines a generating partition for all subsequent times.

Chapter 1. Cat map

Solution 1.1 - Cat map Green's function, infinite lattice.

- (a) It's just the roots of a quadratic equation, with $s = \Lambda + \Lambda^{-1}$, and $\sqrt{D} = \Lambda - \Lambda^{-1}$.
- (b) The Green's function (1.136)

$$g_{tt'} = \frac{1}{\sqrt{D}} \frac{1}{\Lambda^{|t'-t|}} \quad (1.142)$$

for the discrete damped Poisson equation (1.36) was first computed explicitly by Percival and Vivaldi [80], using the methods introduced in Mestel and Percival [73]. It should satisfy

$$(\mathcal{D}g)_{ij} = \sum_k \mathcal{D}_{ik} g_{kj} = \delta_{ij}. \quad (1.143)$$

Since we are considering infinite 1D lattice, we do not need to specify the boundary conditions. \mathcal{D} is a Toeplitz matrix

$$\mathcal{D}_{ik} = s\delta_{ik} - \delta_{i-1,k} - \delta_{i+1,k} \quad (1.144)$$

Substituting (1.144) into (1.143)

$$\sum_k \mathcal{D}_{ik} g_{kj} = s g_{ij} - g_{i-1,j} - g_{i+1,j} = \delta_{ij}, \quad (1.145)$$

and substituting (1.136)

$$g_{ij} = \frac{1}{\sqrt{D}} \frac{1}{\Lambda^{|j-i|}} = \begin{cases} \frac{1}{\sqrt{D}} \frac{1}{\Lambda^{i-j}} & \text{if } j < i \\ \frac{1}{\sqrt{D}} & \text{if } j = i \\ \frac{1}{\sqrt{D}} \frac{1}{\Lambda^{j-i}} & \text{if } j > i \end{cases}. \quad (1.146)$$

Exercises boy scout

into (1.145), one verifies that (1.136) is indeed the Green's function for the infinite lattice. By translational invariance, for $i = j$ consider

$$sg_{00} - g_{-1,0} - g_{10} = \frac{1}{\sqrt{D}} \left(s - \frac{2}{\Lambda} \right) = \frac{1}{\sqrt{D}} \left(\Lambda - \frac{1}{\Lambda} \right) = 1. \quad (1.147)$$

For $i > j$ consider

$$sg_{10} - g_{00} - g_{20} = \frac{1}{\sqrt{D}} \left(\frac{s}{\Lambda} - 1 - \frac{1}{\Lambda^2} \right) = \frac{1}{\sqrt{D}} \frac{1}{\Lambda} \left(s - \Lambda - \frac{1}{\Lambda} \right) = 0. \quad (1.148)$$

(c) The orbit is recovered by:

$$x_n = \sum_{n' \in \mathbb{Z}} g_{nn'} m_{n'} = \frac{1}{\sqrt{D}} \sum_{n' \in \mathbb{Z}} \Lambda^{-|n-n'|} m_{n'}. \quad (1.149)$$

(Han Liang)

Solution 1.2 - Cat map Green's function for a periodic orbit. Express the periodic orbit Green's function in terms of the infinite lattice by using a periodic source $m_{n'} = m_{n'} + n_p$,

$$\begin{aligned} \sum_{n'=-\infty}^{\infty} g_{nn'} m_{n'} &= \sum_{r=-\infty}^{\infty} \sum_{n'=rn_p}^{rn_p+n_p-1} g_{nn'} m_{n'} = \sum_{r=-\infty}^{\infty} \sum_{n'=0}^{n_p-1} g_{n,n'+rn_p} m_{n'+rn_p} \\ &= \sum_{r=-\infty}^{\infty} \sum_{n'=0}^{n_p-1} g_{n-n',rn_p} m_{n'} \end{aligned} \quad (1.150)$$

Comparing with the expression for the Green's function of a periodic orbit:

$$\sum_{n'=0}^{n_p-1} g_{nn'}^{n_p} m_{n'} \quad (1.151)$$

we see that

$$g_{nn'}^{n_p} = \sum_{r=-\infty}^{\infty} g_{n-n',rn_p} \quad (1.152)$$

Substituting (1.136) into (1.152) we have:

$$\begin{aligned} g_{nn'}^{n_p} &= \frac{1}{\sqrt{D}} \sum_{r=-\infty}^{\infty} \frac{1}{\Lambda^{|n-n'-rn_p|}} \\ &= \frac{1}{\sqrt{D}} \left(\frac{1}{\Lambda^{|n-n'|}} + \sum_{r=1}^{\infty} \frac{1}{\Lambda^{rn_p-(n-n')}} + \sum_{r=-1}^{-\infty} \frac{1}{\Lambda^{(n-n')-rn_p}} \right) \\ &= \frac{1}{\sqrt{D}} \left(\frac{1}{\Lambda^{|n-n'|}} + \frac{1}{\Lambda^{-|n-n'|}} \frac{1}{\Lambda^{n_p}-1} + \frac{1}{\Lambda^{|n-n'|}} \frac{1}{\Lambda^{n_p}-1} \right) \\ &= \frac{1}{\sqrt{D}} \frac{1}{1-\Lambda^{-n_p}} (\Lambda^{-|n-n'|} + \Lambda^{-n_p+|n-n'|}) \end{aligned} \quad (1.153)$$

This verifies (1.138).

Bird and Vivaldi [16] show that for an n -cycle $x_{n'}$ are rational functions of Λ , given by the quotient of two reflexive polynomials (for example, $P_t(\Lambda) = \Lambda^n P_t(1/\Lambda)$),

$$\begin{aligned} x_t &= \Lambda P_t(\Lambda)/Q(\Lambda) \\ P_t(\Lambda) &= \sum_{\tau=1}^{n-1} \Lambda^{n-\tau} (\Lambda m_{t+\tau-1} + m_{t-\tau}) \\ Q(\Lambda) &= (\Lambda^2 - 1)(\Lambda^n - 1) \end{aligned} \quad (1.154)$$

Bird and Vivaldi [16] then discuss pruning, give formulas for the numbers of orbits for integer s , etc..

(Han Liang)

Solution 1.3 - $d = 2$ cat map guess Green's function, infinite lattice. The Green's function g for the Toeplitz matrix (tensor) in 2 dimensions

$$\begin{aligned} \mathcal{D}_{lt,l't'} &= [-\square + 2(s/2 - 2)]_{lt,l't'} \\ &= \left(\frac{s}{2} \delta_{ll'} - \delta_{l-1,l'} - \delta_{l+1,l'} \right) \delta_{tt'} \\ &\quad + \delta_{ll'} \left(\frac{s}{2} \delta_{tt'} - \delta_{t-1,t'} - \delta_{t+1,t'} \right). \end{aligned} \quad (1.155)$$

should satisfy (1.140), or, substituting (1.155) into (1.140),

$$\begin{aligned} 2\delta_{ll'}\delta_{tt'} &= \frac{s}{2} g_{ll',tt'} - g_{l-1,l',tt'} - g_{l+1,l',tt'} \\ &\quad + \frac{s}{2} g_{ll',tt'} - g_{ll',t-1,t'} - g_{ll',t+1,t'}. \end{aligned} \quad (1.156)$$

Let's check this. By translational invariance, need to look only at different values of $l - l'$ and $t - t' = 0$. For $l = l'$ and $t = t'$ it suffices that we consider the $l = l' = t = t' = 0$ case. Using (1.141) we have

$$\begin{aligned} &\frac{s}{2} g_{00,00} - g_{-1,0,00} - g_{10,00} \\ &+ \frac{s}{2} g_{00,00} - g_{00,-1,0} - g_{00,10} \\ &= \frac{2}{\sqrt{D}} \left(\frac{s}{2} - \frac{2}{\Lambda} \right) = \frac{2}{\sqrt{D}} \left(\Lambda - \frac{1}{\Lambda} \right) = 2, \end{aligned} \quad (1.157)$$

verifies (1.155).

For $l > l'$ and $t = t'$ it suffices to consider $l = 1, l' = 0, t = t' = 0$ case.

$$\begin{aligned} &\frac{s}{2} g_{10,00} - g_{00,00} - g_{20,00} \\ &+ \frac{s}{2} g_{10,00} - g_{10,-1,0} - g_{10,10} \\ &= \frac{1}{2\sqrt{D}} \left(\frac{s/2}{\Lambda} - 1 - \frac{1}{\Lambda^2} \right) + \frac{1}{2\sqrt{D}} \left(\frac{s/2}{\Lambda} - \frac{2}{\Lambda^2} \right) \\ &= \frac{1}{2\Lambda\sqrt{D}} \left(\frac{s}{2} - \frac{2}{\Lambda} \right) = \frac{1}{2\Lambda\sqrt{D}} \left(\Lambda - \frac{1}{\Lambda} \right) = \frac{1}{2\Lambda}. \end{aligned} \quad (1.158)$$

So, the guess (1.139) already does not work.

Substitute (1.139) into (1.156) we get:

$$\sum_{z''} \mathcal{D}_{zz''} g_{z''z'} = \begin{cases} \frac{1}{\sqrt{D}} \frac{1}{\Lambda^{|\ell'-\ell|+|t'-t|}} (s - 2\Lambda - 2\Lambda^{-1}) & \text{if } l \neq l' \text{ and } t \neq t' \\ \frac{1}{\sqrt{D}} (s - 4\Lambda^{-1}) & \text{if } l = l' \text{ and } t = t' \end{cases}. \quad (1.159)$$

To satisfy (1.140), s , \sqrt{D} and Λ must satisfy:

$$\begin{cases} s = 2\Lambda + 2\Lambda^{-1} \\ \sqrt{D} = 2\Lambda - 2\Lambda^{-1} \end{cases}. \quad (1.160)$$

So we will have:

$$\begin{cases} \Lambda = \frac{1}{4}(s + \sqrt{s^2 - 16}) \\ \Lambda^{-1} = \frac{1}{4}(s - \sqrt{s^2 - 16}) \end{cases}. \quad (1.161)$$

Now the problem is, if $l \neq l'$ but $t = t'$, (1.159) become:

$$\sum_{z''} \mathcal{D}_{zz''} g_{z''z'} = \frac{1}{\sqrt{D}} \frac{1}{\Lambda^{|\ell'-\ell|+|t'-t|}} (s - \Lambda - 3\Lambda^{-1}) \quad (1.162)$$

and this is not satisfied by (1.161). So (1.139) does not work for the 2-dimensional case. I haven't figured out the correct Green's function for the 2 dimensions.

(Han Liang)

Solution 1.3 - $d = 2$ cat map guess Green's function, infinite lattice. The guess Green's function (1.139) doesn't work. For $l = 2$, $l' = 0$ and $t = t' = 0$, the correct form of (1.158) is:

$$\begin{aligned} & \frac{s}{2} g_{10,00} - g_{00,00} - g_{20,00} \\ & + \frac{s}{2} g_{10,00} - g_{10,10} - g_{10,-10} \end{aligned} \quad (1.163)$$

$$= \frac{1}{2\sqrt{D}} \left(\frac{s}{2\Lambda} - 1 - \frac{1}{\Lambda^2} \right) + \frac{1}{2\sqrt{D}} \left(\frac{s}{2\Lambda} - \frac{1}{\Lambda^2} - \frac{1}{\Lambda^2} \right) \quad (1.164)$$

$$= \frac{1}{2\sqrt{D}} \frac{1}{\Lambda} \left(\frac{s}{2} - \Lambda - \frac{1}{\Lambda} \right) + \frac{1}{2\sqrt{D}} \frac{1}{\Lambda} \left(\frac{s}{2} - \frac{1}{\Lambda} - \frac{1}{\Lambda} \right) \quad (1.165)$$

$$= 0 + \frac{1}{2\Lambda}. \quad (1.166)$$

As in (1.158), this does not work.

(Han Liang)

Solution 1.4 - Periodic orbits of Arnol'd cat map. No solution available.

Solution 1.5 - The second iterate generating partition. Figure 1.19 is the generating partition with $s = 3$ evolved after 2 steps. In the Markov diagram figure 1.19 (d) there are 7 self cycles, two of which are the over-counted fixed points at the origin. So there are actually 5 periodic points with period 2, including 1 fixed point and 2 length-2 orbits, as given by (1.70).

Figure 1.19 is a very nice illustration of a generating partition subrectangles being further subdivided.

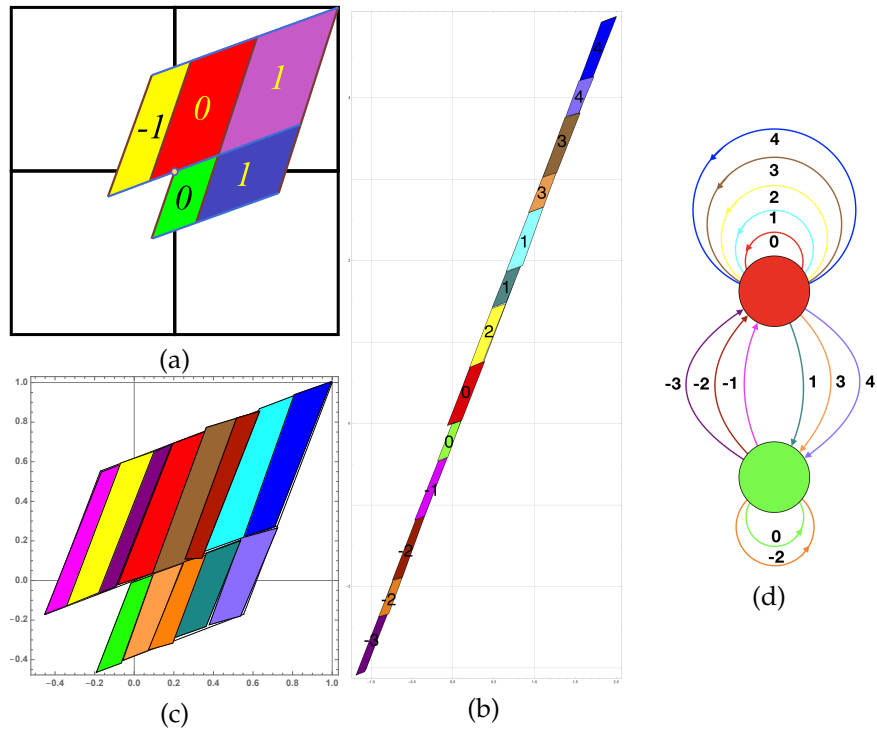


Figure 1.19: (a) An Adler-Weiss one step forward in time partition of the unit torus for the $s = 3$ Percival-Vivaldi cat map figure 1.9 (c). (b) Mapped two steps forward in time, the rectangles are stretched along the unstable direction and shrunk along the stable direction. Sub-rectangles \mathcal{M}_j that have to be translated back into the partition are indicated by color and labeled by their lattice translation m_j . (c) The sub-rectangles \mathcal{M}_j translated back into the unit square yield a two steps forward in time generating partition (a subpartition of rectangles in (a)), with (d) the finite grammar given by the transition graph for this partition. The nodes refer to the rectangles A and B , and the 13 links correspond to the 13 sub-rectangles induced by two step forward-in-time dynamics.

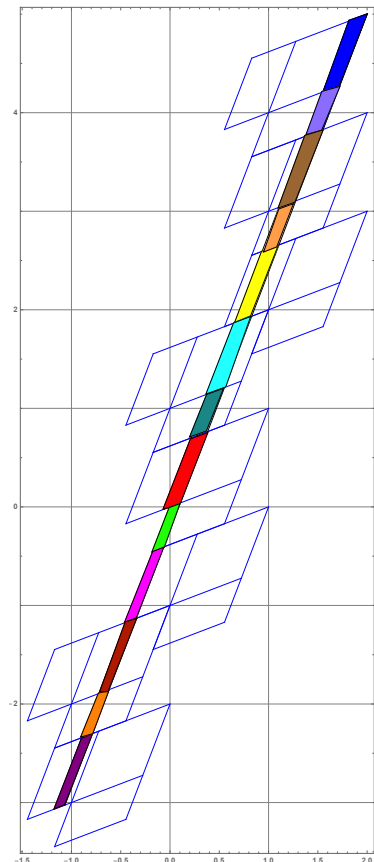


Figure 1.20: This figure is used to track where each sub-rectangle in figure 1.19 goes. Note that two step forward-in-time requires both vertical and horizontal shifts, unlike the one step forward-in-time Percival-Vivaldi cat map (1.101).

Chapter 2

Temporal Hénon

2.1 Hénon blog

2021-02-17 Predrag Predrag's key 2005 result is presumably the time-reversal symmetry induced, temporal lattice cycle by cycle full square (2.16) and (2.15).

2021-02-15 Predrag Added Hénon map examples, mostly for Sidney (to be edited and returned to ChaosBook):

example 2.1 *Hénon map*

example 2.2 *Temporal Hénon*

example 2.4 *Temporal Hénon stability*

example 2.5 *Hamiltonian Hénon map, reversibility*

example 2.6 *Symmetry lines of the standard map*

example 2.7 *Symmetry lines of the cat map*

2.1.1 Temporal Hénon; anti-integrable limit

2021-12-23 Predrag See also sect. 5.7.3 *Classical ϕ^4 lattice field theory*

2021-12-22 Jim Meiss: "The concept of anti-integrability was introduced by Aubry and Abramovici [4] in 1983 for the standard map (PC: 1983? maybe he means Aubry and Le Daeron [5]?), viewed as a linear chain of particles connected by springs in a periodic potential. They reasoned that the integrable limit corresponded to vanishing potential energy, so that the springs dominated giving equal spacing at equilibrium. By contrast, anti-integrability corresponds to vanishing kinetic energy, so that particles sit at critical points of the potential. What is most interesting about this limit is that it is relatively easy, using a contraction mapping style argument, to show that AI states persist, and this gives conjugacy to a shift on a symbolic dynamics."

2021-06-04 Predrag David Meiss' student David G. Sterling [49] much (undeservedly) un-cited [PhD thesis](#), Univ. of Colorado, *Anti-Integrable Continuation and the Destruction of Chaos* has much to teach us. He studies *coupled Hénon map lattices* in both Hamiltonian and Lagrangian formulations; his definition seems pretty much consistent with our (15.12), though he has a coupling parameter c used to make spatial couplings weak. The “anti-integrable” refers to our choice $a \geq 6$, I believe - parameter regimes in which all of the horseshoe orbits exists.

“Specifying the anti-integrable state for an orbit of a coupled map lattice requires a multidimensional symbolic object which we call a symbol tensor.”

His Figures 6.7, 6.18 are reminiscent of my pruning front.

Thesis abstract: [...] Recurrent phenomena, the simplest of which is periodic motion, are particularly interesting and practical objects of study. Scientists have long been captivated by the near periodic motions of the planets. Among them, Poincaré was the first to truly recognize the importance of periodic solutions in understanding more complex dynamical behavior. [...] This research has two complementary aspects. Not only do we develop a technique for locating periodic orbits in discrete dynamical systems, but we then use these orbits to study bifurcations, most significantly the global bifurcation that signals the destruction of chaos. Our technique embodies the following basic principles:
 (1) periodic orbits are conveniently described by a variational principle,
 (2) in a special case, the variation principle simplifies, and
 (3) continuation from this limiting case is an effective method for studying periodic orbits. We illustrate this approach on the Hénon map.

2021-09-12 Sidney, Predrag In the $a \rightarrow \infty$, *anti-integrable* limit [51] the Hénon's original map (2.4) goes to $a(x^*)^2 = 1$, so

$$x_t = m_t x^*, \quad x^* = a^{-1/2}, \quad m_t \in \{-, +\}. \quad (2.1)$$

The small perturbation parameter for the problem is $x^* = a^{-1/2}$, so replace

$$x_t = m_t x^* + \hat{x}_t, \quad (2.2)$$

study the temporal Hénon equations for \hat{x}_t .

2021-09-12 Sidney The process for perturbations that you're describing sounds very reminiscent of what is in chapter 11 of Townsend, would that be worth trying to copy here?

2021-12-22 Predrag Moved ‘generalized Hénon maps’ AKA ϕ^4 field theory posts to sect. 5.7.3 *Classical ϕ^4 lattice field theory*.

2021-06-04 Predrag Read also

Aubry and Le Daeron [5] *The discrete Frenkel-Kontorova model and its extensions. I. Exact results for the ground-states* (1983)

Sterling and Meiss [51] *Computing periodic orbits using the anti-integrable limit* (1988)

Aubry and Abramovici [4], *Chaotic trajectories in the standard map. The concept of anti-integrability*, (1990)

Aubry [3] *Anti-integrability in dynamical and variational problems* (1995)

2021-06-04 Predrag They are probably deep and good, but I find

Bolotin and MacKay [11] *Multibump orbits near the anti-integrable limit for Lagrangian systems*, (1997)

Bolotin and Treschev [10] *The anti-integrable limit* (2015)

hard to read. Gave up.

2021-06-04 Predrag We all might find the Sect. III of Wen's 2014 project [Chaos-Book.org/projects/Wen14.pdf](#) interesting.

Wen says that the original Hénon's [33] Hamiltonian Hénon map is equivalent to the harmonic oscillator system. By that he means it can be interpreted as a kicked driven harmonic oscillator with a nonlinear, cubic potential kicking term [32]. If we write anything about temporal Hénon, we should include this as a physical motivation.

Check out also Zalmond C. Barney [Master's Thesis Derivation of planar diffeomorphisms from Hamiltonians with a kick](#).

Butusov *et al.* [15] *Discrete chaotic maps obtained by symmetric integration* might be of interest for adding a reflection symmetry to the Hénon map.

2021-09-07 Predrag 2 Sidney .

1. Plot lattice field values for $a \gg 1$, then try to look at a perturbation theory treatment of this.
2. Learn about the perturbative treatments of field theories.

2021-09-09 Predrag Re. 1. above: I quickly tried to sketch how $a \gg 1$, did not get anything sensible. Might be yet another crazy idea that met instant death, do not worry about it for now.

2021-09-12 Sidney I did some preliminary calculations of $a \gg 1$ using the Gallas scaling (so not quite field theory, but a good test) and as a got larger, the less variation in lattice site values occurred. There were still negative, and positive values, but in the large a limit the lattice site values all approached an equal absolute value. I am not sure if that is useful, perhaps if we looked at the asymptotic behavior of both large and small a we could come up with some interesting "asymptotic temporal Hénon" theory.

2021-09-12 Predrag That sounds very good: in this limit the fields are apparently $x_t = m_t x^*$, $m_t \in \{-, +\}$, where $- \rightarrow 0$, $+ \rightarrow 1$ is the binary label corresponding to lattice site t .

Basically you get a theory even simpler than the temporal cat.

Perturbation theory for large but finite a would come from replacement $x_t \rightarrow x^* + \epsilon \hat{x}_t$ in the equations, and ordering terms by powers ϵ^k and $a^{-\ell}$. Probably $a^{-\ell}$ only.

2021-09-12 Predrag Do you have the analytic value of x^* ?

2021-09-13 Sidney I have changed my code so that it can be easily switched between the Hénon [33] (2.4), and Endler and Gallas [24] rescaled (2.20), I have added this updated code *Relaxation Method Henon with Orbit Jacobian.py* to *siminos/williams/python/relax*.

So, let's see if I understand, if we plug (2.1) into the Hénon form (2.4), expand and keep only linear terms of \hat{x}_t , we get a new temporal Hénon of form:

$$\hat{x}_{t+1} + 2m_t a^{1/2} \hat{x}_t + \hat{x}_{t-1} = -(m_{t+1} + m_{t-1})x^*, \quad (2.3)$$

where m_t is determined by the cycle itinerary. Is that the form you were thinking of? If this is the correct procedure, I can't see a way of extending this to a second-order perturbation theory, as that is just reproducing temporal Hénon.

2021-09-13 Predrag I have not thought through your (2.3) yet. Maybe $\hat{x}_t \rightarrow x^* \hat{x}_t$ helps a bit.

You have analytic formulas for fixed points (??), period-2 lattice states (??). You might find useful approximate large a formulas for all period- n lattice states. They might already be in David Sterling's [PhD thesis](#).

Maybe Hill determinants have interesting expansions in powers of $a^{-\ell/2}$...

For the contraction parameter value $b = -1$ the Hénon map [33] is orientation and area preserving, and can be written as a 3-term recurrence relation

$$x_{t-1} = 1 - ax_t^2 - x_{t+1}. \quad (2.4)$$

Multiply both sides by $-2a$ and define the Hénon 'field' at lattice site t to be $x_t = -2ax_t$. We shall refer to this form of Hénon as the *temporal Hénon*:

$$x_{t+1} - \frac{1}{2}x_t^2 + x_{t-1} = -2a. \quad (2.5)$$

or we can multiply both sides by -2 and define the Hénon 'field' at lattice site t to be $x_t = -2x_t$, yielding temporal Hénon of form:

$$x_{t+1} - \frac{a}{2}x_t^2 + x_{t-1} = -m_t, \quad m_t = 2, \quad (2.6)$$

with the ‘coupling constant’ a the analogue of the stretching factor s in temporal cat (4.13), and a constant source m_t .

The fixed points $x_j = x$ satisfy

$$x^2 - \frac{4}{a}x - \frac{4}{a} = 0, \quad x_{\pm} = \frac{2}{a} \pm \sqrt{\frac{4}{a^2} + \frac{16}{a}} \quad (2.7)$$

Temporal Hénon is ϕ^3 lattice field theory. Biham-Wenzel [8] find Hénon lattice states by constructing a cubic action density (15.53),

$$S[x]_t - m_t x_t = x_{t+1}x_t + x_t x_{t-1} - \frac{a}{3!} x_t^3 - m_t x_t, \quad m_t = 2. \quad (2.8)$$

Still to check: is $m_t = \pm 2$ the Biham-Wenzel method? Looks like it, as that amounts to flipping the sign of the cubic term while keeping the variation across there sits of the same magnitude.

I took $+2x_n$ out of $S[x]$ to treat it as a source density term $m_t x_t$.

Now the orbit Jacobian matrix (2.9) is of the same form as the temporal cat orbit Jacobian matrix (4.16),

$$\mathcal{J}[X] = \begin{pmatrix} s_0 & -1 & 0 & 0 & \cdots & 0 & 0 & -1 \\ -1 & s_1 & -1 & 0 & \cdots & 0 & 0 & 0 \\ 0 & -1 & s_2 & -1 & \cdots & 0 & 0 & 0 \\ \vdots & \vdots & \vdots & \vdots & \ddots & \vdots & \vdots & \vdots \\ 0 & 0 & 0 & 0 & \cdots & -1 & s_{n-2} & -1 \\ -1 & 0 & 0 & 0 & \cdots & 0 & -1 & s_{n-1} \end{pmatrix}, \quad (2.9)$$

but with the stretching factor at site t depending on the particular lattice state, $s_t = x_t$, and once you have an expression for Hill determinant $\|\mathcal{J}[X]\|$ in terms of traces $\text{Tr } \mathcal{J}^k$, i.e., the D_n invariant orbital sums for products of fields on consecutive lattice sites, they will be the same for the temporal cat and the temporal Hénon.

2.2 Hénon map symmetries

We note here the symmetries of the Hénon map (15.14). For $b \neq 0$ the Hénon map is reversible: the backward iteration of (2.42) is given by

$$x_{n-1} = -\frac{1}{b}(1 - ax_n^2 - x_{n+1}). \quad (2.10)$$

Hence the time reversal amounts to $b \rightarrow 1/b$, $a \rightarrow a/b^2$ symmetry in the parameter plane, together with $x \rightarrow -x/b$ in the coordinate plane, and there is no need to explore the (a, b) parameter plane outside the strip $b \in \{-1, 1\}$. For $b = -1$ the map is orientation and area preserving Hamiltonian Hénon map

$$x_{n-1} = 1 - ax_n^2 - x_{n+1}, \quad (2.11)$$

the backward and the forward iteration are the same, and the non-wandering set is symmetric across the $x_{n+1} = x_n$ diagonal. We can write this as a nonlinear field equation with a Laplacian (5.106) and a “cubic” potential (15.53)

$$\square x_n + (a x_n + 2) x_n = 1. \quad (2.12)$$

Endler and Gallas [24] prefer the equivalent, rescaled form (2.20).

This is one of the simplest models of a return map for a Hamiltonian flow.

For the orientation reversing $b = 1$ case we have ‘golden Hénon’ (in analogy with (4.179))

$$x_{n-1} = 1 - ax_n^2 + x_{n+1}, \quad (2.13)$$

and the non-wandering set is symmetric across the $x_{n+1} = -x_n$ diagonal.

2.3 “Center of mass” puzzle

Some of Predrag’s unpublished 2004 drafts and calculations are in

```
% dasbuch/book/FigSrc/gnu/Gallas % just a link
dasbuch/WWW/library/Gallas-chiral.pdf
dasbuch/WWW/projects/revHenon/Gallas0101305.txt etc
dasbuch/book/Fig/COM0001011.eps COM0001101.eps COM000111.eps
                           COM0011.eps      COM011.eps
dasbuch/book/OldProblems/soluCOM011005.tex
```

predrag/reports/referee/Gallas.txt on the unpublished

Periodic orbits are not necessarily independent from each other

Some of Predrag’s unpublished 2004 drafts and calculations of Jan 26, 1999 suggests many references where similar work was published. The revised paper appeared as Gallas [26] *Nonlinear dependencies between sets of periodic orbits*, I believe.

Gallas-chiral.pdf ([click here](#)) has the Endler-Gallas Hénon map polynomials up to period 8, and nothing else.

[ChaosBook.org/projects/revHenon](#) has lots of stuff:

1. *chiral.pdf* is an unfinished draft of Endler, Gallas and Cvitanović paper, based on *Gallas-chiral.pdf*. Much of the introduction is utterly delirious. Notation for ‘orbits’, eq. (10) is redundant and the indices of x_j are useless, they label roots of different polynomials, ordered by increasing x_j . Figures illustrate ‘chiral’ orbit pairs, $A_n = 0$; $B_n = 0$ and $C_n = 0$ self-dual orbits. Fig. 4 might be $C_n = 0$ for value of a other than 6.
2. From: Jason Alfredo Carlson Gallas (14 Jan 2005) fortran *plot_orbit.f*, generates *.eps files, see *Fig-7cycles.txt*, *Gallas0101305.txt*.
3. *per7.pdf* 18 period-7 orbits.

4. *chiral_p8.pdf*: 3 period-8 time-asymmetric pairs.
5. *per8.pdf*: 18 self-dual period-8 orbits (not sure that is a complete list).
6. *FourClasses.pdf*: defines four classes of orbits under time reversal; perhaps useful, still need to find the LaTeX file.
7. *tres.pdf*: period-6, symmetries with respect to the main diagonal of 3 6-cycles “corresponding to a σ^3 factor,” plotted for $a = 7$. No idea what that is...
8. *Gallas0101305.txt* says he does not understand me.
9. *Predrag011304.txt* my last attempt to explain symbolic dynamics and why is this a time-reversal symmetry. “Please use ‘time reversal’ rather than ‘chiral’. It is a standard part of the lore of Hamiltonian dynamics, and especially Hamiltonian/symplectic mappings.” Hopeless.
10. *puzzle.pdf*, *puzzle.tex* is January 25, 2005 version of Endler and Gallas [24] (submitted December 25, 2005?) that uses ChaosBook notation - Table 1 can be used as a check on Sidney’s periodic orbits. Other versions: *puzzle011305.tex* of 13 Jan 2005; *puzzle.tex* and *puzzle2dasbuch.tex* of 27 Jan 2005;
They published in *Reductions and simplifications of orbital sums in a Hamiltonian repeller* [25] without me as a coauthor. Algebraic number expressions for periodic points show interesting patterns, their eqs. (22), (23) and (28), that would not be noticed from their numerical values.
They use binary labelling also in Endler and Gallas [23] *Conjugacy classes and chiral doublets in the Hénon Hamiltonian repeller*, without mentioning me or ChaosBook at all.
11. *citation.txt* and *puzzle.end* is the footnote which Gallas would not accept:
endnote27 This exact equation was discovered by P. Cvitanović during discussion and in collaboration with the authors.
12. *old/puzzle011805.pdf* has my comments
13. *solRevHen.pdf* is extracted from [ChaosBook.org/projects](#), version 11.2.2, Mar 10 2005. I believe all that is in ChaosBook, ignore.
14. *revHenon.pdf*, *revHenon.zip* is a template for a [ChaosBook.org/projects](#) extracted from Jason Gallas, Predrag edited *puzzle.tex*, Gallas text removed 18 Feb 2006. I believe no one took up the project.

To summarize, this 2005 work agrees with current Han’s work, but does not clarify the problems we are dealing with now. The figures might be useful as crosschecks for Sidney’s Hénon orbits.

2021-02-16 Predrag ¹ Here are my notes on the work of Gallas and collaborators; they have written many papers on polynomial maps [21–25, 28–30]. What I had contributed (unpublished, I believe) is to show Gallas how to use time-reversal, (??), (2.15) and (2.38), wrote a draft of a paper (click on [chiral.pdf](#)), and –when he was not interested in it– requested my traditional citation,

This exact equation was discovered by P. Cvitanović during discussion and in collaboration with the authors.

but he refused to credit me for that, so I - what's the point - I stopped following their papers. I remember him being stubborn in a male kind of way. Absolutely refuses to understand binary symbolic dynamics, that what he understands [27] to be 'spatial $x \leftrightarrow y$ symmetry'

"[...] three algebraic conjugacy classes with respect to a spatial reflection $R(x, y) = (y, x)$ about the $y = x$ symmetry diagonal in phase-space."

is time reversal, and he would not try to understand ChaosBook symmetry factorizations. But it is quite possible that they (or younger me?) did the right thing and quotiented the time reversal... Check the papers and the papers they refer to.

As he has worked on this for at least 20 years, there are many details specific to quadratic mappings that I think we can ignore here. Here is an overview from my point of view: Gallas *et al.* observe that

1. for polynomial mapping (2.23) the *orbital sum*

$$\sigma_p = \sum_{i \in p} x_{p,i} \quad (2.14)$$

is a *prime* cycle p *invariant* that satisfies a (factorized!) polynomial equation $\mathbb{S}_n(\sigma) = 0$ of the order n_p , the period of the cycle, see for example (??).

Predrag addendum: Hill determinants are *symmetric polynomials* in lattice fields $\{\phi_1, \phi_2, \dots, \phi_n\}$, which are, by construction, all *prime* cycle p *invariants*. The orbital sum (2.14) is one example. Another one is the bilinear (15.21).

2. the cycle-points $x_{p,i}$ of a given cycle are roots of a polynomial (2.23) of order n_p , see for example (??). This is remarkable, as higher iterates of a polynomial mapping are polynomials of a horrendous order.

¹Predrag 27dec2004: Extracted from the ChaosBook.org boyscout, version of 2018-08-02 tex files. Edited here, so eventually return to ChaosBook.

3. time-reversal invariance (my interpretation, not theirs) induces the

$$\mathbb{S}_n = C_n^2 D_n N_n . \quad (2.15)$$

factorization of such polynomials, where D =‘diagonal’ class, N =‘non-diagonal’ class, and ‘C=‘chiral’ class, see below.

For me this is the key result.

This \mathbb{S}_n is very smart, as it has a zero for every *prime* orbit. Perhaps we can bring this to a full square, by including the boundary into the definition of the temporal lattice fundamental domain, with (CDN) orbits (perhaps in the Fourier space - they talk about ‘cyclotomic polynomials’)

$$\mathbb{S} = \frac{(CDN)^2}{DN} \quad (2.16)$$

by taking care of the temporal fundamental domain boundary by the inclusion-exclusion principle (18.278), and proceed to zeta-function factorization in the spirit of (4.39), (4.47), for each Hamiltonian Hénon cycle separately.

I believe factorization (2.16) should apply to periodic orbits of *any time-reversible* mapping, not just Hénon and temporal cat, but the ‘N class’ worries me.

(4.39)

$$\begin{aligned} (d - \mathbf{1}) &= \tilde{d}\tilde{\partial} \\ (d^{-1} - \mathbf{1})(d - \mathbf{1}) &= -\tilde{\partial}^2 = \square \\ \mathcal{J} &= \square - \mu^2 \mathbf{1} = (\tilde{\partial} + \mu \mathbf{1})(\tilde{\partial} - \mu \mathbf{1}) \\ \tilde{\mathcal{J}} &= \tilde{\partial} - \mu \mathbf{1} = \tilde{d} - \mu \mathbf{1} - \tilde{d}^{-1} \end{aligned} \quad (2.17)$$

2021-02-19 Predrag Gallas [27] *Counting orbits in conjugacy classes of the Hénon Hamiltonian repeller* counts the numbers C_n, D_n, N_n of (2.16) orbits (switched to calling ‘prime cycles’ orbits, like Gallas does) in each class, for any arbitrary period n .

D_n is sensible, relatively simply related to the number of points on the time-reversal diagonal; one expects something like that for any system.

N_n is funky, has to do with the parabola symmetry line, might be what we call “dynamical”.

C_n is just the remainder $M_n - D_n - N_n$: $C_1 = \dots = C_5 = 0$, and then (Gallas Table 1), starting with $C_6/2 = 1$:

$$1, 2, 6, 14, 30, 62, 127, 252, 500, 968, 25446, \dots \quad (2.18)$$

n	1	2	3	4	5	6	7	8	9	10	11
N_n	2	4	8	16	32	64	128	256	512	1024	.
M_n	2	1	2	3	6	9	18	30	56	99	186

Table 2.1: Lattice states and orbit counts for the $a = 6$ Hénon map. Compare with the golden (Fibonacci [6]) cat map table 4.2 and (4.182).

n	1	2	3	4	5	6	7	8	9	10	11	12	13	14	15
\tilde{N}_n	2	2	4	4	8	8	16	16	32	32
\tilde{M}_n	3

Table 2.2: Temporal lattice states and $\mu = 1$ golden cat map. See (4.182) and the counting of walks on the “half time-step” Markov graph figure 4.2.

This is not in *On-Line Encyclopedia of Integer Sequences* OEIS, (It is close to OEIS:A000918 A000918 $a(n) = 2^n - 2$ and $a(n+1) = 2 + 2a(n)$) so it has to be reverse engineered to find the \tilde{N}_n , the numbers of periodic points of the yet to be written down $\sqrt{\text{Hénon map}}$.

The number of $C_n/2$ periodic points:

$$\tilde{N}_6 = 1 * 6 = 6, \tilde{N}_7 = 2 * 7 = 14, \tilde{N}_8 = 6 * 8 = 48, \tilde{N}_9 = 14 * 9 = 126,$$

Actually, $\tilde{N}_n = n C_n/2 + n(D_{2n} + N_{2n})$ looks more sensible

$$\tilde{N}_6 = **, \tilde{N}_7 = 2 * 7 + 1 = 5, \tilde{N}_8 = 6 * 8 + 1 = 19, \tilde{N}_9 = 14 * 9 + 2 * 2 + 1 = 61,$$

MacKay had these numbers already listed in Table 1.2.3.5.1 of his 1982 PhD thesis [38] ([click here](#)).

Assuming that (4.47) applies, we can compute $\tilde{N}(\mu)_n$ from $N(s)_n$

$$\begin{aligned} 2^n &= \tilde{N}(\mu)_n^2, & n \text{ odd} \\ 2^n &= \tilde{N}(\mu)_{2n}, & n \text{ even}. \end{aligned} \quad (2.19)$$

2004-12-27 Predrag These extracts from ChaosBook.org are meant to complement and perhaps add to the Endler and Gallas explanation [24] of the “center of mass” puzzle for the cycles listed in table 2.4, first observed numerically by G. Vattay in ref. [7].

2016-09-19 Predrag ²

²Predrag 2021-02-15: Copied from DBblog.tex - return eventually, as there are edits here. Not sure where the next few paragraphs came from.

We present exact formulas solving the problem of partitioning the total number M_k of period- k orbits of the area-preserving Hénon map into the number of orbits building its three possible conjugacy classes. The formulas are valid for any arbitrary period n . They are derived with combinatorial methods, by an application of the number-theoretic Moebius inversion formula to a key problem in physics and dynamical systems. A handy MAPLE implementation of the formulas is also provided.

A number of orbital symmetries and asymmetries computed analytically and systematically for the Hamiltonian (area-preserving) $b = -1$ limit of the Hénon map have been studied in refs. [23, 25].

Endler and Gallas [24] prefer the equivalent, rescaled form $x \rightarrow x/a$ of the Hamiltonian Hénon map (2.12):

$$x_{n-1} - 2x_n + x_{n+1} + (x_n + 2)x_n = a, \quad (2.20)$$

They write: “ The advantage of this equation is that it generates *monic* minimal polynomials, i.e. polynomials having 1 as the leading coefficient.”

The key result reported was the existence of a natural segregation of all orbits into three algebraic conjugacy classes with respect to a spatial reflection $R(x,y)=(y,x)$ about the $y=x$ symmetry diagonal in state space. Under reflection, every periodic orbit was found to fall into one of three classes:

D diagonal class, formed by symmetric orbits with points on the time-reversal symmetry diagonal. An odd period symmetric cycle has an odd number of points on the boundary, see figure 2.1(a). An even period symmetric cycle has an even number of points on the boundary, see figure 2.1 (b).

N non-diagonal class, formed by self-symmetric orbits without points on the symmetry diagonal, see figure 2.1 (c).

C chiral class, formed by pairs of asymmetric cycles that map into each other, see figure 2.1 (d,e).

Each class contains a characteristic algebraic signature embodied by a specific orbital decompositions (factorizations) [23]. The orbital segregation is independent of the control parameters and is specially interesting for $a_h > 5.69931 \dots$, the value beyond which there is a complete Smale horseshoe and all orbits are real. This Letter reports exact analytical expressions that count the numbers C_n , D_n , N_n of orbits in each class, for any arbitrary period n .

2CB

The problem of counting periodic orbits and its partitions is among the first problems that one needs to address [9, 12, 14, 16, 17, 36, 37, 52]. For the paradigmatic quadratic map it was addressed very early by Myrberg, in what appears to be one of the first applications of computers

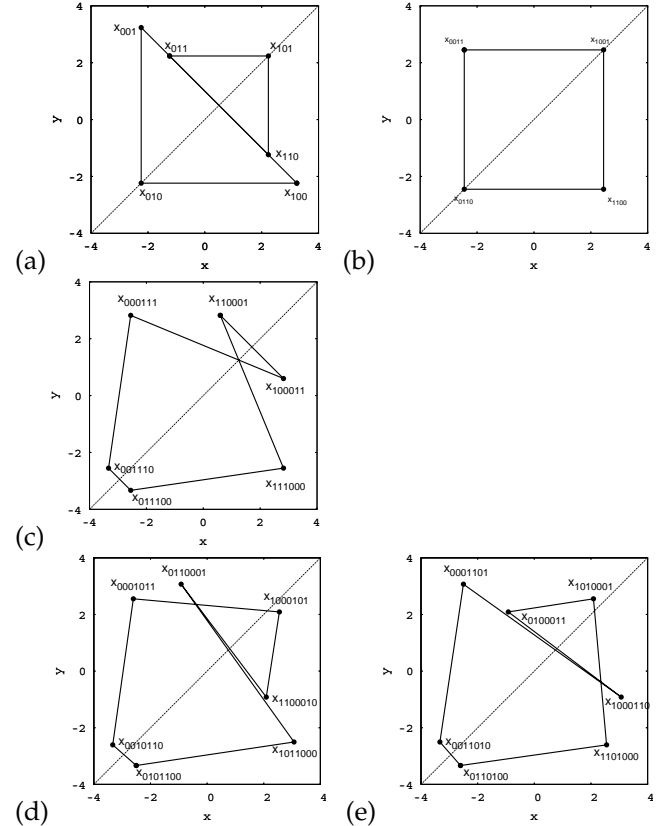


Figure 2.1: Periodic orbits of the Hamiltonian Hénon map (2.11): (a) An odd-period orbit can have a point on the boundary, and thus belong to the diagonal class D. Example: the 3-cycles $\overline{001}$, $\overline{011}$. (b) An even-period orbit can have two points on the boundary, and thus belong to the diagonal class D. Example: the 4-cycle $\overline{0011}$. (c) An even-period orbit can belong to the non-diagonal class N. Example: the 6-cycle $\overline{000111}$, with no points on the boundary. (d) Almost all longer orbits are asymmetric, ‘chiral’ class C. Example: the 7-cycle $\overline{0001011}$, and (e) its partner $\overline{0001101}$ under flip across the diagonal and time-reversal. Under the time reversal periodic points symbol sequences are mirrored into their symmetry partners point by point. For spatiotemporal cat examples, see figure 18.5, figure 18.6, figure 18.18, figure 18.20, figure 18.22.

to dynamics [41–45]. Apart from counting orbits, he knew well how to exploit symbolic dynamics and what was later named “itineraries” and “kneading sequences” [40] to efficiently tabulate parameters with no less than 11 digits of accuracy. The problem of counting orbits for the Hénon map was also addressed very early, in a pioneering work by Simó [47] using an approach centered in the strange attractor creation/destruction.

The direct combinatorial problem of determining the partitions C_n , D_n , N_n individually seems to be very hard. However there is an efficient way of getting indirectly to them by counting the orbital points lying on symmetry axis of the problem. This is what we do. The approach is a nice application of enumerative combinatorics and the number-theoretic Moebius inversion formula to a key problem in physics and dynamical systems. Several complementary aspects of combinatorial dynamics are discussed in ref. [1].

2021-02-18 Predrag Predrag: as the logistic map (??) is not invertible map, I expect no information about the time reversal factorization from this group of papers:

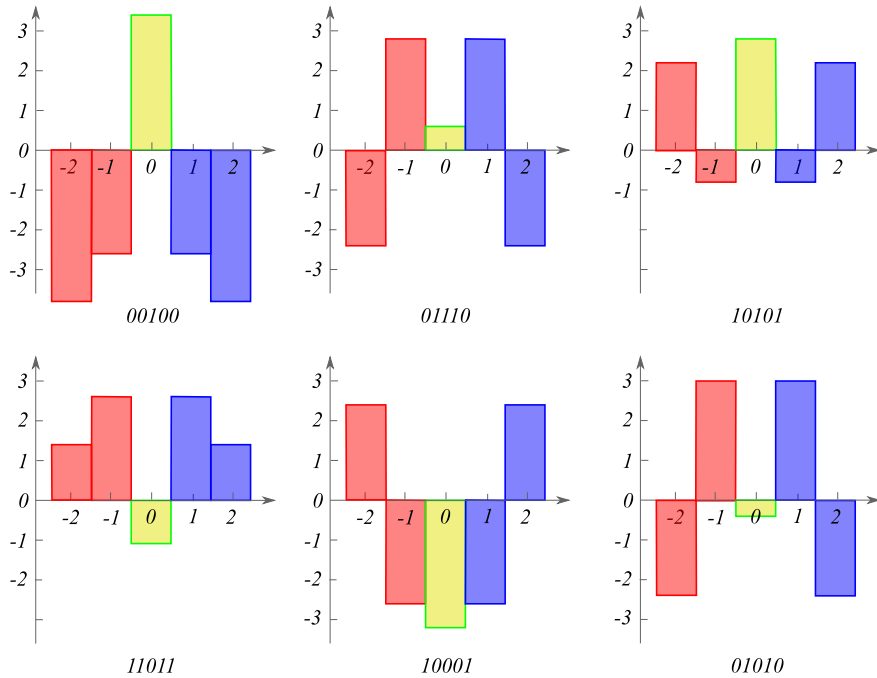


Figure 2.2: Temporal Hénon (2.44), $a = 6$: Odd period (3.158) $n = 5$ lattice states $x_{-2}x_{-1}|x_0|x_1x_2|$ of table 2.3, plotted as in figure 3.13. Compare also with forward-in time plots of figure 2.3. They are all reflection symmetric, with the fixed lattice field x_0 colored gold. Note that the symbolic dynamics is given by the signs of lattice site fields. The most striking feature of these lattice states is how far is $a = 6$ temporal Hénon from a $0 \leftrightarrow 1$ symmetry: stretching close to $\bar{0}$ constant lattice state is much stronger than close to the almost marginal $\bar{1}$ constant lattice state. Probably for somewhat lower bifurcation value of a than the ‘critical’ value $a_h = 5.69931 \dots$, the fixed lattice sites x_0 for 01110 and 01010 coalesce and vanish, so the bifurcation happens on the even symmetry site. **If anybody ever gives some thought to orbit Jacobian matrix eigenvalues of figure 15.2 (right), the corresponding eigenvectors might illuminate this point.** As $a \rightarrow \infty$ I expect this symmetry to be restored.

Table 2.3: The temporal Hénon period-5 and -6 symmetric lattice states of type figure 3.13 (b), with symmetry indicated in the σ -reflection format (3.164). For odd $n = 2m + 1$, symmetric orbits reduce to blocks of length $m + 1$. For even $n = 2m$, their lengths are either $m + 1$ or m . The period-5 lattice states are plotted in figure 2.2 (to supersede figure 15.2 (left)). There is no asymmetric period-5, the first C_n asymmetric pair is period-6. Indicated: the binary code m_j of the field x_j at the lattice site $j = 0, 1, 2, 3, 4$.

C_5	$x_{-2}x_{-1} x_0 x_1x_2 $	D_5	C_6	$x_0x_1x_2x_3x_4x_5$	D_6
11110	11 0 11	0 11	001011	001011	001011
00011	10 0 01	0 01	110100	110100	
00101	01 0 10	0 10		x_0 x_1x_2 x_3 x_2x_1	
00001	00 1 00	1 00		010001 0 10 0 01	0 10 0
11010	10 1 01	1 01		011111 0 11 1 11	0 11 1
11100	01 1 10	1 10		001110 0 01 1 10	0 01 1
				100000 1 00 0 00	1 00 0
				101110 1 01 1 10	1 01 1
					$x_0x_1x_2 x_2x_1x_0 $
			001100	001 100	001
			011110	011 110	011

Gallas [28] *Equivalence among orbital equations of polynomial maps* arXiv:1809.05399

Gallas [29] *Orbital carriers and inheritance in discrete-time quadratic dynamics* arXiv:2008.01073:

[...] may be all conveniently extracted from just a single mathematical object, a polynomial called an *orbital carrier*, see for example (??). All orbits may be encoded simultaneously by a single carrier, with p orbit parameterized by the orbital sum σ_p .

recurrence

from Pincherle's relation

Simó [47] *On the Hénon-Pomeau attractor* is a very fine early paper. Cite it in Hénon remark. No mention of symmetry lines, though.

MacKay [38] 1982 PhD thesis, published as *Renormalisation in Area-preserving Maps* has a chapter on reversible maps. Do cite in our paper(s).

The theory comes from deVogelaere [20] *On the structure of symmetric periodic solutions of conservative systems, with applications* (1958)

Orbits and periodic points A *periodic point* is a solution (x, n) , $x \in \mathbb{R}^d$, $n \in \mathbb{Z}$ of the *periodic orbit condition*

$$x = f^n(x) \quad (2.21)$$

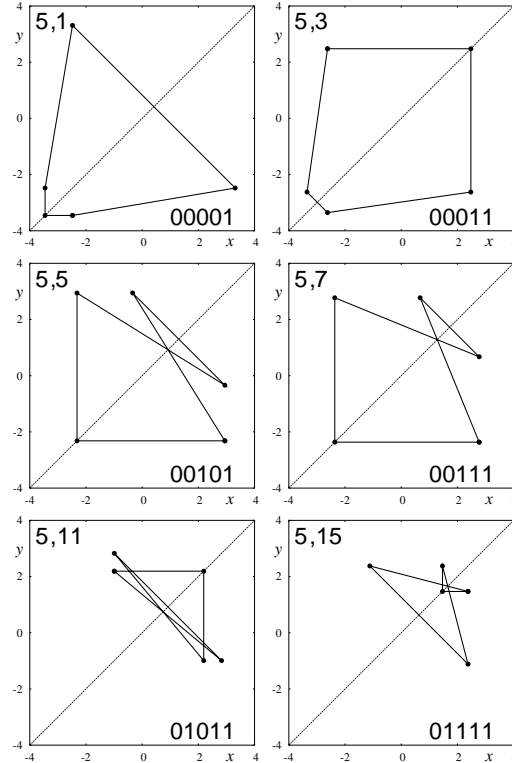


Figure 2.3: The 6 period-5 orbits are of Engler-Gallas class D (here called odd period symmetric cycles (\circ), see (3.158)): they are symmetric under reflection across the diagonal, have a single point on it, corresponding to 2 successive field values of an even-reflection pair. Compare with the lattice state plots of figure 2.2. The pairs 5,1 & 5,3 and 5,1 & 5,3 have an additional symmetry under reflection and stretch (Predrag: what is that? I do not see it) across the other diagonal.

for a given mapping f . Each periodic point $x = x_{p,i} \in p$ belongs to a *time orbit*, a *orbit* p of period n_p , and its n_p distinct images

$$f^k(x_{p,i}) = x_{p,i+k}, \quad i + k \bmod n_p$$

are the successive periodic points along the cycle.

A *orbit* p of period n_p is a single traversal of the orbit.

We list the number of orbits up to length 10 for the 2-letter complete symbolic dynamics in tables ?? and ??.

³ ⁴ Consider the n -periodic point condition $0 = f^n(x) - x$. This polynomial of order 2^n has zeros at all shorter, period d orbits if d is a divisor of n . Dividing those out, we arrive at the polynomial [39]

$$Q_n(x) = \prod_{d|n} (f^d(x) - x)^{\mu(n/d)}, \quad (2.22)$$

with nM_n zeros corresponding to the n periodic points for each orbit p of pe-

³Predrag 27dec2004: table ?? derived from knead.tex

⁴Predrag 27dec2004: extracted from smale.tex

riod $n_p = n$, $Q_n(x) = \prod_p P_p(x)$, where the n th order polynomial

$$P_p(x) = \prod_{i \in p} (x - x_{p,i}) = 0, \quad n_p = n \quad (2.23)$$

has zeros at all periodic points in orbit p . Except for some values of a , at which bifurcations occur, these are simple zeros.

The coefficients in the expansion of (2.26) are symmetric polynomials in x_i , all reducible to powers of the orbital sum σ_p (2.14), a orbit p invariant, For example, the x^{n-2} coefficient

$$2 \sum_{i < j} x_i x_j = \sigma^2 - \sum_i x_i^2 = \sigma^2 + 2\sigma - n_p a$$

can be expressed in terms of σ^2 , σ and a

$$P_p(x) = x^{n_p} - \sigma_p x^{n_p-1} + (\sigma^2 + 2\sigma - n_p a)x^{n_p-2} + \dots \pm (\sigma^{n_p} \dots). \quad (2.24)$$

We refer to σ as the “center of mass” of cycle p (up to an overal prefactor of $1/n_p$).

By cyclic invariance of periodic points in p , σ_p is invariant under $x \rightarrow f(x)$, so it is an intrinsic property of the orbit p , hence it can take at most M_n distinct values corresponding to the M_n orbits p of period $n_p = n$.

Endler and Gallas [24] succeeded - after considerable algebra - in computing explicitly the M_n -th order polynomials

$$S_n(\sigma) = 0, \quad (2.25)$$

⁵ for $n_p \leq n$. The M_n root $\sigma = \sigma_p$ substituted into the n th order polynomial

$$P_n(x, \sigma_p, a) = \prod_{i \in p} (x - x_i) = 0, \quad (2.26)$$

yields the n periodic points $x = x_{p,i}$ belonging to the orbit p as the roots of $P_n(x, \sigma_p, a) = 0$. As the reduction of symmetric polynomial coefficients does not rely on the shape of a given orbit p , P_n has the same form for all $n_p = n$.

Smale horseshoe Smale horseshoes and symbolic dynamics labeling of the dynamics - it's really great, once you get it, because the label tells you everything about the periodic point and the cycle it belongs too. From table ?? you can read off the shape and symmetry of individual cycles, and the factorization of S - at least the highest power of σ in each of the monic polynomials it factors into.

The Jacobian matrix for the n th iterate of the Hamiltonian Hénon map is

$$M^n(x_0) = \prod_{m=n}^1 \begin{bmatrix} -2x_m & -1 \\ 1 & 0 \end{bmatrix}, \quad x_m = f_1^m(x_0, y_0). \quad (2.27)$$

⁵Predrag 27dec2004: fill in the explanation

⁶ The determinant of the Hénon one time-step Jacobian matrix (2.27) is constant,

$$\det M = \Lambda_1 \Lambda_2 = 1 \quad (2.28)$$

so only one eigenvalue $\Lambda_1 = 1/\Lambda_2$ needs to be determined.

Iterating $x_{n+1} = f(x_n)$. and checking the sign of x_k associates a *temporally* ordered topological itinerary $m_{-m} \cdots m_{-1} m_0$ with a given trajectory,

$$m_k = \begin{cases} 1 & \text{if } x_k > 0 \\ 0 & \text{if } x_k < 0 \end{cases} . \quad (2.29)$$

Time reversal symmetry Under the time reversal (2.40) the points in the symbol square for an orientation preserving map are symmetric across the diagonal $\gamma = \delta$. Consequently the periodic orbits appear either in dual pairs $p = m_1 m_2 m_3 \dots m_n$, $\bar{p} = m_n m_{n-1} m_{n-2} \dots m_1$, or are self-dual under time reversal, $S_p = S_{\bar{p}}$.

⁷ For the orientation preserving case a self-dual cycle of odd period has at least one point (or odd number of points) on the symmetry diagonal. In particular, all fixed points lie on the symmetry diagonal.

A self-dual cycle of even period has no, or even number of points on the symmetry diagonal.

One distinguishes three kinds of cycles: asymmetric cycles a , symmetric cycles s built by repeats of irreducible segments \tilde{s} , and boundary cycles b .

Asymmetric cycles C ('chiral' class): A periodic orbit is not symmetric if $\{x_a\} \cap \{\mathbf{R}x_a\} = \emptyset$, where $\{x_a\}$ is the set of periodic points belonging to the cycle a . Thus \mathbf{R} generates a second orbit with the same number of points and the same stability properties.

For this class of cycles for any n ,

$$P_a(x, \sigma, a) = \prod^p (x - x_{a,i}) \quad (2.30)$$

has n distinct roots $\{x_{a,i}\}$. The associated equation for is $C(\sigma)^2 = 0$.

Example : Follow the successive periodic points in the orbit $\overline{0001011}$, figure 2.1 (d); then flip across the diagonal, reverse the direction along the cycle, and you are now on the orbit $\overline{0001101}$, the time reversed partner of $\overline{0001011}$.

Symmetric cycles, no boundary point N ('non-diagonal' class): A cycle s is reflection symmetric if operating with \mathbf{R} on the set of periodic points reproduces the set. The period of a symmetric cycle is always even ($n_s = 2m$) and the

⁶Predrag 27dec2004: main text - explain the order of multiplication

⁷Predrag 27dec2004: insert this into the book

mirror image of the x_s periodic point is reached by traversing the irreducible segment \tilde{s} of length m , $f^m(x_s) = \mathbf{R}x_s$.

$$P_N(x, \sigma, a) = (x - x_1)(x - x_2)^2 \cdots (x - x_m)^2(x - x_{m+1}) \quad (2.31)$$

has $m + 1$ distinct roots.

$$\sigma_p = x_1 + 2x_2 + \cdots + 2x_m + x_{m+1} \quad (2.32)$$

Example : Symmetric (or self-dual orbit):

Draw 4-cycles $\overline{0001}$ and $\overline{0111}$. They map into themselves under flip and time reversal. That means that if you know 2 periodic points, the other 2 are given by symmetry.

Even symmetric cycles, 2 boundary points D ('diagonal' class):

$$P_D(x, \sigma, a) = \prod_{i=1}^p (x - x_{s,i})^2 \quad (2.33)$$

has $n_{\tilde{s}}$ distinct roots.

$$\sigma_p = 2 \sum_i^{n_{\tilde{s}}} x_{p,i} \quad (2.34)$$

3 or more boundary points are not possible for orbits.

Cycle $\overline{0011}$ is an example of even-period boundary orbit. Two periodic points x_{1001}, x_{0110} are on the symmetry diagonal, and reflection symmetry of the remaining x_{0011}, x_{1100} pair forces a square-shaped trajectory in the $[x, y]$ plane, see figure 2.1:⁸

$$\left[\begin{bmatrix} x_{1001} \\ x_{1001} \end{bmatrix}, \begin{bmatrix} -x_{1001} \\ x_{1001} \end{bmatrix}, \begin{bmatrix} -x_{1001} \\ -x_{1001} \end{bmatrix}, \begin{bmatrix} x_{1001} \\ -x_{1001} \end{bmatrix} \right]$$

Hence $\sigma_{0011} = 0$, and

$$P_{0011} = (x^2 - x_{0011}^2)^2. \quad (2.35)$$

with $x_{0011} = \sqrt{a}$. Note that this 4-cycle is more robust than the 2-cycle given in (??) - it exists for $a > 0$, and is not the period-doubling relative of the 2-cycle.

Odd symmetric cycles $n = 2m + 1$, 1 boundary point D ('diagonal' class):

$$P_B(x, \sigma, a) = (x - x_1)^2 \cdots (x - x_m)^2(x - x_{m+1}) \quad (2.36)$$

has $m + 1$ distinct roots.

$$\sigma_p = 2x_1 + 2x_2 + \cdots + 2x_m + x_{m+1} \quad (2.37)$$

⁸Predrag 27dec2004: make into an exercise

Example Boundary cycles:

Draw 3-cycles $\overline{001}$ and $\overline{011}$. They have a point on the diagonal, indicated in the table S.1.

The time reversal symmetry of the state space (this is true for *all* Hamiltonian time-reversible flows whose Poincaré section is symmetric under $[q, p] \rightarrow [p, q]$ diagonal flip, not just polynomial mappings) implies - but we need to cleanly explain it for this case that $S_n(\sigma)$ *always* factorizes into form (2.15). Endler and Gallas [24] indeed observe that the polynomials $S = S_n(\sigma)$ factorize into product of polynomials over the above three kinds of cycles.

For each n , the $P_n(x, \sigma, a)$ polynomial should be written explicitly for each of the 3 symmetry classes $[a, s, b]$. In particular, for $P_s(x, \sigma, a)$ the factorization over 1/2 of the state space

$$P_s(x, \sigma, a) = \left(\prod_{i=1}^{\tilde{s}} (x - x_{\tilde{s},i}) \right)^2 \quad (2.38)$$

is expected, as exemplified by the 6-cycle figure 2.1 (c).

Remark 2.1. “Center of mass” puzzle. The “center of mass” notions play important role in a number of physical problems, such as: (1) the periodic-orbit formulation of the deterministic drift and diffusion (2) the kinematic dynamo problem [7, 31], and (3) Sullivan’s formulation [2, 18, 35, 46] of the Feigenbaum δ eigenvalue problem in the period-doubling renormalization theory.

The “center of mass” puzzle for the cycles listed in table 2.4 was first observed numerically by G. Vattay in ref. [7], and was resolved by Endler and Gallas [24]. Their method of solution resembles the methods earlier employed for quadratic polynomials (and their Julia sets) by Brown [13]⁹ and Stephenson [48]. Brown gives cycles up to length 6 for the logistic map, employing symmetric functions of periodic points. Hitzl and Zele [34] study the Hénon map for cycle lengths up to period 6.

All explicit values of periodic points for the Hamiltonian Hénon map displayed here are taken from ref. [24]. Method of ref. [24] applies to cycles of polynomial maps only, in this case the quadratic map.

Remark 2.2. Complete Smale horseshoe, Hamiltonian Hénon map. It was proved by Devaney and Nitecki [19, 51] that there is indeed a hyperbolic horseshoe when $a > 5 + 2\sqrt{5}$. Numerical studies indicate that [50, 51]

$$a > 5.699310786700 \dots . \quad (2.39)$$

2.4 Symmetries of the symbol square

¹⁰ Depending on the type of dynamical system, the symbol square might have a variety of symmetries. Under the time reversal

$$\cdots m_{-2}m_{-1}m_0.m_1m_2m_3 \cdots \rightarrow \cdots m_3m_2m_1.m_0m_{-1}m_{-2} \cdots \quad (2.40)$$

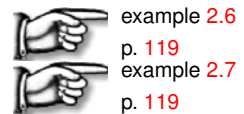
⁹ Predrag : Brown [13] did all the right algebra for the logistic case. but computed approximate numbers rather than algebraic ones.

¹⁰ Predrag 2021-04-03: Moved to here from ChaosBook *appendFiniteGr*. Return once updated here.

the points in the symbol square for an orientation preserving map are symmetric across the diagonal $\gamma = \delta$, and for the orientation reversing case they are symmetric with respect to the $\gamma = 1 - \delta$ diagonal. Consequently the periodic orbits appear either in dual pairs $p = m_1 m_2 m_3 \dots m_n$, $\bar{p} = m_n m_{n-1} m_{n-2} \dots m_1$, or are self-dual under time reversal, $S_p = S_{\bar{p}}$. For the orientation preserving case a self-dual cycle of odd period has at least one point on the symmetry diagonal. In particular, all fixed points lie on the symmetry diagonal. Determination of such symmetry lines can be of considerable practical utility, as it reduces some of the periodic orbit searches to 1-dimensional searches.¹¹

2.4.1 Symmetry lines

discuss symmetry lines



References

- [1] L. Alseda, J. Llibre, and M. Misiurewicz, *Combinatorial Dynamics and Entropy in Dimension One* (World Scientific, Singapore, 2000).
- [2] R. Artuso, E. Aurell, and P. Cvitanović, “Recycling of strange sets: II. Applications”, *Nonlinearity* **3**, 361–386 (1990).
- [3] S. Aubry, “Anti-integrability in dynamical and variational problems”, *Physica D* **86**, 284–296 (1995).
- [4] S. Aubry and G. Abramovici, “Chaotic trajectories in the standard map. The concept of anti-integrability”, *Physica D* **43**, 199–219 (1990).
- [5] S. Aubry and P. Y. Le Daeron, “The discrete Frenkel-Kontorova model and its extensions. I. Exact results for the ground-states”, *Physica D* **8**, 381–422 (1983).
- [6] M. Baake, N. Neumärker, and J. A. G. Roberts, “Orbit structure and (reversing) symmetries of toral endomorphisms on rational lattices”, *Discrete Continuous Dyn. Syst.* **33**, 527–553 (2013).
- [7] N. J. Balmforth, P. Cvitanović, G. R. Ierley, E. A. Spiegel, and G. Vattay, “Advection of vector fields by chaotic flows”, *Ann. New York Acad. Sci.* **706**, 148–160 (1993).
- [8] O. Biham and W. Wenzel, “Characterization of unstable periodic orbits in chaotic attractors and repellers”, *Phys. Rev. Lett.* **63**, 819 (1989).

¹¹Predrag 2021-03-24: create appendix chapter/appendCont.tex, include add JH Jan 18, 2008 Desymmetrization of large spaces, thinking is extra price version from halcrow/blog/TEX/symm.tex; create Problems/exerAppCont.tex, Problems/soluAppCont.tex, include halcrow/blog/TEX/zeghlache.tex; create chapter/refsAppCont.tex.

- [9] R. L. Bivins, J. D. Louck, N. Metropolis, and M. L. Stein, “Classification of all cycles of the parabolic map”, *Physica D* **51**, 3–27 (1991).
- [10] S. V. Bolotin and D. V. Treschev, “The anti-integrable limit”, *Russ. Math. Surv.* **70**, 975–1030 (2015).
- [11] S. Bolotin and R. MacKay, “Multibump orbits near the anti-integrable limit for Lagrangian systems”, *Nonlinearity* **10**, 1015–1029 (1997).
- [12] A. Bridy and R. A. Pérez, “A count of maximal small copies in Multibrot sets”, *Nonlinearity* **18**, 1945–1953 (2005).
- [13] A. Brown, “Equations for periodic solutions of a logistic difference equation”, *J. Austral. Math. Soc. Ser. B* **23**, 78–94 (1981).
- [14] K. M. Brucks, “MSS sequences, colorings of necklaces, and periodic points of $f(z) = z^2 - 2$ ”, *Adv. Appl. Math.* **8**, 434–445 (1987).
- [15] D. N. Butusov, A. I. Karimov, N. S. Pyko, S. A. Pyko, and M. I. Bogachev, “Discrete chaotic maps obtained by symmetric integration”, *Physica A* **509**, 955–970 (2018).
- [16] O. Chavoya-Aceves, F. Angulo-Brown, and E. Piña, “Symbolic dynamics of the cubic map”, *Physica D* **14**, 374–386 (1985).
- [17] W. Y. C. Chen and J. D. Louck, “Necklaces, MSS sequences, and DNA sequences”, *Adv. Appl. Math.* **18**, 18–32 (1997).
- [18] F. Christiansen, P. Cvitanović, and H. H. Rugh, “The spectrum of the period-doubling operator in terms of cycles”, *J. Phys. A* **23**, 713–717 (1999).
- [19] R. L. Devaney and Z. Nitecki, “Shift automorphisms in the Hénon mapping”, *Commun. Math. Phys.* **67**, 137–146 (1979).
- [20] R. DeVogelaere, “IV. On the structure of symmetric periodic solutions of conservative systems, with applications”, in *Contributions to the Theory of Nonlinear Oscillations (AM-41), Volume IV* (Princeton Univ. Press, 1958), pp. 53–84.
- [21] A. Endler and J. A. C. Gallas, “Period four stability and multistability domains for the Hénon map”, *Physica A* **295**, 285–290 (2001).
- [22] A. Endler and J. A. C. Gallas, “Arithmetical signatures of the dynamics of the Hénon map”, *Phys. Rev. E* **65**, 036231 (2002).
- [23] A. Endler and J. A. C. Gallas, “Conjugacy classes and chiral doublets in the Hénon Hamiltonian repeller”, *Phys. Lett. A* **356**, 1–7 (2006).
- [24] A. Endler and J. A. C. Gallas, “Reductions and simplifications of orbital sums in a Hamiltonian repeller”, *Phys. Lett. A* **352**, 124–128 (2006).
- [25] A. Endler and J. A. C. Gallas, “Reductions and simplifications of orbital sums in a Hamiltonian repeller”, *Phys. Lett. A* **352**, 124–128 (2006).
- [26] J. A. C. Gallas, “Nonlinear dependencies between sets of periodic orbits”, *Europhysics Lett.* **47**, 649–655 (1999).

- [27] J. A. C. Gallas, “Counting orbits in conjugacy classes of the Hénon Hamiltonian repeller”, *Phys. Lett. A* **360**, 512–514 (2007).
- [28] J. A. C. Gallas, “Equivalence among orbital equations of polynomial maps”, *Int. J. Modern Phys. C* **29**, 1850082 (2018).
- [29] J. A. C. Gallas, “Orbital carriers and inheritance in discrete-time quadratic dynamics”, *Int. J. Modern Phys. C* **31**, 2050100 (2020).
- [30] J. A. C. Gallas, “Preperiodicity and systematic extraction of periodic orbits of the quadratic map”, *Int. J. Modern Phys. C* **31**, 2050174 (2020).
- [31] A. D. Gilbert and S. Childress, *Stretch, Twist, Fold: the Fast Dynamo* (Springer, Berlin, 1995).
- [32] J. F. Heagy, “A physical interpretation of the Hénon map”, *Physica D* **57**, 436–446 (1992).
- [33] M. Hénon, “A two-dimensional mapping with a strange attractor”, *Commun. Math. Phys.* **50**, 94–102 (1976).
- [34] D. L. Hitzl and F. Zele, “An exploration of the Hénon quadratic map”, *Physica D* **14**, 305–326 (1985).
- [35] Y. Jiang, T. Morita, and D. Sullivan, “Expanding direction of the period doubling operator”, *Commun. Math. Phys.* **144**, 509–520 (1992).
- [36] M. Lutzky, “Counting stable cycles in unimodal iterations”, *Phys. Lett. A* **131**, 248–250 (1988).
- [37] M. Lutzky, “Counting hyperbolic components of the Mandelbrot set”, *Phys. Lett. A* **177**, 338–340 (1993).
- [38] R. S. MacKay, *Renormalisation in Area-preserving Maps* (World Scientific, Singapore, 1993).
- [39] J. W. Milnor, *Orbits, externals rays and the Mandelbrot set: An expository account*, 1999.
- [40] J. Milnor and W. Thurston, “On iterated maps of the interval”, in *Dynamical Systems*, edited by J. C. Alexander (Springer, New York, 1988), pp. 465–563.
- [41] P. J. Myrberg, “Iteration der reellen Polynome zweiten Grades I”, *Ann. Acad. Sc. Fenn. A* **256**, 1–10 (1958).
- [42] P. J. Myrberg, “Iteration von quadratwurzeloperationen”, *Ann. Acad. Sc. Fenn. A* **259**, 1–10 (1958).
- [43] P. J. Myrberg, “Iteration der reellen Polynome zweiten Grades II”, *Ann. Acad. Sc. Fenn. A* **268**, 1–13 (1959).
- [44] P. J. Myrberg, “Sur l’itération des polynomes réels quadratiques”, *J. Math. Pures Appl.* **41**, 339–351 (1962).
- [45] P. J. Myrberg, “Iteration der reellen Polynome zweiten Grades III”, *Ann. Acad. Sc. Fenn. A* **336**, 1–13 (1963).

- [46] M. Pollicott, “A note on the Artuso-Aurell-Cvitanovic approach to the Feigenbaum tangent operator”, *J. Stat. Phys.* **62**, 257–267 (1991).
- [47] C. Simó, “On the Hénon-Pomeau attractor”, *J. Stat. Phys.* **21**, 465–494 (1979).
- [48] J. Stephenson and D. T. Ridgway, “Formulae for cycles in the Mandelbrot set II”, *Physica A* **190**, 104–116 (1992).
- [49] G. Sterling D., *Anti-integrable Continuation and the Destruction of Chaos*, PhD thesis (Univ. Colorado, Boulder, CO, 1999).
- [50] D. G. Sterling, H. R. Dullin, and J. D. Meiss, “Homoclinic bifurcations for the Hénon map”, *Physica D* **134**, 153–184 (1999).
- [51] D. Sterling and J. D. Meiss, “Computing periodic orbits using the anti-integrable limit”, *Phys. Lett. A* **241**, 46–52 (1998).
- [52] F.-G. Xie and B. L. Hao, “Counting the number of periods in one-dimensional maps with multiple critical points”, *Physica A* **202**, 237–263 (1994).

Example 2.1. Hénon map. The map

$$\begin{aligned} x_{n+1} &= 1 - ax_n^2 + by_n \\ y_{n+1} &= x_n \end{aligned} \quad (2.41)$$

is a nonlinear 2-dimensional map frequently employed in testing various hunches about chaotic dynamics. Written as a 2nd-order inhomogeneous difference equation (3-term recurrence relation), the temporal Hénon is

$$x_{n+1} = 1 - ax_n^2 + bx_{n-1}. \quad (2.42)$$

An $(n+1)$ -term recurrence relation is the discrete-time analogue of an n th order differential equation, and it can always be replaced by a set of n 1-step relations.

Always plot the dynamics of such maps in the (x_n, x_{n+1}) plane, rather than in the (x_n, y_n) plane, and make sure that the ordinate and abscissa scales are the same, so $x_n = x_{n+1}$ is the 45° diagonal. There are several reasons why one should plot this way: (a) we think of the Hénon map as a model return map $x_n \rightarrow x_{n+1}$, and (b) as parameter b varies, the attractor will change its y -axis scale, while in the (x_n, x_{n+1}) plane it goes to a parabola as $b \rightarrow 0$, as it should.

Example 2.2. Temporal Hénon. For $b = -1$ parameter value the Hénon map (15.14) is the simplest example of a nonlinear Hamiltonian map, a 2-dimensional orientation preserving, area preserving map, often studied to better understand topology and symmetries of Poincaré sections of 2-degrees of freedom Hamiltonian flows.

We find it convenient [24] to multiply (2.42) by a and absorb the a factor into the definition the lattice field $\phi = a x$. This brings the Hamiltonian Hénon map to the form

$$\begin{aligned} \phi_{n+1} &= a - \phi_n^2 - p_n \\ p_{n+1} &= \phi_n, \end{aligned} \quad (2.43)$$

or, equivalently, the temporal Hénon (2.20) 3-term recurrence relation of form

$$\phi_{i+1} + \phi_i^2 + \phi_{i-1} = a, \quad i = 1, \dots, n_p. \quad (2.44)$$

We can write this as a lattice field equation with lattice Laplacian (5.106)

$$\square \phi_n + (\phi_n + 2) \phi_n = a. \quad (2.45)$$

The field equation is nonlinear, with the cubic potential (15.53).

For definitiveness, in numerical calculations in examples to follow we shall fix (arbitrarily) the stretching parameter value to $a = 6$, a value large enough to guarantee that all roots of $0 = f^n(x) - x$ (periodic points) are real.

exercise ??

click to return: p. ?? **Example 2.3. Temporal Hénon fixed points.** Since we are looking for fixed points p_q of (2.43), each successive step is the same as the previous,

$$\begin{pmatrix} \phi_q \\ p_q \end{pmatrix} = \begin{pmatrix} a - \phi_q^2 - p_q \\ \phi_q \end{pmatrix}.$$

Thus there two fixed points, given by the roots of the quadratic equation $\phi^2 - 2\phi - a = 0$,

$$\begin{aligned} \phi_0 &= -1 - \sqrt{1+a} \\ \phi_1 &= -1 + \sqrt{1+a}. \end{aligned} \quad (2.46)$$

¹²Predrag 2021-04-28: agrees with Endler and Gallas [24] $a = 6$ values

¹³ $\overline{01}$ periodic points are (??)

$$\phi_{10} = 1 + \sqrt{a - 3}, \quad \phi_{01} = 1 - \sqrt{a - 3}. \quad (2.47)$$

click to return: p. ??

Example 2.4. Temporal Hénon stability. For the Hénon map (2.43) the temporal evolution Jacobian matrix for the n th iterate of the map is the product of consecutive one time-step Jacobian matrices

$$J^n(\phi_0) = \prod_{m=n}^1 \begin{bmatrix} -2\phi_m & -1 \\ 1 & 0 \end{bmatrix}, \quad \phi_m = f_1^m(\phi_0, p_0). \quad (2.48)$$

The decreasing order in the indices of the products in above formulas is a reminder that the successive time steps correspond to multiplication from the left, $J_p(\phi_1) = J(\phi_{n_p}) \cdots J(\phi_1)$.

The determinant of the Hénon one time-step Jacobian matrix in (3.52) is a constant,

$$\det J = 1, \quad (2.49)$$

so the map is Hamiltonian (symplectic) in the sense that it preserves areas in the $[\phi, p]$ plane.

The Floquet matrix J_p for a orbit p of length n_p of the Hénon map (2.43) is evaluated by picking any periodic point as a starting point, running once around a orbit, and multiplying the individual periodic point Jacobian matrices (3.52),

$$J_p(x_0) = \prod_{k=n_p}^1 \begin{bmatrix} -2\phi_k & -1 \\ 1 & 0 \end{bmatrix}, \quad \phi_k \in \mathcal{M}_p, \quad (2.50)$$

Once we have a periodic orbit of Hénon map, we also have its Floquet matrix. Only the expanding eigenvalue $\Lambda_1 = 1/\Lambda_2$ needs to be determined, as $\det J = \Lambda_1 \Lambda_2 = 1$.

The orbit Jacobian matrix is the $\delta/\delta\phi_k$ derivative of the temporal Hénon (2.44) 3-term recurrence relation

$$\begin{aligned} \mathcal{J}_p &= \sigma + 2 \mathbb{X}_p + \sigma^{-1} \\ &= \begin{bmatrix} 2\phi_0 & 1 & 0 & 0 & \dots & 0 & 1 \\ 1 & 2\phi_1 & 1 & 0 & \dots & 0 & 0 \\ 0 & 1 & 2\phi_2 & 1 & \dots & 0 & 0 \\ \vdots & \vdots & \vdots & \vdots & \ddots & \vdots & \vdots \\ 0 & 0 & \dots & \dots & \dots & 2\phi_{n-2} & 1 \\ 1 & 0 & \dots & \dots & \dots & 1 & 2\phi_{n-1} \end{bmatrix}, \end{aligned} \quad (2.51)$$

where \mathbb{X}_p is a diagonal matrix with p -lattice state ϕ_k in the k th row/column, and the '1's in the upper right and lower left corners enforce the periodic boundary conditions.

The trace of the orbit Jacobian matrix is twice the orbital sum [30]

$$\sigma_p = \sum_{i \in p} \phi_{p,i} \quad (2.52)$$

a prime cycle p invariant that satisfies a polynomial equation $\mathbb{S}_n(\sigma) = 0$ of the order n_p , the period of the cycle. ¹⁴

¹³Predrag 2021-04-28: make into na exercise: Show that (2.46)...

¹⁴Predrag 2021-05-04: Perhaps include the example (??)?

The two fixed points (2.47) are hyperbolic for $a > 3$, with expanding eigenvalues

$$\begin{aligned}\Lambda_0 &= 1 + \sqrt{1+a} + (1+a)^{1/4} \sqrt{\sqrt{1+a} + 2} \\ \Lambda_1 &= 1 - \sqrt{1+a} - (1+a)^{1/4} \sqrt{\sqrt{1+a} - 2},\end{aligned}\quad (2.53)$$

The action of the temporal Hénon orbit Jacobian matrix can be hard to visualize, as a period-2 lattice state is a 2-torus, period-3 lattice state a 3-torus, etc.. Still, the fundamental parallelepiped for the period-2 and period-3 lattice states, should suffice to convey the idea. The fundamental parallelepiped basis vectors (3.90) are the columns of \mathcal{J} . The $[2 \times 2]$ orbit Jacobian matrix and its Hill determinant follow from (2.46)

$$\mathcal{J} = \begin{pmatrix} 2\phi_0 & 2 \\ 2 & 2\phi_1 \end{pmatrix}, \quad \text{Det } \mathcal{J} = 4(\phi_0\phi_1 - 1) = -4(a-3). \quad (2.54)$$

The resulting fundamental parallelepiped shown in figure ?? (a). Period-3 lattice states for $s = 3$ are contained in the half-open fundamental parallelepiped of figure ?? (b), defined by the columns of $[3 \times 3]$ orbit Jacobian matrix

$$\mathcal{J} = \begin{pmatrix} 2\phi_0 & 1 & 1 \\ 1 & 2\phi_1 & 1 \\ 1 & 1 & 2\phi_2 \end{pmatrix}, \quad \text{Det } \mathcal{J} = 8\phi_0\phi_1\phi_2 - 2(\phi_0 + \phi_2 + \phi_3) + 2, \quad (2.55)$$

and for an period- n lattice state,¹⁵

$$\text{Det } \mathcal{J} = 2^n \phi_0\phi_1\phi_2 \cdots \phi_{n-1}, \quad n > 3. \quad (2.56)$$

Example 2.5. Hamiltonian Hénon map, reversibility. The Hénon map (??) is reversible, with its inverse interchanging the roles of x and y :

$$\begin{aligned}x_{n-1} &= y_n \\ y_{n-1} &= a - y_n^2 - x_n,\end{aligned}\quad (2.57)$$

hence the dynamics is symmetric in the $[x, y]$ plane: a trajectory maps into a trajectory under the flip across the $x = y$ diagonal

$$\begin{bmatrix} y \\ x \end{bmatrix} = R \begin{bmatrix} x \\ y \end{bmatrix} = \begin{bmatrix} 0 & 1 \\ 1 & 0 \end{bmatrix} \begin{bmatrix} x \\ y \end{bmatrix} \quad (2.58)$$

and the time reversal. The reversor R is orientation reversing, $\det[\partial R] = -1$, and is an involution, $R^2 = \mathbf{1}$. In other words, the Hamiltonian Hénon map is conjugate to its inverse $f \circ R = R \circ f^{-1}$, and can be factored into a pair of orientation reversing involutions, $f = (fR) \circ R = T \circ R$, with

$$T \begin{bmatrix} x \\ y \end{bmatrix} = \begin{bmatrix} x \\ a - x^2 - y \end{bmatrix}. \quad (2.59)$$

Equivalently, writing $f = S \circ (Sf) = S \circ U$, the reversor

$$U \begin{bmatrix} x \\ y \end{bmatrix} = \begin{bmatrix} a - y^2 - x \\ y \end{bmatrix} \quad (2.60)$$

factorizes the Hénon map as $f = ST$.

click to return: p. ??

¹⁵Predrag 2021-05-04: A guess, absolutely wrong - Fix!

Example 2.6. Symmetry lines of the standard map. In practice the search for important classes of periodic orbits for the standard map takes advantage of its remarkable symmetry: A can be written as the product of two involutions, $A = T_2 \cdot T_1$, (involution means that the square of the map is the identity):

[remark 1.5](#)

$$\begin{aligned} T_1(x, y) &= (-x, y - k \sin x) \\ T_2(x, y) &= (-x + y, y). \end{aligned} \quad (2.61)$$

Now define symmetry lines \mathcal{L}_1 and \mathcal{L}_2 as the sets of fixed points of the corresponding involution: \mathcal{L}_1 consists of the lines $x = 0, \pi$, \mathcal{L}_2 of $x = y/2 \bmod(2\pi)$. There are deep connections between symmetry lines and periodic orbits: we just give an example with the following statement: if $(x_0, y_0) \in \mathcal{L}_1$ and $A^M(x_0, y_0) \in \mathcal{L}_1$ (i.e. they are both fixed points of T_1), then (x_0, y_0) is a periodic point of period $2M$. ¹⁶ As a matter of fact

$$\begin{aligned} A^{2M}(x_0, y_0) &= A^{M-1}T_2T_1A^{M-1}T_2T_1(x_0, y_0) \\ &= A^{M-1}T_2A^{M-1}T_2(x_0, y_0) \end{aligned} \quad (2.62)$$

by the fixed point property. Now the involution property implies

$$T_2A = T_1 \quad AT_1 = T_2 \quad (2.63)$$

and thus

$$AT_2AT_2 = AT_1T_2 = \mathbf{1} \quad (2.64)$$

and

$$A^P T_2 A^P T_2 = A^{P-1} T_2 A^{P-1} T_2 \quad (2.65)$$

from which it easily follows that (x_0, y_0) belongs to a $2M$ cycle.

(Continued in example 2.7.)

[click to return: p. 112](#)

Example 2.7. Symmetry lines of the cat map. (Continued from example 2.6.) Instead of standard map, consider its linear relative, the cat map, obtained by substituting $k \sin x \rightarrow Kx$ in (2.61). A can now be written as the matrix product of two involutions, $A = T_2 T_1$,

$$\begin{aligned} T_1(x, p) &= (-x, p - Kx) \Rightarrow T_1 = \begin{bmatrix} -1 & 0 \\ s-2 & 1 \end{bmatrix} \\ T_2(x, p) &= (-x + p, p) \Rightarrow T_2 = \begin{bmatrix} -1 & 1 \\ 0 & 1 \end{bmatrix} \\ \Rightarrow A &= \begin{bmatrix} s-1 & 1 \\ s-2 & 1 \end{bmatrix}. \end{aligned} \quad (2.66)$$

T_1 and T_2 are involutions as their squares are the identity. We have substituted $K = -s + 2$, where $s = \text{tr } A$.

¹⁷ Now define symmetry lines \mathcal{L}_1 and \mathcal{L}_2 as the sets of fixed points of the corresponding involution: \mathcal{L}_1 consists of the lines $x = 0 \bmod 1$, \mathcal{L}_2 of $p = 2x$. There are deep connections between symmetry lines and periodic orbits: we just give an example

¹⁶Predrag 2021-04-03: Bad notation - M is monodromy matrix

¹⁷Predrag 2021-04-10: complete the rewrite here.

with the following statement: if $(x_0, p_0) \in \mathcal{L}_1$ and $A^M(x_0, p_0) \in \mathcal{L}_1$ (i.e. they are both fixed points of T_1), then (x_0, p_0) is a periodic point of period $2M$. As a matter of fact

$$\begin{aligned} A^{2M}(x_0, p_0) &= A^{M-1}T_2T_1A^{M-1}T_2T_1(x_0, p_0) \\ &= A^{M-1}T_2A^{M-1}T_2(x_0, p_0) \end{aligned} \quad (2.67)$$

by the fixed point property. Now the involution property implies

$$T_2A = T_1 \quad AT_1 = T_2 \quad (2.68)$$

and thus

$$AT_2AT_2 = AT_1T_2 = \mathbf{1} \quad (2.69)$$

and

$$A^P T_2 A^P T_2 = A^{P-1} T_2 A^{P-1} T_2 \quad (2.70)$$

from which it easily follows that (x_0, p_0) belongs to a $2M$ cycle.

I see no $\mathcal{J} = \tilde{\mathcal{J}}^\top \tilde{\mathcal{J}}$ factorization in style of (4.40)

click to return: p. 112

2.5 *

Exercises boy scout

2CB

2.1. Inverse iteration method for a Hénon repeller.

^{18 19} Consider the Hénon map (15.14) for the area-preserving (“Hamiltonian”) parameter value $b = -1$. The coordinates of a periodic orbit of length n_p satisfy the equation

$$x_{p,i+1} + x_{p,i-1} = 1 - ax_{p,i}^2, \quad i = 1, \dots, n_p, \quad (2.71)$$

with the periodic boundary condition $x_{p,0} = x_{p,n_p}$. Verify that the itineraries and the stabilities of the short periodic orbits for the Hénon repeller (2.71) at $a = 6$ are as listed in table 2.4.

Hint: you can use any cycle-searching routine you wish, but for the complete repeller case (all binary sequences are realized), the cycles can be evaluated by inverse iteration $x_{p,i}^{(m+1)} \rightarrow x_{p,i}^\infty = x_{p,i}$, estimating the midpoint by square-root of (2.71)

$$x_{p,i}^{(m+1)} = \sigma_{p,i} \sqrt{\frac{1 - x_{p,i+1}^{(m)} - x_{p,i-1}^{(m)}}{a}}. \quad (2.72)$$

Here $\sigma_{p,i}$ are the signs of the corresponding periodic point coordinates, $\sigma_{p,i} = x_{p,i}/|x_{p,i}|$, related in the obvious way to desired periodic orbit’s binary itinerary,

$$\sigma_i + 1 = 2 m_i, \quad m_i \in \{0, 1\}. \quad (2.73)$$

see figure 2.2.

G. Vattay

¹⁸Predrag 14oct2021: Return to ChaosBook eventually

¹⁹Predrag 27dec2004: give the center of mass paper reference somewhere

Table 2.4: All periodic orbits up to $n = 6$ for the Hamiltonian Hénon map repeller (2.71) with $a = 6$. Listed are the cycle itinerary, its expanding eigenvalue Λ_p , and its “center of mass.” The “center of mass” is listed because it turns out that it is often a simple rational or a quadratic irrational. All orbits up to topological length $n = 20$ have been computed.

p	Λ_p	$\sum x_{p,i}$
0	0.715168×10^1	-0.607625
1	-0.295285×10^1	0.274292
10	-0.989898×10^1	0.333333
100	-0.131907×10^3	-0.206011
110	0.558970×10^2	0.539345
1000	-0.104430×10^4	-0.816497
1100	0.577998×10^4	0.000000
1110	-0.103688×10^3	0.816497
10000	-0.760653×10^4	-1.426032
11000	0.444552×10^4	-0.606654
10100	0.770202×10^3	0.151375
11100	-0.710688×10^3	0.248463
11010	-0.589499×10^3	0.870695
11110	0.390994×10^3	1.095485
100000	-0.545745×10^5	-2.034134
110000	0.322221×10^5	-1.215250
101000	0.513762×10^4	-0.450662
111000	-0.478461×10^4	-0.366025
110100	-0.639400×10^4	0.333333
101100	-0.639400×10^4	0.333333
111100	0.390194×10^4	0.548583
111010	0.109491×10^4	1.151463
111110	-0.104338×10^4	1.366025

- 2.2. “Center of mass” puzzle. Why is the “center of mass,” tabulated in exercise 2.1, often a rational number?

Chapter 2. Hénon map

Solution 2.1 - Inverse iteration method for a Hamiltonian repeller. For the complete repeller case (all binary sequences are realized), the cycles can be evaluated variationally, as follows. According to (15.14), the coordinates of a periodic orbit of length n_p satisfy the equation

$$x_{p,i+1} + x_{p,i-1} = 1 - ax_{p,i}^2, \quad i = 1, \dots, n_p, \quad (2.74)$$

with the periodic boundary condition $x_{p,0} = x_{p,n_p}$.

In the complete repeller case, the Hénon map is a realization of the Smale horseshoe, and the symbolic dynamics has a very simple description in terms of the binary alphabet $\epsilon \in \{0, 1\}$, $\epsilon_{p,i} = (1+S_{p,i})/2$, where $S_{p,i}$ are the signs of the corresponding periodic point coordinates, $S_{p,i} = x_{p,i}/|x_{p,i}|$. We start with a preassigned sign sequence $S_{p,1}, S_{p,2}, \dots, S_{p,n_p}$, and a good initial guess for the coordinates $x'_{p,i}$. Using the inverse of the equation (2.71)

$$x''_{p,i} = S_{p,i} \sqrt{\frac{1 - x'_{p,i+1} - x'_{p,i-1}}{a}} \quad i = 1, \dots, n_p$$

we converge iteratively, at exponential rate, to the desired periodic points $x_{p,i}$. Given the periodic points, the cycle stabilities and periods are easily computed using (3.52). The itineraries and the stabilities of the short periodic orbits for the Hénon repeller (2.74) for $a = 6$ are listed in table 2.4; in actual calculations all orbits up to topological length $n = 20$ have been computed.

G. Vattay

Chapter 3

LC21: A chaotic lattice field theory in one dimension

3.1 LC21: Introduction

We use lattice-discretized scalar field theories, in particular spatiotemporal cat, Hénon ϕ^3 and ϕ^4 theories to explain how to reformulate dynamics of spatiotemporally ‘chaotic’ or ‘turbulent’ PDEs in

Motivated by a Gutzwiller’s ideas of periodic orbits of deterministic dynamics serving as WKB ‘skeleton’ for chaotic quantum mechanics, in this paper we focus on deterministic chaotic field theory.

We abandon initial state evolution, local in time, and seek instead to determine global solutions compatible with system’s defining equations.

The reformulation aligns ‘chaos theory’ with the standard solid state, field theory and statistical mechanics partition functions, related to the well-known forward-in-time Gutzwiller trace formulas by Hill’s formulas.

In spatiotemporal, crystallographer formulation, time-periodic orbits of dynamical systems theory are replaced by periodic d -dimensional Bravais cell tilings (d -tori) of spacetime. In contrast to conventional solid state calculations, due to hyperbolic shadowing of large cells by smaller ones, the predictions of the theory are dominated by the smallest Bravais cells.

In the field-theoretical formulation, there is no evolution in time, and there is no ‘Lyapunov horizon’; every contributing *lattice state* is a robust global solution of a spatiotemporal fixed point condition.

CHAPTER 3. LC21: A CHAOTIC LATTICE FIELD THEORY IN ONE DIMENSION

The form of the partition function of a given field theory is determined by the group of its spatiotemporal symmetries, i.e., by the space group of its lattice discretization, and its reciprocal lattice.

In particular, from a spatiotemporal field theory perspective, ‘time’-reversal is a purely crystallographic notion, a reflection point group, leading to a perhaps unfamiliar symmetry quotienting of time-reversible theories.

The theory is compactly summarized by its topological zeta function that counts Bravais lattices.

On the level of counting lattice-states, their topological zeta functions are purely group-theoretic Lind zeta functions.

Dedicated to Fritz Haake 1941–2019 [73]

The year was 1988. Roberto Artuso, Erik Aurell and P.C. had just worked out the cycle expansions formulation of the deterministic and semiclassical chaotic systems [7, 8], and a Niels Bohr Institute “Quantum Chaos Symposium” was organized to introduce the new-fangled theory to unbelievers (for a history, see [ChaosBook Append. A.4 Periodic orbit theory](#)). In the first row of the famed auditorium, where long ago Niels Bohr and his colleagues used to nod off, sat a man with an impressive butterfly and a big smile. At the end of our presentation, Fritz –for that was Fritz Haake– stood up and exclaimed

“Amazing! I did not understand a single word!”

And indeed, there is a problem of understanding what is ‘chaos’ as encountered in different disciplines, so we start this offering to Fritz Haake’s memory by ‘a fair coin toss’ theory of chaos, sect. 3.3, as was presented in the 1988 symposium, but in a modern, field theorist’s vision. In those days ‘chaos’ was a phenomenon exhibited by low-dimensional systems. In this and companion papers [43, 79] we explain how to think of ‘chaotic’ or ‘turbulent’ ∞ -dimensional deterministic field theories. Chaotic field theory is of interest on its merits, as a method of describing turbulence in strongly nonlinear deterministic field theories, such as Navier-Stokes or Kuramoto-Sivashinsky [78, 79], or as a Gutzwiller WKB ‘skeleton’ for a chaotic quantum field theory [32, 82] or a stochastic field theory [40, 41, 44, 45, 102]. The lattice reformulation aligns ‘chaos’ with standard solid state, field theory and statistical mechanics, but the claims are radical: we’ve been doing ‘turbulence’ all wrong. In “explaining” chaos we talk the talk as though we have never moved beyond Newton; here is an initial state of a system, at an instant in time, and here are the differential equations that evolve it forward in time. But when we -all of us- walk the walk, we do something altogether different (see the references preceding (7.1)), much closer to the 20th century spacetime physics. Our papers realign the theory to what we actually *do* when solving ‘chaos’ equations, using not much more than linear algebra. In the field-theoretical formulation, there is no evolution in time, and there is no ‘Lyapunov horizon’; every contributing *lattice*

state is a robust global solution of a spatiotemporal fixed point condition, there is no dynamicist's exponential blowup of initial state perturbations.

To a field theorist, the fundamental object is *global*, the partition function sum over probabilities of all possible spacetime field configurations. To a dynamicist, the fundamental notion is *local*, an ordinary or partial differential time-evolution equation. From the field-theoretic perspective, the spacetime formulation is fundamental, elegant and computationally powerful, while moving in step-lock with time is only one of the methods, an inelegant 'transfer matrix' method for construction of the partition sum, awkward and computationally unstable. The two ways of constructing partition sums are related by Hill's formulas, sect. 3.9. Hill's formula says that a higher-order derivative equation can be written as a set of first order ODEs, a relation equally applicable to mechanical, energy conserving systems, as to the viscous, dissipative systems.

As a gentle introduction for a reader too busy [33] to study the book [37], we disguise a brief course on chaos theory as something everyone understands, a Bernoulli coin toss, sect. 3.3. In sect. 3.3.2 we reformulate the forward-in-time Bernoulli map as the 'temporal Bernoulli' discrete lattice problem.

The second time, as a 'temporal cat', a 1-dimensional lattice of coupled rotors that all dynamicists understand, sect. 3.4. In sect. 3.4.2 we introduce the 'temporal cat', a lattice reformulation of the cat map.

Its spacetime generalization, the simplest of all chaotic field theories, the 'spatiotemporal cat' [43, 80, 81], is a discretization of the Klein-Gordon equation, a deterministic scalar field theory on a d -dimensional hyper-cubic lattice, with an unstable "anti-harmonic" rotor ϕ_z at each lattice site z , a rotor that gives, rather than pushes back, coupled to its nearest neighbors. In contrast to its elliptic sister, the Helmholtz equation and its oscillatory solutions, spatiotemporal cat's lattice states are hyperbolic and 'turbulent', just as in contrast to oscillations of a harmonic oscillator, Bernoulli coin flips are unstable and chaotic.

The third time, we generalize the approach in sect. 3.5 to nonlinear field theories.

The deep insight here is the realization that the *Hill determinant*, i.e., the volume of the *orbit Jacobian matrix* (figure 3.7 and 3.8) partitions system's state space.

The deep insight here is that the two formulations of mechanics, the forward-in-time Hamiltonian evolution, and the global, Lagrangian, temporal cat formulation are related by the *Hill's formula*.

Next, we address two questions: (i) how is the high-dimensional orbit Jacobian matrix \mathcal{J} related to the temporal $[d \times d]$ Jacobian matrix \mathbb{J} ? (sect. 3.9), and (ii) how does one evaluate the orbit Jacobian matrix \mathcal{J} ? (sects. 3.8.4 and 3.8.4).

In sect. 3.10 we show that the partition function of a given field theory is determined by the group of its symmetries, i.e., by the space group of its lattice discretization, and its reciprocal lattice, sect. 3.8.4. In particular, from a spatiotemporal field theory perspective, 'time'-reversal is a purely crystallographic notion, leading to a perhaps unfamiliar symmetry quotienting of 'time-

reversible' theories.

The theory is compactly summarized by its topological zeta function (3.190) that counts Bravais lattices.

On the level of counting lattice-states, their topological zeta functions are purely group-theoretic Lind zeta functions, see sect. 3.13.

Our results are summarized and open problems discussed in the sect. 3.14.

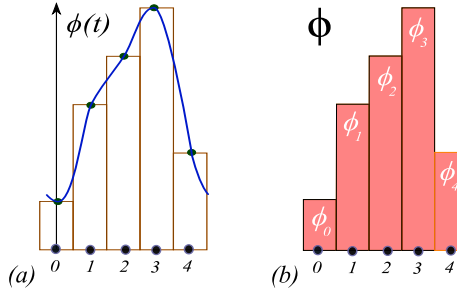


Figure 3.1: (Color online) Discretization of a 1-dimensional field theory. Horizontal: t coordinate, with lattice sites marked by dots and labelled by $t \in \mathbb{Z}$. (a) A periodic field $\phi(t)$, plotted as a function of continuous coordinate t . (b) A corresponding discretized period-5 lattice state $\Phi = \overline{\phi_0\phi_1\phi_2\phi_3\phi_4}$, with discretized field ϕ_t plotted as a bar centred at lattice site t . In what follows we use ‘lattice units’ $a = 1$.

3.2 Deterministic lattice field theory

A scalar field $\phi(x)$ over d Euclidean coordinates can be discretized by replacing the continuous space by a d -dimensional hypercubic integer lattice \mathcal{L} , with lattice spacing a , and evaluating the field only on the lattice points [111, 113]

$$\phi_z = \phi(x), \quad x = az = \text{lattice point}, \quad z \in \mathbb{Z}^d, \quad (3.1)$$

see figure 3.1. A given *field configuration* (here in one spatiotemporal dimension)

$$\Phi = \cdots \phi_{-3}\phi_{-2}\phi_{-1}\phi_0\phi_1\phi_2\phi_3\phi_4 \cdots, \quad (3.2)$$

taking any value in system’s ∞ -dimensional *state space* $\phi_z \in \mathbb{R}$, occurs with probability

$$p(\Phi) = \frac{1}{Z} e^{-S[\Phi]}, \quad Z = Z[0]. \quad (3.3)$$

Here Z is a normalization factor, given by the *partition function*, the integral over probabilities of all configurations,

$$Z[\mathbf{M}] = \int d\Phi e^{-S[\Phi] + \Phi \cdot \mathbf{M}}, \quad d\Phi = \prod_z^{\mathcal{L}} d\phi_z, \quad (3.4)$$

where $\mathbf{M} = \{m_z\}$ is an external ‘source’ that one can twiddle at will, site-by-site, and $S[\Phi]$ is the action that defines the theory. The dimension of the partition function integral is the number of lattice sites $N_{\mathcal{L}}$.

Motivated by WKB ‘semi-classical’ or saddle-point approximations [82] to the partition function (3.4), in this paper we describe their deterministic underpinning, the corresponding *deterministic* field theory, with partition function

built from solutions to the variational saddle-point condition

$$F[\Phi_c]_z = -S[\Phi_c]_z + m_z = 0, \quad S[\Phi]_z = \frac{\delta S[\Phi]}{\delta \phi_z}, \quad (3.5)$$

with a global deterministic solution Φ_c satisfying this local extremal condition on every lattice site. In order to distinguish a *solution* to the Euler–Lagrange equations (3.5) from an arbitrary *field configuration* (3.2), we refer to the solutions as *lattice states*, each a set of lattice site field values

$$\Phi_c = \{\phi_z\}, \quad (3.6)$$

that satisfies the local condition (3.5) globally, over all lattice sites. For a finite lattice segment Φ , one needs to specify the boundary conditions (bc's). The companion article ref. [80] tackles the Dirichlet bc's, a difficult, time-translation symmetry breaking, and from the periodic orbit theory perspective, a wholly unnecessary, self-inflicted pain. All that one needs to solve the temporal cat are the T -periodic, time-translation enforced bc's that we shall use here.¹ An example is the 1 spatiotemporal dimension block of fields of period $n = 5$ sketched in figure 3.1 (b),

$$\Phi_c = \overline{\phi_0 \phi_1 \phi_2 \phi_3 \cdots \phi_{n-1}}, \quad (3.7)$$

with its infinite repetition –for a sketch, see figure 3.11 (1)– denoted by an overbar. The first field value ϕ_0 in the block is evaluated on the lattice site 0, the second ϕ_1 on the lattice site 1, the n th $\phi_n = \phi_0$ on the lattice site n , with k th lattice site field value $\phi_k = \phi_\ell$, where $\ell = k \text{ (mod } n)$.

What we call here a chaotic ‘field’ at a discretized spacetime lattice site z , a solid state physicist would call the state of a ‘particle’ at crystal site z , coupled to its nearest neighbors. A solid state physicist endeavours to understand N -particle chaotic systems in many-body or ‘large N ’ settings, where in practice any N larger than 2 is ‘large’. Chaotic field theory is *ab initio* formulated for infinite time and infinite space lattice, but its periodic theory description is –thanks to hyperbolicity– computationally powerful already for $N = 2, 3, \dots$, where N is the number of sites in Bravais cells that tile the spacetime.

Each lattice state is a distinct deterministic solution Φ_c to the discretized Euler–Lagrange equations (3.5), so its probability is a N_L -dimensional Dirac delta function (that’s what we mean by the system being *deterministic*)

$$p_c(\Phi) = \frac{1}{Z} \delta(F[\Phi_c - \Phi]). \quad (3.8)$$

In sect. 3.9.1 we verify that this definition agrees with the customary forward-in-time Perron-Frobenius probability evolution [39] (see [ChaosBook sect. 19.2](#)). The new, field-theoretical formulation is vastly preferable to the forward-in-time formulation when it comes to higher spatiotemporal dimensions [43].

¹Predrag 2020-02-08: Complain about that stupidity clearly both in the intro and in conclusions.

As is case for a WKB approximation [82], the deterministic field theory partition sum has support only on lattice field values that are solutions to the variational saddle-point condition (3.5), and the partition function (3.3) is now a sum over configuration state space (3.2) *points*,

$$\begin{aligned} Z_c[M] &= \sum_c e^{N_L W_c[M]} \\ e^{N_L W_c[M]} &= \int_{\mathcal{M}_c} d\Phi \delta(F[\Phi]) = \frac{1}{|\text{Det } \mathcal{J}_c|}, \end{aligned} \quad (3.9)$$

where \mathcal{M}_c is a small neighborhood of Φ_c , and we refer to the $[N_c \times N_c]$ matrix of second derivatives

$$(\mathcal{J}_c)_{z'z} = \frac{\delta F[\Phi_c]_{z'}}{\delta \phi_z} = S[\Phi_c]_{z'z} \quad (3.10)$$

as the *orbit Jacobian matrix*.

In what follows, we shall almost exclusively deal only with deterministic field theory and omit the subscript ‘ c ’ in Φ_c throughout.

3.2.1 Lattice Laplacian

Let's have a look at the lattice free field theory action

$$S_0[\Phi] = \frac{1}{2} \Phi^\top (-\square + \mu^2 1) \Phi, \quad (3.11)$$

where the ‘discrete Laplace operator’, ‘central difference operator’, or the ‘graph Laplacian’ [27, 74, 112, 123, 126, 127]

$$\square \phi_z = \sum_{||z'-z||=1} (\phi_{z'} - \phi_z) \text{ for all } z, z' \in \mathcal{L} \quad (3.12)$$

is the average of the lattice field variation $\phi_{z'} - \phi_z$ over the sites nearest to the site z . For example, for a hypercubic lattice in one and two dimensions this discretized Laplacian is given by

$$\square \phi_t = \phi_{t+1} - 2\phi_t + \phi_{t-1} \quad (3.13)$$

$$\square \phi_{jt} = \phi_{j,t+1} + \phi_{j+1,t} - 4\phi_{jt} + \phi_{j,t-1} + \phi_{j-1,t}. \quad (3.14)$$

For action (3.11) this is the discretized screened Poisson equation [64], also known as the Yukawa or Klein–Gordon equation, where $\mu^2 > 0$ is the Klein–Gordon mass-squared. An example is the Gutkin and Osipov [81] spatiotemporal cat in $d = 2$ dimensions [43], an Arnold cat map-inspired scalar field theory of form (3.11) for which the Euler–Lagrange equation (3.5) is a 5-term recurrence relation

$$-\phi_{j,t+1} - \phi_{j,t-1} + 2s\phi_{jt} - \phi_{j+1,t} - \phi_{j-1,t} = m_{jt}, \quad (3.15)$$

where we refer to parameter s , related to the Klein–Gordon mass in (3.11) by $\mu^2 = d(s - 2)$, as the ‘stretching parameter’.

3.2.2 1-dimensional lattice field theories

Discrete time evolution is frequently recast into a 1-dimensional temporal lattice field theory form, essentially by anyone who rewrites a dynamical systems discrete time evolution problem as a k -point recurrence, for example in refs. [40, 41, 45, 63]. As already in one spatiotemporal dimension there is much to be learned about the role symmetries play in solving lattice field theories, that is what we will focus on in this paper (time-reversal sects. 3.10 and 3.13), with the 2-dimensional spatiotemporal field theories discussed in the sequel [43].

We shall consider scalar field theories of polynomial type, with a local potential [2–4, 55, 66, 97]

$$V(\phi_t) = \frac{g}{k} \phi_t^k - m_t \phi_t \quad (3.16)$$

on each 1-dimensional lattice site t added to the free field theory action (3.11). The discrete Euler–Lagrange equations (3.5) now take form of 3-term recurrence, second-order difference equations

$$-\phi_{t+1} + V'(\phi_t) - \phi_{t-1} = 0. \quad (3.17)$$

We start with the first order difference equation that we call ‘temporal Bernoulli’ (sect. 3.3),

$$-\phi_{t+1} + s \phi_t = m_t \quad (3.18)$$

in order to motivate the second-order difference Euler–Lagrange equations (3.17) that we call, in the cases considered here, the ‘temporal cat’ (sect. 3.4), ‘temporal Hénon’ (sect. 3.5), and ‘temporal ϕ^4 theory’ (sect. 3.6), respectively:

$$-\phi_{t+1} + s \phi_t - \phi_{t-1} = m_t \quad (3.19)$$

$$-\phi_{t+1} + a \phi_t^2 - \phi_{t-1} = m_t \quad (3.20)$$

$$-\phi_{t+1} + g \phi_t^3 - \phi_{t-1} = m_t \quad (3.21)$$

Qualifier ‘temporal’ is used here to emphasize that we view 1-dimensional examples as special cases of ‘spatiotemporal’ field theories; much of our methodology for d -dimensional deterministic field theories can be profitably explained by working out 1-dimensional field theories. Lurking here is the totality of the map-iteration dynamical systems theory, but the reader will find it more profitable, and less confusing, to think of these simply as lattice problems, and forget that the index t often stands for ‘time’.

So, what is a ‘chaotic’, or ‘turbulent’ field theory? As we shall see, all of the above, as well as their higher-dimensional spatiotemporal siblings are ‘chaotic’ for sufficiently strong ‘stretching parameters’ or ‘coupling constants’ s , a or g . Our goal here is to make this ‘spatiotemporal chaos’ tangible and precise, by acquainting the reader what we believe are some of the simplest, most elegant examples chaotic field theories.

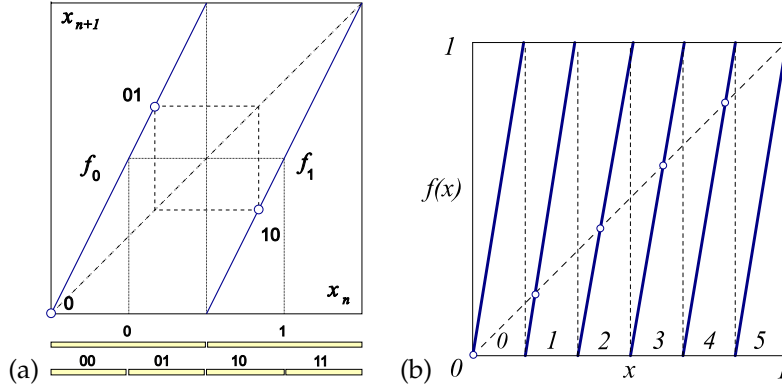


Figure 3.2: (Color online) (a) The ‘coin toss’ map (3.22), together with the $\bar{0}$ fixed point, and the $\bar{0}\bar{1}$ 2-cycle. Preimages of the critical point $x_c = 1/2$ partition the unit interval into $\{\mathcal{M}_0, \mathcal{M}_1\}, \{\mathcal{M}_{00}, \mathcal{M}_{01}, \mathcal{M}_{10}, \mathcal{M}_{11}\}, \dots$, subintervals. (b) The base- s Bernoulli map, here with the ‘dice throw’ stretching parameter $s = 6$, partitions the unit interval into 6 subintervals $\{\mathcal{M}_m\}$, labeled by the 6-letter alphabet (3.26). As the map is a circle map, $x_5 = 1 = 0 = x_0 \pmod{1}$.

3.3 A fair coin toss

The very simplest example of a deterministic law of evolution that gives rise to ‘chaos’ is the *Bernoulli map*, figure 3.2(a), which models a [coin toss](#). Starting with a random initial state, the map generates, deterministically, a sequence of tails and heads with the 50-50% probability.

We introduce the model in its conventional, time-evolution dynamical formulation, than reformulate it as a lattice field theory, solved by enumeration of all admissible *lattice states*, field configurations that satisfy a global fixed point condition, and use this simple setting to motivate (1) the *fundamental fact*: for a given lattice period, the *Hill determinant* of stabilities of global solutions counts their number (sect. 3.8.3), and (2) the topological zeta function counts their translational symmetry group orbits (sect. 3.12).

3.3.1 Bernoulli map

The base-2 *Bernoulli shift map*,

$$x_{t+1} = \begin{cases} f_0(x_t) = 2x_t, & x_t \in \mathcal{M}_0 = [0, 1/2) \\ f_1(x_t) = 2x_t \pmod{1}, & x_t \in \mathcal{M}_1 = [1/2, 1) \end{cases}, \quad (3.22)$$

is shown in figure 3.2(a). If the linear part of such map has an integer-valued slope, or ‘stretching’ parameter $s \geq 2$,

$$x_{t+1} = sx_t \quad (3.23)$$

that maps state x_t into a state in the ‘extended state space’, outside the unit interval, the (mod 1) operation results in the base- s Bernoulli circle map,

$$\phi_{t+1} = s\phi_t \pmod{1}, \quad (3.24)$$

sketched as a **dice throw** in figure 3.2(b). The (mod 1) operation subtracts $m_t = \lfloor s\phi_t \rfloor$, the integer part of $s\phi_t$, or the circle map *winding number*, to keep ϕ_{t+1} in the unit interval $[0, 1)$, and partitions the unit interval into s subintervals $\{\mathcal{M}_m\}$,

$$\phi_{t+1} = s\phi_t - m_t, \quad \phi_t \in \mathcal{M}_{m_t}, \quad (3.25)$$

where m_t takes values in the s -letter alphabet

$$m \in \mathcal{A} = \{0, 1, 2, \dots, s-1\}. \quad (3.26)$$

The Bernoulli map is a highly instructive example of a hyperbolic dynamical system. Its symbolic dynamics is simple: the base- s expansion of the initial point ϕ_0 is also its temporal itinerary, with symbols from alphabet (3.26) indicating that at time t the orbit visits the subinterval \mathcal{M}_{m_t} . The map is a ‘shift’: a multiplication by s acts on the base- s representation of $\phi_0 = .m_1m_2m_3\dots$ (for example, binary, if $s = 2$) by shifting its digits,

$$\phi_1 = f(\phi_0) = .m_2m_3\dots. \quad (3.27)$$

Periodic points can be counted by observing that the preimages of critical points $\{\phi_{c1}, \phi_{c2}, \dots, \phi_{cs-1}\} = \{1/s, 2/s, \dots, (s-1)/s\}$ partition the unit interval into $\{\mathcal{M}_0, \mathcal{M}_1, \dots, \mathcal{M}_{s-1}\}$, $\{\mathcal{M}_{m_1m_2}\}, \dots, s^n$ subintervals, each containing one unstable period- n periodic point $\phi_{m_1m_2\dots m_n}$, with stability multiplier s^n , see figure 3.2. The Bernoulli map is a full shift, in the sense that every itinerary is admissible, with one exception: on the circle, the rightmost fixed point is the same as the fixed point at the origin, $\phi_{s-1} = \phi_0 \pmod{1}$, so these fixed points are identified and counted as one, see figure 3.2. The total number of periodic points of period n is thus

$$N_n = s^n - 1. \quad (3.28)$$

3.3.2 Temporal Bernoulli

To motivate our formulation of a spatiotemporal chaotic field theory to be developed below, we now recast the local initial value, time-evolution Bernoulli map problem as a *temporal lattice* fixed point condition, the problem of enumerating and determining all global solutions.

‘Temporal’ here refers to the lattice site field ϕ_t and the source (winding number) m_t taking their values on the lattice sites of a 1-dimensional *temporal* integer lattice $t \in \mathbb{Z}$. Over a finite lattice segment, these can be written compactly as a *lattice state* and the corresponding *symbol block*

$$\Phi^\top = (\phi_{t+1}, \dots, \phi_{t+n}), \quad M^\top = (m_{t+1}, \dots, m_{t+n}), \quad (3.29)$$

where $(\dots)^\top$ denotes a transpose. The Bernoulli equation (3.25), rewritten as a first-order difference equation

$$-\phi_{t+1} + s\phi_t - m_t = 0, \quad \phi_t \in [0, 1], \quad (3.30)$$

takes the matrix form

$$\mathcal{J}\Phi - M = 0, \quad \mathcal{J} = -r + s\mathbf{1}, \quad (3.31)$$

where the $[n \times n]$ matrix

$$r_{jk} = \delta_{j+1,k}, \quad r = \begin{pmatrix} 0 & 1 & & & \\ & 0 & 1 & & \\ & & \ddots & & \\ & & & 0 & 1 \\ 1 & & & & 0 \end{pmatrix}, \quad (3.32)$$

implements the shift operation (3.27), a cyclic permutation that translates forward-in-time lattice state Φ by one site, $(r\Phi)^\top = (\phi_2, \phi_3, \dots, \phi_n, \phi_1)$. The time evolution law (3.25) must be of the same form for all times, so the shift operator r has to be time-translation invariant, with $r_{n+1,n} = r_{1n} = 1$ matrix element enforcing the periodicity. After n shifts, a lattice state returns to the initial state,

$$r^n = \mathbf{1}. \quad (3.33)$$

As the temporal Bernoulli condition (3.31) is a linear relation, a given block M , or ‘code’ in terms of alphabet (3.26), corresponds to a unique temporal lattice state Φ . That is why Percival and Vivaldi [123] refer to such symbol block M as a *linear code*.

3.3.3 Bernoulli as a continuous time dynamical system

The discrete time derivative of a lattice configuration Φ evaluated at the lattice site t is given by the difference operator [57]

$$\dot{\phi}_t = \left[\frac{\partial \Phi}{\partial t} \right]_t = \frac{\phi_{t+1} - \phi_t}{\Delta t}. \quad (3.34)$$

The temporal Bernoulli condition (3.31) can be thus viewed as a time-discretized, first-order ODE dynamical system

$$\dot{\Phi} = v(\Phi), \quad (3.35)$$

where the ‘velocity’ vector field v is given by

$$v(\Phi) = (s-1)\Phi - M,$$

with the time increment set to $\Delta t = 1$, and perturbations that grow (or decay) with rate $(s-1)$. By inspection of figure 3.2(a), it is clear that for *shrinking*,

$s < 1$ parameter values the orbit is stable forward-in-time, with a single linear branch, 1-letter alphabet $\mathcal{A} = \{0\}$, and the only lattice states being the single fixed point $\phi_0 = 0$, and its repeats $\Phi = (0, 0, \dots, 0)$. However, for *stretching*, $s > 1$ parameter values, the Bernoulli system (more generally, Rényi's beta transformations [128]) that we study here, every lattice state Φ_M is unstable, and there is a lattice state for each admissible symbol block M .²

A fair coin toss, summarized. We refer to the *global* temporal lattice condition (3.31) as the '*temporal* Bernoulli', in order to distinguish it from the one-time step Bernoulli evolution map (3.24), in preparation for the study of *spatiotemporal* systems to be undertaken in ref. [43]. In the lattice formulation, a *global* temporal lattice state Φ_M is determined by the requirement that the *local* temporal lattice condition (3.30) is satisfied at every lattice site. In spatiotemporal formulation there is no need for forward-in-time, close recurrence searches for the returning periodic points. Instead, one determines each global temporal lattice state Φ_M at one go, by solving the fixed point condition (3.77). The most importantly for what follows, the spatiotemporal field theory of ref. [43], this calculation requires no recourse to any *explicit coordinatization and partitioning of system's state space*, and *no explicit symbolic dynamics*.³

3.4 A kicked rotor

Temporal Bernoulli is perhaps the simplest chaotic lattice field theory. Our next task is to formulate a deterministic spatiotemporally chaotic field theory, Hamiltonian and energy conserving, because (a) that is physics, and (b) one cannot do quantum theory without it. We need a system as simple as the Bernoulli map, but mechanical. So, we move on from running in circles, to a mechanical rotor to kick.

The 1-degree of freedom maps that describe kicked rotors subject to discrete time sequences of angle-dependent force pulses $P(q_t)$, $t \in \mathbb{Z}$,

$$q_{t+1} = q_t + p_{t+1} \pmod{1}, \quad (3.36)$$

$$p_{t+1} = p_t + P(q_t), \quad (3.37)$$

with $2\pi q$ the angle of the rotor, p the momentum conjugate to the angular coordinate q , and the angular pulse $P(q_t) = P(q_{t+1}) = -V'(q_t)$ lattice periodic with period 1, play a key role in the theory of deterministic and quantum chaos in atomic physics, from the Taylor, Chirikov and Greene standard map [24, 99], to the cat maps that we turn to now. The equations are of the Hamiltonian form: eq. (3.36) is $\dot{q} = p/m$ in terms of discrete time derivative (3.34), i.e., the configuration trajectory starting at q_t reaches $q_{t+1} = q_t + p_{t+1}\Delta t/m$ in one time step Δt . Eq. (3.37) is the time-discretized $\dot{p} = -\partial V(q)/\partial q$: at each kick the angular momentum p_t is accelerated to p_{t+1} by the force pulse $P(q_t)\Delta t$, with the time step and the rotor mass set to $\Delta t = 1$, $m = 1$.

²Predrag 2021-08-23: Should we include "Quotienting the temporal Bernoulli system" (1.85)?

³Predrag 2020-12-17: Link to the ChaosBook. Maybe refer to Adler-Weiss.

3.4.1 Cat map

The simplest kicked rotor is subject to force pulses $P(q) = \kappa q$ proportional to the angular displacement q : in that case, the map (3.36,3.37) is of form

$$\begin{pmatrix} q_{t+1} \\ p_{t+1} \end{pmatrix} = \mathbb{J} \begin{pmatrix} q_t \\ p_t \end{pmatrix} \pmod{1}, \quad \mathbb{J} = \begin{pmatrix} \kappa + 1 & 1 \\ \kappa & 1 \end{pmatrix}. \quad (3.38)$$

The $(\text{mod } 1)$ makes the map a discontinuous ‘sawtooth,’ unless κ is a positive integer. The map is then a Continuous Automorphism of the Torus known as the Thom-Anosov-Arnol’d-Sinai ‘cat map’ [5, 46, 137], extensively studied as the simplest example of a chaotic Hamiltonian system.

The determinant of the one-time-step Jacobian is $\det \mathbb{J} = 1$, i.e., the mapping is area-preserving. Let $s = \text{tr } \mathbb{J} = \kappa + 2$ be the trace of the Jacobian. For $|s| > 2$ the \mathbb{J} characteristic equation

$$\Lambda^2 - s\Lambda + 1 = 0, \quad (3.39)$$

has real roots (Λ, Λ^{-1}) and a positive Lyapunov exponent $\lambda > 0$,

$$\Lambda = e^\lambda = \frac{1}{2}(s + \sqrt{(s-2)(s+2)}), \quad s = \text{tr } \mathbb{J} = \Lambda + \Lambda^{-1}. \quad (3.40)$$

The eigenvalues are functions of the stretching parameter s , and for $|s| > 2$ the cat map (3.38) is a fully chaotic Hamiltonian dynamical system.

3.4.2 Temporal cat

In order to motivate our formulation of higher-dimensional spatiotemporal chaotic field theories, to be developed in ref. [43], we now recast the *local* initial value, Hamiltonian time-evolution as a *global* solution to the Euler–Lagrange equations.

The 2-component field at the temporal lattice site t , $\phi_t = (q_t, p_t) \in (0, 1] \times (0, 1]$ is kicked rotor’s the angular position and momentum. Hamilton’s equations (3.36,3.37) induce forward-in-time evolution on a 2-torus (q_t, p_t) phase space. Eliminating the momentum by Hamilton’s discrete time velocity eq. (3.36),

$$(q_t, p_t) = \left(\phi_t, \frac{\phi_t - \phi_{t-1}}{\Delta t} \right), \quad (3.41)$$

and setting the time step to $\Delta t = 1$, the forward-in-time Hamilton’s first order difference equations are brought to the second order difference, 3-term recurrence Euler–Lagrange equations for scalar field $\phi_t = q_t$,

$$\phi_{t+1} - 2\phi_t + \phi_{t-1} = P(\phi_t). \quad (3.42)$$

But that is Newton’s Second Law: “acceleration equals force,” so Percival and Vivaldi [123] refer to this formulation as ‘Newtonian’. Here we follow Allroth [1], Mackay, Meiss, Percival, Kook & Dullin [54, 94, 106–108], and Li and Tomsovic [96] in referring to it as ‘Lagrangian’.

For the cat map (3.38), the Lagrangian passage (3.41) to the scalar field ϕ_t leads to the Percival-Vivaldi ‘two-configuration representation’ [123]

$$\begin{pmatrix} \phi_t \\ \phi_{t+1} \end{pmatrix} = \mathbb{J}_{PV} \begin{pmatrix} \phi_{t-1} \\ \phi_t \end{pmatrix} - \begin{pmatrix} 0 \\ m_t \end{pmatrix}, \quad \mathbb{J}_{PV} = \begin{pmatrix} 0 & 1 \\ -1 & s \end{pmatrix}, \quad (3.43)$$

with matrix \mathbb{J}_{PV} acting on the 2-dimensional space of successive configuration points $(\phi_{t-1}, \phi_t)^\top$. As was case for the Bernoulli map (3.30), the cat map (mod 1) condition (3.38) is enforced by integers $m_t \in \mathcal{A}$, where for a given integer stretching parameter s the alphabet \mathcal{A} ranges over $|\mathcal{A}| = s+1$ possible values for m_t ,

$$\mathcal{A} = \{\underline{1}, 0, \dots, s-1\}, \quad (3.44)$$

necessary to keep ϕ_t for all times t within the unit interval $[0, 1]$. (We find it convenient to have symbol \underline{m}_t denote m_t with the negative sign, i.e., ‘ $\underline{1}$ ’ stands for symbol ‘ -1 ’.)

Written out as a second-order difference equation, the Percival-Vivaldi map (3.43) takes a particularly elegant form, that we shall refer to as the *temporal cat* (3.19),

$$-\phi_{t+1} + s\phi_t - \phi_{t-1} = m_t, \quad (3.45)$$

or, in terms of a lattice state Φ , the corresponding symbol block M (3.29), and the $[n \times n]$ shift operator r (3.32),

$$(-r + s\mathbb{1} - r^{-1})\Phi = M, \quad (3.46)$$

very much like the temporal Bernoulli condition (3.31), and the winding numbers (sources) M taking their values on the lattice sites of a 1-dimensional *temporal lattice* $t \in \mathbb{Z}$.

As was the case for temporal Bernoulli (3.31), the condition (3.43) is a linear relation: a given ‘code’ $\{m_t\}$ in terms of alphabet (3.44) corresponds to a unique temporal sequence $\{\phi_t\}$. That is why Percival and Vivaldi [123] refer to such symbol block M as a *linear code*. As for the Bernoulli system, m_t can also be interpreted as ‘winding numbers’ [92], or, as they shepherd stray points back into the unit torus, as ‘stabilising impulses’ [123]. Here we use the field-theoretical parlance, and refer to them as ‘sources’.

3.4.3 Temporal cat as a continuous time dynamical system

Recall that the Bernoulli first-order difference equation could be viewed as a time-discretization of the first-order linear ODE (3.35). The second-order difference equation (3.45) can be interpreted as the second order discrete time derivative d^2/dt^2 , or the temporal lattice Laplacian (3.13),

$$\square \phi_t \equiv \phi_{t+1} - 2\phi_t + \phi_{t-1} = (s-2)\phi_t - m_t, \quad (3.47)$$

with the time step set to $\Delta t = 1$. In other words, if we include the cat map forcing pulse (3.37) $P(\phi_t) = -V'(\phi_t) = -(s-2)\phi + m_t$ into the definition of

the on-site potential (3.17),

$$V(\Phi, M) = \sum_{t \in \mathcal{L}} \left(\frac{1}{2} \mu^2 \phi_t^2 - m_t \phi_t \right), \quad (3.48)$$

the force is linear in the angular displacement ϕ , so the temporal cat Euler–Lagrange equation takes form (see free action (3.11))

$$(-\square + \mu^2 \mathbf{1}) \Phi = M, \quad (3.49)$$

where the Klein-Gordon mass μ is related to the cat-map stretching parameter s by $\mu^2 = s - 2$.

For small stretching parameter values, $s < 2$, this discretized Euler–Lagrange equation (3.5) describes a set of coupled penduli, with oscillatory solutions, known as the discrete Helmholtz equation in applied math [48, 64, 100], as the tight-binding model, the Harper’s or Azbel-Hofstadter model in solid state physics [29, 30, 56, 110, 122], and the critical almost Mathieu operator in mathematical physics [131], with quadratic action (3.11) written as Hamiltonian

$$H = \sum_{\ell} |\ell\rangle \epsilon_0 \langle \ell| + \sum_{\ell m} |\ell\rangle V_{\ell m} \langle m|, \quad V_{\ell m} = \begin{cases} V & \text{if } \ell, m \text{ nearest neighbors} \\ 0 & \text{otherwise} \end{cases}$$

with the stretching factor $s = -\epsilon_0/V$ in (3.47).

Here we study the strong stretching, $s > 2$ case, known as the discrete screened Poisson equation [52, 64, 75, 87, 88, 127], whose solutions are hyperbolic. We refer to the Euler–Lagrange equation (3.49) as the ‘temporal cat’, both to distinguish it from the forward-in-time Hamiltonian cat map (3.38), and in the anticipation of the spatiotemporal cat to be discussed in the sequel ref. [43]. Spatiotemporal cat differs from all of the above model because the field ϕ_t compactification to unit circle makes it a strongly nonlinear deterministic field theory, with nontrivial symbolic dynamics.

Temporal cat, summarized. In the spatiotemporal formulation a *global* temporal lattice state

$$\Phi^\top = (\phi_t, \phi_{t+1}, \dots, \phi_{t+k}) \quad (3.50)$$

is not determined by a forward-in-time ‘cat map’ evolution (3.38), but rather by the fixed point condition (3.5) that the *local*, 3-term discrete temporal lattice Euler–Lagrange equations (3.45) are satisfied at every lattice point. This temporal 1-dimensional lattice reformulation is the bridge that takes us from the single cat map (3.38) to the higher-dimensional coupled “multi-cat” spatiotemporal lattices refs. [43, 80, 81].

And, did you know that the cute Arnold cat is but the screened Poisson equation in disguise? And that the lattice form (3.45) of the theory is so much more elegant than the cat-map form (3.38)? A cat is Hooke’s wild, ‘anti-harmonic’ sister. For $s < 2$ Hooke rules: restoring oscillations around the sleepy resting state. For $s > 2$ cats rule: exponential runaway, wrapped globally around a state space torus. Cat is to chaos what harmonic oscillator is to order. There is no more fundamental example of chaos in mechanics.

3.5 A ϕ^3 field theory

The ‘mod 1’ in the definition of the ‘linear’ kicked rotor, the cat map (3.38), makes cat map a highly nonlinear, discontinuous map. In contrast, field theory action $S[\Phi]$ is typically polynomial and smooth. The simplest such nonlinear action turns out to correspond to the paradigmatic dynamicist’s model of a 2-dimensional nonlinear dynamical system, the Hénon map [84]

$$\begin{aligned} x_{t+1} &= 1 - a x_t^2 + b y_t \\ y_{t+1} &= x_t. \end{aligned} \quad (3.51)$$

For the contraction parameter value $b = -1$ this is a Hamiltonian map.

The *temporal evolution* Jacobian matrix for the n th iterate of the Hamiltonian Hénon map is the product of consecutive one time-step Jacobian matrices

$$J^n(x_0, y_0) = \prod_{m=n-1}^0 \begin{pmatrix} -2a x_m & -1 \\ 1 & 0 \end{pmatrix}, \quad x_m = f_1^m(x_0, y_0), \quad (3.52)$$

where the successive 1-time step Jacobian matrices are multiplied in the order they are applied, as $J^n(x_0) = J(x_{n-1}) \cdots J(x_0)$. So, once we have a Hénon map periodic orbit, we also have its Floquet matrix (monodromy matrix). When J^n is hyperbolic, only the expanding eigenvalue $\Lambda_1 = 1/\Lambda_2$ needs to be determined, as the determinant of the Hénon 1-time step Jacobian matrix is unity,

$$\det J = \Lambda_1 \Lambda_2 = 1. \quad (3.53)$$

The map is Hamiltonian in the sense that it preserves areas in the $[x, y]$ plane.

The Hénon map is the simplest map that captures chaos that arises from the smooth stretch & fold dynamics of nonlinear return maps of flows such as Rössler [129]. Written as a 2nd-order inhomogeneous difference equation [55], (3.51) takes the *temporal Hénon* 3-term recurrence form, explicitly time-translation and time-reversal invariant Euler–Lagrange equation

$$-\phi_{t+1} + a\phi_t^2 - \phi_{t-1} = 1. \quad (3.54)$$

Just as the kicked rotor (3.36, 3.37), the map can be interpreted as a kicked driven anaharmonic oscillator [83], with the nonlinear, cubic Biham-Wenzel [13] lattice site potential (3.16)

$$V(\Phi, M) = \sum_{t \in \mathcal{L}} \left(\frac{a}{3} \phi_t^3 - m_t \phi_t \right), \quad m_t = -1, \quad (3.55)$$

giving rise to kicking pulse (3.37). ⁴ Devaney, Nitecki, Sterling and Meiss [47, 135, 136] have shown that the Hamiltonian Hénon map has a complete Smale horseshoe for sufficiently large ‘stretching parameter’ values

$$a > 5.699310786700 \dots . \quad (3.56)$$

⁴Predrag 2021-12-10: Note the cubic Biham-Wenzel potential includes the source term, as (3.17). Please recheck the signs!

In numerical [37] and analytic [61] calculations we fix (arbitrarily) the stretching parameter value to $a = 6$, in order to guarantee that all 2^n periodic points $\phi = f^n(\phi)$ of the Hénon map (3.51) exist.⁵
⁶

Politi and Torcini [125] note that a problem in reconstructing the statistical properties of an spatiotemporal Hénon attractor is ensuring that all invariant 2-tori used are embedded into the inertial manifold. For instance, in the single Hénon map, one of the two fixed points is isolated and it does not belong to the strange attractor.

We resolve this problem by construction, all our solutions belong to the non-wandering set.

Politi and Torcini [125] *Periodic orbits in coupled Hénon maps: Lyapunov and multifractal analysis*

They study *spatiotemporal Hénon*, a (1+1)-spacetime lattice of Hénon maps orbits which are periodic both in space and time.

Their numerical method is an extension of Biham and Wenzel [13] for the single Hénon map, with symbols m_{nt} in $\mathcal{A} = \{0, 1\}$. Any fixed point in fictitious time corresponds to a spatio-temporal cycle $[L \times T]_S$.

3.6 A ϕ^4 field theory

If a potential that is bounded from below is needed to make sense of the probabilistic interpretation of the configuration weight (3.3), or a symmetry forbids the odd-power potentials such as (3.55), one starts instead with a quartic potential $\sim g\phi_t^4$, leading to the ‘ ϕ^4 lattice field theory’ (3.21). As ϕ^4 example adds little to understanding over what is learned from temporal Hénon, we will not discuss is further in this paper.⁷

⁵Predrag 2021-12-10: Explain that ϕ^3 theory is correspond to the unimodal temporal Hénon, with the Smale horseshoe repeller cleanly split into the left (negative) and right (positive) lattice site field values. This is very much like the temporal Bernoulli, in contrast to the temporal cat which has nontrivial pruning, see table 4.1.

⁶Predrag 2021-06-04: S. Aubry [9] *Anti-integrability in dynamical and variational problems*

The equilibria and relative equilibria of Frenkel-Kontorova models [10, 112], widely studied in literature, might be closely related to temporal Hénon and ϕ^4 lattices.

D. G. Sterling [134] much (undeservedly) un-cited PhD thesis, Univ. of Colorado, *Anti-Integrable Continuation and the Destruction of Chaos* has much to teach us. He studies *coupled Hénon map lattices* in both Hamiltonian and Lagrangian formulations; his definition seems pretty much consistent with our (15.12), though he has a coupling parameter c used to make spatial couplings weak. The “anti-integrable” refers to our choice $a \geq 6$, I believe - parameter regimes in which all of the horseshoe orbits exists.

“Specifying the anti-integrable state for an orbit of a coupled map lattice requires a multidimensional symbolic object which we call a symbol tensor.”

His Figures 6.7, 6.18 are reminiscent of my pruning front.

Sterling and Meiss [136] *Computing periodic orbits using the anti-integrable limit*

⁷Predrag 2021-12-10: No! Explain that ϕ^4 theory is the bimodal extension of what we had learned for the unimodal temporal Hénon.

3.6.1 Computing lattice states for nonlinear theories

Unlike the temporal Bernoulli (3.18) and the temporal cat (3.19), for which the lattice state fixed point condition (3.5) is linear and easily solved, for nonlinear lattice field theories the lattice states are roots of polynomials of arbitrarily high order. While Gallas and collaborators [58–62, 68–70] have developed a powerful theory that yields Hénon map periodic orbits in analytic form, it would be unrealistic to demand such explicit solutions for general field theories on multi-dimensional lattices. We take a pragmatic, numerical route, and search for the fixed-point solutions (3.5) starting with the deviation of an approximate trajectory from the 3-term recurrence (3.17), given by the lattice deviation vector

$$v_t = -\phi_{t+1} + (V'(\phi_t) - m_t) - \phi_{t-1}, \quad (3.59)$$

and minimizing this error term by any convenient variational or optimization method, perhaps in conjunction with a high-dimensional variant of the Newton method [42, 95].⁹

3.6.2 Papers to refer to?

Simó [130] *On the Hénon-Pomeau attractor* is a very fine early paper. Cite it in Hénon remark.

Miguel, Simó and Vieir [109] *From the Hénon conservative map to the Chirikov standard map for large parameter values* ([click here](#)):

Endler and Gallas [62]. method resembles the methods earlier employed for quadratic polynomials (and their Julia sets) by Brown [19] and Stephenson [133].

The Hénon map/ ϕ^3 approaches should be safe for multimodal maps with complete repelling sets, and it should work for finite-grammar Smale horseshoe repellers. Smale's original horseshoe [132], his fig. 1 was unimodal, but he also explicitly gives our ϕ^4 bimodal repeller, his fig. 5.

⁸Predrag 2021-10-13: RECHECK, maybe applies to spatiotemporal cat: Equilibria or steady solutions of Frenkel-Kontorova lattices, the smooth function $V : \mathbb{R} \rightarrow \mathbb{R}$ is a periodic onsite potential, $V[\phi + 1] = V[\phi]$ for all $\xi \in \mathbb{R}$.

The d -dimensional Frenkel-Kontorova Hamiltonian lattice differential equation [10, 112]

$$\frac{d^2\phi_i}{dt^2} + V'[\phi_i] - \square\phi_i = 0 \text{ for all } i \in \mathbb{Z}^d. \quad (3.57)$$

describes the motion of particles under the competing influence of an onsite periodic potential field and nearest neighbor attraction.

the goal is to find a d -dimensional “lattice configuration” (for us, lattice state) $x : \mathbb{Z}^d \rightarrow \mathbb{R}$ that satisfies

$$V'[\phi_i] - \square\phi_i = 0 \text{ for all } i \in \mathbb{Z}^d. \quad (3.58)$$

Eq. (3.58) is relevant for statistical mechanics [112], because it is related to Eq. (??)FKeq) describes its stationary solutions.

⁹Predrag 2021-12-10: Form $(V'(\phi_t) - m_t)$ looks like the most convenient definition of the “ m -centered” subregion \mathcal{M}_m potential, applicable to both linear and nonlinear field theories?

*CHAPTER 3. LC21: A CHAOTIC LATTICE FIELD THEORY IN ONE
DIMENSION*

Brown gives cycles up to length 6 for the logistic map, employing symmetric functions of periodic points.

Hitzl and Zele [86] study the of the Hénon map for cycle lengths up to period 6.

3.7 Reciprocal lattice

ChaosBook conventions:

$$\begin{aligned}\omega &= e^{2i\pi/n} \\ \tilde{\phi}_k &= x_k + i y_k = |\tilde{\phi}_k| e^{i\theta_k} \\ q_k &= 2\pi k/n, \\ n &\text{ is the Bravais cell period}\end{aligned}$$

No self-respecting crystallographer would be drawing longer and longer Bravais lattice states (3.158)-(3.160) - they eventually run off the sheet of paper, no matter how wide. A professional crystallographer plots all lattice states snugly together in the first Brillouin zone, where the translational orbit of a lattice state is -literally- a circle, symmetric lattice states sit on boundaries of point group's fundamental domain, and everything is maximally diagonalized in terms of space group G irreps.

Still, when we think of a temporal lattice as 'time': no dynamicist does that. Embarrassing.

It is all breathtakingly simple on the reciprocal lattice. Period- n Bravais cell maps onto a regular n -gon in the reciprocal lattice, with the usual D_n symmetry axes. Time reversal fixes the symmetric solutions to sit on the symmetry axes, the boundaries of the fundamental domain. Lattice shift r_j maps out the G -orbit by running on circles, and orbits visit the $1/2n$ wedge only once, so the points in the fundamental domain represent an orbit each.

Here is a simple way to explain what the problem is:

Think of a discrete time dynamical system (iterations of a map) as a 1-dimensional lattice with the field on each site labeled by integer time. An period- n lattice state lives on a discrete 1-torus (a ring or necklace) of period- n , and if the law is time-independent, sets of solutions are invariant under cyclic perturbations. The symmetry is C_n , and one needs to distinguish C_n orbits ("prime cycles" in ChaosBook parlance; one per each orbit). The right way to do this is by going to C_n irreps, ie, by the discrete Fourier transform, with all reciprocal lattice Brillouin zone solutions orbits in an $1/n$ sliver of a n -gon. If n is prime, this is irreducible; if it is a multiple of a prime, one should remove those solutions, as they have already been accounted for.

If, in addition, the law is time-reversal (or time-inversion) invariant, the symmetry includes time-reflection, ie, it is dihedral group D_n with $2n$ elements, so the reciprocal lattice should be a half of the above $1/n$ sliver of a n -gon, and irreps are now either 1 or 2 dimensional. Even n is different from odd n , and solutions either appear in pairs, or are self dual under reflection in 3 different ways.

The symmetry is C_n , and one needs to distinguish C_n orbits ("prime cycles" in ChaosBook; one per each orbit). The right way to do this is by going to C_n irreps, ie, by the discrete Fourier transform, with all reciprocal lattice Brillouin zone solutions orbits in an $1/n$ sliver of a n -gon. If n is prime, this is irreducible; if it is a multiple of a prime, one should remove those solutions, as they have already been accounted for.

The quantum-mechanical calculations are executed by approximating the infinite crystal by a periodic one, and going to the *reciprocal* space by deploying C_N discrete Fourier transform. This implements the G/T quotienting by translations and reduces the calculation to a finite *Brillouin zone*. That is the content of the '*Bloch theorem*' of solid state physics. Further work is then required to reduce the calculations to the point group irreps.

In the reciprocal lattice k takes on the values in the first Brillouin zone interval $(-\pi/a, \pi/a]$.

Consider

$$\rho_{\vec{G}}(\vec{x}) = e^{i\vec{G} \cdot \vec{r}(\vec{x})},$$

where \vec{G} is a reciprocal lattice vector. By definition, $\vec{G} \cdot \vec{a}$ is an integer multiple of 2π , $\rho_{\vec{G}} = 1$ for lattice vectors. For any other state, reciprocal lattice state is given by

$$e^{i\vec{G} \cdot \vec{u}(\vec{x})} \neq 1.$$

When a cube is a building block that tiles a 3D cubic lattice, it is referred to as the 'elementary' or 'Wigner-Seitz' cell, and its Fourier transform is called 'the first Brillouin zone' in 'the reciprocal space'.

For a 1-dimensional lattice with lattice spacing 1, the reciprocal lattice has spacing $2\pi/1 = 2\pi$, with the (first) Brillouin zone from $k = -\pi$ to $k = \pi$. Due to the time reversal, all $k = 2\pi/5$ irrep states are the same as the $k = 4\pi/5$ irrep states.

the time-reversal pairs to be the complex-conjugate pairs in Fourier space, as C_∞ shift moves them in opposite directions.

the reciprocal lattice is:

$$\bar{\mathcal{L}}_b = \{n\mathbf{b} \mid n \in \mathbb{Z}\}, \quad (3.60)$$

where the vector \mathbf{b} satisfies:

$$\mathbf{b} \cdot \mathbf{a} = 2\pi. \quad (3.61)$$

The eigenvectors of the translation operator which satisfy the periodicity of the Bravais lattice are plane waves of form:

$$f_{\mathbf{k}}(\mathbf{z}) = e^{i\mathbf{k} \cdot \mathbf{z}}, \quad \mathbf{k} \in \bar{\mathcal{L}}, \quad (3.62)$$

where the wave vector \mathbf{k} is on the reciprocal lattice $\bar{\mathcal{L}}$.

A general plane wave does not satisfy the periodicity, unless

$$e^{i\mathbf{k} \cdot \mathbf{R}} = 1. \quad (3.63)$$

Since \mathbf{R} is a vector from the Bravais lattice \mathcal{L} , the wave vector \mathbf{k} must lie in the reciprocal lattice of \mathcal{L} :

$$\mathbf{k} \in \mathcal{L}^*, \quad \mathcal{L}^* = \{m\mathbf{b} \mid m \in \mathbb{Z}\}, \quad (3.64)$$

where the primitive reciprocal lattice vectors \mathbf{b} satisfies:

$$\mathbf{b} \cdot \mathbf{a} = 2\pi. \quad (3.65)$$

Barvinok [arXiv:/math/0504444](https://arxiv.org/abs/math/0504444):

Let V be a d -dimensional real vector space with the scalar product $\langle \cdot, \cdot \rangle$ and the corresponding Euclidean norm $\| \cdot \|$. Let $\mathcal{L} \subset V$ be a lattice and let $\mathcal{L}^* \subset V$ be the *dual* or the *reciprocal* lattice

$$\mathcal{L}^* = \left\{ x \in V : \quad \langle x, y \rangle \in \mathbb{Z} \quad \text{for all} \quad y \in \mathcal{L} \right\}.$$

3.7.1 Reciprocal lattice state

An infinite lattice state is periodic if the state is invariant under the action of a translation group. A translation group can be described by a Bravais lattice, the vector in which determines the direction and distance of the translation. When the dynamical system has time translation symmetry, the defining equation of the system is invariant under translations. So it is natural to use the eigenvectors of the translation operator to study the lattice states of the system.

The eigenvectors of translation operators are plane waves defined on the lattice. But to study the lattice states, we need to require that the plane wave also satisfies the periodic condition. Generally, a d -dimensional Bravais lattice can be described by:

$$\mathcal{L} = \left\{ \sum_{i=1}^d n_i \mathbf{b}_i | n_i \in \mathbb{Z} \right\}, \quad (3.66)$$

where \mathbf{b}_i is the i th primitive vector of the Bravais lattice. And a plane wave on the d -dimensional lattice is:

$$f_{\mathbf{k}}(\mathbf{z}) = e^{i\mathbf{k} \cdot \mathbf{z}}, \quad (3.67)$$

where \mathbf{z} is the position of a lattice site, and \mathbf{k} is the wave vector. The periodicity given by the Bravais lattice \mathcal{L} requires that:

$$f_{\mathbf{k}}(\mathbf{z} + \mathbf{R}) = f_{\mathbf{k}}(\mathbf{z}), \quad \mathbf{R} \in \mathcal{L}. \quad (3.68)$$

This condition can only be satisfied if the wave vector \mathbf{k} exists on the reciprocal lattice of the lattice \mathcal{L} :

$$\overline{\mathcal{L}} = \left\{ \sum_{j=i}^d n_j \mathbf{b}_i | n_j \in \mathbb{Z} \right\}, \quad (3.69)$$

the basis vectors of which satisfy:

$$\mathbf{b}_i \cdot \mathbf{a}_j = 2\pi\delta_{ij}. \quad (3.70)$$

Using these eigenvectors we can transform lattice states into reciprocal lattice states by discrete Fourier transform. Any lattice state with the periodicity given by the Bravais lattice \mathcal{L} can be spanned by the plane waves with wave vectors

in the reciprocal lattice $\overline{\mathcal{L}}$. And since a lattice state only has values on lattice sites, we only need a finite number of plane waves to span the lattice state. For example, if the period of a 1-dimensional lattice state is n , the lattice state can be written as an n -dimensional vector, $(\phi_0, \phi_1, \phi_2, \dots, \phi_{n-1})$, which is spanned as:

$$(\phi_0, \phi_1, \phi_2, \dots, \phi_{n-1}) = \tilde{\phi}_0 \tilde{e}_0 + \tilde{\phi}_1 \tilde{e}_1 + \dots + \tilde{\phi}_{n-1} \tilde{e}_{n-1}, \quad (3.71)$$

where

$$\tilde{e}_k = \frac{1}{\sqrt{n}}(1, \omega^k, \omega^{2k}, \dots, \omega^{k(n-1)}), \quad k = 0, 1, \dots, n-1, \omega = e^{2\pi i/n} \quad (3.72)$$

are normalized lattice states of plane waves, or Fourier modes.

3.7.2 Irreducible representations of the symmetry group

Cyclic groups

When we write period- n lattice states as n -dimensional vectors, and write the shift operator r as a $[n \times n]$ matrix (3.32) which applies cyclic permutation to the lattice state, the matrix representation of shift operators forms a permutation representation of the cyclic translation group C_n . This permutation representation is a reducible representation, i.e., it can be block diagonalized by a similarity transformation. Each block on the diagonal is an irreducible representation (irrep).

The abelian group C_n only has 1-dimensional irreps. The permutation representation of C_n can be diagonalized by discrete Fourier transform. After the transform the representation of the shift operator becomes,

$$r^m = \begin{pmatrix} 1 & & & & \\ & \omega^m & & & \\ & & \omega^{2m} & & \\ & & & \ddots & \\ & & & & \omega^{(n-1)m} \end{pmatrix}, \quad \omega = e^{2\pi i/n}, \quad (3.73)$$

with lattice states projected onto 1-dimensional subspaces in which action of the shift operators is given by corresponding irrep. As we transform the permutation representation of the shift operator into the block diagonal form, the lattice states $(\phi_0, \phi_1, \phi_2, \dots, \phi_{n-1})$ are spanned by the Fourier modes basis, with components $(\tilde{\phi}_0, \tilde{\phi}_1, \tilde{\phi}_2, \dots, \tilde{\phi}_{n-1})$. When the shift operator acts on the lattice state: $\Phi \rightarrow r\Phi$, the irreducible representations act on the components in the corresponding subspace: $\tilde{\phi}_k \rightarrow \omega^k \tilde{\phi}_k$.

As a concrete example, consider the temporal Bernoulli period-3 Bravais lattice. It's a linear problem and all lattice states are easily computed by hand. There is always the fixed point lattice state $(0, 0, 0)$, and for the stretching parameter value $s = 2$, there are 6 lattice states organized into 2 period-3 orbits,

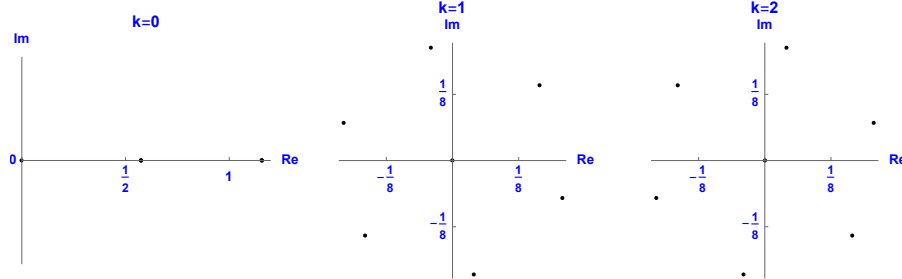


Figure 3.3: Period-3 lattice states of the temporal Bernoulli with $s = 2$, plotted in the C_3 permutation irreps subspaces.

which we mark by a single lattice state per orbit, for example $(\frac{1}{7}, \frac{2}{7}, \frac{4}{7})$ and $(\frac{3}{7}, \frac{6}{7}, \frac{5}{7})$. The remaining lattice states are their cyclic permutations.

Discrete Fourier transform, figure 3.3, maps these 7 lattice states into 7 reciprocal lattice states.¹⁰ The $k = 1$ and $k = 3 - 1$ wave-numbers reciprocal lattice states are complex conjugates of each other because the lattice states are real.

Consider next the action of the shift operator r on the reciprocal lattice states. In the $k = 0$ subspace, the eigenvalue of any shift is 1, so the $k = 0$ component of any reciprocal lattice state is invariant under the shift. In the $k = 1$ and $k = 2$ subspaces, the shift r acts by complex phase rotations $\exp(2\pi i/3)$ and $\exp(4\pi i/3)$, with the two subspaces rotating counter clockwise and clockwise by $2\pi/3$ in the complex plane: reciprocal lattice states that belong to the same orbit lie on a circle in the complex plane, related by complex rotations. Figure 3.4 illustrates this; the two orbits, built from reciprocal lattice states that are related by shifts, are connected by blue lines.

Dihedral group

In the n -dimensional space of the period- n lattice states, the permutation representation of the Dihedral group D_n can be generated by the shift operator matrix representation (3.32) and the reflection operator matrix representation:

$$\sigma = \begin{pmatrix} 1 & & & 0 & \\ & & & 0 & 1 \\ & & \ddots & 1 & \\ & 0 & & \ddots & \\ 0 & 1 & & & \end{pmatrix}. \quad (3.74)$$

¹⁰Predrag 2021-09-02: Why do you mark 1/8 in figures 3.3 and 3.4, when the units are 1/7's? I see. You have $1/\sqrt{3}$ and π 's floating around, unless you redefine units...

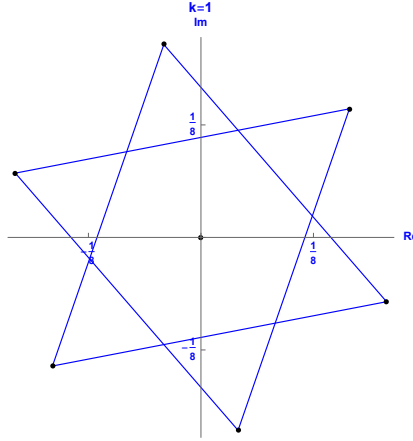


Figure 3.4: Period-3 lattice states of the temporal Bernoulli with $s = 2$ in the subspace of $k = 1$ irrep. Lattice states that are related by cyclic permutations are connected by blue lines. The two triangles are $2 C_3$ orbits. The state in the center is the fixed point.

The Dihedral group D_n has: 2 1-dimensional irreps and $[(n - 1)/2]$ 2-dimensional irreps if n is odd, or 4 1-dimensional irreps and $(n/2 - 1)$ 2-dimensional irreps if n is even. If n is odd, the permutation representation can be block diagonalized into irreps: $A_0 \oplus E_1 \oplus \dots \oplus E_{(n-1)/2}$. If n is even, the permutation representation can be block diagonalized into irreps: $A_0 \oplus B_1 \oplus E_1 \oplus \dots \oplus E_{n/2-1}$.

When we use the similarity transformation to diagonalize the permutation representation, the lattice states are transformed into the subspaces of the irreps. The example of period-3 lattice states of temporal cat with $s = 3$ is shown in figures 3.5 and 3.6. The permutation representation is block diagonalized by basis vectors: $e_0 = 1/\sqrt{3}(1, 1, 1)$, $e_1 = \sqrt{2/3}(\cos(2\pi/3), \cos(4\pi/3), 1)$ and $e_2 = \sqrt{2/3}(\sin(2\pi/3), \sin(4\pi/3), 0)$. The basis vector e_0 spans the subspace of the 1-dimensional irrep A_0 . Basis vectors e_1 and e_2 span the subspace of the 2-dimensional irrep E .

Period-3 lattice states of cat map with $s = 3$ are mapped into the subspace of the irreps A_0 and E in figure 3.5. The irrep A_0 is the symmetric 1-dimensional irrep, so in the subspace of A_0 the components of lattice states are invariant under the action of the D_3 group. In the 2-dimensional subspace of the irrep E , the shift operator r rotates the lattice states clockwise by $2\pi/3$, while the reflection operator σ reflects the lattice states over the axis passing through the origin and pointing toward $(\cos(2\pi/3), \sin(2\pi/3))$. In figure 3.6 lattice states that are related by shifts are connected by blue lines. The red dashed lines are reflection axis of the reflection operators. The 2 big triangles in figure 3.6 (a) are lattice states that belong to 2 orbits which are related by time reflection. The rest 3 triangles are lattice states from 3 orbits which are invariant under time

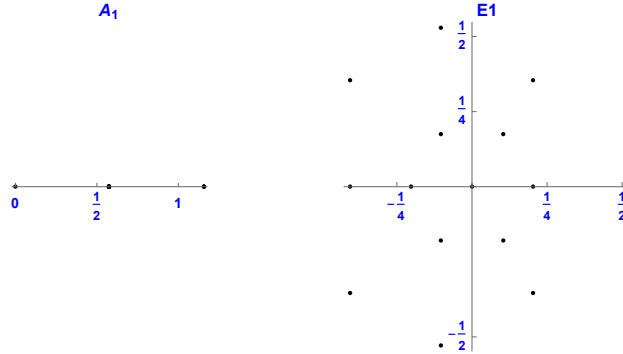


Figure 3.5: Period-3 lattice states of the $s = 3$ temporal cat, plotted in the D_3 permutation irreps subspaces $A_0 + E$. In contrast with the C_n complex irreps (see the C_3 example figure 3.3), the 2-dimensional irrep $E \in \mathbb{R}^2$ is real.

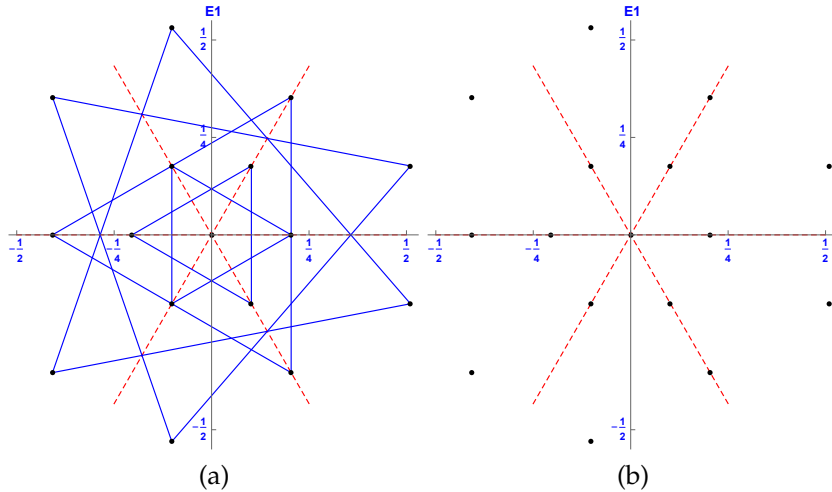


Figure 3.6: Period-3 lattice states of the Temporal cat with $s = 3$ in the subspace of E_1 irrep. (a): Lattice states that are related by cyclic permutations are connected by blue lines. The two big triangles are a single D_3 6-lattice states orbit, what for C_3 is a pair of 3-lattice states orbits without time reversal symmetry. The remaining three smaller triangles are 3 time-reversal symmetric orbits; the pair in the middle is presumably related by the $D_1 : S\phi_i = 1 - \phi_i$ invariance specific to the temporal cat, a symmetry not yet taken into account. The state in the center is the fixed point. (b): Red dashed lines are the reflection axes of the D_3 group. There are 4 states on each reflection axis.

reflection.

3.7.3 Fundamental domain

Given the space of the field configuration and the symmetry group acting on it, we can find a fundamental domain such that each orbit in this space visits the fundamental domain only once. Each lattice state in the fundamental domain is a representative lattice state of an orbit.¹¹

One method to find the fundamental domain is based on the decomposition of the space into the subspaces of the irreps of the symmetry group. A natural way to choose the fundamental domain is to divide in the subspace of an irrep, where the irrep divides the subspace into the number of copies that is equal to the order of the symmetry group.

For example, in the space of the field configuration with C_n symmetry, the $k = 1$ subspace spanned by the eigenstate \tilde{e}_1 , defined in (3.72), can be divided into n copies. One can choose the region in the complex plane of $k = 1$ subspace with argument $0 \leq \arg(\tilde{\phi}_1) < 2\pi/n$ to be the fundamental domain. Each orbit can visit the fundamental domain only once. As shown in figure 3.4, there are 3 points in this region, which are representative lattice states of two different period-3 orbits and the fixed point 0.

If the space of the field configuration has D_n symmetry, the subspace of the 2-dimensional irrep E_1 can be divided into $2n$ copies by the irrep. One can choose the fundamental domain to be the region with polar angle between 0 and π/n , assuming that the horizontal axis is one of the reflection axis of the irrep E_1 . Each orbit only appears once in the fundamental domain, as shown in figure 3.6. Note that the two orbits related by the time reflection are considered one orbit of the dihedral group.

What happens when lattice states appear on the boundary of the fundamental domain? There are two possible situations. The first situation is that the lattice state belongs to an orbit with multiplicity less than the order of the symmetry group. For example, in figure 3.6, there are 3 points in the fundamental domain with polar angle equal to 0 or $\pi/3$. These 3 points are representative lattice states of orbits with time reflection symmetry. The multiplicities of these orbits are 3 instead of 6.

The second situation is that the multiplicity of the orbit of the lattice state is equal to the order of the symmetry group but the component in the subspace is 0. For example,

$$\Phi = \frac{1}{104}(17, 51, 49, 43, 25, 75)$$

is a period-6 lattice state of the temporal Bernoulli (3.18) with $s = 3$. Using the discrete Fourier transform this lattice state becomes:

$$\tilde{\phi} = \left(\frac{5}{2\sqrt{6}}, 0, \frac{-5 - 3i\sqrt{3}}{13\sqrt{6}}, -\frac{\sqrt{3}}{4\sqrt{2}}, \frac{-5 + 3i\sqrt{3}}{13\sqrt{6}}, 0 \right).$$

¹¹Predrag 2021-10-12: Please read our draft [98], and either follow our definition (3.6) of *lattice state*, or replace it with some other definition.

This is a period-6 lattice state. It belongs to an orbit that contains 6 different lattice states. The $k = 1$ component of this lattice state is 0, which is on the boundary of the fundamental domain. To put this kind of lattice states into the fundamental domain one needs to divide other subspaces. For this lattice state the $k = 2$ and $k = 3$ components are not 0. The irreps divide the $k = 2$ subspace into 3 copies and the $k = 3$ subspace into 2 copies. One way to choose the fundamental domain in these subspaces is: the argument of the component in the $k = 1$ subspace is $0 \leq \arg(\tilde{\phi}_1) < \pi/3$; if the $k = 1$ component is 0, the arguments of the components in the $k = 2$ and $k = 3$ subspaces are $0 \leq \arg(\tilde{\phi}_2) < 2\pi/3$ and $0 \leq \arg(\tilde{\phi}_3) < \pi$. Each orbit is guaranteed to visit this fundamental domain exactly once.

3.8 Orbit stability

The temporal lattice reformulation gives us deep insights into how to enumerate and determine all global solutions (lattice states) of lattice field theories.

The discretized Euler–Lagrange $F[\Phi_c] = 0$ fixed point condition (3.5) is central to the theory of global methods for finding periodic orbits. Instead of utilizing local, forward-in-time numerical integrations, in global multi-shooting, collocation [25, 51, 77], and Lindstedt–Poincaré [140–142] searches for periodic orbits, one discretizes a periodic orbit into n segments [42, 49, 50, 95] temporal lattice configuration, and lists the field value at a point of each segment

$$\Phi^\top = (\phi_0, \phi_1, \dots, \phi_{n-1}). \quad (3.75)$$

Starting with an initial guess for Φ , the zero of function $F[\Phi_c]$ can then be found by Newton iteration, which requires an evaluation of the $[n \times n]$ *orbit Jacobian matrix*

$$\mathcal{J}_{tt'} = \frac{\delta F[\Phi_c]_t}{\delta \phi_{t'}}. \quad (3.76)$$

3.8.1 Temporal Bernoulli, temporal cat

The temporal Bernoulli condition (3.31) and the temporal cat discretized Euler–Lagrange equation (4.42) can be viewed as searches for zeros of the vector of n functions

$$F[\Phi_M] = \mathcal{J}\Phi - M = 0 \quad (3.77)$$

$$\text{temporal Bernoulli: } \mathcal{J} = -r + s \mathbf{1} \quad (3.78)$$

$$\text{temporal cat: } \mathcal{J} = -r + s \mathbf{1} - r^{-1}, \quad (3.79)$$

with the entire periodic *lattice state* Φ_M treated as a single fixed *point* $(\phi_0, \phi_1, \dots, \phi_{n-1})$ in the n -dimensional state space unit hyper-cube $\Phi \in [0, 1]^n$, and the $[n \times n]$ orbit Jacobian matrix \mathcal{J} .

The $[n \times n]$ orbit Jacobian matrix \mathcal{J} is a Toeplitz matrix, i.e., matrix constant along each diagonal, $\mathcal{J}_{k\ell} = j_{k-\ell}$, of circulant form, for the temporal Bernoulli,

$$\mathcal{J} = \begin{pmatrix} s & -1 & 0 & 0 & \dots & 0 & 0 \\ 0 & s & -1 & 0 & \dots & 0 & 0 \\ 0 & 0 & s & -1 & \dots & 0 & 0 \\ \vdots & \vdots & \vdots & \vdots & \ddots & \vdots & \vdots \\ 0 & 0 & 0 & 0 & \dots & s & -1 \\ -1 & 0 & 0 & 0 & \dots & 0 & s \end{pmatrix}. \quad (3.80)$$

and for temporal cat

$$\mathcal{J} = \begin{pmatrix} s & -1 & 0 & 0 & \dots & 0 & -1 \\ -1 & s & -1 & 0 & \dots & 0 & 0 \\ 0 & -1 & s & -1 & \dots & 0 & 0 \\ \vdots & \vdots & \vdots & \vdots & \ddots & \vdots & \vdots \\ 0 & 0 & 0 & 0 & \dots & s & -1 \\ -1 & 0 & 0 & 0 & \dots & -1 & s \end{pmatrix}. \quad (3.81)$$

3.8.2 Nonlinear field theories

The key to understanding their chaoticity are the eigenvalues of the orbit Jacobian matrix,

The temporal Bernoulli condition (3.31) can be thus viewed as a time-discretized, first-order ODE dynamical system

$$\dot{\Phi} = v(\Phi), \quad (3.82)$$

where the ‘velocity’ vector field v is given by

$$v(\Phi) = (s - 1)\Phi - M,$$

with the time increment set to $\Delta t = 1$, and perturbations that grow (or decay) with rate $(s - 1)$.

consider a temporal lattice with a set of d fields $\phi_t = \{\phi_{t,1}, \phi_{t,2}, \dots, \phi_{t,d}\}$ on each lattice site t , and time evolution given by a d -dimensional map $\phi_{t+1} = \hat{f}(\phi_t)$. A period- n lattice state (3.29) thus satisfies site-by-site the first-order difference equation

$$\phi_t - \hat{f}(\phi_{t-1}) = 0, \quad t = 1, 2, \dots, n. \quad (3.83)$$

the matrix of second variations of the action $S[\Phi]_{tt'}$,

$$\mathcal{J}[\Phi] = \begin{pmatrix} s_0 & -1 & 0 & 0 & \dots & 0 & -1 \\ -1 & s_1 & -1 & 0 & \dots & 0 & 0 \\ 0 & -1 & s_2 & -1 & \dots & 0 & 0 \\ \vdots & \vdots & \vdots & \vdots & \ddots & \vdots & \vdots \\ 0 & 0 & 0 & 0 & \dots & s_{n-2} & -1 \\ -1 & 0 & 0 & 0 & \dots & -1 & s_{n-1} \end{pmatrix}, \quad (3.84)$$

evaluated on a lattice state Φ , and its Hill determinant $\text{Det } \mathcal{J}[\Phi]$, with the ‘stretching factor’ $s_t = V''(\phi_t)$ at lattice site t in general a function of the site field ϕ_t for the given lattice state Φ . ¹²

¹²Predrag 2020-06-01: Cite Gade and Amritkar [67] as an early investigation of a lattice orbit Jacobian matrix. They did not know about ‘Hill’s formula.

The *orbit Jacobian matrix* is the $\delta/\delta\phi_k$ derivative of the temporal Hénon 3-term recurrence relation (3.84)

$$\mathcal{J}_p = -r + 2\mathbb{X}_p - r^{-1}, \quad (3.85)$$

where \mathbb{X}_p is a diagonal matrix with p -lattice state ϕ_k in the k th row/column, and the '1's in the upper right and lower left corners enforce the periodic boundary conditions.

The action of the temporal Hénon orbit Jacobian matrix can be hard to visualize, as a period-2 lattice state is a 2-torus, period-3 lattice state a 3-torus, etc.. Still, the fundamental parallelepiped for the period-2 and period-3 lattice states, should suffice to convey the idea. The fundamental parallelepiped basis vectors (3.90) are the columns of \mathcal{J} . The $[2 \times 2]$ orbit Jacobian matrix and its Hill determinant follow from (2.46)

$$\mathcal{J} = \begin{pmatrix} 2\phi_0 & -2 \\ -2 & 2\phi_1 \end{pmatrix}, \quad \text{Det } \mathcal{J} = 4(\phi_0\phi_1 - 1) = -4(a - 3). \quad (3.86)$$

The resulting fundamental parallelepiped shown in figure ??(a). Period-3 lattice states for $s = 3$ are contained in the half-open fundamental parallelepiped of figure ??(b), defined by the columns of $[3 \times 3]$ orbit Jacobian matrix

$$\mathcal{J} = \begin{pmatrix} 2\phi_0 & -1 & -1 \\ -1 & 2\phi_1 & -1 \\ -1 & -1 & 2\phi_2 \end{pmatrix}, \quad \text{Det } \mathcal{J} = 8\phi_0\phi_1\phi_2 - 2(\phi_0 + \phi_1 + \phi_2) + 2, \quad (3.87)$$

3.8.3 Fundamental fact

The orbit Jacobian matrix \mathcal{J} stretches the state space unit hyper-cube $\Phi \in [0, 1]^n$ into the n -dimensional *fundamental parallelepiped*, and maps each periodic point Φ_M into an integer lattice \mathbb{Z}^n site, which is then translated by the winding numbers M into the origin, in order to satisfy the fixed point condition (3.77). Hence N_n , the total number of the solutions of the fixed point condition equals the number of integer lattice points within the fundamental parallelepiped, a number given by what Baake *et al.* [11] call the '*fundamental fact*',

$$N_n = |\text{Det } \mathcal{J}|, \quad (3.88)$$

i.e., fact that the number of integer points in the fundamental parallelepiped is equal to its volume, or, what we refer to as the 'Hill determinant' below. In two dimensions this formula is known since 1899 as [Pick's theorem](#), in higher dimensions it was given by Nielsen [18, 119] in 1920, and rederived several times since in different contexts, for example by Baake *et al.* [11]. For the task at hand, Barvinok [12] [lectures](#) offer a clear and simple introduction to integer lattices, and a proof of (3.88).

The action of orbit Jacobian matrix \mathcal{J} for the period-2 lattice states (periodic points) of the Bernoulli map of figure 3.2 (a), suffices to convey the idea. In this

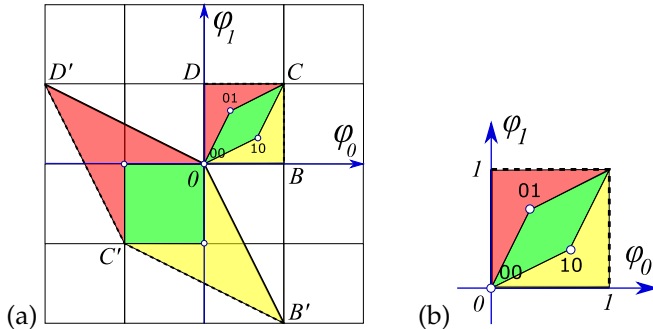


Figure 3.7: (Color online) (a) The Bernoulli map (3.22) periodic points $\Phi_M = (\phi_0, \phi_1)$ of period 2 are the $\bar{0} = (0, 0)$ fixed point, and the 2-cycle $\Phi_{01} = (1/3, 2/3)$, see figure 3.2(a). They all lie within the unit square $[0BCD]$, which is mapped by the orbit Jacobian matrix \mathcal{J} (3.89) into the fundamental parallelepiped $[0B'C'D']$. Periodic points Φ_M are mapped by \mathcal{J} onto the integer lattice, $\mathcal{J}\Phi_M \in \mathbb{Z}^n$, and are sent back into the origin by integer translations M , in order to satisfy the fixed point condition (3.77). Note that this fundamental parallelepiped is covered by 3 unit area quadrilaterals, hence $|\text{Det } \mathcal{J}| = 3$. (b) Conversely, in the flow conservation sum rule (3.183) sum over all lattice states M of period n , the inverse of the Hill determinant defines the ‘neighborhood’ of a lattices state as the corresponding fraction of the unit hypercube volume.

case, the $[2 \times 2]$ orbit Jacobian matrix (3.31), the unit square basis vectors, and their images are

$$\begin{aligned}\mathcal{J} &= \begin{pmatrix} 2 & -1 \\ -1 & 2 \end{pmatrix} \\ \Phi^{(B)} &= \begin{pmatrix} 1 \\ 0 \end{pmatrix} \rightarrow \Phi^{(B')} = \mathcal{J} \Phi^{(B)} = \begin{pmatrix} 2 \\ -1 \end{pmatrix}, \quad \dots\end{aligned}$$

i.e., the columns of the orbit Jacobian matrix are the edges of the fundamental parallelepiped,

$$\mathcal{J} = (\Phi^{(B')} \Phi^{(D')}) , \quad (3.89)$$

see figure 3.7(a), and $N_2 = |\text{Det } \mathcal{J}| = 3$, in agreement with the periodic orbit count (3.28).

In general, the unit vectors of the state space unit hyper-cube $\Phi \in [0, 1]^n$ point along the n axes; orbit Jacobian matrix \mathcal{J} stretches them into a fundamental parallelepiped basis vectors $\Phi^{(j)}$, each one a column of the $[n \times n]$ matrix

$$\mathcal{J} = (\Phi^{(1)} \Phi^{(2)} \dots \Phi^{(n)}) . \quad (3.90)$$

The Hill determinant

$$\text{Det } \mathcal{J} = \text{Det} (\Phi^{(1)} \Phi^{(2)} \dots \Phi^{(n)}) , \quad (3.91)$$

is then the volume of the fundamental parallelepiped whose edges are basis vectors $\Phi^{(j)}$. Note that the unit hypercubes and fundamental parallelepipeds are half-open, as indicated by dashed lines in figure 3.7(a), so that their translates form a partition of the extended state space (3.23). For another example of fundamental parallelepipeds, see figure 3.8.

Note that in the temporal lattice reformulation, the Bernoulli system involves two distinct lattices:

- (i) Any lattice field theory: in the discretization (5.101) of the time continuum, one replaces *any* dynamical system's time-dependent field $\phi(t) \in \mathbb{R}$ at time $t \in \mathbb{R}$ by a discrete set of its values $\phi_t = \phi(at)$ at time instants $t \in \mathbb{Z}$. Here the index t is a *coordinate* over which the field ϕ is defined.
- (ii) Specific to the Bernoulli system: the site t field value ϕ_t (3.24) is confined to the unit interval $[0, 1]$, imparting integer lattice structure onto the intermediate calculational steps in the extended state space (3.23) on which the orbit Jacobian matrix \mathcal{J} (3.31) acts.

¹³

¹³Predrag 2021-10-25: Combine the above with the temporal cat page ?? discussion into a remark that temporal Bernoulli and temporal cat also have a *dynamical* D_1 symmetry, not utilized in this paper, as nonlinear field theories such as temporal Hénon do not have such symmetries. Here we study only the symmetries of the floor, not the dancer.

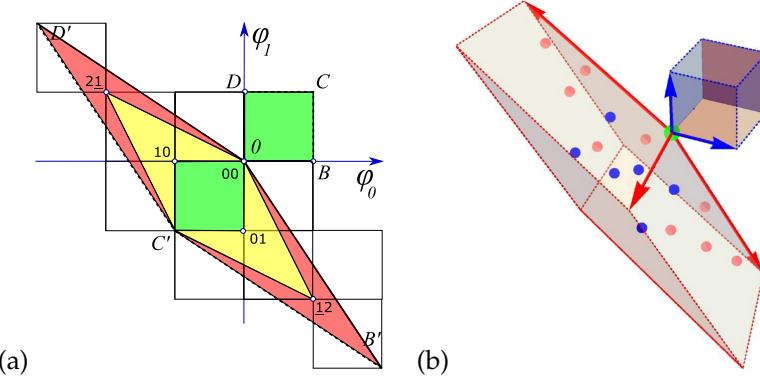


Figure 3.8: (Color online) (a) For $s = 3$, the temporal cat (4.42) has 5 period-2 lattice states $\Phi_M = (\phi_0, \phi_1)$: Φ_{00} fixed point and 2-cycles $\{\Phi_{01}, \Phi_{10}\}$, $\{\Phi_{12}, \Phi_{21}\}$. They lie within the unit square $[0BCD]$, and are mapped by the $[2 \times 2]$ orbit Jacobian matrix J (3.93) into the fundamental parallelepiped $[0B'C'D']$, as in, for example, Bernoulli figure 3.7. The images of periodic points Φ_M land on the integer lattice, and are sent back into the origin by integer translations $M = m_0 m_1$, in order to satisfy the fixed point condition $J\Phi_M + M = 0$. (b) A 3-dimensional [blue basis vectors] unit-cube stretched by J (4.66) into the [red basis vectors] fundamental parallelepiped. For $s = 3$, the temporal cat (4.42) has 16 period-3 lattice states: a Φ_{000} fixed point at the vertex at the origin, [pink dots] 3 period-3 orbits on the faces of the fundamental parallelepiped, and [blue dots] 2 period-3 orbits in its interior. An n -dimensional state space unit hyper-cube $\Phi \in [0, 1]^n$ and the corresponding fundamental parallelepiped are half-open, as indicated by dashed lines, so the integer lattice points on the far corners, edges and faces do not belong to it.

For temporal cat the total number of lattice states is again, as for the Bernoulli system (3.88), given by the ‘fundamental fact’ (3.88). However, while for the temporal Bernoulli every sequence of alphabet letters (3.26) but one is admissible, for temporal cat the condition (3.45) constrains admissible source blocks M .

For period-1, constant field lattice states $\phi_{t+1} = \phi_t = \phi_{t-1}$ it follows from (3.45) that

$$(s - 2)\phi_t = m_t ,$$

so the orbit Jacobian matrix is a $[1 \times 1]$ matrix, and there are

$$N_1 = s - 2 \quad (3.92)$$

period-1 lattice states. This is easy to verify by counting the admissible m_t values. Since $\phi_t \in [0, 1)$, the range of m_t is $m_t \in [0, s - 2)$. So three of the (3.44) temporal cat letters are not admissible: $\underline{1}$ is below the range, and $s - 2$ and $s - 1$ are above it.

The action of the temporal cat orbit Jacobian matrix can be hard to visualize, as a period-2 lattice field is a 2-torus, period-3 lattice field a 3-torus, etc.. Still, the fundamental parallelepiped for the period-2 and period-3 lattice states, figure 3.8, should suffice to convey the idea. The fundamental parallelepiped basis vectors are the columns of \mathcal{J} . The $[2 \times 2]$ orbit Jacobian matrix (3.81) and its Hill determinant are

$$\mathcal{J} = \begin{pmatrix} s & -2 \\ -2 & s \end{pmatrix}, \quad N_2 = \text{Det } \mathcal{J} = (s-2)(s+2), \quad (3.93)$$

(compare with the lattice states count (13.78)), with the resulting fundamental parallelepiped shown in figure 3.8(a). Period-3 lattice states for $s = 3$ are contained in the half-open fundamental parallelepiped of figure 3.8 (b), defined by the columns of $[3 \times 3]$ orbit Jacobian matrix

$$\mathcal{J} = \begin{pmatrix} s & -1 & -1 \\ -1 & s & -1 \\ -1 & -1 & s \end{pmatrix}, \quad N_3 = \text{Det } \mathcal{J} = (s-2)(s+1)^2, \quad (3.94)$$

again in agreement with the periodic orbit count (13.78). The 16 period-3, $s = 3$ lattice states $\Phi_M = (\phi_0, \phi_1, \phi_3)$ are the Φ_{000} fixed point at the vertex at the origin, 3 period-3 orbits on the faces of the fundamental parallelepiped, and 2 period-3 orbits in its interior.¹⁴

In this example there is no need to go further with the fundamental fact Hill determinant evaluations, as the explicit formula for the numbers of periodic lattice states is well known [89, 92]. The temporal cat equation (3.45) is a linear 2nd-order inhomogeneous difference equation (3-term recurrence relation) with constant coefficients that can be solved by standard methods [57] that parallel the theory of linear differential equations. Inserting a solution of form $\phi_t = \Lambda^t$ into the $m_t=0$ homogenous 2nd-order temporal cat condition (3.45) yields the characteristic equation (3.39) with roots $\{\Lambda, \Lambda^{-1}\}$. The result is that the number of temporal lattice states of period n is

$$N_n = |\text{Det } \mathcal{J}| = \Lambda^n + \Lambda^{-n} - 2, \quad (3.95)$$

often written as

$$N_T = 2T_T(s/2) - 2, \quad (3.96)$$

where $T_T(s/2)$ is the Chebyshev polynomial of the first kind.

Note that in the temporal lattice reformulation, the temporal cat happens to involve two unrelated lattices:

- (i) In the latticization of a time continuum, one replaces a time-dependent field $\phi(t)$ at time $t \in \mathbb{R}$ of *any* dynamical system by a discrete set of its values $\phi_t = \phi(t\Delta T)$, $t \in \mathbb{Z}$. Here the index ‘ t ’ is a *coordinate* over which the field ϕ lives.
- (ii) A peculiarity of the temporal cat is that the *field* ϕ_t (3.43) is confined to the unit interval $[0, 1]$, imparting a \mathbb{Z}^1 lattice structure onto the calculationally intermediate fundamental parallelepiped \mathcal{J} basis vectors (3.90).

¹⁴Predrag 2021-10-29: Dropped: , all five of form $\{\Phi_{m_0 m_1 m_2}, \Phi_{m_1 m_2 m_0} \Phi_{m_2 m_0 m_1}\}$.

3.8.4 Orbit Jacobian matrix on reciprocal lattice

¹⁵ we show how compute the orbit Jacobian matrix or Hill determinants $|\text{Det } \mathcal{J}|$ using crystallographer's favorite tool, the discrete Fourier transform.

¹⁵Predrag 2021-08-28: Define the Hill determinant somewhere, refer to it here.

3.9 Stability of an orbit vs. its time-evolution stability

In 1878-1886 a study of stability of the planar motion of the moon around the earth led Hill to the *Hill's formula* [85]

$$|\text{Det } \mathcal{J}_c| = |\det (\mathbf{1} - \mathbb{J}_c)| \quad (3.97)$$

which relates the characteristic polynomial of the forward-in-time evolution periodic orbit Floquet stability matrix (monodromy matrix) \mathbb{J}_p to the determinant of the global orbit Jacobian matrix \mathcal{J}_p (in Lagrangian settings, the Hessian, the second variation of the action functional). The discrete-time Lagrangian systems' Hill's formula that we use here was derived by Mackay and Meiss [106] in 1983.

Hill was lucky: he computed $\text{Det } \mathcal{J}_c$ in a 3×3 Fourier modes matrix approximation, which turned out to be quite a good approximation. But this is a remarkable formula, especially in the limit of $n \rightarrow \infty$ infinitesimal time steps, that relates a field-theoretic, ∞ -dimensional *functional* Hill determinant $\text{Det } \mathcal{J}_c$ to a determinant of the finite, $[d \times d]$ matrix \mathbb{J}_c , and it took Poincaré [124] to prove that Hill's Fourier modes calculation is correct in the continuum limit.

the orbit Jacobian matrix and the temporal evolution (8.23) stability $\hat{\mathbb{J}}_p$ are related by the remarkable (discrete time) Hill's formula [16, 106] which expresses the Hill determinant of the arbitrarily large orbit Jacobian matrix \mathcal{J} in terms of a determinant of a small $[2L \times 2L]$ time-evolution Jacobian matrix $\hat{\mathbb{J}}_p$.

While first discovered in a Lagrangian setting, Hill's formulas are much more general, with the Lagrangian formalism of refs. [16, 94, 106, 139] –just a special case– only getting in way of understanding them. As the formula is fundamental to the formulation of the spatiotemporal chaotic field theory, we shall rederive it here in several ways, relying on nothing more than elementary linear algebra, in order to emphasize that formula applies to dissipative dynamical systems as well, from the Bernoulli map to Navier-Stokes and Kuramoto-Sivashinsky [78, 79].

Assume that a periodic orbit $\phi(T_p + t) = \phi(t)$ of a continuous time flow $\dot{\phi} = v(\phi)$ is known ‘numerically exactly’, that is to say, to arbitrary (but not infinite) precision. One way to present the solution is to give a single point $\phi(0)$ in the orbit, and let the reader reconstruct the orbit p by integrating forward in time, $\phi(t) = \hat{f}^t(\phi(0))$, $t \in [0, T_p]$.

However, for a linearly unstable periodic orbit a single point does not suffice to present the orbit, because there is always a finite ‘Lyapunov time’ t_{Lyap} beyond which $\hat{f}^t(\phi(0))$ has lost all memory of the periodic orbit p . This problem is particularly severe in searches for ‘exact coherent structures’ embedded in turbulence, where even the shortest period solutions have to be computed to the (for everyday fluid dynamics excessive) machine precision [71, 72, 143] in order to complete the first return to the initial state.

Instead of relying on forward-in-time numerical integration, *global methods* for finding periodic orbits [25] view them as equations for the vector fields $\dot{\phi}$ on spaces of closed curves. In numerical implementations one discretizes the periodic orbit p into sufficiently many short segments [25, 49–51, 77], and lists a point for each segment

$$p = (\phi_1, \phi_2, \dots, \phi_{n_p}). \quad (3.98)$$

For a k -dimensional discrete time map \hat{f} obtained by cutting the flow by a set of Poincaré sections, with the periodic orbit p of discrete period n_p , every segment can be reconstructed by a short time integration, and satisfies

$$\phi_{k+1} = \hat{f}(\phi_k), \quad (3.99)$$

to high accuracy, as for sufficiently short times the exponential instabilities are numerically controllable.

The temporal Bernoulli orbit Jacobian matrix $\mathcal{J} = \partial/\partial t - (s - 1)r^{-1}$ is a differential operator whose determinant one usually computes by a Fourier transform diagonalization (see sect. 3.8.4). The Fourier discretization approach goes all the way back to Hill's 1886 paper [85];

In preparing this summary we have found expositions of Lagrangian dynamics for discrete time systems by MacKay, Meiss and Percival [107, 108], and Li and Tomsovic [96] particularly helpful.

This formula was derived by Mackay and Meiss [106] and Allroth [1] (Allroth eq. (12)). It applies to general “one-degree-of-freedom” systems, i.e., 1D lattices with only the nearest neighbor interactions. For a finite set of neighbors, i.e., higher-dimensional discrete-time systems, Allroth [1] has some partial results in the context of Frenkel-Kontorova models.

Hill determinant [16, 28, 106]; discrete Hill's formula and the Hill discriminant, Toda lattice [138].

Toda [138] Chapt. 4. *Periodic Systems*

Toda studies the classical mechanics of one-dimensional lattices (chains) of particles with nearest neighbor interaction; they are discrete and infinite in space, continuous in time.

The *inverse scattering method* for an infinite lattice makes use of the discrete Schrodinger equation. For periodic systems this gives a discrete Hill's equation, and in place of the scattering data, it is convenient to use the spectrum of the discrete Hill's equation. Thus the initial value problem reduces to the inverse problem (Jacobi's inverse problem), or inverse spectral theory.

Toda discrete Hill's equation is continuous in time, so presumably the most of the work is for stationary states.

He works with a 3-term recurrence (4.1.3a), and defines a 2-configuration monodromy matrix (4.1.11).

For special values of A , the solution of (4.1.4) can be periodic, but more generally it is relative periodic (4.1.16), or the Bloch function (it's existence given

by the Floquet theorem). His orbit Jacobian matrix (4.1.28) has variable diagonal and off diagonal elements, corresponding to nontrivial nonlinear solutions for $d = 1$ lattice.

Historically, in periodic orbit theory calculations one always computes \mathbb{J}_M . However, as we shall show here, and in more generality in sect. ??, it is the Hill determinant $\text{Det } \mathcal{J}$ that is the computationally robust quantity that one should evaluate.

A succinct explanation of the Hill's formula:

If you evaluate stability of the 3-term recurrence (13.109) on a periodic lattice you get the orbit Jacobian matrix \mathcal{J} ; if you evaluate it by multiplying the ‘two-configuration representation’ matrix J , you get the ‘time evolution’ side of the Hill’s formula.

3.9.1 Hill determinant for a d -component lattice field

The orbit Jacobian matrix $\mathcal{J}_{tt'}$ (3.76) is a high-dimensional linear stability matrix for the extremum condition $F[\Phi_c] = 0$, evaluated on the lattice state Φ_c . How is the stability so computed related to the conventional dynamical systems’ forward-in-time stability? To motivate the answer in its generality, consider a temporal lattice with a set of d fields $\phi_t = \{\phi_{t,1}, \phi_{t,2}, \dots, \phi_{t,d}\}$ on each lattice site t , and time evolution given by a d -dimensional map $\phi_{t+1} = \hat{f}(\phi_t)$. A period- n lattice state (3.29) thus satisfies site-by-site the first-order difference equation

$$\phi_t - \hat{f}(\phi_{t-1}) = 0, \quad t = 1, 2, \dots, n. \quad (3.100)$$

A small deviation $\Delta\Phi$ from Φ_p then satisfies the linearized condition

$$\Delta\phi_t - r^{-1} \mathbb{J}_t \Delta\phi_t = 0, \quad (\mathbb{J}_t)_{ij} = \frac{\partial f(\phi_t)_i}{\partial \phi_j}, \quad (3.101)$$

where \mathbb{J}_t is the 1-time step $[d \times d]$ Jacobian matrix, evaluated on lattice site t .

It suffices to work out a temporal period $n = 3$ example to understand the calculation for any period. In terms of the $[3d \times 3d]$ generalized (3.32) block shift matrix r , the orbit Jacobian matrix (3.76) has block matrix form

$$\mathcal{J}_p = \mathbb{1} - r^{-1} \mathbb{J}, \quad r = \begin{bmatrix} 0 & \mathbb{1}_d & 0 \\ 0 & 0 & \mathbb{1}_d \\ \mathbb{1}_d & 0 & 0 \end{bmatrix}, \quad \mathbb{J} = \begin{bmatrix} \mathbb{J}_1 & 0 & 0 \\ 0 & \mathbb{J}_2 & 0 \\ 0 & 0 & \mathbb{J}_3 \end{bmatrix}, \quad (3.102)$$

where $\mathbb{1}$ is the d -dimensional identity matrix. Next, consider

$$r^{-1} \mathbb{J} = \begin{bmatrix} 0 & 0 & \mathbb{J}_3 \\ \mathbb{J}_1 & 0 & 0 \\ 0 & \mathbb{J}_2 & 0 \end{bmatrix}, \quad (r^{-1} \mathbb{J})^2 = \begin{bmatrix} 0 & \mathbb{J}_3 \mathbb{J}_2 & 0 \\ 0 & 0 & \mathbb{J}_1 \mathbb{J}_3 \\ \mathbb{J}_2 \mathbb{J}_1 & 0 & 0 \end{bmatrix}, \quad (3.103)$$

and note that the $n = 3$ repeat of $r^{-1} \mathbb{J}$ is block-diagonal

$$(r^{-1} \mathbb{J})^3 = \begin{bmatrix} \mathbb{J}_3 \mathbb{J}_2 \mathbb{J}_1 & 0 & 0 \\ 0 & \mathbb{J}_1 \mathbb{J}_3 \mathbb{J}_2 & 0 \\ 0 & 0 & \mathbb{J}_2 \mathbb{J}_1 \mathbb{J}_3 \end{bmatrix}, \quad (3.104)$$

with $[d \times d]$ blocks cyclic permutations of each other.^f In general, the trace of the $[nd \times nd]$ matrix for a period n lattice state

$$\mathrm{Tr} (r^{-1} \mathbb{J})^k = \delta_{k, rn} n \mathrm{tr} \mathbb{J}_p^r, \quad \mathbb{J}_p = \mathbb{J}_n \mathbb{J}_{n-1} \cdots \mathbb{J}_2 \mathbb{J}_1$$

is non-vanishing only if k is a multiple of n , where \mathbb{J}_p is the forward-in-time $[d \times d]$ Floquet matrix of the periodic orbit p .

Now we can evaluate the Hill determinant $\mathrm{Det} \mathcal{J}_p$ by expanding

$$\begin{aligned} \ln \mathrm{Det} \mathcal{J}_p &= \mathrm{Tr} \ln (\mathbf{1} - r^{-1} \mathbb{J}) = - \sum_{k=1}^{\infty} \frac{1}{k} \mathrm{Tr} (r^{-1} \mathbb{J})^k \\ &= -\mathrm{tr} \sum_{r=1}^{\infty} \frac{1}{r} \mathbb{J}_p^r = \ln \det (\mathbf{1}_d - \mathbb{J}_p). \end{aligned} \quad (3.105)$$

The orbit Jacobian matrix \mathcal{J}_p evaluated on a lattice state Φ_p satisfying the temporal lattice first-order difference equation (3.100), and the dynamical, forward-in-time Jacobian matrix \mathbb{J}_p are thus related by *Hill's formula*

$$\mathrm{Det} \mathcal{J}_p = \det (\mathbf{1} - \mathbb{J}_p), \quad (3.106)$$

which relates the global orbit stability to the Floquet, forward-in-time evolution stability.

As far as the time-evolution stability is concerned, the $|\mathrm{Det} \mathcal{J}_M| = |\det (\mathbf{1} - \mathbb{J}_M)|$ formula (3.106) is correct for all first-order difference equations (systems whose evolution laws are first order in time), for any $[d \times d]$ one-time-step Jacobian matrix. For the Bernoulli system that is a $[1 \times 1]$ matrix $\mathbb{J} = s$, with the periodic points count (4.272) trivially verified.

The temporal Bernoulli (3.31) is a particularly simple, linear example. The site field ϕ_t is a scalar, the 1-time step $[1 \times 1]$ time-evolution Jacobian matrix (7.20) at every lattice point t is simply $\mathbb{J}_t = s$, and the orbit Jacobian matrix (3.31) is the same for all lattice states of period n , so

$$\text{temporal Bernoulli: } N_n = |\mathrm{Det} \mathcal{J}| = s^n - 1, \quad (3.107)$$

in agreement with the time-evolution count (3.28); all itineraries are allowed, except that the periodicity of $r^n = \mathbf{1}$ accounts for $\bar{0}$ and $\bar{s-1}$ fixed points (see figure 3.2) being a single periodic point.

3.9.2 Hill determinant of a forward-in-time map

For a d -dimensional deterministic map $\phi_{t+1} = \hat{f}(\phi_t)$, the Perron-Frobenius operator

$$\mathcal{L} \rho(\phi_{t+1}) = \int_M d\phi_t \delta(\phi_{t+1} - \hat{f}(\phi_t)) \rho(\phi_t) \quad (3.108)$$

maps a density distribution $\rho(\phi_t)$ forward-in-time. Its kernel, a d -dimensional Dirac delta function

$$\mathcal{L}(\phi_{t+1}, \phi_t) = \delta(\phi_{t+1} - \hat{f}(\phi_t)), \quad (3.109)$$

applied repeatedly satisfies the group property

$$\mathcal{L}^2(\phi_{t+2}, \phi_t) = \int_{\mathcal{M}} d\phi_{t+1} \mathcal{L}(\phi_{t+2}, \phi_{t+1}) \mathcal{L}(\phi_{t+1}, \phi_t) = \delta(\phi_{t+2} - f^2(\phi_t)). \quad (3.110)$$

The time-evolution periodic orbit theory [37] relates the long time chaotic averages to the traces of the Perron-Frobenius operator

$$\text{tr } \mathcal{L}^n = \int_{\mathcal{M}} d\phi \mathcal{L}^n(\phi, \phi) = \int_{\mathcal{M}} d\phi_c \delta(\phi_c - f^n(\phi_c)) \quad (3.111)$$

and its weighted, evolution operator generalizations, with support on all periodic points / lattice states $\phi_c = f^n(\phi_c)$ of period cl .

To evaluate the trace of the n th iterate of the Perron-Frobenius operator, one can either use the kernel of the operator $\mathcal{L}^n(\phi_n, \phi_0) = \delta(\phi_n - f^n(\phi_0))$,

$$\text{tr } \mathcal{L}^n = \int_{\mathcal{M}} d\phi_0 \delta(\phi_0 - f^n(\phi_0)), \quad (3.112)$$

or, using the group property (3.110) to insert integrations over intermediate lattice sites, the product of one-time-step operators \mathcal{L} :

$$\begin{aligned} \text{tr } \mathcal{L}^n &= \int d\Phi \prod_{t=0}^{n-1} \delta(\phi_{t+1} - \hat{f}(\phi_t)), \\ \phi_n &= \phi_0, \quad d\Phi = \prod_{t=0}^{n-1} d\phi_t. \end{aligned} \quad (3.113)$$

The field ϕ_t on every lattice site t is a d -dimensional vector, so a period- n lattice state Φ is a nd -dimensional vector, with the Dirac function also nd -dimensional. In matrix notation this trace takes a compact form:

$$\text{tr } \mathcal{L}^n = \int d\Phi \delta(r\Phi - \hat{f}(\Phi)), \quad (3.114)$$

where Φ and $\hat{f}(\Phi)$ are nd -dimensional column vectors with $(id + j)$ th components $(\phi_t)_j$ and $[\hat{f}(\phi_t)]_j$, where $0 \leq i < n - 1$, $0 \leq j < d - 1$, and r is the cyclic $[nd \times nd]$ shift operator (compare with (3.32)):

$$r = \begin{pmatrix} 0 & \mathbf{1} & & \\ & 0 & \mathbf{1} & \\ & & \ddots & \\ \mathbf{1} & & 0 & \mathbf{1} \\ & & & 0 \end{pmatrix}, \quad (3.115)$$

where $\mathbf{1}$ is the d -dimensional identity matrix. Note that the vector in the nd -dimensional Dirac delta function is the defining equation (3.5) of the system:

$$F[\Phi] = r\Phi - \hat{f}(\Phi).$$

(3.5) with a global deterministic solution Φ_c satisfying this local extremal condition on every lattice site.

Restricting the integration to an infinitesimal neighborhood \mathcal{M}_p around a periodic point ϕ_p , the contribution from this periodic point is:

$$\text{tr } \mathcal{L}^n|_p = \int_{\mathcal{M}_p} d\phi_0 \delta(\phi_0 - f^n(\phi_0)) = \frac{1}{|\det(\mathbf{1} - \mathbb{J}_p)|}, \quad (3.116)$$

where \mathbb{J}_p is the $[d \times d]$ forward-in-time Floquet matrix of the periodic orbit (7.20) started from the periodic point ϕ_p with period n . Compute the trace using the integral on n points:

$$\begin{aligned} \text{tr}_p \mathcal{L}^n &= \int_{\mathcal{M}_p} d\Phi \prod_{i=0}^{n-1} \delta(\phi_{t+1} - \hat{f}(\phi_t)) = \int_{\mathcal{M}_p} d\Phi \delta(F[\Phi]) \\ &= \frac{1}{|\text{Det } \mathcal{J}_p|}, \end{aligned} \quad (3.117)$$

where

$$\mathcal{J}_p = \frac{\partial F[\Phi]}{\partial \Phi} \quad (3.118)$$

is the $[nd \times nd]$ orbit Jacobian matrix of the period- n lattice state started with ϕ_p . \mathcal{M}_p is a region in the nd -dimensional state space of Φ whose first d components are the infinitesimal neighborhood around ϕ_p . Comparing the trace (3.116) and (3.117), we have proved the Hill's formula (3.106).

3.9.3 Hill determinant for a 2nd order difference equation

An n -step recurrence relation is the discrete-time analogue of an n th order differential equation. In formulating dynamical systems problems, one almost always replaces higher order derivatives (Euler-Lagrange equations) by sets of fields satisfying first order equations (Hamilton's equations), and the same is true for discrete time systems. For example, the Hamiltonian temporal cat and Hénon map are usually formulated as time-evolution over a 2-dimensional phase space (3.38) and (3.51), rather than the 3-term recurrence configuration space conditions (3.45) and (3.54).

A k th order differential equation can be discretized as a k th order difference equation. Just as a scalar field satisfying a k th order differential equation can be replaced by a set of k fields, each satisfying a first order equation, a k th order difference equation for a scalar field can be replaced by a k -dimensional vector field, satisfying k 1st order difference equations.

One can compute the orbit stability of a scalar field lattice state of such system using the forward-in-time Hill's formula for the k -dimensional vector field representation of dynamics, and the corresponding the determinant of the $[kn \times kn]$ orbit Jacobian matrix (3.117). However, with the recurrence relation, the orbit Jacobian matrix has a simpler form.

Consider a map with a 3-term recurrence relation, $\phi_{t+1} = f(\phi_{t-1}, \phi_t)$, where ϕ_{t-1} , ϕ_t and ϕ_{t+1} are scalars. This map can be replaced by a pair of 1st order difference equations $(\phi_t, \phi_{t+1}) = \hat{f}(\phi_{t-1}, \phi_t) = (\phi_t, f(\phi_{t-1}, \phi_t))$. The trace of the n th iterate of the Perron-Frobenius operator can be evaluated using the Dirac delta kernel of the operator \mathcal{L}^n , or the product of \mathcal{L} and the recurrence relation:

$$\begin{aligned}\text{tr } \mathcal{L}^n &= \int d\phi_0 d\phi_1 \delta((\phi_0, \phi_1) - \hat{f}^n(\phi_0, \phi_1)) \\ &= \int [d\Phi] \prod_{i=0}^{n-1} \delta(\phi_{t+1} - f(\phi_{t-1}, \phi_t)), \\ \phi_n &= \phi_0, \quad \phi_{-1} = \phi_{n-1}, \quad [d\Phi] = \prod_{i=0}^{n-1} d\phi_t.\end{aligned}\quad (3.119)$$

Using the matrix notation, the trace computed by the integral on n points along a discrete periodic orbit is:

$$\text{tr } \mathcal{L}^n = \int [d\Phi] \delta(r\Phi - f(r^{-1}\Phi, \Phi)), \quad (3.120)$$

where Φ and $f(r^{-1}\Phi, \Phi)$ are n -dimensional column vectors with i th components ϕ_t and $f((r^{-1}\Phi)_i, \Phi_i)$, and r is the cyclic $[n \times n]$ shift operator (3.32). The vector in the Dirac delta function is the defining equation of the system:

$$F[\Phi] = r\Phi - f(r^{-1}\Phi, \Phi). \quad (3.121)$$

Restricting the integration to an infinitesimal neighborhood \mathcal{M}_p around a periodic point $(\phi_{p,0}, \phi_{p,1})$ with period n , the contribution from this periodic point is:

$$\text{tr}_p \mathcal{L}^n = \int_{\mathcal{M}_p} d\phi_0 d\phi_1 \delta((\phi_0, \phi_1) - \hat{f}^n(\phi_0, \phi_1)) = \frac{1}{|\det(\mathbf{1} - \mathbb{J}_p)|}, \quad (3.122)$$

where

$$\mathbb{J}_p = \frac{\partial \hat{f}^n(\phi_{p,0}, \phi_{p,1})}{\partial(\phi_{p,0}, \phi_{p,1})} \quad (3.123)$$

is the $[2 \times 2]$ forward-in-time Floquet matrix of the periodic orbit started from the periodic point $(\phi_{p,0}, \phi_{p,1})$ with period n . Compute the trace using the integral on n points:

$$\begin{aligned}\text{tr}_p \mathcal{L}^n &= \int_{\mathcal{M}_{\Phi_p}} [d\Phi] \delta(r\Phi - f(r^{-1}\Phi, \Phi)) = \int_{\mathcal{M}_{\Phi_p}} [d\Phi] \delta(F[\Phi]) \\ &= \frac{1}{|\text{Det } \mathcal{J}_p|},\end{aligned}\quad (3.124)$$

where

$$\mathcal{J}_p = \frac{\partial F[\Phi_p]}{\partial \Phi_p} \quad (3.125)$$

is the $[n \times n]$ orbit Jacobian matrix of the period- n lattice state started with $(\phi_{p,0}, \phi_{p,1})$. \mathcal{M}_{Φ_p} is a region in the n -dimensional space of Φ whose first 2 components are the infinitesimal neighborhood around $(\phi_{p,0}, \phi_{p,1})$. Compare the trace (3.122) and (3.124), we have proved the Hill's formula (3.106).
¹⁶

Our task is to compute the Hill determinant $|\det \mathcal{J}|$. We first show how to do that directly, by computing the volume of the fundamental parallelepiped.

3.9.4 Hill determinant: fundamental parallelepiped evaluation

As a concrete example consider the Bravais lattice with basis vector

3.9.5 Hill determinant: time-evolution evaluation

However, in classical and statistical mechanics, one often computes the Hill determinant using a Hamiltonian, or 'transfer matrix' formulation.

Define

$$\hat{\phi}_t = \begin{bmatrix} \phi_{t-1} \\ \phi_t \end{bmatrix}, \quad \hat{m}_t = \begin{bmatrix} 0 \\ m_t \end{bmatrix},$$

where the hat $\hat{\cdot}$ indicates a 2-dimensional 'two-configuration' [123] lattice site t state.

The 1-dimensional field theory 3-term recurrence (3.17) written in the Percival-Vivaldi [123] 'two-configuration representation' (3.43).

\mathcal{J}_1 is the spatial $[L \times L]$ orbit Jacobian matrix of $d = 1$ temporal cat form (3.79),

This proves that $\det \hat{\mathcal{J}}$ of the 'Hamiltonian' or 'two-configuration' $[2Ln \times 2Ln]$ 'phase space' orbit Jacobian matrix $\hat{\mathcal{J}}$ defined by (8.31) equals the 'Lagrangian' Hill determinant of the $[Ln \times Ln]$ orbit Jacobian matrix \mathcal{J} .

3.9.6 Hill determinant: Reciprocal lattice evaluation

$$\omega = e^{2i\pi/n}$$

$$\tilde{\phi}_k = x_k + i y_k = |\tilde{\phi}_k| e^{i\theta_k}$$

$$q_k = 2\pi k/n,$$

n is the Bravais cell period

The temporal Bernoulli orbit Jacobian matrix $\mathcal{J} = \partial/\partial t - (s-1)r^{-1}$ is a differential operator whose determinant one usually computes by a Fourier transform diagonalization (see sect. 3.8.4). The Fourier discretization approach goes all the way back to Hill's 1886 paper [85].

¹⁶Han 2021-12-16: The rest of this section is from the old version.

The first advantage of using the reciprocal lattice is that it provides a way to compute the Hill determinant. If the orbit Jacobian matrix (3.76) commutes with the translation operator, the plane waves are eigenvectors of the orbit Jacobian matrix. Using these eigenvectors one can find the eigenvalues and the determinant of the orbit Jacobian matrix. In the n -dimensional space of lattice states with period- n , the one-lattice spacing translation operator is a shift matrix (3.32), whose eigenvectors are plane waves \tilde{e}_k :

$$r \tilde{e}_k = \omega^k \tilde{e}_k . \quad (3.126)$$

For example, the eigenvalues of the temporal Bernoulli orbit Jacobian matrix (3.31) are

$$(s \mathbb{1} - r) \tilde{e}_k = (s - \omega^k) \tilde{e}_k , \quad (3.127)$$

and the Hill determinant is simply a polynomial whose roots are the n th roots of unity,

$$\text{Det}(s \mathbb{1} - r) = \prod_{k=0}^{n-1} (s - \omega^k) = s^n - 1 . \quad (3.128)$$

see (3.33). The eigenvalues of the temporal cat orbit Jacobian matrix (3.79) are:

$$(-r + s \mathbb{1} - r^{-1}) \tilde{e}_k = (s - 2 \cos(2\pi k/n)) \tilde{e}_k , \quad (3.129)$$

and the Hill determinant is:

$$\begin{aligned} \text{temporal cat: } \text{Det}(-r + s \mathbb{1} - r^{-1}) &= \prod_{k=0}^{n-1} (s - 2 \cos(2\pi k/n)) \\ &= 2T_n(s/2) - 2 , \end{aligned} \quad (3.130)$$

where T_n is the Chebyshev polynomial of the first kind.

Explain figure 3.9.

¹⁷

3.9.7 Remarks

Two remarks. First, the reformulation of the spatiotemporal cat 3-term recurrence as the ‘two-configuration’ map (8.23) is a passage from the Lagrangian to the Hamiltonian formulation, also known as ‘transfer matrix’ formulation of lattice field theories [111, 113] and Ising models [90, 120]. We chose to prove it here using only elementary linear algebra, not only because the Lagrangian formalism [16] is not needed for the problem at hand, but because it actually

¹⁷Predrag 2021-09-02: I think I prefer some version of the identity (10.51), (18.272), no mention of Chebyshev polynomials. Not important, will revisit later.

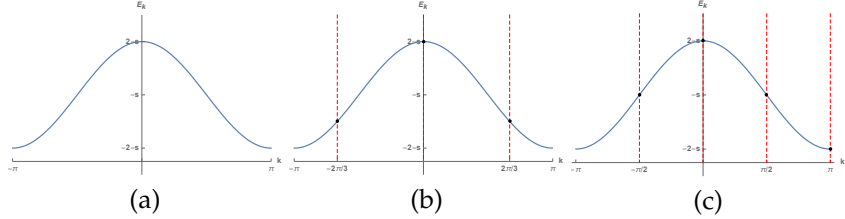


Figure 3.9: (a) The eigenvalue E_k of the orbit Jacobian matrix on the infinite lattice as a function of the wave vector k in the first Brillouin zone. The orbit Jacobian matrix has the reflection symmetry so the eigenvalue is also invariant under the reflection $k \rightarrow -k$. (b) For period 3 lattice states, the wave vectors of the eigenstates exist on the reciprocal lattice spanned by $2\pi/3$. These lattice sites are labeled by the red dashed lines. There are only 3 period 3 eigenstates, with eigenvalues $-1 - s$, $2 - s$ and $-1 - s$. (c) For period 4 lattice states, the wave vectors of the eigenstates exist on the reciprocal lattice spanned by $\pi/2$. These lattice sites are labeled by the red dashed lines. There are only 4 period 4 eigenstates, with eigenvalues $-s$, $2 - s$, $-s$ and $-2 - s$. $k = \pi$ and $k = -\pi$ are different by a reciprocal lattice translation, so they are a same wave vector and should be only counted once.

obscures the generality of Hill's formula, which works equally well for dissipative systems (see Bernoulli Hill's formula (3.43)), systems with no Lagrangian formulation.

Second, for Hamiltonian evolution (3.38), the $[2 \times 2]$ Jacobian matrix \mathbb{J}^n (the monodromy matrix of a periodic orbit) describes the growth of an initial state perturbation in n steps. For the corresponding Lagrangian system with action S , the first variation of the action $\delta S = 0$ yields the temporal cat condition (4.42), while the second variation, the $[n \times n]$ orbit Jacobian matrix (3.79), describes the stability of the *entire* given periodic orbit. In this, classical mechanics context, Bolotin and Treschev [16] refer to \mathcal{J} as the 'Hessian operator', but, as it is clear from our Bernoulli discussion of sect. 3.8, and applications to Kuramoto-Sivashinsky and Navier-Stokes systems [79], this notion of global stability of orbits is general, and applies to all dynamical systems, not only the Hamiltonian ones.

3.10 Translations and reflections

2CB

Though this exposition is nominally about ‘evolution in time’, ‘time’ is such a loaded notion, a straightjacket hard to escape, that it is best to forget about ‘time’ for time being, and think instead like a crystallographer, about lattices and the space groups that describe their symmetries.

Of necessity, there many group-theoretic notions a crystallographer must juggle (see [ChaosBook sect. 11.2](#)), but only a few key things to understand:

- (i) For a 1-dimensional lattice, there are only two kinds of qualitatively different symmetry transformations, translations ([3.142](#)) and
- (ii) reflections ([3.134](#)) which reverse the direction of translation.
- (iii) There are two kinds of reflections ([3.144](#)), across a lattice site, and across a mid-point between lattice sites, figure [3.10](#).
- (iv) Even though both the lattice \mathcal{L} and its space group G are infinite, *orbits* of lattice states are finite and described by finite cyclic and dihedral groups, figure [3.11](#).

Should the reader find symmetries of infinite lattices too obtruse: to understand all that one needs to know about translations and reflections, it suffices to understand the symmetries of a triangle and a square, figure [3.12](#).

3.10.1 Symmetries of 1-dimensional lattices, sublattices

A space group G is the set of all translations and rotations that puts a crystallographic structure \mathcal{L} in coincidence with itself. To make the exposition as simple as possible, here we focus on 1-dimensional crystals, with sites labeled by integer lattice $\mathcal{L} = \mathbb{Z}$. Their space groups crystallographers [53] call *line groups*. There are only two [1-dimensional space groups](#) G : $p1$, or the *infinite cyclic group* C_∞ of all lattice translations, and $p1m$, the *infinite dihedral group* D_∞ of all translations and reflections [93],

$$D_\infty = \{\dots, r_{-2}, \sigma_{-2}, r_{-1}, \sigma_{-1}, 1, \sigma, r_1, \sigma_1, r_2, \sigma_2, \dots\}. \quad (3.131)$$

A half of the elements are translations (‘shifts’; for finite period lattices, ‘rotations’). $r_0 = 1$ denotes the identity, and the $r_1 = r, r_2 = r^2, \dots, r_k = r^k, \dots$, denote translations by $1, 2, \dots, k, \dots$ lattice points. They form the *infinite cyclic group*

$$C_\infty = \{\dots, r_{-2}, r_{-1}, 1, r_1, r_2, r_3, \dots\}, \quad (3.132)$$

a subgroup of D_∞ , in crystallography called the translation group.

The other half of elements are reflections $\sigma_k^2 = 1$ (‘inversions’, ‘time reversals’, ‘flips’), defined by first translating by k steps, and then reflecting, resulting in a ‘translate-reflect’ operation

$$\sigma_k = \sigma r_k. \quad (3.133)$$

The defining property of translate & reflect groups ('dihedral' groups, 'flip systems' [93]) is that any reflection reverses the direction of the translation

$$\sigma_k r = r^{-1} \sigma_k . \quad (3.134)$$

The group multiplication (or 'Cayley') table for successive group actions $g_i g_j$ follows:

	r_j	σ_j	
r_i	r_{i+j}	σ_{j-i}	
σ_i	σ_{i+j}	r_{j-i}	

(3.135)

Multiplication either adds up translations, or shifts and then reverses their direction. The order in which the elements $g_i g_j$ act is right to left, i.e., a group element acts on the expression to its right.

A crystallographer organizes the *subgroups* of a space group G by means of *Bravais lattices* $\mathcal{L}_{\mathbf{a}}$, sublattices of the lattice \mathbb{Z} , each defined here by a 1-dimensional *Bravais cell* of period n , given by a lattice vector \mathbf{a} of integer length n ,

$$\mathcal{L}_{\mathbf{a}} = \{j\mathbf{a} \mid j \in \mathbb{Z}\} , \quad (3.136)$$

with the lattice generated by the infinite translation group of all discrete translations replaced by

$$r_j \rightarrow r_{j\mathbf{a}}$$

multiples of \mathbf{a} , resulting in

$$H_{\mathbf{a}} = \{\dots, r_{-2\mathbf{a}}, r_{-\mathbf{a}}, 1, r_{\mathbf{a}}, r_{2\mathbf{a}}, \dots\} , \quad (3.137)$$

infinite translation subgroup of the infinite translation group C_∞ . You can visualize a lattice state invariant under subgroup $H_{\mathbf{a}}$ as a tiling of the lattice \mathbb{Z} by a generic lattice state over tile of length n .

Another family of subgroups of D_∞ is obtained by substituting elements of D_∞ (3.131) by

$$r_j \rightarrow r_{j\mathbf{a}}, \quad \sigma \rightarrow \sigma_k \quad 0 \leq k < n ,$$

resulting in n infinite dihedral groups

$$H_{\mathbf{a},k} = \{\dots, r_{-2\mathbf{a}}, \sigma_k r_{-2\mathbf{a}}, r_{-\mathbf{a}}, \sigma_k r_{-\mathbf{a}}, 1, \sigma_k, r_{\mathbf{a}}, \sigma_k r_{\mathbf{a}}, r_{2\mathbf{a}}, \sigma_k r_{2\mathbf{a}}, \dots\} , \quad (3.138)$$

each given by a Bravais cell of period n , with reflection across a symmetry point shifted k half-steps, see (3.147).

3.10.2 Classes

Definition: A class is the set of elements left invariant by conjugation with all elements g of the group G , where an element b is conjugate to element a if

$$b = g a g^{-1} . \quad (3.139)$$

By (3.134), a conjugation by any reflection reverses the direction of translation

$$\sigma_i r_j \sigma_{-i} = r_{-j}, \quad (3.140)$$

so every translation pairs up with the equal counter-translation to form

$$\text{identity class} \quad \{1\}, \quad j = 0 \quad (3.141)$$

$$\text{translation classes} \quad \{r_j, r_{-j}\}, \quad j = 1, 2, 3, \dots. \quad (3.142)$$

The $r_0 = 1$ commutes with all group elements, and is thus always a class by itself.

From the multiplication table (3.135) it follows that a conjugate of a reflection

$$r_i \sigma_j r_i^{-1} = \sigma_{j-2i}, \quad \sigma_i \sigma_j \sigma_i^{-1} = \sigma_{2i-j}. \quad (3.143)$$

is a reflection related to it by a $2i$ translation. Hence the even subscript reflections belong to one class, and the odd subscript reflections to the other:

$$\begin{aligned} \text{even} & \quad \{\sigma_{2m}\}, \quad m \in \mathbb{Z} \\ \text{odd} & \quad \{\sigma_{2m+1}\}. \end{aligned} \quad (3.144)$$

By (3.143) $r H_{n,k} r^{-1} = H_{n,k-2}$, so for odd n , there are n Bravais sublattices in the class, and for even n , $H_{n,k}$ separate into 2 classes (3.144),

$$\begin{aligned} \text{even} & \quad \{H_{2m,2j}\}, \quad 0 \leq j < n/2 \\ \text{odd} & \quad \{H_{2m,2j+1}\}, \end{aligned} \quad (3.145)$$

each containing m Bravais sublattices.

3.10.3 Reflections

What's the difference between an 'odd' and an 'even' reflection? Every element in a class is equivalent to any other of its elements. So, to understand what everybody in a given class does, it suffices to work out what a single representative does: it suffices to analyse the $H_{n,0}$ and $H_{n,1}$ to account for all $H_{n,k}$.

So far, we have only discussed the abstract structure of the space group D_∞ and its subgroups. But the difference between an 'odd' and an 'even' is easiest to grasp by working out the action of σ_k on a lattice state.

Even class. Take $\sigma = \sigma_0$ as a representative of all even reflections σ_{2m} , and act on a lattice state (3.6):

$$\begin{aligned} \Phi &= \cdots \phi_{-3} \phi_{-2} \phi_{-1} \phi_0 \phi_1 \phi_2 \phi_3 \phi_4 \cdots \\ \sigma \Phi &= \cdots \phi_5 \phi_4 \phi_3 \phi_2 \phi_1 \boxed{\phi_0} \phi_{-1} \phi_{-2} \phi_{-3} \cdots, \end{aligned} \quad (3.146)$$

with $\boxed{\phi_0}$ indicating that the field at the lattice site 0 is unchanged by the reflection, see figure 3.10 (even).

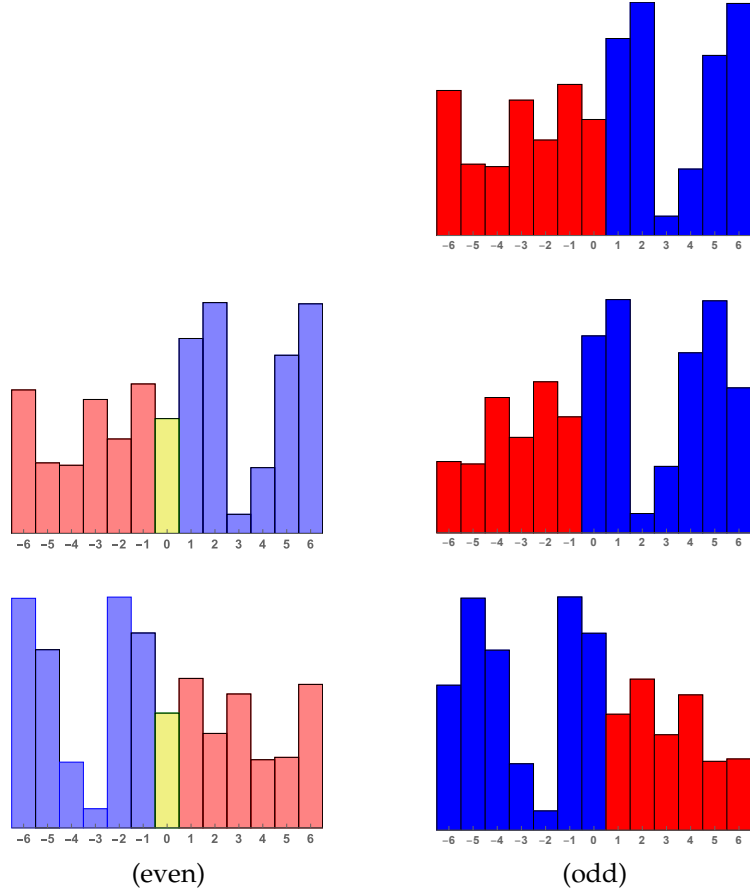


Figure 3.10: (Color online) There are two classes of lattice state reflections, even (3.146) and odd (3.147). (Even) reflection σ exchanges (blue ϕ_j) \leftrightarrow (red ϕ_{-j}) while leaving the yellow field ϕ_0 at lattice site 0 fixed. (Odd) reflection $\sigma_1 = \sigma r$ swaps the ‘blues’ and the ‘reds’ by a lattice translation $\Phi \rightarrow r\Phi$, followed by a reflection σ . The result is a reflection across the midpoint of the [01] interval, marked ‘|’. See figure 3.1 (b) for the notation.

Odd class. Take σ_1 as a representative of all odd reflections σ_{2m+1} . The result is:

$$\begin{aligned}\Phi &= \cdots \phi_{-3} \phi_{-2} \phi_{-1} \underline{\phi}_0 \phi_1 \phi_2 \phi_3 \phi_4 \cdots \\ r\Phi &= \cdots \phi_{-3} \phi_{-2} \phi_{-1} \phi_0 \underline{\phi}_1 \phi_2 \phi_3 \phi_4 \phi_5 \cdots \\ \sigma_1 \Phi = \sigma r\Phi &= \cdots \phi_6 \phi_5 \phi_4 \phi_3 \phi_2 \underline{\phi}_1 | \phi_0 \phi_{-1} \phi_{-2} \phi_{-3} \cdots ,\end{aligned}\quad (3.147)$$

where $\underline{\phi}_j$ indicates the field value at the lattice site 0, and $|$ indicates a reflection across midpoint between lattice sites 0 and 1, see figure 3.10 (odd).

More generally, one can say that the index k in the ‘translate-reflection’ (3.133) operation $\sigma_k = \sigma r_k$ advances the reflection point by $k/2$ steps, and then reflects across it.¹⁸

If you do not find the two kinds of reflections intuitive, the distinction becomes crystal clear once you have a look at the finite periodic lattices of figure 3.12.

3.10.4 Symmetries of a system and of its solutions

What’s the deal about classes? A ‘class’ is a refinement of our intuitive notion that “rotations are rotations, and translations are translations.” Translated into a more familiar language, conjugation (3.139) is central to all of physics: a ‘law’ $f(\Phi)$ is invariant if it retains its form in all symmetry related coordinate frames,

$$f(\Phi) = g^{-1} f(g \Phi), \quad (3.148)$$

where g is a representation of group element $g \in G$. If this holds, we say that G is the *symmetry* of the system.

For example, the ‘temporal Bernoulli’ defining equation (3.30) retains its form under conjugation by any C_∞ translation (3.132),

$$r_i(s\phi_t - \phi_{t+1})r_i^{-1} = (s\phi_{t+i} - \phi_{t+i+1})r_i^{-1} = s\phi_t - \phi_{t+1}, \quad (3.149)$$

while the Euler–Lagrange second-order difference equations (3.17), ‘temporal cat’, ‘temporal Hénon’, and ‘temporal ϕ^4 theory’ defining equations (3.19), (3.20) and (3.21) retain their form also under any D_∞ reflection,¹⁹

$$\sigma_i(-\phi_{t+1} + g V'(\phi_t) - \phi_{t-1})\sigma_i^{-1} = -\phi_{-t+1} + g V'(\phi_{-t}) - \phi_{-t-1}. \quad (3.150)$$

Given that G is the symmetry of the system does not mean that G is also the symmetry of its solutions, or what we here call *lattice states*. They can satisfy all of system’s symmetries, a subgroup of them, or have no symmetry at all. For example, a generic lattice state (3.6) sketched in figure 3.10 has no symmetry beyond the identity, so its symmetry group is the trivial subgroup $\{e\}$; any

¹⁸Predrag 2021-08-17: Before publication, fine tune figure 3.10 using LaTex, as in figure 18.65.

¹⁹Predrag 2021-08-22: This is not quite right, one does not ‘conjugate’ a vector ϕ_j . Not sure how to elegantly deal with ϕ_{-t}^k term. Could have defined actions, but that does not work for the Bernoulli (3.149).

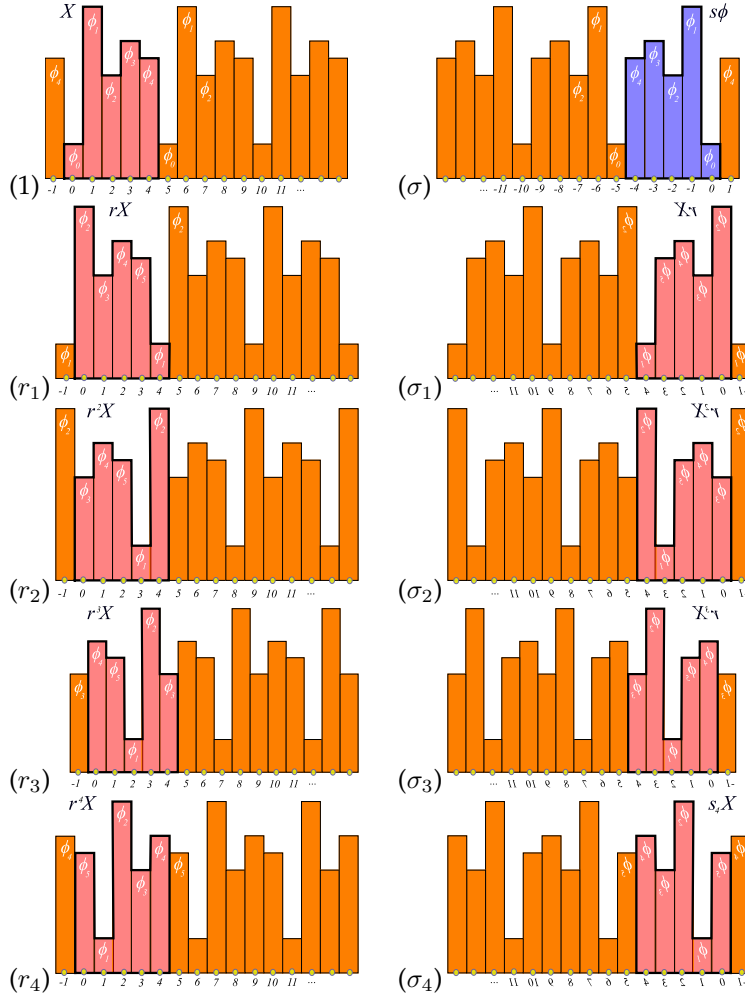


Figure 3.11: (Color online) (1) A Bravais cell \mathbf{a} with lattice state $\Phi = \phi_0\phi_1\phi_2\phi_3\phi_4$ with no reflection symmetry, outlined in bold, invariant under the translation group H_5 . Its C_∞ orbit are the $n = 5$ distinct lattice states (1) to (r_4) , obtained by all of the C_5 translations. Its D_∞ -orbit are $2n = 10$ distinct lattice states, 5 translations (1) to (r_4) and 5 translate-reflections (σ) to (σ_4) , obtained by all of the D_5 actions. See figure 3.1 (b) for the notation. Continued in figure 3.13.

translation r_j or reflection σ_k maps it into a different, distinct lattice state, as shown in figure 3.11. At the other extreme, the constant lattice state $\phi_j = \phi$ is invariant under any translation or reflections - its symmetry group is the full G , the symmetry of the system. In between, there are lattice states whose symmetry is any subgroup of G .

3.10.5 What are 'lattice states'? Orbits?

Remember, for evolution-in-time, every period- n periodic point is a fixed point of the n th iterate of the 1 time-step map. In the lattice formulation, the totality of finite-period lattice states is the *set of fixed points* of all H_a and $H_{a,k}$ subgroups of D_∞ .

You can visualize a lattice state invariant under ("fixed by") subgroup $H_{a,k}$ as a tiling of the lattice \mathbb{Z} by a lattice state tile of length n , symmetric under reflection σ_k , see figure 3.13 (b-c).

Definition: Orbit or G -orbit of a lattice state Φ is the set of all lattice states

$$\mathcal{M}_\Phi = \{g \Phi \mid g \in G\} \quad (3.151)$$

into which Φ is mapped under the action of group G . We label the orbit \mathcal{M}_Φ by any lattice state Φ belonging to it.

As an example, the D_∞ orbit of the period-5 lattice state is shown in figure 3.11.
²⁰

Definition: Symmetry of a solution. We shall refer to the maximal subgroup $G_\Phi \subseteq G$ of actions on lattice states within the orbit \mathcal{M}_Φ , which leave the orbit invariant, as the symmetry G_Φ of the orbit \mathcal{M}_Φ ,

$$G_\Phi = \{g \in G_\Phi \mid g\Phi \in \mathcal{M}_\Phi\}. \quad (3.152)$$

An orbit \mathcal{M}_Φ is G_Φ -symmetric (symmetric, set-wise symmetric, self-dual) if the action of elements of G_Φ on the set of lattice states \mathcal{M}_Φ reproduces the orbit.

Definition: Multiplicity of orbit \mathcal{M}_Φ is given by

$$m_\Phi = |G|/|G_\Phi|. \quad (3.153)$$

(See ChaosBook p. 166.)

And now, a pleasant surprise, obvious upon an inspection of figures 3.11 and 3.13: what happens in the Bravais cell, stays in the Bravais cell. Even though the lattices \mathcal{L} , \mathcal{L}_a are infinite, and their symmetries D_∞ , H_a , $H_{a,k}$ are *infinite* groups, the Bravais lattice states' orbits are *finite*, described by the finite group permutations of the infinite lattice curled up in a Bravais cell periodic n -site ring.

²⁰Predrag 2021-09-05: This "maximal subgroup" does not seem to me to be defined here. Clean up!

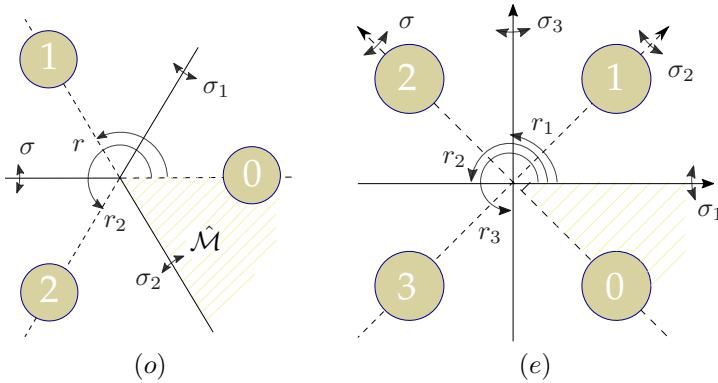


Figure 3.12: Translational and rotational symmetries of (o) an equilateral triangle, $n = 3$ lattice sites; (e) a square, $n = 4$ lattice sites. The n rotations r_j and the n translate-reflect σ_k (elements of dihedral group D_n (3.154), even reflections axes dashed, odd reflections full line) overly an n -sided regular polygon onto itself. They also tile it with the $2n$ copies \hat{M}_ℓ of the fundamental domain, indicated by the shaded wedge.

Indeed, to grasp everything one needs to know about translations r_j (for regular polygons, ‘rotations’), and reflections σ_k , it suffices to understand the symmetries of an equilateral triangle (dihedral group D_3) and a square (dihedral group D_4), depicted in figure 3.12. It is clear by inspection that an n -sided regular polygon has n -fold translational symmetry and n reflection symmetry axes. The group of such symmetries is the finite dihedral group

$$D_n = \{1, \sigma, r, \sigma_1, r_2, \sigma_2, \dots, r_{n-1}, \sigma_{n-1}\} \quad (3.154)$$

of order $2n$. A half of its elements are the n cyclic group C_n translations r_j . The other half are the n reflections σ_k , one for the reflection across each symmetry axis. The group multiplication table is the same as the D_∞ (3.135), but with all subscripts mod n . As in (3.140), conjugation by any reflection reverses the direction of translation

$$\sigma_i r_j \sigma_{-i} = r_{n-j}, \quad 0 < j < n, \quad (3.155)$$

now mod n , so every translation pairs up with the equal counter-translation to form a 2-element class (3.142).

The distinction between the classes of even and odd reflections (3.144) is visually self-evident by inspection of figure 3.12: the symmetry axes either connect opposite lattice sites, or bisect the edges, or both, if n is odd (a triangle, for example). One can say that the index k in the ‘translate-reflection’ (3.133) operation σ_k advances the reflection point by $k 1/2$ steps, and then reflects across it.

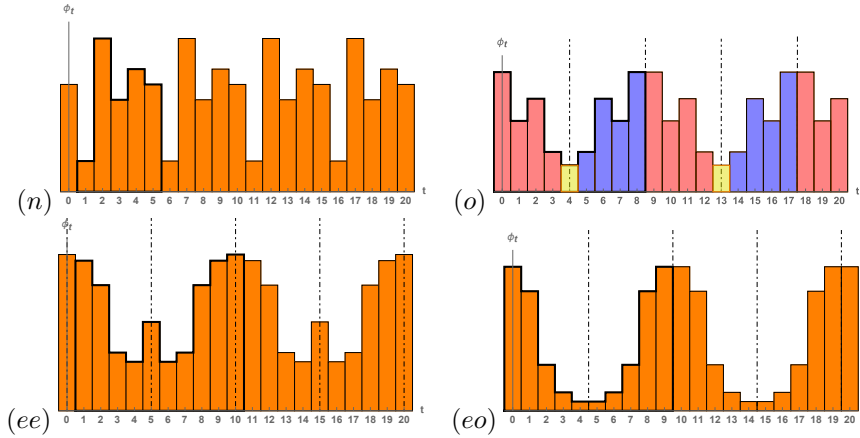


Figure 3.13: (Color online) A Bravais lattice state Φ has one of the 4 possible symmetries, illustrated by: (n) *No reflection symmetry*: an H_5 invariant period-5 lattice state (3.157). For its G -orbit, see figure 3.11. (o) *Odd period, reflection-symmetric*: an $H_{9,8}$ invariant period-9 lattice state (3.158), reflection symmetric over the lattice sites interval [8-9] midpoint and over the lattice site 4. (ee) *Even period, even reflection-symmetric*: an $H_{10,0}$ invariant period-10 lattice state (3.159), reflection symmetric over lattice sites 0 and 5. (eo) *Even period, odd reflection-symmetric*: an $H_{10,9}$ invariant period-10 lattice state (3.160), reflection symmetric over the [4-5] and [9-10] interval midpoints. Horizontal: lattice sites labelled by $t \in \mathbb{Z}$. Vertical: value of field ϕ_t , plotted as a bar centred at lattice site t . Even reflection axes dashed, odd reflections full line.

For a polygon with an *odd* number of lattice sites (a triangle, for example), we see by contemplating the triangle of figure 3.12, as well as by taking mod n of the conjugation relation (3.143), that all reflections are in the same conjugacy class $\{\sigma_j\}$: there is no splitting into odd and even cases, in contrast to the infinite lattice case (3.144).

For a polygon with an *even* number of lattice sites (a square, for example), one must distinguish the ‘long’ axes that connect lattice sites (we label them by even numbers $0, 2, \dots$) from the ‘short’ symmetry axes that bisect opposite edges (labelled by odd numbers $1, 3, \dots$). The corresponding reflections belong to different D_n (subclasses of (3.144)),

$$\begin{array}{ll} \text{even reflections} & \{\sigma, \sigma_2, \sigma_4, \dots, \sigma_{n/2}\} \\ \text{odd reflections} & \{\sigma_1, \sigma_3, \dots, \sigma_{n/2+1}\}. \end{array} \quad (3.156)$$

3.10.6 Symmetries of lattice states

A Bravais lattice state Φ has one of the four symmetries:

$$(n) \quad \begin{array}{c} \text{no reflection symmetry} \\ \overline{\phi_0\phi_1\phi_2\phi_3 \cdots \phi_{n-1}} \\ \text{multiplicity } m_\Phi = 2n \end{array} \quad (3.157)$$

lattice state invariant under the translation group H_n . Its G -orbit, generated by all actions of D_∞ , results in $2n$ distinct, D_n related lattice states. This is illustrated by the H_5 -invariant lattice state Φ of figure 3.11. Its D_5 orbit are $2n = 10$ lattice states, 5 translations and 5 translate-reflections.²¹

Next, the reflection-symmetric lattice states. As illustrated in figures 3.10 and 3.12, there are two classes (3.144) of lattice state reflections: even, across a lattice site, and odd, across the mid-point between a pair of adjacent lattice sites. However, as is evident by inspection of figure 3.12, curling up the lattice \mathcal{L} into a Bravais cell periodic n -site ring implies that an axis cuts the ring twice, and constrains the possible reflection points to three configurations:

$$(o) \quad \begin{array}{c} \text{odd period } n = 2m + 1 \\ \boxed{\phi_0} \phi_1 \phi_2 \cdots \phi_m | \phi_m \cdots \phi_2 \phi_1 \\ \text{multiplicity } m_\Phi = n \end{array} \quad (3.158)$$

lattice state invariant under the dihedral group $H_{n,k}$, illustrated by the $H_{9,8}$ invariant lattice state Φ of figure 3.13(o).²²

$$(ee) \quad \overline{\phi_0 \phi_1 \phi_2 \cdots \phi_m \boxed{\phi_{m+1}} \phi_m \cdots \phi_2 \phi_1} \quad (3.159)$$

multiplicity $m_\Phi = n/2$

lattice state invariant under the dihedral group $H_{n,k}$, k even, illustrated by the $H_{10,0}$ invariant lattice state Φ of figure 3.13 (ee).

$$(eo) \quad \begin{array}{c} \text{even period } n = 2m, \text{ odd reflection } k \\ \overline{\phi_1\phi_2\phi_3 \cdots \phi_m | \phi_m \cdots \phi_2\phi_1} \\ \text{multiplicity } m_\Phi = n/2 \end{array} \quad (3.160)$$

lattice state invariant under the dihedral group $H_{n,k}$, k odd, illustrated by the $H_{10,9}$ invariant lattice state Φ of figure 3.13 (eo).

For long periods n , almost all orbits are of no-symmetry type (3.157). So why do we care about the symmetric orbits so much? The reason is that the periodic orbit expansions are dominated by the short orbits, and many, if not the most of those are reflection-symmetric.

²¹Predrag 2021-08-20: Merge figure 3.13(n) with 1dLatStatC 5 0x3.svg.

²²Predrag 2021-08-28: Merge figure 8.18 (n) with Figure 8.33 as suggested.

²²Predrag 2021-08-17: See (18.372). We also MUST explain the relation to literature, as in the post including (18.371).

The lattice state symmetry G_Φ (3.152) of the above (o)-(eo) reflection-symmetric lattice states Φ is the reflection group $D_1 = \{1, \sigma_k\}$, but we will spare the reader the group-theorist's cosets and group quotients. For us, this symmetry means two things:

- (1) The D_∞ orbits of reflection-symmetric lattice states contain only translations, as any reflection amounts to a cyclic group C_n translation. (Try reflecting a lattice state in figure 3.13(b-d) over any lattice site or mid-interval.)
- (2) lattice state is a 'half' of it, the length m orbit,

$$\tilde{\Phi} = \phi_1 \phi_2 \phi_3 \cdots \phi_m. \quad (3.161)$$

Reflection breaks the translational invariance, and how one reconstructs the period- n orbit from this length- m block is a bit tricky. To develop intuition about that, it is helpful to have a look at a matrix representation of D_n .

3.11 Permutation representation

A lattice state Φ over a Bravais cell a can be assembled into an n -dimensional vector whose components are lattice site fields

$$\Phi^\top = (\phi_0, \phi_1, \phi_2, \phi_3, \dots, \phi_{n-1}), \quad (3.162)$$

with the first field in such vector placed at the lattice site 0, the second at the lattice site 1, and so on. Matrices that reshuffle the components of such vectors form the *permutation representation* of a finite group G , which gives us a different and helpful perspective on the three kinds of symmetric solutions of the preceding section.

The permutation representation of 1-step lattice translation r acts on a Bravais lattice state by the off-diagonal $[n \times n]$ matrix (3.32). This is a cyclic C_n permutation that translates the lattice state Φ "forward-in-time" by one site,

$$(r\Phi)^\top = (\phi_1, \phi_2, \dots, \phi_{n-1}, \phi_0).$$

A permutation representation of a D_n translate-reflect should morally be an anti-diagonal matrix that reverses the order of site fields,

$$(\sigma_k \Phi)^\top = (\phi_{n-1}, \dots, \phi_2, \phi_1, \phi_0).$$

Symmetries of triangles and squares help us make this precise.

Odd period: In odd dimensions, the n translate-reflect matrices of D_n are related by translations (3.143).

A period-3 example: For $n = 3$ lattice state with out symmetry $\Phi^\top = (\phi_0, \phi_1, \phi_2)$, they are

$$\sigma = \begin{pmatrix} 1 & 0 & 0 \\ 0 & 0 & 1 \\ 0 & 1 & 0 \end{pmatrix}, \quad \sigma_1 = \begin{pmatrix} 0 & 1 & 0 \\ 1 & 0 & 0 \\ 0 & 0 & 1 \end{pmatrix}, \quad \sigma_2 = \begin{pmatrix} 0 & 0 & 1 \\ 0 & 1 & 0 \\ 1 & 0 & 0 \end{pmatrix}.$$

In agreement with (3.158), figure 3.12 (o) and figure 3.13 (o), reflections keep one lattice site fixed (for each permutation matrix σ_k there is only one ‘1’ on the diagonal), swap the rest.

A period-5 example: reflection symmetric lattice states tiles the infinite lattice \mathcal{L} with a reflection-fixed $\boxed{\phi_0}$ and a length-2 block (ϕ_1, ϕ_2) ,

$$\Phi = \cdots \phi_2 \phi_1 \boxed{\phi_0} \phi_1 \phi_2 | \phi_2 \phi_1 \boxed{\phi_0} \phi_1 \phi_2 | \cdots . \quad (3.163)$$

D_5 permutation representation of reflections of a pentagon, illustrates that fix-points Φ of σ_k are cyclicly related:

$$\begin{aligned} \sigma \Phi &= \begin{pmatrix} 1 & 0 & 0 & 0 & 0 \\ 0 & 0 & 0 & 0 & 1 \\ 0 & 0 & 0 & 1 & 0 \\ 0 & 0 & 1 & 0 & 0 \\ 0 & 1 & 0 & 0 & 0 \end{pmatrix} \begin{pmatrix} \boxed{\phi_0} \\ \phi_1 \\ \phi_2 \\ \phi_2 \\ \phi_1 \end{pmatrix} = \begin{pmatrix} \boxed{\phi_0} \\ \phi_1 \\ \phi_2 \\ \phi_2 \\ \phi_1 \end{pmatrix} \\ \sigma_4(r_{-2}\Phi) &= \begin{pmatrix} 0 & 0 & 0 & 0 & 1 \\ 0 & 0 & 0 & 1 & 0 \\ 0 & 0 & 1 & 0 & 0 \\ 0 & 1 & 0 & 0 & 0 \\ 1 & 0 & 0 & 0 & 0 \end{pmatrix} \begin{pmatrix} \phi_2 \\ \phi_1 \\ \boxed{\phi_0} \\ \phi_1 \\ \phi_2 \end{pmatrix} = \begin{pmatrix} \phi_2 \\ \phi_1 \\ \boxed{\phi_0} \\ \phi_1 \\ \phi_2 \end{pmatrix} . \end{aligned} \quad (3.164)$$

The symmetry conditions are the Bravais lattice site 5-periodicity mod 5, and the even reflection across $\boxed{\phi_0}$:

$$\phi_i = \phi_{i+5}, \quad \phi_{-i} = \phi_i . \quad (3.165)$$

A lattice state satisfies the defining equation (3.17)

$$-\phi_{t-1} + V'(\phi_t) - \phi_{t+1} = m_t , \quad (3.166)$$

on the period-5 Bravais cell,

$$\begin{aligned} V'(\phi_0) - 2\phi_1 &= m_0 \\ -\phi_0 + V'(\phi_1) - \phi_2 &= m_1 \\ -\phi_1 + V'(\phi_2) - \phi_2 &= m_2 \\ -\phi_1 + V'(\phi_2) - \phi_2 &= m_2 \\ -\phi_0 + V'(\phi_1) - \phi_2 &= m_1 \end{aligned} \quad (3.167)$$

where we have used (3.165). The result is a length-3 block lattice state condition for $\boxed{\phi_0}$ followed by the 2-block (ϕ_1, ϕ_2) ,

$$\begin{aligned} V'(\phi_0) - 2\phi_1 &= m_0 \\ -\phi_0 + V'(\phi_1) - \phi_2 &= m_1 \\ -\phi_1 + V'(\phi_2) - \phi_2 &= m_2 \end{aligned} \quad (3.168)$$

with a 3-dimensional orbit Jacobian matrix (3.84)

$$\mathcal{J}_+ = \begin{pmatrix} s_0 & -2 & 0 \\ -1 & s_1 & -1 \\ 0 & -1 & s_2 - 1 \end{pmatrix}, \quad (3.169)$$

While the translational symmetry is broken, the even ϕ_0 and odd ϕ_1 reflection bc's only affect the top and the bottom rows.

The orbit Jacobian matrix (3.84), 3 symmetry cases:

Odd period Bravais cell (3.158), is $[(m+1) \times (m+1)]$ -dimensional (compare with (18.334)): ²³

$$\mathcal{J}[\Phi] = \begin{pmatrix} s_0 & -2 & 0 & 0 & \cdots & 0 & 0 & 0 \\ -1 & s_1 & -1 & 0 & \cdots & 0 & 0 & 0 \\ 0 & -1 & s_2 & -1 & \cdots & 0 & 0 & 0 \\ \vdots & \vdots & \vdots & \vdots & \ddots & \vdots & \vdots & \vdots \\ 0 & 0 & 0 & 0 & \cdots & -1 & s_{m-1} & -1 \\ 0 & 0 & 0 & 0 & \cdots & 0 & -1 & s_m - 1 \end{pmatrix}. \quad (3.170)$$

Even period $n = 2m + 2$, *even reflection* k (3.159) (compare with (18.336)):

$$\mathcal{J}[\Phi] = \begin{pmatrix} s_0 & -2 & 0 & 0 & \cdots & 0 & 0 & 0 \\ -1 & s_1 & -1 & 0 & \cdots & 0 & 0 & 0 \\ 0 & -1 & s_2 & -1 & \cdots & 0 & 0 & 0 \\ \vdots & \vdots & \vdots & \vdots & \ddots & \vdots & \vdots & \vdots \\ 0 & 0 & 0 & 0 & \cdots & -1 & s_m & -1 \\ 0 & 0 & 0 & 0 & \cdots & 0 & -2 & s_{m+1} \end{pmatrix}. \quad (3.171)$$

Even period $n = 2m$, *odd reflection* k (3.160) (compare with (18.335)):

$$\mathcal{J}[\Phi] = \begin{pmatrix} s_1 - 1 & -1 & 0 & \cdots & 0 & 0 & 0 \\ -1 & s_2 & -1 & \cdots & 0 & 0 & 0 \\ \vdots & \vdots & \vdots & \ddots & \vdots & \vdots & \vdots \\ 0 & 0 & 0 & \cdots & -1 & s_{m-1} & -1 \\ 0 & 0 & 0 & \cdots & 0 & -1 & s_m - 1 \end{pmatrix}. \quad (3.172)$$

orbit Jacobian matrix \mathcal{J} evaluated on the lattice state commutes with σ ,

$$\mathcal{J}\sigma = \begin{pmatrix} s_0 & -1 & 0 & 0 & -1 \\ -1 & s_1 & -1 & 0 & 0 \\ 0 & -1 & s_2 & -1 & 0 \\ 0 & 0 & -1 & s_2 & -1 \\ -1 & 0 & 0 & -1 & s_1 \end{pmatrix} \begin{pmatrix} 1 & 0 & 0 & 0 & 0 \\ 0 & 0 & 0 & 0 & 1 \\ 0 & 0 & 0 & 1 & 0 \\ 0 & 0 & 1 & 0 & 0 \\ 0 & 1 & 0 & 0 & 0 \end{pmatrix} = \sigma\mathcal{J}. \quad (3.173)$$

²³Predrag 2021-09-01: The bottom, odd, looks like Neumann boundary condition, see Pozrikidis [127] ([click here](#)) eq. (1.5.4). The top, time-direction symmetry breaking b.c. I do not recognize.

Even period examples: For even dimensions, there are two classes of reflections, the even ones, figure 3.13 (ee), that leave two ‘yellow’ site fields fixed, swap the rest, and the odd ones, figure 3.13 (eo), that swap the ‘reds’ and ‘blues’. This is illustrated by the D_4 permutation representation of the even σ , odd σ_3 reflection symmetries of a square, figure 3.12 (e):

$$\sigma = \begin{pmatrix} 1 & 0 & 0 & 0 \\ 0 & 0 & 0 & 1 \\ 0 & 0 & 1 & 0 \\ 0 & 1 & 0 & 0 \end{pmatrix}, \quad \sigma_3 = \begin{pmatrix} 0 & 0 & 0 & 1 \\ 0 & 0 & 1 & 0 \\ 0 & 1 & 0 & 0 \\ 1 & 0 & 0 & 0 \end{pmatrix}. \quad (3.174)$$

The even reflection keeps two site fields fixed,

$$(\sigma\Phi)^\top = (\boxed{\phi_0}, \phi_3, \boxed{\phi_2}, \phi_1),$$

in agreement with (3.159). while the odd reflection reverses the order of site fields

$$(\sigma_3\Phi)^\top = (\phi_3, \phi_2 | \phi_1, \phi_0),$$

in agreement with (3.160),

(18.356) is invariant under the 1/2 lattice spacing reflection:

$$\sigma = \begin{pmatrix} 0 & 0 & 0 & 0 & 0 & 0 & 0 & 1 \\ 0 & 0 & 0 & 0 & 0 & 0 & 1 & 0 \\ 0 & 0 & 0 & 0 & 0 & 1 & 0 & 0 \\ 0 & 0 & 0 & 0 & 1 & 0 & 0 & 0 \\ 0 & 0 & 0 & 1 & 0 & 0 & 0 & 0 \\ 0 & 0 & 1 & 0 & 0 & 0 & 0 & 0 \\ 0 & 1 & 0 & 0 & 0 & 0 & 0 & 0 \\ 1 & 0 & 0 & 0 & 0 & 0 & 0 & 0 \end{pmatrix}. \quad (3.175)$$

(18.360) the corresponding reflection operator leaves sites 1 and 4 invariant:

$$\sigma_1 = \begin{pmatrix} 1 & 0 & 0 & 0 & 0 & 0 & 0 & 0 \\ 0 & 0 & 0 & 0 & 0 & 0 & 0 & 1 \\ 0 & 0 & 0 & 0 & 0 & 0 & 1 & 0 \\ 0 & 0 & 0 & 0 & 0 & 1 & 0 & 0 \\ 0 & 0 & 0 & 0 & 1 & 0 & 0 & 0 \\ 0 & 0 & 0 & 1 & 0 & 0 & 0 & 0 \\ 0 & 0 & 1 & 0 & 0 & 0 & 0 & 0 \\ 0 & 1 & 0 & 0 & 0 & 0 & 0 & 0 \end{pmatrix}. \quad (3.176)$$

Combination $r + r^{-1}$ commutes with σ_k , and σ_k conjugacy reverses \mathbb{S}

$$\begin{aligned} \sigma_k \mathcal{J} \sigma_k &= -r + \sigma_k \mathbb{S} \sigma_k - r^{-1} \\ &= \begin{pmatrix} s_{n-1} & -1 & 0 & 0 & \dots & 0 & -1 \\ -1 & s_{n-2} & -1 & 0 & \dots & 0 & 0 \\ 0 & -1 & s_2 & -1 & \dots & 0 & 0 \\ \vdots & \vdots & \vdots & \vdots & \ddots & \vdots & \vdots \\ 0 & 0 & \dots & \dots & \dots & s_2 & -1 \\ -1 & 0 & \dots & \dots & \dots & -1 & s_1 \end{pmatrix} \end{aligned} \quad (3.177)$$

where \mathbb{S} is a diagonal matrix with the lattice site k ‘stretching’ factor s_k in the k th row/column.

If a period-9 orbit is invariant under the reflection operator (see (18.361))

$$\sigma = \begin{pmatrix} 0 & 0 & 0 & 0 & 0 & 0 & 0 & 0 & 1 \\ 0 & 0 & 0 & 0 & 0 & 0 & 0 & 1 & 0 \\ 0 & 0 & 0 & 0 & 0 & 0 & 1 & 0 & 0 \\ 0 & 0 & 0 & 0 & 0 & 1 & 0 & 0 & 0 \\ 0 & 0 & 0 & 0 & 1 & 0 & 0 & 0 & 0 \\ 0 & 0 & 0 & 1 & 0 & 0 & 0 & 0 & 0 \\ 0 & 0 & 1 & 0 & 0 & 0 & 0 & 0 & 0 \\ 0 & 1 & 0 & 0 & 0 & 0 & 0 & 0 & 0 \\ 1 & 0 & 0 & 0 & 0 & 0 & 0 & 0 & 0 \end{pmatrix}. \quad (3.178)$$

If a period-8 orbit is of form (see (3.159))

$$\overline{\phi_0 \phi_1 \phi_2 \phi_3 \phi_4 \phi_3 \phi_2 \phi_1}, \quad (3.179)$$

the corresponding reflection operator leaves sites 0 and 4 invariant (see (18.361)):

$$\sigma = \begin{pmatrix} 1 & 0 & 0 & 0 & 0 & 0 & 0 & 0 & 0 \\ 0 & 0 & 0 & 0 & 0 & 0 & 0 & 0 & 1 \\ 0 & 0 & 0 & 0 & 0 & 0 & 1 & 0 & 0 \\ 0 & 0 & 0 & 0 & 0 & 1 & 0 & 0 & 0 \\ 0 & 0 & 0 & 0 & 1 & 0 & 0 & 0 & 0 \\ 0 & 0 & 0 & 1 & 0 & 0 & 0 & 0 & 0 \\ 0 & 0 & 1 & 0 & 0 & 0 & 0 & 0 & 0 \\ 0 & 1 & 0 & 0 & 0 & 0 & 0 & 0 & 0 \end{pmatrix}. \quad (3.180)$$

Table 3.1: The temporal Hénon period-5 and -6 symmetric lattice states of type figure 3.13 (b), with symmetry indicated in the σ -reflection format (3.164). For odd $n = 2m + 1$, symmetric orbits reduce to blocks of length $m + 1$. For even $n = 2m$, their lengths are either $m + 1$ or m . The period-5 lattice states are plotted in figure 2.2 (to supersede figure 15.2 (left)). There is no asymmetric period-5, the first C_n asymmetric pair is period-6. Indicated: the binary code m_j of the field ϕ_j at the lattice site $j = 0, 1, 2, 3, 4$.

C_6	$\phi_0\phi_1\phi_2\phi_3\phi_4\phi_5$	D_6
001011	001011	001011
110100	110100	
C_5	$\phi_{-2}\phi_{-1} \phi_0 \phi_1\phi_2 $	D_5
11110	11 0 11	0 11
00011	10 0 01	0 01
00101	01 0 10	0 10
00001	00 1 00	1 00
11010	10 1 01	1 01
11100	01 1 10	1 10
	$\phi_0\phi_1\phi_2 \phi_3\phi_2\phi_1 $	
010001	0 10 0 01	0 10 0
011111	0 11 1 11	0 11 1
001110	0 01 1 10	0 01 1
100000	1 00 0 00	1 00 0
101110	1 01 1 10	1 01 1
	$\phi_0\phi_1\phi_2 \phi_2\phi_1\phi_0 $	
001100	001 100	001
011110	011 110	011

3.12 Periodic orbit theory

Recurrent phenomena, the simplest of which is periodic motion, are particularly interesting and practical objects of study. Scientists have long been captivated by the near periodic motions of the planets. Among them, Poincaré was the first to truly recognize the importance of periodic solutions in understanding more complex dynamical behavior.

The problem of counting periodic orbits and how they partition the state space partitions is among the first problems that one needs to address [6, 15, 17, 20, 22, 23, 35, 103, 104, 144]. For the quadratic map it was addressed in 1950's by [Myrberg](#), in perhaps the first application of computers to dynamics [114–118].

The problem of counting orbits for the Hénon map was also addressed very early, in a pioneering work by Simó [130] using an approach centered in the strange attractor creation/destruction.

MacKay [105] 1982 PhD thesis, published as *Renormalisation in Area-preserving Maps* has a chapter on reversible maps. Do cite in our paper(s). MacKay had these numbers already listed in Table 1.2.3.5.1 of his 1982 PhD thesis [105].

This is the ‘periodic orbit theory’. And if you don’t know, [now you know](#).

3.12.1 Periodic orbit theory

How come that a ‘Det’ in (3.88) counts lattice states?

n	1	2	3	4	5	6	7	8	9	10	11
N_n	2	4	8	16	32	64	128	256	512	1024	.
M_n	2	1	2	3	6	9	18	30	56	99	186

Table 3.2: Lattice states and orbit counts for the $a = 6$ Hénon map.

For a general, nonlinear fixed point condition $F[\Phi] = 0$, expansion (7.22) in terms of traces is a cycle expansion [7, 31, 37], with support on *periodic orbits*. Ozorio de Almeida and Hannay [121] were the first to relate the number of periodic points to a Jacobian matrix generated volume; in 1984 they used such relation as an illustration of their ‘principle of uniformity’: “periodic points of an ergodic system, counted with their natural weighting, are uniformly dense in phase space.” In periodic orbit theory [31, 36] this principle is stated as a **flow conservation** sum rule, where the sum is over all lattice states M of period n ,

$$\sum_{|M|=n} \frac{1}{|\det(\mathbf{1} - \mathbb{J}_M)|} = 1, \quad (3.181)$$

or, by Hill’s formula (3.106),

$$\sum_{|M|=n} \frac{1}{|\text{Det } \mathcal{J}_M|} = 1. \quad (3.182)$$

For the Bernoulli system the ‘natural weighting’ takes a particularly simple form, as the Hill determinant of the orbit Jacobian matrix is the same for all periodic points of period n , $\text{Det } \mathcal{J}_M = \text{Det } \mathcal{J}$, whose number is thus given by (3.107). For example, the sum over the $n = 2$ lattice states is,

$$\frac{1}{|\text{Det } \mathcal{J}_{00}|} + \frac{1}{|\text{Det } \mathcal{J}_{01}|} + \frac{1}{|\text{Det } \mathcal{J}_{10}|} = 1, \quad (3.183)$$

see figure 3.7 (b). Furthermore, for any piece-wise linear system all curvature corrections [35] for orbits of periods $k > n$ vanish, leading to explicit lattice state-counting formulas of kind reported in this paper.

In the case of temporal Bernoulli or temporal cat, the hyperbolicity is the same everywhere and does not depend on a particular solution Φ_p , counting periodic orbits is all that is needed to solve a cat-map dynamical system completely; once periodic orbits are counted, all cycle averaging formulas [34] follow.

A zeta function relates the totality of admissible states to the orbits generated by all symmetries of a given theory.

3.12.2 Topological zeta function

Now that we have the numbers of lattice states N_n for any period n , we can combine them all into a single generating function by substituting N_n into the

topological or *Artin-Mazur* zeta function [6, 35],²⁴

$$1/\zeta_{\text{top}}(z) = \exp \left(- \sum_{n=1}^{\infty} \frac{z^n}{n} N_n \right), \quad (3.184)$$

which, when expanded as a Taylor series in z , is built from *primitive* (or *prime*), i.e., non-repeating lattice states [31]. Conversely, given the topological zeta function, the number of periodic points of period n is given by the logarithmic derivative of the topological zeta function (see *ChaosBook* [35])

$$\sum_{n=1} N_n z^n = - \frac{1}{1/\zeta_{\text{top}}} z \frac{d}{dz} (1/\zeta_{\text{top}}). \quad (3.185)$$

For a Bernoulli system (4.272),

$$\begin{aligned} 1/\zeta_{\text{top}}(z) &= \exp \left(- \sum_{n=1}^{\infty} \frac{z^n}{n} (s^n - 1) \right) = \exp [\ln(1 - sz) - \ln(1 - z)] \\ &= \frac{1 - sz}{1 - z}. \end{aligned} \quad (3.186)$$

The numerator $(1 - sz)$ says that a Bernoulli system is a full shift [35]: there are s fundamental lattice states, in this case fixed points $\{\phi_0, \phi_1, \dots, \phi_{s-1}\}$, and every other lattice state is built from their concatenations and repeats. The denominator $(1 - z)$ compensates for the single overcounted lattice state, the fixed point $\phi_{s-1} = \phi_0 \pmod{1}$ of figure 3.2 and its repeats.

For non-integer values of the stretching factor $s = \beta$, the map (3.24) is called the ' β -transformation'. For its topological zeta function see ref. [65].

3.12.3 Counting temporal Bernoulli prime periodic orbits

Substituting the Bernoulli map topological zeta function (13.81) into (3.185) we obtain

$$\begin{aligned} \sum_{n=1} N_n z^n &= z + 3z^2 + 7z^3 + 15z^4 + 31z^5 + 63z^6 + 127z^7 \\ &\quad + 255z^8 + 511z^9 + 1023z^{10} + 2047z^{11} \dots, \end{aligned} \quad (3.187)$$

in agreement with the lattice states count (3.107). The number of *prime* cycles of period n is given recursively by subtracting repeats of shorter prime cycles [35],

$$M_n = \frac{1}{n} \left(N_n - \sum_{d|n}^{d < n} d M_d \right), \quad (3.188)$$

²⁴Predrag 2020-02-16: Do I need to derive this, rather than refer to ChaosBook?

where d 's are all divisors of n , hence

$$\begin{aligned} \sum_{n=1} M_n z^n &= z + z^2 + 2z^3 + 3z^4 + 6z^5 + 9z^6 + 18z^7 \\ &\quad + 30z^8 + 56z^9 + 99z^{10} + 186z^{11} \dots, \end{aligned} \quad (3.189)$$

in agreement with the usual numbers of binary symbolic dynamics prime cycles [35].

3.12.4 Topological zeta function

Substituting the numbers of lattice states N_n (3.95) into the *topological zeta function* (3.184), Isola [89] obtains

$$\begin{aligned} 1/\zeta_{\text{top}}(z) &= \exp \left(- \sum_{n=1}^{\infty} \frac{z^n}{n} N_n \right) = \exp \left(- \sum_{n=1}^{\infty} \frac{z^n}{n} (\Lambda^n + \Lambda^{-n} - 2) \right) \\ &= \exp [\ln(1 - z\Lambda) + \ln(1 - z\Lambda^{-1}) - 2\ln(1 - z)] \\ &= \frac{(1 - z\Lambda)(1 - z\Lambda^{-1})}{(1 - z)^2} = \frac{1 - sz + z^2}{(1 - z)^2}. \end{aligned} \quad (3.190)$$

Topological zeta functions count *prime orbits*, i.e., time invariant sets of equivalent lattice states related by translations (cyclic permutations), and other symmetries [35].

Conversely, given the topological zeta function, the generating function for the number of temporal lattice states of period n is given by the logarithmic derivative of the topological zeta function (3.185),

$$\begin{aligned} \sum_{n=0}^{\infty} N_n z^n &= \frac{2 - sz}{1 - sz + z^2} - \frac{2}{1 - z} \\ &= (s - 2) [z + (s + 2)z^2 + (s + 1)^2 z^3 \\ &\quad + (s + 2)s^2 z^4 + (s^2 + s - 1)^2 z^5 + \dots], \end{aligned} \quad (3.191)$$

which is indeed the generating function for $T_n(s/2)$, the *Chebyshev polynomial of the first kind* (3.96).

Why Chebyshev? Essentially because $T_k(x)$ are also defined by a 3-term recurrence:

$$\begin{aligned} T_0(x) &= 1, \quad T_1(x) = x \\ T_k(x) &= 2xT_{k-1}(x) - T_{k-2}(x) \quad \text{for } k \geq 2, \end{aligned} \quad (3.192)$$

The numbers of periodic points and *prime* cycles M_n (given by (3.188)) are tabulated in table 4.1.

n	1	2	3	4	5	6	7	8	9	10	11
N_n	1	5	16	45	121	320	841	2205	5776	15125	39601
M_n	1	2	5	10	24	50	120	270	640	1500	3600

Table 3.3: Lattice states and prime orbit counts for the $s = 3$ cat map (Bird and Vivaldi [14]).

3.13 Topological D_∞ -zeta function

We use the temporal 1D lattice for systems with time-reversal symmetry to explain how such zeta functions are constructed.

A topological zeta function is the generating function of all distinct orbits (3.151) for a given system.

We shall refer to G -orbit (3.151) counting generating function for a symmetry group G as the topological G -zeta function, or the Lind zeta function [101]. The classic example is (3.184), the *Artin-Mazur* zeta function [6, 35] for the *infinite cyclic group* C_∞ of all integer time translations. Here we focus on the *infinite dihedral group* topological D_∞ -zeta function (Kim-Lee-Park [93] or flip-zeta function).

The *infinite dihedral group* D_∞ (4.7)
the trace formula for maps: ²⁵

$$\sum_p n_p \sum_{r=1}^{\infty} \frac{z^{n_p r}}{|\det(\mathbf{1} - M_p^r)|}. \quad (3.193)$$

the trace formula (3.193) can be recovered from the spectral determinant by taking a derivative

$$-z \frac{d}{dz} \ln \det(1 - z\mathcal{L}). \quad (3.194)$$

For every integer temporal period n , we first determine N_n , the number of all periodic *lattice state* Φ_M solutions on a tile of length n .

Due to the time invariance of the defining equations, there are n_p physically equivalent copies of a given solution in the orbit of every Φ_p . So all we really have to do is to enumerate M_n orbits of the time-invariance equivalent periodic orbit solutions, whose generating function is the topological zeta function.

That Hill determinant factors as $\text{Det } \mathcal{J} = \text{Det } \mathcal{J}_- \text{Det } \mathcal{J}_+$ for all symmetric states must propagate into the factorization of the dynamical zeta function, mirroring the Kim *et al.* [93] topological (counting) Lind eta function (4.149).

multiplicity m_Φ of orbit \mathcal{M}_Φ (3.153)

Let G be a group, \mathcal{M} a set and $f : G \times \mathcal{M} \rightarrow \mathcal{M}$ a G -action on \mathcal{M} . The Lind

²⁵Predrag : box this relation

zeta function [101] is defined by

$$\zeta_{Lind}(t) = \exp \left(\sum_H \frac{N_H}{|G/H|} t^{|G/H|} \right), \quad (3.195)$$

where the sum is over all finite-index subgroups H of G , such that $|G/H| < \infty$, and N_H is defined by (see (3.201)):

$$N_H = |\{\phi \in \mathcal{M} : \text{all } h \in H \quad f(h, \phi) = \phi\}|. \quad (3.196)$$

A flip system (\mathcal{M}, f, σ) is a dynamical system, where \mathcal{M} is a topological space and $f : \mathcal{M} \rightarrow \mathcal{M}$ is a homeomorphism. $\sigma : \mathcal{M} \rightarrow \mathcal{M}$ is flip for (\mathcal{M}, f) that satisfy:

$$\sigma \circ f \circ \sigma = f^{-1} \quad \text{and} \quad \sigma^2 = \mathbf{1}. \quad (3.197)$$

Kim *et al.* [93] showed that the zeta function ζ_σ of a flip system (\mathcal{M}, f, σ) can be defined as a Lind zeta function ζ_{Lind} of the D_∞ -action $f : D_\infty \times \mathcal{M} \rightarrow \mathcal{M}$ that is given by:

$$f(r, x) = f(x) \quad \text{and} \quad f(\sigma, x) = \sigma(x). \quad (3.198)$$

Every finite index subgroup of the infinite dihedral group D_∞ is either

$$H_n = \langle r^n \rangle \quad \text{or} \quad H_{n,k} = \langle r^n, r^k \sigma \rangle, \quad (3.199)$$

with indices

$$|D_\infty/H_n| = 2|n| \quad \text{or} \quad |D_\infty/H_{n,k}| = |n|. \quad (3.200)$$

If n is a positive integer and k is an integer, then $N_{n,k}$ will denote the number of points in \mathcal{M} fixed by f^n and $f^k \circ \sigma$:

$$N_{n,k} = |\{\phi \in \mathcal{M} : f^n(\phi) = f^k \circ \sigma(\phi) = \phi\}|. \quad (3.201)$$

They obtain²⁶

$$\zeta_\sigma(t) = \exp \left(\sum_{n=1}^{\infty} \frac{N_n}{2n} t^{2n} + \sum_{n=1}^{\infty} \sum_{k=0}^{n-1} \frac{N_{n,k}}{n} t^n \right). \quad (3.202)$$

The first sum factors as an Artin-Mazur zeta function (4.226):

$$\exp \left(\sum_{n=1}^{\infty} \frac{t^{2n}}{2n} N_n \right) = \sqrt{\zeta_{top}(t^2)} \quad (3.203)$$

The class count (3.145), (3.156) tells us that

$$N_{n,k} = \begin{cases} N_{n,0} & \text{if } n \text{ is odd,} \\ N_{n,0} & \text{if } n \text{ and } k \text{ are even,} \\ N_{n,1} & \text{if } n \text{ is even and } k \text{ is odd.} \end{cases} \quad (3.204)$$

²⁶Predrag 2021-07-04, 2021-08-25: our notation, replaced subscript f, σ by noting.

Hence

$$\sum_{k=0}^{n-1} \frac{N_{n,k}}{n} = \begin{cases} N_{n,0} & \text{if } n \text{ is odd,} \\ \frac{N_{n,0} + N_{n,1}}{2} & \text{if } n \text{ is even.} \end{cases} \quad (3.205)$$

so the Lind zeta function of the flip triple system (\mathcal{M}, f, σ) is

$$\zeta_\sigma(t) = \sqrt{\zeta_{top}(t^2)} e^{h(t)}, \quad (3.206)$$

where ζ_{top} is the Artin-Mazur zeta function ArtMaz5, and the counts of symmetric orbits

$$h(t) = \sum_{m=1}^{\infty} \left\{ N_{2m-1,0} t^{2m-1} + (N_{2m,0} + N_{2m,1}) \frac{t^{2m}}{2} \right\}. \quad (3.207)$$

The $\exp(h(t))$ in (3.206) can be factored into terms that presumably correspond –in the particular, Hénon case– to the $D_n N_n$ factors in (2.15), but this is now totally general, in the spirit of table 18.3, for any time-reversal discrete time dynamical system. Should be generalizable also to systems with continuous time.

The zeta function ζ_σ can be written as a product over orbits. Let O_1 be the collection of finite orbits with time reversal (flip) symmetry, and O_2 be the collection of the pairs of orbits without time reversal symmetry, each an orbit and the flipped orbit. A finite orbit p is a periodic points set

$$p = \{\phi, f(\phi), \dots, f^{n_p-1}(\phi)\}$$

if $p \in O_1$, and

$$p = \{\phi, f(\phi), \dots, f^{k-1}(\phi)\} \cup \{\sigma(\phi), f \circ \sigma(\phi), \dots, f^{k-1} \circ \sigma(\phi)\}$$

if $p \in O_2$, where $k = n_p/2$.

If $p \in O_1$,

$$\zeta_p(t) = \sqrt{\frac{1}{1-t^{2n_p}}} \exp\left(\frac{t^{n_p}}{1-t^{n_p}}\right), \quad (3.208)$$

and if $p \in O_2$,

$$\zeta_p(t) = \frac{1}{1-t^{n_p}}. \quad (3.209)$$

The product form of the zeta function is:

$$1/\zeta_\sigma(t) = \sqrt{\prod_{p_1 \in O_1} (1-t^{2n_{p_1}})} \exp\left(-\frac{t^{n_{p_1}}}{1-t^{n_{p_1}}}\right) \prod_{p_2 \in O_2} (1-t^{n_{p_2}}). \quad (3.210)$$

3.13.1 Counting temporal cat lattice states

(4.177), (5.27) introduce μ . See also (18.57), (18.101), (18.268), (18.273), (18.337),

For $s > 2$ the stability multipliers $(\Lambda^+, \Lambda^-) = (\Lambda, \Lambda^{-1})$ are real,

$$\Lambda^\pm = \frac{1}{2}(s \pm \sqrt{D}), \quad \Lambda = e^\lambda, \quad (3.211)$$

where

$$\begin{aligned} s &= \Lambda + \Lambda^{-1} = 2 \cosh(\lambda) \\ s - 2 &= \mu^2 \\ \sqrt{D} &= \Lambda - \Lambda^{-1} = 2 \sinh(\lambda) \\ \text{discriminant } D &= s^2 - 4 = \mu^2(\mu^2 + 4) \end{aligned} \quad (3.212)$$

The sine, sinh, cos, cosh are related by the identities (5.29) and (5.30). For D_n irreps, I think we should use the (4.43) form of eigenvalues, and Klein-Gordon mass μ

$$\begin{aligned} \lambda_m &= \mu^2 + 4 \sin^2(\alpha_m/2) \\ &= \left(\mu - i 2 \sin\left(\frac{\alpha_m}{2}\right) \right) \left(\mu + i 2 \sin\left(\frac{\alpha_m}{2}\right) \right) \\ \alpha_m &= 2\pi m/n, \end{aligned} \quad (3.213)$$

rather than (18.323) and stretching s , which is appropriate to C_n irreps. Identities like (13.5), (18.191), (13.90) and Gradshteyn and Ryzhik [76] Eq. 1.317.1 ([click here](#))

$$2 \sin^2(\theta/2) = 1 - \cos(\theta) \quad (3.214)$$

are also suggestive in this context.

How to count the number of lattice states for temporal cat?

No symmetry lattice states Hill determinant:

$$N_n = \prod_{j=0}^{n-1} \left(s - 2 \cos \frac{2\pi j}{n} \right).$$

The products of eigenvalues for the C_n discrete Fourier case follows from (10.52):

$$\prod_{j=0}^{n-1} \left(s - 2 \cos \frac{2\pi j}{n} \right) = (\Lambda^{n/2} - \Lambda^{-n/2})^2, \quad (3.215)$$

It's a square, because of the D_n symmetry. Consider even, odd cases, use $\cos 0 = 1$, $\cos \pi = -1$, $\cos(-\theta) = \cos \theta$. The product over non-trivial eigenvalues is:

$$n = 2m \quad M_{n,0} = \prod_{j=1}^{m-1} \left(s - 2 \cos \frac{\pi j}{m} \right) = \frac{|\Lambda^{n/2} - \Lambda^{-n/2}|}{\mu \sqrt{\mu^2 + 4}}, \quad (3.216)$$

$$n = 2m - 1 \quad M_{n,1} = \prod_{j=1}^{m-1} \left(s - 2 \cos \frac{2j\pi}{2m-1} \right) = \frac{|\Lambda^{n/2} - \Lambda^{-n/2}|}{\mu} \quad (3.217)$$

Next, look at the *symmetric* lattice states Hill determinants:

For odd $n = 2m - 1$,

$$N_{n,1} = \prod_{j=0}^{m-1} \left(s - 2 \cos \frac{2\pi j}{n} \right) = \mu M_{n,1}. \quad (3.218)$$

For $n = 2m$,

$$\begin{aligned} N_{n,1} &= \prod_{j=0}^{m-1} \left(s - 2 \cos \frac{2\pi j}{n} \right) \\ N_{n,0} &= (s+2) N_{n,1}, \end{aligned} \quad (3.219)$$

and

$$\frac{1}{2} (N_{n,0} + N_{n,1}) = \frac{\mu^2 + 5}{2} \prod_{j=0}^{m-1} \left(s - 2 \cos \frac{2\pi j}{n} \right) = \frac{\mu^2 + 5}{2\mu} \sqrt{\frac{(\Lambda^n + \Lambda^{-n} - 2)}{\mu^2 + 4}} \quad (3.220)$$

The number of lattice states can be written as polynomials: For $n = 2m - 1$:

$$\begin{aligned} N_{n,0} &= \mu \left(\Lambda^{n/2} - \Lambda^{-n/2} \right) \\ &= \mu^2 \Lambda^{-1/2} (\Lambda^m - \Lambda^{-m+1}). \end{aligned} \quad (3.221)$$

For $n = 2m$:

$$\begin{aligned} \frac{1}{2} (N_{n,0} + N_{n,1}) &= \frac{s+3}{2(\Lambda - \Lambda^{-1})} \left(\Lambda^{n/2} - \Lambda^{-n/2} \right) \\ &= \frac{\mu^2 + 5}{2\mu\sqrt{\mu^2 + 4}} |\Lambda^m - \Lambda^{-m}|. \end{aligned} \quad (3.222)$$

Now we can compute the $h(t)$ from (3.207)

$$\begin{aligned} h(t) &= \sum_{m=1}^{\infty} \left[N_{2m-1,0} t^{2m-1} + (N_{2m,0} + N_{2m,1}) \frac{t^{2m}}{2} \right] \\ &= \mu \frac{\Lambda^{1/2} t}{1 - \Lambda t^2} - \mu \frac{\Lambda^{-1/2} t}{1 - \Lambda^{-1} t^2} \\ &\quad + \frac{\mu^2 + 5}{2(\Lambda - \Lambda^{-1})} \frac{\Lambda t^2}{1 - \Lambda t^2} - \frac{\mu^2 + 5}{2(\Lambda - \Lambda^{-1})} \frac{\Lambda^{-1} t^2}{1 - \Lambda^{-1} t^2}. \end{aligned} \quad (3.223)$$

Using (3.206) we have the "flip" part of the zeta function. Testing this zeta function using (3.233), we have:

$$\begin{aligned} -t \frac{\partial}{\partial t} (\ln e^{-h(t)}) &= t + 6t^2 + 12t^3 + 36t^4 + 55t^5 + 144t^6 \\ &\quad + 203t^7 + 504t^8 + 684t^9 + 1650t^{10} + \dots, \end{aligned} \quad (3.224)$$

which is in agreement with (3.233) and table 18.3.

3.13.2 Counting lattice states

Given the topological zeta function (3.202) we can count the number of lattice states from the generating function: ²⁷

$$\frac{-t \frac{d}{dt} (1/\zeta_\sigma(t))}{1/\zeta_\sigma(t)} = \sum_{n=1}^{\infty} N_n t^{2n} + \sum_{n=1}^{\infty} \sum_{k=0}^{n-1} N_{n,k} t^n = \sum_{m=1}^{\infty} a_m t^m, \quad (3.225)$$

where the coefficients are:

$$a_m = \begin{cases} \sum_{k=0}^{m-1} N_{m,k}^\sigma = mN_{m,0}^\sigma, & m \text{ is odd}, \\ N_{m/2} + \sum_{k=0}^{m-1} N_{m,k}^\sigma = N_{m/2} + \frac{m}{2} (N_{m,0}^\sigma + N_{m,1}^\sigma), & m \text{ is even}. \end{cases} \quad (3.226)$$

Using the product formula of topological zeta function (3.210) and the numbers of orbits with length up to 5 from the table 18.3, we can write the topological zeta function:

$$\begin{aligned} 1/\zeta_\sigma(t) &= \sqrt{1-t^2} \exp\left(-\frac{t}{1-t}\right) (1-t^4) \exp\left(-\frac{2t^2}{1-t^2}\right) \left(\sqrt{1-t^6}\right)^3 \\ &\quad \exp\left(-\frac{3t^3}{1-t^3}\right) (1-t^6)(1-t^8)^3 \exp\left(-\frac{6t^4}{1-t^4}\right) \\ &\quad (1-t^8)^2(1-t^{10})^5 \exp\left(-\frac{10t^5}{1-t^5}\right) (1-t^{10})^6 \dots. \end{aligned} \quad (3.227)$$

The generating function is:

$$\frac{-t \frac{d}{dt} (1/\zeta_\sigma)}{1/\zeta_\sigma} = t + 7t^2 + 12t^3 + 41t^4 + 55t^5 + \dots, \quad (3.228)$$

which is in agreement with (3.226), where the N_n and N_n^σ are the C_n and SF_n in the table 18.3.

²⁷Predrag 2021-08-25: We have the counts of the Bravais lattice states N_n , $N_{n,k}$ already, from (3.204), so why don't we reverse the logic, start here, and get the zeta function (3.206) by integration? Mention that this is an example of Lind zeta function [101] (3.195) without ever writing it down, so we do not have to explain it? It's a side issue for us, really.

We are not able to retrieve the numbers of fixed points by their symmetry groups using this topological zeta function (3.202), unless we rewrite the topological zeta function with two variables:

$$\zeta_\sigma(t, u) = \exp \left(\sum_{n=1}^{\infty} \frac{N_n}{2n} t^{2n} + \sum_{n=1}^{\infty} \sum_{k=0}^{n-1} \frac{N_{n,k}}{n} u^n \right). \quad (3.229)$$

Using this topological zeta function $\zeta_\sigma(t, u)$ we can write two generating functions:

$$\frac{-t \frac{\partial}{\partial t} (1/\zeta_\sigma(t, u))}{1/\zeta_\sigma(t, u)} = \sum_{n=1}^{\infty} N_n t^{2n}, \quad (3.230)$$

and

$$\frac{-u \frac{\partial}{\partial u} (1/\zeta_\sigma(t, u))}{1/\zeta_\sigma(t, u)} = \sum_{n=1}^{\infty} \sum_{k=0}^{n-1} N_{n,k} u^n. \quad (3.231)$$

Using the product formula of this topological zeta function and the numbers of orbits with length up to 5 from the table 18.3, the topological zeta function is:

$$\begin{aligned} 1/\zeta_\sigma(t, u) &= \sqrt{1-t^2} \exp \left(-\frac{u}{1-u} \right) (1-t^4) \exp \left(-\frac{2u^2}{1-u^2} \right) \left(\sqrt{1-t^6} \right)^3 \\ &\quad \exp \left(-\frac{3u^3}{1-u^3} \right) (1-t^6)(1-t^8)^3 \exp \left(-\frac{6u^4}{1-u^4} \right) \\ &\quad (1-t^8)^2(1-t^{10})^5 \exp \left(-\frac{10u^5}{1-u^5} \right) (1-t^{10})^6 \dots . \end{aligned} \quad (3.232)$$

And the generating function from this topological zeta function is:

$$\frac{-u \frac{\partial}{\partial u} (1/\zeta_\sigma(t, u))}{1/\zeta_\sigma(t, u)} = u + 6u^2 + 12u^3 + 36u^4 + 55u^5 + \dots, \quad (3.233)$$

which is in agreement with (3.231), where the N_n^σ is the SF_n in the table 18.3.

3.14 Summary

How to think about matters spatiotemporal? While dynamics of a turbulent system might appear so complex to defy any precise description, the laws of motion drive a spatially extended system (clouds, say) through a repertoire of unstable patterns, each defined over a finite spatiotemporal region [78, 79]. The local dynamics, observed through such finite spatiotemporal windows, can be thought of as a visitation sequence of a finite repertoire of finite patterns. To make predictions about such system, one needs to know how often a given pattern occurs, and that is a purview of periodic orbit theory [33].

However, the initial rapid progress in description of turbulence in terms of such ‘exact coherent structures’ [72, 91] has slowed down to a crawl due to our inability to extend the theory and the computations to spatially large or infinite computational domains [21].

But in dynamics, we have no fear of the infinite extent in time. That is periodic orbit theory’s [38] *raison d’être*; the dynamics itself describes the infinite time strange sets by a hierarchical succession of periodic orbits, of longer and longer, but always finite periods (with no artificial external periodicity imposed along the time axis). And, since 1996 we know how to deal with both spatially and temporally infinite regions by tiling them with finite spatiotemporally periodic tiles [26, 72]. More precisely: a time periodic orbit is computed in a finite time, with period T , but its repeats “tile” the time axis for all times. Similarly, a spatiotemporally periodic “tile” or “invariant 2-torus” is computed on a finite spatial region L , for a finite period T , but its repeats in both time and space directions tile the infinite spacetime.

Taken together, these open a path to determining exact solutions on *spatially infinite* regions. This is important, as many turbulent flows of physical interest come equipped with D continuous spatial symmetries. For example, in a pipe flow at transitional Reynolds number, the azimuthal and radial directions (measured in viscosity length units) are compact, while the pipe length is infinite. If the theory is recast as a d -dimensional space-time theory, $d = D + 1$, spatiotemporally translational invariant recurrent solutions are invariant d -tori (and *not* the 1-dimensional periodic orbits of the traditional periodic orbit theory), and the symbolic dynamics is likewise d -dimensional (rather than what is today taken for given, a single 1-dimensional temporal string of symbols).

This changes everything. Instead of studying time evolution of a chaotic system, one now studies the repertoire of spatiotemporal patterns allowed by a given PDE, or, in the discretized spacetime, partial difference equations. To put it more provocatively: junk your old equations and look for guidance in clouds’ repeating patterns. There is no more *time* in this vision of nonlinear *dynamics*! Instead, there is the space of all spatiotemporal patterns, and the likelihood that a given finite spatiotemporally pattern can appear, like the mischievous grin of Cheshire cat, anywhere in the turbulent evolution of a flow. A bold vision, but how does it work?

and thus a d -dimensional spatiotemporal pattern is mapped one-to-one

onto a d -dimensional discrete lattice state, symbolic dynamics labelled configuration - a configuration very much like that of an Ising model of statistical mechanics.

In this paper we have analyzed
in particular, a spatiotemporal lattice formulation of time reversal.
corresponding dynamical zeta functions should be sums over d -dimensional Bravais cells, rather than 1-dimensional time-periodic orbits.

While the setting is classical, such deterministic field-theory advances offer new semi-classical approaches to quantum field theory and many-body problems.

References

- [1] E. Allroth, “Ground state of one-dimensional systems and fixed points of $2n$ -dimensional map”, *J. Phys. A* **16**, L497 (1983).
- [2] S. Anastassiou, “Complicated behavior in cubic Hénon maps”, *Theoret. Math. Phys.* **207**, 572–578 (2021).
- [3] S. Anastassiou, A. Bountis, and A. Bäcker, “Homoclinic points of 2D and 4D maps via the parametrization method”, *Nonlinearity* **30**, 3799–3820 (2017).
- [4] S. Anastassiou, A. Bountis, and A. Bäcker, “Recent results on the dynamics of higher-dimensional Hénon maps”, *Regul. Chaotic Dyn.* **23**, 161–177 (2018).
- [5] V. I. Arnol’d and A. Avez, *Ergodic Problems of Classical Mechanics* (Addison-Wesley, Redwood City, 1989).
- [6] M. Artin and B. Mazur, “On periodic points”, *Ann. Math.* **81**, 82–99 (1965).
- [7] R. Artuso, E. Aurell, and P. Cvitanović, “Recycling of strange sets: I. Cycle expansions”, *Nonlinearity* **3**, 325–359 (1990).
- [8] R. Artuso, E. Aurell, and P. Cvitanović, “Recycling of strange sets: II. Applications”, *Nonlinearity* **3**, 361–386 (1990).
- [9] S. Aubry, “Anti-integrability in dynamical and variational problems”, *Physica D* **86**, 284–296 (1995).
- [10] S. Aubry and G. Abramovici, “Chaotic trajectories in the standard map. The concept of anti-integrability”, *Physica D* **43**, 199–219 (1990).
- [11] M. Baake, J. Hermisson, and A. B. Pleasants, “The torus parametrization of quasiperiodic LI-classes”, *J. Phys. A* **30**, 3029–3056 (1997).
- [12] A. Barvinok, *Lattice Points, Polyhedra, and Complexity*, tech. rep. (Univ. of Michigan, Ann Arbor MI, 2004).
- [13] O. Biham and W. Wenzel, “Characterization of unstable periodic orbits in chaotic attractors and repellers”, *Phys. Rev. Lett.* **63**, 819 (1989).

- [14] N. Bird and F. Vivaldi, “Periodic orbits of the sawtooth maps”, *Physica D* **30**, 164–176 (1988).
- [15] R. L. Bivins, J. D. Louck, N. Metropolis, and M. L. Stein, “Classification of all cycles of the parabolic map”, *Physica D* **51**, 3–27 (1991).
- [16] S. V. Bolotin and D. V. Treschev, “Hill’s formula”, *Russ. Math. Surv.* **65**, 191 (2010).
- [17] A. Bridy and R. A. Pérez, “A count of maximal small copies in Multibrot sets”, *Nonlinearity* **18**, 1945–1953 (2005).
- [18] R. B. S. Brooks, R. F. Brown, J. Pak, and D. H. Taylor, “Nielsen numbers of maps of tori”, *Proc. Amer. Math. Soc.* **52**, 398–398 (1975).
- [19] A. Brown, “Equations for periodic solutions of a logistic difference equation”, *J. Austral. Math. Soc. Ser. B* **23**, 78–94 (1981).
- [20] K. M. Brucks, “MSS sequences, colorings of necklaces, and periodic points of $f(z) = z^2 - 2$ ”, *Adv. Appl. Math.* **8**, 434–445 (1987).
- [21] N. B. Budanur, K. Y. Short, M. Farazmand, A. P. Willis, and P. Cvitanović, “Relative periodic orbits form the backbone of turbulent pipe flow”, *J. Fluid Mech.* **833**, 274–301 (2017).
- [22] O. Chavoya-Aceves, F. Angulo-Brown, and E. Piña, “Symbolic dynamics of the cubic map”, *Physica D* **14**, 374–386 (1985).
- [23] W. Y. C. Chen and J. D. Louck, “Necklaces, MSS sequences, and DNA sequences”, *Adv. Appl. Math.* **18**, 18–32 (1997).
- [24] B. V. Chirikov, “A universal instability of many-dimensional oscillator system”, *Phys. Rep.* **52**, 263–379 (1979).
- [25] W. G. Choe and J. Guckenheimer, “Computing periodic orbits with high accuracy”, *Computer Meth. Appl. Mech. and Engin.* **170**, 331–341 (1999).
- [26] F. Christiansen, P. Cvitanović, and V. Putkaradze, “Spatiotemporal chaos in terms of unstable recurrent patterns”, *Nonlinearity* **10**, 55–70 (1997).
- [27] D. Cimasoni, “The critical Ising model via Kac-Ward matrices”, *Commun. Math. Phys.* **316**, 99–126 (2012).
- [28] Y. Colin de Verdière, “Spectrum of the Laplace operator and periodic geodesics: thirty years after”, *Ann. Inst. Fourier* **57**, 2429–2463 (2007).
- [29] J. Cserti, “Application of the lattice Green’s function for calculating the resistance of an infinite network of resistors”, *Amer. J. Physics* **68**, 896–906 (2000).
- [30] J. Cserti, G. Széchenyi, and G. Dávid, “Uniform tiling with electrical resistors”, *J. Phys. A* **44**, 215201 (2011).
- [31] P. Cvitanović, “Invariant measurement of strange sets in terms of cycles”, *Phys. Rev. Lett.* **61**, 2729–2732 (1988).
- [32] P. Cvitanović, “Chaotic Field Theory: A sketch”, *Physica A* **288**, 61–80 (2000).

- [33] P. Cvitanović, “Recurrent flows: The clockwork behind turbulence”, *J. Fluid Mech. Focus Fluids* **726**, 1–4 (2013).
- [34] P. Cvitanović, “Trace formulas”, in *Chaos: classical and quantum*, edited by P. Cvitanović, R. Artuso, R. Mainieri, G. Tanner, and G. Vattay (Niels Bohr Inst., Copenhagen, 2017).
- [35] P. Cvitanović, “Counting”, in *Chaos: Classical and Quantum* (Niels Bohr Inst., Copenhagen, 2020).
- [36] P. Cvitanović, “Why cycle?”, in *Chaos: Classical and Quantum*, edited by P. Cvitanović, R. Artuso, R. Mainieri, G. Tanner, and G. Vattay (Niels Bohr Inst., Copenhagen, 2020).
- [37] P. Cvitanović, R. Artuso, R. Mainieri, G. Tanner, and G. Vattay, *Chaos: Classical and Quantum* (Niels Bohr Inst., Copenhagen, 2020).
- [38] P. Cvitanović, R. Artuso, R. Mainieri, G. Tanner, and G. Vattay, *Chaos: Classical and Quantum* (Niels Bohr Inst., Copenhagen, 2020).
- [39] P. Cvitanović, R. Artuso, L. Rondoni, and E. A. Spiegel, “Transporting densities”, in *Chaos: Classical and Quantum*, edited by P. Cvitanović, R. Artuso, R. Mainieri, G. Tanner, and G. Vattay (Niels Bohr Inst., Copenhagen, 2017).
- [40] P. Cvitanović, C. P. Dettmann, R. Mainieri, and G. Vattay, “Trace formulas for stochastic evolution operators: Weak noise perturbation theory”, *J. Stat. Phys.* **93**, 981–999 (1998).
- [41] P. Cvitanović, C. P. Dettmann, R. Mainieri, and G. Vattay, “Trace formulae for stochastic evolution operators: Smooth conjugation method”, *Nonlinearity* **12**, 939 (1999).
- [42] P. Cvitanović and Y. Lan, Turbulent fields and their recurrences, in *Correlations and Fluctuations in QCD : Proceedings of 10. International Workshop on Multiparticle Production*, edited by N. Antoniou (2003), pp. 313–325.
- [43] P. Cvitanović and H. Liang, *Spatiotemporal cat: A chaotic field theory*, In preparation, 2021.
- [44] P. Cvitanović and D. Lippolis, Knowing when to stop: How noise frees us from determinism, in *Let's Face Chaos through Nonlinear Dynamics*, edited by M. Robnik and V. G. Romanovski (2012), pp. 82–126.
- [45] P. Cvitanović, N. Søndergaard, G. Palla, G. Vattay, and C. P. Dettmann, “Spectrum of stochastic evolution operators: Local matrix representation approach”, *Phys. Rev. E* **60**, 3936–3941 (1999).
- [46] R. L. Devaney, *An Introduction to Chaotic Dynamical systems*, 2nd ed. (Westview Press, Cambridge, Mass, 2008).
- [47] R. L. Devaney and Z. Nitecki, “Shift automorphisms in the Hénon mapping”, *Commun. Math. Phys.* **67**, 137–146 (1979).

- [48] A. Dienstfrey, F. Hang, and J. Huang, “Lattice sums and the two-dimensional, periodic Green’s function for the Helmholtz equation”, Proc. Roy. Soc. Ser A **457**, 67–85 (2001).
- [49] X. Ding, H. Chaté, P. Cvitanović, E. Siminos, and K. A. Takeuchi, “Estimating the dimension of the inertial manifold from unstable periodic orbits”, Phys. Rev. Lett. **117**, 024101 (2016).
- [50] X. Ding and P. Cvitanović, “Periodic eigendecomposition and its application in Kuramoto-Sivashinsky system”, SIAM J. Appl. Dyn. Syst. **15**, 1434–1454 (2016).
- [51] E. J. Doedel, A. R. Champneys, T. F. Fairgrieve, Y. A. Kuznetsov, B. Sandstede, and X. Wang, *AUTO: Continuation and Bifurcation Software for Ordinary Differential Equations* (2007).
- [52] F. W. Dorr, “The direct solution of the discrete Poisson equation on a rectangle”, SIAM Rev. **12**, 248–263 (1970).
- [53] M. S. Dresselhaus, G. Dresselhaus, and A. Jorio, *Group Theory: Application to the Physics of Condensed Matter* (Springer, New York, 2007).
- [54] H. R. Dullin and J. D. Meiss, “Stability of minimal periodic orbits”, Phys. Lett. A **247**, 227–234 (1998).
- [55] H. R. Dullin and J. D. Meiss, “Generalized Hénon maps: the cubic diffeomorphisms of the plane”, Physica D **143**, 262–289 (2000).
- [56] E. N. Economou, *Green’s Functions in Quantum Physics* (Springer, Berlin, 2006).
- [57] S. Elaydi, *An Introduction to Difference Equations*, 3rd ed. (Springer, Berlin, 2005).
- [58] A. Endler and J. A. C. Gallas, “Period four stability and multistability domains for the Hénon map”, Physica A **295**, 285–290 (2001).
- [59] A. Endler and J. A. C. Gallas, “Arithmetical signatures of the dynamics of the Hénon map”, Phys. Rev. E **65**, 036231 (2002).
- [60] A. Endler and J. A. C. Gallas, “Conjugacy classes and chiral doublets in the Hénon Hamiltonian repeller”, Phys. Lett. A **356**, 1–7 (2006).
- [61] A. Endler and J. A. C. Gallas, “Reductions and simplifications of orbital sums in a Hamiltonian repeller”, Phys. Lett. A **352**, 124–128 (2006).
- [62] A. Endler and J. A. C. Gallas, “Reductions and simplifications of orbital sums in a Hamiltonian repeller”, Phys. Lett. A **352**, 124–128 (2006).
- [63] M. J. Feigenbaum and B. Hasslacher, “Irrational decimations and path-integrals for external noise”, Phys. Rev. Lett. **49**, 605–609 (1982).
- [64] A. L. Fetter and J. D. Walecka, *Theoretical Mechanics of Particles and Continua* (Dover, New York, 2003).
- [65] L. Flatto, J. C. Lagarias, and B. Poonen, “The zeta function of the beta transformation”, Ergodic Theory Dynam. Systems **14**, 237–266 (1994).

- [66] S. Friedland and J. Milnor, “Dynamical properties of plane polynomial automorphisms”, *Ergodic Theory Dynam. Systems* **9**, 67–99 (1989).
- [67] P. M. Gade and R. E. Amritkar, “Spatially periodic orbits in coupled-map lattices”, *Phys. Rev. E* **47**, 143–154 (1993).
- [68] J. A. C. Gallas, “Equivalence among orbital equations of polynomial maps”, *Int. J. Modern Phys. C* **29**, 1850082 (2018).
- [69] J. A. C. Gallas, “Orbital carriers and inheritance in discrete-time quadratic dynamics”, *Int. J. Modern Phys. C* **31**, 2050100 (2020).
- [70] J. A. C. Gallas, “Preperiodicity and systematic extraction of periodic orbits of the quadratic map”, *Int. J. Modern Phys. C* **31**, 2050174 (2020).
- [71] J. F. Gibson, *Channelflow: A spectral Navier-Stokes simulator in C++*, tech. rep., Channelflow.org (U. New Hampshire, 2019).
- [72] J. F. Gibson, J. Halcrow, and P. Cvitanović, “Visualizing the geometry of state-space in plane Couette flow”, *J. Fluid Mech.* **611**, 107–130 (2008).
- [73] S. Gnutzmann, T. Guhr, H. Schomerus, and K. Życzkowski, “Special issue in honour of the life and work of Fritz Haake”, *J. Phys. A* **54**, 130301 (2021).
- [74] C. Godsil and G. . Royle, *Algebraic Graph Theory* (Springer, New York, 2013).
- [75] G. H. Golub and C. F. Van Loan, *Matrix Computations*, 4th ed. (J. Hopkins Univ. Press, Baltimore, MD, 2013).
- [76] I. S. Gradshteyn and I. M. Ryzhik, *Tables of Integrals, Series and Products*, 8th ed. (Elsevier LTD, Oxford, New York, 2014).
- [77] J. Guckenheimer and B. Meloon, “Computing periodic orbits and their bifurcations with automatic differentiation”, *SIAM J. Sci. Comput.* **22**, 951–985 (2000).
- [78] M. N. Gudorf, *Spatiotemporal Tiling of the Kuramoto-Sivashinsky Equation*, PhD thesis (School of Physics, Georgia Inst. of Technology, Atlanta, 2020).
- [79] M. N. Gudorf, N. B. Budanur, and P. Cvitanović, *Spatiotemporal tiling of the Kuramoto-Sivashinsky flow*, In preparation, 2021.
- [80] B. Gutkin, L. Han, R. Jafari, A. K. Saremi, and P. Cvitanović, “Linear encoding of the spatiotemporal cat map”, *Nonlinearity* **34**, 2800–2836 (2021).
- [81] B. Gutkin and V. Osipov, “Classical foundations of many-particle quantum chaos”, *Nonlinearity* **29**, 325–356 (2016).
- [82] M. C. Gutzwiller, *Chaos in Classical and Quantum Mechanics* (Springer, New York, 1990).
- [83] J. F. Heagy, “A physical interpretation of the Hénon map”, *Physica D* **57**, 436–446 (1992).

- [84] M. Hénon, “A two-dimensional mapping with a strange attractor”, *Commun. Math. Phys.* **50**, 94–102 (1976).
- [85] G. W. Hill, “On the part of the motion of the lunar perigee which is a function of the mean motions of the sun and moon”, *Acta Math.* **8**, 1–36 (1886).
- [86] D. L. Hitzl and F. Zele, “An exploration of the Hénon quadratic map”, *Physica D* **14**, 305–326 (1985).
- [87] G. Y. Hu and R. F. O’Connell, “Analytical inversion of symmetric tridiagonal matrices”, *J. Phys. A* **29**, 1511 (1996).
- [88] G. Y. Hu, J. Y. Ryu, and R. F. O’Connell, “Analytical solution of the generalized discrete Poisson equation”, *J. Phys. A* **31**, 9279 (1998).
- [89] S. Isola, “ ζ -functions and distribution of periodic orbits of toral automorphisms”, *Europhys. Lett.* **11**, 517–522 (1990).
- [90] B. Kastening, “Simplified transfer matrix approach in the two-dimensional Ising model with various boundary conditions”, *Phys. Rev. E* **66**, 057103 (2002).
- [91] G. Kawahara and S. Kida, “Periodic motion embedded in plane Couette turbulence: Regeneration cycle and burst”, *J. Fluid Mech.* **449**, 291 (2001).
- [92] J. P. Keating, “The cat maps: quantum mechanics and classical motion”, *Nonlinearity* **4**, 309–341 (1991).
- [93] Y.-O. Kim, J. Lee, and K. K. Park, “A zeta function for flip systems”, *Pacific J. Math.* **209**, 289–301 (2003).
- [94] H.-T. Kook and J. D. Meiss, “Application of Newton’s method to Lagrangian mappings”, *Physica D* **36**, 317–326 (1989).
- [95] Y. Lan and P. Cvitanović, “Variational method for finding periodic orbits in a general flow”, *Phys. Rev. E* **69**, 016217 (2004).
- [96] J. Li and S. Tomsovic, “Exact relations between homoclinic and periodic orbit actions in chaotic systems”, *Phys. Rev. E* **97**, 022216 (2017).
- [97] M.-C. Li and M. Malkin, “Bounded nonwandering sets for polynomial mappings”, *J. Dynam. Control Systems* **10**, 377–389 (2004).
- [98] H. Liang and P. Cvitanović, Time reversal for discrete time dynamical systems, In preparation, 2021.
- [99] A. J. Lichtenberg and M. A. Lieberman, *Regular and Chaotic Dynamics*, 2nd ed. (Springer, New York, 2013).
- [100] W. J. Lick, *Difference Equations from Differential Equations* (Springer, Berlin, 1989).
- [101] D. A. Lind, “A zeta function for Z^d -actions”, in *Ergodic Theory of Z^d Actions*, edited by M. Pollicott and K. Schmidt (Cambridge Univ. Press, 1996), pp. 433–450.

- [102] D. Lippolis and P. Cvitanović, “How well can one resolve the state space of a chaotic map?”, *Phys. Rev. Lett.* **104**, 014101 (2010).
- [103] M. Lutzky, “Counting stable cycles in unimodal iterations”, *Phys. Lett. A* **131**, 248–250 (1988).
- [104] M. Lutzky, “Counting hyperbolic components of the Mandelbrot set”, *Phys. Lett. A* **177**, 338–340 (1993).
- [105] R. S. MacKay, *Renormalisation in Area-preserving Maps* (World Scientific, Singapore, 1993).
- [106] R. S. MacKay and J. D. Meiss, “Linear stability of periodic orbits in Lagrangian systems”, *Phys. Lett. A* **98**, 92–94 (1983).
- [107] R. S. MacKay, J. D. Meiss, and I. C. Percival, “Transport in Hamiltonian systems”, *Physica D* **13**, 55–81 (1984).
- [108] J. D. Meiss, “Symplectic maps, variational principles, and transport”, *Rev. Mod. Phys.* **64**, 795–848 (1992).
- [109] N. Miguel, C. Simó, and A. Vieiro, “From the Hénon conservative map to the Chirikov standard map for large parameter values”, *Regul. Chaotic Dyn.* **18**, 469–489 (2013).
- [110] J. W. Mintmire, B. I. Dunlap, and C. T. White, “Are Fullerene tubules metallic?”, *Phys. Rev. Lett.* **68**, 631–634 (1992).
- [111] I. Montvay and G. Münster, *Quantum Fields on a Lattice* (Cambridge Univ. Press, Cambridge, 1994).
- [112] B. Mramor and B. Rink, “Ghost circles in lattice Aubry-Mather theory”, *J. Diff. Equ.* **252**, 3163–3208 (2012).
- [113] G. Münster and M. Walzl, *Lattice gauge theory - A short primer*, 2000.
- [114] P. J. Myrberg, “Iteration der reellen Polynome zweiten Grades I”, *Ann. Acad. Sc. Fenn. A* **256**, 1–10 (1958).
- [115] P. J. Myrberg, “Iteration von quadratwurzeloperationen”, *Ann. Acad. Sc. Fenn. A* **259**, 1–10 (1958).
- [116] P. J. Myrberg, “Iteration der reellen Polynome zweiten Grades II”, *Ann. Acad. Sc. Fenn. A* **268**, 1–13 (1959).
- [117] P. J. Myrberg, “Sur l’itération des polynomes réels quadratiques”, *J. Math. Pures Appl.* **41**, 339–351 (1962).
- [118] P. J. Myrberg, “Iteration der reellen Polynome zweiten Grades III”, *Ann. Acad. Sc. Fenn. A* **336**, 1–13 (1963).
- [119] J. Nielsen, “Über die Minimalzahl der Fixpunkte bei den Abbildungstypen der Ringflächen”, *Math. Ann.* **82**, 83–93 (1920).
- [120] L. Onsager, “Crystal statistics. I. A Two-dimensional model with an order-disorder transition”, *Phys. Rev.* **65**, 117–149 (1944).

- [121] A. M. Ozorio de Almeida and J. H. Hannay, “Periodic orbits and a correlation function for the semiclassical density of states”, *J. Phys. A* **17**, 3429 (1984).
- [122] R. Peierls, “Zur Theorie des Diamagnetismus von Leitungselektronen”, *Z. Phys.* **80**, 763–791 (1933).
- [123] I. Percival and F. Vivaldi, “A linear code for the sawtooth and cat maps”, *Physica D* **27**, 373–386 (1987).
- [124] H. Poincaré, “Sur les déterminants d’ordre infini”, *Bull. Soc. Math. France* **14**, 77–90 (1886).
- [125] A. Politi and A. Torcini, “Periodic orbits in coupled Hénon maps: Lyapunov and multifractal analysis”, *Chaos* **2**, 293–300 (1992).
- [126] M. Pollicott, *Dynamical zeta functions*, in *Smooth Ergodic Theory and Its Applications*, Vol. 69, edited by A. Katok, R. de la Llave, Y. Pesin, and H. Weiss (2001), pp. 409–428.
- [127] C. Pozrikidis, *An Introduction to Grids, Graphs, and Networks* (Oxford Univ. Press, Oxford , UK, 2014).
- [128] A. Rényi, “Representations for real numbers and their ergodic properties”, *Acta Math. Acad. Sci. Hung.* **8**, 477–493 (1957).
- [129] O. E. Rössler, “An equation for continuous chaos”, *Phys. Lett. A* **57**, 397–398 (1976).
- [130] C. Simó, “On the Hénon-Pomeau attractor”, *J. Stat. Phys.* **21**, 465–494 (1979).
- [131] B. Simon, “Almost periodic schrödinger operators: A review”, *Adv. Appl. Math.* **3**, 463–490 (1982).
- [132] S. Smale, “Differentiable dynamical systems”, *Bull. Amer. Math. Soc.* **73**, 747–817 (1967).
- [133] J. Stephenson and D. T. Ridgway, “Formulae for cycles in the Mandelbrot set II”, *Physica A* **190**, 104–116 (1992).
- [134] G. Sterling D., *Anti-integrable Continuation and the Destruction of Chaos*, PhD thesis (Univ. Colorado, Boulder, CO, 1999).
- [135] D. G. Sterling, H. R. Dullin, and J. D. Meiss, “Homoclinic bifurcations for the Hénon map”, *Physica D* **134**, 153–184 (1999).
- [136] D. Sterling and J. D. Meiss, “Computing periodic orbits using the anti-integrable limit”, *Phys. Lett. A* **241**, 46–52 (1998).
- [137] R. Sturman, J. M. Ottino, and S. Wiggins, *The Mathematical Foundations of Mixing* (Cambridge Univ. Press, 2006).
- [138] M. Toda, *Theory of Nonlinear Lattices* (Springer, Berlin, 1989).
- [139] D. Treschev and O. Zubelevich, “Hill’s formula”, in *Introduction to the Perturbation Theory of Hamiltonian Systems* (Springer, Berlin, 2009), pp. 143–162.

- [140] D. Viswanath, “The Lindstedt-Poincaré technique as an algorithm for finding periodic orbits”, *SIAM Rev.* **43**, 478–496 (2001).
- [141] D. Viswanath, “Symbolic dynamics and periodic orbits of the Lorenz attractor”, *Nonlinearity* **16**, 1035–1056 (2003).
- [142] D. Viswanath, “The fractal property of the Lorenz attractor”, *Physica D* **190**, 115–128 (2004).
- [143] A. P. Willis, *Openpipeflow: Pipe flow code for incompressible flow*, tech. rep., Openpipeflow.org (U. Sheffield, 2014).
- [144] F.-G. Xie and B. L. Hao, “Counting the number of periods in one-dimensional maps with multiple critical points”, *Physica A* **202**, 237–263 (1994).

Chapter 4

Group theory

We used to be stuck on reflection-symmetry reduction needed to factorize the zeta functions. But no more - see sect. 4.4 *A Lind zeta function for flip systems*.
classical field theory on d -dimensional lattice

$$(\square - \mu^2) \Phi + F[\Phi] = -M \quad (4.1)$$

Definitions:

The matrix *symmetry group* G of a matrix M :

$$S(M) = \{g \in G \mid gMg^{-1} = M\}. \quad (4.2)$$

The *reversing matrix symmetry group* R of a matrix M :

$$\mathcal{R}(M) = \{s \in R \mid sMs^{-1} = M^{-1}\}. \quad (4.3)$$

A matrix M is *reversible* if it is conjugate to its inverse within matrix group R .

Park [74] refers to (3.134) as ‘skew-commuting’:

“The ‘covering space’ has two actions, f and s , where f is a \mathbb{Z} -action, s is a map of order two, and s and T skew-commute; that is, $sfs = f^{-l}$.”

Let (\mathcal{M}, f) be an invertible dynamical system. A homeomorphism $s : \mathcal{M} \rightarrow \mathcal{M}$ is a *flip* if

$$s \circ f \circ s = f^{-1}, \quad s^2 = 1. \quad (4.4)$$

The triple (\mathcal{M}, f, s) is called a *flip system* [58].

For a shift space a flip is a non-abelian group action, see (4.7). A flip system (\mathcal{M}, f, s) is *shift-flip system of finite type* if (\mathcal{M}, f) is a shift of finite type.

Notation follows [Dihedral group](#) and [Regular polygons](#) wikis.

T is a normal subgroup of G .

For space groups, the cosets by translation subgroup T (the set all translations) form the *factor* (also known as *quotient*) group G/T , isomorphic to the point group g . The normal subgroup of a line group G is its translational subgroup T , with its factor group G/T isomorphic to the *isogonal point group* P of discrete symmetries of its 1-dimensional unit cell $x \in [0, 1]$.

$$r_i r_j = r_{i+j}, \quad r_i s_j = s_{i+j}, \quad s_i r_j = s_{i-j}, \quad s_i s_j = r_{i-j}, \quad (4.5)$$

As the order in which a translation and a reflection are applied is not commutative, dihedral groups are nonabelian.

¹

To omit from the paper:

As any two flips result in a rotation, alternative presentation for D_n , n even, is generated by a horizontal (short axis) reflection, and a diagonal (long axis) reflection, rather than the usual (r, s) set. (I have not checked this for the odd n .)

an even index $2k$ reflection s_{2k} reflects the lattice across the k th lattice site, while an odd index reflection s_{2k+1} reflects the lattice across the midpoint between sites k and $k+$.

Definition: Coset. Let $H = \{e, b_2, b_3, b_4, \dots\} \subseteq G$ be a subgroup of G . The set of h elements $\{c, cb_2, cb_3, cb_4, \dots\}$, $c \in G$ but not in H , is called left coset cH . For a given subgroup H the group elements are partitioned into H and $m - 1$ cosets, where $m = |G|/|H|$.

There are $2n$ left cosets of subgroup $H(n)$ in D_∞ (4.229), with the quotient group $D_\infty/H(n)$ isomorphic to the dihedral group D_n .

There are n infinite dihedral $H(n, k)$ subgroups of D_∞ , with n left cosets (4.230) and the quotient group $D_\infty/H(n, k)$ isomorphic to the cyclic group C_n .

A typical turbulent trajectory of fluid flow has no symmetry beyond the identity, so its symmetry group is the trivial subgroup $\{e\}$.

In summary: You can visualize an lattice states invariant under a translation subgroup $H(a)$, figure 3.13 (a), as a tiling of the lattice \mathbb{Z} by a lattice state tiles with a fish painted on it, swimming upstream, and no reflection symmetry.

Note that as $H(10, 9)$ and $H(10, 0)$ are not conjugate subgroups, there is no translation or reflection that maps lattice state of the first type into lattice state of the second.

An orbit is by construction a *symmetry invariant* notion: as the set of all lattice states that can be reached Φ by symmetries, it is an invariant set, as any group action merely permutes it. The full state space \mathcal{M} is a union of such orbits.

If G is a symmetry, intrinsic properties of an orbit p (period, Floquet multipliers) evaluated anywhere along its G -orbit are the same.

A symmetry thus reduces the number of inequivalent lattice states \mathcal{M}_p . So we also need to describe the symmetry of a *solution*, as opposed to the symmetry of the *system*.

A generic orbit might be ergodic, unstable and essentially uncontrollable. The ChaosBook strategy is to populate the state space by a hierarchy of orbits which are *compact invariant sets* (equilibria, periodic orbits, invariant tori, ...),

¹Predrag 2021-07-17: Fig. 2.1 in [Damnjanović and Milošević](#) is cute:) So is [this illustration](#) of the group elements D_8 .

each computable in a finite time. They are to a generic orbit what fractions are to normal numbers on the unit interval.

While for the infinite lattice case there are no ‘long axes’, ‘short axes’, an even index $2k$ reflection s_{2k} still reflects the lattice across the k th lattice site (a ‘vertex’ of a triangle or a square in the finite example), while an odd index $2k-1$ reflection s_{2k-1} reflects the lattice across the midpoint between sites $k-1$ and k (an ‘edge’ of a square in the finite example).²

Not sure we need this, so I dropped it for now: “For odd n , there are $(n-1)/2$ such classes. For even n , there are $(n-2)/2$ such pairs, with the rotation by half a circle a class $\{r_{n/2}\}$ by itself.”

Dihedral groups are *ambivalent* groups – every element is conjugate to its inverse. Thus, all the irreducible representations of a dihedral group over the complex numbers can be realized over the real numbers. Etc.

As D_n elements are combinations of one-step translations and reflections, its group presentation is

$$D_n = \langle r, s \mid r^n = s^2 = 1, rs = sr^{n-1} \rangle . \quad (4.6)$$

A presentation of the *infinite dihedral group* [58] is

$$D_\infty = \langle r, s \mid srs = r^{-1}, s^2 = 1 \rangle . \quad (4.7)$$

$D_1, D_2, D_3, D_4, \dots$

Examples are the D_3 Cayley table 4.11 and the D_6 Cayley table 4.12.

So far, ChaosBook works out zeta function factorizations for D_1 (example 4.11), D_2 (known as Klein four-group), D_3 (symmetric group S_3), and D_4 .



example 4.15
p. 278



example 4.17
p. 280



example 4.18
p. 280

4.1 Temporal lattice systems

4.1.1 Temporal Bernoulli system

To motivate our formulation of a spatiotemporal chaotic field theory to be developed in the sequel [29], we recast the local initial value, time-evolution Bernoulli map problem as a *temporal lattice* fixed point condition, the problem of enumerating and determining all global solutions.

‘Temporal’ here refers to the state (field) ϕ_t , and the winding number (source) m_t taking their values on the lattice sites of a 1-dimensional *temporal* integer lattice $t \in \mathbb{Z}$. Over a finite lattice segment, these can be written compactly as a *lattice state* and the corresponding *symbol block*

$$\Phi^\top = (\phi_{t+1}, \dots, \phi_{t+n}), \quad M^\top = (m_{t+1}, \dots, m_{t+n}), \quad (4.8)$$

²Han 2021-08-13: This is correct only when we define that s is the reflection across the 0th lattice site.

where $(\dots)^\top$ denotes a transpose. The Bernoulli equation, rewritten as a first-order difference equation

$$\phi_t - s\phi_{t-1} = -m_t, \quad \phi_t \in [0, 1], \quad (4.9)$$

takes the matrix form

$$\mathcal{J}\Phi = -M, \quad \mathcal{J} = \mathbb{1} - sr^{-1}, \quad (4.10)$$

where the $[n \times n]$ matrix

$$r_{jk} = \delta_{j+1,k}, \quad r = \begin{pmatrix} 0 & 1 & & & \\ & 0 & 1 & & \\ & & \ddots & & \\ & & & 0 & 1 \\ 1 & & & & 0 \end{pmatrix}, \quad (4.11)$$

implements the shift operation, a cyclic permutation that translates forward in time the lattice state Φ by one site, $(r\Phi)^\top = (\phi_2, \phi_3, \dots, \phi_n, \phi_1)$. The time evolution law must be of the same form for all times, so the shift operator r has to be time-translation invariant, with $r_{n+1,n} = r_{1n} = 1$ matrix element enforcing the periodicity. After n shifts, a lattice state returns to the initial state,

$$r^n = \mathbb{1}. \quad (4.12)$$

4.1.2 Temporal cat

Written out as a second-order difference equation, the Percival-Vivaldi map takes a particularly elegant, *temporal cat* form

$$\phi_{t+1} - s\phi_t + \phi_{t-1} = -m_t, \quad (4.13)$$

or, in terms of a lattice state Φ , the corresponding symbol block M (4.8), and the $[n \times n]$ shift operator r (4.11),

$$(r - s\mathbb{1} + r^{-1})\Phi = -M, \quad (4.14)$$

very much like the temporal Bernoulli condition (4.10). ‘Temporal’ again refers to the global lattice state (field) Φ , and the winding numbers (sources) M taking their values on the lattice sites of a 1-dimensional *temporal* lattice $t \in \mathbb{Z}$.

where the $[n \times n]$ orbit Jacobian matrix \mathcal{J} is now given by

$$\mathcal{J} = r - s\mathbb{1} + r^{-1} \quad (4.15)$$

a tri-diagonal Toeplitz matrix (constant along each diagonal, $\mathcal{J}_{k\ell} = j_{k-\ell}$) of circulant form,

$$\mathcal{J} = \begin{pmatrix} -s & 1 & \cdot & \cdot & \dots & \cdot & 1 \\ 1 & -s & 1 & \cdot & \dots & \cdot & \cdot \\ \cdot & 1 & -s & 1 & \dots & \cdot & \cdot \\ \vdots & \vdots & \vdots & \vdots & \ddots & \vdots & \vdots \\ \cdot & \cdot & \dots & \dots & \dots & -s & 1 \\ 1 & \cdot & \dots & \dots & \dots & 1 & -s \end{pmatrix}. \quad (4.16)$$

4.1.3 Lattice states

A lattice state Φ is *periodic* if it satisfies

$$\Phi(x + R) = \Phi(x) \quad (4.17)$$

for any discrete translation $R = n\mathbf{a} \in \mathcal{L}$, where n is any integer, and \mathbf{a} is the integer lattice vector that defines the *Bravais cell* (or, the Bravais sublattice of \mathbb{Z}).

The basic ‘atom’ of a reflection-symmetric period n lattice state is a ‘half’ of it, the length m orbit, and its reflection

$$\tilde{\Phi} = \phi_1 \phi_2 \phi_3 \cdots \phi_m, \quad s\tilde{\Phi} = \phi_m \cdots \phi_3 \phi_2 \phi_1, \quad (4.18)$$

in terms of which a Bravais lattice state Φ has one of the four symmetries:

$$(1) \quad \tilde{\Phi} \quad m = n \quad (4.19)$$

$$(2) \quad \boxed{\phi_0} \tilde{\Phi} | s\tilde{\Phi} \quad m = (n - 1)/2, \quad n \text{ odd} \quad (4.20)$$

$$(3) \quad \boxed{\phi_0} \tilde{\Phi} \boxed{\phi_{m+1}} | s\tilde{\Phi} \quad m = (n - 2)/2, \quad n \text{ even} \quad (4.21)$$

$$(4) \quad \tilde{\Phi} | s\tilde{\Phi} \quad m = n/2, \quad n \text{ even} \quad (4.22)$$

While the defining equation for temporal cat or temporal Hénon is equivariant under the integer lattice *space group* $p1m$ symmetry operations, the individual lattice states either have no symmetry at all (they are, after all, ‘turbulent’), or are invariant under subgroups of space group $p1m$.

In addition, the temporal cat (but not the temporal Hénon) has a *dynamical symmetry* under the inversion S through the center of the $0 \leq \phi_j < 1$ unit interval,

$$\bar{\phi}_j = S\phi_j = 1 - \phi_j, \quad \text{for all } j \in \mathcal{L}. \quad (4.23)$$

Indeed, if $\Phi_M = \{\phi_t\}$ is a lattice state, its conjugation symmetry partner $\bar{\Phi} = \{1 - \phi_t\}$ is also a lattice state. So, every lattice state either belongs to a conjugate pair $\{\Phi, \bar{\Phi}\}$, or is self-dual under conjugation.

The temporal cat happens to involve two quite distinct lattices:

- (i) In the latticization of a continuous time, one replaces a time-dependent field $\phi(t)$ at time $t \in \mathbb{R}^d$ by a discrete set of its values $\phi_t = \phi(t\Delta T)$ on lattice sites, where the subscript $t \in \mathbb{Z}$ is a discrete time *coordinate*.
- (ii) A peculiarity of the temporal cat is that the *field* ϕ_t is confined to the unit interval $[0, 1]$, imparting a \mathbb{Z} lattice structure onto the calculationally intermediate fundamental parallelepiped \mathcal{J} basis vectors.

4.1.4 Reflection-symmetric lattice states

2021-08-14 Predrag Almost everything in this section is misguided or wrong.
Delete eventually...

Consider a lattice state

$$\cdots \phi_{-3} \phi_{-2} \phi_{-1} \phi_0 \phi_1 \phi_2 \phi_3 \phi_4 \cdots \quad (4.24)$$

over an infinite 1-dimensional integer lattice \mathbb{Z} . Assume for the moment that the system is linear so a sum of lattice states is also a lattice state.

If the lattice state is antisymmetric under an even reflection, the antisymmetric subspace is 2-dimensional. The lattice state tiles the infinite lattice as:

$$\overline{0} \phi_1 \phi_2 \overline{0} \phi_2 \phi_1, \quad (4.25)$$

Go to any lattice site k , reflect the lattice state and average the two, using the translate-reflect operator³

$$P_k = \frac{1}{2}(\mathbf{1} + s_k). \quad (4.26)$$

The result is a lattice state reflection-symmetric across lattice site k . From (3.143) it follows that for odd k , all P_k operators are in the same conjugacy class as P_1 , and for even k , all P_k are in the same conjugacy class as P_0 . It suffices to do the computation only once for each class.

$$P_{\pm} = (1 \pm s)/2$$

$$P_+ = \frac{1}{2} \begin{pmatrix} 2 & 0 & 0 & 0 & 0 \\ 0 & 1 & 0 & 0 & 1 \\ 0 & 0 & 1 & 1 & 0 \\ 0 & 0 & 1 & 1 & 0 \\ 0 & 1 & 0 & 0 & 1 \end{pmatrix}, \quad \text{Tr } P_+ = 3 \quad (4.27)$$

with two orthogonal null eigenvectors

$$e_4 = 2^{-1/2}(0, 0, 1, -1, 0), e_5 = 2^{-1/2}(0, 1, 0, 0, -1),$$

suggesting an orthogonal basis

$$e_1 = (1, 0, 0, 0, 0), e_2 = 2^{-1/2}(0, 0, 1, 1, 0) e_3 = 2^{-1/2}(0, 1, 0, 0, 1)$$

Stack them up into a diagonalization matrix

$$V = \begin{pmatrix} 1 & 0 & 0 & 0 & 0 \\ 0 & 0 & 1 & 0 & 1 \\ 0 & 1 & 0 & 1 & 0 \\ 0 & 1 & 0 & -1 & 0 \\ 0 & 0 & 1 & 0 & -1 \end{pmatrix}, \quad V^{-1} = \frac{1}{2} \begin{pmatrix} 2 & 0 & 0 & 0 & 0 \\ 0 & 0 & 1 & 1 & 0 \\ 0 & 1 & 0 & 0 & 1 \\ 0 & 0 & 1 & -1 & 0 \\ 0 & 1 & 0 & 0 & -1 \end{pmatrix} \quad (4.28)$$

(I gave up on this - too manual)

$$P_- = \frac{1}{2} \begin{pmatrix} 0 & 0 & 0 & 0 & 0 \\ 0 & 1 & 0 & 0 & -1 \\ 0 & 0 & 1 & -1 & 0 \\ 0 & 0 & -1 & 1 & 0 \\ 0 & -1 & 0 & 0 & 1 \end{pmatrix}, \quad \text{Tr } P_- = 2. \quad (4.29)$$

³Predrag 2021-10-08: Was 'shift-reflect', but Burak says in fluid dynamics translation is one direction, but 'reflect' is in a transverse direction; changed to avoid confusion.

The determinant of a $[3 \times 3]$ matrix can be written as the antisymmetrized trace of the matrix [25]:

$$\begin{aligned}\text{Det } M &= \text{Tr}_3 AM = \frac{1}{3} \sum_{k=1}^3 (-1)^{k-1} (\text{Tr}_{3-k} AM) \text{Tr } M^k \\ &= \frac{1}{3} ((\text{Tr}_2 AM) \text{Tr } M - (\text{Tr } M) \text{Tr } M^2 + \text{Tr } M^3) \\ \text{Tr}_2 AM &= \frac{1}{2} ((\text{Tr } M)^2 - \text{Tr } M^2),\end{aligned}\quad (4.30)$$

where A is the antisymmetrization projection operator, and 3 is the dimension of the matrix M . Evaluating this seems a bit not smart...

Apply the (4.26) operator $P_0 = (\mathbf{1} + s)/2$ to lattice state (4.24). We obtain a lattice state

$$\cdots \tilde{\phi}_4 \tilde{\phi}_3 \tilde{\phi}_2 \tilde{\phi}_1 |\tilde{\phi}_0| \tilde{\phi}_1 \tilde{\phi}_2 \tilde{\phi}_3 \tilde{\phi}_4 \cdots, \quad (4.31)$$

symmetric under reflection, where $\tilde{\phi}_j = (\phi_{-j} + \phi_j)/2$, are pairwise symmetric under the reflection s , with $|\tilde{\phi}_0| = (\phi_0 + \phi_0)/2$ indicating that the field at the lattice site 0 is unchanged by reflection.

Next apply the projection operator $P_1 = (\mathbf{1} + sr)/2$ from (4.26) to a lattice state (4.24). We obtain a lattice state

$$\cdots \tilde{\phi}_4 \tilde{\phi}_3 \tilde{\phi}_2 \tilde{\phi}_1 | \tilde{\phi}_1 \tilde{\phi}_2 \tilde{\phi}_3 \tilde{\phi}_4 \cdots, \quad (4.32)$$

where $|$ indicates that the state is symmetric under reflection across midpoint between lattice sites 0 and 1, and the successive lattice pair averages $\tilde{\phi}_j = (\phi_j + \phi_{1-j})/2$, $j = 1, 2, 3, \dots$, are pairwise symmetric under the reflection s_1 .

In summary, as reflection operators $s_0 = s$ and $s_1 = sr$ belong to the two dihedral group D_∞ classes, all other lattice states symmetric with respect to reflection s_k , for any integer k , are conjugate to the above two types of symmetric lattice states.

2021-08-23 Predrag I still worry about the antisymmetric states (18.338), (18.339); here (4.33) and (4.33) look wrong as they force the fixed lattice site fields to be zero. Cannot be true for nonlinear field theories, such as temporal Hénon. Presumably, individual symmetric lattice states are either symmetric or antisymmetric under the swap, not just the reflection-reduced orbit Jacobian matrix \mathcal{J} . I wish someone would actually show me how this works for individual temporal cat or temporal Hénon lattice states? I'll plod on...

2021-08-28 Predrag For example, if the period of the lattice states is 6, we have two kinds of reflections. If the lattice state is antisymmetric under an odd reflection, the antisymmetric subspace is 3-dimensional, and the Bravais lattice state tiles \mathcal{L} as:

$$\tilde{\phi}_1 \tilde{\phi}_2 \tilde{\phi}_3 | \tilde{\phi}_3 \tilde{\phi}_2 \tilde{\phi}_1 |, \quad (4.33)$$

where the underline is a shorthand for $\underline{\phi}_j = -\phi_j$.

2021-08-29 Predrag A period-5 reflection *antisymmetric lattice state* tiles the infinite lattice as:

$$\cdots \underline{\phi_2} \underline{\phi_1} \overline{\phi_0} \phi_1 \phi_2 | \underline{\phi_2} \underline{\phi_1} \overline{\phi_0} \phi_1 \phi_2 | \cdots , \quad (4.34)$$

The thing to get used to is that a reflection of the Bravais cell leads to

$$s \overline{\phi_0} \phi_1 \phi_2 | \underline{\phi_2} \underline{\phi_1} = \overline{\phi_0} \underline{\phi_1} \underline{\phi_2} | \overline{\phi_2} \overline{\phi_1} ,$$

which is not a translation; length-2 block (ϕ_1, ϕ_2) lattice fields have changed signs. I assume that is OK because the overall number of '-'s does not change.

$$\begin{aligned} -s_0 \phi_0 &= -m_0 \\ \phi_0 - s_2 \phi_1 + \phi_2 &= -m_1 . \\ \phi_1 - (s_3 + 1) \phi_2 &= -m_2 \end{aligned}$$

Note, this differs from (18.339), where it is assumed that the antisymmetry forces $\phi_0 = 0$ (which is indeed the case for a multiplicative symmetrization operator with eigenvalue -1, but we are not doing that here, I think).

orbit Jacobian matrix

$$\begin{aligned} \mathcal{J}_- &= \begin{pmatrix} -s_0 & 0 & 0 \\ 1 & -s_1 & 1 \\ 0 & 1 & -s_2 - 1 \end{pmatrix} \text{ or } \begin{pmatrix} -s_1 & 1 \\ 1 & -s_2 - 1 \end{pmatrix} \\ \text{Det } \mathcal{J}_- &= -s_0(s_1 s_2 + s_2 - 1) \end{aligned} \quad (4.35)$$

where the $[2 \times 2]$ matrix comes from assuming that separately fixed.

As temporal cat fields are always presented mod 1, there the asymmetric states do not look asymmetric. That would be much easier to see in plots of temporal Hénon lattice states of table 2.3 and figure 2.3.

For $s_j = 3$ the determinant of this orbit Jacobian matrix is 3^*11 or 11. Are there 11 antisymmetric lattice states, i.e., the corresponding 2 antisymmetric 5-orbits? I assume $\phi_j = 0$ fixed point counts as 'antisymmetric'. Seems to agree with table 18.3.

Starting with the block (ϕ_2, ϕ_1) , followed by $\overline{\phi_0}$ presumably results in a time-reversed orbit Jacobian matrix $s \mathcal{J}_s$. From this construction it is not clear how to connect this to the 5-dimensional Bravais cell; so, see also (3.164), and the continuation in (18.334).

4.2 Time reversal symmetry reduction

4.2.1 Laplacians (and time reversal?)

The symmetric (self-adjoint) Laplacian $\square = -\partial^\top \partial$ suggests that time-reversal desymmetrized dynamics is given by a first order derivative $\partial = r - \mathbf{1}$ (also known as the integer lattice forward difference operator, see (5.103), (5.104)). The symmetric (self-adjoint) combination $\square = -\partial^\top \partial$ is the Laplacian

$$\mathcal{J} = \square - \mu^2 \mathbf{1} = -(r^{-1} - \mathbf{1})(r - \mathbf{1}) - \mu^2 \mathbf{1}, \quad (4.36)$$

where

$$\mu = \sqrt{s - 2}. \quad (4.37)$$

is the Yukawa mass parameter (5.27) in $d = 1$ dimension.

For purposes of the time-reversal desymmetrization its is more convenient to work with the centered, reflection antisymmetric difference operators (5.106),

$$\begin{aligned} \tilde{\partial} &= \tilde{r} - \tilde{r}^{-1}, & \tilde{r} &= r^{1/2} \\ &= -\tilde{\partial}^\top, \end{aligned} \quad (4.38)$$

constructed by interpolating 1/2-unit spacing lattice $\tilde{\mathcal{L}}$ points between the integer lattice \mathcal{L} points, with the derivatives written as

$$\begin{aligned} (r - \mathbf{1}) &= \tilde{r} \tilde{\partial} \\ (r^{-1} - \mathbf{1})(r - \mathbf{1}) &= -\tilde{\partial}^2 = \square \\ \mathcal{J} &= \square - \mu^2 \mathbf{1} = \tilde{\mathcal{J}}^\top \tilde{\mathcal{J}} \\ \tilde{\mathcal{J}} &= \tilde{\partial} - \mu \mathbf{1} = \tilde{r} - \mu \mathbf{1} - \tilde{r}^{-1} \\ \tilde{\mathcal{J}}^\top &= \tilde{\partial} + \mu \mathbf{1} = \tilde{r} + \mu \mathbf{1} - \tilde{r}^{-1} \end{aligned} \quad (4.39)$$

Written out in the matrix form, the $\mathcal{J} = \tilde{\mathcal{J}}^\top \tilde{\mathcal{J}}$ factorization can be checked by matrix multiplication ⁴

$$\begin{aligned} \mathcal{J}[\Phi] &= \begin{pmatrix} -s_0 & 0 & 1 & 0 & \dots & 1 & 0 \\ 0 & -s_1 & 0 & 1 & \dots & 0 & 1 \\ 1 & 0 & -s_2 & 0 & \dots & 0 & 0 \\ \vdots & \vdots & \vdots & \ddots & \vdots & \vdots & \vdots \\ 0 & 0 & \dots & 0 & -s_{n-3} & 0 & 1 \\ 1 & 0 & \dots & 1 & 0 & -s_{n-2} & 0 \\ 0 & 1 & \dots & 0 & 1 & 0 & -s_{n-1} \end{pmatrix} \\ \tilde{\mathcal{J}} &= \begin{pmatrix} -\mu_0 & -1 & 0 & 0 & \dots & 0 & 1 \\ 1 & -\mu_1 & -1 & 0 & \dots & 0 & 0 \\ 0 & 1 & -\mu_2 & -1 & \dots & 0 & 0 \\ \vdots & \vdots & \vdots & \vdots & \ddots & \vdots & \vdots \\ 0 & 0 & \dots & \dots & \dots & -\mu_{n-2} & -1 \\ -1 & 0 & \dots & \dots & \dots & 1 & -\mu_{n-1} \end{pmatrix}, \quad (4.40) \end{aligned}$$

⁴Predrag 2021-09-14: Checked that factorization (4.40), metal temporal lattice condition (4.41) works also for the orbit Φ dependent case (3.84).

where $\mu_t^2 = s_t - 2$ is the lattice site "Klein-Gordon mass", "stretching factor", respectively, and $\mathcal{J}, \tilde{\mathcal{J}}^\top, \tilde{\mathcal{J}}$ act on the 1/2-unit spacing lattice $\tilde{\mathcal{L}}$, i.e., remember (perhaps reintroduce Δt lattice spacing explicitly?) that $\tilde{r} = r^{1/2}$ in (4.39) is the shift operator on the 1/2 lattice spacing. So two applications of 1/2 lattice shift operator give you one full lattice spacing.

Written out as a second-order difference equation, the metal map takes a temporal lattice form

$$\tilde{\phi}_{t+1} - \mu_t \tilde{\phi}_t - \tilde{\phi}_{t-1} = -\tilde{m}_t, \quad (4.41)$$

or, in terms of a lattice state Φ , the corresponding symbol block' M , and the $[n \times n]$ shift operator r ,

$$(\tilde{r} - \mu[\Phi] \mathbb{1} - \tilde{r}^{-1}) \tilde{\Phi} = -\tilde{M}, \quad (4.42)$$

where $\mu[\Phi] \mathbb{1}$ stands for site-dependent diagonal Klein-Gordon mass matrix.

$\tilde{\mathcal{J}}$ discrete Fourier diagonalization

$$\begin{aligned} \lambda_m &= \mu^2 + 2 - 2 \cos \alpha_m = \mu^2 + 4 \sin^2(\alpha_m/2) \\ &= \left(\mu - i 2 \sin\left(\frac{\alpha_m}{2}\right) \right) \left(\mu + i 2 \sin\left(\frac{\alpha_m}{2}\right) \right) \\ &= \left(\mu + e^{i\alpha_m/2} - e^{-i\alpha_m/2} \right) \left(\mu + e^{i\alpha_m/2} - e^{-i\alpha_m/2} \right)^* \\ \text{where } \alpha_m &= 2\pi m/n \end{aligned} \quad (4.43)$$

i.e., the $\sin^2(\alpha_m/2)$ version of the eigenvalues is there for a reason, a consequence of the time-reversal symmetry, with $\tilde{\mathcal{J}}$ eigenvalues being

$$-2i \sin(\alpha_m/2) = e^{i\alpha_m/2} - e^{-i\alpha_m/2}.$$

Phase is $\alpha_m/2$ because the fundamental domain is 1/2 of the full line. The square root is natural because the Yukawa mass $\mu^2 = d(s-2)$ parameter (5.27).

Discrete Fourier diagonalization $\mathcal{J} = \mathcal{J}_- \mathcal{J}_+$, turns \tilde{r} into its eigenvalues $\exp(i\alpha_k/2)$, and the temporal cat Hill determinant (18.268) factorizes as

$$\begin{aligned} \text{Det } \mathcal{J} &= \text{Det } \mathcal{J}_- \text{ Det } \mathcal{J}_+ \\ \text{Det } \mathcal{J}_+ &= \mu \prod_{k=1}^{T-1} (\mu + 2i \sin(\alpha_k/2)), \quad \alpha_k = 2\pi k/T \\ \text{Det } \mathcal{J}_- &= \mu \prod_{k=1}^{T-1} (\mu - 2i \sin(\alpha_k/2)). \end{aligned} \quad (4.44)$$

By derivation (do it!) analogous to the Isola's cat map $\zeta(Z)$ (1.30), the topological zeta function for metal cat maps is

$$\frac{1}{\tilde{\zeta}(t)} = \frac{1 - \mu t - t^2}{(1-t)^2}, \quad (4.45)$$

n	1	2	3	4	5	6	7	8	9	10	11
N_n	1	5	16	45	121	320	841	2205	5776	15125	39601
M_n	1	2	5	10	24	50	120	270	640	1500	3600

Table 4.1: Lattice states and orbit counts for the $s = 3$ cat map. Compare with the golden (Fibonacci [8]) cat map table 4.2 and (4.182).

n	1	2	3	4	5	6	7	8	9	10	11	12	13	14	15
\tilde{N}_n	1	1	4	5	11	16	29	45	76	121	199	320	521	841	1364
\tilde{M}_n	1	0	1	1	2	2	4	5	8	11	18	25	40	58	90

Table 4.2: Temporal lattice states and orbit counts for the $\mu = 1$ golden cat map. See (4.182) and the counting of walks on the “half time-step” Markov graph figure 4.2.

where $z = t^2$, in agreement with (4.181) for $\mu = 1$. See also (5.233).

Denote the $[\tilde{n} \times \tilde{n}]$ orbit Jacobian matrix $\tilde{\mathcal{J}}(\mu)$ of the 1/2 time-step lattice $\tilde{\mathcal{L}}$ as $\tilde{\mathcal{J}}_{\tilde{n}}$, where \tilde{n} is the period of the lattice state Φ on the half interval lattice $\tilde{\mathcal{L}}$. Denote the orbit Jacobian matrix $\mathcal{J}(s)$ of the temporal cat lattice \mathcal{L} as \mathcal{J}_n , where n is the period of the lattice state Φ on the integer lattice \mathcal{L} . For odd, respectively even periods, the determinants of $\tilde{\mathcal{J}}$ and \mathcal{J} are related as:

$$\begin{aligned} \det(\tilde{\mathcal{J}}_{2m+1}^\top \tilde{\mathcal{J}}_{2m+1}) &= \det(\mathcal{J}_{2m+1}) \\ \det(\tilde{\mathcal{J}}_{2n}^\top \tilde{\mathcal{J}}_{2n}) &= \det(\mathcal{J}_n)^2, \end{aligned} \quad (4.46)$$

hence⁵

$$\begin{aligned} N(s)_n &= \det \mathcal{J}_n = (\det \tilde{\mathcal{J}}_n)^2 = \tilde{N}(\mu)_n^2, \quad n \text{ odd} \\ N(s)_n &= |\det \mathcal{J}_n| = |\det \tilde{\mathcal{J}}_{2n}| = \tilde{N}(\mu)_{2n}, \quad n \text{ even}. \end{aligned} \quad (4.47)$$

For odd n , see (4.66) and compare odd entries in table 4.1 and table 4.2.

For even n , compare the n entries in table 4.1 with the $\tilde{n} = 2n$ entries in table 4.2.

$\hat{\mathcal{J}} = \tilde{\mathcal{J}}^\top \tilde{\mathcal{J}}$ is the orbit Jacobian matrix of the temporal cat on the half interval lattice $\tilde{\mathcal{L}}$ (denoted \mathcal{J} in (4.40)). $\hat{\mathcal{J}}_{2n} = \tilde{\mathcal{J}}_{2n}^\top \tilde{\mathcal{J}}_{2n}$ is the orbit Jacobian matrix of the temporal cat on the half lattice with period $2n$, which is period n in the unit lattice. But $\hat{\mathcal{J}}_{2n}$ is different from \mathcal{J}_n , the orbit Jacobian matrix of the temporal cat on the unit lattice, because it has more lattice sites. Note that:

$$\hat{\mathcal{J}}_{2n} = \mathcal{J}_n \otimes \mathbf{1}_{[2 \times 2]}.$$

⁵Predrag 2021-02-13: Have not checked whether absolute values $|\dots|$ are needed for the even case.

Using the second identity in (8.20) we can get the second relation in (4.46).

$\hat{\mathcal{J}}_{2n+1} = \tilde{\mathcal{J}}_{2n+1}^\top \tilde{\mathcal{J}}_{2n+1}$ is the orbit Jacobian matrix of the temporal cat on the half lattice with period $2n + 1$, which has period $n + 1/2$ on the unit lattice. $\hat{\mathcal{J}}_{2n+1}$ is same as the \mathcal{J}_{2n+1} after a permutation, which leads to the first relation in (4.46).

The “functional equation” [2]

$$\zeta(z) = \zeta(1/z) \quad (4.48)$$

is for us the obvious statement of time-reversal invariance. Note also under the time reversal $t \rightarrow 1/t$

$$\frac{1}{\tilde{\zeta}(1/t)} = -\frac{1}{\tilde{\zeta}(-t)}. \quad (4.49)$$

4.2.2 Time reversal blog

2007-11-20 Keating, Marklof and Williams The cat map A acting on (q_t, p_t) must be symplectic, and time-reversal symmetric,

$$TAT = A^{-1} \quad (4.50)$$

where T is the time-reversal operator

$$T = \begin{bmatrix} 1 & 0 \\ 0 & -1 \end{bmatrix} \quad (4.51)$$

An example is

$$A = \begin{bmatrix} 2 & 1 \\ 3 & 2 \end{bmatrix} \quad (4.52)$$

The Percival-Vivaldi 2-configuration map (1.5) acts on a 2-dimensional state space point (ϕ_{n-1}, ϕ_n) , so time reversal permutes the two entries,

$$A = \begin{bmatrix} 0 & 1 \\ -1 & s \end{bmatrix}, \quad T = \begin{bmatrix} 0 & 1 \\ 1 & 0 \end{bmatrix}. \quad (4.53)$$

Not sure what T is for cat map of form (5.62).

2004-11-01 Predrag and Lan We implemented the “half-step” figure 4.2 reduction for the Kuramoto-Sivashinsky spatial reflection symmetry in *Unstable recurrent patterns in Kuramoto-Sivashinsky dynamics* [63], see figure 4.1. It happens in sect. B *Curvilinear coordinates, center repeller* of the paper, and the result is the 3-letter bimodal return map of figure 4.1 (c). Without quotienting the D_1 symmetry, the return map would have up to 11 letters, and be an unmaneagable holly mess.

2018-04-12 Predrag For our many (failed) attempts to find an Adler-Weiss forward and backward in time symmetric partition, see sect. 18.3 *Time reversal*.

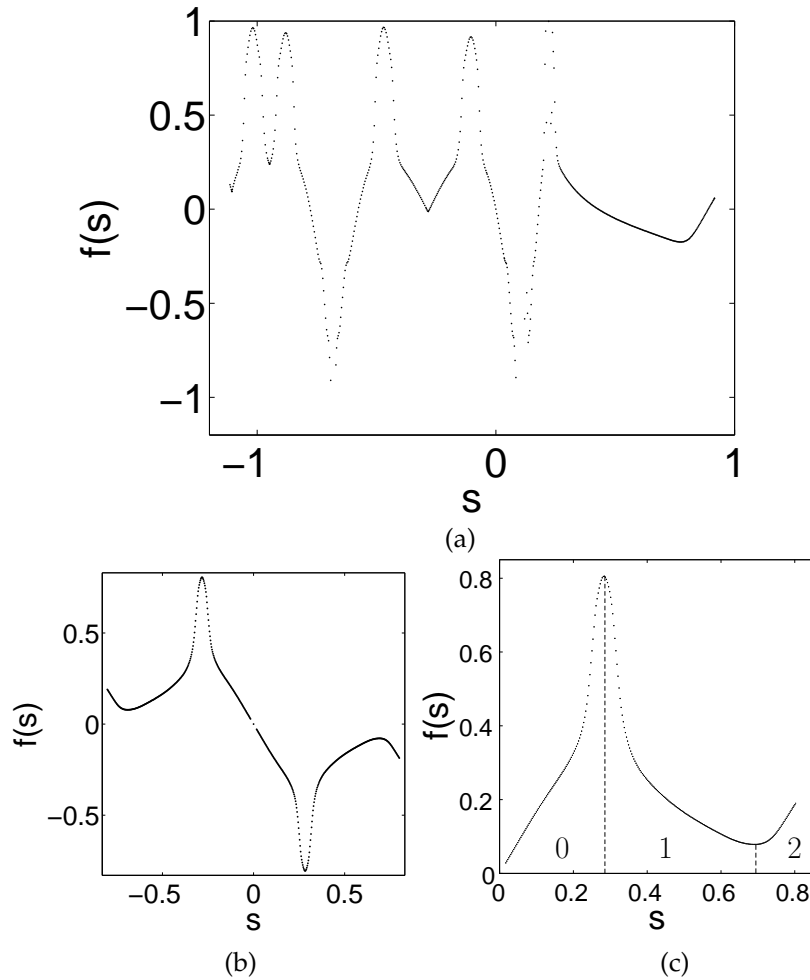


Figure 4.1: The return map on the Poincaré section \mathcal{P}_C of the unstable manifold of equilibrium C , antisymmetric subspace of Kuramoto-Sivashinsky, the intrinsic coordinate: (a) There are 11 monotone segments, requiring an 11-letter alphabet. However, in the (Kuramoto-Sivashinsky)/ D_1 -spatial reflection symmetry reduced state space, (b) the return map simplifies to an antisymmetric return map, which becomes (c) a 3-letter bimodal return map in the fundamental domain, with the symbolic dynamics given by three symbols $\{0, 1, 2\}$. It's a **wild** $\sqrt{\text{time}}$ simplification of the dynamics! enabling us to populate the neighboring strange attractor with many periodic orbits. (Taken from fig. 8 (e) of Lan and Cvitanović [63]).

2018-04-12 Predrag Birdtracks.eu Sect. 8.2.3 Time reversal symmetry might be relevant to spatiotemporal cat: when the Hamiltonian is invariant under time reversal, the symmetry group is enlarged.

2016-11-16 Predrag Maillard group, Anglès d'Auriac, Boukraa and Maillard [2] *Functional relations in lattice statistical mechanics, enumerative combinatorics, and discrete dynamical systems* state the “functional equation”

$$\zeta(z) = \zeta(1/z) \quad (4.54)$$

which for us is the obvious statement of time-reversal invariance.

2016-11-16 Predrag Note also (4.49) under the presumed time reversal $t \rightarrow 1/t$. This all has to do with time reversibility - we should exploit time and space reversal symmetries in this way, and - who knows - understand Ihara zeta functions better.

2020-12-24 Predrag Note that in the discussion of time-reversal invariant recurrence relations (5.248) (see (1.40), etc.) the characteristic equation factors as $a(\phi) = \ell(\phi) \ell(l/\phi)$ where the factors $\ell(\phi)$ and $\ell(l/\phi)$ of $a(\phi)$ are known as the *Hurwitz factors*.

2020-01-10 Predrag The “square root” C (4.173) might be related to resistor networks’s Laplace-like operator factorization $L = RR^\top$, see (5.286), with no transpose needed in this example, as C is symmetric.

2020-02-06 Predrag $\mathcal{J} = \tilde{\mathcal{J}}^\top \tilde{\mathcal{J}}$ factorization [75], as in (18.297):

$$\tilde{\mathcal{J}} = \begin{pmatrix} \mu & -1 & 0 & 0 & \dots & 0 & 1 \\ 1 & \mu & -1 & 0 & \dots & 0 & 0 \\ 0 & 1 & \mu & -1 & \dots & 0 & 0 \\ \vdots & \vdots & \vdots & \vdots & \ddots & \vdots & \vdots \\ 0 & 0 & \dots & \dots & \dots & \mu & -1 \\ -1 & 0 & \dots & \dots & \dots & 1 & \mu \end{pmatrix}. \quad (4.55)$$

$$\tilde{\mathcal{J}}^\top = \begin{pmatrix} \mu & 1 & 0 & 0 & \dots & 0 & -1 \\ -1 & \mu & 1 & 0 & \dots & 0 & 0 \\ 0 & -1 & \mu & 1 & \dots & 0 & 0 \\ \vdots & \vdots & \vdots & \vdots & \ddots & \vdots & \vdots \\ 0 & 0 & \dots & \dots & \dots & \mu & 1 \\ 1 & 0 & \dots & \dots & \dots & -1 & \mu \end{pmatrix}. \quad (4.56)$$

Note that Pozrikidis [75] $L = RR^\top$ factorization (5.286) the factors R are bi-diagonal, as in the forward difference operator (4.36). He does not seem to introduce 1/2 lattice spacing central difference operator (4.38), and considers only the Helmholtz equation $\mu = 0$ case, not our tri-diagonal map. I do not see our symmetry reduction there...

\mathcal{J} is time reversal (4.60) invariant (self-adjoint; Hermitian), $R\mathcal{J}R^\top = \mathcal{J}$, but $\tilde{\mathcal{J}}^\top = \tilde{R}\tilde{\mathcal{J}}\tilde{R}^\top$ is time reversed, as a first order derivative should.

2020-09-30 Predrag Note that in (4.183) Maillard *et al.* [2] quotient the time reversal (reflection) symmetry for $s = 3$ temporal cat.

The reflection-symmetric operator

$$T_{ij} = \sum_{\mu=1}^d [(r^\mu)_{ij} + (r^\mu)_{ji}], \quad (4.57)$$

generates all steps of length 1. The symmetric (self-adjoint) combination $\Delta = -\partial^\top \partial = \partial^2$ (note this notation for \square)

$$\begin{aligned} \Delta - \mu^2 \mathbf{1} &= - \sum_{\mu=1}^d \{(r_\mu^{-1} - \mathbf{1})(r_\mu - \mathbf{1}) + \mu^2 \mathbf{1}\} \\ &= \mathcal{J} = \sum_{\mu=1}^d (r_\mu^{-1} + r_\mu - s \mathbf{1}) \\ &= (T - ds \mathbf{1}) \end{aligned} \quad (4.58)$$

relates the walker T to the lattice Laplacian and the orbit Jacobian matrix \mathcal{J} .

2020-10-31 Predrag Han, what does Gradshteyn and Ryzhik [45] have to say about formulas (4.44)? Sine is a cosine rotated by $\pi/2$.

Still have to factorize the zeta function, as in (4.183). Clearly $\det \mathcal{J}_+(\mu) = (-1)^T \det \mathcal{J}_-(-\mu)$, so, up to a complex phase, $\det \mathcal{J}_+$ is a square root of \mathcal{J} . Not sure anything is attained by computing one rather than the other...

A guess for factorization in d dimensions (still wrong) is something like

$$\begin{aligned} \Delta - d(s-2)\mathbf{1} &= - \sum_{\mu=1}^d \{(r_\mu^{-1} - \mathbf{1})(r_\mu - \mathbf{1}) + (s-2)\mathbf{1}\} \\ &= - \sum_{\mu=1}^d \{-i(r_\mu^{-1} - \mathbf{1}) + \sqrt{s-2}\mathbf{1}\} \\ &\quad \{i(r_\mu - \mathbf{1}) + \sqrt{s-2}\mathbf{1}\} \end{aligned} \quad (4.59)$$

2020-09-30 Predrag Failed attempt, can safely ignore. In $d = 1$ temporal cat case the time reflection operator R , $R^2 = \mathbf{1}$, is

$$R = \begin{pmatrix} 0 & 0 & 0 & 0 & \dots & 0 & 1 \\ 0 & 0 & 0 & 0 & \dots & 1 & 0 \\ 0 & 0 & 0 & \dots & 1 & 0 & 0 \\ \vdots & \vdots & \vdots & \vdots & \ddots & \vdots & \vdots \\ 0 & 1 & \dots & \dots & \dots & 0 & 0 \\ 1 & 0 & \dots & \dots & \dots & 0 & 0 \end{pmatrix}. \quad (4.60)$$

with projection operators (for $n = 3$)

$$P_{A_1} = \frac{1}{2} \begin{pmatrix} 1 & 0 & 1 \\ 0 & 2 & 0 \\ 1 & 0 & 1 \end{pmatrix}, \quad P_{A_2} = \frac{1}{2} \begin{pmatrix} 1 & 0 & -1 \\ 0 & 0 & 0 \\ -1 & 0 & 1 \end{pmatrix} \quad (4.61)$$

$$d_{A_1} = \text{Tr } P_{A_1} = 2, \quad d_{A_2} = \text{Tr } P_{A_2} = 1 \quad (4.62)$$

For any n

$$d_{A_1} = \text{Tr } P_{A_1} = \frac{1}{2}(\text{Tr } \mathbf{1} + \text{Tr } R) = \frac{1}{2}(n+1), \quad d_{A_2} = \frac{1}{2}(n-1) \quad (4.63)$$

This can only work for n odd. For even ones there must be another irrep?

$$\mathcal{J}_{A_1} = \frac{1}{2} \begin{pmatrix} 1-s & 2 & 1-s \\ 2 & -2s & 2 \\ 1-s & 2 & 1-s \end{pmatrix}, \quad \mathcal{J}_{A_2} = \frac{1}{2} \begin{pmatrix} -1-s & 0 & 1+s \\ 0 & 0 & 0 \\ 1+s & 0 & -1-s \end{pmatrix} \quad (4.64)$$

$$\mathcal{J}_{A_1} = \mathbf{1} + \begin{pmatrix} -\frac{1+s}{2} & 1 & \frac{1-s}{2} \\ 1 & -(1+s) & 1 \\ \frac{1-s}{2} & 1 & -\frac{1+s}{2} \end{pmatrix} \quad (4.65)$$

We know that for $[3 \times 3]$ orbit Jacobian matrix

$$\begin{aligned} \mathcal{J} &= \begin{pmatrix} -s & 1 & 1 \\ 1 & -s & 1 \\ 1 & 1 & -s \end{pmatrix} \\ N_3 &= |\text{Det } \mathcal{J}| = (s-2)(s+1)^2 = [\mu(\mu^2+3)]^2, \end{aligned} \quad (4.66)$$

but clearly

$$\text{Det } \mathcal{J}_{A_1} = 0, \quad \text{Det } \mathcal{J}_{A_2} = \frac{1}{4} (0(1+s)^2 - 0(1+s)^2) = 0. \quad (4.67)$$

As det of sum is not sum of det's, \mathcal{J}_{A_1} , \mathcal{J}_{A_2} are not fundamental parallelepipeds, and have no geometrical meaning, both have vanishing determinants. Actually, \mathcal{J}_{A_1} should be invariant under time reversal, so what did I screw up? Failed attempt, done.

2021-03-22 Predrag Grava *et al.* [46] eq. (4.108) suggests what went wrong with the above failed D_1 factorization attempt: we should have started from the Hamiltonian formulation, decompose the one-time step temporal evolution $[2 \times 2]$ Jacobian matrix $\hat{\mathcal{J}}_1$ that generates a time orbit by acting on the 2-dimensional ‘phase space’ of successive temporal lattice points (8.24) with time reversal T (4.53) decomposing the 2nd order Percival-Vivaldi

time-evolution equation into two 1st order invariant subspace evolution equations:

$$\mathbf{T} = \begin{bmatrix} 0 & 1 \\ 1 & 0 \end{bmatrix}, \quad \mathbf{P}^+ = \frac{1}{2} \begin{bmatrix} 1 & 1 \\ 1 & 1 \end{bmatrix}, \quad \mathbf{P}^- = \frac{1}{2} \begin{bmatrix} 1 & -1 \\ -1 & 1 \end{bmatrix}. \quad (4.68)$$

so

$$\hat{\mathbf{J}}_1 = \begin{bmatrix} 0 & 1 \\ -1 & s \end{bmatrix}; \quad \hat{\mathbf{J}}_1^+ = \frac{1}{2} \begin{bmatrix} 1 & 1 \\ s-1 & s-1 \end{bmatrix}, \quad \hat{\mathbf{J}}_1^- = \frac{1}{2} \begin{bmatrix} -1 & 1 \\ -s-1 & s+1 \end{bmatrix}. \quad (4.69)$$

Next: verify the Hill's formula, sect. 7.1.4, and/or sect. 5. *Hill determinant: stability of an orbit vs. its time-evolution stability* of *siminos/kittens/CL18.tex* for period- n lattice states;

$$\text{Det } \mathcal{J}_\pm = \det \left[\mathbf{1} - (\hat{\mathbf{J}}_1^\pm)^n \right]. \quad (4.70)$$

This establishes, following Fejér [43, 78] (1916) Fejér and Riesz lemma sect. 4.3.1, -doubting Thomases notwithstanding- that the time reversal invariance leads to factorization of zeta functions for -hopefully- any temporal lattice systems with time-inversion $t \rightarrow -t$ invariance.

As far as I can tell, we are the first to make this claim for time evolution, not for spatially discrete or N -body systems.

Sidney and Han, please go to sect. 24.4 *Pow wow* 2021-03-22 and do the homework. Call me any time for any clarifications you need. As always, everything prof says might be wrong, so remain vigilant. And stay safe.

2021-03-22 Predrag The above might be a failed attempt again..., as Percival-Vivaldi form is not right: $[\mathbf{T}, \mathbf{J}_1] \neq 0$:

$$\mathbf{T} = \begin{bmatrix} 0 & 1 \\ 1 & 0 \end{bmatrix}, \quad \mathbf{P}^+ = \frac{1}{2} \begin{bmatrix} 1 & 1 \\ 1 & 1 \end{bmatrix}, \quad \mathbf{P}^- = \frac{1}{2} \begin{bmatrix} 1 & -1 \\ -1 & 1 \end{bmatrix}. \quad (4.71)$$

so

$$\hat{\mathbf{J}}_1 = \begin{bmatrix} 0 & 1 \\ -1 & s \end{bmatrix}; \quad \hat{\mathbf{J}}_1^+ = \frac{1}{2} \begin{bmatrix} 1 & 1 \\ s-1 & s-1 \end{bmatrix}, \quad \hat{\mathbf{J}}_1^- = \frac{1}{2} \begin{bmatrix} -1 & 1 \\ -s-1 & s+1 \end{bmatrix}. \quad (4.72)$$

2020-11-18 Predrag Factorization (1.2)

$$A = \begin{bmatrix} 2 & 1 \\ 1 & 1 \end{bmatrix} = \begin{bmatrix} 1 & 1 \\ 0 & 1 \end{bmatrix} \begin{bmatrix} 1 & 0 \\ 1 & 1 \end{bmatrix} = LL^\top \quad (4.73)$$

leads to

$$\det(1 - tL^\top) \det(1 + tL) = \det(1 - zA) \quad (4.74)$$

which also verifies (4.183). Both (4.170), (1.2) are symmetric under transposition. What about the asymmetric Percival-Vivaldi (1.5)? The similarity transformation (5.191) that maps (1.1) into (1.5),

$$\mathbf{A} = \begin{bmatrix} 2 & 1 \\ 1 & 1 \end{bmatrix}, \quad \mathbf{B} = \begin{bmatrix} 0 & 1 \\ -1 & 3 \end{bmatrix}, \quad (4.75)$$

is

$$\mathbf{B} = \mathbf{S}^{-1} \mathbf{A} \mathbf{S}, \quad (4.76)$$

where

$$\mathbf{S} = \mathbf{S}^{-1} = \begin{bmatrix} -1 & 2 \\ 0 & 1 \end{bmatrix}.$$

See also discussion around (5.192) and (18.43).

2021-02-10 Predrag I looked cursorily at it and did not spot anything, but it is of possible interest:

Terry Loring and Fredy Vides *Computing Floquet Hamiltonians with Symmetries* [arXiv:2007.06112](https://arxiv.org/abs/2007.06112)

2021-04-10 Predrag For specializing example 2.6 *Symmetry lines of the standard map* to cat map, see example 2.7 *Symmetry lines of the cat map*.

2021-04-10 Predrag For a scholarly discussion of many facets of “time-reversal”, see the essay *Time Reversal* by Bryan W. Roberts (2019).

2021-04-14 Predrag to Stephen In spirit of our ‘square root’ philosophy, [Wolfram Physics Project](#) writes:

Another promising possibility relates to the distinction between fermions and bosons. We’re not sure yet, but it seems as if Fermi–Dirac statistics may be associated with multiway graphs where we see only non-merging branches, while Bose–Einstein statistics may be associated with ones where we see all branches merging. Spinors may then turn out to be as straightforward as being associated with directed rather than undirected spatial hypergraphs.

The problem is that I cannot find a technical paper on that, if it exists. I do not find any hint of this in his Wolfram [93] *A Project to Find the Fundamental Theory of Physics*.

That jives with our spatiotemporal cat work. There the graph is just a d-dimensional undirected hypercubic lattice, but reflection symmetry reduces the graph to a pair of directed graphs, much like reducing the Klein-Gordon Laplacian to two Dirac operators.

CHAPTER 4. GROUP THEORY

2021-04-15 Stephen There's nothing yet on our home pages.

Very interesting! Now I just went searching in your material ... and couldn't find this either. Can you point me to this?

I'm wondering if it's at all related to the (disappointingly vague) [notes-9-16-discrete-quantum-mechanics](#). (2021-04-16 Predrag: Read this, do not see any connection to our work.)

I saw various Klein-Gordan-like equations in your works ... but nothing Dirac like (did I miss it?)

The d-dimensional hypercubic lattice obviously has certain discrete symmetry. Does the "square root lattice" have some other identifiable, and perhaps spinorial, symmetry?

By the way ... if you're up for it sometime, I'd love to try to talk through the geodesic-balls-in-hypergraphs-have-limiting-symmetries-that-are-Lie-groups story. Your hypercubic lattice is too "special" ... but imagine a random d-dimensional lattice (for integer d). Then presumably the invariances of the geodesic ball limit to $SO(d)$. But what happens with one-way vs two-way connections? How does it affect representations? What about fractional d? Etc. etc. I have a suspicion that with your help this might be able to be cracked...

2021-04-17 Predrag to Tony Kennedy <Tony.Kennedy@ed.ac.uk>

You might be The Man for the job:

We are stuck on reflection-symmetry reduction needed to factorize the zeta functions. Here is a simple way to explain what the problem is:

Think of a discrete time dynamical system (iterations of a map) as a 1-dimensional lattice with the field on each site labeled by integer time. A period- n lattice state lives on a discrete 1-torus (a ring or necklace) of period n , and if the law is time-independent, sets of solutions are invariant under cyclic perturbations. The symmetry is C_n , and one needs to distinguish C_n orbits ("prime cycles" in ChaosBook; one per each orbit). The right way to do this is by going to C_n irreps, ie, by the discrete Fourier transform, with all reciprocal lattice Brillouin zone solutions orbits in an $1/n$ sliver of a n -gon. If n is prime, this is irreducible; if it is a multiple of a prime, one should remove those solutions, as they have already been accounted for.

If, in addition, the law is time-reversal (or time-inversion) invariant, the symmetry includes time-reflection, ie, it is dihedral group D_n with $2n$ elements, so the reciprocal lattice should be a half of the above $1/n$ sliver of a n -gon, and irreps are now either 1 or 2 dimensional. Even n is different from odd n , and solutions either appear in pairs, or are self dual under reflection in 3 different ways.

ChaosBook works out zeta function factorizations for D_1 , D_2 (known as [Klein four-group](#)), D_3 (symmetric group S_3), and D_4 , but somehow I get

confused by all the invariant subspaces of solutions for D_n , so we are stuck... Not to mention counting orbits for a Bravais lattices (doubly periodic lattice states) for spatiotemporal cat. There we do not know how to write down the zeta function, let alone factorize it into irreps of the discrete symmetry group of a given Bravais lattice.

For more detail, see sect. 3.10 *Dihedral groups*.

2021-05-04 Predrag Can one write the orbit Jacobian matrix of a repeat of a p -cycle as a product of p -cycle orbit Jacobian matrices?

(2021-06-14 Predrag) This is now accomplished by the block matrix formulation (18.345).)

$$\begin{aligned} \mathcal{J}_p^{(2)} \mathcal{J}_p^{(1)} &= \begin{bmatrix} 1 & 0 & 0 & 0 & 0 & 0 \\ 0 & 1 & 0 & 0 & 0 & 0 \\ 0 & 0 & 1 & 0 & 0 & 0 \\ 0 & 0 & 0 & \phi_0 & 1 & 1 \\ 0 & 0 & 0 & 1 & \phi_1 & 1 \\ 0 & 0 & 0 & 1 & 1 & \phi_2 \end{bmatrix} \begin{bmatrix} \phi_0 & 1 & 1 & 0 & 0 & 0 \\ 1 & \phi_1 & 1 & 0 & 0 & 0 \\ 1 & 1 & \phi_2 & 0 & 0 & 0 \\ 0 & 0 & 0 & 1 & 0 & 0 \\ 0 & 0 & 0 & 0 & 1 & 0 \\ 0 & 0 & 0 & 0 & 0 & 1 \end{bmatrix} \\ &\neq \begin{bmatrix} \phi_0 & 1 & 0 & 0 & 0 & 1 \\ 1 & \phi_1 & 1 & 0 & 0 & 0 \\ 0 & 1 & \phi_2 & 1 & 0 & 0 \\ 0 & 0 & 1 & \phi_0 & 1 & 0 \\ 0 & 0 & 0 & 1 & \phi_1 & 1 \\ 1 & 0 & 0 & 0 & 1 & \phi_2 \end{bmatrix}, \end{aligned} \quad (4.77)$$

Another try:

$$\begin{aligned} \mathcal{J}_p^{(2)} \mathcal{J}_p^{(1)} &= \begin{bmatrix} 1 & 0 & 0 & 0 & 0 & 1 \\ 0 & 1 & 0 & 0 & 0 & 0 \\ 0 & 0 & 1 & 1 & 0 & 0 \\ 0 & 0 & 1 & \phi_0 & 1 & 0 \\ 0 & 0 & 0 & 1 & \phi_1 & 1 \\ 1 & 0 & 0 & 0 & 1 & \phi_2 \end{bmatrix} \begin{bmatrix} \phi_0 & 1 & 0 & 0 & 0 & 1 \\ 1 & \phi_1 & 1 & 0 & 0 & 0 \\ 0 & 1 & \phi_2 & 1 & 0 & 0 \\ 0 & 0 & 1 & 1 & 0 & 0 \\ 0 & 0 & 0 & 0 & 1 & 0 \\ 1 & 0 & 0 & 0 & 0 & 1 \end{bmatrix} \\ &\neq \begin{bmatrix} \phi_0 + 1 & 1 & 0 & 0 & 0 & 2 \\ 1 & \phi_1 & 1 & 0 & 0 & 0 \\ 0 & 1 & \phi_2 + 1 & 2 & 0 & 0 \\ 0 & 0 & 1 & \phi_0 + 1 & 1 & 0 \\ 0 & 0 & 0 & 1 & \phi_1 & 1 \\ \phi_0 + \phi_2 & 0 & 0 & 0 & 1 & \phi_2 + 1 \end{bmatrix}, \end{aligned} \quad (4.78)$$

(partly wrong, but does not matter), so orbit Jacobian matrices do not multiply.

But they do not add up, either, cannot reconcile the small block periodic bc's with the repeated block bc's. Defeated again.

4.2.3 Poles of dynamical zeta functions

1993-03-11 Predrag A clip from (boyscouts only) ChaosBook Chapter *Quantum pinball*, taken from Predrag's `c.tex` [40], Casati and Shilnikov [20].

2020-11-07 Predrag In 1993 I have not thought of (4.81) as clue to time-reversal factorization, but the Hamiltonian weight, one per each degree of freedom,

$$\det(\mathbf{1} - \mathbf{J}_p) = (1 - \Lambda_p)(1 - 1/\Lambda_p) = -\Lambda_p + 2 - 1/\Lambda_p \quad (4.79)$$

sure looks suggestive, in the spirit of (18.269). It leads to factorization (4.88),

$$1/\zeta_j = \frac{F_j}{F_{j+1}} \frac{F_{j+2}}{F_{j+1}}, \quad (4.80)$$

compare with (4.183).

For a Hamiltonian two degree of freedom system, \mathbf{J}_p is a $[2 \times 2]$ matrix with unit determinant. If the cycle is unstable, the eigenvalues Λ_p and $1/\Lambda_p$ are real, and we denote the expanding eigenvalue by Λ_p . The denominator can then be expanded in a geometric series

$$1/|\det(\mathbf{J}_p - \mathbf{1})| = |\Lambda_p|^{-1}(1 - 1/\Lambda_p)^{-2} = |\Lambda_p|^{-1} \sum_{j=0}^{\infty} (j+1)\Lambda_p^{-j}. \quad (4.81)$$

Performing the r summation and interchanging sums and logarithms one ends up with $\Omega(s) = \frac{\partial}{\partial s} \ln F(s)$, where $F(s)$ is the *classical Fredholm determinant*

$$F(s) = \prod_p \prod_{j=0}^{\infty} \left(1 - |\Lambda_p|^{-1} \Lambda_p^{-j} e^{sT_p}\right)^{j+1}. \quad (4.82)$$

As $\Omega(s)$ is a logarithmic derivative, its poles are given by the zeros and poles of $F(s)$. Denoting the classical weight of the cycle p by

$$t_p = z^{n_p} e^{sT_p} / |\Lambda_p| \quad (4.83)$$

and defining *dynamical zeta functions* [83]

$$1/\zeta_j = \exp \left(- \sum_p \sum_{r=1}^{\infty} \frac{1}{r} (t_p/\Lambda_p^j)^r \right) = \prod_p (1 - t_p/\Lambda_p^j), \quad (4.84)$$

the Fredholm determinant (4.82) can be written as an infinite product over $1/\zeta_j$:

$$F(s) = \prod_p \prod_{j=0}^{\infty} (1 - t_p/\Lambda_p^j)^{j+1} = \prod_{j=0}^{\infty} 1/\zeta_j^{j+1}. \quad (4.85)$$

We have introduced a bookkeeping variable z raised to the power of the topological length (number of disk collisions in a cycle) in order to be able to systematically expand the infinite products in terms of increasing topological cycle length.

The double pole is not as surprising as it might seem at the first glance; indeed, the theorem that establishes that the classical Fredholm determinant (4.85) is entire implies that the poles in $1/\zeta_j$ must have right multiplicities in order that they be cancelled in the $F = \prod 1/\zeta_j$ product. More explicitly, $1/\zeta_j$ can be expressed in terms of weighted Fredholm determinants

$$F_j = \exp \left(- \sum_p \sum_{r=1}^{\infty} \frac{1}{r} \frac{(t_p/\Lambda_p^j)^r}{(1-1/\Lambda_p^r)^2} \right) \quad (4.86)$$

by inserting the identity

$$1 = \frac{1}{(1-1/\Lambda)^2} - \frac{2}{\Lambda} \frac{1}{(1-1/\Lambda)^2} + \frac{1}{\Lambda^2} \frac{1}{(1-1/\Lambda)^2} \quad (4.87)$$

into the exponential representation (4.84) of $1/\zeta_j$. This yields

$$1/\zeta_j = \frac{F_j F_{j+2}}{F_{j+1}^2}, \quad (4.88)$$

and we conclude that for 2-dimensional Hamiltonian flows the dynamical zeta function $1/\zeta_j$ has a *double* leading pole coinciding with the leading zero of the F_{j+1} Fredholm determinant.

4.3 Time reversal literature

4.3.1 Grava et al. 2021 paper GKMM21

Notes on Grava, Kriecherbauer, Mazzuca and McLaughlin [46] *Correlation functions for a chain of short range oscillators*, arXiv:2010.09612:

[C]onsider a system of $N = 2M + 1$ particles interacting with a short range harmonic potential with Hamiltonian of the form

$$H = \sum_{j=0}^{N-1} \frac{p_j^2}{2} + \sum_{s=1}^m \frac{\kappa_s}{2} \sum_{j=0}^{N-1} (q_j - q_{j+s})^2, \quad (4.89)$$

and Hamiltonian density

$$e_j = \frac{p_j^2}{2} + \frac{1}{2} \left(\sum_{s=1}^m \tau_s (q_{j+s} - q_j) \right)^2,$$

local in the variables (\mathbf{p}, \mathbf{q}) for fixed m . If we let $N \rightarrow \infty$, the quantity e_j involves a finite number of physical variables (\mathbf{p}, \mathbf{q}) . We always take periodic boundary conditions, the indices j are taken from $\mathbb{Z}/N\mathbb{Z}$ and therefore

$$q_{N+j} = q_j, \quad p_{N+j} = p_j$$

holds for all j .

The relative shift S boundary condition $q_{N+1} = q_1 + S$ can be also be considered (see e.g. ref. [89]). The periodic boundary condition is recovered by change of coordinates $q_j \rightarrow q_j - \frac{S}{N}(j-1)$.

The coefficients τ_s are the entries of the circulant localized square root T of the matrix A by which we mean a solution of the equation (4.94) of the form (4.95).

The Hamiltonian (4.89) can be rewritten in the form

$$H(\mathbf{p}, \mathbf{q}) := \frac{1}{2} \langle \mathbf{p}, \mathbf{p} \rangle + \frac{1}{2} \langle \mathbf{q}, A\mathbf{q} \rangle, \quad (4.90)$$

where $\mathbf{p} = (p_0, \dots, p_{N-1})$, $\mathbf{q} = (q_0, \dots, q_{N-1})$, $\langle \cdot, \cdot \rangle$ denotes the standard scalar product in \mathcal{R}^N and where $A \in \text{Mat}(N, \mathcal{R})$ is a positive semidefinite symmetric circulant matrix generated by the vector $\mathbf{a} = (a_0, \dots, a_{N-1})$ namely $A_{kj} = a_{(j-k) \bmod N}$ or

$$A = \begin{bmatrix} a_0 & a_1 & \dots & a_{N-2} & a_{N-1} \\ a_{N-1} & a_0 & a_1 & & a_{N-2} \\ \vdots & a_{N-1} & a_0 & \ddots & \vdots \\ a_2 & & \ddots & \ddots & a_1 \\ a_1 & a_2 & \dots & a_{N-1} & a_0 \end{bmatrix}, \quad (4.91)$$

The harmonic oscillator with only nearest neighbour interactions is recovered by choosing

$$a_0 = 2\kappa_1, \quad a_1 = a_{N-1} = -\kappa_1,$$

and the remaining coefficients are set to zero.

The equations of motion for the Hamiltonian H take the form

$$\frac{d^2}{dt^2}q_j = \sum_{s=1}^m \kappa_s(q_{j+s} - 2q_j + q_{j-s}), \quad j \in \mathbb{Z}/N\mathbb{Z}. \quad (4.92)$$

The integration is obtained by studying the dynamics in Fourier space. [...] Following the standard procedure in the case of nearest neighbour interactions we replace the vector of position \mathbf{q} by a new variable \mathbf{r} so that the Hamiltonian takes the form

$$H = \frac{1}{2}\langle \mathbf{p}, \mathbf{p} \rangle + \frac{1}{2}\langle \mathbf{r}, \mathbf{r} \rangle.$$

Such a change of variables may be achieved by any linear transformation

$$\mathbf{r} = T\mathbf{q}, \quad (4.93)$$

with an $N \times N$ matrix T that satisfies

$$A = T^\top T, \quad (4.94)$$

where T^\top denotes the transpose of T .

In the case of nearest neighbour interactions one may choose

$$r_j = \sqrt{\kappa_1}(q_{j+1} - q_j)$$

corresponding to a circulant matrix T generated by the vector

$$\boldsymbol{\tau} = \sqrt{\kappa_1}(-1, 1, 0, \dots, 0).$$

We show that short range interactions given by matrices A of the form (4.91) also admit such a *localized square root*. More precisely, there exists a circulant $N \times N$ matrix T of the form

$$T = \begin{bmatrix} \tau_0 & \tau_1 & \dots & \tau_m & 0 & \dots & 0 \\ 0 & \tau_0 & \tau_1 & \dots & \tau_m & 0 & \dots \\ \ddots & \ddots & \ddots & \ddots & \ddots & & \\ \tau_m & 0 & \ddots & \ddots & \ddots & \ddots & \ddots \\ \ddots & \ddots & \ddots & \ddots & \ddots & \ddots & \ddots \\ \tau_2 & \dots & \tau_m & 0 & \dots & \tau_0 & \tau_1 \\ \tau_1 & \tau_2 & \dots & \tau_m & 0 & 0 & \tau_0 \end{bmatrix}. \quad (4.95)$$

that satisfies (4.94). The crucial point here is that T is not the standard (symmetric) square root of the positive semidefinite matrix A but a localized version

generated by some vector τ with zero entries everywhere, except possibly in the first $m + 1$ components. [...] Note that $\mathbf{1} = (1, \dots, 1)^\top$ satisfies $T\mathbf{1} = 0$ since $\langle \mathbf{1}, A\mathbf{1} \rangle = 0$. This implies

$$\sum_{s=0}^m \tau_s = 0, \quad r_j = \sum_{s=1}^m \tau_s (q_{j+s} - q_j) \quad \text{and} \quad \sum_{j=0}^{N-1} r_j = (1, \dots, 1)^\top T \mathbf{q} = 0.$$

The local energy e_j takes the form

$$e_j = \frac{1}{2} p_j^2 + \frac{1}{2} r_j^2.$$

Due to the spatial translation invariance of the Hamiltonian

$$H(\mathbf{p}, \mathbf{q}) = H(\mathbf{p}, \mathbf{q} + \lambda \mathbf{1}),$$

$\lambda \in \mathcal{R}$, that corresponds to the conservation of total momentum, we reduce the Hamiltonian system by one degree of freedom, with the reduced phase space

$$\mathcal{M} := \left\{ (\mathbf{p}, \mathbf{q}) \in \mathcal{R}^N \times \mathcal{R}^N : \sum_{k=0}^{N-1} p_k = 0; \sum_{k=0}^{N-1} q_k = 0 \right\}. \quad (4.96)$$

[...] the dispersion relation $|\omega(k)|$ for the harmonic oscillator with short range interaction in the limit $N \rightarrow \infty$ obtaining

$$f(k) = |\omega(k)| = \sqrt{2 \sum_{\ell=1}^m \kappa_\ell (1 - \cos(2\pi k\ell))}, \quad (4.97)$$

[...] we show that the evolution equations for the generalized position, momentum can be written in the form of conservation laws which have a potential function. For the case of the harmonic oscillator with nearest neighbour interaction, we show that this function is a Gaussian random variable and determine the leading order behaviour of its variance as $t \rightarrow \infty$.

[...] some notation. First of all, a matrix A of the form (4.91) with $\mathbf{a} \in \mathcal{R}^N$ is called a circulant matrix generated by the vector \mathbf{a} .

m -physical vector and half- m -physical vector Fix $m \in \mathbb{N}$. For any odd $N > 2m$, a vector $\tilde{\mathbf{x}} \in \mathcal{R}^N$ is said to be m -physical generated by $\mathbf{x} = (x_0, x_1, \dots, x_m) \in \mathcal{R}^{m+1}$ if $x_0 = -2 \sum_{s=1}^m x_s$ and

$$\tilde{x}_0 = x_0, \quad (4.98)$$

$$\tilde{x}_1 = \tilde{x}_{N-1} = x_1 < 0, \quad \tilde{x}_m = \tilde{x}_{N-m} = x_m < 0, \quad (4.99)$$

$$\tilde{x}_k = \tilde{x}_{N-k} = x_k \leq 0, \quad \text{for } 1 < k < m, \quad (4.100)$$

$$\tilde{x}_k = 0, \quad \text{otherwise,} \quad (4.101)$$

while the vector $\tilde{\mathbf{x}} \in \mathcal{R}^N$ is called *half-m-physical* generated by $\mathbf{y} \in \mathcal{R}^{m+1}$ if $y_0 = -\sum_{s=1}^m y_s$ and

$$\begin{aligned}\tilde{x}_k &= y_k, \text{ for } 0 \leq k \leq m \\ \tilde{x}_k &= 0, \text{ for } m < k \leq N-1.\end{aligned}$$

Following the proof of a lemma by Fejér and Riesz, one can show that a circulant symmetric matrix A of the form (4.90) generated by a m -physical vector \mathbf{a} always has a circulant localized square root T that is generated by a half- m -physical vector $\boldsymbol{\tau}$.

Fejér and Riesz [78, pg. 117 f] lemma asserts that every positive trigonometric polynomial can be represented by the square of the absolute value of another trigonometric polynomial whose coefficients are, in general, complex.

Fix $m \in \mathbb{N}$. Let the circulant matrix A be generated by an m -physical vector \mathbf{a} , then there exist a circulant matrix T generated by an half- m -physical vector $\boldsymbol{\tau}$ such that:

$$A = T^\top T. \quad (4.102)$$

Moreover, we can choose $\boldsymbol{\tau}$ such that $\sum_{s=1}^m s\tau_s > 0$. Then one has $\sum_{s=1}^m s\tau_s = \sqrt{\sum_{s=1}^m s^2 \kappa_s}$.

For example, if we consider $m = 1$, and $a_0 = 2\kappa_1$ and $a_1 = a_{N-1} = -\kappa_1$. The matrix T is generated by the vector $\boldsymbol{\tau} = (\tau_0, \tau_1)$ with $\tau_0 = -\sqrt{\kappa_1}$ and $\tau_1 = \sqrt{\kappa_1}$. When $m = 2$ and $a_0 = 2\kappa_1 + 2\kappa_2$, $a_1 = a_{N-1} = -\kappa_1$, $a_2 = a_{N-2} = -\kappa_2$. The matrix T is generated by the vector $\boldsymbol{\tau} = (\tau_0, \tau_1, \tau_2)$ with

$$\begin{aligned}\tau_0 &= -\frac{\sqrt{\kappa_1}}{2} - \frac{1}{2}\sqrt{\kappa_1 + 4\kappa_2}, \quad \tau_1 = \sqrt{\kappa_1}, \\ \tau_2 &= -\frac{\sqrt{\kappa_1}}{2} + \frac{1}{2}\sqrt{\kappa_1 + 4\kappa_2},\end{aligned}$$

so that the quantities r_j are defined as

$$r_j = \tau_1(q_{j+1} - q_j) + \tau_2(q_{j+2} - q_j), \quad j \in \mathbb{Z}/N\mathbb{Z}.$$

[...] The Hamiltonian $H(\mathbf{p}, \mathbf{q})$ represents clearly an integrable system that can be integrated passing through Fourier transform. Let \mathcal{F} be the discrete Fourier transform with entries $\mathcal{F}_{j,k} := \frac{1}{\sqrt{N}} e^{-2\pi jk/N}$ with $j, k = 0, \dots, N-1$. It is immediate to verify that

$$\mathcal{F}^{-1} = \bar{\mathcal{F}} \quad \mathcal{F}^\top = \mathcal{F}. \quad (4.103)$$

Thanks to the above properties, the transformation defined by

$$(\dot{\mathbf{p}}, \dot{\mathbf{q}}) = (\bar{\mathcal{F}}\mathbf{p}, \mathcal{F}\mathbf{q}) \quad (4.104)$$

is canonical. Furthermore $\bar{\mathbf{p}}_j = \hat{\mathbf{p}}_{N-j}$ and $\bar{\mathbf{q}}_j = \hat{\mathbf{q}}_{N-j}$, for $j = 1, \dots, N-1$, while $\hat{\mathbf{p}}_0$ and $\hat{\mathbf{q}}_0$ are real variables. The matrices T and A are circulant matrices and so they are reduced to diagonal form by \mathcal{F} :

$$\mathcal{F}A\mathcal{F}^{-1} = \mathcal{F}T^\top T\mathcal{F}^{-1} = (\overline{\mathcal{F}T\mathcal{F}^{-1}})^\top (\mathcal{F}T\mathcal{F}^{-1}).$$

Let ω_j denote the eigenvalues of the matrix T ordered so that $\mathcal{F}T\mathcal{F}^{-1} = \text{diag}(\omega_j)$. Then $|\omega_j|^2$ are the (non negative) eigenvalues of the matrix A and

$$|\omega_j|^2 = \sqrt{N}(\mathcal{F}\tilde{\mathbf{a}})_j, \quad \omega_j = \sqrt{N}(\mathcal{F}\tilde{\boldsymbol{\tau}})_j, \quad j = 0, \dots, N-1, \quad (4.105)$$

where $\tilde{\mathbf{a}}$ is the m -physical vector generated by \mathbf{a} and $\tilde{\boldsymbol{\tau}}$ is the half m -physical vector generated by $\boldsymbol{\tau}$. It follows that

$$\omega_0 = 0, \quad \omega_j = \overline{\omega}_{N-j}, \quad j = 1, \dots, N-1, \quad (4.106)$$

which implies $|\omega_j|^2 = |\omega_{N-j}|^2$, $j = 1, \dots, N-1$.

Circulant hierarchy of integrals

In this section we construct a complete set of conserved quantities that have local densities. The harmonic oscillator with short range interaction is clearly an integrable system. A set of integrals of motion is given by the harmonic oscillators in each of the Fourier variables: $\hat{H}_j = \frac{1}{2}(|\hat{\mathbf{p}}_j|^2 + |\omega_j|^2|\hat{\mathbf{q}}_j|^2)$, $j = 0, \dots, \frac{N-1}{2}$. However, when written in the physical variables \mathbf{p} and \mathbf{q} , the quantities

$$\hat{H}_j = \frac{1}{2} \sum_{k,l=0}^{N-1} \mathcal{F}_{j,k} \overline{\mathcal{F}_{j,l}} (p_k p_l + |\omega_j|^2 q_k q_l)$$

depend on all components of the physical variables. We now construct integrals of motion each having a density that involves only a limited number of components of the physical variables and this number only depends on the range m of interaction.

For this purpose we denote by $\{\mathbf{e}_k\}_{k=0}^{N-1}$ the canonical basis in \mathcal{R}^N .

Local conserved quantities Let us consider the Hamiltonian

$$H(\mathbf{p}, \mathbf{q}) = \frac{1}{2}\mathbf{p}^\top \mathbf{p} + \frac{1}{2}\mathbf{q}^\top A\mathbf{q}, \quad (4.107)$$

with the symmetric circulant matrix A as in (4.90), (4.91). Define the matrices $\{G_k\}_{k=1}^M$ to be the symmetric circulant matrix generated by the vector $\frac{1}{2}(\mathbf{e}_k + \mathbf{e}_{N-k})$ and $\{S_k\}_{k=1}^M$ to be the antisymmetric circulant matrix generated by the

vector $\frac{1}{2}(\mathbf{e}_k - \mathbf{e}_{N-k})$. Then the family of Hamiltonians defined as

$$H_k(\mathbf{p}, \mathbf{q}) = \frac{1}{2}\mathbf{p}^\top G_k \mathbf{p} + \frac{1}{2}\mathbf{q}^\top T^\top G_k T \mathbf{q} = \frac{1}{2} \sum_{j=0}^{N-1} [p_j p_{j+k} + r_j r_{j+k}], \quad (4.108)$$

$$H_{k+\frac{N-1}{2}}(\mathbf{p}, \mathbf{q}) = \mathbf{p}^\top T^\top S_k T \mathbf{q} = \frac{1}{2} \sum_{j=0}^{N-1} \left[\left(\sum_{\ell=0}^m \tau_\ell p_{j+\ell} \right) (r_{j+k} - r_{j-k}) \right], \quad k = 1, \dots, \frac{N-1}{2} \quad (4.109)$$

together with $H_0 := H$ forms a complete family $(H_j)_{0 \leq j \leq N-1}$ of integrals of motion that, moreover, is in involution. [...] Now we introduce the local densities corresponding to the just defined integrals of motion

$$e_j^{(k)} = \begin{cases} \frac{1}{2}(p_j p_{j+k} + r_j r_{j+k}), & \text{for } k = 1, \dots, \frac{N-1}{2} \\ (\sum_{l=0}^m \tau_l p_{j+l})(r_{j+k} - r_{j-k}), & \text{for } k = \frac{N+1}{2}, \dots, N. \end{cases} \quad (4.110)$$

[...]

Nonlinear regime

In this section we consider a nonlinear perturbation of the harmonic oscillators with short range interactions of the form

$$H(\mathbf{p}, \mathbf{q}) = \sum_{j=0}^{N-1} \frac{p_j^2}{2} + \sum_{s=1}^m \kappa_s \left(\frac{1}{2} \sum_{j=0}^{N-1} (q_j - q_{j+s})^2 + \frac{\chi}{3} \sum_{j=0}^{N-1} (q_j - q_{j+s})^3 + \frac{\gamma}{4} \sum_{j=0}^{N-1} (q_j - q_{j+s})^4 \right). \quad (4.111)$$

We consider examples with different strengths of nonlinearity namely

$$\begin{aligned} m = 2, \kappa_1 = 1, \kappa_2 = \frac{1}{4}, & \quad \begin{cases} \chi = 0.01 \text{ and } \gamma = 0.001 \\ \chi = 0.1 \text{ and } \gamma = 0.01 \end{cases} \\ m = 3, \kappa_1 = 1, \kappa_2 = \frac{1}{8}, \kappa_3 = \frac{7}{72}, & \quad \begin{cases} \chi = 0.01 \text{ and } \gamma = 0.001 \\ \chi = 0.1 \text{ and } \gamma = 0.01 \end{cases}. \end{aligned}$$

4.3.2 Baake et al. 2008 paper BaRoWe08

2017-09-27, 2021-02-03 Predrag reading Baake, Roberts and Weiss [10] *Periodic orbits of linear endomorphisms on the 2-torus and its lattices* arXiv:0808.3489.

2021-02-03 Predrag Summary

1. The main result is the third matrix invariant: the ‘gmc’ that fixes the conjugacy class of a given lattice in an invariant way, unlike the Hermite normal form (5.204) that breaks the ‘spatiotemporal’ symmetry; mention and cite in CL18 [29], even if we do not use it.

2. They do counting for the golden (Fibonacci [8]) cat map (4.179), see table 4.2 and (4.182), as the simplest example; we do not need to cite their counting in CL18 [29], cite 1997 sect. 4.3.3 *Baake, Hermisson and Pleasants* [7] instead. (I'm somewhat sure that name 'golden cat' is not already in 1967 Smale [88], or 1995 Katok and Hasselblatt [56]. Perhaps better to call it "Fibonacci" [8]?) There is no mention that this is a time-reversal reduction of the $s = 3$ cat map in Baake *et al.* [10]. Perhaps Katok and Hasselblatt [56] mention that?
3. They do not mention any time-reversal symmetry reduction connection to the lattice states and orbit counts for the $s = 3$ cat map table 4.1; do not cite them for that.

Their focus on the relation between global and local aspects and between the dynamical zeta function on the torus and its analogue on finite lattices. The situation on the lattices, up to local conjugacy, is completely determined by the determinant, the trace and a third invariant of the matrix defining the toral endomorphism.

In introduction they refer to much literature on cat maps on lattices, and I've not read much of it.

[...] the system (Ω, T) is called *chaotic* when the periodic orbits of T are dense in Ω and when also a dense orbit exists, see Banks *et al.* [12] *On Devaney's definition of chaos* for details. Knowledge of the periodic orbits can be used to detect characteristic properties of T . For example, if T' represents another continuous mapping of Ω , then a necessary condition for T and T' to be topologically conjugate is that they share the same number of periodic points of each period.

[...] endomorphisms of the 2-torus, represented by the action (mod 1) of an integer matrix $M \in \text{Mat}(2, \mathbb{Z})$ on $\mathbb{T}^2 \simeq \mathbb{R}^2 / \mathbb{Z}^2$. A well-studied subclass consists of the toral automorphisms, represented by elements of the group $GL(2, \mathbb{Z})$, being the subgroup of matrices with determinant ± 1 within the ring $\text{Mat}(2, \mathbb{Z})$. Particularly important are the hyperbolic ones (meaning that no eigenvalue is on the unit circle), which are often called *cat maps*. Since these are expansive, all periodic point counts are finite. Hyperbolic toral automorphisms are also topologically mixing and intrinsically ergodic, see refs. [56, 92]. By the Bowen-Sinai theorem, this has the consequence that the integral of a continuous function over \mathbb{T}^2 equals its average value over the points fixed by M^m in the limit as $m \rightarrow \infty$.

The topological entropy of a hyperbolic toral automorphism $M \in GL(2, \mathbb{Z})$ is given by $\log |\lambda_{\max}|$, where λ_{\max} is the eigenvalue of M with modulus > 1 . This is also the metric (or Kolmogorov-Sinai) entropy of M , and completely determines the dynamics up to metric isomorphism, compare ref. [1]. This does not imply topological conjugacy though, and one important difference emerges from the periodic orbits, which live on a set of measure 0. Indeed, on \mathbb{T}^2 , it is well-known that the periodic orbits of hyperbolic linear endomorphisms lie on the invariant lattices given by the sets of rational points with a given denominator n , also known as n -division points. One of our main themes in this paper

is the interplay between the periodic orbit statistics on a certain lattice (which we call *local statistics*) versus periodic orbit statistics on the union of all lattices (which we call *global statistics*). What determines when two cat maps have the same global statistics? What determines when two cat maps have the same local statistics on a certain lattice or on all lattices?

The time of recurrence of a hyperbolic $M \in GL(2, \mathbb{Z})$ on the toral rational lattice with denominator n is denoted by $\text{per}(M, n)$, where this is the least common multiple of the periods present on the n -division points.

[...] for symmetries or (time) reversing symmetries of a cat map, these being automorphisms of the torus that commute with the cat map, respectively conjugate it into its inverse.

[...] there has been quite some interest in dealing with this challenge of so-called pseudo-symmetries of quantum maps that are not quantisations of symmetries of the cat map on the torus, but instead are manifestations of local symmetries of the cat map restricted to some lattice [57, 60].

Conjugacy of $GL(2, \mathbb{Z})$ matrices is another topic that has arisen in a broad variety of contexts and has been considered by many. Conjugacy is determined by a triple of invariants, namely the determinant, the trace and one other invariant which can be related to ideal classes, representation by binary quadratic forms or topological properties. Conjugacy in $GL(2, \mathbb{Z})$ can also be completely decided by using the amalgamated free product structure of $PGL(2, \mathbb{Z})$, which attaches a finite sequence of integers to each element which corresponds to its normal form as a word in the generators of the amalgamated free product [9].

There are various ways of deciding $GL(2, \mathbb{Z})$ -conjugacy, amounting to exploiting a third and final conjugacy invariant.

Result of this paper: The matrix gcd is a key quantity. It is preserved by $GL(2, \mathbb{Z})$ conjugacy, so it provides a quick tool to see that two $GL(2, \mathbb{Z})$ matrices with different matrix gcd are not conjugate on the torus. If two integer matrices share the same determinant, trace and matrix gcd they are linearly conjugate on all rational lattices of the torus. As an illustration of this result, consider cat maps and time-reversal symmetry. The fact that any $M \in SL(2, \mathbb{Z})$ shares determinant, trace and matrix gcd with M^{-1} means that the two matrices are conjugate on *all* rational lattices, though not necessarily by matrices that derive from one and the same matrix on the torus.

Consider a compact space Ω and some (continuous) mapping T of Ω into itself. Let $\text{Fix}_m(T) := \{x \in X \mid T^m x = x\}$ be the set of fixed points of T^m . Of particular interest are the *fixed point counts*, defined as

$$a_m := \text{card}\{x \in \Omega \mid T^m x = x\} = \text{card}(\text{Fix}_m(T)). \quad (4.112)$$

The quantity a_m has the disadvantage that one keeps recounting the contributions a_ℓ for all $\ell|m$. Clearly, the fixed points of *genuine* order m permit a partition into disjoint cycles, each of length m . If c_m is the number of such cycles, one thus has the relation

$$a_m = \sum_{d|m} d c_d. \quad (4.113)$$

An application of a standard inclusion-exclusion argument, here by means of the Möbius inversion formula from elementary number theory, results in the converse identity,

$$c_m = \frac{1}{m} \sum_{d|m} \mu\left(\frac{m}{d}\right) a_d, \quad (4.114)$$

where $\mu(k)$ is the Möbius function.

[...] a toral endomorphism $M \in \text{Mat}(2, \mathbb{Z})$ is *hyperbolic* if it has no eigenvalue on the unit circle S^1 . The standard 2-torus is $\mathbb{T}^2 \simeq \mathbb{R}^2 / \mathbb{Z}^2$, where \mathbb{Z}^2 is the square lattice in the plane. It is a compact Abelian group, which can be written as $\mathbb{T}^2 := [0, 1]^2$, with addition defined mod 1.

[...] the abbreviation $\mathbb{Z}_n = \mathbb{Z}/n\mathbb{Z}$ for the finite integer ring mod n , and $\mathbb{Z}_n^\times = \{1 \leq k \leq n \mid \gcd(k, n) = 1\}$ for its unit group.

Some ‘obvious’ number theory defines gcd, but I have not put in the effort needed to understand it.

For counting orbits, this might be useful:

Let $M \in \text{Mat}(2, \mathbb{C})$ be a non-singular matrix, with $D := \det(M) \neq 0$ and $T := \text{tr}(M)$. Define a two-sided sequence of (possibly complex) numbers p_m by the initial conditions $p_{-1} = -1/D$ and $p_0 = 0$ together with the recursion

$$\begin{aligned} p_{m+1} &= Tp_m - Dp_{m-1}, \quad \text{for } m \geq 0, \\ p_{m-1} &= \frac{1}{D}(Tp_m - p_{m+1}), \quad \text{for } m \leq -1. \end{aligned} \quad (4.115)$$

This way, as $D \neq 0$, p_m is uniquely defined for all $m \in \mathbb{Z}$. Note that the sequence $(p_m)_{m \in \mathbb{Z}}$ depends only on the determinant and the trace of M . When $M \in \text{Mat}(2, \mathbb{Z})$, one has $p_m \in \mathbb{Q}$, and $p_m \in \mathbb{Z}$ for $m \geq 0$. When $M \in \text{GL}(2, \mathbb{Z})$, all p_m are integers.

Note an interesting property, which follows from a straight-forward induction argument (in two directions):

The two-sided sequence of rational numbers defined by the recursion (4.115) satisfies the relation

$$p_m^2 - p_{m+1}p_{m-1} = D^{m-1}, \quad (4.116)$$

for all $m \in \mathbb{Z}$.

To deal with combinatorial quantities such as the fixed point counts a_m , it is advantageous to employ generating functions. Here, the concept of a *dynamical zeta function* is usually most appropriate. Consequently, given a matrix $M \in \text{Mat}(2, \mathbb{Z})$, we set

$$\zeta_M(t) := \exp\left(\sum_{m=1}^{\infty} \frac{a_m}{m} t^m\right), \quad (4.117)$$

where, from now on, $a_m := \text{card}\{x \in \text{Fix}_m(M) \mid x \text{ is isolated}\}$ is the number of *isolated* fixed points of M^m .

The ordinary power series generating function for the counts a_m can be calculated from $\zeta_M(t)$ as $\sum_{m \geq 1} a_m t^m = t \frac{d}{dt} \log(\zeta_M(t))$. The significance of the

formulation used in Eq. (4.117) follows from the fact that it has a unique Euler product decomposition as

$$\frac{1}{\zeta_M(t)} = \prod_{\text{cycles } \mathcal{C}} (1 - t^{|\mathcal{C}|}) = \prod_{m \geq 1} (1 - t^m)^{c_m}, \quad (4.118)$$

where $|\mathcal{C}|$ stands for the length of the cycle \mathcal{C} and c_m is now the number of *isolated* cycles of M on \mathbb{T}^2 of length m , as determined from Formula (4.114). Consequently, the role of cycles in dynamics is similar to that of primes in elementary number theory.

The dynamical zeta function, a special case of which was also given in ref. [42].

Let $M \in GL(2, \mathbb{Z})$ be hyperbolic, and define $\sigma = \text{sgn}(\text{tr}(M))$. Then, with the coefficients $a_m = \text{card}\{x \in \mathbb{T}^2 \mid M^m x = x \pmod{1}\}$, the dynamical zeta function (4.117) of M on \mathbb{T}^2 is given by

$$\zeta_M(t) = \frac{(1 - \sigma t)(1 - \sigma t \det(M))}{\det(1 - \sigma t M)} = \frac{(1 - \sigma t)(1 - \sigma \det(M)t)}{1 - |\text{tr}(M)|t + \det(M)t^2}.$$

In particular, $\zeta_M(t)$ is a rational function, with numerator and denominator in $\mathbb{Z}[t]$. The denominator is a quadratic polynomial that is irreducible over \mathbb{Z} . Its zero t_{\min} closest to 0 gives the radius of convergence of $\zeta_M(t)$, as a power series around 0, via $r_c = |t_{\min}|$.

If M is hyperbolic, the general formula for the a_m

$$a_m = \sigma^m (\text{tr}(M^m) - (1 + \det(M)^m))$$

can be derived by observing that the two eigenvalues of A can be written as λ and $\det(A)/\lambda$. For the detailed argument, one may assume $|\lambda| > 1$ and check the different cases. Note that a hyperbolic toral automorphism is never of trace 0.

The formula for the zeta function now follows from (4.117) by inserting the expression for a_m . The statement on the nature of the rational function is then clear. With $M \in GL(2, \mathbb{Z})$, the denominator only factorises for $\text{tr}(M) = 0$, $\det(M) = -1$ or for $\text{tr}(M) = \pm 2$, $\det(M) = 1$, both cases being impossible for hyperbolic matrices.

Two hyperbolic $GL(2, \mathbb{Z})$ -matrices with the same trace and determinant possess the same dynamical zeta function, hence the same fixed point counts. The converse is slightly more subtle.

3.3. Generating functions on lattices: I tried reading this before, I tried on 2017-09-27 again, and on 2021-02-03 again, and I still do not get it.

Consider a 2×2 -matrix

$$M = \begin{pmatrix} a & b \\ c & d \end{pmatrix} \quad (4.119)$$

If $M \in \text{Mat}(2, \mathbb{Z})$, the quantity

$$\text{mgcd}(M) := \text{gcd}(b, c, d - a),$$

is called the *matrix gcd* of M , or *mgcd* for short. Here, we take the gcd to be a non-negative integer, and set $\text{mgcd}(M) = 0$ when $b = c = d - a = 0$. The last convention matches that of the ordinary gcd, and is compatible with modular arithmetic.

For $M \in \text{Mat}(2, \mathbb{Z})$, the following statements are equivalent:

- (a) The matrix gcd satisfies $\text{mgcd}(M) = 0$.
- (b) $M = k\mathbf{1}$ for some $k \in \mathbb{Z}$.
- (c) The minimal polynomial of M is of degree 1.

Consequently, whenever $\text{mgcd}(M) = r \in \mathcal{N}$, M cannot be a multiple of the identity, and its characteristic and minimal polynomials coincide.

Most significantly, the matrix gcd satisfies the following invariance property:

If $M, M' \in \text{Mat}(2, \mathbb{Z})$ are two integer matrices that are conjugate via a $GL(2, \mathbb{Z})$ -matrix, one has $\text{mgcd}(M') = \text{mgcd}(M)$. In particular, the matrix gcd is constant on the conjugacy classes of $GL(2, \mathbb{Z})$.

consider the integer matrices

$$M = \begin{pmatrix} a & b \\ c & d \end{pmatrix} \quad \text{and} \quad C = \begin{pmatrix} 0 & -D \\ 1 & T \end{pmatrix} \quad (4.120)$$

with $D = \det(M)$ and $T = \text{tr}(M)$. Here, C is the standard companion matrix for the characteristic polynomial

$$x^2 - Tx + D \quad (4.121)$$

of the matrix M . [...]

2017-09-27, 2021-02-03 Predrag read superficially Llibre and Neumärker [68]
Period sets of linear toral endomorphisms on T^2 ; did not understand much.

4.3.3 Baake *et al.* 1997 paper BaHePl97

In 1997 Baake, Hermisson and Pleasants [7] *The torus parametrization of quasiperiodic LI-classes* ([click here](#)) refer to time-reversal as ‘*inversion*’ symmetry, and discuss the golden (Fibonacci [8]) cat map. Before giving up on them, do have a look at their eq. (18) zeta function and Table 2. *Inflation orbit counts for 1D cut-and-project patterns with inflation*, compare with table 4.2; compare their Table 4. with table 4.1. Their eq. (18) zeta function is not our Kim *et al.* [58] (4.149). **Do cite in CL18 [29]!**

Sect. 2.3 Symmetry The only kind of point symmetry possible for 1D chains is mirror symmetry, which we shall usually refer to as *inversion symmetry* in order to have the same terminology for all dimensions (‘*inversion*’ meaning

the isometry $x \rightarrow -x$). Inversion symmetric chains correspond to points \mathbf{t} on the torus with $\mathbf{t} = -\mathbf{t}$, i.e. $2\mathbf{t} = \mathbf{0}$. There are four such points

$$(0, 0) \quad \left(\frac{1}{2}, 0\right) \quad \left(0, \frac{1}{2}\right) \quad \left(\frac{1}{2}, \frac{1}{2}\right), \quad (4.122)$$

that form the discrete subgroup of ‘two-division points’ of T^2 , isomorphic to $C_2 \times C_2$.

They count many inversion-symmetric patterns in various dimensions, but I do not think any of that applies to temporal cat or spatiotemporal cat.

4.3.4 Baake 2018 paper Baake18

Read this:

Michael Baake [6] *A brief guide to reversing and extended symmetries of dynamical systems* arXiv:1803.06263.

4.3.5 Lamb and Roberts 1998 paper lamb98

Lamb and Roberts [61] *Time reversal symmetry in dynamical systems: A survey* (1998) is a very extensive compendium of references on reversibility. Even though they touch upon discrete lattice settings (the Frenkel-Kontorova model [5]) I see no place a reference to group-theoretic description of D_∞ lattices that we undertake in LC21 [64].

section 13.6 Example 3.4. Symmetric difference equations of the form

$$\phi_{n+1} - f(\phi_n) + \phi_{n-1} = 0 \quad (4.123)$$

the Frenkel-Kontorova model which is equivalent to the area-preserving Chirikov-Taylor standard mapping.

Remarkably, (4.123) is not only reversible, but the associate ‘time’ mapping is also area-preserving. Many area-preserving (symplectic) mappings studied in the literature are reversible (e.g. the well-studied area-preserving Hénon map, cf. Roberts and Quispel [80] (1992) and references therein).

2021-03-25 Predrag See example 2.5; shouldn’t “time-reversal operator” just reverse momentum/velocity (4.51)? The definitive review of the nomenclature is Roberts and Quispel [80] *Chaos and time-reversal symmetry. Order and chaos in reversible dynamical systems*.

It turns out that symmetry naturally arises in the study of return maps of flows of time-periodic vector fields with mixed space-time symmetries. In a natural way these space-time symmetries form a group under composition.

4.1. Symmetric periodic orbits

a result on periodic orbits is by far the most well known and used result in reversible dynamical systems. In 1915, Birkhoff [Birkhoff, 1915] described the use of reversibility to find periodic orbits of the restricted three-body problem. In 1958 De Vogelaere [30] described the method again, but now as a tool for searching for symmetric periodic orbits of reversible systems (by computer).

Definition 4.1 (Symmetric orbits). An orbit of a dynamical system is s -symmetric or symmetric with respect to s when the orbit is setwise invariant under s .

Theorem 4.2 (Symmetric orbits for maps) is the same as LC21 [64] classification of 3 kinds of symmetric orbits (Predrag believes).

Theorem 4.1 or 4.2 is used in almost every paper discussing reversible dynamical systems. In particular, these theorems imply efficient techniques for tracking down s -symmetric periodic orbits, as it justifies searching for them in only a subset of the full phase space.

A well-known property of linear reversible systems is that their eigenvalue structure is similar to that of Hamiltonian systems.

Theorem 4.4 (Eigenvalues of linear reversible systems)...

4.3.6 Calogero 2007 paper BrCaDr07

Bruschi, Calogero and Droghei [17] *Tridiagonal matrices, orthogonal polynomials and Diophantine relations: I.*

If the equations of motion and the solution of their initial-value problems involve only algebraic operations: finding the zeros of explicitly known polynomials of degree N , finding the eigenvectors and eigenvalues of explicitly known $N \times N$ matrices, the dynamical system is called *solvabile*.

It is well known that the eigenvalues of tridiagonal matrices can be identified with the zeros of polynomials satisfying three-term recursion relations and being therefore members of an orthogonal set. They consider the class of monic polynomials $p_n(s)$, of degree n in the variable s , defined by the three-term recursion relation

$$p_{n+1}(s) - (s + a_n)p_n(s) - b_n p_{n-1}(s) = 0, \quad (4.124)$$

They associate a tridiagonal $[n \times n]$ matrix M with it, related to $p_n(s)$ via the “well-known” formula

$$p_n(s) = \det(s - M). \quad (4.125)$$

The n zeros of the polynomial $p_n(s)$ coincide with the n eigenvalues of the tridiagonal matrix M .

Favard’s theorem: a sequence of polynomials satisfying a suitable 3-term recurrence relation of the form $p(s)_{n+1} = (s - c_n)p(s)_n - d_n p(s)_{n-1}$ for some numbers c_n and d_n , then the polynomials $p(s)_n$ form a sequence of orthogonal polynomials. We are interested in this, because we would like to understand Hill determinants polynomials factorization, such as in (13.78).

See also **Jacobi operator**. The self-adjoint Jacobi operators act on the Hilbert space of square summable sequences over the $\ell^2(\mathbb{N})$:

$$Jf_0 = a_0 f_1 + b_0 f_0, \quad Jf_n = a_n f_{n+1} + b_n f_n + a_{n-1} f_{n-1}, \quad n > 0,$$

where the coefficients are assumed to satisfy

$$a_n > 0, \quad b_n \in \mathbb{R}.$$

The solution $p_n(s)$ of the recurrence relation

$$J p_n(s) = s p_n(s), \quad p_0(s) = 1 \text{ and } p_{-1}(s) = 0,$$

is a polynomial of degree n and these polynomials are orthonormal. Here J can be interpreted as a lattice right-shift operator, i.e., for a temporal lattice this is related to the evolution in time. This recurrence relation can also be written as

$$a_{n+1}p_{n+1}(s) - (s - b_n)p_n(s) + a_n p_{n-1}(s) = 0, \quad (4.126)$$

(Compare with (5.239).)

or (if one replaces $s \rightarrow \mu^2$)

$$(-J + \mu^2)p_n(\mu^2) = 0,$$

reminiscent of the Klein–Gordon equation (5.26). The operator will be bounded if and only if the coefficients are bounded. The case $a(n) = 1$ is known as the discrete one-dimensional Schrödinger operator. It also arises in:

- The Lax pair of the Toda lattice (see 2020-08-02 Predrag Toda post)
- The three-term recurrence relationship of orthogonal polynomials.
- Algorithms devised to calculate Gaussian quadrature rules, derived from systems of orthogonal polynomials.

4.3.7 Variational method, Dong 2020 paper DoLiLi20

Some of the text that follows is copy & paste from Dong, Liu and Li [36] *Unstable periodic orbits analysis in the generalized Lorenz-type system* 2020). That is probably copy & paste from earlier Dong papers, have not checked that.

Their description of our variational method [28, 62] looks better than our own, or the ChaosBook text (which is not in the public edition yet).

[...] a local, time-dependent scaling factor is used to adjust the period

$$\lambda(s_n) \equiv \Delta t_n / \Delta s_n, \quad (4.127)$$

where $\Delta s_n = s_{n+1} - s_n, n = 1, \dots, N - 1$, $\Delta s_N = 2\pi - (s_N - s_1)$ and Δt_n follows the same pattern. The scaling factor guarantees the loop increment Δs_n is proportional to its counterpart $\Delta t_n + \delta t_n$ on the periodic orbit when the loop approaches the cycle, with $\delta t_n \rightarrow 0$ as $L \rightarrow p$.

The Jacobian matrix $\mathbf{J}(x, t) = dx(t)/dx(0)$ is obtained by integrating

$$\frac{d\mathbf{J}}{dt} = \mathbf{A}\mathbf{J}, \quad \mathbf{A}_{ij} = \frac{\partial \mathbf{v}_i}{\partial \mathbf{x}_j}, \quad \text{with} \quad \mathbf{J}(x, 0) = 1. \quad (4.128)$$

[Predrag is getting tired of copying LaTeX from Dong, Liu and Li [36]. Whoever continues this, remember to turn on *MathJax*, upper right corner of paper's homepage.]

The variational evolution equation containing the crux of the method of finding periodic orbits

$$\frac{\partial^2 \tilde{x}}{\partial s \partial \tau} - \lambda A \frac{\partial \tilde{x}}{\partial \tau} - v \frac{\partial \lambda}{\partial \tau} = \lambda v - \tilde{v}. \quad (4.129)$$

Rewriting as

$$\frac{\partial \tilde{v}}{\partial \tau} - \lambda \frac{\partial v}{\partial \tau} = -(\tilde{v} - \lambda v), \quad (4.130)$$

yields

$$(\tilde{v} - \lambda v) = e^{-\tau} (\tilde{v} - \lambda v) |_{\tau=0}, , \quad (4.131)$$

a minimizing cost function:

$$F^2 [\tilde{x}] = \frac{1}{2\pi} \oint_{L(\tau)} d\tilde{x} [\tilde{v}(\tilde{x}) - \lambda v(\tilde{x})]^2. \quad (4.132)$$

As the loop descends toward a periodic orbit, the cost function decreases monotonically the differences between $\tilde{v}(\tilde{x})$ and $v(\tilde{x})$, converging in the $\tau \rightarrow \infty$ limit to the periodic orbit. On the periodic orbit, by (4.127), $\lambda(s, \infty) = (dt/ds)(\tilde{x}(s, \infty))$, and the period is given by

$$T_P = \int_0^{2\pi} \lambda(\tilde{x}(s, \infty)) ds. \quad (4.133)$$

The finite difference scheme is employed in a discretization of a loop

$$\tilde{v}_n \equiv \left. \frac{\partial \tilde{x}}{\partial s} \right|_{\tilde{x}=\tilde{x}(s_n)} \approx (\hat{D} \tilde{x})_n \quad (4.134)$$

and the five-point approximation is adopted

$$\hat{D} = \frac{1}{12h} \begin{pmatrix} 0 & 8 & -1 & & & & 1 & -8 \\ -8 & 0 & 8 & -1 & & & & 1 \\ 1 & -8 & 0 & 8 & -1 & & & \\ & & & & \ddots & & & \\ & & & & & 1 & -8 & 0 & 8 & -1 \\ & & & & & & 1 & -8 & 0 & 8 \\ -1 & & & & & & & 1 & -8 & 0 \\ 8 & -1 & & & & & & & 1 & -8 & 0 \end{pmatrix}, \quad (4.135)$$

where $h = 2\pi/N$, and each entry represents a $[d \times d]$ matrix in (4.135), $8 \rightarrow 8\mathbf{1}$, etc; the blanks in the matrix represent zeros. The two $[2d \times 2d]$ matrices, found in the upper right-corner and the lower-left corner of (4.135), respectively, can be written as

$$M_1 = \begin{pmatrix} \mathbf{1} & -8\mathbf{1} \\ 0 & \mathbf{1} \end{pmatrix}, \quad M_2 = \begin{pmatrix} -\mathbf{1} & 0 \\ 8\mathbf{1} & -\mathbf{1} \end{pmatrix},$$

and are related to the periodic boundary conditions.

After discretization, (4.129) can be written as

$$\begin{pmatrix} \hat{\mathbf{A}} & -\hat{\mathbf{v}} \\ \hat{\mathbf{a}} & 0 \end{pmatrix} \begin{pmatrix} \delta\tilde{x} \\ \delta\lambda \end{pmatrix} = \delta\tau \begin{pmatrix} \lambda\hat{\mathbf{v}} - \hat{\mathbf{v}} \\ 0 \end{pmatrix}, \quad (4.136)$$

where $\hat{\mathbf{A}} = \hat{\mathbf{D}} - \lambda \text{diag}[A_1, A_2, \dots, A_N]$ and $A_n = \mathbf{A}(\tilde{x}(s_n))$ is defined in (4.128).

$$\hat{\mathbf{v}} = (v_1, v_2, \dots, v_N)^T \quad \text{with} \quad \mathbf{v}_n = \mathbf{v}(\tilde{x}(s_n)),$$

are the two column vectors that we match everywhere during the evolution of the loop. $\hat{\mathbf{a}}$ is an Nd -dimensional row vector that restricts the coordinate variations. The deformation of the loop coordinates $\delta\tilde{x}$ and period $\delta\lambda$ can be calculated by inverting the $[(Nd+1) \times (Nd+1)]$ matrix on the left-hand side of (4.136).

We use the banded lower-upper (LU) decomposition scheme. Due to the structure of the matrix in (4.136), the Woodbury formula is adopted on the cyclic and boundary terms in the calculations [76], thus enabling an efficient search for periodic orbits.

The variational approach is a good choice to search cycles in a low-dimensional dissipative system. This method is not only suitable for the determination of periodic orbits but also for the homoclinic and heteroclinic orbits [34]. In the previous work, the periodic orbits in various chaotic systems were calculated efficiently using the variational method [32, 33, 35], which illustrates the practicability of this method in the GLTS.

The variational method can also be used to analyze bifurcation phenomena. When the parameters of a dynamical system change continuously, we can observe the conditions under which the periodic orbit is created or disappears through deformations of the periodic orbit.

4.3.8 Dong 2021 paper LDJL21

Liu, Dong, Jie, and Li [67] *Topological classification of periodic orbits in the generalized Lorenz-type system with diverse symbolic dynamics* (2021) ([click here](#)).

I like their explanation of the variational method for finding periodic orbits, and their use of it to study bifurcations by homotopy evolution, which I believe to be authors' original contribution to the subject.

I wish they would consider quotienting symmetries of a given dynamical system prior to their symbolic dynamics analysis. For the 3-disk system quotienting the D_3 symmetry vastly improves the convergence of cycle expansions, see [ChaosBook Table 23.2](#), with symmetry reduction illustrated by [ChaosBook Figure 11.1](#), and explained at length in ChaosBook, also for the Lorenz flow, see [ChaosBook Example 14.4](#), and the text leading up to it.

Reduction of the Lorenz D_1 symmetry might not seem like much, but even that is pretty impressive - the period of a prime or pre-periodic orbit is $|G|/|G_p|$ -th root of the full state space orbit period, and that leads to a significant simplification of the given problem. For example, in ref. [63], [Figure 8 \(e\)](#) that led

CHAPTER 4. GROUP THEORY

to the 3-letter, bi-modal return map instead of a numerically unmanageable 9-letter return map in the symmetry-unreduced, original state space.

In authors' example, symmetry reduction would reduce their Table 1 cycles 0,1; 001, 011; 0001,0111 etc to a single cycle, and 01 to repeat 1-cycle, 0011 to a repeat of a prime 2-cycle, and in general of 1/2 period. Table 2 is another illustration, with 2,3; barred 2,3 to a single letter, 23 a repeat of 1-cycle, ..., etc, and the co-existing attractors of Figure 9 reduced to a single attractor. Would be nice to visualize self-linking in the symmetry-reduced state space.

How the reduced symbolic dynamics is related to unreduced one (the kind used by the authors) is explained in ref. [34] [ChaosBook Sect. 25.5 D₁ factorization](#).

4.3.9 Letter from Ping Ao

2020-12-16 from [Ping Ao](#), aoping@sjtu.edu.cn

*Distinguished Professor Shanghai Center for Quantitative Life Sciences
and Physics Department Shanghai University; and Shanghai Center for
Systems Biomedicine Shanghai Jiao Tong University Shanghai, China*

Dear Prof. Predrag Cvitanović, Many thanks for your inspiring pandemic talk on "Spatiotemporal Cat: A Chaotic Field Theory". It is very interesting to use "chaotic attractors" as building blocks for field theories. Here I have one remark and one question which may be of an interest to you.

In dynamical systems it is known that there are three generic classes of systems: fixed points or linear; limit cycles; chaotic attractors. The last two must be nonlinear, as well explained during your talk. For dissipative dynamical systems we have explicitly constructions for all three:

1. *Structure of stochastic dynamics near fixed points*, C Kwon, P Ao, DJ Thouless. PNAS 102 (2005) 13029 ([click here](#))
2. *Limit cycle and conserved dynamics*, XM Zhu, L Yin, P Ao. Intl J Modern Physics B20 (2006) 817 ([click here](#))
3. *Exploring a noisy van der Pol type oscillator with a stochastic approach*, Yuan, R.-S.; Wang, X.-A.; Ma, Y.-A.; Yuan, B. & Ao, P. . Phys Rev E87 (2013) 062109 ([click here](#))
4. *Potential function in a continuous dissipative chaotic system: Decomposition scheme and role of strange attractor*, Yian Ma, Qijun Tan, Ruoshi Yuan, Bo Yuan and Ping Ao. Intl J Bifur Chaos 24 (2014) 1450015 ([click here](#))
5. A summary of our method is here: *SDE decomposition and A-type stochastic interpretation in nonequilibrium processes*, Ruoshi Yuan, Ying Tang, Ping Ao Frontiers of Physics 12 (2017) 120201 ([click here](#))

To my knowledge, we were the first group to explicitly construct the "Hamiltonian" for limit cycles and chaotic attractors, thought not possible before our work. I would be happy to be updated on this, due to our limited knowledge.

My remark is that, our explicit construction for chaotic attractors revealed a hidden structure which may be useful for your construction, too.

My question is, is there a field theory constructed upon limit cycles?
Will be happy to receive your feedback.

4.4 A Lind zeta function for flip systems

Let G be a group, \mathcal{M} a set and $f : G \times \mathcal{M} \rightarrow \mathcal{M}$ a G -action on \mathcal{M} . The Lind zeta function [65] is defined by

$$\zeta_{Lind}(t) = \exp \left(\sum_H \frac{N_H}{|G/H|} t^{|G/H|} \right), \quad (4.137)$$

where the sum is over all finite-index subgroups H of G , such that $|G/H| < \infty$, and N_H is defined by (see (4.143)):

$$N_H = |\{x \in \mathcal{M} : \text{all } h \in H \quad f(h, x) = x\}|. \quad (4.138)$$



example 4.16
p. 279

A flip system (\mathcal{M}, f, s) is a dynamical system, where \mathcal{M} is a topological space and $f : \mathcal{M} \rightarrow \mathcal{M}$ is a homeomorphism. $s : \mathcal{M} \rightarrow \mathcal{M}$ is flip for (\mathcal{M}, f) that satisfy:

$$s \circ f \circ s = f^{-1} \quad \text{and} \quad s^2 = \mathbf{1}. \quad (4.139)$$

Kim *et al.* [58] showed that the zeta function ζ_s of a flip system (\mathcal{M}, f, s) can be defined as a Lind zeta function ζ_{Lind} of the D_∞ -action $f : D_\infty \times \mathcal{M} \rightarrow \mathcal{M}$ that is given by:

$$f(r, x) = f(x) \quad \text{and} \quad f(s, x) = s(x). \quad (4.140)$$

Every finite index subgroup of the infinite dihedral group D_∞ is either

$$H(n) = \langle r^n \rangle \quad \text{or} \quad H(n, k) = \langle r^n, r^k s \rangle, \quad (4.141)$$

with indices

$$|D_\infty/H(n)| = 2|n| \quad \text{or} \quad |D_\infty/H(n, k)| = |n|. \quad (4.142)$$

⁶

If n is a positive integer and k is an integer, then $N_{n,k}^s$ will denote the number of points in \mathcal{M} fixed by f^n and $f^k \circ s$:⁷

$$N_{n,k}^s = |\{x \in \mathcal{M} : f^n(x) = f^k \circ s(x) = x\}|. \quad (4.143)$$

They obtain⁸

$$\zeta_s(t) = \exp \left(\sum_{n=1}^{\infty} \frac{N_n}{2n} t^{2n} + \sum_{n=1}^{\infty} \sum_{k=0}^{n-1} \frac{N_{n,k}^s}{n} t^n \right). \quad (4.144)$$

⁶Han 2021-07-16: The infinite dihedral group D_∞ is the point group of a 1-dimensional Bravais lattice.

The subgroup $H(n)$ is a translation group of a sublattice of the 1-dimensional Bravais lattice.
The subgroup $H(n, k)$ is the symmetry group of a 1-dimensional lattice with a picture in the unit cell that is invariant under $s_k = sr^k$.

⁷Predrag 2021-07-04, 2021-08-25: our notation, replaced subscript f,s by noting.

⁸Predrag 2021-07-04: my own notation, replaced subscript f,s by superscript s .

The first sum factors as an Artin-Mazur zeta function (4.226):

$$\exp \left(\sum_{n=1}^{\infty} \frac{t^{2n}}{2n} N_n \right) = \sqrt{\zeta_{top}(t^2)} \quad (4.145)$$

The definition of a flip (4.143) tells us that

$$N_{n,k}^s = N_{n,k+n}^s = N_{n,k+2}^s \quad (4.146)$$

and this implies

$$N_{n,k}^s = \begin{cases} N_{n,0}^s & \text{if } n \text{ is odd,} \\ N_{n,0}^s & \text{if } n \text{ and } k \text{ are even,} \\ N_{n,1}^s & \text{if } n \text{ is even and } k \text{ is odd.} \end{cases} \quad (4.147)$$

Hence ⁹

$$\sum_{k=0}^{n-1} \frac{N_{n,k}^s}{n} = \begin{cases} N_{n,0}^s & \text{if } n \text{ is odd,} \\ \frac{N_{n,0}^s + N_{n,1}^s}{2} & \text{if } n \text{ is even.} \end{cases} \quad (4.148)$$

so the Lind zeta function of the flip triple system (\mathcal{M}, f, s) is

$$\zeta_s(t) = \sqrt{\zeta_{top}(t^2)} e^{h(t)}, \quad (4.149)$$

where ζ_{top} is the Artin-Mazur zeta function (4.226), and the counts of symmetric orbits

$$h(t) = \sum_{m=1}^{\infty} \left\{ N_{2m-1,0}^s t^{2m-1} + (N_{2m,0}^s + N_{2m,1}^s) \frac{t^{2m}}{2} \right\}. \quad (4.150)$$

they call the “generating function.”

The $\exp(h(t))$ in (4.149) can be factored into terms that presumably correspond –in the particular, Hénon case– to the $D_n N_n$ factors in (2.15), but this is now totally general, in the spirit of table 18.3, for any time-reversal discrete time dynamical system. Should be generalizable also to systems with continuous time.

⁹Han 2021-07-07: To understand $N_{n,k} = N_{n,k+2}$: Note that $rH_{n,k}r^{-1} = H_{n,k+2}$. Let x be a periodic point that is fixed by group $H_{n,k}$:

$$h \cdot x = x, \forall h \in H_{n,k}.$$

For simplicity here I denote $f(h, x)$ as $h \cdot x$. There is a periodic point $r \cdot x$ that is fixed by group $H_{n,k+2} = rH_{n,k}r^{-1}$:

$$rhr^{-1} r \cdot x = rh \cdot x = r \cdot x, \forall h \in H_{n,k}.$$

So the numbers of periodic points fixed by group $H_{n,k}$ and $H_{n,k+2}$ are equal.

The zeta function ζ_s can be written as a product over orbits. Let O_1 be the collection of finite orbits with time reversal (flip) symmetry, and O_2 be the collection of the pairs of orbits without time reversal symmetry, each an orbit and the flipped orbit. A finite orbit p is a periodic points set

$$p = \{x, f(x), \dots, f^{n_p-1}(x)\}$$

if $p \in O_1$, and

$$p = \{x, f(x), \dots, f^{k-1}(x)\} \cup \{s(x), f \circ s(x), \dots, f^{k-1} \circ s(x)\}$$

if $p \in O_2$, where $k = n_p/2$.

If $p \in O_1$,

$$\zeta_p(t) = \sqrt{\frac{1}{1-t^{2n_p}}} \exp\left(\frac{t^{n_p}}{1-t^{n_p}}\right), \quad (4.151)$$

and if $p \in O_2$,

$$\zeta_p(t) = \frac{1}{1-t^{n_p}}. \quad (4.152)$$

The product form of the zeta function is:

$$1/\zeta_s(t) = \sqrt{\prod_{p_1 \in O_1} (1-t^{2n_{p_1}})} \exp\left(-\frac{t^{n_{p_1}}}{1-t^{n_{p_1}}}\right) \prod_{p_2 \in O_2} (1-t^{n_{p_2}}). \quad (4.153)$$

4.4.1 Counting lattice states

Given the topological zeta function (4.144) we can count the number of fixed points from the generating function:

$$\frac{-t \frac{d}{dt} (1/\zeta_s(t))}{1/\zeta_s(t)} = \sum_{n=1}^{\infty} N_n t^{2n} + \sum_{n=1}^{\infty} \sum_{k=0}^{n-1} N_{n,k}^s t^n = \sum_{m=1}^{\infty} a_m t^m, \quad (4.154)$$

where the coefficients are:

$$a_m = \begin{cases} \sum_{k=0}^{m-1} N_{m,k}^s = m N_{m,0}^s, & m \text{ is odd}, \\ N_{m/2} + \sum_{k=0}^{m-1} N_{m,k}^s = N_{m/2} + \frac{m}{2} (N_{m,0}^s + N_{m,1}^s), & m \text{ is even}. \end{cases} \quad (4.155)$$

Using the product formula of topological zeta function (4.153) and the numbers of orbits with length up to 5 from the table 18.3, we can write the topological zeta function:

$$\begin{aligned} 1/\zeta_s(t) = & \sqrt{1-t^2} \exp\left(-\frac{t}{1-t}\right) (1-t^4) \exp\left(-\frac{2t^2}{1-t^2}\right) \left(\sqrt{1-t^6}\right)^3 \\ & \exp\left(-\frac{3t^3}{1-t^3}\right) (1-t^6)(1-t^8)^3 \exp\left(-\frac{6t^4}{1-t^4}\right) \\ & (1-t^8)^2(1-t^{10})^5 \exp\left(-\frac{10t^5}{1-t^5}\right) (1-t^{10})^6 \dots \end{aligned} \quad (4.156)$$

The generating function is:

$$\frac{-t \frac{d}{dt}(1/\zeta_s)}{1/\zeta_s} = t + 7t^2 + 12t^3 + 41t^4 + 55t^5 + \dots, \quad (4.157)$$

which is in agreement with (4.155), where the N_n and N_n^s are the C_n and SF_n in the table 18.3.

We are not able to retrieve the numbers of fixed points by their symmetry groups using this topological zeta function (4.144), unless we rewrite the topological zeta function with two variables:

$$\zeta_s(t, u) = \exp \left(\sum_{n=1}^{\infty} \frac{N_n}{2n} t^{2n} + \sum_{n=1}^{\infty} \sum_{k=0}^{n-1} \frac{N_{n,k}^s}{n} u^n \right). \quad (4.158)$$

Using this topological zeta function $\zeta_s(t, u)$ we can write two generating functions:

$$\frac{-t \frac{\partial}{\partial t}(1/\zeta_s(t, u))}{1/\zeta_s(t, u)} = \sum_{n=1}^{\infty} N_n t^{2n}, \quad (4.159)$$

and

$$\frac{-u \frac{\partial}{\partial u}(1/\zeta_s(t, u))}{1/\zeta_s(t, u)} = \sum_{n=1}^{\infty} \sum_{k=0}^{n-1} N_{n,k}^s u^n. \quad (4.160)$$

Using the product formula of this topological zeta function and the numbers of orbits with length up to 5 from the table 18.3, the topological zeta function is:

$$\begin{aligned} 1/\zeta_s(t, u) &= \sqrt{1-t^2} \exp \left(-\frac{u}{1-u} \right) (1-t^4) \exp \left(-\frac{2u^2}{1-u^2} \right) \left(\sqrt{1-t^6} \right)^3 \\ &\quad \exp \left(-\frac{3u^3}{1-u^3} \right) (1-t^6)(1-t^8)^3 \exp \left(-\frac{6u^4}{1-u^4} \right) \\ &\quad (1-t^8)^2(1-t^{10})^5 \exp \left(-\frac{10u^5}{1-u^5} \right) (1-t^{10})^6 \dots. \end{aligned} \quad (4.161)$$

And the generating function from this topological zeta function is:

$$\frac{-u \frac{\partial}{\partial u}(1/\zeta_s(t, u))}{1/\zeta_s(t, u)} = u + 6u^2 + 12u^3 + 36u^4 + 55u^5 + \dots, \quad (4.162)$$

which is in agreement with (4.160), where the N_n^s is the SF_n in the table 18.3.

4.5 Permutation representations

Burnside's *Table of marks*, whose rows are the orbit types, and the columns are the subgroups seems related to ChaosBook determinant factorizations.

Marks wiki: Much as character theory simplifies working with group representations, ‘marks’ simplify working with permutation representations and the Burnside ring (for the D_3 example, see (18.346)).

See also [ncatlab Table of marks](#). Possibly DOI contains the tables we might want to use.

GAP is an amazing system for computational discrete algebra. In particular, it computes [tables of marks](#).

[Permutation representations wiki](#):

Associated to a lattice state X is a vector space with the X lattice sites as the basis. An action of a finite group G on X induces a linear action on this vector space, called a *permutation representation*.

$H \subseteq G$ is a subgroup of G .

The table of marks of the group G is computed from the *lattice of subgroups* of G .

The *mark* of H on X is the number of elements of X that are fixed by every element of H : $m_X(H) = |X^H|$, where

$$X^H = \{x \in X \mid h \cdot x = x, \forall h \in H\}.$$

If H and K are conjugate subgroups, then $m_X(H) = m_X(K)$ for any finite G -set X ; indeed, if $K = gHg^{-1}$ then $X^K = gX^H$.

Let $G_1 = \mathbf{1}, G_2, \dots, G_N = G$ be representatives of the N conjugacy classes of subgroups of G , ordered in such a way that whenever G_i is conjugate to a subgroup of G_j , then $i \leq j$. Now define the $[N \times N]$ table (square matrix) whose (i, j) th entry is $m(G_i, G_j)$. This matrix is lower triangular, and the elements on the diagonal are non-zero so it is invertible.

The table of marks (Burnside matrix) entries are the number of elements in the orbit G/K fixed by the subgroup H .

The first column is the degree of the representation. The bottom row is 1’s because G/G is a single point. The diagonal terms are (CONTINUE)

D_3 table of marks is given in table 4.3, and D_6 table of marks in table 18.4. Corresponding sets of lattice states are given by Burnside rings (18.346) and (18.350)

Theorem (Burnside 1897): If X is a G -set, and $u_i = m_X(G_i)$ its row vector of marks, then X decomposes as a disjoint union of a_i copies of the orbit of type G_i , where the vector a satisfies (18.348)

$$\mathbf{a}M = \mathbf{u}, \tag{4.163}$$

and M is the matrix of the table of marks.

2021-06-27 Predrag Study example 4.30 discussion of the D_3 symmetry: compact and elegant.

Table 4.3: D_3 table of marks, from [Montaldi](#). For D_6 see table 18.4.

D_3	$\mathbf{1}$	D_2	C_3	D_3
$D_3/\mathbf{1}$	6			
D_3/D_2	3	1		
D_3/C_3	2	0	2	
D_3/D_3	1	1	1	1

D_3 permutation representation on the

- 3 vertices of an equilateral triangle is $A_0 + E$

D_4 permutation representation on the

- 4 vertices of the square is $A_0 + B_1 + E$
- not used: 4 edges of the square is $A_0 + B_2 + E$
- not used: 2 diagonals of the square is $A_0 + A_1$

D_5 permutation representation on the

- 5 vertices of the pentagon is $A_0 + E_1 + E_2$

D_6 permutation representation on the

- 6 vertices of the hexagon is $A_0 + B_1 + E_1 + E_2$
- not used: 3 diagonals joining opposite vertices of the hexagon is $A_0 + E_2$

 Table 4.4: D_n permutation representation irreps (from [J. Montaldi](#)).

2021-06-21 Predrag Montaldi discussion of D_3 is instructive.

In agreement with our results, his D_3 *permutation representation* is

$$D_3 : \quad A_0 + E, \tag{4.164}$$

see for example figure 3.6.

His “orientation permutation” representation on the set of 3 edges of the triangle, is $A_1 + E$. I do not think we use that representation.

Montaldi *Product structure in Burnside Ring* seems to be a variant of the class operators multiplication tables.

2021-06-21 Predrag James Montaldi has a cute overview of the D_2 to D_6 irreps.

Our fields ϕ_t are defined on n lattice sites, not on links

Dihedral irrep:

2021-06-21 Predrag Character tables in physics and chemistry use the *Mulliken symbols* as the representations names, such as A_1 or T_{2g} . Montaldi adheres to that notation, except that he denotes the trivial representation by A_0 rather than A_1 .

Montaldi *Notes on circulant matrices* (2012) are very pedagogical. He discusses (as we do, calling this the permutation rep) the representation theory of the cyclic group (or dihedral group in the symmetric case) acting on \mathbb{R}^n .

For each $\ell = 1, \dots, [(n-1)/2]$ let A_ℓ be the irreducible 1-dimensional real representation of D_n : let the rotation r act by rotation through $2\pi\ell/n$ and let s act by a reflection (this is independent of the choice of reflection as any two reflections are conjugate, and the resulting irreps equivalent).

Here $[q]$ denotes the greatest integer less than or equal to q .

A_0 is the trivial rep and if n is even, $A_n/2$ is the 1-dimensional rep where r and s act by multiplication by -1. These irreducible representations are also irreps for the cyclic group C_n (ignoring s). The real 1-dimensional reps E_r are irreducible but not absolutely irreducible, and their complexification splits as a sum of two 1-d reps.

Proposition 1 The above (permutation) representation decomposes as a sum of irreps:

$$A_0 \oplus A_1 \cdots \oplus A_{n/2} \quad (4.165)$$

This is called the *isotypic decomposition* of \mathbb{R}^n for this action (or representation).

The eigenvectors of M are the same for any circulant matrix M . Define the vectors $u^{(\ell)}, v^{(\ell)} \in \mathbb{R}^n$, with components

$$u_j^{(\ell)} = \cos(2\pi j\ell/n), \quad v_j^{(\ell)} = \sin(2\pi j\ell/n). \quad (4.166)$$

Note that $u^{(n-\ell)} = u^{(\ell)}$ and $v^{(n-\ell)} = -v^{(\ell)}$. In particular, $v^{(0)} = 0$ and if n is even then $v^{(n/2)} = 0$. There is therefore a total of n linearly independent vectors

$$u^{(\ell)} \quad (\ell = 0, \dots, \left[\frac{n}{2} \right]) \text{ and } v^{(\ell)} \quad (\ell = 1, \dots, \left[\frac{n-1}{2} \right]). \quad (4.167)$$

They form a basis for \mathbb{R}^n (there is more complex components detail in Montaldi notes).

In particular, $u^{(0)} = (1, 1 \cdots, 1)^\top$ and $u^{(n/2)} = (1, -1, 1 \dots, -1)^\top$ (the latter if n is even) are real eigenvectors.

Proposition 2 The component A_ℓ is spanned by the vectors u_ℓ, v_ℓ .

Proposition 3 A matrix M is circulant iff it commutes with the action of C_n , and it is symmetric and circulant iff it commutes with D_n . λ_0 and (if n is even) $\lambda_{n/2}$ are simple, while the other λ_ℓ are double eigenvalues.

2021-06-27 Predrag The *markaracter table* of a finite group was introduced by Shinsaku Fujita.

2021-07-04 Predrag For a bit of history, see J. E. Humphreys review of [Pioneers of representation theory](#).

2021-07-07 Predrag Dirac characters (Harter's central operators, see [Harter's Sect. 3.2 First stage of non-Abelian symmetry analysis](#)) were introduced by Dirac [31] in *The Principles of Quantum Mechanics* (1930) ([click here](#)): "[...]" what is called in group theory a character of the group of permutations."

Corson [24] *Note on the Dirac character operators* (1948) writes:

[...] the evaluation of Dirac and similar character operators is all that is required for the solution of the standard molecular problems in the spirit of Dirac's original program which avoids appeal to formal group theory.

Dirac characters (??) use not only the abstract group information, but also account for the symmetry information contained in the basis set used. The diagonalization of Dirac characters has three main advantages:

1. It can be realized by means of a quite simple and general algorithm.
2. The projective irreps obtained are just the ones that are needed to reduce the starting basis set into irreducible sets.
3. No tabulated quantities are required to construct the projective irreps.

The scheme is completely general, in the sense that it applies to all space groups.

Cini and Stefanucci [22] *Antiferromagnetism of the two-dimensional Hubbard model at half-filling: The analytic ground state for weak coupling*, [arXiv:cond-mat/0009058](#), uses Dirac characters to diagonalize a square integer $[N \times N]$ lattice with D_4 symmetry. Might help us with the temporal cat desymmetrization.

Cini [21] *Topics and Methods in Condensed Matter Theory* (2007) ([click here](#))

Jacobs [53] *Group Theory with Applications in Chemical Physics*, ([click here](#)) (2005)

El-Batanouny and Wooten [13] *Symmetry and Condensed Matter Physics: A Computational Approach* (2008) ([click here](#)). In sect. 4.3 they describe the Burnside's method. They give an example of Mathematica code that constructs the character table. If needed, one might use Dixon's method, which is more clever for numerical computations.

Big Chemical Encyclopedia, [Dirac character](#)

The [CRYSTAL](#) package performs ab initio calculations of the ground state energy, energy gradient, electronic wave function and properties of periodic systems. Uses Dirac characters.

CHAPTER 4. GROUP THEORY

2021-07-08 Predrag Ananda Dasgupta had 1.68K followers on YouTube, now he has one more.

▶ playlist for his *Symmetries in Physics* course:

▶ *Lecture 15* (start at about 35 min into the lecture) has a nice discussion of Dirac characters, their relation to characters, and motivates the algorithmic Burnside's method for computing characters via class multiplication tables $(H_i)_{jk}$.

example 4.22

▶ *PH4213 Discussion Class 8* applies Burnside's method to D_4 .

Less interesting, but anyway, you might learn something:

▶ *PH4213 Discussion Class 9* gets projection operators out of characters.

▶ *Lecture 16* Projection operators, the Wigner-Eckart theorem.

A discussion from the Group Theory course:

Sect. 2.10 What are cosets good for?

Henriette Roux asks: What are cosets good for? Apologies for glossing over their meaning in the lecture. I try to minimize group-theory jargon, but cosets cannot be ignored.

Dresselhaus *et al.* [37] ([click here](#)) Chapter 1 *Basic Mathematical Background: Introduction* needs them to show that the dimension of a subgroup is a divisor of the dimension of the group. For example, C_3 of dimension 3 is a subgroup of D_3 of dimension 6.

In [ChaosBook Chapter 10. Flips, slides and turns](#) cosets are absolutely essential. The significance of the coset is that if a lattice state has a symmetry, then the elements in a coset act on the lattice state the same way, and generate all equivalent copies of this lattice state. Example 10.7. *Subgroups, cosets of D_3* should help you understand that.

Henriette Roux writes: When talking about the cosets of a subgroup we demonstrated multiplication between cosets with a specific example, but this wasn't leading to something along the lines of that the set of all left cosets of a subgroup (or the set of all the right cosets of a subgroup) form a group, correct? It didn't appear so in the example since the "unit" $\{E, A\}$ we looked appears to only have the properties of an identity with multiplication from one direction (the direction depending on if it is the set of left cosets or the set of right cosets). In the context of the lecture I think this point was related to Lagrange's theorem (although we didn't call it that) and I vaguely remember cosets being used in the proof of Lagrange's theorem but I wasn't connecting it today. Are we going to cover that in a future lecture?

Predrag You are right - Lagrange's theorem (see the [wiki](#)) simply says the order of a subgroup has to be a divisor of the order of the group. We used cosets to partition elements of G to prove that. But what we really need

cosets for is to define (see Dresselhaus *et al.* [37] Sect. 1.7) *Factor Groups* whose elements are cosets of a self-conjugate subgroup ([click here](#)). I will not cover that in a subsequent lecture, so please read up on it yourself.

Henriette Roux You talked about the period of an element X , and said that that *period* is the set

$$\{E, X, \dots, X^{n-1}\}, \quad (4.168)$$

where n is the *order* of the element X . I had thought that set was the subgroup generated by the element X and that the period of the element X was a synonym for the order of the element X ? Is that incorrect?

2CB

Predrag To keep things as simple as possible, in Thursday's lecture I followed Sect. 1.3 *Basic Definitions* of Dresselhaus *et al.* textbook [37], to the letter. In Def. 3 the *order* of an element X is the smallest n such that $X^n = E$, and they call the set (4.168) the *period* of X . I do not like that usage (and do not remember seeing it anywhere else). As you would do, in ChaosBook.org Chap. *Flips, slides and turns* I also define the smallest n to be the *period* of X and refer to the set (4.168) as the *orbit* generated by X . When we get to compact continuous groups, the orbit will be a (great) circle generated by a given Lie algebra element, and look more like what we usually think of as an orbit.

I am not using my own [ChaosBook.org](#) here, not to confuse things further by discussing both time evolution and its discrete symmetries. Here we focus on the discrete group only (typically spatial reflections and finite angle rotations).

- o Sect. 4.6 *Reduction to the reciprocal lattice*
- o See (5.197) for Dudgeon and Mersereau [38] explaining clearly how to get the “quotient” Q when “dividing” by P . $|\det \Lambda|/|\det Q| = |\det P|$ is then the number of cosets.

 Canals and Schober [18] *Introduction to group theory*. It is very concise and precise, a bastard child of Bourbaki and Hamermesh [49]. Space groups show up only once, on p. 24: “By working with the cosets we have effectively factored out the translational part of the problem.”

4.6 Reduction to the reciprocal lattice

My Phys 7143 zipped! World Wide Quest to Tame Group Theory course notes [are here](#).

[/birdtracks.eu Sect. 8.2.2](#), here copied as sect. ?? *One-dimensional line groups*

Gutkin [lecture notes](#) Lecture 7 *Applications III. Energy Band Structure*, Sects. 1. *Lattice symmetries* and 2. *Band structure*. Also good reads: Dresselhaus *et al.* [37] ([click here](#)) chapter 9. *Space Groups in Real Space*, and Cornwell [23] ([click here](#))

CHAPTER 4. GROUP THEORY

chapter 7. *Crystallographic Space Groups*. Walt De Heer learned this stuff from Herzberg [52] *Molecular Spectra and Molecular Structure*. Condensed matter people like Kittel [59] *Introduction to Solid State Physics*, but I am not a fan, because simple group theoretical facts are there presented as solid state phenomena. Quinn and Yi [77] *Solid State Physics: Principles and Modern Applications* introduction to space groups looks compact and sensible.

Martin Mourigal found the Presqu'ile Giens, May 2009 *Contribution of Symmetries in Condensed Matter Summer School* very useful. Villain [91] *Symmetry and group theory throughout physics* gives a readable overview. The overheads are [here](#), many of them are of potential interest. Mourigal recommends Ballou [11] *An introduction to the linear representations of finite groups* appears rather formal (and very erudite). Grenier, B. and Ballou [47] *Crystallography: Symmetry groups and group representations*.

Schober [84] *Symmetry characterization of electrons and lattice excitations* gives an eminently readable discussion of space groups.

Rodríguez-Carvajal and Bourée [81] *Symmetry and magnetic structures*

Schweizer [85] *Conjugation and co-representation analysis of magnetic structures* deals with black, white and gray groups that Martin tries not to deal with, so all Mourigal groups are gray.

If you are curious about graphene, work out Gutkin [lecture notes](#) Lecture 7 *Applications III. Energy Band Structure, Sect. 7.3 Band structure of graphene*. Villain discusses graphene in the Appendix A of *Symmetry and group theory*

The symmetry is C_n , and one needs to distinguish C_n orbits ("prime cycles" in ChaosBook; one per each orbit). The right way to do this is by going to C_n irreps, ie, by the discrete Fourier transform, with all reciprocal lattice Brillouin zone solutions orbits in an $1/n$ sliver of a n -gon. If n is prime, this is irreducible; if it is a multiple of a prime, one should remove those solutions, as they have already been accounted for.

The translation group T , the set of translations \vec{t} that put the crystallographic structure in coincidence with itself, constitutes the *lattice*. T is a normal subgroup of G . It defines the *Bravais lattice*. In 1 dimension translations are of the form

$$\vec{t} = \vec{t}_{\vec{n}} = n\vec{a}, \quad n \in \mathbb{Z}.$$

The basis vector \vec{a} spans the *unit cell*. The lattice unit cell is always a *generating region* (a tile that tiles the entire space), but the smallest generating region –the *fundamental domain*– may be smaller than the lattice unit. At each lattice point the identical group of "atoms" constitutes the *motif*. A *primitive cell* is a minimal region repeated by lattice translations. The lattice and the motif completely characterize the crystal.

The cosets by translation subgroup T (the set all translations) form the *factor* (AKA *quotient*) group G/T , isomorphic to the point group g (rotations). All irreducible representations of a space group G can be constructed from irreducible representations of g and T . This step, however, is tricky, as, due to

the non-commutativity of translations and rotations, the quotient group G/T is not a normal subgroup of the space group G .

The quantum-mechanical calculations are executed by approximating the infinite crystal by a periodic one, and going to the *reciprocal* space by deploying C_N discrete Fourier transform. This implements the G/T quotienting by translations and reduces the calculation to a finite *Brillouin zone*. That is the content of the '*Bloch theorem*' of solid state physics. Further work is then required to reduce the calculations to the point group irreps.

One would think that the one-dimensional *line groups*, which describe systems exhibiting translational periodicity along a line, such as carbon nanotubes, would be simpler still. But even they are not trivial – there are 13 of them.

The normal subgroup of a line group L is its translational subgroup T , with its factor group L/T isomorphic to the *isogonal point group* P of discrete symmetries of its 1-dimensional unit cell $x \in (-a/2, a/2]$. In the reciprocal lattice k takes on the values in the first Brillouin zone interval $(-\pi/a, \pi/a]$. In *Irreducible representations of the symmetry groups of polymer molecules. I*, Božović, Vujičić and Herbut [16] construct all the reps of the line groups whose isogonal point groups are C_n , C_{nv} , C_{nh} , S_{2n} , and D_n . For some of these line groups the irreps are obtained as products of the reps of the translational subgroup and the irreps of the isogonal point group.

According to W. De Heer, the Mintmire, Dunlap and White [72] paper *Are Fullerene tubules metallic?* which took care of chiral rotations for nanotubes by a tight-binding calculation, played a key role in physicists' understanding of line groups.

Consequences of time-reversal symmetry on line groups are discussed by Božović [15]; In the case when the Hamiltonian is invariant under time reversal [51], the symmetry group is enlarged: $L + \theta L$. It is interesting to learn if the degeneracy of the levels is doubled or not.

Johnston [55] *Group theory in solid state physics* is one of the many reviews that discusses Wigner's time-reversal theorems for a many-electron system, including the character tests for time-reversal degeneracy, the double space groups, and the time-reversal theorems (first discussed by Herring [51] in *Effect of time-reversal symmetry on energy bands of crystals*).

Consider

$$\rho_{\vec{G}}(\vec{x}) = e^{i\vec{G} \cdot \vec{r}(\vec{x})},$$

where \vec{G} is a reciprocal lattice vector. By definition, $\vec{G} \cdot \vec{a}$ is an integer multiple of 2π , $\rho_{\vec{G}} = 1$ for lattice vectors. For any other state, reciprocal lattice state is given by

$$e^{i\vec{G} \cdot \vec{u}(\vec{x})} \neq 1.$$

When a cube is a building block that tiles a 3D cubic lattice, it is referred to as the 'elementary' or 'Wigner-Seitz' cell, and its Fourier transform is called 'the first Brillouin zone' in 'the reciprocal space'.

2018-03-18 Predrag Check sect. 18.2.1 *Reduction to the reciprocal lattice* for possibly useful material.

2018-05-22 Han For the Fourier transform of all the admissible period-5 see figure 18.35. For a 1-dimensional lattice with lattice spacing 1, the reciprocal lattice has spacing $2\pi/1 = 2\pi$, with the (first) Brillouin zone from $k = -\pi$ to $k = \pi$. Due to the time reversal, all $k = 2\pi/5$ irrep states are the same as the $k = 4\pi/5$ irrep states.

2018-04-18 Predrag I would expect the time-reversal pairs to be the complex-conjugate pairs in Fourier space, as C_4 shift moves them in opposite directions.

2020-01-10 Predrag A very pedagogical, down to earth textbook: Pozrikidis [75] *An introduction to grids, graphs, and networks*, ([click here](#)).

He discusses Sect 2.6.1 *Bravais Lattices*, the reciprocal lattice, the discrete Brillouin zone or Wigner-Seitz cell.

2020-01-23 Predrag Barvinok [arXiv:/math/0504444](#):

Let V be a d -dimensional real vector space with the scalar product $\langle \cdot, \cdot \rangle$ and the corresponding Euclidean norm $\|\cdot\|$. Let $\mathcal{L} \subset V$ be a lattice and let $\mathcal{L}^* \subset V$ be the *dual* or the *reciprocal* lattice

$$\mathcal{L}^* = \left\{ x \in V : \quad \langle x, y \rangle \in \mathbb{Z} \quad \text{for all } y \in \mathcal{L} \right\}.$$

For $\tau > 0$, we introduce the *theta function*

$$\begin{aligned} \theta_{\mathcal{L}}(x, \tau) &= \tau^{d/2} \sum_{m \in \mathcal{L}} \exp \left\{ -\pi \tau \|x - m\|^2 \right\} \\ &= (\det \mathcal{L})^{-1} \sum_{l \in \mathcal{L}^*} \exp \left\{ -\pi \|l\|^2 / \tau + 2\pi i \langle l, x \rangle \right\}, \end{aligned} \quad (4.169)$$

where $x \in V$. The last equality is the reciprocity relation for theta series (essentially, the Poisson summation formula).

2021-02-27 Sidney Figure 15.1 shows all Hamiltonian Hénon (2.11), $a = 6$ lattice states of period $n = 6$, in the C_6 reciprocal lattice.

Compare with Han's figure 18.60.

4.7 Dynamical symmetry factorization

Here we shall distinguish "geometrical symmetry" (invariance of a shape of an object under coordinate translations, reflections, and rotations).

Physical Symmetry *vs.* Symmetry

A dynamical symmetry is often a *hidden* symmetry. The classic example would be the Hydrogen atom. Naively, we would only expect an $SO(3)$ symmetry associated with rotational symmetry. This would be the geometrical symmetry, which leads to the conserved angular momentum vector. In fact,

the full symmetry of the system is SO(4); this is exhibited by there being another conserved vector, the Laplace-Runge-Lenz (LRL) vector. Since the LRL vector is peculiar to the particular potential of the hydrogen atom and does not emerge as the result of some general geometrical feature shared by a whole class of systems (like rotational symmetry), it is referred to as a *dynamical symmetry*.

Noether?

the symmetry of a particular figure or lattice in a two- or three-dimensional Euclidean space is defined by a subgroup of the group of all translations, rotations, reflections and inversions — the subgroup that converts the object into itself.

Associated with each geometric object is the set of symmetry operations that leave invariant the relation between the object and a coordinate system. These conceptions of symmetry and operations of symmetry have their basis in Euclidean geometry.

Symmetry in physics means invariance under any kind of transformation, for example arbitrary coordinate transformations.

The invariance group of an equation is an intrinsic property of the equation.

To avoid this problem, we will henceforth use the words intrinsic symmetry and intrinsic symmetry groups when speaking of invariance properties of equations and functions. If functions or equations are left invariant by the operations of a group of transformations, the group will be said to be an intrinsic symmetry group of the functions or equations.

The hyperspherical symmetry of Kepler Hamiltonians is a truly dynamical symmetry — a symmetry present when there is motion. It is a symmetry that exists only when motion is allowed.

The phrase hidden symmetry is sometimes used to signify the presence of dynamical symmetry greater than ordinary geometrical symmetry.

Note; we do not know yet how this section relates to sect. 4.2.1 *Laplacians and (time) reversal*.

4.7.1 Dynamical symmetry blog

2016-11-16 Predrag Note that [3] the canonical Thom-Arnol'd cat map (1.1) can be written as

$$\begin{bmatrix} 2 & 1 \\ 1 & 1 \end{bmatrix} = \begin{bmatrix} 1 & 1 \\ 1 & 0 \end{bmatrix}^2, \quad (4.170)$$

so each of equivalence classes with respect to centralizer is split into two equivalence classes with respect to the group $\{\pm A^n \mid n \in \mathbb{Z}\}$. (See also (4.174).)

Jaidee, Moss and Ward [54] *Time-changes preserving zeta functions* say that

$$N_n = \text{tr} \begin{bmatrix} 1 & 1 \\ 1 & 0 \end{bmatrix}^n, \quad (4.171)$$

is a ‘golden mean’ system, and N_n is the n th Lucas number $(1, 3, 4, 7, 11, \dots)$, with zeta function

$$\frac{1}{\tilde{\zeta}(t)} = 1 - t - t^2, \quad (4.172)$$

(compare with (4.181)).

2016-11-16 Predrag Maillard group, Anglès d’Auriac, Boukraa and Maillard [2] *Functional relations in lattice statistical mechanics, enumerative combinatorics, and discrete dynamical systems* note that (see (4.170), (1.2))

$$A = \begin{pmatrix} 2 & 1 \\ 1 & 1 \end{pmatrix} = \begin{pmatrix} 1 & 1 \\ 1 & 0 \end{pmatrix}^2 = C^2. \quad (4.173)$$

Anosov, Klimenko and Kolutsky [3] say: “so each of equivalence classes with respect to centralizer is split into two equivalence classes with respect to the group $\{\pm A^n \mid n \in \mathbb{Z}\}$.“ (whatever that means)

Factorization

$$\det(1 - tC) \det(1 + tC) = \det(1 - zC^2) \quad (4.174)$$

leads then to (4.183) (see (1.30), (1.20), (13.74); here corrected by Han (4.183))

2020-09-30 Predrag (I have no generalization guess of (4.174) yet.)

The Yukawa massive field mass parameter is related to the spatiotemporal cat stretching parameter s by (5.27)

$$\mu^2 = d(s - 2). \quad (4.175)$$

Observe that

$$\begin{aligned} \left(1 - \frac{t^2}{\mu^2}\right)^2 - t^2 &= 1 - sz + z^2, \quad t^2 = \mu^2 z \\ &= \left(1 - t - \frac{t^2}{\mu^2}\right) \left(1 + t - \frac{t^2}{\mu^2}\right) \\ (\mu^2 - t^2)^2 - \mu^4 t^2 &= \mu^4(1 - sz + z^2) \\ &= (\mu^2(1 - t) - t^2)(\mu^2(1 + t) - t^2) \\ \frac{(\mu^2 - t^2)^2}{\mu^4} &= (1 - z)^2, \end{aligned} \quad (4.176)$$

so Predrag gets (see (4.183)) time-reflection factorized $1/\tilde{\zeta}(t)$.

$$\begin{aligned} \frac{1}{\zeta(z)} &= \frac{1 - sz + z^2}{(1 - z)^2} = \frac{1}{\zeta_{A_1}(t)} \frac{1}{\zeta_{A_1}(-t)} \\ \frac{1}{\zeta_{A_1}(t)} &= \frac{\mu^2(1 - t) - t^2}{\mu^2 - t^2} = 1 - \frac{\mu^2 t}{\mu^2 - t^2}. \end{aligned} \quad (4.177)$$

The antisymmetric A_2 subspace dynamical zeta function ζ_{A_2} differs from ζ_{A_1} only by a minus sign for cycles with an odd number of 0's, see (4.270). This is presumably the same as metal cat map zeta (4.45) except here I chose to count the symmetry-reduced cycles by the $t = \sqrt{\mu^2 - z}$ expansion. I suspect that the factorization (5.252) is another example of such factorization, but for a cubic lattice.

2020-10-31 Predrag Note that time-reversal factorization of zeta functions naturally leads to formulas in terms of the mass $\mu = \sqrt{s - 2}$, see (4.43) and (4.59).

2020-11-06 Han

$$\frac{1}{\zeta(z)} = \frac{\det(1 - zA)}{\det(1 - zB)}, \quad B = \begin{pmatrix} 1 & 0 \\ 0 & 1 \end{pmatrix}.$$

Using the factorization:

$$\det(1 - tB) \det(1 + tB) = \det(1 - zB)$$

we have (4.183).

2020-12-09, 2020-12-11 Predrag Reread the “quotienting the temporal Bernoulli system” (1.85) by its *dynamical* $D_1 = \{e, s\}$ symmetry (1.86); figure 1.17.

2020-12-29 Predrag Temporal cat *dynamical* $D_1 = \{e, s\}$ symmetry is (18.286)

$$sx_t = 1 - xt, \quad ss_t = \mu^2 - st, \quad \text{for all } t \in \mathbb{Z}, \quad (4.178)$$

where s_t takes values in the s -letter alphabet (18.285).

2021-01-13 Han The factorization of (4.183) can be interpreted as the product of the topological zeta function of a half time step cat map, see (18.290) and what follows.

2017-09-27, 2021-02-03 Predrag reading Baake, Roberts and Weiss [10] *Periodic orbits of linear endomorphisms on the 2-torus and its lattices* arXiv:0808.3489, see sect. 4.3.2:

They discuss zeta functions of toral automorphisms, see their Table 1. Fixed point and orbit counts for the golden cat map. Example 2 is amusing:

The best known hyperbolic toral automorphism is the ‘classic’ or golden (Fibonacci [8]) cat map (see also (5.233))

$$M = \begin{pmatrix} 0 & 1 \\ 1 & 1 \end{pmatrix}. \quad (4.179)$$

It has $\det(M) = -1$ and is thus orientation reversing (sometimes, as in ref. [56], its square is used instead). One obtains

$$\zeta_M(t) = \frac{1 - t^2}{1 - t - t^2} = \prod_{m \geq 1} (1 - t^m)^{-c_m}$$

with $a_m = f_{m+1} + f_{m-1} - (1 + (-1)^m)$ and c_m according to Eq. (4.114), see also entries A001350 and A060280. Here, f_m are the Fibonacci numbers, defined by the recursion $f_{m+1} = f_m + f_{m-1}$, for $m \geq 0$, together with the initial condition $f_0 = 0$ and $f_{-1} = 1$. The first few terms of the counts are given in table 4.2. Note that $\zeta_M(t) = 1 + \sum_{m=0}^{\infty} f_m t^m$, and one has $M^m = f_m M + f_{m-1} \mathbf{1}$, the latter being valid for all $m \in \mathbb{Z}$.

2021-02-12 Han By derivation ([do it!](#)) analogous to the Isola's cat map $\zeta(Z)$ (1.30), the topological zeta function for metal cat maps is (4.45) where $z = t^2$, in agreement with (4.181) for $\mu = 1$. See also (5.233).

2021-02-12 Predrag What is this square root of z ? This is expected, see [Chaos-Book sect. 25.5](#) $Z_2 = D_1$ factorization: [...] if a cycle p is invariant under the symmetry subgroup $\mathcal{H}_p \subseteq G$ of order h_p , its weight can be written as a repetition of a fundamental domain cycle

$$t_p = t_{\hat{p}}^{h_p} \quad (4.180)$$

computed on the irreducible segment that corresponds to a fundamental domain cycle. [...] In the D_1 case, t_p is a orbit, or a double repeat of a orbit, $t_p = t_{\hat{p}}^2$, hence the square root.

For the $\mu = 1$ golden (Fibonacci [8]) cat zeta function (18.291) or (4.183) or [54] (4.172):

$$\frac{1}{\tilde{\zeta}(t)} = \frac{1-t-t^2}{(1-t)^2}, \quad (4.181)$$

\tilde{N}_n , the number of *lattice states* of period n is given by the logarithmic derivative of the golden cat zeta function (3.185),

$$\begin{aligned} \sum_{n=1} \tilde{N}_n t^n &= -\tilde{\zeta} t \frac{d}{dt} \frac{1}{\tilde{\zeta}} \\ &= t + t^2 + 4t^3 + 5t^4 + 11t^5 + 16t^6 + 29t^7 \\ &\quad + 45t^8 + 76t^9 + 121t^{10} + 199t^{11} + \dots \end{aligned} \quad (4.182)$$

So this is the golden (Fibonacci [8]) cat map count, table 4.2 of Baake *et al.* [10] *Periodic orbits of linear endomorphisms on the 2-torus and its lattices*. It is also the number of walks on Han's reduced Markov diagram, figure 4.2.

$$\frac{1}{\zeta(z)} = \frac{1}{\tilde{\zeta}(t)\tilde{\zeta}(-t)} = \frac{1-t-t^2}{(1-t)^2} \cdot \frac{1+t-t^2}{(1+t)^2} = \frac{1-3z+z^2}{(1-z)^2}, \quad (4.183)$$

where $z = t^2$.

2021-04-03 Predrag The temporal Hénon (2.20) is a 3-term recurrence relation of form (2.44)

$$\phi_{i+1} + \phi_i^2 + \phi_{i-1} = a, \quad i = 1, \dots, n_p. \quad (4.184)$$

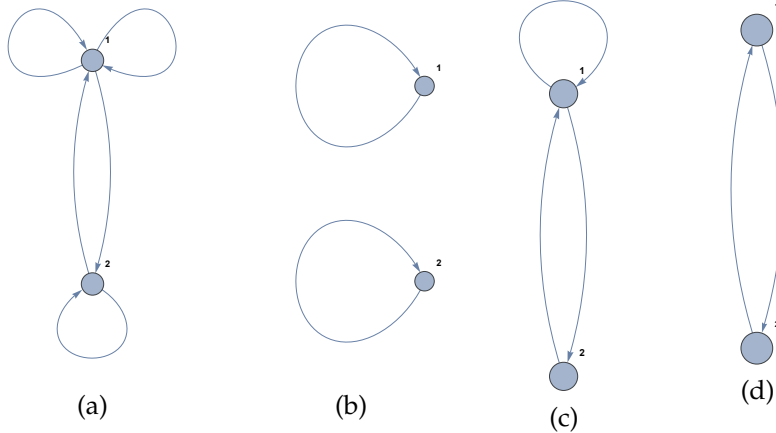


Figure 4.2: (a), (b), (c) and (d) are the Markov diagrams corresponding to the transition matrices A , B , A' and B' . We can get (a) and (b) by mapping (c) and (d) two time steps forward. $1/\zeta(z)$ is the topological zeta function of the Markov diagram (a) with periodic orbits in (b) eliminated. $1/\tilde{\zeta}(t)$ is the topological zeta function of the Markov diagram (c) with periodic orbits in (d) eliminated.

4.8 Symmetry factorization blog

For the latest entry, go to the bottom of this section

2018-09-02 Predrag Miles [71] *A dynamical zeta function for group actions*, [arXiv:1506.08555](https://arxiv.org/abs/1506.08555): “ introduces and investigates the basic features of a dynamical zeta function for group actions, motivated by the classical dynamical zeta function of a single transformation. A product formula for the dynamical zeta function is established that highlights a crucial link between this function and the zeta function of the acting group.

The zeta function of a dynamical system is a fundamental invariant that has warranted considerable attention since the definitive work of Artin and Mazur [4]. Ruelle [82] provides an introduction to various guises of this function, and Sharp [86] (seems to be lacking from [here](#)) provides a comprehensive survey by in the context of periodic orbits of hyperbolic flows. ”

“ The relevance of the dynamical zeta function in questions of orbit growth is also considered. ”

2020-09-24, 2020-12-16 Predrag to Robert S. MacKay (see discussion around (6.4))
My thoughts in that directions (that is in my temporal cat talk, and in this

blog, see (5.248), (13.70), (13.73), (13.84)) are that for the 1-dimensional temporal cat [29, 48]

$$x_{n,t+1} + x_{n,t-1} - 2s x_t + x_{n+1,t} + x_{n-1,t} = -s_t, \quad s_t \in \mathcal{A}, \quad (4.185)$$

with alphabet

$$\mathcal{A} = \{-3, -2, -1, 0, \dots, \mu^2 + 1, \mu^2 + 2, \mu^2 + 3\}, \quad (4.186)$$

and the Yukawa mass squared of the scalar field x

$$\mu^2 = 2(s - 2). \quad (4.187)$$

The ζ function has to satisfy all spatiotemporal symmetries of the square lattice

$$D_4 = \{1, r, r^2, r^3, s, s_1, s_2, s_3, \}. \quad (4.188)$$

See [ChaosBook sect. A25.1](#).

In the international crystallographic notation, this square lattice space point group is referred to as $p4mm$ [37].

2CB

2019-01-28 Predrag Useful wikis:

[Dihedral group \$D_4\$](#)

[Wolfram Demonstrations](#):

[Dihedral Group n of Order 2n](#)

[Cosine and Sine Identities with Dihedral Transformations](#)

[The symmetry group of a square](#): I find their “different Cayley graph” interesting: here D_4 is generated by a horizontal (short axis) reflection, and a diagonal (long axis) reflection, rather than the usual (r, s) set.

[Linear representation theory of dihedral groups](#) summarizes everything worth knowing:

2021-01-08 Predrag taken from [ChaosBook remark 11.2: Examples of systems with discrete symmetries](#).

$D_2 = C_{2v} = V_4 = Z_2 \times Z_2$ symmetry in the stadium billiard [79]. Cvitanović, Davidchack and Siminos [27] [eq. \(2.13\)](#)

See [ChaosBook sect. A25.2](#).

$D_4 = C_{4v}$ symmetry: in quartic oscillators [39, 69], in the pure x^2y^2 potential [19, 70] and in hydrogen in a magnetic field [41].

D_n symmetry: see [Ding thesis example 2.9](#).

Pdflatex `siminos/lyapunov/blog.tex`, read sect. 7.11.2 *Factorization of C_n and D_n* .

2020-12-20 Predrag This square lattice symmetry group is the space group $p4mm$, with point group D_4 (4.188), so all calculations should be carried out on the reciprocal lattice, with a 1/8th of a square Brillouin zone, figure 4.3.

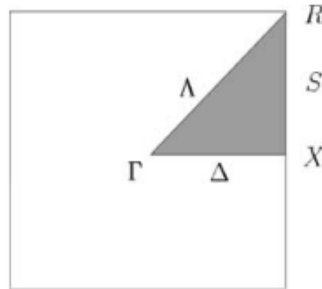


Figure 4.3: The shaded (or yellow) area indicates a *fundamental domain*, i.e., the smallest part of the pattern whose repeats tile the entire plane. For the most symmetric 2D square lattice, with point group $p4mm$, the fundamental domain is indicated by the shaded triangle $\Gamma\Lambda RSX\Delta\Gamma$ which constitutes 1/8 of the Brillouin zone, and contains the basic wave vectors and the high symmetry points (Fig. 10.2 of Dresselhaus *et al.* [37]).

Furthermore, one should quotient the temporal cat (6.4) by its $D_1 = \{e, \sigma\}$ dynamical symmetry

$$\sigma x_t = 1 - x_t, \quad \sigma s_t = \mu^2 - s_t, \quad \text{for all } t \in \mathbb{Z}, \quad (4.189)$$

where s_t takes values in the s -letter alphabet (6.5). Define the fundamental domain to be $\hat{x}_t \in [0, 1/2]$. We construct the temporal cat fundamental domain lattice system, with '1/2' unit hypercube $\hat{X} \in [0, 1/2]^n$, as in [ChaosBook Group \$D_1\$ and reduction to the fundamental domain](#), see figure 1.17(b), and the fundamental domain symbolic dynamics $\hat{\mathcal{A}}$. That leads to [ChaosBook chapter 25 Discrete symmetry factorization of zeta functions](#).

2021-06-08 Predrag [Lecture 7](#) (Unedited as of 2021-06-18)

- We work out the symmetry reduction and a breaking of the D_3 symmetry in the $[3 \times 3]$ permutation matrices representation

2021-06-20 Predrag I'll have to rerecord the above video from scratch, example 4.30 discussion of the D_3 symmetry is much more compact and elegant.

2021-06-20 Predrag This analysis of D_n irreps does not apply to symmetric orbits. For that one has to look at the subgroup structure of dihedral groups, see [groupprops wiki](#), the subgroup called there $\langle x \rangle$. Han's discussion of (4.249), (4.250) and (18.341) counts the broken rotational invariance solutions.

2021-06-21 Predrag Paul Garrett (2014) course notes [Harmonic analysis of dihedral group](#) contain a nice discussion of use of discrete Fourier basis for

representation of fields (i.e., scalar functions) on D_n lattices. His *Representation theory* course contains many interesting nuggets.

2018-07-04 Predrag Siemaszko and Wojtkowski [87] *Counting Berg partitions* describe symmetries of Adler-Weiss partitions. They are present for reversible toral automorphisms.

2021-07-04 Predrag The full symmetry group of a toral automorphism was studied by Baake and Roberts [9].

2021-07-04 Predrag The *infinite dihedral group* D_∞ (4.7) was introduced by Kim, Lee and Park [58] *A zeta function for flip systems* (2003).

Kim, Lee and Park [58] give the explicit formula (4.149) for the Lind zeta function [65] ζ_s (search for “Lind96” to find more about it) of a flip system (\mathcal{M}, f, s) (4.4).

[...] investigate dynamical systems with flip maps (4.4), regarded as infinite dihedral group actions. We introduce a zeta function for flip systems, and find its basic properties including a product formula. When the underlying C_n -action is conjugate to a topological Markov shift, the flip system is represented by a pair of matrices, and its zeta function is expressed explicitly in terms of the representation matrices.

[...] Any topological Markov shift whose transition matrix is symmetric has a natural flip.

[...] establish a zeta function for flip systems which is a conjugacy invariant, and give a finite description of the function when the underlying \mathbb{Z} -action is conjugate to a topological Markov shift.

2021-07-04 Predrag The much desired -see (2.16)- square root and dependence on t^2 finally makes an appearance in the Lind zeta function (4.149)!

2021-07-04 Predrag S. Ryu *The Lind Zeta functions of reversal systems of finite order* arXiv:1712.03519 (2017) deals with a more general case of reversing operators, but the LaTeX file was useful for clip & paste.

If (\mathcal{M}, f) is a shift of finite type, then there exists a square matrix A with non-negative integer entries such that the number of fixed points N_n can be expressed in terms of matrices [66]

$$N_n = \text{tr } A^n \quad (m = 1, 2, \dots) \quad (4.190)$$

Similarly, when (\mathcal{M}, f, s) is a shift-flip system of finite type, the number of fixed points N_n^s can be expressed in terms of matrices [58].

They write: “ Since there is a dynamical system (X, T) which is not conjugate to its time reversal (X, T^{-1}) , not every dynamical system has a flip. See p. 104 of Boyle, Marcus and Trow [14].

Note: Predrag does not understand that page. Worse still, Predrag does not understand any page in the entire monograph :(

In Park [74] it is shown that if the underlying \mathbb{Z} -actions are Kolmogorov and isomorphic, there are examples of non-isomorphic D_∞ -actions. "

2021-08-11 Predrag Park [74] *On ergodic foliations* (1988).

The 'covering space' has two actions, f and s , where f is a \mathbb{Z} -action, s is a map of order two, and s and T skew-commute; that is, $sfs = f^{-l}$.

Note: Predrag does not understand this paper, not at all.

2021-07-04 Predrag Still to read:

Boyle, Marcus and Trow [14] *Resolving maps and the dimension group for shifts of finite type* (1987).

Nordin and Noorani [73] *Counting finite orbits for the flip systems of shifts of finite type* (2021).

Yumiko Hironaka *Zeta functions of finite groups by enumerating subgroups*, arXiv:1410.4326 (2014) is potentially interesting: Hironaka forms zeta function like Riemann, rather than Artin-Mazur.

Richard Miles *Orbit growth for algebraic flip systems* DOI (2014)

Sieye Ryu PhD thesis *The Lind Zeta Function and Williams' Decomposition Theorem for Sofic Shift-Reversal Systems of Finite Order* (2014)

Golubitsky and Stewart [44] *The Symmetry Perspective*, chapters *Time Periodicity and Spatio-Temporal Symmetry* and *Periodic Solutions of Symmetric Hamiltonian Systems* (2002)



example 4.11

p. 275



example 4.30

p. 288



example 4.35

p. 292



example 4.31

p. 288



example 4.32

p. 290

4.9 Group theory and symmetries: a review

^{10 11} In quantum mechanics, whenever a system exhibits some symmetry, the corresponding symmetry group commutes with the Hamiltonian of this system, namely, $[U(g), H] = U(g)H - HU(g) = 0$. Here $U(g)$ denotes the operation corresponding to symmetry g whose meaning will be explained soon. The set of eigenstates with degeneracy ℓ , $\{\phi_1, \phi_2, \dots, \phi_\ell\}$, corresponding to the same system energy $H\psi_i = E_n\psi_i$, is invariant under the symmetry since $U(g)\psi_i$ are also eigenvectors for the same energy. This information helps us understand the spectrum of a Hamiltonian and the quantum mechanical selection rules. We now apply the same idea to the classical evolution operator $\mathcal{L}^t(x_e, x_s)$ for a system $f^t(x)$ equivariant under a discrete symmetry group $G = \{e, g_2, g_3, \dots, g_{|G|}\}$ of order $|G|$:

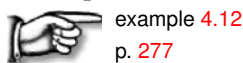
$$f^t(D(g))x = D(g)f^t(x) \quad \text{for } \forall g \in G. \quad (4.191)$$

We start with a review of some basic facts of the group representation theory. Some examples of good references on this topic are ref. [50, 90].

Suppose group G acts on a linear space V and function $\rho(x)$ is defined on this space $x \in V$. Each element $g \in G$ will transform point x to $D(g)x$. At the same time, $\rho(x)$ is transformed to $\rho'(x)$. The value $\rho(x)$ is unchanged after state point x is transformed to $D(g)x$, so $\rho'(D(g)x) = \rho(x)$. Denote $U(g)\rho(x) = \rho'(x)$, so we have

$$U(g)\rho(x) = \rho(D(g)^{-1}x). \quad (4.192)$$

This is how functions are transformed by group operations. Note, $D(g)$ is the representation of G in the form of space transformation matrices. The operator $U(g)$, which acts on the function space, is not the same as group operation $D(g)$, so (4.192) does not mean that $\rho(x)$ is invariant under G . Example 4.12 gives the space transformation matrices of C_3 .



4.9.1 Regular representation

An operator $U(g)$ which acts on an infinite-dimensional function space is too abstract to analyze. We would like to represent it in a more familiar way. Suppose there is a function $\rho(x)$ with symmetry G defined in full state space \mathcal{M} , then full state space can be decomposed as a union of $|G|$ tiles each of which is obtained by transforming the fundamental domain,

$$\mathcal{M} = \bigcup_{g \in G} g\hat{\mathcal{M}}, \quad (4.193)$$

¹⁰Predrag 2021-06-19: A copy of the 2017-03-09 section from Xiong Ding's thesis siminos/xiong/thesis/chapters/symGroup.tex.

¹¹Predrag 2021-06-19: Update/replace the ChaosBook version, as now $Z_2 \rightarrow D_1, Z_3 \rightarrow C_3$.

where $\hat{\mathcal{M}}$ is the chosen fundamental domain. So $\rho(x)$ takes $|G|$ different forms by (4.192) in each sub-domain in (4.193). Now, we obtained a natural choice of a set of bases in this function space called the *regular basis*,

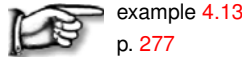
$$\{\rho_1^{reg}(\hat{x}), \rho_2^{reg}(\hat{x}), \dots, \rho_{|G|}^{reg}(\hat{x})\} = \{\rho(\hat{x}), \rho(g_2\hat{x}), \dots, \rho(g_{|G|}\hat{x})\}. \quad (4.194)$$

Here, for notation simplicity we use $\rho(g_i\hat{x})$ to represent $\rho(D(g_i\hat{x}))$ without ambiguity. These bases are constructed by applying $U(g^{-1})$ to $\rho(\hat{x})$ for each $g \in G$, with \hat{x} a point in the fundamental domain. The $[|G| \times |G|]$ matrix representation of the action of $U(g)$ in basis (4.194) is called the (*left*) *regular representation* $D^{reg}(g)$. Relation (4.192) says that $D^{reg}(g)$ is a permutation matrix, so each row or column has only one nonzero element.

We have a simple trick to obtain the regular representation quickly. Suppose the element at the i th row and the j th column of $D^{reg}(g)$ is 1. It means $\rho(g_i\hat{x}) = U(g)\rho(g_j\hat{x})$, which is $g_i = g^{-1}g_j \implies g^{-1} = g_i g_j^{-1}$. Namely,

$$D^{reg}(g)_{ij} = \delta_{g^{-1}, g_i g_j^{-1}}. \quad (4.195)$$

So if we arrange the columns of the multiplication table by the inverse of the group elements, then setting positions with g^{-1} to 1 defines the regular representation $D^{reg}(g)$. Note, the above relation can be further simplified to $g = g_j g_i^{-1}$, but it exchanges the rows and columns of the multiplication table, so $g = g_j g_i^{-1}$ should not be used to get $D^{reg}(g)$. On the other hand, it is easy to see that the regular representation of group element e is always the identity matrix.



4.9.2 Irreducible representations

$U(g)$ is a linear operator under the regular basis. Any linearly independent combination of the regular bases can be used as new basis, and then the representation of $U(g)$ changes respectively. So we ask a question: can we find a new set of bases

$$\rho_i^{irr} = \sum_j S_{ij} \rho_j^{reg} \quad (4.196)$$

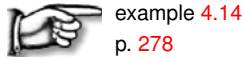
such that the new representation $D^{irr}(g) = SD^{reg}(g)S^{-1}$ is block-diagonal for any $g \in G$?

$$D^{irr}(g) = \begin{bmatrix} D^{(1)}(g) & & & \\ & D^{(2)}(g) & & \\ & & \ddots & \\ & & & \ddots \end{bmatrix} = \bigoplus_{\mu=1}^r d_\mu D^{(\mu)}(g). \quad (4.197)$$

In such a block-diagonal representation, the subspace corresponding to each diagonal block is invariant under G and the action of $U(g)$ can be analyzed subspace by subspace. It can be easily checked that for each μ , $D^{(\mu)}(g)$ for all

$g \in G$ form another representation (*irreducible representation*, or *irrep*) of group G . Here, r denotes the total number of irreps of G . The same irrep may show up more than once in the decomposition (4.197), so the coefficient d_μ denotes the number of its copies. Moreover, it is proved [50] that d_μ is also equal to the dimension of $D^{(\mu)}(g)$ in (4.197). Therefore, we have a relation

$$\sum_{\mu=1}^r d_\mu^2 = |G|.$$



Character tables. Finding a transformation S which simultaneously block-diagonalizes the regular representation of each group element sounds difficult. However, suppose it can be achieved and we obtain a set of irreps $D^{(\mu)}(g)$, then according to Schur's lemmas [50], $D^{(\mu)}(g)$ must satisfy a set of orthogonality relations:

$$\frac{d_\mu}{|G|} \sum_g D_{il}^{(\mu)}(g) D_{mj}^{(\nu)}(g^{-1}) = \delta_{\mu\nu} \delta_{ij} \delta_{lm}. \quad (4.198)$$

Denote the trace of irrep $D^{(\mu)}$ as $\chi^{(\mu)}$, which is referred to as the *character* of $D^{(\mu)}$. Properties of irreps can be derived from (4.198), and we list them as follows:

1. The number of irreps is the same as the number of classes.

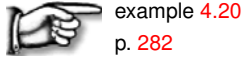
2. Dimensions of irreps satisfy $\sum_{\mu=1}^r d_\mu^2 = |G|$

3. Orthonormal relation I : $\sum_{i=1}^r |K_i| \chi_i^{(\mu)} \chi_i^{(\nu)*} = |G| \delta_{\mu\nu}$.

Here, the summation goes through all classes of this group, and $|K_i|$ is the number of elements in class i . This weight comes from the fact that elements in the same class have the same character. Symbol * means the complex conjugate.

4. Orthonormal relation II : $\sum_{\mu=1}^r \chi_i^{(\mu)} \chi_j^{(\mu)*} = \frac{|G|}{|K_i|} \delta_{ij}$.

The characters for all classes and irreps of a finite group are conventionally arranged into a *character table*, a square matrix whose rows represent different classes and columns represent different irreps. Rules 1 and 2 help determine the number of irreps and their dimensions. As the matrix representation of class $\{e\}$ is always the identity matrix, the first row is always the dimension of the corresponding representation. All entries of the first column are always 1, because the symmetric irrep is always one-dimensional. To compute the remaining entries, we should use properties 3, 4 and the class multiplication tables. Spectroscopists conventions use labels A and B for symmetric, respectively antisymmetric nondegenerate irreps, and E, T, G, H for doubly, triply, quadruply, quintuply degenerate irreps.



example 4.20

p. 282

4.9.3 Projection operator

We have listed the properties of irreps and the techniques of constructing a character table, but we still do not know how to construct the similarity transformation S which takes a regular representation into a block-diagonal form. Think of it in another way, each irrep is associated with an invariant subspace, so by projecting an arbitrary function $\rho(x)$ into its invariant subspaces, we find the transformation (4.196). One of these invariant subspaces is $\sum_g \rho(g\hat{x})$, which is the basis of the one-dimensional symmetric irrep A . For C_3 , it is (4.214). But how to get the others? We resort to the projection operator:

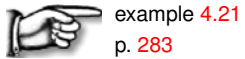
$$P_i^{(\mu)} = \frac{d_\mu}{|G|} \sum_g \left(D_{ii}^{(\mu)}(g) \right)^* U(g). \quad (4.199)$$

It projects an arbitrary function into the i th basis of irrep $D^{(\mu)}$ provided the diagonal elements of this representation $D_{ii}^{(\mu)}$ are known. $P_i^{(\mu)} \rho(x) = \rho_i^{(\mu)}$. Here, symbol $*$ means the complex conjugate. For unitary groups $\left(D_{ii}^{(\mu)}(g) \right)^* = D_{ii}^{(\mu)}(g^{-1})$. Summing i in (4.199) gives

$$P^{(\mu)} = \frac{d_\mu}{|G|} \sum_g \left(\chi^{(\mu)}(g) \right)^* U(g). \quad (4.200)$$

This is also a projection operator which projects an arbitrary function onto the sum of the bases of irrep $D^{(\mu)}$.

Note, for one-dimensional representations, (4.200) is equivalent to (4.199). The projection operator is known after we obtain the character table, since the character of an one-dimensional matrix is the matrix itself. However, for two-dimensional or higher-dimensional representations, we need to know the diagonal elements $D_{ii}^{(\mu)}$ in order to get the basis of invariant subspaces. That is to say, (4.199) should be used instead of (4.200) in this case. Example 4.21 illustrates this point. The two one-dimensional irreps are obtained by (4.200), but the other four two-dimensional irreps are obtained by (4.199).



example 4.21

p. 283

The C_3 and D_3 examples used in this section can be generalized to any C_n and D_n . For references, Example 4.26, example 4.33 and example 4.34 give the character tables of C_n and D_n .



example 4.26

p. 285



example 4.33

p. 291



example 4.34

p. 292

Commentary

Remark 4.1. Time reversal. Some background on D_∞ symmetry of the temporal cat and ϕ^4 1d lattice field theory, sect. 3.10 *Translations and reflections*. Time-reversed lattice states (if not self-dual under reflection) are counted as pairs, see for example ChaosBook fig. 11.6, ChaosBook example 11.11, ChaosBook Example 15.6 C_2 recoded, ChaosBook fig. 15.15, ChaosBook table 18.1 *The 4-disk orbits up to period 8*, ChaosBook table 34.1, the time-reversal discussion in ChaosBook section 42.2.3, and ChaosBook fig. 42.5.

This is a many-years outstanding frustration, see ChaosBook Remark 16.3 *Symmetries of the symbol square* and ChaosBook Remark 25.2 *Other symmetries*.

The zeta functions are still to be factorized in the $z \rightarrow t^2$ sense, perhaps as in (4.181). Then the corresponding ChaosBook chapters have to be rewritten.

4.10 Examples

Example 4.1. Discrete groups of order 2 on \mathbb{R}^3 . Three types of discrete group of order 2 can arise by linear action on our 3-dimensional Euclidean space \mathbb{R}^3 :



$$\begin{aligned} \text{reflections: } s(x, y, z) &= (x, y, -z) \\ \text{rotations: } r(x, y, z) &= (-x, -y, z) \\ \text{inversions: } P(x, y, z) &= (-x, -y, -z). \end{aligned} \quad (4.201)$$

s is a reflection (or an inversion) through the $[x, y]$ plane. r is $[x, y]$ -plane, constant z rotation by π about the z -axis (or an inversion thorough the z -axis). $P = rs$ is an inversion (or parity operation) through the point $(0, 0, 0)$. Singly, each operation generates a group of order 2: $D_1 = \{e, s\}$, $C_2 = \{e, r\}$, and $D_1 = \{e, P\}$. Together, they form the dihedral group $D_2 = \{e, s, r, sr\}$ of order 4. (continued in example 4.2)

[click to return: p. ??](#)

Example 4.2. Discrete operations on \mathbb{R}^3 . (Continued from example 4.1.) The matrix representation of reflections, rotations and inversions defined by (4.201) is

$$D(s) = \begin{pmatrix} 1 & 0 & 0 \\ 0 & 1 & 0 \\ 0 & 0 & -1 \end{pmatrix}, \quad D(r) = \begin{pmatrix} -1 & 0 & 0 \\ 0 & -1 & 0 \\ 0 & 0 & 1 \end{pmatrix}, \quad D(P) = \begin{pmatrix} -1 & 0 & 0 \\ 0 & -1 & 0 \\ 0 & 0 & -1 \end{pmatrix}, \quad (4.202)$$

with $\det D(r) = 1$, $\det D(s) = \det D(P) = -1$; that is why we refer to r as a rotation, and s , P as inversions. As $g^2 = e$ in all three cases, these are groups of order 2. (continued in example 4.3)

[click to return: p. ??](#)

Example 4.3. Equivariance of the Lorenz flow. (Continued from example 4.2) The velocity field in Lorenz equations (??)

[exercise ??](#)

$$\begin{bmatrix} \dot{x} \\ \dot{y} \\ \dot{z} \end{bmatrix} = \begin{bmatrix} \sigma(y - x) \\ \rho x - y - xz \\ xy - bz \end{bmatrix} \quad (4.203)$$

is equivariant under the action of cyclic group $C_2 = \{e, r\}$ acting on \mathbb{R}^3 by a π rotation about the z axis,

$$r(x, y, z) = (-x, -y, z). \quad (4.204)$$

(continued in example 4.4)

[click to return: p. ??](#)

Example 4.4. Desymmetrization of Lorenz flow. (Continuation of example 4.3) Lorenz^{CB} equation (4.203) is equivariant under (4.204), the action of order-2 group $C_2 = \{e, r\}$, where r is $[x, y]$ -plane, half-cycle rotation by π about the z -axis:

$$(x, y, z) \rightarrow r(x, y, z) = (-x, -y, z). \quad (4.205)$$

$r^2 = 1$ condition decomposes the state space into two linearly irreducible subspaces $\mathcal{M} = \mathcal{M}^+ \oplus \mathcal{M}^-$, the z -axis \mathcal{M}^+ and the $[x, y]$ plane \mathcal{M}^- , with projection operators onto the two subspaces given by (see sect. ??)

$$P^+ = \frac{1}{2}(1+r) = \begin{pmatrix} 0 & 0 & 0 \\ 0 & 0 & 0 \\ 0 & 0 & 1 \end{pmatrix}, \quad P^- = \frac{1}{2}(1-r) = \begin{pmatrix} 1 & 0 & 0 \\ 0 & 1 & 0 \\ 0 & 0 & 0 \end{pmatrix}. \quad (4.206)$$

As the flow is C_2 -invariant, so is its linearization $\dot{x} = Ax$. Evaluated at E_0 , A commutes with r , and, as we have already seen in example ??, the E_0 stability matrix decomposes into $[x, y]$ and z blocks.¹²

The 1-dimensional \mathcal{M}^+ subspace is the fixed-point subspace, with the z -axis pointwise invariant under the group action

$$\mathcal{M}^+ = \text{Fix}(C_2) = \{x \in \mathcal{M} \mid g x = x \text{ for } g \in \{e, r\}\} \quad (4.207)$$

(here $x = (x, y, z)$ is a 3-dimensional vector, not the coordinate x). A C_2 -fixed point $x(t)$ in $\text{Fix}(C_2)$ moves with time, but according to (??) remains within $x(t) \in \text{Fix}(C_2)$ for all times; the subspace $\mathcal{M}^+ = \text{Fix}(C_2)$ is flow invariant. In case at hand this jargon is a bit of an overkill: clearly for $(x, y, z) = (0, 0, z)$ the full state space Lorenz equation (4.203) is reduced to the exponential contraction to the E_0 equilibrium,¹³

$$\dot{z} = -bz. \quad (4.208)$$

However, for higher-dimensional flows the flow-invariant subspaces can be high-dimensional, with interesting dynamics of their own. Even in this simple case this subspace plays an important role as a topological obstruction: the orbits can neither enter it nor exit it, so the number of windings of a trajectory around it provides a natural, topological symbolic dynamics.

The \mathcal{M}^- subspace is, however, not flow-invariant, as the nonlinear terms $\dot{z} = xy - bz$ in the Lorenz equation (4.203) send all initial conditions within $\mathcal{M}^- = (x(0), y(0), 0)$ into the full, $z(t) \neq 0$ state space $\mathcal{M}/\mathcal{M}^+$. (continued in example ??)

(E. Siminos and J. Halcrow)

click to return: p. 737

Example 4.5. Discrete symmetries of the plane Couette flow. The plane Couette flow is a fluid flow bounded by two countermoving planes, in a cell periodic in streamwise and spanwise directions. The Navier-Stokes equations for the plane Couette flow have two discrete symmetries: reflection through the (streamwise, wall-normal) plane, and rotation by π in the (streamwise, wall-normal) plane. That is why the system has equilibrium and periodic orbit solutions, as well as relative equilibrium and relative periodic orbit solutions discussed in chapter ??). They belong to discrete symmetry subspaces. (continued in example ??)

click to return: p. ??

Example 4.6. A reflection-symmetric 1d map. Consider a 1-dimensional bimodal

¹²Predrag 2017-07-24: create example in sect. ?? from the last sentence

¹³Predrag 2017-07-24: pointer to turbulence chapter here

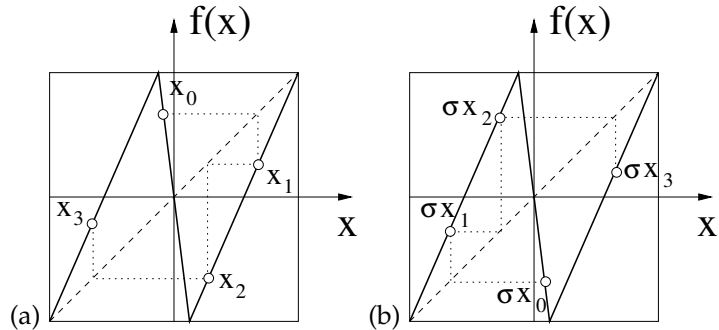


Figure 4.4: The bimodal Ulam sawtooth map with the D_1 symmetry $f(-x) = -f(x)$. If the trajectory (a) $x_0 \rightarrow x_1 \rightarrow x_2 \rightarrow \dots$ is a solution, so is its reflection (b) $\sigma x_0 \rightarrow \sigma x_1 \rightarrow \sigma x_2 \rightarrow \dots$. (work through example 4.6; continued in figure 4.5).

'sawtooth' map f shown in figure 4.4.

$$x_{t+1} = \begin{cases} f_L(x_t) = \Lambda(x_t + 1) - 1, & x_t \in \mathcal{M}_0 = [-1, -\ell/2] \\ f_C(x_t) = \Lambda_C x_t, & x_t \in \mathcal{M}_0 = [-\ell/2, \ell/2] \\ f_R(x_t) = \Lambda(x_t - 1) + 1, & x_t \in \mathcal{M}_1 = (\ell/2, 1], \end{cases} \quad (4.209)$$

with $\ell = 2/|\Lambda_C|$, and $2/|\Lambda| + 1/|\Lambda_C| = 1$. The map is piecewise-linear on the state space $\mathcal{M} = [-1, 1]$, a compact 1-dimensional line interval, split into three regions $\mathcal{M} = \mathcal{M}_L \cup \mathcal{M}_C \cup \mathcal{M}_R$. The map is reflection-symmetric, $f(-x) = -f(x)$.

Denote the reflection operation by $\sigma x = -x$. The 2-element group $G = \{e, \sigma\}$ goes by many names, such as Z_2 or C_2 . Here we shall refer to it as D_1 , dihedral group generated by a single reflection. The G -equivariance of the map implies that if $\{x_n\}$ is a trajectory, than also $\{\sigma x_n\}$ is a symmetry-equivalent trajectory because $\sigma x_{n+1} = \sigma f(x_n) = f(\sigma x_n)$.

In the temporal lattice formulation, there is a triplet of fields $\phi_t = (\phi_t^L, \phi_t^C, \phi_t^R)$ at each lattice site t . Just like the temporal Bernoulli (1.76), temporal lattice states satisfy a linear first-order difference equation

$$\phi_t - f \circ \phi_{t-1} = 0, \quad (4.210)$$

but now for a triplet of fields satisfying the local condition (4.209) at each lattice site. As the local slope can be either Λ or Λ_C , the $[3n \times 3n]$ orbit Jacobian matrix \mathcal{J} takes a block-diagonal form, and depends on the symbol block of a particular lattice state.

Challenge: write down the Hill determinant for a given symbol block, not only using Hill's formula, but also directly, without time evolution.

(continued in example 4.7)¹⁴

click to return: p. ??

Example 4.7. D_1 -asymmetric cycles. (Continued from example 4.6)¹⁵ The D_1 -equivariance of a map, $D_1 = \{e, \sigma\}$, implies that, in particular, if a finite set of states $\mathcal{M}_p = \{x_n\}$ constitutes a periodic orbit p , so does its reflection $\mathcal{M}_{\sigma p} = \{\sigma x_n\}$, with the same period and the same stability properties.

Label the three regions $\mathcal{M} = \{\mathcal{M}_L, \mathcal{M}_C, \mathcal{M}_R\}$ of the bimodal 'sawtooth' map of figure 4.5, with a 3-letter alphabet L(left), C(enter), and R(right). This symbolic dynamics

¹⁴Predrag 2021-06-12: write up exercise exer:ReflectA: write down the formula for the map of figure 4.4, verify its D_1 -equivariance.

¹⁵Predrag 2019-02-18: REPLACE discreteD1.mp4, eventually.

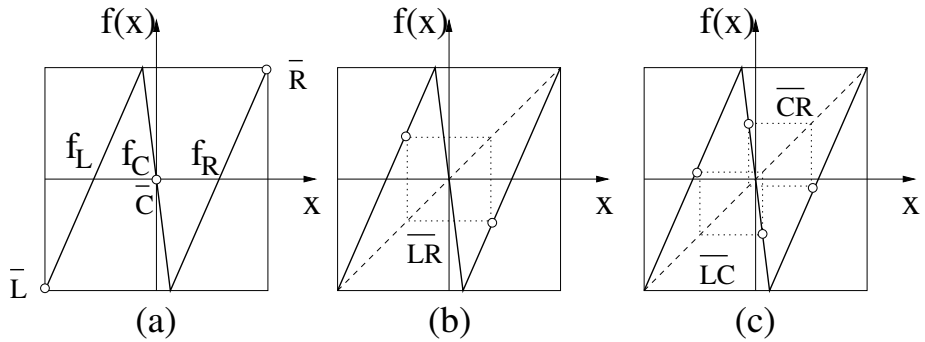


Figure 4.5: The D_1 -equivariant bimodal sawtooth map of figure 4.4 has three types of periodic orbits: (a) D_1 -fixed point \bar{C} , asymmetric fixed points pair $\{\bar{L}, \bar{R}\}$. (b) D_1 -symmetric (setwise invariant) 2-cycle \bar{LR} , composed of the relative cycle segment from L to R and its repeat from R to L . (c) Asymmetric 2-cycles pair $\{\bar{LC}, \bar{CR}\}$. (study example 4.7; continued in figure 4.6) (Y. Lan,)

is complete ternary dynamics, with any sequence of letters $\mathcal{A} = \{L, C, R\}$ corresponding to an admissible trajectory ('complete' means no additional grammar rules required, see example ?? below).

If a is an asymmetric cycle $\tilde{\mathcal{M}}_a$, σ maps it into the reflected cycle $\sigma\tilde{\mathcal{M}}_a$, with no points in common, $\tilde{\mathcal{M}}_a \cap \sigma\tilde{\mathcal{M}}_a = \emptyset$. Examples are the fixed points pair $\{\bar{L}, \bar{R}\}$ and the 2-cycles pair $\{\bar{LC}, \bar{CR}\}$ in figure 4.5(c).

[click to return: p. ??](#)

Example 4.8. D_1 -symmetric cycles. (Continued from example 4.7) For D_1 the period of a set-wise symmetric cycle is even ($n_s = 2n_{\bar{s}}$), and the mirror image of the x_s periodic point is reached by traversing the relative periodic orbit segment \bar{s} of length $n_{\bar{s}}$, $f^{n_{\bar{s}}}(x_s) = \sigma x_s$, see figure 4.5(b).

[click to return: p. ??](#)

Example 4.9. D_1 -invariant cycles.

Fix (G) , the set of points invariant under group action of D_1 , $\tilde{\mathcal{M}} \cap \sigma\tilde{\mathcal{M}}$, is just this fixed point $x = 0$, the reflection symmetry point.

In the example at hand there is only one G -invariant (point-wise invariant) orbit, the fixed point \bar{C} at the origin, see figure 4.5(a). As reflection symmetry is the only discrete symmetry that a map of the interval can have, this example completes the group-theoretic analysis of 1-dimensional maps. We shall continue analysis of this system in example 4.10, and work out the symbolic dynamics of such reflection symmetric systems in example 4.11).

[click to return: p. ??](#)

Example 4.10. D_1 reduction to the fundamental domain. Consider again the reflection-symmetric bimodal Ulam sawtooth map $f(-x) = -f(x)$ of example 4.7, with symmetry group $D_1 = \{e, \sigma\}$. The state space $\mathcal{M} = [-1, 1]$ can be tiled by half-line $\mathcal{M} = [0, 1]$, and $\sigma\mathcal{M} = [-1, 0]$, its image under a reflection across $x = 0$ point. The dynamics can then be restricted to the fundamental domain $\tilde{x}_k \in \tilde{\mathcal{M}} = [0, 1]$; every time a trajectory leaves this interval, it is mapped back using σ .

Figure 4.6: The bimodal Ulam sawtooth map of figure 4.5 with the D_1 symmetry $f(-x) = -f(x)$, restricted to the fundamental domain. $f(x)$ is indicated by the thin line, and fundamental domain map $\tilde{f}(\tilde{x})$ by the thick line. (a) Boundary fixed point \bar{C} is the fixed point $\bar{0}$. The asymmetric fixed point pair $\{\bar{L}, \bar{R}\}$ is reduced to the fixed point $\bar{2}$, and the full state space symmetric 2-cycle \bar{LR} is reduced to the fixed point $\bar{1}$. (b) The asymmetric 2-cycle pair $\{\bar{LC}, \bar{CR}\}$ is reduced to 2-cycle $\bar{01}$. (c) All fundamental domain fixed points and 2-cycles. (work through example 4.10) (Y. Lan,)

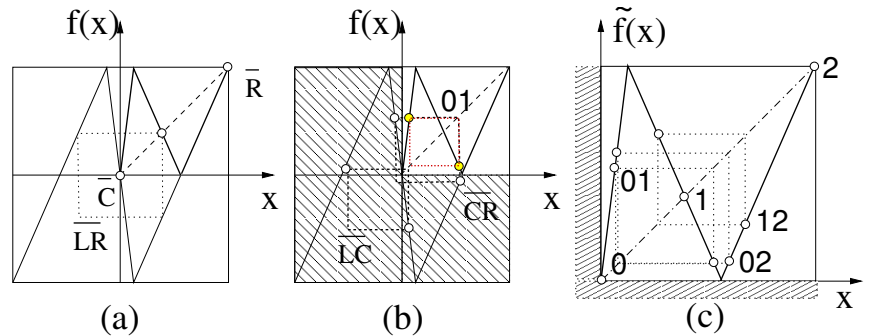
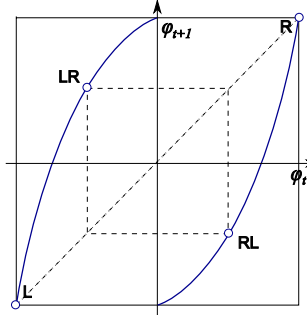


Figure 4.7: The D_1 -equivariant ‘bent Bernoulli’ map has two types of periodic orbits: (a) asymmetric pairs, such as the fixed points pair $\{\bar{L}, \bar{R}\}$. (b) D_1 -symmetric (setwise invariant) periodic orbits, such as the 2-cycle \bar{LR} , composed of the relative cycle segment from L to R and its repeat from R to L . (study example 4.11; continued in figure 4.8)



In figure 4.6 the fundamental domain map $\tilde{f}(\tilde{x})$ is obtained by reflecting $x < 0$ segments of the global map $f(x)$ into the upper right quadrant. \tilde{f} is also bimodal and piecewise-linear, with $\tilde{\mathcal{M}} = [0, 1]$ split into three regions $\tilde{\mathcal{M}} = \{\tilde{\mathcal{M}}_0, \tilde{\mathcal{M}}_1, \tilde{\mathcal{M}}_2\}$ which we label with a 3-letter alphabet $\tilde{\mathcal{A}} = \{0, 1, 2\}$. The symbolic dynamics is again complete ternary dynamics, with any sequence of letters $\{0, 1, 2\}$ admissible.

However, the interpretation of the ‘desymmetrized’ dynamics is quite different - the multiplicity of every periodic orbit is now 1, and relative periodic segments of the full state space dynamics are all periodic orbits in the fundamental domain. Consider figure 4.6:

In (a) the boundary fixed point \bar{C} is also the fixed point $\bar{0}$. The asymmetric fixed point pair $\{\bar{L}, \bar{R}\}$ is reduced to the fixed point $\bar{2}$, and the full state space symmetric 2-cycle \bar{LR} is reduced to the fixed point $\bar{1}$. (b) The asymmetric 2-cycle pair $\{\bar{LC}, \bar{CR}\}$ is reduced to the 2-cycle $\bar{01}$. Finally, the symmetric 4-cycle \bar{LCRC} is reduced to the 2-cycle $\bar{02}$. This completes the conversion from the full state space for all fundamental domain fixed points and 2-cycles, frame (c).¹⁶

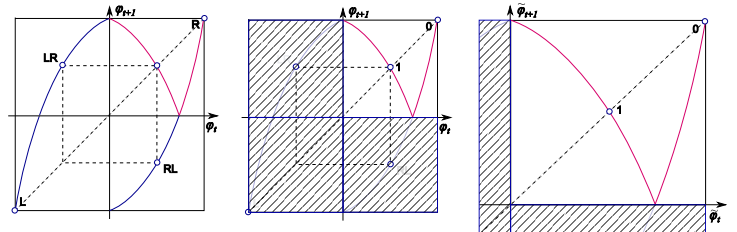
[click to return: p. ??](#)

Example 4.11. D_1 -reduced binary symbolic dynamics.

2CB

¹⁶Predrag 2019-02-18: draw this cycle both in the full and in the fundamental domain. in figure 4.6(a) double label, with $\bar{0}, \bar{1}$ and $\bar{2}$.

Figure 4.8: The ‘bent Bernoulli’ map of figure 4.7 with the D_1 symmetry $f(-\phi) = -f(\phi)$, restricted to the fundamental domain. $f(\phi)$ is indicated by a blue line, and fundamental domain map $\tilde{f}(\tilde{\phi})$ by the purple line. The asymmetric fixed point pair $\{\bar{L}, \bar{R}\}$ is reduced to the fixed point $\bar{0}$, and the full state space symmetric 2-cycle \bar{LR} is reduced to the fixed point $\bar{1}$. (work through example 4.11)



¹⁷ Consider a nonlinear, D_1 -symmetric ‘bent Bernoulli’ map of figure 4.7; like the bimodal map figure 4.5, but with the middle interval squeezed to a point, so the symbolic dynamics is simpler, complete binary with a 2-letter alphabet L (eft), R (ight).

In figure 4.8 the fundamental domain map $\tilde{f}(\tilde{\phi})$ is obtained by reflecting $\phi < 0$ segments of the global map $f(\phi)$ into the upper right quadrant. \tilde{f} also has two branches, with $\tilde{\mathcal{M}} = [0, 1]$ split into two regions $\tilde{\mathcal{M}} = \{\tilde{\mathcal{M}}_0, \tilde{\mathcal{M}}_1\}$ which we label with a 2-letter alphabet $\tilde{\mathcal{A}} = \{0, 1\}$. While the full state space map has two monotone branches with positive slopes, the symmetry reduced map is a unimodal map, with negative slope branch \tilde{f}_1 .

The negative slope branch is the consequence of relative periodicity: the mirror image of the x_s periodic point is reached by traversing the relative periodic orbit segment \tilde{s} of length $n_{\tilde{s}}$, $f^{n_{\tilde{s}}}(x_s) = \sigma x_s$, see the LR 2-cycle in figure 4.7, so the relative periodic orbit temporal Jacobian matrix carries a minus sign.

We could have illustrated this with the Bernoulli piecewise linear map, figure 3.2, whose symmetry-reduced map is the Ulam tent map, but there the D_1 symmetry is so obvious that it is hidden in the plain sight.¹⁸

The symbolic dynamics is again complete binary dynamics, with any sequence of letters $\{0, 1\}$ admissible. Assume that all periodic orbits are strictly unstable, $|\Lambda_p| > 0$, so that each orbit or orbit is uniquely labeled by an infinite string $\{s_i\}$, $s_i \in \{R, L\}$, and that the dynamics is invariant under the $R \leftrightarrow L$ interchange, i.e., it is D_1 symmetric. The periodic orbits separate into the symmetric orbits $s \in \{RL, RRLL, RRRLLL, RLLRLRRL, \dots\}$, with multiplicity $m_s = 1$, and the asymmetric orbit pairs $a \in \{R, L, RRL, LLR, \dots\}$, with multiplicity $m_a = 2$. For example, as there is no distinction between the “left” or the “right” branch of the map, the weights $t_R = t_L$, $t_{RRL} = t_{LRL}$, are equal, and so on.

exercise ??

The symmetry reduced labeling $\tilde{s}_i \in \{0, 1\}$ is related to the full state space labels $s_i \in \{L, R\}$ by

$$\begin{aligned} \text{If } s_i &= s_{i-1} \text{ then } \tilde{s}_i = 0 \\ \text{If } s_i &\neq s_{i-1} \text{ then } \tilde{s}_i = 1 \end{aligned} \quad (4.211)$$

For example, both $\bar{L} = \dots LLLL \dots$ and $\bar{R} = \dots RRRR \dots$ map into $\dots 000 \dots = \bar{0}$, $\bar{LR} = \dots LRLR \dots$ maps into $\dots 111 \dots = \bar{1}$, $\bar{LRRR} = \dots LLRLLLRR \dots$ maps

¹⁷Predrag 2017-09-20: Extracted this from ChaosBook symm.tex Discrete symmetry factorization, ChaosBook sect. 25.5 $Z_2 = D_1$ factorization (version of 2015-04-07).

¹⁸Predrag 2021-08-03: Make up the Bernoulli D_1 -symmetry example, setting up example 4.36, will need it for LC21.

Table 4.5: Correspondence between the D_1 symmetry reduced cycles \tilde{p} and the full state space periodic orbits p , together with their multiplicities m_p . Also listed are the two shortest cycles (length 6) related by time reversal, but distinct under D_1 .

\tilde{p}	p	m_p
0	R	2
1	LR	1
01	$LLRR$	1
011	LLR	2
001	$LLLRRR$	1
0111	$LRLRLR$	1
0001	$LRRR$	2
0011	$LLLLRRR$	1
01111	$LRLRL$	2
00111	$LRLRLRLRR$	1
11010	$LRLRLRLRR$	1
00011	$LRLRLRLRR$	1
10100	$LLRRR$	2
00001	$LLLLRRRRR$	1
110100	$LRLRLRLRLRR$	1
110010	$LRLRLRLRLRR$	1

into $\cdots 0101 \cdots = \overline{01}$, and so forth. A list of such reductions is given in table 4.5.¹⁹ (continued in example 4.35, illustrated by the Bernoulli example 4.36)

[click to return: p. 266](#)

Example 4.12. A matrix representation of cyclic group C_3 . A 3-dimensional matrix representation of the 3-element cyclic group $C_3 = \{e, r, r^2\}$ is given by the three rotations by $2\pi/3$ around the z -axis in a 3-dimensional state space,

$$D(e) = \begin{bmatrix} 1 & & \\ & 1 & \\ & & 1 \end{bmatrix}, \quad D(r) = \begin{bmatrix} \cos \frac{2\pi}{3} & -\sin \frac{2\pi}{3} & \\ \sin \frac{2\pi}{3} & \cos \frac{2\pi}{3} & \\ & & 1 \end{bmatrix},$$

$$D(r^2) = \begin{bmatrix} \cos \frac{4\pi}{3} & -\sin \frac{4\pi}{3} & \\ \sin \frac{4\pi}{3} & \cos \frac{4\pi}{3} & \\ & & 1 \end{bmatrix}.$$

(continued in example 4.13)

(X. Ding,)

[click to return: p. 267](#)

Example 4.13. The regular representation of cyclic group C_3 . (continued from example 4.12) Take an arbitrary function $\rho(x)$ over the state space $x \in \mathcal{M}$, and define a fundamental domain $\hat{\mathcal{M}}$ as a 1/3 wedge, with axis z as its (symmetry invariant) edge. The state space is tiled with three copies of the wedge,

$$\mathcal{M} = \hat{\mathcal{M}}_1 \cup \hat{\mathcal{M}}_2 \cup \hat{\mathcal{M}}_3 = \hat{\mathcal{M}} \cup r\hat{\mathcal{M}} \cup r^2\hat{\mathcal{M}}.$$

Function $\rho(x)$ can be written as the 3-dimensional vector of functions over the fundamental domain $\hat{x} \in \hat{\mathcal{M}}$,

$$(\rho_1^{reg}(\hat{x}), \rho_2^{reg}(\hat{x}), \rho_3^{reg}(\hat{x})) = (\rho(\hat{x}), \rho(r\hat{x}), \rho(r^2\hat{x})). \quad (4.212)$$

¹⁹Predrag 2021-08-02: please recheck table 4.5: I have interchanged '0' and '1' compared to ChaosBook, might have introduced errors.

Table 4.6: The multiplication tables of the dihedral group D_1 , and cyclic group C_3 .

D_1	e	s	C_3	e	r^{-1}	r^{-2}
e	e	s	e	e	r^2	r
s	s	e	r	r	e	r^2
			r^2	r^2	r	e

The multiplication table of C_3 is given in table 4.6. By (4.195), the regular representation matrices $D^{reg}(g)$ have '1' at the location of g^{-1} in the multiplication table, '0' elsewhere. The actions of the operator $U(g)$ are now represented by permutations matrices (blank entries are zeros):

$$D^{reg}(e) = \begin{bmatrix} 1 & & \\ & 1 & \\ & & 1 \end{bmatrix}, \quad D^{reg}(r) = \begin{bmatrix} & 1 & \\ 1 & & \\ & & 1 \end{bmatrix}, \quad D^{reg}(r^2) = \begin{bmatrix} & & 1 \\ 1 & & \\ & 1 & \end{bmatrix}. \quad (4.213)$$

(X. Ding,)

click to return: p. 268

2CB

Example 4.14. Irreps of cyclic group C_3 . (continued from example 4.13) For D_1 , whose multiplication table is in table 4.6, we can form the symmetric base $\rho(\hat{x}) + \rho(s\hat{x})$ and the antisymmetric base $\rho(\hat{x}) - \rho(s\hat{x})$. You can verify that in this new basis, D_1 is block-diagonalized. We would like to generalize this symmetric-antisymmetric decomposition to the order 3 group C_3 . Symmetrization can be carried out on any number of functions, but there is no obvious anti-symmetrization. We draw instead inspiration from the Fourier transformation for a finite periodic lattice, and construct from the regular basis (4.212) a new set of bases

$$\rho_0^{irr}(\hat{x}) = \frac{1}{3} [\rho(\hat{x}) + \rho(r\hat{x}) + \rho(r^2\hat{x})] \quad (4.214)$$

$$\rho_1^{irr}(\hat{x}) = \frac{1}{3} [\rho(\hat{x}) + \omega \rho(r\hat{x}) + \omega^2 \rho(r^2\hat{x})] \quad (4.215)$$

$$\rho_2^{irr}(\hat{x}) = \frac{1}{3} [\rho(\hat{x}) + \omega^2 \rho(r\hat{x}) + \omega \rho(r^2\hat{x})]. \quad (4.216)$$

Here $\omega = e^{2i\pi/3}$. The representation of group C_3 in this new basis is block-diagonal by inspection:

$$D^{irr}(e) = \begin{bmatrix} 1 & & \\ & 1 & \\ & & 1 \end{bmatrix}, \quad D^{irr}(r) = \begin{bmatrix} 1 & 0 & 0 \\ 0 & \omega & 0 \\ 0 & 0 & \omega^2 \end{bmatrix}, \quad D^{irr}(r^2) = \begin{bmatrix} 1 & 0 & 0 \\ 0 & \omega^2 & 0 \\ 0 & 0 & \omega \end{bmatrix}. \quad (4.217)$$

So C_3 has three 1-dimensional irreps. Generalization to any C_n is immediate: this is just a finite lattice, discrete Fourier transform.

(X. Ding,)

click to return: p. 269

2CB

Example 4.15. C_∞ group. Consider the integer lattice \mathbb{Z} . The infinite cyclic group C_∞ is generated by r , the right shift by one lattice spacing

$$C_\infty = \langle r \mid r^\ell, \ell \in \mathbb{Z} \rangle. \quad (4.218)$$

Table 4.7: C_∞ cyclic group multiplication adds up translations. D_∞ dihedral group multiplication adds up translations, or translates and then reverses their direction.

C_∞	r_j	D_∞	r_j	s_j
r_i	r_{i+j}	r_i	r_{i+j}	s_{j-i}
		s_i	s_{i+j}	r_{j-i}

Every finite index subgroup of the infinite cyclic group C_∞ is also cyclic, isomorphic to C_n

$$H(n) = \langle r^n \rangle, \quad (4.219)$$

with index

$$|C_\infty/H(n)| = |n|. \quad (4.220)$$

The infinite cyclic group elements are all shifts

$$\begin{aligned} C_\infty &= \langle r_j \mid r_j = r^j; j \in \mathbb{Z} \rangle \\ &= \{\dots, r_{-2}, r_{-1}, 1, r_1, r_2, r_3, \dots\}, \end{aligned} \quad (4.221)$$

where $r_j = r^j$ denotes translation by j lattice sites. $r_0 = 1$ denotes the identity. Cyclic group multiplication adds translations.

[click to return: p. 207](#)

Example 4.16. Marching forward in time: Artin-Mazur zeta function. Consider the integer lattice \mathbb{Z} , invariant under infinite cyclic group shifts by one or integer number of lattice spacings (see example 4.15):

$$C_\infty = \langle r \mid r^\ell, \ell \in \mathbb{Z} \rangle. \quad (4.222)$$

Every period n sublattice is n -steps infinite cyclic group,

$$H(n) = \langle r^n \rangle, \quad (4.223)$$

with the quotient $C_\infty/H(n)$ isomorphic to C_n , with multiplicity

$$|C_\infty/H(n)| = |n|. \quad (4.224)$$

Let N_n denote the number of points in \mathcal{M} fixed by f^n :

$$N_n = |\{x \in \mathcal{M} : f^n(x) = x\}|. \quad (4.225)$$

The corresponding Lind zeta function (4.137) is known as the Artin-Mazur zeta function [4, 26]

$$1/\zeta_{top}(t) = \exp \left(- \sum_{n=1}^{\infty} \frac{t^n}{n} N_n \right) \quad (4.226)$$

[click to return: p. 245](#)

Example 4.17. D_∞ group multiplication table. The infinite dihedral group [58] 2CB elements are all shifts and translate-reflections

$$\begin{aligned} D_\infty &= \langle r_i, s_j \mid r_i s_j = s_j r_{-i}; s_j^2 = 1; i, j \in \mathbb{Z} \rangle \\ &= \{\dots, r_{-2}, s_{-2}, r_{-1}, s_{-1}, 1, s, r_1, s_1, r_2, s_2, \dots\}. \end{aligned} \quad (4.227)$$

where $r_j = r^j$ denotes translation by j lattice sites, and $s_j = sr^j$ denotes reflection across the j th lattice site. $r_0 = 1$ denotes the identity, and by definition $s_0 = s$. Dihedral group multiplication table 4.7 adds up translations, or translates and then reverses their direction.

click to return: p. 207

Example 4.18. D_∞ subgroups and cosets. $H(n)$, any n , is a translation subgroup of D_∞ (a 1-dimensional Bravais sublattice \mathcal{L} ??), with a basis vector a that defines the Bravais cell of length n) with group elements $\langle r^n \rangle$, or, more explicitly:

$$H(n) = \{\dots, r_{-2n}, r_{-n}, 1, r_n, r_{2n}, \dots\}. \quad (4.228)$$

There are $2n$ left cosets of subgroup $H(n)$ in D_∞ :

$$\begin{aligned} H(n) &= \{\dots, r_{-2n}, r_{-n}, 1, r_n, r_{2n}, \dots\} \\ sH(n) &= \{\dots, s_{-2n}, s_{-n}, s, s_n, s_{2n}, \dots\} \\ rH(n) &= \{\dots, r_{-2n+1}, r_{-n+1}, r, r_{n+1}, r_{2n+1}, \dots\} \\ s_1H(n) &= \{\dots, s_{-2n+1}, s_{-n+1}, s_1, s_{n+1}, s_{2n+1}, \dots\} \\ &\vdots \\ r_{n-1}H(n) &= \{\dots, r_{-n-1}, r_{-1}, r_{n-1}, r_{2n-1}, r_{3n-1}, \dots\} \\ s_{n-1}H(n) &= \{\dots, s_{-n-1}, s_{-1}, s_{n-1}, s_{2n-1}, s_{3n-1}, \dots\}. \end{aligned} \quad (4.229)$$

Using elements $\{1, s, r, s_1, \dots, r_{n-1}, s_{n-1}\}$ as representatives of these cosets we see that the quotient group $D_\infty/H(n)$ is isomorphic to the dihedral group D_n .

There are n infinite dihedral $H(n, k)$ subgroups of D_∞ , for any $n, 0 \leq k < n$ (Bravais cell of length n , with reflection point shifted k steps):

$$H(n, k) = \{\dots, r_{-2n}, s_{-2n+k}, r_{-n}, s_{-n+k}, 1, s_k, r_n, s_{n+k}, r_{2n}, s_{2n+k}, \dots\}.$$

The left cosets of the subgroup $H(n, k)$ in D_∞ are:²⁰

$$\begin{aligned} H(n, k) &= \{\dots, r_{-2n}, s_{-2n+k}, r_{-n}, s_{-n+k}, 1, \\ &\quad s_k, r_n, s_{n+k}, r_{2n}, s_{2n+k}, \dots\} \\ rH(n, k) &= \{\dots, r_{-2n+1}, s_{-2n+k+1}, r_{-n+1}, s_{-n+k+1}, r \\ &\quad s_{k+1}, r_{n+1}, s_{n+k+1}, r_{2n+1}, s_{2n+k+1}, \dots\} \\ &\vdots \\ r_{n-1}H(n, k) &= \{\dots, r_{-n-1}, s_{-n+k-1}, r_{-1}, s_{k-1}, r_{n-1}, \\ &\quad s_{n+k-1}, r_{2n-1}, s_{2n+k-1}, r_{3n-1}, s_{3n+k-1}, \dots\}. \end{aligned} \quad (4.230)$$

Using $\{1, r, \dots, r_{n-1}\}$ as representatives of these cosets we see that the quotient group $D_\infty/H(n, k)$ is isomorphic to the cyclic group C_n .

²⁰Predrag 2021-07-24: Explain that $s_j H(n, k)$ is a rearrangement.

Table 4.8: D_3 group and class operator multiplication tables.

D_3	1	r	r_2	s_1	s_2	s_3	\mathcal{C}_1	\mathcal{C}_2	\mathcal{C}_3
1	1	r	r_2	s_1	s_2	s_3	\mathcal{C}_1	\mathcal{C}_2	\mathcal{C}_3
r	r	r_2	1	s_3	s_1	s_2	\mathcal{C}_1	\mathcal{C}_2	\mathcal{C}_3
r_2	r_2	1	r	s_2	s_3	s_1	\mathcal{C}_2	$2\mathcal{C}_1+\mathcal{C}_2$	$2\mathcal{C}_3$
s_1	s_1	s_2	s_3	1	r	r_2	\mathcal{C}_3	$2\mathcal{C}_3$	$3\mathcal{C}_1+3\mathcal{C}_2$
s_2	s_2	s_3	s_1	r_2	1	r			
s_3	s_3	s_1	s_2	r	r_2	1			

To show that $H(n, k)$ is not a normal subgroup: using (3.143) we have: $r_i s_k r_i^{-1} = s_{k-2i}$. For $i \neq n$, generally $s_{k-2i} = r_{2i}s_k$ is not an element of $H(n, k)$.

Let $\phi(n)$ be a lattice state that is invariant under the action of subgroup $H(n)$:

$$H(n)\phi(n) = \phi(n), \quad (4.231)$$

and $\phi(n, k)$ be a lattice state that is invariant under the action of subgroup $H(n, k)$:

$$H(n, k)\phi(n, k) = \phi(n, k). \quad (4.232)$$

Since $H(n)$ is a normal subgroup of D_∞ , we have:

$$\begin{aligned} H(n)g\phi(n) &= gH(n)g^{-1}g\phi(n) \\ &= gH(n)\phi(n) \\ &= g\phi(n), \quad g \in D_\infty. \end{aligned} \quad (4.233)$$

So $g\phi(n)$ with $g \in D_\infty$ is also a lattice state that is invariant under $H(n)$. For the lattice state $\phi(n, k)$ we have:

$$\begin{aligned} gH(n, k)g^{-1}g\phi(n, k) &= gH(n, k)\phi(n, k) \\ &= g\phi(n, k), \quad g \in D_\infty. \end{aligned} \quad (4.234)$$

Since $H(n, k)$ is not a normal subgroup, $gH(n, k)g^{-1}$ is a conjugate subgroup of $H(n, k)$. So $g\phi(n, k)$ with $g \in D_\infty$ is not invariant under $H(n, k)$, but invariant under a conjugate subgroup of $H(n, k)$.

(H. Liang, 2021-07-28) [click to return: p. 207](#)



example 4.19

p. 281

Example 4.19. The regular representation of dihedral group D_3 .

2CB

$D_3 = \{e, r, r_2, s, s_1, s_2\}$ represents the symmetries of a triangle with equal sides. r and r_2 are rotations by $2\pi/3$ and $4\pi/3$ respectively. s, s_1 and s_2 are the 3 reflections. The regular basis in this case are

$$(\rho(\hat{x}), \rho(s\hat{x}), \rho(s_1\hat{x}), \rho(s_2\hat{x}), \rho(r\hat{x}), \rho(r_2\hat{x})).$$

It helps us obtain the multiplication table quickly by the following relations

$$s_2 = s_1r, \quad s_1 = r_2s, \quad rs = sr_2, \quad r_2s = sr. \quad (4.235)$$

Table 4.9: The multiplication table of D_3 , the group of symmetries of an equilateral triangle.

D_3	e	s	s_{-1}	s_{-2}	r_{-1}	r_{-2}
e	e	s	s_1	s_2	r_2	r
s	s	e	r	r_2	s_2	s_1
s_1	s_1	r_2	e	r	s	s_2
s_2	s_2	r	r_2	e	s_1	s
r	r	s_2	s	s_1	e	r_2
r_2	r_2	s_1	s_2	s	r	e

The multiplication table of D_3 is given in table 4.9. By (4.195), the 6 regular representation matrices $D^{reg}(g)$ have '1' at the location of g^{-1} in the multiplication table, '0' elsewhere. For example, the regular representation of the action of operators $U(s_1)$ and $U(r_2)$ are, respectively:

$$D^{reg}(s_1) = \begin{bmatrix} 0 & 0 & 1 & 0 & 0 & 0 \\ 0 & 0 & 0 & 0 & 0 & 1 \\ 1 & 0 & 0 & 0 & 0 & 0 \\ 0 & 0 & 0 & 0 & 1 & 0 \\ 0 & 0 & 0 & 1 & 0 & 0 \\ 0 & 1 & 0 & 0 & 0 & 0 \end{bmatrix}, \quad D^{reg}(r) = \begin{bmatrix} 0 & 0 & 0 & 0 & 1 & 0 \\ 0 & 0 & 0 & 1 & 0 & 0 \\ 0 & 1 & 0 & 0 & 0 & 0 \\ 0 & 0 & 1 & 0 & 0 & 0 \\ 0 & 0 & 0 & 0 & 0 & 1 \\ 1 & 0 & 0 & 0 & 0 & 0 \end{bmatrix}.$$

click to return: p. 281

(X. Ding,)

 Table 4.10: Character tables of D_1 , C_3 and D_3 . The classes $\{s_{12}, s_{13}, s_{14}\}$, $\{r, r^2\}$ are denoted $3s, 2C$, respectively.

D_1	A	B	C_3	A	E	D_3	A	B	E
e	1	1	e	1	1	1	1	1	2
s	1	-1	r	1	ω	ω^2	1	-1	0
			r^2	1	ω^2	ω	1	1	-1

Example 4.20. Character table of D_3 . (continued from example ??) Let us construct table 4.10. one-dimensional representations are denoted by A and B , depending on whether the basis function is symmetric or antisymmetric with respect to transpositions s_{ij} . E denotes the two-dimensional representation. As D_3 has 3 classes, the dimension sum rule $d_1^2 + d_2^2 + d_3^2 = 6$ has only one solution $d_1 = d_2 = 1, d_3 = 2$. Hence there are two one-dimensional irreps and one two-dimensional irrep. The first row is 1, 1, 2, and the first column is 1, 1, 1 corresponding to the one-dimensional symmetric representation. We take two approaches to figure out the remaining 4 entries. First, since B is an antisymmetric one-dimensional representation, so the characters should be ± 1 . We anticipate $\chi^B(s) = -1$ and can quickly figure out the remaining 3 positions. Then we check that the obtained table satisfies the orthonormal relations. Second, denote $\chi^B(s) = x$ and $\chi^E(s) = y$, then from the orthonormal relation of the second column

with the first column and itself, we obtain $1+x+2y=0$ and $1+x^2+y^2=6/3$. Then we get two sets of solutions, one of which is incompatible with other orthonormal relations, so we are left with $x=-1, y=0$. Similarly, we can get the other two characters. (X. Ding,)

[click to return: p. 270](#)

Example 4.21. Bases for irreps of D_3 . (continued from example ??) We use 2CB projection operator (4.200) to obtain a basis of irreps of D_3 . From table 4.10, we have

$$P^A \rho(\hat{x}) = \frac{1}{6} [\rho(\hat{x}) + \rho(s\hat{x}) + \rho(s_2\hat{x}) + \rho(s_1\hat{x}) + \rho(r\hat{x}) + \rho(r^2\hat{x})] \quad (4.236)$$

$$P^B \rho(\hat{x}) = \frac{1}{6} [\rho(\hat{x}) - \rho(s\hat{x}) - \rho(s_2\hat{x}) - \rho(s_1\hat{x}) + \rho(r\hat{x}) + \rho(r^2\hat{x})]. \quad (4.237)$$

For projection into irrep E , we need to figure out the explicit matrix representation first. Obviously, the following 2 by 2 matrices are E irreps.

$$D^E(e) = \begin{bmatrix} 1 & 0 \\ 0 & 1 \end{bmatrix}, \quad D^E(r) = \begin{bmatrix} \omega & 0 \\ 0 & \omega^2 \end{bmatrix}, \quad D^E(r^2) = \begin{bmatrix} \omega^2 & 0 \\ 0 & \omega \end{bmatrix} \quad (4.238)$$

$$D^E(s) = \begin{bmatrix} 0 & 1 \\ 1 & 0 \end{bmatrix}, \quad D^E(s_2) = \begin{bmatrix} 0 & \omega^2 \\ \omega & 0 \end{bmatrix}, \quad D^E(s_1) = \begin{bmatrix} 0 & \omega \\ \omega^2 & 0 \end{bmatrix}. \quad (4.239)$$

So apply projection operator (4.199) on $\rho(\hat{x})$ and $\rho(s\hat{x})$, we get

$$P_1^E \rho(\hat{x}) = \frac{1}{6} [\rho(\hat{x}) + \omega\rho(r\hat{x}) + \omega^2\rho(r^2\hat{x})] \quad (4.240)$$

$$P_2^E \rho(\hat{x}) = \frac{1}{6} [\rho(\hat{x}) + \omega^2\rho(r\hat{x}) + \omega\rho(r^2\hat{x})] \quad (4.241)$$

$$P_1^E \rho(s\hat{x}) = \frac{1}{6} [\rho(s\hat{x}) + \omega\rho(s_1\hat{x}) + \omega^2\rho(s_2\hat{x})] \quad (4.242)$$

$$P_2^E \rho(s\hat{x}) = \frac{1}{6} [\rho(s\hat{x}) + \omega^2\rho(s_1\hat{x}) + \omega\rho(s_2\hat{x})]. \quad (4.243)$$

The above derivation has used formulas (4.235). In the invariant basis

$$\left\{ P^A \rho(\hat{x}), P^B \rho(\hat{x}), P_1^E \rho(\hat{x}), P_2^E \rho(s\hat{x}), P_1^E \rho(s\hat{x}), P_2^E \rho(\hat{x}) \right\},$$

we have

$$D^{irr}(s_2) = \begin{bmatrix} 1 & 0 & 0 & 0 & 0 & 0 \\ 0 & -1 & 0 & 0 & 0 & 0 \\ 0 & 0 & 0 & \omega^2 & 0 & 0 \\ 0 & 0 & \omega & 0 & 0 & 0 \\ 0 & 0 & 0 & 0 & 0 & \omega^2 \\ 0 & 0 & 0 & 0 & \omega & 0 \end{bmatrix} \quad D^{irr}(r) = \begin{bmatrix} 1 & 0 & 0 & 0 & 0 & 0 \\ 0 & 1 & 0 & 0 & 0 & 0 \\ 0 & 0 & \omega & 0 & 0 & 0 \\ 0 & 0 & 0 & \omega^2 & 0 & 0 \\ 0 & 0 & 0 & 0 & \omega & 0 \\ 0 & 0 & 0 & 0 & 0 & \omega^2 \end{bmatrix}.$$

(X. Ding,)

[click to return: p. 270](#)

Example 4.22. The class multiplication table for D_3 .

2CB

See table 4.11.

Table 4.11: D_3 group and class operator multiplication tables.

D_3	1	r	r_2	s	s_1	s_2
1	1	r	r_2	s	s_1	s_2
r	r	r_2	1	s_2	s	s_1
r_2	r_2	1	r	s_1	s_2	s
s	s	s_1	s_2	1	r	r_2
s_1	s_1	s_2	s	r_2	1	r
s_2	s_2	s	s_1	r	r_2	1

D_3	$\mathbf{1}$	\mathcal{R}	\mathcal{S}
$\mathbf{1}$	$\mathbf{1}$	\mathcal{R}	\mathcal{S}
\mathcal{R}	\mathcal{R}	$2\mathbf{1} + \mathcal{R}$	$2\mathcal{S}$
\mathcal{S}	\mathcal{S}	$2\mathcal{S}$	$3(\mathbf{1} + \mathcal{R})$

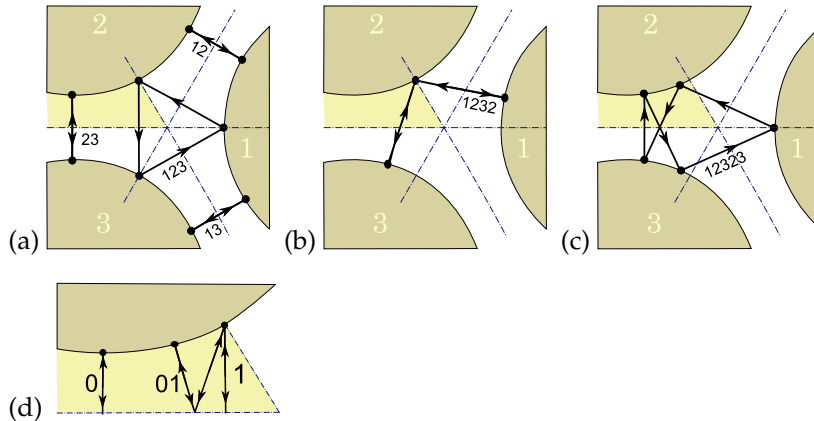


Figure 4.9: The 3-disk pinball orbits: (a) $\bar{1}2$, $\bar{1}3$, $\bar{2}3$, $\bar{1}23$; the clockwise $\bar{1}32$ not drawn. (b) Orbit $\bar{1}232$; the symmetry related $\bar{1}213$ and $\bar{1}323$ not drawn. (c) Orbit $\bar{1}2323$; orbits $\bar{1}2123$, $\bar{1}2132$, $\bar{1}2313$, $\bar{1}3131$ and $\bar{1}3232$ not drawn. (d) The fundamental domain, i.e., the light-shaded 1/6th wedge in (a), consisting of a section of a disk, two segments of symmetry axes acting as straight mirror walls, and the escape gap to the left. The above 14 full-space orbits restricted to the fundamental domain and recoded in binary reduce to the two fixed points $\bar{0}$, $\bar{1}$, period-2 orbit $\bar{1}\bar{0}$, and period-5 orbit 00111 (not drawn).

CHAPTER 4. GROUP THEORY

Example 4.23. Subgroups, cosets of D_3 . (Continued from example ??) 2CB
The 3-disks symmetry group, the D_3 dihedral group (??) has six subgroups

$$\{e\}, \quad \{e, s\}, \quad \{e, s_1\}, \quad \{e, s_2\}, \quad \{e, r, r_2\}, \quad D_3. \quad (4.244)$$

The left cosets of subgroup $D_1 = \{e, s\}$ are $\{r, s_1\}, \{r_2, s_2\}$. The coset of subgroup $C_3 = \{e, r, r_2\}$ is $\{s, s_1, s_2\}$. The significance of the coset is that if a solution has a symmetry H , for example the symmetry of a 3-cycle $\overline{123}$ is C_3 , then all elements in a coset act on it the same way, for example $\{s, s_1, s_2\}\overline{123} = \overline{132}$.

The nontrivial subgroups of D_3 are $D_1 = \{e, \sigma\}$, consisting of the identity and any one of the reflections, of order 2, and $C_3 = \{e, r, r_2\}$, of order 3, so possible cycle multiplicities are $|G|/|G_p| = 1, 2, 3$ or 6. Only the fixed point at the origin has full symmetry $G_p = G$. Such equilibria exist for smooth potentials, but not for the 3-disk billiard. Examples of other multiplicities are given in figure 4.9 and figure ???. (continued in example 4.24)

[click to return: p. ??](#)

Example 4.24. Classes of D_3 . (Continued from example 4.23) 2CB
The three classes of the 3-disk symmetry group $D_3 = \{e, r, r_2, s, s_1, s_2\}$, are the identity, any one of the reflections, and the two rotations,

$$\{e\}, \quad \left\{ \begin{array}{c} s \\ s_1 \\ s_2 \end{array} \right\}, \quad \left\{ \begin{array}{c} r \\ r_2 \end{array} \right\}. \quad (4.245)$$

In other words, the group actions either flip or rotate. (continued in example ??)

[click to return: p. ??](#)

Example 4.25. Cyclic groups. The cyclic group $C_n \subset SO(2)$ (sometimes called Z_n) of order n is generated by one element a shift r , the $1/n$ circle rotation by $2\pi/n$.

2CB

[click to return: p. ??](#)

Example 4.26. Character table of cyclic group C_n . The symmetry under a discrete rotation by angle $2\pi/n$ gives birth to a cyclic group $C_n = \{e, r, r^2, \dots, r^{n-1}\}$. Since C_n is Abelian, each element forms a separate class, and thus C_n has n one-dimensional irreducible representations. The characters multiply as group elements: $\chi_\alpha(r^i)\chi_\alpha(r^j) = \chi_\alpha(r^{i+j}) \pmod{n}$. Therefore, we get table 4.14. (X. Ding,)

[click to return: p. 270](#)

Example 4.27. Dihedral groups. The dihedral group $D_n \subset O(2)$, $n = 1, 2, 3, \dots$ (sometimes called C_{nv}), can be generated by two elements one at least of which must orientation reversing. For example, take s corresponding to reflection across the x -axis. $s^2 = e$; such operation is called an involution. r to rotation through $2\pi/n$, then $D_n = \langle s, r \rangle$, and the defining relations are $s^2 = r^n = e, (rs)^2 = e$.

2CB

[click to return: p. ??](#)

Example 4.28. D_4 reflection symmetric, antisymmetric permutation representation subspaces. The characteristic equation $s^2 = 1$, with eigenvalues $\{+1, -1\}$, enables us to start the symmetry reduction of the n -dimensional permutation representation of D_n by splitting it into the reflection symmetric or antisymmetric subspaces by means of projection operators.

When the period n of the lattice states is even, there are two classes of reflections. For example, when the period of the lattice states is 4, reflection operators s and $s_1 = sr$ (see example 4.17) belong to distinct dihedral group D_4 classes:

$$s = \begin{bmatrix} 0 & 0 & 0 & 1 \\ 0 & 0 & 1 & 0 \\ 0 & 1 & 0 & 0 \\ 1 & 0 & 0 & 0 \end{bmatrix}, \quad s_1 = \begin{bmatrix} 0 & 0 & 1 & 0 \\ 0 & 1 & 0 & 0 \\ 1 & 0 & 0 & 0 \\ 0 & 0 & 0 & 1 \end{bmatrix}, \quad (4.246)$$

where r is the shift matrix. Either one splits the n -dimensional permutation representation of D_n into the reflection symmetric and antisymmetric subspaces. For s the two projection operators are

$$\begin{aligned} P_{0+} &= \frac{s - (-1)\mathbf{1}}{1 - (-1)} = \frac{1}{2} \begin{bmatrix} 1 & 0 & 0 & 1 \\ 0 & 1 & 1 & 0 \\ 0 & 1 & 1 & 0 \\ 1 & 0 & 0 & 1 \end{bmatrix} \\ P_{0-} &= \frac{s - \mathbf{1}}{-1 - 1} = \frac{1}{2} \begin{bmatrix} 1 & 0 & 0 & -1 \\ 0 & 1 & -1 & 0 \\ 0 & -1 & 1 & 0 \\ -1 & 0 & 0 & 1 \end{bmatrix}, \end{aligned} \quad (4.247)$$

and for s_1 they are

$$\begin{aligned} P_{1+} &= \frac{\mathbf{1} - (-1)s_1}{1 + 1} = \frac{1}{2} \begin{bmatrix} 1 & 0 & 1 & 0 \\ 0 & 2 & 0 & 1 \\ 1 & 0 & 1 & 0 \\ 0 & 0 & 0 & 2 \end{bmatrix} \\ P_{1-} &= \frac{\mathbf{1} + (-1)s_1}{1 + 1} = \frac{1}{2} \begin{bmatrix} 1 & 0 & -1 & 0 \\ 0 & 0 & 0 & 0 \\ -1 & 0 & 1 & 0 \\ 0 & 0 & 0 & 0 \end{bmatrix}. \end{aligned} \quad (4.248)$$

Either splits the n -dimensional permutation representation, but in a different way. The dimensions $d_\alpha = \text{Tr } P_\alpha$ of the pairs of subspaces are $d_{s+} = 2$, $d_{s-} = 2$, and $d_{s_1+} = 3$, $d_{s_1-} = 1$. They are reducible further by each other, and by the translation operator characteristic equation $r^4 = 1$. Of course, there is no reason to single out reflection operators s and s_1 . For a systematic, all commuting operator approach, see example 4.31 for the Burnside, class operator full reduction.

[click to return: p. 737](#)

Example 4.29. D_6 reflection symmetric, antisymmetric permutation representation subspaces. The characteristic equation $s^2 = 1$, with eigenvalues $\{+1, -1\}$, enables us to start the symmetry reduction of the n -dimensional permutation representation of D_n by splitting it into the reflection symmetric or antisymmetric subspaces by means of projection operators.

When the period n of the lattice states is even, there are two classes of reflections. For example, when the period of the lattice states is 6, reflection operators s and r_s belong to distinct dihedral group D_6 classes:

$$s = \begin{bmatrix} 0 & 0 & 0 & 0 & 0 & 1 \\ 0 & 0 & 0 & 0 & 1 & 0 \\ 0 & 0 & 0 & 1 & 0 & 0 \\ 0 & 0 & 1 & 0 & 0 & 0 \\ 0 & 1 & 0 & 0 & 0 & 0 \\ 1 & 0 & 0 & 0 & 0 & 0 \end{bmatrix}, \quad (4.249)$$

CHAPTER 4. GROUP THEORY

and²¹

$$rs = \begin{bmatrix} 1 & 0 & 0 & 0 & 0 & 0 \\ 0 & 0 & 0 & 0 & 0 & 1 \\ 0 & 0 & 0 & 0 & 1 & 0 \\ 0 & 0 & 0 & 1 & 0 & 0 \\ 0 & 0 & 1 & 0 & 0 & 0 \\ 0 & 1 & 0 & 0 & 0 & 0 \end{bmatrix}, \quad (4.250)$$

where r is the shift matrix. Either one splits the n -dimensional permutation representation of D_n into the reflection symmetric and antisymmetric subspaces. For s the two projection operators are

$$\begin{aligned} P_{0+} &= \frac{s - (-1)\mathbf{1}}{1 - (-1)} = \frac{1}{2} \begin{bmatrix} 1 & 0 & 0 & 0 & 0 & 1 \\ 0 & 1 & 0 & 0 & 1 & 0 \\ 0 & 0 & 1 & 1 & 0 & 0 \\ 0 & 0 & 1 & 1 & 0 & 0 \\ 0 & 1 & 0 & 0 & 1 & 0 \\ 1 & 0 & 0 & 0 & 0 & 1 \end{bmatrix} \\ P_{1-} &= \frac{rs - \mathbf{1}}{-1 - 1} = \frac{1}{2} \begin{bmatrix} 0 & 0 & 0 & 0 & 0 & 0 \\ 0 & 1 & 0 & 0 & 0 & -1 \\ 0 & 0 & 1 & 0 & -1 & 0 \\ 0 & 0 & 0 & 0 & 0 & 0 \\ 0 & 0 & -1 & 0 & 1 & 0 \\ 0 & -1 & 0 & 0 & 0 & 1 \end{bmatrix}, \end{aligned} \quad (4.251)$$

and for rs they are

$$\begin{aligned} P_{0-} &= \frac{s - \mathbf{1}}{-1 - 1} = \frac{1}{2} \begin{bmatrix} 1 & 0 & 0 & 0 & 0 & -1 \\ 0 & 1 & 0 & 0 & -1 & 0 \\ 0 & 0 & 1 & -1 & 0 & 0 \\ 0 & 0 & -1 & 1 & 0 & 0 \\ 0 & -1 & 0 & 0 & 1 & 0 \\ -1 & 0 & 0 & 0 & 0 & 1 \end{bmatrix} \\ P_{1+} &= \frac{rs - (-1)\mathbf{1}}{1 - (-1)} = \frac{1}{2} \begin{bmatrix} 2 & 0 & 0 & 0 & 0 & 0 \\ 0 & 1 & 0 & 0 & 0 & 1 \\ 0 & 0 & 1 & 0 & 1 & 0 \\ 0 & 0 & 0 & 2 & 0 & 0 \\ 0 & 0 & 1 & 0 & 1 & 0 \\ 0 & 1 & 0 & 0 & 0 & 1 \end{bmatrix}. \end{aligned} \quad (4.252)$$

Either splits the n -dimensional permutation representation, but in a different way. The dimensions $d_\alpha = \text{Tr } P_\alpha$ of the pairs of subspaces are $d_{0+} = 3$, $d_{0-} = 3$, and $d_{1+} = 4$, $d_{1-} = 2$. They are reducible further by each other, and by the translation operator characteristic equation $r^6 = 1$. Of course, there is no reason to single out reflection operators s and rs . For a systematic, all commuting operator approach, see example 4.31 for the Burnside, class operator full reduction.

(H. Liang, 2021-05-11)

[click to return: p. 930](#)

²¹Predrag 2021-07-25: I would prefer $s_1 = sr$, to be consistent with the wiki convention of example 4.17.

Example 4.30. *D₃ multiplication tables and the permutation rep.* For period-3 lattice states, the class operators are the identity $\mathbf{1}$ and

$$\mathcal{R} = \begin{bmatrix} 0 & 1 & 1 \\ 1 & 0 & 1 \\ 1 & 1 & 0 \end{bmatrix}, \quad \mathcal{S} = \begin{bmatrix} 1 & 1 & 1 \\ 1 & 1 & 1 \\ 1 & 1 & 1 \end{bmatrix} = \mathbf{1} + \mathcal{R}, \quad (4.253)$$

so either \mathcal{R} or \mathcal{S} can be eliminated from the class multiplication table 4.11. In the spirit of the presentation of a dihedral group in terms of two flips, let's eliminate $\mathcal{R} = \mathcal{S} - \mathbf{1}$:

D ₃	$\mathbf{1}$	\mathcal{S}	
$\mathbf{1}$	$\mathbf{1}$	\mathcal{S}	
\mathcal{S}	\mathcal{S}	$3\mathcal{S}$	

(4.254)

From this D₃ class operator multiplication table follows the Hamilton-Cayley equation for its 3-dimensional permutation rep, with two eigenvalues,

$$\mathcal{S}(\mathcal{S} - 3\mathbf{1}) = 0, \quad (4.255)$$

with projection operators

λ	projection op.	d
3	$P_3 = \mathcal{S}/3$	1
0	$P_0 = (3\mathbf{1} - \mathcal{S})/3$	2

(4.256)

Note that the zero-eigenvalue P_0 is the Laplacian operator.

Take orbit Jacobian matrix of form common to both the temporal cat (5.83) and the temporal Hénon (3.85), and use the spectral resolution $\mathbf{1} = P_0 + P_3$:

$$d = 3 \quad \mathcal{J} = \begin{bmatrix} -\mathcal{J}_{00} & 1 & 1 \\ 1 & -\mathcal{J}_{11} & 1 \\ 1 & 1 & -\mathcal{J}_{22} \end{bmatrix} = P_0 - (\mathcal{J} - \mathbf{1}), \quad (4.257)$$

Study also [wiki: Character of the permutation representation](#).

Dixon, J. D. and Mortimer, Permutation Groups, Springer

click to return: p. 266

Example 4.31. *D₆ multiplication tables.* From the D₆ class operator multiplication table follow the Hamilton-Cayley equations (for any matrix representation; in our application (??) that is the 6-dimensional matrix representation of permutations), with 16 eigenvalues as listed,²²

$$\begin{aligned} (\mathcal{R}_3 - \mathbf{1})(\mathcal{R}_3 + \mathbf{1}) &= 0 \\ (\mathcal{R}_1 - \mathbf{1})(\mathcal{R}_1 + \mathbf{1})(\mathcal{R}_1 - 2\mathbf{1})(\mathcal{R}_1 + 2\mathbf{1}) &= 0 \\ (\mathcal{R}_2 - \mathbf{1})(\mathcal{R}_2 + \mathbf{1})(\mathcal{R}_2 - 2\mathbf{1})(\mathcal{R}_2 + 2\mathbf{1}) &= 0 \\ \mathcal{S}_0(\mathcal{S}_0 - 3\mathbf{1})(\mathcal{S}_0 + 3\mathbf{1}) &= 0 \\ \mathcal{S}_1(\mathcal{S}_1 - 3\mathbf{1})(\mathcal{S}_1 + 3\mathbf{1}) &= 0, \end{aligned} \quad (4.258)$$

²²Predrag 2021-06-16: \mathcal{R}_2 is a guess, I have not derived it.

Table 4.12: The D_6 Cayley table (group multiplication (3.135) table), and the class operator multiplication table. The class operator multiplication table is symmetric under transposition, so it suffices to fill up the upper half-triangular region. The 6 classes correspond to 4 1-dimensional irreps, and the 2 1-dimensional irreps.

D_6	1	r^3	r	r^5	r^2	r^4	s	s_2	s_4	s_1	s_3	s_5
1	1	r^3	r	r^5	r^2	r^4	s	s_2	s_4	s_1	s_3	s_5
r^3	r^3	1	r^4	r^2	r^5	r	s_3	s_5	s_1	s	s_1	s_2
r	r	r^4	r^2	1	r^3	r^5	s_1	s_3	s_5	s_2	s_4	s
r^5	r^5	r^2	1	r^4	r	r^3	s_5	s_1	s_3	s	s_2	s_4
r^2	r^2	r^5	r^3	r	r^4	1	s_2	s_4	s	s_3	s_5	s_1
r^4	r^4	r	r^5	r^3	1	r^2	s_4	s	s_2	s_5	s_1	s_3
s	s	s_3	s_1	s_5	s_2	s_4	1	r^4	r^2	r^5	r^3	r
s_2	s_2	s_5	s_3	s_1	s_4	s	r^2	1	r^4	r	r^5	r^3
s_4	s_4	s_2	s_5	s_3	s	s_2	r^4	r^2	1	r^3	r	r^5
s_1	s_1	s_4	s_2	s	s_3	s_5	r	r^5	r^3	1	r^4	r^2
s_3	s_3	s	s_4	s_2	s_5	s_1	r^3	r	r^5	r^2	1	r^4
s_5	s_5	s_3	s	s_4	s_1	s_3	r^5	r^3	r	r^4	r^2	1

D_6	$\mathbf{1}$	\mathcal{R}_3	\mathcal{R}_1	\mathcal{R}_2	\mathcal{S}_0	\mathcal{S}_1
$\mathbf{1}$	$\mathbf{1}$	\mathcal{R}_3	\mathcal{R}_1	\mathcal{R}_2	\mathcal{S}_0	\mathcal{S}_1
\mathcal{R}_3	.	$\mathbf{1}$	\mathcal{R}_2	\mathcal{R}_1	\mathcal{S}_1	\mathcal{S}_0
\mathcal{R}_1	.	.	$2\mathbf{1}+\mathcal{R}_2$	$2\mathcal{R}_3+\mathcal{R}_1$	$2\mathcal{S}_1$	$2\mathcal{S}_0$
\mathcal{R}_2	.	.	.	$2\mathbf{1}+\mathcal{R}_2$	$2\mathcal{S}_0$	$2\mathcal{S}_1$
\mathcal{S}_0	$3(\mathbf{1}+\mathcal{R}_2)$	$3(\mathcal{R}_3+\mathcal{R}_1)$
\mathcal{S}_1	$3(\mathbf{1}+\mathcal{R}_2)$

so there is lots of redundancy - there are only 6 irreps.

$$\begin{aligned}
 \mathcal{R}_3 : \lambda = 1 &\rightarrow P_1 = (\mathbf{1} + \mathcal{R}_3)/2 \\
 \mathcal{R}_3 : \lambda = -1 &\rightarrow P_{-1} = (\mathbf{1} - \mathcal{R}_3)/2 \\
 \mathcal{S}_0 : \lambda = 0 &\rightarrow P_{0,0} = (2\mathbf{1} - \mathcal{R}_2)/3 \\
 \mathcal{S}_0 : \lambda = 3 &\rightarrow P_{0,3} = (\mathbf{1} + \mathcal{R}_2 + \mathcal{S}_0)/6 \\
 \mathcal{S}_0 : \lambda = -3 &\rightarrow P_{0,-3} = (\mathbf{1} + \mathcal{R}_2 - \mathcal{S}_0)/6 \\
 \mathcal{S}_1 : \lambda = 0 &\rightarrow P_{1,0} = P_{0,0} \\
 \mathcal{S}_1 : \lambda = 3 &\rightarrow P_{1,3} = (\mathbf{1} + \mathcal{R}_2 + \mathcal{S}_1)/6 \\
 \mathcal{S}_1 : \lambda = -3 &\rightarrow P_{1,-3} = (\mathbf{1} + \mathcal{R}_2 - \mathcal{S}_1)/3. \tag{4.259}
 \end{aligned}$$

Split $P_{0,-3}$ using P_1 :

$$P_1 P_{0,-3} = (\mathbf{1} + \mathcal{R}_3 + \mathcal{R}_1 + \mathcal{R}_2 - \mathcal{S}_0 - \mathcal{S}_1)/12. \tag{4.260}$$

\mathcal{S}_j equations are the same form as for D_3 1-dimensional irrep, so the number of such equations presumably equals the number of 1-dimensional irrep, and the same for \mathcal{R}_j , $j \neq n/2$ equations.

\mathcal{S}_j equations presumably contain symmetric/antisymmetric solutions, in the spirit of (4.249) and (4.250).

For even dimensions $\mathcal{R}_{n/2}$ presumably leads to 4 1-dimensional irreps, of which I assume the two antisymmetric ones do not contribute to then-dimensional matrix representation of permutations, while all 1-dimensional irrep do.

That is probably easier to count using the character formulas.

click to return: p. 266

Example 4.32. D_6 permutation rep. For period-6 lattice states, the class operators are the identity, and:

$$\mathcal{R}_3 = \begin{bmatrix} 0 & 0 & 0 & 1 & 0 & 0 \\ 0 & 0 & 0 & 0 & 1 & 0 \\ 0 & 0 & 0 & 0 & 0 & 1 \\ 1 & 0 & 0 & 0 & 0 & 0 \\ 0 & 1 & 0 & 0 & 0 & 0 \\ 0 & 0 & 1 & 0 & 0 & 0 \end{bmatrix}, \tag{4.261}$$

$$\mathcal{R}_1 = \left[\begin{array}{ccc|ccc} 0 & 1 & 0 & 0 & 0 & 1 \\ 1 & 0 & 1 & 0 & 0 & 0 \\ 0 & 1 & 0 & 1 & 0 & 0 \end{array} \right], \quad \mathcal{R}_2 = \left[\begin{array}{ccc|ccc} 0 & 0 & 1 & 0 & 1 & 0 \\ 0 & 0 & 0 & 1 & 0 & 1 \\ 1 & 0 & 0 & 0 & 1 & 0 \end{array} \right]. \tag{4.262}$$

$$\mathcal{S}_0 = \left[\begin{array}{ccc|ccc} 0 & 1 & 0 & 1 & 0 & 1 \\ 1 & 0 & 1 & 0 & 1 & 0 \\ 0 & 1 & 0 & 1 & 0 & 1 \\ 1 & 0 & 1 & 0 & 1 & 0 \\ 0 & 1 & 0 & 1 & 0 & 1 \\ 1 & 0 & 1 & 0 & 1 & 0 \end{array} \right], \quad \mathcal{S}_1 = \left[\begin{array}{ccc|ccc} 1 & 0 & 1 & 0 & 1 & 0 \\ 0 & 1 & 0 & 1 & 0 & 1 \\ 1 & 0 & 1 & 0 & 1 & 0 \\ 0 & 1 & 0 & 1 & 0 & 1 \\ 1 & 0 & 1 & 0 & 1 & 0 \\ 0 & 1 & 0 & 1 & 0 & 1 \end{array} \right]. \tag{4.263}$$

CHAPTER 4. GROUP THEORY

The reflection operators eigenvalues are $+1$ and -1 , corresponding to the reflection symmetric and antisymmetric subspaces.

To compute the dimensions of irreps obtained from (4.258), we need the characters of the permutation representation class operators:

$$\text{tr } \mathbf{1} = 6, \text{tr } \mathcal{R}_3 = 0, \text{tr } \mathcal{R}_1 = 0, \text{tr } \mathcal{R}_2 = 0, \text{tr } \mathcal{S}_0 = 0, \text{tr } \mathcal{S}_1 = 6. \quad (4.264)$$

(Predrag: I do not see why \mathcal{S}_1 is special...) In particular, we have a vanishing dimension $\lambda = -3$ representation, so

$$\mathcal{S}_1, \lambda = -3 \rightarrow P_{1,-3} = (\mathbf{1} + \mathcal{R}_2 - \mathcal{S}_1)/2 = 0, \quad (4.265)$$

Taking trace of (4.260) we find that also $P_1 P_{0,-3}$ is 0-dimensional, so, 6-dimensional permutation representation is not faithful, and the classes are not independent (you can check this by inspecting eqs. (4.263) to (4.262)):

$$\begin{aligned} \mathcal{S}_0 &= \mathcal{R}_3 + \mathcal{R}_1 \\ \mathcal{S}_1 &= \mathbf{1} + \mathcal{R}_2, \end{aligned} \quad (4.266)$$

so forget the last two equations in (4.258) for the n -dimensional permutation representations of D_n . I think it is clear from (4.260) that this means no antisymmetric 1-dimensional reps.

Lecturing about the "projector analysis" of D_3 I was such a fool - I forgot to follow [birdtracks.eu](#), which explains very clearly that whenever there is a matrix equation $=0$, that means a relationship between matrices, they are not independent.

Now one can eliminate S_j from projection operators (4.259):

$$\begin{aligned} \mathcal{S}_0 : \lambda = 3 &\rightarrow P_{0,3} = (\mathbf{1} + \mathcal{R}_3 + \mathcal{R}_1 + \mathcal{R}_2)/6 \\ \mathcal{S}_1 : \lambda = 3 &\rightarrow P_{1,3} = (\mathbf{1} + \mathcal{R}_2)/3, \end{aligned} \quad (4.267)$$

To summarize - this is rather inelegant, but the main result is that the flip classes $\mathcal{S}_0, \mathcal{S}_1, \mathcal{S}_2, \dots$ do not contribute to the reduction of the permutation representation; is can be done purely in terms of the rotation classes $\mathcal{R}_1, \mathcal{R}_3, \mathcal{R}_3, \dots$. This strikes me as a big deal, as this is isomorphic - I believe - to the cyclic group $C_{n/2}$ (for the even period n). I tentative submit table 4.13 being sufficient to construct all irreducible projection operators. Of course, C_6 is the only normal subgroup of D_6 , but we do not use that - we use only 4 classes rather than the 6 of C_6 . Looks pretty illegal:)

Can you check that you get 2 symmetric 1-dimensional irreps, and the two 1-dimensional ones?

[click to return: p. 266](#)

Example 4.33. Character table of dihedral group D_n , n odd. The D_n group

2CB

$$D_n = \{e, r, r^2, \dots, r^{n-1}, s, rs, \dots, r^{n-1}s\}$$

has n rotation elements and n reflections. Group elements satisfies $r^i \cdot r^j s = r^j s \cdot r^{n-i}$, so r^i and r^{n-i} form a class. Also, $r^{n-i} \cdot r^{2i+j}s = r^j s \cdot r^{n-i}$ implies that $r^j s$ and $r^{2i+j}s$ are in the same class. Therefore, there are only three different types of classes: $\{e\}$, $\{r^k, r^{n-k}\}$ and $\{s, rs, \dots, r^{n-1}s\}$. The total number of classes is $(n+3)/2$. In this case, there are 2 one-dimensional irreducible representations (symmetric A_1 and antisymmetric A_2) and $(n-1)/2$ two-dimensional irreducible representations. In the j th two-dimensional irreducible representation, class $\{e\}$ has form $(\begin{smallmatrix} 1 & 0 \\ 0 & 1 \end{smallmatrix})$, class $\{r^k, r^{n-k}\}$ has form $(\begin{smallmatrix} \exp(\frac{i2\pi kj}{n}) & 0 \\ 0 & \exp(-\frac{i2\pi kj}{n}) \end{smallmatrix})$, and class $\{s, rs, \dots, r^{n-1}s\}$ has form $(\begin{smallmatrix} 0 & 1 \\ 1 & 0 \end{smallmatrix})$. We get table 4.15.

(X. Ding,)

[click to return: p. 270](#)

Table 4.13: A tentative D_6 class operator multiplication table restricted to the permutations matrix representation, with flip classes eliminated using (4.266).

D_6	$\mathbf{1}$	\mathcal{R}_3	\mathcal{R}_1	\mathcal{R}_2
$\mathbf{1}$	$\mathbf{1}$	\mathcal{R}_3	\mathcal{R}_1	\mathcal{R}_2
\mathcal{R}_3	.	$\mathbf{1}$	\mathcal{R}_2	\mathcal{R}_1
\mathcal{R}_1	.	.	$2\mathbf{1} + \mathcal{R}_2$	$2\mathcal{R}_3 + \mathcal{R}_1$
\mathcal{R}_2	.	.	.	$2\mathbf{1} + \mathcal{R}_2$

Table 4.14: Character table of cyclic group C_n . Here $k, j = 1, 2, \dots, n - 1$.

C_n	A	Γ_j
e	1	1
r^k	1	$\exp\left(\frac{i2\pi kj}{n}\right)$

Example 4.34. Character table of dihedral group D_n , n even. In this case, there are $\frac{(n+6)}{2}$ classes: $\{e\}$, $\{r_{n/2}\}$, $\{r_k, r_{n-k}\}$, $\{s, sr_2, \dots, sr_{n-2}\}$ and $\{sr_1, sr_3, \dots, sr_{n-1}\}$. There are four different one-dimensional irreducible representations, whose characters are ± 1 under reflection s and translate-reflect operation sr_1 . We get table 4.16. (X. Ding,)

click to return: p. 270

Example 4.35. D_1 factorization. (Continued from example 4.11)

Depending on the maximal symmetry group \mathcal{H}_p that leaves an orbit p invariant (see refsects degene Dynami as well as example 4.7), the contributions to the full state space dynamical zeta function factor as

$$\begin{aligned} \mathcal{H}_p = \{e\} : \quad (1 - t_{\hat{p}})^2 &= (1 - t_{\hat{p}})(1 - t_{\hat{p}}) \\ \mathcal{H}_p = \{e, s\} : \quad (1 - t_{\hat{p}}^2) &= (1 - t_{\hat{p}})(1 + t_{\hat{p}}), \end{aligned} \quad (4.268)$$

For example:

$$\begin{aligned} \mathcal{H}_{RRL} = \{e\} : \quad (1 - t_{RRL})^2 &= (1 - t_{001})(1 - t_{001}) \\ \mathcal{H}_{RL} = \{e, s\} : \quad (1 - t_{RL}) &= (1 - t_0)(1 + t_0), \quad \text{where } t_{RL} = t_0^2. \end{aligned}$$

The A_1 subspace dynamical zeta function has the same form as the full state space \mathcal{M} binary expansion refeq curvbin:

$$\begin{aligned} 1/\zeta_{A_1} &= 1 - t_0 - t_1 - (t_{01} - t_1 t_0) - (t_{001} - t_0 t_{10}) - (t_{011} - t_1 t_{10}) \\ &\quad - (t_{0001} - t_0 t_{001}) - (t_{0111} - t_1 t_{011}) \\ &\quad - (t_{0011} - t_{001} t_1 - t_0 t_{011} + t_0 t_{01} t_1) - \dots. \end{aligned} \quad (4.269)$$

The form is the same, however, the weights $t_{\hat{p}}$ are different - a symmetric orbit weight is a square root of the corresponding full state space orbit weight. The asymmetric orbits retain the same weight, but contribute only once.

Table 4.15: Character table of dihedral group D_n , n odd.

D_n (n odd)	A_1	A_2	E_j
e	1	1	2
r^k, r^{n-k}	1	1	$2 \cos(\frac{2\pi k j}{n})$
s, sr^1, \dots, sr^{n-1}	1	-1	0

Table 4.16: Character table of dihedral group D_n , n even. Here $k, j = 1, 2, \dots, n - 1$.

D_n (n even)	A_1	A_2	B_1	B_2	E_j
e	1	1	1	1	2
$r_{1/2}$	1	1	$(-1)^{n/2}$	$(-1)^{n/2}$	$2(-1)^j$
r_k, r_{n-k} (k odd)	1	1	-1	-1	$2 \cos(\frac{2\pi k j}{n})$
r_k, r_{n-k} (k even)	1	1	1	1	$2 \cos(\frac{2\pi k j}{n})$
s, sr_2, \dots, sr_{n-2}	1	-1	1	-1	0
$sr_1, sr_3, \dots, sr_{n-1}$	1	-1	-1	1	0

The antisymmetric A_2 subspace dynamical zeta function ζ_{A_2} differs from ζ_{A_1} by a minus sign for cycles with an odd number of 0's:

$$\begin{aligned}
 1/\zeta_{A_2} &= (1 + t_0)(1 - t_1)(1 + t_{10})(1 - t_{100})(1 + t_{101})(1 + t_{1000}) \\
 &\quad (1 - t_{1001})(1 + t_{1011})(1 - t_{10000})(1 + t_{10001}) \\
 &\quad (1 + t_{10010})(1 - t_{10011})(1 - t_{10101})(1 + t_{10111}) \dots \\
 &= 1 + t_0 - t_1 + (t_{10} - t_1 t_0) - (t_{100} - t_{10} t_0) + (t_{101} - t_{10} t_1) \\
 &\quad - (t_{1001} - t_1 t_{100} - t_{101} t_0 + t_{10} t_0 t_1) - \dots \dots \tag{4.270}
 \end{aligned}$$

Note that the group theory factors do not destroy the curvature corrections (the cycles and pseudo cycles are still arranged into shadowing combinations).

If the system under consideration has a boundary orbit (cf. respect bound- σ) with group-theoretic factor $h_p = (e + \sigma)/2$, the boundary orbit does not contribute to the antisymmetric subspace

$$\text{boundary: } (1 - t_p) = (1 - t_{\bar{p}})(1 - 0t_{\bar{p}}) \tag{4.271}$$

This is the $1/\zeta$ part of the boundary orbit factorization discussed in example 4.7, where the factorization of the corresponding spectral determinants for the 1-dimensional reflection symmetric maps is worked out in detail.

[click to return: p. 266](#)

Example 4.36. D_1 -symmetry factorization of the temporal Bernoulli zeta function.

²³ For the particularly simple, linear Bernoulli case at hand, the field x_t is a scalar, the

²³Predrag 2021-08-03: Making up the Bernoulli D_1 -symmetry example, will need it for LC21.

1-time step [1×1] time-evolution Jacobian matrix (7.20) at every lattice point t is simply $\mathbb{J}_t = s$, and the orbit Jacobian matrix (3.31) is the same for all, in general distinct lattice states of period n , so

$$N_n = |\text{Det } \mathcal{J}| = s^n - 1; \quad (4.272)$$

all itineraries are allowed, except that the periodicity of $r^n = 1$ accounts for $\bar{0}$ and $\bar{s-1}$ fixed points (see figure 3.2) being a single periodic point.

For a Bernoulli system (4.272),

$$\begin{aligned} 1/\zeta_{top}(z) &= \exp\left(-\sum_{n=1}^{\infty} \frac{z^n}{n}(s^n - 1)\right) = \exp[\ln(1-sz) - \ln(1-z)] \\ &= \frac{1-sz}{1-z}. \end{aligned} \quad (4.273)$$

The numerator $(1-sz)$ says that a Bernoulli system is a full shift [26]: there are s fundamental lattice states, in this case fixed points $\{x_0, x_1, \dots, x_{s-1}\}$, and every other lattice state is built from their concatenations and repeats. The denominator $(1-z)$ compensates for the single overcounted lattice state, the fixed point $x_{s-1} = x_0 \pmod{1}$ of figure 3.2 and its repeats.

The dynamical D_1 -symmetry factorized zeta function, analogous to (4.183), follows from (4.268):

$$\begin{aligned} \frac{1}{\zeta(z)} &= \frac{1}{\zeta_{A_1}(t)} \frac{1}{\zeta_{A_1}(-t)}, \quad z = t^2, s = \mu^2 \\ \frac{1}{\zeta_{A_1}(t)} &= \frac{1-\mu t}{1-t}. \end{aligned} \quad (4.274)$$

The antisymmetric A_2 subspace dynamical zeta function ζ_{A_2} differs from ζ_{A_1} only by a minus sign for cycles with an odd number of 1's, see (4.270). At the level of the linear Bernoulli map, this seems a triviality, but for a nonlinear example 4.11, it is not; all cycles are computed numerically in the D_1 -symmetry-reduced fundamental domain figure 4.8.

click to return: p. ??

Example 4.37. XXX.

4.11 Discrete factorization of the dynamical zeta function

²⁴ When a dynamical system has a discrete symmetry, the cycle averaging formula can be simplified substantially, and the expansion needs much fewer orbits to achieve the desired accuracy. In this section, we discuss how the dynamical zeta function can be factorized by a product of contributions from each irreps of this discrete symmetry.

4.11.1 Factorization of C_3 and D_3

C_3 has two subgroups $\{e\}$ and $\{e, r, r_2\}$, so there are two types of periodic orbits as shown in figure 4.10. A type-(a) orbit has symmetry $\{e\}$, i.e., no sym-

²⁴Predrag 2021-06-19: A copy of the 2017-03-09 Xiong Ding's section, not included in his thesis siminos/xiong/thesis/chapters/symFactor.tex.

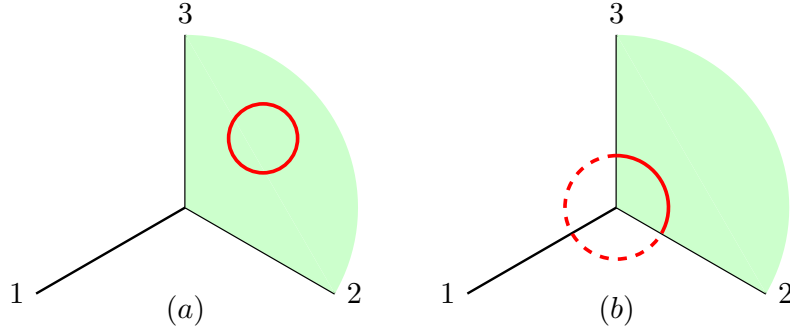


Figure 4.10: The two different kinds of periodic orbits in a system with C_3 symmetry. The green region is the chosen fundamental domain. The red cycles are periodic orbits.

metry, and it has two replicas by rotation r and r_2 respectively, which are not shown in this figure. So the contribution from a type-(a) orbit to the dynamical zeta function is $(1 - t_p)^3$. The cubic order refers to the fact that there are three sibling orbits together. Also, since the entire orbit is in the fundamental domain, we have

$$1/\zeta_a = (1 - t_{\hat{p}})^3.$$

The hat on p means that $t_{\hat{p}}$ is evaluated only on the part of the orbit that is in the fundamental domain. A type-(b) orbit is invariant under e , r and r_2 . This orbit has no siblings and only one third of this orbit is in the fundamental domain. The other two thirds are replicas by rotation r and r_2 of the part in the fundamental domain. So, its contribution to dynamical zeta function is

$$1/\zeta_b = 1 - t_p = 1 - t_{\hat{p}}^3.$$

Here, relation $t_p = t_{\hat{p}}^3$ is easily obtained by its definition in (??). On the other hand, by example 4.13, we know that the regular representations of e , r , and r_2 are respectively

$$D^{reg}(e) = \begin{bmatrix} 1 & & \\ & 1 & \\ & & 1 \end{bmatrix}, \quad D^{reg}(r) = \begin{bmatrix} & 1 \\ 1 & \end{bmatrix}, \quad D^{reg}(r_2) = \begin{bmatrix} & 1 \\ 1 & \end{bmatrix}.$$

You can easily verify that

$$(1 - t_{\hat{p}})^3 = \det(1 - D^{reg}(e)t_{\hat{p}}), \quad 1 - t_{\hat{p}}^3 = \det(1 - D^{reg}(r)t_{\hat{p}}) = \det(1 - D^{reg}(r_2)t_{\hat{p}}).$$

Therefore, you see that the contribution from periodic orbits to the dynamical zeta function in a system with C_3 symmetry are related to the regular representation of C_3 .

Let us check out another example - a system with D_3 symmetry. D_3 has four different kinds of subgroups $\{e\}$, $\{e, s\}$, $\{e, r, r_2\}$, and D_3 itself. Here s can be

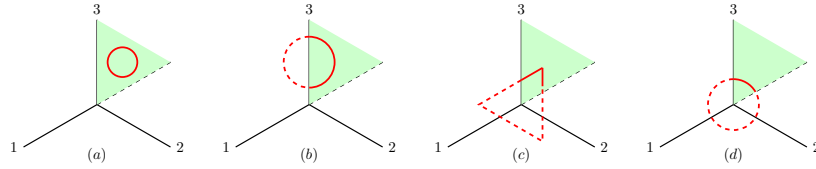


Figure 4.11: The four different kinds of periodic orbits in a system with D_3 symmetry. The green region is the chosen fundamental domain. The red cycles are periodic orbits.

any one of s_{12} , s_{23} or s_{31} . Accordingly, there are four types of periodic orbits as shown in figure 4.11. The fundamental domain is one sixth of the full state space. Similar to the analysis of the two orbits in the C_3 case, we have

$$1/\zeta_a = (1 - t_{\hat{p}})^6, \quad 1/\zeta_b = (1 - t_{\hat{p}}^2)^3, \quad 1/\zeta_c = (1 - t_{\hat{p}}^3)^2, \quad 1/\zeta_d = 1 - t_{\hat{p}}^6.$$

Example ?? gives the regular representation of D_3 . You can also verify that

$$\begin{aligned} (1 - t_{\hat{p}})^6 &= \det(1 - D^{reg}(e)t_{\hat{p}}), & (1 - t_{\hat{p}}^2)^3 &= \det(1 - D^{reg}(s)t_{\hat{p}}) \\ (1 - t_{\hat{p}}^3)^2 &= \det(1 - D^{reg}(r)t_{\hat{p}}), & 1 - t_{\hat{p}}^6 &=? \end{aligned}$$

I leave a question mark above since no analogous expression exists for it. We will come back to it after proving the identity (4.275).

We can generalize the above observation for a system invariant under a general discrete group $G = \{e, g_2, g_3, \dots, g_{|G|}\}$. Let h be an element of G with order (period) m , i.e., m is the smallest positive integer such that $h^m = e$. Then we have

$$(1 - t^m)^{\frac{|G|}{m}} = \det(1 - D^{reg}(h)t). \quad (4.275)$$

The proof starts from the matrix identity $\ln \det = \text{tr } \ln$, by which we have

$$\ln \det(1 - D^{reg}(h)t) = \text{tr} \ln(1 - D^{reg}(h)t) = - \sum_{k=1}^{\infty} \frac{\text{tr } D^{reg}(h^k)t^k}{k}.$$

The last identity above comes from the Taylor expansion $\ln(1-x) = -\sum_{k=1}^{\infty} \frac{x^k}{k}$. As we know, the regular representation of a group element has nonzero trace if and only if this group element is e . So we have,

$$\ln \det(1 - D^{reg}(h)t) = - \sum_{k=1}^{\infty} \frac{|G|t^{mk}}{mk} = - \frac{|G|}{m} \sum_{k=1}^{\infty} \frac{t^{mk}}{k} = \frac{|G|}{m} \ln(1 - t^m).$$

Therefore, we obtain (4.275). This is why we have the observation in the C_3 and D_3 example. However, for the type-(d) orbit in figure 4.11, the symmetry group of this orbit is $\{e, s_{12}, s_{32}, s_{13}, r, r_2\}$. The order of s is 2 while the order of r is 3. The least common multiple is 6. Therefore, the contribution to the dynamical

zeta function is $(1 - t_{\hat{p}}^6)^1$ and it cannot be written as form $\det(1 - D^{reg}(h)t_{\hat{p}})$ with some $h \in G$.

Actually, we can write

$$1 - t_{\hat{p}}^6 = \det(1 - D^{reg}(r)t_{\hat{p}}^2), \quad \text{or} \quad 1 - t_{\hat{p}}^6 = \det(1 - D^{reg}(s)t_{\hat{p}}^3)$$

With $D^{reg}(r)$ the $[3 \times 3]$ representation of r in group C_3 and $D^{reg}(s)$ the $[2 \times 2]$ representation of s in reflection group $\{e, s\}$. Anyway, for the type-(d) orbit we have no choice but to give up the regular representation of D_3 .

4.11.2 Factorization of C_n and D_n

for a discrete symmetry group $G = \{e, g_2, \dots, g_{|G|}\}$. The orthogonality and completeness of projection operator can be easily verified by the orthogonality relation among characters of irreducible representation. Define $\mathcal{L}_\alpha = \mathcal{P}_\alpha \mathcal{L}$, then the trace of evolution operator \mathcal{L} can be decomposed into a sum of $\sum_\alpha \text{tr } \mathcal{L}_\alpha$ because of the completeness of projection operators.²⁵ So we only need to investigate the projected trace formula:

$$\begin{aligned} \text{tr } \mathcal{L}_\alpha &= \frac{d_\alpha}{|G|} \sum_{hg \in G} \chi_\alpha(h) \mathbf{h}^{-1} \int_{\mathcal{M}} dx \mathcal{L}(x, x) \\ &= \frac{d_\alpha}{|G|} \sum_{hg \in G} \chi_\alpha(h) \mathbf{h}^{-1} \sum_{ag \in G} \int_{\tilde{\mathcal{M}}} d(a\tilde{x}) \mathcal{L}(a\tilde{x}, a\tilde{x}) \\ &= \frac{d_\alpha}{|G|} \sum_{hg \in G} \chi_\alpha(h) \mathbf{h}^{-1} \cdot |G| \int_{\tilde{\mathcal{M}}} d(\tilde{x}) \mathcal{L}(\tilde{x}, \tilde{x}) \\ &= d_\alpha \sum_{hg \in G} \chi_\alpha(h) \int_{\tilde{\mathcal{M}}} d\tilde{x} \mathcal{L}(\mathbf{h}^{-1}\tilde{x}, \tilde{x}) \end{aligned}$$

In the above derivation, we have used the invariance of evolution operator under group transform. For a periodic orbit in the fundamental domain \tilde{p} , we follow the standard argument in Chaosbook and get

$$\int_{\tilde{\mathcal{M}}} d\tilde{x} \mathcal{L}(\mathbf{h}^{-1}\tilde{x}, \tilde{x}) = n_{\tilde{p}} \sum_{r=1}^{\infty} \frac{e^{r\beta \cdot A_{\tilde{p}}}}{|\det(\mathbf{1} - \tilde{M}_{\tilde{p}}^r)|} \delta_{n, n_{\tilde{p}} r} \delta_{h, h_{\tilde{p}}^r};$$

so, the spectral determinant is

$$\begin{aligned} F(z) &= \prod_\alpha F_\alpha(z)^{d_\alpha} \\ F_\alpha(z) &= \exp \left(-\sum_{\tilde{p}} \sum_{r=1}^{\infty} \frac{1}{r} \frac{\chi_\alpha(h_{\tilde{p}}^r) z^{n_{\tilde{p}} r} e^{r\beta \cdot A_{\tilde{p}}}}{|\det(\mathbf{1} - \tilde{M}_{\tilde{p}}^r)|} \right), \end{aligned} \quad (4.276)$$

²⁵XD 2014-05-03: Here the decomposition of trace just relies on the completeness of projection operators, we haven't used the commuting relation between evolution operator and group transform. Am I right?

which is discrete factorization for maps. The same method can be applied to flows with discrete symmetry:

$$F_\alpha(z) = \exp \left(-\sum_{\tilde{p}} \sum_{r=1}^{\infty} \frac{1}{r} \frac{\chi_\alpha(h_{\tilde{p}}^r) e^{r(\beta \cdot A_{\tilde{p}} - s T_{\tilde{p}})}}{|\det(\mathbf{1} - \tilde{M}_{\tilde{p}}^r)|} \right)$$

Making an approximation $|\det(\mathbf{1} - \tilde{M}_{\tilde{p}}^r)| \approx |\Lambda_{\tilde{p}}|$ where $\Lambda_{\tilde{p}}$ is the product of all expanding multipliers, we get the factorized zeta function:

$$F_\alpha(z) = \exp \left(-\sum_{\tilde{p}} \sum_{r=1}^{\infty} \frac{1}{r} \chi_\alpha(h_{\tilde{p}}^r) t_{\tilde{p}}^r \right) \quad (4.277)$$

Formula (4.277) is the ultimate goal of Discrete Factorization, which basically tells us that, equipped with character table of the group in question, we can write down all the factorized zeta function for all classes of this group. On the other hand, in order to verify our result, let's calculate the zeta function in the full state space.

$$\begin{aligned} F(z) &= \prod_{\alpha} F_\alpha(z)^{d_\alpha} \\ &= \exp \left(-\sum_{\tilde{p}} \sum_{r=1}^{\infty} \frac{1}{r} \sum_{\alpha} (d_\alpha \chi_\alpha(h_{\tilde{p}}^r)) t_{\tilde{p}}^r \right) \\ &= \exp \left(-\sum_{\tilde{p}} \sum_{r=1}^{\infty} \frac{1}{r} |G| \delta_{h_{\tilde{p}}^r} t_{\tilde{p}}^r \right) \\ &= \exp \left(-\sum_{\tilde{p}} \sum_{k=1}^{\infty} \frac{|G|}{mk} t_{\tilde{p}}^{mk} \right), \end{aligned}$$

that is

$$F(z) = \left(1 - t_{\tilde{p}}^m \right)^m, \quad (4.278)$$

where m is the smallest positive number such that $h_{\tilde{p}}^m = e$, namely the multiplicity of the periodic orbit in the full state space. Formula (4.278) is just the left side of

$$(1 - t_{\tilde{p}}^{h_p})^{g/h_p} = \det(1 - D(h_{\tilde{p}})t_{\tilde{p}}) = \prod_{\alpha} \det(1 - D_{\alpha}(h_{\tilde{p}})t_{\tilde{p}})^{d_{\alpha}} \quad (4.279)$$

in Chaosbook and actually formula (4.277) is the right side of it. For completeness, I derive their equivalence here. By the definition of character and representation of a group, $\chi_{\alpha}(h_{\tilde{p}}^r) = \text{tr } D_{\alpha}(h_{\tilde{p}}^r) = \text{tr } (D_{\alpha}(h_{\tilde{p}}))^r$ where D is the

regular representation of this group, so (4.277) can be rewritten as follows,

$$\begin{aligned} F_\alpha(z) &= \exp \left(-\text{tr} \sum_{\tilde{p}} \sum_{r=1}^{\infty} \frac{1}{r} (D_\alpha(h_{\tilde{p}}))^r t_{\tilde{p}}^r \right) \\ &= \exp \left(\text{tr} \sum_{\tilde{p}} \ln(1 - D_\alpha(h_{\tilde{p}})) \right) \\ &= \prod_{\tilde{p}} \det(1 - D_\alpha(h_{\tilde{p}})) \end{aligned}$$

Here, we have used relation $\text{tr} \ln = \ln \det$. All calculation of factorized zeta function in Chaosbook is conducted by $\det(1 - D_\alpha(h_{\tilde{p}}))$, but I am apt to use (4.277) because it doesn't contain information about any specific representation.²⁶ All the following examples are analyzed by (4.277).

C_n case

When $h_{\tilde{p}} = e$,

$$F_A = F_{\Gamma_j} = \exp \left(- \sum_{r=1}^{\infty} \frac{1}{r} t_{\tilde{p}}^r \right) = 1 - t_{\tilde{p}},$$

Where we only investigate the contribution from one specific periodic orbit and ignore the summation $\sum_{\tilde{p}}$.

When $h_{\tilde{p}} = C_n^k$, Similarly,

$$F_A = 1 - t_{\tilde{p}}$$

$$F_{\Gamma_j} = \exp \left(- \sum_{r=1}^{\infty} \frac{1}{r} e^{\frac{i2\pi k j r}{n}} t_{\tilde{p}}^r \right) = 1 - e^{\frac{i2\pi k j}{n}} t_{\tilde{p}},$$

In sum,

$$\begin{array}{rcl} h_{\tilde{p}} & & A \\ e: & (1 - t_{\tilde{p}})^n & = (1 - t_{\tilde{p}}) & \Gamma_j \\ C_n^k: & (1 - t_{\tilde{p}}^m)^{\frac{n}{m}} & = (1 - t_{\tilde{p}}) & (1 - \exp(\frac{i2\pi k j}{n}) t_{\tilde{p}}) \end{array}$$

D_n (n odd) case: When $h_{\tilde{p}} = e$,

$$F_{A_1} = F_{A_2} = \exp \left(- \sum_{r=1}^{\infty} \frac{1}{r} t_{\tilde{p}}^r \right) = 1 - t_{\tilde{p}}$$

²⁶XD 2014-05-05: I am not sure whether I understand it correctly here.

$$F_{E_j} = \exp\left(-\sum_{r=1}^{\infty} \frac{2}{r} t_{\tilde{p}}^r\right) = (1 - t_{\tilde{p}})^2$$

When $h_{\tilde{p}} = C_n^k$, the same goes for A_1 and A_2 : $F_{A_1} = F_{A_2} = 1 - t_{\tilde{p}}$, but for E_j , it requires a little special treatment.

$$\begin{aligned} F_{E_j} &= \exp\left(-\sum_{r=1}^{\infty} \frac{1}{r} 2 \cos \frac{2\pi k j r}{n} t_{\tilde{p}}^r\right) \\ &= \exp\left(-\sum_{r=1}^{\infty} \frac{1}{r} (\exp(\frac{i2\pi k j r}{n}) + \exp(-\frac{i2\pi k j r}{n})) t_{\tilde{p}}^r\right) \\ &= \left(1 - \exp(\frac{i2\pi k j}{n}) t_{\tilde{p}}\right) \left(1 - \exp(-\frac{i2\pi k j}{n}) t_{\tilde{p}}\right) \\ &= 1 - 2 \cos \frac{2\pi k j}{n} t_{\tilde{p}} + t_{\tilde{p}}^2 \end{aligned}$$

When $h_{\tilde{p}} \in \{s, s_1, \dots, s_{n-1}\}$, $h_{\tilde{p}}^2 = e$.

$$\begin{aligned} F_{A_1} &= 1 - t_{\tilde{p}} \\ F_{A_2} &= \exp\left(-\sum_{r=even}^{\infty} \frac{1}{r} t_{\tilde{p}}^r + \sum_{r=odd}^{\infty} \frac{1}{r} t_{\tilde{p}}^r\right) = (1 + t_{\tilde{p}}) \\ F_{E_j} &= \exp\left(-\sum_{r=even}^{\infty} \frac{1}{r} 2 t_{\tilde{p}}^r\right) = (1 - t_{\tilde{p}}^2) \end{aligned}$$

In sum,

$$\begin{array}{lllll} h_{\tilde{p}} & A_1 & A_2 & E_j \\ e: & (1 - t_{\tilde{p}})^{2n} & = & (1 - t_{\tilde{p}}) & (1 - t_{\tilde{p}})^4 \\ C_n^k, C_n^{n-k}: & (1 - t_{\tilde{p}}^m)^{\frac{2n}{m}} & = & (1 - t_{\tilde{p}}) & (1 - t_{\tilde{p}})^4 \\ s, s_1, \dots, s_{n-1}: & (1 - t_{\tilde{p}}^2)^n & = & (1 - t_{\tilde{p}}) & (1 - t_{\tilde{p}}^2)^2 \end{array}$$

D_n (n even) case:

Similar calculation gives us the following factorized zeta function table.

$$\begin{array}{lllllll} h_{\tilde{p}} & A_1 & A_2 & B_1 & B_2 & E_j \\ e: & (1 - t_{\tilde{p}})^{2n} & = & (1 - t_{\tilde{p}}) & (1 - t_{\tilde{p}}) & (1 - t_{\tilde{p}})^4 \\ r_{n/2}: & (1 - t_{\tilde{p}}^2)^n & = & (1 - t_{\tilde{p}}) & (1 - t_{\tilde{p}}) & (1 - (-1)^{\frac{n}{2}} t_{\tilde{p}}) & (1 - (-1)^j t_{\tilde{p}})^4 \\ r_k \\ (\text{odd}): & (1 - t_{\tilde{p}}^m)^{\frac{2n}{m}} & = & (1 - t_{\tilde{p}}) & (1 - t_{\tilde{p}}) & (1 + t_{\tilde{p}}) & (1 + t_{\tilde{p}}) & (1 - 2 \cos(\frac{2\pi k j}{n}) t_{\tilde{p}} + t_{\tilde{p}}^2) \\ r_k \\ (\text{even}): & (1 - t_{\tilde{p}}^m)^{\frac{2n}{m}} & = & (1 - t_{\tilde{p}}) & (1 - t_{\tilde{p}}) & (1 - t_{\tilde{p}}) & (1 - t_{\tilde{p}}) & (1 - 2 \cos(\frac{2\pi k j}{n}) t_{\tilde{p}} + t_{\tilde{p}}^2) \\ s: & (1 - t_{\tilde{p}}^2)^n & = & (1 - t_{\tilde{p}}) & (1 + t_{\tilde{p}}) & (1 - t_{\tilde{p}}) & (1 + t_{\tilde{p}}) & (1 - t_{\tilde{p}}^2)^2 \\ rs: & (1 - t_{\tilde{p}}^2)^n & = & (1 - t_{\tilde{p}}) & (1 + t_{\tilde{p}}) & (1 + t_{\tilde{p}}) & (1 - t_{\tilde{p}}) & (1 - t_{\tilde{p}}^2)^2 \end{array}$$

When it comes to continuous symmetry, projection operator is

$$P_m = d_m \int_G dg \chi_m(g^{-1}) O_g. \quad (4.280)$$

The corresponding trace formula in the irreducible subspace is

$$\sum_{\beta=0}^{\infty} \frac{1}{s - s_{m,\beta}} = d_m \sum_p T_p \sum_{r=1}^{\infty} \chi_m(g_p^r) \frac{e^{r(\beta A_p - s T_p)}}{\left| \det \left(\mathbf{1} - \tilde{M}_{m,p}^r \right) \right|}. \quad (4.281)$$

Therefore the spectral determinant is factorized as

$$\begin{aligned} \det(s - \mathcal{A}) &= \prod_{\alpha} F_{\alpha}(z)^{d_{\alpha}} \\ F_{\alpha}(z) &= \exp \left(- \sum_{\tilde{p}} \sum_{r=1}^{\infty} \frac{1}{r} \frac{\chi_{\alpha}(g_{\tilde{p}}^r) z^{n_{\tilde{p}} r} e^{r \beta \cdot A_{\tilde{p}}}}{\left| \det \left(\mathbf{1} - \tilde{M}_{\tilde{p}}^r \right) \right|} \right) \end{aligned} \quad (4.282)$$

It differs from the discrete case on that now the group operator $g_{\tilde{p}}$ is continuous and the factorization may have infinite terms.

Used formulas Here I list several formulas used in the above post.

$$\frac{1}{2\pi} \sum_{n=-\infty}^{\infty} e^{inx} = \delta(x) \quad (4.283)$$

This identity comes from one definition of delta function $\delta(x) = \lim_{N \rightarrow \infty} \frac{1}{2\pi} \frac{\sin(N+1/2)x}{\sin(\frac{1}{2}x)}$ and simple calculation gives $\sum_{n=-N}^N e^{inx} = \frac{\sin(N+1/2)x}{\sin(\frac{1}{2}x)}$.

$$\sum_R \chi_{\alpha}(R) \chi_{\beta}(SR^{-1}) = \frac{|G|}{d_{\alpha}} \delta_{\alpha,\beta} \chi_{\alpha}(S) \quad (4.284)$$

This is the orthogonality between characters of irreducible representations. If we set $S = e$, then it reduces to $\sum_R \chi_{\alpha}(R) \chi_{\beta}(R^{-1}) = |G| \delta_{\alpha,\beta}$. The orthogonality of projection operators can be checked:

$$\begin{aligned} P_{\alpha} P_{\beta} &= \frac{d_{\alpha}}{|G|} \frac{d_{\beta}}{|G|} \sum_{h, sg \in G} \chi_{\alpha}(h) \chi_{\alpha}(s) \mathbf{h}^{-1} \mathbf{s}^{-1} \\ &= \frac{d_{\alpha}}{|G|} \frac{d_{\beta}}{|G|} \sum_{sg \in G} \frac{|G|}{d_{\alpha}} \delta_{\alpha,\beta} \chi_{\alpha}(sh) (\mathbf{s}\mathbf{h})^{-1} \\ &= \delta_{\alpha,\beta} \frac{d_{\alpha}}{|G|} \sum_{sg \in G} \chi_{\alpha}(s) \mathbf{s}^{-1} \\ &= \delta_{\alpha,\beta} P_{\alpha} \end{aligned}$$

The last formula is

$$\sum_{\alpha} d_{\alpha} \chi_{\alpha}(R) = |G| \delta_{e,R} \quad (4.285)$$

which comes from orthogonality relation above. For regular representation, the trace of R in terms of irreducible representations is $\chi(R) = \sum_{\alpha} a_{\alpha} \chi_{\alpha}(R)$, so the summation of all group elements gives

$$\sum_R \chi(R) \chi_{\alpha}(R^{-1}) = \sum_{\alpha} a_{\alpha} \sum_R \chi_{\alpha}(R) \chi_{\alpha}(R^{-1}) = |G| a_{\alpha}$$

On the other hand, $\chi(R) = |G| \delta_{e,R}$ for regular representation, then the left side of the above expression is just $|G| \chi_{\alpha}(e)$, so $a_{\alpha} = \chi_{\alpha}(e) = d_{\alpha}$ the dimension of α_{th} irreducible representation. In this way, we obtain (4.285). Now the completeness of projection operator can be checked:

$$\sum_{\alpha} P_{\alpha} = \sum_{\alpha} \frac{d_{\alpha}}{|G|} \sum_{hg \in G} \chi_{\alpha}(h) \mathbf{h}^{-1} = \frac{1}{|G|} \sum_{hg \in G} \left(\sum_{\alpha} d_{\alpha} \chi_{\alpha}(h) \right) \mathbf{h}^{-1} = e$$

References

- [1] R. L. Adler and B. Weiss, “Entropy, a complete metric invariant for automorphisms of the torus”, Proc. Natl. Acad. Sci. USA **57**, 1573–1576 (1967).
- [2] J.-C. Anglès d’Auriac, S. Boukraa, and J.-M. Maillard, “Functional relations in lattice statistical mechanics, enumerative combinatorics, and discrete dynamical systems”, Ann. Comb. **3**, 131–158 (1999).
- [3] D. V. Anosov, A. V. Klimenko, and G. Kolutsky, *On the hyperbolic automorphisms of the 2-torus and their Markov partitions*, 2008.
- [4] M. Artin and B. Mazur, “On periodic points”, Ann. Math. **81**, 82–99 (1965).
- [5] S. Aubry and G. Abramovici, “Chaotic trajectories in the standard map. The concept of anti-integrability”, Physica D **43**, 199–219 (1990).
- [6] M. Baake, “A brief guide to reversing and extended symmetries of dynamical systems”, in *Ergodic Theory and Dynamical Systems in their Interactions with Arithmetics and Combinatorics*, edited by S. Ferenczi, J. Kułaga-Przymus, and M. Lemańczyk (2018), pp. 117–135.
- [7] M. Baake, J. Hermisson, and A. B. Pleasants, “The torus parametrization of quasiperiodic LI-classes”, J. Phys. A **30**, 3029–3056 (1997).
- [8] M. Baake, N. Neumärker, and J. A. G. Roberts, “Orbit structure and (reversing) symmetries of toral endomorphisms on rational lattices”, Discrete Continuous Dyn. Syst. **33**, 527–553 (2013).

- [9] M. Baake and J. A. G. Roberts, “Reversing symmetry group of $\text{Gl}(2, \mathbb{Z})$ and $\text{PGL}(2, \mathbb{Z})$ matrices with connections to cat maps and trace maps”, *J. Phys. A* **30**, 1549 (1997).
- [10] M. Baake, J. A. G. Roberts, and A. Weiss, “Periodic orbits of linear endomorphisms on the 2-torus and its lattices”, *Nonlinearity* **21**, 2427 (2008).
- [11] R. Ballou, “An introduction to the linear representations of finite groups”, *EPJ Web Conf.* **22**, 00005 (2012).
- [12] J. Banks, J. Brooks, G. Cairns, G. Davis, and P. Stacey, “On Devaney’s definition of chaos”, *Amer. Math. Monthly* **99**, 332–334 (1992).
- [13] M. El-Batanouny and F. Wooten, *Symmetry and Condensed Matter Physics: A Computational Approach* (Cambridge Univ. Press, Cambridge UK, 2008).
- [14] M. Boyle, B. Marcus, and P. Trow, *Resolving Maps and the Dimension Group for Shifts of Finite Type*, Vol. 70, 377 (Amer. Math. Soc., 1987).
- [15] I. B. Božović, “Irreducible representations of the symmetry groups of polymer molecules. III. Consequences of time-reversal symmetry”, *J. Phys. A* **14**, 1825 (1981).
- [16] I. B. Božović, M. Vujičić, and F. Herbut, “Irreducible representations of the symmetry groups of polymer molecules. I”, *J. Phys. A* **11**, 2133 (1978).
- [17] M. Bruschi, F. Calogero, and R. Droghei, “Tridiagonal matrices, orthogonal polynomials and Diophantine relations: I”, *J. Phys. A* **40**, 9793–9817 (2007).
- [18] B. Canals and H. Schober, “Introduction to group theory”, *EPJ Web Conf.* **22**, 00004 (2012).
- [19] A. Carnegie and I. C. Percival, “Regular and chaotic motion in some quartic potentials”, *J. Phys. A* **17**, 801 (1984).
- [20] G. Casati and B. V. Chirikov, *Quantum Chaos: Between Order and Disorder* (Cambridge Univ. Press, Cambridge UK, 1995).
- [21] M. Cini, *Topics and Methods in Condensed Matter Theory - From Basic Quantum Mechanics to the Frontiers of Research* (Springer, Berlin, 2007).
- [22] M. Cini and G. Stefanucci, “Antiferromagnetism of the two-dimensional Hubbard model at half-filling: The analytic ground state for weak coupling”, *J. Phys.: Condens. Matter* **13**, 1279–1294 (2001).
- [23] J. F. Cornwell, *Group theory in physics: an introduction* (Academic, New York, 1997).
- [24] E. M. Corson, “Note on the Dirac character operators”, *Phys. Rev.* **73**, 57–60 (1948).
- [25] P. Cvitanović, *Group Theory: Birdtracks, Lie’s and Exceptional Groups* (Princeton Univ. Press, Princeton NJ, 2008).
- [26] P. Cvitanović, “Counting”, in *Chaos: Classical and Quantum* (Niels Bohr Inst., Copenhagen, 2020).

- [27] P. Cvitanović, R. L. Davidchack, and E. Siminos, “On the state space geometry of the Kuramoto-Sivashinsky flow in a periodic domain”, SIAM J. Appl. Dyn. Syst. **9**, 1–33 (2010).
- [28] P. Cvitanović and Y. Lan, Turbulent fields and their recurrences, in *Correlations and Fluctuations in QCD : Proceedings of 10. International Workshop on Multiparticle Production*, edited by N. Antoniou (2003), pp. 313–325.
- [29] P. Cvitanović and H. Liang, *Spatiotemporal cat: A chaotic field theory*, In preparation, 2021.
- [30] R. DeVogelaere, “IV. On the structure of symmetric periodic solutions of conservative systems, with applications”, in *Contributions to the Theory of Nonlinear Oscillations (AM-41), Volume IV* (Princeton Univ. Press, 1958), pp. 53–84.
- [31] P. A. M. Dirac, *The Principles of Quantum Mechanics* (Oxford Univ. Press, 1930).
- [32] C. Dong, “Topological classification of periodic orbits in Lorenz system”, Chin. Phys. B **27**, 080501 (2018).
- [33] C. Dong, “Topological classification of periodic orbits in the Yang-Chen system”, Europhys. Lett. **123**, 20005 (2018).
- [34] C. Dong and Y. Lan, “A variational approach to connecting orbits in nonlinear dynamical systems”, Phys. Lett. A **378**, 705–712 (2014).
- [35] C. Dong and Y. Lan, “Organization of spatially periodic solutions of the steady Kuramoto-Sivashinsky equation”, Commun. Nonlinear Sci. Numer. Simul. **19**, 2140–2153 (2014).
- [36] C. Dong, H. Liu, and H. Li, “Unstable periodic orbits analysis in the generalized Lorenz-type system”, J. Stat. Mech. **2020**, 073211 (2020).
- [37] M. S. Dresselhaus, G. Dresselhaus, and A. Jorio, *Group Theory: Application to the Physics of Condensed Matter* (Springer, New York, 2007).
- [38] D. Dudgeon and R. M. Mersereau, *Multidimensional Digital Signal Processing* (Prentice-Hall, Englewood Cliffs, NJ, 1984).
- [39] B. Eckhardt, G. Hose, and E. Pollak, “Quantum mechanics of a classically chaotic system: Observations on scars, periodic orbits, and vibrational adiabaticity”, Phys. Rev. A **39**, 3776–3793 (1989).
- [40] B. Eckhardt, G. Russberg, P. Cvitanović, P. E. Rosenqvist, and P. Scherer, “Pinball scattering”, in *Quantum Chaos: Between Order and Disorder*, edited by G. Casati and B. Chirikov (Cambridge Univ. Press, Cambridge UK, 1995).
- [41] B. Eckhardt and D. Wintgen, “Symbolic description of periodic orbits for the quadratic Zeeman effect”, J. Phys. B **23**, 355–363 (1990).
- [42] M. D. Esposti and S. Isola, “Distribution of closed orbits for linear automorphisms of tori”, Nonlinearity **8**, 827–842 (1995).

- [43] L. Fejér, “Über trigonometrische Polynome”, *J. Reine Angew. Math. (Crelle)* **1916**, 53–82 (1916).
- [44] M. Golubitsky and I. Stewart, *The Symmetry Perspective* (Birkhäuser, Boston, 2002).
- [45] I. S. Gradshteyn and I. M. Ryzhik, *Tables of Integrals, Series and Products*, 8th ed. (Elsevier LTD, Oxford, New York, 2014).
- [46] T. Grava, T. Kriecherbauer, G. Mazzuca, and K. D. T.-R. McLaughlin, “Correlation functions for a chain of short range oscillators”, *J. Stat. Phys.* **183**, 1 (2021).
- [47] B. Grenier and R. Ballou, “Crystallography: Symmetry groups and group representations”, *EPJ Web Conf.* **22**, 00006 (2012).
- [48] B. Gutkin, L. Han, R. Jafari, A. K. Saremi, and P. Cvitanović, “Linear encoding of the spatiotemporal cat map”, *Nonlinearity* **34**, 2800–2836 (2021).
- [49] M. Hamermesh, *Group Theory and Its Application to Physical Problems* (Dover, New York, 1962).
- [50] M. Hamermesh, *Group Theory and Its Application to Physical Problems* (Dover, New York, 1962).
- [51] C. Herring, “Effect of time-reversal symmetry on energy bands of crystals”, *Phys. Rev.* **52**, 361–365 (1937).
- [52] G. Herzberg, *Molecular Spectra and Molecular Structure* (Van Nostrand, Princeton NJ, 1950).
- [53] P. Jacobs, *Group Theory with Applications in Chemical Physics* (Cambridge Univ. Press, 2005).
- [54] S. Jaidee, P. Moss, and T. Ward, “Time-changes preserving zeta functions”, *Proc. Amer. Math. Soc.* **147**, 4425–4438 (2019).
- [55] D. F. Johnston, “Group theory in solid state physics”, *Rep. Prog. Phys.* **23**, 66 (1960).
- [56] A. Katok and B. Hasselblatt, *Introduction to the modern theory of dynamical systems* (Cambridge Univ. Press, Cambridge, 1995).
- [57] J. P. Keating and F. Mezzadri, “Pseudo-symmetries of Anosov maps and spectral statistics”, *Nonlinearity* **13**, 747–775 (2000).
- [58] Y.-O. Kim, J. Lee, and K. K. Park, “A zeta function for flip systems”, *Pacific J. Math.* **209**, 289–301 (2003).
- [59] C. Kittel, *Introduction to Solid State Physics*, 8th ed. (Wiley, 2004).
- [60] P. Kurlberg and Z. Rudnick, “Hecke theory and equidistribution for the quantization of linear maps of the torus”, *Duke Math. J.* **103**, 47–77 (2000).
- [61] J. S. W. Lamb and J. A. G. Roberts, “Time reversal symmetry in dynamical systems: A survey”, *Physica D* **112**, 1–39 (1998).

- [62] Y. Lan and P. Cvitanović, “Variational method for finding periodic orbits in a general flow”, *Phys. Rev. E* **69**, 016217 (2004).
- [63] Y. Lan and P. Cvitanović, “Unstable recurrent patterns in Kuramoto-Sivashinsky dynamics”, *Phys. Rev. E* **78**, 026208 (2008).
- [64] H. Liang and P. Cvitanović, Time reversal for discrete time dynamical systems, In preparation, 2021.
- [65] D. A. Lind, “A zeta function for Z^d -actions”, in *Ergodic Theory of Z^d Actions*, edited by M. Pollicott and K. Schmidt (Cambridge Univ. Press, 1996), pp. 433–450.
- [66] D. A. Lind and B. Marcus, *An Introduction to Symbolic Dynamics and Coding* (Cambridge Univ. Press, Cambridge, 1995).
- [67] H. Liu, C. Dong, Q. Jie, and H. Li, “Topological classification of periodic orbits in the generalized Lorenz-type system with diverse symbolic dynamics”, *Chaos, Solitons & Fractals* **154**, 111686 (2022).
- [68] J. Llibre and N. Neumärker, “Period sets of linear toral endomorphisms on T^2 ”, *Topology Appl.* **185-186**, 41–49 (2015).
- [69] C. C. Martens, R. L. Waterland, and W. P. Reinhardt, “Classical, semi-classical, and quantum mechanics of a globally chaotic system: integrability in the adiabatic approximation”, *J. Chem. Phys.* **90**, 2328 (1989).
- [70] S. G. Matanyan, G. K. Savvidy, and N. G. Ter-Arutyunyan-Savvidy, “Classical Yang-Mills mechanics. Nonlinear color oscillations”, *Sov. Phys. JETP* **53**, 830–838 (1981).
- [71] R. Miles, “A dynamical zeta function for group actions”, *Monatsh. Math.* **182**, 683–708 (2016).
- [72] J. W. Mintmire, B. I. Dunlap, and C. T. White, “Are Fullerene tubules metallic?”, *Phys. Rev. Lett.* **68**, 631–634 (1992).
- [73] A. Nordin and M. S. M. Noorani, “Counting finite orbits for the flip systems of shifts of finite type”, *Discrete Continuous Dyn. Syst.* **41**, 4515–4529 (2021).
- [74] K. Park, “On ergodic foliations”, *Ergod. Theor. Dyn. Syst.* **8**, 437–457 (1988).
- [75] C. Pozrikidis, *An Introduction to Grids, Graphs, and Networks* (Oxford Univ. Press, Oxford , UK, 2014).
- [76] W. H. Press, B. P. Flannery, S. A. Teukolsky, and W. T. Vetterling, *Numerical Recipes*, 3rd ed. (Cambridge Univ. Press, Cambridge UK, 2007).
- [77] J. J. Quinn and K. . Yi, *Solid State Physics: Principles and Modern Applications* (Springer, Berlin, 2009).
- [78] F. Riesz and B. Sz.-Nagy, *Functional Analysis* (Dover Publ., Mineola, NY, 1955).
- [79] J. M. Robbins, “Discrete symmetries in periodic-orbit theory”, *Phys. Rev. A* **40**, 2128–2136 (1989).

- [80] J. A. G. Roberts and G. R. W. Quispel, “Chaos and time-reversal symmetry. Order and chaos in reversible dynamical systems”, *Phys. Rep.* **216**, 63–177 (1992).
- [81] J. Rodríguez-Carvajal and F. Bourée, “Symmetry and magnetic structures”, *EPJ Web Conf.* **22**, 00010 (2012).
- [82] D. Ruelle, “Dynamical zeta functions and transfer operators”, *Notices Amer. Math. Soc.* **95**, 887–895 (2002).
- [83] D. Ruelle, *Thermodynamic Formalism: The Mathematical Structure of Equilibrium Statistical Mechanics*, 2nd ed. (Cambridge Univ. Press, Cambridge, 2004).
- [84] H. Schober, “Symmetry characterization of electrons and lattice excitations”, *EPJ Web Conf.* **22**, 00012 (2012).
- [85] J. Schweizer, “Conjugation and co-representation analysis of magnetic structures”, *EPJ Web Conf.* **22**, 00011 (2012).
- [86] R. Sharp, “Periodic orbits of hyperbolic flows”, in *On Some Aspects of the Theory of Anosov Systems*, edited by G. A. Margulis (Springer, Berlin, 2004), pp. 73–138.
- [87] A. Siemaszko and M. P. Wojtkowski, “Counting Berg partitions”, *Nonlinearity* **24**, 2383–2403 (2011).
- [88] S. Smale, “Differentiable dynamical systems”, *Bull. Amer. Math. Soc.* **73**, 747–817 (1967).
- [89] H. Spohn, “Nonlinear fluctuating hydrodynamics for anharmonic chains”, *J. Stat. Phys.* **154**, 1191–1227 (2014).
- [90] M. Tinkham, *Group theory and quantum mechanics* (Dover, New York, 2003).
- [91] J. Villain, “Symmetry and group theory throughout physics”, *EPJ Web Conf.* **22**, 00002 (2012).
- [92] P. Walters, *An Introduction to Ergodic Theory* (Springer, New York, 1982).
- [93] S. Wolfram, *A Project to Find the Fundamental Theory of Physics* (Wolfram Media Inc., 2020).

Chapter 5

Spatiotemporal cat

2016-09-09 Predrag I have added this chapter with intention to include it as several examples in ChaosBook.org.

2020-12-16 Predrag The abstract of my online Mathematical Physics Webinar, Rutgers University - the most attended of the series :)

▶ *Spatiotemporal cat - a chaotic field theory* (55 min seminar)

When I refer to a physical phenomenon -such as motions of a Navier-Stokes fluid- as 'chaotic', or 'turbulent', I am often told: We understand 'chaos' for a system such as Lorenz attractor, but what is a 'chaotic' field, a field with infinitely many degrees of freedom?

The goal of the seminar is to answer this question pedagogically, as a sequence of pencil and paper calculations. First I will explain what is 'deterministic chaos' by walking you through its simplest example, the coin toss or Bernoulli map, but reformulated as problem of enumerating admissible global solutions on an integer-time lattice. Then I will do the same with the 'kicked rotor', the simplest mechanical system that is chaotic. Finally, I will take an infinity of 'rotors' coupled together on a spatial lattice to explain what 'chaos' or 'turbulence' looks like in the spacetime.

What emerges is a spacetime which is very much like a big spring mattress that obeys the familiar harmonic oscillator field theory equations, the discrete Helmholtz equation (or the tight-binding model), but instead of being 'springy', this metamaterial is a discretization of the Euclidean Klein-Gordon equation, with an unstable rotor at every lattice site, that gives, rather than pushes back, a theory formulated in terms of Hill determinants and zeta functions. We call this mother of all chaotic field theories the 'spatiotemporal cat'.

This is the simplest example of reformulating a space and time translationally invariant, exponentially unstable 'turbulent' field theory as a

(D+1)-dimensional spatiotemporal system which treats space and time on equal footing. Here there is no ‘evolution in time’: there is only the enumeration of the repertoire of admissible tilings of spacetime by invariant (D+1)-dimensional tori, or ‘periodic orbits’, very much as the partition function of the Ising model is a weighted sum formed by enumerating its lattice states. But that is a story for another seminar.

And if you don’t know, **now you know**

5.1 Coupled map lattices

Diffusive coupled map lattices (CML) were introduced by Kaneko [158, 159]:

$$x_{n,t+1} = g(x_{n,t}) + \frac{\epsilon}{2}[g(x_{n-1,t}) - 2g(x_{n,t}) + g(x_{n+1,t})] = (1 + \epsilon \square)g(x_{n,t}) \quad (5.1)$$

where the individual site dynamical system $g(x)$ is a 1D map such as the logistic map.

In the discretization of a spacetime field $q(x, t)$ on lattice points (x_n, t_j) , the field is replaced by its lattice point value $q_{n,j} = q(x_n, t_j)$. For a Hamiltonian set of fields we also have $p_{n,j} = p(x_n, t_j)$. In the spatiotemporal cat, a cat map at each periodic lattice site is coupled diffusively to its nearest neighbors:

$$\begin{aligned} q_{n,j+1} &= p_{n,j} + (s - 3)q_{n,j} - (q_{n+1,j} - 2q_{n,j} + q_{n-1,j}) - m_{n,j+1}^q \\ p_{n,j+1} &= p_{n,j} + (s - 4)q_{n,j} - (q_{n+1,j} - 2q_{n,j} + q_{n-1,j}) - m_{n,j+1}^p \end{aligned} \quad (5.2)$$

The spatiotemporal symbols follow from the Newtonian equations in d spatiotemporal dimensions

$$\begin{aligned} (q_{n,j+1} - 2q_{n,j} + q_{n,j-1}) + (q_{n+1,j} - 2q_{n,j} + q_{n-1,j}) - (s - 4)q_{n,j} &= m_{n,j} \\ (-\square + \mu^2 \mathbf{1}) \mathbf{q} &= -\mathbf{m}. \end{aligned} \quad (5.3)$$

The $\square + 2d\mathbf{1}$ part is the standard statistical mechanics diffusive inverse propagator that counts paths on a d -dimensional lattice [73], $\mu^2 = d(s - 2)$ is the Yukawa mass parameter (5.27), and $-s\mathbf{1}$ is the on-site cat map dynamics, described by the stretching parameter s . For $d = 1$ lattice, $s = 3$ is the usual Arnol’d cat map.

2018-12-15 Predrag Frahm and Shepelyansky [104] *Small world of Ulam networks for chaotic Hamiltonian dynamics*, and the related **Shepelyansky** work is of potential interest.

“Ulam method” replaces discrete dynamics by an Ulam approximate [103] of the Perron-Frobenius operator (UPFO). The Ulam method produces directed “Ulam networks” with weighted probability transitions between

nodes corresponding to phase-space cells. From a physical point of view the finite cell size of UPFO corresponds to the introduction of a finite noise with amplitude given by a discretization cell size. Ulam networks have small-world properties, meaning that almost any two nodes are indirectly connected by a small number of links.

They show that the Ulam method applied to symplectic maps generates Ulam networks which belong to the class of small-world networks. They analyze the small-world examples of the Chirikov standard map and the Arnold cat map, showing that the number of degrees of separation grows logarithmically with the network size for the regime of strong chaos, due to the instability of chaotic dynamics. The presence of stability islands leads to an algebraic growth with the network size.

The usual case of the cat map corresponds to $L = 1$. The map on a torus of longer integer size $L > 1$ generates a diffusive dynamics [92]. For $L \gg 1$ the diffusive process for the probability density is described by the Fokker-Planck equation.

The time scales related with the degrees of separation and the relaxation times of the Perron-Frobenius operator have different behaviors. The largest relaxation times remain size independent in the case of a diffusive process, like for the Arnold cat map on a long torus.

In the Appendix they show that the exact linear form of the cat map allows for very efficient and direct *exact Ulam network* network size 10^8 computation of the transition probabilities needed for the UPFO. Shepelyansky tends to omit boring formulas, so I see no stability multipliers which are so important in our computations.

In UPFO discretizations of the standard map they use the Arnoldi method. The main idea of the Arnoldi method is to construct a subspace of “modest”, but not too small, dimension (the Arnoldi-dimension) generated by the vectors that span a Krylov space); the Arnoldi method in ref. [103] is quite interesting.

The construction of the Ulam networks is (verbally?) described in ref. [103], but I have not understood it. As graphs are directed (?), there is probably no Laplacian. There might be a related undirected network model, with a graph Laplacian (13.53). In that case a Lagrangian formulation (in terms of graph Laplacians) might be a more powerful formulation than their Hamiltonian one. “Arrow of time” is perhaps encoded by the orientations of the links in a directed complex network.

2CB

2018-12-15 Predrag Ermann and Shepelyansky [92] *The Arnold cat map, the Ulam method and time reversal* show that the “Ulam method” coarse-graining leads to irreversibility.

2020-02-19 Predrag In Berenstein and García-García15 [35] *A universal quantum constraints on the butterfly effect*, arXiv:1510.08870, cat maps were generalized to products of such vector spaces that can be put on a lattice, with

a variables at each site and variables at different sites commuting with each other, for nearest neighbors on a lattice in any dimension. As they write, "This generates a system with nearest neighbor hopping and local scrambling." They write down a periodic (circulant) banded matrix, so the eigenvalues have a band structure similar to a periodic potential with nearest neighbor hopping. The evolve forward in time, i.e., their is a quantized Hamiltonian formulation.

Berenstein [34] *A toy model for time evolving QFT on a lattice with controllable chaos*, arXiv:1803.02396 from UC Santa Barbara. is perhaps a precursor to Gutkin and our spatiotemporal cat.

He discusses two points of view on how the Lyapunov exponents appear in real time correlation functions in quantum field theory and will them compute them in the case of the cat map dynamics. The Kubo's formula point if view is in semiclassical physics, and the second point of view is statistical. They both amount to different ways of making a quantity with an indefinite sign positive.

He considers 1-dimensional spatial lattice, and caries out computations on a spatial lattice with only two sites. He composes a local cat map at each site with a nearest neighbor entangler and after the system is constructed one iterates the automorphism. The system will also be determined by a $[2m \times 2m]$ matrix. Each $[2 \times 2]$ block on the diagonal represents $(P_i; Q_i)$. The local cat map acts on each of these as a $[2 \times 2]$ matrix, and the nearest neighbor entangler is a matrix that, at least for a lattice on a line, is near the diagonal giving rise to a banded matrix. The eigenvalues of this bigger matrix are the Lyapunov exponent of the system.

Iterating over a general M produces a cat map dynamics on the Q, and the 'inverse' cat dynamics on the P. The dynamics on P is actually built from the inverse transpose, but that has the same eigenvalues as the inverse of M.

As noted in ref. [35], models with nearest neighbor properties also mimic the Lieb-Robinson bound [18] for propagation of information and thus can in principle serve as toy models for relativistic field theories (they have the equivalent of a speed of light).

He sets up a one dimensional spatial lattice, with nearest neighbor entanglers whose dynamics can be encoded by an 'Dirichlet' upper triangular matrix, his eq. (64) and sketch (65), with eigenvalues 1, and thus not chaotic. However, with periodic bc's it is chaotic. The paper here falls short of Gutkin and Osipov [120].

Berenstein and Teixeira [34] *Maximally entangling states and dynamics in one dimensional nearest neighbor Floquet systems*, arXiv:1901.02944, describe conditions for generating entanglement between two regions at the optimal rate in a class of one-dimensional quantum circuits with Floquet dynamics. I do not get it, but it does cite Prosen [36] see 2019-11-18 Boris below.

I do not think we need to cite him, but should send him links to our papers: [David Berenstein](#)

2020-05-31 Predrag Houlrik [135] *Periodic orbits in a two-variable coupled map* computes periodic orbits in $1 + 1$ spacetime CML for a linear map composed of two coupled Chaté-Manneville maps [53] [tent map + linear branch] (see (5.1))

$$x_{n,t+1} = f(x_{n,t}) + \frac{\epsilon}{2}[f(x_{n-1,t}) - 2f(x_{n,t}) + f(x_{n+1,t})] \quad (5.4)$$

what we call the $[2 \times n]_0$ family periodic orbits, using symbolic dynamics blocks M defined as the direct product of the single-map symbols $\mathcal{A} = \{0, 1, 2\}$. He credits Bunimovich and Sinai [49] with introducing the $(D+1)$ -dimensional spatiotemporal symbolic dynamics.

The $[2 \times 2]$ matrix

$$A = \begin{pmatrix} 1-\epsilon & \epsilon \\ \epsilon & 1-\epsilon \end{pmatrix} = (1-\epsilon)\mathbf{1} + \epsilon(d + d^{-1}) \quad (5.5)$$

and sources

$$B(M) = \sum_{n=1}^{k=0} J(s_{n-1}) \cdots J(s_{k+1}) A \mathbf{b} \quad (5.6)$$

He finds the $[2 \times n]_0$ periodic orbits by solving

$$(1 - J(M)) X = B(M) \quad (5.7)$$

The fixed point condition (5.7) has a periodic orbit solution

$$X = \frac{1}{1 - J(M)} B(M) \quad (5.8)$$

for each admissible brick M , where this needs still to be rewritten in the n -dimensional temporal lattice state formulation, hence the partial products of $[2 \times 2]$ stability matrices in (5.6). The admissible lattice states and the pruning criterion are easily visualized in the $(\phi_{1,0}, \phi_{2,0})$ plane.

2020-06-01 Predrag Gade and Amritkar [107] *Spatially periodic orbits in coupled-map lattices* (a preliminary version of a part of this work was published as Amritkar, Gade, Gangal and Nandkumaran [9] *Stability of periodic orbits of coupled-map lattices*):

They take CMLs with periodic orbits over $[L \times T]_0$ and study the stability of their periodic orbit ‘replicas’ $[kL \times T]_0$ obtained by repeating $[L \times T]_0$ k times in the spatial direction, and show that orbit Jacobian matrix eigenvalues of the replica follow from the small periodic orbit. Not obvious, as the replica periodic orbit has more directions to be stable/unstable in.

The trick is observing that the replica orbit Jacobian matrix is a block circulant with circulant blocks.

Cite Gade and Amritkar [107] as an early investigation of a lattice orbit Jacobian matrix. They did not know about 'Hill's formula.

2016-01-12, 2016-08-04 PC Literature related to Gutkin and Osipov [120] *Classical foundations of many-particle quantum chaos*:

The existence of 2D symbolic dynamics was demonstrated in ref. [221], for a particular model of coupled lattice map.

"In general, calculating periodic orbits of a non-integrable system is a non-trivial task. To this end a number of methods have been developed," and then, for some reason, they refer to ref. [27].

Pethel *et al.* [220] *Symbolic dynamics of coupled map lattices*

Pethel *et al.* [221] *Deconstructing spatiotemporal chaos using local symbolic dynamics*

Amigó, Zambrano and Sanjuán [8] *Permutation complexity of spatiotemporal dynamics* study diffusive logistic coupled map lattices (CML) (5.1). Sun *et al.* [252] *A method of recovering the initial vectors of globally coupled map lattices based on symbolic dynamics* study CMLs with logistic, Bernoulli, and tent chaotic maps. They cite Refs. [220, 221]. Gundlach and Rand [118] study coupled circle maps (the results of subsequent papers in this series are claimed to be wrong, see Jiang [150]), which is too mathematical for me to understand. Sad.

Just [153] *Equilibrium phase transitions in coupled map lattices: A pedestrian approach*. A class of piecewise linear coupled map lattices with simple symbolic dynamics is constructed. It can be solved analytically in terms of the statistical mechanics of spin lattices. The corresponding Hamiltonian is written down explicitly in terms of the parameters of the map. The method works only for map lattices with repelling invariant sets.

Just [154] *On symbolic dynamics of space-time chaotic models*

Sakaguchi [234] *Breakdown of the phase dynamics* was the first to study a coupled Bernoulli maps lattice (in $D = 2$).

Kawasaki and Sasa [166] *Statistics of unstable periodic orbits of a chaotic dynamical system with a large number of degrees of freedom*, study a coupled Bernoulli maps lattice (in spatial $D = 1$); Bernoulli forward in time, but tanh-coupled to the nearest spatial neighbors, so that the natural invariant measure for spin configurations coincides with the canonical distribution for an Ising spin Hamiltonian. The most significant feature of the Bernoulli CML is that it respects a detailed balance and the resulting measure coincides with the canonical distribution of the 1D Ising model. There is a one-to-one correspondence between symbol sequences and periodic orbits, as proven by Yutaka Ishii, *Note on a paper by Kawasaki and Sasa on Bernoulli coupled map lattices*. Then they commit the Japanese

heresy: “In summary, we have demonstrated that the macroscopic properties of the Bernoulli CML can be calculated with high accuracy using only one periodic orbit sampled from the special periodic orbit ensemble.”

Takeuchi and Sano [255] *Role of unstable periodic orbits in phase transitions of coupled map lattices* also study the spatially periodic Bernoulli CML (in spatial $D = 1$).

Atay, Jalan and Jost [17] study coupled map networks with multiple time delays; of no current interest for us.

Chen, Chen, and Yuan [56] *Topological horseshoes in travelling waves of discretized nonlinear wave equations* is a mathematical paper. They concentrate on describing relative equilibria of a discretized version of a PDE that has Kuramoto-Sivashinsky, KdV and Burgers as special cases. They define discretized derivatives up to the 5th, if we ever need them. They write “ Applying the concept of anti-integrable limit to coupled map lattices originated from space-time discretized nonlinear wave equations, we show that there exist topological horseshoes in the phase space formed by the initial states of travelling wave solutions. In particular, the coupled map lattices display spatiotemporal chaos on the horseshoes. ”

Afraimovich and Pesin [2] *Hyperbolicity of infinite-dimensional drift systems* study the discrete versions of the complex Ginzburg-Landau equation

$$u_{n,t+1} = u_{n,t} + \tau(u_{n,t}, \sigma) + \gamma(u_{n,t} - u_{n,t-1}) + \frac{\epsilon}{2}[u_{n-1,t} - 2u_{n,t} + u_{n+1,t}], \quad (5.9)$$

where $\tau(u_{n,t}, \sigma)$ is local time dynamics, γ is a parameter of “connection”, a memory of the previous step, so this has a time evolution component that could be written as a time Laplacian, with remainder presumably playing role of a friction. Not sure why this would be a good idea, as Ginzburg-Landau is the first order in time. Literature worries about the stability of of the space-homogeneous state in chains of maps. They consider a special ‘drift’ type of perturbation, at which point they lost me.

Elder *et al.* [91] *Spatiotemporal chaos in the damped Kuramoto-Sivashinsky equation:* “ A discretized version of the damped Kuramoto-Sivashinsky (DKS) equation is constructed to provide a simple computational model of spatiotemporal chaos in one dimension. The discrete map is used to study the transition from periodic solutions to disordered solutions (i.e., spatiotemporal chaos). The numerical evidence indicates a jump discontinuity at this transition. ”

5.2 Helmholtz type equations

The inhomogeneous *Helmholtz equation* is an elliptical equation of form

$$(\square + k^2) \phi(x) = -4\pi\rho(x), \quad x \in \mathbb{R}^d, \quad (5.10)$$

where the field $\phi(x)$ is a C^2 function of coordinates, and $\rho(x)$ is a density function with compact support. Its Green's function satisfies

$$(\square + k^2) g(x, x') = \delta(x - x'). \quad (5.11)$$

For example, in $d = 3$ dimensions the stationary wave, the outgoing wave and the incoming wave Green's functions are:

$$\begin{aligned} g_0(x, x') &= -\frac{\cos(k|x - x'|)}{4\pi|x - x'|} \\ g_+(x, x') &= -\frac{e^{ik|x - x'|}}{4\pi|x - x'|} \\ g_-(x, x') &= -\frac{e^{-ik|x - x'|}}{4\pi|x - x'|}. \end{aligned} \quad (5.12)$$

Furthermore, to these any solution to the homogeneous Helmholtz equation

$$(\square + k^2) f_0(x, x') = 0$$

can be added. On infinite space, the solution of (15.1) is of the form

$$\phi(x) = \phi_0(x) - \int_V d^d x' \rho(x') g(x, x'), \quad (5.13)$$

where $(\square + k^2) \phi_0(x) = 0$.

5.2.1 Poisson and Laplace's equations

The *Poisson equation* is the $k \rightarrow 0$ limit of the Helmholtz equation;

$$\square \phi(x) = -4\pi\rho(x), \quad x \in \mathbb{R}^d, \quad (5.14)$$

with Green's function

$$g(x, x') = -\frac{1}{4\pi|x - x'|}. \quad (5.15)$$

For $\rho = 0$, the equation is known as *Laplace's equation*.

5.2.2 Screened Poisson equation

For the $\mu^2 = -k^2 > 0$ (imaginary k), the equation

$$(-\square + \mu^2) \phi(x) = 4\pi\rho(x), \quad x \in \mathbb{R}^d, \quad (5.16)$$

is known as the *screened Poisson equation* [95], Klein–Gordon or *Yukawa equation*.

The name arises from its applications to electric field screening in plasmas. In chemistry the equation governs steady-state diffusion in presence of the solute $\rho(x)$ piped in or generated by a chemical reaction, or of heat diffusion in presence of heat sources.

The solutions of the screened Poisson equation (5.16) are of the same form as for the Helmholtz equation, but with the oscillatory \sin , \cos , and $\exp(i\cdots)$ solutions replaced by the hyperbolic \sinh , \cosh , and $\exp(-\cdots)$.

The outgoing Green's function (5.12) is here known as the *Yukawa potential*, the static, spherically symmetric solution

$$g(x, x') = -\frac{e^{-\mu|x-x'|}}{4\pi|x-x'|}. \quad (5.17)$$

to the Klein–Gordon equation. The Fourier transform relates the Yukawa potential to the massive scalar particle propagator, i.e., Green's function of the static Klein–Gordon equation (5.25),

$$V(\mathbf{r}) = \frac{-g^2}{(2\pi)^3} \int e^{i\mathbf{k}\cdot\mathbf{r}} \frac{4\pi}{k^2 + \mu^2} dk^3.$$

In $d = 2$ this integral can be explicitly evaluated as a Bessel function,¹

$$g(\mathbf{r}, 0) = \frac{1}{2\pi} \int_0^{+\infty} dk_r \frac{k_r J_0(k_r r)}{k_r^2 + \mu^2} = \frac{1}{2\pi} K_0(r\mu). \quad (5.18)$$

5.2.3 Klein–Gordon equation

wiki says: The Klein–Gordon equation for a scalar particle of mass m and complex-valued function $\psi(t, \mathbf{x})$ of the time variable t and space variables \mathbf{x} ,

$$\frac{1}{c^2} \frac{\partial^2}{\partial t^2} \psi - \nabla^2 \psi + \frac{m^2 c^2}{\hbar^2} \psi = 0, \quad (5.19)$$

is derived by requiring that its plane-wave solutions

$$\psi = e^{-i\omega t + i\mathbf{k}\cdot\mathbf{x}} = e^{ik_\mu x^\mu} \quad (5.20)$$

obey the energy–momentum relation of special relativity,

$$-p_\mu p^\mu = E^2 - \mathbf{p}^2 = \omega^2 - \mathbf{k}^2 = -k_\mu k^\mu = \mu^2, \quad (5.21)$$

with $(-, +, +, +)$ metric. It is written compactly in *natural units*,

$$(\square + \mu^2)\psi = 0, \quad (5.22)$$

¹Predrag 2020-10-31: Recheck the 2π factors

where $\mu = mc/\hbar$, and

$$\square = -\partial_\nu \partial^\nu = \frac{1}{c^2} \frac{\partial^2}{\partial t^2} - \nabla^2 \quad (5.23)$$

is the *d'Alembert operator*, while the scalar operator

$$\Delta = \nabla^2 = \frac{\partial^2}{\partial x^2} + \frac{\partial^2}{\partial y^2} + \frac{\partial^2}{\partial z^2}, \quad (5.24)$$

is called the *Laplacian* or the *Laplace operator*.

Writing the equation as

$$-\partial_t^2 \psi + \nabla^2 \psi = \mu^2 \psi, \quad (5.25)$$

we note that for the time-independent solutions, the Klein–Gordon equation becomes the homogeneous *screened Poisson equation*

$$(\nabla^2 - \mu^2) \psi(\mathbf{r}) = 0. \quad (5.26)$$

5.2.4 Spatiotemporal cat equation

The Yukawa massive field mass parameter is related to the spatiotemporal cat stretching parameter s by

$$\mu^2 = d(s - 2). \quad (5.27)$$

The d -dimensional, purely hyperbolic $\mu^2 > 0$ spatiotemporal cat

$$(-\square + \mu^2 \mathbf{1})_{zz'} \phi_{z'} = -m_z, \quad \phi_z \in \mathbb{T}^1, \quad m_z \in \mathcal{A}^1, \quad z \in \mathbb{Z}^d, \quad (5.28)$$

that we study is a discretization of the inhomogeneous *screened Poisson equation* (5.26), while the discretization of the Helmholtz equation corresponds to $s < 2$.

We denote the differential operator by the *d'Alembert* \square rather than the Laplacian Δ (5.24) to emphasize that we are studying the spatiotemporal spatiotemporal cat rather than the temporally static solutions (5.26).

5.2.5 Helmholtz blog

wiki: In the inhomogeneous case, the only difference between the inhomogeneous screened Poisson equation and the inhomogeneous Helmholtz equation is the the sign of the μ^2 parameter.

2020-10-31 Predrag In sect. 1.30 *Introduction*, Gradshteyn and Ryzhik write:

The trigonometric and hyperbolic sines are related by the identities

$$\sinh x = \frac{1}{i} \sin(ix), \quad \sin x = \frac{1}{i} \sinh(ix). \quad (5.29)$$

The trigonometric and hyperbolic cosines are related by the identities

$$\cosh x = \cos(ix), \quad \cos x = \cosh(ix). \quad (5.30)$$

Because of this duality, every relation involving trigonometric functions has its formal counterpart involving the corresponding hyperbolic functions, and vice versa. In many cases, both pairs of relationships are meaningful.

In sect. 6.94 *Relationships between eigenfunctions of the Helmholtz equation in different coordinate systems* they define the scalar Helmholtz equation as

$$(\nabla^2 + k^2)\Psi = 0, \quad (5.31)$$

with a 3-dimensional Laplacian (5.24), and a Cartesian particular solution of form

$$\Psi_{k_x k_y k_z}(x, y, z) \propto e^{i(k_x x + k_y y + k_z z)} \text{ with } k^2 = k_x^2 + k_y^2 + k_z^2. \quad (5.32)$$

2017-09-09 Predrag Hu and O'Connell [136] also state the discretized version of the solution (5.15) for $s = 2$, which, unlike (1.54) has no exponentials - it's a power law.

I find [Robert E. Hunt notes](#) quite good, both for the continuum case, and for solving the lattice discretization.

2020-10-31 Predrag In publications, it would be nice if we could refer to Gradshteyn and Ryzhik [114] whenever we mention continuum limits of our discretized equations. It's the best known, classical reference.

Unfortunately, Gradshteyn and Ryzhik [114] do not define the Laplace equation and (damped?) screened Poisson equation, see [wiki](#). For that, we should combine our definitions (5.11), (5.57), (5.282), (5.283), see also **2017-09-09 Predrag, 2020-01-13 Predrag**, and discretizations of Helmholtz [82, 181] and screened Poisson [50, 83, 113, 136, 137] (also known as Klein–Gordon or Yukawa) equations.

2020-10-31 Predrag Relation to field theory is discussed in sect. 5.7 *Lattice discretization of a field theory*.

2018-09-26 Predrag The Lagrangian formulation (5.3) suggests that the action (integral over the Lagrangian density, one-step generating function (5.73)) is given by

$$Z[M] = e^{W[M]} = \int [dX] e^{S[X] + X \cdot M}, \quad (5.33)$$

$$W[M] = \Gamma[X] + X \cdot M. \quad (5.34)$$

with “source” symbol block M , free action

$$S[X] = -\frac{1}{2} X^\top (-\square + \mu^2 1) X, \quad (5.35)$$

and the Yukawa mass parameter $\mu^2 = d(s - 2)$ related to the spatiotemporal cat stretching parameter s by (5.27).

Were X not confined to a unit hypercube, the Gaussian integral for quadratic action

$$S[X] = -\frac{1}{2} X^\top (-\square + \mu^2 1) X \quad (5.36)$$

could be integrated out in the usual way,

$$Z[M] = |\det(-\square + \mu^2 1)|^{-1/2} e^{\frac{1}{2} M^\top (-\square + \mu^2 1)^{-1} M}, \quad (5.37)$$

leading to determinants and traces

$$W[0] = \ln Z[0] = -\frac{1}{2} \ln \det(-\square + \mu^2 1) = -\frac{1}{2} \text{tr} \ln(-\square + \mu^2 1). \quad (5.38)$$

2020-09-24 Predrag The trace formula is logarithmic derivative of the determinant,

$$\text{tr} \frac{1}{-\square + \mu^2} = \frac{d}{d\mu^2} \ln \det(-\square + \mu^2). \quad (5.39)$$

To recover $\det(-\square + \mu^2)$ integrate both sides with respect to μ^2 ,

$$\int_{\mu_0^2}^{\mu^2} du \text{tr} \frac{1}{-\square + u} = \ln \frac{\det(-\square + \mu^2)}{\det(-\square + \mu_0^2)},$$

and exponentiate. In this form, the determinant is regularized, as the divergent, large wave-numbers k contribution cancels out

$$\begin{aligned} \frac{\det(-\square + \mu^2)}{\det(-\square + \mu_0^2)} &= \exp \left(\int_{\mu_0^2}^{\mu^2} du \text{tr} \frac{1}{-\square + u} \right) \\ &= \exp \left(\int_0^\infty dt \int_{\mu_0^2}^{\mu^2} du \text{tr} e^{-t(-\square + u)} \right) \\ &= \exp \left(- \int_0^\infty dt \frac{1}{t} \text{tr} (e^{-t(-\square + \mu^2)} - e^{-t(-\square + \mu_0^2)}) \right). \end{aligned}$$

This appears to be the natural form of topological zeta functions, see (13.73), with the Laplacian value $\mu_0 = 0$.

(Another variant, following worldline formalism:) The free scalar propagator for the Euclidean Klein-Gordon equation [5, 236] is

$$g_{zz'} = \left(\frac{1}{-\square + \mu^2} \right)_{zz'}. \quad (5.40)$$

Exponentiate the denominator following Schwinger,

$$g_{zz'} = \int_0^\infty dt e^{-\mu^2 t} \left(e^{-t(-\square)} \right)_{zz'}, \quad (5.41)$$

Replace the operator in the exponent by a path integral, i.e., the sum over random walks (see [Wanderings of a drunken snail](#))

$$g_{zz'} = \int_0^\infty dt e^{-\mu^2 t} \int_{x(0)=x'}^{x(t)=x} \mathcal{D}x(\tau) e^{-\int_0^t d\tau \frac{1}{4} \dot{x}^2}, \quad (5.42)$$

where τ is a proper-time parameter (the fifth parameter [101]), and the dot denotes a derivative with respect to the proper time. This is the *worldline path integral* representation of the relativistic propagator of a scalar particle in Euclidean space-time. In the vacuum (no background field), it is easily evaluated by standard methods and leads to the usual space and momentum space free propagators,²

$$\int_{x(0)=x'}^{x(t)=x} \mathcal{D}x(\tau) e^{-\int_0^t d\tau \frac{1}{4} \dot{x}^2} = \frac{1}{(4\pi t)^{d/2}}, \quad (5.43)$$

should be one derivation of (5.17).

Let $g(x, x')$, with $x, x' \in \mathcal{R}$ be the corresponding Green's function on a bounded, simply connected domain $\mathcal{R} \subset \mathbb{R}^d$, satisfying some boundary condition (e.g., periodic, Dirichlet or Neumann) at $\partial\mathcal{R}$. The Green's function identity allows us to connect the values of x_z inside of \mathcal{R} with the ones attained at the boundary ([an arbitrary Soviet citation](#)):

$$\begin{aligned} x(z) &= \int_{\mathcal{R}} g(z, z') m(z') dz' \\ &- \int_{\partial\mathcal{R}} \nabla_n g(z, z'') x(z'') dz'' + \int_{\partial\mathcal{R}} \nabla_n x(z'') g(z, z'') dz''. \end{aligned} \quad (5.44)$$

The Neumann boundary condition can be imposed by extending the original field symmetrically across its sides, so that the extended field, which is four times bigger, is symmetric and periodic.

At the risk of sounding repetitive: it's crazy to formulate this problem in terms of the symmetry-breaking domains with Dirichlet boundary conditions, when all that is needed are the trivial periodic solutions on 2-dimensional tori. To appreciate how difficult the Dirichlet problem is, you can at your leisure study the paper *On the solution of the Helmholtz equation on regions with corners* by Soviet mathematicians Serkh and Rokhlin [237] (one of them a Member of The National Academy of Sciences of The USA), who solve several boundary value problems for the Helmholtz equation on polygonal domains. In terms of the boundary integral equations of potential theory, the solutions are representable by series of appropriately chosen Bessel functions. Making the space discrete does not make these calculations any easier.

²Predrag 2017-06-17: Here a study of Sect. 6. *Worldline formalism* of Gelis and Tanji [109] might be helpful - it reexpresses the integral as an average over Wilson loops.

5.3 Green's function for 2-dimensional square lattice

Copied to here from *siminos/cats/GHJSC16.tex*

2019-10-31

The free Green's function $g(z, z') \equiv g(z - z', 0) \equiv g_{zz'}$ solves the equation

$$(-\square + \mu^2)g_{zz'} = \delta_{zz'}, \quad z = (n, t) \in \mathbb{Z}^2. \quad (5.45)$$

The solution is given by the double integral [193]

$$g_{z0} = \frac{1}{\pi^2} \int_0^\pi \int_0^\pi \frac{\cos(nx) \cos(ty)}{s - 2 \cos x - 2 \cos y} dx dy, \quad (5.46)$$

an expression which can, in turn, be recast into single integral form,

$$\begin{aligned} g_{z0} &= \frac{1}{2\pi^3} \int_{-\infty}^{+\infty} d\eta \int_0^\pi \int_0^\pi \frac{\cos(nx) \cos(ty)}{(s/2 - 2 \cos x - i\eta)(s/2 - 2 \cos y + i\eta)} dx dy \\ &= \frac{1}{2\pi} \int_{-\infty}^{+\infty} d\eta \frac{\mathcal{L}(\eta)^{-n} \mathcal{L}^*(\eta)^{-t}}{|\mathcal{L}(\eta) - \mathcal{L}(\eta)^{-1}|^2}, \end{aligned} \quad (5.47)$$

where

$$\mathcal{L}(\eta) + \mathcal{L}(\eta)^{-1} = s/2 + i\eta, \quad |\mathcal{L}(\eta)| > 1. \quad (5.48)$$

The above equation can be thought as the integral over a product of two \mathbb{Z}^1 functions:

$$g_{z0} = \frac{1}{2\pi} \int_{-\infty}^{+\infty} d\eta g_{n0}(s/2 + i\eta) g_{t0}(s/2 - i\eta). \quad (5.49)$$

An alternative representation is given by modified Bessel functions $I_n(x)$ of the first kind [193]:

$$g_{z0} = \int_0^{+\infty} d\eta e^{-s\eta} I_n(\eta) I_t(\eta), \quad (5.50)$$

which demonstrates that $g_{zz'}$ is positive for all $z = (n, t)$. The representation (5.50) enables explicit evaluation of the $n = t$ diagonal elements in terms of a Legendre function,

$$g_{z0} = \frac{1}{2\pi i} Q_{n-1/2}(s^2/8 - 1), \quad s^2/8 - 1 > 1, \quad z = (n, n).$$

Dirichlet boundary conditions. Consider next the Green's function $g_{zz'}$ which satisfies (5.45) within the rectangular domain $\mathcal{R} = \{(n, t) \in \mathbb{Z}^2 | 1 \leq n \leq \ell_1, 1 \leq t \leq \ell_2\}$ and vanishes at its boundary $\partial\mathcal{R}$. By applying the same method as in the case of 1-dimensional lattices we get

$$\begin{aligned} g_{zz'} &= \sum_{j_1, j_2=-\infty}^{+\infty} g_{n-n'+2j_1(\ell_1+1), t-t'+2j_2(\ell_2+1)} + g_{n+n'+2j_1(\ell_1+1), t+t'+2j_2(\ell_2+1)} \\ &\quad - g_{n-n'+2j_1(\ell_1+1), t+t'+2j_2(\ell_2+1)} - g_{n+n'+2j_1(\ell_1+1), t-t'+2j_2(\ell_2+1)}, \end{aligned}$$

where $g_{zz'}$ is the free Green's function (5.46). Substituting (5.49) yields the spatiotemporal Green's function as a convolution of the two 1-dimensional Green's functions (??)

$$g_{zz'} = \frac{1}{2\pi} \int_{-\infty}^{+\infty} d\eta g_{nn'}(s/2 + i\eta) g_{tt'}(s/2 - i\eta). \quad (5.51)$$

³

5.4 Toeplitz tensors

In refsect s-lattProp we worked out the propagator in the only in $d = 1$ configuration space, and stated the result for $d > 1$ after the Fourier transform diagonalization. What are the generalizations of Toeplitz matrices to $d > 1$? They are called *Toeplitz tensors*.

2018-02-24 Predrag This one I think is not relevant to us: Lim [183] *Singular values and eigenvalues of tensors: A variational approach* - “A theory of eigenvalues, eigenvectors, singular values, and singular vectors for tensors based on a constrained variational approach much like the Rayleigh quotient for symmetric matrix eigenvalues. An illustration: a multilinear generalization of the Perron-Frobenius theorem.”

2018-02-24 Predrag Khoromskaia and Khoromskij [170] *Block circulant and Toeplitz structures in the linearized Hartree-Fock equation on finite lattices: Tensor approach* seems quite relevant to our project - they work out the $D = 3$ lattice case: “grid-based tensor approach to solution of the elliptic eigenvalue problem for the 3D lattice-structured systems. We consider the linearized Hartree-Fock equation over a spatial $L_1 \times L_2 \times L_3$ lattice for both periodic and non-periodic case. In the periodic case the low-rank tensor structure in the diagonal blocks of the Fock matrix in the Fourier space reduces the conventional 3D FFT to the product of 1D FFTs.”

Xie, Jin and Wei [273] *A fast algorithm for solving circulant tensor systems*: “Circulant tensors is a generalization of the circulant matrix. We define the generalized circulant tensors which can be diagonalized by a Fourier matrix, and solve the circulant tensor system by a fast FFT algorithm.”

Cui *et al.* [70] *An eigenvalue problem for even order tensors with its applications*: “Using the matrix unfolding of even order tensors, we can establish the relationship between a tensor eigenvalue problem and a multi-level matrix eigenvalue problem. We show that higher order singular values are the square root of the eigenvalues of the product of the tensor and its conjugate transpose, as in the matrix case. Also we study an eigenvalue problem for Toeplitz/circulant tensors, and give the lower and upper bounds of eigenvalues of Toeplitz tensors.”

³Boris 2017-07-18, 2019-10-31: TO NEVER BE CONTINUED

Rezghi and Eldén [230] *Diagonalization of tensors with circulant structure:* “A tensor of arbitrary order, which is circulant with respect to two modes, can be diagonalized in those modes by discrete Fourier transforms. This property can be used in the efficient solution of linear systems involving contractive products of tensors with circulant structure. Tensors with circulant structure occur in models with periodic boundary conditions.”

2018-02-24 Predrag In 2007 the N-way Toolbox, Tensor Toolbox, and Multilinear Engine were software packages for working with tensors.
block-Toeplitz matrix

A tensor can be regarded as a multidimensional array of data. The order of a tensor is the number of dimensions. The dimensions of a tensor also are known as *ways* or *modes*.

Multilevel matrices arise in multidimensional applications.

5.5 Green's blog

2016-07-13 Predrag Cat map Green's functions are standard 'lattice propagators' for discrete lattices, obtained by discrete Fourier transform diagonalization of discrete Laplacian. Working through ChaosBook sections *D.3 Lattice derivatives* to *D.5.2 Lattice Laplacian diagonalized* might help you understand this material.

Note: All eq. numbers refer to svn ver. 5020 of [160521Gutkin.pdf](#) and ChaosBook.org [ver. 15.7](#). You can also use [current ver.](#), but the chapter numbering is different.

2017-02-17 Predrag For diffusion, a linear (symmetric, Vivaldi) code is needed.
For spatiotemporal cat

1. linear code seems needed. Have not proven that.
2. its partition volumes have no relation to 2-tori weights
3. linear code pruning rules undercount 2-tori pruning rules
4. 2-tori are intrinsic to the flow, there might exist Markov partitions

Boris 2017-02-17 Markov partitions for spatiotemporal cats exist, but their complexity grows exponentially with number of cats.

Predrag 2017-03-04 That is what you keep saying, but if you mean *finite* Markov partitions for *the* spatiotemporal cat, even on a finite spatially periodic domain, I have never seen it. It would require high-dimensional unstable/stable manifolds of the fixed point at the origin to map onto each other, in order to get a generating partition consisting of a finite number of volumes. Pretty amazing.

2017-08-25 Predrag I have not understood this before, but the $\mathcal{R} = [2 \times 1]$ block

$$M = \begin{bmatrix} s_{11} s_{21} \end{bmatrix}$$

is not just a 1D temporal cat - the Dirichlet boundary conditions make this nasty as well,

$$M \cup \partial R = \begin{bmatrix} x_{12}x_{22} \\ x_{01}s_{11}s_{21}x_{31} \\ x_{10}x_{20} \end{bmatrix}.$$

2017-08-25 Predrag $\partial R = \{x_1, x_2, \dots, x_8\}$ is not consistent with our notation: they live on sites, and should be labelled by index pairs $\partial R = \{x_z\}$, in $R = [2 \times 1]$ example as $\partial R = \{x_{01}, x_{02}, x_{13}, \dots, x_{10}\}$. That is consistent with the cat map, where the corresponding block + boundary points is correctly labelled as $x_0s_1s_2x_3$. The crazy thing is that even with the correct notation, there is no rhyme nor reason in the above 8 inequalities.

$$\begin{aligned} 0 &\leq (x_{01} + x_{10} - s_{12})(s^2 - 2) + (x_{13} + x_{02} + x_{31} + x_{20} - s_{22} - s_{11})s + (x_{23} + x_{32} - s_{21})2 \leq \nu_s \\ 0 &\leq (x_{02} + x_{13} - s_{22})(s^2 - 2) + (x_{01} + x_{10} + x_{23} + x_{32} - s_{12} - s_{21})s + (x_{20} + x_{31} - s_{11})2 \leq \nu_s \\ 0 &\leq (x_{20} + x_{31} - s_{11})(s^2 - 2) + (x_{01} + x_{10} + x_{23} + x_{32} - s_{12} - s_{21})s + (x_{02} + x_{13} - s_{22})2 \leq \nu_s \\ 0 &\leq (x_{23} + x_{32} - s_{21})(s^2 - 2) + (x_{13} + x_{02} + x_{31} + x_{20} - s_{22} - s_{11})s + (x_{01} + x_{10} - s_{12})2 \leq \nu_s \end{aligned}$$

2017-08-30 Boris In principle you are right, but keeping 2 indices would only make things look terribly "heavy" (without a good justification, as anyway "there is no rhyme nor reason"). The single index notation for the boundary points seems to me the least evil. **2017-09-09 Predrag** not convinced, but this is really a minor point. We follow Boris' convention.

2017-09-09 Predrag Dorr [83] *The direct solution of the discrete Poisson equation on a rectangle*

Hu, Ryu and O'Connell [137] *Analytical solution of the generalized discrete Poisson equation* " present an analytical solution to the generalized discrete Poisson equation (DPE), a matrix equation which has a tridiagonal matrix with fringes having an arbitrary value for the diagonal elements."

Many physical problems require the numerical solution of the Poisson equation on a rectangle. In general, one uses the finite-difference method [83], where the rectangle is replaced by an $N \times k$ grid, and the Poisson equation is solved in the finite-difference representation. In this way, the problem is reduced to the discrete Poisson equation (DPE) on an $[N \times k]$ grid, a matrix equation $Dx = s$ having a tridiagonal matrix $[k \times k]$ with fringes, of form

$$D = \begin{pmatrix} M & 1 & 0 & 0 & \dots & 0 & 0 \\ 1 & M & 1 & 0 & \dots & 0 & 0 \\ 0 & 1 & M & 1 & \dots & 0 & 0 \\ \vdots & \vdots & \vdots & \vdots & \ddots & \vdots & \vdots \\ 0 & 0 & \dots & \dots & \dots & M & 1 \\ 0 & 0 & \dots & \dots & \dots & 1 & M \end{pmatrix}, \quad (5.52)$$

where M is a $[N \times N]$ symmetric tridiagonal matrix (1.40), with constant $-s$ along the diagonal, and the $[N \times N]$ identity matrix I as the off-diagonal elements. Thus, the matrix \mathcal{D} consists of $[k \times k]$ submatrices of $[N \times N]$ elements. An important special case is $s = 4$, which is the matrix form for the Poisson equation on a rectangle arising from the difference method.

They invert \mathcal{D} in three steps:

1. By applying the results of ref. [136], invert \mathcal{D} into \mathcal{D}^{-1} . This generalizes (1.54) to a (sub)matrix formula, with g_{jk} replaced by submatrix Θ_{jk} , where Θ is an $[N \times N]$ matrix defined by

$$-2 \cosh \Theta = M$$

2. The eigenvalues and eigenfunctions for the submatrices of the block matrix $g = \mathcal{D}^{-1}$ are given by (1.52).
3. Evaluate analytically each of the individual elements in the inverted matrix \mathcal{D}^{-1} by the Schur decomposition scheme [113].

I find the procedure inelegant and cumbersome, as the two dimensions are treated in different ways. The result is, however, a bit more symmetric (but not written fully symmetric), written in terms of coefficients such as:

$$\alpha_{lm}(n) = \sqrt{\frac{2}{N+1}} \sinh \frac{ln\pi}{N+1} \sinh \frac{mn\pi}{N+1}.$$

In contrast, Boris formulation (5.46) is symmetric.

My intuition is explained in refsect s-lattProp - the d translations commute, so should compute eigenvalues for each direction separately. Works out for periodic boundary conditions.

As a wild guess, in d -dimensional the Jacobian (1.43) for Dirichlet b.c. would generalize to the product of d Jacobians, one for each direction

$$\det(\mathcal{D}_{\ell_1 \times \ell_2 \times \dots \times \ell_d}) = U_{\ell_1}(s/2)U_{\ell_2}(s/2) \cdots U_{\ell_d}(s/2). \quad (5.53)$$

For example,

$$\det(\mathcal{D}_{1 \times 1}) = U_1(s/2)U_1(s/2) = s^2, \quad (5.54)$$

and

$$\det(\mathcal{D}_{2 \times 2}) = U_2(s/2)U_2(s/2) = (s^2 - 1)^2. \quad (5.55)$$

This naive guess is almost certainly wrong...

How does one get cosh's and sinh's in the circulant matrix case?

2017-09-09 Predrag A few more links to digest:

Eigenvalues of periodic lattice Laplacian? uses the Kronecker product, and Harshaw gives sensible, symmetric eigenvalues for a doubly-periodic torus, something like

$$\lambda_{jk}^{[\ell_1 \times \ell_2]} = -\mu^2 - 2 \cos \frac{j\pi}{\ell_1} - 2 \cos \frac{k\pi}{\ell_2}, \quad (5.56)$$

where, , $0 \leq j \leq \ell_1 - 1$, $0 \leq k \leq \ell_2 - 2$, and $d = 2$. Their problem is the usual diffusive Laplacian on a square lattice, has no s term, so this is still only a guess.

Andreas Wipf [268] *Statistical Approach to Quantum Field Theory: An Introduction* ([click here](#)).

[arXiv:math/0010135](#) *Integrable Lattices: Random Matrices and Random Permutations*

[arXiv:1702.00339](#) *Block circulant and Toeplitz structures in the linearized Hartree-Fock equation on finite lattices: tensor approach*

2017-09-08 Predrag Giles and Thorn [110] *Lattice approach to string theory*. The Giles-Thorn (GT) discretization of the worldsheet begins with a representation of the free closed or open string propagator as a lightcone worldsheet path integral defined on a lattice.

The sequel Papathanasiou and Thorn [213] *Worldsheet propagator on the lightcone worldsheet lattice* give in Appendix B 2D lattice Neumann open string, Dirichlet open string, and closed string propagators.

Discrete Green's functions are explained, for example, by Chung and Yau [59] who give explicitly, in their Theorem 6, a 2-dimensional lattice Green's function for a rectangular $R^{[\ell_1 \times \ell_2]}$. I do not understand the paper - in any case, I see no determinants in it. This paper is cited over 100 times, maybe there is a better answer in that list.

2017-09-11 Predrag Bhat and Osting [37] *Diffraction on the two-dimensional square lattice* write: The lattice Green's function is quite well known [89, 162].

Katsura [164] *Lattice Green's function. Introduction:* The Helmholtz equation for the wavefunction $\psi(r)$ in the continuous space is given by

$$\left(\frac{1}{2} \Delta + E \right) \psi = 0 \quad (5.57)$$

The Green's function $g(E, r)$ is the solution of

$$\left(\frac{1}{2} \Delta + E \right) g = \delta(r) \quad (5.58)$$

The real part of the square lattice Green's function (5.46) is odd or even function of s , and the imaginary part is even or odd function of s , if the sum of n and t is even or odd, respectively.

Morita and Horiguchi [204] *Calculation of the lattice Green's function for the bcc, fcc, and rectangular lattices*: see the appendix *The lattice Green's functions for the rectangular lattice* (includes the square lattice as a special case). They integrate (5.46) and express it as the complete elliptic integral of the first kind (5.251).

Katsura, Inawashiro and Abe [163] *Lattice Green's function for the simple cubic lattice in terms of a Mellin-Barnes type integral*

Horiguchi [132] *Lattice Green's function for the simple cubic lattice* - GaTech does not have online access to it.

Horiguchi and Morita [133] *Note on the lattice Green's function for the simple cubic lattice*: “A simple recurrence relation connecting the lattice Green's function at (l, m, n) and the first derivatives of the lattice Green's function at $(l \pm 1, m, n)$, is presented for the simple cubic lattice. By making use of that recurrence relation, the lattice Green's functions at $(2, 0, 0)$ and $(3, 0, 0)$ are obtained in closed forms, which contain a sum of products of the complete elliptic integrals of the first and the second kind, see (5.251).”

Asad [16] *Differential equation approach for one- and two-dimensional lattice Green's function* seems a continuation of ref. [133]: “A first-order differential equation of Green's function, at the origin $G(0)$, for the one-dimensional lattice is derived by simple recurrence relation. Green's function at site (m) is then calculated in terms of $G(0)$. A simple recurrence relation connecting the lattice Green's function at the site (m, n) and the first derivative of the lattice Green's function at the site $(m \pm 1, n)$ is presented for the two-dimensional lattice, a differential equation of second order in $G(0, 0)$ is obtained. By making use of the latter recurrence relation, lattice Green's function at an arbitrary site is obtained in closed form.”

2017-09-11 Boris Some caution on Green's functions: In 1D everything is explicit and simple. The real problem is 2D. For the paper we need two facts – positivity of its elements, and exponential decay (both for Dirichlet boundary conditions). I was unable to extract them from the literature (which is bizarre), but checked numerically. Proofs are still lacking, but should be within reach.

2017-09-20 Predrag Continued feline misery. From the periodic orbit theory point of view, it is insane to work with finite lattice blocks with Dirichlet boundary conditions. The theory demands periodic boundary conditions. They preserve translational invariance which makes Green's matrices trivially diagonalizable by discrete Fourier transforms. Now that Boris is such a mensch that he can do it, I am writing up a pedagogical Dirichlet/periodic b.c.'s Green's matrices appendix to ref. [119] (or per chance even a section of the paper proper, as this is no afterthought - this is the central point of the paper), an appendix whose ultimate goal is to show

that the matrix elements are decaying exponentially as

$$\mathcal{D}_{zz'} \approx e^{-\lambda|z-z'|^d}, \quad (5.59)$$

i.e., in our humble $d = 2$ example as $\exp(-\lambda|z - z'|^2)$. If the coauthors were to understand or (gasp!) contribute to the write up, we would be in cat heaven.

So far, still writing up the $d = 1$ temporal cat example of sect. 1.4, but the determinant of the Helmholtz operator for any finite $d = 2$ rectangular lattice region of sect. 5.4 should play out the same way.

To Matt and Andy: This goes lock, stock and barrel into the continuum field theories, such as Kuramoto-Sivashinsky, with the Euclidian metric in (5.59) replaced by the (still to be thought through) correct Kuramoto-Sivashinsky spacetime metric.

2017-10-18 Predrag Glaser [111] *Numerical solution of waveguide scattering problems by finite-difference Green's functions* computes a 2-dimensional Green's function with boundary conditions on arbitrary shape approximated by a discrete boundary: “A finite-difference Green's function method for solving time-harmonic wave guide scattering problems involving metallic obstacles of finite size is applied to the two-dimensional problem of a TE10 mode impinging on cylindrical metallic posts of arbitrary shape in a rectangular waveguide.”

2017-10-19 Predrag de la Llave [187] *Variational methods for quasiperiodic solutions of partial differential equations* has a pedagogical discussion of the discrete lattices gradient flows.

2017-09-11 Predrag Katsura and Inawashiro [162] *Lattice Green's functions for the rectangular and the square lattices at arbitrary points*. They start with product of two Bessel functions (5.50), then go hypergeometric, or $K(u)$ complete elliptic. In the appendix they study lattice Green's function of the linear lattice (i.e., $d = 1$ lattice), and relate it to Chebyshev $T_m(u)$ and in turn to the hypergeometric ${}_2F_1$.

2019-11-04 Predrag Doyle and Snell [84] [arXiv:math/0001057](https://arxiv.org/abs/math/0001057) present the connection between random walks and electric networks.

2020-05-09 Predrag Sunada [254] *Topological Crystallography* ([click here](#)) Chap. 9 is all about random walks on lattices.

2CB

2020-05-10 Predrag Some general graph-theory definitions, from different sources, will eventually be all in ChaosBook *appendMarkov.tex*:

Many follow the definitions in Serre [238] and Stark and Terras [249].

Let $G = (V, E)$ be a connected *non-directed* graph, with V the set of $|V|$ vertices or nodes (assume that there are no 1-degree vertices), E the set

of $|E|$ unoriented edges (possibly multiple edges and 1-loops) labeled $e_1, \dots, e_{|E|}$.

The *adjacency matrix* for an undirected graph with n nodes is an $[n \times n]$ matrix (13.42) with (i,j) -th entry specifying the number of non-directed edges from node i to j with i -th diagonal entry being twice the number of self-adjoining loops on i -th node.

A graph is *finite* if it has a finite number of nodes and edges. It is *connected* if every node can be reached by traversing a path.

A *rooted graph* is a pair (G, v) , where G is a graph and $v \in V$ is a vertex of G , called the root.

A graph is *simple* if it has no loops, i.e., no edges of the form (u, u) $u \in V$ and there is at most a single edge between any two vertices.

A graph is *bi-partite* if its vertices can be partitioned into two disjoint sets U and W such that no vertex in U is adjacent to any other vertex in U and likewise for W ; the graph has edges only between “ U ” and “ W ” vertices.

In order to define a closed path in a non-directed graph orient the edges in an arbitrary but fixed way. Oriented edge $e = (u, v) \in E(G)$ joins two vertices, the origin $u = o(e)$ to the tip $v = t(e)$.

The vertices $o(e)$ and $t(e)$ are the *extremities* of the edge E . Two vertices are *adjacent* if they are extremities of an edge.

The *degree* of a vertex v is $\deg v = \text{Card}\{e \in E_v : o(e) = v\}$. A graph is d -regular if each vertex has degree d .

The in-degree (respectively out-degree) of any vertex of a directed graph is the number of in-coming (respectively out-going) edges. For a *directed regular* graph all vertices have equal in-degrees and out-degrees.

A graph is *vertex transitive* if there is a group of automorphisms which is transitive on the vertices. Such a graph is *regular*.

In the physics literature regular trees are called Bethe lattices.

Denote by $e^{-1} = (v, u)$ the inverse of $e = (u, v)$, with the origin v and the tip u .

Let G' be the graph with $2|E|$ oriented edges built from such oriented graph G by adding the opposing oriented edges $e_{|E|+1} = (e_1)^{-1}, \dots, e_{2|E|} = (e_{|E|})^{-1}$.

If e_i belongs to an oriented loop, $e_{i+|E|} = (e_i)^{-1}$ belongs to oriented loop going through the same pair of vertices.

A path $P = (e_1, \dots, e_n)$ has a backtracking if $e_{i+1}^{-1} = e_i$. The path has a *tail* if $e_0 = e_{n-1}^{-1}$.

The *inverse cycle* of a cycle $C = (e_1, \dots, e_n)$ is the cycle $C^{-1} = (e_n^{-1}, \dots, e_1^{-1})$.

The cycle C is called reduced if C^2 has no backtrack, and prime if it can not be expressed as $C = D^f$ for any cycle D and $f \geq 2$.

A cycle C is prime if it is not a repeat of a strictly smaller cycle.

Cycles $C_1 = (e_1, \dots, e_n)$ and $C_2 = (f_1, \dots, f_n)$ are called *equivalent* if there exists k such that $f_j = e_j + k$ for all j . Let $[C]$ be the equivalence class which contains a cycle C .

For a cycle C , the equivalence class $[C]$ is the set of cyclic permutations of C , i.e., cycles are equivalent up to choice of the initial/terminal vertex.

A ‘prime cycle’ (‘orbit’) is non-backtracking, tailless and not a r -multiple cycle.

A geodesic in a graph is a path without back-tracking, consistent with Riemannian geometry where a geodesic is a path which is locally distance minimizing. A closed geodesic is a closed path without back-tracking or tails.

A *tree* is a connected nonempty graph without geodesic loops.

In Riemannian geometry geodesics are locally distance minimizing paths and the difference between a *geodesic loop* and a *closed geodesic* is that the latter is required to be differentiable also at the starting/ending point.

A path is closed if $e_0 = e_n$. A geodesic is a path without backtracking. A geodesic loop (or circuit in Serre’s terminology) is a closed path that is a geodesic. A closed geodesic is a closed path with no tail and without backtracking.

The path of length zero counts as a closed geodesic and, therefore, is a geodesic loop. Additionally, every closed path with one edge counts as a closed geodesic. Any length two geodesic loop is also a closed geodesic, but the closed path $e e^{-1}$ is neither.

A *prime* geodesic is an equivalence class of closed geodesics $[C]$ (where the equivalence class is forgetting the starting point) which is primitive in the sense that it is not a power of another closed geodesic. The latter means by definition that there is no closed geodesic d and integer $n > 1$ such that $[C] = [d^n]$, which says in words that c is not just a geodesic that traverses another one n number of times.

In graph theory the names for “closed geodesics” or “geodesic loops”, range from circuits, loops etc, to closed paths without backtracking and no tails.

In terms of a graph $G = (V, E)$, a random walk is a stochastic process associated with a positive-valued function p on E satisfying

$$\sum_{e \in E_v} p(e) = 1.$$

$p(e)$ is the transition probability that a random walker at $o(e)$ moves to $t(e)$ along the edge e . The transition operator $P : C(V) \rightarrow C(V)$

the space of functions on V , is defined by

$$Pf(x) = \sum_{e \in E_v} p(e)f(t(e)).$$

The n -step transition probability $p(n, x, y)$ is the probability that after the n -steps a random walker at the initial site x is found at y ,

$$(P^n)f(x) = \sum_{y \in V} p(n, x, y)f(y).$$

The *simple random walk* on $G = (V, E)$ is the walk such that the probabilities moving along out-going edges from a vertex are the same, with the transition probability $p(e) = 1/\deg o(e)$.

The operator $P - I$ is the discrete Laplacian associated with the weight functions $m_V(v) = \deg v$, $m_E = 1$,

$$((P^n - I)f)(v) = \frac{1}{\deg v} \sum_{e \in E_v} [f(t(e)) - f(o(e))]. \quad (5.60)$$

$P_v - I$ is the discrete analogue of the *twisted Laplacian* [253]⁴⁵

Let Λ be a Bravais lattice. Then P is Λ -equivariant, and is related to the transition operator P_0 associated with the simple random walk on over a finite graph $G_0 = (V_0, E_0)$ as

$$P(f \circ \omega) = (P_0(f)) \circ \omega,$$

where f is an arbitrary function on V_0 , and $\omega : G \rightarrow G_0$ is the covering map.

2020-05-11 Predrag Bharatram Rangarajan *A combinatorial proof of Bass's determinant formula for the zeta function of regular graphs*, arXiv:1706.00851:

For an integer $d \geq 2$, let $G = (V, E)$ be a finite d -regular undirected graph with adjacency matrix A . A *walk* on the graph G is a sequence $v_0v_1 \dots v_k$ where v_0, v_1, \dots, v_k are (not necessarily distinct) vertices in V , and for every $0 \leq i \leq k-1$, $(v_i, v_{i+1}) \in E$. The vertex v_0 is referred to as the *root* (or origin) of the above walk, v_k is the terminus of the walk, and the walk is said to have length k .

It is often useful to equivalently define a walk as a sequence of directed or oriented edges. Associate each edge $e = (v, w) \in E$ with two directed edges (or rays) denoted

$$\vec{e} = (v \rightarrow w)$$

$$\vec{e}^{-1} = (w \rightarrow v)$$

⁴Predrag 2020-05-05: Looked at Sunada [253], but still not sure what is a ‘twisted’ Laplacian.

⁵Predrag 2020-05-13: Why $1/\deg v$ in (5.60)?

Note that the origin $org(\vec{e})$ is the vertex v and its terminus $ter(\vec{e})$ is the vertex w . Similarly, the origin $org(\vec{e}^{-1})$ is the vertex w and its terminus $ter(\vec{e})$ is the vertex v . Let \vec{E} denote the set of $m = nd$ directed edges of G . So a walk of length k can equivalently be described as a sequence $\vec{e}_1 \vec{e}_2 \dots \vec{e}_k$ of k (not necessarily distinct) oriented edges in \vec{E} such that for every $1 \leq i \leq k - 1$,

$$ter(\vec{e}_i) = org(\vec{e}_{i+1})$$

This is a walk that starts at $org(\vec{e}_1)$ and ends at $ter(\vec{e}_k)$.

It is easy to show that for any $k \in \mathbb{Z}$, the number of walks of length k between vertices $u, v \in V$ is exactly $(A^k)_{u,v}$. In particular, the total number of rooted cycles of length k in G is exactly

$$\text{Tr}(A^k)$$

A *non-backtracking walk* of length k from $v_0 \in V$ to $v_k \in V$ is a walk $v_0 v_1 \dots v_k$ such that for every $1 \leq i \leq k - 1$,

$$v_{i-1} \neq v_{i+1}$$

Equivalently, a non-backtracking walk of length k from $v \in V$ to $w \in V$ is a walk $\vec{e}_1 \vec{e}_2 \dots \vec{e}_k$ such that $org(\vec{e}_1) = v$, $ter(\vec{e}_k) = w$ and for every $1 \leq i \leq k - 1$,

$$\vec{e}_{k+1} \neq \vec{e}_k^{-1}$$

Non-backtracking random walks on graphs have been studied in the context of mixing time [cite alon], cut-offs [cite peres], and exhibit more useful statistical properties than ordinary random walks. In [cite peres], the authors obtain further interesting results on the eigendecomposition of the Hashimoto matrix H .

A rooted, non-backtracking cycle of length k with root v is a non-backtracking walk $v, v_1, v_2, \dots, v_{k-1}, v$ with the additional boundary constraint that

$$v_1 \neq v_{k-1}$$

Let \mathcal{C} denote the set of all rooted, non-backtracking, closed walks in G , and for $C \in \mathcal{C}$, let $|C|$ denote the length of the walk C . There are two elementary constructions we can carry out to generate more elements of \mathcal{C} from a given cycle C :

- *Powering:* Given a rooted, non-backtracking closed walk $C \in \mathcal{C}$ of length k of the form

$$C = \vec{e}_1 \vec{e}_2 \dots \vec{e}_k$$

then for $m \geq 1$ define a power

$$C^m = \underbrace{\vec{e}_1 \dots \vec{e}_k \vec{e}_1 \dots \vec{e}_k \dots \vec{e}_1 \dots \vec{e}_k}_{m \text{ times}}$$

which is a concatenation of the string of edges corresponding to the walk C with itself m times. Note that C^m is also a rooted, non-backtracking closed walk in G of length mk . Essentially, C^m represents the walk obtained by repeating or winding the walk C m times. Also note that C and C^m are both rooted at the same vertex.

- *Cycle class:* Given a rooted, non-backtracking closed walk $C \in \mathcal{C}$ of length k of the form

$$C = \vec{e}_1 \vec{e}_2 \dots \vec{e}_k$$

we can form another walk

$$C^{(2)} = \vec{e}_2 \vec{e}_3 \dots \vec{e}_k \vec{e}_1$$

which is also a rooted, non-backtracking closed walk in G of length k , but now rooted at the origin of the directed edge \vec{e}_2 (or the terminus of \vec{e}_1). More generally, for $1 \leq j \leq k$, define

$$C^{(j)} = \vec{e}_j \vec{e}_{j+1} \dots \vec{e}_k \vec{e}_1 \vec{e}_2 \dots \vec{e}_{j-1}$$

which is a cyclic permutation of the walk C obtained by choosing a different root. So given a walk $C \in \mathcal{C}$ of length k , we get $k - 1$ additional walks in \mathcal{C} of length k for free this way. In fact, this defines an equivalence class \sim on \mathcal{C} , and the set

$$[C] = \{C^{(1)}, C^{(2)}, \dots, C^{(k)}\}$$

is called the equivalence class of C . An element $[C] \in \mathcal{C}/\sim$ represents a non-backtracking closed walk modulo a choice of root.

2019-10-31 Predrag Guttmann [121] *Lattice Green's functions in all dimensions* starts the way I understand, with random walks on lattices ([Wanderings of a drunken snail](#)), apparently discussed eruditely by Hughes [139] and also used in the calculation of the effective resistance of resistor networks [68], but then quickly leads to an amazing range of deep mathematics which we can safely ignore (though not some of the references).

" for a translationally invariant walk on a d -dimensional periodic Bravais lattice, a natural question to ask is the probability that a walker starting at the origin of a lattice will be at position z after n steps. The probability-generating function is known as the lattice Green's function $g_{z,0}$. [...] the *structure function* of the lattice and is given by the discrete Fourier transform of the individual step probabilities. For example, for the d -dimensional hypercubic lattice, the structure function is

$$\lambda(k) = \frac{1}{d}(\cos k_1 + \cos k_2 + \dots + \cos k_d).$$

Harshaw (5.56) seem to be in the same spirit.

[...] The probability of returning to the origin is

$$1 - 1/g_{0,0}.$$

Since $g_{0,0}$ diverges for two-dimensional lattices, the probability of returning to the origin by a random walker in two dimensions is certain. [...] For the infinite square lattice, the result is remarkably simple:

$$g_{z,0}(u) = \frac{2}{\pi} K(u)$$

where $K(u)$ is the complete elliptic integral of the first kind (5.251), with hypergeometric representation

$$K(u) = \frac{\pi}{2} {}_2F_1\left(\frac{1}{2}, \frac{1}{2}; 1; u\right)$$

For the square lattice, we can also use the equivalent structure function

$$\lambda(k) = \cos k_1 \cos k_2,$$

demonstrating that structure functions for a given lattice are not unique. [...] In $d = 3$ the result for the simple cubic case is a saga in itself. [...] "

2020-02-09 Predrag Chen [54] *On the solution of circulant linear systems*: In the case where multidimensional problems are concerned, the matrices of coefficients of the resulting linear systems are block circulant matrices. After some transformations and permutations we are led to a block diagonal matrix with circulant blocks on the diagonal. This reduces the problem to the solution of n circulant linear systems, which may be performed in parallel. An important example is the finite difference approximate solution of elliptic equations over a rectangle with periodic boundary conditions [50, 269].

Sect. 4: A block matrix is a matrix defined by smaller matrices, called blocks. A block matrix M , where each of the blocks M_i it self an circulant, is called block circulant with circulant blocks. He first extracts eigenvalues of circulant blocks, then inserts them into the large matrix.

It is well known [50] that the approximation of Poisson's equation on a rectangle subject to periodic boundary conditions in both directions by the standard five-term difference scheme on a uniform mesh results in the block circulant linear system.

He also solves biharmonic (Laplacian squared) equation with the standard 13-term difference approximation.

2020-02-16 Predrag An example computed for
CL18.tex, using *siminos/mathematica/Tensors.nb*

Block circulant with circulant blocks [50, 54] $\mathcal{J}_{[4 \times 2]} =$

$$\left(\begin{array}{cc|cc} \begin{pmatrix} -2s & 2 \\ 2 & -2s \end{pmatrix} & \begin{pmatrix} 1 & 0 \\ 0 & 1 \end{pmatrix} & \begin{pmatrix} 0 & 0 \\ 0 & 0 \end{pmatrix} & \begin{pmatrix} 1 & 0 \\ 0 & 1 \end{pmatrix} \\ \begin{pmatrix} 1 & 0 \\ 0 & 1 \end{pmatrix} & \begin{pmatrix} -2s & 2 \\ 2 & -2s \end{pmatrix} & \begin{pmatrix} 1 & 0 \\ 0 & 1 \end{pmatrix} & \begin{pmatrix} 0 & 0 \\ 0 & 0 \end{pmatrix} \\ \begin{pmatrix} 0 & 0 \\ 0 & 0 \end{pmatrix} & \begin{pmatrix} 1 & 0 \\ 0 & 1 \end{pmatrix} & \begin{pmatrix} -2s & 2 \\ 2 & -2s \end{pmatrix} & \begin{pmatrix} 1 & 0 \\ 0 & 1 \end{pmatrix} \\ \begin{pmatrix} 1 & 0 \\ 0 & 1 \end{pmatrix} & \begin{pmatrix} 0 & 0 \\ 0 & 0 \end{pmatrix} & \begin{pmatrix} 1 & 0 \\ 0 & 1 \end{pmatrix} & \begin{pmatrix} -2s & 2 \\ 2 & -2s \end{pmatrix} \end{array} \right) \quad (5.61)$$

is of $[L \times L]$ block form, $L = 4$, with $[T \times T]$ blocks, $T = 2$.

Lagrangian systems are conservative dynamical systems which have a variational formulation. To understand the relation between the discrete time Hamiltonian and Lagrangian formulations, one needs to understand the discrete mapping generating function, such as (7.73).⁶

Consider a cat map [14] of form

$$\begin{pmatrix} q_{t+1} \\ p_{t+1} \end{pmatrix} = A \begin{pmatrix} q_t \\ p_t \end{pmatrix} \quad \text{mod } 1, \quad A = \begin{pmatrix} s-1 & 1 \\ s-2 & 1 \end{pmatrix}, \quad (5.62)$$

with both q_t and p_t in the unit interval, A a linear, state space (area) preserving map of a 2-torus onto itself, and $s = \text{tr } A > 2$ an integer. Implement explicitly, as in (1.101), the mod 1 operation by introducing m^q and m^p winding numbers,

$$\begin{pmatrix} q_{t+1} \\ p_{t+1} \end{pmatrix} = A \begin{pmatrix} q_t \\ p_t \end{pmatrix} - \begin{pmatrix} m_{t+1}^q \\ m_{t+1}^p \end{pmatrix}. \quad (5.63)$$

This is a non-autonomous, time-forced Hamiltonian equation of motion of form (12.2,12.1):

$$q_{t+1} = q_t + p_{t+1} + (s_{t+1}^p - s_{t+1}^q) \quad (5.64)$$

$$p_{t+1} = p_t + \mu^2 q_t - s_{t+1}^p, \quad (5.65)$$

with the force and the corresponding potential energy given by

$$P(q_t) = -\frac{dV(q_t)}{dq_t} = \mu^2 q_t - s_{t+1}^p, \quad (5.66)$$

$$V(q_t) = -\frac{1}{2}\mu^2 q_t^2 + s_{t+1}^p q_t. \quad (5.67)$$

As always, the Lagrangian, or, in the parlance of discrete time dynamics, the *generating function* $L(q_i, q_{i+1})$, is given by the difference of the kinetic and potential energies, where in the literature [39, 189, 190, 196] there are different choices of the instant in time at which $V(q)$ is be evaluated. We define the generating function as

$$L(q_t, q_{t+1}) = \frac{1}{2}p_{t+1}^2 - V(q_t).$$

Next one eliminates momenta in favor of velocities, using (5.64)

$$\begin{aligned} L(q_t, q_{t+1}) &= \frac{1}{2}(q_{t+1} - q_t - s_{t+1}^p + s_{t+1}^q)^2 + \frac{1}{2}\mu^2 q_t^2 - s_{t+1}^p q_t \\ &= \frac{1}{2}q_{t+1}^2 + \frac{s-1}{2}q_t^2 - q_t q_{t+1} \\ &\quad - q_{t+1}s_{t+1}^p + q_{t+1}s_{t+1}^q - q_t s_{t+1}^q + \text{constant}. \end{aligned} \quad (5.68)$$

⁶Predrag 2019-08-05: In preparing this summary we have found expositions of Lagrangian dynamics for discrete time systems by MacKay, Meiss and Percival [190, 196], and Li and Tomsovic [178] particulary helpful.

And this generating function satisfies (5.78).

Consider a symplectic (“area preserving”) map acting on phase space

$$x_{t+1} = M(x_t), \quad x_t = (q_t, p_t)$$

that maps x_t to x_{t+1} while preserving the symplectic area.

A *path* is any set of successive *configuration space* points

$$\{q_i\} = \{q_t, q_{t+1}, \dots, q_{t+k}\}. \quad (5.69)$$

In a Lagrangian system each path of finite length in the configuration space is assigned an *action*.⁷

To get the action of an orbit from time t_0 to t_n , we only need to sum (5.68) over intermediate time steps:

$$S(q_{t_0}, q_{t_0+1}, \dots, q_{t_n-1}, q_{t_n}) = \sum_{t=t_0}^{t_n-1} L(q_t, q_{t+1}). \quad (5.70)$$

For example, in a discrete-time one-degree-of-freedom Lagrangian system with the configuration coordinate q_i at the discrete time i , and *generating function* (“Lagrangian density”) $L(q_i, q_{i+1})$, the action of path $\{q_i\}$ is

$$S_{t,t+k} \equiv \sum_{i=t}^{t+k-1} L(q_i, q_{i+1}), \quad (5.71)$$

For 1-dof systems, the geometrical interpretation of the action $S_{t,t+k}$ is that $L(q_t, q_{t+1})$ is, up to an overall constant, the phase-space area below the p_t to p_{t+k} graph for the (q_t, q_{t+k}) path in the (q, p) phase plane.⁸

Denoting the derivatives of the generating function $L(q, q')$ as

$$\begin{aligned} L_1(q, q') &= \frac{\partial}{\partial q} L(q, q'), & L_2(q, q') &= \frac{\partial}{\partial q'} L(q, q') \\ L_{12}(q, q') &= L_{21}(q, q') = \frac{\partial^2}{\partial q \partial q'} L(q, q'), \end{aligned} \quad (5.72)$$

the *momenta* are given by [190, 196]

$$p_n = -L_1(q_n, q_{n+1}), \quad p_{n+1} = L_2(q_n, q_{n+1}). \quad (5.73)$$

The twist condition

$$\partial p_{n+1} / \partial q_n \neq 0 \text{ for all } p_{n+1}, q_n, \quad (5.74)$$

⁷Predrag 2019-08-04: repeat of text in catLagrang.tex; 2020-07-04 no recollection of where that is?

⁸Predrag 2016-11-11, 2018-09-26: What follows is (initially) copied from Li and Tomsovic [178], *Exact relations between homoclinic and periodic orbit actions in chaotic systems* arXiv source file, then merged with the MacKay-Meiss-Percival action principle refs. [190, 196].

ensures that

$$L_{12}(q_n, q_{n+1}) \neq 0. \quad (5.75)$$

We distinguish a *path* (5.69), which is any set of successive points $\{q_n\}$ in the configuration space, from the *orbit segment* $M^k(x_n)$ from x_n to x_{n+k} , a set of successive *phase space* points

$$\{x_i\} = \{x_n, x_{n+1}, \dots, x_{n+k}\}. \quad (5.76)$$

that extremizes the *action* (5.71), with momenta given by (5.73). In other words, not only q_n , but also p_n have to align from phase space point to phase space point [218],

$$\frac{\partial}{\partial q_n} (L(q_{n-1}, q_n) + L(q_n, q_{n+1})) = 0. \quad (5.77)$$

Any finite path for which the action is stationary with respect to variations of the segment keeping the endpoints fixed, is called an orbit segment or *trajectory* [73]. Infinite paths for which each finite segment is an orbit segment are called *orbits*.

Given by Keating [168], for the 1-dimensional cat map (1.101), the action of a one-step orbit (which is the generating function) from (x_t, p_t) to (x_{t+1}, p_{t+1}) can be written as (5.88). And the map (5.63) can be generated using [190, 196]:

$$p_t = -\partial L(x_t, x_{t-1})/\partial x_t, \quad p_{t+1} = \partial L(x_t, x_{t-1})/\partial x_{t+1} \quad (5.78)$$

⁹

Setting the first variation of the action δS to 0 we get:

$$\frac{\partial S}{\partial x_t} = \frac{\partial L(x_t, x_{t+1})}{\partial x_t} + \frac{\partial L(x_{t-1}, x_t)}{\partial x_t} = 0 \quad (5.79)$$

$$\Rightarrow -x_{t-1} + s x_t - x_{t+1} = s_{t+1}^x - s_t^x + s_t^p. \quad (5.80)$$

This is the Percival-Vivaldi second-order difference equation of the cat map with $s_t = s_{t+1}^x - s_t^x + s_t^p$.

Using (5.68–5.70) we can compute the action of any finite trajectory. For a trajectory $\dots x_{t-1} x_t x_{t+1} x_{t+2} \dots$, the action can be written as:

$$S(\mathbf{x}) = -\frac{1}{2} \mathbf{x}^\top \mathcal{J} \mathbf{x} - \mathbf{s}^\top \mathbf{x}, \quad (5.81)$$

where \mathbf{x} and \mathbf{s} are column vectors,

$$\mathbf{x} = \begin{bmatrix} \vdots \\ x_{t-1} \\ x_t \\ x_{t+1} \\ x_{t+2} \\ \vdots \end{bmatrix}, \quad \mathbf{s} = \begin{bmatrix} \vdots \\ s_{t-1} \\ s_t \\ s_{t+1} \\ s_{t+2} \\ \vdots \end{bmatrix}, \quad (5.82)$$

⁹Han 2019-08-01: (5.88) is given by Keating [168] but I cannot find the derivation of this generating function in that paper and the papers referred [167, 219]. The following derivation of generating function is from our blog.

and the orbit Jacobian matrix \mathcal{J} is a Toeplitz matrix

$$-\mathcal{J} = \begin{bmatrix} \ddots & \ddots \\ \ddots & s & -1 & 0 & 0 & \dots & 0 & 0 & \ddots \\ \ddots & -1 & s & -1 & 0 & \dots & 0 & 0 & \ddots \\ \ddots & 0 & -1 & s & -1 & \dots & 0 & 0 & \ddots \\ \ddots & \vdots & \vdots & \ddots & \ddots & \ddots & \vdots & \vdots & \ddots \\ \ddots & 0 & 0 & \dots & \dots & \dots & s & -1 & \ddots \\ \ddots & 0 & 0 & \dots & \dots & \dots & -1 & s & \ddots \\ \ddots & \ddots \end{bmatrix}. \quad (5.83)$$

For an orbit with finite length, we need to know the bc's to find the action at boundaries. Note that the action computed in this way will not have the constant terms in (5.68). The matrix \mathcal{J} has same effect as $(s - \square - 2)$ where the \square is the discrete one-dimensional Laplacian defined in (12.3).

5.6.1 Lagrangian formulation

¹⁰ While introduction of ‘temporal Bernoulli’ might have seem unmotivated (as we had already shown, there are many way to skin a cat), in mechanics the ‘temporal’ formulation is as old as the modern mechanics itself, and known as the Lagrangian, or variational formulation, the additional twist being phase space volume conservation. In the simplest, 1-degree of freedom kicked rotor example, that means area preservation.

An area-preserving map (12.2,12.1) that describes a kicked rotor subject to a discrete time sequence of angle-dependent impulses $P(x_t)$ has a Lagrangian (*generating function*) for a particle moving in potential $V(x)$ at the *lattice site* (time instant) t ,

$$L(x_t, x_{t+1}) = \frac{1}{2}(x_t - x_{t+1})^2 - V(x_t), \quad P(x) = -\frac{dV(x)}{dx}. \quad (5.84)$$

In the Lagrangian formulation a global lattice state X is assigned an *action* functional $S[X] = \sum_t L(x_t, x_{t+1}) + X^\top M$, for a prescribed symbol block M of sources s_t . The action can be written down by inspection,

$$S[X] = \frac{1}{2}X^\top \mathcal{J} X + X^\top M = \frac{1}{2} \sum_{t,t'=1}^{\ell} x_{t'} \mathcal{J}_{t't} x_t + \sum_{t=1}^{\ell} s_t x_t, \quad (5.85)$$

as its first variation $\delta S / \delta X^\top = 0$ has to yield $\mathcal{J}X_M + M = 0$, the temporal cat fixed point condition (3.49). The solutions X_M of the variational condition of

¹⁰Predrag 2020-07-24: This is a former subsection *Lagrangian formulation of cat.tex*, called by *CL18.tex*.

$\delta S/\delta \mathbf{X}^\top = 0$ are stationary points of the action, so they are sometimes called *stationary* configurations; here we refer to them as ‘lattice states’. The form is the same as the Bernoulli fixed point condition `refeq{tempFixPoint}`, but with the temporal cat orbit Jacobian matrix \mathcal{J} given by the symmetric $[n \times n]$ matrix of second variations `refeq{Hessian}` $\mathcal{J}_{tt'} = \partial^2 S/\partial x_t \partial x_{t'}$, in mechanics often referred to as the *Hessian* matrix. Here, due to the fact that the temporal stability multipliers `refeq{StabMtlpr}` are the same for all temporal lattice states of the same period ℓ , this orbit Jacobian matrix depends only on the period of the lattice state. That does not hold for general nonlinear cat maps [67], where each periodic temporal lattice state \mathbf{X}_M has its own stability.

2020-01-17 Han In my previous computation, the orbit Jacobian matrix is $\mathcal{J} = -d + s\mathbf{1} - d^{-1}$. And I think my \mathcal{J} is correct. One way to show this is: $S[\mathbf{X}] = \sum_t L(x_t, x_{t+1}) + \mathbf{X}^\top \mathbf{M}$, and in the Lagrangian (5.84) if you expand the first term there will be a $-x_t x_{t+1}$ term. So the subdiagonal elements of \mathcal{J} should be -1 .

And $\square = \partial^\top \partial = d^\top d - 2\mathbf{1}$ is not right. In the first chapter of your Quantum Field Theory notes, section of Lattice Laplacian, you have $\square = -\partial^\top \partial$.

$\partial^\top \partial = 2\mathbf{1} - d^\top d$. So using my orbit Jacobian matrix $\mathcal{J} = -d + s\mathbf{1} - d^{-1}$ the action has form:

$$S[\mathbf{X}] = \sum_{t=1}^n \left\{ \frac{1}{2}(\partial x_t)^2 - \frac{1}{2}\mu^2 x_t^2 \right\} + \sum_{t=1}^n s_t x_t. \quad (5.86)$$

2020-01-31 Predrag I would love to have your convention $\mathcal{J} = -d + s\mathbf{1} - d^{-1}$. But there is no avoiding the pesky overall “-” sign; it arises from $s_{t+1} = \lfloor sx_t \rfloor$, being the integer part of sx_t . This leads to (3.25), and there is no logically clean rational for changing the sign of s_t . But I do have to ponder again the meaning of $\partial^\top \partial = 2\mathbf{1} - d^\top d$ for the Lagrangian formulation

2021-12-14 Predrag I now avoid the pesky overall “-” sign; it arises from $s_{t+1} = \lfloor sx_t \rfloor$, being the integer part of sx_t by having redefined the temporal Bernoulli. Han’s (5.86) is the way to go.

By noting that the temporal lattice Laplacian can be written as $\square = \partial^\top \partial = d^\top d - 2\mathbf{1}$, where the $[n \times n]$ matrix $\partial = (\mathbf{1} - d)/\Delta t$ is the discrete time derivative `refeq{1stepVecEq}`, the temporal cat Lagrangian density (5.84) and the action (18.200) can be written in the more familiar, field-theoretic form

$$S[\mathbf{X}] = \sum_{t=1}^n \left\{ \frac{1}{2}(\partial x_t)^2 + \frac{1}{2}\mu^2 x_t^2 \right\} + \sum_{t=1}^n s_t x_t. \quad (5.87)$$

For $0 \leq s < 2$ this is the action for a 1-dimensional chain of nearest-neighbor coupled harmonic oscillators. Here we are, however, interested in the everywhere hyperbolic, unstable, anti-harmonic or inverted parabolic potential, $s \geq 2$ case.

5.6.2 Temporary: Cat map in the Lagrangian formulation

===== the rest: TEMPORARY TEXT =====

Rewrite (1.101) back to (5.62)'s form, and let m^q and m^p be the winding numbers, we can get (5.63).

¹¹ The action of the system in this one-step motion is [168] ¹²

$$L(q_t, q_{t-1}) = \frac{1}{2}[(s-1)q_{t-1}^2 - 2q_{t-1}(q_t + m_t^q) + (q_t + m_t^q)^2 - 2m_t^p q_t]. \quad (5.88)$$

The action of a longer orbit is the sum of the one-step actions at each time step. The Lagrangian equations of motion are obtained by demanding that the first variation of the action vanishes:

$$\frac{\partial L(q_{t+1}, q_t)}{\partial q_t} + \frac{\partial L(q_t, q_{t-1})}{\partial q_t} = 0 \quad (5.89)$$

$$-q_{t-1} + sq_t - q_{t+1} = m_{t+1}^q - m_t^q + m_t^p = m_t, \quad (5.90)$$

which gives us the screened Poisson equation (1.118) with $m_t = m_{t+1}^q - m_t^q + m_t^p$. If the orbit has periodic bc's with period n , $q_t = q_{t+n}$, the action of the periodic orbit can be written as (18.200), where the $n \times n$ matrix \mathcal{J} is given by refeq{Hessian}, and

$$\mathbf{x} = \begin{bmatrix} x_1 \\ x_2 \\ x_3 \\ \vdots \\ x_n \end{bmatrix}, \quad \mathbf{m} = \begin{bmatrix} m_1 \\ m_2 \\ m_3 \\ \vdots \\ m_n \end{bmatrix}. \quad (5.91)$$

\mathcal{J}_n is called the orbit Jacobian matrix (or the Hessian matrix) of period n . The element of matrix $-\mathcal{J}_n$ is $-(\mathcal{J}_n)_{ij} = \partial^2 L(\mathbf{x}) / \partial x_i \partial x_j$. Letting the first derivative of action (18.200) be 0, we can see that a periodic point of cat map with

¹¹Predrag 2019-08-04: Percival-Vivaldi [218] (3.1) uses only m^p , no need for this confusing additional m^q , for their Hamiltonian (2.1), with no specialization to the Percival-Vivaldi cat map.

¹²Predrag 2019-08-04: By MacKay, Meiss and Percival [190, 196] convention (3.2), and Li and Tomovic [178] convention (9) we should always have $L(q_t, q_{t+1})$. Unfortunately Keating [168] definition (3) corresponds to $L(q_t, q_{t-1})$, but we do not take that one.

period n satisfies:

$$\begin{bmatrix} s & -1 & 0 & \dots & -1 \\ -1 & s & -1 & \dots & 0 \\ 0 & -1 & s & \dots & 0 \\ \vdots & \vdots & \vdots & \ddots & \vdots \\ -1 & 0 & 0 & \dots & s \end{bmatrix} \begin{bmatrix} x_1 \\ x_2 \\ x_3 \\ \vdots \\ x_n \end{bmatrix} = \begin{bmatrix} m_1 \\ m_2 \\ m_3 \\ \vdots \\ m_n \end{bmatrix}, \quad (5.92)$$

¹³

$$L(x_{t+1}, x_t) = \frac{1}{2}[(s-1)x_t^2 - 2x_t(x_{t+1} + m_{t+1}^x) + (x_{t+1} + m_{t+1}^x)^2 - 2m_{t+1}^p x_{t+1}]. \quad (5.93)$$

¹⁴ ¹⁵

Consider cat map of form (5.62).

$$L(q_t, q_{t+1}) = \frac{1}{2}(q_{t+1} - q_t)^2 - V(q_t), \quad P(q) = -\frac{dV(q)}{dq}, \quad (5.94)$$

The problem with formulation (5.67) is that the potential energy contribution is defined asymmetrically in (5.94). We should really follow Bolotin and Treschev [39] eq. (2.5), and define a symmetric generating function

$$L(q_t, q_{t+1}) = \frac{1}{2}(q_{t+1} - q_t)^2 - \frac{1}{2}[V(q_t) + V(q_{t+1})], \quad (5.95)$$

The first variation (8.13) of the action vanishes,

$$\begin{aligned} 0 &= L_2(q_{t+1}, q_t) + L_1(q_t, q_{t-1}) \\ &= q_t - q_{t+1} + \mu^2 q_t - s_{t+1}^p + q_t - q_{t-1} \\ &= -q_{t+1} + s q_t - q_{t-1} - s_{t+1}^p, \end{aligned} \quad (5.96)$$

hence

$$q_{t+1} - s q_t + q_{t-1} = -s_{t+1}^p. \quad (5.97)$$

Defining $s_t = -s_{t+1}^p$, we recover the screened Poisson equation (1.118).

Alternatively, Han's generating function (1-step Lagrangian density) is:

$$\begin{aligned} L(q_{n+1}, q_n) &= \frac{1}{2}[p_{n+1}(q_{n+1}, q_n)]^2 - V(q_n) \\ &= \frac{1}{2}(q_{n+1} - q_n + m_{n+1}^q - m_{n+1}^p)^2 + \frac{1}{2}\mu^2 q_n^2 - m_{n+1}^p q_n. \end{aligned} \quad (5.98)$$

¹³Predrag 2019-05-27: For a more detailed discussion, see for example (7.58) in *spatiotemp/chapter/Hill.tex*; *spatiotemp/chapter/examCatMap.tex* text: generating function (5.94) This generating function is the discrete time Lagrangian for a particle moving in potential $V(x)$.

¹⁴Han 2019-06-10: (5.88) is already given by Keating [168]. Do we want to add our procedure here? I got the Lagrangian (7.62) which is different from (5.93) only by a constant.

¹⁵Han 2019-06-12: The generating function of a 2-dimensional spatiotemporal cat (7.73) is given by Gutkin and Osipov [120].

The action is the sum over the Lagrangian density over the orbit. The first variation (8.13) of the action vanishes,

$$\begin{aligned}
 0 &= L_2(q_{n+1}, q_n) + L_1(q_n, q_{n-1}) \\
 &= q_n - q_{n+1} + m_{n+1}^p - m_{n+1}^q \\
 &\quad + \mu^2 q_n - m_{n+1}^p + q_n - q_{n-1} + m_n^q - m_n^p \\
 &= -q_{n+1} + sq_n - q_{n-1} - (m_{n+1}^q - m_n^q + m_n^p),
 \end{aligned} \tag{5.99}$$

hence

$$-q_{n+1} + sq_n - q_{n-1} = m_{n+1}^q - m_n^q + m_n^p. \tag{5.100}$$

Letting $m_n = m_{n+1}^q - m_n^q + m_n^p$, we recover the Lagrangian formulation refeq{eq:CatMapNewt}, except for the wrong sign for m_n . Now we see why m_n 's are called 'sources'.

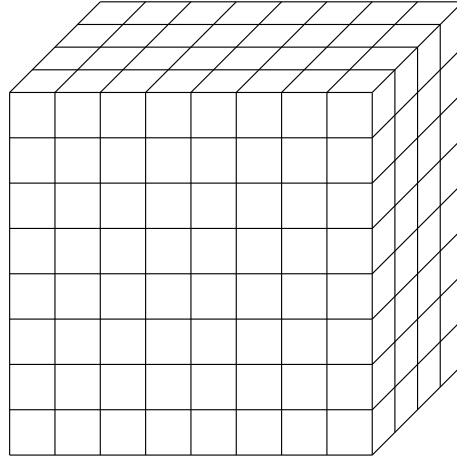


Figure 5.1: 3-dimensional lattice. From ref. [205].

5.7 Lattice discretization of a field theory

¹⁶

In Euclidean field theory the fields $\phi(x)$ depend on the d Euclidean coordinates, so introduce a discretized spacetime in form of a d -periodic hypercubic *integer lattice* \mathbb{Z}^d/L^d (see figure 5.1), with lattice spacing $a_i = \Delta x_i$ and lattice period $L_i = 1/\Delta x_i$ along the unit vector

$$\hat{n}_i \in \{\hat{n}_1, \hat{n}_2, \dots, \hat{n}_d\}$$

pointing in the i th positive direction. The (scalar) *field* $\phi(x)$ is evaluated only on the lattice points

$$\phi_z = \phi(x), \quad x = az = \text{lattice point}, \quad z \in \mathbb{Z}^d/L^d. \quad (5.101)$$

It is periodic

$$\phi_z = \phi_{z+L_i \hat{n}_i}.$$

in all directions. We refer to the set of values of $\Phi = \{\phi_z\}$ as a *lattice state*.

In order to discretize field-theoretic partial differential equations, we need to lattice derivatives. The *forward partial lattice derivative*

$$(\partial_i \phi)_z = \frac{\phi(x + \Delta x_i \hat{n}_i) - \phi(x)}{\Delta x_i} = \frac{\phi_{z+\hat{n}_i} - \phi_z}{\Delta x_i} \quad (5.102)$$

¹⁶Predrag 2020-03-15: Some of the formulas initially extracted from G. Münster and M. Walzl [205] *Lattice Gauge Theory - A Short Primer*, arXiv:hep-lat/0012005, to use in CL18 [77]
Maybe already used:

for CL18 [77]:
 $x_\ell = x(a\ell)$, where $x(a\ell)$ is defined by the value of the continuum field $x(x)$ at the lattice point $x_\ell = a\ell$
 (Here we work in Euclidean space.)

depends explicitly on the lattice spacing. For our purposes it is convenient to reformulate the problem as a discretization on an integer lattice. This is attained by converting all continuum partial *derivatives* into discrete partial *differences* by $\partial_i \rightarrow L_i \partial_i$ rescaling of the partial derivatives. After this rescaling ∂_i is an integer lattice forward partial *difference operator*

$$\partial_i = r_i - \mathbf{1}. \quad (5.103)$$

Higher lattice partial difference operators can be defined as [90]

$$\partial_i^k = \sum_{j=0}^k (-1)^j \binom{k}{j} r_i^{k-j}, \quad (5.104)$$

with support on $k + 1$ forward points. For example

$$\begin{aligned} \partial_i^2 &= r_i^2 - 2r_i + \mathbf{1} \\ \partial_i^3 &= r_i^3 - 3r_i^2 + 3r_i - \mathbf{1}. \end{aligned} \quad (5.105)$$

The even ones can be centered to be reflection symmetric (symmetric under transposition) by translation by k sites,

$$\begin{aligned} \square_i &= -\partial_i^\top \partial_i = r_i - 2\mathbf{1} + r_i^{-1} \\ \square_i^2 &= r_i^2 - 4r_i + 6\mathbf{1} - 4r_i^{-1} + 6r_i^{-2}, \end{aligned} \quad (5.106)$$

where $\square = \sum \square_i$ stands for the lattice Laplacian (or d'Alambertian).

Spacetime integrals are now replaced by sums,

$$\int d^d x \longrightarrow \sum_x a^d,$$

¹⁷ and the lattice free field action is

$$\begin{aligned} S &= \sum_x a^d \left\{ \frac{1}{2} \sum_{i=1}^d (\partial_\mu \phi(x))^2 + \frac{m^2}{2} \phi(x)^2 \right\} \\ &= \sum_z a^d \left\{ \frac{1}{2} \sum_{i=1}^d \phi_z (-\square_i + m^2)_{zz'} \phi_{z'} \right\}. \end{aligned} \quad (5.107)$$

In the functional integrals the measure

$$\mathcal{D}\phi = \prod_x d\phi(x)$$

¹⁷Predrag 2020-03-15:

$$\partial_\mu x(x) = \frac{1}{a}(x(x + a\hat{\mu}) - x(x)),$$

and spacetime integrals by sums:

$$\int d^4 x \longrightarrow \sum_x a^4.$$

involves the lattice points x only, so for a finite lattice this is a finite dimensional integral.

involves the lattice points x only, so we have a discrete set of variables to integrate. If the lattice is taken to be finite, we just have finite dimensional integrals.

¹⁸

The momenta are also discretized,

$$p_\mu = \frac{2\pi}{a} \frac{l_\mu}{L_\mu} \quad \text{with } l_\mu = 0, 1, 2, \dots, L_\mu - 1,$$

and the momentum-space integration is replaced by finite sums

$$\int \frac{d^4 p}{(2\pi)^4} \rightarrow \frac{1}{a^4 L^3 T} \sum_{l_\mu} .$$

All “functional integrals” are now regularized, finite expressions.

To recover physics in a continuous and infinite spacetime, one needs to take the infinite volume limit,

$$L, T \rightarrow \infty ,$$

and the continuum limit,

$$a \rightarrow 0.$$

We shall not discuss the continuum limit of a lattice field theory here.

5.7.1 Transfer matrix

Picking out a ‘time direction’ and evolving in time slices (what we call Hamiltonian formulation) is here called ‘transfer matrix’, presumably in reference to the similar formulation for the Ising model.

Split the 4D hypercubic lattice $z = (z_1, z_2, z_3, z_4)$ into 3-dimensional ‘spatial’ directions $\mathbf{z} = (z_1, z_2, z_3)$ and the ‘temporal’ direction $z_4 = t$. Let

$$\Phi_t = \{\phi_z | z_4 = t\} \tag{5.108}$$

be a field configuration on a Euclidean time slice $z_4 = t$. Decompose the lattice action as

$$S[\phi] = \sum_t L[\Phi_{t+1}, \Phi_t] \tag{5.109}$$

¹⁸Predrag 2020-03-15: Let us assume a hypercubic lattice with length $L_1 = L_2 = L_3 = L$ in every spatial direction and length $L_4 = T$ in Euclidean time,

$$x_\mu = a n_\mu, \quad n_\mu = 0, 1, 2, \dots, L_\mu - 1,$$

with finite volume $V = L^3 T$, and periodic boundary conditions

$$x(x) = x(x + a L_\mu \hat{\mu}),$$

where $\hat{\mu}$ is the unit vector in the μ -direction.

This sum looks like the usual 1D temporal lattice action (8.3). Here

$$L[\Phi_{t+1}, \Phi_t] = \sum_z \frac{1}{2} (\phi_{z,t+1} - \phi_{zt})^2 + \frac{1}{2} (L_1[\Phi_t] + L_1[\Phi_{t+1}]) \quad (5.110)$$

with (here I drop a non-harmonic potential terms)

$$L_1[\Phi_t] = \sum_z \frac{1}{2} \left\{ \sum_{k=1}^3 (\phi_{z+\hat{k},t} - \phi_{zt})^2 + \frac{m^2}{2} \phi_{zt}^2 \right\} \quad (5.111)$$

Eq. (5.110) looks like a sensible generalization of the temporal lattice generating function (5.84).

The transfer matrix is defined as

$$T[\Phi_{t+1}, \Phi_t] = e^{-L[\Phi_{t+1}, \Phi_t]} \quad (5.112)$$

As the matrices are presumably not commuting, it is not obvious to me that repeated application of the transfer operator adds up to the lattice action $S[\phi]$ (5.109) in the exponent. Take a field Ψ_t defined on t time-slice. Then the transfer operator evolves the initial time-slice by matrix multiplication,

$$T^n \Psi_t = \Psi_{t+n} \quad (5.113)$$

As it stands, it is not obvious how this is supposed to work, but Montvay and Münster [202] do give the standard differential formulation, explain correlations, etc., so it's probably OK. For a time-periodic lattice of time period T they say that

$$Z = \text{Tr } T^n \quad (5.114)$$

is the *partition function*.

2020-07-04 Predrag Would be happier if (5.114) were a Det , i.e., if there were a $T = 1 - zJ$ kind of expression. But ... I do not see a quick way from here to the Hill's formula, so I abandon this path for now.

5.7.2 Classical ϕ^3 lattice field theory

2021-12-23 Predrag All ϕ^k lattice field theories fit under the "generalized Hénon map" umbrella, so $\phi^3, \phi^k, k > 4$ are covered in sect. 2.1.1 *Temporal Hénon; anti-integrable limit*

5.7.3 Classical ϕ^4 lattice field theory

Field theorists do not like odd potentials, such as the temporal Hénon (2.8), as they are not bounded from below.

We should be able to write (5.119) action $S[\Phi]$ such that the derivative of the quartic term yields classical ϕ^4 theory (5.118) on d -dimensional lattice

$$-x_{t+1} + \frac{g}{3!} x_t^3 - x_{t-1} = s_t . \quad (5.115)$$

To get some intuition, find the 3 steady states $x_t = x$ by plotting

$$V'[x] = 2x - \frac{g}{3!}x^3 = 2x(1 - \frac{g}{12}x^2) \quad (5.116)$$

as a function of (sufficiently strong) stretching g , and then picking a sensible constant source $s_t = s$ value (or 3 values $s_t \in \{L, C, R\}$, see example 4.6 A reflection-symmetric 1d map.) for which not only the 3 fixed points are real, but all 3^n 3-symbol bimodal map itineraries are realized.

Continued around (5.122).

The Hill determinant $\|\mathcal{J}[\Phi]\|$ is again of the same form (2.9), with the stretching factor at site t depending on the coupling constant g , the lattice site field for the given lattice state.

For example, the Hill determinant of the $[4 \times 4]$ orbit Jacobian matrix \mathcal{J} is (correct this!):

$$\begin{aligned} \text{Det}(\mathcal{J}) &= \begin{vmatrix} s_1 & -1 & 0 & -1 \\ -1 & s_2 & -1 & 0 \\ 0 & -1 & s_3 & -1 \\ -1 & 0 & -1 & s_4 \end{vmatrix} \\ &= s_1s_2s_3s_4 + s_1s_2s_3 + s_2s_3s_4 \\ &\quad + s_1s_2 + s_2s_3 + s_1s_4 + s_3s_4 + s_1 + s_2 + s_3 + s_4. \end{aligned} \quad (5.117)$$

2016-08-20 Predrag Might be worth a look - several papers on coupled map lattices, see also ref. [131] on order and chaos in a continuous time, 1-dimensional latticel ϕ^4 model - if you read that literature, please share what you have learned by writing it up there.

2021-08-11 Predrag Karimipour and Zarei [160] Completeness of classical ϕ^4 theory on two-dimensional lattices arXiv:1201.4558:

The 2-dimensional ϕ^4 Hamiltonian for all discrete scalar field theories on a two dimensional square lattice with periodic boundary conditions

$$H_c = \sum_{\langle r,s \rangle} K_{r,s} (\phi_r - \phi_s)^2 + \sum_r h_r \phi_r + m_r \phi_r^2 + q_r \phi_r^4, \quad (5.118)$$

where $K_{r,s} \in \{i, -i\}$, $i = \sqrt{-1}$ and the real parameters h_r , m_r and q_r denote respectively the inhomogeneous external field, the quadratic (mass term) and quartic coupling strengths. The linear terms $\{h_r\}$ are also necessary for completeness.

From Scholarpedia: action

$$S = \sum_z \left[\varphi_z^2 + \lambda (\varphi_z^2 - 1)^2 \right] - 2\kappa \sum_{\langle zz' \rangle} \varphi_z \varphi_{z'}. \quad (5.119)$$

2021-12-05 Predrag ϕ^4 theory also shows up in Brézin & Zinn-Justin (see sect. 13.7) *Mean field theory for the Ising model*. Their formulation suggests that the partition function (3.4) should be written as (13.122) where $f[\Phi]$ is free energy (the large-deviation potential)

$$Z[M] = e^{-N_{\mathcal{L}} f[M]} . \quad (5.120)$$

and $N_{\mathcal{L}}$ is the number of lattice sites.

2021-12-07 Predrag Vierhaus's masters thesis [261] *Simulation of ϕ^4 theory in the strong coupling expansion beyond the Ising Limit* has a clear discussion of the *Ising limit of ϕ^4* . Note the reformulation (5.119) of the action, his eq. (2.15).

2021-12-21 Predrag Hagiwara and Shudo [122] *An algorithm to prune the area-preserving Hénon map* (2004) describes Sterlings anti-integrable method.

Starting with the temporal Hénon second-order difference equation (2.6), changing variables to $z = \epsilon x$, $\epsilon = a^{-1/2}$ gives

$$-\epsilon(z_{t-1} + z_{t+1}) + z_t^2 - 1 = 0 . \quad (5.121)$$

At the anti-integrable limit $\epsilon \rightarrow 0$, the map reduces to $z_t^2 = 1$, with every orbit an arbitrary sequence of ± 1 .

2021-12-22 Predrag An unchecked reverse engineering guess: Starting with the second-order difference equation for ϕ^4 theory:

$$-\epsilon(z_{t-1} + z_{t+1}) + z_t(z_t - 1)(z_t + 1) = 0 . \quad (5.122)$$

At the anti-integrable limit $\epsilon \rightarrow 0$, the map reduces to $z_t(z_t - 1)(z_t + 1) = 0$, with every orbit an arbitrary sequence of $\{-1, 0, 1\}$. Then go back to (5.115), using $x = z/\epsilon$, $\epsilon = g^{-1/3}$.

$$-x_{j-1} + g x_j^3 - x_{j+1} = g^{2/3} x_j . \quad (5.123)$$

Probably not the right thing; note that (5.129) scales the linear term differently, by ϵ .

2021-12-22 Predrag Anastassiou, Bountis and Bäcker [11] *Homoclinic points of 2D and 4D maps via the parametrization method* (2017):

the dynamics of discrete breather solutions on 1-dimensional lattices (or chains) of nonlinearly interacting particles

The discrete nonlinear Klein-Gordon system of ordinary differential equations

$$\ddot{u}_n = -V'(u_n) + \alpha(u_{n+1} - 2u_n + u_{n-1}) , \quad V(x) = \frac{1}{2}Kx^2 + \frac{1}{4}x^4 , \quad (5.124)$$

where u_n for $-\infty < n < \infty$ is the amplitude of the n -th particle, $\alpha > 0$ is a parameter indicating the strength of coupling between nearest neighbors, and $V(x)$ is the on-site potential with primes denoting differentiation with respect to the argument of $V(x)$.

Discrete nonlinear Schrödinger equation is similar.

2021-12-22 Predrag Must study Anastassiou [10] *Complicated behavior in cubic Hénon maps*, (2021). He defines the generalized Hénon map of the plane onto itself as

$$H: \mathbb{R}^2 \rightarrow \mathbb{R}^2, \quad H(x, y) = (y, b x + p(y)), \quad (5.125)$$

The determinant of the Jacobian matrix connected to the dissipation of the system is equal to $-b$. If the polynomial $p(y)$ is odd, then the map $H(x, y)$ is symmetric under the transformation

$$\sigma(x, y) = (-x, -y). \quad (5.126)$$

For $-b = 1$, the map is a symplectomorphism (or symplectic map) because it preserves the natural symplectic form of the plane, $dx \wedge dy$.

The dynamics of $H(x, y)$, where $p(y)$ is a third-degree polynomial, was studied in ref. [88], sufficient conditions for hyperbolicity in generalized Hénon maps for arbitrary polynomials $p(y)$ were given in ref. [276]. Anastassiou studies cubic polynomial $p(y)$ Hénon maps,

$$H: \mathbb{R}^2 \rightarrow \mathbb{R}^2, \quad H(x, y) = (y, -b x + g(y^3 - y)), \quad (5.127)$$

studied from a different perspective in his earlier articles [11, 12]. He locates the region of the state space

$$\mathcal{A} = \left\{ (x, y) \in \mathbb{R}^2 : |x|, |y| \leq \sqrt{1 + \frac{2}{g}} \right\}, \quad (5.128)$$

where the bounded nonwandering invariant set exists, and finds parameter values $g > 4$ for which this nonwandering set is hyperbolic. Read his proof - it is instructive. Remember that these are just very crude bounds - the stable/unstable manifolds will give tight bounds. He shows that his map is conjugate to the Bernoulli three-shift, using the anti-integrability technique [19, 23, 40, 55].

$$-x_{n+1} + g x_n^3 - g x_n - x_{n-1} = 0,$$

Define $\epsilon = 1/g$

$$- \epsilon(x_{n+2} + x_{n+1}) + x_{n+1}^3 = \epsilon x_n, \quad (5.129)$$

It is customary to say that such a complex behavior is ‘chaotic’ because of Devaney’s definition [26].

2021-06-04 Predrag Friedland and Milnor [105] *Dynamical properties of plane polynomial automorphisms* (1989) introduced the generalized Hénon map. Their theorem 2.6 on the normal form of such maps is nice. In their fig. 2 they do the 0th order version of the plot I hope Harrison and Ibrahim will plot: the three-fold horseshoe associated with a real cubic polynomial. Dullin and Meiss [88] do that, their fig. 13 (right).

2021-06-04 Predrag See also Anastassiou, Bountis and Bäcker [12] (2018) *Recent results on the dynamics of higher-dimensional Hénon maps*, their fig. 1. They take

$$p(y) = cy + 3y^3 \quad (5.130)$$

They chose $c = -\frac{5}{2}$ throughout their publication (we should too, to compare results). "This choice is pictorially convenient, since c values in that range produce large scale manifolds that are clearly visible in the figures."

The cubic mapping possesses three fixed points: saddle point at the origin, for all parameter values, a symmetric pair at

$$\left(\pm \sqrt{(2-c)/3}, \pm \sqrt{(2-c)/3} \right).$$

The $(0, 0)$ fixed point Floquet multipliers are

$$\frac{1}{2} \left(c - \sqrt{c^2 - 4} \right), \frac{1}{2} \left(c + \sqrt{c^2 - 4} \right). \quad (5.131)$$

Since $c = -5/2$ and $\delta = 1$, the Floquet multipliers of the origin are $\Lambda_u = -2$ and $\Lambda_s = -1/2$ with normalized eigenvectors $(-1/\sqrt{5}, 2/\sqrt{5})$ and $(-2/\sqrt{5}, 1/\sqrt{5})$. The origin is thus a saddle, with a 1-dimensional stable and a 1-dimensional unstable manifold, whose parametric computation they explain.

2021-06-04 Predrag Dullin and Meiss [88] *Generalized Hénon maps: the cubic diffeomorphisms of the plane* (2000):

The Euler–Lagrange equation associated with this action is

$$m(x_{t-1} + x_{t+1}) = U'(x_t) \quad (5.132)$$

which is the Lagrangian form of the Hénon map. They concentrate on the area-preserving cubic maps. [...] These are reversible and have an additional symmetry on a codimension-one line in parameter space (Predrag currently calls that 'dynamical symmetry').

2021-06-04 Predrag The Arneodo–Coullet–Tresser maps (referred to in [179]) are 5-term recurrence equations with x_t^k nonlinear term, ignore for now.

Li and Malkin [179] *Bounded nonwandering sets for polynomial mappings* (2004)

5.8 Normalizing flows

Predrag: What is here called

'normalizing flow' $f : \mathcal{X} \rightarrow \mathcal{X}$, invertible and differentiable

Jacobian factor $J(z) = |\det \partial f_i(z)/\partial z_j|$

is the main idea of our refs. [72, 75]); what they call their 'latent' space probability distribution being set to Gaussian is what we call 'free field theory'. One pays a determinant of the Jacobian matrix of that field transformation, the same as for us. But Miranda Cheng says that this determinant "can be easily computed/approximated" which is news to me.

2021-11-01 **Predrag** Miranda Cheng

 *Machine learning and theoretical physics: some applications.*

Lattice field theory is the main tool for doing nonperturbative calculations in field theory. The idea of ML techniques, such as Normalizing Flows, is that if we can learn an invertible map that trivializes an interacting model to a free theory, we can easily sample the latter and push back the samples through the inverse map to obtain (proposed) samples from the original non-trivial distribution.

Predrag: this is the main idea of our ref. [72, 75]); what they call their 'latent' space probability distribution being set to Gaussian is what we call 'free field theory'. One pays a determinant of the Jacobian matrix of that field transformation, the same as for us. But she says that this determinant "can be easily computed/approximated" which is news to me.

In the talk she defines the "observable" the way we would; I have not seen the definition yet in their papers.

The first part is based on

Pim de Haan, Corrado Rainone, Miranda Cheng and Roberto Bondesan *Scaling Up Machine Learning For Quantum Field Theory with Equivariant Continuous Flows*, arXiv:2110.02673. Cheng has typos in her presentation (probability density " + " $\text{Det } |J|$ rather than \times).

the contributions of their paper:

- They extend and develop continuous normalizing flows for lattice field theories that are fully equivariant under lattice symmetries as well as the internal $\phi \mapsto -\phi$ symmetry of the ϕ^4 model.
- They train our model for the ϕ^4 theory and for the 32×32 lattice we improve the effective sample size from 1% to 66% w.r.t. a real NVP baseline of similar size.
- They study equivariance violations of real NVP models and contrast it with the exact equivariance of our flows.

If the vector field g is equivariant, the resulting distribution on ϕ is invariant. They show how to construct a g equivariant to the square lattice symmetries.

The ϕ^4 theory possesses non-trivial symmetry properties and a phase transition. In the case of ϕ^4 theory in two dimensions, the *field configuration* is a real function on

the vertex set V_L of the square lattice

with periodic boundaries and size $L \times L$: $\phi : V_L \rightarrow \mathbb{R}$. The ϕ^4 theory is described by a probability density

$$p(\phi) = \exp(-S(\phi))/Z, \quad (5.133)$$

with action

$$S(\phi) = \sum_{x,y \in V_L} \phi(x) \Delta_{x,y} \phi(y) + \sum_{x \in V_L} m^2 \phi(x)^2 + \lambda \phi(x)^4 \quad (5.134)$$

Here Δ is Laplacian matrix of the square lattice $(\mathbb{Z}/L\mathbb{Z})^{2 \times 2}$, m and λ are numerical parameters. In the case of this and other non-trivial field theoretical densities, Z is the normalisation factor that is not known analytically for $\lambda \neq 0$.

Probability densities over those state space manifolds:

- Prior density $r(z)$
- Model density $q(x)$
- Target density $p(x)$

Note that, besides the space-time symmetries of the periodic lattice, the theory possesses a

discrete global symmetry $\phi \mapsto -\phi$.

We shall choose the couplings in such a way that only one minimum of the action, invariant under this symmetry, exists. See [??] for relevant work in the case of a symmetry-broken case.

(Was commented out:) We will work in the "unbroken" phase with $m^2 > 0$, where the minimum of the action is invariant under the global symmetry. See [arXiv:2107.00734](#) for relevant work in the broken phase.

The periodic lattice V_L has spatial symmetry group $G = C_L^2 \rtimes D_4$, the semi-direct product of two cyclic groups C_L of translations and dihedral group D_4 of right angle rotations and mirrors. To ensure spatial equivariance of the vector field model, we should have that

$$\forall g \in G, x, y, a, f, W_{g(x)g(y)a f} = W_{xyaf}.$$

Using the translation subgroup, we can map any point x to a fixed point x_0 . This allows us to write $W_{xyaf} = W_{x_0 t_x(y) a f}$, $t_x(y) = y - x + x_0$.

(Predrag - they seem to be defining the point group here:)

Then let $H \simeq D_4$ be the subgroup of G such that $g(x_0) = x_0$ for all $g \in H$, and denote the orbit of y under H by $[y] = \{y' \mid \exists g \in H, g(y) = y'\}$.

For each such orbit $[y]$ and dimension a and f , a free parameter $W_{[y]af}$ exists, so that the other parameters are generated by $W_{xyaf} = W_{[t_x(y)]af}$.

(Was commented out; Predrag - they ignore symmetric lattice states here:) As most orbits are of size 8, the number of free parameters per a and f is approximately $L^2/8$.

The orbits of D_4 , leaving point $(0, 0)$ invariant, for $L = 16$ are shown in Fig. 4. For each color in that figure, for each dimensions a and f , we have a free parameter.

(Predrag - that figure says the 1/8th fundamental domain tiles the square lattice, and ignores the symmetry boundaries. The “free parameter” is just the values of the field in the fundamental domain.)

2021-12-05 Predrag These papers seem to be more informative:

Rezende and Mohamed (2015) “normalizing flows” [arXiv:1505.05770](#) cites Jordan, Ghahramani, Jaakkola and Saul [151] *An introduction to variational methods for graphical models* (1999)

Del Debbio, Rossney and Wilson *Efficient Modelling of Trivializing Maps for Lattice ϕ^4 Theory Using Normalizing Flows: A First Look at Scalability* [arXiv:2105.12481](#)

2021-12-05 Predrag Albergo, Boyda, Hackett, Kanwar, Cranmer, Racanière, Jimenez Rezende and Shanahan, *Introduction to Normalizing Flows for Lattice Field Theory* (2021), [arXiv:2101.08176](#):

This notebook tutorial demonstrates a method for sampling Boltzmann distributions of lattice field theories using a class of machine learning models known as normalizing flows. The ideas and approaches proposed in

[arXiv:1904.12072](#)

[arXiv:2002.02428](#)

[arXiv:2003.06413](#)

are reviewed and a concrete implementation of the framework is presented. We apply this framework to a lattice scalar field theory and to U(1) gauge theory, explicitly encoding gauge symmetries in the flow-based approach to the latter.

The Box-Muller transform is an example of a ‘normalizing’ transformation: to produce Gaussian random variables, draw two variables U_1 and U_2 from $\text{unif}(0, 1)$, then change variables to

$$(Z_1, Z_2) = (r \cos(2\pi U_2), r \sin(2\pi U_2)), \quad r = \sqrt{-2 \ln U_1}. \quad (5.135)$$

The resulting variables Z_1, Z_2 are then distributed according to an uncorrelated, unit-variance Gaussian distribution; U_1 controls the radius, and U_2 the angle of a 2d Gaussian.

Predrag: This might relate Bernoulli and temporal cat to Gaussian field theories (see sect. 13.2), i.e., this maps fields in $[0, 1]$ to fields in \mathbb{R} .

The density associated with output samples is computed by the *change-of-variables formula* relating the *prior density* $\rho(U_1, U_2) = 1$ to the *output density*

$$\begin{aligned} q(Z_1, Z_2) &= \rho(U_1, U_2) \left| \det \frac{\partial Z_k(U_1, U_2)}{\partial U_l} \right|^{-1} \\ &= 1 \times \left| \det \begin{pmatrix} \frac{-1}{U_1 r} \cos(2\pi U_2) & -2\pi r \sin(2\pi U_2) \\ \frac{-1}{U_1 r} \sin(2\pi U_2) & 2\pi r \cos(2\pi U_2) \end{pmatrix} \right|^{-1} \quad (5.136) \\ &= \left| \frac{2\pi}{U_1} \right|^{-1}. \end{aligned}$$

$J(U_1, U_2) \equiv \det(\partial Z / \partial U)$ is the determinant of the Jacobian of the coordinates transformation $(U_1, U_2) \rightarrow (Z_1, Z_2)$. The Jacobian factor is a change in volume element, therefore the change-of-variables formula must contain the inverse of this factor (spreading out volume decreases density).

As

$$U_1 = \exp(-(Z_1^2 + Z_2^2)/2)$$

and the initial density $\rho(U_1, U_2)$ over the unit square was uniform, the transformed density is

$$q(Z_1, Z_2) = \frac{1}{2\pi} e^{-(Z_1^2 + Z_2^2)/2}. \quad (5.137)$$

This example has no free parameters because no extra parameters were needed to create a transform that exactly reproduced the desired target distribution, independent, unit-variance Gaussian. In general, we may not know a normalizing flow that exactly produces our desired distribution, and so instead construct parametrized models that we can variationally optimize to *approximate* that target distribution, and because we can compute the density these can be corrected to nevertheless guarantee exactness.

In some cases, it is easy to compute the Jacobian factor even when the whole Jacobian matrix is intractable; for example, only the diagonal elements are needed if the Jacobian matrix is known to be triangular.

The hypercubic lattice discretization of the derivatives of the continuum Euclidean action gives rise to a lattice Euclidean action,

$$\begin{aligned} S_{\text{cont}}^E[\phi] &= \int d^2 \vec{x} (\partial_\mu \phi(\vec{x}))^2 + m^2 \phi(\vec{x})^2 + \lambda \phi(\vec{x})^4 \\ \rightarrow S(\phi) &= \sum_{\vec{n}} \phi(\vec{n}) \left[\sum_{\mu \in \{1, 2\}} -\phi(\vec{n} + \hat{\mu}) + 2\phi(\vec{n}) - \phi(\vec{n} - \hat{\mu}) \right] + m^2 \phi(\vec{n})^2 + \lambda \phi(\vec{n})^4 \end{aligned} \quad (5.138)$$

where now $\phi(\vec{n})$ is only defined on the sites of the $L_x \times L_y$ lattice, $\vec{n} = (n_x, n_y)$, with integer n_x, n_y . The discretized field ϕ can be thought of as an $(L_x \times L_y)$ -dimensional vector. We use periodic boundary conditions in all directions, i.e. $\phi(L_x, y) \equiv \phi(0, y)$, etc.

More details on ϕ^4 lattice scalar field theory can be found in Vierhaus's masters thesis [261] *Simulation of ϕ^4 theory in the strong coupling expansion beyond the Ising Limit*.

The lattice action then defines a probability distribution over configurations ϕ ,

$$p(\phi) = \frac{1}{Z} e^{-S(\phi)}, \quad Z \equiv \int \prod_{\vec{n}} d\phi(\vec{n}) e^{-S(\phi)}, \quad (5.139)$$

where $\prod_{\vec{n}}$ runs over all lattice sites \vec{n} . This is the distribution we are training the normalizing flows to reproduce. While Z is difficult to calculate, in practice we only need $p(\phi)$ up to a constant. The action can be efficiently calculated on arbitrary configurations using Pytorch. Note that while the theory describes 2D spacetime, the dimensionality of distribution $p(\phi)$ is the number of lattice sites, scaling with the volume of the lattice.

The theory has a symmetric phase and a broken symmetry phase, corresponding respectively to nearly one mode of the distribution or two widely separated modes (with intermediate configurations suppressed exponentially in volume). The broken symmetry phase can be accessed for $m^2 < 0$ and λ less than a critical λ_c . For simplicity, we restrict focus to the **symmetric phase**, but remain close to this phase transition such that the system has a non-trivial correlation length.

A selection of references to related works (find the links in [arXiv:2101.08176](#)):

- **Normalizing flows:** Agnelli *et al.* (2010); Tabak and Vanden-Eijnden (2010); Dinh *et al.* (2014); Dinh *et al.* (2016); Papamakarios *et al.* *Normalizing flows for probabilistic modeling and inference* (2019), [arXiv:1912.02762](#);
- **Symmetries and equivariance:** Cohen and Welling (2016); Cohen *et al.* (2019); Rezende *et al.* (2019); Köhler *et al.* (2020); Luo *et al.* (2020); Favoni *et al.* (2020);
- **Flows on manifolds:** Gemici *et al.* (2016); Falorsi *et al.* (2019); Finzi *et al.* (2020); Mathieu and Nickel (2020); Falorsi and Forré (2020);
- **Applications of flows:** Müller *et al.* (2018); Noé *et al.* (2019); Wu *et al.* (2020); Dibak *et al.* (2020); Nicoli *et al.* (2021) [DOI](#)

2021-12-13 Predrag Sara liked very much this morning's talk by [Max Welling](#) on ML for PDEs – the way he controls the PDE grid, incorporates symmetries into the NN part of the algorithm.

Garcia Satorras, Victor and Hoogeboom, Emiel and Fuchs, Fabian and Posner, Ingmar and Welling, Max [E\(n\) Equivariant Normalizing Flows](#) Advances in Neural Information Processing Systems 34 (2021):

This paper introduces a generative model equivariant to Euclidean symmetries: E(n) Equivariant Normalizing Flows (E-NFs). To construct E-NFs, we take the discriminative E (n) graph neural networks and integrate them as a differential equation to obtain an invertible equivariant function: a continuous-time normalizing flow. We demonstrate that E-NFs considerably outperform baselines and existing methods from the literature on particle systems such as DW4 and LJ13, and on molecules from QM9 in terms of log-likelihood. To the best of our knowledge, this is the first flow that jointly generates molecule features and positions in 3D.

5.9 Noise is your friend

2021-11-27 Predrag Excerpts (mashed together in random order) from Cvitanović, Dettmann, Mainieri and Vattay *Trace formulae for stochastic evolution operators*:

Weak noise perturbation theory [74] (1998), [arXiv:chao-dyn/9807034](https://arxiv.org/abs/chao-dyn/9807034), and *Smooth conjugation method* [75] (1998) [arXiv:chao-dyn/9811003](https://arxiv.org/abs/chao-dyn/9811003).

These are the first two papers to treat time evolution as a 1-dimensional temporal lattice field theory. They start out by expressing the weak noise expansions in terms of Dirac δ and its derivatives. In what is excerpted here we omit all correction terms, as we are interested only into the leading behavior.

The central object in the theory, the trace of the evolution operator, is a discrete path integral, similar to those found in field theory and statistical mechanics.

The theory is cast in the standard field theoretic formalism, and weak noise perturbation theory written in terms of Feynman diagrams.

The noise tends to regularize the theory, replacing the deterministic delta function evolution operators by smooth distributions. While in this paper we are interested in effects of weak but *finite* noise, the $\sigma \rightarrow 0$ limit is also important as a tool for identifying the natural measure [41, 233, 243] for deterministic flows.

We have cast the theory in the standard field theoretic language [71], in the spirit of approaches such as the Martin-Siggia-Rose [194] formalism, the Parisi-Wu [214] stochastic quantization, and the Feigenbaum and Hasslacher [93] study of noise renormalization in period doubling.

The form of the perturbative expansions is reminiscent of perturbative calculations of field theory, but in some aspects the calculations undertaken here are relatively more difficult. The main difference is that there is no translational invariance along the chain, so unlike the case of usual field theory, the propagator is not diagonalized by a Fourier transform. We do our computations in configuration coordinates. Unlike the most field-theoretic literature, we are neither “quantizing” around a trivial vacuum, nor a countable infinity of stable soliton saddles, but around an infinity of nontrivial unstable hyperbolic saddles.

[...] our results are *a priori* far from obvious: [...] a more subtle and surprising result, repeats of prime cycles can be resummed and theory reduced to the dynamical zeta functions and spectral determinants of the same form as the for the deterministic systems.

[...] a discrete time 1-dimensional discrete Langevin equation [157, 173],

$$x_{n+1} = f(x_n) + \sigma \xi_n , \quad (5.140)$$

with ξ_n independent normalized random variables, suffices to reveal the structure of the perturbative corrections.

We shall treat a chaotic system with such Gaussian weak external noise by replacing the deterministic evolution δ -function kernel by \mathcal{L}_{FP} , the Fokker-Planck kernel corresponding to (5.140), a sharply peaked noise distribution function

$$\mathcal{L}_{FP} = \delta_\sigma(y - f(x)), \quad (5.141)$$

where δ_σ is the Gaussian kernel

$$\delta_\sigma(z) = \frac{1}{\sqrt{2\pi\sigma^2}} e^{-z^2/2\sigma^2}. \quad (5.142)$$

In the weak noise limit the kernel is sharply peaked, so it makes sense to expand it in terms of the Dirac delta function and its derivatives:

$$\delta_\sigma(y) = \sum_{m=0}^{\infty} \frac{a_m \sigma^m}{m!} \delta^{(m)}(y) = \delta(y) + a_2 \frac{\sigma^2}{2} \delta^{(2)}(y) + \dots \quad (5.143)$$

where

$$\delta^{(k)}(y) = \frac{\partial^k}{\partial y^k} \delta(y),$$

and the coefficients a_m depend on the choice of the kernel. We have omitted the $\delta^{(1)}(y)$ term in the above because in our applications we shall impose the saddle-point condition, that is, we shift f by a constant to ensure that the noise peak corresponds to $y = 0$, so $\delta'_\sigma(0) = 0$. For example, if $\delta_\sigma(y)$ is a Gaussian kernel, it can be expanded as

$$\delta_\sigma(y) = \frac{1}{\sqrt{2\pi\sigma^2}} e^{-y^2/2\sigma^2} = \delta(y) + \frac{\sigma^2}{2} \delta^{(2)}(y) + \dots \quad (5.144)$$

We start our computation of the weak noise corrections to the spectrum of \mathcal{L}_{FP} by calculating the trace of the n th iterate of the stochastic evolution operator \mathcal{L}_{FP} for a one-dimensional analytic map $f(x)$ with additive noise σ . This trace is an n -dimensional integral on n points along a discrete periodic chain, so x becomes an n -vector x_a with indices a, b, \dots ranging from 0 to $n-1$ in a cyclic fashion

$$\begin{aligned} \text{tr } \mathcal{L}_{FP}^n &= \int \prod_{a=0}^{n-1} dx_a \delta_\sigma(y_a) \\ y_a(x) &= f(x_a) - x_{a+1}, \quad x_n = x_0. \end{aligned} \quad (5.145)$$

If the map is smooth, the periodic points of given finite period n are isolated and the noise broadening σ sufficiently small so that they remain separated, the dominant contributions come from neighborhoods of periodic points; in the *saddlepoint approximation* the trace (5.145) is given by

$$\text{tr } \mathcal{L}_{FP}^n \longrightarrow \sum_{x_c \in \text{Fix } f^n} e^{W_c}, \quad (5.146)$$

As traces are cyclic, e^{W_c} is the same for all periodic points in a given cycle, independent of the choice of the starting point x_c . Hence it is customary to rewrite this sum in terms of prime cycles and their repeats,

$$\text{tr } \mathcal{L}_{FP}^n|_{\text{saddles}} = \sum_p n_p \sum_{r=1}^{\infty} e^{W_{p^r}}, \quad (5.147)$$

where p^r labels the r th repeat of prime cycle p .

A fixed point and its repeats are of particular interest having the same interaction at every site, as does the usual field theory. What we do here is to formulate [...] the field theory on finite periodic 1-dimensional discrete chains.

Defining $y = f(x) - x$, we can write the fixed point trace as

$$\text{tr } \mathcal{L}_{FP} = \int dx \delta_\sigma(f(x) - x) = \int dy \frac{1}{|y'(x)|} \delta_\sigma(y). \quad (5.148)$$

We start by calculating the trace of the n th iterate of the stochastic evolution operator \mathcal{L}_{FP} for a one-dimensional analytic map $f(x)$ with additive Gaussian noise σ . This trace is an n -dimensional integral on n points along a discrete periodic chain, so x becomes an n -vector x_a with indices a, b, \dots ranging from 0 to $n-1$ in a cyclic fashion

$$\begin{aligned} \text{tr } \mathcal{L}_{FP}^n &= \int [dx] \exp \left\{ -\frac{1}{2\sigma^2} \sum_a [x_{a+1} - f(x_a)]^2 \right\} \\ x_n &= x_0, \quad [dx] = \prod_{a=0}^{n-1} \frac{dx_a}{\sqrt{2\pi\sigma^2}}. \end{aligned} \quad (5.149)$$

As we are dealing with a path integral on a finite discrete chain, we find it convenient to rewrite the exponent in matrix notation

$$\text{tr } \mathcal{L}_{FP}^n = \int [dx] e^{-[r^{-1}x - f(x)]^2 / 2\sigma^2}, \quad r_{ab} = \delta_{a,b+1}, \quad (5.150)$$

where x and $f(x)$ are column vectors with components x_a and $f(x_a)$ respectively, and r is the left cyclic shift or hopping matrix satisfying $r^n = 1$, $r^{-1} = r^T$. Unless stated otherwise, we shall assume the repeated index summation convention throughout, and that the Kronecker δ function is the periodic one, defined by

$$\delta_{ab} = \frac{1}{n} \sum_{k=0}^{n-1} e^{i2\pi(a-b)k/n}. \quad (5.151)$$

[...] if the noise is weak, the path integral (5.149) is dominated by periodic deterministic trajectories. Assuming that the periodic points of given finite period n are isolated and the trajectory broadening σ sufficiently small so that

they remain clearly separated, the dominant contributions come from neighborhoods of periodic points; in the *saddlepoint approximation* the trace (5.149) is given by

$$\text{tr } \mathcal{L}_{FP}^n \longrightarrow \sum_{x_c \in \text{Fix } f^n} e^{W_c}, \quad (5.152)$$

where the sum goes over all periodic points $x_c = x_{c+n}$ of period n , $f^n(x_c) = x_c$. The contribution of the x_c neighborhood is obtained by shifting the origin of integration to

$$x_a \rightarrow x_a + \phi_a,$$

where from now on x_a refers to the position of the a -th periodic point, and expanding f in Taylor series around each of the periodic points in the orbit of x_c .

The contribution of the neighborhood of the periodic point x_c is given by

$$\begin{aligned} e^{W_c} &= \int [d\phi] e^{-(M^{-1}\phi - V'(\phi))^2/2\sigma^2} \\ &= |\det M| \int [d\varphi] e^{\sum \frac{1}{k} \text{tr}(MV''(\phi))^k} e^{-\varphi^2/2\sigma^2} \end{aligned} \quad (5.153)$$

where the propagator and interaction terms are collected in

$$M^{-1}_{ab}\phi_b = -f'(x_a)\phi_a + \phi_{a+1}, \quad V(\phi) = \sum_a \sum_{m=2}^{\infty} f^{(m)}(x_a) \frac{\phi_a^{m+1}}{(m+1)!}. \quad (5.154)$$

We find it convenient to also introduce a bidirectional propagator $C = MM^T$ for reasons that will become apparent below. In the second line of (5.153) we have changed coordinates,

$$\varphi = M^{-1}\phi - V'(\phi), \quad (5.155)$$

and used the matrix identity $\ln \det M = \text{tr} \ln M$ on the Jacobian

$$\frac{1}{\det(M^{-1} - V'')} = \frac{\det M}{\det(1 - MV'')} = \det M e^{-\text{tr} \ln(1 - MV'')}. \quad (5.156)$$

The functional dependence of $\phi = \phi(\varphi)$ is recovered by iterating (5.155)

$$\phi_a = M_{ab}\varphi_b + M_{ab}V'_b(\phi). \quad (5.157)$$

The above manipulations are standard [194] and often used in the stochastic quantization literature [78, 214].

As the sum is cyclic, e^{W_c} is the same for all periodic points in a given cycle, independent of the choice of the starting point x_c . In the saddlepoint approximation we assume that the map is analytic and the extrema f^n are isolated.

From the second path integral representation in (5.153) it follows that M can be interpreted as the “free” propagator. As M will play a central role in what follows, we write its inverse in its full $[n \times n]$ matrix form:

$$M^{-1} = r^{-1} - \mathbf{f}' = \begin{pmatrix} -f'_0 & 1 & & & \\ & -f'_1 & 1 & & \\ & & -f'_2 & 1 & \\ & & & \ddots & \\ 1 & & & & -f'_{n-1} \end{pmatrix} \quad (5.158)$$

where \mathbf{f}' is a diagonal matrix with elements $f'_a = f'(x_a)$ a shorthand notation for stability of the map at the periodic point x_a . The determinant of M is

$$\det M = \frac{(-1)^n}{\Lambda_c - 1}, \quad \Lambda_c = \prod_{a=0}^{n-1} f'(x_a), \quad (5.159)$$

with Λ_c the *stability* of the n cycle going through the periodic point x_c . We shall assume that we are dealing with a chaotic dynamical system, and that all cycles are unstable, $|\Lambda_c| > 1$.

The formula for propagator itself is obtained by inverting (5.158) and using relation $(r\mathbf{f}')^n = \Lambda_c$, (due to the periodicity of the chain):

$$\begin{aligned} M &= -\frac{1}{1 - \mathbf{f}'^{-1} r^{-1}} \mathbf{f}'^{-1} = -\sum_{k=0}^{\infty} (\mathbf{f}'^{-1} r^{-1})^k \mathbf{f}'^{-1} \\ &= -\frac{1}{\Lambda_c - 1} \sum_{k=0}^{n-1} r(\mathbf{f}' r)^k \end{aligned} \quad (5.160)$$

In the full matrix form, the propagator is given by

$$M = \frac{-1}{\Lambda_c - 1} \begin{pmatrix} f'_1 \dots f'_{n-1} & f'_2 \dots f'_{n-1} & f'_3 \dots f'_{n-1} & \dots & 1 \\ 1 & f'_2 \dots f'_0 & f'_3 f'_4 \dots f'_0 & \dots & f'_0 \\ f'_1 & 1 & f'_3 \dots f'_0 f'_1 & \dots & f'_0 f'_1 \\ f'_1 f'_2 & f'_2 & 1 & \ddots & f'_0 f'_1 f'_2 \\ f'_1 f'_2 f'_3 & f'_2 f'_3 & f'_3 & \ddots & \vdots \\ \vdots & \vdots & \vdots & \vdots & \vdots \\ f'_1 \dots f'_{n-2} & f'_2 \dots f'_{n-2} & \dots & \dots & 1 & f'_0 \dots f'_{n-2} \end{pmatrix} \quad (5.161)$$

or, more compactly,

$$M_{ab} = \frac{-1}{\Lambda_c - 1} \prod_{d=b+1}^{a-1} f'(x_d), \quad M_{a,a-1} = \frac{-1}{\Lambda_c - 1}, \quad (5.162)$$

where d increases cyclically through the range $b + 1$ to $a - 1$; for example, if $a = 0, a - 1 = n - 1$. We note that M is invertible only for cycles which are not marginal, $|\Lambda_c| \neq 1$.

The saddlepoint approximation (5.153) is a discrete path integral on periodic chain of n points which we shall evaluate by standard field-theoretic methods. Separating the quadratic terms we obtain

$$e^{W_c} = \frac{1}{|\Lambda_c - 1|} \int [d\varphi] e^{-S_0(\varphi) - S_I(\varphi)}, \quad (5.163)$$

where

$$S_0(\varphi) = \varphi^2/2\sigma^2, \quad S_I(\varphi) = - \sum_{k=1}^{\infty} \frac{1}{k} \text{tr} [MV''(\phi(\varphi))]^k \quad (5.164)$$

The terms collected in $S_I(\varphi)$, linear or higher in φ , are the interaction vertices.

Next introduce a source term J_a and define a partition function

$$\begin{aligned} e^{W_c(J)} &= \frac{1}{|\Lambda_c - 1|} \int [d\varphi] e^{-S_0(\varphi) - S_I(\varphi) + J_a \varphi_a} \\ &= \frac{1}{|\Lambda_c - 1|} e^{-S_I(\frac{d}{dJ})} \int [d\varphi] e^{-S_0(\varphi) + J_a \varphi_a} \\ &= \frac{1}{|\Lambda_c - 1|} e^{-S_I(\frac{d}{dJ})} e^{\frac{\sigma^2}{2} J^2}. \end{aligned} \quad (5.165)$$

Here we have used standard formulas for Gaussian integrals together with the normalization (5.149).

[...] yields the perturbation expansion

$$W_c = -\ln |\Lambda_c - 1| + \sum_{k=1}^{\infty} W_{c,2k} \sigma^{2k}. \quad (5.166)$$

In field-theoretic calculations the $W_{c,0}$ term is usually an overall volume term that drops out in the expectation value computations. In contrast, here the $W_{c,0} = -\ln |\Lambda_c - 1|$ term is the classical weight of the cycle which plays the key role both in the classical and stochastic trace formulas.

If efficient methods are found for computing numerical periodic solutions of spatially extended systems, the method might apply to the field theory as well.

5.9.1 Noisy Gábor

1998-03-04 Gábor Vattay The initial version.

2021-12-08 Predrag Tweaked Gábor's note a bit. The approach is safe for multimodal maps, and it should work for finite-grammar Smale horseshoe

repellers (Smale's original horseshoe [244], his fig. 1 was unimodal, but he also explicitly gives our ϕ^4 bimodal map, his fig. 5.

For generic, no finite grammar case, who knows... Will be messier, pruning front style. Perhaps.

Suppose we have a 'bimodal' system with three distinct, monotone segments such as (4.209), with map $f_i(x_t)$ for i th segment. Associate with each monotone segment one of three Perron-Frobenius operators (18.394),

$$\mathcal{L}_i(x, y) = \delta(x - f_i(y)), \quad i = \{0, 1, 2\}. \quad (5.167)$$

To compute the spectral determinant

$$F(z) = \det(1 - z(\mathcal{L}_0 + \mathcal{L}_1 + \mathcal{L}_2)), \quad (5.168)$$

write

$$F(z) = \exp(\text{tr} \log(1 - z(\mathcal{L}_0 + \mathcal{L}_1 + \mathcal{L}_2))) = \exp\left(-\sum_n \frac{z^n}{n} \text{tr}(\mathcal{L}_0 + \mathcal{L}_1 + \mathcal{L}_2)^n\right), \quad (5.169)$$

expand the n th power,

$$\text{tr}(\mathcal{L}_0 + \mathcal{L}_1 + \mathcal{L}_2)^n = \sum_p \sum_{r|n=n_p, r} n_p \text{tr} \mathcal{L}_p^r, \quad (5.170)$$

where p denotes a period n_p prime symbol sequence composed of 0, 1, 2, and r is its repetition number. Say $p = 011$, then $\mathcal{L}_{011} = \mathcal{L}_0 \mathcal{L}_1 \mathcal{L}_1 = \mathcal{L}_0 \mathcal{L}_1^2$, up to a cyclic permutation. For a given n we get contributions only from primitive orbits for which $n_n = r n_p$. Then, as usual one can write

$$F(z) = \exp\left(-\sum_{p,r} \frac{z^{n_p r}}{r} \text{tr} \mathcal{L}_p^r\right), \quad (5.171)$$

and after r summation we get

$$F(z) = \prod_p \det(1 - z^{n_p} \mathcal{L}_p). \quad (5.172)$$

In case of the noisy maps we can introduce -let's say- the three branches of the map $f_i(x)$ corresponding to the symbols $f(x) = f_i(x)$ if x is in the state space region \mathcal{M}_i , and define operators

$$\mathcal{L}_i(x', x) = \frac{1}{\sqrt{2\pi}\sigma} e^{-\frac{1}{2\sigma^2}(x' - f_i(x))^2}. \quad (5.173)$$

Map f_i acts only on the state space region \mathcal{M}_i , but it maps to all regions \mathcal{M}_j allowed by system's transition graph. If you visualize this operator as a matrix, \mathcal{L} is an $[n \times n]$ matrix, while \mathcal{L}_i is -say- $[n \times n/3]$ matrix, the matrix elements

where the initial x is in the state space region $\mathcal{M}_j \neq \mathcal{M}_i$ are all zero. For these operators we can apply (5.172) and get the spectral determinant as a product of spectral determinants of primitive orbits. The operators are defined on piecewise monotonic maps, so there is only one periodic point on each.

So, this way can get rid of repeats in an early stage, and concentrate only on computing prime orbits. Tomorrow (March 4, 1998 - tomorrow never came) on the train I will try to give the matrix representation elements [74] of L_p in the unperturbed basis (eg. on x^k) and hope to end up with simpler formulas.

5.10 Kuramoto-Sivashinsky equation

Assume a 2-dimensional square lattice with period L in the spatial direction and period T in the temporal direction, finite volume LT , and periodic boundary conditions. We use $L = 1/\Delta x$, $T = 1/\Delta t$ discretization.

Given the Kuramoto-Sivashinsky equation of form

$$u_t + u u_x + u_{xx} + u_{xxxx} = 0, \quad x \in [0, L]. \quad (5.174)$$

the corresponding discretized Kuramoto-Sivashinsky equation is

$$T\partial_t U + \frac{L}{2}\partial_x U^2 + L^2 \square_x U + L^4 \square_x^2 U = 0. \quad (5.175)$$

In continuum the Kuramoto-Sivashinsky equation is Galilean invariant: if $u(x, t)$ is a solution, then $v + u(x - vt, t)$, with v an arbitrary constant velocity, is also a solution. On a spacetime torus, the velocity have to be 'quantized', satisfy something like $n\Delta x - vt\Delta t = \frac{n}{L} - v\frac{t}{T} \in \mathbb{Z}$, i.e., if you have relative periodic orbit $[L \times T]_S$, allowed velocities are

$$v = k\frac{n}{t}\frac{T}{L}, \quad k \in \mathbb{Z}.$$

FIX S dependence in THIS! But would like to check that one gets a sensible spatiotemporal orbit Jacobian matrix \mathcal{J} and $\text{Det } \mathcal{J}$, at least for the $U = 0$ fixed point...

5.11 Field theory blog

2021-07-20 Chris Crowley I am looking for a good citation to use that suggests that periodic orbit theory like thinking could be useful for quantum field theories. I have a few references at the very end of a paper, see that try to establish that this framework could extend to other systems and want to add quantum field theory to the list because it sounds sexy in the current zeitgeist.

2021-08-04 Predrag For the Quantum Field Theory I think I am still the main proponent, I tend to cite [72]

```
@Article{CFTsketch,
  author  = {P. Cvitanovi\'c},
  journal = {Physica A},
  title   = {Chaotic field theory: {A} sketch},
  year    = {2000},
  pages   = {61},
  volume  = {288},
  doi     = {10.1016/s0378-4371(00)00415-5},
}
```

2020-05-15 Predrag .

Kadanoff [155] ([click here](#)) 3.4 Lattice Green Function discussion of the “Gaussian model” coefficient matrix of his (3.12)

$$-\frac{1}{K} C_{nm} = \begin{cases} K^{-1} & \text{if } x_n = x_m \\ 1 & \text{if nearest neighbors} \end{cases} \quad (5.176)$$

is the same as our \mathcal{J} with $d s = 1/K$.

He writes “As we shall see this simple and exactly solvable problem is in fact closely related to several different situations involving phase transitions. The Gaussian problem itself undergoes a kind of phase transition at a point at which one of the eigenvalues of C approaches zero. When that happens, the correlation matrix G goes to infinity, and very large correlations tend to develop in the system. Some thermodynamic derivatives for the system become very large, and the system shows every sign of doing something interesting. We shall explore this interesting behavior in considerable detail below.”

He looks at the Fourier transformed \mathcal{J} and observes 0-Fourier mode is of form

$$C(0) = 1 - 2dK = 1 - 2/s, \quad (5.177)$$

so there is a phase transition as K approaches $1/(2d)$ from below, or s approaches -2 from above. He writes “We shall investigate this point in considerable detail in several of the chapters below.”

He returns to it in his eq. (4.38), where he notes (for 1-dimensional chain) that $-1/2 < K < 1/2$, i.e., $|s| > 2$, so the Gaussian field theory operates in the same regime as the spatiotemporal cat. But I have not found a discussion in higher dimensions, or rather, while the Gaussian model is used throughout the book as the ‘opposite of’ the Ising model, I do not see what to make out of it from our perspective...

His lecture [is nice](#).

2018-10-09 Predrag I have been trying to write up a standard Euclidean lattice field theory formulation of generating functions $Z[J]$ and $W[J]$, mostly

following Montvay and Münster [202] *Quantum Fields on a Lattice*, though there are many references, and some others might be smarter.

What I have done so far is in section *Lattice action* of the course [QFT notes](#).

Like Han, they single out one “time” direction, and reformulate the theory as a “transfer matrix” calculation, which is essentially the Hamiltonian formulation, I believe. I have not written that part up yet.

2020-06-11 Nathan Seiberg Institute for Advanced Study talk: *Continuum Quantum Field Theories for Fractons*: “ Starting with a lattice system at short distances, its long-distance behavior is captured by a continuum Quantum Field Theory (QFT). This description is universal, i.e. it is independent of most of the details of the microscopic system. Surprisingly, certain recently discovered lattice systems, and in particular models of fractons, seem to violate this general dogma. We present exotic continuum QFTs that describe these systems. ”

I had a brief scan through

Exotic Symmetries, Duality, and Fractons in 2+1-Dimensional Quantum Field Theory [arXiv:2003.10466](#);

Exotic U(1) Symmetries, Duality, and Fractons in 3+1-Dimensional Quantum Field Theory [arXiv:2004.00015](#);

Exotic Z_N Symmetries, Duality, and Fractons in 3+1-Dimensional Quantum Field Theory [arXiv:2004.06115](#),

but I do not get them. Ignore for now.

2021-02-04 Predrag van der Kamp [156] *Initial value problems for lattice equations* studies periodic solutions of *partial difference equations* ($P\Delta E$ s):

consider (s_1, s_2) relative periodic initial value problem. [...] In the Cauchy directions, assuming the equation to be multi-linear, the periodic solution can be obtained uniquely by iteration of a simple mapping, whose dimension is a piecewise linear function of (s_1, s_2) .

van der Kamp [156] paper offers geometric understanding, and shows how to pose initial value problems for general lattice equations. He provides explicit reductions of an integrable 5-point equation.

If well-posed, the periodic solutions are uniquely determined by iteration of single-valued mappings. Here, s -periodicity on the band of initial values implies s periodicity of the solution on $\mathbb{Z} \times \mathbb{Z}$.

His mappings can be obtained by using the equation only $r = \gcd(s_1, s_2)$ times.

He performs different reductions for the integrable 5-point equation of Bruschi, Calogero and Droghei [48] *Tridiagonal matrices, orthogonal polynomials and Diophantine relations: I*. Also, read sect. 4.3.6, add your notes to the subsection there.

Do have a look at:

Papageorgiou, Nijhoff and Capel [212] *Integrable mappings and nonlinear integrable lattice equations*: Periodic reductions for lattice equations defined on a square.

Quispel, Capel, Papageorgiou and Nijhoff [227] *Integrable mappings derived from soliton equations*: They realized that such reductions provide traveling wave solutions.

A general description of s-reduction, with $s \in \mathbb{Z} \times \mathbb{Z}$, is given in Rojas, van der Kamp and Quispel [231] *Lax representations for integrable maps $O\Delta Es$* .

Adler and Veselov [1] *Cauchy problem for integrable discrete equations on quad-graphs* give a criterion for the well-posedness of Cauchy problems for integrable equations defined on the square, on a so-called quad-graph (a planar graph with quadrilateral faces).

Commentary

Remark 5.1. Lattice field theory. In his 1983 *Six Lectures on Lattice Field Theory* Michael Stone explains that the free, non-interacting partition function (??) is the sum over all loop (returning walks), i.e., related to the trace of the propagator (??). ¹⁹ This goes back to Symanzik, and is probably explained at length in Federico Camia *Brownian Loops and Conformal Fields*, arXiv:1501.04861.

Check Rosenfelder *Path Integrals in Quantum Physics*, arXiv:1209.1315.

Meyer [198] *Lattice QCD: A brief introduction*.

Check out also online Simons, Lecture I: Simons courses *Collective Excitations: From Particles to Fields Free Scalar Field Theory: Phonons*; and *Quantum Condensed Matter Field Theory*; as well as Piers Coleman [65] *Introduction to Many-Body Physics* ([click here](#)) + ([click here](#)).

Further reading on lattice field theories: Sommer [246] *Introduction to Lattice Gauge Theories*; Wiese [265] *An Introduction to Lattice Field Theory*; Rothe [232] *Lattice Gauge Theories*; Jansen [148] *Lattice field theory* focuses on the lattice QCD; Smit [245] *Introduction to Quantum Fields on a Lattice*; Münster and M. Walzl [205] *Lattice gauge theory - A short primer*, arXiv:hep-lat/0012005; Montvay and G. Münster [202] *Quantum Fields on a Lattice*.

¹⁹ Predrag 2018-10-07: Incorporate Stone explanation, with hops weighted by fugacity $h = \exp(-\mu)$.

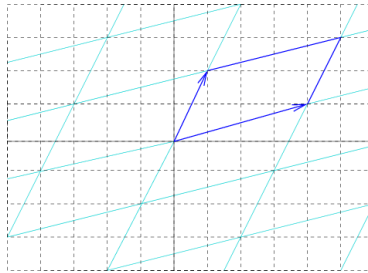


Figure 5.2: A fundamental parallelogram spanned by $(4,1)$ and $(1,2)$ contains $\text{Det } \mathcal{L} = 7$ points. Note that the far vertices $(4,1)$, $(1,2)$ and $(5,3)$ are not counted, as they belong to other tiles.

5.12 Lattice points enumeration

God made the integers, all else is the work of man.
— Leopold Kronecker

5.12.1 Complex plane

[wiki](#): Gaussian integers have many nice properties (factorization, primes, etc) but I do not feel the complex plane relevant to our problem; for us it is only the $d = 2$ case of general lattice point counting of the next section..

2020-01-23 Predrag .

[wiki](#): A fundamental pair of periods is a pair of complex numbers $\omega_1, \omega_2 \in \mathbb{C}$ such that, considered as vectors in \mathbb{R}^2 , the two are not collinear. The lattice generated by ω_1 and ω_2 is

$$\mathcal{L} = \{m\omega_1 + n\omega_2 \mid m, n \in \mathbb{Z}\}$$

The two generators ω_1 and ω_2 are called the *lattice basis*. The parallelogram defined by the vertices $0, \omega_1$ and ω_2 is called the *fundamental parallelogram*, see figure 5.2. The fundamental parallelogram contains no further lattice points in its interior or boundary. Conversely, any pair of lattice points with this property constitute a fundamental pair, and furthermore, they generate the same lattice.

A fundamental parallelogram spanned by $(4,1)$ and $(1,2)$ contains

$$\text{Det} \begin{pmatrix} 4 & 1 \\ 1 & 2 \end{pmatrix} = 7$$

points, see figure 5.2.

There is no unique fundamental pair; an infinite number of fundamental pairs correspond to the same lattice. Any pair of fundamental parallelograms is related by a modular group matrix $\in SL_n \mathbb{Z}$. This equivalence

of lattices underlies many of the properties of elliptic functions (especially the Weierstrass elliptic function - I think not relevant to us) and modular forms.

The abelian group \mathbb{Z}^2 maps the complex plane into the fundamental parallelogram. That is, every point $z \in \mathbb{C}$ can be written as $z = p + m\omega_1 + n\omega_2$ for integers m, n , with a point p in the fundamental parallelogram.

If one identifies opposite sides of the parallelogram as being the same, the fundamental parallelogram has the topology of a torus; the quotient manifold \mathbb{C}/\mathcal{L} is a torus. We are possibly interested in functions on $\mathbb{C}/(\text{lattice})$, functions on \mathbb{C} with a certain periodicity condition. These doubly periodic, meromorphic functions are called *elliptic*.

5.12.2 Integer lattice in d dimensions

Since we are interested in combinatorial rather than metric properties, it suffices to consider the case of the standard integer lattice $\mathbb{Z}^d \subset \mathbb{R}^d$. The case of a general lattice \mathcal{L} in \mathbb{R}^d reduces to that of \mathbb{Z}^d by a change of the coordinates.

2020-01-23 Predrag .

wiki: *Lattice (group)*: A lattice \mathcal{L} in \mathbb{R}^d has the form

$$\mathcal{L} = \left\{ \sum_{i=1}^d a_i v_i \mid a_i \in \mathbb{Z} \right\}$$

where

$$\{v_1, v_2, \dots, v_d\} \quad (5.178)$$

is a basis (or ‘integral basis’) that defines the Bravais cell. One convention is that an integral basis is ordered according to the length of its elements; i.e. $|v_1| \leq |v_2| \leq \dots \leq |v_d|$.

wiki: A *lattice graph*, mesh graph, or grid graph, is a graph whose drawing, embedded in \mathbb{R}^d , forms a regular tiling. In $d = 2$ a lattice graph (or a square grid graph) is the graph whose vertices correspond to the points in the plane with integer coordinates.

The determinant (‘discriminant’ or ‘volume’) of lattice \mathcal{L} is

$$d(\mathcal{L}) = |\det(v_1|v_2|\dots|v_d)|. \quad (5.179)$$

The determinant is the reciprocal of the average density of points in the lattice. Different bases can generate the same lattice, but the absolute value of the determinant is uniquely determined by \mathcal{L} . If one thinks of a lattice as dividing the whole of \mathbb{R}^d into equal polyhedra (copies of an d -dimensional parallelepiped, the ‘fundamental region’ of the lattice), then $d(\mathcal{L})$ is equal to the d -dimensional volume of this polyhedron. This is why $d(\mathcal{L})$ is sometimes called the *covolume* of the lattice. If it equals 1, the lattice is called unimodular.

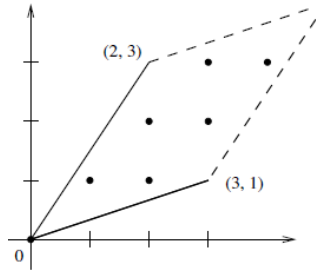


Figure 5.3: A parallelepiped spanned by $(3,1)$ and $(2,3)$ contains $\text{Det} \begin{pmatrix} 3 & 2 \\ 1 & 3 \end{pmatrix} = 7$ points. Note that $(3,1)$, $(2,3)$ and the far vertex $(5,4)$ are not counted. Barvinok [28] Fig. 81.

The master of counting integer lattice points in various domains (and all dimensions) is Alexander Barvinok. Barvinok lectures are very clear and simple. On p. 20 he defines the fundamental parallelepiped, and then shows that

Theorem 2. The number of integer points in the fundamental parallelepiped is equal to the volume of the parallelepiped.

Note that the fundamental parallelepiped is half-open, as indicated by dashed lines in figure 5.3 so that its translates form a partition of the whole space.

Barvinok [28] *A Course in Convexity*, ([click here](#))

Barvinok [29] *Integer Points in Polyhedra*, ([click here](#)) seems to be a harder read, and not helpful for our integer lattice points counting.

1831 pages *Handbook of Discrete and Computational Geometry* might be of some use.

Hadamard's inequality. Let v_1, v_2, \dots, v_d be any basis for \mathcal{L} . Then

$$d(\mathcal{L}) \leq |v_1||v_2| \cdots |v_d|, \quad (5.180)$$

as the volume of a parallelepiped is never greater than the product of the lengths of its sides. Hadamard's inequality is an equality if and only if the basis vectors are orthogonal. A theorem of Hermite says that every lattice has a basis that is reasonably orthogonal (see (5.204)), where the amount of nonorthogonality is bounded solely in terms of the dimension. A *reduced basis* is an integral basis that minimizes the product of lengths (5.180) over all bases of the lattice. Lattice \mathcal{L} is *bounded* by T , if it has a reduced basis consisting of vectors of length at most T .

LattE is an “Lattice point Enumeration” program that count lattice points contained in convex polyhedra defined by linear equations and inequalities with integer coefficients [80]. In 1994 Barvinok [30] gave an algorithm

that counts lattice points in convex rational polyhedra in polynomial time when the dimension of the polytope is fixed. LattE counts the lattice points using multivariate generating functions $P(a)$, $z^a = z^{a_1}z^{a_2}\cdots z^{a_d}$, implementing Barvinok algorithm. At the end, $f(P)$ is written as a sum of "short" rational functions.

Latte [home page](#).

[Maple](#) code.

Simplicial cone: Let (5.178) be a set of k linearly independent integral vectors in \mathbb{R}^d , where $k \leq d$. Consider simplicial cone K and parallelepiped S generated by (5.178),

$$K = \{\lambda_1 v_1 + \lambda_2 v_2 + \cdots + \lambda_k v_k\}, \quad 0 \leq \lambda_i \quad (5.181)$$

$$S = \{\lambda_1 v_1 + \lambda_2 v_2 + \cdots + \lambda_k v_k\}, \quad 0 \leq \lambda_i < 1 \quad (5.182)$$

The generating function for the lattice points in K equals [248]²⁰

$$\sum_{\beta \in K \cap \mathbb{Z}^d} z^\beta = \left(\sum_{\tau \in S \cap \mathbb{Z}^d} z^\tau \right) \prod_{i=1}^k \frac{1}{1 - z^{v_i}} \quad (5.183)$$

A unimodular cone is a simplicial cone with all $\lambda = 1$ which forms an integral basis for the lattice $\mathbb{R}\{v_1, v_2, \dots, v_k\} \cap \mathbb{Z}^d$. In this case the numerator of the formula has a single monomial; in other words, the parallelepiped has only one lattice point. The number of points in the parallelepiped is obtained by setting $z_i = 1$ in the generating function

$$f(S; z) = \left(\sum_{\tau \in S \cap \mathbb{Z}^d} z^\tau \right) \quad (5.184)$$

However, the generating function is not constructed by enumerating all the integer points in S , but rather as a signed sum of rational functions that can be derived from the description of S . They all count points in a general polyhedron; counting them in a parallelepiped should be a simple special case, but I have not seen that discussed separately.

Note that this count does not identify opposing sides of the parallelepiped.

If we need to enumerate periodic points one-by-one, John Voight [mathoverflow](#) question might be a start.

[Stumbling Robot](#) derives the area of a polygon whose vertices are lattice points.

The study of integer points in convex polyhedra is motivated by questions such as "how many nonnegative integer-valued solutions does a

²⁰Predrag 2020-01-25: I cannot find this formula in Stanley [248], ([click here](#)).

system of linear equations with nonnegative coefficients have" or "how many solutions does an integer linear program have".

[wiki](#): *Minkowski's theorem* relates the number $d(\mathcal{L})$ and the volume of a symmetric convex set S to the number of lattice points contained in S . The number of lattice points contained in a polytope all of whose vertices are elements of the lattice is described by the polytope's Ehrhart polynomial. Formulas for some of the coefficients of this polynomial involve $d(\mathcal{L})$ as well.

[wiki](#): An integral polytope has an associated *Ehrhart polynomial* that encodes the relationship between the volume of a polytope and the number of integer points the polytope contains. A generating function for the Ehrhart polynomials, or the Ehrhart series is a rational function - this suggest that we should able to convert this series into a zeta function. This wiki has some intriguing explicit examples.

2020-09-18 Predrag Subramaniam and Balani have an [E-book](#) with a cute chapter on [lattices](#), but it standard Bravais lattice crystallography, of no use to us. Ignore

2020-07-31 Predrag The spatiotemporal cat orbit Jacobian matrix (8.22) in the Hill determinant $\det \mathcal{J}$ computation for a $[L \times T]_0$ rectangular Bravais cell is expressed naturally and spacetime symmetrically in terms of 'horizontal', 'vertical' translation generators r_1, r_2 .

I expect that for an arbitrary Bravais cell, such as figure 5.3, the corresponding translation generators should act along the 'integral basis' vectors (5.178) that define the Bravais cell \mathcal{L} , i.e., the spatiotemporal cat Hill determinant should be given by

$$\det \mathcal{J} = \det (\mathcal{J}\mathcal{L})/\det \mathcal{L}, \quad (5.185)$$

where spatiotemporal cat orbit Jacobian matrix \mathcal{J} should be expressed in terms of translations along the Bravais cell basis vectors, and the Hill determinant should be expressed terms of invariant quantities that can be constructed from them. The simplest is the volume (5.179), the others are presumably related to traces $\text{tr } \mathcal{L}^k$ and the corresponding subvolumes. Not sure what they are, but someone has surely thought about that. My understanding is summarized in [birdtracks.eu](#).

Han and I have an answer of asymmetric form for the orbit Jacobian matrix (8.22) for a tilted Bravais domain (relative periodic orbit) (8.46), with the relative periodicity all in the 'comoving frame' translation generator $r_1^{-S/T} \otimes r_2$.

This space-time asymmetry is a consequence of choosing the Hermite normal form (5.204) to define the Bravais cell. So - even though we are computing the representation-independent determinants, we do not have an invariant statement of cell's 'tilt'. There must be a more elegant

answer to this. Some of this discussion is in the [2020-07-11 Predrag](#) post, around eq. (5.197).

But that might lead us too deep into the role that prime numbers play in characterizing equivalent Bravais cells \mathcal{L} and their volumes. Whenever you result depends on factorization in primes, it is time to sound a potentially deep number theory red alert :)

2020-01-23 Predrag Oded Regev is good on this - will post more links. He uses Micciancio and Goldwasser [199] *Complexity of Lattice Problems - A Cryptographic Perspective* ([click here](#)) as his course textbook.

Oded Regev: Definition 5 defines $d(\mathcal{L})$, the determinant of a lattice in terms of the Bravais basis that might be useful to us.

Lattices, Convexity and Algorithms lecture notes from 2013 might be better. Check out "Gram Schmidt Orthogonalization," which I think is his construction of the Hermite normal basis, and "Equivalence of Lattice Definitions." Also check out his *Fundamental Parallelepiped and the Determinant lecture*.

2CB

2020-12-12 Predrag Haviv and Regev [arXiv:1311.0366](#) address the Lattice Isomorphism Problem (LIP). I like their definitions.

Two lattices \mathcal{L}_1 and \mathcal{L}_2 are isomorphic if there exists an orthogonal linear transformation mapping \mathcal{L}_1 to \mathcal{L}_2 .

An *orthogonal* linear transformation (or *isometry*) $O : V_1 \rightarrow V_2$ is a linear transformation that preserves inner products, that is, $\langle x, y \rangle = \langle O(x), O(y) \rangle$ for every $x, y \in V_1$. For a set $A \subseteq V_1$ we use the notation $O(A) = \{O(x) \mid x \in A\}$.

For a matrix B we denote its i th column by b_i , and $O(B)$ stands for the matrix whose i th column is $O(b_i)$. $\text{span}(B)$ stands for the subspace spanned by the columns of B .

Let B and D be two matrices satisfying $B^T \cdot B = D^T \cdot D$. Then there exists an orthogonal linear transformation $O : \text{span}(B) \rightarrow \text{span}(D)$ for which $D = O(B)$.

An m -dimensional *lattice* $\mathcal{L} \subseteq \mathbb{R}^m$ is the set of all integer combinations of a set of linearly independent vectors $\{b_1, \dots, b_n\} \subseteq \mathbb{R}^m$, i.e., $\mathcal{L} = \{\sum_{i=1}^n a_i b_i \mid \forall i. a_i \in \mathbb{Z}\}$. The set $\{b_1, \dots, b_n\}$ is called a *basis* of \mathcal{L} and n , the number of vectors in it, is the *rank* of \mathcal{L} . Let B be the m by n matrix whose i th column is b_i . We identify the matrix and the basis that it represents and denote by $\mathcal{L}(B)$ the lattice that B generates.

A basis of a lattice is not unique: two bases B_1 and B_2 generate the same lattice of rank n if and only if $B_1 = B_2 \cdot U$ for a *unimodular* matrix $U \in \mathbb{Z}^{n \times n}$, i.e., an integer matrix satisfying $|\det(U)| = 1$.

The determinant of a lattice \mathcal{L} is defined by

$$\det(\mathcal{L}) = \sqrt{\det(B^T B)}, \quad (5.186)$$

where B is a basis that generates \mathcal{L} . $\det(\mathcal{L})$ is independent of the choice of the basis. A set of (not necessarily linearly independent) vectors that generate a lattice is called a *generating set* of the lattice.

A lattice \mathcal{M} is a *sublattice* of a lattice \mathcal{L} if $\mathcal{M} \subseteq \mathcal{L}$, and it is a *strict sublattice* if $\mathcal{M} \subsetneq \mathcal{L}$. If a lattice \mathcal{L} and its sublattice \mathcal{M} span the same subspace, then the *index* of \mathcal{M} in \mathcal{L} is defined by $|\mathcal{L} : \mathcal{M}| = \det(\mathcal{M})/\det(\mathcal{L})$. If \mathcal{M} is a sublattice of \mathcal{L} such that $|\mathcal{L} : \mathcal{M}| = 1$ then $\mathcal{M} = \mathcal{L}$.

They define lattices by their *Gram matrices*. The *Gram matrix* of a matrix B is defined to be the matrix

$$G = B^T \cdot B, \quad (5.187)$$

or equivalently,

$$G_{ij} = \langle b_i, b_j \rangle, \quad \text{for every } i \text{ and } j. \quad (5.188)$$

A Gram matrix specifies a basis only up to rotation.

In the Lattice Isomorphism Problem the input consists of two Gram matrices G_1 and G_2 , and the goal is to decide if there exists a unimodular matrix U for which $G_1 = U^T \cdot G_2 \cdot U$.

The *dual lattice* of a lattice \mathcal{L} , denoted by \mathcal{L}^* , is defined as the set of all vectors in $\text{span}(\mathcal{L})$ that have integer inner product with all the lattice vectors of \mathcal{L} , that is,

$$\mathcal{L}^* = \{u \in \text{span}(\mathcal{L}) \mid \forall v \in \mathcal{L}. \langle u, v \rangle \in \mathbb{Z}\}.$$

The *dual basis* of a lattice basis B is denoted by B^* and is defined as the one which satisfies $B^T \cdot B^* = I$ and $\text{span}(B) = \text{span}(B^*)$, that is, $B^* = B(B^T B)^{-1}$. It is well known that the dual basis generates the dual lattice, i.e., $\mathcal{L}(B)^* = \mathcal{L}(B^*)$.

The relations between parameters of lattices and parameters of their dual are known as *transference theorems*.

2020-02-14 Predrag Given a nondegenerate lattice \mathcal{L} , we can construct an invariant by choosing a basis, and taking the determinant of the matrix whose (i,j) entry is the inner product of the i-th basis vector with the j-th basis vector. The matrix is called the Gram matrix of the basis, and the determinant is a rough measure of how loosely packed the lattice vectors are in $\mathcal{L} \otimes \mathbb{R}$.

2020-02-14 Predrag I have run (once) into ‘fundamental parallelepiped’ being called ‘fundamental parallelotope’.

2020-12-12 Predrag For our choice of Hermite normal form (5.205), (18.228), the Gram matrix (5.187) is

$$G = \begin{bmatrix} L^2 & LS \\ LS & L^2 + T^2 \end{bmatrix}. \quad (5.189)$$

2020-09-08 Predrag Daniele Micciancio is very economical. I propose we follow his exposition, and use Micciancio and Goldwasser [199] *Complexity of Lattice Problems - A Cryptographic Perspective* ([click here](#)). They say (I have not looked at any of these, so they might be even better than Micciancio and Goldwasser, for our purposes):

"Classical references about lattices are Cassels [52] (or 1971) ([click here](#)) and Gruber and Lekkerkerker [116] ([click here](#)). Another very good reference is Siegel [240] ([click here](#)). For a brief introduction to the applications of lattices in various areas of mathematics and science the reader is referred to (Lagarias 1995) and (Gritzmann and Wills 1993), which also touch some complexity and algorithmic issues. A very good survey of algorithmic application of lattices is (Kannan 1987a)."

Lattices are regular arrangements of points in Euclidean space. The simplest example of lattice in n -dimensional space is \mathbb{Z}^d , the set of all d -dimensional vectors with integer entries. More generally, a lattice is the result of applying a nonsingular linear transformation $B \in \mathbb{R}^{m \times d}$ to the integer lattice \mathbb{Z}^d , to obtain the set $B(\mathbb{Z}^d) = \{Bx : x \in \mathbb{Z}^d\}$. etc. - you fill it in.

To Han: can you replace our 'Bravais' by Micciancio and Goldwasser [199] lattice definitions?

Is the 'Hermite normal form' the same as the 'Gram-Schmidt orthogonalization method'?

2020-09-11 Han See sect. 18.6.3. Gram Schmidt Orthogonalization constructs orthogonal with basis vectors whose tips are not on \mathbb{Z}^d lattice; not Hermite normal form, forget it.

2018-01-31 Han The similarity transformation S that maps (1.1) into (1.5),

$$\mathbf{A} = \begin{bmatrix} 2 & 1 \\ 1 & 1 \end{bmatrix}, \quad \mathbf{B} = \begin{bmatrix} 0 & 1 \\ -1 & 3 \end{bmatrix}, \quad (5.190)$$

is

$$\mathbf{B} = \mathbf{S}^{-1} \mathbf{A} \mathbf{S}, \quad (5.191)$$

where

$$\mathbf{S} = \mathbf{S}^{-1} = \begin{bmatrix} -1 & 2 \\ 0 & 1 \end{bmatrix}.$$

2018-04-27 Predrag Note that $\det \mathbf{S} = -1$. Why? That can be fixed by multiplying it by i , but why? It is also not unique, one could, for example, use

$$\mathbf{S}' = \mathbf{S}'^{-1} = \begin{bmatrix} 0 & -1 \\ 1 & 0 \end{bmatrix} \begin{bmatrix} -1 & 2 \\ 0 & 1 \end{bmatrix} \begin{bmatrix} 0 & 1 \\ -1 & 0 \end{bmatrix} = \begin{bmatrix} 1 & 0 \\ -2 & -1 \end{bmatrix}.$$

For a systematic discussion, see sect. 4. *Global versus local conjugacy and orbit statistics* of Baake *et al.* [22], and sect. 2.5. *Results for $d = 2$* of Baake

et al. [21] *Orbit structure and (reversing) symmetries of toral endomorphisms on rational lattices.* The main point (for us) is that maps that are in the same conjugacy class need to have 3 invariants in common; the trace, the determinant, and the mgcd (the matrix greatest common denominator). For the Thom-Arnol'd cat map (1.1), $\text{mgcd}(A) = 1$

Baake *et al.* [21] discuss “pretails” to periodic orbits at length.

2018-04-27 Predrag Next, one can transform Arnold cat map “square root” C (or, according to Baake *et al.* [22], the ‘classic’ or golden orientation reversing cat map, or the Fibonacci cat map [21], with $\det(C) = -1$)

$$A = C^2, \quad C = \begin{bmatrix} 1 & 1 \\ 1 & 0 \end{bmatrix} \quad (5.192)$$

to the Percival-Vivaldi version

$$B = \tilde{C}^2, \quad \tilde{C} = S^{-1}CS = \begin{bmatrix} -2 & 1 \\ -1 & 1 \end{bmatrix}. \quad (5.193)$$

As noted in (4.183), taking this “square root” expresses the zeta function as a product of a time-reversal pair of zeta’s. B and \tilde{C} have the same eigenvectors, but as $\det(\tilde{C}) = -1$, one of the stability multipliers is a negative square root of the B multipliers (1.6),

$$\tilde{\Lambda} = \tilde{\Lambda}_1 = \frac{1 + \sqrt{5}}{2}, \quad \tilde{\Lambda}_2 = \frac{1 - \sqrt{5}}{2}. \quad (5.194)$$

The issue of reversibility seems complicated [21]. When $M \in \text{SL}(2, \mathbb{Z})$, also its inverse is in $M^{-1} \in \text{SL}(2, \mathbb{Z})$, and M and M^{-1} share the same determinant, trace and mgcd:

$$M = \begin{bmatrix} a & b \\ c & d \end{bmatrix}, \quad M^{-1} = \begin{bmatrix} d & -b \\ -c & a \end{bmatrix}.$$

The golden (Fibonacci [21]) cat map (5.192) is not reversible in $\text{GL}(2, \mathbb{Z})$ (while its square A is [21]).

2020-02-19 Predrag *Linear recurrences with constant coefficients: the multivariate case* by Mireille Bousquet-Mélou1a and Marko Petkovšek, (DOI) has the right feel and a few 2-dimensional integer lattice recurrences and the corresponding functional equations, but I do not see how to apply it to the 2-dimensional spatiotemporal cat.

2020-07-11 Predrag Woods [270] (2012) ([click here](#)) is very clear, what follows is excerpted from it. As Woods says, his starting chapters are taken from Lim [182] *Two-dimensional Signal and Image Processing* ([click here](#)) ([click here](#)), who copies from Dudgeon and Mersereau [87] (1984) *Multidimensional Digital Signal Processing* ([click here](#)) which cover the same ground.

A 2-dimensional field ϕ_{nt} is periodic with period $[L \times T]_0$, if the following equalities hold for all integers n, t :

$$\phi_{nt} = \phi_{n+L,t} = \phi_{n,t+T}, \quad (5.195)$$

where L and T are positive integers. This type of periodicity occurs often for 2-dimensional signals and is referred to as *rectangular periodicity*. We call the resulting period the *rectangular period*.

Given a periodic function, the period effectively defines a basic cell in the plane, which can be repeated to form the function over all integers n, t . As such, we often want the minimum size unit cell for efficiency of both specification and storage. In the case of the rectangular period, we seek the smallest nonzero integers that will suffice for $[L \times T]_0$ to form this basic cell.

Horizontal Wave. Consider the sine wave $\phi_{nt} = \sin(2\pi n/4)$. The horizontal period is $L = 4$. In the vertical direction, the signal is constant, so we can use any positive integer T . The smallest such value is $T = 1$. Thus the rectangular period is $[L \times T]_0 = [4 \times 1]_0$, and the basic cell consists of the set of points $\{(nt) = [(0,0), (1,0), (2,0), (3,0)]\}$ or any translate of this set.

In general, ‘periodicity’ refers to a repetition of blocks, not necessarily rectangular blocks or blocks occurring on a rectangular repeat grid, with the periodicity represented with two integer vectors,

$$v_1 = \begin{pmatrix} L \\ c_{21} \end{pmatrix}, \quad v_2 = \begin{pmatrix} S \\ T \end{pmatrix}.$$

While they note the nonuniqueness of Bravais cells with respect to unimodular transformations, image processing textbooks seem not to use the Hermite normal form (5.204) to eliminate c_{21} .

The 2-dimensional field ϕ_{nt} is periodic with period $(v_1, v_2) = \Lambda$ if the following hold for all integers n, t :

$$\phi_{nt} = \phi_{n+L,t+c_{21}} = \phi_{n+S,t+T}, \quad (5.196)$$

To avoid degenerate cases, restrict the integers in v_j with the condition

$$\det(v_1, v_2) \neq 0.$$

“We leave it to the reader to show that” the number of samples in this region is $\det \Lambda$, i.e., the absolute value of the determinant of the periodicity matrix gives the number of samples of ϕ_n contained in one period.

The matrix Λ is called the *periodicity matrix*. In matrix notation, the periodic field satisfies

$$\phi_n = \phi_{n+\Lambda r}, \quad r = \begin{pmatrix} r_1 \\ r_2 \end{pmatrix}.$$

Two integer vectors \mathbf{m} and \mathbf{n} are *congruent* with respect to the matrix modulus Λ if $\mathbf{m} = \mathbf{n} + \Lambda\mathbf{r}$ for some integer vector \mathbf{r} .

In the case that Λ is a diagonal matrix, $\phi_{\mathbf{n}}$ is *rectangularly periodic*.

If P is any integer matrix, then $P\Lambda$ is also be a periodicity matrix for $\phi_{\mathbf{n}}$. Thus the periodicity matrix is not unique for any periodic sequence.

A matrix E for which $\det E = 1$ is called a *unimodular matrix*. E^{-1} is then also a unimodular matrix. Unimodular matrices are the only integer matrices whose inverses are also integer matrices. If $\det \Lambda$ is a prime number, we will say that Λ is a *prime matrix*. If Λ is neither prime nor unimodular, we say that it is *composite*, and can be decomposed, nonuniquely - up to a unimodular transformation - into a product of two non-unimodular matrices

$$\Lambda = PQ. \quad (5.197)$$

If either P or Q is composite, one continues the process, until $\det \Lambda$ is the product of its prime factors.

Dudgeon and Mersereau [87] then explain clearly how to get the “quotient” Q when “dividing” by P . $|\det \Lambda|/|\det Q| = |\det P|$ is then the number of cosets. In the image-processing, Fourier transforms trade this non-prime factorization is known as “decimation-in-time Cooley-Tukey FFT algorithm,” “twiddle factors,” and “butterflies.”²¹

Example Relative equilibrium field $\sin[2\pi(n/8 + t/16)]$ is constant along the line $2n + t = 16$. The basis vectors are

$$v_1 = \begin{pmatrix} 4 \\ 8 \end{pmatrix}, \quad v_2 = \begin{pmatrix} 1 \\ -2 \end{pmatrix}, \quad \text{with } \det \Lambda = 16.$$

Definition 1.1-1: Linear System [· · ·]

Definition 1.1-2: Shift Invariance [· · ·]

“Linear shift-invariant discrete systems are generally implemented using difference equations. Although multidimensional difference equations represent a generalization of 1-dimensional difference equations, they are considerably more complex and are, in fact, quite different. A number of important issues associated with multidimensional difference equations, such as the direction of recursion and the ordering relation, are really not issues in the 1-dimensional case.

[· · ·] they define multidimensional recursive systems and consider the issues associated with multidimensional difference equations; [· · ·] define the multidimensional Z-transform. ”

²¹ Predrag 2020-07-15: Use this to define prime factorization in ref. [77]?

2-dimensional Convolution If a system is *linear shift-invariant* (LSI), then [...] the field h is called the LSI system's *impulse response*. [...] He defines the 2-dimensional convolution operator [...]

Properties of 2-dimensional Convolution or Convolution Algebra [...] All 5 properties of convolution hold for any 2-dimensional fields x, y , and z , for which convolution is defined (i.e., for which the infinite sums exist). His Figure 1.1-9 illustrates a convolution.

Stability in 2-dimensional Systems²² Stable systems are those for which a small change in the input gives a small change in the output. We define bounded-input bounded-output (BIBO) stability for 2-dimensional systems analogously to that in 1-dimensional system theory. A spatial or 2-dimensional system will be stable if the response to every uniformly bounded input is itself uniformly bounded. For an LSI system the condition is equivalent to the impulse response being absolutely summable,

$$\sum_{k_1, k_2} |h_{k_1, k_2}| < \infty. \quad (5.198)$$

Sect. 1.2 2-dimensional discrete-space Fourier transform The Fourier transform is important in 1-dimensional signal processing because it effectively explains the operation of linear time-invariant (LTI) systems via the concept of frequency response, i.e., the Fourier transform of the system impulse response. While convolution provides a complicated description of the LTI system operation, with the input at all locations n affects the output at all locations, the frequency response provides a simple interpretation as a scalar weighting in the Fourier domain, where the output at each frequency ω depends only on the input at that same frequency. A similar result holds for 2-dimensional systems that are LSI.

2020-07-15 Predrag Note that the discrete Fourier transform of a Bravais lattice always carries the prefactor $1/\det \Lambda$. Going back involves a volume $(2\pi)^d$.

Definition 1.2-1: 2-dimensional Fourier Transform [...] In the 2-dimensional Fourier transform the frequency variable ω_1 is called *horizontal frequency*, and the variable ω_2 is called *vertical frequency*. [...] As n, t are integers, the 2-dimensional Fourier transform is periodic with rectangular period $2\pi \times 2\pi$, and only needs be calculated for one period, usually taken to be $[-\pi, \pi] \times [-\pi, \pi]$.

[...] the 2-dimensional Fourier transform is a *separable operator*, because it can be performed as the concatenation of 1-dimensional operations on the rows followed by 2-dimensional operations on the columns.

Inverse 2-dimensional Fourier Transform [...]

²²Predrag 2020-07-11: I do not understand BIBO, but maybe we should?

Fourier Transform of 2-dimensional or Spatial Convolution

Theorem 1.211: Fourier Convolution Theorem [· · ·]

[· · ·] As a 2-dimensional or spatial LSI system is characterized by its impulse response $h_{n,t}$, its frequency response H_{ω_1, ω_2} suffices to characterize such a system. And the Fourier transform Y of the output equals the product of the frequency response H and the Fourier transform X of the input. When the frequency response H takes on only values 1 and 0, the system is an *ideal filter*, filtering out some frequencies and passing others unmodified. More generally, the term filter include all such LSI systems, and has been extended to shift-variant and even nonlinear systems through the concept of the Volterra series of operators.²³

Some Important Properties of the FT Operator [· · ·]

Some Useful Fourier Transform Pairs [· · ·]

Example 1.2-4: Fourier Transform of Separable Signal [· · ·]

Symmetry Properties of the Fourier Transform [· · ·]

Generally, we think of the Fourier transform as the evaluation of the Z-transform on the unit polycircle $\{|z_1| = |z_2| = 1\}$; however, this assumes the polycircle is in the region of convergence of $X(z_1, z_2)$, which is not always true.

[· · ·] linear shift-invariant systems with sinusoidal excitations are naturally described by the Fourier transform. The Z-transform is a generalization of the Fourier transform which allows us to treat exponential inputs.

[· · ·] Exponentials of the form $x_{n_1 n_2} = z^{n_1} z^{n_2}$ are eigenfunctions of 2-dimensional linear shift invariant systems.

The 2-dimensional Z-transform of a discrete field X is defined as

$$X_{z_1 z_2}^Z = \sum_{n_1=-\infty}^{\infty} \sum_{n_2=-\infty}^{\infty} x_{n_1 n_2} z_1^{-n_1} z_2^{-n_2}. \quad (5.199)$$

Example 3.4-5: Comparison of Fourier Transform and Z-Transform [· · ·]

The Fourier transform is not strictly a subset of the Z-transform, because it can use impulses and other singularity functions, which are not permitted to Z-transforms.

²³Predrag 2020-07-11: ‘Volterra series of operators’? Defined in S. Thurnhofer and S. K. Mitra, *A General Framework for Quadratic Volterra Filters for Edge Enhancement*, IEEE Trans. Image Process., vol. 5, June, pp. 950-963, 1996.

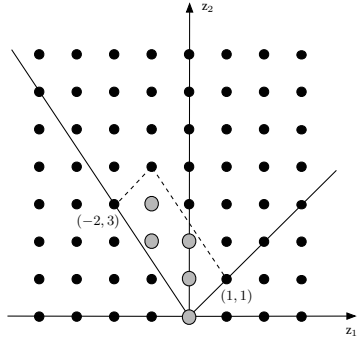


Figure 5.4: The cone \mathcal{K} and its fundamental parallelogram, fig 3.3 from ref. [33].

[...] The Fourier transform is used primarily to describe signals and to describe the actions that systems will have on them. The Z-transform is used to describe systems and to provide an additional tool for manipulating difference equations. While the 2-dimensional Z-transform is related to its 1-dimensional counterpart, the two transforms are actually quite different.

For $z_1 = e^{i\omega_1}$, $z_2 = e^{i\omega_2}$ the Z-transform reduces to the Fourier transform. The corresponding surface in the Z-domain is the called 2-dimensional unit *bicircle*. 2-dimensional Z-transform converges on the *Reinhardt domain*, the 2-dimensional analog of the annulus for 1-dimensional case.

2020-02-23 Predrag Continuing on the multivariate generating functions, the *integer-point transform* introduced in this textbook in integer lattices counting: Beck and Robins [33] *Computing the Continuous Discretely*, ([click here](#)), might be helpful:

Let $\mathbf{a} = (a_1, \dots, a_d) \in \mathbb{Z}^d$ be an integer point. The Laurent monomial $\mathbf{z}^\mathbf{a}$ is defined as

$$\mathbf{z}^\mathbf{a} := z_1^{a_1} z_2^{a_2} \cdots z_d^{a_d}, \quad \mathbf{z}^0 := 1 \quad (5.200)$$

where $\mathbf{0} := (0, 0, \dots, 0)$. For a given rational cone or rational polytope $S \subset \mathbb{R}^d$,

$$\sigma_S(\mathbf{z}) = \sigma_S(z_1, z_2, \dots, z_d) := \sum_{\mathbf{a} \in S \cap \mathbb{Z}^d} \mathbf{z}^\mathbf{a} \quad (5.201)$$

is called the *integer-point transform* of S . The function σ_S lists all integer points in S not as a list of vectors, but as a sum of monomials. This σ_S also goes by the name *moment generating function* or simply *generating function* of S .

They start with the usual trivial example of a geometric series in Example 3.3, and work out a 2-dimensional $\{(1, 1), (-2, 3)\}$ Bravais lattice in example Example 3.4, see figure 5.4. They call the \mathbb{R}^2 interior of the half-open

Bravais cell ‘fundamental parallelogram II’, and tile the two-dimensional cone \mathcal{K} with its non-negative translations. That results in the rational polynomial formula for the integer-point transform of the cone \mathcal{K}

$$\sigma_{\mathcal{K}}(\mathbf{z}) = \frac{1 + z_2 + z_2^2 + z_1^{-1}z_2^2 + z_1^{-1}z_2^3}{(1 - z_1z_2)(1 - z_1^{-2}z_2^3)} \quad (5.202)$$

of the form that I had suggested to Han for the spatiotemporal cat.

Check also:

- **2020-03-02 Predrag** notes below, on Wilf [267] sect. 1.5 *Two independent variables*.
- *Characteristic function* or “five-point stencil” (5.249)

2020-03-03 Predrag OK, the fundamental parallelepiped determinant (5.179) counts integer points

$$N_n = |\text{Det } \mathcal{J}| = |\text{Det}(v_1|v_2|\cdots|v_n)|. \quad (5.203)$$

What does $\text{tr } \mathcal{J}$ do? That is also an invariant under $SLG(n)$ lattice transformations.

5.12.3 Primitive parallelogram

2020-01-25 Predrag A lattice vector is called *primitive*, if there is no other lattice points on the segment between 0 and the tip.

or:

An integer vector $v \in \mathbb{Z}^d$ is *primitive* if it cannot be written as an integer multiple $m \neq 1$ of some other integer vector $w \in \mathbb{Z}^d$.

or:

A lattice point is a primitive lattice point if it is not a multiple of any other lattice point, that is, the greatest common divisor of its coordinates is one.

or:

A primitive lattice point is a lattice point visible from the origin.

Let A be an integer $[d \times d]$ -matrix with nonzero determinant k and primitive row vectors. The common divisors of the entries of each row of A are preserved under multiplication on the right by any matrix $X \in SLnd\mathbb{Z}$.

A lower triangular integer matrix

$$C = \begin{pmatrix} c_{11} & 0 & \cdots & 0 \\ c_{21} & c_{22} & \ddots & 0 \\ \vdots & & \ddots & 0 \\ c_{d1} & \cdots & c_{d(d-1)} & c_{dd} \end{pmatrix} \quad (5.204)$$

is said to be in (lower) *Hermite normal form* if $0 < c_{11}$ and $0 \leq c_{ij} < c_{ii}$ for all $j < i$.

I would prefer the vectors to be column vectors, as in Lind (18.166). In particular, in the case of 2-dimensional square lattice,

$$C = \begin{pmatrix} L & S \\ 0 & T \end{pmatrix} \quad (5.205)$$

The Bravais cell basis column vectors are

$$v_1 = \begin{pmatrix} L \\ 0 \end{pmatrix}, \quad v_2 = \begin{pmatrix} S \\ T \end{pmatrix},$$

where $0 \leq S < L$ is the relative-periodic ‘shift,’ or ‘screw’ for a screw-boundary condition, and our convention is $L \geq T$, the rest obtained by discrete symmetries.

Orbit of Λ , a matrix in Hermite normal form with primitive row vectors, is denoted $\{A\Lambda | A \in SL_n 2\mathbb{Z}\}$.

Lemma[Cohen [64], Theorem 2.4.3] Assume $k > 0$. Given an arbitrary matrix $A \in M_{n,k}$, the orbit $ASL_n d\mathbb{Z}$ contains a unique matrix Λ in Hermite normal form.

Samuel Holmin PhD thesis [130] is a user-friendly overview of his papers, such as *Counting nonsingular matrices with primitive row vectors* [129] arXiv:1211.2716. Holmin defines a *primitive parallelogram*: “Consider a parallelogram with integer coordinates which cannot be decomposed into smaller parallelograms with integer coordinates. We will call such an object a primitive parallelogram; see figure 5.5 for an illustration. How many primitive parallelograms are there with an area of 10? There are infinitely many such primitive parallelograms: in fact, starting with a single primitive parallelogram, we can produce another one with the same area by for example shifting it an integer distance up or to the right, or by shearing it, and by repeating either of these operations we can produce arbitrarily many different parallelograms, all of which are primitive and have the same area.”

Curiously, even though in his 2nd papers he mentions that different Bravais cells correspond to the same *lattice*, his claim of figure 5.5 is wrong.

Wigman [266] *Counting singular matrices with primitive row vectors*: “Let us consider the set of singular $[n \times n]$ matrices with integer entries. We are interested in the question how many among these matrices have primitive row vectors, that is each row is not a nontrivial multiple of an integer vector. We count the matrices according to the maximal allowed Euclidean length of the rows. Without the constraint of primitivity the problem of counting such matrices was solved by Katznelson [??].”

Wigman [266] and Katznelson focus on asymptotic counting, which we probably do not need.

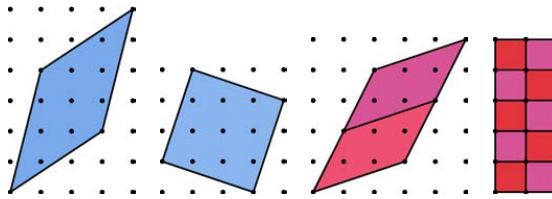


Figure 5.5: Four Bravais cells of area 10, a figure from Holmin's PhD thesis [130]. The two blue Bravais cells are not 'primitive' (i.e., prime), as they are clearly tiled by smaller prime Bravais cells. Holmin claims that the two blue Bravais cells are primitive, but that is wrong, see (18.243).

2020-02-19 Predrag Alexander Gorodnik [lecture notes](#) discuss cat map ($A^n - 1$) and says "The number of such solutions is exactly the area $\det(A^n - 1)$ of fundamental parallelepiped in virtue of the

Pick's theorem (Gorodnik's Theorem 1.5.3, and A.4.1). Let i be the number of points with integer coordinates in the interior of parallelogram P and b be the number of points with integer coordinates on the perimeter of P . Then, $\text{Area}(P) = i + (b/2) + 1$, with points on the edges are counted as half and all vertices count as a single point.

He proves the theorem. As usual, Pick's theorem is for \mathbb{R}^2 , not general enough for us.

2020-02-19 Predrag Baake, Hermisson and Pleasants [20] *The torus parametrization of quasiperiodic LI-classes* call this theorem a "Fundamental fact" (their eq. (10)), and prove it, in Appendix for d -dimensional tori maps, i.e., in the case that we need. They use it to count all manner of tilings. What they emphasize, and what we might have to pay attention to, is the structure of the symmetry solutions on \mathbb{T}^d .

2020-02-21 Predrag Jezierski and Marzantowicz [149] ([click here](#)) write:

let $f : X \rightarrow X$ be a self-map of a set X .

(1.0.4) Definition. If $x \in X$ is a periodic point of f then any $m \in N$ such that $f^m(x) = x$ is called a period of x . The smallest period of x is called the minimal period of x with respect to f . The set of all minimal periods of $x \in X$ is called the set of minimal periods of f and denoted by $\text{Per}(f)$.

We will define the fundamental algebraic invariants of a map f which allow us to study the following notions:

- Lefschetz number $L(f)$ (cf. (2.3.12)), correspondingly Lefschetz numbers $L(f^m)$ of all iterations and their algebraic combinations, informing about the existence of fixed, respectively periodic points.
- Nielsen number $N(f)$ (cf. (4.1.2)), correspondingly Nielsen periodic numbers $NF_m(f)$ (cf. (5.1.16)), $NP_m(f)$ (cf. (5.1.14)) estimating from

below the number of fixed, respectively points of period m and m -periodic points.

[...] This theory was initiated by Jakob Nielsen [206] in 1920 by the observation that every self-map of the two-dimensional torus $f : \mathbb{T}^2 \rightarrow \mathbb{T}^2$ has at least $|\det(I-A)|$ fixed points (here $I, A \in M_{2 \times 2}(\mathbb{Z})$) are respectively the identity matrix and the matrix representing the induced homotopy homomorphism $f_\#$ of $\pi_1(\mathbb{T}^2) = \mathbb{Z}^2$.

In 1975 R. Brooks, B. Brown J. Pak, and D. Taylor [46] derived a nice formula for the Nielsen number $N(f)$ for the torus map: the Nielsen number equals the absolute value of the Lefschetz number. [...] The following theorem has been proved in ref. [46].

(4.3.14) Theorem. For every self-map of the torus $f : \mathbb{T}^d \rightarrow \mathbb{T}^d$, $L(f) = \det(I-A)$ and $N(f) = |L(f)|$.

Proof. Since the Lefschetz and Nielsen numbers are homotopy invariants we may assume that $f = f_A$, i.e. f is induced by the linear map A .

1. f_A has exactly $|\det(I-A)|$ fixed points,
2. no two fixed points of f_A are Nielsen related,
3. the index of each fixed point equals $\text{sgn}(\det(I-A))$.

[...] the fundamental theorem which allows us to extend the Nielsen fixed point theory from tori into nilmanifolds. This theorem was proved simultaneously by Anosov [An], and also Fadell and Husseini [FaHu2].

(6.3.13) Theorem. Let $f : X \rightarrow X$ be a self-map of a compact nilmanifold. Then $N(f) = |L(f)|$ and $L(f) = \det(I-A)$, where A denotes the linearization matrix of f (cf. Definition (6.3.4), Proposition (6.3.6)).

2020-02-22 Predrag Brooks *et al.* [46] *Nielsen numbers of maps of tori*:

If $f : X \rightarrow X$ is any map on a k -dimensional torus X , then the Nielsen number and Lefschetz number of f are related by the formula $N(f) = |L(f)|$. Thus, on the torus, the Lefschetz number gives information, not just on the existence of fixed points, but on the number of fixed points as well. No other compact Lie group has this property.

1995-09-08, 2020-12-08 Predrag Fel'shtyn and Hill [94] *Trace formulae, Zeta functions, congruences and Reidemeister torsion in Nielsen theory* [arXiv:chao-dyn/9509009](https://arxiv.org/abs/math/9509009) paper is rich in examples of trace formulas and zeta functions, but it's probably safe to ignore all this...

“The Artin-Mazur zeta function and its modification count periodic points of a map geometrically, the Lefschetz's type zeta functions do this algebraically (with weight given by index theory). Another way to count the periodic points is given by Nielsen theory.

The Lefschetz zeta function is always rational function of z and is given by a determinant formula. Manning [191] proved the rationality of the

Artin-Mazur zeta function for diffeomorphisms of a compact smooth manifold satisfying Smale's Axiom A.

In Nielsen theory the ‘fixed point class’ is determined by the ‘lifting class’. A fixed point class is called *essential* if its index is nonzero. The number of lifting classes (and hence the number of fixed point classes, empty or not) is called the *Reidemeister Number*. Generating functions for these numbers are called the Reidemeister zeta and Nielsen zeta functions. They are homotopy invariants. ”

5.12.4 Tensor eigenvalues

In principle Han has solved the periodic states counting problem for d -dimensional hypercubic lattices by the discrete Fourier transform diagonalization formula (18.179). A conceptual problem is that the answer is stated in terms of cos's of rational angles, and it is not obvious how those combine to yield an integer as the final result, the number of periodic states.

For that reason it might be nice to perform the inverse Fourier transform to the configuration space, to see what the basis vectors and the fundamental parallelogram of the 2-dimensional integer lattice look like, and unify the treatment of the 1-dimensional and higher-dimensional lattice points counting. We have looked at the relationship between the lattice states and their Fourier representation in (18.32), figure 18.24, (18.56), etc..

Also we have some suggestive lattice solutions, such as (18.65), figure 18.29 (unit cube have been preferable - this is in the cube center coordinates).

There is much literature on eigenvectors of tensors - probably we can figure it out on our own, but I'm recording possible references just for record here:

2018-02-06 Predrag A job candidate Glen Evenly talked about “Tensor Networks”, (also known as “birdtracks”, but getting a citation out of computer nerds who do it is harder than pulling teeth - at best I can pass under “Penrose diagrams”). If you want to see a lot of non-birdtracky pictures, Román Orús [has them](#). Basically, if you are solving a 1D lattice problem, the transfer operator is a matrix. However, if you are acting on a 2-dimensional or higher lattice, the transfer operator has pairs of more indices replacing each index of the 1D matrix, hence “tensor.” We need to understand that as we go from cat map Toeplitz matrices to their d -dimensional generalizations.

2020-02-14 Predrag Mateusz Michałek and Bernd Sturmfels [200] *Invitation to Nonlinear Algebra*, ([click here](#)) discuss symmetric $[n \times n]$ matrices tensor eigenvectors in Sect. 9.1.

The main monograph in this subject is Qi, Chen and Chen [226] *Tensor Eigenvalues and Their Applications*, ([click here](#)).

They find convenient to replace the n -dimensional affine space with the $(n-1)$ -dimensional projective space, where two nonzero vectors are identified if they are parallel.

Papers not looked at yet:

All Real Eigenvalues of Symmetric Tensors DOI:

Generalized Tensor Eigenvalue Problems DOI:

On determinants and eigenvalue theory of tensors DOI:

5.13 Difference equations

sect. 2.3 Linear homogenous equations with constant coefficients, Elaydi [90]

Consider k th-order difference equation

$$\phi_{n+k} + p_1 \phi_{n+k-1} + p_2 \phi_{n+k-2} + \cdots + p_k \phi_n = 0, \quad (5.206)$$

where p_i are constants and $p_k \neq 0$. A k th-order difference equation with constant coefficients is often referred to as $(k+1)$ -term recurrence relation, see sect. 5.14. Assuming a solution of form $\phi_n = \Lambda^n$ leads to the *characteristic equation* (see also ‘characteristic function’ (5.248))

$$\Lambda^k + p_1 \Lambda^{k-1} + p_2 \Lambda^{k-2} + \cdots + p_k = 0, \quad (5.207)$$

with characteristic roots $\{\Lambda_1, \Lambda_2, \dots, \Lambda_k\}$. If the roots are distinct,

$$\{\Lambda_1^n, \Lambda_2^n, \dots, \Lambda_k^n\}$$

is a set of fundamental solutions, and the general solution is of form

$$\phi_n = \sum_{i=1}^k a_i \Lambda_i^n, \quad (5.208)$$

where constants a_i are determined by the initial conditions $\{\phi_0, \phi_1, \dots, \phi_{k-1}\}$.

If the roots are not distinct, one also has fundamental solutions of form $n^m \Lambda_i^n$.

sect. 2.4 Linear inhomogenous equations, Elaydi [90]

$$\phi_{n+k} + p_1 \phi_{n+k-1} + p_2 \phi_{n+k-2} + \cdots + p_k \phi_n = g_n \quad (5.209)$$

represents a physical system in which the *forcing term* (or *external force*, or *control*, or *input*) g_n is the input, and ϕ_n the output,

$$g_n \rightarrow \text{system} \rightarrow \phi_n.$$

The solutions of (5.209) do not form a vector space, i.e., their linear combinations are not also solutions. However, a difference of any pair of solutions is a solution of the homogenous difference equation (5.206), and a general solution of the linear inhomogenous system (5.209) is a sum of the *complementary* solution (a homogenous solution ϕ_c of (5.206), and a *particular* solution ϕ_p

$$\phi_n = \phi_{c,n} + \phi_{p,n} \quad (5.210)$$

A simple example of a particular solution: if $g_n = a^n$, then $\phi_{p,n} = c_1 a^n$.

2020-03-28 Predrag There are many books on difference equations.

I like Elaydi [90] ([click here](#)), but I have also downloaded

Kelley and Peterson [169] ([click here](#))

Agarwal [3] ([click here](#))

Agarwal [4] ([click here](#))

Allen, Aulbach, Elaydi and Sacker [7] ([click here](#))

Galor [108] ([click here](#))

Ozisik, Orlande, Colaco and Cotta [211] ([click here](#))

Micciancio and Goldwasser [199]

2020-04-13 Predrag Dannan, Elaydi and Liu [79] *Periodic solutions of difference equations* is a treasure trove of results on periodic solutions of difference equations: marginal eigenvalues, Floquet exponents and multipliers, Fredholm alternative.

2020-08-10 Predrag Lick [181] *Difference Equations from Differential Equations* ([click here](#)) we probably do not need.

The most general, quasi-linear, second-order PDE in two independent variables is his eq. (2.0.2). Depending on coefficients, the equation can be *hyperbolic*, such as the $d = 2$ spacetime wave equation (2.0.3). He focuses on *parabolic* ($s = 2$ for us), such as the time dependent diffusion equation given by (2.0.4).

Elliptic equations usually describe the steady-state limit of problems where the time-dependent problem is described by parabolic or hyperbolic partial differential equations. The most common elliptic equation is $d = 2$ space'time' symmetric Laplace's equation (2.0.5).

He defines Helmholtz equation (4.0.5), Laplace's equation (4.0.6), and Poisson's equation (4.0.7). His emphasis is on the discretized Helmholtz equation (4.1.3).

Sect. 2.4 *Algorithms for Two-Dimensional Problems* has the 5-term recurrence, his eq. (2.4.3) and (4.1.3).

Difference equations arising from elliptic equations generally necessitate the solution of a large set of linear algebraic equations. The matrix corresponding to this set of equations is generally sparse and good solution methods take advantage of this fact. [...] the direct solution of these difference equations is quite time consuming. When the number of equations is large, iterative methods of solution are usually more efficient.

(4.2.8) defines *Jacobi iteration*, a method of improving initial guess solution. (4.2.9) method is known as Gauss-Seidel iteration or the method of successive relaxation.

2016-07-11 Predrag Boris cites P. A. Martin [193] *Discrete scattering theory: Green's function for a square lattice*

The *lattice Green's function* is the main subject of the paper.

We consider the simplest problem, with a two-dimensional, square lattice. Each lattice point can move out of the plane of the lattice, and that each point is connected to its neighbours by springs; only nearest-neighbour interactions are included. This leads to a system of partial difference equations. The same equations are obtained if the two-dimensional Helmholtz equation is discretized using the central-difference approximation (lattice d'Alembert operator) for the Laplacian.

2017-09-11 Predrag Morita [203] *Useful procedure for computing the lattice Green's function - square, tetragonal, and bcc lattices:* "A recurrence relation, which gives the values of the lattice Green's function along the diagonal direction from a couple of the elliptic integrals of the first (5.251) and second kind, is derived for the square lattice by an elementary partial integration. The values of the square lattice Green's function at an arbitrary site are then calculated in a successive way with the aid of the difference equation defining the function." The method yields a recursion formula for a peculiar lattice Green's function on a 2d lattice, but not the LGF itself.

2017-09-09 Predrag Simons [242] uses (5.208) in his (1.57) to invert a particular banded matrix.

See also example 1.11 *Tent map linear code*.

Compare characteristic equation (5.207) to the characteristic function $a(z)$ (5.248).

5.13.1 Time quasilattices

2018-10-10, 2020-03-12 Predrag Felix Flicker writes: "My student Leon Zaporski and I have been investigating the topological entropy of substitution sequences in the symbolic dynamics of periodic orbits in discrete-time dynamical systems. We were hoping you might be willing to take a look at our draft, Zaporski and Flicker [275] *Superconvergence of topological entropy in the symbolic dynamics of substitution sequences*, arXiv:1811.00331, and to send any thoughts you might have, both in terms of whether you think the results would be of interest to the community, and if there is a journal you might recommend for us to submit to."

2CB

I failed to read it. But it needs to be included in ChaosBook, as well as many of the references.

Their Fig. 1 is the topological entropy as a function of a control parameter of the logistic map [217]. [...] In the cases that accumulation points correspond to generalised time quasilattices, the Boyle-Steinhardt class [45] is indicated above the curve.

Predrag: I made several attempts to get some kind of renormalization theory for the Sharkovsky sequence, with no interesting results to report. Dahlquist wrote up his attempt [ChaosBook \(click here\)](#).

[...] Period doubling continues to be of importance to cutting edge research: recent experiments established the existence of (discrete) time crystals, which spontaneously break the symmetry of a periodic driving by returning a robust period-doubled response, made rigid to perturbations and finite temperature by the local interactions of many degrees of freedom. [...] periodically-driven nonlinear systems can feature not just period-doubled responses, but robust responses with the symmetries of one-dimensional (generalised) *time quasilattices* [99]. [...] Quasilattice substitution rules fall within the set we consider, and, by considering a simple generalisation of the basic quasilattice concept, we find that we are able to identify aperiodic orbits corresponding to all physically relevant quasilattices, extending previous results identifying two cases. Generalizing further we consider a set of substitutions additionally covering, for example, the period-doubling cascade. [...] Whereas the topological entropy is zero for all sequences in the period-doubling cascade, for other substitution sequences it increases monotonically. [...] We find that the topological entropy of the wide class of substitution sequences we consider converges as a double exponential onto its accumulation point. [...] We demonstrate that all one-dimensional quasilattices can appear as stable orbits in nonlinear dynamical systems.

Here is something we might find useful for spatiotemporal cat:

[...] we focus on the *generalised composition rules*, which systematically generate admissible words by a substitution process [47].

[...] The universal order of periodic windows coincides with the *parity-lexicographic order* of words, defined through the relation ' \prec ' in the following way:

$$L \prec C \prec R$$

and for two admissible words they state it in a way that is perhaps superior to [ChaosBook](#) [ChaosBook](#). Cite it there.

[...] Word operations

- $\bar{A}\bar{B}$ indicates the concatenation of words \bar{A} and \bar{B}
- $|\bar{A}|$ returns the number of letters in \bar{A}
- $|\bar{A}|_{R,L}$ returns the number of letters R, L in \bar{A}
- $\bar{A}|_C$ substitutes the final letter of \bar{A} with the letter C .

Inverse words are defined as follows (Predrag - I do not understand this):

$$\begin{aligned} \bar{A}^{-1}(\bar{A}\bar{B}) &= \bar{B} \\ (\bar{A}\bar{B})\bar{B}^{-1} &= \bar{A}. \end{aligned} \tag{5.211}$$

Theorem 5.1. Substitution rules generating a cascade with initial word $\bar{\mathbf{W}}_1 = R$ and $\bar{\mathbf{W}}_2 = \bar{\mathbf{R}}$ can be restated as a second order linear recursive relation $\bar{\mathbf{W}}_{n+2} = g(\bar{\mathbf{W}}_n, \bar{\mathbf{W}}_{n+1})$ under concatenation if $\bar{\mathbf{W}}_3 = g(\bar{\mathbf{W}}_1, \bar{\mathbf{W}}_2)$.

[...] Consider a $[2 \times 2]$ growth matrix

$$A = \begin{pmatrix} a & b \\ c & d \end{pmatrix} \quad (5.212)$$

which quantifies the growth in the numbers of each letter type:

$$\left(\begin{array}{c} |\bar{\mathbf{W}}_n|_R \\ |\bar{\mathbf{W}}_n|_L \end{array} \right) \rightarrow \left(\begin{array}{cc} a & b \\ c & d \end{array} \right) \left(\begin{array}{c} |\bar{\mathbf{W}}_n|_R \\ |\bar{\mathbf{W}}_n|_L \end{array} \right) = \left(\begin{array}{c} |\bar{\mathbf{W}}_{n+1}|_R \\ |\bar{\mathbf{W}}_{n+1}|_L \end{array} \right) \quad (5.213)$$

The class of substitutions we consider can then be written as

$$\bar{\mathbf{W}}_n = \bar{\mathbf{W}}_{n-1} \mathcal{P} \left(\bar{\mathbf{W}}_{n-1}^{\text{tr}(A)-1} \bar{\mathbf{W}}_{n-2}^{-\det(A)} \right) \quad (5.214)$$

for $n > 2$, with $\bar{\mathbf{W}}_1 = R$, and $\bar{\mathbf{W}}_2$ a specified word. The symbol \mathcal{P} indicates an unspecified permutation. The characteristic equation of the growth matrix A is

$$\lambda^2 - \text{tr}(A)\lambda + \det(A) = 0. \quad (5.215)$$

The eigenvalues of A must be real, either integer or quadratic irrational (when we consider quasilattices). The ratio of the components of the eigenvector associated to the largest eigenvalue gives the relative frequencies of the two cell types [45]. Eq. (5.215) can be seen as the $n \rightarrow \infty$ limit of the defining equation of some integer sequence W_n given by

$$W_n = \text{tr}(A)W_{n-1} - \det(A)W_{n-2} \quad (5.216)$$

for $n > 2$, $W_1 = |\bar{\mathbf{W}}_1| = 1$, and $W_2 = |\bar{\mathbf{W}}_2|$. The ratio W_n/W_{n-1} gives the best possible rational approximation, for denominators not larger than W_{n-1} , to the largest eigenvalue of the growth matrix, *i.e.* the larger of the solutions to Eq. (5.215).

[...] As an example, the period-doubling substitutions lead to the integer sequence

$$W_n = W_{n-1} + 2W_{n-2} \quad (5.217)$$

for $n > 2$, with $W_1 = |\bar{\mathbf{W}}_1| = |R| = 1$ and $W_2 = |\bar{\mathbf{W}}_2| = |RL| = 2$. Explicitly, the first few terms are

$$1, 2, 4, 8, 16, 32, 64, \dots \quad (5.218)$$

i.e. $W_n = 2^{n-1}$.

Predrag: This is perhaps related to $s = 2$ version of (1.119).

Then they do Fibonacci. [...] The eigenvalues of a $[2 \times 2]$ growth matrix A are real and given by

$$\lambda_{\pm} = \frac{1}{2} \left(s \pm \sqrt{s^2 - 4 \det A} \right), \quad s = \text{tr } A. \quad (5.219)$$

If $s^2 = 4\det A$ they are integers. Otherwise, the larger eigenvalue is a quadratic irrational ‘Pisot-Vijayaraghavan’ (PV) number: the largest root of an irreducible monic polynomial, all of whose Galois conjugates have modulus strictly less than one. [...] The three conditions are necessary and sufficient for the substitutions to correspond to quasilattice inflation rules [45]:

1. the growth matrix must be unimodular, $|\det A| = 1$
 2. there must be two spacings between each symbol
 3. the largest eigenvalue of the growth matrix must be a PV number.

The condition $|\det A| = 1$, implies the inverse of the growth matrix is also an integer matrix. The inflation (substitution) of any quasilattice sequence can therefore be undone with a well-defined deflation. This endows quasilattices with a discrete scale invariance [44]. The third, PV numbers condition is necessary for the interpretation of the quasilattice sequence in terms of a cut through a higher-dimensional regular lattice.

The concept of quasilattices relating to higher-dimensional lattices is discussed at length in refs. [45, 99].

Predrag: So our $s = 3$ temporal cat $\lambda^2 - 3\lambda + 1 = 0$ eigenvalue $\frac{3+\sqrt{5}}{2}$ turns out to be a PV number. So is $s = 4$ temporal cat $\lambda^2 - 4\lambda + 1 = 0$ eigenvalue $2 + \sqrt{3}$. Both are the Boyle-Steinhardt [45] quasilattices, of class 1, respectively 3.

[...] Starting from an orbit described by the word R , repeated application of the inflation rules will lead to a cascade of stable periodic orbits of increasing length. After an infinite number of substitutions, *i.e.* at the accumulation point of the sequence, lies a stable orbit described by an aperiodic word: a *time quasilattice*. [...] Characteristic equation

$$\lambda^2 = 4\lambda - 1. \quad (5.220)$$

leads to the (modulus of the) Clapeyron numbers C_n (A125905 in the [On-Line Encyclopedia of Integer Sequences](#))

$$C_n = 4C_{n-1} - C_{n-2} \quad (5.221)$$

for $n \geq 2$ with $C_1 = 1, C_2 = 4$.

Predrag: In conclusion, temporal cat is related to counting of quasi-lattice words. Not sure it is of any use to us.

5.14 Generating functions

(Note, there is also a totally unrelated Lagrangian ‘generating function’, sect. 7.6, nothing to do with this section of the blog.)

Definition [33]. Let $f(x)$ be a series in powers of x . Then by the symbol $[x^n]f(x)$ we will mean the coefficient of x^n in the series $f(x)$.

2CB

2020-03-20 Predrag The theory generating function (AKA Z-transforms) is pedagogically explained by Elaydi [90], including a table of common Z-transform pairs, in analogy with the familiar Laplace transform tables.

2CB

2020-09-30 Predrag Online [Signals and Systems](#) has pedagogical chapters on Z-transforms.

2020-07-11 Predrag Woods [270] *Multidimensional signal, image, and video processing and coding*, Chap. 3 *Two-Dimensional Systems and Z-Transforms* (2012) ([click here](#)).

2020-01-23 Predrag For multivariate generating functions

$$N(z), \quad z^n = z^{n_1} z^{n_2} \cdots z^{n_d}, \quad (5.222)$$

see (5.183), (5.200), (5.201), (5.202).

Other examples of generating functions: (1.46), (5.271), (13.24).

2020-04-07 Han Perhaps we need three generating function variables

$$N(z_1, z_2, z_3) = \sum_{L=1} N_{[L \times T]_S} z_1^L z_2^T z_3^S, \quad (5.223)$$

Here z_3^S sum is finite, $-L < S < L$, and that feels not sufficiently invariant, as it depends on Hermite normal form convention. Need something invariant...

2020-03-01 Predrag Cute but true; Wilf [267] *Generatingfunctionology* defines the periodic points counting generating function as

$$N(z) = \sum_{n \geq 0} N_n z^n, \quad (5.224)$$

and starts out in his sect. 1.1 *An easy 2-term recurrence*, with our Bernoulli periodic points count (for the $s = 2$ case only)

$$N_n = s^n - 1, \quad (5.225)$$

as a trivial example of a two-term recurrence (first-order difference equation [90])

$$N_{n+1} = 2N_n + 1, \quad (s = 2; n \geq 0, N_0 = 0), \quad (5.226)$$

and (Predrag's insert) for $s \neq 2$,

$$N_{n+1} - s N_n = (s-1), \quad (n \geq 0, N_0 = 0), \quad (5.227)$$

and its conversion to the periodic points count generating function (5.224). For (5.226) he derives and expands in partial fractions

$$N(z; 2) = \frac{z}{(1-z)(1-2z)} = \frac{2z}{1-2z} - \frac{z}{1-z}, \quad (5.228)$$

and (Predrag's addition) for $s \neq 1$,

$$N(z; s) = (s-1)z + (s-1)(s+1)z^2 + (s-1)(s^2+s+1)z^3 + \dots, \quad (5.229)$$

verifying the Bernoulli periodic points count (5.225). Take $N_n = (s-1)\hat{N}_n$, then (5.227) leads to

$$\hat{N}_{n+1} - s \hat{N}_n = 1, \quad (n \geq 0, \hat{N}_0 = 0, \hat{N}_1 = 1). \quad (5.230)$$

$$\hat{N}(z; s) = z + (s+1)z^2 + (s^2+s+1)z^3 + \dots, \quad (5.231)$$

For $s = 1$ this is a complicated way to generate integers.

Then he does, as an example of a 3-term recurrence (second-order difference equation [90]), the Fibonacci recurrence

$$F_{n+1} = F_n + F_{n-1} : , \quad (n \geq 1, F_0 = 0, F_1 = 1), \quad (5.232)$$

and derives

$$N(z) = \frac{z}{1-z-z^2} = \frac{1}{z^{-1}-1-z}. \quad (5.233)$$

Here the expansion in partial fractions is in terms of roots of the ('golden mean') polynomial $1 - z - z^2$.

He notes that the Stirling numbers of the first kind satisfy a 3-term recurrence relation.

2020-06-20 Predrag Oscar Levin *Discrete Mathematics: An Open Introduction* Sect. 5.1 Generating Functions works out a 3-term recurrence $a_n = 3a_{n-1} - 2a_{n-2}$, with $a_0 = 1, a_1 = 3$ in Example 5.1.6. Surprisingly, one gets again (!)

$$a_n = 2^{n+1} - 1.$$

2020-06-20 Predrag Check out also Al Doerr and Ken Levasseur *Applied Discrete Structures*:

Sect. 8.3 Recurrence relations.

Sect. 8.5.2 Solution of a Recurrence Relation Using Generating Functions.

2020-03-04 Predrag Ron Knott writes:

The series of natural numbers $1, 2, 3, 4, \dots$ has the generating function

$$\frac{1}{(1-z)^2} = \frac{1}{1-2z+z^2} \quad (5.234)$$

and the 3-term recurrence (second-order difference equation [90])

$$\phi_n - 2\phi_{n-1} + \phi_{n-2} = 0$$

and compare that with the denominator of the generating function, namely:

$$1 - 2z + z^2$$

which might be a way to understand why $s = 2$ is special.

A variant of Fibonnaci: 0,1,3,8,21,...is generated by

$$\frac{z}{z^2 - 3z + 1} = \frac{1}{z - 3 + z^{-1}}$$

which looks temporal cat-like.

2020-03-02 Predrag In sect. 1.4 *A three term boundary value problem* Wilf [267] considers a 3-term recurrence with Dirichlet bc's

$$au_{n+1} + bu_n + cu_{n-1} = d_n, \quad (n = 1, 2, \dots, N-1; u_0 = u_N = 0) \quad (5.235)$$

where the positive integer N , the constants a, b, c and the sequence $\{d_n\}_{n=1}^{N-1}$ are given in advance. The eqs (5.235) determine the sequence $\{u_i\}_0^N$ uniquely. Such boundary value problems arise in applications such as the interpolation by spline functions.

2020-03-01 Predrag Compare (5.227) to our [77] Bernoulli 1-step difference condition

$$\phi_t - s\phi_{t-1} = -s_t, \quad \phi_t \in [0, 1]. \quad (5.236)$$

This suggests that the periodic points count is obtained by

$$\phi_t \rightarrow N_n, s_t \rightarrow 1 - s. \quad (5.237)$$

The temporal cat second-order difference equation is

$$\phi_{t+1} - s\phi_t + \phi_{t-1} = -s_t, \quad (5.238)$$

Mimicking (5.237), my guess for the recurrence for periodic points count is

$$N_{n+1} - sN_n + N_{n-1} = 2(s-2), \quad (n \geq 1, N_0 = 0, N_1 = s-2). \quad (5.239)$$

$$N_{n+1} - (\mu^2 + 2) N_n + N_{n-1} = 2\mu^2, \quad (n \geq 1, N_0 = 0, N_1 = \mu^2). \quad (5.240)$$

Indeed, this generates the correct series for arbitrary s (compare with (1.120), (4.126).)

$$\begin{aligned} N(z; s) &= (s-2)z + (s-2)(s+2)z^2 + (s-2)(s+1)^2 z^3 \\ &\quad + (s-2)(s+2)s^2 z^4 + \end{aligned} \quad (5.241)$$

$$\begin{aligned} N(z : \mu^2) &= \mu^2 z + \mu^2(\mu^2 + 4)z^2 + \mu^2(\mu^2 + 3)^2 z^3 \\ &\quad + \mu^2(\mu^2 + 4)(\mu^2 + 2)^2 z^4 + \end{aligned} \quad (5.242)$$

Take $N_n = \mu^2 \hat{N}_n$, then (5.239) leads to

$$\hat{N}_{n+1} - s \hat{N}_n + \hat{N}_{n-1} = 2, \quad (n \geq 1, \hat{N}_0 = 0, \hat{N}_1 = 1). \quad (5.243)$$

$$\begin{aligned} \hat{N}(z; s) &= z + (s+2)z^2 + (s+1)^2 z^3 + (s+2)s^2 z^4 \\ &\quad + (s^2 + s - 1)^2 z^5 + (s^2 - 1)^2(s+2)z^6 + \end{aligned} \quad (5.244)$$

$$\begin{aligned} \hat{N}(z; s) &= z + (\mu^2 + 4)z^2 + (\mu^2 + 3)^2 z^3 + (\mu^2 + 4)(\mu^2 + 2)^2 z^4 \\ &\quad + (\mu^4 + 3\mu^2 + 5)^2 z^5 + (\mu^2 + 1)^2(\mu^2 + 3)^2(\mu^2 + 4)z^6 + \end{aligned} \quad (5.245)$$

For $\mu = 0$ this is a complicated way to generate integers squared (see also (5.234))

$$\hat{N}(z; 2) = z + 4z^2 + 9z^3 + 16z^4 + 25z^5 + 36z^6 + \quad (5.246)$$

Recurrence (5.241) appears correct for the $s = 3$ count (have not rechecked)

$$\begin{aligned} N(z; 3) &= z + 5z^2 + 16z^3 + 45z^4 + 121z^5 + 320z^6 + 841z^7 \\ &\quad + 2205z^8 + 5776z^9 + 15125z^{10} + 39601z^{11} + \dots \end{aligned} \quad (5.247)$$

2020-03-02 Predrag In sect. 1.5 *Two independent variables* and 1.6 *Another 2-variable case* Wilf [267] considers problems that involve functions of two discrete variables. His example is combinatorial, probably not what we need.

A generating function with the $1/n!$'s thrown into the coefficients, is called an *exponential generating function*. After his eq. (1.6.12), he explains the

$$x(d/dx) \log$$

operation. He works it out for the “Bell numbers”, and derives that the Bell numbers satisfy the recurrence depending on all previous Bell numbers, much like the ChaosBook formulas for cumulants.

He says, comfortingly: “[...] there’s no need for the guilt, because the various manipulations can be carried out in the ring of formal power series, where questions of convergence are nonexistent.”

2012-06-19 Predrag In [ChaosBook example 18.12](#) (edition 16.4.5), I show that for alphabet $\mathcal{A} = \{a, cb^k; \bar{b}\}$, the cycle counting ζ -function is

$$1/\zeta_{\text{top}} = 1 - 3z + z^2,$$

i.e., the Isola [142] ζ -function (1.30) for $s = 3$, without the $(1 - z)^2$ factor (see (3.190), (1.20), (4.183), (13.74)). That might be a simple statement of the cat map symbolic dynamics.

2020-02-09 Predrag Fischer, Golub, Hald, Leiva and Widlund [97] *On Fourier-Toeplitz methods for separable elliptic problems* solve linear equations, where M arises from a finite difference approximation to an elliptic partial differential equation.

Such a situation arises for those problems that can be handled by the classical separation-of-variables technique. Their methods are a computer implementation of the separation of variables carried out on a discretized model of the elliptic differential equation.

In one-dimensional lattice, the *characteristic function* $a(x)$ of a symmetric $2k$ -banded Toeplitz matrix A is defined as

$$a(x) = a_k x^k + \cdots + a_0 + \cdots + a_k x^{-k} \quad (5.248)$$

(see (1.40), for example). Such matrices occur in fourth, or higher, order accurate finite difference approximation to second order elliptic problems, when solving the bi-harmonic problem by a Fourier method, in higher order spline interpolation, etc.

For a 1-dimensional lattice one assumes that the characteristic function $a(x)$ has no roots on the unit circle. Then they factor $a(x) = \ell(x) \ell(l/x)$, where $\ell(x) = b_0 + \cdots + b_k x^k$, $b_0 > 0$, is a real polynomial with no roots inside the unit circle, their Lemma 1. The factors $\ell(x)$ and $\ell(l/x)$ of $a(x)$ are known as the *Hurwitz factors*. Predrag has not found any useful literature on these.

Their algorithm applied to the temporal cat tri-diagonal case (1.47) with $a_1 = -1$ and $a_0 > 2$, has linear convergence; see obscure references

[3] F. L. Bauer, "Ein direktes Iterationsverfahren zur Hurwitz-Zerlegung eines Polynoms," Arch. Elec. Ubertr., v. 9, 1955, pp. 285-290.

[4] F. L. Bauer, "Beiträge zur Entwicklung numerischer Verfahren für programmgesteuerte Rechenanlagen. II. Direkte Faktorisierung eines Polynoms," Bayer. Akad. Wiss. Math.-Nat. Kl. S.-B., v. 1956, pp. 163-203.

[18] M. Malcolm & J. Palmer, A Fast Method for Solving a Class of Tri-Diagonal Linear Systems, Computer Science Report 323, Stanford University, 1972,

[24] V. Thomée, "Elliptic difference operators and Dirichlet's problem," Contributions to Differential Equations, v. 3, 1964, pp. 301-324.

[25] O. B. Widlund, "On the use of fast methods for separable finite difference equations for the solution of general elliptic problems," Sparse Matrices and Their Applications, edited by D. J. Rose and R. A. Willoughby,

Plenum Press, New York, 1972.

which we hopefully can ignore.

In the *semidefinite case*, $a_0 = 2$, one still has convergence, but the error decreases only as l/n .

2-dimensional lattice: When the characteristic function depends on several variables, a factorization like the one of their Lemma 1 is possible only in exceptional cases. They seek an appropriate factorization of the *characteristic function* for 2-dimensional lattice Laplacian

$$a(x_1, x_2) = -x_1 - x_2 + 4 - x_1^{-1} - x_2^{-1} \quad (5.249)$$

which cannot be factored in a useful way. They turn to the separation of variables technique.

“Characteristic function” (5.248) does not seem to be a commonly used name; compare with (5.248).

our preference is to call this *characteristic equation*, as in (5.207).

Lothar Reichel refers to (5.249) as the standard “five-point stencil” for discretization of the Poisson equation on a rectangle by finite differences.

2020-06-15 Predrag Insert into (5.249) $x_i^{n_i} \rightarrow \Lambda_i^{n_i}$ to get characteristic equation for the 2-dimensional homogenous linear 2nd-order difference equation

$$\frac{1}{x_1}(x_1^2 - sx_1 + 1) + c \frac{1}{x_2}(x_2^2 - sx_2 + 1) = 0,$$

where $[c] = [\ell_1]/[\ell_2]$ is dimensionally the ‘velocity’ parameter.

We can write

$$x_2(\Lambda - x_1)(\Lambda^{-1} - x_1) + c x_1(\Lambda - x_2)(\Lambda^{-1} - x_2) = 0,$$

with each term separately zero for $x_1 = x_2 = 0$ and 4 combinations $x_i \in \{\Lambda, 1/\Lambda\}$. Though there is no reason to set terms separately to zero, so there are 1-dimensional families of roots,

$$\begin{aligned} x_2(\Lambda - x_1)(\Lambda^{-1} - x_1) &= b \\ c x_1(\Lambda - x_2)(\Lambda^{-1} - x_2) &= -b, \end{aligned} \quad (5.250)$$

parametrized by b . So I too am lost as to how to use characteristic equations in higher dimensions...

5.15 Resistor networks

2017-09-11 Predrag A textbook: Blanchard and Volchenkov [38] *Random Walks and Diffusions on Graphs and Databases*, ([click here](#)); Chapter 6 *Random walks and electric resistance networks*. They cite Doyle and Snell 1984; Tetali 1991; Chandra et al. 1996; Bollobas 1998 (have not looked at any of these).

They define the discrete representation of the Laplace operator on a lattice in their eq. (4.22). The matrix (4.38) corresponds to the normalized Laplace operator.

“ It was established in Tetali (1991) and Chandra et al. (1996) that the effective resistance might be interpreted as the expected number of times a random walker visits all nodes of the network in a random round trip from i to j and back. ”

2020-01-10 Predrag A textbook: A very pedagogical, down to earth textbook: Pozrikidis [225] *An introduction to grids, graphs, and networks*, ([click here](#)) discusses this in Chap. 6 *Network performance*. In part based on Wu [271], cited below. My notes are bellow, search for **2020-01-10 Predrag**.

2020-01-13 Predrag A textbook: Grimmett [115] *Probability on Graphs: Random Processes on Graphs and Lattices*, ([click here](#)). Not sure we need this now, but it is a modern stat mech book on percolation, Schramm–Löwner evolution, Gibbs states and Markov fields, the Ising and Potts models.

Chapter 1 is devoted to the relationship between random walks (on graphs) and electrical networks. This leads to the Thomson and Rayleigh principles, and thence to a proof of Pólya’s theorem.

Early papers are

Venezian [260] *On the resistance between two points on a grid*

Atkinson and van Steenwijk [18] *Infinite resistive lattices*

leading to much cited:

Cserti [68] *Application of the lattice Green’s function for calculating the resistance of an infinite network of resistors*:

In the network of resistors it is assumed here that the resistances of all the edges of the hypercube are the same, say R . The goal is to find the resistance between the origin and a given lattice point of the infinite hypercube. Ohm’s and Kirchhoff’s laws for potential at a lattice site are expressed in terms of the lattice Laplacian. To find the resistance one solves a Poisson-type equation by using the lattice Green’s function.

The 1-dimensional case, his eq. (23) is very simple.

The energy-dependent lattice Green’s function of the tight-binding Hamiltonian for a square lattice, his eq. (30), has energy E playing the role of our stretching parameter s .

He does the actual derivations on finite d -tori, but only as a step preliminary to taking the infinite-lattice limit; no actual calculations for finite d -tori.

[...] The value of $G(0,0,0)$ was evaluated for the first time by Watson [21] and subsequently by Joyce [22] in a closed form in terms of the complete elliptic integral of the first kind

$$K(k) = \int_0^{\pi/2} d\theta \frac{1}{\sqrt{1 - k^2 \sin^2 \theta}} \quad (5.251)$$

It is worth mentioning that a simpler result was obtained by Glasser and Zucker [23] (see also Doyle and Snell's book [84]), [arXiv:math/0001057](https://arxiv.org/abs/math/0001057), who calculated the integrals in terms of gamma functions:

$$2G(0,0,0) = \frac{\sqrt{3}-1}{96\pi^3} \Gamma^2(1/24)\Gamma^2(11/24). \quad (5.252)$$

Predrag finds this form intriguing, as he expects symmetry factorizations in the spirit of (4.181).

Glasser and Montaldi [27] gave other useful integral representations of the lattice Green's function for the hypercubic lattice for arbitrary dimension d . It was shown by Joyce [22] that the function $G(E;0,0,0)$ can be expressed in the form of a product of two complete elliptic integrals of the first kind. (Predrag: presumably a symmetry factorization.)

This work is continued in ref. [69]:

2019-11-04 Predrag Cserti, Széchenyi and Dávid [69] *Uniform tiling with electrical resistors*: "The resistance between two arbitrary nodes of a network of resistors is studied when the network is perturbed by connecting an extra resistor between two arbitrary nodes in the perfect lattice. The lattice Green's function and the resistance of the perturbed network are expressed in terms of those of the perfect lattice by solving Dyson's equation. A comparison is carried out between numerical and experimental results for a square lattice."

The electric resistance between two arbitrary nodes on any infinite lattice structure of resistors that is a periodic tiling of space is obtained, using the lattice Green's function of the Laplacian matrix associated with the network. The method can be extended to the random walk problem or to electron dynamics in solid state physics. The results may be used to calculate the wavefunctions at the lattice points for complicated lattice structures.

I do not think we need this paper at the present stage - understanding 'undecorated' square lattice is all we need...

2019-11-01 Predrag Introduction of Owaidat, Asad and Tan [210] *Resistance computation of generalized decorated square and simple cubic network lattices*

has a very exhaustive lattice Green functions literature discussion, starting with

Kirchhoff [171] *Üeber die Auflösung der Gleichungen, auf welche man bei der Untersuchung der linearen Vertheilung galvanischer Ströme geführt wird*, which, weirdly enough, reminds me that I've computed for my PhD [76] the determinants for QED that we here seek to compute for a much simpler lattice problem.

Their work follows the Green's function theory presented by Cserti [68]. They say that the lattice Green functions are usually evaluated as the elliptic integrals (5.251) or by recurrence relations methods.

They do display a determinant of a Laplacian, eq. (B.11) in their Appendix B. *The matrix elements of the Green's function for the generalized decorated simple cubic lattice*, but it is a determinant of a single Fourier mode (in each of the three directions of a cubic lattice). Han has the analogue for the square lattice - what we do not have is the product formula, in which all eigenvalues (cosines, etc) average out, and all that is left is a polynomial in s

2019-11-04 Predrag Jafarizadeh, Sufiani and Jafarizadeh [147] *Calculating two-point resistances in distance-regular resistor networks* provide an algorithm for the calculation of the resistance between two arbitrary nodes in an arbitrary distance-regular resistor network.

Past efforts have been focused mainly on infinite lattices, with little attention paid to finite networks. They present a general formulation for computing two-point resistances in finite networks.

Their starting point is the Laplacian matrix associated with a network. The Laplacian is a matrix whose off-diagonal entries are the conductances connecting pairs of nodes. Just as in graph theory where everything about a graph is described by its adjacency matrix (whose element is 1 if two vertices are connected and 0 otherwise), everything about an electric network is described by its Laplacian.

The two-point resistances on a network depend only on the Stieltjes function $G_\mu(x)$ corresponding to the network. The Stieltjes function corresponding to an infinite network possesses a unique representation as an infinite continued fraction. In the cases for which the parameters iterate themselves after some finite steps, one can find a closed form for the infinite continued fraction. This situation takes place, for instance, in the infinite line network. But in most cases, this situation does not occur and one cannot obtain a closed form for the Stieltjes function of the network.

2019-11-04 Predrag Wu [271] *Theory of resistor networks: the two-point resistance* is a foundational paper, where a theory to calculate the resistance between arbitrary nodes for a finite lattice of resistors is given in terms of the eigenvalues and eigenvectors of the graph Laplacian matrix.

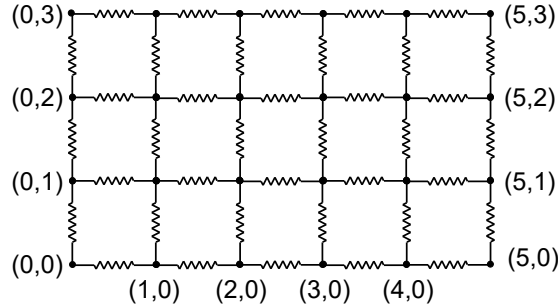


Figure 5.6: A $[5 \times 4]$ rectangular resistor network: resistors with resistances r and s on edges of the network in, respectively, horizontal and vertical directions.

Wu gives a closed-form expression, his eq. (43), for the resistance $R_{z_1 z_2}^{[L \times T]}$ of a finite square lattice between nodes $z_1 = (x_1, y_1)$ and $z_2 = (x_2, y_2)$ for free, periodic and cylindrical boundary conditions.

The paper is very clear and explicit, with many examples, including the 1-dimensional periodic chain (sect. 3.2. *Periodic boundary conditions*) and the doubly periodic $[L \times T]$ square lattice, his sect. 5. *Two-dimensional network* and figure 5.6. His eq. (43) gives the resistance between nodes $z_1 = (x_1, y_1)$ and $z_2 = (x_2, y_2)$

$$\begin{aligned}
 R_{z_1 z_2}^{[L \times T]} &= \sum_{m=0}^{M-1} \sum_{n=0}^{N-1} \frac{\left| \psi_{(m,n);(x_1,y_1)} - \psi_{(m,n);(x_2,y_2)} \right|^2}{\lambda_{(m,n)}} \\
 &= \frac{r}{N} \left[|x_1 - x_2| - \frac{(x_1 - x_2)^2}{M} \right] + \frac{s}{M} \left[|y_1 - y_2| - \frac{(y_1 - y_2)^2}{N} \right] \\
 &\quad + \frac{1}{MN} \sum_{m=1}^M \sum_{n=1}^N \frac{1 - \cos \left[2(x_1 - x_2)\theta_m + 2(y_1 - y_2)\phi_n \right]}{r^{-1}(1 - \cos 2\theta_m) + s^{-1}(1 - \cos 2\phi_n)},
 \end{aligned} \tag{5.253}$$

The result depends only on the differences $|x_1 - x_2|$ and $|y_1 - y_2|$, as it should by translational invariance. This is a double sum over Fourier modes, and I see no determinant calculation where these are summed over and what remains is some sensible polynomial.

However, his sect. 10. *Summation and product identities* might be just what we need:

He shows that

$$\begin{aligned} F_N(\ell) &= \frac{1}{N} \sum_{n=1}^{N-1} \frac{1 - \cos(\ell\phi_n)}{1 - \cos\phi_n} \\ &= |\ell| - \frac{1}{N} \left(\frac{\ell^2 + |\ell|}{2} - \left[\frac{|\ell|}{2} \right] \right) \end{aligned} \quad (5.254)$$

where $[x]$ denotes the integral part of x . Similarly

$$G_N(\ell) = \frac{1}{N} \sum_{n=1}^{N-1} \frac{1 - \cos(2\ell\phi_n)}{1 - \cos 2\phi_n}.$$

is evaluated as a special case of the identity (5.257), using the recursion relation

$$G_N(\ell) - G_N(\ell - 1) = 1 - \frac{1}{N}(2\ell - 1)$$

which yields

$$G_N(\ell) = |\ell| - \ell^2/N. \quad (5.255)$$

Proposition: Define

$$I_\alpha(\ell) = \frac{1}{N} \sum_{n=0}^{N-1} \frac{\cos(\alpha \ell \frac{n\pi}{N})}{\cosh \lambda - \cos(\alpha \frac{n\pi}{N})}, \quad \alpha = 1, 2.$$

Then the following identities hold for $\lambda \geq 0$, $N = 1, 2, \dots$,

$$I_1(\ell) = \frac{\cosh(N - \ell)\lambda}{(\sinh \lambda) \sinh(N\lambda)} + \frac{1}{N} \left[\frac{1}{\sinh^2 \lambda} + \frac{1 - (-1)^\ell}{4 \cosh^2(\lambda/2)} \right], \quad 0 \leq \ell < 2N, \quad (5.256)$$

$$I_2(\ell) = \frac{\cosh(\frac{N}{2} - \ell)\lambda}{(\sinh \lambda) \sinh(N\lambda/2)}, \quad 0 \leq \ell < N. \quad (5.257)$$

Remarks:

3. In the $N \rightarrow \infty$ limit both (5.256) and (5.257) become the integral

$$\frac{1}{\pi} \int_0^\pi \frac{\cos(\ell\theta)}{\cosh \lambda - \cos \theta} d\theta = \frac{e^{-\ell\lambda}}{\sinh \lambda} \quad \ell \geq 0.$$

4. Set $\ell = 0$ in (5.256), multiply by $\sinh \lambda$ and integrate over λ , we obtain the product identity

$$\prod_{n=0}^{N-1} \left(\cosh \lambda - \cos \frac{n\pi}{N} \right) = (\sinh N\lambda) \tanh(\lambda/2). \quad (5.258)$$

5. Set $\ell = 0$ in (5.257), multiply by $\sinh \lambda$ and integrate over λ . We obtain the product identity

$$\prod_{n=0}^{N-1} \left(\cosh \lambda - \cos \frac{2n\pi}{N} \right) = \sinh^2(N\lambda/2). \quad (5.259)$$

Proof:

Introduce

$$S_\alpha(\ell) = \frac{1}{N} \sum_{n=0}^{N-1} \frac{\cos(\ell \theta_n)}{1 + a^2 - 2a \cos \theta_n}, \quad a < 1, \quad \alpha = 1, 2 \quad (5.260)$$

so that

$$I_\alpha(\ell) = 2a S_\alpha(\ell), \quad a = e^{-\lambda}. \quad (5.261)$$

It is readily seen that we have the identity

$$S_\alpha(1) = \frac{1}{2a} \left[(1 + a^2) S_\alpha(0) - 1 \right]. \quad (5.262)$$

1. Proof of (5.256):

First we evaluate $S_1(0)$ by carrying out the following summation, where $\Re e$ denotes the real part, in two different ways. First we have

$$\begin{aligned} \Re e \frac{1}{N} \sum_{n=0}^{N-1} \frac{1}{1 - a e^{i\theta_n}} &= \Re e \frac{1}{N} \sum_{n=0}^{N-1} \frac{1 - a e^{-i\theta_n}}{\left| 1 - a e^{i\theta_n} \right|^2} \\ &= \frac{1}{N} \sum_{n=0}^{N-1} \frac{1 - a \cos \theta_n}{1 + a^2 - 2a \cos \theta_n} \\ &= S_1(0) - a S_1(1) \\ &= \frac{1}{2} \left[1 + (1 - a^2) S_1(0) \right]. \end{aligned} \quad (5.263)$$

Secondly by expanding the summand we have

$$\Re e \frac{1}{N} \sum_{n=0}^{N-1} \frac{1}{1 - a e^{i\theta_n}} = \Re e \frac{1}{N} \sum_{n=0}^{N-1} \sum_{\ell=0}^{\infty} a^\ell e^{i\ell n \pi/N}$$

and carry out the summation over n for fixed ℓ . It is clear that all $\ell =$ even terms vanish except those with $\ell = 2mN, m = 0, 1, 2, \dots$ which yield $\sum_{m=0}^{\infty} a^{2mN} = 1/(1 - a^{2N})$. For $\ell = \text{odd} = 2m+1, m = 0, 1, 2, \dots$ we have

$$\Re e \sum_{n=0}^{N-1} e^{i(2m+1)n\pi/N} = \Re e \frac{1 - (-1)^{2m+1}}{1 - e^{i(2m+1)\pi/N}} = 1$$

after making use of

$$\operatorname{Re} \left(\frac{1}{1 - e^{i\theta}} \right) = \frac{1}{2}, \quad 0 < \theta < 2\pi. \quad (5.264)$$

So the summation over $\ell = \text{odd}$ terms yields $N^{-1} \sum_{m=0}^{\infty} a^{2m+1} = a/N(1 - a^2)$, and we have

$$\operatorname{Re} \sum_{n=0}^{N-1} \frac{1}{1 - a e^{i\theta_n}} = \frac{1}{1 - a^{2N}} + \frac{a}{N(1 - a^2)} \quad (5.265)$$

Equating (5.263) with (5.265) we obtain

$$S_1(0) = \frac{1}{1 - a^2} \left[\left(\frac{1 + a^{2N}}{1 - a^{2N}} \right) + \frac{2a}{N(1 - a^2)} \right]. \quad (5.266)$$

To evaluate $S_1(\ell)$ for general ℓ , we consider the summation

$$\begin{aligned} \operatorname{Re} \frac{1}{N} \sum_{n=0}^{N-1} \frac{1 - (a e^{i\theta_n})^\ell}{1 - a e^{i\theta_n}} &= \operatorname{Re} \frac{1}{N} \sum_{n=0}^{N-1} \frac{(1 - a^\ell e^{i\ell\theta_n})(1 - a e^{-i\theta_n})}{|1 - a e^{i\theta_n}|^2} \\ &= S_1(0) - a S_1(1) - a^\ell S_1(\ell) + a^{\ell+1} S_1(\ell - 1), \end{aligned} \quad (5.267)$$

where the second line is obtained by writing out the real part of the summand as in (5.263). On the other hand, by expanding the summand we have

$$\begin{aligned} \operatorname{Re} \frac{1}{N} \sum_{n=0}^{N-1} \frac{1 - (a e^{i\theta_n})^\ell}{1 - a e^{i\theta_n}} &= \operatorname{Re} \frac{1}{N} \sum_{n=0}^{N-1} \sum_{m=0}^{\ell-1} a^m e^{i\pi mn/N} \\ &= 1 + \operatorname{Re} \frac{1}{N} \sum_{m=1}^{\ell-1} a^m \left(\frac{1 - (-1)^m}{1 - e^{i\pi m/N}} \right) \\ &= 1 + \frac{a(1 - a^\ell)}{N(1 - a^2)}, \quad \ell = \text{even} < 2N \\ &= 1 + \frac{a(1 - a^{\ell-1})}{N(1 - a^2)}, \quad \ell = \text{odd} < 2N \end{aligned} \quad (5.268)$$

where again we have used (5.264).

Equating (5.268) with (5.267) and using (5.262) and (5.266), we obtain the recursion relation

$$S_N(\ell) - a S_N(\ell - 1) = A a^{-\ell} + B_\ell \quad (5.269)$$

where

$$A = \frac{a^{2N}}{1 - a^{2N}}, \quad B_\ell = \frac{a^{(1+(-1)^\ell)/2}}{N(1 - a^2)}. \quad (5.270)$$

The recursion relation (5.269) can be solved by standard means. Define the generating function

$$G_\alpha(t) = \sum_{\ell=0}^{\infty} S_\alpha(\ell) t^\ell, \quad \alpha = 1, 2. \quad (5.271)$$

Multiply (5.269) by t^ℓ and sum over ℓ . We obtain

$$(1 - at)G_1(t) - S_1(0) = \frac{A a^{-1} t}{1 - a^{-1} t} + \frac{t + at^2}{N(1 - a^2)(1 - t^2)}. \quad (5.272)$$

This leads to

$$\begin{aligned} G_1(t) &= \frac{1}{1 - at} \left[S_1(0) + \frac{A a^{-1} t}{1 - a^{-1} t} + \frac{t + at^2}{N(1 - a^2)(1 - t^2)} \right] \\ &= \frac{1}{(1 - a^2)(1 - a^{2N})} \left[\frac{1}{1 - at} + \frac{a^{2N}}{1 - a^{-1} t} \right] \\ &\quad + \frac{1}{2N(1 - a)^2(1 - t)} - \frac{1}{2N(1 + a)^2(1 + t)}, \end{aligned}$$

from which one obtains

$$\begin{aligned} S_1(\ell) &= \frac{a^\ell + a^{2N-\ell}}{(1 - a^2)(1 - a^{2N})} + \frac{1}{2N(1 - a)^2} - \frac{(-1)^\ell}{2N(1 + a)^2} \\ &= \frac{a^\ell + a^{2N-\ell}}{(1 - a^2)(1 - a^{2N})} + \frac{1}{2N} \left[\frac{4a}{(1 - a^2)^2} + \frac{1 - (-1)^\ell}{(1 + a^2)^2} \right] \end{aligned} \quad (5.273)$$

It follows that using $I_1(\ell) = 2a S_1(\ell)$ we obtain (5.256) after setting $a = e^{-\lambda}$.

2. Proof of (5.257):

Again, we first evaluate $S_2(0)$ by carrying out the summation

$$\mathcal{R}e \frac{1}{N} \sum_{n=0}^{N-1} \frac{1}{1 - a e^{i2\theta_n}}, \quad a < 1$$

in two different ways. First as in (5.263) we have

$$\mathcal{R}e \frac{1}{N} \sum_{n=0}^{N-1} \frac{1}{1 - a e^{i2\theta_n}} = \frac{1}{2} \left[1 + (1 - a^2) S_2(0) \right], \quad (5.274)$$

where $S_2(\ell)$ is defined in (5.260). Secondly by expanding the summand we have

$$\frac{1}{N} \sum_{n=0}^{N-1} \frac{1}{1 - a e^{i2\theta_n}} = \frac{1}{N} \sum_{n=0}^{N-1} \sum_{\ell=0}^{\infty} a^\ell e^{i2\ell n \pi / N} = \frac{1}{1 - a^N} \quad (5.275)$$

where by carrying out the summation over n for fixed ℓ all terms in (5.265) vanish except those with $\ell = mN, m = 0, 1, 2, \dots$. Equating (5.275) with (5.274) we obtain

$$S_2(0) = \frac{1}{1-a^2} \left(\frac{1+a^N}{1-a^N} \right) \quad (5.276)$$

and from (5.262)

$$S_2(1) = \frac{1}{1-a^N}.$$

We consider next the summation

$$\mathcal{R}e \frac{1}{N} \sum_{n=0}^{N-1} \frac{1 - (a e^{i2\theta_n})^\ell}{1 - a e^{i2\theta_n}} \quad a < 1. \quad (5.277)$$

Evaluating the real part of the summand directly as in (5.267), we obtain

$$\mathcal{R}e \frac{1}{N} \sum_{n=0}^{N-1} \frac{1 - (a e^{i2\theta_n})^\ell}{1 - a e^{i2\theta_n}} = S_2(0) - a S_2(1) - a^\ell S_2(\ell) + a^{\ell+1} S_2(\ell-1) \quad (5.278)$$

Secondly, expanding the summand in (5.277) we obtain

$$\begin{aligned} \frac{1}{N} \sum_{n=0}^{N-1} \frac{1 - (a e^{i2\theta_n})^\ell}{1 - a e^{i2\theta_n}} &= \frac{1}{N} \sum_{n=0}^{N-1} \sum_{m=0}^{\ell-1} a^m e^{i2\pi mn/N} \\ &= \frac{1}{N} \left[N + \sum_{m=1}^{\ell-1} \frac{1 - e^{i2m\pi}}{1 - e^{i2m\pi/N}} \right] \\ &= 1 \quad m < \ell \leq N. \end{aligned} \quad (5.279)$$

Equating (5.279) and (5.278) and making use of (5.276) for $S_2(0)$, we obtain

$$S_2(\ell) - a S_2(\ell-1) = \frac{a^{N-\ell}}{1-a^N} \quad (5.280)$$

The recursion relation (5.280) can be solved as in the above. Define the generating function $G_2(t)$ by (5.271). We find

$$\begin{aligned} G_2(t) &= \frac{1}{1-at} \left[S_2(0) + \frac{a^{N-1}t}{(1-a^N)(1-a^{-1}t)} \right] \\ &= \frac{1}{(1-a^2)(1-a^{2N})} \left[\frac{1}{1-at} + \frac{a^N}{1-a^{-1}t} \right], \end{aligned} \quad (5.281)$$

from which one reads off

$$S_2(\ell) = \frac{a^\ell + a^{N-\ell}}{(1-a^2)(1-a^{2N})}.$$

Using the relation $I_2(\ell) = 2a S_2(\ell)$ with $a = e^{-\lambda}$, we obtain (5.257).

2019-11-04 Predrag Tzeng and Wu have extended this impedance networks, where the Laplacian matrix has complex matrix elements; I think we do not care about this at this time.

2019-11-04 Predrag The corner-to-corner resistance and its asymptotic expansion for various boundary conditions were calculated by Izmailian and Huang [146] *Asymptotic expansion for the resistance between two maximally separated nodes on an M by N resistor network*: “ The computation of the asymptotic expansion of the corner to-corner resistance, in other word the resistance between two maximally separated nodes of a rectangular resistor network is of interest as its value provides a lower bound to the resistance of compact percolation clusters in the Domany-Kinzel model of a directed percolation [15]. ”

They take a $[L \times T]$ array, use a ton of funky identities, and manage to reduce Wu’s double sum (5.253) to a single, highly non-obvious sum, their eq. (33). Then there are Kronecker’s double series expressed in terms of the complete elliptic integrals $K(s)$ and $E(s)$.

2020-01-11 Predrag Dienstfrey, Hang and Huang [82] *Lattice sums and the two-dimensional, periodic Green’s function for the Helmholtz equation*. They compute the Green’s function for the Helmholtz equation in two dimensions with doubly periodic boundary conditions, on a fundamental cell $[-1/2, 12]^2$. I believe this is not relevant to us, it solves a continuous problem over the unit cell, rather than a problem on discrete lattice.

Due to the translation invariance, the Green’s function has a convolution structure, $G(x, x_0) = G(y)$, $y = x - x_0 \in [-1, 1]^2$. A periodic Helmholtz equation can be computed via the method of images over the zeroth-order Hankel function of the first-kind. The sums can also be evaluated by recognizing an identity between the so-called ‘spectral’ and ‘spatial’ representations of G . For a square array, there are symmetries which allow for further simplification.

2020-01-10 Predrag Stewart and Gökaydin [250] *Symmetries of quotient networks for doubly periodic patterns on the square lattice*, ([click here](#)). Read for sect. 18.4 *Reduction to the fundamental domain* that has still to be completed.

2020-01-10 Predrag A very pedagogical, down to earth textbook: Pozrikidis [225] *An introduction to grids, graphs, and networks*, ([click here](#)):

Graphs are finite or infinite sets of vertices connected by edges in structured or unstructured configurations.

Infinite lattices and tiled surfaces are described by highly ordered graphs parametrized by an appropriate number of indices.

Networks consist of nodes connected by physical or abstract links with an assigned conductance in spontaneous or engineered configurations. In

physical and engineering applications, networks are venues for conducting or convecting a transported entity, such as heat, mass, or digitized information according to a prevailing transport law.

Finite difference and finite element *grids* can be regarded as networks whose link conductance is determined by the differential equation, as well as by the chosen finite difference or finite element approximation.

A finite difference grid for solving ordinary or partial differential equations consists of rectilinear grid lines that can be regarded as conveying links intersecting at nodes.

Topics: The node adjacency, Laplacian, and Kirchhoff matrices; The computation of the regular and generalized lattice Green's function describing the response to a nodal source; The pairwise resistance of any two nodes.

Consider the Poisson equation in one dimension for an unknown function of one variable, $f(x)$,

$$\frac{d^2f}{dx^2} + g(x) = 0, \quad (5.282)$$

to be solved in a finite domain, $[a, b]$, where $g(x)$ is a given source function. When $g(x) = 0$, the Poisson equation reduces to Laplace's equation. When $g(x) = \alpha f(x)$, the Poisson equation reduces to the Helmholtz's equation,

$$\left(\frac{d^2}{dx^2} + \alpha \right) f(x) = 0, \quad (5.283)$$

where α is a real or complex constant. (See also sect. 5.2 *Helmholtz and screened Poisson equations*.)

Applying the Poisson equation at the i th node, approximating the second derivative with a central difference

$$f_{i+1} - 2f_i + f_{i-1} = -g_i \quad (5.284)$$

where $f_i = f(x_i)$, $g_i = g(x_i)$. He says: "The signs on the left- and right-hand sides of (5.284) were chosen intentionally to conform with standard notation in graph theory regarding the Laplacian, as discussed in Section 1.7."

The discretized Helmholtz's equation:

$$f_{i+1} - 2f_i + f_{i-1} + \alpha f_i = 0, \quad (5.285)$$

so for us $\alpha = 2 - s$.

For any boundary conditions -Neumann, Dirichlet, or periodic- the coefficient matrix of the linear system admits the factorization

$$L = RR^\top \quad (5.286)$$

where R is a square or rectangular matrix. This factorization is the discrete counterpart of the second derivative constructed as the sequential application of the first derivative. Note that the commutative property $RR^\top = R^\top R$ is not always satisfied.

When the Dirichlet boundary condition is specified at both ends of the solution domain, the first and last values, f_1 and f_{n+1} , are known. Collecting the difference equations (5.284) for the interior nodes, $i = 2, \dots, n$, we obtain a system of linear equations where L is $(n - 1) \times (n - 1)$ symmetric tridiagonal Toeplitz matrix, a matrix with constant diagonal lines. The $m = 1, 2, \dots, n - 1$ eigenvalues of L are

$$\lambda_m = 2 - 2 \cos \alpha_m = 4 \sin^2 (\frac{1}{2} \alpha_m), \quad \alpha_m = \pi \frac{m}{n} \quad (5.287)$$

He also lists eigenvectors and factorizes as in (5.286), and discusses the Neumann boundary condition, in which case L is a “nearly Toeplitz matrix.” as well. In factorization (5.286), R is now a rectangular matrix.

For periodic boundary conditions, L is a “nearly tridiagonal matrix.” Because of the zero eigenvalue of the Laplacian, $\lambda_0 = 0$, corresponding to a constant eigenvector, the matrix L is singular. The rest of the eigenvectors are pure harmonic waves. The identity

$$f^\top \cdot L \cdot f = \sum_{i=1}^n (f_{i+1} - f_i)^2 \geq 0 \quad (5.288)$$

for arbitrary periodic field f demonstrates that the matrix L is positive semidefinite.

The periodic Laplacian is a circulant matrix.

He defines the graph Laplacian.

The adjacency matrix A , defined as $A_{ij} = 1$ if nodes i and j are connected by a grid line or link, 0 otherwise, with the convention that $A_{ii} = 0$. Thus, by convention, the diagonal line of the adjacency matrix is zero..

The number of paths that return to an arbitrary node after s steps have been made, summed over all starting nodes, is

$$n_s = \sum_{j=1}^n \mu_j^s \quad (5.289)$$

where μ_j are eigenvalues of A .

The degree of the i th node, denoted by d_i , is defined as the number of links attached to the node, which is equal to the sum of the elements in the corresponding row or column of the adjacency matrix. The Laplacian equals $L = D - A$, where D is a diagonal matrix whose i th diagonal element is equal to the corresponding node degree d_i .

He introduces the oriented incidence matrix R , by labeling nodes and links sequentially, and shows it leads to the factorization (5.286). All of these notions generalize to graphs.

A uniform two-dimensional Cartesian (square) lattice.

An Archimedean lattice consists of an infinite doubly periodic array regular polygons. In particular, each node is surrounded by the same sequence of polygons. There are 11 Archimedean lattices.

The Archimedean 4^4 lattice, also known as the square lattice, is a Bravais lattice consisting of a doubly periodic array of empty squares.

Laves lattices are the duals of the Archimedean lattices. A Laves lattice arises by introducing vertices in the middle of the tiles (faces) of an Archimedean lattice and then connecting the vertices to cross the edges of the Archimedean lattice. The dual of the square lattice is the same square lattice.

The nodes of a two- or three-dimensional regular lattice, regarded as a structured network, can be identified by two or three indices assigned to the individual lattice directions. The spectra of lattice networks Laplacians are used in computing of lattice Green's functions.

His figure 5.7 is interesting: I think it is a plot of the lowest eigenstates ("spectral partitioning") of a $[17 \times 17]$ square lattice ("Cartesian network") consisting of a complete set of horizontal and vertical links. As an example, the spectral partitioning of a square network is shown in Figure 2.2.1.

In spectral partitioning (a weighed sum of eigenvectors of the Laplacian matrix) roughly an equal number of eigenvector components with positive and negative sign appear. Eigenvector corresponding to the zero eigenvalue of the Laplacian matrix is uniform over the nodes of a network; the eigenvector corresponding to the zero eigenvalue is filled with ones. Orthogonality of the set of eigenvectors requires that all other eigenvectors have mean zero, his Eq. (2.2.8). Higher eigenvectors partition the network into two or a higher number of pieces (spectral partitioning). To partition a network, we may group together nodes whose eigenvector components corresponding to a specified eigenvalue have the same sign. The eigenvalue with the second smallest magnitude, is chosen for division into two fragments, while higher eigenvalues are chosen for division into a higher number of fragments.

A network whose structure is isomorphic to that of a square lattice consists of two intersecting one-dimensional arrays of links. A theorem due to Fiedler [13, 96] states that the eigenvectors of the Laplacian matrix for certain types of boundary conditions are tensor products of those of the constituent one-dimensional graphs, and the eigenvalues are the sums of the eigenvalues of the Laplacian of the constituent one-dimensional graphs. This property reflects the separability of the discrete Laplace operator in Cartesian coordinates.

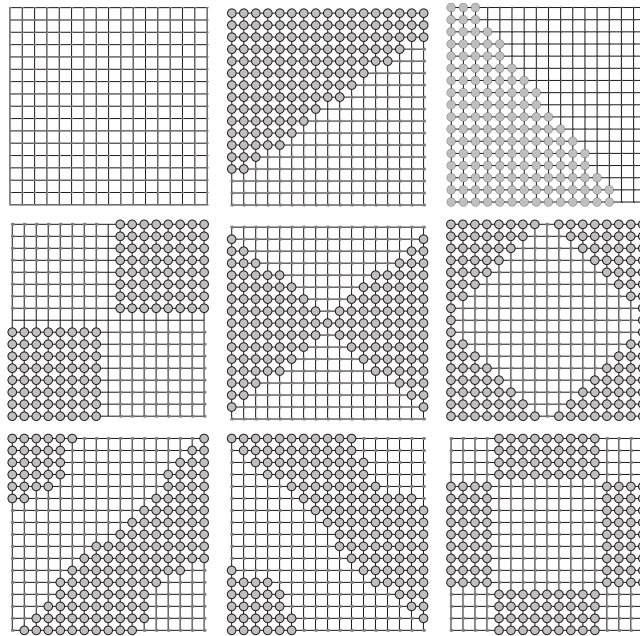


Figure 5.7: A $[17 \times 17]$ rectangular Helmholtz (5.285) network. Positive components of an eigenvector are marked as filled circles, negative components are marked as dots, and zero components are unmarked. The network shown consists of $N = 17^2 = 289$ nodes connected by $L = 544$ links. The degree of the 4 corner nodes is 2, the 60 edge nodes is 3, and 225 interior nodes is 4. Exact expressions for the eigenvalues and eigenvectors of the Laplacian of the square network are discussed in Pozrikidis Chapter 3. The first nine eigenvalues corresponding to the eigenvectors shown here are $\lambda_i = 0, 0.0341$ (double), $0.0681, 0.1351$ (double), 0.1691 (double), and 0.2701 . Pozrikidis [225] Fig 2.2.1.

We need to understand spatiotemporal cat eigenmodes. If $s < 2$ lattice is a spring mattress, with spring constant $2 - s$, what are the normal modes of the $s > 2$ spatiotemporal cat? In the above he discusses the Helmholtz, $s = 2$ Laplacian eigenmodes case (5.285).

2020-01-21 Predrag Fruchart, Zhou and Vitelli [106] *Dualities and non-Abelian mechanics* seems interesting. The abstract: “ Dualities are mathematical mappings that reveal links between apparently unrelated systems in virtually every branch of physics. Systems mapped onto themselves by a duality transformation are called self-dual and exhibit remarkable properties, as exemplified by the scale invariance of an Ising magnet at the critical point. Here we show how dualities can enhance the symmetries of a dynamical matrix (or Hamiltonian), enabling the design of metamaterials with emergent properties that escape a standard group theory analysis. As an illustration, we consider twisted kagome lattices, reconfigurable mechanical structures that change shape by means of a collapse mechanism. We observe that pairs of distinct configurations along the mechanism exhibit the same vibrational spectrum and related elastic moduli. We show that these puzzling properties arise from a duality between pairs of configurations on either side of a mechanical critical point. The critical point corresponds to a self-dual structure with isotropic elasticity even in the absence of spatial symmetries and a twofold-degenerate spectrum over the entire Brillouin zone. The spectral degeneracy originates from a version of Kramers’ theorem in which fermionic time-reversal invariance is replaced by a hidden symmetry emerging at the self-dual point. The normal modes of the self-dual systems exhibit non-Abelian geometric phases that affect the semiclassical propagation of wavepackets, leading to non-commuting mechanical responses. ”

Mechanical structures are described at the linear level by normal modes of vibration and their oscillation frequencies. Both are determined by the dynamical matrix \hat{D} , which summarizes the Newton equations of motion in the harmonic approximation [...] our analysis also applies when \hat{D} is replaced by other linear operators, such as the Maxwell operator of a photonic crystal[ref28], the mean-field Hamiltonian of a quantum system (in which case the eigenvalues are energies) or the dynamical matrix of an electrical circuit [6, 174, 207].

A *symmetry* is a transformation that maps a system onto itself. A *duality* relates distinct models or structures. In self-dual systems, the distinction between dualities and symmetries is blurred: additional symmetries can emerge at a self-dual point even if the spatial symmetries are unchanged. Such dualities can be harnessed to engineer material properties from wave propagation to static responses that are not predicted by a standard symmetry analysis based on space groups.

This one as well: Souslov and Vitelli [247] *Geometry for mechanics*: “ The mechanics of many materials can be modelled by a network of balls con-

nected by springs. A bottom-up approach based on differential geometry now captures changes in mechanics upon network growth or merger, going beyond the linear deformation regime. ”

2021-01-09 Predrag Fruchart, Zhou and Vitelli [106] cite

Ningyuan *et al.* [207] *Time- and site-resolved dynamics in a topological circuit:* I think we can ignore this paper. Though supplemental material explains: (1) The Harper-Hofstadter model, and its extension to spinful systems. (2) Photonic lattices, in both massive and massless limits. (3) Adding topology to photonic lattice models. (4) Mathematical tools for the calculation of band-structure, corresponding band Chern numbers, and two-point response of photonic lattice models. (5) Mathematical tools for calculating band- and edge- structure of finite strips.

Albert, Glazman and Jiang [6] *Topological properties of linear circuit lattices* have a 3-site lattice example, where the Lagrangian contribution of the link between neighboring sites is built from a (kinetic) capacitive part with what we call orbit Jacobian matrix \mathcal{J} , and a (potential) inductive part with what we call shift matrix r .

2021-01-09 Predrag Fruchart, Zhou and Vitelli [106] cite Lee *et al.* [174] *Topological circuits.* The normal mode frequency matrix of our circuit is unitarily equivalent to the hopping matrix of a quantum spin Hall insulator.

Circuits consisting of resistor, inductor and capacitor (RLC) components are governed by its circuit Laplacian, which is analogous to the Hamiltonian describing the energetics of a physical system. Here we show that topological insulating and semimetallic states can be realized in a periodic RLC circuit.

Any electrical circuit network can be represented by a graph whose nodes and edges correspond to the circuit junctions and connecting wires/elements. The circuit behavior is fundamentally described by Kirchhoff’s law. As an initial step towards identifying circuits with tight-binding lattice models, they rewrite Kirchhoff’s law in a matrix form, and consider circuits made up of periodic sublattices, with periodic boundary conditions (i.e. without grounded terminations).

What we call orbit Jacobian matrix \mathcal{J} they call ‘the grounded Laplacian’ \mathcal{J} .

The regularized inverse of \mathcal{J} known as the circuit Green’s function (regularization in this context means that 0 modes are omitted). The Laplacian is defined in terms of the conductances by $L = D - C$, where C is the (adjacency) matrix of conductances and D lists the total conductances out of each node. They call the set of eigenvalues the bandstructure of the circuit, and also refer to the nodes as sites.

RLC circuits obey a linear 2nd order ordinary differential equation (ODE), just like a mechanical system with springs, dampers and masses.

5.16 Counting invariant 2-tori

²⁴ An invariant 2-torus on a 2-dimensional spatiotemporally infinite \mathbb{Z}^2 lattice has more complicated pattern than a cat map periodic orbit. An invariant 2-torus can tile the infinitely large 2-dimensional space not only by repeating in the time or space direction, but also by moving in both of the spatiotemporal directions. The repeating pattern can generally be described by a Bravais lattice:

$$\mathcal{L} = \{n_1\mathbf{a}_1 + n_2\mathbf{a}_2 | n_i \in \mathbb{Z}\}. \quad (5.290)$$

And the invariant 2-tori tile the infinitely large 2-dimensional space by:

$$x_{\mathbf{z}} = x_{\mathbf{z}+\mathbf{R}}, \quad \mathbf{R} \in \mathcal{L}. \quad (5.291)$$

The \mathbf{z} here is a two-dimensional vector which labels the position and time of the field. The screened Poisson equation (??) can be written as:

$$(-2s + \sigma_1 + \sigma_1^\top + \sigma_2 + \sigma_2^\top)x_{\mathbf{z}} = -m_{\mathbf{z}}, \quad (5.292)$$

where the σ_i is a translation operator which can translate the field in the positive i th direction by length one and σ_i^\top is the inverse of the operator σ_i which translates the field in the negative i th direction. Here we can assume that σ_1 is a translation in the time and σ_2 is a translation in space. But since the system is invariant under the exchange of space and time, we don't need to distinguish these two directions.

Note that in (5.292) the operators, field and source are defined on infinitely large 2-dimensional space (lattice). For an invariant 2-torus, which is a periodic tile, the screened Poisson equation (5.292) is also satisfied on this finite tile. But in this case, the translation operators need to satisfy the periodic bc's specified by this invariant 2-torus. And the $-2s + \sigma_1 + \sigma_1^\top + \sigma_2 + \sigma_2^\top$ on the finite region is the orbit Jacobian matrix matrix of this specific periodic pattern.

Following the same procedure as counting the periodic points of a cat map, we know that the number of periodic points is given by the determinant of the orbit Jacobian matrix. To find the determinant and the inverse of the orbit Jacobian matrix, we need to first find the eigenvectors and eigenvalues.

The eigenvectors here are fields defined in this finite tile. The elements of these eigenvectors are generally complex numbers. If we tile the whole 2-dimensional space with one of these finite fields using the periodic condition, we will get an eigenvector of the operator in (5.292) defined in the infinite 2-dimensional space. And the eigenvalue remains unchanged. So we can find the eigenvectors and eigenvalues in the infinite 2-dimensional space then reduce the field into the finite tiles.

²⁵

²⁴Han 2019-06-25: This section is a version of kittens refsect s:dDcatMap that starts from 2D cat map without giving the formula of general d -dimensional spatiotemporal cat. I feel this is less clear than start with the d -dimensional spatiotemporal cat, but it directly follows the section of spatiotemporal cat map. Eventually this text was not used not used in kittens [77].

²⁵Han 2019-06-17: I will need to rewrite this paragraph to make it clearer.

For a 2-dimensional spatiotemporal cat map, we want to find eigenvectors with periodicity given by the Bravais lattice (5.290), where \mathbf{a}_1 and \mathbf{a}_2 are two 2-dimensional basis vectors. The general form of these basis vectors are $\mathbf{a}_1 = \{l_1, l_2\}$ and $\mathbf{a}_2 = \{l_3, l_4\}$. For a given Bravais lattice, the choice of basis vectors is not unique. It is shown by Lind [184], ([click here](#)) that we can choose basis vectors with form $\mathbf{a}_1 = \{l_1, 0\}$ and $\mathbf{a}_2 = \{l_3, l_4\}$ without loss of generality.²⁶ Then the reciprocal lattice is:

$$\bar{\mathcal{L}} = \{n_1 \mathbf{b}_1 + n_2 \mathbf{b}_2 | n_i \in \mathbb{Z}\}, \quad (5.293)$$

where the vectors \mathbf{b}_1 and \mathbf{b}_2 satisfy:

$$\mathbf{b}_i \cdot \mathbf{a}_j = 2\pi\delta_{ij}. \quad (5.294)$$

The eigenvectors of the translation operator which satisfy the periodicity of the Bravais lattice (5.290) are plane waves of form:

$$f_{\mathbf{k}}(\mathbf{z}) = e^{i\mathbf{k} \cdot \mathbf{z}}, \quad \mathbf{k} \in \bar{\mathcal{L}}, \quad (5.295)$$

where the wave vector \mathbf{k} is on the reciprocal lattice $\bar{\mathcal{L}}$. For the basis vectors $\mathbf{a}_1 = \{l_1, 0\}$ and $\mathbf{a}_2 = \{l_3, l_4\}$, the basis vectors of the corresponding reciprocal lattice are $\mathbf{b}_1 = 2\pi/l_1 l_4 \{l_4, -l_3\}$ and $\mathbf{b}_2 = 2\pi/l_1 l_4 \{0, l_1\}$. The expression of eigenvector with wave vector $\mathbf{k} = n_1 \mathbf{b}_1 + n_2 \mathbf{b}_2$ is:

$$f_{\mathbf{k}}(\mathbf{z}) = e^{i\mathbf{k} \cdot \mathbf{z}} = \exp[i\frac{2\pi}{l_1 l_4}(n_1 l_4 z_1 - n_1 l_3 z_2 + n_2 l_1 z_2)], \quad (5.296)$$

where the $\mathbf{z} = (z_1, z_2)$. The eigenvalue of the operator $s - \sigma_1 - \sigma_1^\top - \sigma_2 - \sigma_2^\top$ corresponding to this eigenvector is:

$$\lambda_{\mathbf{k}} = s - 2\cos(\frac{2\pi n_1}{l_1}) - 2\cos(-\frac{2\pi n_1 l_3}{l_1 l_4} + \frac{2\pi n_2}{l_4}). \quad (5.297)$$

It is sufficient to use the wave vectors \mathbf{k} with n_1 from 0 to $l_1 - 1$ and n_2 from 0 to $l_4 - 1$ to get all of the eigenvectors. Any wave vector on the reciprocal lattice outside of this range will give an eigenvector which is equivalent to an eigenvector with the wave vector in the range. So the number of eigenmodes we can get is $l_1 l_4$, which is the number of lattice sites in a smallest repeating tile.

Using the counting formula (??), we can find the number of the periodic points by computing the determinant of the orbit Jacobian matrix, which is the operator $-2s + \sigma_1 + \sigma_1^\top + \sigma_2 + \sigma_2^\top$ defined on the finite tile with periodic bc's:

$$N = \prod_{\mathbf{k}} \lambda_{\mathbf{k}} = \prod_{n_1=0}^{l_1-1} \prod_{n_2=0}^{l_4-1} \left[2s - 2\cos(\frac{2\pi n_1}{l_1}) - 2\cos(-\frac{2\pi n_1 l_3}{l_1 l_4} + \frac{2\pi n_2}{l_4}) \right]. \quad (5.298)$$

This is the number of periodic points with the periodicity given by Bravais lattice (5.290) with the basis vectors $\mathbf{a}_1 = \{l_1, 0\}$ and $\mathbf{a}_2 = \{l_3, l_4\}$.

Using the eigenvectors we can do a Fourier transform to the orbit Jacobian matrix and get the inverse which is the Green's function.

²⁶Predrag 2020-02-15: This is called 'Hermite normal form', see (5.204).

5.17 Elastodynamic equilibria of 2D solids

Predrag 2018-08-23 this section is now in *book/chapters/mattress.tex*, removed from here.

5.18 Integer lattices literature

There are many reasons why one needs to compute an “orbit Jacobian matrix” Hill determinant $|\text{Det } \mathcal{J}|$, in fields ranging from number theory to engineering, and many methods to accomplish that:

- discretizations of Helmholtz [82, 95, 181] and screened Poisson or Klein–Gordon or Yukawa [83, 113, 136, 137] equations
- Green’s functions on integer lattices [13, 16, 37, 50, 54, 59, 96, 111, 132, 133, 162–164, 187, 193, 197, 203, 204, 218, 250, 269]
- linearized Hartree-Fock equation on finite lattices [170]
- random walks, resistor networks, electrical circuits [6, 18, 38, 68, 69, 84, 115, 121, 139, 171, 174, 207, 225, 254, 260, 271]
- Gaussian model [102, 155, 192, 239]
- tight-binding Hamiltonians [68, 69, 89]
- discrete Schrödinger equation [216], Harper or Hofstadter model [123, 128]
- or almost Mathieu operator [241]
- quasilattices [45, 99]
- circulant tensor systems [50, 54, 200, 226, 230, 273]
- Ising model [32, 125, 126, 138, 140, 143–145, 165, 180, 188, 195, 208, 222, 272], Ising model transfer matrices [209, 272]
- lattice field theory [148, 198, 202, 205, 232, 245, 246, 265]
- modular transformations [51, 279]
- lattice string theory [110, 213]
- spatiotemporal stability in coupled map lattices [9, 107, 277]
- Van Vleck determinant, Laplace operator spectrum, semiclassical Gaussian path integrals [66, 176, 177, 259]
- Jacobi operator
- time reversal
- Hill determinant [39, 66, 189]; discrete Hill’s formula and the Hill discriminant, Toda lattice [258]
- Lindstedt-Poincaré technique [262–264]
- heat kernel [57, 86, 90, 152, 161, 197, 218, 274]
- chronotopic models [223]
- lattice points enumeration [28, 29, 33, 80]
- cryptography [199]
- primitive parallelogram [20, 46, 206, 266]
- difference equations [79, 97, 251]
- Bernoulli map [43, 85, 127], beta transformation [98, 215, 229]
- digital signal processing [87, 182, 270]
- generating functions, Z-transforms [90, 267]
- integer-point transform [33]
- graph Laplacians [60, 112, 185, 224]
- graph zeta functions [15, 25, 31, 42, 61–63, 81, 86, 117, 124, 134, 141, 172, 175, 224, 228, 235, 238, 249, 256, 257, 278]
- zeta functions for multi-dimensional shifts [24, 184, 186, 201]
- zeta functions on discrete tori [57, 58, 274]

References

- [1] V. E. Adler and A. P. Veselov, “Cauchy problem for integrable discrete equations on quad-graphs”, *Acta Appl. Math.* **84**, 237–262 (2004).
- [2] V. S. Afraimovich and Y. B. Pesin, “Hyperbolicity of infinite-dimensional drift systems”, *Nonlinearity* **3**, 1–19 (1990).
- [3] R. P. Agarwal, *Difference Equations and Inequalities* (Taylor & Francis, 2000).
- [4] R. P. Agarwal and K. Perera, *Proc. Conf. Differential & Difference Eqs. and Appl.* (Hindawi, New York, 2006).
- [5] N. Ahmadiniaz, A. Bashir, and C. Schubert, “Multiphoton amplitudes and generalized Landau-Khalatnikov-Fradkin transformation in scalar QED”, *Phys. Rev. D* **93**, 045023 (2016).
- [6] V. V. Albert, L. I. Glazman, and L. Jiang, “Topological properties of linear circuit lattices”, *Phys. Rev. Lett.* **114**, 173902 (2015).
- [7] L. Allen, B. Aulbach, S. Elaydi, and R. Sacker, eds., *Difference Equations and Discrete Dynamical Systems : Proc. 9th Intern. Conf.* (World Sci., Singapore, 2005).
- [8] J. M. Amigó, S. Zambrano, and M. A. F. Sanjuán, “Permutation complexity of spatiotemporal dynamics”, *Europhys. Lett.* **90**, 10007 (2010).
- [9] R. E. Amritkar, P. M. Gade, A. D. Gangal, and V. M. Nandkumaran, “Stability of periodic orbits of coupled-map lattices”, *Phys. Rev. A* **44**, R3407–R3410 (1991).
- [10] S. Anastassiou, “Complicated behavior in cubic Hénon maps”, *Theoret. Math. Phys.* **207**, 572–578 (2021).
- [11] S. Anastassiou, A. Bountis, and A. Bäcker, “Homoclinic points of 2D and 4D maps via the parametrization method”, *Nonlinearity* **30**, 3799–3820 (2017).
- [12] S. Anastassiou, A. Bountis, and A. Bäcker, “Recent results on the dynamics of higher-dimensional Hénon maps”, *Regul. Chaotic Dyn.* **23**, 161–177 (2018).
- [13] W. N. Anderson and T. D. Morley, “Eigenvalues of the Laplacian of a graph”, *Lin. Multilin. Algebra* **18**, 141–145 (1985).
- [14] V. I. Arnol'd and A. Avez, *Ergodic Problems of Classical Mechanics* (Addison-Wesley, Redwood City, 1989).
- [15] F. Arrigo, P. Grindrod, D. J. Higham, and V. Noferini, “On the exponential generating function for non-backtracking walks”, *Linear Algebra Appl.* **556**, 381–399 (2018).
- [16] J. H. Asad, “Differential equation approach for one- and two-dimensional lattice green's function”, *Mod. Phys. Lett. B* **21**, 139–154 (2007).

- [17] F. M. Atay, S. Jalan, and J. Jost, “Symbolic dynamics and synchronization of coupled map networks with multiple delays”, *Phys. Lett. A* **375**, 130–135 (2010).
- [18] D. Atkinson and F. J. van Steenwijk, “Infinite resistive lattices”, *Am. J. Phys* **67**, 486–492 (1999).
- [19] S. Aubry, “Anti-integrability in dynamical and variational problems”, *Physica D* **86**, 284–296 (1995).
- [20] M. Baake, J. Hermisson, and A. B. Pleasants, “The torus parametrization of quasiperiodic LI-classes”, *J. Phys. A* **30**, 3029–3056 (1997).
- [21] M. Baake, N. Neumärker, and J. A. G. Roberts, “Orbit structure and (reversing) symmetries of toral endomorphisms on rational lattices”, *Discrete Continuous Dyn. Syst.* **33**, 527–553 (2013).
- [22] M. Baake, J. A. G. Roberts, and A. Weiss, “Periodic orbits of linear endomorphisms on the 2-torus and its lattices”, *Nonlinearity* **21**, 2427 (2008).
- [23] C. Baesens, Y.-C. Chen, and R. S. MacKay, “Abrupt bifurcations in chaotic scattering: view from the anti-integrable limit”, *Nonlinearity* **26**, 2703–2730 (2013).
- [24] J.-C. Ban, W.-G. Hu, S.-S. Lin, and Y.-H. Lin, *Zeta Functions for Two-dimensional Shifts of Finite Type*, Vol. 221, Memoirs Amer. Math. Soc. (Amer. Math. Soc., Providence RI, 2013).
- [25] R. Band, J. M. Harrison, and C. H. Joyner, “Finite pseudo orbit expansions for spectral quantities of quantum graphs”, *J. Phys. A* **45**, 325204 (2012).
- [26] J. Banks, J. Brooks, G. Cairns, G. Davis, and P. Stacey, “On Devaney’s definition of chaos”, *Amer. Math. Monthly* **99**, 332–334 (1992).
- [27] M. Baranger, K. T. R. Davies, and J. H. Mahoney, “The calculation of periodic trajectories”, *Ann. Phys.* **186**, 95–110 (1988).
- [28] A. Barvinok, *A Course in Convexity* (Amer. Math. Soc., New York, 2002).
- [29] A. Barvinok, *Integer Points in Polyhedra* (European Math. Soc. Pub., Berlin, 2008).
- [30] A. I. Barvinok, “A polynomial time algorithm for counting integral points in polyhedra when the dimension is fixed”, *Math. Oper. Res.* **19**, 769–779 (1994).
- [31] H. Bass, “The Ihara-Selberg zeta function of a tree lattice”, *Int. J. Math.* **3**, 717–797 (1992).
- [32] R. J. Baxter, “The bulk, surface and corner free energies of the square lattice Ising model”, *J. Phys. A* **50**, 014001 (2016).
- [33] M. Beck and S. Robins, *Computing the Continuous Discretely* (Springer, New York, 2007).
- [34] D. Berenstein, *A toy model for time evolving QFT on a lattice with controllable chaos*, 2018.

- [35] D. Berenstein and A. M. García-García, *A universal quantum constraints on the butterfly effect*, 2015.
- [36] B. Bertini, P. Kos, and T. Prosen, “Entanglement spreading in a minimal model of maximal many-body quantum chaos”, *Phys. Rev. X* **9**, 021033 (2019).
- [37] H. S. Bhat and B. Osting, “Diffraction on the two-dimensional square lattice”, *SIAM J. Appl. Math.* **70**, 1389–1406 (2010).
- [38] P. Blanchard and D. Volchenkov, *Random Walks and Diffusions on Graphs and Databases* (Springer, Berlin, 2011).
- [39] S. V. Bolotin and D. V. Treschev, “Hill’s formula”, *Russ. Math. Surv.* **65**, 191 (2010).
- [40] S. Bolotin and R. MacKay, “Multibump orbits near the anti-integrable limit for Lagrangian systems”, *Nonlinearity* **10**, 1015–1029 (1997).
- [41] R. Bowen, *Equilibrium States and the Ergodic Theory of Anosov Diffeomorphisms* (Springer, Berlin, 1975).
- [42] R. Bowen and O. Lanford, Zeta functions of restrictions of the shift transformation, in *Global Analysis (Proc. Sympos. Pure Math., Berkeley, CA, 1968)*, Vol. 1, edited by S.-S. Chern and S. Smale (1970), pp. 43–50.
- [43] A. Boyarsky and P. Góra, *Laws of Chaos: Invariant Measures and Dynamical Systems in One Dimension* (Birkhäuser, Boston, 1997).
- [44] L. Boyle, M. Dickens, and F. Flicker, “Conformal quasicrystals and holography”, *Phys. Rev. X* **10**, 011009 (2020).
- [45] L. Boyle and P. J. Steinhardt, *Self-similar one-dimensional quasilattices*, 2016.
- [46] R. B. S. Brooks, R. F. Brown, J. Pak, and D. H. Taylor, “Nielsen numbers of maps of tori”, *Proc. Amer. Math. Soc.* **52**, 398–398 (1975).
- [47] N. G. de Bruijn, “Sequences of zeros and ones generated by special production rules”, *Indag. Math. Proc.* **84**, 27–37 (1981).
- [48] M. Bruschi, F. Calogero, and R. Droghei, “Tridiagonal matrices, orthogonal polynomials and Diophantine relations: I”, *J. Phys. A* **40**, 9793–9817 (2007).
- [49] L. A. Bunimovich and Y. G. Sinai, “Spacetime chaos in coupled map lattices”, *Nonlinearity* **1**, 491 (1988).
- [50] B. L. Buzbee, G. H. Golub, and C. W. Nielson, “On direct methods for solving Poisson’s equations”, *SIAM J. Numer. Anal.* **7**, 627–656 (1970).
- [51] J. L. Cardy, “Operator content of two-dimensional conformally invariant theories”, *Nucl. Phys. B* **270**, 186–204 (1986).
- [52] J. W. S. Cassels, *An Introduction to the Geometry of Numbers* (Springer, Berlin, 1959).

- [53] H. Chaté and P. Manneville, “Transition to turbulence via spatiotemporal intermittency”, *Phys. Rev. Lett.* **58**, 112 (1987).
- [54] M. Chen, “On the solution of circulant linear systems”, *SIAM J. Numer. Anal.* **24**, 668–683 (1987).
- [55] Y.-C. Chen, “Anti-integrability in scattering billiards”, *Dyn. Sys.* **19**, 145–159 (2004).
- [56] Y.-C. Chen, S.-S. Chen, and J.-M. Yuan, “Topological horseshoes in travelling waves of discretized nonlinear wave equations”, *J. Math. Phys.* **55**, 042701 (2014).
- [57] G. Chinta, J. Jorgenson, and A. Karlsson, “Zeta functions, heat kernels, and spectral asymptotics on degenerating families of discrete tori”, *Nagoya Math. J.* **198**, 121–172 (2010).
- [58] G. Chinta, J. Jorgenson, and A. Karlsson, “Heat kernels on regular graphs and generalized Ihara zeta function formulas”, *Monatsh. Math.* **178**, 171–190 (2014).
- [59] F. Chung and S.-T. Yau, “Discrete Green’s functions”, *J. Combin. Theory A* **91**, 19–214 (2000).
- [60] D. Cimasoni, “The critical Ising model via Kac-Ward matrices”, *Commun. Math. Phys.* **316**, 99–126 (2012).
- [61] B. Clair, “The Ihara zeta function of the infinite grid”, *Electron. J. Combin.* **21**, P2–16 (2014).
- [62] B. Clair and S. Mokhtari-Sharghi, “Zeta functions of discrete groups acting on trees”, *J. Algebra* **237**, 591–620 (2001).
- [63] B. Clair and S. Mokhtari-Sharghi, “Convergence of zeta functions of graphs”, *Proc. Amer. Math. Soc.* **130**, 1881–1887 (2002).
- [64] H. Cohen, *A Course in Computational Algebraic Number Theory* (Springer, Berlin, 1993).
- [65] P. Coleman, *Introduction to Many-Body Physics* (Cambridge Univ. Press, Cambridge UK, 2015).
- [66] Y. Colin de Verdière, “Spectrum of the Laplace operator and periodic geodesics: thirty years after”, *Ann. Inst. Fourier* **57**, 2429–2463 (2007).
- [67] S. C. Creagh, “Quantum zeta function for perturbed cat maps”, *Chaos* **5**, 477–493 (1995).
- [68] J. Cserti, “Application of the lattice Green’s function for calculating the resistance of an infinite network of resistors”, *Amer. J. Physics* **68**, 896–906 (2000).
- [69] J. Cserti, G. Széchenyi, and G. Dávid, “Uniform tiling with electrical resistors”, *J. Phys. A* **44**, 215201 (2011).
- [70] L.-B. Cui, C. Chen, W. Li, and M. K. Ng, “An eigenvalue problem for even order tensors with its applications”, *Lin. Multilin. Algebra* **64**, 602–621 (2015).

- [71] P. Cvitanović, *Field Theory*, Notes prepared by E. Gyldenkerne (Nordita, Copenhagen, 1983).
- [72] P. Cvitanović, “Chaotic Field Theory: A sketch”, *Physica A* **288**, 61–80 (2000).
- [73] P. Cvitanović, R. Artuso, R. Mainieri, G. Tanner, and G. Vattay, *Chaos: Classical and Quantum* (Niels Bohr Inst., Copenhagen, 2020).
- [74] P. Cvitanović, C. P. Dettmann, R. Mainieri, and G. Vattay, “Trace formulae for stochastic evolution operators: Weak noise perturbation theory”, *J. Stat. Phys.* **93**, 981–999 (1998).
- [75] P. Cvitanović, C. P. Dettmann, R. Mainieri, and G. Vattay, “Trace formulae for stochastic evolution operators: Smooth conjugation method”, *Nonlinearity* **12**, 939 (1999).
- [76] P. Cvitanović and T. Kinoshita, “Feynman-Dyson rules in parametric space”, *Phys. Rev. D* **10**, 3978–3991 (1974).
- [77] P. Cvitanović and H. Liang, Spatiotemporal cat: A chaotic field theory, In preparation, 2021.
- [78] P. H. Damgaard, H. Hüffel, and A. Rosenblum, eds., *Probabilistic Methods in Quantum Field Theory and Quantum Gravity* (Springer, New York, 1990).
- [79] F. Dannan, S. Elaydi, and P. Liu, “Periodic solutions of difference equations”, *J. Difference Equations and Applications* **6**, 203–232 (2000).
- [80] J. A. De Loera, R. Hemmecke, J. Tauzer, and R. Yoshida, “Effective lattice point counting in rational convex polytopes”, *J. Symbolic Comp.* **38**, 1273–1302 (2004).
- [81] A. Deitmar, “Ihara zeta functions of infinite weighted graphs”, *SIAM J. Discrete Math.* **29**, 2100–2116 (2015).
- [82] A. Dienstfrey, F. Hang, and J. Huang, “Lattice sums and the two-dimensional, periodic Green’s function for the Helmholtz equation”, *Proc. Roy. Soc. Ser A* **457**, 67–85 (2001).
- [83] F. W. Dorr, “The direct solution of the discrete Poisson equation on a rectangle”, *SIAM Rev.* **12**, 248–263 (1970).
- [84] P. G. Doyle and J. L. Snell, “Random walks and electric networks”, in *Intelligent Systems, Control and Automation: Science and Engineering* (Springer, 2012), pp. 259–265.
- [85] D. J. Driebe, *Fully Chaotic Maps and Broken Time Symmetry* (Springer, New York, 1999).
- [86] J. Dubout, *Zeta functions of graphs, their symmetries and extended Catalan numbers*.
- [87] D. Dudgeon and R. M. Mersereau, *Multidimensional Digital Signal Processing* (Prentice-Hall, Englewood Cliffs, NJ, 1984).

- [88] H. R. Dullin and J. D. Meiss, “Generalized Hénon maps: the cubic diffeomorphisms of the plane”, *Physica D* **143**, 262–289 (2000).
- [89] E. N. Economou, *Green's Functions in Quantum Physics* (Springer, Berlin, 2006).
- [90] S. Elaydi, *An Introduction to Difference Equations*, 3rd ed. (Springer, Berlin, 2005).
- [91] K. R. Elder, H. Xi, M. Deans, and J. D. Gunton, “Spatiotemporal chaos in the damped Kuramoto-Sivashinsky equation”, *AIP Conf. Proc.* **342**, 702–708 (1995).
- [92] L. Ermann and D. L. Shepelyansky, “The Arnold cat map, the Ulam method and time reversal”, *Physica D* **241**, 514–518 (2012).
- [93] M. J. Feigenbaum and B. Hasslacher, “Irrational decimations and path-integrals for external noise”, *Phys. Rev. Lett.* **49**, 605–609 (1982).
- [94] A. Fel'shtyn and R. Hill, “Trace formulae, Zeta functions, congruences and Reidemeister torsion in Nielsen theory”, *Forum Mathematicum* **10**, 641–664 (1998).
- [95] A. L. Fetter and J. D. Walecka, *Theoretical Mechanics of Particles and Continua* (Dover, New York, 2003).
- [96] M. Fiedler, “Algebraic connectivity of graphs”, *Czech. Math. J* **23**, 298–305 (1973).
- [97] D. Fischer, G. Golub, O. Hald, C. Leiva, and O. Widlund, “On Fourier-Toeplitz methods for separable elliptic problems”, *Math. Comput.* **28**, 349–349 (1974).
- [98] L. Flatto, J. C. Lagarias, and B. Poonen, “The zeta function of the beta transformation”, *Ergodic Theory Dynam. Systems* **14**, 237–266 (1994).
- [99] F. Flicker, “Time quasilattices in dissipative dynamical systems”, *SciPost Phys.* **5**, 001 (2018).
- [100] F. Flicker, S. H. Simon, and S.-A. Parameswaran, “Classical dimers on Penrose tilings”, *Phys. Rev. X* **10**, 011005 (2020).
- [101] V. Fock, “Die Eigenzeit in der klassischen und in der Quantenmechanik”, *Physik. Z. Sowjetunion* **12**, Transl. Proper time in classical and quantum mechanics, 404–425 (1937).
- [102] E. Fradkin, *Field Theories of Condensed Matter Physics* (Cambridge Univ. Press, Cambridge UK, 2013).
- [103] K. M. Frahm and D. L. Shepelyansky, “Ulam method for the Chirikov standard map”, *Eur. Phys. J. B* **76**, 57–68 (2010).
- [104] K. M. Frahm and D. L. Shepelyansky, “Small world of Ulam networks for chaotic Hamiltonian dynamics”, *Phys. Rev. E* **98**, 032205 (2018).
- [105] S. Friedland and J. Milnor, “Dynamical properties of plane polynomial automorphisms”, *Ergodic Theory Dynam. Systems* **9**, 67–99 (1989).

- [106] M. Fruchart, Y. Zhou, and V. Vitelli, “Dualities and non-Abelian mechanics”, *Nature*, **1–5** (2020).
- [107] P. M. Gade and R. E. Amritkar, “Spatially periodic orbits in coupled-map lattices”, *Phys. Rev. E* **47**, 143–154 (1993).
- [108] O. Galor, *Discrete Dynamical Systems* (Springer, Berlin, 2007).
- [109] F. Gelis and N. Tanji, “Schwinger mechanism revisited”, *Prog. Part. Nucl. Phys.* **87**, 1–49 (2016).
- [110] R. Giles and C. B. Thorn, “Lattice approach to string theory”, *Phys. Rev. D* **16**, 366–386 (1977).
- [111] J. I. Glaser, “Numerical solution of waveguide scattering problems by finite-difference Green’s functions”, *IEEE Trans. Microwave Theory Tech.* **18**, 436–443 (1970).
- [112] C. Godsil and G. . Royle, *Algebraic Graph Theory* (Springer, New York, 2013).
- [113] G. H. Golub and C. F. Van Loan, *Matrix Computations*, 4th ed. (J. Hopkins Univ. Press, Baltimore, MD, 2013).
- [114] I. S. Gradshteyn and I. M. Ryzhik, *Tables of Integrals, Series and Products*, 8th ed. (Elsevier LTD, Oxford, New York, 2014).
- [115] G. Grimmett, *Probability on Graphs: : Random Processes on Graphs and Lattices* (Cambridge Univ. Press, 2009).
- [116] P. Gruber and C. G. Lekkerkerker, *Geometry of numbers* (North-Holland, Amsterdam, 1987).
- [117] D. Guido, T. Isola, and M. L. Lapidus, “A trace on fractal graphs and the Ihara zeta function”, *Trans. Amer. Math. Soc.* **361**, 3041–3041 (2009).
- [118] V. M. Gundlach and D. A. Rand, “Spatio-temporal chaos. I. Hyperbolicity, structural stability, spatio-temporal shadowing and symbolic dynamics”, *Nonlinearity* **6**, 165 (1993).
- [119] B. Gutkin, L. Han, R. Jafari, A. K. Saremi, and P. Cvitanović, “Linear encoding of the spatiotemporal cat map”, *Nonlinearity* **34**, 2800–2836 (2021).
- [120] B. Gutkin and V. Osipov, “Classical foundations of many-particle quantum chaos”, *Nonlinearity* **29**, 325–356 (2016).
- [121] A. J. Guttmann, “Lattice Green’s functions in all dimensions”, *J. Phys. A* **43**, 305205 (2010).
- [122] R. Hagiwara and A. Shudo, “An algorithm to prune the area-preserving Hénon map”, *J. Phys. A* **37**, 10521 (2004).
- [123] P. G. Harper, “Single band motion of conduction electrons in a uniform magnetic field”, *Proc. Phys. Soc. London, Sect. A* **68**, 874–878 (1955).
- [124] K. Hashimoto, “Zeta functions of finite graphs and representations of p -adic groups”, *Adv. Stud. Pure Math.* **15**, 211–280 (1989).

- [125] H. Hobrecht and F. Hucht, “Anisotropic scaling of the two-dimensional Ising model I: the torus”, *SciPost Phys.* **7**, 026 (2019).
- [126] H. Hobrecht and F. Hucht, “Anisotropic scaling of the two-dimensional Ising model II: surfaces and boundary fields”, *SciPost Physics* **8**, 032 (2020).
- [127] F. Hofbauer and G. Keller, “Zeta-functions and transfer-operators for piecewise linear transformations”, *J. Reine Angew. Math. (Crelle)* **1984**, 100–113 (1984).
- [128] D. R. Hofstadter, “Energy levels and wave functions of Bloch electrons in rational and irrational magnetic fields”, *Phys. Rev. B* **14**, 2239–2249 (1976).
- [129] S. Holmin, “Counting nonsingular matrices with primitive row vectors”, *Monatsh. Math.* **173**, 209–230 (2013).
- [130] S. Holmin, Geometry of Numbers, Class Group Statistics and Free Path Lengths, PhD thesis (KTH Royal Inst. Technology, Stockholm, 2015).
- [131] W. G. Hoover and K. Aoki, “Order and chaos in the one-dimensional ϕ^4 model : N-dependence and the Second Law of Thermodynamics”, *Commun. Nonlinear Sci. Numer. Simul.* **49**, 192–201 (2017).
- [132] T. Horiguchi, “Lattice Green’s function for the simple cubic lattice”, *J. Phys. Soc. Jpn.* **30**, 1261–1272 (1971).
- [133] T. Horiguchi and T. Morita, “Note on the lattice Green’s function for the simple cubic lattice”, *J. Phys. C* **8**, L232 (1975).
- [134] M. D. Horton, “Ihara zeta functions of digraphs”, *Linear Algebra Appl.* **425**, 130–142 (2007).
- [135] J. M. Houlrik, “Periodic orbits in a two-variable coupled map”, *Chaos* **2**, 323–327 (1992).
- [136] G. Y. Hu and R. F. O’Connell, “Analytical inversion of symmetric tridiagonal matrices”, *J. Phys. A* **29**, 1511 (1996).
- [137] G. Y. Hu, J. Y. Ryu, and R. F. O’Connell, “Analytical solution of the generalized discrete Poisson equation”, *J. Phys. A* **31**, 9279 (1998).
- [138] A. Hucht, “The square lattice Ising model on the rectangle I: finite systems”, *J. Phys. A* **50**, 065201 (2017).
- [139] B. D. Hughes, *Random Walks and Random Environments: Vol. I, Random Walks* (Clarendon Press, Oxford, 1995).
- [140] C. A. Hurst and H. S. Green, “New solution of the Ising problem for a rectangular lattice”, *J. Chem. Phys.* **33**, 1059–1062 (1960).
- [141] Y. Ihara, “On discrete subgroups of the two by two projective linear group over p-adic fields”, *J. Math. Soc. Japan* **18**, 219–235 (1966).
- [142] S. Isola, “ ζ -functions and distribution of periodic orbits of toral automorphisms”, *Europhys. Lett.* **11**, 517–522 (1990).

- [143] E. V. Ivashkevich, N. S. Izmailian, and C.-K. Hu, “Kronecker’s double series and exact asymptotic expansions for free models of statistical mechanics on torus”, *J. Phys. A* **35**, 5543–5561 (2002).
- [144] N. S. Izmailian, “Finite-size effects for anisotropic 2D Ising model with various boundary conditions”, *J. Phys. A* **45**, 494009 (2012).
- [145] N. S. Izmailian and C.-K. Hu, “Finite-size effects for the Ising model on helical tori”, *Phys. Rev. E* **76**, 041118 (2007).
- [146] N. S. Izmailian and M.-C. Huang, “Asymptotic expansion for the resistance between two maximally separated nodes on an M by N resistor network”, *Phys. Rev. E* **82**, 011125 (2010).
- [147] M. A. Jafarizadeh, R. Sufiani, and S. Jafarizadeh, “Calculating two-point resistances in distance-regular resistor networks”, *J. Phys. A* **40**, 4949–4972 (2007).
- [148] K. Jansen, “Lattice field theory”, *Int. J. Mod. Phys. E* **16**, 2638–2679 (2007).
- [149] J. Jeziorski and W. Marzantowicz, *Homotopy Methods in Topological Fixed and Periodic Points Theory* (Springer, Berlin, 2006).
- [150] M. Jiang, “Equilibrium states for lattice models of hyperbolic type”, *Nonlinearity* **8**, 631–659 (1995).
- [151] M. I. Jordan, Z. Ghahramani, T. S. Jaakkola, and L. K. Saul, “An introduction to variational methods for graphical models”, *Machine Learning* **37**, 183–233 (1999).
- [152] J. Jorgenson and S. Lang, “The ubiquitous heat kernel”, in *Mathematics Unlimited - 2001 and Beyond* (Springer, Berlin, 2001), pp. 655–683.
- [153] W. Just, “Equilibrium phase transitions in coupled map lattices: A pedestrian approach”, *J. Stat. Phys.* **105**, 133–142 (2001).
- [154] W. Just, “On symbolic dynamics of space-time chaotic models”, in *Collective Dynamics of Nonlinear and Disordered Systems* (Springer, 2005), pp. 339–357.
- [155] L. P. Kadanoff, *Statistical Physics: Statics, Dynamics and Renormalization* (World Scientific, Singapore, 2000).
- [156] P. H. van der Kamp, “Initial value problems for lattice equations”, *J. Phys. A* **42**, 404019 (2009).
- [157] N. G. van Kampen, *Stochastic Processes in Physics and Chemistry*, 3rd ed. (Elsevier, Amsterdam, 2007).
- [158] K. Kaneko, “Transition from torus to chaos accompanied by frequency lockings with symmetry breaking: In connection with the coupled-logistic map”, *Prog. Theor. Phys.* **69**, 1427–1442 (1983).
- [159] K. Kaneko, “Period-doubling of kink-antikink patterns, quasiperiodicity in antiferro-like structures and spatial intermittency in coupled logistic lattice: Towards a prelude of a “field theory of chaos””, *Prog. Theor. Phys.* **72**, 480–486 (1984).

- [160] V. Karimipour and M. H. Zarei, “Completeness of classical ϕ^4 theory on two-dimensional lattices”, *Phys. Rev. A* **85**, 032316 (2012).
- [161] A. Karlsson and M. Neuhauser, “Heat kernels, theta identities, and zeta functions on cyclic groups”, *Contemp. Math.* **394**, 177–190 (2006).
- [162] S. Katsura and S. Inawashiro, “Lattice Green’s functions for the rectangular and the square lattices at arbitrary points”, *J. Math. Phys.* **12**, 1622–1630 (1971).
- [163] S. Katsura, S. Inawashiro, and Y. Abe, “Lattice Green’s function for the simple cubic lattice in terms of a Mellin-Barnes type integral”, *J. Math. Phys.* **12**, 895–899 (1971).
- [164] S. Katsura, T. Morita, S. Inawashiro, T. Horiguchi, and Y. Abe, “Lattice Green’s function. Introduction”, *J. Math. Phys.* **12**, 892–895 (1971).
- [165] B. Kaufman, “Crystal statistics. II. Partition function evaluated by spinor analysis”, *Phys. Rev.* **76**, 1232–1243 (1949).
- [166] M. Kawasaki and S. Sasa, “Statistics of unstable periodic orbits of a chaotic dynamical system with a large number of degrees of freedom”, *Phys. Rev. E* **72**, 037202 (2005).
- [167] J. P. Keating, “Asymptotic properties of the periodic orbits of the cat maps”, *Nonlinearity* **4**, 277 (1991).
- [168] J. P. Keating, “The cat maps: quantum mechanics and classical motion”, *Nonlinearity* **4**, 309–341 (1991).
- [169] W. G. Kelley and A. C. Peterson, *Difference Equations : An Introduction with Applications* (Academic, San Diego, 2001).
- [170] V. Khoromskaia and B. N. Khoromskij, “Block circulant and Toeplitz structures in the linearized Hartree-Fock equation on finite lattices: Tensor approach”, *Comput. Methods Appl. Math.* **17**, 43–455 (2017).
- [171] G. Kirchhoff, “Über die Auflösung der Gleichungen, auf welche man bei der Untersuchung der linearen Vertheilung galvanischer Ströme geführt wird”, *Ann. Phys. Chem.* **148**, 497–508 (1847).
- [172] M. Kotani and T. Sunada, “Zeta functions of finite graphs”, *J. Math. Sci. Univ. Tokyo* **7**, 7–25 (2000).
- [173] A. Lasota and M. MacKey, *Chaos, fractals, and noise; stochastic aspects of dynamics* (Springer, New York, 1994).
- [174] C. H. Lee, S. Imhof, C. Berger, F. Bayer, J. Brehm, L. W. Molenkamp, T. Kiessling, and R. Thomale, “Topoelectrical circuits”, *Commun. Phys.* **1**, 39 (2018).
- [175] D. Lenz, F. Pogorzelski, and M. Schmidt, “The Ihara zeta function for infinite graphs”, *Trans. Amer. Math. Soc.* **371**, 5687–5729 (2018).
- [176] S. Levit and U. Smilansky, “A new approach to Gaussian path integrals and the evaluation of the semiclassical propagator”, *Ann. Phys.* **103**, 198–207 (1977).

- [177] S. Levit and U. Smilansky, “A theorem on infinite products of eigenvalues of Sturm-Liouville type operators”, Proc. Amer. Math. Soc. **65**, 299–299 (1977).
- [178] J. Li and S. Tomsovic, “Exact relations between homoclinic and periodic orbit actions in chaotic systems”, Phys. Rev. E **97**, 022216 (2017).
- [179] M.-C. Li and M. Malkin, “Bounded nonwandering sets for polynomial mappings”, J. Dynam. Control Systems **10**, 377–389 (2004).
- [180] T. M. Liaw, M. C. Huang, Y. L. Chou, S. C. Lin, and F. Y. Li, “Partition functions and finite-size scalings of Ising model on helical tori”, Phys. Rev. E **73**, 041118 (2006).
- [181] W.J. Lick, *Difference Equations from Differential Equations* (Springer, Berlin, 1989).
- [182] J. S. Lim, *Two-dimensional Signal and Image Processing* (Prentice Hall, Englewood Cliffs, N.J, 1990).
- [183] L.-H. Lim, Singular values and eigenvalues of tensors: A variational approach, in *1st IEEE International Workshop on Computational Advances in Multi-Sensor Adaptive Processing* (2005).
- [184] D. A. Lind, “A zeta function for Z^d -actions”, in *Ergodic Theory of Z^d Actions*, edited by M. Pollicott and K. Schmidt (Cambridge Univ. Press, 1996), pp. 433–450.
- [185] D. A. Lind and B. Marcus, *An Introduction to Symbolic Dynamics and Coding* (Cambridge Univ. Press, Cambridge, 1995).
- [186] D. Lind and K. Schmidt, “Symbolic and algebraic dynamical systems”, in *Handbook of Dynamical Systems*, Vol. 1, edited by B. Hasselblatt and A. Katok (Elsevier, New York, 2002), pp. 765–812.
- [187] R. de la Llave, Variational methods for quasiperiodic solutions of partial differential equations, in *Hamiltonian Systems and Celestial Mechanics (HAMSYS-98)*, edited by J. Delgado, E. A. Lacomba, E. Pérez-Chavela, and J. Llibre (2000).
- [188] I. Lyberg, “Free energy of the anisotropic Ising lattice with Brascamp-Kunz boundary conditions”, Phys. Rev. E **87**, 062141 (2013).
- [189] R. S. MacKay and J. D. Meiss, “Linear stability of periodic orbits in Lagrangian systems”, Phys. Lett. A **98**, 92–94 (1983).
- [190] R. S. MacKay, J. D. Meiss, and I. C. Percival, “Transport in Hamiltonian systems”, Physica D **13**, 55–81 (1984).
- [191] A. Manning, “Axiom A diffeomorphisms have rational zeta function”, Bull. London Math. Soc. **3**, 215–220 (1971).
- [192] E. C. Marino, *Quantum Field Theory Approach to Condensed Matter Physics* (Cambridge Univ. Press, Cambridge UK, 2017).
- [193] P. A. Martin, “Discrete scattering theory: Green’s function for a square lattice”, Wave Motion **43**, 619–629 (2006).

- [194] P. C. Martin, E. D. Siggia, and H. A. Rose, “Statistical dynamics of classical systems”, *Phys. Rev. A* **8**, 423–437 (1973).
- [195] B. M. McCoy and T. T. Wu, *The Two-Dimensional Ising Model*, 2nd ed. (Dover, 1973).
- [196] J. D. Meiss, “Symplectic maps, variational principles, and transport”, *Rev. Mod. Phys.* **64**, 795–848 (1992).
- [197] B. D. Mestel and I. Percival, “Newton method for highly unstable orbits”, *Physica D* **24**, 172 (1987).
- [198] H. B. Meyer, “Lattice QCD: A brief introduction”, in *Lattice QCD for Nuclear Physics*, edited by H.-W. Lin and H. B. Meyer (Springer, York New, 2015), pp. 1–34.
- [199] D. Micciancio and S. Goldwasser, *Complexity of Lattice Problems - A Cryptographic Perspective* (Springer, New York, 2002).
- [200] M. Michałek and B. Sturmfels, *Invitation to Nonlinear Algebra* (MPI Leipzig, 2020).
- [201] R. Miles, “A dynamical zeta function for group actions”, *Monatsh. Math.* **182**, 683–708 (2016).
- [202] I. Montvay and G. Münster, *Quantum Fields on a Lattice* (Cambridge Univ. Press, Cambridge, 1994).
- [203] T. Morita, “Useful procedure for computing the lattice Green’s function - square, tetragonal, and bcc lattices”, *J. Math. Phys.* **12**, 1744–1747 (1971).
- [204] T. Morita and T. Horiguchi, “Calculation of the lattice Green’s function for the bcc, fcc, and rectangular lattices”, *J. Math. Phys.* **12**, 986–992 (1971).
- [205] G. Münster and M. Walzl, *Lattice gauge theory - A short primer*, 2000.
- [206] J. Nielsen, “Über die Minimalzahl der Fixpunkte bei den Abbildungstypen der Ringflächen”, *Math. Ann.* **82**, 83–93 (1920).
- [207] J. Ningyuan, C. Owens, A. Sommer, D. Schuster, and J. Simon, “Time- and site-resolved dynamics in a topological circuit”, *Phys. Rev. X* **5**, 021031 (2015).
- [208] Y. Okabe, K. Kaneda, M. Kikuchi, and C.-K. Hu, “Universal finite-size scaling functions for critical systems with tilted boundary conditions”, *Phys. Rev. E* **59**, 1585–1588 (1999).
- [209] L. Onsager, “Crystal statistics. I. A Two-dimensional model with an order-disorder transition”, *Phys. Rev.* **65**, 117–149 (1944).
- [210] M. Q. Owaidat, J. H. Asad, and Z.-Z. Tan, “Resistance computation of generalized decorated square and simple cubic network lattices”, *Results Phys.* **12**, 1621–1627 (2019).
- [211] N. Ozisik, H. R. B. Orlande, M. J. Colaco, and R. M. Cotta, *Finite Difference Methods in Heat Transfer* (Apple Academic Press, 2017).

- [212] V. G. Papageorgiou, F. W. Nijhoff, and H. W. Capel, “Integrable mappings and nonlinear integrable lattice equations”, *Phys. Lett. A* **147**, 106–114 (1990).
- [213] G. Papathanasiou and C. B. Thorn, “Worldsheet propagator on the light-cone worldsheet lattice”, *Phys. Rev. D* **87**, 066005 (2013).
- [214] G. Parisi and Y. S. Wu, “Perturbation-theory without gauge fixing”, *Scientia Sinica* **24**, 483–496 (1981).
- [215] W. Parry, “On the β -expansions of real numbers”, *Acta Math. Acad. Sci. Hung.* **11**, 401–416 (1960).
- [216] R. Peierls, “Zur Theorie des Diamagnetismus von Leitungselektronen”, *Z. Phys.* **80**, 763–791 (1933).
- [217] S.-L. Peng, K.-F. Cao, and Z.-X. Chen, “Devil’s staircase of topological entropy and global metric regularity”, *Phys. Lett. A* **193**, 437–443 (1994).
- [218] I. Percival and F. Vivaldi, “A linear code for the sawtooth and cat maps”, *Physica D* **27**, 373–386 (1987).
- [219] I. Percival and F. Vivaldi, “Arithmetical properties of strongly chaotic motions”, *Physica D* **25**, 105–130 (1987).
- [220] S. D. Pethel, N. J. Corron, and E. Boltt, “Symbolic dynamics of coupled map lattices”, *Phys. Rev. Lett.* **96**, 034105 (2006).
- [221] S. D. Pethel, N. J. Corron, and E. Boltt, “Deconstructing spatiotemporal chaos using local symbolic dynamics”, *Phys. Rev. Lett.* **99**, 214101 (2007).
- [222] A. Poghosyan, N. Izmailian, and R. Kenna, “Exact solution of the critical Ising model with special toroidal boundary conditions”, *Phys. Rev. E* **96**, 062127 (2017).
- [223] A. Politi, A. Torcini, and S. Lepri, “Lyapunov exponents from node-counting arguments”, *J. Phys. IV* **8**, 263 (1998).
- [224] M. Pollicott, *Dynamical zeta functions*, in *Smooth Ergodic Theory and Its Applications*, Vol. 69, edited by A. Katok, R. de la Llave, Y. Pesin, and H. Weiss (2001), pp. 409–428.
- [225] C. Pozrikidis, *An Introduction to Grids, Graphs, and Networks* (Oxford Univ. Press, Oxford , UK, 2014).
- [226] L. Qi, H. Chen, and Y. Chen, *Tensor Eigenvalues and Their Applications* (Springer, Singapore, 2018).
- [227] G. R. W. Quispel, H. W. Capel, V. G. Papageorgiou, and F. W. Nijhoff, “Integrable mappings derived from soliton equations”, *Physica A* **173**, 243–266 (1991).
- [228] P. Ren, T. Aleksić, D. Emms, R. C. Wilson, and E. R. Hancock, “Quantum walks, Ihara zeta functions and cospectrality in regular graphs”, *Quantum Inf. Process.* **10**, 405–417 (2010).

- [229] A. Rényi, “Representations for real numbers and their ergodic properties”, *Acta Math. Acad. Sci. Hung.* **8**, 477–493 (1957).
- [230] M. Rezghi and L. Eldén, “Diagonalization of tensors with circulant structure”, *Linear Algebra Appl.* **435**, 422–447 (2011).
- [231] P. H. Rojas O. van der Kamp and G. R. W. Quispel, *Lax representations for integrable maps OΔEs*, 2007.
- [232] H. J. Rothe, *Lattice Gauge Theories - An Introduction* (World Scientific, Singapore, 2005).
- [233] D. Ruelle, *Thermodynamic Formalism: The Mathematical Structure of Equilibrium Statistical Mechanics*, 2nd ed. (Cambridge Univ. Press, Cambridge, 2004).
- [234] H. Sakaguchi, “Breakdown of the phase dynamics”, *Progr. Theor. Phys.* **84**, 792–800 (1990).
- [235] I. Sato, “Bartholdi zeta functions of group coverings of digraphs”, *Far East J. Math. Sci.* **18**, 321–339 (2005).
- [236] C. Schubert, “Lectures on the worldline formalism”, in *School of Spinning Particles in Quantum Field Theory: Worldline Formalism, Higher Spins and Conformal Geometry*, edited by C. Schubert (2012).
- [237] K. Serkh and V. Rokhlin, “On the solution of the Helmholtz equation on regions with corners”, *Proc. Natl. Acad. Sci. USA* **113**, 9171–9176 (2016).
- [238] J.-P. Serre, *Trees* (Springer, Berlin, 1980).
- [239] R. Shankar, *Quantum Field Theory and Condensed Matter* (Cambridge Univ. Press, Cambridge UK, 2017).
- [240] C. L. Siegel and K. Chandrasekharan, *Lectures on the Geometry of Numbers* (Springer Berlin Heidelberg, Berlin, Heidelberg, 1989).
- [241] B. Simon, “Almost periodic schrödinger operators: A review”, *Adv. Appl. Math.* **3**, 463–490 (1982).
- [242] S. Simons, “Analytical inversion of a particular type of banded matrix”, *J. Phys. A* **30**, 755 (1997).
- [243] Y. G. Sinai, “Gibbs measures in ergodic theory”, *Russian Math. Surveys* **27**, 21 (1972).
- [244] S. Smale, “Differentiable dynamical systems”, *Bull. Amer. Math. Soc.* **73**, 747–817 (1967).
- [245] J. Smit, *Introduction to Quantum Fields on a Lattice* (Cambridge Univ. Press, Cambridge, 2002).
- [246] R. Sommer, *Introduction to Lattice Gauge Theories*, tech. rep. (Humboldt Univ., 2015).
- [247] A. Souslov and V. Vitelli, “Geometry for mechanics”, *Nature Physics* **15**, 623–624 (2019).

- [248] R. P. Stanley, *Enumerative Combinatorics*, Vol. 1 (Cambridge Univ. Press, 2009).
- [249] H. M. Stark and A. A. Terras, “Zeta functions of finite graphs and coverings”, *Adv. Math.* **121**, 124–165 (1996).
- [250] I. Stewart and D. Gökaydin, “Symmetries of quotient networks for doubly periodic patterns on the square lattice”, *Int. J. Bifur. Chaos* **29**, 1930026 (2019).
- [251] R. Suarez, “Difference equations and a principle of double induction”, *Math. Mag.* **62**, 334–339 (1989).
- [252] L.-S. Sun, X.-Y. Kang, Q. Zhang, and L.-X. Lin, “A method of recovering the initial vectors of globally coupled map lattices based on symbolic dynamics”, *Chin. Phys. B* **20**, 120507 (2011).
- [253] T. Sunada, “Unitary representations of fundamental groups and the spectrum of twisted Laplacians”, *Topology* **28**, 125–132 (1989).
- [254] T. Sunada, *Topological Crystallography* (Springer, Tokyo, 2013).
- [255] K. Takeuchi and M. Sano, “Role of unstable periodic orbits in phase transitions of coupled map lattices”, *Phys. Rev. E* **75**, 036201 (2007).
- [256] A. Tarfulea and R. Perlis, “An Ihara formula for partially directed graphs”, *Linear Algebra Appl.* **431**, 73–85 (2009).
- [257] A. Terras, *Zeta Functions of Graphs: A Stroll through the Garden* (Cambridge Univ. Press, 2010).
- [258] M. Toda, *Theory of Nonlinear Lattices* (Springer, Berlin, 1989).
- [259] J. H. Van Vleck, “The correspondence principle in the statistical interpretation of quantum mechanics”, *Proc. Natl. Acad. Sci.* **14**, 178–188 (1928).
- [260] G. Venezian, “On the resistance between two points on a grid”, *Am. J. Phys* **62**, 1000–1004 (1994).
- [261] I. Vierhaus, Simulation of ϕ^4 Theory in the Strong Coupling Expansion beyond the Ising Limit, MA thesis (Humboldt-Univ. Berlin, Math.-Naturwissen. Fakultät I, 2010).
- [262] D. Viswanath, “The Lindstedt-Poincaré technique as an algorithm for finding periodic orbits”, *SIAM Rev.* **43**, 478–496 (2001).
- [263] D. Viswanath, “Symbolic dynamics and periodic orbits of the Lorenz attractor”, *Nonlinearity* **16**, 1035–1056 (2003).
- [264] D. Viswanath, “The fractal property of the Lorenz attractor”, *Physica D* **190**, 115–128 (2004).
- [265] U.-J. Wiese, *An Introduction to Lattice Field Theory*, tech. rep. (Univ. Bern, 2009).
- [266] I. Wigman, “Counting singular matrices with primitive row vectors”, *Monatsh. Math.* **144**, 71–84 (2005).

- [267] H. S. Wilf, *Generatingfunctionology* (Academic Press, New York, 1994).
- [268] A. Wipf, *Statistical Approach to Quantum Field Theory: An Introduction* (Springer, Berlin, 2013).
- [269] W. L. Wood, “Periodicity effects on the iterative solution of elliptic difference equations”, *SIAM J. Numer. Anal.* **8**, 439–464 (1971).
- [270] J. Woods, *Multidimensional Signal, Image, and Video Processing and Coding* (Academic Press, Amsterdam, 2012).
- [271] F. Y. Wu, “Theory of resistor networks: the two-point resistance”, *J. Phys. A* **37**, 6653–6673 (2004).
- [272] M.-C. Wu and C.-K. Hu, “Exact partition functions of the Ising model on $M \times N$ planar lattices with periodic-aperiodic boundary conditions”, *J. Phys. A* **35**, 5189–5206 (2002).
- [273] Z.-J. Xie, X.-Q. Jin, and Y.-M. Wei, “A fast algorithm for solving circulant tensor systems”, *Lin. Multilin. Algebra* **65**, 1894–1904 (2016).
- [274] Y. Yamasaki, “An explicit prime geodesic theorem for discrete tori and the hypergeometric functions”, *Math. Z.* **289**, 361–376 (2017).
- [275] L. Zaporski and F. Flicker, “Superconvergence of topological entropy in the symbolic dynamics of substitution sequences”, *SciPost Phys.* **7**, 018 (2019).
- [276] X. Zhang, “Hyperbolic invariant sets of the real generalized Hénon maps”, *Chaos Solit. Fract.* **43**, 31–41 (2010).
- [277] Q. Zhilin, A. Gangal, M. Benkun, and T. Gang, “Spatiotemporally periodic patterns in symmetrically coupled map lattices”, *Phys. Rev. E* **50**, 163–170 (1994).
- [278] D. Zhou, Y. Xiao, and Y.-H. He, “Seiberg duality, quiver gauge theories, and Ihara’s zeta function”, *Int. J. Mod. Phys. A* **30**, 1550118 (2015).
- [279] R. M. Ziff, C. D. Lorenz, and P. Kleban, “Shape-dependent universality in percolation”, *Physica A* **266**, 17–26 (1999).

Chapter 6

Zeta functions in 2D

“symbols” are sometimes called “colors”.

2CB

¹ Let \mathbb{Z}^2 be a two-dimensional planar lattice. For any $m, n \geq 1$ and $(i, j) \in \mathbb{Z}^2$, the $m \times n$ rectangular lattice with the left-bottom vertex (i, j) is denoted by

$$\mathbb{Z}_{m \times n}((i, j)) = \{(i + m', j + n') \mid 0 \leq m' \leq m - 1, 0 \leq n' \leq n - 1\}.$$

and $\mathbb{Z}_{m \times n} = \mathbb{Z}_{m \times n}((0, 0))$. Let \mathcal{S}_p be an alphabet of p (≥ 2) symbols. For $m, n \geq 1$, $\Sigma_{m \times n}(p) = \mathcal{S}_p^{\mathbb{Z}_{m \times n}}$ is the set of all $m \times n$ local patterns or rectangular blocks, and $\Sigma_{m \times n}(\mathcal{B})$ is the set of admissible $m \times n$ patterns. $\Sigma(\mathcal{B})$ is the set of all admissible patterns in \mathcal{B} .

2016-11-07 Predrag There is much literature on multi-dimensional shifts [2–6, 8, 9, 16, 20, 22, 23, 31, 32, 41, 43]. It does not seem to directly relevant to the 2-dimensional spatiotemporal symbolic dynamics studied by us.

2016-05-04 Predrag There is much literature on multi-dimensional shifts that we have to understand (or at least understand whether it is relevant to our 2-dimensional symbolic dynamics):

Ward [44] *An algebraic obstruction to isomorphism of Markov shifts with group alphabets* introduced \mathbb{Z}^2 -subshift, or the space of doubly indexed sequences over a finite abelian compact group G .

Ward [43] *Automorphisms of \mathbb{Z}^d -subshifts of finite type*

Ward and Miles [45] *A directional uniformity of periodic point distribution and mixing:* “For mixing actions generated by commuting automorphisms of a compact abelian group, we investigate the directional uniformity of the rate of periodic point distribution and mixing. When each of these automorphisms has finite entropy, it is shown that directional mixing and directional convergence of the uniform measure supported on periodic points to Haar measure occurs at a uniform rate independent of the direction.”

¹Predrag 2016-10-11: From Ban *et al.* [3], on two-dimensional \mathbb{Z}^2 -shifts of finite type

Miles and Ward [34] *The dynamical zeta function for commuting automorphisms of zero-dimensional groups:* “ For a \mathbb{Z}^d -action α by commuting homeomorphisms of a compact metric space, Lind [25], ([click here](#)) introduced a dynamical zeta function that generalizes the dynamical zeta function of a single transformation. We investigate this function when α is generated by continuous automorphisms of a compact abelian zero-dimensional group. We address Lind’s conjecture concerning the existence of a natural boundary for the zeta function and prove this for two significant classes of actions, including both zero entropy and positive entropy examples. The finer structure of the periodic point counting function is also examined and, in the zero entropy case, we show how this may be severely restricted for subgroups of prime index in \mathbb{Z}^d . ”

Ward and Miles [46] *Directional uniformities, periodic points, and entropy:* “ For dynamical systems generated by $d \geq 2$ commuting homeomorphisms, dynamical invariants like entropy and periodic point data, become more complex and permit multiple definitions. A powerful theory of directional entropy and periodic points can be built. An underlying theme is uniformity in dynamical invariants as the direction changes, and the connection between this theory and problems in number theory; we explore this for several invariants and highlight Fried’s notion of average entropy and its connection to uniformities in growth properties. ”

Al Refaei 2011 “The group Z^2 acts natural on the space ?? via left and upward shifts” is gibberish, ignore it.

Roettger [42], *Periodic points classify a family of Markov shifts*, writes:

Ledrappier introduced the following type of space of doubly indexed sequences over a finite abelian group G ,

$$X_G = \{(x_{s,t}) \in G^{\mathbb{Z}^2} \mid x_{s,t+1} = x_{s,t} + x_{s+1,t} \text{ for all } s, t \in \mathbb{Z}\}.$$

The group \mathbb{Z}^2 acts naturally on the space X_G via left and upward shifts.

Chow, Mallet-Paret and Van Vleck [8, 9, 31, 32] *Pattern formation and spatial chaos in spatially discrete evolution equations*

(Actually, Bunimovich might have worked on this)

Friedland [16] *On the entropy of \mathbb{Z}^d subshifts of finite type*

Quas and Trow [41] *Subshifts of multi-dimensional shifts of finite type*

Desai [11] *Subsystem entropy for \mathbb{Z}^d sofic shifts*

Ban and Lin [4, 5] *Patterns generation and transition matrices in multi-dimensional lattice models*

Boyle, Pavlov and Schraudner [6] *Multidimensional sofic shifts without separation and their factors*

Hochman and Meyerovitch [20] *A characterization of the entropies of multi-dimensional shifts of finite type*

Ban, Hu, Lin, and Lin [3], *Verification of mixing properties in two-dimensional shifts of finite type*

Hu and Lin [22] *Nonemptiness problems of plane square tiling with two colors*

Hu and Lin [23], *On spatial entropy of multi-dimensional symbolic dynamical systems*, discuss multi-dimensional shift space for a rectangular spatial entropy which is the limit of growth rate of admissible local patterns on finite rectangular sublattices.

2016-05-04 Predrag Ban, Hu, Lin, and Lin [2], *Zeta functions for two-dimensional shifts of finite type* seems to be a [must read](#), with exhaustive references. The zeta functions of two-dimensional shifts of finite type which generalizes the Artin-Mazur [1] zeta function was given by Lind [25], ([click here](#)) for \mathbb{Z}^2 -action. The rotationally symmetric trace operator is the transition matrix for x -periodic patterns with period n and height 2. The rotational symmetry induces the reduced trace operator, and the zeta function in the x -direction is now a reciprocal of an infinite product of polynomials. The zeta function can be presented in the y -direction and in the coordinates of any unimodular transformation in $GL_2(\mathbb{Z})$. Therefore, there exists a family of zeta functions that are meromorphic extensions of the same analytic function. The Taylor series for these zeta functions at the origin are equal with integer coefficients, yielding a family of identities, which are of interest in number theory.

Their **Example 7.2**

Let $F_2 = \{0, 1\}$ and

$$\mathbb{Z} = \{\phi_{nt} = \phi_{n,t+1} + \phi_{n,t-1} + \phi_{n+1,t} + \phi_{n-1,t} \text{ for all } nt \in \mathbb{Z}^2\}$$

is about the harmonic patterns on square-cross lattice \mathcal{L} studied by F. Ledrappier, *Un champ markovien peut être d'entropie nulle et mélangeant*, C. R. Acad. Sc. Paris Ser. A 287 (1978), 561-562. For us, this is a bit strange - our 'harmonic' value would be $4\phi_{nt}$, not ϕ_{nt} .

2016-10-11 Predrag Boris has explained the strategy of Ban *et al.* [2], approach that he himself has used: one constructs ζ functions for finite periodic domain in one direction, i.e., infinite strip $\mathbb{Z}_{\infty \times L}$ or $\mathbb{Z}_{T \times \infty}$, with a transfer operator generating the other, infinite direction, as in figure 6.1 (b). Those zeta functions are multiplied. The infinite products, a different formula for each direction, describe the same set of admissible patterns, resulting in some unexpected identities.

I find this very unnatural - intelligent zeta should account for all commuting directions democratically.

2020-03-05 Predrag Douglas Lind's [website](#).

Lind [25]: Let $f : X \rightarrow X$ be a homeomorphism of a compact space and $N_n(f)$ denote the number of points in X fixed by f . We assume

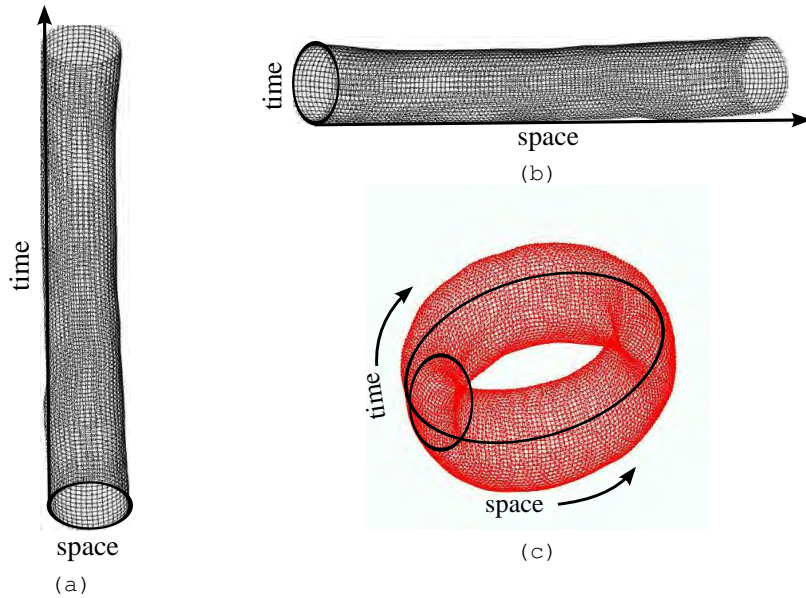


Figure 6.1: (a) A fixed L periodic spatial domain, all t . (b) A fixed T periodic temporal domain, all x . (c) A fixed LT , doubly periodic spatiotemporally invariant 2-torus.

that $N_n(f)$ is finite for all $n \geq 1$. [· · ·] The zeta function has the product formula

$$1/\zeta_{\text{top}}(z) = \prod_p (1 - z^{n_p}) \quad (6.1)$$

where the product is over all finite orbits p of f and n_p denotes the number of points in p .

To compute $e_d(n)$ we use the Hermite normal form of an integer matrix (see ref. [28], Thm. 22.I.).

[10] Mac Duffee [28] *The Theory of Matrices*, (Chelsea, New York, 1956) ([click here](#)); Y. Katznelson, Ergodic automorphisms of T^n are Bernoulli, Israel J. Math. 10 (1971), 186-195.

The following question was suggested to us by David Ruelle:

Problem 7.5. Compute explicitly the thermodynamic zeta function for the 2-dimensional Ising model, where α is the \mathbb{Z}^2 shift action on the space of configurations.

2021-07-28 Predrag Here is a cute “interesting zeta function” over \mathbb{Z} with the product formula, apparently known to Gauss:

$$\prod_n \frac{1}{1 - z^n} = \sum_{\ell} p_{\ell} z^{\ell} \quad (6.2)$$

where p_ℓ of is the number of partitions of ℓ .

2018-10-09 Predrag Lind and Schmidt [26] *Symbolic and algebraic dynamical systems*, ([click here](#)) studies zeta functions for \mathbb{Z}^d actions.

2018-09-02, 2018-10-09 Predrag Einsiedler, Lindenstrauss, Michel and Venkatesh [13] *Distribution of periodic torus orbits and Duke's theorem for cubic fields*: “ We study periodic torus orbits on spaces of lattices. Using the action of the group of adelic points of the underlying tori, we define a natural equivalence relation on these orbits, and show that the equivalence classes become uniformly distributed. This is a cubic analogue of Duke's theorem about the distribution of closed geodesics on the modular surface: suitably interpreted, the ideal classes of a cubic totally real field are equidistributed [...] ”

Homogeneous toral sets do not seem to be defined. They generalize the groupings of compact orbits (I believe these compact orbits are what we call -at this moment- prime tori).

They define two invariants for homogeneous toral sets, *volume* (defined in their eq. (13), measuring how “large” it is) and *discriminant* (measuring its arithmetic complexity). I have no intuition about what this discriminant is in our applications.

The periodic orbits are grouped into equivalence classes, equivalent orbits having the same volume and discriminant. An equivalence class of compact orbits is a *packet*. Compact orbits in the same packet have the same stabilizer and the same discriminant.

2020-12-18 Predrag Espositi and Isola [14] *Distribution of closed orbits for linear automorphisms of tori* (1995) develop zeta functions for d -dimensional tori; then they specialized to D dof symplectic matrices acting on $2D$ -dimensional tori, of which Isola's $d = 2$ is a special case. But I'm confused. I do not think that has to do with lattice zeta functions we seek...

2020-11-22 RSM The November 20, 2020 Matthew Gudorf *Spatiotemporal tiling of the Kuramoto-Sivashinsky system* thesis dissertation defense interests me. At the conceptual level it was already in Pesin & Sinai [37] 1988 *Space-time chaos in the system of weakly interacting hyperbolic systems*, for CML, and in my MacKay [29] *Space-time phases* 2012 lecture notes, but claiming it applies to Kuramoto-Sivashinsky is bold. I suppose it does not fit perfectly, but interesting if it fits approximately.

Is there a paper I can read?

2020-11-22 Predrag to Han: please read MacKay [29] *Space-time phases: Statistical properties of dynamics on large networks* ([click here](#)), Sect. 2.2 *Statistical Phases for Uniformly Hyperbolic Attractors of Finite-Dimensional Deterministic Dynamical Systems* and related, and please take notes here on anything that is related to our project.

2020-12-16 RSM Cf. section 7.2.3 *Uniformly hyperbolic dynamics on networks* in our 2013 LMS lecture notes [29] “Masters of Complexity Science” ([click here](#)).

2020-12-16 Predrag Han Liang and I have been studying your *Space-time phases: Statistical properties of dynamics on large networks* [29], and I was supposed to report back to you. I like the proof of hyperbolicity for the spatiotemporal CML. Other than sect. 9.1 *Chronotopic literature*, this is the closest to our spatiotemporal work.

2020-12-16 RSM Perhaps the analogue of the MM formula that is relevant is the formula on line 4 of p. 436, of which I am proud but it was also found by Bricmont and Kupiainen, and they published before I did.

2020-12-23 Predrag Bricmont and Kupiainen, *High temperature expansions and dynamical systems* [arXiv:chao-dyn/9504015](#): “ We develop a resummed high-temperature expansion for lattice spin systems with long range interactions, in models where the free energy is not, in general, analytic. We establish uniqueness of the Gibbs state and exponential decay of the correlation functions. Then, we apply this expansion to the Perron-Frobenius operator of weakly coupled map lattices.”

They credit D. L. Volevich, *Kinetics of coupled map lattices*, Nonlinearity 4, 37-45 (1991); *The Sinai -Bowen-Ruelle measure for a multidimensional lattice of interacting hyperbolic mappings*, Russ. Acad. Dokl. Math.47, 117-121 (1993); and *Construction of an analogue of Bowen-Ruelle-Sinai measure for a multidimensional lattice of interacting hyperbolic mappings*, Russ. Acad. Math. Sbornik 79, 347-363 (1994).

2020-12-16 Predrag Spatially homogenous lattice models also invariant under discrete space translations were studied by Bunimovich and Sinai [7] in the case when $g(\phi_{nt})$ is a one-dimensional expanding map.

Regarding you “symbol tables” (what we call symbol blocks): the previous examples of $(D+1)$ -dimensional spatiotemporal symbolic dynamics: Pesin and Sinai [37], Bunimovich and Sinai [7], Pethel, Corron and Boltt [38, 39]. In other literature, I noticed that Houlrik [21] gives Bunimovich and Sinai [7] the credit.

The key insight [7, 19] –an insight that applies to coupled-map lattices [38–40], and field theories modeled by them, not only the system considered here– is that a field $X = \{\phi_z\}$ over a d -dimensional spacetime lattice $z \in \mathbb{Z}^d$ has to be described by a corresponding symbol block $M = \{m_z\}$, over the same d -dimensional spacetime lattice $z \in \mathbb{Z}^d$, rather than a 1-dimensional temporal symbol sequence (1.68), as one does when describing a finite coupled “ N -particle” system in the Hamiltonian formalism.

Other than the “symbol tables”, Bunimovich and Sinai [7] (1988) and Pesin and Sinai [37] are profoundly different, nothing to do with the spatiotemporal cat. Bunimovich has heard me talk about it, Sinai not.

As spatiotemporal cat equations are symmetric under interchange of the ‘space’ and the ‘time’ directions, their temporal and spatial dynamics are strongly coupled, corresponding to $\epsilon \approx O(1)$ in (5.1), in contrast to the traditional spatially weakly coupled CML [7].

The conventional CML models start out with chaotic on-site dynamics weakly coupled to neighboring sites, with strong spacetime asymmetry. In order to establish the desired statistical properties of CML, such as the continuity of their SRB measures, refs. [7, 37] and most of the subsequent mathematical literature rely on the structural stability of Anosov automorphisms under small perturbations. Contrast this with the non-perturbative 2-dimensional Gutkin-Osipov [19] *spatiotemporal cat* (18.46).

Unlike the systems studied in ref. [7], spatiotemporal cat cannot be conjugated to a product of non-interacting cat maps; a way to see that is to compare the numbers of invariant 2-tori in the two cases – they differ.

In all other coupled maps literature I am aware of, the starting point is time evolution of a non-interacting particle at each site, with its 1-dimensional temporal symbolic dynamics, with spatial coupling to D spatial neighbors subsequently tacked on. While the spacetime coordinate of site is $(D+1)$ -dimensional, its symbolic dynamics is 1-dimensional.

Your paper I found most eye-opening was the Hill’s formula of [30] *Linear stability of periodic orbits in Lagrangian systems*.

We do not derive the formula the way you did it (ours also works for dissipative systems), but the paper made the light bulb turn on...

Is there something else?

The thing we’ve been struggling with the most, that has kept the paper from a publication is unimodular invariance of the defining cell (Bravais cell) of a lattice (tiling of spacetime) so I have not been able to write down a rational spatiotemporal topological zeta function in terms of prime (non-repeating) 2-tori (spatiotemporal periodic orbits). Should be doable (the Green’s function is elliptic K function), but I just do not get it:

2020-12-16 RSM Yes, neat to consider cat map as a second order recurrence on one variable rather than a first order one on two variables (I hadn’t appreciated the advantage when Vivaldi was talking about it way back then) and then it indeed looks like a discrete field theory and extends naturally to space-time and you can code all solutions by lattices of integers, one for each point in space-time.

In the general “uniformly hyperbolic” situation (in quotes because it is the way to connect with dyn sys, but the point is to escape from time-evolution view, as you do, and consider solutions as being zeroes of some function from states on spatiotemporal lattice to the spatiotemporal lattice and then u hyp just means the derivative of the function has

bounded inverse), expect to be able to code all solutions by some set of allowed symbol tables, via spatiotemporal shadowing (which is just shadowing in the more general context, again having nothing to do with time-evolution). Not sure to what extent I mentioned this in my lecture notes, but perhaps it appears in the article I wrote for Chazottes & Fernandez earlier. I have certainly waved spatiotemporal shadowing around as providing an answer, but never really done it for any particular system. Will think about it.

Will also think about your question of zeta fn for the Gutkin-Osipov CML. It will be a straightforward answer once we have thought of it, but a question of keeping everything straight in one's mind. I'm not clear where your obstacle is. We can count all spatiotemporal periodic solutions and so make a zeta fn; you want to reduce it to an expression in terms of prime ones? or to one in terms of collections of disjoint elementary cycles? (I put elementary in there because graph theorists use closed walk for what you might call a cycle and cycle for what I'm calling an elementary one) "Just" need to work out the spatiotemporal analogue. Maybe I need to wake up fresh tomorrow morning to do it. Or have a whisky now to do it (except I don't have any in the house right now!).

2020-12-17 RSM I found the Percival-Vivaldi [35] paper (having first found their other one [36] from 1987 on the periodic orbits). As I remembered, they do not appear to derive finite-type conditions on their coding. I suspect it is not of finite type. Thus I'd say it is pretty useless, compared to the Adler-Weiss partition.

I wasn't convinced by Percival-Vivaldi [35] as it is not obvious (to me) what are the constraints on the sequence of integers m_t . Do you know? Say we take $\phi_{t+1} - 3\phi_t + \phi_{t-1} = 0 \pmod{1}$, $\phi \in [-1/2, 1/2)$ then we can get $\{-2, -1, 0, 1, 2\}$, but not all sequences of such integers are possible because that would give entropy $\log 5$ whereas it is supposed to be $\log(3 + \sqrt{5})/2$, or $\log(s + \sqrt{(s-2)(s+2)})/2$ in general. There should be a simple finite-type condition. Do you know it?

2020-12-18 Predrag I agree. It's ridiculous, arbitrary frame on the unit torus, contra natura, ignoring stable/unstable manifolds, painful to implement – Dirichlet conditions destroy the time-translational invariance of the lattice. That is why I included figure 2 and table 2 – an impossible number-theoretic problem created by ignoring the well-known generating partition construction. There Vivaldi and Percival got it wrong.

Aside: Nobody listens to me, and in particular Russians, so I had to watch and assist Gutkin and 3 grad students push this pointless torture of a paper. The problem is that quantum chaos crowd profoundly lacks understanding of periodic orbit theory – I wrote a whole book to explain that periodic orbit calculations are general nonlinear coordinate transformation invariant, that one does not need nowhere differentiable probability

measures, to no avail. Russians make it worse by idolizing Sinai and believing that one has to construct explicit, coordinate-dependent generating partitions – that never works except in 3 or so examples which are the only ones they are always taught.

2020-12-17 RSM Do you have a way around it?

2020-12-18 Predrag Yes, we construct the Adler-Weiss generating partition for Percival-Vivaldi 2-configuration map in ChaosBook.org (not polished yet, but for you I've promoted it from internal to publicly readable text): [ChaosBook Example 14.12 Adler-Weiss partition of the cat map state space](#). Our construction is sufficiently clever that my very smart collaborator Gutkin still does not get it:

While Percival and Vivaldi were well aware of Adler-Weiss partitions, they felt that their “coding is less efficient in requiring more symbols, but it has the advantage of linearity.” Our construction demonstrates that one can have both: an Adler-Weiss generating cat map partition, and a linear code. The only difference from the Percival-Vivaldi formulation [35] is that one trades the single unit-square cover of the torus of (1.101) for the dynamically intrinsic, two-rectangles cover, but the effect is magic - now every infinite walk on the transition graph corresponds to a unique admissible orbit $\{\phi_t\}$, and the transition graph generates all admissible itineraries $\{m_t\}$.

But the Hamiltonian formulation is stupid. The great advantage of the Lagrangian, temporal lattice formulation is that the fundamental fact yields the number of periodic solutions and the zeta function without any explicit time-evolution generating partition. I believe that explicit time-evolution generating partitions are impossible to generalize to spatial lattices evolving in time.

2020-12-17 RSM You cited Isola [24] for the ζ -function for the cat map but I thought people like Manning had calculated it earlier. I looked up his 1971 paper on rationality of zeta for Axiom A and see he cites Smale's 1967 review for toral automorphisms.

2020-12-18 Predrag I doubt it. In his 1971 *Axiom A diffeomorphisms have rational zeta function* [33] he explains rationality of topological (orbit counting) of Smale's school zeta functions in terms of ‘Manning multiples’, what I understand as inclusion-exclusion principle (when sets share boundaries, boundary has to be –recursively- subtracted not to be overcounted).

It is easy enough to construct, but I have not seen cat map zeta function earlier than the one written down by Isola. Will change the citation if we find an earlier one.

2020-12-18 RSM OK, you map the Adler-Weiss partition into (x, x') coordinates and then reduce by translation into that fundamental domain instead of the standard one. Got it. I thought you had some magic for the

standard fundamental domain. I agree the tedious thing about counting periodic orbits of toral automorphisms is the ambiguity of coding for orbits on the partition boundaries. A cute thing is that if you consider the map on a sphere (with 4 conical points) induced by quotienting by reflection through 0,0 then you get exactly $\text{tr } A^n$ fixed points of A^n , see Llibre and MacKay [27] *Pseudo-Anosov homeomorphisms on a sphere with four punctures have all periods* (1992).

2020-12-18 Predrag A very cute paper, but it will not help me here, will it?

2020-12-18 RSM OK, I might look up Pollicott on zeta fns for toral autos because I think he has some lecture notes in which he gives history.

On your big question, can I phrase it as how many orbits under $\text{SL}_2(\mathbb{Z})$ are there for its action on integer parallelograms of given area (based at 0)? Equivalently, how many sublattices of given area are there in \mathbb{Z}^2 ?

2020-12-18 Predrag It's the first step, a warm-up exercise - we all can do it. But then you have to count the number of invariant 2-tori that live on each parallelogram. The paper explains that we know how to do it, but if we had the zeta functions, it would generate all these numbers.

It could be that the sensible zeta function is a double series in (z_1^L, z_2^T) , in which case we want to count integer parallelograms of periods (L, T) , not lump them into areas $A = LT$, and have a zeta function which is a series in single z^A .

2020-12-18 RSM It is the sort of thing Marklof probably knows. But we can think about it too. For area 1 I get 1 because I can map any unit parallelogram to the unit square by the inverse of the matrix representing its sides, which is in $\text{SL}_2(\mathbb{Z})$. For area 2, I think I get two, by observing that to have area 2, the matrix has one row or column divisible by 2 and then dividing that out and using its inverse to map to one of the two standard rectangles. For area 3 I didn't get an answer yet. But I wonder if it is something trivial like the area. This would fit with your fundamental fact.

2020-12-18 RSM I see I was wrong in getting only two orbits of parallelograms for area 2. There's also the diamond. I must have missed something with the rows and columns calculation (which admittedly I did while in bed)! Ah yes, I remember I did see one more solution and then forgot it by the time I go up. Here it is done properly:

Number of sublattices of \mathbb{Z}^2 . "I would like to count the number of sublattices \mathcal{L} of \mathbb{Z}^2 of index $n = |\det \mathcal{L}|$."

2020-12-19 Predrag This example lists $\det \mathcal{L} = 2$ parallelograms as (columns are their basis vectors)

$$\begin{bmatrix} 2 & 0 \\ 0 & 1 \end{bmatrix}, \begin{bmatrix} 0 & 1 \\ 2 & 0 \end{bmatrix}, \begin{bmatrix} 1 & -1 \\ 1 & 1 \end{bmatrix}. \quad (6.3)$$

The third one is not in the Hermite normal form, but presumably a unimodular transformation (have not checked it) brings it to the upper diagonal form $[2 \times 1]_1$ invariant 2-torus that we use.

This example counts parallelograms under distinct translations (must make sure that each unimodular orbit is counted only once). Guido, Isola and Lapidus [17] (or [ChaosBook chapter 25 Discrete symmetry factorization](#)) count parallelograms distinct under reflections.

I think counting $\det \mathcal{L} = A$ parallelograms is easy. What we need is a generating function that counts numbers of invariant 2-tori, and the related zeta that counts the numbers of prime invariant 2-tori.

2020-12-18 Predrag If it is any help, for small areas answers are listed in [table 2](#).

2020-12-18 RSM The question is how to make a zeta fn from these counts. Take simplest case of Bernoulli on s symbols. For each area n , we have $T_n = \sum d$ over divisors of n , sublattices. Each can be populated by s^n patterns (not worrying about patterns with a smaller lattice), so there are $s^n T_n$ patterns with an area n . I suppose it is natural to divide by n because we could move the origin to any of the n points. So propose $\zeta(z) = \exp \sum_n s^n z^n T_n / n$ for this example. Need to look up some number theory to simplify this but I think it is some standard formula.

2020-12-18 RSM Ah, I see from (86) of your draft paper that I have made a mistake. Yes, have identified my error now. Here is [a useful page](#). So, OK, number of Bravais lattices has zeta fn (with respect to area) = $\prod_L (1 - z^L)$. But you already knew this. Your question at the bottom of p. 21 is to count prime lattices or perhaps the more subtle one of counting prime periodic patterns taking the finite-type conditions of spatiotemporal cat into account.

2020-12-19 RSM If define $\zeta(z) = \exp \sum_n z^n / n N_n$ where N_n is the number of lattice states that have a period parallelogram of area n , and we let prime patterns be ones that are not repetitions of ones with a smaller area, and regarded as equivalent if differ by a translation, then I get $\zeta(z) = \prod_\gamma F(z^{|\gamma|})$ over orbits γ , where $F(x) = \prod_m (1 - x^m)^{-1/m}$. Not sure if F can be simplified.

2020-12-16 Predrag We have not been able to make that one work. Square lattice is separable, so one hopes for something like that. The problem is that in the addition to double periodicity, there is a third integer – parallelogram come with different tilts (screw bc's). Some details are towards the end of the current draft [10], Predrag Cvitanović and Han Liang *Spatiotemporal cat: A chaotic field theory* rough draft, (November 2020) on [spatiotemporal homemade](#).

2020-12-20 RSM I have some thoughts about the 2D ζ function, in particular the question of how to generalise $\det(I - zW)$ from finite type conditions

(or more generally weights W) for nearest nbr chains to finite type conditions (or more generally weights from cliques) for 2D lattices. I think it proceeds in same way as I did for Gibbs measures for CML.

2020-09-24, 2020-12-16 Predrag My thoughts in that directions (that is in my spatiotemporal cat talk, and in this blog, see (5.248), (13.70), (13.73), (13.84)) are that for the 2-dimensional spatiotemporal cat [10, 18]

$$\phi_{n,t+1} + \phi_{n,t-1} - 2s \phi_{nt} + \phi_{n+1,t} + \phi_{n-1,t} = -m_{nt}, \quad m_{nt} \in \mathcal{A}, \quad (6.4)$$

with alphabet

$$\mathcal{A} = \{-3, -2, -1, 0, \dots, \mu^2 + 1, \mu^2 + 2, \mu^2 + 3\}, \quad (6.5)$$

and the Yukawa mass squared of the scalar field ϕ

$$\mu^2 = 2(s - 2). \quad (6.6)$$

The ζ function has to satisfy all spatiotemporal symmetries of the square lattice (4.188)

$$C_{4v} = D_4 = \{E, C_{4z}^+, C_{4z}^-, C_{2z}, \sigma_y, \sigma_x, \sigma_a, \sigma_b\}. \quad (6.7)$$

See [ChaosBook sect. A25.1](#).

In the international crystallographic notation, this square lattice space point group is referred to as $p4mm$ [12].

2020-12-16 Predrag The simplest rational ζ function that satisfies these symmetries is of form

$$1/\zeta_{\text{top}}(z_1, z_2) = d(s)/d(2) = 1 - \mu^2/d(2), \quad (6.8)$$

where

$$d(s) = z_1 + z_2 - 2s + z_1^{-1} + z_2^{-1} \quad (6.9)$$

$d(s)$ is the Z-transform (discrete Laplace transform) of (6.4). Fischer *et al.* [15] call this the *characteristic function*, a somewhat over-abused nothing-saying appellation.

Anything more complicated would be a disappointment :)

2020-12-20 Predrag Its massless $\mu^2 = 0$, Poisson equation value $d(2)$ is the Z-transform of the $d = 2$ lattice Laplacian. $d(s)$ can be written in a D_4 -symmetric form

$$\begin{aligned} d(s) &= (1 - \Lambda z_1)(1/z_1 - 1/\Lambda) + (1 - \Lambda z_2)(1/z_2 - 1/\Lambda) \\ d(2) &= (1 - z_1)(1/z_1 - 1) + (1 - z_2)(1/z_2 - 1). \end{aligned} \quad (6.10)$$

Here $(\Lambda, 1/\Lambda)$ are the roots of the $d = 1$ characteristic equation

$$\Lambda^2 - s\Lambda + 1 = 0, \quad (6.11)$$

which, for $|s| > 2$, has two real roots $\{\Lambda, \Lambda^{-1}\}$,

$$\Lambda = \frac{1}{2}(s + \sqrt{(s-2)(s+2)}), \quad (6.12)$$

$$\Lambda = \frac{1}{2}(\mu^2 + 2 + \mu^2 \sqrt{1 + \left(\frac{2}{\mu}\right)^2}), \quad (6.13)$$

$$s = \Lambda + \Lambda^{-1} = e^\lambda + e^{-\lambda} = 2 \cosh \lambda, \quad \lambda > 0. \quad (6.14)$$

Derivatives, integrations with respect to the parameter (z_1, z_2) , should relate this to the numbers of lattice states generating function, but Han, my graduate student, tells me that does not work. Perhaps, in the spirit of Schwinger and Feynman ‘tricks’ derivatives, integrations with respect to the stretching parameter s or squared mass μ^2 do the job.

Decomposition (6.10) is dodgy - in higher dimensions there are other eigenvalues than (6.12).

2020-12-17 RSM I found [...] Percival-Vivaldi [35] [...] see above [...] There should be a simple finite-type condition. Do you know it?

2CB

2020-12-20 Predrag As for the cat map, we split the $\mu^2 + 7$ letter alphabet $\mathcal{A} = \mathcal{A}_0 \cup \mathcal{A}_1$ into the interior \mathcal{A}_0 and exterior \mathcal{A}_1 alphabets [18]

$$\mathcal{A}_0 = \{0, \dots, \mu^2\}, \quad \mathcal{A}_1 = \{-3, -2, -1\} \cup \{\mu^2 + 1, \mu^2 + 2, \mu^2 + 3\}. \quad (6.15)$$

For example, for $\mu^2 = 1$ (ie, $s = 5/2$) the interior, respectively exterior alphabets are

$$\mathcal{A}_0 = \{0, 1\}, \quad \mathcal{A}_1 = \{-3, -2, -1\} \cup \{2, 3, 4\}. \quad (6.16)$$

If all $m_z \in M$ belong to \mathcal{A}_0 , M is admissible, i.e., $\mathcal{A}_0^{\mathbb{Z}^2}$ is a full shift [18]. All grammar rules involve exterior alphabet \mathcal{A}_1 . I do not know whether there is a finite grammar, or the grammar is the infinite one investigated by Gutkin et al. [18]. My claim is that it does not matter, as we know how to count all $[L \times T]_S$, and for each we can read off all admissible M by listing all integer points within the \mathcal{J}_M fundamental parallelepiped.

Curiously, even the Poisson $\mu = 0$ case looks chaotic, numerically (though how would our graduate students notice logarithmic corrections due to the 0-mode?), see figure 5(c) of Gutkin et al. [18]. That presumably arises from the intersection set (the boundary) of the (4.189) fundamental domain and its reflection.

References

- [1] M. Artin and B. Mazur, “On periodic points”, Ann. Math. 81, 82–99 (1965).

- [2] J.-C. Ban, W.-G. Hu, S.-S. Lin, and Y.-H. Lin, *Zeta Functions for Two-dimensional Shifts of Finite Type*, Vol. 221, Memoirs Amer. Math. Soc. (Amer. Math. Soc., Providence RI, 2013).
- [3] J.-C. Ban, W.-G. Hu, S.-S. Lin, and Y.-H. Lin, *Verification of mixing properties in two-dimensional shifts of finite type*, 2015.
- [4] J.-C. Ban and S.-S. Lin, “Patterns generation and transition matrices in multi-dimensional lattice models”, *Discrete Continuous Dyn. Syst. Ser. A* **13**, 637–658 (2005).
- [5] J.-C. Ban, S.-S. Lin, and Y.-H. Lin, “Patterns generation and spatial entropy in two-dimensional lattice models”, *Asian J. Math.* **11**, 497–534 (2007).
- [6] M. Boyle, R. Pavlov, and M. Schraudner, “Multidimensional sofic shifts without separation and their factors”, *Trans. Amer. Math. Soc.* **362**, 4617–4653 (2010).
- [7] L. A. Bunimovich and Y. G. Sinai, “Spacetime chaos in coupled map lattices”, *Nonlinearity* **1**, 491 (1988).
- [8] S.-N. Chow, J. Mallet-Paret, and W. Shen, “Traveling waves in lattice dynamical systems”, *J. Diff. Equ.* **149**, 248–291 (1998).
- [9] S.-N. Chow, J. Mallet-Paret, and E. S. Van Vleck, “Pattern formation and spatial chaos in spatially discrete evolution equations”, *Random Comput. Dynam.* **4**, 109–178 (1996).
- [10] P. Cvitanović and H. Liang, *Spatiotemporal cat: A chaotic field theory*, In preparation, 2021.
- [11] A. Desai, “Subsystem entropy for Z^d sofic shifts”, *Indag. Math.* **17**, 353–359 (2006).
- [12] M. S. Dresselhaus, G. Dresselhaus, and A. Jorio, *Group Theory: Application to the Physics of Condensed Matter* (Springer, New York, 2007).
- [13] M. Einsiedler, E. Lindenstrauss, P. Michel, and A. Venkatesh, “Distribution of periodic torus orbits and Duke’s theorem for cubic fields”, *Ann. Math.* **173**, 815–885 (2011).
- [14] M. D. Espositi and S. Isola, “Distribution of closed orbits for linear automorphisms of tori”, *Nonlinearity* **8**, 827–842 (1995).
- [15] D. Fischer, G. Golub, O. Hald, C. Leiva, and O. Widlund, “On Fourier-Toeplitz methods for separable elliptic problems”, *Math. Comput.* **28**, 349–349 (1974).
- [16] S. Friedland, “On the entropy of Z^d subshifts of finite type”, *Linear Algebra Appl.* **252**, 199–220 (1997).
- [17] D. Guido, T. Isola, and M. L. Lapidus, “Ihara zeta functions for periodic simple graphs”, in *C*-algebras and Elliptic Theory II*, edited by D. Burghelea, R. Melrose, A. S. Mishchenko, and E. V. Troitsky (Birkhäuser, Basel, 2008), pp. 103–121.

- [18] B. Gutkin, L. Han, R. Jafari, A. K. Saremi, and P. Cvitanović, “Linear encoding of the spatiotemporal cat map”, *Nonlinearity* **34**, 2800–2836 (2021).
- [19] B. Gutkin and V. Osipov, “Classical foundations of many-particle quantum chaos”, *Nonlinearity* **29**, 325–356 (2016).
- [20] M. Hochman and T. Meyerovitch, “A characterization of the entropies of multidimensional shifts of finite type”, *Ann. Math.* **171**, 2011–2038 (2010).
- [21] J. M. Houlrik, “Periodic orbits in a two-variable coupled map”, *Chaos* **2**, 323–327 (1992).
- [22] W.-G. Hu and S.-S. Lin, “Nonemptiness problems of plane square tiling with two colors”, *Proc. Amer. Math. Soc.* **139**, 1045–1059 (2011).
- [23] W.-G. Hu and S.-S. Lin, “On spatial entropy of multi-dimensional symbolic dynamical systems”, *Discrete Continuous Dyn. Syst. Ser. A* **36**, 3705–3717 (2016).
- [24] S. Isola, “ ζ -functions and distribution of periodic orbits of toral automorphisms”, *Europhys. Lett.* **11**, 517–522 (1990).
- [25] D. A. Lind, “A zeta function for Z^d -actions”, in *Ergodic Theory of Z^d Actions*, edited by M. Pollicott and K. Schmidt (Cambridge Univ. Press, 1996), pp. 433–450.
- [26] D. Lind and K. Schmidt, “Symbolic and algebraic dynamical systems”, in *Handbook of Dynamical Systems*, Vol. 1, edited by B. Hasselblatt and A. Katok (Elsevier, New York, 2002), pp. 765–812.
- [27] J. Llibre and R. S. MacKay, “Pseudo-Anosov homeomorphisms on a sphere with four punctures have all periods”, *Math. Proc. Cambridge Philos. Soc.* **112**, 539–549 (1992).
- [28] C. C. Mac Duffee, *The Theory of Matrices* (Springer, Berlin, 1933).
- [29] R. S. MacKay, “Space-time phases: Statistical properties of dynamics on large networks, The Warwick Master’s Course”, in *Complexity Science*, edited by R. Ball, V. Kolokoltsov, and R. S. MacKay (Cambridge Univ. Press, Cambridge UK, 2013).
- [30] R. S. MacKay and J. D. Meiss, “Linear stability of periodic orbits in Lagrangian systems”, *Phys. Lett. A* **98**, 92–94 (1983).
- [31] J. Mallet-Paret and S. N. Chow, “Pattern formation and spatial chaos in lattice dynamical systems. I”, *IEEE Trans. Circuits Systems I Fund. Theory Appl.* **42**, 746–751 (1995).
- [32] J. Mallet-Paret and S. N. Chow, “Pattern formation and spatial chaos in lattice dynamical systems. II”, *IEEE Trans. Circuits Systems I Fund. Theory Appl.* **42**, 752–756 (1995).
- [33] A. Manning, “Axiom A diffeomorphisms have rational zeta function”, *Bull. London Math. Soc.* **3**, 215–220 (1971).

- [34] R. Miles and T. Ward, “The dynamical zeta function for commuting automorphisms of zero-dimensional groups”, *Ergod. Th. & Dynam. Sys.* **38**, 1564–1587 (2016).
- [35] I. Percival and F. Vivaldi, “A linear code for the sawtooth and cat maps”, *Physica D* **27**, 373–386 (1987).
- [36] I. Percival and F. Vivaldi, “Arithmetical properties of strongly chaotic motions”, *Physica D* **25**, 105–130 (1987).
- [37] Y. B. Pesin and Y. G. Sinai, “Space-time chaos in the system of weakly interacting hyperbolic systems”, *J. Geom. Phys.* **5**, 483–492 (1988).
- [38] S. D. Pethel, N. J. Corron, and E. Boltt, “Symbolic dynamics of coupled map lattices”, *Phys. Rev. Lett.* **96**, 034105 (2006).
- [39] S. D. Pethel, N. J. Corron, and E. Boltt, “Deconstructing spatiotemporal chaos using local symbolic dynamics”, *Phys. Rev. Lett.* **99**, 214101 (2007).
- [40] A. Politi and A. Torcini, “Towards a statistical mechanics of spatiotemporal chaos”, *Phys. Rev. Lett.* **69**, 3421–3424 (1992).
- [41] A. N. Quas and P. B. Trow, “Subshifts of multi-dimensional shifts of finite type”, *Ergod. Theor. Dynam. Syst.* **20**, 859–874 (2000).
- [42] C. G. J. Roettger, “Periodic points classify a family of markov shifts”, *J. Number Theory* **113**, 69–83 (2005).
- [43] T. Ward, “Automorphisms of Z^d -subshifts of finite type”, *Indag. Math.* **5**, 495–504 (1994).
- [44] T. B. Ward, “An algebraic obstruction to isomorphism of Markov shifts with group alphabets”, *Bull. London Math. Soc.* **25**, 240–246 (1993).
- [45] T. Ward and R. Miles, “A directional uniformity of periodic point distribution and mixing”, *Discrete Continuous Dyn. Syst.* **30**, 1181–1189 (2011).
- [46] T. Ward and R. Miles, “Directional uniformities, periodic points, and entropy”, *Discrete Continuous Dyn. Syst. Ser. B* **20**, 3525–3545 (2015).

Chapter 7

Spatiotemporal stability

7.1 Temporal lattice

Assume that a periodic orbit $x(T_p + t) = x(t)$ of a continuous time flow $\dot{x} = v(x)$ is known ‘numerically exactly’, that is to say, to arbitrary (but not infinite) precision. One way to present the solution is to give a single point $x(0)$ in the orbit, and let the reader reconstruct the orbit p by integrating forward in time, $x(t) = f^t(x(0))$, $t \in [0, T_p]$.

However, for a linearly unstable periodic orbit a single point does not suffice to present the orbit, because there is always a finite ‘Lyapunov time’ t_{Lyap} beyond which $f^t(x(0))$ has lost all memory of the periodic orbit p . This problem is particularly severe in searches for ‘exact coherent structures’ embedded in turbulence, where even the shortest period solutions have to be computed to the (for everyday fluid dynamics excessive) machine precision [22, 23, 60] in order to complete the first return to the initial state.

Instead of relying on forward-in-time numerical integration, *global methods* for finding periodic orbits [7] view them as equations for the vector fields \dot{x} on spaces of closed curves. In numerical implementations one discretizes the periodic orbit p into sufficiently many short segments [7, 13, 14, 16, 24], and lists a point for each segment

$$p = (x_1, x_2, \dots, x_{n_p}). \quad (7.1)$$

For a d -dimensional discrete time map f obtained by cutting the flow by a set of Poincaré sections, with the periodic orbit p of discrete period n_p , every segment can be reconstructed by a short time integration, and satisfies

$$x_{k+1} = f(x_k), \quad (7.2)$$

to high accuracy, as for sufficiently short times the exponential instabilities are numerically controllable.

So, how accurate is such an orbit, i.e., how fast do errors grow for such globally specified orbit? In numerical work we know the cycle points only to a

finite precision

$$\hat{p} = (\hat{x}_1, \hat{x}_2, \dots, \hat{x}_{n_p}), \quad \hat{x}_k = x_k + \Delta x_k, \quad (7.3)$$

where x_k are the exact periodic orbit points. Define the error field by $F(\hat{p}) = f(\hat{p}) - \sigma\hat{p}$, an operator which compares the forward map of every point in \hat{p} with the next point $\sigma\hat{p}$, a $(n_p \times d)$ -dimensional vector field obtained by stacking n_p state space points \hat{x}_k

$$F(\hat{x}) = F \begin{pmatrix} \hat{x}_1 \\ \hat{x}_2 \\ \dots \\ \hat{x}_{n_p} \end{pmatrix} = \begin{pmatrix} \hat{x}_1 - \hat{f}_{n_p} \\ \hat{x}_2 - \hat{f}_1 \\ \dots \\ \hat{x}_{n_p} - \hat{f}_{n_p-1} \end{pmatrix}, \quad \hat{f}_k = f(\hat{x}_k), \quad (7.4)$$

which measures the misalignment of every finite forward-in-time segment $f(\hat{x})_k$ with the next listed point \hat{x}_{k+1} on the periodic orbit.

By (7.2), the exact discretized cycle (7.1) is a zero of this vector field, $F(x) = 0$. Assuming that the d -dimensional vectors Δx_k are small in magnitude, and Taylor expanding the one discrete time-step map f to linear order around the exact solution,

$$f(x_t + \Delta x_t) = x_{t+1} + \mathbb{J}_t \Delta x + (\dots),$$

where

$$[\mathbb{J}_t]_{ij} = \frac{\partial f_i(x_t)}{\partial x_j}, \quad t = (1, 2, \dots, n_p), \quad i, j = (1, 2, \dots, d) \quad (7.5)$$

one finds that the neighborhood of entire cycle p is linearly deformed by the $[n_p d \times n_p d]$ orbit Jacobian matrix

$$\Delta x' = \mathcal{J}(x) \Delta x, \quad \mathcal{J}_{ij}(x) = \frac{\partial F(x)_i}{\partial x_j}, \quad (7.6)$$

with

$$\mathcal{J} = 1 - \sigma \mathbb{J},$$

the one discrete time-step temporal $[d \times d]$ diagonal Jacobian matrix \mathbb{J} evaluated on the entire cycle p , and σ the shift matrix

$$\sigma = \begin{pmatrix} 0 & & & \mathbf{1} \\ \mathbf{1} & 0 & & \\ & \mathbf{1} & 0 & \\ & & \mathbf{1} & \\ & & & \ddots & 0 \\ & & & & \mathbf{1} & 0 \end{pmatrix}, \quad \mathbb{J} = \begin{pmatrix} \mathbb{J}_1 & & & & \\ & \mathbb{J}_2 & & & \\ & & \mathbb{J}_3 & & \\ & & & \ddots & \\ & & & & \mathbb{J}_{n_p-1} \\ & & & & & \mathbb{J}_{n_p} \end{pmatrix}, \quad (7.7)$$

with $\mathbf{1}$ in the upper right corner assuring periodicity, $\sigma^{n_p} = \mathbf{1}$.¹

Next, we address two questions: (i) how is the high-dimensional orbit Jacobian matrix \mathcal{J} related to the temporal $[d \times d]$ Jacobian matrix \mathbb{J} ? and (ii) how does one evaluate the orbit Jacobian matrix \mathcal{J} ?

¹Predrag 2019-10-10: this is σ^{-1} shift operator as defined in ChaosBook.

7.1.1 Second-order difference equation

²

2CB

A second-order difference equation with constant coefficients has the form

$$x_{t+2} + p_1 x_{t+1} + p_2 x_t = 0 \quad (7.8)$$

Let $x_{0,t} = x_t$, $x_{1,t} = x_{t+1}$, and rewrite this as a pair of coupled first-order difference equations

$$\begin{aligned} \mathbf{x}_{t+1} &= A \mathbf{x}_t, & \mathbf{x}_t &= (x_{0,t}, x_{1,t})^\top \\ A &= \begin{pmatrix} 0 & 1 \\ -p_2 & -p_1 \end{pmatrix}. \end{aligned} \quad (7.9)$$

The characteristic equation

$$\lambda^2 + p_1 \lambda + p_2 = 0 \quad (7.10)$$

can be obtained by substitution $x_t = \lambda^n$ into the two-term recursion (7.8).

If $\lambda_1 \neq \lambda_2$, λ_j real, then the solution of (7.8) is

$$x_t = c_1 \lambda_1^t + c_2 \lambda_2^t. \quad (7.11)$$

If $\lambda_1 = \lambda_2 = \lambda$, then the solution is

$$x_t = c_1 \lambda^t + c_2 t \lambda^t. \quad (7.12)$$

If $\lambda_1 = \alpha + i\beta$, $\lambda_2 = \alpha - i\beta$, then the solution is

$$x_t = |\lambda|^t (c_1 \cos t\omega + c_2 \sin t\omega), \quad (7.13)$$

where $\omega = \arctan(\beta/\alpha)$. To solve such second-order difference equation, one has to specify initial conditions, for example $x_0 = 1, x_1 = 0$.

(Based on Elaydi [20])

7.1.2 Third-order difference equation

One can always reformulate an k -term recursion relation (5.206) as a set of k coupled first-order difference equations (delay equations). For example, one can rewrite the three-term recursion relation (third-order difference equation)

$$x_{t+3} + p_1 x_{t+2} + p_2 x_{t+1} + p_3 x_t = 0 \quad (7.14)$$

as three coupled first-order difference equations

$$\begin{aligned} x_{0,t+1} &= x_{1,t}, \\ x_{1,t+1} &= x_{2,t}, \\ x_{2,t+1} &= -p_3 x_{0,t} - p_2 x_{1,t} - p_1 x_{2,t}. \end{aligned} \quad (7.15)$$

²Predrag 2020-12-15: Transfer to ChaosBook.org. Once incorporated, remove from here)

where $x_{0,t} = x_t$, $x_{1,t} = x_{t+1}$, $x_{2,t} = x_{t+2}$. Compactly

$$\begin{aligned}\mathbf{X}_{t+1} &= A \mathbf{X}_t, \quad \mathbf{X}_t = (x_{0,t}, x_{1,t}, x_{2,t})^\top \\ A &= \begin{pmatrix} 0 & 1 & 0 \\ 0 & 0 & 1 \\ -p_3 & -p_2 & -p_1 \end{pmatrix}. \end{aligned}\tag{7.16}$$

The eigenvalues of A are the characteristic roots of (7.14), see (5.207) and (5.248).

The discrete time derivative of a lattice state \mathbf{X} evaluated at the lattice site t is given by the *difference operator*

$$\dot{\mathbf{X}}_t = \left[\frac{\partial \mathbf{X}}{\partial t} \right]_t = \frac{x_t - x_{t-1}}{\Delta t} \tag{7.17}$$

Eq. (7.16) can be viewed as a time-discretized, first-order ODE dynamical system

$$\dot{\mathbf{X}} = v(\mathbf{X}), \tag{7.18}$$

with the time increment set to $\Delta t = 1$

(Based on Elaydi [19])

7.1.3 Hill's formula for a first-order system

³

Consider an period- n lattice state X_p , with d fields $\{x_{t,1}, x_{t,2}, \dots, x_{t,d}\}$ on each temporal lattice site t satisfying the condition

$$x_t - f(x_{t-1}) = 0, \quad t = 1, 2, \dots, n, \quad (7.19)$$

where $f(x)$ is a d -dimensional function. A deviation ΔX from X_p then satisfies the linearized condition

$$\Delta x_t - \mathbb{J}_{t-1} \Delta x_{t-1} = 0, \quad (\mathbb{J}_t)_{ij} = \left. \frac{\partial f(x)_i}{\partial x_j} \right|_{x_j=x_{t,j}}, \quad (7.20)$$

where \mathbb{J}_t is the 1-time step $[d \times d]$ Jacobian matrix.

It suffices to work out a temporal period $n = 3$ example to understand the calculation for any period. In terms of the $[3d \times 3d]$ matrix shift matrix r , the orbit Jacobian matrix can be written as

$$\mathcal{J}_p = \mathbf{1} - r^{-1} \mathbb{J}, \quad r^{-1} = \begin{bmatrix} 0 & 0 & \mathbf{1}_d \\ \mathbf{1}_d & 0 & 0 \\ 0 & \mathbf{1}_d & 0 \end{bmatrix}, \quad \mathbb{J} = \begin{bmatrix} \mathbb{J}_1 & 0 & 0 \\ 0 & \mathbb{J}_2 & 0 \\ 0 & 0 & \mathbb{J}_3 \end{bmatrix}, \quad (7.21)$$

where $\mathbf{1}_d$ is the d -dimensional identity matrix. Next, note that

$$(r^{-1} \mathbb{J})^2 = r^{-2} \begin{bmatrix} \mathbb{J}_2 \mathbb{J}_1 & 0 & 0 \\ 0 & \mathbb{J}_3 \mathbb{J}_2 & 0 \\ 0 & 0 & \mathbb{J}_1 \mathbb{J}_3 \end{bmatrix}, \quad (r^{-1} \mathbb{J})^3 = \begin{bmatrix} \mathbb{J}_2 \mathbb{J}_1 \mathbb{J}_3 & 0 & 0 \\ 0 & \mathbb{J}_3 \mathbb{J}_2 \mathbb{J}_1 & 0 \\ 0 & 0 & \mathbb{J}_1 \mathbb{J}_3 \mathbb{J}_2 \end{bmatrix},$$

as $r^{-3} = \mathbf{1}$. Likewise, as $r^n = \mathbf{1}$ for any period n , the trace of $[nd \times nd]$ matrix

$$\text{tr}(r^{-1} \mathbb{J})^k = \delta_{k,n} n \text{tr} \mathbb{J}_p^r, \quad \mathbb{J}_p = \mathbb{J}_n \mathbb{J}_{n-1} \cdots \mathbb{J}_1$$

is non-vanishing only if k is a multiple of n , with \mathbb{J}_p the forward-in-time $[d \times d]$ Jacobian matrix of the periodic orbit p .

Now we can evaluate the Hill determinant (5.203) by expanding

$$\begin{aligned} \ln \text{Det}(\mathcal{J}_p) &= \text{tr} \ln(\mathbf{1} - r^{-1} \mathbb{J}) = - \sum_{k=1}^{\infty} \frac{1}{k} \text{tr}(r^{-1} \mathbb{J})^k \\ &= -\text{tr} \sum_{r=1}^{\infty} \frac{1}{r} \mathbb{J}_p^r = \ln \det(\mathbf{1}_d - \mathbb{J}_p). \end{aligned} \quad (7.22)$$

The Hill determinant for a 2-term difference equation (3.100) on a temporal lattice

$$\text{Det}(\mathcal{J}_p) = \det(\mathbf{1}_d - \mathbb{J}_p)$$

³Predrag 2020-12-15: Transfer to CL18.tex. Once incorporated, remove from here - too much duplication, as is.)

thus relates the global orbit stability to the Floquet, temporal evolution stability. In the temporal Bernoulli case, the field x_t is a scalar, and the 1-time step $[1 \times 1]$ time-evolution Jacobian matrix (7.20) at every lattice point t is simply $\mathbb{J}_t = s$, so

$$N_n = |\text{Det } \mathcal{J}| = s^n - 1, \quad (7.23)$$

in agreement with the time-evolution count.

7.1.4 Hill's formula for a second-order system

⁴

Consider an period- n lattice state X_p , with d fields $\{x_{t,1}, x_{t,2}, \dots, x_{t,d}\}$ on each temporal lattice site t satisfying the condition

$$x_{t+1} - f(x_{t-1}) + x_{t-1} = 0, \quad t = 1, 2, \dots, n, \quad (7.24)$$

where $f(x)$ is a d -dimensional function.

Consider one-dimensional Schrödinger equation [27, 29, 46, 51], $H = -d^2/dx^2 + V(x)$ with $V(x)$ almost periodic and the discrete (= tight binding) analog, i.e., the doubly infinite Jacobi matrix

$$h_{ij} = \delta_{i,j+1} + V_i \delta_{i,j} + \delta_{i,j-1} \quad (7.25)$$

with V_n almost periodic on the integers.

A deviation ΔX from X_p then satisfies the linearized condition

$$\Delta x_t - \mathbb{J}_{t-1} \Delta x_{t-1} = 0, \quad (\mathbb{J}_t)_{ij} = \left. \frac{\partial f(x)_i}{\partial x_j} \right|_{x_j=x_{t,j}}, \quad (7.26)$$

where \mathbb{J}_t is the two-configuration $[d \times d]$ Jacobian matrix.

in our notation (13.109) is written as (1.118)

$$x_{\ell+1} - s_\ell x_\ell + x_{\ell-1} = -s_\ell, \quad (7.27)$$

He, as everybody else, sooner or later, rewrites (13.112) in the “Percival-Vivaldi” two-configuration representation’ [29, 47] matrix J (1.5),

$$\begin{bmatrix} \Delta\phi_t \\ \Delta\phi_{t+1} \end{bmatrix} = \begin{bmatrix} 0 & \mathbf{1}_d \\ -\mathbf{1}_d & \mathbb{J}_t \end{bmatrix} \begin{bmatrix} \Delta\phi_{t-1} \\ \Delta\phi_t \end{bmatrix}. \quad (7.28)$$

(note ‘upside-down’ 2D vector), and concerns himself with the rational, energy $\text{tr } J^m < 2$, oscillatory case.

Note, it’s only about the order of recurrence, nobody says the systems should be Hamiltonian / Lagrangian, works for dissipative systems as well.

A deviation ΔX from X_p then satisfies the linearized condition

$$\Delta x_t - \mathbb{J}_{t-1} \Delta x_{t-1} = 0, \quad (\mathbb{J}_t)_{ij} = \left. \frac{\partial f(x)_i}{\partial x_j} \right|_{x_j=x_{t,j}}, \quad (7.29)$$

where \mathbb{J}_t is the two-configuration $[d \times d]$ Jacobian matrix.

It suffices to work out a temporal period $n = 3$ example to understand the calculation for any period. In terms of the $[3d \times 3d]$ matrix shift matrix r , the orbit Jacobian matrix can be written as

$$\mathcal{J}_p = \mathbf{1} - r^{-1} \mathbb{J}, \quad r^{-1} = \begin{bmatrix} 0 & 0 & \mathbf{1}_d \\ \mathbf{1}_d & 0 & 0 \\ 0 & \mathbf{1}_d & 0 \end{bmatrix}, \quad \mathbb{J} = \begin{bmatrix} \mathbb{J}_1 & 0 & 0 \\ 0 & \mathbb{J}_2 & 0 \\ 0 & 0 & \mathbb{J}_3 \end{bmatrix}, \quad (7.30)$$

⁴Predrag 2020-12-15: Merge sect. 8.5 Spatiotemporal cat Hill's formula into his, to transfer to CL18.tex. Once incorporated, remove from here (too much duplication, as is)

where $\mathbf{1}_d$ is the d -dimensional identity matrix. Next, note that

$$(r^{-1}\mathbb{J})^2 = r^{-2} \begin{bmatrix} \mathbb{J}_2\mathbb{J}_1 & 0 & 0 \\ 0 & \mathbb{J}_3\mathbb{J}_2 & 0 \\ 0 & 0 & \mathbb{J}_1\mathbb{J}_3 \end{bmatrix}, \quad (r^{-1}\mathbb{J})^3 = \begin{bmatrix} \mathbb{J}_2\mathbb{J}_1\mathbb{J}_3 & 0 & 0 \\ 0 & \mathbb{J}_3\mathbb{J}_2\mathbb{J}_1 & 0 \\ 0 & 0 & \mathbb{J}_1\mathbb{J}_3\mathbb{J}_2 \end{bmatrix},$$

as $r^{-3} = \mathbf{1}$. Likewise, as $r^n = \mathbf{1}$ for any period n , the trace of $[nd \times nd]$ matrix

$$\text{tr}(r^{-1}\mathbb{J})^k = \delta_{k,rn} n \text{tr} \mathbb{J}_p^r, \quad \mathbb{J}_p = \mathbb{J}_n \mathbb{J}_{n-1} \cdots \mathbb{J}_2 \mathbb{J}_1$$

is non-vanishing only if k is a multiple of n , with \mathbb{J}_p the forward-in-time $[d \times d]$ Jacobian matrix of the periodic orbit p .

Now we can evaluate the Hill determinant (5.203) by expanding

$$\begin{aligned} \ln \text{Det}(\mathcal{J}_p) &= \text{tr} \ln(\mathbf{1} - r^{-1}\mathbb{J}) = - \sum_{k=1}^{\infty} \frac{1}{k} \text{tr}(r^{-1}\mathbb{J})^k \\ &= -\text{tr} \sum_{r=1}^{\infty} \frac{1}{r} \mathbb{J}_p^r = \ln \det(\mathbf{1}_d - \mathbb{J}_p). \end{aligned} \quad (7.31)$$

The Hill determinant for a 2-term difference equation (3.100) on a temporal lattice

$$\text{Det}(\mathcal{J}_p) = \det(\mathbf{1}_d - \mathbb{J}_p)$$

thus relates the global orbit stability to the Floquet, temporal evolution stability. In the temporal Bernoulli case, the field x_t is a scalar, and the 1-time step $[1 \times 1]$ time-evolution Jacobian matrix (7.20) at every lattice point t is simply $\mathbb{J}_t = s$, so

$$N_n = |\text{Det } \mathcal{J}| = s^n - 1, \quad (7.32)$$

in agreement with the time-evolution count.

Example 7.1. Temporal lattice stability of a 3-cycle. For a 1-dimensional map f , orbit Jacobian matrix is an $[n_p \times n_p]$ matrix:

$$\mathcal{J}(x) = \begin{pmatrix} 1 & & & -f'_{n_p} \\ -f'_1 & 1 & & \\ \cdots & \cdots & 1 & \\ & & \cdots & 1 \\ & & & -f'_{n_p-1} & 1 \end{pmatrix}. \quad (7.33)$$

Let us invert a 3-cycle orbit Jacobian matrix $\mathcal{J}(x)$ for such 1-dimensional map by hand, step by step. According to (7.6), the initial small Δx deviations from the periodic orbit (7.3) are mapped into deviations $\Delta x'$ a time step later by

$$\begin{pmatrix} \Delta x'_1 \\ \Delta x'_2 \\ \Delta x'_3 \end{pmatrix} = \begin{pmatrix} 1 & 0 & -f'_3 \\ -f'_1 & 1 & 0 \\ 0 & -f'_2 & 1 \end{pmatrix} \begin{pmatrix} \Delta x_1 \\ \Delta x_2 \\ \Delta x_3 \end{pmatrix},$$

where the d -dimensional vector $\Delta x_i = \hat{x}_i - x_i$ is the error at i th periodic point. In terms of the shift matrix σ , the one-time step cycle Jacobian matrix (7.33) can be written as

$$\mathcal{J} = \mathbf{1} - \sigma f', \quad \sigma = \begin{pmatrix} 0 & 0 & 1 \\ 1 & 0 & 0 \\ 0 & 1 & 0 \end{pmatrix}, \quad f' = \begin{pmatrix} f'_1 & 0 & 0 \\ 0 & f'_2 & 0 \\ 0 & 0 & f'_3 \end{pmatrix}. \quad (7.34)$$

Suppose all $|f'_k| > 1$, so forward in time the errors are growing. We can make errors contract by going backwards in time, i.e., evaluating the inverse matrix \mathcal{J} , and noting that every 3rd power $(\sigma f')^3 = J_p \mathbf{1}$ is diagonal,

$$\begin{aligned} \frac{1}{1 - \sigma f'} &= \sum_{j=0}^{\infty} (\sigma f')^j = \sum_{k=0}^{\infty} J_p^k \sum_{\ell=0}^2 (\sigma f')^\ell = \frac{1}{1 - J_p} [\mathbf{1} + \sigma f' + (\sigma f')^2] \\ &= \frac{1}{1 - J} \left[\mathbf{1} + \sigma \begin{pmatrix} f'_1 & 0 & 0 \\ 0 & f'_2 & 0 \\ 0 & 0 & f'_3 \end{pmatrix} + \sigma^2 \begin{pmatrix} f'_1 f'_2 & 0 & 0 \\ 0 & f'_2 f'_3 & 0 \\ 0 & 0 & f'_1 f'_3 \end{pmatrix} \right], \end{aligned} \quad (7.35)$$

where $J_p = f'_3 f'_2 f'_1$ is the forward-in-time stability of the cycle p , so

$$\begin{pmatrix} \Delta x_1 \\ \Delta x_2 \\ \Delta x_3 \end{pmatrix} = \frac{1}{1 - J_p} \begin{pmatrix} \Delta x'_1 + f'_3 \Delta x'_3 + f'_3 f'_2 \Delta x'_2 \\ \Delta x'_2 + f'_1 \Delta x'_1 + f'_1 f'_3 \Delta x'_3 \\ \Delta x'_3 + f'_2 \Delta x'_2 + f'_2 f'_1 \Delta x'_1 \end{pmatrix}.$$

For an unstable cycle, the error gets contracted by overall factor $1/(1 - J)$, with the earlier errors amplified by the orbit instability; for example, Δx_3 receives a contribution from two time steps in the past of form $f'_2 f'_1 \Delta x'_1$.

By explicit evaluation, for 1-dimensional maps⁵ $\mathcal{J}(x)^3 = (1 - J_p)\mathbf{1} + (\dots)$ and

$$\text{Det } \mathcal{J}_p = \det(1 - J_p) \quad (7.36)$$

for the d -dimensional case. $\mathcal{J}(x)$ is a cycle rotation by one time step; for a 3-cycle we are back, times a constant, uniform factor multiplying all errors by the rotation invariant scalar quantity $\det(1 - J_p)$, whose inverse happens to be the cycle-expansions' size of the neighborhood of cycle p .

⁶

⁵Predrag 2019-10-10: Still have to derive this formula, probably by $\ln \det = \text{tr} \ln$ relation

⁶Predrag 2019-09-28: I have inverted this Newton Jacobian matrix often, see for example

Example 7.2. Temporal lattice stability of a 3-cycle.

Consider an period- n lattice state X_p , with d fields $\{x_{t,1}, x_{t,2}, \dots, x_{t,d}\}$ on each lattice site t satisfying the condition

$$x_t - f(x_{t-1}) = 0, \quad t = 1, 2, \dots, n, \quad (7.37)$$

where d -dimensional time evolution function. A deviation ΔX from X_p must satisfy the linearized condition

$$\Delta x_t - \mathbb{J}_{t-1} \Delta x_{t-1} = 0, \quad (\mathbb{J}_t)_{ij} = \left. \frac{\partial f(x)_i}{\partial x_j} \right|_{x_i=x_{t,i}}, \quad (7.38)$$

where \mathbb{J}_t the 1-time step $[d \times d]$ time-evolution Jacobian matrix. Let $\mathbf{1}_d$ be a d -dimensional identity matrix. For an period- n lattice state X_p , the orbit Jacobian matrix $\mathcal{J}_p \Delta X = 0$ is an $[nd \times nd]$ matrix

$$\mathcal{J}_p = \mathbf{1} - r^{-1} \mathbb{J} = \begin{pmatrix} \mathbf{1}_d & & & & -\mathbb{J}_n \\ -\mathbb{J}_1 & \mathbf{1}_d & & & \\ & -\mathbb{J}_2 & \ddots & & \\ & & & \mathbf{1}_d & \\ & & & -\mathbb{J}_{n-1} & \mathbf{1}_d \end{pmatrix}, \quad (7.39)$$

where the $[nd \times nd]$ matrix

$$r = \begin{pmatrix} 0 & \mathbf{1}_d & & & \\ & 0 & \mathbf{1}_d & & \\ & & \ddots & & \\ & & & 0 & \mathbf{1}_d \\ \mathbf{1}_d & & & 0 & 0 \end{pmatrix}, \quad (7.40)$$

implements the shift operation, a cyclic permutation that translates forward in time the lattice state X_p by one site, $(rX)^\top = (x_2, x_3, \dots, x_n, x_1)$.

To evaluate the Hill determinant (3.88), note that $r^n = \mathbf{1}$, that $\text{tr}(r^{-1} \mathbb{J})^k = n \delta_{k,rn} \text{tr} \mathbb{J}_p^r$ is non-vanishing only if k is a multiple of n , and expand

$$\begin{aligned} \ln \text{Det}(\mathcal{J}_p) &= \text{tr} \ln(\mathbf{1} - r^{-1} \mathbb{J}) = - \sum_{k=1}^{\infty} \frac{1}{k} \text{tr}((r^{-1} \mathbb{J})^k) \\ &= -\text{tr} \sum_{r=1}^{\infty} \frac{1}{r} \mathbb{J}_p^r = \ln \det(\mathbf{1}_d - \mathbb{J}_p). \end{aligned} \quad (7.41)$$

So, the Hill determinant for any hyperbolic 2-term difference equation on a temporal lattice is

$$\text{Det}(\mathcal{J}_p) = \det(\mathbf{1}_d - \mathbb{J}_p).$$

eq. (16) and onward in Cvitanović, Dettmann, Mainieri and Vattay [9], [click here](#). I have also introduced the notation for finite-time (shorter than the period) Jacobian matrices, see for example eq. (69) in Cvitanović and Lippolis [11], [click here](#). But I have never done it the way I should have, by a discrete Fourier transform, into sum of irreps of C_n (AKA Fourier modes) and using characters for discrete Fourier transforms.

In the temporal Bernoulli case, the field x_t is a scalar, and the 1-time step $[d \times d]$ time-evolution Jacobian matrix (7.38) at any time is simply $\mathbb{J}_t = s$, so

$$N_n = |\text{Det } \mathcal{J}| = s^n - 1, \quad (7.42)$$

in agreement with the time-evolution count.

In terms of the shift matrix r , the one-time step cycle Jacobian matrix (7.33) can be written as

$$\mathcal{J}_p = \mathbf{1} - r^{-1} \mathbb{J}, \quad r = \begin{pmatrix} 0 & 0 & \mathbf{1}_d \\ \mathbf{1}_d & 0 & 0 \\ 0 & \mathbf{1}_d & 0 \end{pmatrix}, \quad \mathbb{J} = \begin{pmatrix} \mathbb{J}_1 & 0 & 0 \\ 0 & \mathbb{J}_2 & 0 \\ 0 & 0 & \mathbb{J}_3 \end{pmatrix}. \quad (7.43)$$

Suppose all $\mathbb{J}_p \neq 1$. Note that every n th power $(r\mathbb{J})^3 = \mathbb{J}_p\mathbb{J}$ is diagonal,

$$\begin{aligned} \frac{1}{1 - r\mathbb{J}} &= \sum_{j=0}^{\infty} (r\mathbb{J})^j = \sum_{k=0}^{\infty} \mathbb{J}_p^k \sum_{\ell=0}^2 (r\mathbb{J})^{\ell} = \frac{1}{1 - \mathbb{J}_p} [\mathbb{J} + r\mathbb{J} + (r\mathbb{J})^2] \\ &= \frac{\mathbf{1}}{\mathbf{1} - \mathbb{J}} \left[\mathbb{J} + r \begin{pmatrix} \mathbb{J}_1 & 0 & 0 \\ 0 & \mathbb{J}_2 & 0 \\ 0 & 0 & \mathbb{J}_3 \end{pmatrix} + r^2 \begin{pmatrix} \mathbb{J}_2\mathbb{J}_1 & 0 & 0 \\ 0 & \mathbb{J}_3\mathbb{J}_2 & 0 \\ 0 & 0 & \mathbb{J}_1\mathbb{J}_3 \end{pmatrix} \right], \end{aligned} \quad (7.44)$$

where $\mathbb{J}_p = \mathbb{J}_3\mathbb{J}_2\mathbb{J}_1$ is the forward-in-time stability of the cycle p .

To summarize, a discretized, temporal lattice periodic orbit linear stability can be computed in two ways - either by computing the $[n_p d \times n_p d]$ Jacobian matrix $\mathcal{J}(x)$, or by computing \mathbb{J}_p

$$|\text{Det } \mathcal{J}_p| = |\det(1 - \mathbb{J}_p)|, \quad (7.45)$$

where \mathbb{J}_p is the n_p time-steps $[d \times d]$ forward-time Jacobian matrix. In the limit of discretization $n_p \rightarrow \infty$ the left hand side is a *functional* determinant of an ∞ -dimensional *operator*. Nevertheless, thanks to the discrete Fourier diagonalization of $\mathcal{J}(x)$, appendix ??, the determinant $\text{Det } \mathcal{J}_p$ is easier to compute than the ill-posed \mathbb{J}_p .^{7,8}

The projection operator on the k th Fourier mode is

$$P_k = \prod_{j \neq k} \frac{r - \omega_j \mathbf{1}}{\omega_k - \omega_j}. \quad (7.46)$$

The set of the projection operators is complete,

$$\sum_k P_k = \mathbf{1}, \quad (7.47)$$

and orthonormal

$$P_k P_j = \delta_{kj} P_k \quad (\text{no sum on } k). \quad (7.48)$$

[TO BE CONTINUED]

7.2 Spatiotemporal lattice

In spatiotemporal settings, \mathbb{J}_p can be defined only for finite numbers of spatial sites, and it gets funkier and funkier as the spatial direction increases (that is why we are able to work only with very small spatial domain Kuramoto-Sivashinsky discretizations). But, as shown for the spatiotemporal cat in ref. [10], $\text{Det } \mathcal{J}_p$ works just fine on any spatiotemporal torus. In particular, for any invariant 2-torus Kuramoto-Sivashinsky discretization.

7.3 Noether's theorem

2018-05-04 Predrag Moved this section to `spatiotemp/blog.tex`

⁷Predrag 2019-10-10: $\mathcal{J}(x)$ is block-diagonalized by the discrete Fourier transform on a periodic lattice of three sites. Write up next the discrete Fourier evaluation of $\text{Det } \mathcal{J}_p$.

⁸Predrag 2019-10-10: Rewrite the derivation of the Hill-Poincaré-Van Vleck stability matrix (18.187) for symplectic / Lagrangian Hessians (orbit Jacobian matrix) using the shift matrix (7.34).

7.4 Stability blog

2016-09-28 Predrag Amritkar *et al.* [2, 21] have investigated the stability of spatiotemporally periodic orbits in one- and two-dimensional coupled map lattices, i.e., $1 + 1$ and $1 + 2$ spatiotemporal dimensions. The stability matrices for such lattice states are block circulant and hence can be brought onto a block diagonal form through a unitary transformation. They derive conditions for the stability of periodic solutions in terms of the criteria for smaller orbits.

Zhilinet *et al.* [62] *Spatiotemporally periodic patterns in symmetrically coupled map lattices* write: “ The stability of the deduced orbits is investigated and we can reduce the problem to analyze much smaller matrices corresponding to the building block of their spatial periodicity or to the building block of the spatial periodicity of the original orbits from which we construct the new orbits. In the two-dimensional case the problem is considerably simplified. ”

2019-10-10 Predrag Reread Lindstedt-Poincaré [57] Fourier method papers by Viswanath [58, 59]; his most accurate resolution of fractal structure of the Lorenz attractor. It is a very thin fractal, stable manifold thickness is of the order 10^{-4} . He has computed all 111011 periodic orbits corresponding to symbol sequences of length 20 or less, all with 14 digits accuracy.

2019-10-13 Predrag Viswanath [57] writes: “ The Lindstedt-Poincaré technique uses a nearby periodic orbit of the unperturbed differential equation as the first approximation to a perturbed differential equation. One of the examples presents what is possibly the most accurate computation of Hill’s orbit of lunation since its justly celebrated discovery in 1878.

The eigenvalues excluding 1 are called characteristic multipliers.

AUTO [15, 16] collocation method, Guckenheimer and Meloon [24], Choe and Guckenheimer [7] all set up their periodic orbits as in (7.4). Since the linear systems that they form are sparse, the cost of solution is only linear in the number of mesh points.

There are other variants of this forward multiple shooting algorithm: one is a symmetric multiple shooting algorithm and another is based on Hermite interpolation.

He dismisses harmonic balance methods for computing periodic orbits (Lau, Cheung and Wu [?15], and Ling and Wu [?16]) as being too expensive, of order $O(n^3)$, where the Fourier series are of width n , whereas his method is of order $O(n \ln n)$.

Wisvanath algorithm for computing periodic orbits is a “polyphony of three themes:” the Lindstedt-Poincaré technique from perturbation theory, Newton’s method for solving nonlinear systems, and Fourier interpolation.

To compute n Fourier coefficients of $x(t)$, the fast Fourier transform (FFT) is applied to the function evaluated at n equispaced points in $[0, 2\pi]$. The width n of the Fourier series must be sufficiently large to pick up all the coefficients above a desired accuracy threshold.

If (x_1, x_2, \dots, x_m) are 2π periodic, so is $f(x_1, x_2, \dots, x_m)$. To obtain its Fourier series from those of the x_i , interpolate x_i at equispaced points, evaluate f at those points, and apply the FFT. The inverse FFT can be used to interpolate a Fourier series at equispaced points [54]. In d state space dimensions, one needs d Fourier series, one for each coordinate in \mathbb{R}^d .

His 4 coupled Josephson junctions (10-dimensional state space) uses 64 Fourier modes.

"

The implementation of the algorithm must pay attention to the possibility of aliasing.

2019-10-13 Predrag Viswanath [58] writes: "The representation of periodic orbits by Fourier series is both accurate and efficient because, when a periodic orbit is analytic, the Fourier coefficients decrease exponentially fast, making its Fourier representation compact.

"

2019-10-13 Predrag Guckenheimer and Meloon [24] set up their periodic orbits as in (7.4), and have the same d -dimensional orbit Jacobian matrix variant of (7.33), but with extra, time-direction fixing diagonals, as they are looking at continuous time flows. Instead of the cyclic group, they use LU factorization. They get $1 - J_p$ matrix.

2019-10-14 Predrag Notes on Choe and Guckenheimer [7], a clear and enjoyable read:

Instead of relying on forward-in-time numerical integration, *global methods* for finding periodic orbits view the vector field as an equation on a function space of closed curves. Here f is a Lipschitz continuous vector field on a smooth manifold \mathcal{M} , and $p : S^1 \rightarrow \mathcal{M}$ is a C^1 closed curve in \mathcal{M} .

Computer implementation of global methods for computing periodic orbits requires discretization of closed curves and approximation of the periodic orbit equations. One defines finite-dimensional submanifolds of the space of closed curves and approximates the periodic orbit equations as a map defined on this space.

They keep the number of discretization points fixed and increase the accuracy by *automatic differentiation*, constructing the Taylor series of trajectories at discretization points. They also compute stability matrix derivatives of the Taylor series coefficients with respect to the state space variables for use in the Newton iteration. As the degree of the computed

Taylor series increases, their curves converge since the trajectories are analytic.

The Taylor series is obtained by repeated differentiation of the differential equation $\dot{x} = v(x)$ and recursive substitution of the values of derivatives $x^{(k)}(t)$ of increasing degree. To make the approximate curve smooth and continuous, they use a somewhat funky interpolation function they call $\beta(t)$.

[Predrag's aside: hopefully our strategy of using Fourier transforms has much faster convergence than Taylor series. Even if one wants polynomials, I suspect Chebyshev or Hermite or some other orthogonal sets would be better.]

Indeed, the Hermite splines, interpolating functions that are polynomials of degree $2d + 1$, gave the best results in their computations.

They eliminate the time translation marginal eigenvalue by using sets of Poincaré section hyperplanes transverse to the vector field, and solving for points that lie on the intersection of Poincaré section with the periodic orbit. They use the orthogonal complements to the vector field $v(x_i)$ at the mesh points x_i . The normal subspace to the vector field at x_i is determined by computing the QR factorization of the $[d \times (d + 1)]$ matrix. There is a whole PhD thesis worth of detail here.

The structure of the Jacobian matrices that are used in the root finding has a simple sparsity pattern that can be exploited in its inversion. Explicit inversion of this block matrix in terms of the inverses of the individual blocks yields a relationship between the regularity of the root finding problem and the hyperbolicity of the periodic orbit. They relate the regularity of orbit Jacobian matrix \mathcal{J} to the periodic orbit's monodromy matrix, their sect. 3. *Analysis*, using LU factorization. They show that \mathcal{J} is invertible (needed for Newton schemes) if and only if the monodromy matrix M of the Poincaré section does not have 1 as an eigenvalue.

Since their methods produce smooth approximations to periodic orbits, they can evaluate the distance between the tangent vectors to a computed curve and the vector field along that curve. These error estimates enable them to develop strategies for mesh refinement that balance the error in different mesh intervals. Since the approximating solution in a mesh interval is determined entirely by its endpoints, mesh refinement is a simple process and does not change the structure of the discretized periodic orbit equations.

They define the error field (7.4) as operator $F(p) = f(p) - \sigma p$, with periodic orbits solutions satisfying $F = 0$. p are analytic curves, but Choe-Guckenheimer approximations are not analytic.

The starting data is an N -point *discrete closed curve* (7.3), a cyclically ordered collection of N points. Given a map S , one seeks systems of $(n_p \times d)$ -dimensional vector field equations $F_S = 0$ whose solutions yield

good approximations to periodic orbits of f . The convergence is takes place on a fixed mesh, but with increasing degree d of map S_d . They compute the orbit Jacobian matrix \mathcal{J} and invert it to use in the Newton routine, but do not mention or discuss computing $\det \mathcal{J}$.

They test their algorithm with the Hodgkin-Huxley equations, a moderately stiff 4-dimensional vector field with strongly stable directions. They do not boast, but their residual errors are of order 10^{-11} .

7.5 Hill's formula blog

For the latest entry, go to the bottom of this section

2019-10-13 Predrag Viswanath [57] describes, and numerically solves Hill's problem: " In 1878, Hill [28] derived the equations that describe the planar motion of the moon around the earth:

$$\begin{aligned}\ddot{x} - 2\dot{y} &= \frac{\partial \Omega}{\partial x} \\ \ddot{y} + 2\dot{x} &= \frac{\partial \Omega}{\partial y}, \quad \Omega = \frac{3}{2}x^2 + (x^2 + y^2)^{-1/2}.\end{aligned}\quad (7.49)$$

The Jacobi integral $2\Omega - \dot{x}^2 - \dot{y}^2$ is constant along the solutions of Hill's equation, so each orbit is characterized by a "Jacobi constant." The orbits Viswanath (and Hill) computes are symmetric with respect to both the x and the y axes - $C_2 \times C_2$ -symmetric, so it suffices to compute them to quarter-period $T/4$. He uses a Fourier series of width 64 and filters out 20% of the frequencies at the high end after each iteration.

I do not see Hill's formula in this paper. "

2018-10-27 Predrag Petrisor [48] *Twist number and order properties of periodic orbits* works mostly with the standard-like maps, but we might find her article useful both as a review of the standard literature, as well as an aid in understanding the \mathcal{J} of the cat map, and perhaps the twisted bc's (relative) invariant 2-tori of spatiotemporal cat as well.

Petrisor [49] *Monotone gradient dynamics and the location of stationary (p, q) -configurations* might also be of interest.

A standard-like map is a twist map F_ϵ , defined by a Lagrangian generating function of the form

$$h(x, x') = \frac{1}{2}(x - x')^2 - \epsilon V(x),$$

where V is a fixed 1-periodic even function. Classical standard map corresponds to the potential $V(x) = -\frac{1}{(2\pi)^2} \cos(2\pi x)$. The twist map F_ϵ is

reversible, i.e. it factorizes as $F_\epsilon = I \circ R$, where R and I are the involutions. [...] The R -invariant orbits are called symmetric orbits.

A numerical characteristic associated with a periodic orbit is the rotation number, which measures the average rotation of the orbit around the annulus. Mather [45] defined also the amount of rotation, which is called twist number or torsion number. [...] Angenent [3] proved that in the space of (p, q) -sequences a critical point of the W_{pq} action [...] is connected by the negative gradient flow of the action.

The 1-cone function is defined on the phase space of a twist map and takes negative values within the region where the map exhibits strong folding property. We prove that the restriction of this function to a periodic orbit gives information on the eigenvalues of the orbit Jacobian matrix \mathcal{J}_q associated with that orbit.

[...] we revisit the definition and properties of the twist number of a periodic orbit based on the structure of the universal covering group of the group $SL_2(\mathbb{R})$. The twist number is defined as the translation number of a circle map induced by the monodromy matrix associated with the periodic orbit. [...] we give the relationship between the twist number value of a (p, q) -periodic orbit, and the position of the real number 0 with respect to the sequence of interlaced eigenvalues of the orbit Jacobian matrix \mathcal{J}_q , associated with the corresponding (p, q) -sequence, and of a symmetric matrix derived from H_q .

Petrisor eq. (11) expresses the Hessian in terms of the 1-step forward Jacobian matrix, and gives references to the related literature. In particular, the discrete Hill's formula, the characteristic polynomial of a periodic Jacobi matrix, and the Hill discriminant are presented in Toda [53].

The orbit Jacobian matrix \mathcal{J}_q of the W_{pq} action associated with a (p, q) -periodic orbit, $q \leq 3$, is a Jacobi periodic matrix (i.e. a symmetric tridiagonal matrix with non-null entries in the upper right, and left lower corners, and the next-to-diagonal entries have the same sign), see Petrisor eq. (19). For $q = 2$, H_q is simply a symmetric matrix.

Let \mathcal{J}_q be the orbit Jacobian matrix of the action W_{pq} at a critical point $x = (x_n)$. The signature (the number of negative and positive eigenvalues) of the Hessian \mathcal{J}_q , at a non-degenerate minimizing sequence is $(0, q)$, while at the corresponding mini-maximizing sequence it is $(1, q-1)$. The number of negative eigenvalues is called the Morse index of the critical sequence.

2020-08-02 Predrag Toda [53] *Theory of Nonlinear Lattices* ([click here](#)), Chapt. 4. *Periodic Systems* has way more wisdom than what I am capable of learning this Sunday.

Toda studies the classical mechanics of one-dimensional lattices (chains) of particles with nearest neighbor interaction; they are discrete and infinite in space, continuous in time.

When the force is proportional to displacement, that is, when Hooke's law is obeyed, the spring is said to be linear, the potential is quadratic. While for us that leads to site stretching rate s , for Toda it leads to the Laplacian ($s = 2$), not sure why..

The *inverse scattering method* for an infinite lattice makes use of the discrete Schrodinger equation. For periodic systems this gives a discrete Hill's equation, and in place of the scattering data, it is convenient to use the spectrum of the discrete Hill's equation and the auxiliary spectrum for fixed boundary conditions of the same equation. In this case the fundamental solutions and the discriminant of the discrete Hill's equation play important roles. The discriminant is a polynomial of the spectrum, and the integral of motion is given in terms of elliptic integrals. Thus the initial value problem reduces to the inverse problem (Jacobi's inverse problem), or inverse spectral theory.

His discrete Hill's equation is continuous in time, so presumably most work is for stationary states; I have probably misunderstood the formulation....

He works with a 3-term recurrence (4.1.3a), and defines a 2-configuration monodromy matrix (4.1.11).

For special values of A, the solution of (4.1.4) can be periodic, but more generally it is relative periodic (4.1.16), or the Bloch function (it's existence given by the Floquet theorem) which he relates to the trace of the monodromy matrix (4.1.19). The simplest example is his (4.1.23). His orbit Jacobian matrix (4.1.28) has variable diagonal and off diagonal elements, corresponding to nontrivial nonlinear solutions for $d = 1$ lattice.

He says that the $L = 3$ three-particle system [4.8] is important because, though the simplest, it shows nearly all the characteristic features which L -particle systems exhibit.

2020-07-24 Predrag Bolotin and Treschev [4] *Hill's formula*: give two multidimensional generalizations of Hill's formula:

1. to discrete Lagrangian systems (symplectic twist maps)
2. to continuous Lagrangian systems

They discuss additional aspects which appear in the presence of symmetries or reversibility.

1. study the change of the Morse index of a periodic trajectory after the reduction of order in a system with symmetries
2. applications to stability of periodic orbits

"In his study of periodic orbits of the 3 body problem, Hill obtained a formula relating the characteristic polynomial of the monodromy matrix of a periodic orbit and an infinite determinant of the Hessian of the action

functional. A mathematically correct definition of the Hill determinant and a proof of Hill's formula were obtained later by Poincaré."

Hill computed $\det H$ approximately replacing H by a 3×3 matrix, which gave quite a good approximation. Hill did not prove convergence for the infinite determinant $\det H$. Poincaré [50] (Vol. I: Solutions périodiques. Non-existence des intégrales uniformes. Solutions asymptotiques) explained the meaning of the Hill determinant and presented a rigorous proof of Hill's formula. The equation appeared in 1983 for discrete Lagrangian systems in ref. [43] and independently in ref[4]. Here H is the finite Hessian matrix associated with the action functional at the critical point generated by the periodic solution. In ref{5} (see also ref{6}) a general form of Hill's formula was obtained for a periodic solution of an arbitrary Lagrangian system on a manifold. In this case H is a properly regularized Hessian operator of the action functional at the critical point determined by a periodic solution.

Hill's relates P , the monodromy matrix of the periodic trajectory, to the second variation of the action functional at the periodic trajectory, with H the corresponding Hessian operator.

2CB

The first dynamical application of Hill's formula is the well known statement that the Poincaré degeneracy of a periodic trajectory (that is, the condition that 1 is an eigenvalue of P) is equivalent to the variational degeneracy (the condition $\det H = 0$).

2019-01-30 Predrag Downloaded the monograph by Treschev and Zubelevich [55] *Introduction to the Perturbation Theory of Hamiltonian Systems* ([click here](#)) which contains a chapter *Hill's formula*. Here are some clippings:

"In 1886, in his study of stability of the lunar orbit, Hill [28] published a formula which expresses the characteristic polynomial of the monodromy matrix for a second order time periodic equation in terms of the determinant of a certain infinite matrix."

2018-09-29 Predrag Some papers that follow up on Bolotin and Treschev [4]:

Xu and Weng [61] *The calculation for characteristic multiplier of Hill's equation in case with positive mean*

Hu and Wang [32] *Conditional Fredholm determinant for the S-periodic orbits in Hamiltonian systems*

Hu and Wang [33] *Conditional Fredholm determinant and trace formula for Hamiltonian systems: a survey*

Hu, Ou and Wang [30] *Trace formula for linear Hamiltonian systems with its applications to elliptic Lagrangian solutions*. Their eq. (1.17) Krein formula for eigenvalues of a linear Hamiltonian systems with D degree of freedoms is intriguing.

Krein [39] *The basic propositions of the theory of λ -zones of stability of a canonical system of linear differential equations with periodic coefficients* (have not found a free version on line)

Davletshin [12] *Hill's formula for g -periodic trajectories of Lagrangian systems*

Hu and Wang [34] *Eigenvalue problem of Sturm-Liouville systems with separated bc's*

Hu and Wang [35] *Hill-type formula and Krein-type trace formula for S -periodic solutions in ODEs*, [arXiv:1504.01815](https://arxiv.org/abs/1504.01815)

Hu, Ou and Wang [31] *Hill-type formula for Hamiltonian system with Lagrangian bc's*, [arXiv:1711.09182](https://arxiv.org/abs/1711.09182): "The Hill-type formula connects the infinite determinant of the Hessian of the action functional with the determinant of matrices which depend on the monodromy matrix and bc's. Consequently, we derive the Krein-type trace formula and give nontrivial estimation for the eigenvalue problem."

Hu, Wu and Yang [36] *Morse index theorem of Lagrangian systems and stability of brake orbit*

Sunada [52] *Trace formula for Hill's operators*

Carlson [6] *Eigenvalue estimates and trace formulas for the matrix Hill's equation*

2019-01-28 Predrag Downloaded monographs (have not started studying them as yet):

Maybe [encyclopediaofmath.org](https://encyclopediaofmath.org/Hill%27s%20equation) *Hill equation* is a starting point for this literature.

A whole book on the subject that we might have to have a look at: Magnus and Winkler [44] *Hill's Equation* ([click here](#))

Added a Bolotin conference abstract ([click here](#)) and a Hu conference abstract ([click here](#)).

2019-04-21 Predrag Kozlov [38] *Problem of stability of two-link trajectories in a multidimensional Birkhoff billiard* has a simple derivation of Hill's formula for billiards, where the Hessian is the second derivative of the length function.

2018-09-29 Predrag Agrachev [1] *Spectrum of the second variation*, [arXiv:1807.10527](https://arxiv.org/abs/1807.10527) writes: Second variation of a smooth optimal control problem at a regular extremal is a symmetric Fredholm operator. We study the spectrum of this operator and give an explicit expression for its determinant in terms of solutions of the Jacobi equation.

We study the spectrum of the second variation $D_u^2\varphi$ that is a symmetric Fredholm operator of the form $I + K$, where K is a compact Hilbert-Schmidt operator. K is NOT a trace class operator so that the trace of K and the determinant of $I + K$ are not well-defined in the standard sense.

[...] A simple example: for the 1-dimensional linear control system $\dot{x} = ax + u$ with the quadratic cost $\varphi(u) = \int_0^1 u^2(t) - (a^2 + b^2)x^2(t) dt$ our determinantal identity reads:

$$\prod_{n=1}^{\infty} \left(1 - \frac{a^2 + b^2}{a^2 + (\pi n)^2} \right) = \frac{a \sin b}{b \sinh a}; \quad (7.50)$$

the case $a = 0$ corresponds to the famous Euler identity

$$\prod_{n=1}^{\infty} \left(1 - \frac{b^2}{(\pi n)^2} \right) = \frac{\sin b}{b}. \quad (7.51)$$

The example is simple, but, unfortunately, the paper itself is a hell to read...

2018-12-07 Predrag Reread Kook and Meiss [37] *Application of Newton's method to Lagrangian mappings*. They describe an Newton's method algorithm for finding periodic orbits of Lagrangian mappings. The method is based on block-diagonalization of the orbit Jacobian matrix of the action function. The explicit form of the Hessian displayed by Kook and Meiss reminds me of Bolotin discrete Hill's formula (sect. 8.2, Predrag post 2018-09-29 above, eq. (7.59)), maybe that's the way to derive it.

2018-09-26 Han I worked through the example ?? cat map example. The equation of motion is:

$$\begin{bmatrix} q_{n+1} \\ p_{n+1} \end{bmatrix} = \begin{bmatrix} s-1 & 1 \\ s-2 & 1 \end{bmatrix} \begin{bmatrix} q_n \\ p_n \end{bmatrix} \quad \text{mod } 1. \quad (7.52)$$

Rewrite this equation as:

$$\begin{aligned} q_{n+1} &= q_n + p_n + (s-2)q_n - s_{n+1}^q \\ p_{n+1} &= p_n + (s-2)q_n - s_{n+1}^q - (s_{n+1}^p - s_{n+1}^q). \end{aligned} \quad (7.53)$$

and compare with (7.55),

$$q_{n+1} = q_n + p_{n+1} \quad \text{mod } 1, \quad (7.54)$$

$$p_{n+1} = p_n + P(q_n), \quad (7.55)$$

so

$$\begin{aligned} q_{n+1} &= q_n + p_{n+1} \\ p_{n+1} &= p_n + (s-2)q_n - s_{n+1}^p. \end{aligned} \quad (7.56)$$

where the s_{n+1}^q seems happily absorbed into p_{n+1} . The generating function (1-step Lagrangian density) is

$$L(q_n, q_{n+1}) = \frac{1}{2}(q_{n+1} - q_n)^2 - V(q_n), \quad P(q) = -\frac{dV(q)}{dq}, \quad (7.57)$$

and the potential energy is:

$$V(q_n) = -\frac{s-2}{2}q_n^2 + s_{n+1}^p q_n. \quad (7.58)$$

The problem with this formulation is that the potential energy contribution is defined asymmetrically in (5.94). We should really follow Bolotin and Treschev [4] eq. (2.5), and define a symmetric generating function

$$L(q_n, q_{n+1}) = \frac{1}{2}(q_{n+1} - q_n)^2 - \frac{1}{2}[V(q_n) + V(q_{n+1})], \quad (7.59)$$

The first variation (8.13) of the action vanishes,

$$\begin{aligned} 0 &= L_2(q_{n+1}, q_n) + L_1(q_n, q_{n-1}) \\ &= q_n - q_{n+1} + (s-2)q_n - s_{n+1}^p + q_n - q_{n-1} \\ &= -q_{n+1} + sq_n - q_{n-1} - s_{n+1}^p, \end{aligned} \quad (7.60)$$

hence

$$q_{n+1} - sq_n + q_{n-1} = -s_{n+1}^p. \quad (7.61)$$

Letting $s_n = -s_{n+1}^p$, we recover the Lagrangian formulation (1.118).

Alternatively, Han's generating function (1-step Lagrangian density) is:

$$\begin{aligned} L(q_{n+1}, q_n) &= \frac{1}{2}[p_{n+1}(q_{n+1}, q_n)]^2 - V(q_n) \\ &= \frac{1}{2}(q_{n+1} - q_n + m_{n+1}^q - m_{n+1}^p)^2 + \frac{s-2}{2}q_n^2 - m_{n+1}^p q_n. \end{aligned} \quad (7.62)$$

The action is the sum over the Lagrangian density over the orbit. The first variation (8.13) of the action vanishes,

$$\begin{aligned} 0 &= L_2(q_{n+1}, q_n) + L_1(q_n, q_{n-1}) \\ &= q_n - q_{n+1} + m_{n+1}^p - m_{n+1}^q \\ &\quad + (s-2)q_n - m_{n+1}^p + q_n - q_{n-1} + m_n^q - m_n^p \\ &= -q_{n+1} + sq_n - q_{n-1} - (m_{n+1}^q - m_n^q + m_n^p), \end{aligned} \quad (7.63)$$

hence

$$-q_{n+1} + sq_n - q_{n-1} = m_{n+1}^q - m_n^q + m_n^p. \quad (7.64)$$

Letting $m_n = m_{n+1}^q - m_n^q + m_n^p$, we recover the Lagrangian formulation (1.118), except for the wrong sign for m_n . Now I see why m_n 's are called 'sources'.

But I think I missed something. I believe (5.36) is correct. Because $\square - \mu^2 \mathbf{1}$ has negative determinant, so we can do the Gaussian integral. But it seems like the action $S[X]$ is the negative of the sum of Lagrangian along the orbit? Because if we sum (7.62) along the orbit, the sign before s should be positive but in (5.36) it is negative...

2019-09-25 PC Levit and Smilansky [42] *A theorem on infinite products of eigenvalues of Sturm-Liouville type operators* computes a Gaussian path integral with a Laplacian kernel. Looks simple, but I do not understand it.

Levit and Smilansky [41] *A new approach to Gaussian path integrals and the evaluation of the semiclassical propagator.*

2019-09-25 PC Han, can you clean up the rest, make it (7.66) and beyond into a derivation of the Hill's formula for our paper - what follows is just a sketch in (close to) our notations:

Colin de Verdière [8] *Spectrum of the Laplace operator and periodic geodesics: thirty years after* discusses the mathematical history of "Semi-classical trace formula," a formula expressing the smoothed density of states of the Laplace operator on a compact Riemannian manifold in terms of the periodic geodesics. This seems to be an elaboration of [these lectures](#) from which one can clip & paste.

Colin de Verdière [8] and Levit and Smilansky [41] are deriving "semi-classical" or "Gaussian path integral" evolution trace formulas, which lead to $|\det(\mathbf{1} - M_p)|^{\frac{1}{2}}$ rather than the classical $|\det(\mathbf{1} - M_p)|$. That does not matter for our purposes, which is the derivation of the Hill's formula, sketched in (7.66), and on.

What we call periodic orbit's monodromy matrix M he seems to call (linear) Poincaré map Π a closed orbit computed on a hypersurface transverse to the orbit, an "inversible (symplectic) endomorphism of the tangent space". The periodic orbit weight $|\det(\mathbf{1} - M_p)|$ shows up in his eq. (5.5).

In his Theorem 11, Sect. 11, Colin de Verdière evaluates the integral over $\exp(iS(x)/\hbar)$ in the stationary phase approximation, with $S(W)$ having support on a critical manifold W has a measure $d\mu_W$ given by the quotient of the measure $|dx|$ by the "Riemannian measure" on the normal bundle to W associated to the Hessian of S

$$d\mu_W = \frac{|dx|}{|\det(\partial_{\alpha\beta}^2 S)|^{\frac{1}{2}} |dz|}, \quad (7.65)$$

where $z = (z_\alpha)$ are the coordinates on the normal bundle.

The Hessian is associated to a periodic Sturm-Liouville operator for which many regularizations have been proposed.

Elsewhere [41, 56] $\det(\partial_{\alpha\beta}^2 S)$ is known as the Van Vleck determinant. Irrelevant to the problem at hand, but a fun history read [Nicholas Wheeler](#) is [here](#). In Sect. 11.6 *Regularized Determinants of continuous Sturm-Liouville operators* he discretizes the n -cycle Hessian just as we do (except he allows

s to vary along the path), with Dirichlet, or periodic boundary conditions,

$$\mathcal{H}_n = \begin{pmatrix} A & B & 0 & \dots & 0 & B^\top \\ B^\top & A & B & \dots & 0 & 0 \\ 0 & B^\top & A & \dots & 0 & 0 \\ \vdots & \vdots & \vdots & \ddots & \vdots & \vdots \\ 0 & 0 & 0 & \dots & A & B \\ B & 0 & 0 & \dots & B^\top & A \end{pmatrix} \quad (7.66)$$

In general the $[2 \times 2]$ matrices

$$A = \frac{1}{*} \begin{pmatrix} a_{11} & a_{12} \\ a_{21} & a_{22} \end{pmatrix}, \quad B = -\frac{1}{*} \begin{pmatrix} * & * \\ * & * \end{pmatrix} \quad (7.67)$$

are time dependent, (A_t, B_t) , but for our simple temporal cat they are constant, $(A_t, B_t) = (A, B)$. For some choices, see sect. [22.2 Adrien's blog](#). Denote $b = -\det B$, and by

$$\begin{pmatrix} x_1 \\ x_2 - x_1 \end{pmatrix} = J \begin{pmatrix} x_0 \\ x_1 - x_0 \end{pmatrix} \quad (7.68)$$

the 1-time step symplectic (canonical) transformation

$$J = \begin{pmatrix} \alpha & \beta \\ \gamma & \delta \end{pmatrix}. \quad (7.69)$$

From his theorem 13 he gets Hill's formula $\det H = \det(1 - J_p)$ for the periodic case.

2019-09-28 PC It is clearer and clearer that the smart way of doing the multi-shooting Newton and various related "noisy" dynamics problems is by discrete Fourier (C_n cyclic group) irreps diagonalization. So I might have to rework several earlier papers:

I had inverted Newton Jacobian matrix often, see for example eq. (16) and onward in Cvitanović, Dettmann, Mainieri and Vattay [9], [click here](#). I have also introduced the notation for finite-time (shorter than the period) Jacobian matrices, see for example eq. (69) in Cvitanović and Lipolis [11], [click here](#). But I have never done it the way I should have, by a discrete Fourier transform, into sum of irreps of C_n (AKA Fourier modes). Probably best to use characters?

2019-09-28 PC I think I have finally committed the long awaited conceptual breakthrough. To remind everyone - one unsolved problem in Matt and my work [25] is "Hill's formula" for the first-order time derivative dissipative dynamics, which relates linear stability of a spatiotemporal pattern to $(1 - J)$ temporal evolution stability.

I'm writing this up in chapter [7 Spatiotemporal stability](#).

2019-10-01 PC Cao and Voth [5] *Semiclassical approximations to quantum dynamical time correlation functions* ([click here](#)): “ find an alternative to evaluate the Jacobi matrices and have thereby found it necessary to derive the initial-value expression from a new perspective. Straight-forward and self-contained, this derivation leads to a discretized expression for the Jacobi matrices and a simple interpretation of the Maslov-like index. ”

They derive the Jacobi equations from a discretization, their Appendix B. These equations evolve subblocks of the Jacobian that maintain the symplectic invariance.

Langouche, Roekaerts and Tirapegui [40] *WKB Expansion for arbitrary Hamiltonians* might be of interest, but I have not studied it.

2019-10-13 Predrag Guckenheimer and Meloon [24] define a “symmetric multiple shooting algorithm” as is a small modification of the forward multiple shooting method that makes the method time reversible. Let $p = (x_1, x_2, \dots, x_{n_p})$, as in (7.1). They evaluate some “Taylor polynomials” at time-interval midpoints, I admit not to see how their formulas are time reversible. I believe they replace (7.4) by segments that traverse a time interval in both direction

$$F_{GM}(\hat{x}) = \begin{pmatrix} \hat{f}_{n_p} - \hat{f}_1^{-1} \\ \hat{f}_1 - \hat{f}_2^{-1} \\ \dots \\ \hat{f}_{n_p-1} - \hat{f}_{n_p}^{-1} \end{pmatrix}, \quad \hat{f}_k = f(\hat{x}_k), \quad (7.70)$$

Now the orbit Jacobian matrix (7.33) picks up the derivatives of inverse map along the diagonal (instead of the identity matrices). They manipulate it and show it is the same Jacobian as the forward shooting one.

For my taste having a diagonal and sub-diagonal is not time-symmetric enough. Inspired by the formula for the discrete Laplacian (12.3), I suggest trying the tri-diagonal vector field

$$H(\hat{x}) = \begin{pmatrix} \hat{f}_2^{-1} - 2\hat{x}_1 + \hat{f}_{n_p} \\ \hat{f}_3^{-1} - 2\hat{x}_2 + \hat{f}_1 \\ \dots \\ \hat{f}_{n_p-1}^{-1} - 2\hat{x}_{n_p} + \hat{f}_{n_p-1} \end{pmatrix}, \quad \hat{f}_k = f(\hat{x}_k), \quad (7.71)$$

that reverses its direction under time reversal. The orbit Jacobian matrix

$$\mathcal{H} = (\sigma J)^{-1} - 2J + \sigma J, \quad (7.72)$$

is of self-adjoint form. We have to show that its determinant is the Hill’s formula.

Is it what we need for the Hessian / Lagrangian case? I suspect that the temporal cat case - uniform stretching, is easily brought to the temporal

cat orbit stability form, by rescaling (7.72) so that off-diagonal J 's are absorbed into the diagonal μ^2 factors.

Read Doedel *et al.* [17] ([click here](#)). They show how two-point boundary value problem continuation software like AUTO [Doedel *et al.*, 1997; Doedel *et al.*, 2000] can be used to compute families of periodic solutions of conservative systems, i.e. systems having a first integral. Seems the same as chaos book as far as adding and additional constraint is concerned. See no word “determinant” anywhere...

2020-08-01 Predrag I guess I should have looked more closely. The original the Hill determinant (see [mathworld.wolfram](#)) is, with various terms absorbed into our stretching parameter s , a 3-term recurrence which is *exactly* our $d = 1$ temporal cat, with our Hill determinant, except Hill did it for the oscillatory parameter value $\mu^2 < 0$.

Check Morse, P. M. and Feshbach, H. *Methods of Theoretical Physics*, Part I. New York: McGraw-Hill, pp. 555-562, (1953).

Magnus and Winkler [44] *Hill's Equation* ([click here](#)).

Dan Rothman told me to look at J. J. Stoker (but it is not in *Differential geometry*), so it's in the wave mechanics book... Have not found it yet.

7.6 Generating function literature

For the latest entry, go to the bottom of this section

2016-11-11 Predrag I still cannot get over how elegant the Gutkin-Osipov [26] spatiotemporal cat is. It is *linear!* ($\mod 1$, that is - the map is continuous for integer s). A 1-dimensional cat map has a Hamiltonian (1.34), and they have written down the 2-dimensional Lagrangian, their Eq. (3.1) (or the “generating function”, as this is a mapping). Their spatiotemporal cat generating function is defined on a spatiotemporal cylinder, infinite in time direction,

$$\begin{aligned} S(q_t, q_{t+1}) = & - \sum_{n=1}^N q_{nt} q_{1+n,t} - \sum_{n=1}^N q_{nt} (q_{n,t+1} + m_{n,t+1}^q) + \frac{a}{2} \sum_{n=1}^N q_{nt}^2 \\ & + \frac{b}{2} \sum_{n=1}^N (q_{n,t+1} + m_{n,t+1}^q)^2 - m_{n,t+1}^p q_{n,t+1}, \end{aligned} \quad (7.73)$$

where $q_t = \{q_{nt}\}_{n=1}^N$ is a spatially periodic state at time t , with q_{nt} being the coordinate of n th “particle” $n = 1 \dots N$ at the moment of time $t \in \mathbb{Z}$, and $m_{n,t+1}^q, m_{n,t+1}^p$ are integer numbers which stand for winding numbers along the q and p directions of the $2N$ -torus. Note that $x_{1+n,t} = x_{1+(n \bmod N),t}$. The coefficients $a, b, s = a + b$ are integers which they specify. Gutkin and Osipov refer to the map generated by the action (7.73) as non-perturbed *coupled cat map*, and to an invariant 2-torus p as a “many-particle periodic orbit” (MPO) if q_{nt} is doubly-periodic, or “closed,” i.e.,

$$q_{nt} = q_{n+L,t+T}, \quad n = 1, 2, \dots, L, \quad t = 1, 2, \dots, T.$$

2D symbolic representation Encode each invariant 2-torus (many-particle periodic orbit) p by a two dimensional (periodic) lattice of symbols a_{nt} , $(nt) \in \mathbb{Z}^2$, where symbols a_{nt} belong to some alphabet \mathcal{A} of a small size. Each invariant 2-torus p is represented by $L \times T$ toroidal array of symbols:

$$\bar{\mathcal{A}}_p = \{a_{nt} \mid (nt) \in \mathbb{Z}_{LT}^2\}.$$

The Hamiltonian equations of motion can be generated using (5.73) but who needs them? Remember, a field theorist would formulate a space-time symmetric field theory in a Lagrangian way, with the invariant action.

2016-11-11 Predrag Percival and Vivaldi [47] state the Lagrangian variational principle in Sect. 6. *Codes, variational principle and the static model:* ⁹

⁹Predrag 2016-11-12: eventually move to remark 12.1

The Lagrangian variational principle for the sawtooth map on the real line states that the action sum (5.94) is stationary with respect to variations of any finite set of configurations x_t . Their discussion of how “elasticity” works against the “potential” is worth reading. For large values of stretching parameter s , the potential wins out, and the state x_t falls into the m_t th well: “the code may be considered as a labelling of the local minima of the Lagrangian variational principle.”

Dullin and Meiss [18] *Stability of minimal periodic orbits* does the calculations in great detail.

2016-11-11 Predrag “mean action” = the action divided by the period

2018-12-07 Predrag as shown in (copied here from ChaosBook) example 1.7, example 1.8, and example 1.9 Hamiltonian spectral determinant and dynamical zeta function have a special form. Recheck against our cat map $1/\zeta_{\text{top}}$.

2019-10-14 Predrag The Jacobi operator acts on a discrete periodic lattice as

$$L u(t) = a(t+1)u(t+1) + b(t)u(t) + a(t-1)u(t-1),$$

where $a(t)$ and $b(t)$ are real valued for each $t \in \mathbb{Z}$, and M -periodic in t . Jacobi operators are the discrete analogue of Sturm–Liouville operators, with many similarities to Sturm–Liouville theory.

References

- [1] A. Agrachev, *Spectrum of the second variation*, 2018.
- [2] R. E. Amritkar, P. M. Gade, A. D. Gangal, and V. M. Nandkumaran, “*Stability of periodic orbits of coupled-map lattices*”, Phys. Rev. A **44**, R3407–R3410 (1991).
- [3] S. B. Angenent, “*The periodic orbits of an area preserving twist-map*”, Commun. Math. Phys. **115**, 353–374 (1988).
- [4] S. V. Bolotin and D. V. Treschev, “*Hill’s formula*”, Russ. Math. Surv. **65**, 191 (2010).
- [5] J. Cao and G. A. Voth, “*Semiclassical approximations to quantum dynamical time correlation functions*”, J. Chem. Phys. **104**, 273–285 (1996).
- [6] R. Carlson, “*Eigenvalue estimates and trace formulas for the matrix Hill’s equation*”, J. Diff. Eqn. **167**, 211–244 (2000).
- [7] W. G. Choe and J. Guckenheimer, “*Computing periodic orbits with high accuracy*”, Computer Meth. Appl. Mech. and Engin. **170**, 331–341 (1999).
- [8] Y. Colin de Verdière, “*Spectrum of the Laplace operator and periodic geodesics: thirty years after*”, Ann. Inst. Fourier **57**, 2429–2463 (2007).

- [9] P. Cvitanović, C. P. Dettmann, R. Mainieri, and G. Vattay, “Trace formulas for stochastic evolution operators: Weak noise perturbation theory”, *J. Stat. Phys.* **93**, 981–999 (1998).
- [10] P. Cvitanović and H. Liang, *Spatiotemporal cat: A chaotic field theory*, In preparation, 2021.
- [11] P. Cvitanović and D. Lippolis, Knowing when to stop: How noise frees us from determinism, in *Let’s Face Chaos through Nonlinear Dynamics*, edited by M. Robnik and V. G. Romanovski (2012), pp. 82–126.
- [12] M. N. Davletshin, “Hill’s formula for g -periodic trajectories of Lagrangian systems”, *Trans. Moscow Math. Soc.* **74**, 65–96 (2014).
- [13] X. Ding, H. Chaté, P. Cvitanović, E. Siminos, and K. A. Takeuchi, “Estimating the dimension of the inertial manifold from unstable periodic orbits”, *Phys. Rev. Lett.* **117**, 024101 (2016).
- [14] X. Ding and P. Cvitanović, “Periodic eigendecomposition and its application in Kuramoto-Sivashinsky system”, *SIAM J. Appl. Dyn. Syst.* **15**, 1434–1454 (2016).
- [15] E. J. Doedel, “Nonlinear numerics”, *J. Franklin Inst.* **334**, 1049–1073 (1997).
- [16] E. J. Doedel, A. R. Champneys, T. F. Fairgrieve, Y. A. Kuznetsov, B. Sandstede, and X. Wang, *AUTO: Continuation and Bifurcation Software for Ordinary Differential Equations* (2007).
- [17] E. J. Doedel, R. C. Paffenroth, H. B. Keller, D. J. Dichmann, J. Galan, and A. Vanderbauwhede, “Computation of periodic solutions of conservative systems with application to the 3-body problem”, *Int. J. Bifur. Chaos* **13**, 1353–1381 (2003).
- [18] H. R. Dullin and J. D. Meiss, “Stability of minimal periodic orbits”, *Phys. Lett. A* **247**, 227–234 (1998).
- [19] S. Elaydi, *An Introduction to Difference Equations*, 3rd ed. (Springer, Berlin, 2005).
- [20] S. N. Elaydi, *Discrete Chaos* (Chapman and Hall/CRC, 2007).
- [21] P. M. Gade and R. E. Amritkar, “Spatially periodic orbits in coupled-map lattices”, *Phys. Rev. E* **47**, 143–154 (1993).
- [22] J. F. Gibson, *Channelflow: A spectral Navier-Stokes simulator in C++*, tech. rep., Channelflow.org (U. New Hampshire, 2019).
- [23] J. F. Gibson, J. Halcrow, and P. Cvitanović, “Visualizing the geometry of state-space in plane Couette flow”, *J. Fluid Mech.* **611**, 107–130 (2008).
- [24] J. Guckenheimer and B. Meloon, “Computing periodic orbits and their bifurcations with automatic differentiation”, *SIAM J. Sci. Comput.* **22**, 951–985 (2000).
- [25] M. N. Gudorf, N. B. Budanur, and P. Cvitanović, *Spatiotemporal tiling of the Kuramoto-Sivashinsky flow*, In preparation, 2021.

- [26] B. Gutkin and V. Osipov, “Classical foundations of many-particle quantum chaos”, *Nonlinearity* **29**, 325–356 (2016).
- [27] P. G. Harper, “Single band motion of conduction electrons in a uniform magnetic field”, *Proc. Phys. Soc. London, Sect. A* **68**, 874–878 (1955).
- [28] G. W. Hill, “On the part of the motion of the lunar perigee which is a function of the mean motions of the sun and moon”, *Acta Math.* **8**, 1–36 (1886).
- [29] D. R. Hofstadter, “Energy levels and wave functions of Bloch electrons in rational and irrational magnetic fields”, *Phys. Rev. B* **14**, 2239–2249 (1976).
- [30] X. Hu, Y. Ou, and P. Wang, “Trace formula for linear Hamiltonian systems with its applications to elliptic Lagrangian solutions”, *Arch. Ration. Mech. Anal.* **216**, 313–357 (2014).
- [31] X. Hu, Y. Ou, and P. Wang, “Hill-type formula for Hamiltonian system with Lagrangian boundary conditions”, *J. Diff. Equ.* **267**, 2416–2447 (2019).
- [32] X. Hu and P. Wang, “Conditional Fredholm determinant for the S-periodic orbits in Hamiltonian systems”, *J. Funct. Analysis* **261**, 3247–3278 (2011).
- [33] X. Hu and P. Wang, “Conditional Fredholm determinant and trace formula for Hamiltonian systems: a survey”, in *Emerging Topics on Differential Equations and Their Applications* (World Scientific, Singapore, 2013), pp. 12–23.
- [34] X. Hu and P. Wang, “Eigenvalue problem of Sturm-Liouville systems with separated boundary conditions”, *Math. Z.* **283**, 339–348 (2015).
- [35] X. Hu and P. Wang, “Hill-type formula and Krein-type trace formula for S-periodic solutions in ODEs”, *Discrete Continuous Dyn. Syst. Ser. A* **36**, 763–784 (2016).
- [36] X. Hu, L. Wu, and R. Yang, *Morse index theorem of Lagrangian systems and stability of brake orbit*, 2018.
- [37] H.-T. Kook and J. D. Meiss, “Application of Newton’s method to Lagrangian mappings”, *Physica D* **36**, 317–326 (1989).
- [38] V. V. Kozlov, “Problem of stability of two-link trajectories in a multidimensional Birkhoff billiard”, *Proc. Steklov Inst. of Math.* **273**, 196–213 (2011).
- [39] M. G. Krein, “The basic propositions of the theory of λ -zones of stability of a canonical system of linear differential equations with periodic coefficients”, in *Operator Theory: Advances and Applications* (Birkhäuser, Basel, 1983), pp. 1–105.
- [40] F. Langouche, D. Roekaerts, and E. Tirapegui, “WKB expansion for arbitrary Hamiltonians”, *Il Nuovo Cimento A* **64**, 357–377 (1981).

- [41] S. Levit and U. Smilansky, “A new approach to Gaussian path integrals and the evaluation of the semiclassical propagator”, *Ann. Phys.* **103**, 198–207 (1977).
- [42] S. Levit and U. Smilansky, “A theorem on infinite products of eigenvalues of Sturm-Liouville type operators”, *Proc. Amer. Math. Soc.* **65**, 299–299 (1977).
- [43] R. S. MacKay and J. D. Meiss, “Linear stability of periodic orbits in Lagrangian systems”, *Phys. Lett. A* **98**, 92–94 (1983).
- [44] W. Magnus and S. Winkler, *Hill’s Equation* (Dover, 1966).
- [45] J. N. Mather, “Amount of rotation about a point and the Morse index”, *Commun. Math. Phys.* **94**, 141–153 (1984).
- [46] R. Peierls, “Zur Theorie des Diamagnetismus von Leitungselektronen”, *Z. Phys.* **80**, 763–791 (1933).
- [47] I. Percival and F. Vivaldi, “A linear code for the sawtooth and cat maps”, *Physica D* **27**, 373–386 (1987).
- [48] E. Petrisor, “Twist number and order properties of periodic orbits”, *Physica D* **263**, 57–73 (2013).
- [49] E. Petrisor, “Monotone gradient dynamics and the location of stationary (p,q)-configurations”, *J. Phys. A* **47**, 045102 (2014).
- [50] H. Poincaré, *Les méthodes nouvelles de la mécanique céleste*, For a very readable exposition of Poincaré’s work and the development of the dynamical systems theory up to 1920’s see ref. [JBG97]. (Guthier-Villars, Paris, 1899).
- [51] B. Simon, “Almost periodic Schrödinger operators: A review”, *Adv. Appl. Math.* **3**, 463–490 (1982).
- [52] T. Sunada, “Trace formula for Hill’s operators”, *Duke Math. J.* **47**, 529–546 (1980).
- [53] M. Toda, *Theory of Nonlinear Lattices* (Springer, Berlin, 1989).
- [54] L. N. Trefethen, *Spectral Methods in MATLAB* (SIAM, Philadelphia, 2000).
- [55] D. Treschev and O. Zubelevich, “Hill’s formula”, in *Introduction to the Perturbation Theory of Hamiltonian Systems* (Springer, Berlin, 2009), pp. 143–162.
- [56] J. H. Van Vleck, “The correspondence principle in the statistical interpretation of quantum mechanics”, *Proc. Natl. Acad. Sci.* **14**, 178–188 (1928).
- [57] D. Viswanath, “The Lindstedt-Poincaré technique as an algorithm for finding periodic orbits”, *SIAM Rev.* **43**, 478–496 (2001).
- [58] D. Viswanath, “Symbolic dynamics and periodic orbits of the Lorenz attractor”, *Nonlinearity* **16**, 1035–1056 (2003).

- [59] D. Viswanath, “The fractal property of the Lorenz attractor”, *Physica D* **190**, 115–128 (2004).
- [60] A. P. Willis, *Openpipeflow: Pipe flow code for incompressible flow*, tech. rep., Openpipeflow.org (U. Sheffield, 2014).
- [61] R. Xu and A. Weng, “The calculation for characteristic multiplier of Hill’s equation in case with positive mean”, *Nonlinear Anal. Real World Appl.* **9**, 949–962 (2008).
- [62] Q. Zhilin, A. Gangal, M. Benkun, and T. Gang, “Spatiotemporally periodic patterns in symmetrically coupled map lattices”, *Phys. Rev. E* **50**, 163–170 (1994).

Chapter 8

Hill's formula

8.1 An overview over “Hill’s formulas”

A succinct explanation of the Hill’s formula:

If you evaluate stability of the 3-term recurrence (13.109) on a periodic lattice you get the orbit Jacobian matrix \mathcal{J} ; if you evaluate it by multiplying the ‘two-configuration representation’ matrix J , you get the ‘time evolution’ side of the Hill’s formula.

We should emphasize that, while discovered first in Lagrangian setting, Hill’s formulas are much more general, they apply also to dissipative dynamical systems as well, see

CL18 [sect. 1.5 Stability of an orbit vs. its time-evolution stability](#)

CL18 [appendix C Spatiotemporal stability](#)

[sect. 8.2 Generating functions; action](#)

[sect. 8.4 Hill’s formula, Lagrangian setting](#)

[sect. 8.5 Spatiotemporal cat Hill’s formula](#)

[sect. 8.6 Hill’s formula for relative periodic orbits](#)

[sect. 8.7 Han’s temporal cat Hill’s formula](#)

[sect. 8.8 Han’s spatiotemporal cat Hill’s formula](#)

[sect. 8.8.1 Han’s relative-periodic Hill’s formula](#)

[sect. 8.9 Han’s Hénon map Hill’s formula](#)

8.2 Generating functions; action

¹ For discrete-time one-degree-of-freedom Lagrangian systems satisfying a periodicity condition (i.e., cat map):

$$L(q + 1, q' + 1) = L(q, q') + C, \quad (8.1)$$

¹Predrag 2016-11-11, 2018-09-26: What follows is (initially) copied from Li and Tomsovic [13], *Exact relations between homoclinic and periodic orbit actions in chaotic systems* arXiv source file, then merged with the MacKay-Meiss-Percival action principle refs. [15, 16].

one can consider relative periodic paths (or pre-periodic paths, also called periodic paths of type (d, n) by Mackay and Meiss [14]), with²

$$q_{i+n} = q_i + d. \quad (8.2)$$

Every q_i returns to its value after time period n , but shifted by d . Orbits satisfying (8.2) are given by stationary points of the action

$$S = \sum_{i=0}^{q-1} L(q_i, q_{i+1}) \quad (8.3)$$

in the space of periodic paths of type (d, n) . For periodic paths, it suffices to consider one period, because an orbit is periodic if and only if it is a stationary point of the action of one period in the space of periodic paths.

If the constant C (the Calabi invariant [5]) in the periodicity condition (8.1) is zero, and the Lagrangian satisfies a convexity condition

$$L_{12}(q, q') < 0, \quad (8.4)$$

where subscript k refers to the derivative with respect to the k th argument, then the action of periodic paths of type (d, n) is bounded below, so there is a minimising path. Since its action is stationary, it gives a periodic orbit of type (d, n) .

³ For orbit p of period n_p , the action of the orbit is:

$$S_p \equiv \sum_{n=0}^{n_p-1} L(q_n, q_{n+1}). \quad (8.5)$$

S_p is the generating function that maps a point along the orbit for one (prime) period. For the case of a fixed point p of period $n_p = 1$, the action is

$$S_p = L(q_p, q_p), \quad (8.6)$$

where the generating function $L(q_p, q_p)$ maps x_p into itself in one iteration.

8.3 Homoclinic and periodic orbit actions in chaotic systems

⁴ For an aperiodic orbit $\{x_0\}$ going through the point x_0 , the action, evaluated as the sum over an infinity of successive mappings,

$$S_{\{x_0\}} \equiv \lim_{N \rightarrow \infty} \sum_{n=-N}^{N-1} L(q_n, q_{n+1}) = \lim_{N \rightarrow \infty} S_{-N, N}, \quad (8.7)$$

²Predrag 2018-09-29: presumably they are relative periodic orbits, or pre-periodic orbits, with a rational winding number p/q .

³Predrag 2018-01-21: Is this true? To go from the Hamiltonian (x_t, p_t) phase space formulation to the Newtonian (or Lagrangian) (x_{t-1}, x_t) state space formulation, replace p_t by $p_t = (x_t - x_{t-1})/\Delta t$, where $\Delta t = 1$.

⁴Predrag 2018-09-29: What follows is copied from Li and Tomsovic [13].

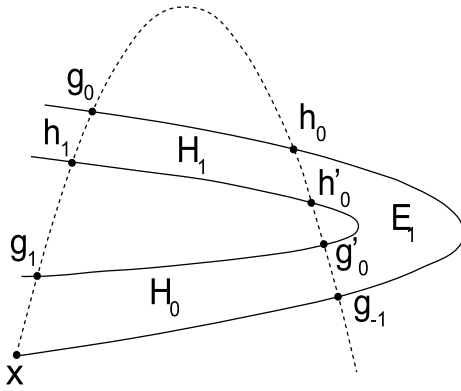


Figure 8.1: A sketch of a partial homoclinic tangle which forms a complete horseshoe structure. The unstable (stable) manifold of x is the solid (dashed) curve. There are two primary homoclinic orbits $\{h_0\}$ and $\{g_0\}$. \mathcal{R} is the closed region bounded by loop $\mathcal{L}_{USUS[x, g_{-1}, h_0, g_0]}$. (From ref. [13])

is not necessarily convergent. However, the MacKay-Meiss-Percival action principle [15, 16] can be applied to obtain well defined action differences between pairs of orbits. For example, the *relative action* $\Delta S_{\{h_0\}\{x_p\}}$ between a fixed point x_p and its homoclinic orbit $\{h_0\}$, where $h_{\pm\infty} \rightarrow x_p$:

$$\begin{aligned} \Delta S_{\{h_0\}\{x_p\}} &\equiv \lim_{N \rightarrow \infty} \sum_{i=-N}^{N-1} [L(h_i, h_{i+1}) - L(x_p, x_p)] \\ &= \int_{U[x_p, h_0]} pdq + \int_{S[h_0, x_p]} pdq = \oint_{US[x_p, h_0]} pdq \\ &= \mathcal{A}_{US[x_p, h_0]}^{\circ} \end{aligned} \quad (8.8)$$

where $U[x_p, h_0]$ is the segment of the unstable manifold from x_p to h_0 , and $S[h_0, x_p]$ the segment of the stable manifold from h_0 to x_p . The \circ superscript on the last line indicates that the area is interior to a path that forms a closed loop, and the subscript indicates the path: $US[x_p, h_0] = U[x_p, h_0] + S[h_0, x_p]$. The clockwise enclosure of an area is positive, counterclockwise negative. $\Delta S_{\{h_0\}\{x_p\}}$ gives the action difference between the homoclinic orbit segment $[h_{-N}, \dots, h_N]$ and the length- $(2N + 1)$ fixed point orbit segment $[x_p, \dots, x_p]$ in the limit $N \rightarrow \infty$. In later sections, upon specifying the symbolic code of the homoclinic orbit $\{h_0\} \Rightarrow \bar{0}\gamma\bar{0}$, we also denote $\Delta S_{\{h_0\}\{x_p\}}$ alternatively as

$$\Delta S_{\{h_0\}\{x_p\}} = \Delta S_{\bar{0}\gamma\bar{0}, \bar{0}} \quad (8.9)$$

by replacing the orbits in the subscript with their symbolic codes.

Likewise, a second important case is for the relative action between a pair

of homoclinic orbits $\{h'_0\} \Rightarrow \bar{0}\gamma'\bar{0}$ and $\{h_0\} \Rightarrow \bar{0}\gamma\bar{0}$, which results in

$$\begin{aligned}
 \Delta S_{\{h'_0\}\{h_0\}} &\equiv \lim_{N \rightarrow \infty} \sum_{i=-N}^{N-1} [L(h'_i, h'_{i+1}) - L(h_i, h_{i+1})] \\
 &= \lim_{N \rightarrow \infty} [L(h'_{-N}, h'_N) - L(h_{-N}, h_N)] \\
 &= \int_{U[h_0, h'_0]} pdq + \int_{S[h'_0, h_0]} pdq = \mathcal{A}_{US[h_0, h'_0]}^\circ \\
 &= \Delta S_{\bar{0}\gamma'\bar{0}, \bar{0}\gamma\bar{0}}
 \end{aligned} \tag{8.10}$$

where $U[h_0, h'_0]$ is the segment of the unstable manifold from h_0 to h'_0 , and $S[h'_0, h_0]$ the segment of the stable manifold from h'_0 to h_0 . Due to the fact that the endpoints approach x_p forward and backward in time, one can also write

$$\begin{aligned}
 \Delta S_{\{h'_0\}\{h_0\}} &= \lim_{N \rightarrow \infty} [L(h'_{-(N+n)}, h'_{N+m}) - L(h_{-N}, h_N)] \\
 &\quad -(n+m)\mathcal{F}_0.
 \end{aligned} \tag{8.11}$$

8.4 Hill's formula, Lagrangian setting

⁵ There can be more than one minimising path. In particular, translating one minimising path by an integer in time or space or both gives another. This implies existence of saddle points of the action in between the minima, with one downward direction [1-3]. They are called minimax points, and give rise to minimax periodic orbits of type (d, n) . The statement of the existence of at least two periodic orbits of each type (d, n) is known as the Poincaré-Birkhoff theorem.

As a corollary, Mackay and Meiss [14] rederive the old result that when the convexity condition is satisfied, the multipliers of a minimising orbit are a reciprocal pair of positive reals, and those of a minimax orbit are either a complex conjugate pair on the unit circle, or a reciprocal pair of negative reals. The result for minimising orbits was shown by Poincaré [20] for two-degree-of-freedom continuous-time systems, and Birkhoff [1] discusses the minimax case.

The linear stability of a periodic orbit is determined by its multipliers, the eigenvalues of the derivative of the return map round the orbit. While the first variation of the action is by definition zero for an orbit, the multipliers of a periodic orbit can be related to the second variations of the action in the space of periodic paths. This has been shown in various cases. Hill [9] and Poincaré [20] derived a formula for the multipliers in the case of one-degree-of-freedom systems of the form kinetic minus potential [9], using a Fourier representation for periodic paths. In his study of periodic orbits of the three-body problem, Hill obtained a formula connecting the characteristic polynomial of the monodromy matrix of a periodic orbit with the infinite determinant of the Hessian of the action functional. Mackay and Meiss [14] derived a formula (8.17) for the multipliers of a periodic orbit for general discrete-time one-degree-of-freedom systems. Bolotin and Treschev [3] give two multidimensional generalizations of Hill's formula: for discrete Lagrangian systems (symplectic twist maps) and for continuous Lagrangian systems, and discuss implications of symmetries and reversibility. Bountis and Helleman [4] and Greene [8] treated the case of discrete-time one-degree-of-freedom systems with

$$L_{12}(q, q') = -1. \quad (8.12)$$

Schmidt [21] determined n -tupling bifurcations by the criterion that the matrix of second variations of the action with respect to periodic paths of n times the period have a zero eigenvalue.

Mackay and Meiss [14] relate the multipliers of a periodic orbit to the second variations of the action about the orbit, and compute the Hill determinant of the matrix of second variations of the action in the space of periodic paths of period T .

⁵Predrag 2016-11-11, 2018-09-26: The current draft of this section starts out with excerpts from Mackay and Meiss [14] *Linear stability of periodic orbits in Lagrangian systems*, and Bolotin and Treschev [3] *Hill's formula*.

Stationarity (5.77) of the action for an orbit of a discrete-time one-degree-of-freedom system implies that

$$L_2(q_{i-1}, q_i) + L_1(q_i, q_{i+1}) = 0. \quad (8.13)$$

Thus the tangent orbits δx_i satisfy [...]. The multipliers Λ of a periodic orbit of period q are defined by existence of a tangent orbit satisfying [...] residue of a periodic orbit one can easily solve for multipliers. [... losing steam]

Mackay and Meiss [14] formulas for the multipliers of minimising and minimax orbits follow. Under the convexity condition (8.4), the denominator is positive. At a minimum of action (whether local or global):

$$D(1) \leq 0, \quad (8.14)$$

so the multipliers are real and positive. At a minimax with one downward direction:

$$D(1) \geq 0, \quad (8.15)$$

so the multipliers are on the unit circle or the negative real axis.

Residue [8] R of a periodic orbit p of period n_p

$$4R = \det(\mathbf{1} - J_p) = \text{tr}(\mathbf{1} - J_p) = 2 - \Lambda_p - 1/\Lambda_p \quad (8.16)$$

is related to the Hill determinant $D(\Lambda)$ by what the discrete Hill's formula [3]:
⁶

$$\det(\mathbf{1} - J_p) = -D(1) \left(\prod_{i=0}^{n_p-1} (-L_{12}[i, i+1]) \right)^{-1}. \quad (8.17)$$

This formula was derived by Mackay and Meiss [14] and Allroth [1] (Allroth eq. (12)). It applies to general “one-degree-of-freedom” systems, i.e., 1D lattices with only the nearest neighbor interactions. For a finite set of neighbors, i.e., higher-dimensional discrete-time systems, Allroth [1] has some partial results in the context of Frenkel-Kontorova models.

$D(1)$ is the Hill determinant of the matrix of second variations of the action in the space of periodic paths of period q . So we have related the multipliers of a periodic orbit to the second variations of the action about the orbit.

⁶Predrag 2018-09-30: See Bolotin and Treschev [3] eqs. (2.8) and (2.13)

8.5 Spatiotemporal cat Hill's formula

2020-07-23 Predrag I have everything in place for deriving spatiotemporal cat (and temporal catas a special case) Hill's formula from the elementary Kronecker product (8.18) block matrix rules

1. multiplication (8.19) leads to shift (8.35) accruing correctly.
2. Hill determinant (8.20), (8.36); yields correct $\ln \det = \text{tr} \ln$ reduction to periodic J_p
3. $\mathbf{A} \otimes \mathbf{B}$ being similar to $\mathbf{B} \otimes \mathbf{A}$ by (8.21) explains why $[2L \times 2L]$ phase space is equivalent to the $[L \times L]$ orbit stability.

2020-07-23 Predrag Next: streamline, move to CL18.tex

2020-07-27 Predrag Essential parts copied to CL18.tex, *siminos/kittens/Hill.tex*

The $d = 2$ lattice spatiotemporal cat equations can be recast in a matrix form, by rewriting the defining equations as block matrices [6, 7, 11], constructed by the **Kronecker product** $\mathbf{A} \otimes \mathbf{B}$,⁷ an operation that replaces elements of the $[n \times n]$ matrix \mathbf{A} by $[m \times m]$ matrix 'blocks' \mathbf{B} , resulting in an $[mn \times mn]$ block matrix [2, 26]

$$\mathbf{A} \otimes \mathbf{B} = \begin{bmatrix} a_{11}\mathbf{B} & \cdots & a_{1n}\mathbf{B} \\ \vdots & \ddots & \vdots \\ a_{n1}\mathbf{B} & \cdots & a_{nn}\mathbf{B} \end{bmatrix}. \quad (8.18)$$

Consider \mathbf{A}, \mathbf{C} square matrices of size $[n \times n]$, and \mathbf{B}, \mathbf{D} square matrices of size $[m \times m]$. The matrix product of two block matrices is a block matrix [2, 25],

$$(\mathbf{A} \otimes \mathbf{B})(\mathbf{C} \otimes \mathbf{D}) = (\mathbf{AC}) \otimes (\mathbf{BD}). \quad (8.19)$$

The trace and the determinant of a block matrix are given by

$$\begin{aligned} \text{tr}(\mathbf{A} \otimes \mathbf{B}) &= \text{tr} \mathbf{A} \text{tr} \mathbf{B} \\ \det(\mathbf{A} \otimes \mathbf{B}) &= \det(\mathbf{A}^m) \det(\mathbf{B}^n). \end{aligned} \quad (8.20)$$

The two $[mn \times mn]$ block matrices $\mathbf{A} \otimes \mathbf{B}$ and $\mathbf{B} \otimes \mathbf{A}$ are equivalent by a similarity transformation

$$\mathbf{B} \otimes \mathbf{A} = \mathbf{P}^\top (\mathbf{A} \otimes \mathbf{B}) \mathbf{P}, \quad (8.21)$$

where \mathbf{P} is permutation matrix. As $\det \mathbf{P} = 1$, the block matrix determinant $\det(\mathbf{A} \otimes \mathbf{B}) = \det(\mathbf{B} \otimes \mathbf{A})$ is independent of the order in which blocks are constructed.

⁷Predrag 2020-08-01: The Zehfuss product (1858), really. The Hill determinant is from 1886, though it does not look recognizably anything like out the Hill determinants... These things are everywhere!

Now, apply this formalism to a $[L \times T]_0$ rectangular Bravais cell. In the Kronecker product block matrix notation (8.18), the orbit Jacobian matrix `refeq{eq:BxAtempJ}` can be written as a $[LT \times LT]$ block matrix

$$\mathcal{J} = \mathbf{1}_1 \otimes (d_2 + d_2^{-1}) - 2s \mathbf{1}_1 \otimes \mathbf{1}_2 + (d_1 + d_1^{-1}) \otimes \mathbf{1}_2, \quad (8.22)$$

where the (8.18) matrix \mathbf{A} and identity $\mathbf{1}_1$ matrix are ‘spatial’ $[L \times L]$ matrices, with blocks \mathbf{B} and identity $\mathbf{1}_2$ ‘temporal’ $[T \times T]$ matrices, with indices ‘1’, ‘2’ referring to ‘spatial’, ‘temporal’ lattice directions, respectively.

Our goal is to compute the Hill determinant $|\det \mathcal{J}|$. As we have shown in the example `refsect{s:catLattRel3x2}`, this is best done directly, by computing the volume of the fundamental parallelepiped.⁸

However, in classical and statistical mechanics, one often computes the Hill determinant using a Hamiltonian, or ‘transfer matrix’ formulation. An example is the temporal cat 3-term recurrence (5.238) in the Percival-Vivaldi [19] ‘two-configuration’ cat map representation (1.101)

$$\hat{\mathbf{x}}_{t+1} = \hat{\mathbf{J}}_1 \hat{\mathbf{x}}_t - \hat{\mathbf{s}}_t, \quad (8.23)$$

with the one-time step temporal evolution $[2 \times 2]$ Jacobian matrix $\hat{\mathbf{J}}_1$ generating a time orbit by acting on the 2-dimensional ‘phase space’ of successive configuration points

$$\hat{\mathbf{J}}_1 = \begin{bmatrix} 0 & 1 \\ -1 & s \end{bmatrix}, \quad \hat{\mathbf{x}}_t = \begin{pmatrix} x_{t-1} \\ x_t \end{pmatrix}, \quad \hat{\mathbf{s}}_t = \begin{pmatrix} 0 \\ s_t \end{pmatrix}, \quad (8.24)$$

Similarly, for the $d = 2$ spatiotemporal cat lattice at hand, one can recast the 5-term recurrence (XX) (compare with the (5.248))

$$\begin{aligned} x_{nt} &= x_{nt} \\ x_{n,t+1} &= -x_{n,t-1} + (-x_{n-1,t} + 2s x_{nt} - x_{n+1,t}) - s_{nt} \end{aligned} \quad (8.25)$$

in the ‘two-configuration’ matrix form (8.23) by picking the vertical direction (indexed ‘2’) as the ‘time’, with temporal 1-time step Jacobian $[2L \times 2L]$ block matrix

$$\hat{\mathbf{J}}_1 = \left[\begin{array}{c|c} \mathbf{0} & \mathbf{1}_1 \\ \hline -\mathbf{1}_1 & -\mathcal{J}_1 \end{array} \right], \quad (8.26)$$

(known as a transfer matrix in statistical mechanics [17, 18]) generating a time orbit by acting on a $2L$ -dimensional ‘phase space’ lattice strip $\hat{\mathbf{x}}_t$ along the ‘spatial’ direction (indexed ‘1’),

$$\hat{\mathbf{x}}_t = \begin{bmatrix} \mathbf{x}_{t-1} \\ \mathbf{x}_t \end{bmatrix}, \quad \hat{\mathbf{s}}_t = \begin{bmatrix} \mathbf{0} \\ \mathbf{s}_{1t} \end{bmatrix}, \quad \mathbf{x}_t = \begin{bmatrix} x_{1t} \\ \vdots \\ x_{Lt} \end{bmatrix}, \quad \mathbf{s}_t = \begin{bmatrix} s_{1t} \\ \vdots \\ s_{Lt} \end{bmatrix}, \quad (8.27)$$

⁸Predrag 2020-07-27: Insert `refsect{s:catLattRel3x2}` example here?

where the hat $\hat{\cdot}$ indicates a $2L$ -dimensional ‘two-configuration’ state, and \mathcal{J}_1 is the spatial $[L \times L]$ orbit Jacobian matrix of form (XX),

$$\mathcal{J}_1 = d_1^{-1} - 2s\mathbf{1}_1 + d_1 \quad (8.28)$$

The ‘two-configuration’ coupled cat maps system (8.23) is a generalization of the Bernoulli map time evolution formulation (XX) to a higher-dimensional spatially-coupled lattice. Just as in the temporal Bernoulli condition refeq {tempFixPoint}, the first order in time difference equation (8.23) can be viewed as a lattice state fixed point condition refeq{tempFixPoint}, a zeros of the function $F[\hat{X}] = \hat{\mathcal{J}}\hat{X} + \hat{M} = 0$, with the entire periodic *lattice state* \hat{X}_M treated as a single fixed *point* in the $2LT$ -dimensional unit hyper-cube, and the $[2LT \times 2LT]$ block matrix orbit Jacobian matrix given either by

$$\hat{\mathcal{J}} = \hat{\mathbf{1}} - \hat{\mathbf{J}}_1 \otimes d_2^{-1}, \quad (8.29)$$

or by

$$\hat{\mathcal{J}}' = \hat{\mathbf{1}} - d_2^{-1} \otimes \hat{\mathbf{J}}_1. \quad (8.30)$$

Here the unity $\hat{\mathbf{1}} = \hat{\mathbf{1}}_1 \otimes \mathbf{1}_2$ is a $[2LT \times 2LT]$ block matrix, and the time-evolution Jacobian matrix $\hat{\mathbf{J}}_1$ (8.26) is a $[2L \times 2L]$ matrix.

The order in which the block matrix blocks are composed does not matter, yielding the same the Hill determinant $\det \hat{\mathcal{J}} = \det \hat{\mathcal{J}}'$ by (8.21). However, written out explicitly, the two orbit Jacobian matrices (8.31) and (8.34) are of a very different form.

For example, for the $[L \times T]_0$ rectangular Bravais cell, the spatiotemporal cat orbit Jacobian matrix (XX) involves the $[T \times T]$ time shift operator block matrix d_2 (XX) with the one-time-step $[2L \times 2L]$ time-evolution Jacobian matrix $\hat{\mathbf{J}}_1$ (8.26)

$$\hat{\mathcal{J}} = \left[\begin{array}{c|c} \mathbf{1}_1 \otimes \mathbf{1}_2 & -\mathbf{1}_1 \otimes d_2^{-1} \\ \hline \mathbf{1}_1 \otimes d_2^{-1} & \mathbf{1}_1 \otimes \mathbf{1}_2 + \mathcal{J}_1 \otimes d_2^{-1} \end{array} \right], \quad (8.31)$$

and for spatiotemporal cat (8.25) this is a time-periodic $[T \times T]$ shift operator block matrix d_2 (XX), each block now a space-periodic $[2L \times 2L]$ matrix $\hat{\mathbf{J}}_1$ (8.26).

If a block matrix is composed of four blocks, its determinant can be factorized by Schur's (1917) formula [22, 25]

$$\det \left[\begin{array}{c|c} \mathbf{A} & \mathbf{B} \\ \hline \mathbf{C} & \mathbf{D} \end{array} \right] = \det(\mathbf{A}) \det(\mathbf{D} - \mathbf{C}\mathbf{A}^{-1}\mathbf{B}). \quad (8.32)$$

so, noting (8.19), (8.22) and (8.28), we find that the $[2LT \times 2LT]$ ‘phase space’ $\det \hat{\mathcal{J}}$ defined by (8.31) is actually the desired Hill determinant of $[LT \times LT]$

orbit Jacobian matrix \mathcal{J} ,

$$\begin{aligned}
 \det \hat{\mathcal{J}} &= \det \left[\begin{array}{c|c} \mathbf{1}_1 \otimes \mathbf{1}_2 & -\mathbf{1}_1 \otimes d_2^{-1} \\ \mathbf{1}_1 \otimes d_2^{-1} & \mathbf{1}_1 \otimes \mathbf{1}_2 + \mathcal{J}_1 \otimes d_2^{-1} \end{array} \right] \\
 &= \det [\mathbf{1}_1 \otimes \mathbf{1}_2 + \mathcal{J}_1 \otimes d_2^{-1} + (\mathbf{1}_1 \otimes d_2^{-1})(\mathbf{1}_1 \otimes \mathbf{1}_2)(\mathbf{1}_1 \otimes d_2^{-1})] \\
 &= \det [\mathbf{1}_1 \otimes \mathbf{1}_2 + \mathcal{J}_1 \otimes d_2^{-1} + \mathbf{1}_1 \otimes d_2^{-2}] \\
 &= \det(d_2^{-1}) \det [\mathbf{1}_1 \otimes d_2^{-1} + (d_1^{-1} - 2s\mathbf{1}_1 + d_1) \otimes \mathbf{1}_2 + \mathbf{1}_1 \otimes d_2] \\
 &= \det \mathcal{J},
 \end{aligned} \tag{8.33}$$

where we have used $\det \mathbf{1}_1 = \det \mathbf{1}_2 = \det d_1 = \det d_2 = 1$.

Consider next (8.30), the equivalent way of forming of the block matrix for the $[L \times T]_0$ rectangular Bravais cell, with temporal period taken for definitiveness $T = 4$. The spatiotemporal cat orbit Jacobian matrix (8.30) is now constructed as the $[4 \times 4]$ time shift operator block matrix d_2 (XX), with the one-time-step $[2L \times 2L]$ time-evolution Jacobian matrix $\hat{\mathbf{J}}_1$ (8.26) and unit matrix $\hat{\mathbf{1}}_1$ as blocks

$$\hat{\mathcal{J}}' = \mathbf{1}_2 \otimes \hat{\mathbf{1}}_1 - d_2^{-1} \otimes \hat{\mathbf{J}}_1 = \left[\begin{array}{c|c|c|c} \hat{\mathbf{1}}_1 & \mathbf{0} & \mathbf{0} & -\hat{\mathbf{J}}_1 \\ \hline -\hat{\mathbf{J}}_1 & \hat{\mathbf{1}}_1 & \mathbf{0} & \mathbf{0} \\ \hline \mathbf{0} & -\hat{\mathbf{J}}_1 & \hat{\mathbf{1}}_1 & \mathbf{0} \\ \hline \mathbf{0} & \mathbf{0} & -\hat{\mathbf{J}}_1 & \hat{\mathbf{1}}_1 \end{array} \right]. \tag{8.34}$$

To evaluate the Hill determinant $\det \hat{\mathcal{J}}'$, note that from the block-matrix multiplication rule (8.19) and the determinant rule (8.20) it follows that

$$(d_2^{-1} \otimes \hat{\mathbf{J}}_1)(d_2^{-1} \otimes \hat{\mathbf{J}}_1) = d_2^{-2} \otimes \hat{\mathbf{J}}_1^2, \quad (d_2^{-1} \otimes \hat{\mathbf{J}}_1)^k = d_2^{-k} \otimes \hat{\mathbf{J}}_1^k, \tag{8.35}$$

and

$$\det(d_2^{-1} \otimes \hat{\mathbf{J}}_1) = (\det d_2)^{-L} (\det \hat{\mathbf{J}}_1)^T = \det \hat{\mathbf{J}}_p, \quad \hat{\mathbf{J}}_p = \hat{\mathbf{J}}_1^T, \tag{8.36}$$

where $\hat{\mathbf{J}}_p$ is the Jacobian matrix of a temporal periodic orbit p . Expand $\ln \det \hat{\mathcal{J}}' = \text{tr} \ln \hat{\mathcal{J}}'$ as a series using (8.20) and (8.35),

$$\text{tr} \ln \hat{\mathcal{J}}' = \text{tr} \ln (\mathbf{1} - d_2^{-1} \otimes \hat{\mathbf{J}}_1) = - \sum_{k=1}^{\infty} \frac{1}{k} \text{tr}(d_2^{-k}) \text{tr} \hat{\mathbf{J}}_1^k, \tag{8.37}$$

and use $\text{tr } d_2^k = T$ if k is a multiple of T , 0 otherwise (follows from $d_2^T = \mathbf{1}$):

$$\ln \det (\mathbf{1} - d_2^{-1} \otimes \hat{\mathbf{J}}_1) = - \sum_{r=1}^{\infty} \frac{1}{r} \text{tr} \hat{\mathbf{J}}_p^r = \ln \det (\hat{\mathbf{1}}_1 - \hat{\mathbf{J}}_p).$$

So for the spatiotemporal cat the orbit Jacobian matrix and the temporal evolution (8.23) stability $\hat{\mathbf{J}}_p$ are related by the remarkable Hill's formula

$$|\det \mathcal{J}| = |\det(\hat{\mathbf{1}}_1 - \hat{\mathbf{J}}_p)|. \tag{8.38}$$

which expresses the Hill determinant of the arbitrarily large orbit Jacobian matrix $\hat{\mathcal{J}}'$ in terms of a determinant of a small $[2L \times 2L]$ time-evolution Jacobian matrix $\hat{\mathbf{J}}_1$.

Remark From (10.89) we have

2CB

$$\det \hat{\mathbf{J}}_1 = \det \begin{bmatrix} \mathbf{0} & \mathbf{1}_1 \\ -\mathbf{1}_1 & -\mathcal{J}_1 \end{bmatrix} = \det(\mathcal{J}_1) \det(\mathcal{J}_1^{-1}) = 1, \quad (8.39)$$

so $\hat{\mathbf{J}}_1$ is a canonical, or phase-space volume preserving transformation, as one expects of Hamiltonian systems.

Remark The reformulation of the spatiotemporal cat 5-term recurrence (8.25) as the ‘two-configuration’ form (8.23) is really just the usual passage from Lagrangian to the Hamiltonian formulation, but we chose to short-circuit it, as all that heavy general formalism is not needed for the problem at hand.⁹

Remark I am not a big fan of the Kronecker product (8.18) as it treats the time and the space differently. Nicer notion would be a tensor product that treats all directions in d -dimensional on equal, symmetric footing. Perhaps the ‘outer product’ does that (see the [wiki](#)) explains the outer product of tensors, and its relation to the Kronecker product. Arfken, Weber & Harris [2] *Mathematical Methods for Physicists: A Comprehensive Guide* ([click here](#)) call it the *direct tensor* or *Kronecker* product, see [AWH eq. \(2.55\)](#).

Perhaps Steeb and Hardy [24] *Matrix Calculus, Kronecker Product and Tensor Product* (I have not downloaded the book) deals with that. Not sure if that is different from Steeb and Hardy [23] *Matrix Calculus and Kronecker Product - A Practical Approach to Linear and Multilinear Algebra*.

Kowalski and Steeb [12] *Nonlinear Dynamical Systems and Carleman Linearization* ([click here](#)) already goes beyond the other Kronecker product references I had looked at, as it emphasizes commutators of Kronecker products.

Horn and Johnson [10] *Matrix Analysis* ([click here](#)) promises to do Kronecker product in the companion volume Horn and JohnsonHoJo94 *Topics in Matrix Analysis* that I have not looked yet.

Schur’s (1917) formula (8.32) is derived in exercise A.12 of Stone and GoldbartStGo09 *Mathematics for Physics* ([click here](#)).

8.6 Hill's formula for relative periodic orbits

As a first try, let’s reverse-engineer relative periodicity for the more familiar ‘two-configuration’ spatiotemporal cat (8.23). The stability matrix of a temporally periodic orbit

$$\delta\hat{\mathbf{x}}_T = \hat{\mathbf{J}}_1^T \delta\hat{\mathbf{x}}_0, \quad (8.40)$$

corresponds spatiotemporally to a $[L \times T]_0$ rectangular Bravais cell, while the stability matrix of a relative periodic orbit includes the relative shift S ,

$$\delta\hat{\mathbf{x}}_T = d_1^S \hat{\mathbf{J}}_1^T \delta\hat{\mathbf{x}}_0, \quad (8.41)$$

⁹Predrag 2020-07-15: Perhaps refer to [ChaosBook 8.1 Hamiltonian flows](#). Mention transfer matrix formulation of lattice field theories?

and corresponds spatiotemporally to a $[L \times T]_S$ parallelepipedal Bravais cell, which can be convert into a rectangular cell by going into a co-moving frame, with the temporal 1-time step Jacobian $[2L \times 2L]$ block matrix (8.26) replaced by

$$\tilde{\mathbf{J}}_1 \Rightarrow d_1^{S/T} \tilde{\mathbf{J}}_1 = \left[\begin{array}{c|c} \mathbf{0} & d_1^{S/T} \\ \hline -d_1^{S/T} & -d_1^{S/T} \mathcal{J}_1 \end{array} \right], \quad (8.42)$$

and $\hat{\mathcal{J}}'_{[L \times T]_S}$ is of the rectangular cell form, with replacement $\hat{\mathbf{J}}_1 \rightarrow \tilde{\mathbf{J}}_1$ in (8.34). In evaluating the corresponding determinants we can use (8.36),

$$\det(d_2^{-1} \otimes \tilde{\mathbf{J}}_1) = (\det d_2)^{-L} (\det \tilde{\mathbf{J}}_1)^T = \det \tilde{\mathbf{J}}_p, \quad \tilde{\mathbf{J}}_p = d_1^S \hat{\mathbf{J}}_1^T, \quad (8.43)$$

where $\tilde{\mathbf{J}}_p$ is the Jacobian matrix of the temporal prime relative periodic orbit p .

Now we can reverse-engineer relative periodicity for the $d = 2$ lattice. We have just worked out $\hat{\mathcal{J}}'$ defined by (8.30). Consider next $\hat{\mathcal{J}}$ (8.29), with ‘time’ and ‘space’ blocked in the other order, defined by (8.29), (8.31) and (8.42),

$$\hat{\mathcal{J}} = \left[\begin{array}{c|c} \mathbf{1}_1 \otimes \mathbf{1}_2 & -d_1^{S/T} \otimes d_2^{-1} \\ \hline d_1^{S/T} \otimes d_2^{-1} & \mathbf{1}_1 \otimes \mathbf{1}_2 + \mathcal{J}_1 d_1^{S/T} \otimes d_2^{-1} \end{array} \right], \quad (8.44)$$

We next evaluate the $[2LT \times 2LT]$ ‘phase space’ $\det \hat{\mathcal{J}}$ defined by (8.31), and show again that it equals the Hill determinant of $[LT \times LT]$ orbit Jacobian matrix \mathcal{J} ,

$$\begin{aligned} \det \hat{\mathcal{J}} &= \det \left[\mathbf{1}_1 \otimes \mathbf{1}_2 + \mathcal{J}_1 d_1^{S/T} \otimes d_2^{-1} + d_1^{2S/T} \otimes d_2^{-2} \right] \\ &= \det \left[d_1^{S/T} \otimes d_2^{-1} + (d_1^{-1} - 2s\mathbf{1}_1 + d_1) \otimes \mathbf{1}_2 + d_1^{-S/T} \otimes d_2 \right] \\ &= \det \mathcal{J}, \end{aligned} \quad (8.45)$$

The orbit Jacobian matrix (8.22) for a tilted Bravais domain (relative periodic orbit) is thus a $[LT \times LT]$ block matrix

$$\mathcal{J}_{[L \times T]_S} = \left(d_1^{S/T} \otimes d_2^{-1} + d_1^{-S/T} \otimes d_2 \right) - 2s \mathbf{1}_1 \otimes \mathbf{1}_2 + (d_1 + d_1^{-1}) \otimes \mathbf{1}_2. \quad (8.46)$$

All the relative periodicity is in the $d_1^{-S/T} \otimes d_2$. This space-time asymmetry is a consequence of choosing the Hermite normal form (5.204) to define the Bravais cell, so we are not home yet - even though we are computing the representation-independent determinants, we do not have an invariant statement of cell’s ‘tilt’.

What do I mean? An example of an invariant condition is the statement that a prime lattice \mathcal{L}_p tiles the given lattice \mathcal{L} only if the area spanned by the two ‘tilted’ basis vectors

$$\mathbf{a}_2 \times \mathbf{a}_2^p = ST_p - TS_p \quad (8.47)$$

is a multiple of the prime tile area $L_p T_p$.

Remark Perhaps we can use Floquet theory analogue of a comoving frame (8.42) to put the generally time-varying $(\hat{\mathbf{J}}_1)_t$ into an average, constant per time step form $\tilde{\mathbf{J}}_1$, in order to use the block-matrix formalism.

8.7 Han's temporal cat Hill's formula

The orbit Jacobian matrix of the $T = 4$ temporal cat has form:

$$\mathcal{J} = \begin{pmatrix} -s & 1 & 0 & 1 \\ 1 & -s & 1 & 0 \\ 0 & 1 & -s & 1 \\ 1 & 0 & 1 & -s \end{pmatrix}.$$

For example, the $T = 4$ the orbit Jacobian matrix expressed in the terms of the one-step $[2 \times 2]$ temporal Jacobian matrix (8.23) is:

$$\begin{aligned} \hat{\mathbf{J}}_1 &= \mathbf{1} - d^{-1} \otimes J \\ &= \left(\begin{array}{cc|cc|cc|cc} 1 & 0 & 0 & 0 & 0 & 0 & 0 & -1 \\ 0 & 1 & 0 & 0 & 0 & 0 & 1 & -s \\ \hline 0 & -1 & 1 & 0 & 0 & 0 & 0 & 0 \\ 1 & -s & 0 & 1 & 0 & 0 & 0 & 0 \\ \hline 0 & 0 & 0 & -1 & 1 & 0 & 0 & 0 \\ 0 & 0 & 1 & -s & 0 & 1 & 0 & 0 \\ \hline 0 & 0 & 0 & 0 & 0 & -1 & 1 & 0 \\ 0 & 0 & 0 & 0 & 1 & -s & 0 & 1 \end{array} \right). \end{aligned} \quad (8.48)$$

$$\det(\mathbf{1} - d^{-1} \otimes J) = \det(\mathbf{1} - J \otimes d^{-1}) = \det[(\mathbf{1} - J \otimes d^{-1})(\mathbf{1}_{[2 \times 2]} \otimes d)],$$

where:

$$\mathbf{1} - J \otimes d^{-1} = \left(\begin{array}{cccc|cccc} 1 & 0 & 0 & 0 & 0 & 0 & 0 & -1 \\ 0 & 1 & 0 & 0 & -1 & 0 & 0 & 0 \\ 0 & 0 & 1 & 0 & 0 & -1 & 0 & 0 \\ 0 & 0 & 0 & 1 & 0 & 0 & -1 & 0 \\ \hline 0 & 0 & 0 & 1 & 1 & 0 & 0 & -s \\ 1 & 0 & 0 & 0 & -s & 1 & 0 & 0 \\ 0 & 1 & 0 & 0 & 0 & -s & 1 & 0 \\ 0 & 0 & 1 & 0 & 0 & 0 & -s & 1 \end{array} \right),$$

and

$$(\mathbf{1} - J \otimes d^{-1})(\mathbf{1}_{[2 \times 2]} \otimes d) = \left(\begin{array}{cccc|cccc} 0 & 1 & 0 & 0 & -1 & 0 & 0 & 0 \\ 0 & 0 & 1 & 0 & 0 & -1 & 0 & 0 \\ 0 & 0 & 0 & 1 & 0 & 0 & -1 & 0 \\ 1 & 0 & 0 & 0 & 0 & 0 & 0 & -1 \\ \hline 1 & 0 & 0 & 0 & -s & 1 & 0 & 0 \\ 0 & 1 & 0 & 0 & 0 & -s & 1 & 0 \\ 0 & 0 & 1 & 0 & 0 & 0 & -s & 1 \\ 0 & 0 & 0 & 1 & 1 & 0 & 0 & -s \end{array} \right).$$

A block matrix is a matrix defined by smaller matrices, called blocks. The determinant of a block matrix is [25] (see [wiki](#)):

$$\det \begin{pmatrix} A & B \\ C & D \end{pmatrix} = \det(A) \det(D - CA^{-1}B). \quad (8.49)$$

or

$$\det \begin{pmatrix} A & B \\ C & D \end{pmatrix} = \det(D) \det(A - BD^{-1}C). \quad (8.50)$$

8.8 Han's spatiotemporal cat Hill's formula

Consider a $[L \times T]_0$ rectangular Bravais cell. In the Kronecker product block matrix notation (8.18), the orbit Jacobian matrix `refeq{eq:BxAtempJ}` is the $[LT \times LT]$ block matrix (8.22):

$$\mathcal{J} = \mathbf{1}_1 \otimes (d_2 + d_2^{-1}) - 2s\mathbf{1} + (d_1 + d_1^{-1}) \otimes \mathbf{1}_2.$$

The temporal Jacobian matrix \mathbf{J} is:

$$\mathbf{J} = \begin{pmatrix} \mathbf{0}_1 & \mathbf{1}_1 \\ -\mathbf{1}_1 & -\hat{\mathcal{J}}_1 \end{pmatrix},$$

where $\hat{\mathcal{J}}_1$ is a $[L \times L]$ matrix (8.28):

$$\hat{\mathcal{J}}_1 = d_1^{-1} - 2s\mathbf{1}_1 + d_1.$$

There is another $[2LT \times 2LT]$ orbit Jacobian matrix:

$$\mathcal{J}' = \mathbf{1} - d_2^{-1} \otimes \mathcal{J}_1.$$

Here we will show that:

$$\det \mathcal{J} = \det \mathcal{J}'.$$

$$\begin{aligned} \det \mathcal{J}' &= \det (\mathbf{1} - d_2^{-1} \otimes \mathcal{J}_1) = \det (\mathbf{1} - \mathcal{J}_1 \otimes d_2^{-1}) \\ &= \det [(\mathbf{1} \otimes d_2)(\mathbf{1} - \mathcal{J}_1 \otimes d_2^{-1})] \\ &= \det (\mathbf{1} \otimes d_2 - \mathcal{J}_1 \otimes \mathbf{1}_2) \\ &= \det \left\{ \begin{pmatrix} \mathbf{1}_1 \otimes d_2 & 0 \\ 0 & \mathbf{1}_1 \otimes d_2 \end{pmatrix} - \begin{pmatrix} 0 & \mathbf{1}_1 \otimes \mathbf{1}_2 \\ -\mathbf{1}_1 \otimes \mathbf{1}_2 & -\hat{\mathcal{J}}_1 \otimes \mathbf{1}_2 \end{pmatrix} \right\} \\ &= \det \begin{pmatrix} \mathbf{1}_1 \otimes d_2 & -\mathbf{1}_1 \otimes \mathbf{1}_2 \\ \mathbf{1}_1 \otimes \mathbf{1}_2 & \mathbf{1}_1 \otimes d_2 + \hat{\mathcal{J}}_1 \otimes \mathbf{1}_2 \end{pmatrix} \\ &= \det (\mathbf{1}_1 \otimes d_2 + \hat{\mathcal{J}}_1 \otimes \mathbf{1}_2 + \mathbf{1}_1 \otimes d_2^{-1}) \\ &= \det \mathcal{J}. \end{aligned} \quad (8.51)$$

8.8.1 Han's relative-periodic Hill's formula

Consider a ‘tilted’ or ‘relative periodic’ $[L \times T]_S$ Bravais cell for which we have after one time period:

$$\hat{\mathbf{J}}_p \hat{\mathbf{u}}_t = \hat{\mathbf{u}}_{t+T} = \mathbf{g}_S^{-1} \hat{\mathbf{u}}_t,$$

so

$$(\hat{\mathbf{I}}_1 - \mathbf{g}_S \hat{\mathbf{J}}_p) \hat{\mathbf{u}}_t = 0.$$

First we will show that:

$$\det \hat{\mathcal{J}}' = \det (\hat{\mathbf{I}}_1 - \mathbf{g}_S \hat{\mathbf{J}}_p), \quad (8.52)$$

where

$$\mathbf{g}_S = \left[\begin{array}{c|c} d_1^S & 0 \\ \hline 0 & d_1^S \end{array} \right], \quad (8.53)$$

The right hand side of (8.52) is different from (8.38), because ...

Note that \mathbf{g}_S and $\hat{\mathbf{J}}_1$ commute. Let u_{nt} be a variation on the field x_{nt} .

$$\hat{\mathbf{u}}_t = \begin{bmatrix} \mathbf{u}_{t-1} \\ \mathbf{u}_t \end{bmatrix}, \quad \mathbf{u}_t = \begin{bmatrix} u_{1t} \\ \vdots \\ u_{Lt} \end{bmatrix}.$$

Now we need to know the form of $\hat{\mathcal{J}}'$ in (8.52). Let:

$$\hat{\mathbf{u}} = \begin{bmatrix} \hat{\mathbf{u}}_1 \\ \hline \hat{\mathbf{u}}_2 \\ \hline \vdots \\ \hline \hat{\mathbf{u}}_{T-1} \\ \hline \hat{\mathbf{u}}_T \end{bmatrix}.$$

Then

$$\hat{\mathcal{J}}' = \begin{bmatrix} \hat{\mathbf{I}}_1 & & -\hat{\mathbf{J}}_1 \mathbf{g}_S \\ -\hat{\mathbf{J}}_1 & \hat{\mathbf{I}}_1 & \\ & \ddots & \\ & -\hat{\mathbf{J}}_1 & \hat{\mathbf{I}}_1 \end{bmatrix},$$

where \mathbf{g}_S is the ‘tilt’ (8.53), and $\hat{\mathcal{J}}' \hat{\mathbf{u}} = 0$ for a periodic perturbation field. In an analogy with the usual construction of Floquet matrices, let $\mathbf{g}_S^{1/T}$ be a T th root of the total relative shift \mathbf{g}_S . Change the field to a co-moving frame $\hat{\mathbf{u}}_t \rightarrow \hat{\mathbf{w}}_t$, where $\hat{\mathbf{u}}_t = \mathbf{g}_S^{-t/T} \hat{\mathbf{w}}_t$. Now $\hat{\mathcal{J}}'$ is replaced by $\hat{\mathcal{J}}'_S$:

$$\hat{\mathcal{J}}'_S = \hat{\mathbf{I}} - d_2^{-1} \otimes (\hat{\mathbf{J}}_1 \mathbf{g}_S^{1/T}).$$

Then we have $\hat{\mathcal{J}}'_S \hat{\mathbf{w}} = 0$ when $\hat{\mathcal{J}}' \hat{\mathbf{u}} = 0$. Using the method from (8.37),

$$\det \hat{\mathcal{J}}'_S = \det \left[\hat{\mathbf{1}}_1 - \left(\hat{\mathbf{J}}_1 \mathbf{g}_S^{1/T} \right)^T \right] = \det \left(\hat{\mathbf{1}}_1 - \hat{\mathbf{J}}_1^T \mathbf{g}_S \right) = \det \left(\hat{\mathbf{1}}_1 - \mathbf{g}_S \hat{\mathbf{J}}_1^T \right).$$

When we change to the co-moving frame $\hat{\mathbf{u}}_t \rightarrow \hat{\mathbf{w}}_t$, all of the operators are changed by a similarity transformation:

$$\hat{\mathcal{J}}'_S = \hat{\mathbf{P}} \hat{\mathcal{J}}' \hat{\mathbf{P}}^{-1},$$

where

$$\hat{\mathbf{P}} = \text{diag} \left(\mathbf{g}_S^{1/T}, \mathbf{g}_S^{2/T}, \dots, \mathbf{g}_S^{(T-1)/T}, \mathbf{g}_S \right)$$

is a $[2LT \times 2LT]$ block diagonal matrix. In the co-moving frame, we have $\hat{\mathbf{w}}_t = \mathbf{g}_S^{t/T} \hat{\mathbf{u}}_t$, $\hat{\mathbf{w}} = \hat{\mathbf{P}} \hat{\mathbf{u}}$ and $\mathbf{w} = \mathbf{P} \mathbf{u}$, where

$$\mathbf{u} = \begin{bmatrix} \mathbf{u}_1 \\ \hline \mathbf{u}_2 \\ \hline \vdots \\ \hline \mathbf{u}_{T-1} \\ \hline \mathbf{u}_T \end{bmatrix},$$

and

$$\mathbf{P} = \text{diag} \left(d_1^{S/T}, d_1^{2S/T}, \dots, d_1^{(T-1)S/T}, d_1^S \right).$$

Now we can prove that (8.46) is the orbit Jacobian matrix for the tilted Bravais domain in the co-moving frame. The orbit Jacobian matrix for the tilted Bravais domain in the original frame is:

$$\mathcal{J}_{[L \times T]_S} = \begin{pmatrix} \mathcal{J}_1 & \mathbf{1}_1 & & & d_1^S \\ \mathbf{1}_1 & \mathcal{J}_1 & \mathbf{1}_1 & & \\ & \ddots & \ddots & \ddots & \\ & & \mathbf{1}_1 & \mathcal{J}_1 & \mathbf{1}_1 \\ d_1^{-S} & & & \mathbf{1}_1 & \mathcal{J}_1 \end{pmatrix},$$

which can also be written as:

$$\mathcal{J}_{[L \times T]_S} = 2s \mathbf{1}_2 \otimes \mathbf{1}_1 + \mathbf{1}_2 \otimes (d_1 + d_1^{-1}) + \mathbf{B},$$

where

$$\mathbf{B} = \begin{pmatrix} 0 & \mathbf{1}_1 & & & d_1^S \\ \mathbf{1}_1 & 0 & \mathbf{1}_1 & & \\ & \ddots & \ddots & \ddots & \\ & & \mathbf{1}_1 & 0 & \mathbf{1}_1 \\ d_1^{-S} & & & \mathbf{1}_1 & 0 \end{pmatrix}$$

and the rest of $\mathcal{J}_{[L \times T]_S}$ is the diagonal part. The diagonal part commutes with \mathbf{P} since \mathcal{J}_1 and $d_1^{-S/T}$ commute. So the diagonal part is unchanged after the similarity transformation. The block matrix \mathbf{B} becomes:

$$\mathbf{PB}\mathbf{P}^{-1} = \begin{pmatrix} 0 & d_1^{-S/T} & & d_1^{S/T} \\ d_1^{S/T} & 0 & d_1^{-S/T} & \\ & \ddots & \ddots & \ddots \\ & & d_1^{S/T} & 0 & d_1^{-S/T} \\ d_1^{-S/T} & & & d_1^{S/T} & 0 \end{pmatrix} = d_2 \otimes d_1^{-S/T} + d_2^{-1} \otimes d_1^{S/T}.$$

So the orbit Jacobian matrix in the co-moving frame is:

$$\mathbf{P} \mathcal{J}_{[L \times T]_S} \mathbf{P}^{-1} = d_2 \otimes d_1^{-S/T} + d_2^{-1} \otimes d_1^{S/T} + \mathbf{1}_2 \otimes (d_1 + d_1^{-1}) + 2s \mathbf{1}_2 \otimes \mathbf{1}_1.$$

8.9 Han's Hénon map Hill's formula

The temporal evolution Jacobian matrix of the Hénon map (2.43) is:

$$J(\phi_n) = \frac{\partial(\phi_n, \phi_{n+1})}{\partial(\phi_{n-1}, \phi_n)} = \begin{bmatrix} 0 & 1 \\ -1 & -2a\phi_n \end{bmatrix}.$$

For the periodic orbit X_p with period n , we have two orbit Jacobian matrices: The $[n \times n]$ orbit Jacobian matrix from the 3-term recurrence relation (2.44),

$$\mathcal{J}_p = \begin{bmatrix} 2\phi_0 & 1 & 0 & 0 & \dots & 0 & 1 \\ 1 & 2\phi_1 & 1 & 0 & \dots & 0 & 0 \\ 0 & 1 & 2\phi_2 & 1 & \dots & 0 & 0 \\ \vdots & \vdots & \vdots & \vdots & \ddots & \vdots & \vdots \\ 0 & 0 & \dots & \dots & \dots & 2\phi_{n-2} & 1 \\ 1 & 0 & \dots & \dots & \dots & 1 & 2\phi_{n-1} \end{bmatrix},$$

and the $[2n \times 2n]$ orbit Jacobian matrix from the first-order difference equation,

$$\hat{\mathcal{J}}_p = \begin{bmatrix} \mathbf{1} & & & -J(\phi_0) \\ -J(\phi_1) & \mathbf{1} & & \\ & \ddots & \ddots & \\ & & -J(\phi_{n-2}) & \mathbf{1} \\ & & & -J(\phi_{n-1}) & \mathbf{1} \end{bmatrix},$$

where $\mathbf{1}$ is the $[2 \times 2]$ identity matrix.

To show

$$|\text{Det } \mathcal{J}_p| = |\text{Det } \hat{\mathcal{J}}_p|,$$

we need to use the $[2n \times 2n]$ permutation matrix P to change the form of $\hat{\mathcal{J}}_p$. The matrix elements of P is the Kronecker (circular) delta function:

$$P_{kj} = \delta_{2k-2+\lceil k/n \rceil, j} = \frac{1}{2n} \sum_{l=0}^{2n-1} e^{i\frac{2\pi}{2n}(2k-2+\lceil k/n \rceil-j)l}, \quad (8.54)$$

where the $\lceil x \rceil$ is the ceiling function. Using the permutation matrix P , the orbit Jacobian matrix $\hat{\mathcal{J}}_p$ can be transformed into a block matrix:

$$P \hat{\mathcal{J}}_p P^\top = \left[\begin{array}{cc|cc|ccccc} 1 & 0 & \cdots & 0 & 0 & 0 & 0 & \cdots & 0 & -1 \\ 0 & 1 & \cdots & 0 & 0 & -1 & 0 & \cdots & 0 & 0 \\ \vdots & \vdots & \ddots & \vdots & \vdots & \vdots & \ddots & \ddots & \vdots & \vdots \\ 0 & 0 & \cdots & 1 & 0 & 0 & \cdots & -1 & 0 & 0 \\ 0 & 0 & \cdots & 0 & 1 & 0 & \cdots & 0 & -1 & 0 \\ \hline 0 & 0 & \cdots & 0 & 1 & 1 & 0 & \cdots & 0 & 2a\phi_0 \\ 1 & 0 & \cdots & 0 & 0 & 2a\phi_1 & 1 & \cdots & 0 & 0 \\ \vdots & \ddots & \ddots & \vdots & \vdots & \vdots & \ddots & \ddots & \vdots & \vdots \\ 0 & \cdots & 1 & 0 & 0 & 0 & \cdots & 2a\phi_{n-2} & 1 & 0 \\ 0 & \cdots & 0 & 1 & 0 & 0 & \cdots & 0 & 2a\phi_{n-1} & 1 \end{array} \right].$$

Then use (8.32) we have $|\text{Det } \mathcal{J}_p| = |\text{Det } \hat{\mathcal{J}}_p|$.

Now we will evaluate the Hill determinant $|\det(\hat{\mathcal{J}}_p)|$ and prove the Hill's formula:

$$|\det(\hat{\mathcal{J}}_p)| = |\det(\mathbf{1} - J_p)|,$$

Where $J_p = J(\phi_{n-1})J(\phi_{n-2})\dots J(\phi_1)J(\phi_0)$.

Write the orbit Jacobian matrix $\hat{\mathcal{J}}_p$ as:

$$\hat{\mathcal{J}}_p = \hat{\mathbf{1}} - \tilde{\mathcal{J}}_p,$$

where $\hat{\mathbf{1}}$ is the $[2n \times 2n]$ identity matrix and $\tilde{\mathcal{J}}_p$ is a block matrix:

$$\tilde{\mathcal{J}}_p = \left[\begin{array}{cccc} 0 & & & J(\phi_0) \\ J(\phi_1) & 0 & & \\ \ddots & \ddots & & \\ J(\phi_{n-2}) & 0 & J(\phi_{n-1}) & 0 \end{array} \right].$$

Expand $\ln \det \hat{\mathcal{J}}_p = \text{tr} \ln \hat{\mathcal{J}}_p$ as a series:

$$\text{tr} \ln \hat{\mathcal{J}}_p = \text{tr} \ln (\hat{\mathbf{1}} - \tilde{\mathcal{J}}_p) = - \sum_{k=1}^{\infty} \frac{1}{k} \text{tr} \tilde{\mathcal{J}}_p^k.$$

Note that $\text{tr } \tilde{\mathcal{J}}_p^k$ is non-zero only when k is a multiple of n , and

$$\tilde{\mathcal{J}}_p^n = \begin{bmatrix} J(\phi_0)J(\phi_{n-1})\dots J(\phi_1) & & & \\ & J(\phi_1)\dots J(\phi_2) & & \\ & & \ddots & \\ & & & J(\phi_{n-2})\dots J(\phi_{n-1}) \\ & & & & J(\phi_{n-1})\dots J(\phi_0) \end{bmatrix},$$

is a block diagonal matrix, with the j th block on the diagonal:

$$\begin{bmatrix} (\tilde{\mathcal{J}}_p^n)_{2j-1,2j-1} & (\tilde{\mathcal{J}}_p^n)_{2j-1,2j} \\ (\tilde{\mathcal{J}}_p^n)_{2j,2j-1} & (\tilde{\mathcal{J}}_p^n)_{2j,2j} \end{bmatrix} = J(\phi_{j-1})J(\phi_{j-2})\dots J(\phi_1)J(\phi_0)J(\phi_{n-1})J(\phi_{n-2})\dots J(\phi_{j+1})J(\phi_j).$$

So we have:

$$\ln \det \hat{\mathcal{J}}_p = - \sum_{k=1}^{\infty} \frac{1}{k} \text{tr } \tilde{\mathcal{J}}_p^k = - \sum_{r=1}^{\infty} \frac{1}{r} \text{tr } J_p^r = \text{tr } \ln (\mathbf{1} - J_p) = \ln \det (\mathbf{1} - J_p).$$

And we have proved the Hill's formula:

$$|\det (\hat{\mathcal{J}}_p)| = |\det (\mathbf{1} - J_p)|.$$

section 7.5

References

- [1] E. Allroth, "Ground state of one-dimensional systems and fixed points of 2n-dimensional map", *J. Phys. A* **16**, L497 (1983).
- [2] G. B. Arfken, H. J. Weber, and F. E. Harris, *Mathematical Methods for Physicists: A Comprehensive Guide*, 7th ed. (Academic, New York, 2013).
- [3] S. V. Bolotin and D. V. Treschev, "Hill's formula", *Russ. Math. Surv.* **65**, 191 (2010).
- [4] T. Bountis and R. H. G. Helleman, "On the stability of periodic orbits of two-dimensional mappings", *J. Math. Phys.* **22**, 1867–1877 (1981).
- [5] E. Calabi, "On the group of automorphisms of a symplectic manifold", in *Problems in Analysis: A Symposium in Honor of Salomon Bochner* (Princeton Univ. Press, Princeton NJ, 1970), pp. 1–26.
- [6] M. Chen, "On the solution of circulant linear systems", *SIAM J. Numer. Anal.* **24**, 668–683 (1987).
- [7] F. W. Dorr, "The direct solution of the discrete Poisson equation on a rectangle", *SIAM Rev.* **12**, 248–263 (1970).
- [8] J. M. Greene, "A method for determining a stochastic transition", *J. Math. Phys.* **20**, 1183–1201 (1979).

- [9] G. W. Hill, “On the part of the motion of the lunar perigee which is a function of the mean motions of the sun and moon”, *Acta Math.* **8**, 1–36 (1886).
- [10] R. A. Horn and C. R. Johnson, *Matrix Analysis* (Cambridge Univ. Press, Cambridge, 1990).
- [11] G. Y. Hu, J. Y. Ryu, and R. F. O’Connell, “Analytical solution of the generalized discrete Poisson equation”, *J. Phys. A* **31**, 9279 (1998).
- [12] K. Kowalski and W.-H. Steeb, *Nonlinear Dynamical Systems and Carleman Linearization* (World Scientific, Singapore, 1991).
- [13] J. Li and S. Tomsovic, “Exact relations between homoclinic and periodic orbit actions in chaotic systems”, *Phys. Rev. E* **97**, 022216 (2017).
- [14] R. S. MacKay and J. D. Meiss, “Linear stability of periodic orbits in Lagrangian systems”, *Phys. Lett. A* **98**, 92–94 (1983).
- [15] R. S. MacKay, J. D. Meiss, and I. C. Percival, “Transport in Hamiltonian systems”, *Physica D* **13**, 55–81 (1984).
- [16] J. D. Meiss, “Symplectic maps, variational principles, and transport”, *Rev. Mod. Phys.* **64**, 795–848 (1992).
- [17] I. Montvay and G. Münster, *Quantum Fields on a Lattice* (Cambridge Univ. Press, Cambridge, 1994).
- [18] L. Onsager, “Crystal statistics. I. A Two-dimensional model with an order-disorder transition”, *Phys. Rev.* **65**, 117–149 (1944).
- [19] I. Percival and F. Vivaldi, “A linear code for the sawtooth and cat maps”, *Physica D* **27**, 373–386 (1987).
- [20] H. Poincaré, “Sur les déterminants d’ordre infini”, *Bull. Soc. Math. France* **14**, 77–90 (1886).
- [21] G. Schmidt, “Hamilton’s principle and the splitting of periodic orbits”, in *Statistical Physics and Chaos in Fusion Plasmas*, edited by C. W. Horton Jr. and L. E. Reichl (John Wiley and Sons, 1984), p. 57.
- [22] I. Schur, “Über Potenzreihen, die im Innern des Einheitskreises beschränkt sind”, *J. reine angewandte Math.* **147**, 205–232 (1917).
- [23] W.-H. Steeb and Y. Hardy, *Matrix Calculus and Kronecker Product - A Practical Approach to Linear and Multilinear Algebra*, 2nd ed. (World Scientific, Singapore, 2011).
- [24] W.-H. Steeb and Y. Hardy, *Matrix Calculus, Kronecker Product and Tensor Product* (World Scientific, Singapore, 2011).
- [25] Wikipedia contributors, [Block matrix — Wikipedia, The Free Encyclopedia](#), 2020.
- [26] Wikipedia contributors, [Kronecker product — Wikipedia, The Free Encyclopedia](#), 2020.

Chapter 9

Chronotopic musings

2020-10-25 **Predrag** ChaosBook.org [spatiotemporal homepage](#)

2020-10-25 **Predrag** 2021 APS March Meeting (held virtually) March 15 - 19
Abstracts deadline has been extended to Friday, **November 6** at 5:00 p.m.
ET.

Sorting Categories

03.0 Statistical and Nonlinear Physics (GSNP)
03.07.00 Pattern Formation and Spatio-temporal Chaos
03.08.00 Chaos and Nonlinear Dynamics

2020-10-25 **Predrag** SIAM DS21 May 23 - 27, 2021
Minisymposium Proposal [Submission Deadline](#): **November 23, 2020**,
11:59 p.m. ET

2020-10-25 **Predrag** 2021 Dynamics Days DD21-Europe
August 24-28, 2020, Nice, France
Minisymposium Proposal [Submission Deadline](#): not announced yet.

9.1 Chronotopic literature

The latest entry at the bottom for this blog

2016-03-02 **Boris** Just stumbled upon Lepri, Politi and Torcini [10] *Chronotopic Lyapunov analysis. I. A detailed characterization of 1D systems.*

Are you familiar with this? Somewhere in the direction I thought about.

2016-03-02, 2016-09-03 **Predrag** Politi and collaborators work is very close to our way of spatiotemporal thinking. See sect. ??, sect. ??, sect. ?? and sect. 9.4. If you read that literature, please share what you have learned by writing it up there.

2016-03-02 Predrag Also Pazó *et al.* [14] *Structure of characteristic Lyapunov vectors in spatiotemporal chaos*. Actually (I hesitated to bring it up) this line of inquiry goes smoothly into Xiong Ding's inertial manifold dimension project.

Not sure Li *et al.* [12] *Lyapunov spectra of coupled chaotic maps* is of any interest, but we'll know only if we read it.

2016-09-06 Matt Chronotopic Approach I've been reading refs. [6, 10, 11, 21] on chronotopic approach to spatiotemporal chaos.

2016-09-06 Matt Branching out to get a better grasp of what's out there, I read Pikovsky and Politi [15] *Dynamic localization of Lyapunov vectors in space-time chaos*, It discusses the complex Ginzburg-Landau, two types of coupled maps, as well as Kuramoto-Sivashinsky equation, so I thought it might be useful somehow.

2016-09-06 Predrag Pikovsky and Politi [15] is a stat mech paper about using KPZ equations in pattern formation, do not waste time on it right now.

Rafael 2016-09-29 I spent a lot of time in the coupled cat maps, but in the regime of small coupling. One thing I did explore numerically is when the conjugacy given by the structural stability breaks down as one turns up the coupling.

Rafael 2016-10-10 The main paper about the coupled maps is the paper with Miaoqua Jiang. We show that the local chains of Anosov remain Anosov under local couplings. The partitions remain the same if you make changes of coordinates that are essentially local.

Of course, the fact that there is a regime of large perturbations in which this does not happen begs the question of studying the transition. Some of this has been studied also by Bastien Fernandez [4].

I have done some preliminary numerics (too crude to show). One possibility is that some of the Lyapunov exponents go to zero. Another is that the Lyapunov exponents remain away from zero but that the angle between the splittings goes to zero. There are heuristic arguments that the second possibility should occur. (Almost a proof when there is a system small coupling to another more massive one).

There were other points of the discussion. The space dynamics for PDE's. This contains references to older papers notably Kirchgassner and Mielke as well as applications to some papers.

I think Weinstein [22] is related.

2011-02-17 PC *A large-deviation approach to space-time chaos* by Pavel V. Kuptsov and Antonio Politi [9], arXiv:1102.3141. They say:

“ We show that the analysis of Lyapunov-exponents fluctuations contributes to deepen our understanding of high-dimensional chaos. This is

achieved by introducing a Gaussian approximation for the entropy function that quantifies the fluctuation probability. More precisely, a diffusion matrix D (a dynamical invariant itself) is measured and analyzed in terms of its principal components. The application of this method to four (conservative, as well as dissipative) models, allows: (i) quantifying the strength of the effective interactions among the different degrees of freedom; (ii) unveiling microscopic constraints such as those associated to a symplectic structure; (iii) checking the hyperbolicity of the dynamics. ”

2016-09-28 Predrag Isola, Politi, Ruffo and Torcini [8] *Lyapunov spectra of coupled map lattices.*

Fontich, de la Llave and Martín [5] *Dynamical systems on lattices with decaying interaction I: A functional analysis framework.* [...] consider weakly coupled map lattices with a decaying interaction. [...] applications of the framework are the study of the structural stability of maps with decay close to uncoupled possessing hyperbolic sets and the decay properties of the invariant manifolds of their hyperbolic sets, in the companion paper by Fontich et al. (2011).

2016-11-18 Matt : There is a storm in the distance however, as this general procedure is ruined for the spatial problem. According to the chronotopic literature [6, 10, 11, 21], iteration in space typically does not converge to the same attractor as iteration in time, and generally corresponds to a strange repeller. Therefore I cannot hope to form an initial guess loop from using a Poincaré section in the spatial direction, as typically all of my Fourier coefficients go off to infinity before a recurrence is found.

2017-03-02 Predrag I asked GaTech library to order Pikovsky and Politi [16] *Lyapunov Exponents: A Tool to Explore Complex Dynamics.*

2017-11-07 Matt My *spatiotemp/blog* comments of 2017-11-02 were mainly predicated by the fact that once we find these roots, I don't think we can apply the same type of reasoning as Politi and Torcini [19] as they aren't truly fixed points of a fictitious dynamical system, like so, $F(\hat{a}_{kj}, T, L) = \hat{a}_{kj}, T, L$. But rather, like I have already described, they are the roots of a system of nonlinear algebraic equations, $F(\hat{a}_{kj}, T, L) = 0$.

2019-05-11 Predrag My extensive notes on extensivity in Carlu, Ginelli, Lu- carini and Politi [2] *Lyapunov analysis of multiscale dynamics: the slow bundle of the two-scale Lorenz 96 model* are in `lyapunov/dailyBlog.tex`.

2020-12-16 Alessandro Torcini `alessandro.torcini@u-cergy.fr`
to Domenico:

si avevo visto l'annuncio della tesi di Gudorf ma alla fine non avevo partecipato, se ho capito bene lui e' riuscito a fare nello spazio-tempo continuo una cosa che io e Politi avevamo tentato nel 1990 in tempo discreto e spazio discreto (mappe accoppiate), cioè riscrivere come un modello Markoviano la evoluzione spazio-temporiale di un sistema con caos

spazio temporale in termini di unità spazio temporali, tipo i mattoncini del Tetris.

(I had seen the announcement of the thesis of Gudorf but in the end I had not participated, if I understood well he was able to do in continuous space-time something that Politi and I had tried in 1990 in discrete time and discrete space (coupled maps), that is to rewrite as a Markovian model the spatio-temporal evolution space-time evolution of a system with space-time chaos in terms of space-time units time-space units, like Tetris bricks.)

Io ci ho speso 6 mesi sopra e credo di avere ancora quaderni su quaderni, ma alla fine non pubblicammo mai nulla con Politi. A parte un PRL del 1992 molto poco citato ed un Chaos.

(I spent 6 months on it and I think I still have notebooks upon notebooks, but in the end we never published anything with Politi. Except for a 1992 PRL very little cited and a Chaos.)

Poi scrivemmo 3 lavori con Lepri su chronotopic approach al caos spazio temporale, questa roba e' finita in 2 o 3 libri, ma di fatto la linea di ricerca e' stata molto poco seguita , infine nel 2013 siamo riusciti a calcolare tutto lo spettro dei i comoving Lyapunov exponents (lavoro ignoto ai piu),

(Then we wrote 3 papers with Lepri on chronotopic approach to space-time chaos. time chaos, this stuff ended up in 2 or 3 books, but in fact the research line of research was very little followed, finally in 2013 we managed to calculate the whole spectrum of the the whole spectrum of comoving Lyapunov exponents, work unknown to most,)

A. K. Jrotsa, A. Politi, and A. Torcini, *Convective Lyapunov Spectra* J. Phys. A 46 (2013) 254013.

potete trovare tutto nella mia web page e scaricare tutto

(you can find everything in my web page and download everything)

perso.u-cergy.fr/atorcini/pri.html

Per la review a SIAM grazie va bene, per i fondi sino al 31 marzo non ho problemi, dopo si, spero di poter pagare prima la FEE.

(For the review in SIAM thank you is fine, for the funds until March 31 I don't have any problem, after that I hope to be able to pay before the FEE)

Spero di riuscire a studiare la tesi di Gudorf prima o poi.

(I hope to be able to study Gudorf's thesis sooner or later.)

A presto

9.2 PolTor92b Towards a statistical mechanics of spatiotemporal chaos

2017-10-31 Burak I looked everywhere but could not find Politi and Torcini [19] *Towards a statistical mechanics of spatiotemporal chaos* (1992) in this blog. The abstract:

Coupled Hénon maps are introduced to model in a more appropriate way chaos in extended systems. An effective technique allows the extraction of spatiotemporal periodic orbits, which are then used to approximate the invariant measure. A further implementation of the ζ -function formalism reveals the extensive character of entropies and dimensions, and allows the computation of the associated multifractal spectra. Finally, the analysis of short chains indicates the existence of distinct phases in the invariant measure, characterized by a different number of positive Lyapunov exponents.

We should all read it very carefully. They use Biham-Wenzel [1] to infer spatiotemporal periodic orbits and their symbolic dynamics by introducing a continuous fictitious time.

I'm not sure if they are using periodic orbits of different chain spatial period L in order to estimate the statistics of the system at thermodynamic limit $L \rightarrow \infty$. If that's the case and the dynamical ζ function is designed for this purpose, then this paper is very similar to what we have in mind.

2017-10-31 Matt I find it interesting that they use a continuous fictitious Biham-Wenzel [1] dynamics for a spatiotemporal system of mappings, while I have a discrete fictitious time (in the form of my spatiotemporal mapping) introduced for continuous (albeit discretized) spatiotemporal equations.

If a paper is worth something, other people cite it. Currently it has 13 APS and 22 Google Scholar citations.

To motivate the Politi and Torcini [19] coupled Hénon map lattice, we start by a review a single Hénon map, written using the conventions of [Chaos-Book.org](#).

Note: Politi and Torcini say that in the case of $\epsilon = 0$ that the original Hénon map is retrieved, but if you actually do this then indices don't match the original equation.

$$\begin{aligned} x_{n+1} &= 1 - ay_{n+1}^2 + bx_{n-1} \\ y_{n+1} &= x_n, \end{aligned} \tag{9.1}$$

or, as a 3-term recurrence

$$\phi_{n+1} + a\phi_n^2 - b\phi_{n-1} = 1.$$

The parameter a quantifies the “stretching” and b quantifies the “contraction”.

The single Hénon map is nice because the system is not linear, but has binary dynamics.

The deviation of an approximate trajectory from the 3-term recurrence is

$$v_n = \phi_{n+1} - (1 - a\phi_n^2 + b\phi_{n-1})$$

In classical mechanics force is the gradient of potential, which Biham-Wenzel [1] construct as a cubic potential

$$V_n = \phi_n(\phi_{n+1} - b\phi_{n-1} - 1) + a\phi_n^3$$

With the cubic potential of a single Hénon map we can start to look for orbits with initial conditions of two points (two point recurrence relation requires this) and make the guess as we iterate in time. A particular guess is to choose a sequence of maxima/minima of the potential.

In order to accurately enumerate the orbit with symbolic dynamics, in order to choose which way you “roll” the potential needs to be modified by ± 1 , as when viewed from the perspective of the cubic potential, trajectories roll downhill, so in order to flip the direction one must apply a flip. The symbolic dynamics is therefore binary and determined by these flips. One can just list the binary sequences and see if the orbit is realized by the system. [Chaosbook](#) does this up to sequences of length 13, while it has been done by Grassberger, Kantz and Moenig [7] to symbol length 32. This means that there could be as many as $2^{32}/32$ distinct periodic orbits.

In the Politi-Torcini [19] coupled Hénon map equations t is the index associated to time, while n is the index associated with space:¹

$$\begin{aligned} \phi_{n,t+1} + y_{nt}^2 - b\phi_{n,t-1} &= a \\ y_{nt} &= \phi_{nt} + \frac{\epsilon}{2}(\phi_{n+1,t} - 2\phi_{nt} + \phi_{n-1,t}) \end{aligned} \quad (9.3)$$

In the Hamiltonian $b = -1$ case the only parameter is the stretching a ; when it is small some orbits become stable, not everyone is unstable. If there’s not strong stretching then there is a mixture as the hyperbolicity isn’t dominating. All of these coupled maps, say something wild happens at each site (alternating between 1 and -1 is far in this case), and THEN you couple it weakly to its neighbors.

But when the coupling with neighbors is very strong, its a very different phenomena. The cats have written a Helmholtz in space and time where the

¹Matt 2017-11-08: Politi-Torcini Hénon map form differs from the ChaosBook convention (9.1). If we take their claim that in the $\epsilon = 0$ case we should retrieve the classical Hénon equations very strictly, this is how they should appear I believe. The difference lies in the time index $t + 1$ versus t of the y terms.

$$\begin{aligned} \phi_{n,t+1} &= 1 - a(y_{n,t+1})^2 + b\phi_{n,t-1} \\ y_{n,t+1} &= (1 + \epsilon)\phi_{nt} + \frac{\epsilon}{2}(\phi_{n+1,t} + \phi_{n-1,t}). \end{aligned} \quad (9.2)$$

CHAPTER 9. CHRONOTOPIC MUSINGS

Laplacian is weighted by +1 as opposed to 1, -1 in the Minkowski case. Second order operator that has different weights (as determined by some metric) its called the Beltrami operator. Predrag also thinks the sign is different. This is 1992 though, and there's not much there because its Phys. Rev. Lett. so there must be real work somewhere.

They cite the fact that most people don't use it for invertible dynamics. Then they say the spatially and temporally periodic orbits are extracted using the Newton method. What they actually do, they take $L = 1, 2, 3, 4$ only. They don't elucidate on interesting tricks, like how to use the method for coupled maps. The density of periodic orbits in the invariant measure is stated, but this is only really known for single maps, Predrag doubts this.

Politi and Torcini [19] is one of the first papers that uses spatiotemporal symbolic dynamics, as seen by Predrag in the literature. Symbol of a torus is really just a lattice label. Politi and Torcini use doubly periodic boundary conditions, with canonical values from Hénon for the parameters.

When you write the equations in diagonal, form you'll likely take a square root of it. Then, they say some orbits are pruned, some exist only with uncoupled case. That helps them because if you can prove you only lose orbits and never gain orbits you can see if certain orbits are realized or not.

It is important to realize that not all invariant 2-tori belong to the inertial manifold. There are isolated orbits, corresponding to fixed points.

The orbits are found with Newton method.

They discarded all of the cycles that had a sequence, specifically $\bar{0}\bar{0}$ in symbolic dynamics, is not allowed. The application of the zeta function, "they don't know what they are doing, so ignore it".

Their intuition is that the inertial manifold is extensive: if you double the spatial length, you should double the number of physical Lyapunov exponents as you go in time. They compute some Jacobian, they are just the normal Jacobians in time. Using these they compute $2J \times 2J$ sized matrices for the spatiotemporal domain, (thinks Bloch theorem doesn't apply, maybe). They also say to take the logarithm and divide it by the size of the domain. Their entropy is a sum of temporal Lyapunov exponents divided by L . They have an intuition but its hard to check because of the small L . One possible solution is to use the fixed point, as its a representative of the stretching rate in the neighborhood. "Let's just say the typical stretching rate is roughly the same no matter the domain size." I.e. they assume its a frozen state so it doesn't matter how big the domain gets. Grand canonical formalism for the Zeta function, but it can be "safely ignored". Multifractal stuff seems useless, look at this h , instead of plotting everything from infinity to infinity, but can subtract something and it works out and they get a plot. But there seems to be an envelope which may be connected to the quantity they try to claim, maybe.

Different phases, but they notice that different periodic orbits have different number of positive Lyapunov exponents. They interpret periodic orbits with the same number belong to the same 'phase'.

The problem only uses Biham in time; Not clear why they did it because they say its invertible, which makes sense because Hamiltonian.

For a particular solution, the potential is just a set of numbers, even though it depends on x . It will have to be evaluated at the linearization of the nonlinear equations and evaluated along the orbit. e.g. stability of orbits do not look like constant anything. PC Thinks the Jacobian will work out somehow.

2017-10-31 Matt Part Two: Discussions from the Invariant Solns Meeting

Ignore the last third of the paper. The one thing PC doesn't understand, is that they are studying coupled Hénon maps because they're invertible, but he doesn't understand why they care.

They uses the standard parameter values of Hénon.

Fictitious time isn't important, the method is the method of Biham where they derive a cubic potential such that its derivative is the Hénon map.

The coupling is what determines the type of behavior here, in the weak coupling limit, everything looks unstable on its own, but when the coupling is strong The model is then determined to be an ergodic model, because it is fully developed due to the length scale imposed but no laminar patches (No point where there are a different number of unstable directions).

If we write it carefully, take a Hamiltonian map, rewrite in terms of Beltrami operator (Laplacian with metric). Looking at this operator, its bilinear in derivative, but the derivatives have different weights and can have opposite signs.

Elliptic structure in PC's case, but thinks the Hénon there should be a negative sign.

If you have a spatially periodic chain, (they still think of a chain in space evolved in time, but they change this in the future). They say if you have periodic lattice, you should use Bloch theorem, which is what is done in condensed matter. They write the Bloch theorem, but we don't know why. PC believes it may be because the coupling is weak, so deformations are long wavelength deformations.

Explicitly the stretching parameter, changed from small to large, the problem becomes hyperbolic and sines and cosines change to hyperbolic sines and cosines.

In order to rewrite the equations in one variable that has a spatiotemporal Beltrami operator, we need to modify (9.2). First we write the set of equations as two step recurrence in one variable,

$$\phi_{n+1}^j + b\phi_{n-1}^j = 1 - a((1 + \epsilon)\phi_n^j + \frac{\epsilon}{2}(\phi_n^{j+1} + \phi_n^{j-1}))^2, \quad (9.4)$$

Then we can add and subtract $2\phi_n^j$ to the LHS of the equation,

$$(\square_t - 2)\phi_n^j = 1 - a((1 + \epsilon)\phi_n^j + \frac{\epsilon}{2}(\phi_n^{j+1} + \phi_n^{j-1}))^2, \quad (9.5)$$

Because the quadratic nonlinearity is where the spatial part of the Beltrami or Laplacian is, I don't know how to get around this and combine space and time currently. I recall Predrag mentioning something about a square root but it doesn't seem very well motivated because the spatial coupling is completely separated from time coupling unless I'm missing some type of approximation.

2020-06-25 Predrag Perhaps the easiest thing would be to replace the Hénon in (9.3) by the Lozi map?

9.3 PolTor92 Periodic orbits in coupled Hénon maps

2020-05-31 Predrag Politi and Torcini [18] *Periodic orbits in coupled Hénon maps: Lyapunov and multifractal analysis* is quite close to our spatiotemporal cat. The problem is harder, as the Hénon map is nonlinear; MUST CITE in ref. [3].

They study *spatiotemporal Hénon*, a (1+1)-spacetime lattice of Hénon maps orbits which are periodic both in space and time, and note that the dependence of the lattice field at time ϕ_{t+1} on the two previous time steps prevents an interpretation of dynamics as the composition of a local chaotic evolution with a diffusion process, and that the $|b| = 1$ case(s) could be important as examples of Hamiltonian lattice field theories. (**Predrag**: they do not comment on the role of the spacetime asymmetry of spatiotemporal Hénon.)

Their numerical method is an extension of Biham and Wenzel [1] for the single Hénon map, with symbols s_{nt} in $\mathcal{A} = \{0, 1\}$. Any fixed point in fictitious time corresponds to a spatio-temporal cycle $[L \times T]_S$.

The search of periodic orbits is further simplified by the fact that a small coupling prunes some of cycles which are present for $\epsilon = 0$. Therefore, the knowledge of the topological structure of the single Hénon map yields a symbolic encoding of the dynamics and allows for restricting the set of candidate admissible symbol blocks to be investigated. For $a = 1.4$, $b = 0.3$ this works well for $\epsilon = 0.1$.

They comment on existence both time-equilibria $[L \times 1]_0$ and time-relative equilibria $[L \times 1]_S$, $S \neq 0$ (seen as stationary patterns in a reference frame moving with a constant velocity).

A problem in reconstructing the statistical properties of an attractor from periodic orbits is ensuring that all orbits used belong to the natural invariant measure. For instance, in the single Hénon map, one of the two fixed points is isolated and it does not belong to the strange attractor. Something similar should occur in the CML.

A family of specific Lyapunov exponents is defined, which estimate the growth rate of spatially inhomogeneous perturbations, related to the co-moving Lyapunov exponents.

The ζ -function formalism is used to analyze the scaling structure of the invariant measure both in space and time.

(**Predrag**: here things fall apart. They do numerics for various small fixed L or T , but have no path to constructing a spacetime ζ -function.)

In the case of a CML, the periodic orbit weights depend exponentially both on space and time variables, $t_j = r_j^{LT}$. This suggests that the ζ -function formalism could be effectively extended, by performing an additional sum over all spatial periods. Unfortunately, a straight implementation of this scheme is not so effective as in the low-dimensional case. Therefore, we limit ourselves to apply the standard formalism, checking afterwards the dependence on the length chain L .

9.4 PoToLe98 Lyapunov exponents from node-counting

Politi, Torcini and Lepri [21] *Lyapunov exponents from node-counting arguments* is a promising start, but there does not seem to have been any followup since 1998...

The *chronotopic approach* aims to extending the concept of Lyapunov spectrum to spatially inhomogeneous perturbations.

The main result of the chronotopic approach is the existence of a dynamical invariant, the entropy potential, the knowledge of which allows to determine all properties of the evolution of localized as well as extended perturbations.

One can describe the spatial structure of a generic Lyapunov vector with a single complex number $\tilde{\mu} = \mu + ik$, the real part of which is the exponential growth rate, while the imaginary part is the wavenumber. The frequency ω can be read as the imaginary part of the complex number $\tilde{\lambda} = \lambda + i\omega$, where λ is the temporal growth rate (i.e. the Lyapunov exponent) of the given perturbation. The analyticity properties of the “dispersion relation” connecting $\tilde{\mu}$ with $\tilde{\lambda}$ furnish the last ingredient to “prove” the existence of an entropy potential [11].

This paper introduces a wavenumber by define “rotation numbers” as the imaginary counterpart of the Lyapunov exponents. They compute the Lyapunov spectrum by using the transfer matrix approach. The approach is limited to a class of coupled map lattices (CMLs) with everywhere expanding multipliers.

(First) they assume a time-stationary spatiotemporal solution and compute the 1 spatial dimension orbit Jacobian matrix. That resembles the tight-binding approximation of the 1D Schrödinger equation (with imaginary time) in the presence of a random potential, i.e., the Anderson model. They note the close analogy with the computation of the vibrational spectrum of a chain with random masses. The spectrum of the Schrödinger problem can be determined without diagonalizing the operator (which is the sum of the discretized spatial Laplacian and a diagonal operator). Its symmetry ensures the applicability of the node theorem which states that the eigenfunctions are ordered according to the number of their zeros [13].

For a time-stationary spatiotemporal solution, one can always redefine site fields ϕ_{nt} to make them all a constant field ϕ_{oo} . Then the spatial structure of the corresponding Lyapunov vector counts the nodes. Furthermore, all eigenvalues are real, i.e., no rotations in tangent space.

(Second), they consider orbits of temporal period $T > 2$. The operator is a banded matrix (of width $2T + 1$) so that we are dealing with a sort of Schrodinger problem with long-range hopping. The fundamental difference is that no similarity transformation can turn the operator into a symmetric matrix, hence generic existence of complex eigenvalues. That's a problem for them, as the node theorem is proved only for operators with a strictly real and positive spectrum. They waffle.

Still, they do a numerical calculation for $[L_{11} \times T_7]_{S_0}$ and $[L_7 \times T_5]_{S_0}$ Bravais cells and get the correct counting, their figs. 2 and 3. They finish with

"More important, in our opinion, is the question whether the same approach can be extended to continuous-time and -space systems. We believe that instead of checking numerically whether this is true or not, it is more important to look for the possibly deep reasons that lie behind the apparent validity of the conjectures presented in this paper."

2020-04-18 Predrag A long shot, but maybe Pastur and Figotin [13] *Spectra of Random and Almost-Periodic Operators* Chap. III offers some estimate of the Kuramoto-Sivashinsky spectra, and provides mean node-count for Kuramoto-Sivashinsky?

9.5 PolPuc92 Invariant measure in coupled maps

2016-11-06 Predrag Politi and Puccioni [17] *Invariant measure in coupled maps* write: "The state of affairs is much less clear when we pass from closed chains (as above) to sub-chains of an-in principle-infinite lattice. This corresponds to the canonical-ensemble picture of statistical mechanics: the system of interest (sub-chain of length E) is coupled with a thermal bath given by the rest of the chain. From the previous considerations, the attractor corresponding to an isolated system would fill, for E sufficiently large, a ρE -dimensional manifold. The main effect of the coupling with the heat bath is to add a sort of "external noise" dressing the manifold along all directions, and thus making the resulting invariant measure to become E -dimensional."

This paper is lots of hand-waving, so I gave up on reading it.

9.6 PolTor09 Stable chaos

Politi and Torcini [20] *Stable chaos* (2009), [arXiv:0902.2545](https://arxiv.org/abs/0902.2545)

Chaos is associated with an exponential sensitivity to tiny perturbations in the initial conditions, so that the presence of at least one positive Lyapunov

exponent is considered as a necessary and sufficient condition for the occurrence of irregular dynamics in deterministic dynamical systems. In fact, the first observation in coupled-map models of stochastic-like behaviour accompanied by a negative maximum Lyapunov exponent came as a big surprise. The unexpected coexistence of local stability and chaotic behaviour, due to the phenomenon was called stable chaos (SC). The irregular behaviour is a transient phenomenon that is restricted to finite-time scales.

We might want to study the ‘chronotopic approach’ of eqs. (10) to (17).

References

- [1] O. Biham and W. Wenzel, “Characterization of unstable periodic orbits in chaotic attractors and repellers”, *Phys. Rev. Lett.* **63**, 819 (1989).
- [2] M. Carlu, F. Ginelli, V. Lucarini, and A. Politi, “Lyapunov analysis of multiscale dynamics: the slow bundle of the two-scale Lorenz 96 model”, *Nonlinear Processes Geophys.* **26**, 73–89 (2019).
- [3] P. Cvitanović and H. Liang, *Spatiotemporal cat: A chaotic field theory*, In preparation, 2021.
- [4] B. Fernandez, “Breaking of ergodicity in expanding systems of globally coupled piecewise affine circle maps”, *J. Stat. Phys.* **154**, 999–1029 (2014).
- [5] E. Fontich, R. de la Llave, and P. Martín, “Dynamical systems on lattices with decaying interaction I: A functional analysis framework”, *J. Diff. Equ.* **250**, 2838–2886 (2011).
- [6] G. Giacomelli, S. Lepri, and A. Politi, “Statistical properties of bidimensional patterns generated from delayed and extended maps”, *Phys. Rev. E* **51**, 3939–3944 (1995).
- [7] P. Grassberger, H. Kantz, and U. Moenig, “On the symbolic dynamics of Hénon map”, *J. Phys. A* **22**, 5217–5230 (1989).
- [8] S. Isola, A. Politi, S. Ruffo, and A. Torcini, “Lyapunov spectra of coupled map lattices”, *Phys. Lett. A* **143**, 365–368 (1990).
- [9] P. V. Kuptsov and A. Politi, “Large-deviation approach to space-time chaos”, *Phys. Rev. Lett.* **107**, 114101 (2011).
- [10] S. Lepri, A. Politi, and A. Torcini, “Chronotopic Lyapunov analysis. I. A detailed characterization of 1D systems”, *J. Stat. Phys.* **82**, 1429–1452 (1996).
- [11] S. Lepri, A. Politi, and A. Torcini, “Chronotopic Lyapunov analysis. II. Towards a unified approach”, *J. Stat. Phys.* **88**, 31–45 (1997).
- [12] X. Li, Y. Xue, P. Shi, and G. Hu, “Lyapunov spectra of coupled chaotic maps”, *Int. J. Bifur. Chaos* **18**, 3759–3770 (2008).

CHAPTER 9. CHRONOTOPIC MUSINGS

- [13] L. Pastur and A. Figotin, *Spectra of Random and Almost-Periodic Operators* (Springer, Berlin, 1992).
- [14] D. Pazó, I. G. Szendro, J. M. López, and M. A. Rodríguez, “Structure of characteristic Lyapunov vectors in spatiotemporal chaos”, *Phys. Rev. E* **78**, 016209 (2008).
- [15] A. Pikovsky and A. Politi, “Dynamic localization of Lyapunov vectors in spacetime chaos”, *Nonlinearity* **11**, 1049–1062 (1998).
- [16] A. Pikovsky and A. Politi, *Lyapunov Exponents: A Tool to Explore Complex Dynamics* (Cambridge Univ. Press, Cambridge, 2016).
- [17] A. Politi and G. P. Puccioni, “Invariant measure in coupled maps”, *Physica D* **58**, 384–391 (1992).
- [18] A. Politi and A. Torcini, “Periodic orbits in coupled Hénon maps: Lyapunov and multifractal analysis”, *Chaos* **2**, 293–300 (1992).
- [19] A. Politi and A. Torcini, “Towards a statistical mechanics of spatiotemporal chaos”, *Phys. Rev. Lett.* **69**, 3421–3424 (1992).
- [20] A. Politi and A. Torcini, “Stable chaos”, in *Understanding Complex Systems* (Springer, Berlin, 2009), pp. 103–129.
- [21] A. Politi, A. Torcini, and S. Lepri, “Lyapunov exponents from node-counting arguments”, *J. Phys. IV* **8**, 263 (1998).
- [22] A. Weinstein, “Periodic nonlinear waves on a half-line”, *Commun. Math. Phys.* **99**, 385–388 (1985).

Chapter 10

Article edits

10.1 Cats' GHJSC16blog

Internal discussions of ref. [34] edits: Move good text not used in ref. [34] to this file, for possible reuse later.

2016-12-06 Boris I prefer a precise title. E.g. :

Linear encoding of cat map lattices

Some earlier titles:

Linear encoding of the spatiotemporal cat

A spatiotemporal cat encoded

A spatiotemporal code for a coupled maps lattice

A spatiotemporal symbolic dynamics for a coupled maps lattice

A spatiotemporal symbolic dynamics for a coupled cat maps lattice

A linear symbolic dynamics for coupled cat maps lattices

A spatiotemporal herding of coupled lattice cats

Herding five cats

2016-11-18 Predrag A theory of turbulence that has done away with *dynamics*?

We rest our case.

2016-10-05 Predrag My approach is that this is written for field theorists, fluid dynamicists etc., who do not see any reason to look at cat maps, so I am trying to be pedagogical, motivate it as that chaotic counterpart of the harmonic oscillator, something that field theorists fell comfortable with (they should not, but they do).

2016-11-13 Predrag The next thing to rethink: Green's functions for periodic lattices are in ChaosBook sections D.3 Lattice derivatives and on, for the Hermitian Laplacian and $s = 2$. For real $s > 2$ cat map, the potential is inverted harmonic oscillator, the frequency is imaginary (Schrödinger in imaginary time), eigenvectors real - should be a straightforward generalization. Have done this already while studying Ornstein-Uhlenbeck

with Lippolis and Henninger - the eigenfunctions are Hermite polynomials times Gaussians.

2016-11-13 Predrag The claim “the cat map $A = \begin{pmatrix} a & c \\ d & b \end{pmatrix}$ is assumed to be time-reversal invariant, i.e. $c = d$.” seems to be in conflict with Boris choice $A = \begin{pmatrix} s-1 & 1 \\ s-2 & 1 \end{pmatrix}$

We write (3.49) as

$$(\square + 2 - s)x_t = m_t, \quad (10.1)$$

Percival and Vivaldi [54] write their Eq. (3.6)

$$(\square + 2 - s)x_t = -b_t \quad (10.2)$$

so their “stabilising impulses” b_t (defined on interval $x \in [-1/2, 1/2]$) have the opposite sign to our “winding numbers” m_t (defined on $x \in [0, 1]$).

Did not replace Arnol'd by PerViv choice.

$$A = \begin{pmatrix} 0 & 1 \\ -1 & s \end{pmatrix}, \quad (10.3)$$

$$\begin{aligned} x_{t+1} &= p_t \mod 1 \\ p_{t+1} &= -x_t + s p_t \mod 1 \end{aligned} \quad (10.4)$$

Predrag's formula, removed by Boris 2017-01-15:

$$\begin{aligned} x_{t+1} &= (s-1)x_t + p_t \mod 1, \\ p_{t+1} &= (s-2)x_t + p_t \end{aligned} \quad (10.5)$$

Predrag's formula, removed by Boris 2017-01-15:

As the 3-point discretization of the second time derivative d^2/dt^2 (central difference operator) is $\square x_t \equiv x_{t+1} - 2x_t + x_{t-1}$ (with the time step set to $\Delta t = 1$), the *temporal* cat map (5.62) can be rewritten as the discrete time Newton equation for inverted harmonic potential,

$$(\square + 2 - s)x_t = m_t. \quad (10.6)$$

Predrag's formula, replaced by a more abstract form by Boris 2017-01-15:
a d -dimensional spatiotemporal pattern $\{x_z\} = \{x_{n_1 n_2 \dots n_d}\}$ requires d -dimensional spatiotemporal block $\{m_z\} = \{m_{n_1 n_2 \dots n_d}\}$,

for definiteness written as

$$A = \begin{pmatrix} 2 & 1 \\ 1 & 1 \end{pmatrix}, \quad (10.7)$$

2016-08-20 Predrag “ The fact that even Dyson [25] counts cat map periods should give us pause - clearly, some nontrivial number theory is afoot. ”

Not sure whether this is related to cat map symbolic dynamics that we use, dropped for now: “ Problems with the discretization of Arnol’d cat map were pointed out in refs. [11, 12]. Ref. [12] discusses two partitions of the cat map unit square. ”

“ and resist the siren song of the Hecke operators [47, 53] ”

While stability multipliers depend only on the trace s , the state space eigenvectors depend on the explicit matrix A , and so do “winding numbers” m_t (which also depend on the defining interval $x \in [-1/2, 1/2]$, Percival and Predrag choice, or Boris choice $x \in [0, 1]$). Time-reversed has different eigenvectors (orthogonal to the forward-time ones), so I am not even sure how time reversed m_t look.

2016-05-21 Predrag Behrends [8, 9] *The ghosts of the cat* is fun - he uncovers various regular patterns in the iterates of the cat map.

2016-09-27 Boris Cat maps and spatiotemporal cats

In the spatiotemporal cat, “particles” (i.e., a cat map at each periodic lattice site) are coupled by the next-neighbor coupling rules:

$$q_{n,t+1} = p_{nt} + (s-1)q_{nt} - q_{n+1,t} - q_{n-1,t} - m_{n,t+1}^q$$

$$p_{n,t+1} = p_{nt} + (s-2)q_{nt} - q_{n+1,t} - q_{n-1,t} - m_{n,t+1}^p$$

The symbols of interest can be found by:

$$m_{nt} = q_{n,t+1} + q_{n,t-1} + q_{n+1,t} + q_{n-1,t} - s q_{nt} .$$

2016-10-27 Boris Gutkin and Osipov [35] write: “In general, calculating periodic orbits of a non-integrable system is a non-trivial task. To this end a number of methods have been developed,” and then, for a mysterious reasons, they refer to ref. [6].

2016-11-07 Predrag The dynamical systems literature tends to focus on *local* problems: bifurcations of a single time-invariant solution (equilibrium, relative equilibrium, periodic orbit or relative periodic orbit) in low-dimensional settings (3-5 coupled ODEs, 1-dimensional PDE). The problem that we face is *global*: organizing and relating *simultaneously* infinities of unstable relative periodic orbits in ∞ -dimensional state spaces, orbits that are presumed to form the skeleton of turbulence (see ref. [28] for a gentle introduction) and are typically not solutions that possess the symmetries of the problem. In this quest we found the standard equivariant bifurcation theory literature not very helpful, as its general focus is on bifurcations of solutions, which admit all or some of the symmetries of the problem at hand.

2016-11-17 Predrag Adler and Weiss [1] discovered that certain mappings from the torus to itself, called hyperbolic toral automorphisms have Markov partitions, and in fact these partitions are parallelograms. One famous example is the Arnol'd Cat Map

(Axiom A; Anosov)

are a family of analytic hyperbolic automorphisms of the 2-dimensional torus which

The “linear code” was introduced and worked out in detail in influential papers of Percival and Vivaldi [10, 54, 55].

For $d = 1$ lattice, $s = 5$ the spatial period 1 fixed point is equivalent to the usual $s = 3$ Arnol'd cat map.

The cat map partitions the state space into $|\mathcal{A}|$ regions, with borders defined by the condition that the two adjacent labels $k, k+1$ simultaneously satisfy (3.49),

$$x_1 - sx_0 + x_{-1} - \epsilon = k, \quad (10.8)$$

$$x_1 - sx_0 + x_{-1} + \epsilon = k + 1, \quad (10.9)$$

$$x_2 - sx_1 + x_0 = m_1, \quad (10.10)$$

$$x_1 - sx_0 + x_{-1} = m_0, \quad (10.11)$$

$$(x_0, x_1) = (0, 0) \rightarrow (0, 0), \quad (1, 0) \rightarrow (0, -1), \quad (0, 1) \rightarrow (1, s), \quad (1, 1) \rightarrow (1, s-1)$$

2016-11-05 Predrag Dropped this:

Note the two symmetries of the dynamics [42]: The calculations generalize directly to any cat map invariant under time reversal [44].

2016-11-11 Boris “Deeper insight” into $d = 2$ symbolic dynamics Information comes locally (both in space and time). Allows to understand correlations between invariant 2-tori. Connection with field theories.

To Predrag: we have similar results on 2×1 blocks, but I think $1 \times 1, 2 \times 2$ is enough. Agree?

2016-12-08 Predrag: I agree

2016-12-06 Boris Confused about Predrag's claim that refs. [15, 29] tile “spatially and temporally infinite domains”(?) In both papers the spatial extension of the system is finite, and the attractors have relatively small dimensions.

2016-12-08 Predrag: I rewrote that now, is it clearer?

2016-12-06 Boris Is this claim true: “Temporally chaotic systems are exponentially unstable with time: double the time, and roughly twice as many periodic orbits are required to describe it to the same accuracy. For large spatial extents, the complexity of the spatial shapes also needs to be taken

[the same plot as figure ??]

Figure 10.1: (Color online) Newtonian Arnol'd cat map (x_0, x_1) state space partition into (a) 4 regions labeled by m_{0+} , obtained from (x_{-1}, x_0) state space by one iteration (the same as figure 1.2). (b) 14 regions labeled by past block $m_{-1}m_0$, obtained from (x_{-2}, x_{-1}) state space by two iterations. (c) 44 regions, past block $m_{-2}m_{-1}m_0$. (d) 4 regions labeled by $.m_1$, obtained from (x_2, x_1) state space by one backward iteration. (e) 14 regions labeled by future block $.m_1m_2$, obtained from (x_3, x_2) state space by two backward iterations. (f) 44 regions, future block $m_3m_2m_1$. Each color has the same total area ($1/6$ for $m_t = 1, 2$, and $1/3$ for $m_t = 0, 1$). All boundaries are straight lines with rational slopes.

into account. A spatiotemporally chaotic system is *extensive* in the sense that ...” Double the time and the number of periodic orbits is squared?

2016-12-08 Predrag: It is true only for discrete time, complete binary dynamics, but any other statement brings in more confusing words. I do not want to say “entropy” here. I rewrote it now.

2016-12-06 Boris Predrag’s statement “Essentially, as the stretching is uniform, distinct admissible symbol patterns count all patterns of a given size, and that can be accomplished by construction the appropriate finite size transition matrices [16].” is true only for symbolic dynamics based on Markov partitions. Wrong e.g., for linear coding.

2016-12-08 Predrag: I rewrote that now, is it correct?

2016-12-12 Predrag My claim (in a conversation with Boris) that spatiotemporal cat symbolic dynamics is “ d -dimensional” was nonsensical. I have now removed this from the draft: “ The key innovation of ref. [35] is the realization (an insight that applies to all coupled-map lattices, and all PDEs modeled by them, not only the system considered here) that d -dimensional spatiotemporal orbit $\{x_z\}$ requires d -dimensional symbolic dynamics code $\{m_z\} = \{(m_1, m_2, \dots, m_d)\}$, rather than a *single* temporal symbol sequence (as one is tempted to do when describing a finite coupled N^{d-1} -“particle” system).”

Li Han text: “ To generate such state space partitions, we start with length $\ell = 1$. Consider first the symbol $m_0 = sx_0 - (x_1 + x_{-1}) = \lfloor sx_0 - x_1 \rfloor$, where $\lfloor \dots \rfloor$ is the floor function. m_0 has symbol boundaries which are equally spaced parallel lines of slope s and passing through $(x_0, x_1) = (0, 0), (1, 1)$. We then look at the time-evolved images of these symbol regions under forward map (1.101). The transformed region therefore means that at coordinate (x_{t+1}, Fx_{t+2}) the point has symbol m_t , which in turn implies that when interpreted back to (x_0, x_1) state space, a point is associated with symbol m_{-1} . As a result, we can generate all length-1 state spaces corresponding to symbols m_t , $t = 0, \pm 1, \pm 2, \dots$ on the (x_0, x_1) state space simply by applying the forward map (1.101) or its in-

[the same plot as figure ??]

Figure 10.2: Newtonian Arnol'd cat map (x_0, x_1) state space partition into (a) 14 regions labeled by block $b = m_0.m_1$, the intersection of one past (figure 10.1(a)) and one future iteration (figure 10.1(d)). (b) block $b = m_{-1}m_0.m_1$, the intersection of two past (figure 10.1(b)) and one future iteration (figure 10.1(d)). (c) block $b = m_{-1}m_0.m_1m_2$, the intersection of two past (figure 10.1(b)) and two future iterations (figure 10.1(e)). Note that while some regions involving external alphabet (such as $_22_$ in (a)) are pruned, the interior alphabet labels a horseshoe, indicated by the shaded regions. Their total area is (a) $4 \times 1/8$, (b) $8 \times 1/21$, and (c) $16 \times 1/55$.

[the same plot as figure ??]

Figure 10.3: (Color online) $\ell = 1$ state spaces on (x_0, x_1) state space with respect to symbols m_t , $t = 0, -1, -2, 1, 2, 3$ for $s = 3$. In each block values of $m_t = -1, 0, 1, 2$ are shaded with light red, green, blue, and yellow, respectively, and each color has the same total area ($1/6$ for $m_t = -1, 2$, $1/3$ for $m_t = 0, 1$) in all blocks. All boundary lines are straight lines with rational slopes, while the slopes tend to irrational values set by stable/unstable directions of the cat map exponentially fast in the limit $t \rightarrow \pm\infty$.

[the same plot as figure ??]

Figure 10.4: $\ell = 2, 3, 4$ state spaces on (x_0, x_1) state space for $s = 3$, using blocks m_0m_1 , $m_{-1}m_0m_1$, and $m_{-1}m_0m_1m_2$ from the $\ell = 1$ diagrams. Shaded diamonds or rectangles correspond to sequences of all interior symbols $(0, 1)^{\otimes \ell}$, having a total area of $4 \times 1/8$, $8 \times 1/21$, $16 \times 1/55$ respectively from left to right.

verse. We plot such length-1 diagrams in figure ?? for symbols m_0, m_{-1}, m_{-2} (top), and m_1, m_2, m_3 (bottom), and call them different blocks. Note that any of the blocks can be used to recover the 1-symbol measure $f_1(m)$ by calculating the total of respective region areas, while with blocks $m_0 = \lfloor sx_0 - x_1 \rfloor$ and $m_1 = \lfloor sx_1 - x_0 \rfloor$ the computations are the easiest, which have symbol boundaries of slopes s and $1/s$ respectively.

The fact that $\mu(m \in \mathcal{A}_0)$ are all equal and twice of $\mu(m \in \mathcal{A}_1)$ is also obvious from the m_0, m_1 blocks of length-1 state spaces.

A length- ℓ state space is then the superposition of any ℓ consecutive blocks of length-1 diagrams, while a choice that is symmetric about block m_0 or m_0 and m_1 will make the amount of calculations minimal. We have evaluated $\mu(m)$ up to $\ell = 12$ from both (??) and symbolic diagrams for $s = 3, 4, 5$, and they are consistent. In figure ?? we plot the symbolic diagrams for 2, 3, and 4 consecutive symbols using blocks $m_{0,1}, m_{-1,0,1}$, and $m_{-1,0,1,2}$ of figure ???. Sequences of all interior symbols correspond to congruent parallelogram regions whose opposite sides are exactly parallel, and for even ℓ the regions are diamonds whose sides are of equal length. Sequences of symbols from both \mathcal{A}_0 and \mathcal{A}_1 are not all admissible, which is the topic of next section. Here we note that the corresponding regions of such sequences have general polygon shapes and are not parallelograms, no matter which consecutive set of blocks we use.

All boundary lines are straight lines with rational slopes, while the slopes tend to irrational values set by stable/unstable directions of the cat map exponentially fast in the limit $t \rightarrow \pm\infty$.

From (??) the measure $\mu(b)$ for a block $b = m_1 m_2 \cdots m_\ell$ is proportional to the area of the polygon defined by inequalities (??).

The full list of measures $\mu(m_1 m_2 \cdots m_\ell)$ has a tensor structure of tensor rank ℓ with each index running over \mathcal{A} and can be interpreted as a joint probability function. "

Boris results.tex text: " whose lower left corner is the (n, t) lattice site

$$\mathcal{R}_{nt} = \{(n+i, t+j) | i = 0, \dots, \ell_1 - 1, j = 0, \dots, \ell_2 - 2\},$$

It is straightforward to see that when M is such that all symbols m_z belong to $\mathcal{A}_0 = \{0, \dots, s-4\}$ then M is always admissible. By positivity of Green's function (see appendix ??) it follows immediately that $0 < x_z$ while the condition $\sum_{z' \in \mathbb{Z}} g_{zz'} = s-2$ implies that $x_z \leq 1$.
"

Predrag text, recycle: " Here the piecewise linearity of the spatiotemporal cat enables us to go far analytically. Essentially, as the cat map stretching is uniform, distinct admissible symbol blocks count all blocks of a given shape (they all have the same stability, and thus the same dynamical weight), and that can be accomplished by linear, Green's function methods. "

Predrag removed Boris poetry: “ The alphabet separation into interior and external parts nicely illustrates the transition of the model from the correlated regime to the uncorrelated Bernoulli process as parameter s in (18.46) tends to ∞ . Indeed, the number of external symbols in \mathcal{A}_1 is fixed within a given differential operator \square structure, while the number of interior symbols in \mathcal{A}_0 grows linearly with the parameter s controlling the strength of chaos in a single map. For cat map this transition can be achieved by merely increasing the time step of time evolution. Increasing the time step from 1 to 2 leaves the form of equation (3.49) intact, but renormalizes the constant $s \rightarrow s^2 - 1$. This reflects the fact that ϕ^2 is more “chaotic” than ϕ . With an increase of k the map ϕ^k resembles more and more uncorrelated Bernoulli process. Similar transition can be observed in the coupled \mathbb{Z} map lattices, with a caveat that switch from Φ to Φ^k renormalizes not only the constant s , but \square itself. The resulting equation of motion will contain an elliptic operator $\square^{(k)}$ of higher order. Still, it is straightforward to see that the number of external symbols is controlled by the order of the operator $\square^{(k)}$ which grows linearly with k . On the other hand, the number of interior symbols grows in the same way as the constant s i.e., exponentially. ”

Replaced N (for N “particles”) by L (for spatial extent) throughout

2019-09-10 Boris Old version, now replaced in results.tex by a more compact paragraph:

To be specific, let \mathcal{R} be a rectangular $[\ell_1 \times \ell_2]$ region, and let $M_{\mathcal{R}}$ be the $[\ell_1 \times \ell_2]$ block of M symbols from the alphabet \mathcal{A} . Let $\mathcal{N}(M_{\mathcal{R}} | M_{[L \times T]})$ be the number of times a given symbol block $M_{\mathcal{R}}$ appears anywhere within a much larger admissible symbol block $M_{[L \times T]}$ cut out from a spatiotemporally infinite generic solution M of the spatiotemporal cat (18.46). The $d = 1$ cat map is known to be fully hyperbolic and ergodic for $s > 2$, with a unique invariant natural measure μ in the state space (5.62) of the system. The $d = 2$ spatiotemporal cat is fully hyperbolic and ergodic for $s > 4$, see (??). In the language of spatially extended systems, we assume that a steady state spatiotemporally chaotic solution is on average spatiotemporally invariant, so the number of times a *given* admissible block $M_{\mathcal{R}}$ shows up over a region $[L \times T]$ is expected to grow linearly with the area LT . Hence a *relative* frequency of the occurrence of the block $M_{\mathcal{R}}$ can be defined as

$$f(M_{\mathcal{R}} | M_{[L \times T]}) = \frac{1}{LT} \mathcal{N}(M_{\mathcal{R}} | M_{[L \times T]}). \quad (10.12)$$

With L and T increasing at comparable rates (for example, take a square $[L \times T]$, with $L = T$), the ergodic measure of finding the block $M_{\mathcal{R}}$ across the infinite spatiotemporal domain is given by

$$\mu(M_{\mathcal{R}}) = \lim_{L, T \rightarrow \infty} f(M_{\mathcal{R}} | M_{[L \times T]}), \quad \sum_{M_{\mathcal{R}}} \mu(M_{\mathcal{R}}) = 1. \quad (10.13)$$

For an ergodic system with a unique invariant natural measure μ , the limiting frequencies $f(M_{\mathcal{R}})$ are equal to the measures $\mu(M_{\mathcal{R}})$ of the cylinder sets $M_{\mathcal{R}}$, defined as sets of state space points $X_{\mathcal{R}}$ having $M_{\mathcal{R}}$ symbolic representation over the region \mathcal{R} . For this reason, we sometimes refer, with a slight abuse of notation, to the frequencies $f(M_{\mathcal{R}})$ defined by (10.12) as measures of $M_{\mathcal{R}}$ in the limit $L, T \rightarrow \infty$, and denote them by $\mu(M_{\mathcal{R}})$ in what follows.

2016-11-20 Boris The spatiotemporal symbols follow from the Newtonian equations in d spatiotemporal dimensions

$$\begin{aligned} m_{n,j} &= (q_{n,j+1} - 2q_{n,j} + q_{n,j-1}) + (q_{n+1,j} - 2q_{n,j} + q_{n-1,j}) - (s-4)q_{n,j} \\ m &= [\square + 2d1 - s1] q. \end{aligned} \quad (10.14)$$

2017-02-16 Predrag To me, the Green's functions look strictly positive. Must harmonize definitions (??), (??), (5.45), (18.46) and (3.49), originating in Boris' flip-flop $m_t \rightarrow -m_t$

Is there a reference to Green's functions in terms of Chebyshevs?

2017-08-02 Boris Yes, and it is OK with our present convention - Green's functions must be positive.

2017-08-02 Boris Rule-of-thumb - internal symbols are non-negative, Green's functions are positive.

2017-07-31 Boris "As every Anosov automorphism is topologically conjugate to a linear cat map ..." Is it really true ?

2017-08-11 Predrag That's what I read in some of the articles cited. But no need to say it here, so now this is removed from our article.

2016-11-13 Predrag to all cats - where we write (3.49), Percival and Vivaldi [54] write their Eq. (3.6) $(\square + 2 - s)x_t = -b_t$ so their "stabilising impulses" b_t have the opposite sign to our "winding numbers" m_t (defined on $x \in [0, 1]$).

To all cats: keep checking that after your flip of signs of m_t 's Eqs. (18.46), (3.49), (??) and (10.14) are consistent.

2017-07-31 Boris Changed time ago. They should have the same sign as Percival and Vivaldi i.e., our m are positive!

2017-08-11 Predrag I now get it. LT is the area of \mathcal{R} . The total number of blocks grows exponentially with the size of \mathcal{R} and is bounded from above by $(LT)^{|A|}$. You are saying that the number of times a *single* admissible block $M_{\mathcal{R}}$ shows up over a region $[L \times T]$ grows linearly with the area LT , and so does the sum over frequencies of all distinct admissible blocks

M'_R ? These “frequencies” are *relative*, in the sense that correct normalization is not (10.13), but

$$\mu(M_R) = \frac{f(M_R)}{\sum_{M'_R} f(M'_R)}. \quad (10.15)$$

2017-08-05 Predrag Cylinder sets are subtle: if we were counting only *admissible* X , the cylinder set would be much smaller. But we almost never know all inadmissible states.

2017-07-31 Boris Li subsection *Blocks of length ℓ* , was siminos/cats/catGenerL.tex 2017-02-17, mostly contained repetitions of the previous stuff. Did not think we needed it. Few usable things could be brought to other places. Agree?

2017-08-23 Predrag Done.

2017-08-26 Predrag Removed: “The term $\square + 2d1$ is the standard statistical mechanics diffusive inverse propagator that counts paths on a d -dimensional lattice [60], and $-s1$ is the on-site cat map dynamics (for the Hamiltonian formulation, see appendix ??).

2017-08-05 Boris Something unclear here (at least for me). “The iteration of a map $g(x_t)$ generates a group of *time translations*”. Why translations? g is a (time) map acting on all sites of lattice independently (no interaction). Note: I think the models in [56] and [14] are of the same type. Both can be thought of as products of two maps: “Interactions” · “Single particle propagations” (i.e., product of g 's)

2017-09-04 Predrag: You are right, I have rewritten that text now.

2017-08-28 Predrag For the Dirichlet (as opposed to periodic) boundary condition, which breaks the translational symmetry, we take the very unphysical b.c. $x_z = 0$ for $z \in \mathcal{R}$. Finite windows into turbulence that we describe by our symbol blocks never have such edges. Methinks...

2017-09-12 Boris This equation

$$\begin{aligned} x_{n,t+1} &= p_{nt} + (s - 3)x_{nt} - (x_{n+1,t} - 2x_{nt} + x_{n-1,t}) - m_{n,t+1}^x \\ p_{n,t+1} &= p_{nt} + (s - 4)x_{nt} - (x_{n+1,t} - 2x_{nt} + x_{n-1,t}) - m_{n,t+1}^p \end{aligned} \quad (10.16)$$

seems wrong. We use (??).

2017-09-14 Boris Recall that (the Dirichlet) $g_{zz''}$ is a function of both z and z'' and not just of the distance between them $|z - z''|$.

2017-09-04 Predrag “integer $s > 4$ ” is not the correct condition, for $d = 2$ $s = 4$ is presumably already hyperbolic. To add to the confusion, in his report Adrien computes for $s = 3$, the case with no interior alphabet symbols. So $s > 2$ is the correct hyperbolicity condition for all d ? Give the correct condition on s , explain it.

2017-09-12 Boris Here are the answers to this and co. questions over the paper.

1. The system is uniformly (fully) hyperbolic for $s > 2d$. This means all eigenvalues of linearized map (see (??) for $d = 2$) are either $|\Lambda| < 1$ (stable subspaces) or $|\Lambda| > 1$ (unstable subspaces).
2. For $s = 2d$ the system is partially hyperbolic. This means everything as above except two Lyapunovs for which $\Lambda = 1$ (neutral subspaces).
3. For $|s| < 2d$ system is non-hyperbolic. Apparently for everything in this paper 1 & 2 is OK. But
4. drastically changes everything (suspect a phase transition in physics jargon i.e., non-unique SRB measure). So whatever we consider in the paper should be for $s \geq 2d$.

2017-09-14 Boris A comment on $s = 2d$ case (do not know how much of it we need for the paper). Our results in this paper require in principle $s > 2d$ (all Lyapunovs are positive). However certain things still work (by whatever reason) for $s = 2d$ as two figs in sect. ?? show. In this case the total momentum $\sum_{n=1}^L p_{nt}$ is preserved. This can be seen from the invariance of (18.46) under translation $x_{nt} \rightarrow x_{nt} + \alpha$. So the system is not ergodic and linear encoding is not one to one (different trajectories might have the same symbolic representation). However, it is (probably) ergodic on the shell $\sum_{n=1}^L p_{nt} = \text{const}$. This is probably the reason why our formulas for frequencies of M_R still work.

2017-09-26 Boris Dropped this: “with the corresponding probability of occurrence of a fixed symbol block M_R given by

$$\mu(M_R | M_{[L \times T]}) = \frac{f(M_R | M_{[L \times T]})}{\sum_{M'_R} f(M'_R | M_{[L \times T]})}, \quad \sum_{M_R} \mu(M_R | M_{[L \times T]}) = 1,$$

where the sum goes over all distinct admissible blocks M'_R .”

The point is that

$$\sum_{M_R} N(M_R | M_{[L \times T]}) = LT - \text{“Terms linear in L and T”}.$$

So no need in an artificial normalization - normalization in (10.13) would follow anyhow.

2017-09-14 Boris Replaced this eq.

$$M \cup \partial R = \begin{bmatrix} x_{12} \\ x_{01} & m_{11} & x_{21} \\ x_{10} \end{bmatrix} = \begin{bmatrix} x_2 \\ x_1 & m_{11} & x_3 \\ x_4 \end{bmatrix} \quad (10.17)$$

by the first plot in figure ??.

CHAPTER 10. ARTICLE EDITS

2016-11-15, 2017-08-28 Predrag Note: When I look at the intersection of the diagonal with the partition strips in by inspecting figure ??, I find that the Fibonacci numbers 1,2,3,5, ... give the numbers of periodic points, in agreement with the Adler-Weiss Markov partition. So the linear code is not a generating partition, but periodic orbits do the right thing anyway.

2018-04-05 to Adrien from Predrag I think figure 10.8 is really hard to explain to a reader; why these axes, how did all points get mapped into the same unit square, why there are huge empty swaths - all stuff that distracts from the main point which is that x_z 's within the center of the shared symbol block are exponentially close.

2018-04-05 Predrag I think we can simplify this greatly, using the fact that the (damped) screened Poisson equation (??) is linear, so one can subtract patterns in order to visualize their distance.

In order to have a 2-dimensional visualization for each block, color the symbol M_j $[\ell_1 \times \ell_2]$ block with discrete color alphabet \mathcal{A}_0 , as in figure 10.6, and the corresponding state X_j $[\ell_1 \times \ell_2]$ block with colors chosen from a continuum color strip.

As this is a linear problem, you can also represent closeness of two $[\ell_1 \times \ell_2]$ blocks by using this coloring scheme for $M_2 - M_1$ and $X_2 - X_1$.

For pairs of distinct 2-tori which share the same region of m_z 's, or a single 2-torus in which the same region of m_z 's appears twice, the states x_z in the center of the region should be exponentially close, in order to demonstrate that they shadow each other.

So, replace figure 10.8 by (a) $M_2 - M_1$ from figure 10.6 (it will be all the same color in the shared region), and (b) plot $X_2 - X_1$. Mark the lattice point z with the minimal value of $|x_z^{(2)} - x_z^{(1)}|$ on this graph, and in the text state the minimal value of $|x_z^{(2)} - x_z^{(1)}|$. You can also state the mean Euclidean (or L2) distance between the two invariant 2-tori:

$$d_{X_2 - X_1} = \left(\frac{1}{LT} \sum_z (x_z^{(2)} - x_z^{(1)})^2 \right)^{1/2}, \quad (10.18)$$

or distance averaged over the lattice points restricted a region \mathcal{R} .
(taken care of by AKS)

2018-04-13 Adrien After reconstructing the orbits separately, I plotted the distance between the positions in (q, p) space for each lattice site z , see the new figure 10.5, meant to replace the current figure 10.8. Still have to use sensible color ranges, and compute figure 10.5 (b).
(taken care of by AKS)

2018-04-13 to Adrien from Predrag Also of interest might be the color-coded plot of value of $x_{q,p}$ for at least one of them. Would be nice to check

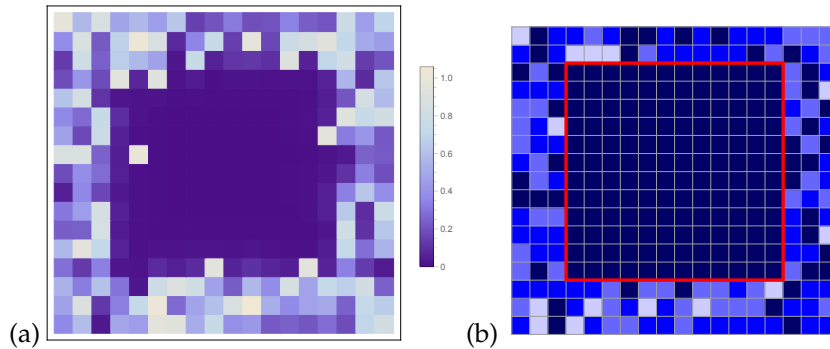


Figure 10.5: (Color online) (a) $X_{2,z} - X_{1,z}$, the site-wise distance between the invariant 2-tori fields corresponding to the two $[18 \times 18]$ blocks M_1, M_2 (colored tiles) of figure 10.6 (a,b). (b) The plot of the site-wise symbol difference $|M_{2,z} - M_{1,z}|$ of figure 10.6 (b) and (b) (for a better visualization, see figure 10.9).

-at least once- whether there is any relation to the corresponding $m_{q,p}$ (probably there is no relation).

We'll have to rethink coloring (should be the same as $m_{q,p}$, more or less).

As the distance decreases exponentially towards the center, you probably want a color plot of $\ln |x_{q,p}^{(2)} - x_{q,p}^{(1)}|$ to resolve the small distances towards the center of the square.

(taken care of by AKS)

2017-08-02 Boris The representation figure ?? has changed from digits to colors figure 10.6 (PC 2019-08-26 reverted this figure to digits).

Was it try and see, or is it going to stay? In my opinion it is more colorful, but less informative. The reason is a) digits are directly m_{nt} - no need to translate colors into numbers + make sense without colors (on line). b) the encounters (regions with the same coding) can be visualized by coloring.¹

2019-08-21 Boris Now that we got rid of the color figure 10.8, there's no point in having two different colors in figure ?? for the overlapping regions of symbols, light blue for the outer region called \mathcal{R}_1 in the paper, dark blue for the inner one called \mathcal{R}_0 .

ToDo

(taken care of by AKS)

2019-08-21 Boris I like including the differences plot figure 10.5 or figure ?? (we have something similar in Our Paper [35] with Vladimir Osipov) (im-

¹Predrag 2017-08-11: Well, that's a bit subjective - it is unintelligible to a human eye either way. I would keep this one figure as an illustration that color coding is an alternative to number coding. (taken care of by AKS)

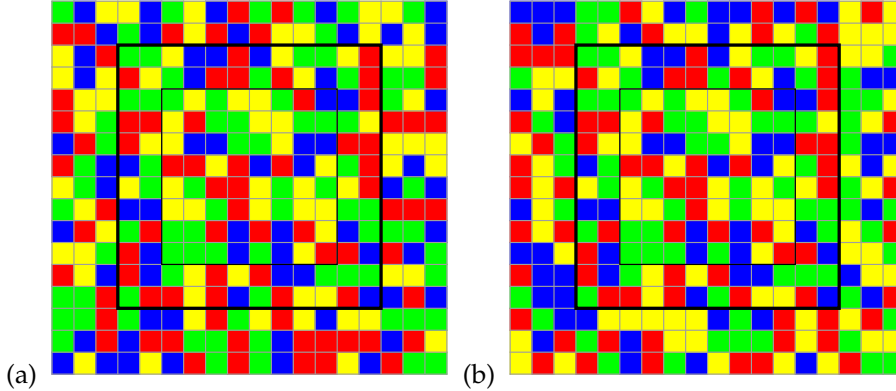


Figure 10.6: Figure nixed by Boris 2019-08-21, replaced by digits figure ??.
 Symbolic representation (colored tiles) of two $[L \times T] = [18 \times 18]$ invariant 2-torus solutions of (??), $s = 7$, that shadow each other within the shared block $M_R = M_{R_0} \cup M_{R_1}$ (blue). The symbols within R , drawn randomly from the interior alphabet A_0 , are the same for both solutions; the symbols outside R , also drawn randomly from A_0 , differ. The shared block $R = R_0 \cup R_1$ is split into the interior region R_0 (bold blue) and the border strip R_1 (blue).

plemented PC 2019-08-27).

It should be included as addition to figure ??, and not as substitution to it (it substitutes figure 10.8, now removed from the paper). Without figure ?? it would be difficult to digest and explain its content.

2019-10-30 Adrien I think by now we agreed we would keep the digits figure only. The figures of symbolic difference (figure 10.5) and of symbolic coloring (figure 10.6) are either outdated or ugly. We can toss them out of the blog. figure 10.7 and figure 10.8 could be moved to another appendix. We could also move figure 10.9 to another appendix, as it is the most recent “difference of symbols” figure.

(taken care of by AKS)

2019-08-27 Predrag If you mean “metric distances” of Gutkin-Osipov figures A3 and C2, that is quite different than our $\log(\text{distance})$ plots. Problem is that Gutkin-Osipov measure Euclidean distance between symplectic phase-space points, not a meaningful distance. Would have to subtract actions, but this is not a thing for this paper...

2019-08-21 Adrien You mean figure 10.5 here in `GHJSC16blog.tex`, i.e., figure ??(a) which is the log of the norm of the difference of the two trajectories in state space? I agree that if anything, figure ??(a) should substitute figure 10.8 and not figure ???. What do you think on the updated color pattern, figure ??(b)?

(a)	$\begin{pmatrix} 3 & 3 & 1 & 3 & 3 & 0 & 3 & 2 & 2 & 3 & 3 & 0 & 1 & 3 & 3 & 2 & 0 & 1 & 2 \\ 2 & 0 & 3 & 2 & 2 & 1 & 2 & 2 & 3 & 3 & 2 & 1 & 1 & 1 & 0 & 3 & 0 & 1 \\ 1 & 3 & 1 & \textcolor{blue}{0} & 2 & 0 & 0 & 1 & 3 & 1 & 0 & 0 & 0 & 1 & 2 & 0 & 0 & 3 \\ 1 & 2 & 3 & 1 & 1 & 1 & 1 & 2 & 2 & 0 & 1 & 2 & 0 & 2 & 1 & 3 & 0 \\ 1 & 2 & 3 & 1 & 1 & 1 & 1 & 2 & 2 & 0 & 1 & 2 & 0 & 2 & 1 & 2 & 0 \\ 2 & 3 & 1 & 2 & 1 & 0 & 2 & 0 & 1 & 1 & 3 & 1 & 0 & 0 & 0 & 2 & 2 & 2 \\ 2 & 2 & 3 & 0 & 3 & 2 & 3 & 3 & 3 & 2 & 2 & 0 & 0 & 0 & 2 & 0 & 1 & 1 \\ 2 & 3 & 3 & 1 & 1 & 1 & 1 & 3 & 3 & 1 & 1 & 0 & 1 & 2 & 0 & 0 \\ 2 & 2 & 1 & 3 & 2 & 2 & 0 & 2 & 2 & 0 & 2 & 3 & 3 & 0 & 1 & 2 & 2 & 2 \\ 1 & 0 & 2 & 2 & 0 & 0 & 0 & 0 & 3 & 2 & 3 & 0 & 0 & 1 & 2 & 0 & 3 \\ 1 & 0 & 2 & 2 & 1 & 3 & 2 & 3 & 0 & 1 & 1 & 0 & 0 & 0 & 1 & 1 & 2 \\ 2 & 1 & 3 & 0 & 3 & 1 & 1 & 0 & 1 & 0 & 2 & 1 & 3 & 3 & 0 & 0 & 2 \\ 2 & 0 & 0 & 2 & 1 & 1 & 2 & 0 & 0 & 1 & 0 & 1 & 0 & 0 & 0 & 3 & 2 & 0 \\ 3 & 3 & 2 & 1 & 3 & 1 & 1 & 1 & 3 & 3 & 3 & 0 & 1 & 0 & 3 & 2 & 1 & 1 \\ 3 & 1 & 3 & 3 & 3 & 1 & 0 & 2 & 2 & 1 & 3 & 0 & 1 & 3 & 3 & 3 & 0 & 1 & 1 \\ 3 & 1 & 3 & 3 & 1 & 0 & 2 & 2 & 1 & 3 & 0 & 1 & 3 & 3 & 3 & 0 & 1 & 1 & 1 \\ 3 & 1 & 0 & 1 & 3 & 2 & 2 & 0 & 2 & 2 & 0 & 2 & 3 & 3 & 0 & 1 & 1 & 1 & 1 \\ 2 & 2 & 1 & 1 & 1 & 1 & 1 & 1 & 3 & 3 & 3 & 3 & 1 & 1 & 1 & 0 & 0 & 2 & 2 \\ 1 & 1 & 1 & 1 & 3 & 2 & 2 & 0 & 2 & 2 & 0 & 2 & 3 & 3 & 0 & 1 & 2 & 0 & 3 \\ 1 & 0 & 2 & 2 & 0 & 0 & 0 & 0 & 3 & 2 & 3 & 0 & 0 & 1 & 2 & 2 & 3 & 1 \\ 2 & 0 & 2 & 2 & 1 & 3 & 2 & 3 & 0 & 1 & 1 & 1 & 1 & 0 & 0 & 0 & 2 & 0 & 3 \\ 0 & 1 & 0 & 0 & 3 & 1 & 1 & 0 & 1 & 0 & 2 & 1 & 3 & 3 & 0 & 1 & 2 & 1 & 1 \\ 1 & 2 & 1 & 2 & 1 & 1 & 2 & 0 & 0 & 1 & 0 & 1 & 0 & 0 & 0 & 2 & 1 & 3 & 0 \\ 3 & 3 & 0 & 1 & 3 & 1 & 1 & 1 & 3 & 3 & 3 & 3 & 0 & 1 & 0 & 0 & 0 & 2 & 2 & 3 \\ 3 & 0 & 2 & 3 & 3 & 1 & 0 & 2 & 2 & 2 & 1 & 3 & 0 & 1 & 3 & 3 & 3 & 1 & 1 & 1 \\ 3 & 0 & 2 & 3 & 3 & 1 & 0 & 2 & 2 & 2 & 2 & 3 & 2 & 3 & 2 & 2 & 3 & 0 & 2 & 3 & 3 \\ 1 & 0 & 0 & 2 & 3 & 2 & 2 & 2 & 2 & 2 & 2 & 3 & 2 & 3 & 2 & 2 & 3 & 0 & 2 & 3 & 3 \\ 2 & 2 & 1 & 2 & 2 & 2 & 2 & 3 & 1 & 0 & 1 & 2 & 2 & 0 & 2 & 1 & 2 & 0 & 3 & 1 \end{pmatrix}$	(b)
-----	--	-----

Figure 10.7: (Color online) Symbolic representation (numbered tiles) of two $[L \times T] = [18 \times 18]$ invariant 2-torus solutions of (??), $s = 7$, that shadow each other within the shared block $M_{\mathcal{R}} = M_{\mathcal{R}_0} \cup M_{\mathcal{R}_1}$ (blue). The symbols within \mathcal{R} , drawn randomly from the interior alphabet \mathcal{A}_0 , are the same for both solutions; the symbols outside \mathcal{R} , also drawn randomly from \mathcal{A}_0 , differ. The shared block $\mathcal{R} = \mathcal{R}_0 \cup \mathcal{R}_1$ is split into the interior region \mathcal{R}_0 (bold blue) and the border strip \mathcal{R}_1 (blue).

(taken care of by AKS)

2019-08-26 Boris Still not good enough. The coloring is too jumpy. It should range from white or light blue to dark blue. For a more reasonable coloring of this type see figure 14 from Our Paper [35] arXiv:1503.02676. Maybe also the periods of tori L, T should be larger to make things smoother.

(taken care of by AKS)

2019-08-21 Adrien We still need the two symbolic representation figures in figure ?? . In figure 10.7 I have regenerated those symbolic representation as numbers instead of colors, as an alternative to figure ?? . Which one do you prefer?

(taken care of by AKS)

2019-08-21 Boris For figure ?? - a different coloring pattern is indeed needed + the size of the figures (a), (b) should be the same.

AKS I agree. Except for the size, which should be the same as the current figure ??(a).

ToDo

(taken care of by AKS)

2019-08-28 Adrien I am re-generating both figures of figure ?? with larger periods in time and space ($L = 28$ and $T = 27$) so that they appear more smoothly. I've also expanded the shadowing region so we could observe an even larger exponential decay. Finally, I chose a coloring pattern similar to that of Boris's paper [35] arXiv:1503.02676. What do you guys

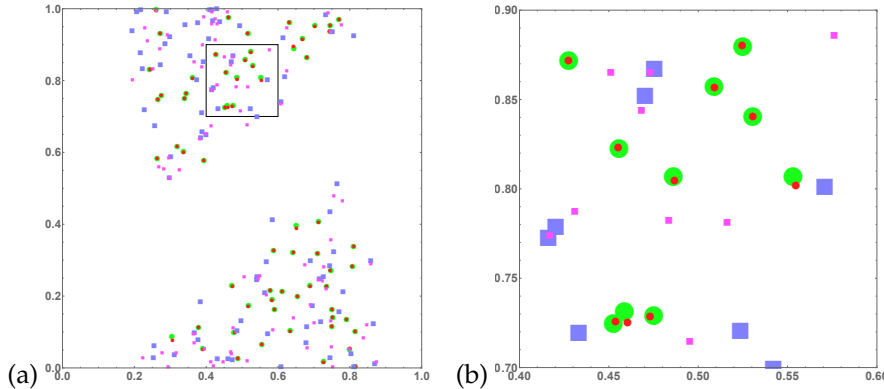


Figure 10.8: (Color online) (a) Phase space representation $(q_z^{(i)}, p_z^{(i)})$, where $i = 1, 2$ refers to the two invariant 2-tori of figure 10.7. (b) A zoom into small rectangular area shown on the left. The state space is covered only partially, as symbols in blocks M are restricted exclusively to the interior alphabet. Only data for $z = (n, t) \in \mathcal{R}$ are shown in the figure. The centers of red (small) circles and green (large) circles are the points $(q_z^{(i)}, p_z^{(i)})$ of the first ($i = 1$) and the second ($i = 2$) invariant 2-torus for z 's from the interior \mathcal{R}_0 . The centers of violet (large) and magenta (small) squares show the respective points from the border \mathcal{R}_1 , see figure 10.7. All $(q_z^{(1)}, p_z^{(1)})$ and $(q_z^{(2)}, p_z^{(2)})$ in the interior are well paired, while the separations are larger for z 's in the border region \mathcal{R}_1 . This illustrates shadowing being exponentially stronger the closer the point is to the center of \mathcal{R} , see (??).

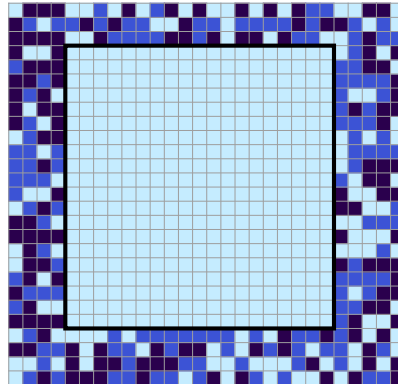


Figure 10.9: The site-wise distance $M_{2,z} - M_{1,z}$ between the $[28 \times 27]$ symbol blocks M_1, M_2 of figure ?? (For a worse visualization, see figure 10.5.)

think?

Here (on the blog/comments) I am attaching the difference of symbols (check figure figure 10.9).

For all the new figures I added, I've labeled them identically to their previous version and re-labeled the old ones "nameindex" so that they're stored in THE CLOUD.

Also I think it's not needed to break down the region \mathcal{R} into $\mathcal{R}_1, \mathcal{R}_2$ as we're no longer distinguishing between outer and inner regions of shared symbols (on figure 6,7 for example).

(taken care of by AKS)

2019-09-09 Predrag The point-wise block difference of figure 10.9 contains mo information - it's obvious from figure ?? that $M_{2,z} - M_{1,z}$ is zero over \mathcal{R} .

2019-08-28 Boris :

1. sect. ?? *Introduction*: there were wide cuts in comparison to the previous version. This was probably justified, but in my opinion it is overdone by now. It is difficult to understand what is a general motivation for our paper. It looks very technical, dry and restricted to concrete model. A bit more poetry on (linear) coding, e.g., why it is useful for description of dynamical systems might improve things.
2. sect. ?? *Model and overview of the main results*: I propose mother figures out how to use LaTex in order how to implement several of my desired changes in today's so deftly emailed GHJSC16_notes.pdf (in yellow).

2019-08-29 Predrag :

1. sect. ?? *Introduction*: I would like Boris to write the general motivation in his own voice, as that is a voice that quantum chaos community will resonate with. Predrag's pitch in the parallel Ref. [21] universe is to the turbulence community, I think having the two introductions, sung in different keys, will serve us better.
2. Text about not knowing the Percival-Vivaldi cat map grammar rules is now moved to just before sect. ?? *From itineraries to orbits and back*. sect. ?? *Model and overview of the main results* (Boris yellow markings) is reshuffled, hopefully as was his desire to have had it reshuffled.

2019-09-07 Boris redundant, removed:

Answer to Q1. *The spatiotemporal cat admits a natural 2-dimensional linear symbolic code with a finite alphabet. In principle, we can compute analytically the measure of a given finite spatiotemporal symbol block $M_{\mathcal{R}}$ over a region \mathcal{R} .*

2019-09-09 Predrag Files AKSLPS12_2.pdf, AKSLPS12_3.pdf are not referred to anywhere. If needed, I think they corresponds to log difference of the two small invariant 2-tori of figure 10.6.

2017-09-04 Predrag Border notation in (??) conflicts with (??). Shouldn't it be $+g_{t,0}x_0 + g_{t,\ell+1}x_{\ell+1}$?

2019-09-12 Boris No way :) I checked, (??) is correct.

2017-09-25 Predrag Eq. (??) would be "average coordinate" for the periodic boundary conditions, i.e., the periodic point (with repeats of the defining block correctly summed. Here $\bar{x}_i(b)$ is at the lower edge (lower corner?) of the admissible polytope.

2019-09-12 Boris I found the calculation following originally upon (??) redundant, so I removed it to here. Hope you understand everything without it.

The \mathcal{M}_b are partitions of the (x_0, x_1) state space, in contrast to the polygons \mathcal{P}_b , plotted in the Lagrangian coordinates $(x_0, x_{\ell+1})$, see figure ??-. Hence the interior alphabet measures $\mu(b)$, $m_i \in \mathcal{A}_0$, are given by the Jacobian (??) of coordinate transformation from the Lagrangian coordinates $(x_0, x_{\ell+1})$ to the state space (x_0, x_1) , $\mu(b) = U_{|b|}(s/2)^{-1}$. The value of $U_{|b|}(s/2)$ is always an integer greater than 1, and thus the (x_0, x_1) state space is "magnified" and wrapped around the $(x_0, x_{\ell+1})$ state space $U_{|b|}(s/2)$ times through ℓ iterations of the cat map. Lagrangian coordinates $(x_0, x_{\ell+1})$ are related to state space coordinates (x_k, p_k) , $p_t = (x_t - x_{t-1})/\Delta t$, at time $t \in (0, \ell + 1)$ by

$$\begin{aligned} x_t &= \bar{x}_t(b) + \frac{U_{\ell-t}(\frac{s}{2})}{U_{\ell}(\frac{s}{2})} x_0 + \frac{U_{t-1}(\frac{s}{2})}{U_{\ell}(\frac{s}{2})} x_{\ell+1} \\ p_{t+1} &= \bar{x}_{t+1}(b) - \bar{x}_t(b) + \frac{U_{\ell-t-1}(\frac{s}{2}) - U_{\ell-t}(\frac{s}{2})}{U_{\ell}(\frac{s}{2})} x_0 + \frac{U_t(\frac{s}{2}) - U_{t-1}(\frac{s}{2})}{U_{\ell}(\frac{s}{2})} x_{\ell+1}. \end{aligned}$$

This is a linear map, so its Jacobian $d_\ell = |\partial(x_0, x_1)/\partial(x_0, x_{\ell+1})|$ is simply

$$d_\ell = \frac{1}{U_\ell(\frac{s}{2})^2} \det \begin{pmatrix} U_\ell(\frac{s}{2}) & U_{-1}(\frac{s}{2}) \\ U_{\ell-1}(\frac{s}{2}) & U_0(\frac{s}{2}) \end{pmatrix} = \frac{1}{U_\ell(\frac{s}{2})}. \quad (10.19)$$

2019-09-12 Predrag Dropped this: “Unlike the systems studied in ref. [14], spatiotemporal cat cannot be conjugated to a product of non-interacting cat maps. A way to see that is, for an example, to compare the numbers of periodic orbits in the two cases – they differ.”

2017-09-14 Boris More straightforward argument is that \mathcal{B}_L (see ??) in appendix ?? is not conjugated to any feline with $B = 0$.

2019-09-27 Boris Checked ???. It is OK. The only question is whether the notation is sufficiently explained? (I plan to improve a bit figure ??.)

2019-09-28 Predrag Has anybody checked that the block of example following ?? is admissible?

2019-09-30 Boris Most probably not. On the other hand it is not terribly important. At the worst case they are all zeroes :)

2019-10-08 Predrag Cannot beat the post-Soviet perfectionism :)

2019-09-30 Boris We need Hamiltonian formulation for two reasons. First, our measure $dp dq$ comes from there. Second, for all numerics we actually use initial data problem i.e., Hamiltonian formulation. We need appendix ??, but should keep it compact.

2019-10-03 Boris A risky statement below. Did anybody checked this? “As X_z take rational values for any finite $[L \times T]$ invariant 2-tori, for sites sufficiently close to the center of \mathcal{R} the cancelation $x_{2,z} - x'_z$ can be exact.” **Predrag:** dropped it.

2017-01-25 Predrag Gutkin and Osipov refer to the map generated by the action (10.21) as non-perturbed *coupled cat map*, and to an invariant 2-torus p as a “many-particle periodic orbit” (MPO) if x_{nt} is doubly-periodic, or “closed,” i.e.,

$$x_{nt} = x_{n+L,t+T}, \quad n = 0, 1, 2, \dots, L-1, \quad t = 0, 1, 2, \dots, T-1. \quad (10.20)$$

Action of an invariant 2-torus p is

$$S_p = -\frac{1}{2} \sum_{t=1}^T \sum_{n=1}^L m_{nt} x_{nt}. \quad (10.21)$$

2019-10-08 Boris Do you want formula for action in the paper?

CHAPTER 10. ARTICLE EDITS

2017-01-25 Predrag Not unless it is necessary to discuss it anywhere in the paper... Besides, to me (10.21) seems almost surely wrong.

2019-01-24 Predrag Some of this invariant 2-torus stuff presumably goes to the kittens paper [21]; this paper does only the Dirichlet b.c..

2019-10-08 Boris Do you mean g_{zz}^0 ? Should we refer here to [21] instead of appendix ???

2017-09-05 Li Han I'm looking at numerical data. The number of total admissible rules of cat map takes an exponential law: $\sim 2.63^n$ for $s=3$, $\sim 3.74^n$ for $s=4$ for example. i.e., effectively $2.63/3.74$ symbols are needed for $s=3/s=4$. They agree with that from the topological entropy and Lyapunov exponent, which are $(3 + \sqrt{5})/2$, $2 + \sqrt{3}$, respectively. Intuitively this should hold (that $\log[\text{number of admissible rules}]/n = \text{topological entropy}$), but is it well-known/justified in symbolic dynamics?

2019-10-10 Boris Now dealt with, in sect. ???. Added concrete numbers to the picture caption.

2017-07-31 Boris Should we change layout of table ?? to the horizontal one?

2017-08-11 Predrag Not sure - easier to see the exponential growth in this format.

2017-09-01 Li Han How about including list of new pruning rules for small lengths as an Appendix?

2019-09-14 Boris Would be fine if you can do this.

2017-08-02 Boris figure ?? "Any 4×4 block of symbols appears one and the same number of times in both representations."

means the following: If we scroll/peep through the (upper) torus symbolic representation with 4×4 window, there are exactly NT different 4×4 blocks of symbols. Each of them appears the same number of times, as well, in the symbolic representation of the bottom tori (but for possibly different window positions).

2019-10-19 Predrag to Boris and Han: I have not checked it, but (??) is very pretty, kind of formula on gets from discrete-Fourier digitalization of Green's functions. You seem to be saying the det of the 2-torus Jacobian matrix counts the numbers of invariant 2-tori, and are computing $\ln \det$ to get a rate per area $|\mathcal{R}|$. Could some Chebyshev polynomials lurk here, and an analytic answer?

2017-09-14 Predrag Spatiotemporal cat metric entropy (??) is presumably exact for spatiotemporal cat as long as ℓ and ℓ' are going large at comparable rates. For systems without the space-time symmetry $t \leftrightarrow x$, h_k should be different along the time and the space directions, so I do not think we

can define one spacetime entropy? Enlightenment on this point would be very welcome.

2019-10-20 Adrien to Predrag and Boris: I can see why we would want to plot the logarithm of the site-wise distance $\ln |x_z - x'_z|$ between the states X, X' . The idea would be to remain in the Lagrangian picture. To be clear, right now:

- figure ?? is actually plotting $\ln \left(\sqrt{(q_z - q'_z)^2 + (p_z - p'_z)^2} \right)$ which is the site-wise distance in the Hamiltonian picture ($q = x$ and p is momentum). I already have generated the figure that corresponds to the Lagrangian site-wise distance, which is simply $\ln |x_z - x'_z|$. We want that one, correct?
- for figure ?? and figure ??, I can also generate the same 'Lagrangian' distance. For the 3 diamond blocks, we would have to generate two site-wise distance, let's say between (X_1, X_2) and (X_1, X_3) . Would that work? It would look something like what's on figure G11 of this blog.

(taken care of by AKS)

2019-10-20 Predrag to Boris - I admit to not understanding to what the title of sect. ?? *Full shadowing* refers to. $X_i - X_j$ shadow each other with the doughnuts, as they should, all distances elsewhere are of $O(1)$. What's *Full shadowing* about that?

2019-10-20 Predrag I would like to give shelter to figure ?? and figure ?? here in Bloglandia - they would require too much explanation - and replace them by the likes of figure 10.10. We could replace both by a single figure, the left frame giving $\ln |x_z - x'_z|$ for figure ??, and using figure 10.10 as the right frame, no need to exhibit the two other pairwise distances, as they should all look very much the same.

We let Boris decide.

(taken care of by AKS)

2019-10-19 Predrag Green's function notation is g_t is not helpful - it's a matrix, so easier to use $g_{tt'}$ throughout. Green's function notation is g_{nt} is not helpful, and here even misleading - it's a tensorial matrix, so less confusing to use $g_{zz'}$ notation throughout.

2019-10-21 Boris Semi-agree :). It is a matter of perception - after all "Green's function" is also (or rather first of all) a function (of z, z'). I have changed the notation. Looks more clumsy, but might be a less evil.

2016-11-08 Predrag Say: THE BIG DEAL is

for d -dimensional field theory, symbolic dynamics is not one temporal sequence with a huge alphabet, but d -dimensional spatiotemporal tiling by a finite alphabet

"Classical foundations of many-particle quantum chaos" I believe could become a game-changer. Corresponding dynamical zeta functions should be sums over invariant 2-tori (as is done in the kittens paper [21]), rather than 1-dimensional periodic orbits.

2016-11-20 Boris All papers that I know were dances around question of uniqueness SRB measure. Either show that measure is unique or opposite way around (phase transitions). We know from the start that system is in the high temperature regime, so the measure is unique.

2019-09-12 Boris Two remarks

1. In several cases you call \mathcal{A}_0 as a "full shift". This looks wrong. As far as I understand (see [Scholarpedia](#)), one can call $\mathcal{A}_0^{\mathbb{Z}}$ (together with the shift map T) as a "full shift", but not \mathcal{A}_0 . "Full shift" is a dynamical system = state space ($\mathcal{A}_0^{\mathbb{Z}}$) + map (shift) not just alphabet.
2. Regarding notion of generating partition. "A partition Q is called a generator or generating partition if μ -almost every point x has a unique symbolic name". So the partitions which we consider here are generating. I think what you mean by "generating" are rather called "Markov partitions".

Predrag 2019-09-17 Thanks, for me these are very important remarks, to be fixed also in ChaosBook. Will chew on them... Until then, keep this remark here, as a reminder.

2019-10-19 Predrag I would like to use only one Green's function notation, i.e., $g_{zz'}^0$, and not $g(z, z')$.

2019-10-19 Boris Do you mean $g_{zz'}$ ($g_{zz'}^0$ is reserved for periodic boundary conditions)? I have changed $g(z, z')$ to $g_{zz'}$, everywhere except section A3. Seems to me - putting there everything downstairs would make things more uglier.

2019-09-30 Boris To be on the safe side it would be nice to check if everything above is compatible with numerics on figure ???. Is there a hero who can do this?

2019-10-20 Predrag to Boris: A typical reader (if there will be any:) of this opus magnum will not be encumbered by precisely your flavor of your quantum chaos baggage. To motivate this funky section full of peculiar doughnuts and their permuted holes, you need to explain why action differences (are they defined anywhere?) need to be small for close periodic orbit encounters in the quantum work that connects periodic orbits and quantum chaos spectral distributions.

2019-10-26 Boris It was done already in our paper with Vladimir. No need to repeat. Motivation here is somewhat different - By using internal symbols you can easily manufacture invariant 2-tori with whatever properties you wish/need (like in baker's map).

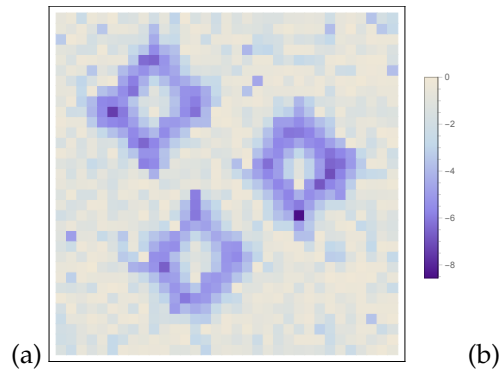


Figure 10.10: (Color online) The plots of the logarithm of the site-wise distance $\ln|x_z - x'_z|$ (a) of the states X_1, X_2 of figure ?? illustrate the exponential fall-off of the site-wise distances within the shared doughnut blocks $M_{\mathcal{R}_1}, M_{\mathcal{R}_2}$; (b) of one of the three pairs of states X_i, X_j of figure ??; the other combinations have similar site-wise distance plots. Outside of the shared domains the distances are of the order 1. **2019-10-30 Boris:** “completely wrong!”

2019-10-26 Boris 1) Brought 2 unnamed figures back from the exile (at least they are correct).

2) Removed some confusion over domains – \mathbb{Z}_{LT}^2 and \mathcal{R} are 2 different domains. \mathcal{R} is sub domain of \mathbb{Z}_{LT}^2 . Removed some unnecessary/confusing indexes

3) If you start to change notation (I prefer not to do this at this stage) - be careful there is high probability you will need to do it all over the paper = lot of work.

4) Did not like ‘doughnut’ slang - everything is pretty flat here (You can sell some topological stuff but only after very long and unnecessary :) discussion = you would need first to make a smooth picture out of this i.e., discuss smooth field theories. Some attempts in this direction are in our paper with Vladimir.) ‘doughnut hole’ is completely misleading. So for the lack of anything better I return back to ‘annular-like domain’ = seems to me much less evil.

(taken care of by AKS)

2017-09-06 Predrag to Boris: Do you have some analytically small number, like $\mu(M_{\mathcal{R}}) = 1/8!s(s^2 - 1)$ for any of the measures in sect. ???

2019-09-30 Boris To Predrag: for this particular M would be a lot of work to get it.

2019-10-28 Boris Returned figure 10.10 back to Blogosiberia

CHAPTER 10. ARTICLE EDITS

2017-08-06 Predrag I have crosschecked (??) with *siminos/spatiotemp/reportRJ.tex*

2017-09-06 Predrag to Rana - explaining figure ?? you write: “relative frequency equal to 0.995755”: how many digits do we trust? we should state only the significant digits.

When you replot, and replot you must, make both plots in figure ?? square, with both axes going from 0 to 1.

2016-11-07 Predrag figure ??: Note 5th bullet on page ?? and appendix ??.
Refer here (within this comment) to the source code (in the repository) that generates these figures.

2019-10-29 Predrag giving up waiting on the response.

2017-09-04 Predrag to Li Han or Adrien or Rana: Please reformat the LaTeX layout of figure ?? (not the plots themselves! and without decreasing the sizes of individual plots) so each plot has in the lower left corner a label (a), (b), ..., (h), (i)

2019-10-29 Predrag giving up waiting on the response.

2019-09-30 Predrag In figure ?? Boris writes “the two invariant 2-tori X_1 and X_2 shadow each other at every point.” I do not know what “every point” he has in mind, but I agree that M_1 and M_2 are identical everywhere except for the A_1, A_2 permutation, so if I stand on my head, I can see it being right in some inexplicable sense.

Happy is the referee who grasps figure ?? without any reference to any explanatory text.

2019-10-28 Adrien I don't know to what extent do Predrag wanted to explain or define the use of momentum coordinates in figure ?? and figure ???. I am satisfied with its current state, but could see that we add the definition for the coordinates $(q_z^{(i)}, p_z^{(i)})$.²

2019-10-29 Predrag Explanation would be nice... When I write in figure ?? caption that “This Hamiltonian representation is explained in appendix ??” I am lying, no?³

2019-10-30 Adrien Added a ([taken care of by AKS](#)) note to each completed blog post which concerned sect. ??.

2019-09-30 Rana dropped this: “ If only a column or row of symbols belongs to the interior alphabet, the value of relative frequency $|\mathcal{P}_{M_R}|$ is typically either close to 1 or 0. For example, for $s = 7$ the block

$$\begin{bmatrix} 5 & 3 \\ 1 & 0 \end{bmatrix},$$

²Adrien 2019-10-30: Those are defined in appendix ??

³Adrien 2019-10-30: Not sure about that...

with the $[3, 0]^T$ column in the interior alphabet, has a relative frequency $\approx 1 - 0.005$. ”

2016-10-10 Predrag RECHECK! Do they still use pacs?

2017-08-31 Boris On my current level of resolution (5 in the morning) the paper is completely ready for submission at any journal of this galaxy.

10.1.1 Cats/nonlin-v2/ GHJSC16 revisions

2020-10-16 Boris dropped formulas

The remarkable feature of the spatiotemporal cat is that its every solution $\{x_z, z \in \mathbb{Z}^d\}$ is uniquely encoded by a linear transformation to the corresponding finite alphabet d -dimensional symbol lattice $\{m_z, z \in \mathbb{Z}^d\}$

2020-10-16 Boris dropped formulas

dropped:

This paper builds explicit 2-dimensional spatiotemporal cat state space partitions using winding numbers m_z . An alternative, generating Adler-Weiss partition for the cat map, and a periodic orbit theory for spatiotemporal cat in higher dimensions are formulated in the parallel paper [21].

inserted instead later:

This paper builds explicit 2-dimensional spatiotemporal cat symbolic dynamics using winding numbers m_z . (An alternative construction, based on generating Adler-Weiss partition for the cat map, and a periodic orbit theory for spatiotemporal cat in higher dimensions are formulated in the parallel paper [21].)

2020-10-17 Predrag Removed:

“(An alternative construction, based on generating Adler-Weiss partition for the cat map, and a periodic orbit theory for spatiotemporal cat in higher dimensions are formulated in the parallel paper [21].)”

The case $s < -2$ can be treated analogously.

2020-10-16 Boris added:

The following theorem allows for evaluation of symbol blocks measures.

Theorem 10.1. Let b be a finite sequence of symbols. The corresponding measure is given by the product

$$\mu(b) = d_\ell |\mathcal{P}_b|, \quad d_\ell = 1/U_\ell(s/2), \quad (10.22)$$

where $|\mathcal{P}_b|$ is the area of the polygon \mathcal{P}_b defined by the inequalities

$$0 \leq \bar{x}_i(b) + \frac{U_{\ell-i}(s/2)}{U_\ell(s/2)} x_0 + \frac{U_{i-1}(s/2)}{U_\ell(s/2)} x_{\ell+1} < 1, \quad i = 1, \dots \quad (10.23)$$

$$0 \leq x_0 < 1, \quad 0 \leq x_{\ell+1} < 1 \quad (10.24)$$

in the plane $(x_0, x_{\ell+1})$.

2020-10-16 Predrag Boris has now renamed refeq FreqDecomp to (??). While Boris-introduced (??) is cited many times, (??) is never cited.

Too many ‘In general,’s

mark as EDITED:

Since all coefficients in (??) are given by rational numbers, the polygon areas $|\mathcal{P}_b|$ are rational too. The same holds for the d_ℓ factor. As a result, measures $\mu(b)$ are always rational (see, for example, table 19.1). This allows for their exact evaluation by integer arithmetic. As the factor d_ℓ in (??) is known explicitly, the

2020-10-16 Boris rewrote:

Interior symbols. For blocks composed of interior symbols only, the inequalities (??) are always satisfied, and \mathcal{P}_b are unit squares of area 1. The corresponding measure

$$\mu(b) = 1/U_{|b|}(s/2), \quad m_i \in \mathcal{A}_0, \quad i = 1, \dots, |b|$$

depends only on the length of the block b .

Rationality. Since all coefficients in (??) are given by rational numbers, the polygon areas $|\mathcal{P}_b|$ are rational too. The same holds for the d_ℓ factor. As a result, measures $\mu(b)$ are always rational (see, for example, table 19.1). This allows for their exact evaluation by integer arithmetic.

2020-10-31 Predrag Dropped: “The always trustworthy but so un-cited Soviet scientists (1781–1840) teach us that...”

2020-10-17 Predrag Edited everything down to $d = 2$ dimensions. Was:

The temporal cat map (??), and the spatiotemporal cat (??) can be brought into uniform notation and generalized to d dimensions by converting the spatiotemporal differences to discrete derivatives. This yields the discrete screened Poisson equation [23, 37] for the d -dimensional *spatiotemporal cat*.

The key insight is that d -dimensional spatiotemporal lattice of integers $\{m_z\} = \{m_z, z \in \mathbb{Z}^d\}$ is the natural encoding of a d -dimensional spatiotemporal state.

Eq. (18.46) was

$$(-\square + 2(s-2)) x_z = m_z, \quad m_z \in \mathcal{A}, \\ \mathcal{A} = \{-2d+1, -2d+2, \dots, s-2, s-1, 0, 1, 2\}$$

2020-11-12 Boris With the redefined stretching parameter s alphabet runs up to $2s - 1$. s can attain half-integer values.

2020-11-15 Predrag Thanks for noticing that $\mathcal{A} = \{-3, -2, \dots, s-2, s-1\}$ in (18.46) was not updated to (??). Fixed now. Yes, $s > 2$ can attain half-integer values, the lowest one is $s = 5/2$.

2020-11-15 Predrag I do not remember the unnumbered equation after (??) any longer. Do I know this identity? Does it follow from Green's function being the inverse of the linear operator in (??)? From appendix ?? *Lattice Green's identity?* I changed it to $2(s-2)$ rather than the old convention $(s-4)$.

2020-11-12 Boris Text below (??) - "from which the above 'generic' state X is assumed to be drawn."

This part is very unclear. To obtain a generic solution X you need to draw generic (with respect to μ) initial conditions and then apply the map which is defined in the appendix. This how we check our results numerically.

2020-11-15 Predrag Ok. Go ahead with the rewrite.

2020-11-12 Boris Have we defined \mathcal{R} before the end of "Answer to Q1"?

2020-11-15 Predrag Yes, see 4 lines above **Q1..**

2020-11-12 Boris $s = 2$ is the marginal case, with one zero Lyapunov exponent. Apparently the results are applicable to this case as well, as numerics shows.

2020-10-17 Predrag In figure ?? we are simulating the marginal, $s = 2$ (Laplace operator) case. I do not trust student's simulations here -it's so easy to miss power laws- but it's too late to do anything about that. We will pass it over in silence, unhappily.

To Boris: This Dirichlet bc is lots of pain for a no gain. Again I do not know what even $\mathcal{R} = [1]$ means. Or Figure 4. (a) A $[5 \times 3]$ domain \mathcal{R} I would like to think of as a $[4 \times 2]$ domain, centered on $(\ell_j + 1)/2$. Will rethink this tomorrow. For now, Good night.

10.2 Kittens' CL18blog

Internal discussions of ref. [21] edits: Move good text not used in ref. [21] to this file, for possible reuse later.

Tentative title: "Is there anything cats cannot do?"

2016-11-18 Predrag A theory of turbulence that has done away with *dynamics*?
We rest our case.

2016-10-05 Predrag My approach is that this is written for field theorists, fluid dynamicists etc., who do not see any reason to look at cat maps, so I am trying to be pedagogical, motivate it as that chaotic counterpart of the harmonic oscillator, something that field theorists fell comfortable with (they should not, but they do).

2016-11-13 Predrag The next thing to rethink: Green's functions for periodic lattices are in ChaosBook sections D.3 Lattice derivatives and on, for the Hermitian Laplacian and $s = 2$. For real $s > 2$ cat map, the potential is inverted harmonic oscillator, the frequency is imaginary (Schrödinger in imaginary time), eigenvectors real - should be a straightforward generalization. Have done this already while studying Ornstein-Uhlenbeck with Lippolis and Henninger - the eigenfunctions are Hermite polynomials times Gaussians.

2016-11-13 Predrag Potential inserts, varied temptations

B. Fernandez and P. Guiraud [26]

B. Fernandez and M. Jiang [27]

W. Just [39, 40]

the cat map is linear and the trivial trajectory located at the origin can be regarded as distinguished

2016-11-13 Predrag We write (3.49) screened Poisson equation as

$$(\square + 2 - s)x_t = m_t, \quad (10.26)$$

Percival and Vivaldi [54] write their Eq. (3.6)

$$(\square + 2 - s)x_t = -b_t \quad (10.27)$$

so their "stabilising impulses" b_t (defined on interval $x \in [-1/2, 1/2]$) have the opposite sign to our "winding numbers" m_t (defined on $x \in [0, 1]$).

Did not replace Arnol'd by PerViv choice.

$$A = \begin{pmatrix} 0 & 1 \\ -1 & s \end{pmatrix}, \quad (10.28)$$

$$\begin{aligned} q_{t+1} &= p_t \pmod{1} \\ p_{t+1} &= -x_t + s p_t \pmod{1} \end{aligned} \quad (10.29)$$

Predrag's formula, removed by Boris 2017-01-15:

$$\begin{aligned} x_{t+1} &= (s-1)x_t + p_t \pmod{1}, \\ p_{t+1} &= (s-2)x_t + p_t \end{aligned} \quad (10.30)$$

Predrag's formula, removed by Boris 2017-01-15:

As the 3-term discretization of the second time derivative d^2/dt^2 (central difference operator) is $\square x_t \equiv x_{t+1} - 2x_t + x_{t-1}$ (with the time step set to $\Delta t = 1$), the *temporal* cat map (10.36) can be rewritten as the discrete time Newton equation for inverted harmonic potential,

$$(\square + 2 - s)x_t = m_t. \quad (10.31)$$

a d -dimensional spatiotemporal pattern $\{x_z\} = \{x_{n_1 n_2 \dots n_d}\}$ requires d -dimensional spatiotemporal block $\{m_z\} = \{m_{n_1 n_2 \dots n_d}\}$,

2016-08-20 Predrag “The fact that even Dyson [25] counts cat map periods should give us pause - clearly, some nontrivial number theory is afoot.”

Not sure whether this is related to cat map symbolic dynamics that we use, dropped for now: “Problems with the discretization of Arnol'd cat map were pointed out in refs. [11, 12]. Ref. [12] discusses two partitions of the cat map unit square.”

“and resist the siren song of the Hecke operators [47, 53]”

2016-05-21 Predrag Behrends [8, 9] *The ghosts of the cat* is fun - he uncovers various regular patterns in the iterates of the cat map.

2016-09-27 Boris Cat maps and spatiotemporal cats

In the spatiotemporal cat, “particles” (i.e., a cat map at each periodic lattice site) are coupled by the next-neighbor coupling rules:

$$\begin{aligned} q_{n,t+1} &= p_{nt} + (s-1)q_{nt} - q_{n+1,t} - q_{n-1,t} - m_{n,t+1}^q \\ p_{n,t+1} &= p_{nt} + (s-2)q_{nt} - q_{n+1,t} - q_{n-1,t} - m_{n,t+1}^p \end{aligned}$$

The symbols of interest can be found by:

$$m_{nt} = q_{n,t+1} + q_{n,t-1} + q_{n+1,t} + q_{n-1,t} - s q_{nt}.$$

2016-10-27 Boris Gutkin and Osipov [35] write: “In general, calculating periodic orbits of a non-integrable system is a non-trivial task. To this end a number of methods have been developed,” and then, for a mysterious reasons, they refer to ref. [6].

2016-11-07 Predrag The dynamical systems literature tends to focus on *local* problems: bifurcations of a single time-invariant solution (equilibrium, relative equilibrium, periodic orbit or relative periodic orbit) in low-dimensional settings (3-5 coupled ODEs, 1-dimensional PDE). The problem that we face is *global*: organizing and relating *simultaneously* infinities of unstable relative periodic orbits in ∞ -dimensional state spaces, orbits that are presumed to form the skeleton of turbulence (see ref. [28] for a gentle introduction) and are typically not solutions that possess the symmetries of the problem. In this quest we found the standard equivariant bifurcation theory literature not very helpful, as its general focus is on bifurcations of solutions, which admit all or some of the symmetries of the problem at hand.

⁴

2016-11-17 Boris Unlike the systems studied in ref. [14], spatiotemporal cat cannot be conjugated to a product of non-interacting cat maps; a way to see that is to compare the numbers of periodic orbits in the two cases – they differ.

2016-11-17 Predrag The cat map partitions the state space into $|\mathcal{A}|$ regions, with borders defined by the condition that the two adjacent labels $k, k+1$ simultaneously satisfy (3.49),

$$x_1 - sx_0 + x_{-1} - \epsilon = k, \quad (10.32)$$

$$x_1 - sx_0 + x_{-1} + \epsilon = k + 1, \quad (10.33)$$

$$x_2 - sx_1 + x_0 = m_1, \quad (10.34)$$

$$x_1 - sx_0 + x_{-1} = m_0, \quad (10.35)$$

$$(x_0, x_1) = (0, 0) \rightarrow (0, 0), \quad (1, 0) \rightarrow (0, -1), \quad (0, 1) \rightarrow (1, s), \quad (1, 1) \rightarrow (1, s-1)$$

2016-11-05 Predrag Dropped this:

Note the two symmetries of the dynamics [42]: The calculations generalize directly to any cat map invariant under time reversal [44].

2016-11-11 Boris “Deeper insight” into $d = 2$ symbolic dynamics Information comes locally (both in space and time). Allows to understand correlations between invariant 2-tori. Connection with field theories.

⁴Predrag 2016-11-15: **Homework for all cats:** Write the correct (??) for an n -cycle. For inspiration: check ChaosBook.org discussion of the kneading theory, where such formula is written down for unimodal maps. Might require thinking.

Hint: the answer is in the paper.)

2016-12-12 Predrag Predrag text, recycle: “ Here the piecewise linearity of the spatiotemporal cat enables us to go far analytically. Essentially, as the cat map stretching is uniform, distinct admissible symbol blocks count all blocks of a given shape (they all have the same stability, and thus the same dynamical weight), and that can be accomplished by linear, Green’s function methods. ”

2017-08-28 Predrag “Average state” depends on bc’s. Average state GHJSC16.tex eq. catMapAverCoord is computed for the very unphysical Dirichlet bc’s $x_z = 0$ for $z \in \mathcal{R}$ which breaks translation invariance. If one takes the much gentler, translationally invariant doubly periodic b.c., the “average state” \bar{x}_z is the invariant 2-torus periodic point, a more natural choice.

2017-08-28 Predrag Probably lots of repeats with existing text:

Consider a linear, area preserving map of a 2-torus onto itself⁵

$$\begin{pmatrix} x_{t+1} \\ p_{t+1} \end{pmatrix} = A \begin{pmatrix} x_t \\ p_t \end{pmatrix} \pmod{1}, \quad A = \begin{pmatrix} s-1 & 1 \\ s-2 & 1 \end{pmatrix}, \quad (10.36)$$

where both x_t and p_t belong to the unit interval. For integer $s = \text{tr } A > 2$ the map is referred to as a cat map [2]. It is a fully chaotic Hamiltonian dynamical system, which, rewritten as a second-order difference equation in (x_t, x_{t-1}) takes a particularly simple form (??) with a unique integer “winding number” m_t at every time step t ensuring that x_{t+1} lands in the unit interval [54]. While the dynamics is linear, the nonlinearity comes through the $(\pmod{1})$ operation, encoded in $m_t \in \mathcal{A}$, where \mathcal{A} is finite alphabet of possible values for m_t .

A generalization to the *spatiotemporal* cat map is now immediate. Consider a 1-dimensional spatial lattice, with field $x_{n,t}$ (the angle of a kicked rotor “particle” at instant t) at site n . If each site couples only to its nearest neighbors $x_{n\pm 1,t}$, and if we require (1) invariance under spatial translations, (2) invariance under spatial reflections, and (3) invariance under the space-time exchange, we arrive at the 2-dimensional Euclidean cat map lattice (3.15). Note that both equations (??), (3.15) can be brought into uniform notation and generalized to d dimensions by converting the spatiotemporal differences to discrete derivatives. This yields the Newton (or Lagrange) equation for the d -dimensional *spatiotemporal cat* (??) where \square is the discrete d -dimensional Euclidean space-time Laplacian, given by $\square x_t \equiv x_{t+1} - 2x_t + x_{t-1}$, $\square x_{n,t+1} \equiv x_{n,t+1} + x_{n,t-1} - 4x_{n,t} + x_{n+1,t} + x_{n-1,t}$ in $d = 1$ and $d = 2$ dimensions, respectively. The key insight (an insight that applies to all coupled-map lattices, and all PDEs modeled by them, not only the system considered here) is that a d -dimensional spatiotemporal pattern $\{x_z\} = \{x_z, z \in \mathbb{Z}^d\}$ is described by the corresponding d -dimensional spatiotemporal symbols block $\{m_z\} = \{m_z, z \in \mathbb{Z}^d\}$, rather

⁵Predrag 2019-10-31: compare with (3.38)

than a *single* temporal symbol sequence (as one is tempted to do when describing a finite coupled N^{d-1} -“particle” system).

the cat map in one dimension (temporal dynamics of a single “particle”) and for the spatiotemporal cat (??) in d dimensions (temporal dynamics of a (d -1)-dimensional spatial lattice of N^{d-1} interacting “particles,” $N \rightarrow \infty$). Linearity of (??) enables us to solve for $\{x_z\}$ given $\{m_z\}$ by lattice Green’s function methods. However, dependence on the parameter s introduces an infinite set of grammar rules for admissible itineraries $\{m_z\}$. In this paper we focus on the $d = 1$ case (introduced in ref. [54]), and the $d = 2$ case (introduced in ref. [35]).

2018-11-16 Predrag some potential verbiage for abstract, introduction:

Recent advances in fluid dynamics reveal that the recurrent patterns observed in turbulent flows result from close passes to unstable invariant solutions of Navier-Stokes equations. While hundreds of such solutions been computed, they are always confined to small computational domains, while the flows of interest (pipe, channel, plane flows), are flows on infinite spatial domains. To describe them, we recast the Navier-Stokes equations as a spacetime theory, with all infinite translational directions treated on equal footing.

We illustrate this by solving what is arguably the simplest classical field theory, the discretized screened Poisson equation, or the “spatiotemporal cat”, and describe its repertoire of admissible spatiotemporal patterns. We encode these by spatiotemporal symbol dynamics (rather than a single temporal string of symbols).

In the spatiotemporal formulation of turbulence there are no periodic orbits, as there is no time evolution. Instead, the theory is formulated in terms of unstable spacetime tori, which are minimal tilings of spacetime. The measure concept here is akin to the statistical mechanics understanding of the Ising model - what is the likelihood of occurrence of a given spacetime configuration?

Herding cats

In the spatiotemporal formulation of turbulence the zeta functions (Fredholm determinants) are presumably 2-d or (1+3)-d Laplace/Fourier transforms of trace formulas, one dimension for each continuous symmetry: one Laplace transform for time, and one Fourier transform for each infinite spatial direction.

We have not written either the trace or the determinant formulas yet. The spatiotemporal cat periodic points (invariant 2-tori) counting suggests a way, so far unexplored.

We sketch how these are to be encoded by spatiotemporal symbol dynamics, in terms of minimal exact coherent structures. To determine

these, radically different kinds of codes will have to be written, with space and time treated on equal footing.

- review cat map in damped Poisson formulation
- explain solution for temporal cat
- show few plots of 2D solutions
- future: computational literature that advocates for spatiotemporal computations

2018-02-16 Predrag We need a simple explanation for why the 2-dimensional $1 - A^n$ and the linearization of the periodic orbit 2n-dimensional orbit Jacobian matrix give the same multipliers. (DONE since)

2019-05-20 Han My action of cat map is different from Keating's action [43] by two constant terms, which do not affect the computation.

2019-05-23 Han I rewrote the section of Perron-Frobenius operators and periodic orbits theory of cat maps and moved the original version here.

2018-02-16 Predrag Dropped this: “ , both for the cat map (??) in one dimension (temporal dynamics of a single “particle”) and for the spatiotemporal cat (??) in d dimensions (temporal dynamics of a ($d-1$)-dimensional spatial lattice of N^{d-1} interacting “particles,” $N \rightarrow \infty$). Given a set of $\{m_z\}$, the linearity of (??) enables us to find solution for $\{x_t\}$ by lattice Green’s function methods.

However, for our purposes, Adler-Weiss codes still have one fatal shortcoming, and are therefore not used in this paper: for L coupled cat maps the size of the alphabet $|\mathcal{A}|$ (the number of partitions of the state space, a $2L$ -dimensional unit hypercube) grows exponentially with L .

⁶

2019-08-10 Predrag .

$$N_n = |\det(A^n - \mathbf{I})| = |\text{tr}(A^n) - 2| = |\Lambda^n + \Lambda^{-n} - 2|, \quad (10.37)$$

if , or

$$N_n = |\text{tr}(A^n)| = |\Lambda^n + \Lambda^{-n}|, \quad (10.38)$$

if $\det(A^n) = -1$. Here Λ is the larger eigenvalue (3.40) of A .

2018-12-01 Predrag Give reference for (10.38). I see it nowhere in Isola [38] or Keating [43].

2019-06-06 Han I cannot find (10.38) either, but it can be proved by explicitly computing the determinant.

⁶Predrag 2018-04-05: In the “Lagrangian” coordinates $\{x_{t-1}, x_{t+1}\}$ formulation the 2-cycles are symmetric, as in (18.37), and the fixed point is very special, as it sits in the maximally invariant subspace.

The orbit Jacobian matrix \mathcal{J}_n is given by (3.81).

For our problem, $-L_{12}[i, i + 1] = 1$.

In practice one can supply only symbol sequences of finite length, in which case the truncated (1.122) returns a finite trajectory x_t , with a finite accuracy. However, a periodic orbit p of period n (an n -cycle) is infinite in duration, but specified by a finite admissible block $p = [m_1 m_2 \cdots m_n]$. To generate all admissible n -cycles for a given n , list all orbit symbol sequences $[m_1 m_2, \cdots m_n]$, (one string per its n cyclic permutations, not composed from repeats of a shorter cycle), apply (1.122) with cyclic $[n \times n]$ $g_{tt'}$, and then apply modulus one to all points in the cycle,

$$x_t = \sum_{t'=t}^{n+t-1} g_{tt'} m_{t'} \quad \text{mod } 1. \quad (10.39)$$

If the cycle is admissible, $\text{mod } 1$ does not affect it. If it is inadmissible, add the string to the list of pruned symbol strings. One can even start with any random sequence $[m_1 m_2 \cdots m_n]$, have $\text{mod } 1$ corral back the stray x_t 's into the unit interval, and in this way map any inadmissible symbol sequence into an admissible trajectory of the same duration.⁷

2016-11-15 Predrag Homework for all cats: Write the correct (10.39) for an n -cycle. For inspiration: check ChaosBook.org discussion of the kneading theory, where such formula is written down for unimodal maps. Might require thinking.

Hint: the answer is *this paper* :)

2019-06-10 Han Currently the argument of ref. [21] (this paper) is organized as:

1. Hamiltonian cat map
2. Periodic orbits theory of cat maps
3. Lagrangian cat map
4. Spatiotemporal cat (Predrag: I call it simply spatiotemporal cat, as it is not a “map”)

In the section of Hamiltonian cat map we also introduced the Adler-Weiss generating partition and used the Markov diagram of this partition to compute the topological zeta function.

We need to introduce temporal cat before the discussion of the periodic orbit theory. Although we can also get the temporal cat (5.92) from the linear code (3.49), we still need to write down the Lagrangian explicitly to define the orbit Jacobian matrix, $(\mathcal{J}_n)_{ij} = \partial^2 L(\mathbf{x}) / \partial x_i \partial x_j$. Then we can use the Hill's formula to show that the two counting methods are equivalent.

⁷Predrag 2018-12-03: Mixing $m_{t'}$ and $\text{mod } 1$ strikes me as profoundly wrong.

2019-06-25 Han I added *Invariant tori in d-dimensional spatiotemporal cat* that introduces the method of finding eigenmodes in d -dimensional spatiotemporal cat.

I also wrote *catMapLatt.tex*, refsect s:2DcatCounting *Counting invariant 2-tori*, which is an alternative version that starts from 2D cat map without giving the formula of general d -dimensional spatiotemporal cat. I feel this is less clear than starting with the d -dimensional spatiotemporal cat, but it follows directly from the section on temporal cat.

2019-08-13 Predrag *catMapLatt.tex* was an experimental, alternative version that starts from $d = 2$ cat map without giving the formula of general d -dimensional spatiotemporal cat. Now kept only in *blogCats.tex*.

2019-08-04 Predrag Note configuration part of the map (12.2) differs from Percival-Vivaldi [54] (2.1). However, it agrees with MacKay, Meiss and Percival [51] definition (3.4), and Meiss [52] (no discussion of cat maps) definition of the standard map (1.36).

2019-08-04 Predrag Percival-Vivaldi [54] get (??) immediately, their (2.2) for any force from their Hamiltonian (2.1), rather than our Hamiltonian of form (12.1).

2019-08-01 Han I changed the letter of action (18.200) from L to W , which is the same letter as in [51, 52]. L is the generating function, and W is the sum of L .

PC 2019-8-03 Yes, but check *defsKittens.tex*. S has been defined your way since 07jan2018.

2019-08-05 Predrag Rewrite (5.63) as:

$$\begin{aligned} q_{t+1} &= q_t + p_t + (s-2)q_t - m_{t+1}^q \\ p_{t+1} &= p_t + (s-2)q_t - m_{t+1}^q - (m_{t+1}^p - m_{t+1}^q). \end{aligned} \quad (10.40)$$

Comparing this with the Hamiltonian mapping (12.2,12.1) we identify the impulse $F(q_t)$

$$\begin{aligned} q_{t+1} &= q_t + p_{t+1} \\ p_{t+1} &= p_t + (s-2)q_t - m_{t+1}^p. \end{aligned} \quad (10.41)$$

where the m_{t+1}^q seems happily absorbed into p_{t+1} . The generating function (1-step Lagrangian density) is

2019-05-16 Han For the cat map, the problem of solving for a periodic string eventually becomes solving the linear equation (5.92) for x 's. For any set of integers \mathbf{m} , there is a solution \mathbf{x} . But the solution is admissible only when each one of the field values in \mathbf{x} is larger or equal to 0 and smaller than 1.

2019-05-16 Han Will need to change the range of x_z to $-1/2 \leq x_z < 1/2$ if we add the shadowing to this paper.

2019-08-06 Predrag We shall refer here to the least unstable of the cat maps (3.38), with $s = 3$, as the ‘Arnol’d’, or ‘Arnol’d-Sinai cat map’ [2, 22].

2019-05-27 Predrag I see no (1.19) in Percival and Vivaldi [54, 55] or Isola [38] - papers preceding Keating [43], though it is implicit in Isola [38] eq. (11).

2019-06-06 Han The method of using the determinant $\det(A^n - \mathbf{I})$ to count periodic points is given by Keating [43] eq.(28) and the following paragraph.

2019-06-26 Predrag Currently the argument flow of ref. [21] (this paper) is:

1. Bernoulli map
 - (a) coin flip map
 - (b) temporal Bernoullii orbits, linear code, discrete Fourier transform appendix ??
2. Hamiltonian cat map
 - (a) Percival-Vivaldi map
 - (b) Appendix: Adler-Weiss generating partition, transition graph
3. Temporal cat
 - (a) Hamiltonian \rightarrow Lagrangian
 - (b) screened Poisson equation
4. Periodic orbits theory of cat maps
 - (a) orbit counting
 - (b) Adler-Weiss zeta function of transition graph
 - (c) Hamiltonian volume formula
 - (d) Lagrangian orbit Jacobian matrix
 - (e) Hill’s formula
5. Spatiotemporal cat (Predrag: spatiotemporal cat, as it is not a “map”)
 - (a) time, space Laplacians \rightarrow screened Poisson equation
 - (b) Lagrangian
 - (c) orbit Jacobian matrix, reciprocal lattice, spectrum formula for volume

In language of statistical mechanics and q state clock models, in this paper we focus on the description of the high-temperature paramagnetic (or disordered) phase.

Although we can also get the temporal cat (5.92) from the linear code (3.49), we still need to write down the Lagrangian explicitly to define the orbit Jacobian matrix, $(\mathcal{J}_n)_{ij} = \delta^2 L[X]/\delta x_i \delta x_j$. Then we can use the Hill’s formula to show that the two counting methods are equivalent.

2019-06-26 Predrag which symbol blocks are admissible?

The linearity of the spatiotemporal cat enables us to standard crystallographic methods [24] and integer lattices counting [7] enable us to count spatiotemporally finite blocks, and give explicit formulas for the number of invariant d -torus solutions for blocks of any size. coupled map lattice models the spacetime discretized dynamics of small-scale spatial structures modeled by discrete time maps single cell dynamics attached to lattice sites, coupling to neighboring sites the Gutkin and Osipov [35] d -dimensional coupled cat maps lattice (“spatiotemporal cat” for short, in what follows), a spatiotemporal generalization of the Percival and Vivaldi [54] linear code for temporal evolution of a single cat map from the cat maps (modeling the Hamiltonian dynamics of individual “particles”) at sites of a $(d-1)$ -dimensional spatial lattice, linearly coupled to their nearest neighbors.

Before turning to the spatially infinite field theory in sect. ??, it is instructive to motivate our formulation of the spatiotemporal cat by investigating the temporal lattice Bernoulli and cat systems (i.e., ‘spatiotemporal lattices’ with only one site in the spatial direction).

2017-01-25 Predrag Do not remember where it came from, but it sure looks wrong: Action of an invariant 2-torus p is

$$S_p = -\frac{1}{2} \sum_{t=1}^T \sum_{n=1}^L m_{nt} x_{nt} \quad (10.42)$$

Still, why the ‘-’ sign?

2017-09-15 Boris The measures of the following blocks are equal by D_4 symmetry, see the example in ref. [34], following ??.

2019-08-06 Predrag For a discrete Euclidean space-time the Laplacian is given by

$$\square x_t \equiv x_{t+1} - 2x_t + x_{t-1} \quad (10.43)$$

$$\square x_{nt} \equiv x_{n,t+1} + x_{n+1,t} - 4x_{nt} + x_{n,t-1} + x_{n-1,t} \quad (10.44)$$

in $d = 1$ and 2 dimensions, respectively.

2018-02-09 Predrag If I understood his remark correctly, Howie Weiss suggested that we read and cite Weiss-Bowen paper. But I cannot find such paper anywhere where?

CHAPTER 10. ARTICLE EDITS

2019-08-04 Predrag By MacKay, Meiss and Percival [51, 52] convention (3.2), and Li and Tomsovic [48] convention (9) we should always have $L(q_t, q_{t+1})$. Unfortunately Keating [43] definition (3) corresponds to $L(q_t, q_{t-1})$, but we do not take that one.

2019-08-08 Han We derived generating function because the orbit Jacobian matrix is defined by the second order partial derivatives of the generating function, $-(\mathcal{J})_{ij} = \partial^2 L(\mathbf{x})/\partial x_i \partial x_j$. This concept is used in the Hill's formula (??) [13]. I think it's fine to keep that in the appendix.

2019-08-08 Han In examples of sect. ?? and sect. ?? I used the symmetric $x \in [-1/2, 1/2]$ field range of values. And the shadowing that we did before is also in the symmetric domain. I can change them back to the asymmetric $x \in [0, 1)$ domain if needed, since in sect. ?? the alphabet (??) is asymmetric.

2019-08-08 Han Invariant 2-tori (??) written out:

$$\begin{aligned} X_{\underline{3}\underline{3}} &= \frac{1}{9} \begin{bmatrix} -3 & 3 \end{bmatrix}, & X_{\underline{2}\underline{2}} &= \frac{1}{9} \begin{bmatrix} -2 & 2 \end{bmatrix}, & X_{\underline{1}\underline{1}} &= \frac{1}{9} \begin{bmatrix} -1 & 1 \end{bmatrix}, \\ X_{00} &= \frac{1}{9} \begin{bmatrix} 0 & 0 \end{bmatrix}, & X_{11} &= \frac{1}{9} \begin{bmatrix} 1 & -1 \end{bmatrix}, & X_{22} &= \frac{1}{9} \begin{bmatrix} 2 & -2 \end{bmatrix}, \\ X_{33} &= \frac{1}{9} \begin{bmatrix} 3 & -3 \end{bmatrix}, & X_{44} &= \frac{1}{9} \begin{bmatrix} 4 & -4 \end{bmatrix}. \end{aligned} \quad (10.45)$$

2019-08-10 Predrag The example of figure ?? is a very important, great you are writing it up. Our notational convention, in the spirit of (1.22), (10.45):

$$X_{44} = \frac{1}{9} \begin{bmatrix} 4 & -4 \end{bmatrix}, \quad (10.46)$$

use M array as a subscript of the periodic state X, (the label for orbit p).

2019-08-12 Han I have figures in the blog tried to visualize the orbit Jacobian matrix (10.50). The figures and the post are moved here. We can only visualize this for $n \leq 3$. A longer period can only be shown in higher dimensional space. The two figures in figure 18.37 are made with asymmetric admissible domain $x \in [0, 1)$. If these two figures are helpful I can redo these using the symmetric domain $x \in [-1/2, 1/2]$.

2019-08-08 Predrag For (3.81), refer to appendix ??, full of Toeplitz, discrete Fourier, Chebyshev

Expand the determinant of \mathcal{J}_n by minors at the first row, use $U_n(x)$ recurrence relations and a relation between $U_n(x)$'s and $T_n(x)$'s to derive (3.96).

2019-01-08 Han I made figure 18.37 to show how the volume (area) of the stretched torus counts the number of periodic points. Consider the cat map with $s = 3$. The periodic solutions satisfy:

$$\mathcal{J} \mathbf{x} = -\mathbf{M}, \quad (10.47)$$

where \mathcal{J}_n is the orbit Jacobian matrix of the periodic orbit with period n . If any \mathbf{x} on the torus satisfies (18.154), this \mathbf{x} is a periodic solution. So we can count the periodic points using \mathcal{J}_n to stretch the torus and counting the number of integer points enclosed in the stretched region. I plotted the stretched region of periodic solutions with $n = 2$ and $n = 3$. The orbit Jacobian matrix for $n = 2$ and $n = 3$ are:

$$-\mathcal{J} = \begin{pmatrix} 3 & -2 \\ -2 & 3 \end{pmatrix} \quad (10.48)$$

$$-\mathcal{J} = \begin{pmatrix} 3 & -1 & -1 \\ -1 & 3 & -1 \\ -1 & -1 & 3 \end{pmatrix} \quad (10.49)$$

Let the range of the field value x be $0 \leq x < 1$. Figure 18.37(a) shows the number of periodic points with length 2. The unit square enclosed by black lines is the available region of (x_n, x_{n+1}) . The parallelogram with red borders are the region of the unit square stretched by the orbit Jacobian matrix \mathcal{J} . There are 4 blue dots which are the integer points in the fundamental parallelepiped. Each one of these blue dots corresponds to a periodic point. The 4 green dots are integer points on the vertices of the fundamental parallelepiped. These 4 points contribute to 1 periodic point. So there are 5 periodic points with period 2, corresponding to 3 periodic solutions (1 fixed point and 2 2-cycles). The area of this fundamental parallelepiped is 5.

Figure 18.37(b) shows the periodic points with length 3. The square cube with black border is the available region of torus (x_n, x_{n+1}, x_{n+2}) . After stretched by orbit Jacobian matrix \mathcal{J} it becomes the fundamental parallelepiped with red border. There are 6 blue dots which are the integer points completely enclosed in the fundamental parallelepiped. The 8 green dots are integer points on the vertices of the fundamental parallelepiped, which contribute to 1 periodic points. There are 18 pink points which are integer points on the surface of the fundamental parallelepiped. These 18 points contribute to 9 periodic points. So the number of periodic points is 16 which is also the volume of the fundamental parallelepiped

. I have a Mathematica notebook with this 3d plot in [siminos/figSrc/han/Mathematica/HLCCountingFigures.nb](#) so you can rotate it.

2019-08-13 Predrag I am starting to worry that you have not only forgotten point groups (4.188) from our group theory course, but also the discrete Fourier transforms?

How do you prove formulas such as (3.96)? Are you sticking the formula into Mathematica? The product of eigenvalues of H ,

$$N_n = \det H = \prod_{j=0}^{n-1} \left[s - 2 \cos\left(\frac{2\pi j}{n}\right) \right], \quad (10.50)$$

goes over all eigenfunctions $\exp 2\pi j/n$, so one presumably uses the orthonormality of discrete Fourier eigenmodes in replacing cos's by a polynomial in s .

Is that how you are trying to simplify (??)?

2019-08-13 Han I get (3.96) by calculating the determinant of the circulant orbit Jacobian matrix directly (basically a recurrence relation). I haven't figured out how to get the Chebyshev polynomial using the orthonormality of discrete Fourier eigenmodes...

2020-01-11 Predrag Where is that derivation written down in this blog, or anywhere?

2019-08-13 Predrag I remember this funky argument from your blog (right?), was never a fan. If you just copied that to here with on further edits, we can erase it again.

Try substituting (10.50) into topological zeta function (3.190), see whether there are some doable sums over discrete Fourier eigenvalues $\exp 2\pi jk/n$?

2019-08-21 Han I redid the shadowing plot in a larger $[18 \times 18]$ block with $s = 5$. The algorithm is same as before:

(1) Start with a random admissible state X^0 with $-1/2 \leq x_z < 1/2$. Calculate the corresponding symbol block M^0 . The m_z 's in this symbol block are not integers. So we need to round these m_z 's to the nearest integers and get symbol block M^1

(2) Use the Green's function and the integer symbol block M^1 to calculate the state X^1 . If the maximum x_{max} is larger or equal to $1/2$, calculate the distance $\delta x_{max} = x_{max} - 1/2$. Round up $s\delta x_{max}$ (and call it δm_{max}). Then change the corresponding symbol m_{max} to $m_{max} - \delta m_{max}$. If the minimum x_{min} is smaller than $1/2$, calculate the distance $\delta x_{min} = -x_{min} - 1/2$. Round up $s\delta x_{min}$ (and call it δm_{min}). Then change the corresponding symbol m_{min} to $m_{min} + \delta m_{min}$.

(3) Now we get a new symbol block M^2 . Repeat step (2) until all x_z in X are in the admissible range.

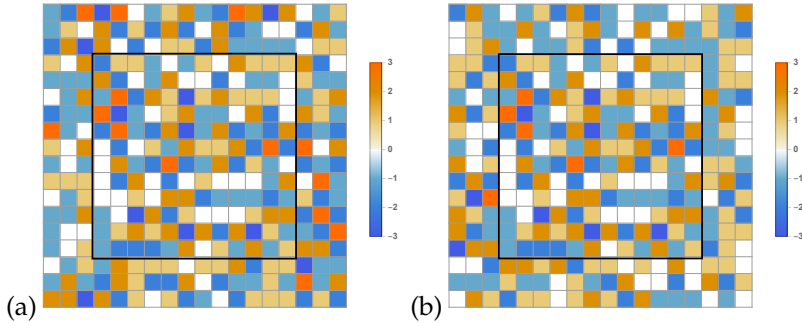


Figure 10.11: (a) and (b) are two admissible $[18 \times 18]$ blocks corresponding to the two distinct invariant 2-tori of figure 10.12. They coincide within the shared $[12 \times 12]$ block M_R , region R indicated by the black border.

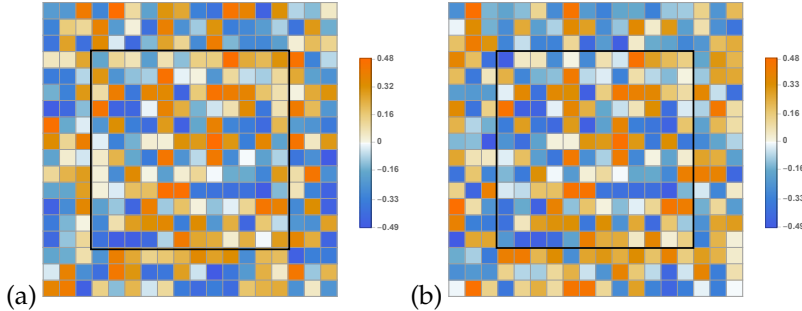


Figure 10.12: (a) and (b) are two invariant 2-tori whose symbol arrays are given by the $[18 \times 18]$ blocks of symbols of figure 10.11.

Using this method we get two periodic blocks of symbols shown in figure 10.11. In these two blocks of symbols the m_z within the $[12 \times 12]$ square region with black borders are the same. The periodic field generated by these two blocks of symbol are shown in figure 10.12. Figure 10.13 shows the pointwise distance and the logarithm of the absolute value of the pointwise distance between the two invariant 2-tori in figure 10.12.

2019-08-21 Han I also did the shadowing plot of $[18 \times 18]$ blocks with a smaller shared region of symbols. As shown in figures 10.14 and 10.15, the shared region is a $[8 \times 8]$ block.

What I'm considering is: the symbols are on invariant 2-tori, so as we go further from the center of the shared region, we are getting closer to the shared region of the next tile. Using a smaller shared region we can probably reduce the effect of the next shared region. But compare figure 10.13 (b) and figure 10.16 (b), the logarithm of the distance is not too different. So I guess we don't need these figures with small shared region...

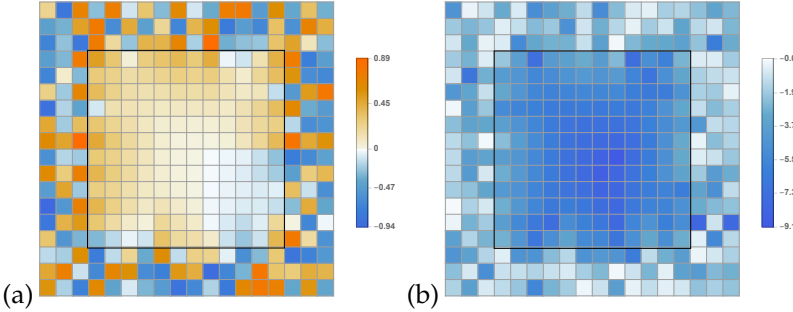


Figure 10.13: (a) The pointwise distance between the two invariant 2-tori of figure 10.12. (b) The logarithm of the absolute value of the distance between the two invariant 2-tori indicate exponential shadowing close to the center of the shared $M_{\mathcal{R}}$.

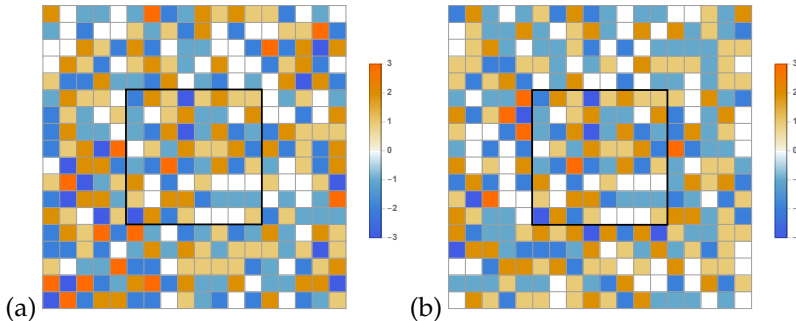


Figure 10.14: (a) and (b) are two admissible $[18 \times 18]$ blocks corresponding to the two distinct invariant 2-tori of figure 10.15. They coincide within the shared $[8 \times 8]$ block $M_{\mathcal{R}}$, region \mathcal{R} indicated by the black border.

Also I think this exponential shadowing only exist in the region with shared symbols? In figure 10.13 (b) and figure 10.16 (b), the distance outside of the shared region looks random, while the distance within the shared region shrink exponentially as we go closer to the center.

2019-08-21 Han Another thing I tried is to generate 11 different $[18 \times 18]$ invariant 2-tori shared a same $[12 \times 12]$ block of symbols. Take one of these invariant 2-tori and compute the distance between this invariant 2-torus and other 10 invariant 2-tori, then compute the ensemble average. The result is shown in figure 10.17, which looks very similar to figure 10.13. Perhaps using a larger group of ensemble we can get a better result?

2019-08-22 Han I generated 500 different invariant 2-tori with a shared $[12 \times 12]$ block of symbols at the center, labeled as X_1, X_2, \dots, X_{500} . Then I compute the distance between X_i and X_{i+250} where i goes from 1 to 250, and get

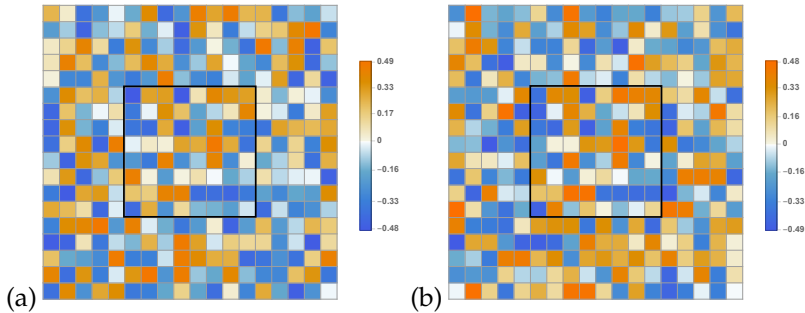


Figure 10.15: (a) and (b) are two invariant 2-tori whose symbol arrays are given by the $[18 \times 18]$ blocks of symbols of figure 10.14.

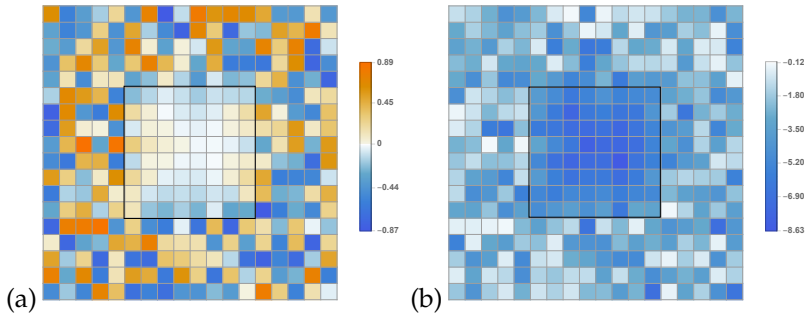


Figure 10.16: (a) The pointwise distance between the two invariant 2-tori of figure 10.15. (b) The logarithm of the absolute value of the distance between the two invariant 2-tori indicate exponential shadowing close to the center of the shared M_R .

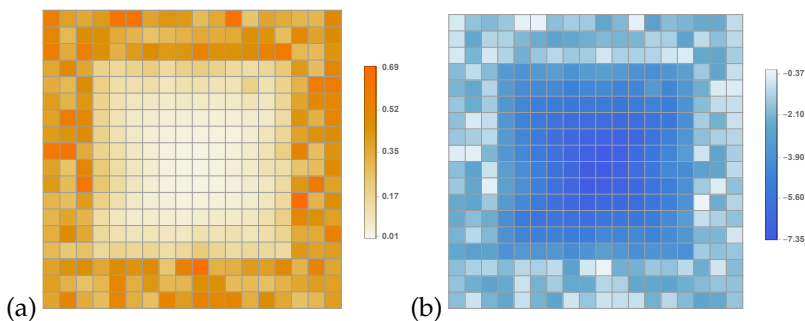


Figure 10.17: (a) The average of the absolute value of the pointwise distance between the one invariant 2-torus and other 10 different invariant 2-tori with shared $[12 \times 12]$ block of symbols. (b) The logarithm of the average of the absolute value of the distance between the invariant 2-tori indicate exponential shadowing close to the center of the shared M_R .

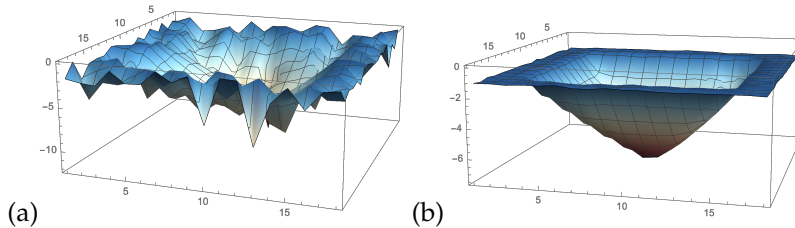


Figure 10.18: (a) The logarithm of the absolute value of the pointwise distance between the solutions X_1 and X_{251} with shared $[12 \times 12]$ block of symbols at the center. (b) The logarithm of the average of the absolute value of 250 different distance fields.

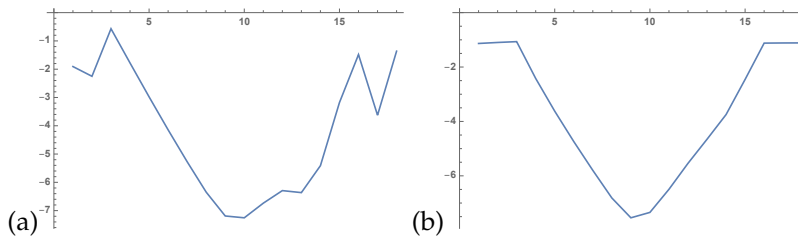


Figure 10.19: (a) The cross section through the center of the figure 10.18 (a). (b) The cross section through the center of the figure 10.18 (b). The logarithm of the distance decreases linearly as the coordinate of the field approaches the center of the shared symbol block.

250 distance field. Figure 10.18 is the log plot of the absolute value of the distance field. Figure 10.18 (a) is the logarithm of the distance between field X_1 and X_{251} , and (b) is the the logarithm of the average of the 250 distance field. By doing the average, the distance field becomes smooth. Figure 10.19 is the cross section of figure 10.18 through the center of the field. In figure 10.19 (b) the logarithm of the distance is straight line in the region with shared symbols, which shows that the distance shrink exponentially as getting closer to the center.

In figure 10.19 (b), the logarithm of the distance outside of the shared symbol block is approximately equal to $\ln(1/3) = -1.0986$, where $1/3$ is the average distance between two random numbers within the range $[-1/2, 1/2]$.

I still need to add axis labels to these figures... (It seems like Mathematica doesn't allow me to use LaTeX for writing the labels.)

2019-09-05 Predrag dropped this:

$$(x \mapsto Ax \mid x \in \mathbb{T}^2 = \mathbb{R}^2 / \mathbb{Z}^2; A \in \mathrm{SL}_2(\mathbb{Z})),$$

on no time-forward map,

In appendix 5.6 we derive the Lagrangian formulation of cat maps.

Cat map is so simple that going from Hamiltonian to Lagrangian formulation amounts to replacement (3.41) of momentum by velocity. Still, for what follows, it might pay off to understand the general theory of transformations from discrete Hamiltonians to discrete Lagrangians; we review that in refappe s:GenFctn.

The new results follow from our determination of state space generating partitions generated by the iterations of the cat map, for different integer values of the stretching parameter s .

, new kinds of determinants, new relations between propagation of temporal vs. spatial disturbances; some of these are derived in XXX eq. s:Green.
the discrete Euler–Lagrange equations (3.5) take form of 3-term, second-order difference equations

$$-x_{t+1} + V'(x_t) - x_{t-1} = m_t .$$

Following eqs. PerViv2.1a and PerViv2.1b: Here $2\pi q$ is the angle of the rotor, p is the momentum conjugate to the angular coordinate q , the angular pulse $P(q) = P(q + 1)$ is periodic with period 1, and the time step has been set to $\Delta t = 1$. Eq. (12.2) says that in one time step Δt the configuration trajectory starting at q_t reaches $q_{t+1} = q_t + p_{t+1}\Delta t$, and (12.1) says that at each kick the angular momentum p_t is accelerated to p_{t+1} by the force $P(q_t)\Delta t$. As the values of q differing by integers are identified, and the momentum p is unbounded, the phase space is a cylinder. However, one can analyze the dynamics just as well on the compactified phase space, with the momentum wrapped around a circle, i.e., adding mod 1 to (12.1). Now the dynamics is a toral automorphism acting on a $(0, 1] \times (0, 1]$ phase space square of unit area, with the opposite edges identified.

We shall refer here to the least unstable of the cat maps (3.38), with $s = 3$, as the ‘Arnol’d cat map’ [2, 22], and to maps with integer $s \geq 3$ as ‘cat maps’.

For spatiotemporal cat (3.15) the field x_{nt} takes values in the ℓT -dimensional unit hyper-cube $X \in [0, 1]^{\ell T}$, where ℓ is the ‘spatial’, and T the ‘temporal’ lattice period.

2019-12-15 Predrag move to GuBuCv17.tex:

Flows described by partial differential equations are in principle infinite dimensional, and, at first glance, turbulent dynamics that they exhibit might appear hopelessly complex. However, what is actually observed in experiments and simulations is that turbulence is dominated by repertoires of identifiable recurrent vortices, rolls, streaks and the like [36]. Dynamics on a low-dimensional chaotic attractor can be visualized as a succession of near visitations to exact unstable periodic solutions of

the equations of motion, interspersed by transient interludes [17]. In the same spirit, the long-term turbulent dynamics of spatially extended systems can be thought of as a sequence of visitations through the repertoire of admissible spatiotemporal patterns, each framed by a finite spatiotemporal window. The question we address here is: can states of a strongly nonlinear field theory be described by such repertoires of admissible patterns explored by turbulence? And if yes, what is the likelihood to observe any such pattern?

Such questions have been studied extensively for systems of small spatial extension, where the attractor dimension is relatively small [15, 18, 20, 46, 59]. However, going from spatially small to spatially infinite systems will require completely new tools. For small systems the long time dynamics can be thought of as motion of a point within an inertial manifold of a moderate dimension.

2019-12-14 Predrag restore this somewhere in cat map discussions:

The key property of hyperbolic flows is that nearby trajectories can *shadow* each other for finite times controlled by their stability exponents. One common way to quantify ‘nearness’ is to determine the minimal Euclidean distance between pairs of trajectories. That kind of distance is not invariant under symplectic transformations, and is thus meaningless in the Hamiltonian phase space. Here the notion of action comes to rescue: *the symplectic invariant distance between a pair of shadowing orbits is given by the difference of their actions* [48].

2019-12-20 Predrag dropped

Incorporate *spatiotemp/Examples/tempStab3cyc.tex*, eq. *tempStab3cyc:inv*

2020-01-13 Predrag Implemented now in the article:

I know LU is a method in textbooks, but in this example, cannot you use the periodicity of d , as I do in sect. ?? *Counting Bernoulli periodic orbits*, sect. 7.1 *Temporal lattice stability of a 3-cycle*, but for d -dimensional example done here? (10.53) is the same as (1.81), but for a d -dimensional Jacobian matrix J , rather than the 1-dimensional matrix s .

2019-08-04 Predrag to Han - Please make sure that all definitions and signs agree with the discrete lattice sections of ChaosBook [17].

2020-01-28 Han To prove that the product of cosines gives Chebyshev polynomial, the simplest way is to use the identity from Grashteyn and Ryzhik [31] *Table of Integrals, Summations and Products* (Academic Press, New York, 1965) 1.395.2:

$$\cosh nx - \cos ny = 2^{n-1} \prod_{k=0}^{n-1} \left\{ \cosh x - \cos\left(y + \frac{2k\pi}{n}\right) \right\}. \quad (10.51)$$

Let $y = 0$, $\cosh x = s/2$, and multiply both side by 2, (10.51) becomes:

$$\prod_{k=0}^{n-1} \left\{ s - 2 \cos\left(\frac{2k\pi}{n}\right) \right\} = 2\{\cosh[n \operatorname{arcosh}(s/2)] - 1\}. \quad (10.52)$$

By the definition of the Chebyshev polynomials of the first kind:

$$T_n(x) = \cosh(n \operatorname{arcosh} x), \quad \text{if } x \geq 1,$$

the right hand side of (10.52) is $2T_n(s/2) - 2$, same as (3.96).

2019-12-18 Predrag turn the final version into *spatiotemp/chapter/examSawtoothLin.tex* examples, then move to ChaosBook.

2020-01-17 Han For a lattice state X_M with period n , the orbit Jacobian matrix (3.76) is a $[nd \times nd]$ block matrix

$$\mathcal{J} = \begin{pmatrix} \mathbf{1} & & & -\mathbb{J} \\ -\mathbb{J} & \mathbf{1} & & \\ & \cdots & \mathbf{1} & \\ & & \cdots & \mathbf{1} \\ & & & -\mathbb{J} & \mathbf{1} \end{pmatrix} = \mathbf{1} - \mathbb{J} \otimes d^{-1}, \quad (10.53)$$

where $\mathbf{1}$ is a d -dimensional identity matrix, \mathbb{J} is the one time step $[d \times d]$ Jacobian matrix (??), and d is the $[n \times n]$ shift operator matrix with period n .

To evaluate the determinant of the orbit Jacobian matrix, expand $\ln \det \mathcal{J} = \operatorname{tr} \ln \mathcal{J}$:

$$\begin{aligned} \ln \det \mathcal{J} &= \operatorname{tr} \ln(\mathbf{1} - \mathbb{J} \otimes d^{-1}) \\ &= - \sum_{k=1}^{\infty} \frac{1}{k} \operatorname{tr} (\mathbb{J} \otimes d^{-1})^k. \end{aligned} \quad (10.54)$$

Note that $(\mathbb{J} \otimes d^{-1})^k = \mathbb{J}^k \otimes d^{-k}$ and $\operatorname{tr} (\mathbb{J}^k \otimes d^{-k}) = \operatorname{tr} (\mathbb{J}^{nr} \otimes \mathbf{1}_{[n \times n]}) \delta_{k,nr} = n \operatorname{tr} (\mathbb{J}^{nr}) \delta_{k,nr}$ which is not 0 only when k is a multiple of n .

$$\begin{aligned} \ln \det \mathcal{J} &= - \sum_{r=1}^{\infty} \frac{n \operatorname{tr} (\mathbb{J}^{rn})}{rn} = \operatorname{tr} \left[- \sum_{r=1}^{\infty} \frac{(\mathbb{J}^n)^r}{r} \right] \\ &= \operatorname{tr} \ln(\mathbf{1} - \mathbb{J}^n) = \ln \det(\mathbf{1} - \mathbb{J}^n). \end{aligned} \quad (10.55)$$

So the determinant of the orbit Jacobian matrix is $\det \mathcal{J} = \det(\mathbf{1} - \mathbb{J}^n)$, hence

$$\det \mathcal{J}_M = \det(\mathbb{J}_M - \mathbf{1}) = \det(\mathbb{J}^n - \mathbf{1}). \quad (10.56)$$

2020-01-21 Han A possible problem is \mathcal{J} could be negative. And here we have the one time step Jacobian matrix instead of a scalar s so I'm not sure if we can expand $\ln(\mathbf{1} - \mathbb{J} \otimes d^{-1})$ as a series in $\mathbb{J} \otimes d^{-1} \dots$

2020-01-13 Han (18.210) is different from (10.56). I think (18.210) is correct. Will check again.

2020-01-13 Predrag You are right about the sign - I was hoping to avoid $N_n = |\det \mathcal{J}|$ in (5.203), but I cannot change the sign of the matrix \mathcal{J} without making the fixed point condition (3.31) look awkward.

2020-01-24 Predrag I think (now commented out) figure 1.12 (b) was illegal - we are not allowed to define a Bravais cell off the unit cell, on the 1/2 integer lattice. Removed, unless Han has a counterargument. It is kept for the record in *spatiotemp/chapter/catHamilton.tex*

2020-01-21 Han A possible problem with (3.106) is that \mathcal{J} could be negative. And here we have the one time step Jacobian matrix instead of a scalar s so I'm not sure if we can expand $\ln(\mathbf{1} - \mathbb{J} \otimes d^{-1})$ as a series in $\mathbb{J} \otimes d^{-1} \dots$

2020-01-27 Predrag Dropped: This overcounting happens if the initial unit square is on the integer lattice. If initial states lie off the integer lattice, within the symmetric unit square $(-1/2, 1/2] \times (-1/2, 1/2]$ (Wigner-Seitz cell?), the fundamental parallelogram figure 1.12 (b) all 5 integer points lie within the fundamental parallelogram, without any over-counting. This is not the situation studied here, so we will not pursue it further.

We are not aware of any useful visualizations of orbit Jacobian matrix fundamental parallelepiped for $n > 3$ temporal cat and 2- and d -dimensional spatiotemporal cat of sect. ??.

$$(-\square + s - 4)_{0,0,i_2,j_2} = (\mathcal{J}_{0,0})_{i_2,j_2} = \begin{bmatrix} -1 & -1 & 0 \\ 5 & -1 & -1 \end{bmatrix}_{i_2,j_2},$$

$$(-\square + s - 4)_{0,1,i_2,j_2} = (\mathcal{J}_{0,1})_{i_2,j_2} = \begin{bmatrix} 5 & -1 & -1 \\ -1 & 0 & -1 \end{bmatrix}_{i_2,j_2},$$

$$(-\square + s - 4)_{1,0,i_2,j_2} = (\mathcal{J}_{1,0})_{i_2,j_2} = \begin{bmatrix} 0 & -1 & -1 \\ -1 & 5 & -1 \end{bmatrix}_{i_2,j_2},$$

$$(-\square + s - 4)_{1,1,i_2,j_2} = (\mathcal{J}_{1,1})_{i_2,j_2} = \begin{bmatrix} -1 & 5 & -1 \\ -1 & -1 & 0 \end{bmatrix}_{i_2,j_2},$$

$$(-\square + s - 4)_{2,0,i_2,j_2} = (\mathcal{J}_{2,0})_{i_2,j_2} = \begin{bmatrix} -1 & 0 & -1 \\ -1 & -1 & 5 \end{bmatrix}_{i_2,j_2},$$

$$(-\square + s - 4)_{2,1,i_2,j_2} = (\mathcal{J}_{2,1})_{i_2,j_2} = \begin{bmatrix} -1 & -1 & 5 \\ 0 & -1 & -1 \end{bmatrix}_{i_2,j_2}.$$

To diagonalize this rank-4 orbit Jacobian matrix we need to use the the eigenvectors (??) to form a rank-4 tensor:

$$U_{i_1,j_1,i_2,j_2} = \exp\left(i\frac{2\pi}{6}(2i_2i_1 - i_2j_1 + 3j_2j_1)\right).$$

The inverse of this tensor is the conjugate transpose U^\dagger :

$$(U^\dagger)_{i_1,j_1,i_2,j_2} = (U_{i_2,j_2,i_1,j_1})^*.$$

The diagonalized orbit Jacobian matrix is:

$$(\mathcal{J}_{\text{diagonalized}})_{i_1,j_1,i_2,j_2} = \sum_{i_3=0}^2 \sum_{j_3=0}^1 \sum_{i_4=0}^2 \sum_{j_4=0}^1 (U^\dagger)_{i_1,j_1,i_3,j_3} \mathcal{J}_{i_3,j_3,i_4,j_4} U_{i_4,j_4,i_2,j_2}.$$

The diagonalized orbit Jacobian matrix's element $(\mathcal{J}_{\text{diagonalized}})_{i_1,j_1,i_2,j_2}$ is not 0 only when $i_1 = i_2$ and $j_1 = j_2$. We can get the inverse of this diagonalized tensor, $\mathcal{J}_{\text{diagonalized}}^{-1}$, by changing the non-zero elements to their inverse. Then inverse of the orbit Jacobian matrix is:

$$(\mathcal{J}^{-1})_{i_1,j_1,i_2,j_2} = \sum_{i_3=0}^2 \sum_{j_3=0}^1 \sum_{i_4=0}^2 \sum_{j_4=0}^1 U_{i_1,j_1,i_3,j_3} (\mathcal{J}_{\text{diagonalized}}^{-1})_{i_3,j_3,i_4,j_4} (U^\dagger)_{i_4,j_4,i_2,j_2}.$$

The elements of the inverse orbit Jacobian matrix are:

$$(\mathcal{J}_{0,0}^{-1})_{i_2,j_2} = \frac{1}{35} \begin{bmatrix} 5 & 5 & 4 \\ 11 & 5 & 5 \end{bmatrix}_{i_2,j_2},$$

$$(\mathcal{J}_{0,1}^{-1})_{i_2,j_2} = \frac{1}{35} \begin{bmatrix} 11 & 5 & 5 \\ 5 & 4 & 5 \end{bmatrix}_{i_2,j_2},$$

$$(\mathcal{J}_{1,0}^{-1})_{i_2,j_2} = \frac{1}{35} \begin{bmatrix} 4 & 5 & 5 \\ 5 & 11 & 5 \end{bmatrix}_{i_2,j_2},$$

$$(\mathcal{J}_{1,1}^{-1})_{i_2,j_2} = \frac{1}{35} \begin{bmatrix} 5 & 11 & 5 \\ 5 & 5 & 4 \end{bmatrix}_{i_2,j_2},$$

$$(\mathcal{J}_{2,0}^{-1})_{i_2,j_2} = \frac{1}{35} \begin{bmatrix} 5 & 4 & 5 \\ 5 & 5 & 11 \end{bmatrix}_{i_2,j_2},$$

$$(\mathcal{J}_{2,1}^{-1})_{i_2,j_2} = \frac{1}{35} \begin{bmatrix} 5 & 5 & 11 \\ 4 & 5 & 5 \end{bmatrix}_{i_2,j_2}.$$

2020-01-30 Predrag Dropped everything mentioning ‘Brillouin zones’, for example figure 18.45(b); they are OK for solid state physics, but our job is to count integer lattice points, and Brillouin zones live off integer lattices.

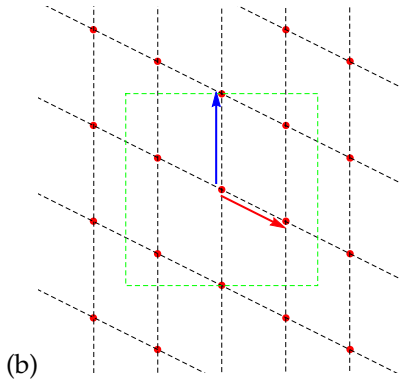


Figure 10.20: (b) The reciprocal lattice (10.81). Each reciprocal lattice point is a wave vector of the eigenvector of the translation operator with periodicity given by the Bravais lattice. The green dashed square encloses the first Brillouin zone of the *square lattice* (not the Bravais lattice). The wave vectors in the first Brillouin zone give all eigenvectors of the translation operator. Any wave vector outside of the first Brillouin zone is equivalent to a wave vector within it.

Dropped: The periodicity of a periodic state $X(z)$ over a d -dimensional lattice, with the state described by repeats of a Bravais cell spanned by basis vectors $(\mathbf{a}_1, \mathbf{a}_2, \dots, \mathbf{a}_d)$,

$$\Lambda = \left\{ \sum_{i=1}^d n_i \mathbf{a}_i \mid n_i \in \mathbb{Z} \right\}. \quad (10.57)$$

and combine them as columns of matrix

$$\Lambda = \begin{pmatrix} \ell & S \\ 0 & T \end{pmatrix} \quad (10.58)$$

$$[\mathbf{a}_1 \mathbf{a}_2] = \begin{bmatrix} \ell & S \\ 0 & T \end{bmatrix}. \quad (10.59)$$

This is the simplest example of a spatiotemporal cat tiling that is not just a 1-dimensional temporal cat periodic orbit solution along one direction, repeated along the other.

2019-09-11 Predrag Perhaps - if that helps: copy to here the nomenclature used in *PHYS-7143-19 week8*.

2019-11-24 Predrag Do you have a closed form formula for counting these? We will need to include it in the paper. My $[2 \times 2]$ count $36 = 9 + 8 + 7 + \dots + 1$ was wrong.

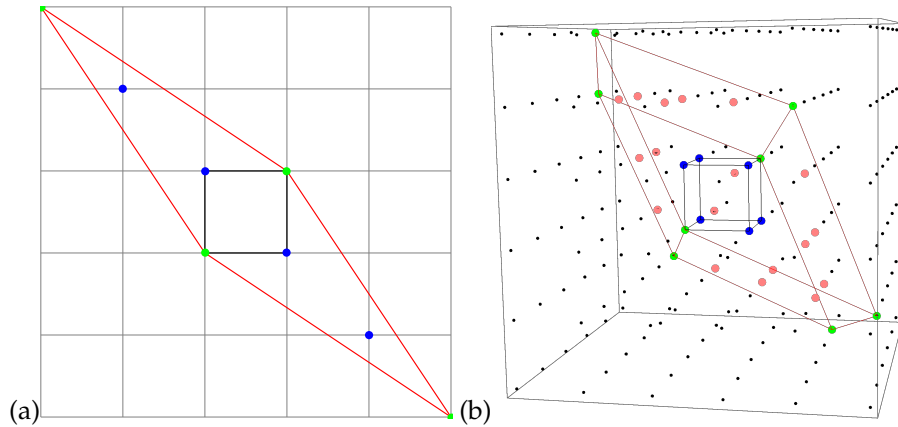


Figure 10.21: (a) A 2-dimensional torus (with black border) stretched by \mathcal{J} . The blue dots are internal integer points in the fundamental parallelepiped (with red border). The green dots are on the vertices of the fundamental parallelepiped. (b) A 3-dimensional torus (with black border) stretched by \mathcal{J} . The blue dots are internal integer points in the stretched fundamental parallelepiped (with red border). The green dots are on the vertices of the fundamental parallelepiped. The pink dots are on the surface of the fundamental parallelepiped.

2018-12-01 Predrag Keep it as elementary as possible. Look at the beginning of the [wiki](#) - you can already see our zeta function there. We need none of these funky trigonometric functions, we only need the recurrence relations - they either already in this wiki, or in `blogCats.tex`, or referred to in `blogCats.tex`.

2020-0131 Predrag Maybe if you plot only the points within (inside, and on the 3 faces connected to the origin) the fundamental parallelepiped of figure 3.8, no other integer points, it might be easier to understand. Also, if you trace out the cubic lattice in light gray, it will be clear the periodic points are on the integer lattice, in the spirit of figure 3.7 (b).

2020-02-08 Predrag To Han: not writing up what you are working on in the blog is self-defeating, as I cannot help you as long as I am not aware of you doing anything. However, not saving figure-generating code in `siminos/mathematica` is also inefficient, as you are making me regenerate all figures from scratch.

2018-06-21 Predrag Your difficulty is that you keep on thinking in Hamiltonian way, where one steps in time, using the Hamilton's equations for (q_t, p_t) , where we had replaced the momentum p_t (at spatial position ℓ) by velocity $p_t = (x_{\ell t} - x_{\ell, t-1})/\Delta t$, and thus initializing the Hamiltonian, a second-order difference equation for *evolution in time* by two horizontal

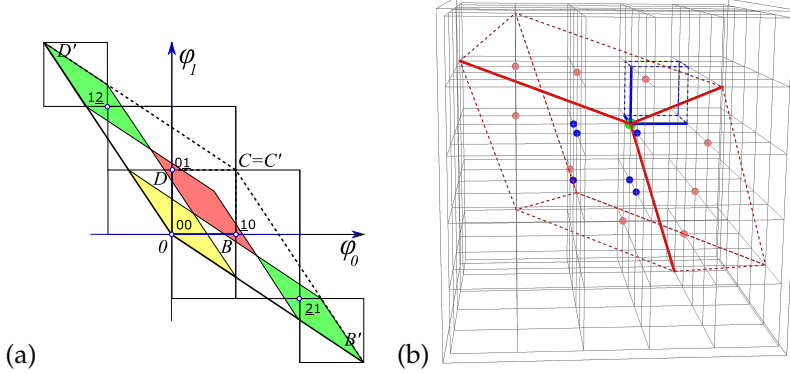


Figure 10.22: Was figure 3.8, now superannuated: (a) $[2 \times 2]$ orbit Jacobian matrix \mathcal{J} (3.93) had a wrong sign, meaningless partition into 9 rectangles. (b) Han 2020-02-11: Intermediate attempt to draw figure 3.8. $[3 \times 3]$ orbit Jacobian matrix \mathcal{J} had tons of irrelevant points plotted, is unintelligible.

rows $(x_{\ell t}, x_{\ell, t-1})$, $\ell \in \mathbb{Z}$ in the spacetime plane.

You have to think in the spacetime, Lagrangian way instead. On each lattice site $z = (\ell, t)$ there is a scalar field $x_{\ell t}$, not a two-torus. The field $x_{\ell, t-1}$ belongs to a neighboring site $z = (\ell, t-1)$. The two fields do not form a dynamical system on a two-torus, as the dynamics is also influenced by spatial neighbors $x_{\ell \pm 1, t}$.

2017-09-16 Predrag Methods described above make it an easy task to obtain a particular class of invariant 2-tori for the spatiotemporal cat.

Invariant 2-torus's coordinate representation $\Gamma = \{x_z, z \in \mathbb{Z}_{LT}^2\}$, is obtained by taking inverse of (??):

$$x_z = \sum_{z' \in \mathbb{Z}_{LT}^2} g_{zz'}^0 m_{z'}, \quad m_{z'} \in \mathcal{A}_0, \quad (10.60)$$

where $g_{zz'}^0$ is the corresponding Green's function with periodic bc's.

2018-12-01 Predrag Include here the song and dance from the remark.

What Hill's formula? Is it (8.17)? Not any longer sure that [50] contains the Hill's formula...

discrete Hill's formula [13]:

$$\det(\mathbb{J}_M - \mathbf{1}) = \frac{(-1)^n \det \mathcal{J}_M}{\prod_{i=1}^n \det B_i}, \quad (10.61)$$

where for the one dimensional cat map the B here is an $[1 \times 1]_0$ matrix:

$$B = -\frac{\delta^2 L[x_{n+1}, x_n]}{\delta x_{n+1} \delta x_n} = 1, \quad (10.62)$$

2020-02-02 Predrag It is hard to find (??) in Gutkin-Osipov [35]. The paper is mostly about the Hamiltonian formulation. Their (3.4) is the equation, once on sets $c = d$ space-time isotropy, and drops their potential V . Their perturbed equation (7.1) comes close to it. Their action (3.9) is a bit mysterious as well.

Gutkin and Osipov [35] refer to an screened Poisson equation invariant 2-torus solution p as a ‘many-particle periodic orbit’, with x_{nt} ‘doubly-periodic’, or ‘closed,’

$$x_{nt} = x_{n+\ell_p, t+T_p}, \quad n = 0, 1, 2, \dots, \ell_p - 1; \quad t = 0, 1, 2, \dots, T_p - 1.$$

2020-02-02 Predrag Note that in (??) and throughout I have redefined the stretching parameter s to be stretching per dimension, i.e., s in (3.15) is replaced by ds . This is consistent with how one defines a diffusion constant on an isotropic d -dimensional hypercubic lattice.

2019-08-06 Predrag I do not think “lattice cell” is the standard terminology, and as you have chosen not to quotient the point group, what you have is not ‘primitive’ - that would be 1/8th triangle that tiles the first Brillouin zone, I think. Please strictly follow the nomenclature of a single reference -presumably Dresselhaus *et al.* [24], or Barvinok [7] or whatever - and state so clearly in your text. Whenever you use a reference, ethics of the profession requires that you clearly cite it.

2020-02-20 Han Figure 10.23 is the fundamental parallelepiped of a $[2 \times 1]_1$ invariant 2-torus. The pattern of this periodic state is shown in figure ?? (a). The orbit Jacobian matrix of this invariant 2-torus can be written as a $[2 \times 2]$ matrix:

$$\mathcal{J} = \begin{pmatrix} -2s & 4 \\ 4 & -2s \end{pmatrix}.$$

The shape of the fundamental parallelepiped is very similar to figure 3.8 (a).

2018-12-13 Predrag Must rethink the DIMENSION of $F[X]$ and \mathcal{J} . $F[X]_i$ is a n -dimensional vector function - is it dimensionally the same as x_j ? Otherwise orbit Jacobian matrix is not dimensionless, and cannot be referred to as a ‘Jacobian’. Relation (3.106) only makes sense for the dimensionless case. I think we are OK, but we have to be sure.

2019-08-11 Predrag to Han: this is wrong alphabet, for the symmetric unit interval $x \in [-1/2, 1/2)$. For all our examples we pick the ‘least stretching’ spatiotemporal cat with $s = 5/2$, with 9-letter alphabet

$$\mathcal{A} = \{\underline{4}, \underline{3}, \underline{2}, \underline{1}, 0, 1, 2, 3, 4\}. \quad (10.63)$$

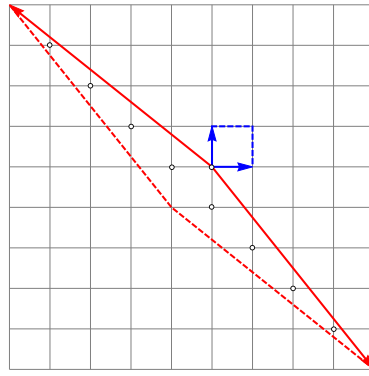


Figure 10.23: The fundamental parallelepiped of a $[2 \times 1]_1$ invariant 2-torus with $s = 5/2$. Admissible field values lie within the unit square with blue boundaries. This unit square is stretched by the orbit Jacobian matrix \mathcal{J} into the fundamental parallelepiped with red boundaries. Integer points in the fundamental parallelepiped are marked by the circles. There are 9 integer points in the fundamental parallelepiped, in agreement with the counting formula.

2020-02-17 Predrag Now in table 11.2:

$$\begin{aligned}
 N_{[1 \times 1]_0}(s) &= 2(s - 2) \\
 N_{[2 \times 1]}(s) &= 4(s - 2)s \\
 N_{[2 \times 1]_1}(s) &= 4(s - 2)(s + 2) \\
 N_{[2 \times 2]}(s) &= 16(s - 2)s^2(s + 2) \\
 N_{[3 \times 2]_0}(s) &= 4(s - 2)s(2s - 1)^2(2s + 3)^2 \\
 N_{[3 \times 2]_1}(s) &= 64(s - 2)s^3(s + 1)^2 \\
 N_{[3 \times 2]_2}(s) &= 64(s - 2)s^3(s + 1)^2 \\
 N_{[3 \times 3]}(s) &= -32(s - 2)(s + 1)^4(2s - 1)^4.
 \end{aligned} \tag{10.64}$$

2019-11-23 Predrag Dropped: For all our examples we pick the ‘least stretching’ hyperbolic spatiotemporal cat with $s = 5$, and restrict the admissible field values x_z at lattice site $z = (n_1, n_2)$ to the symmetric unit interval $x \in [-1/2, 1/2]$, with 9-letter alphabet (10.63)

the code depends on the choice of the unit interval: the alphabet \mathcal{A} for $x_t \in [-1/2, 1/2]$ differs from the alphabet for $x_t \in [0, 1]$.

Here $s = 5/2$ and $x_z \in [-1/2, 1/2]$, so the interior alphabet is one letter alphabet $\mathcal{A}_0 = \{0\}\dots$

2020-02-08 Predrag I think the $N_n = (s - 2) \dots$ factorization is true for all n in (13.78) and table 11.2. Do you understand it? Does in the temporal cat

$s = 2$ case, the Laplacian has a zero mode? A constant x_i eigenvector? If so, why doesn't the spatiotemporal cat have $N = (s - 2)^2 \dots$, one for each direction? Instead, one gets only a factor 2, $N = 2(s - 2) \dots$

2020-02-24 Predrag Not urgent, but can you complete the primitive counts $M_{[\ell \times T]_s}$ and decompositions of $N_{[\ell \times T]_s}$ into primitive invariant 2-tori in table 11.1 and perhaps also in table 11.2?

2020-03-05 Predrag Temporal cat counting (all messed up, fix using *CatMaptopZeta.nb* output):

$$\begin{aligned} \sum_{n=0}^{\infty} N_n z^n &= \frac{2 - sz}{1 - sz + z^2} - \frac{2}{1 - z} \\ \{N_n\} &= s - 2, s^2 - 4, s^3 - 3s - 2, s^4 - 4s^2, \\ &\quad 2(s^5 - 4s^3 + 3s) - s(s^4 - 3s^2 + 1) - 2, \\ &\quad -2(s^3 - 2s) - s(s^4 - 3s^2 + 1) \\ &\quad -2 - s(-1 + 6s^2 - 5s^4 + s^6) + 2(-4s + 10s^3 - 6s^5 + s^7), \\ &\quad -2s(s^5 - 4s^3 + 3s) - 2(s^4 - 3s^2 + 1) - 2, \\ &\quad -2(s^5 - 4s^3 + 3s) + s(s^6 - 5s^4 + 6s^2 - 1) - 2, , \end{aligned} \quad (10.65)$$

2020-03-23 Predrag Lot's of headless Kuramoto-Sivashinsky equation floundering in preparing *BlogCats.tex* sect. 5.10 saved below. Hopefully the resulting discretized Kuramoto-Sivashinsky equation (5.175) is correct...

The discretized Kuramoto-Sivashinsky equation is of the form

$$\partial_t U + \frac{\alpha}{2} \partial_x U^2 - \beta \Delta_x U + \gamma \Delta_x^2 U = 0. \quad (10.66)$$

Rescale $U \rightarrow U/\Delta t$

$$\frac{\partial_t}{\Delta t} U + \frac{(\Delta x)^2}{\Delta t} \frac{\alpha}{2} \frac{\partial_x}{\Delta x} U^2 - \frac{(\Delta x)^2}{\Delta t} \beta \frac{\Delta_x}{(\Delta x)^2} U + \frac{(\Delta x)^4}{\Delta t} \gamma \frac{\Delta_x^2}{(\Delta x)^4} U = 0. \quad (10.67)$$

Our canonical choice is setting these

$$\alpha = \frac{\Delta t}{(\Delta x)^2}, \quad \beta = -\frac{\Delta t}{(\Delta x)^2}, \quad \gamma = \frac{\Delta t}{(\Delta x)^4}, \quad (10.68)$$

equal to 1, parametrizing the problem with $\ell = 1/\Delta x$, $T = 1/\Delta t$,

$$\frac{1}{T} \frac{\partial_t}{\Delta t} U + \frac{1}{\ell} \frac{\alpha}{2} \frac{\partial_x}{\Delta x} U^2 - \frac{1}{\ell^2} \beta \frac{\Delta_x}{(\Delta x)^2} U + \frac{1}{\ell^4} \gamma \frac{\Delta_x^2}{(\Delta x)^4} U = 0. \quad (10.69)$$

Rescale $U \rightarrow U T$

$$\frac{\partial_t}{\Delta t} U + \frac{T^2}{\ell} \frac{\alpha}{2} \frac{\partial_x}{\Delta x} U^2 - \frac{T}{\ell^2} \beta \frac{\Delta_x}{(\Delta x)^2} U + \frac{T}{\ell^4} \gamma \frac{\Delta_x^2}{(\Delta x)^4} U = 0. \quad (10.70)$$

Our canonical choice is setting these

$$\alpha = \ell/T^2, \quad \beta = -\ell^2/T, \quad \gamma = \ell^4/T, \quad (10.71)$$

equal to 1,

$$\frac{\partial_t}{\Delta t} U + \frac{1}{2} \frac{\partial_x}{\Delta x} U^2 + \frac{\Delta_x}{(\Delta x)^2} U + \left(\frac{\Delta_x}{(\Delta x)^2} \right)^2 U = 0, \quad (10.72)$$

2019-12-28 Predrag My argument along the following lines was unnecessarily complicated:

$$\epsilon^0 \epsilon^1 \epsilon^2 \cdots \epsilon^{n-1} = 1. \quad (10.73)$$

can be eliminated by going from products to sums over cyclic eigenvalues. For example, if a polynomial is of form $G(x)/(x - \lambda_0)$, with the zeroth root $(x - \epsilon^0) = (x - 1)$ quotiented out from the characteristic polynomial,

$$\frac{x^N - 1}{x - 1} = (x - \epsilon)(x - \epsilon^2) \cdots (x - \epsilon^{N-1}).$$

Consider a sum of the first N terms of a geometric series, multiplied by $(x - 1)/(x - 1)$:

$$1 + x + \cdots + x^{N-1} = \sum_{m=0}^{N-1} x^m = \frac{1}{x - 1} \sum_{m=0}^{N-1} (x - 1) x^m = \frac{x^N - 1}{x - 1}. \quad (10.74)$$

So, the products can be written as sums

$$(x - \epsilon)(x - \epsilon^2) \cdots (x - \epsilon^{N-1}) = 1 + x + \cdots + x^{N-1}. \quad (10.75)$$

In $C_N P_n$ projection operators, the denominators are evaluated by substituting $x \rightarrow 1$ into (10.75); that adds up to N . The numerator is evaluated by substituting $x \rightarrow \epsilon^{-n} M$. We obtain the projection operator as a discrete Fourier weighted sum of matrices M^m ,

$$P_n = \frac{1}{N} \sum_{m=0}^{N-1} e^{-i \frac{2\pi}{N} nm} M^m, \quad (10.76)$$

instead of the usual product form.

2020-06-08 Predrag dropped: The periodicity of a lattice states is described by the d -dimensional Bravais lattice:

$$\Lambda = \left\{ \sum_{i=1}^d n_i \mathbf{a}_i \mid n_i \in \mathbb{Z} \right\}. \quad (10.77)$$

The orbit Jacobian matrix (??) is constructed from d commuting translation operators d_i with $i = 1, \dots, d$. The eigenvectors of these translation operators are plane waves:

$$f_k(z) = e^{ik \cdot z}, \quad (10.78)$$

where \mathbf{k} is a d -dimensional wave vector. A general plane wave does not satisfy the periodicity (??), unless

$$e^{ik \cdot R} = 1. \quad (10.79)$$

Since R is a vector from the Bravais lattice \mathcal{L} , the wave vector \mathbf{k} must lie in the reciprocal lattice of Λ :

$$\mathbf{k} \in \Lambda^*, \quad \Lambda^* = \left\{ \sum_{i=1}^d m_i \mathbf{b}_i \mid m_i \in \mathbb{Z} \right\}, \quad (10.80)$$

where the primitive reciprocal lattice vectors \mathbf{b}_i satisfy:

$$\mathbf{b}_i \cdot \mathbf{a}_j = 2\pi \delta_{ij}. \quad (10.81)$$

To get the eigenvectors and the corresponding eigenvalues of the orbit Jacobian matrix, note that

$$(d_j + d_j^{-1})e^{ik \cdot z} = e^{i(k \cdot z - k_j)} + e^{i(k \cdot z + k_j)} = (2 \cos k_j)e^{ik \cdot z}, \quad (10.82)$$

where the $\mathbf{k} = (k_1, k_2, \dots, k_d)$. Hence the eigenvalue of the orbit Jacobian matrix (??) corresponding to the eigenvector with the wave vector \mathbf{k} (10.78) is

$$\lambda_k = \sum_{j=1}^d (2 \cos k_j - s). \quad (10.83)$$

and compute its inverse, the Green's function.

The generalization to d spatiotemporal dimensions is immediate. A periodic lattice state $\mathbf{X} = \{x_z\}$, $z \in \mathbb{Z}^d$ is a point within the $(\ell_1 \ell_2 \cdots \ell_d)$ -dimensional unit hyper-cube $[0, 1]^{\ell_1 \ell_2 \cdots \ell_d}$, where ℓ_j is the lattice period in direction j , and the $(\ell_1 \ell_2 \cdots \ell_d)^2$ -dimensional orbit Jacobian matrix $\mathcal{J}_{zz'}$ is given by

$$\mathcal{J} = \sum_{j=1}^d (d_j - s \mathbf{1} + d_j^{-1}). \quad (10.84)$$

Here d_i is a shift operator (3.32) which translates the field in the i th direction by one lattice spacing. Its inverse d_i^{-1} translates the field in the negative i th direction.

From now on we specialize to the 2-dimensional, $z = (n, t) \in \mathbb{Z}^2$ spatiotemporal lattice, and replace the (ℓ_1, ℓ_2) notation for lattice periods by

(ℓ, T) , where ℓ is the ‘spatial’, and T the ‘temporal’ lattice period. The field x_i takes values in the ℓT -dimensional unit hyper-cube $X \in [0, 1]^{\ell T}$.

Throw away all blocks which are repeats of shorter blocks in the temporal direction. What remains in N_k prime periodic blocks p of the same size $[\ell_p \times T_p] = [\ell_k \times T_k]$.

This is essential to all that follows, as the Lagrangian formulation will apply to spatiotemporal cat in any number of spatial dimensions as well.

2020-05-31 Predrag *Periodic orbits in coupled Hénon maps: Lyapunov and multi-fractal analysis* is quite close to our spatiotemporal cat. The problem is harder, as the Hénon map is nonlinear.

2020-05-28 Predrag Track this down: Vicky Weiskopf: “It is better to uncover a little than cover a lot”

10.2.1 Hill’s formula: stability of an orbit vs. its time-evolution stability

2020-07-14 Han

To prove the Hill’s formula (??) for the cat map, first note that both the left hand side and right hand side are polynomials with the same leading terms s^n . The left hand side is the determinant of the tri-diagonal Toeplitz matrix (3.81). From the (3.40) and (1.19), the right hand side can be written in the form

$$\begin{aligned} |\det(\mathbb{J}^n - \mathbf{1})| &= \Lambda^n + \Lambda^{-n} - 2 \\ &= 2 \cosh(n\lambda) - 2 \\ &= 2 \cosh\left[n \operatorname{arcosh}\left(\frac{s}{2}\right)\right] - 2, \end{aligned} \quad (10.85)$$

where we used $s = 2 \cosh(\lambda)$. As the Chebyshev polynomial of the first kind can be written as $T_n(x) = \cosh[n \operatorname{arcosh}(x)]$, the right hand side of (??) is

$$|\det(\mathbb{J}^n - \mathbf{1})| = 2T_n\left(\frac{s}{2}\right) - 2,$$

which has the leading term s^n .

Let $u = (u_j)_{j=1,2,\dots,n}$ be the variation to the periodic orbit X with length n . $\mathcal{J}u = 0$ only if $\mathbb{J}^n w = w$ where $w = (u_1, u_2)$. Then $|\det(\mathbb{J}^n - \mathbf{1})| = 0$ is equivalent to $|\operatorname{Det} \mathcal{J}| = 0$. Then the polynomials $|\operatorname{Det} \mathcal{J}|$ and $|\det(\mathbb{J}^n - \mathbf{1})|$ have the same roots and the same leading terms so they are equal.

2020-07-17 Han

Let s go to infinity. Then the stability multipliers becomes:

$$\begin{aligned} \lim_{s \rightarrow \infty} \Lambda &= \lim_{s \rightarrow \infty} \frac{s + \sqrt{s^2 - 4}}{2} = s, \\ \lim_{s \rightarrow \infty} \Lambda^{-1} &= \lim_{s \rightarrow \infty} \frac{2}{s + \sqrt{s^2 - 4}} = \lim_{s \rightarrow \infty} \frac{1}{s} = 0. \end{aligned} \quad (10.86)$$

Then in the limit:

$$\lim_{s \rightarrow \infty} |\det(\mathbb{J}^n - \mathbf{1}\mathbf{1})| = \lim_{s \rightarrow \infty} \Lambda^n + \Lambda^{-n} - 2 = s^n, \quad (10.87)$$

So the leading term of the right hand side of (??) is s^n .

$$\begin{aligned} |\det(\mathbb{J}^n - \mathbf{1}\mathbf{1})| &= \Lambda^n + \Lambda^{-n} - 2 \\ &= \left(\frac{s + \sqrt{s^2 - 4}}{2} \right)^n + \left(\frac{s - \sqrt{s^2 - 4}}{2} \right)^n - 2 \\ &= \frac{1}{2^n} \sum_{k=0}^{\frac{n}{2}} \binom{2k}{n} s^{n-2k} (s^2 - 4)^k - 2, \end{aligned} \quad (10.88)$$

2020-07-21 Han The orbit Jacobian matrix of the temporal cat has form:

$$\mathcal{J} = \begin{pmatrix} -s & 1 & 0 & 1 \\ 1 & -s & 1 & 0 \\ 0 & 1 & -s & 1 \\ 1 & 0 & 1 & -s \end{pmatrix},$$

while the orbit Jacobian matrix from (10.56) is

$$\mathcal{J}' = \mathbf{1} - d^{-1} \otimes \mathbb{J} = \left(\begin{array}{cc|cc|cc|cc} 1 & 0 & 0 & 0 & 0 & 0 & 0 & -1 \\ 0 & 1 & 0 & 0 & 0 & 0 & 1 & -s \\ \hline 0 & -1 & 1 & 0 & 0 & 0 & 0 & 0 \\ 1 & -s & 0 & 1 & 0 & 0 & 0 & 0 \\ \hline 0 & 0 & 0 & -1 & 1 & 0 & 0 & 0 \\ 0 & 0 & 1 & -s & 0 & 1 & 0 & 0 \\ \hline 0 & 0 & 0 & 0 & 0 & -1 & 1 & 0 \\ 0 & 0 & 0 & 0 & 1 & -s & 0 & 1 \end{array} \right).$$

We know that

$$\det(\mathbf{1} - d^{-1} \otimes \mathbb{J}) = \det(\mathbf{1} - \mathbb{J} \otimes d^{-1}) = \det[(\mathbf{1} - \mathbb{J} \otimes d^{-1})(\mathbf{1}_{[2 \times 2]} \otimes d)],$$

where

$$\mathbf{1} - \mathbb{J} \otimes d^{-1} = \left(\begin{array}{cccc|cccc} 1 & 0 & 0 & 0 & 0 & 0 & 0 & -1 \\ 0 & 1 & 0 & 0 & -1 & 0 & 0 & 0 \\ 0 & 0 & 1 & 0 & 0 & -1 & 0 & 0 \\ 0 & 0 & 0 & 1 & 0 & 0 & -1 & 0 \\ \hline 0 & 0 & 0 & 1 & 1 & 0 & 0 & -s \\ 1 & 0 & 0 & 0 & -s & 1 & 0 & 0 \\ 0 & 1 & 0 & 0 & 0 & -s & 1 & 0 \\ 0 & 0 & 1 & 0 & 0 & 0 & -s & 1 \end{array} \right),$$

and

$$(\mathbf{1} - \mathbb{J} \otimes d^{-1}) (\mathbf{1}_{[2 \times 2]} \otimes d) = \left(\begin{array}{cccc|cccc} 0 & 1 & 0 & 0 & -1 & 0 & 0 & 0 \\ 0 & 0 & 1 & 0 & 0 & -1 & 0 & 0 \\ 0 & 0 & 0 & 1 & 0 & 0 & -1 & 0 \\ 1 & 0 & 0 & 0 & 0 & 0 & 0 & -1 \\ \hline 1 & 0 & 0 & 0 & -s & 1 & 0 & 0 \\ 0 & 1 & 0 & 0 & 0 & -s & 1 & 0 \\ 0 & 0 & 1 & 0 & 0 & 0 & -s & 1 \\ 0 & 0 & 0 & 1 & 1 & 0 & 0 & -s \end{array} \right).$$

The determinant of a block matrix is

$$\det \begin{pmatrix} A & B \\ C & D \end{pmatrix} = \det(A)\det(D - CA^{-1}B).$$

Then we have:

$$\det [(\mathbf{1} - \mathbb{J} \otimes d^{-1}) (\mathbf{1}_{[2 \times 2]} \otimes d)] = \det [-s\mathbf{1} + d - \mathbf{1}d^{-1}(-\mathbf{1})] = \det \mathcal{J}.$$

What happens if we change the order of how we block the matrix, and consider $\mathbb{J}_1 \otimes d_2^{-1}$ instead of $d_2^{-1} \otimes \mathbb{J}_1$ in (8.34)?

In particular, by similarity relation (8.21), (8.34) is equivalent to ...

2020-07-25 Predrag using

$$\det \begin{pmatrix} A & B \\ C & D \end{pmatrix} = \det(D)\det(A - BD^{-1}C). \quad (10.89)$$

so (not rechecked),

$$\begin{aligned} \det(1 - \mathbb{J} \otimes d^{-1}) &= \det \begin{bmatrix} \mathbf{1}_1 & -\mathbf{1}_1 \\ \mathbf{1}_1 & \mathbf{1}_1 + \mathcal{J}_1 \end{bmatrix} = \det(2\mathbf{1}_1 + \mathcal{J}_1)\det(\mathbf{1}_1) \\ &= \det[d - 2(s-1)\mathbf{1} + d^{-1}] = |\det \mathcal{J}|. \end{aligned} \quad (10.90)$$

in time with a $[2\ell \times 2\ell]$ block matrix $\hat{\mathbb{J}}$,⁸

$$\hat{\mathbf{x}}_{t+1} = \hat{\mathbb{J}}\hat{\mathbf{x}}_t - \hat{\mathbf{m}}_t, \quad \hat{\mathbb{J}} = \begin{bmatrix} \mathbf{0} & \mathbf{I} \\ -\mathbf{I} & -\mathcal{J}_t \end{bmatrix}. \quad (10.91)$$

The **Kronecker product** $\mathbf{A} \otimes \mathbf{B}$ is an operation by $[m \times n]$ matrix \mathbf{A} on $[p \times q]$ matrix \mathbf{B} , resulting in an $[pm \times qn]$ block matrix:

$$\mathbf{A} \otimes \mathbf{B} = \begin{pmatrix} a_{11}\mathbf{B} & \cdots & a_{1n}\mathbf{B} \\ \vdots & \ddots & \vdots \\ a_{m1}\mathbf{B} & \cdots & a_{mn}\mathbf{B} \end{pmatrix}, \quad (10.92)$$

⁸Predrag 2020-07-15: Rewriting here (18.258), (18.259) as (8.25); will use U for the variation of \mathbf{x} .

$$\text{tr}(\mathbf{A} \otimes \mathbf{B}) = \text{tr} \mathbf{A} \text{tr} \mathbf{B} \quad \text{and} \quad \det(\mathbf{A} \otimes \mathbf{B}) = (\det \mathbf{A})^m (\det \mathbf{B})^n. \quad (10.93)$$

\mathcal{J}_1 is the spatial $[\ell \times \ell]$ orbit Jacobian matrix of form (XX),

$$\begin{aligned} \mathcal{J}_1 &= d_1^{-1} - 2s \mathbf{1}_1 + d_1 \\ &= \begin{pmatrix} -2s & 1 & 0 & \dots & 1 \\ 1 & -2s & 1 & \dots & 0 \\ \vdots & \vdots & \vdots & \ddots & \vdots \\ 1 & 0 & \dots & 1 & -2s \end{pmatrix}. \end{aligned} \quad (10.94)$$

If \mathbf{A} , \mathbf{B} , \mathbf{C} and \mathbf{D} are matrices of such size that one can form the matrix products \mathbf{AC} and \mathbf{BD} , then the product of two block matrices is a block matrix:

$$(\mathbf{A} \otimes \mathbf{B})(\mathbf{C} \otimes \mathbf{D}) = (\mathbf{AC}) \otimes (\mathbf{BD}). \quad (10.95)$$

If $\lambda_1, \dots, \lambda_n$ are the eigenvalues of \mathbf{A} , and μ_1, \dots, μ_m the eigenvalues of \mathbf{B} , then the eigenvalues of $\mathbf{A} \otimes \mathbf{B}$ are

$$\lambda_i \mu_j, \quad i = 1, \dots, n, j = 1, \dots, m, \quad (10.96)$$

temporal Jacobian matrix

$$\mathbb{J} = \begin{pmatrix} 0 & 1 \\ -1 & s \end{pmatrix} = \omega \left(\mathbf{1} - \omega \begin{pmatrix} 0 & 0 \\ 0 & s \end{pmatrix} \right). \quad (10.97)$$

$$\begin{aligned} \hat{\mathbf{X}}_{t+1} &= \mathbb{J}_{PV} \hat{\mathbf{X}}_t - \hat{\mathbf{m}}_t \\ \mathbb{J}_{PV} &= \begin{bmatrix} \mathbf{0} & \mathbf{I} \\ -\mathbf{I} & -\mathcal{J}_t \end{bmatrix} = \omega - \begin{bmatrix} \mathbf{0} & \mathbf{0} \\ \mathbf{0} & \mathcal{J}_t \end{bmatrix} \end{aligned} \quad (10.98)$$

as a generalization of the $\ell = 1$ cat map (8.23), where

$$\omega = \begin{bmatrix} \mathbf{0} & \mathbf{I} \\ -\mathbf{I} & \mathbf{0} \end{bmatrix}, \quad (10.99)$$

is an antisymmetric $[2\ell \times 2\ell]$ matrix, $\omega^2 = -\mathbf{1}$,

2019-11-23 Predrag For uses of the lexical ordering, ChaosBook table [ChaosBook 18.1: Orbits for the binary symbolic dynamics up to length 9](#), and appendix [ChaosBook A18.2 Prime factorization for dynamical itineraries](#) might be of interest.

In the paper, we will probably first review the temporal cat counting, something along the lines of the above tables.

suggestion of constructing covering prime blocks wildly overcounts the candidates for admissible prime invariant 2-tori, so we should give up this avenue of constructing them - no need to count any larger Bravais lattices.

2019-08-11 Predrag to Han - we need something like

For the $s = 5/2$ example at hand, (??) yields the numbers of relative prime invariant 2-tori $[\ell \times 1]$

$$\{M_{[\ell \times 1]_0}\} = (M_{[1 \times 1]_0}, M_{2 \times 1}, M_{3 \times 1}, \dots) = (1, 9, ?, ?, ?, ?, \dots), \quad (10.100)$$

to be contrasted with temporal cat counting (1.70), this time for $s = 3$,

$$\{M_\ell\} = (M_1, M_2, M_3, M_4, M_5, \dots) = (1, ?, ?, ?, ?, ?, \dots). \quad (10.101)$$

2019-11-24 Han A brute way to determine the *admissible* blocks, is to compute X_p for each prime block M_p , and eliminate every X_p which contains a lattice site or sites on which the value of the field violates the admissibility condition $x_z \in [0, 1]^2$.

The interior alphabet depends on the value of s and the admissible range of x_z . For $s = 5/2$, $x_z \in [0, 1]$, the interior alphabet is $\mathcal{A}_0 = \{0, 1\}$ (see eq. (38) in ref. [34]). For $s = 7/2$, $x_z \in [0, 1]$, the interior alphabet is $\mathcal{A}_0 = \{0, 1, 2, 3\}$ (eq. (46) in ref. [34]).

2020-09-06 Predrag Removed the Mathematica expansion of (13.78)

$$\begin{aligned} \sum_{n=0}^{\infty} N_n z^n &= \frac{2 - sz}{1 - sz + z^2} - \frac{2}{1 - z} \\ &= (s - 2) [z + (s + 2)z^2 + (s + 1)^2 z^3 \\ &\quad + (s + 2) s^2 z^4 + (s^2 + s - 1)^2 z^5 + \dots] \end{aligned} \quad (10.102)$$

$$\begin{aligned} &s - 2, s^2 - 4, s^3 - 3s - 2, s^4 - 4s^2, -2(s^3 - 2s) + s(s^4 - 3s^2 + 1) - 2, \\ &s(s^5 - 4s^3 + 3s) - 2(s^4 - 3s^2 + 1) - 2, -2(s^5 - 4s^3 + 3s) + s(s^6 - 5s^4 + 6s^2 - 1) - 2, \end{aligned}$$

2016-11-01 Boris “Deeper insight” into $d = 2$ symbolic dynamics: Relevance to semiclassics.

“Classical foundations of many-particle quantum chaos” I believe could become a game-changer

2016-12-24 Predrag “Alternatively, one can consider the dynamics on the infinite line, and interpret m_t as a jump to m_t th interval. This leads to the phenomenon of “deterministic diffusion” [32, 58], and its periodic orbit theory [3, 19], with unit circle periodic orbits in one-to-one relation to the relative periodic (“running”) orbits on the line, and symbolic dynamics given by m_t ’s.

For single-parameter, 1-dimensional sawtooth maps, it is possible to find infinitely many values of the parameter such that the grammar is finite

(a finite subshift), and the exact diffusion constant is given by a finite-polynomial topological zeta function [4]. For cat maps, deterministic diffusion constants are not known exactly [5]. ”

2020-07-15 Perhaps refer to ChaosBook [ChaosBook 8.1 Hamiltonian flows](#), when discussing ‘two-configuration’ form (8.23).

2020-09-19 **Predrag** dropped from the abstract: “, with the lattice state and its symbolic encoding related linearly.”

dropped: “the problem of enumerating and determining all global solutions stripped to its bare essentials.”

As a function of the strengths of cell-cell couplings, dynamics can exhibit rich phase-transitions structure [41]. In this paper we chose couplings such that the system is fully turbulent.

“For an explicit example, see sect. ??.”

Hamiltonian, so symplectic or area preserving, but that is not essential. Cite the Hamiltonian zeta function from ChaosBook.

Implementing this program requires several tools not standard in dynamicist’s tool box: lattice Green’s functions; lattice determinants.

Turbulence everywhere in space, with a range of length scales.

We start the paper with a reformulation of the 1 degree of freedom Bernoulli map, because our goal, the spatiotemporal cat is nothing but its generalization to a mechanical system in spacetimes of arbitrary dimension, and thus arguably the simplest possible example of a ‘chaotic field theory’.

, true at all times and at all spatial positions

A reader may skip sect. 3.4.1 to ?? on the first reading.

The reader who already knows everything can start here.

solution X of a global fixed-point condition $F[X] = 0$ is uniquely encoded by a finite alphabet d -dimensional symbol lattice state M

Remarkably, as far as the linear symbolic dynamics is concerned, the above results hold both for the single cat map and its coupled lattice generalization. In both cases the proofs rely only upon ellipticity of the operator \square and the linearity of the equations. It is very plausible that the same results hold for the lattices \mathbb{Z}^d of an arbitrary dimension d .

Furthermore, the restriction to the integer valued matrices in the definitions of maps appears unnecessary. Cat map is a smooth version of the sawtooth map, defined by the same equation (3.49), but for a real (not necessarily integer) value of s . The linear symbolic dynamics for single saw map has been analyzed in [54] and its extension to a coupled \mathbb{Z}^d model along the lines of the present paper seems to be straightforward.

Also, in the current paper we stucked to the Laplacian form of \square . Again this seems to be too restrictive and extension to other elliptic operators of

higher order should be possible. Such operators are necessarily appear within the models with higher range of interactions.

A physically necessary extension of current setting would be addition of an external periodic potential V to (??), rendering this a nonlinear problem,

$$(\square - s + 2d + V'(x_z))x_z = m_z, \quad z \in \mathbb{Z}^d. \quad (10.103)$$

As long as the perturbation V is sufficiently weak, this lattice map can be conjugated to the linear spatiotemporal cat, with $V = 0$. This approach has been used in ref. [35] to construct partner invariant 2-tori for perturbed cat map lattices. On the other hand, for a sufficiently strong perturbation, such a conjugation to linear system is no longer possible. Finally, let us note that the lattice models like (10.103) can be seen as discretized versions of PDEs. In this respect it would be of interest to study whether our results can be extended to the continuous, PDE setting.

In particular, the following questions seem to be of fundamental importance:

- Can an effective $d = 2$ symbolic dynamics with finite alphabet be constructed for an example of a PDE with spatiotemporal chaos, such that (a) Connection between periodic field solutions and their symbolic representation is unique; (b) The local symbolic content would define the values of the corresponding fields with the exponentially decreasing errors?

2020-01-26 Predrag Dropped: Insert the (1.81) step

$$\text{tr} \ln \left(\mathbb{1} - \frac{d}{\mathbb{J}} \right) = - \sum_{k=1}^{\infty} \frac{1}{k} \text{tr}(d^k) \text{tr}(\mathbb{J}^{-k}),$$

2020-09-21 Predrag Following Mephistopheles pedagogical dictum "You have to say it three times" [30], I hereby exorcise Liang-Gudorf-Williams heresy by singing my song thrice:
 sect. ?? *Coin is not the table off which it bounces*
 sect. ?? *Cat is not the floor on which it dances*
 sect. ?? *Cats are not the spacetime over which we herd them*

2020-12-14 Predrag So, every repeat $(d\mathbb{J})^{-3r}$ has cyclic permutations of r th power of $\mathbb{J}_p = \mathbb{J}_3\mathbb{J}_2\mathbb{J}_1$, the forward-in-time stability of the cycle p , along the diagonal.

The 1-time step $[d \times d]$ Jacobian matrix of this dynamical system is

$$\mathbb{J}(x_t)_{ij} = \left. \frac{\partial f(x)_i}{\partial x_j} \right|_{x_i=x_{t,i}}. \quad (10.104)$$

Bernoulli systems stretch uniformly, so for the example at hand it suffices to consider the case of a Jacobian matrix not depending on the field value x_t or time t , $\mathbb{J}(x_t) = \mathbb{J}$. For a period- n lattice state X_M , the orbit Jacobian matrix (3.76) is now a $[nd \times nd]$ matrix function of the $[d \times d]$ block matrix \mathbb{J} ,

$$\mathcal{J}(\mathbb{J}) = \begin{pmatrix} \mathbf{1} & & & -\mathbb{J} \\ -\mathbb{J} & \mathbf{1} & & \\ & -\mathbb{J} & \ddots & \\ & & & \mathbf{1} \\ & & & -\mathbb{J} & \mathbf{1} \end{pmatrix}, \quad (10.105)$$

where $\mathbf{1}$ is a d -dimensional identity matrix.

2020-02-16 Predrag Recheck - is there something called ‘characteristic function’ in integer lattice and other lattice literature?

Note to Predrag - send this paper to Vladimir Rosenhaus <vladr@kitp.ucsb.edu>, Xiangyu Cao <xiangyu.cao08@gmail.com>, George Savvidy, “Demokritos”, Athens, and David Berenstein <dberens@physics.ucsb.edu>

10.3 Kittens' LC21blog

Internal discussions of ref. [49] edits: Move good text not used in ref. [49] to this file, for possible reuse later.

Tentative title: "Is there anything cats cannot do?"

2016-11-18 Predrag A theory of turbulence that has done away with *dynamics*? We rest our case.

one determines the total number of lattice states by computing the Hill determinant (??) of the *orbit Jacobian matrix*

The observation that a Bernoulli system can be viewed as a discretization of a first-order in time ODE, eq. (3.35), with solutions whose temporal global linear stability is described by the orbit Jacobian matrix $\mathcal{J}_{tt'} = \delta F[\mathbf{X}]_t / \delta x_{t'}$, has profound implications for dissipative spatiotemporal systems such as Navier-Stokes and Kuramoto-Sivashinsky [33].

As we shall here have to traverse territory unfamiliar to many, we follow Mephistopheles pedagogical dictum "You have to say it three times" [30], and sing our song thrice.

2021-07-07 Predrag Experimenting with (10.106) by:

a flip across the k th axis, $k = 0, 1, 2, \dots, n - 1$,

$$\text{dihedral } D_n : H_{n,k} = \langle d, \sigma_k = d^k \sigma \mid \sigma_k d \sigma_k = d^{-1}, d^n = \sigma_k^2 \rangle \quad (10.106)$$

that Han had replaced with (??) and n with $|n|$ in (4.142).

2021-07-07 Predrag A presentation of the *infinite dihedral group* [45] is

$$D_\infty = \langle d_i, \sigma_j \mid d_i \sigma_j = \sigma_j d_{-i}; \sigma_j^2 = 1; i, j \in \mathbb{Z} \rangle. \quad (10.107)$$

2021-08-10 Predrag dropped:

Applying the projection operator $P_{0-} = \frac{1}{2}(\mathbf{1} - \sigma_0)/2$ we obtain a lattice state

$$\cdots \underline{y_4} \underline{y_3} \underline{y_2} \underline{y_1} \bar{0} y_1 y_2 y_3 y_4 \cdots, \quad (10.108)$$

antisymmetric under reflection, where the field $\bar{0} = (x_0 - x_0)/2 = 0$ at the reflection lattice site 0 vanishes by antisymmetry, while the rest, $y_j = (x_j - x_{-j})/2$, are pairwise antisymmetric under the reflection σ . The underline indicates the negative of, i.e., $\underline{y_j} = -y_j$.

Applying the antisymmetric projection operator $P_{1-} = \frac{1}{2}(\mathbf{1} - \sigma d)/2$ we obtain a lattice state

$$\cdots \underline{y_4} \underline{y_3} \underline{y_2} \underline{y_1} | y_1 y_2 y_3 y_4 \cdots, \quad (10.109)$$

antisymmetric under reflection, where $y_j = (x_j - x_{1-j})/2$, are pairwise antisymmetric under the reflection σ_1 .

2021-08-21 Predrag The old definition of Bernoulli m_t in (3.21) conflicted with the definition (3.25). I changed (3.25) to current form.

2021-10-29 Predrag Dropped: Cat maps are beloved by ergodicists and statistical mechanicians because, even though the field (q_t, p_t) is 2-dimensional, for integer values of the stretching parameter s , a cat map has a finite alphabet linear code, just like the Bernoulli map, and its unit torus can be tiled by two rectangles,⁹ in analogy with the forward-in-time Bernoulli map subinterval partitioning of figure 3.2. From this it follows that all admissible symbol blocks can be generated as shifts of finite type, and all periodic points determined and counted.

As all that is well known, and a side issue for this paper, we relegate the details of the Hamiltonian cat map dynamics and periodic orbit counting to ??.¹⁰ Here we focus on reformulating the cat dynamics as a temporal lattice (or discrete Lagrangian) problem, as we have done for the Bernoulli system in sect. 3.3.2.

2021-10-29 Predrag Dropped: The Lagrangian formulation requires only temporal lattice states and their actions, replacing the phase space ‘cat map’ (3.38) by a ‘temporal cat’ lattice (3.49). The temporal cat has no generating partition analogue of the Adler-Weiss partition for a Hamiltonian cat map (see¹¹). As we have shown here, no funky Hamiltonian state space partitioning magic (such as¹²) is needed to count the lattice states of a temporal cat. Not only are no such partitions needed to solve the system, but the Lagrangian,

2021-08-12 Predrag Sidney will chuckle at this comment: The usual ax_t^2 form (2.6) might be preferable, as the ‘ a ’ is a stretching parameter, just like in (3.19). See sect. 2.1.1 Temporal Hénon.

2020-12-17 Predrag Link to the ChaosBook? or drop?

In sect. 3.4.1 we review the traditional cat map in its Hamiltonian formulation. (but relegate to the explicit Adler-Weiss generating partition of the cat map state space).

We evaluate and cross-check Hill determinants by two methods, either the ‘fundamental fact’ evaluation, or by the discrete Fourier transform diagonalization, sect. 3.8.4.

2021-10-13 Predrag Is there a - sign specific to Sidney’s definition of the Hénon orbit Jacobian matrix Han and Predrag have to redefine both temporal cat and temporal Hénon orbit Jacobian matrix throughout, so we do not pick up an extraneous ‘-’ sign for odd period lattice states. See also (5.284), and Pozrikidis [57] ([click here](#)) eq. (1.8.2). The main thing is to have a

⁹Predrag 2020-12-17: Link to the ChaosBook.

¹⁰Predrag 2020-12-17: Link to the ChaosBook.

¹¹Predrag 2020-12-17: Link to the ChaosBook.

¹²Predrag 2020-12-17: Link to the ChaosBook.

Laplacian with positive eigenvalues, right? Maybe not, the main thing is to have hyperbolic eigenvalues for $s > 2$. Rethink. determinants in periodic orbit formulas.

$Z[M]$ notation extracted from *lattFTnotat.tex*, called by *lattFT.tex*.

, in field theorist's parlance, m_z are 'sources', and

The orbit Jacobian matrix $\mathcal{J}[X]$ is best understood by starting with the period- n Bravais cell stability.

As in sect. 3.8.3, the fundamental parallelepiped given the stretching of the n -dimensional state space unit hyper-cube $X \in [0, 1]^n$ by the orbit Jacobian matrix counts lattice states, with the admissible lattice states of period T constrained to field values within $0 \leq x_t < 1$. The fundamental parallelepiped contains images of all lattice states X_M , which are then translated by integer winding numbers M into the origin, in order to satisfy the fixed point condition (3.77).

2021-10-21 Predrag Han, RECHECK all m_t , as well as formulas starting with (3.100)!!! Bernoulli m_t in (3.21) conflicted with the old definition (3.25), so I changed (3.25).

When the force is proportional to displacement, that is, when Hooke's law is obeyed, the spring is said to be linear, the potential is quadratic.

A matrix J with no eigenvalue on the unit circle is called hyperbolic.

Ignoring (mod 1) for a moment, we can use (3.36) to eliminate p_t from (3.37) and rewrite the kicked rotor equation as the

For the problem at hand, it pays to go from the Hamiltonian (configuration, momentum) phase space formulation to the discrete Lagrangian (x_{t-1}, x_t) formulation.

temporal lattice condition

'Temporal' again refers to the discretized time 1d lattice

In atomic physics applications, the values of the angle q differing by integers are identified, but the momentum p is unbounded. In dynamical systems theory one compactifies the momentum as well, by adding (mod 1) to (3.37), as for the Bernoulli map (3.24). This reduces the phase space to a square $[0, 1] \times [0, 1]$ of unit area, with the opposite edges identified, i.e., 2-torus.

Thom-Anosov diffeomorphism

Cat maps with the same s are equivalent up to a similarity transformation, so it suffices to work out a single convenient realization, as we shall do here for the Percival-Vivaldi [54] 'two-configuration representation' (3.43).

2021-11-29 Predrag Might need to introduce the inverse temperature $\beta = 1/T$ and the free energy F , as in (5.120), multiplied by 'volume' N the number

of lattice sites;

$$Z[M] = e^{W[M]}, \quad W[M] = \beta N F[X]$$

So, $W[M]$ is not the ‘free energy’.

Hill’s formula here is the discrete Hill’s formula [13, 50] (8.17).

2021-11-29 Predrag !!!WARNING!!! Following Han (5.86), we are changing the sign of the action $S[X]$ and the orbit Jacobian matrix, as in (3.17), **THROUGHOUT!** (Totally Predrag’s fault). This makes spatiotemporal cat and ϕ^4 theory action strictly positive for $s > 2$, as needed for the probability interpretation (3.3). Han, Sidney and Predrag have to redefine temporal cat, spatiotemporal cat and temporal Hénon orbit Jacobian matrices throughout, to avoid the extraneous ‘-’ sign for odd period lattice states. See also (5.284), and Pozrikidis [57] ([click here](#)) eq. (1.8.2).

2016-11-08 Predrag Say: THE BIG DEAL is

for d -dimensional field theory, symbolic dynamics is not one temporal sequence with a huge alphabet, but d -dimensional spatiotemporal tiling by a finite alphabet

2021-12-26 Han I think (3.36–3.37) should be written as:

$$q_{t+1} = q_t + p_{t+1} \pmod{1}, \quad (10.110)$$

$$p_{t+1} = p_t + P(q_t). \quad (10.111)$$

Otherwise the angle of the rotor q is not constrained to $[0, 1)$.

Predrag: you are right, corrected.

Note to Predrag - send this paper to Vladimir Rosenhaus <vladr@kitp.ucsb.edu>, Xiangyu Cao <xiangyu.cao08@gmail.com>, George Savvidy, “Demokritos”, Athens, and David Berenstein <dberens@physics.ucsb.edu>

References

- [1] R. L. Adler and B. Weiss, “Entropy, a complete metric invariant for automorphisms of the torus”, Proc. Natl. Acad. Sci. USA **57**, 1573–1576 (1967).
- [2] V. I. Arnol’d and A. Avez, *Ergodic Problems of Classical Mechanics* (Addison-Wesley, Redwood City, 1989).
- [3] R. Artuso, “Diffusive dynamics and periodic orbits of dynamic systems”, Phys. Lett. A **160**, 528–530 (1991).

- [4] R. Artuso and P. Cvitanović, “Deterministic diffusion”, in *Chaos: Classical and Quantum*, edited by P. Cvitanović, R. Artuso, R. Mainieri, G. Tanner, and G. Vattay (Niels Bohr Inst., Copenhagen, 2016).
- [5] R. Artuso and R. Strepparava, “Recycling diffusion in sawtooth and cat maps”, *Phys. Lett. A* **236**, 469–475 (1997).
- [6] M. Baranger, K. T. R. Davies, and J. H. Mahoney, “The calculation of periodic trajectories”, *Ann. Phys.* **186**, 95–110 (1988).
- [7] A. Barvinok, *Integer Points in Polyhedra* (European Math. Soc. Pub., Berlin, 2008).
- [8] E. Behrends, “The ghosts of the cat”, *Ergod. Theor. Dynam. Syst.* **18**, 321–330 (1998).
- [9] E. Behrends and B. Fielder, “Periods of discretized linear Anosov maps”, *Ergod. Theor. Dynam. Syst.* **18**, 331–341 (1998).
- [10] N. Bird and F. Vivaldi, “Periodic orbits of the sawtooth maps”, *Physica D* **30**, 164–176 (1988).
- [11] M. L. Blank, *Discreteness and Continuity in Problems of Chaotic Dynamics* (Amer. Math. Soc., Providence RI, 1997).
- [12] M. Blank and G. Keller, “Random perturbations of chaotic dynamical systems: stability of the spectrum”, *Nonlinearity* **11**, 1351–1364 (1998).
- [13] S. V. Bolotin and D. V. Treschev, “Hill’s formula”, *Russ. Math. Surv.* **65**, 191 (2010).
- [14] L. A. Bunimovich and Y. G. Sinai, “Spacetime chaos in coupled map lattices”, *Nonlinearity* **1**, 491 (1988).
- [15] F. Christiansen, P. Cvitanović, and V. Putkaradze, “Spatiotemporal chaos in terms of unstable recurrent patterns”, *Nonlinearity* **10**, 55–70 (1997).
- [16] P. Cvitanović, “Counting”, in *Chaos: Classical and Quantum* (Niels Bohr Inst., Copenhagen, 2020).
- [17] P. Cvitanović, R. Artuso, R. Mainieri, G. Tanner, and G. Vattay, *Chaos: Classical and Quantum* (Niels Bohr Inst., Copenhagen, 2020).
- [18] P. Cvitanović, R. L. Davidchack, and E. Siminos, “On the state space geometry of the Kuramoto-Sivashinsky flow in a periodic domain”, *SIAM J. Appl. Dyn. Syst.* **9**, 1–33 (2010).
- [19] P. Cvitanović, P. Gaspard, and T. Schreiber, “Investigation of the Lorentz gas in terms of periodic orbits”, *Chaos* **2**, 85–90 (1992).
- [20] P. Cvitanović and J. F. Gibson, “Geometry of turbulence in wall-bounded shear flows: Periodic orbits”, *Phys. Scr. T* **142**, 014007 (2010).
- [21] P. Cvitanović and H. Liang, Spatiotemporal cat: A chaotic field theory, In preparation, 2021.
- [22] R. L. Devaney, *An Introduction to Chaotic Dynamical systems*, 2nd ed. (Westview Press, Cambridge, Mass, 2008).

- [23] F. W. Dorr, “The direct solution of the discrete Poisson equation on a rectangle”, *SIAM Rev.* **12**, 248–263 (1970).
- [24] M. S. Dresselhaus, G. Dresselhaus, and A. Jorio, *Group Theory: Application to the Physics of Condensed Matter* (Springer, New York, 2007).
- [25] F. J. Dyson and H. Falk, “Period of a discrete cat mapping”, *Amer. Math. Monthly* **99**, 603–614 (1992).
- [26] B. Fernandez and P. Guiraud, “Route to chaotic synchronisation in coupled map lattices: Rigorous results”, *Discrete Continuous Dyn. Syst. Ser. B* **4**, 435–456 (2004).
- [27] B. Fernandez and M. Jiang, “Coupling two unimodal maps with simple kneading sequences”, *Ergod. Theor. Dynam. Syst.* **24**, 107–125 (2004).
- [28] J. F. Gibson and P. Cvitanović, *Movies of plane Couette*, tech. rep. (Georgia Inst. of Technology, 2015).
- [29] J. F. Gibson, J. Halcrow, and P. Cvitanović, “Visualizing the geometry of state-space in plane Couette flow”, *J. Fluid Mech.* **611**, 107–130 (2008).
- [30] J. W. von Goethe, *Faust I, Studierzimmer 2*. M. Greenberg, transl. (Yale Univ. Press, 1806).
- [31] I. S. Gradshteyn and I. M. Ryzhik, *Tables of Integrals, Series and Products*, 8th ed. (Elsevier LTD, Oxford, New York, 2014).
- [32] S. Grossmann and H. Fujisaka, “Diffusion in discrete nonlinear dynamical systems”, *Phys. Rev. A* **26**, 1779–1782 (1982).
- [33] M. N. Gudorf, N. B. Budanur, and P. Cvitanović, *Spatiotemporal tiling of the Kuramoto-Sivashinsky flow*, In preparation, 2021.
- [34] B. Gutkin, L. Han, R. Jafari, A. K. Saremi, and P. Cvitanović, “Linear encoding of the spatiotemporal cat map”, *Nonlinearity* **34**, 2800–2836 (2021).
- [35] B. Gutkin and V. Osipov, “Classical foundations of many-particle quantum chaos”, *Nonlinearity* **29**, 325–356 (2016).
- [36] B. Hof, C. W. H. van Doorne, J. Westerweel, F. T. M. Nieuwstadt, H. Faisst, B. Eckhardt, H. Wedin, R. R. Kerswell, and F. Waleffe, “Experimental observation of nonlinear traveling waves in turbulent pipe flow”, *Science* **305**, 1594–1598 (2004).
- [37] G. Y. Hu and R. F. O’Connell, “Analytical inversion of symmetric tridiagonal matrices”, *J. Phys. A* **29**, 1511 (1996).
- [38] S. Isola, “ ζ -functions and distribution of periodic orbits of toral automorphisms”, *Europhys. Lett.* **11**, 517–522 (1990).
- [39] W. Just, “Analytical approach for piecewise linear coupled map lattices”, *J. Stat. Phys.* **90**, 727–748 (1998).
- [40] W. Just, “Equilibrium phase transitions in coupled map lattices: A pedestrian approach”, *J. Stat. Phys.* **105**, 133–142 (2001).

- [41] K. Kaneko, “Period-doubling of kink-antikink patterns, quasiperiodicity in antiferro-like structures and spatial intermittency in coupled logistic lattice: Towards a prelude of a “field theory of chaos””, *Prog. Theor. Phys.* **72**, 480–486 (1984).
- [42] J. P. Keating, “Asymptotic properties of the periodic orbits of the cat maps”, *Nonlinearity* **4**, 277 (1991).
- [43] J. P. Keating, “The cat maps: quantum mechanics and classical motion”, *Nonlinearity* **4**, 309–341 (1991).
- [44] J. P. Keating and F. Mezzadri, “Pseudo-symmetries of Anosov maps and spectral statistics”, *Nonlinearity* **13**, 747–775 (2000).
- [45] Y.-O. Kim, J. Lee, and K. K. Park, “A zeta function for flip systems”, *Pacific J. Math.* **209**, 289–301 (2003).
- [46] T. Kreilos and B. Eckhardt, “Periodic orbits near onset of chaos in plane Couette flow”, *Chaos* **22**, 047505 (2012).
- [47] P. Kurlberg and Z. Rudnick, “Hecke theory and equidistribution for the quantization of linear maps of the torus”, *Duke Math. J.* **103**, 47–77 (2000).
- [48] J. Li and S. Tomsovic, “Exact relations between homoclinic and periodic orbit actions in chaotic systems”, *Phys. Rev. E* **97**, 022216 (2017).
- [49] H. Liang and P. Cvitanović, Time reversal for discrete time dynamical systems, In preparation, 2021.
- [50] R. S. MacKay and J. D. Meiss, “Linear stability of periodic orbits in Lagrangian systems”, *Phys. Lett. A* **98**, 92–94 (1983).
- [51] R. S. MacKay, J. D. Meiss, and I. C. Percival, “Transport in Hamiltonian systems”, *Physica D* **13**, 55–81 (1984).
- [52] J. D. Meiss, “Symplectic maps, variational principles, and transport”, *Rev. Mod. Phys.* **64**, 795–848 (1992).
- [53] F. Mezzadri, “On the multiplicativity of quantum cat maps”, *Nonlinearity* **15**, 905–922 (2002).
- [54] I. Percival and F. Vivaldi, “A linear code for the sawtooth and cat maps”, *Physica D* **27**, 373–386 (1987).
- [55] I. Percival and F. Vivaldi, “Arithmetical properties of strongly chaotic motions”, *Physica D* **25**, 105–130 (1987).
- [56] Y. B. Pesin and Y. G. Sinai, “Space-time chaos in the system of weakly interacting hyperbolic systems”, *J. Geom. Phys.* **5**, 483–492 (1988).
- [57] C. Pozrikidis, *An Introduction to Grids, Graphs, and Networks* (Oxford Univ. Press, Oxford , UK, 2014).
- [58] M. Schell, S. Fraser, and R. Kapral, “Diffusive dynamics in systems with translational symmetry: A one-dimensional-map model”, *Phys. Rev. A* **26**, 504–521 (1982).

- [59] A. P. Willis, P. Cvitanović, and M. Avila, “Revealing the state space of turbulent pipe flow by symmetry reduction”, *J. Fluid Mech.* **721**, 514–540 (2013).
- [60] A. Wirzba and P. Cvitanović, “Appendix: Discrete symmetries of dynamics”, in *Chaos: Classical and Quantum* (Niels Bohr Inst., Copenhagen, 2016).

Chapter 11

Symbolic dynamics: a glossary

Analysis of a low-dimensional chaotic dynamical system typically starts [4] with establishing that a flow is locally stretching, globally folding. The flow is then reduced to a discrete time return map by appropriate Poincaré sections. Its state space is partitioned, the partitions labeled by an alphabet, and the qualitatively distinct solutions classified by their temporal symbol sequences. Thus our analysis of the cat map and the spatiotemporal cat requires recalling and generalising a few standard symbolic dynamics notions.

Partitions, alphabets. A division of state space \mathcal{M} into a disjoint union of distinct regions $\mathcal{M}_A, \mathcal{M}_B, \dots, \mathcal{M}_Z$ constitutes a *partition*. Label each region by a symbol m from an N -letter *alphabet* $\mathcal{A} = \{A, B, C, \dots, Z\}$, where $N = n_{\mathcal{A}}$ is the number of such regions. Alternatively, one can distinguish different regions by coloring them, with colors serving as the “letters” of the alphabet. For notational convenience, in alphabets we sometimes denote negative integer m by underlining it, as in $\mathcal{A} = \{-2, -1, 0, 1\} = \{\underline{2}, \underline{1}, 0, 1\}$.

Itineraries. For a dynamical system evolving in time, every state space point $x_0 \in \mathcal{M}$ has the *future itinerary*, an infinite sequence of symbols $S^+(x_0) = m_1 m_2 m_3 \dots$ which indicates the temporal order in which the regions shall be visited. Given a trajectory x_1, x_2, x_3, \dots of the initial point x_0 generated by a time-evolution law $x_{n+1} = f(x_n)$, the itinerary is given by the symbol sequence

$$m_n = m \quad \text{if} \quad x_n \in \mathcal{M}_m. \quad (11.1)$$

The *past itinerary* $S^-(x_0) = \dots m_{-2} m_{-1} m_0$ describes the order in which the regions were visited up to arriving to the point x_0 . Each point x_0 thus has associated with it the bi-infinite itinerary

$$S(x_0) = S^- . S^+ = \dots m_{-2} m_{-1} m_0 . m_1 m_2 m_3 \dots, \quad (11.2)$$

or simply ‘itinerary’, if we chose not to use the decimal point to indicate the present,

$$\{m_t\} = \cdots m_{-2} m_{-1} m_0 m_1 m_2 m_3 \cdots \quad (11.3)$$

Shifts. A forward iteration of temporal dynamics $x \rightarrow x' = f(x)$ shifts the entire itinerary to the left through the ‘decimal point’. This operation, denoted by the shift operator d ,

$$d(\cdots m_{-2} m_{-1} m_0.m_1 m_2 m_3 \cdots) = \cdots m_{-2} m_{-1} m_0 m_1.m_2 m_3 \cdots, \quad (11.4)$$

denotes the current partition label m_1 from the future S^+ to the past S^- . The inverse shift d^{-1} shifts the entire itinerary one step to the right.

The set of all itineraries that can be formed from the letters of the alphabet \mathcal{A} is called the *full shift*

$$\hat{\Sigma} = \{(m_k) : m_k \in \mathcal{A} \text{ for all } k \in \mathbb{Z}\}. \quad (11.5)$$

The itinerary is infinite for any trapped (non-escaping or non-wandering set orbit) orbit (such as an orbit that stays on a chaotic repeller), and infinitely repeating for a periodic orbit p of period n_p . A map f is said to be a *horseshoe* if its restriction to the non-wandering set is hyperbolic and topologically conjugate to the full \mathcal{A} -shift.

Lattices. Consider a d -dimensional hypercubic lattice infinite in extent, with each site labeled by d integers $z \in \mathbb{Z}^d$. Assign to each site z a letter m_z from a finite alphabet \mathcal{A} . A particular fixed set of letters m_z corresponds to a particular lattice state $M = \{m_z\}$. In other words, a d -dimensional lattice requires a d -dimensional code $M = \{m_{n_1 n_2 \dots n_d}\}$ for a complete specification of the corresponding state X . In the lattice case, the *full shift* is the set of all d -dimensional symbol blocks that can be formed from the letters of the alphabet \mathcal{A}

$$\hat{\Sigma} = \{\{m_z\} : m_z \in \mathcal{A} \text{ for all } z \in \mathbb{Z}^d\}. \quad (11.6)$$

Commuting discrete translations. For an autonomous dynamical system, the evolution law f is of the same form for all times. If f is also of the same form at every lattice site, the group of lattice translations (sometimes called multi-dimensional shifts), acting along j th lattice direction by shift d_j , is a spatial symmetry that commutes with the temporal evolution. A temporal mapping f that satisfies $f \circ d_j = d_j \circ f$ along the $d-1$ spatial lattice directions is said to be *shift invariant*, with the associated symmetry of dynamics given by the d -dimensional group of discrete spatiotemporal translations.

Assign to each site z a letter m_z from the alphabet \mathcal{A} . A particular fixed set of letters m_z corresponds to a particular lattice symbol array $M = \{m_z\} = \{m_{n_1 n_2 \dots n_d}\}$, which yields a complete specification of the corresponding state X . In the lattice case, the *full shift* is the set of all d -dimensional symbol arrays that can be formed from the letters of the alphabet \mathcal{A}

as in (11.6)

A d -dimensional spatiotemporal field $X = \{x_z\}$ is determined by the corresponding d -dimensional spatiotemporal symbol array $M = \{m_z\}$. Consider next a finite block of symbols $M_{\mathcal{R}} \subset M$, over a finite rectangular $[\ell_1 \times \ell_2 \times \cdots \times \ell_d]$ lattice region $\mathcal{R} \subset \mathbb{Z}^d$. In particular, let M_p over a finite rectangular $[\ell_1 \times \ell_2 \times \cdots \times \ell_d]$ lattice region be the $[\ell_1 \times \ell_2 \times \cdots \times \ell_d]$ d -periodic block of M whose repeats tile \mathbb{Z}^d .

Blocks. In the case of temporal dynamics, a finite itinerary

$M_{\mathcal{R}} = m_{k+1}m_{k+2}\cdots m_{k+\ell}$ of symbols from \mathcal{A} is called a *block* of length $\ell = n_{\mathcal{R}}$. More generally, let $\mathcal{R} \subset \mathbb{Z}^d$ be a $[\ell_1 \times \ell_2 \times \cdots \times \ell_d]$ rectangular lattice region, $\ell_k \geq 1$, whose lower left corner is the $n = (n_1 n_2 \cdots n_d)$ lattice site

$$\mathcal{R} = \mathcal{R}_n^{[\ell_1 \times \ell_2 \times \cdots \times \ell_d]} = \{(n_1 + j_1, \dots, n_d + j_d) \mid 0 \leq j_k \leq \ell_k - 1\}. \quad (11.7)$$

The associated finite block of symbols $m_z \in \mathcal{A}$ restricted to \mathcal{R} , $M_{\mathcal{R}} = \{m_z \mid z \in \mathcal{R}\} \subset M$ is called the block $M_{\mathcal{R}}$ of volume $n_{\mathcal{R}} = \ell_1 \ell_2 \cdots \ell_d$. For example, for a 2-dimensional lattice a $\mathcal{R} = [3 \times 2]$ block is of form

$$M_{\mathcal{R}} = \begin{bmatrix} m_{12} & m_{22} & m_{32} \\ m_{11} & m_{21} & m_{31} \end{bmatrix} \quad (11.8)$$

and volume (in this case, an area) equals $3 \times 2 = 6$. In our convention, the first index is ‘space’, increasing from left to right, and the second index is ‘time’, increasing from bottom up.

Cylinder sets. While a particular admissible infinite symbol array $M = \{m_z\}$ defines a point X (a unique lattice state) in the state space, the *cylinder set* $M_{\mathcal{M}_{\mathcal{R}}}$, corresponds to the totality of state space points X that share the same given finite block $M_{\mathcal{R}}$ symbolic representation over the region \mathcal{R} . For example, in $d = 1$ case

$$M_{\mathcal{M}_{\mathcal{R}}} = \{\cdots a_{-2}a_{-1} \cdot m_1 m_2 \cdots m_{\ell} a_{\ell+1} a_{\ell+2} \cdots\}, \quad (11.9)$$

with the symbols a_j outside of the block $M_{\mathcal{R}} = [m_1 m_2 \cdots m_{\ell}]$ unspecified.

Periodic orbits, invariant d -tori. A state space point $x_z \in X$ is spatiotemporally *periodic*, $x_z = x_{z+\ell}$, if its spacetime orbit returns to it after a finite lattice shift $\ell = (\ell_1, \ell_2, \dots, \ell_d)$ over region \mathcal{R} defined in (11.7). The infinity of repeats of the corresponding block $M_{\mathcal{R}}$ then tiles the lattice. For a spatiotemporally periodic state X , a *prime* block M_p (or p) is a smallest such block $\ell_p = (\ell_1, \ell_2, \dots, \ell_d)$ that cannot itself be tiled by repeats of a shorter block.

The periodic tiling of the lattice by the infinitely many repeats of a prime block is denoted by a bar: \bar{M}_p . We shall omit the bar whenever it is clear from the context that the state is periodic.¹²

In $d = 1$ dimensions, a prime block is called an *orbit* p , a single traversal of the orbit; its label is a block of n_p symbols that cannot be written as a repeat of a shorter block. Each *periodic point* $x_{m_1 m_2 \cdots m_{n_p}}$ is then labeled by the starting

¹Predrag 2019-01-19: eliminate $_m \cdots m_{-1} \cdots m_0$ and $[m_{-m+1} \cdots m_0,]$ notation in favor a single convention

²Predrag 2018-11-07: Generalize to invariant d -tori.

symbol m_1 , followed by the next $(n_p - 1)$ steps of its future itinerary. The set of periodic points \mathcal{M}_p that belong to a given periodic orbit form a *cycle*

$$p = \overline{m_1 m_2 \cdots m_{n_p}} = \{x_{m_1 m_2 \cdots m_{n_p}}, x_{m_2 \cdots m_{n_p} m_1}, \dots, x_{m_{n_p} m_1 \cdots m_{n_p-1}}\}. \quad (11.10)$$

More generally, a state space point is *spatiotemporally periodic* if it belongs to an invariant d -torus, i.e., its symbolic representation is a block over region \mathcal{R} defined by (11.7),

$$\mathbf{M}_p = \mathbf{M}_{\mathcal{R}}, \quad \mathcal{R} = \mathcal{R}_0^{[\ell_1 \times \ell_2 \times \cdots \times \ell_d]}, \quad (11.11)$$

that tiles the lattice state \mathbf{M} periodically, with period ℓ_j in the j th lattice direction.

Generating partitions. A temporal partition is called *generating* if every bi-infinite itinerary corresponds to a distinct point in state space. In practice almost any generating partition of interest is infinite. Even when the dynamics assigns a unique infinite itinerary $\cdots m_{-2} m_{-1} m_0. m_1 m_2 m_3 \cdots$ to each distinct orbit, there generically exist full shift itineraries (11.5) which are not realized as orbits; such sequences are called *inadmissible*, and we say that the symbolic dynamics is *pruned*.

Dynamical partitions. If the symbols outside of given temporal block b remain unspecified, the set of all admissible blocks of length n_b yield a dynamically generated partition of the state space, $\mathcal{M} = \cup_b \mathcal{M}_b$.

Subshifts. A dynamical system (\mathcal{M}, f) given by a mapping $f : \mathcal{M} \rightarrow \mathcal{M}$ together with a partition \mathcal{A} induces *topological dynamics* (Σ, d) , where the *subshift*

$$\Sigma = \{(m_k)_{k \in \mathbb{Z}}\}, \quad (11.12)$$

is the set of all *admissible* itineraries, and $d : \Sigma \rightarrow \Sigma$ is the shift operator (11.4). The designation ‘subshift’ comes from the fact that Σ is a subset of the full shift.

Let $\hat{\Sigma}$ be the full lattice shift (11.5), i.e., the set of all possible lattice state \mathbf{M} labelings by the alphabet \mathcal{A} , and $\hat{\Sigma}(\mathbf{M}_{\mathcal{R}})$ is the set of such blocks over a region \mathcal{R} . The principal task in developing the symbolic dynamics of a dynamical system is to determine Σ , the set of all *admissible* itineraries/lattice states, i.e., all states that can be realized by the given system.

Pruning, grammars, recoding. If certain states are inadmissible, the alphabet must be supplemented by a *grammar*, a set of pruning rules. Suppose that the grammar can be stated as a finite number of pruning rules, each forbidding a block of finite size,

$$\mathcal{G} = \{b_1, b_2, \dots, b_k\}, \quad (11.13)$$

where a *pruned block* b is an array of symbols defined over a finite \mathcal{R} lattice region of size $[\ell_1 \times \ell_2 \times \cdots \times \ell_d]$. In this case we can construct a finite Markov partition by replacing finite size blocks of the original partition by letters of a new alphabet. In the case of a 1-dimensional, the temporal lattice, if the longest forbidden block is of length $L+1$, we say that the symbolic dynamics is Markov, a shift of finite type with L -step memory.

Subshifts of finite type. A topological dynamical system (Σ, d) for which all admissible states M are generated by recursive application of the finite set of pruning rules (11.13) is called a subshift of *finite type*.

If a map can be topologically conjugated to a linear map, the symbolic dynamics of the linear map offers a dramatically simplified description of all admissible solutions of the original flow, with the temporal symbolic dynamics and the state space dynamics related by linear recoding formulas. For example, if a map of an interval, such as a parabola, can be conjugated to a piecewise linear map, the kneading theory [6] classifies *all* of its admissible orbits.

11.1 Symbolic dynamics, inserts

2019-01-19 Predrag Merge everything here to chapter 11 *Symbolic dynamics: a glossary* then `svn rm` this file.

2017-08-05 Predrag Consult / harmonize with ChaosBook.org Chapter *Charting the state space* (source file `knead.tex`).

to Predrag: check that all this is in ChaosBook, then erase:

The set of all bi-infinite itineraries that can be formed from the letters of the alphabet \mathcal{A} is called the *full shift* (or *topological Markov chain*)

Here we refer to this set of all conceivable itineraries as the *covering* symbolic dynamics.

Orbit that starts out as a finite block followed by infinite number of repeats of another block $p = (m_1 m_2 m_3 \dots m_T)$ is said to be *heteroclinic* to the cycle p . An orbit that starts out as p^∞ followed by a different finite block followed by $(p')^\infty$ of another block p' is said to be a *heteroclinic connection* from cycle p to cycle p' .

Suppose that the grammar can be stated as a finite number of pruning rules, each forbidding a block of finite length,

$$\mathcal{G} = \{b_1, b_2, \dots, b_k\}, \quad (11.14)$$

where a *pruned block* b is a sequence of symbols $b = m_1 m_2 \dots m_{n_b}$, $m \in \mathcal{A}$, of finite length n_b .

Subshifts of finite type. A topological dynamical system (Σ, σ) for which all admissible itineraries are generated by a finite transition matrix

$$\Sigma = \{(m_k)_{k \in \mathbb{Z}} : T_{s_k s_{k+1}} = 1 \text{ for all } k\} \quad (11.15)$$

is called a subshift of *finite type*.

Reflection symmetries. Symmetries of the cat map induce invariance with respect to corresponding symbol exchanges. Define $\tilde{m} = s - m - 2$ to be the conjugate of symbol $m \in \mathcal{A}$. For example, the two exterior alphabet \mathcal{A}_1 symbols are conjugate to each other, as illustrated by (1.101). ³ If $b = m_1 m_2 \dots m_\ell$ is a

³Predrag 2019-05-27: fix this eq. reference; edit it away

block, and $\bar{b} = \bar{m}_1 \bar{m}_2 \dots \bar{m}_\ell$ its conjugate, then by reflection symmetry of the cat map we have $|\mathcal{P}_b| = |\mathcal{P}_{\bar{b}}|$. Similarly, if $b^* = m_l m_{l-1} \dots m_1$, the time reversal invariance implies $|\mathcal{P}_b| = |\mathcal{P}_{b^*}|$.

There are many ways to skin a cat. For example, due to the space reflection symmetry about $x = 1/2$ of the Percival-Vivaldi cat map (1.101), it is natural (especially in studies of deterministic diffusion on periodic lattices [1–3]) to center the phase space unit interval [7] as $x \in [-1/2, 1/2]$. In this formulation the Percival-Vivaldi cat map has a 5-letter alphabet $\mathcal{A} = \{\underline{2}, \underline{1}, 0, 1, 2\}$, in which the spatial reflection symmetry is explicit (the “conjugate” of a symbol $m \in \mathcal{A}$ is $\bar{m} = -m$).

References

- [1] R. Artuso and P. Cvitanović, “Deterministic diffusion”, in *Chaos: Classical and Quantum*, edited by P. Cvitanović, R. Artuso, R. Mainieri, G. Tanner, and G. Vattay (Niels Bohr Inst., Copenhagen, 2016).
- [2] R. Artuso and P. Cvitanović, “Deterministic diffusion”, in *Chaos: Classical and Quantum*, edited by P. Cvitanović, R. Artuso, R. Mainieri, G. Tanner, and G. Vattay (Niels Bohr Inst., Copenhagen, 2019).
- [3] R. Artuso and R. Strepparava, “Reycling diffusion in sawtooth and cat maps”, *Phys. Lett. A* **236**, 469–475 (1997).
- [4] P. Cvitanović, R. Artuso, R. Mainieri, G. Tanner, and G. Vattay, *Chaos: Classical and Quantum* (Niels Bohr Inst., Copenhagen, 2020).
- [5] B. Gutkin, L. Han, R. Jafari, A. K. Saremi, and P. Cvitanović, “Linear encoding of the spatiotemporal cat map”, *Nonlinearity* **34**, 2800–2836 (2021).
- [6] J. Milnor and W. Thurston, “On iterated maps of the interval”, in *Dynamical Systems*, edited by J. C. Alexander (Springer, New York, 1988), pp. 465–563.
- [7] I. Percival and F. Vivaldi, “A linear code for the sawtooth and cat maps”, *Physica D* **27**, 373–386 (1987).

11.2 Enumeration of prime invariant 2-tori

2020-08-10 Predrag Copied to *siminos/kittens/prime.tex*, in *CL18.tex* The two versions are from now on edited separately

11.2.1 Covering alphabet

Our algorithm for generating all prime $[\ell \times T]_S$ Bravais lattices consists in picking the lexically lowest block for every set of blocks related by spatial and temporal translations:

1. Fill the first row $[m_{11} m_{21} \cdots m_{\ell 1}]$ by lexically ordered symbols, $m_{j1} \leq m_{j+1,1}$, keep one block for each set of spatially cyclically related permutations.
2. Picking the lexically ordered first row representatives uses up the cyclic invariance under spatial translations, so for the second $[m_{12} m_{22} \cdots m_{\ell 2}]$ and higher rows fill in all $|\mathcal{A}|^T$ combinations of symbols.
3. The count is the same for all $[\ell \times T]_S$ relative-periodic blocks.
4. Group blocks into sets related by cyclic permutations in the time direction. For each such set, pick a representative that has lexically lowest first row, throw away the rest.
5. Throw away all blocks which are repeats of shorter blocks in the spatial direction.
6. Throw away all blocks which are repeats of shorter blocks in the temporal direction. What remains in N_k prime periodic blocks p of the same size $[\ell_p \times T_p] = [\ell_k \times T_k]$.
7. The total number of (doubly) periodic blocks is the sum of all cyclic permutations of prime blocks,

$$|\mathcal{A}|^{\ell T} = \sum_p N_p [\ell_p \times T_p]_{S_p}$$

where the sum goes over prime tilings of the $[\ell \times T]_S$ block.

This completes the list of prime invariant 2-tori, with the alphabet \mathcal{A} taken as a *covering alphabet*, i.e., we have generated all possible prime blocks, under assumption of no grammar rules.

The number of prime invariant 2-tori is given recursively by (see (3.188)),

$$M_p = \frac{1}{\ell T} \left(N_p - \sum_{p'} \ell_{p'} T_{p'} M_{p'} \right), \quad (11.16)$$

where the sum is over p' , the prime ‘divisors’ of p that satisfy tiling conditions (8.47).

Example: $[2 \times 2]_0$ Bravais lattices prime blocks.

Consider $[2 \times 2]_0$ Bravais lattices prime block

$$M_p = \begin{bmatrix} m_{01} & m_{11} \\ m_{00} & m_{10} \end{bmatrix}, \quad (11.17)$$

and the relative-periodic $[2 \times 1]_1$ block with 1 site-shift periodic boundary, which is periodic after the second repeat in the time direction,

$$M_p = \begin{bmatrix} & [m_{00} & m_{10}] \\ [m_{00} & m_{10}] & \end{bmatrix}. \quad (11.18)$$

According to (11.16), the number of prime $[2 \times 2]_0$ lattice states is

$$M_{[2 \times 2]_0} = \frac{1}{2 \cdot 2} (N_{[2 \times 2]_0} - 2M_{[2 \times 1]_0} - 2M_{[1 \times 2]_0} - 2M_{[2 \times 1]_1} - M_{[1 \times 1]_0}) \quad (11.19)$$

We can work this out explicitly as follows:

(1) Fill the first row $[m_{11} m_{21}]$ by lexically ordered symbols, one for each set of spatially cyclically related permutations. For the alphabet (??) there are 36 such length 2 strings.

(2) As we have already ‘used up’ the cyclic invariance under spatial translations by picking the lexically ordered first row representatives, for the second $[m_{12} m_{22}]$ and higher rows all 81 combinations of 9 symbols are allowed. We now have $36 \times 81 = 2916$ blocks in all.

(3) The $[2 \times 1]_1$ relative-periodic block (11.18) is counted as the $[2 \times 2]_0$ invariant 2-torus; as in (1), after spatial cyclic rotations, there are 36 such prime blocks.

(4) Group blocks into sets related by cyclic permutations in the time direction. For each such set, pick a representative that is lexically lowest in the first row, throw away the rest.

(5) Throw away all blocks which are repeats of shorter blocks. There are three kinds of repeating small blocks:

$$[2 \times 1]_0 = \begin{bmatrix} a & b \\ a & b \end{bmatrix}, \quad [1 \times 2]_0 = \begin{bmatrix} b & b \\ a & a \end{bmatrix}, \quad [2 \times 1]_1 = \begin{bmatrix} & a & b \\ a & b & \end{bmatrix}.$$

(6) The result is 1584 $[2 \times 2]_0$ prime blocks.

There are also 36 prime $[2 \times 1]_0$ blocks repeating in time, 36 prime $[1 \times 2]_0$ blocks repeating in space, 36 prime $[2 \times 1]_1$ blocks repeating in time with 1/2-shift periodic boundary, and 9 blocks which are repeats of one-symbol prime $[1 \times 1]_0$ block. The total number of $[2 \times 2]_0$ blocks is recovered by all cyclic permutations of prime blocks (11.19):

$$\begin{aligned} N_{[2 \times 2]_0} &= 9^{2 \times 2} = 6561 \\ &= 1584 [2 \times 2]_0 + 36 [2 \times 1]_0 + 36 [1 \times 2]_0 + 36 [2 \times 1]_1 + 9 [1 \times 1]_0, \end{aligned} \quad (11.20)$$

where \cdots stands for the number of prime blocks of a given shape. This completes the count with the alphabet (??) taken as a *covering* alphabet, i.e., we have generated all possible prime blocks, were there no further grammar rules.

Example: $[3 \times 2]_0$ Bravais lattices prime blocks.

Consider the Bravais lattice

$$M = \begin{bmatrix} m_{12} & m_{22} & m_{32} \\ m_{11} & m_{21} & m_{31} \end{bmatrix}. \quad (11.21)$$

According to (11.16), the number of prime $[3 \times 2]_0$ lattice states is

$$M_{[3 \times 2]_0} = \frac{1}{3 \cdot 2} (N_{[3 \times 2]_0} - 3M_{[3 \times 1]_0} - 2M_{[1 \times 2]_0} - M_{[1 \times 1]_0}), \quad (11.22)$$

Unlike the $[2 \times 2]_0$ case (11.18), there no sub-blocks with relative-periodic boundary contributing to the $[3 \times 2]_0$ blocks count, since $[3 \times 1]_0$ and $[1 \times 2]_0$ sub-blocks cannot fit into the $[3 \times 2]_0$ doubly-periodic Bravais lattice without a shift.

Following the same algorithm as for $[2 \times 2]_0$ blocks, we get 88440 $[3 \times 2]_0$ prime blocks, 240 prime $[3 \times 1]_0$ blocks repeating in time, 36 prime $[1 \times 2]_0$ blocks repeating in space, and 9 blocks which are repeats of one symbol prime $[1 \times 1]_0$ block. The total number of $[3 \times 2]_0$ blocks is recovered by all cyclic permutations of prime blocks:

$$\begin{aligned} N_{[3 \times 2]_0} &= 9^{3 \times 2} = 531441 \\ &= 88440 [3 \times 2]_0 + 240 [3 \times 1]_0 + 36 [1 \times 2]_0 + 9 [1 \times 1]_0. \end{aligned} \quad (11.23)$$

11.2.2 Admissible prime invariant 2-tori

To determine the *admissible* blocks, compute X_p for each prime block M_p , and eliminate every X_p which contains a lattice site or sites on which the value of the field violates the admissibility condition $x_z \in [0, 1]^2$.

2019-11-22 Han For $s = 5/2$ spatiotemporal cat the pruning is very severe.

Of 1584 covering alphabet prime blocks in (11.20), only 52 prime $[2 \times 2]_0$ blocks are admissible. As for the repeats of smaller blocks, there are 2 admissible $[1 \times 2]_0$ blocks repeating in time and 2 $[2 \times 1]_0$ blocks repeating in space. There are 4 admissible $1/2$ -shift periodic boundary $[1 \times 2]_0$ blocks. And there is 1 admissible block $[1 \times 1]_0$ which is a repeat of letter 0. The total number of $[2 \times 2]_0$ of invariant 2-tori is obtained by all cyclic permutations of admissible prime blocks (a significant pruning, compared to the full shift count (11.20)),

$$\begin{aligned} N_{[2 \times 2]_0} &= 225 \\ &= 52 [2 \times 2]_0 + 2 [2 \times 1]_0 + 2 [1 \times 2]_0 + 4 [2 \times 1]_1 + 1 [1 \times 1]_0. \end{aligned} \quad (11.24)$$

Table 11.1: The numbers of the $s = 5/2$ spatiotemporal cat $[\ell \times T]_S$ invariant 2-tori: $M_{[\ell \times T]_S}$ is the number of prime invariant 2-tori, $N_{[\ell \times T]_S}$ is the number of doubly periodic lattice states, and $R_{[\ell \times T]_S}$ is the number of prime invariant 2-tori in the D_4 symmetries orbit.

$[\ell \times T]_S$	M	N	R
$[1 \times 1]_0$	1	1	1
$[2 \times 1]_0$	2	$5 = 2[2 \times 1]_0 + 1[1 \times 1]_0$	2
$[2 \times 1]_1$	4	$9 = 4[2 \times 1]_1 + 1[1 \times 1]_0$	
$[3 \times 1]_0$	5	$16 = 5[3 \times 1]_0 + 1[1 \times 1]_0$	
$[3 \times 1]_1$	16	$49 = 16[3 \times 1]_1 + 1[1 \times 1]_0$	
$[4 \times 1]_0$	10	$45 = 10[4 \times 1]_0 + 2[2 \times 1]_0 + 1[1 \times 1]_0$	
$[4 \times 1]_1$	54	$225 = 54[4 \times 1]_1 + 4[2 \times 1]_1 + 1[1 \times 1]_0$	
$[4 \times 1]_2$	60	$245 = 59[4 \times 1]_2 + 2[2 \times 1]_0 + 1[1 \times 1]_0$	
$[2 \times 2]_0$	52	$225 = 52[2 \times 2]_0 + 2[2 \times 1]_0 + 2[1 \times 2]_0$ $+ 4[2 \times 1]_1 + 1[1 \times 1]_0$	1
$[2 \times 2]_1$	60	$245 = 60[2 \times 2]_1 + 2[1 \times 2]_0 + 1[1 \times 1]_0$	
$[3 \times 2]_0$	850	$5\ 120 = 850[3 \times 2]_0 + 5[3 \times 1]_0$ $+ 2[1 \times 2]_0 + 1[1 \times 1]_0$	
$[3 \times 2]_1$	1 012	$6\ 125 = 1\ 012[3 \times 2]_1 + 16[3 \times 1]_2$ $+ 2[1 \times 2]_0 + 1[1 \times 1]_0$	
$[3 \times 3]_0$	68 281	$614\ 656 = 68\ 281[3 \times 3]_0 + 5[3 \times 1]_0$ $+ 16[3 \times 1]_1 + 16[3 \times 1]_2 + 5[1 \times 3]_0 + 1[1 \times 1]_0$	1
$[3 \times 3]_1$	70 400	$633\ 616 = 70\ 400[3 \times 3]_1 + 5[1 \times 3]_0 + 1[1 \times 1]_0$	

CHAPTER 11. SYMBOLIC DYNAMICS: A GLOSSARY

Table 11.2: The numbers of spatiotemporal cat lattice states for Bravais lattices $\Lambda = [\ell \times T]_s$ up to $[3 \times 3]_2$. Here $N_\Lambda(s)$ is the number of doubly periodic lattice states, $M_\Lambda(s)$ is the number of prime invariant 2-tori, and R_Λ is the number of prime invariant 2-tori in the D_4 symmetries orbit. The stretching parameter s can take half-integer or integer values.

Λ	$N_\Lambda(s)$	$M_\Lambda(s)$	R
$[1 \times 1]_0$	$2(s - 2)$	$2(s - 2)$	1
$[2 \times 1]_0$	$2(s - 2)2s$	$2(s - 2)\frac{1}{2}(2s - 1)$	2
$[2 \times 1]_1$	$2(s - 2)2(s + 2)$	$2(s - 2)\frac{1}{2}(2s + 3)$	
$[3 \times 1]_0$	$2(s - 2)(2s - 1)^2$	$2(s - 2)\frac{4}{3}(s - 1)s$	
$[3 \times 1]_1$	$2(s - 2)4(s + 1)^2$	$2(s - 2)\frac{1}{3}(2s + 1)(2s + 3)$	
$[4 \times 1]_0$	$2(s - 2)8(s - 1)^2s$	$2(s - 2)\frac{1}{2}(2s - 3)(2s - 1)s$	
$[4 \times 1]_1$	$2(s - 2)8s^2(s + 2)$	$2(s - 2)\frac{1}{2}(s + 2)(2s - 1)(2s + 1)$	
$[4 \times 1]_2$	$2(s - 2)8(s + 1)^2s$	$2(s - 2)\frac{1}{2}(2s + 3)(2s + 1)s$	
$[4 \times 1]_3$	$2(s - 2)8s^2(s + 2)$	$2(s - 2)\frac{1}{2}(s + 2)(2s - 1)(2s + 1)$	
$[5 \times 1]_0$	$2(s - 2)(4s^2 - 6s + 1)^2$	$2(s - 2)\frac{4}{5}(s - 1)(2s - 3)(2s - 1)s$	
$[5 \times 1]_1$	$2(s - 2)16(s^2 + s - 1)^2$	$2(s - 2)\frac{1}{5}(2s - 1)(2s + 3)(4s^2 + 4s - 5)$	
$[2 \times 2]_0$	$2(s - 2)8s^2(s + 2)$	$2(s - 2)\frac{1}{2}(2s - 1)(2s^2 + 5s + 1)$	
$[2 \times 2]_1$	$2(s - 2)8s(s + 1)^2$	$2(s - 2)\frac{1}{2}(2s + 1)(2s + 3)s$	
$[3 \times 2]_0$	$2(s - 2)2s(2s - 1)^2(2s + 3)^2$	$2(s - 2)\frac{2}{3}(2s - 1)(4s^3 + 10s^2 + 3s - 5)s$	
$[3 \times 2]_1$	$2(s - 2)32s^3(s + 1)^2$	$2(s - 2)\frac{1}{6}(2s - 1)(2s + 1)(8s^3 + 16s^2 + 10s + 3)$	
$[3 \times 3]_0$	$2(s - 2)16(s + 1)^4(2s - 1)^4$		
$[3 \times 3]_1$	$2(s - 2)(2s - 1)^2(8s^3 + 12s^2 - 1)^2$		

2019-11-23 Han For $s = 5/2$ spatiotemporal cat only 850 prime $[3 \times 2]_0$ blocks are admissible. There are 5 admissible repeating prime $[3 \times 1]_0$ blocks, 2 admissible repeating prime $[1 \times 2]_0$ blocks, and 1 admissible block which is a repeat of 0 . The total number of admissible solutions obtained by all cyclic permutations of admissible prime blocks is:

$$N_{[3 \times 2]_0} = 5120 = 850 [3 \times 2]_0 + 5 [3 \times 1]_0 + 2 [1 \times 2]_0 + 1 [1 \times 1]_0, \quad (11.25)$$

in agreement with the counting formula (??) for the $[3 \times 2]_0$ invariant 2-tori.

2020-06-09 Han The admissible prime invariant 2-tori counts for any half-integer or integer s are listed in table 11.2. Note that $N_{[3 \times T]_1}(s) = N_{[3 \times T]_2}(s)$, by reflection symmetry, as $N_{[3 \times T]_2}(s) = N_{[3 \times T]_{-1}}(s)$.

These two expressions do not fit into the table format:

$$\begin{aligned} M_{[3 \times 3]_0} = & 2(s - 2) \frac{1}{9} (256s^8 + 512s^7 - 128s^6 - 640s^5 \\ & + 16s^4 + 320s^3 - 48s^2 - 72s + 9). \end{aligned} \quad (11.26)$$

The last, currently unreduced formula exemplifies what is nonintuitive

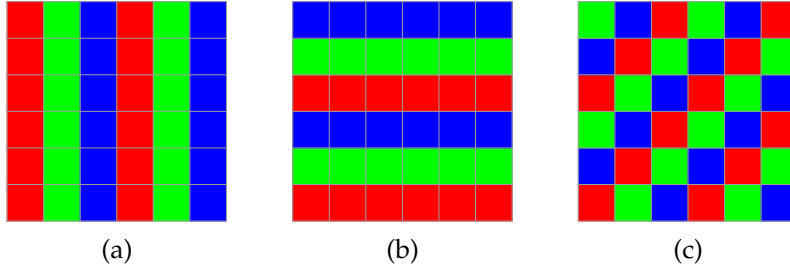


Figure 11.1: Examples of $[\ell \times T]_S$ periodic blocks together with their spatiotemporal Bravais lattice tilings (??). (a) $[3 \times 1]_0$, basis vectors $\mathbf{a}_1 = \{3, 0\}$ and $\mathbf{a}_2 = \{0, 1\}$; (b) $[1 \times 3]_0$, basis vectors $\mathbf{a}_1 = \{1, 0\}$ and $\mathbf{a}_2 = \{0, 3\}$; (c) $[3 \times 1]_1$, basis vectors $\mathbf{a}_1 = \{3, 0\}$ and $\mathbf{a}_2 = \{1, 1\}$;

about the Fourier space results; it is not at all obvious that this

$$\begin{aligned} M_{[3 \times 3]_1} &= M_{[3 \times 3]_2} = 2(s-2) \frac{1}{9} (1-2s)^2 \times \\ &\quad \left\{ \left[2s + 1 - 2 \sin \left(\frac{\pi}{18} \right) \right]^2 \left[2s + 1 + 2 \cos \left(\frac{\pi}{9} \right) \right]^2 \right. \\ &\quad \left. \left[(2s+1 - 2 \cos \left(\frac{2\pi}{9} \right))^2 - 1 \right] \right\} \end{aligned} \quad (11.27)$$

is an integer for any half-integer or integer s . **Predrag** to Han: can you evaluate this using the fundamental fact $N_n = |\text{Det } \mathcal{J}|$?

2020-06-09 Han The admissible prime invariant 2-tori counts are listed in table 11.1. This list verifies the counting formula (??).

2019-11-24 Han The interior alphabet depends on the value of s and the admissible range of x_z . For $s = 5/2$, $x_z \in [0, 1]$, the interior alphabet is $\mathcal{A}_0 = \{0, 1\}$ (see eq. (38) in ref. [5]). For $s = 7/2$, $x_z \in [0, 1]$, the interior alphabet is $\mathcal{A}_0 = \{0, 1, 2, 3\}$ (eq. (46) in ref. [5]).

2020-06-09 Han Figures 11.1 and 11.2 are the plots of the periodic blocks by color. The three figures in figure 11.1 are the blocks with periodicity $[1 \times 3]_0$, $[3 \times 1]_0$ and $[3 \times 1]_1$, which can show the periodicity of the space-equilibria, time-equilibria and time-relative equilibria. Figure 11.2 is the color coding of the periodic blocks with periodicity $[2 \times 1]_1$, $[3 \times 2]_1$ and $[3 \times 2]_0$.

2019-11-23 Predrag We always reduce relative-shift symmetries, so I am not happy about the $[2 \times 1]_1$ relative-periodic block (11.18) being counted as the $[2 \times 2]_0$ invariant 2-torus. We'll have to revisit symmetry reduction...

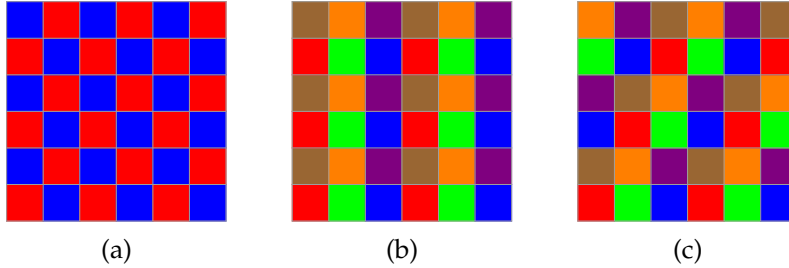


Figure 11.2: Examples of $[\ell \times T]_S$ periodic blocks together with their spatiotemporal Bravais lattice tilings (??). (a) $[2 \times 2]_1$, basis vectors $\mathbf{a}_1 = \{2, 0\}$ and $\mathbf{a}_2 = \{1, 1\}$; (b) $[3 \times 2]_0$, basis vectors $\mathbf{a}_1 = \{3, 0\}$ and $\mathbf{a}_2 = \{0, 2\}$; (c) $[3 \times 2]_1$, basis vectors $\mathbf{a}_1 = \{3, 0\}$ and $\mathbf{a}_2 = \{1, 2\}$;

2019-11-23 Predrag For uses of the lexical ordering, ChaosBook table [ChaosBook 18.1: Orbits for the binary symbolic dynamics up to length 9](#), and appendix [ChaosBook A18.2 Prime factorization for dynamical itineraries](#) might be of interest.

In the paper, we will probably first review the temporal cat counting, something along the lines of the above tables.

suggestion of constructing covering prime blocks wildly overcounts the candidates for admissible prime invariant 2-tori, so we should give up this avenue of constructing them - no need to count any larger Bravais lattices.

2020-03-17 Han *PrimeTiles.nb* generates all prime tiles that can tile a larger tile. It gives some not obvious results. For example, let the large tile be $[3 \times 2]_1$, and consider the full-shift 9-symbol $[3 \times 2]_1$ blocks. The number $[3 \times 2]_0$ blocks is given by (11.23). The program shows that the $[3 \times 2]_0$ tile can only be tiled by $[1 \times 1]_0$, $[1 \times 2]_0$ and $[3 \times 1]_0$ tiles. So we get the result in (11.23):

$$N_{[3 \times 2]_0} = 9^{3 \times 2} = 88440 [3 \times 2]_0 + 240 [3 \times 1]_0 + 36 [1 \times 2]_0 + 9 [1 \times 1]_0 .$$

For the full-shift the number of periodic blocks is given by the area of the larger tile, and number of $[3 \times 2]_S$ blocks is the same for all S . But now $[3 \times 1]_0$ tile cannot tile the $[3 \times 2]_1$ tile. Instead, the $[3 \times 2]_1$ can be tiled by $[1 \times 1]_0$, $[3 \times 1]_2$ and $[1 \times 2]_0$ tiles,

$$N_{[3 \times 2]_1} = 9^{3 \times 2} = 88440 [3 \times 2]_1 + 240 [3 \times 1]_2 + 36 [1 \times 2]_0 + 9 [1 \times 1]_0 .$$

A priori is not obvious that $[3 \times 1]_2$ tile can tile a $[3 \times 2]_1$ tile. But if you stack $[3 \times 1]_2$ tile in the shifted temporal direction by 2 then the left edge of the tile is shifted by 4 in the spatial direction. With the spatial period being 3, shifted by 4 in the spatial direction is same as shifted by 1. So the bc's of $[3 \times 2]_1$ tile are satisfied by the $[3 \times 1]_2$ tiles.

Chapter 12

Statistical mechanics applications

12.1 Cat map

HERE WE WILL DEAL WITH the prototype example of chaotic Hamiltonian maps, *hyperbolic toral automorphisms*, (subspecies of which, known as the as the ‘Arnol’d cat map’, you have most likely already encountered), acting on a cylinder or over \mathbb{R}^2 . Their dynamics restricted to the elementary cell involves maps on T^2 (two-dimensional torus). On such torus an action of a matrix in $SL_2(\mathbb{N})$ with unit determinant and absolute value of the trace bigger than 2 is known as the Anosov map.

12.2 New example: Arnol’d cat map

the Arnol’d-Sinai cat is a practical cat
— Ian Percival and Franco Vivaldi [15]

The ‘standard’ generating partition code of Arnol’d and Avez [2] is rather simple - it is described in Devaney [9].¹ It relies on a 3-rectangles complete partition of the torus. It is a subshift of finite type - it is well suited to the generation and counting of periodic orbits on the torus, see Isola [11] rational topological zeta function in sect. 1.3.7.

However, the Arnol’d-Avez alphabet has no easy translation to the integers shift on the unfolded torus (on the lattice, most of torus periodic orbits are relative periodic orbits). Furthermore, for N coupled cat maps the number of such rectangles would grow exponentially [10].²

¹Predrag 2016-08-03: I do not have either monograph at hand, but Creagh [7] summary in sect. 1.3.8 is pretty clear.

²Predrag 2016-08-03: Have not checked that, or whether this is explained in ref. [10].

There is a general consensus in the cat map community [12] that the ‘linear code’ of Percival and Vivaldi [15] (here sect. 1.3.6) is deeper and more powerful. For deterministic diffusion developed in ChaosBook (chapter 12 here) that is the only choice, as one needs to convert symbolic dynamics of an relative periodic orbit to the integer shift (translation) on the lattice.³ The downside is that the Markov/generating partition is infinite, meaning that for longer and longer orbits there are more and more new pruning (inadmissible blocks) rules, ad infinitum.

⁴ Iterated area preserving maps of the form

$$p' = p + F(x) \quad (12.1)$$

$$x' = x + p' \quad \text{mod } 1, \quad (12.2)$$

where $F(x)$ is periodic of period 1, are widely studied because of their importance in dynamics. They include the standard map of Taylor, Chirikov and Greene [5, 13], and also the sawtooth and cat maps that we describe here. Because values of x differing by integers are identified, whereas the corresponding values of p are not, the phase space for these equations is a cylinder.

These maps describe ‘kicked’ rotors that are subject to a sequence of angle-dependent impulses $F(x)$, with $2\pi x$ as the configuration angle of the rotor, and p as the momentum conjugate to the configuration coordinate x . The time step has been set to $\Delta t = 1$. Eq. (12.1) says that the momentum p is accelerated to p' by the force pulse $F(x)\Delta t$, and eq. (12.2) says in that time the trajectory x reaches $x' = x + p'\Delta t$.

The phase space of the rotor is a cylinder, but it is often convenient to extend it to the plane or contract it to a torus. For the former case the “ mod 1” is removed from (12.2) and for the latter it is included in (12.1).

Eqs. (12.1,12.2) are a discrete time form of Hamilton’s equations. But for many purposes we are only interested in the values of the configuration coordinate x , which satisfy the second-order difference equation (the discrete Laplacian in time)

$$\delta^2 x_t \equiv x_{t+1} - 2x_t + x_{t-1} = F(x_t) \quad \text{mod } 1 \quad (12.3)$$

where t is a discrete time variable that takes only integer values. This equation may be considered as the Lagrangian or Newtonian equation corresponding to the Hamiltonian form (2.1), with $p_t = x_t + x_{t-1}$.

Rewrite (12.3) as

$$x_{t+1} = 2x_t + F(x_t) - x_{t-1} \quad \text{mod } 1 \quad (12.4)$$

Call the 1-step configuration point forward in (12.2) $x_t = y$, and the next configuration point $x_{t+1} = y'$. This recasts the dynamical equation in the form of

³Predrag 2016-08-03: I do not know why this symbolic dynamics is natural for extensions to N nearest-neighbor coupled maps.

⁴Predrag 2016-06-02: verbatim from Percival and Vivaldi [15]

an area preserving map in which only configurations at different times appear,

$$\begin{aligned} x' &= y \\ y' &= 2y + F(y) - x \quad \text{mod } 1. \end{aligned} \quad (12.5)$$

This they call the ‘two-configuration representation’.

The sawtooth map represents a rotor subject to an impulse $F(x)$ that is linear in x , except for a single discontinuity. The impulse is standardised to have zero mean, the origin of x is chosen so that $F(0)=0$, so

$$F(x) = Kx \quad (-1/2 \leq x < 1/2) \quad (12.6)$$

With these conventions Hamilton’s equations for the sawtooth are

$$\begin{aligned} x' &= y \quad \text{mod } 1 \\ y' &= -x + sy \quad \text{mod } 1 \end{aligned} \quad (12.7)$$

in the two-configuration representation, where

$$s = K + 2. \quad (12.8)$$

For $s > 2$ the map is unstable. In the two-configuration representation, Hamilton’s equations can be written in matrix form as

$$\begin{pmatrix} x' \\ y' \end{pmatrix} = M \begin{pmatrix} x \\ y \end{pmatrix} \quad \text{mod } 1 \quad (12.9)$$

with

$$M = \begin{pmatrix} 0 & 1 \\ -1 & s \end{pmatrix}, \quad (12.10)$$

characteristic polynomial

$$\Lambda^2 - s\Lambda + 1. \quad (12.11)$$

and eigenvalues

$$\Lambda = (s + \sqrt{D})/2, \quad \Lambda' = (s - \sqrt{D})/2, \quad (12.12)$$

where $D = s^2 - 4$. When s is an integer, then the map (12.9) is continuous on the torus, because the discontinuity of the sawtooth is an integer absorbed into the modulus. The map is then continuous; it is a toral automorphism, of a class called *cat maps*, of which the Arnol’d-Sinai cat map [2] with $s = 3$ is a special case,

$$M = \begin{pmatrix} 0 & 1 \\ -1 & 3 \end{pmatrix}. \quad (12.13)$$

If instead of (12.4) dynamics on a torus, one considers motion on a line (no mod 1), one can land in any unit interval along the q -axis. Let then $-b_t$ be the sequence of integer shifts that ensures that for all t the dynamics

$$x_{t+1} = 2x_t + F(x_t) - x_{t-1} - b_t \quad (12.14)$$

stays confined to the elementary cell $x_t \in [-1/2, 1/2]$. The Newton equation (12.3) then takes the form

$$(\delta^2 - K)x_t = -b_t \quad (12.15)$$

The linear operator or infinite tridiagonal matrix on the left of (12.15) has a Green's function or inverse matrix given by the unique bounded solution g_{ts} of the inhomogeneous equation ⁵

$$g_{t+1,t'} - s g_{tt'} + g_{t-1,t'} = \delta_{tt'}, \quad (12.16)$$

which is given by

$$g_{tt'} = -\Lambda^{-|t-t'|}/\sqrt{D}. \quad (12.17)$$

This solution is obtained by a method that is directly analogous to the method used for second order linear differential equations [14] ([click here](#)). The solution of (12.15) for the orbit is therefore ⁶

$$t_t = \sum'_t g_{tt'}(-b_t) = \frac{1}{\sqrt{D}} \sum'_t \Lambda^{-|t-t'|} b_{t'} = \delta_{tt'}, \quad (12.18)$$

defining the orbit uniquely in terms of the symbol sequence. That is to say that the code is complete. We shall refer to an integer code such as $\{b_t\}$ for a linear system as a *linear code*: the orbit and the code are related to one another by a linear transformation. Clearly, a shift in the symbol sequence $\{b_t\}$ corresponds to an equivalent time shift of the orbit.

The past and the future sums in (12.18) resembles the expression for a real number in terms of the digits b_t , using a representation of the reals in the non-integral base Λ , in contrast with the past and future coordinates for the baker's transformation, which have a similar form, to base 2. The 'present' symbol b_0 is incorporated with the past in our convention.

Commentary

Remark 12.1. Deterministic diffusion in Hamiltonian maps. (Continued from remark ??) The quasilinear estimate (??) was given in ref. [4] and evaluated in refs. [3, 16]. Circulant matrices are discussed in Aitkenref. [1] (1939). The result (??) agrees with the saw-tooth result of ref. [4]; for the cat maps (??) is the exact value of the diffusion coefficient. This result was also obtained, by using periodic orbits, in ref. [8], where Gaussian nature of the diffusion process is explicitly assumed. Measure polytopes are discussed in ref. [6].

⁷

⁵Predrag 2016-05-29: still have to check this calculation

⁶Predrag 2018-03-11: Mestel and Percival [14] is very systematic, with Wronskians, etc., but I do not see this solution there. Percival and Vivaldi [15] state it, say it can be derived by the method of Mestel and Percival [14], and say "as may be verified by substitution."

⁷Predrag 2018-12-01: Had here Problems/exerAppStatM until 30dec2017, now only copy is the renamed ChaosBook exerAppDiff.tex.

REMEMBER: move the cat map exercises to exerCatMap.tex

References

- [1] A. Aitken, *Determinants & Matrices* (Oliver & Boyd, Edinburgh, 1939).
- [2] V. I. Arnol'd and A. Avez, *Ergodic Problems of Classical Mechanics* (Addison-Wesley, Redwood City, 1989).
- [3] R. Artuso and R. Strepparava, "Reycling diffusion in sawtooth and cat maps", *Phys. Lett. A* **236**, 469–475 (1997).
- [4] J. R. Cary and J. D. Meiss, "Rigorously diffusive deterministic map", *Phys. Rev. A* **24**, 2664–2668 (1981).
- [5] B. V. Chirikov, "A universal instability of many-dimensional oscillator system", *Phys. Rep.* **52**, 263–379 (1979).
- [6] H. S. M. Coxeter, *Regular Polytopes* (Dover, New York, 1948).
- [7] S. C. Creagh, "Quantum zeta function for perturbed cat maps", *Chaos* **5**, 477–493 (1995).
- [8] Dana, "Hamiltonian transport on unstable periodic orbits", *Physica D* **39**, 205 (1989).
- [9] R. L. Devaney, *An Introduction to Chaotic Dynamical systems*, 2nd ed. (Westview Press, Cambridge, Mass, 2008).
- [10] B. Gutkin and V. Osipov, "Classical foundations of many-particle quantum chaos", *Nonlinearity* **29**, 325–356 (2016).
- [11] S. Isola, " ζ -functions and distribution of periodic orbits of toral automorphisms", *Europhys. Lett.* **11**, 517–522 (1990).
- [12] J. P. Keating, "Asymptotic properties of the periodic orbits of the cat maps", *Nonlinearity* **4**, 277 (1991).
- [13] A. J. Lichtenberg and M. A. Lieberman, *Regular and Chaotic Dynamics*, 2nd ed. (Springer, New York, 2013).
- [14] B. D. Mestel and I. Percival, "Newton method for highly unstable orbits", *Physica D* **24**, 172 (1987).
- [15] I. Percival and F. Vivaldi, "A linear code for the sawtooth and cat maps", *Physica D* **27**, 373–386 (1987).
- [16] R. Strepparava, Laurea thesis, MA thesis (Università degli Studi di Milano, 1995).

Chapter 13

Ising model in 2D

ChaosBook Exercise 17.1 Time reversibility. Hamiltonian flows are time reversible. Does that mean that their transition graphs are symmetric in all node → node links, their transition matrices are adjacency matrices, symmetric and diagonalizable, and that they have only real eigenvalues?

Solution 14.1, 2021-12-07 Read sect. 3.10 and on for a group-theoretic solution.

— An open exercise from ChaosBook.org

2CB

2016-02-19 Predrag A wild idea, to keep in mind, if we get to the point where QFT is within reach. ‘Fundamental domain’ appears in an interesting stat mech context in Wipf *et al.* [131, 132] *Generalized Potts-models and their relevance for gauge theories*. They study the 3-state Potts model, a natural extension of the Ising model with 3 vectors at each site, whose global symmetries are point group C_3 , and the 1d lattice of discrete translations. The domain of the traced Polyakov loop variable (?) for $SU(3)$ is a triangle, with a C_3 fundamental domain. Then they compute leading terms in the strong coupling limit using characters χ_{pq} for the $SU(3)$ representation (p, q) . These characters transform under C_3 , so they restrict calculations to the fundamental domain inside the above triangle. Or perhaps D_3 , could not tell in my first, very superficial reading. These articles were immediately followed up by a bunch of other articles - there are too many quantum field theorists out there:)

In other words, Potts model could provide a bridge from Boris’ cat maps to QFT on lattices.

There is also a continuation with G_2 Yang-Mills by the same authors, but that’s for another, more ambitious time...

2016-10-03 Predrag Not quick or easy to explain, but I have a hunch that the spatiotemporal zeta function should be something like the 2D Ising model

zeta function described by Aizenman ([click here](#)). It should assign a weight for every spatiotemporal domain, described by its 2D symbolic dynamics.

2016-10-08 Predrag qmath16 Aizenman talk notes (mostly gibberish - my fault):

It is known (?) that QM is emergent from the *classical* stat mech of Ising models. Key tools: Pfaffians. Random current representation of Ising.

Groenevald-Boel-Kasteleyn'78: describe correlations in the planar Ising model, by boundary segments, ordered cyclically. Pfaffian refers to spin-spin correlations along the boundary. There is a parity sign that makes it a non-interacting fermion model.

Aizenman et al. extend it to nonplanar models, where planarity *emerges* at the critical point. ADTW'16 proof utilizes the *random current representation*. Starts with high temperature expansion. Partition function is a sum over loops. In a correlation, sources are connected pairwise by lines, ie, Gaussian limit. Above critical dimension - four - the theory is free (sum of products over pairs). In 2D, fermionic case, you get Pfaffian. Leads to the integrability of the model. (Read Chelkak-Cimasoni-Kassel '15.)

"Almost planar"

Order-disorder variables.

Aizenman: Two implications of planarity

1) For any planar graph, and a symmetric edge function

$$\mathcal{F}(\{K_\theta\}) = \det(1 - K\mathcal{W})$$

is the *square of a multilinear function* of the parameters $\{K_\theta\}_{\theta \in \epsilon_0}$. This is proven through a reduction to an antisymmetric matrix A , and (Kasteleyn matrix '63):

$$\det(A) = \text{Pf}[A]^2.$$

For planar models, done by Kac-Ward. Works for any planar graph ("amorphous graphs"), not only on a regular lattice.

2) For any planar loop of oriented non-backtracking edges $\{e_1, e_2, \dots\}$

$$\prod_{j=1}^n \mathcal{W}_{e_{j+1}, e_j} = (-1)^{w(\rho^*)} = (-1)^{n(\rho^*)}.$$

with $w(\rho^*)$ = winding number, and $n(\rho^*)$ = # of self crossings [Whitney's Thm].

This is then combined with the *Ihara relation*, for matrices indexed by oriented edges:

$$\det(1 - K\mathcal{W})_{\epsilon_0 \times \epsilon_0} = \prod_{\ell} \left[1 + (-1)^{n(\ell)} \chi_{-K}(\ell) \right]^2.$$

the product being over unoriented loops on \mathbb{G} (hence the power 2).

2020-09-30 Predrag .



Aizenman Rutgers talk (unrecorded) was a modal of clear exposition. It is an audience friendly explanation of the background to, and advance for $d = 4$ explained in Michael Aizenman and Hugo Duminil-Copin *Marginal triviality of the scaling limits of critical 4D Ising and ϕ_4^4 models*, [arXiv:1912.07973](https://arxiv.org/abs/1912.07973). Duminil-Copin will give a tutorial on this work on October 9-10, 2020, in [42nd Midwest Probability Colloquium](#).

I especially liked the ‘reminder’ explaining how ϕ^4 goes to Ising in particular limit.

Related publications to check:

Michael Aizenman and Simone Warzel *Kac-Ward formula and its extension to order-disorder correlators through a graph zeta function*, [arXiv:1709.06052](https://arxiv.org/abs/1709.06052)

Is the *loop-soup expansion* related to my random walk interpretation of the hypercubic orbit Jacobian matrix traces and the determinant? References might be in Michael Aizenman, Hugo Duminil-Copin and Simone Warzel *Dimerization and Néel order in different quantum spin chains through a shared loop representation*, [arXiv:2002.02543](https://arxiv.org/abs/2002.02543).

2016-10-05 Predrag Aizenman, Laínz Valcázar and Warzel [2] *Pfaffian correlation functions of planar dimer covers* does not seem to be what we need (no word ‘zeta’ in this paper). They refer to 2016 preprint of

M. Aizenman H. Duminil-Copin, V. Tassion, S. Warzel, *Fermionic correlation functions and emergent planarity in 2D Ising models*. (that paper does not seem to be available anywhere, as yet)

The structure of the solution of Kac and Ward has been explained in unpublished lectures by Feynman (Aizenman referred to Feynman’s stat mech book).

Sherman [116] *Combinatorial aspects of the Ising model for ferromagnetism. I. A conjecture of Feynman on paths and graphs*

Hurst and Green [62] *New solution of the Ising problem for a rectangular lattice*

Burgoyne [14] *Remarks on the combinatorial approach to the Ising problem*

Vdovichenko [128] *A calculation of the partition function for a plane dipole lattice*. The steps: a) the sum over polygons is reduced to a sum over closed loops without intersections; b) the sum over closed loops without intersections is transformed into a sum over all loops; c) the sum over all loops is reduced to a random-walk problem and is calculated easily.

Cimasoni [23] *A generalized Kac-Ward formula*: “ As a consequence of our second proof, we also obtain the following fact: the Kac–Ward and the Fisher–Kasteleyn methods for solving the Ising model are one and the same. ”

Cimasoni [24] *The critical Ising model via Kac-Ward matrices*: The Kac-Ward formula [72] allows to compute the Ising partition function on any finite graph G from a determinant with quite remarkable properties. First of all, they satisfy some generalized Kramers-Wannier duality: there is an explicit equality relating the determinants associated to a graph and to its dual graph. Also, they are proportional to the determinants of the discrete critical Laplacians on the graph G .

Fisher [43] *On the dimer solution of planar Ising models*

Kasteleyn [76] *The statistics of dimers on a lattice: I. The number of dimer arrangements on a quadratic lattice*

Kasteleyn [77] *Dimer statistics and phase transitions*

H. Au-Yang, J. H. H. Perk. Ising correlations at the critical temperature. Physics Letters A 104, 131–134 (1984).

Kager, Lis and Meester [74] *The signed loop approach to the Ising model: Foundations and critical point*

Lis [89] *A short proof of the Kac-Ward formula*:

$$\det(Id - \Lambda) = \mathbb{Z}^2 \quad (13.1)$$

The original proof of Kac and Ward [72] famously contained an error. We refer the reader to ref. [74] for a longer discussion on the history of this theorem. The main improvement here, in comparison with ref. [74], is that there is no need for expanding the generating functions into generating functions of collections of loops. The combinatorial mechanism of the Kac-Ward formula is here as transparent as the one of the loop-erased walks.

Chertkov, Chernyak and Teodorescu [19] *Belief propagation and loop series on planar graphs*, write: “ We discuss a generic model of Bayesian inference with binary variables defined on edges of a planar graph. The Loop Calculus approach of Chertkov and Chernyak [18] is used to evaluate the resulting series expansion for the partition function. We show that, for planar graphs, truncating the series at single-connected loops reduces, via a map reminiscent of the Fisher transformation [42], to evaluating the partition function of the dimer-matching model on an auxiliary planar graph. Thus, the truncated series can be easily re-summed, using the Pfaffian formula of Kasteleyn [76]. This allows us to identify a big class of computationally tractable planar models reducible to a dimer model via the Belief Propagation (gauge) transformation. The Pfaffian representation can also be extended to the full Loop Series, in which case the expansion becomes a sum of Pfaffian contributions, each associated with dimer matchings on an extension to a subgraph of the original graph. Algorithmic consequences of the Pfaffian representation, as well as relations to quantum and non-planar models, are discussed. ”

“ As the seminal work of Onsager [103] on the two-dimensional Ising model and its combinatorial interpretation by Kac and Ward [72] have shown, the planarity constraint dramatically simplifies statistical calculations. ”

Onsager [103] computed the free energy, and Yang [135] obtained a formula for the magnetization. In particular, this formula implies that the magnetization is zero at criticality. These results have been reproved in a number of papers since then. See Werner [130] for a recent proof.

Onsager’s computation of the free energy is based on the study of the eigenvalues of the so-called transfer matrices. The original strategy used by Onsager is based on the fact that the transfer matrix is the product of two matrices whose commutation relations generate a finite dimensional Lie algebra. Later on, Kaufman [79] gave a simpler solution using Clifford algebra and anti-commuting spinor (free-fermion) operators.

The most famous expansions of the partition function are called the low and high temperature expansions. An expansion in terms of subgraphs of the original graph, called the random-cluster model, was found by Fortuin and Kasteleyn [44]. The strength of all these expansions is that they work for all graphs. They do not lead to an explicit computation of the partition function or the free energy, but they provide new insight and often highlight specific properties of the model.

2019-11-04 Predrag Ivashkevich, Izmailian and Hu [65] Kronecker’s double series and exact asymptotic expansions for free models of statistical mechanics on torus:

Consider a planar square lattice of size $M \times N$ with periodic boundary conditions, i.e. torus. To each site (m, n) of the torus a spin variable is ascribed, s_{mn} , with two possible values: +1 or -1. Two nearest neighbor spins, say s_{mn} and $s_{m,n+1}$ contribute a term $-J s_{mn} s_{m,n+1}$ to the Hamiltonian, where J is some fixed energy. Therefore, the Ising model Hamiltonian is the sum of all such terms, one for each edge of the lattice

$$H(s) = -J \sum_{n=0}^{N-1} \sum_{m=0}^{M-1} (s_{mn} s_{m+1,n} + s_{mn} s_{m,n+1}) \quad (13.2)$$

(Predrag:) Note that this can be written in terms of a shift matrices σ_j as

$$H(s) = -J s^\top \cdot (\sigma_1 + \sigma_2) \cdot s,$$

which looks asymmetric - check whether this has a lattice Laplacian formulation?

The partition function of the Ising model is given by the sum over all spin configurations on the lattice

$$Z_{\text{Ising}}(J) = \sum_{\{s\}} e^{-H(s)}$$

It is convenient to set up another parameterizations of the interaction constant J in terms of the mass variable $\mu = \ln \sqrt{\sinh 2J}$. Critical point corresponds to the massless case $\mu = 0$.

An explicit expression for the partition function of the Ising model on $M \times N$ torus, which was given originally by Kaufmann [79], can be written as

$$Z_{\text{Ising}}(\mu) = \frac{1}{2} \left(\sqrt{2} e^\mu \right)^{MN} \left\{ Z_{\frac{1}{2}, \frac{1}{2}}(\mu) + Z_{0, \frac{1}{2}}(\mu) + Z_{\frac{1}{2}, 0}(\mu) + Z_{0, 0}(\mu) \right\} \quad (13.3)$$

where we have introduced the partition function with twisted boundary conditions

$$Z_{\alpha, \beta}^2(\mu) = \prod_{n=0}^{N-1} \prod_{m=0}^{M-1} 4 \left[\sin^2 \left(\frac{\pi(n+\alpha)}{N} \right) + \sin^2 \left(\frac{\pi(m+\beta)}{M} \right) + 2 \sinh^2 \mu \right] \quad (13.4)$$

Here $\alpha = 0$ corresponds to the periodic boundary conditions for the underlying free fermion in the N -direction while $\alpha = \frac{1}{2}$ stands for anti-periodic boundary conditions. Similarly β controls boundary conditions in M -direction. With the help of the identity [48]

$$4 |\sinh(M\omega + i\pi\beta)|^2 = 4 [\sinh^2 M\omega + \sin^2 \pi\beta] = \prod_{m=0}^{M-1} 4 \left[\sinh^2 \omega + \sin^2 \left(\frac{\pi(m+\beta)}{M} \right) \right] \quad (13.5)$$

partition function the partition function with twisted boundary conditions $Z_{\alpha, \beta}$ can be transformed into simpler form

$$Z_{\alpha, \beta}(\mu) = \prod_{n=0}^{N-1} 2 \left| \sinh \left[M\omega_\mu \left(\frac{\pi(n+\alpha)}{N} \right) + i\pi\beta \right] \right| \quad (13.6)$$

where lattice dispersion relation has appeared

$$\omega_\mu(k) = \operatorname{arcsinh} \sqrt{\sin^2 k + 2 \sinh^2 \mu} \quad (13.7)$$

This is nothing but the functional relation between energy ω_μ and momentum k of a free quasi-particle on the planar square lattice.

2019-11-04 Predrag Ivashkevich, Izmailian and Hu [65] Elliptic Theta Functions. We adopt the following definition of the elliptic θ -functions:

$$\begin{aligned} \theta_{\alpha, \beta}(z, \tau) &= \sum_{n \in \mathbb{Z}} \exp \left\{ \pi i \tau \left(n + \frac{1}{2} - \alpha \right)^2 + 2\pi i \left(n + \frac{1}{2} - \alpha \right) (z + \frac{1}{2} - \beta) \right\} \\ &= \eta(\tau) \exp \left\{ \pi i \tau \left(\alpha^2 - \alpha + \frac{1}{6} \right) + 2\pi i \left(\frac{1}{2} - \alpha \right) (z + \frac{1}{2} - \beta) \right\} \\ &\times \prod_{n=0}^{\infty} \left[1 - e^{2\pi i \tau(n+\alpha) - 2\pi i(z-\beta)} \right] \left[1 - e^{2\pi i \tau(n+1-\alpha) + 2\pi i(z-\beta)} \right] \end{aligned}$$

These should be compared with the notations of Mumford.

The elliptic θ -functions satisfies the heat equation

$$\frac{\partial}{\partial \tau} \theta_{\alpha,\beta}(z, \tau) = \frac{1}{4\pi i} \frac{\partial^2}{\partial z^2} \theta_{\alpha,\beta}(z, \tau) \quad (13.8)$$

2020-12-23 Predrag Kaufman [79] *Crystal statistics. II. Partition function evaluated by spinor analysis* is an impressive paper, bug I hope we do not need it.

2020-06-16 Predrag Machide [92] *An elliptic analogue of generalized Dedekind-Rademacher sums:* “We mention a relation between the generating function of Kronecker’s double series [65] and that of the (Debye) elliptic polylogarithms studied by A. Levin.”

Machide [93] *Sums of products of Kronecker’s double series*

2020-06-16 Predrag Shanker [115] *Exact solution of Ising model in 2d shortcut network*

Janke and Kenna [69] *Finite-size scaling and corrections in the Ising model with Brascamp-Kunz boundary conditions*

Izmailian, Oganesyan and Hu [68] *Exact finite-size corrections for the square-lattice Ising model with Brascamp-Kunz boundary conditions*

Wu and Hu [133] *Exact partition functions of the Ising model on $M \times N$ planar lattices with periodic-aperiodic boundary conditions*

Kastening [78] *Simplified transfer matrix approach in the two-dimensional Ising model with various boundary conditions*

Izmailian [66] *Finite-size effects for anisotropic 2D Ising model with various boundary conditions,*

Lyberg [91] *Free energy of the anisotropic Ising lattice with Brascamp-Kunz boundary conditions*

Poghosyan, Izmailian and Kenna [106] *Exact solution of the critical Ising model with special toroidal boundary conditions*

2020-06-19 Predrag Okabe, Kaneda, Kikuchi and Hu [102] *Universal finite-size scaling functions for critical systems with tilted boundary conditions*, deal with the two-dimensional Ising model on $\ell \times T$ square lattices with periodic boundary conditions in the horizontal ℓ direction and tilted boundary conditions in the vertical T direction, such that the i -th site in the first row is connected with the $\text{mod}(i + c\ell, \ell)$ -th site in the T row of the lattice, where $1 \leq i \leq \ell$; see figure 13.1. They find that the finite-size scaling functions are universal for fixed sets of aspect ratio $a = \ell/T$ and tilt parameter $c = S/\ell$.

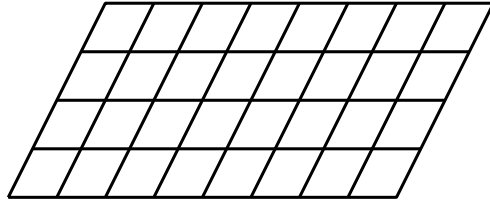


Figure 13.1: $\ell \times T$ square lattice with tilt parameter c . Here, $\ell = 8$, $T = 4$ and $c = 1/4$, so $S = \ell/4$. The i -th site of the first row is identical with the $\text{mod}(i + cl, \ell)$ -th site in the last row. The left-most site and the right-most site on the same horizontal line are identical.

It is interesting to discuss this problem in terms of the modular (conformal) transformation. According to Cardy [15], the shape of the 2D lattice may be represented by the imaginary number

$$z = 1/a + i c. \quad (13.9)$$

Then, Cardy asserted that the partition function becomes invariant under the transformations

$$z \rightarrow z + i \quad (13.10)$$

and

$$z \rightarrow 1/z, \quad (13.11)$$

in the limit that the system size becomes infinite. The first translates, the 2nd inverts: these are easiest to understand in the complex upper half-plane, see figure 13.2.

2021-01-08 Predrag Lecian [85] discusses this group in detail in [arXiv:1303.6343](#), see ‘big billiard’, ‘small billiard’, Sect. III.A. *The modular group*, Maass wavefunctions.

We have another invariant transformation

$$z \rightarrow z^*, \quad (13.12)$$

which corresponds to the fact that we can confine c to the interval of $0 \leq c \leq 1/2$. Starting from the recurrence relation

$$z_{n+1} = \frac{1}{z_n + i} + i, \quad (13.13)$$

we can easily show that (recheck! T, ℓ rewrite wrong as it stands)

$$A = a/(c^2 a^2 + 1) = \frac{T}{\ell} \frac{1}{\frac{S^2}{\ell^2} \frac{T^2}{\ell^2} + 1} \quad (13.14)$$

is an invariant, and can be regarded as the effective aspect ratio.

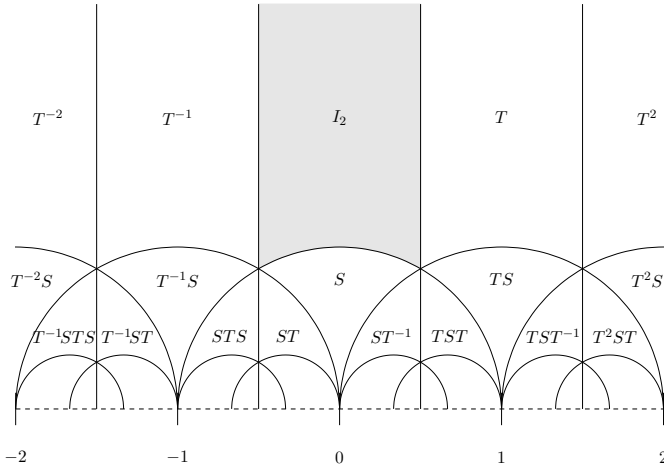


Figure 13.2: Action of $\text{SL}_2(\mathbb{Z})$ on the complex upper half-plane by linear fractional transformations T and S . Taken from Keith Conrad.

2020-10-16 Predrag For me the problem is that I do not see any of the above formulas in Cardy [15], except for (13.9) that might correspond to his figure of a parallelepiped. I understand nothing in the paper. He writes thoug something intriguing: “the symmetry of the parallelogram, which corresponds to the invariance of $Z(\delta)$ under the modular group, has recently been exploited to limit the possible gauge groups in heterotic string theories by D. Gross, J. Harvey, E. Martinec and R. Rohm, Phys. Rev. Lett. 54 (1985) 502.” I would stay far away from such references.

2020-06-19 Predrag Ziff, Lorentz and Kleban [137] *Shape-dependent universality in percolation*, arXiv:cond-mat/9811122.

The torus with a twist has various topological symmetries that apply to any shape-dependent universal quantity $u(r, t)$. We consider a rectangular boundary with base 1 and height r , with a horizontal twist t in the periodic b. c. (Note that having twists in two directions leads to a non-uniform system, so we don’t consider it.) $u(r, t)$ satisfies the obvious symmetries of reflection

$$u(r, t) = u(r, -t) \quad (13.15)$$

and periodicity in the t direction

$$u(r, t) = u(r, 1 + t) \quad (13.16)$$

Another symmetry follows from the observation that the same rhombus can be made into a rectangle in two different ways, leading to:

$$u(r, t) = u\left(\frac{r}{r^2 + t^2}, \frac{t}{r^2 + t^2}\right) \quad (13.17)$$

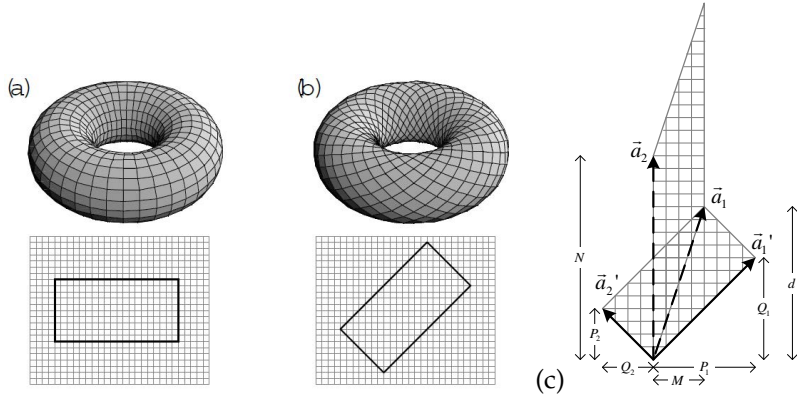


Figure 13.3: A helical tiling is formed by pairwise joining of the edges of the rectangle spanned by an orthogonal set of basis vectors in the \mathbb{Z}^2 lattice: (a) the direction of the basis vectors coincides with the lattice orientations for the conventional toroidal bc's, and (b) a helical torus. (c) Equivalence between the bc's in helical and twisted schemes prescribed by $\{\vec{a}_1, \vec{a}_2\}$ and $\{\vec{a}'_1, \vec{a}'_2\}$ respectively, on a $[M \times N]$ square lattice. For the helical bc's, the setting $Q_1/P_1 = Q_2/P_2$ ensures that the two primitive vectors are orthogonal. On the other hand, twisting is generated by a d -unit traverse shift.

Another construction shows that when $t = 1/n$ where n is an integer,

$$u\left(r, \frac{1}{n}\right) = u\left(\frac{1}{n^2 r}, \frac{1}{n}\right) \quad (13.18)$$

which also follows from Eqs. (13.15-13.17). On the complex $\tau = t + ir$ plane, (13.17) corresponds to $\tau \rightarrow 1/\tau$ while (13.16) corresponds to $\tau \rightarrow \tau + 1$. These transformations generate the modular group, and functions invariant under them are called modular. Thus, $b(r, t)$ must necessarily be a modular function.

Besides the excess number, another universal quantity on a torus is the cross-configuration probability $\pi_+(r, t)$, which can be expressed in a quite compact form. Things veer off to Dedekind eta function and such, and Predrag gives up.

2020-06-19 Predrag Liaw et al. Exact treatment of Ising model on the helical tori, arXiv:cond-mat/0512262, published as Liaw et al. [87] *Partition functions and finite-size scalings of Ising model on helical tori*: The exact closed forms of the partition functions of a two-dimensional Ising model on square lattices with twisted bc's are given.

A helical torus is related to the twisted boundary conditions tiling by an $SL_2(\mathbb{Z})$ transformation. In $d = 2$, the equivalence transformations among the Bravais cell vector-pairs preserve the area and are thus $SL_2(\mathbb{Z})$. This is the prototype of the modular symmetry of the conformal field theory.

In figure 13.3 they make a distinction between the ‘*helical*’, and the equivalent ‘*twisted*’ tiles.

Helical tori are tiled by pairwise joining the edges of the rectangle spanned by any orthogonal set of vectors on the lattice plane. This leads to distinct orientations of the underlying lattice, labelled by the chirality [sahito] as well as the chiral aspect ratio. The conventional periodic BC is referred as the helical Bravais cell with trivial chirality, as depicted in figure 13.3(a).

The twisted BC Bravais cell is a modification to the conventional Bravais cell by cutting the torus and then rejoining after twisting. Twisted tori are what we call Hermite normal form Bravais cells. There are two types of twisting: $Tw_I(M, N, d/M)$ Bravais cell specified by $\{\vec{d}_1 = M\hat{x} + d\hat{y}, \vec{d}_2 = N\hat{y}\}$, and $Tw_{II}(M, N, d/N)$ Bravais cell specified by $\{\vec{d}_1 = M\hat{x}, \vec{d}_2 = d\hat{x} + N\hat{y}\}$ used in ref. [34].

In CL18 [34] notation: $Tw_{II}(\ell, T, S/T)$ Bravais cell is specified by $\{\vec{d}_1 = \ell\hat{x}, \vec{d}_2 = S\hat{x} + T\hat{y}\}$.

It suffices to study the unique correspondence of a helical torus to the one of the above twistings, say Tw_I .

The helical tori Bravais cell is given by the orthogonal basis vector pair,

$$\begin{aligned}\vec{d}'_1 &= \hat{x} P_1 + \hat{y} Q_1, \\ \vec{d}'_2 &= -\hat{x} Q_2 + \hat{y} P_2,\end{aligned}\tag{13.19}$$

where the two radii for the torus are given as $L_i = \sqrt{P_i^2 + Q_i^2}$ for $i = 1, 2$. They denoted the helical system by $Hl(B, L_1, \chi)$, where the chiral aspect ratio $B = L_2/L_1$ and the chirality $\chi = Q_1/P_1 \equiv Q_2/P_2$. In order to furnish the equivalent structure $Hl(B, L_1, \chi) \cong Tw_I(A, M, \alpha)$, $\mathcal{M}_{11} = P_1/M$ and $\mathcal{M}_{21} = -Q_2/M$ implies that

$$\mathcal{M}_{21} = -B\chi\mathcal{M}_{11}\tag{13.20}$$

$$1 = \mathcal{M}_{11}\mathcal{M}_{22} - \mathcal{M}_{21}\mathcal{M}_{12}.\tag{13.21}$$

$$A = \frac{(\mathcal{M}_{21})^2}{B} + B(\mathcal{M}_{11})^2,\tag{13.22}$$

$$\alpha = -\frac{\mathcal{M}_{21}\mathcal{M}_{22}}{B} - B\mathcal{M}_{11}\mathcal{M}_{12}.\tag{13.23}$$

The helical Bravais cell is a subclass of twisted one by an $SL_2(\mathbb{Z})$ equivalence relation, figure 13.3(c) and (13.17).

They refer to $\alpha = d/M$ (our notation: $\alpha = S/T$) as a “twisting factor”.

$Q_{M,N}^\alpha = Q_{M,N}^{-\alpha}$ as twisting either clockwise or counterclockwise is not distinguished by the energy. Note that reversing the sign of a twist factor α is not an $SL_2(\mathbb{Z})$ transformation.

The $[M \times N]$ square lattice with the helicity factor $d = D/M$, the system has periodic boundary conditions in the N direction and helical (tilted)

boundary conditions in the M direction such that the i-site in the first column is connected with the $\mod(i + D, M)$ th site in the N column of the lattice.

R. Sahito, G. Dresselhaus and M. S. Dresselhaus, *Physical properties of Carbon Nanotubes*, (Imperial College Press, London, 1998).

Alexi Morin-Duchesne, Paul A. Pearce and Jorgen Rasmussen *Modular invariant partition function of critical dense polymers*, arXiv:1303.4895: [...] The torus is formed by gluing the top and bottom of the cylinder. This gives rise to a variety of non-contractible loops winding around the torus. [...] a parameter v that keeps track of the winding of defects on the cylinder. [...] The modified trace is constructed as a linear functional on planar connectivity diagrams in terms of matrix traces Tr_d (with a fixed number of defects d) and Chebyshev polynomials of the first kind.

We assume helical boundary conditions in x-direction, i.e., $\phi_{L_x+1,y} = \phi_{1,y+1}$, and periodic boundaries in y-direction.

2020-06-16 Predrag Izmailian and Hu [67] *Finite-size effects for the Ising model on helical tori:* “ We analyze the exact partition function of the Ising model on a square lattice under helical boundary conditions obtained by Liaw *et al.* [87]. We find that finite-size corrections for the free energy, the internal energy, and the specific heat of the model in a crucial way depend on the helicity factor of the lattice. ”

2019-11-04 Predrag Hobrecht and Hucht [56]

Anisotropic scaling of the two-dimensional Ising model I: the torus: They compute the partition function and the free energy of the finite two-dimensional square lattice Ising model with periodic boundary conditions.

The problem of finding the generating function of the closest-packed dimer configurations on an arbitrary planar graph was solved by Kasteleyn in terms of Pfaffians, as it gives the number of *perfect matchings* of a given directed planar graph with an even number of sites. This is especially powerful because of the connection between the Pfaffian and the determinant, namely

$$(\text{Pf } \mathcal{A})^2 = \det \mathcal{A}. \quad (13.24)$$

[...] The nearest-neighbour structure in a row and a column are both represented by the $[n \times n]$ matrix

$$\mathbf{H}_{b,n} = \begin{pmatrix} 0 & 1 & 0 & \cdots & 0 \\ 0 & 0 & 1 & & 0 \\ \vdots & & & \ddots & \vdots \\ 0 & 0 & 0 & & 1 \\ -b & 0 & 0 & \cdots & 0 \end{pmatrix}, \quad (13.25)$$

with $b \in \{+1, 0, -1\}$ accounting for $b = 0$ open, $b = +1$ periodic, and $b = -1$ for anti-periodic boundary conditions. $b = -1$ accounts for periodic boundaries on the directed graph, i.e., in the dimer system, in the sense that all edges are likewise aligned, while it accounts for antiperiodic BCs in the Ising model. However, the topology of the underlying directed graph is not representative for the Ising model, which is emphasised by the fact that the Ising partition function is a combination of four Pfaffians.

[...] the characteristic polynomials are

$$\mathcal{P}_\beta^\pm(N; \varphi) = \prod_{m=0}^{N-1} \left(e^{\pm i\varphi} - e^{i\varphi_m^{(\beta)}} \right) = e^{\pm iN\varphi} + \beta \quad (13.26)$$

with

$$\varphi_m^{(\beta)} = \begin{cases} 2m\pi/N & \text{if } \beta = -1 \\ (2m+1)\pi/N & \text{if } \beta = +1 \end{cases} \quad (13.27)$$

for $m \in \{0, 1, 2, \dots, N-1\}$, and thus we will call $\beta = -1$ even and $\beta = +1$ odd. Note that the eigenvalues lie equidistantly on the unit circle and thus we have a free shifting parameter for the spectrum. We have chosen it in such a way, that the eigenvalue $\varphi_0^{(-)} = 0$ appears in the even spectrum; a shift by $-\pi$ on the other hand would have given rise to a dependency on whether N is even or odd.

Characteristic polynomials (13.26) have a simple scaling form as one only have to replace $\varphi = \Phi/N$ to obtain

$$\mathcal{P}_e^\pm(\Phi) = e^{\pm i\Phi} - 1, \quad (13.28a)$$

$$\mathcal{P}_o^\pm(\Phi) = e^{\pm i\Phi} + 1. \quad (13.28b)$$

They compute variety of determinants. Particularly suggestive is the product formula for translational invariance in both directions, their eq. (2.32), that looks like Han's determinant. This was previously computed by McCoy & Wu for the anisotropic torus [97]. There is an interesting matrix for the torus, their eq. (4.3). All in all, looks harder than what we need for the spatiotemporal cat.

2019-11-04 Predrag Baxter [9] *The bulk, surface and corner free energies of the square lattice Ising model*

Hucht [61] *The square lattice Ising model on the rectangle I: finite systems*

Hobrecht and Hucht [57] *Anisotropic scaling of the two-dimensional Ising model II: surfaces and boundary fields*

13.1 Ihara zeta functions

2020-05-12 Predrag .

- I think it should be little work to verify for temporal cat that the Boss determinant (13.47), (13.60), (13.67) for the Ihara zeta function (that counts undirected loops) is the Isola's Bowen-Ruelle zeta (13.74). This counts walks of the cat map directed Markov graph.
- Clair's square 2D lattice (13.45) presumably counts 1D loops (returning walks) on a 2D lattice. So does Kasteleyn [77] elliptic integral of the first kind (13.49) (see also (5.251)).
- For spatiotemporal cat we count 2D tori (Bravais lattices); expect a variable z_j for every translational symmetry direction, not a single z as in (13.49). In Ising models, one counts the 2D configurations - so how come Ihara functions can do that? Or can they?
- Explain the relation between a discrete torus and the Cayley graph. For example, given $n \in \mathbb{N}^*$, let G_n denote the Cayley graph $(\mathbb{Z}/n\mathbb{Z}, \{\pm 1\})$.

13.1.1 Heat equation

¹ Let T_{nt} be temperature at spatial site n at time t . The heat equation for temperature field $\mathbf{T} = \{T_{nt}\}$ is

$$\partial_t \mathbf{T} = D \Delta_x \mathbf{T}, \quad (13.29)$$

where D is the diffusion constant. Convert this into an integer lattice difference equation over a finite spacetime domain by the same rescaling as for (5.103). Then the heat difference equation for temperature field $\mathbf{T} = \{T_{nt}\}$ over a finite tile $[\ell \times T]_S$ is

$$\partial_t \mathbf{T} = \beta \Delta_x \mathbf{T}, \quad (13.30)$$

In the space and time continuum limits, β is related to the diffusion constant by

$$\beta = \frac{\Delta t}{(\Delta x)^2} D = \frac{\ell^2}{T} D.$$

13.1.2 Heat kernel

2020-05-05 Predrag Jorgenson and Lang [71] *The ubiquitous heat kernel*

2020-05-13 Predrag For general regular graphs with a transitive group action, in particular the discrete tori, a zeta function has been defined in an impressive paper by Chinta, Jorgenson and Karlsson [21] *Heat kernels on regular graphs and generalized Ihara zeta function formulas*: Let q be a positive integer and G be a $(q+1)$ -regular graph. There is an associated heat

¹Predrag 2020-03-15: I like Elaydi [41]'s Sect. 3.5.5 *The heat equation*

kernel $K_G(t, x_0, x)$ corresponding to the Laplacian formed by considering the adjacency matrix on G . The building blocks of K_G are I-Bessel functions, and the number of geodesics from a fixed base point x_0 to x of length m .

N_m^0 denotes the number of closed geodesics of length m in G with base point x_0 .

They give a clear introduction into heat kernels on graphs, the origin of I-Bessel functions, and the relation to the number of paths. They also deduce the classical Ihara determinantal formula.

There is a second expression for the heat kernel coming from spectral considerations. Equating the two expressions for the heat kernel, as in known approaches to the Poisson summation formula or the Selberg trace formula, one obtains an identity which is a type of theta inversion formula. To this identity they apply an integral transform, a Laplace transform with a change of variables, and obtain the logarithmic derivative of the Ihara zeta function.

For finite graphs, the classical Ihara zeta function is their Ihara zeta function raised to the power equaling the number of vertices (by fixing the base point x_0 , they can work with infinite graphs). They give a formula, their Theorem 1.3, for $1/\zeta$ as an integral over the spectral measure for the Laplacian.

They also count geodesics paths, not only closed geodesics paths. That corresponds to computing the Hurwitz zeta function instead of the Riemann zeta function, they say.

2020-05-13 Predrag Chinta, Jorgenson and Karlsson [20] *Zeta functions, heat kernels, and spectral asymptotics on degenerating families of discrete tori:*

By a discrete torus we mean the Cayley graph associated to a finite product of finite cycle groups with the generating set given by choosing a generator for each cyclic factor.

We examine the spectral theory of the combinatorial Laplacian for sequences of discrete tori when the orders of the cyclic factors tend to infinity at comparable rates. First, we show that the sequence of heat kernels corresponding to the degenerating family converges, after rescaling, to the heat kernel on an associated real torus.

We then establish an asymptotic expansion, in the degeneration parameter, of the determinant of the combinatorial Laplacian. The zeta-regularized determinant of the Laplacian of the limiting real torus appears as the constant term in this expansion.

By a classical theorem by Kirchhoff, the determinant of the combinatorial Laplacian of a finite graph divided by the number of vertices equals the number of spanning trees, called the complexity, of the graph. As a result, we establish a precise connection between the complexity of the Cayley graphs of finite abelian groups and heights of real tori.

It is also known that spectral determinants on discrete tori can be expressed using trigonometric functions and that spectral determinants on real tori can be expressed using modular forms on general linear groups. Another interpretation of our analysis is thus to establish a link between limiting values of certain products of trigonometric functions and modular forms. The heat kernel analysis which we employ uses I-Bessel functions. Our methods extend to prove the asymptotic behavior of other spectral invariants through degeneration, such as special values of spectral zeta functions and Epstein-Hurwitz-type zeta functions.

For any $d \geq 1$, let $N = (n_1, \dots, n_d)$ denote a d -tuple of positive integers, and consider the product

$$D(N) = \prod_{K \neq 0} (2d - 2 \cos(2\pi k_1/n_1) - \dots - 2 \cos(2\pi k_d/n_d)); \quad (13.31)$$

where the product is over all d -tuples $K = (k_1, \dots, k_d)$ of non-negative integers with $k_j < n_j$, omitting the zero vector in the product.

One can view $D(N)$ as a determinant of a naturally defined matrix from graph theory. Quite generally, associated to any finite graph, there is a discrete Laplacian which acts on the finite dimensional space of complex valued functions whose domain of definition is the space of vertices of the graph. $D(N)$ is equal to the product of the non-zero eigenvalues of the Laplacian associated to a graph which we call a discrete torus.

The d -dimensional discrete torus is defined as the product space

$$DT_N = \prod_{j=1}^d \ell_j \mathbb{Z} \backslash \mathbb{Z},$$

See also

Yamasaki [134] *An explicit prime geodesic theorem for discrete tori and the hypergeometric functions*

Anders Karlsson *Spectral zeta functions*, [arXiv:1907.01832](https://arxiv.org/abs/1907.01832)

2020-06-04 Predrag Evgeny L. Korotyaev and Jacob Schach Møller [82], korotyaev@gmail.com, jacob@math.au.dk, [arXiv:1701.03605](https://arxiv.org/abs/1701.03605): *Weighted estimates for the Laplacian on the cubic lattice*:

The starting point for their analysis is a representation of the summation kernel of the free resolvent (the propagator) in terms of a product of Bessel functions.

The momentum representation of the discrete Laplacian: one may diagonalize the discrete Laplacian, using the (unitary) Fourier transform $\Phi: \ell^2(\mathbb{Z}^d) \rightarrow L^2(\mathbb{T}^d)$, where $\mathbb{T} = \mathcal{R}/(2\pi\mathbb{Z})$. It is defined by

$$(\Phi f)(k) = \widehat{f}(k) = 1/(2\pi)^{d/2} \sum_{n \in \mathbb{Z}^d} f_n e^{in \cdot k}, \quad \text{where } k = (k_j)_{j=1}^d \in \mathbb{T}^d.$$

Here $k \cdot n = \sum_{j=1}^d k_j n_j$ is the scalar product in \mathcal{R}^d . In the resulting momentum representation of the discrete Laplacian Δ , we write $\widehat{\Delta} = \Phi \Delta \Phi^*$. The Laplacian is transformed into a multiplication operator

$$(\widehat{\Delta} \widehat{f})(k) = \left(\sum_{j=1}^d \cos k_j \right) \widehat{f}.$$

The operator $e^{it\Delta}$, $t \in \mathcal{R}$ is unitary on $L^2(\mathbb{T}^d)$ and has the kernel $(e^{it\Delta})(n - n')$, where for $n \in \mathbb{Z}^d$:

$$\begin{aligned} (e^{it\Delta})(n) &= 1(2\pi)^d \int_{\mathbb{T}^d} e^{-in \cdot k + it \sum_{j=1}^d \cos(k_j)} dk \\ &= \prod_{j=1}^d \left(\frac{1}{2\pi} \int_0^{2\pi} e^{-in_j k + it \cos(k)} dk \right) = i^{|n|} \prod_{j=1}^d J_{n_j}(t), \end{aligned}$$

where $|n| = n_1 + \cdots + n_d$. Here $J_n(z)$ denotes the Bessel function:

$$J_n(t) = (-i)^n 2\pi \int_0^{2\pi} e^{ink - it \cos(k)} dk \quad \forall (n, z) \in \mathbb{Z} \times \mathbb{R}.$$

The rest is all about bounds, we can safely ignore it.

2020-05-14 Predrag Jérémie Dubout Jeremy.Dubout@unige.ch is a smart cookie. I'm very impressed by Dubout [39] *Zeta functions of graphs, their symmetries and extended Catalan numbers*, arXiv:1909.01659:

It is natural to form symmetric functions of the eigenvalues of operators, in finite dimensions one has the trace and determinant. In infinite dimensions things become more complicated. For example, the determinant of the Laplace operator on a manifold cannot be directly defined, but the following the heat kernel function can

$$\zeta_M(s) = \sum_{n \in \mathbb{N}} \lambda_n^{-s} = \frac{1}{\Gamma(s)} \int_0^\infty \text{tr} (e^{-t\Delta}) t^s \frac{dt}{t}, \quad (13.32)$$

for s in the half-plane $\{s | \text{Re}(s) > 0\}$. Since graphs have a natural Laplacian Δ , Dubout considers sums over the eigenvalues as in (13.32), and introduces the *spectral zeta function* of a graph G as

$$\zeta_G(s) = \int_{\sigma(\Delta)} x^{-s} \mu_\Delta^{\delta_v, \delta_v}(dx),$$

where $\mu_\Delta^{\delta_v, \delta_v}(dx)$ is a spectral measure of the Laplacian. ζ_G provides an analogue of the right hand side of (13.32) for graphs. Dubout introduces a heat function H_t for infinite graphs [46] as an analogue of the heat kernel for manifolds:

$$\zeta_G(s) = \frac{1}{\Gamma(s)} \int_0^\infty H_t^G t^s \frac{dt}{t}.$$

This spectral zeta function recovers both previous definitions for finite graphs, the lattice \mathbb{Z}^d and the infinite d -regular tree. Dubout extends the \mathbb{Z} functional equation [46] to \mathbb{Z}^2 . For more general s and $d > 2$ the existence of such symmetries remains unknown. The formula acts can interpreted as a symmetry for Catalan numbers. Dubout is able to describe ζ_G explicitly for $G = \mathbb{Z}^d$ as well as for products for integers values.

Contrary to the compact manifold case, the heat kernel of an infinite graph is not always a trace-class operator. Instead of taking its trace, Dubout therefore evaluates it on the rooted graph, at some cost.

The resolvent

$$R(z, \Delta) = \frac{1}{z - \Delta}.$$

The heat kernel of \mathbb{Z} is given by

$$H_t^{\mathbb{Z}} = \int_0^4 \frac{e^{-tx}}{\pi \sqrt{x(4-x)}} dx = e^{-2t} I_0(2t),$$

where I_0 a modified Bessel function of first kind, the same as ref. [75] (up to a factor 2, coming from their normalization of the Laplacian). Dubout extends this result to \mathbb{Z}^d with

$$H_t^{\mathbb{Z}^d} = e^{-2dt} I_0(2t)^d.$$

The spectral zeta function of \mathbb{Z} is given by

$$\begin{aligned} \zeta_{\mathbb{Z}}(s) &= \int_0^4 x^{-s} \frac{1}{\pi \sqrt{x(4-x)}} dx = \frac{1}{\pi} \int_0^1 4^{-s} x^{-s-\frac{1}{2}} (1-x)^{-\frac{1}{2}} dx \\ &= \frac{4^{-s}}{\pi} \mathbf{B}\left(\frac{1}{2} - s, \frac{1}{2}\right) = \frac{4^{-s}}{\sqrt{\pi}} \frac{\Gamma\left(\frac{1}{2} - s\right)}{\Gamma(1-s)}, \end{aligned} \quad (13.33)$$

where \mathbf{B}, Γ are the beta and gamma functions.

The function $\zeta_{\mathbb{Z}}$ is meromorphic over $\mathbb{C} \setminus \{\frac{1}{2}, \frac{3}{2}, \dots\}$ and satisfies

$$\zeta_{\mathbb{Z}}(s) = \binom{-2s}{-s}$$

for any s .

For a finite transitive graph G with n vertices, the spectral zeta function ζ_G can be written in explicit form, similar to the one in the first part of Equation 13.32, and analytically continued over \mathbb{C} with the formula

$$\zeta_G(s) = \frac{1}{n} \sum_{\lambda \neq 0} \lambda^{-s}, \quad (13.34)$$

where the sum is over the non-zero eigenvalues of Δ_G . The Lebesgue's decomposition theorem allows us to split the spectral measure into an

absolutely continuous part, a singular continuous part and a pure point part. The only issue with ζ_G 's analyticity is the presence of 0 in the spectrum: A graph G is finite if and only if 0 belongs to the pure point part. Dubout then does some serious analysis.

Dubout introduces a *regularized* determinant. If G is finite and transitive, then $\det^*(x + \Delta) = \det(x\mathbf{1} + \Delta)^{\frac{1}{|V_G|}}$. In the case of the regularized determinant for \mathbb{Z} , Dubout almost gets the generating function of the Catalan numbers:

$$\det^*(x + \Delta_{\mathbb{Z}}) = \frac{x}{2} + 1 + \frac{1}{2}\sqrt{x(4+x)} = x + 2 + \sum_{n \geq 1} C_n \frac{(-1)^n}{x^n}, \quad (13.35)$$

where $C_n = \frac{1}{n+1} \binom{2n}{n}$ is the n -th Catalan number.

Predrag: Amusing, but I've also run into Catalan numbers while counting rooted trees, back in 1976: Cvitanović [32] *Group theory for Feynman diagrams in non-Abelian gauge theories*

Dubout computes the standard characteristic polynomial of the Laplacian of a cyclic graph, by a new, completely analytical way of obtaining the coefficients. Given $n \in \mathbb{N}^*$, let G_n denote the Cayley graph $(\mathbb{Z}/n\mathbb{Z}, \{\pm 1\})$. Then

$$\det(x + \Delta_{G_n}) = \sum_{l=0}^{n-1} \binom{2n-l}{l} \frac{2n}{2n-l} x^{n-l}. \quad (13.36)$$

The coefficients of $\det(x + \Delta_{G_n})$ can be computed numerically using the eigenvalues of Δ_{G_n} . Dubout gets the our usual discrete Fourier product formula

$$\det(x + \Delta_{G_n}) = \prod_{k=0}^{n-1} \left(x + 4 \sin^2 \left(\frac{k\pi}{n} \right) \right),$$

but he did not find a way to expand this product into a polynomial with integers coefficients.

Predrag: we should alert him to our integer-points counting formulas!

Dubout then relates the Ihara zeta function Z_G [126] of a d -regular finite graph G

$$Z_G(u) = \left((1 - u^2)^{\frac{(d-2)|V_G|}{2}} \det(1 - (d - \Delta_G)u + (d - 1)u^2) \right)^{-1}. \quad (13.37)$$

to his spectral zeta function. Given a d -regular finite graph G with n vertex, the Ihara zeta function of G can be computed as

$$Z_G(u) = (y_u \det^*(x_u + \Delta_G))^{-n}, \quad (13.38)$$

with $y_u = u(1 - u^2)^{\frac{d}{2}-1}$ and $x_u = (1 - \frac{1}{u})(u(d - 1) - 1)$.

The appearance of $|V_G|$ in (13.38) as only an exponent provides good motivation for defining a modified Ihara zeta function that extends to infinite graphs:

The *regularized Ihara zeta function* of a (possibly infinite) d -regular graph G is defined as

$$Z_G^*(u) = u^{-1}(1-u^2)^{1-\frac{d}{2}} \det^* \left(\left(1 - \frac{1}{u}\right) (u(d-1)-1) + \Delta_G \right)^{-1}. \quad (13.39)$$

This coincides with the known one for the Cayley graph of a finitely generated group.

It follows from (13.38) that if G is finite then $Z_G^*(u)^{|V_G|} = Z_G(u)$. This allows us to extend the functional equations to infinite regular graphs.

The regularized determinant of \mathbb{Z} was calculated in (13.35), and following (13.39) he obtains the regularized Ihara zeta function of \mathbb{Z} :

$$Z_{\mathbb{Z}}^*(u) = \begin{cases} 1 & \text{if } 0 < |u| < 1, \\ u^2 & \text{if } |u| > 1. \end{cases} \quad (13.40)$$

Note the functional equation

$$Z_{\mathbb{Z}}^*\left(\frac{1}{u}\right) = \frac{1}{u^2} Z_{\mathbb{Z}}^*(u).$$

That $Z_{\mathbb{Z}}^*(u) = 1$ for $0 < u < 1$ is a natural result, as the original definition of the Ihara zeta function is a generating function of weighted loops, and \mathbb{Z} does not have any, giving us only 1 as generating function. The same argument holds for any tree-like graph.

2020-05-14 Predrag Lenz, Pogorzelski and Schmidt [86] *The Ihara zeta function for infinite graphs*, arXiv:1408.3522, a very lengthy and ambitious paper, apparently gives yet another definition of an Ihara zeta function for infinite graphs. Dubout was unable to determine how it compares to his (13.37). I'm not frisky enough to read this paper, after having gone through Dubout already today...

13.1.3 Clair / Clair14

For the two dimensional integer lattice a zeta function has been defined and computed in Clair [25] *The Ihara zeta function of the infinite grid*

Bryan Clair is a great fan of *Ihara zeta functions*.

Shahriar Mokhtari-Sharghi [26, 27] have shown that Ihara's construction can be extended to infinite graphs on which a discrete group acts isomorphically and with finite quotient. Their works seems to deal with trees, not lattices, though Clair [25] does discuss infinite square lattice, see (13.44).

The Ihara zeta function may be considered as a modification of the Selberg zeta function [8], and was originally written in terms of the variable s , where $z = q^{-s}$. One of main properties of the Ihara zeta function is the *determinant formula*, i.e., that its inverse is the determinant of a matrix-valued polynomial. A consequence of the determinant formula is that the Ihara zeta function meromorphically extends to the whole complex plane, and its completions satisfy a functional equation.

The main formula in all these papers gives a connection between the zeta function, originally defined as an infinite product, and the Laplacian of the graph.

Pollicott [108] explains in *Dynamical zeta functions* Sect. 3.3 what the Laplacian for a undirected graph is, relates it to the adjacency matrix in a somewhat obvious way, as we are used to on a lattice. He defines Ihara for undirected graph

1. the graph G has valency $q+1$ with $q \geq 2$ (i.e., every vertex has $q+1$ edges attached)
2. there is at most one edge between any two vertices
3. there are no edges starting and finishing at the same vertex

He outlines a proof of the Bass determinant formula for the Bowen-Lanford zeta function.

2CB

Loop: A closed path in G , up to cyclic equivalence, without backtracking.

Prime: A loop p which is not a power (a repeat) of another loop.

Back-track: A path has a back-tracking if a subsequence of the form \dots, x, y, x, \dots appears.

The Ihara zeta function of a finite graph G

$$\zeta(z) = \prod_p \frac{1}{1 - z^{n_p}} \quad (13.41)$$

It is instructive to have a look at the octahedral graph in Clair's talk above. There is no self-crossing condition, so $\zeta(z)$ always has an infinity of prime cycles, of arbitrary length (as does any topological zeta function).

As a power series in z , the Ihara zeta has non-negative coefficients, and thus a finite radius of convergence. However, the inverse of the Ihara zeta is a polynomial.

Ihara considered the special case of regular graphs (those all of whose vertices have the same degree; i.e., the same number of oriented edges coming out of the vertex). A graph is k -regular if every vertex has degree k .

Terras [126] defines the $m \times m$ adjacency matrix as,

$$A_{ij} = \begin{cases} k & \text{if a transition } \mathcal{M}_j \rightarrow \mathcal{M}_i \text{ is possible in } k \text{ ways} \\ 2\ell_j & \text{if } i = j \\ 0 & \text{otherwise,} \end{cases} \quad (13.42)$$

where ℓ_j is the number of loops at vertex j . She then assigns to every of the e unoriented edges a pair of oriented edges. Her graphs are finite, connected and undirected, without "backtracks" and "tails". It will usually be assumed that they contain no degree 1 vertices (called "leaves" or "hair" or "danglers"). We will also usually assume the graphs are not cycles or cycles with hair. A cycle graph is obtained by arranging the vertices in a circle and connecting each vertex to the 2 vertices next to it on the circle. We will allow our graphs to have loops and multiple edges. For any closed loop, the equivalence class is the set of all its cyclic permutations. Two loops are equivalent if they differ only by the starting vertex.

Terras: We do not consider zeta functions of infinite graphs here. Nor do we consider directed graphs. Zeta functions for such graphs are discussed, for example, by Matthew Horton [60].

There is no unique factorization into primes. The only nonprimes are powers of primes. We distinguish prime p from p^{-1} which is the loop traversed in the opposite direction. All graphs have infinity of primes, with exception of the cycle graph that has only 2 primes p, p^{-1} , traversing the vertices in the opposite directions.

Theorem [8, 63]: Consider a finite connected graph G (without degree 1 vertices) with m vertices, e unoriented (or undirected) edges, $\deg m_i$ the number of (undirected) edges going into vertex i . Let A be the adjacency matrix, Q be the $m \times m$ diagonal matrix with $Q_{ii} = \deg m_i - 1$, and $\Delta_z = I - zA + z^2Q$. The (vertex) adjacency matrix A of G is a $m \times m$ matrix whose i,j entry is the number of directed edges from vertex i to vertex j . The matrix Q is a diagonal matrix whose j -th diagonal entry is 1 less than the degree of the j -th vertex. If there is a loop at a vertex, it contributes 2 to the degree.

$$1/\zeta(z) = (1 - z^2)^{e-m} \det \Delta_z \quad (13.43)$$

(then comes Riemann Hypothesis for the spectrum of a regular graph G , and Ramanujan graphs).

See 2020-05-11 Bharatram Rangarajan (13.66) below for another derivation of the same.

Next, consider the 'grid' zeta function for G the infinite grid, i.e., a square 2D lattice. Let $\pi = \mathbb{Z} \times \mathbb{Z}$ be a translation acting on G . The zeta function is still

$$\zeta(z) = \prod_{[p]} \frac{1}{1 - z^{n_p}} \quad (13.44)$$

where $[p]$ is an equivalence class of loops under translation by π :

$$1/\zeta(z) = (1 - z^4)^2(1 - z^6)^4(1 - z^8)^{26}(1 - z^{10})^{152}\dots \quad (13.45)$$

(look at the 8-loops in Clair's talk - there seems to be an extra factor 2 in loop counting. I only see two 6-loops, not four).

On infinite graphs, the adjacency matrix becomes an $\ell^2(\mathbb{Z} \times \mathbb{Z}) \rightarrow \ell^2(\mathbb{Z} \times \mathbb{Z})$ adjacency operator. For the infinite grid,

$$\Delta_z = I - zA + z^3 \quad (13.46)$$

There is still a determinant formula for the zeta function:

$$1/\zeta_\pi(z) = (1 - z^2)\det_\pi \Delta_z. \quad (13.47)$$

With $\pi = \mathbb{Z} \times \mathbb{Z}$, \det_π is an operator determinant:

$$\det_\pi \Delta_z = \exp \text{Tr}_\pi \ln \Delta_z, \quad (13.48)$$

where Tr_π is the trace on the group von Neumann algebra $\mathcal{N}(\pi)$.

The adjacency operator on a square lattice is essentially the 2D Laplacian. Clair throws in the 2D Ising, then Kasteleyn [77] and ends up with

$$1/\zeta_\pi(z) = (1 - z^2)(1 + 3z^2) \exp \mathbf{I}(k), \quad (13.49)$$

with a simple set of singularities, and $\mathbf{I}(k)$ is related to an elliptic integral of the first kind (5.251), expressed in terms of theta functions (whose squares are modular forms of weight 1).

13.1.4 Ihara blog

2016-10-03 Predrag For further discussion, see [Wiki](#), and the notes for equation (13.53).

Ihara zeta function for undirected graphs satisfies a functional equation [126]. The formulation of the graph Riemann Hypothesis in terms of Ihara zeta function is based on the fact that the adjacency matrix of an undirected regular graph is symmetric. There is no analogue of Riemann Hypothesis for directed graphs.

A zeta function of a regular graph G associated to a unitary representation of the fundamental group of G was developed by Sunada [120].

2016-10-03 Predrag I cannot, at the moment, tell the difference between [Ihara](#) and what I call the topological zeta function in [ChaosBook.org](#) (section 18.4; the chapter alone is [here](#)). I find Aizenman's derivation of 2D Onsager solution beautiful - will have to chew on it.

2018-03-22 Predrag Trying to incorporate dynamics into a generalized, time-reversal invariant Laplacian by replacing a time forward cat map A by something like a time reversal invariant combination AA^\top :

Incidence matrix B entries are $b_{ij} = \pm 1$, depending on whether v_i is a target or a source.

For literature and further discussion, see sect. 13.1 *Ihara zeta functions*.

For the finite transition graph figure 18.4 (d) and (18.15) the incidence matrix is (2018-05-02 Predrag as they currently stand, the next two equation are wrong - they should be $[\ell \times \ell]$ matrices, not 2-dimensional ones. Also, the literature discusses only 'simple' graphs, i.e., graphs without 1-loops)

$$\begin{bmatrix} \phi'_A \\ \phi'_B \end{bmatrix} = B\phi = \begin{bmatrix} 2 & 1 \\ -1 & 1 \end{bmatrix} \begin{bmatrix} \phi_A \\ \phi_B \end{bmatrix} \quad (13.50)$$

and

$$BB^\top = \begin{bmatrix} 2 & 1 \\ -1 & 1 \end{bmatrix} \begin{bmatrix} 2 & -1 \\ 1 & 1 \end{bmatrix} = \begin{bmatrix} 5 & -1 \\ -1 & 2 \end{bmatrix}. \quad (13.51)$$

Actually, we need something that acts on the whole chain, some Toeplitz matrix like

$$BB^\top = \begin{bmatrix} -2 & 1 & & & 1 \\ 1 & -2 & 1 & & \\ & 1 & -2 & 1 & \\ & & 1 & \ddots & \\ 1 & & & & 1 \end{bmatrix}, \quad (13.52)$$

but with 2 fields $[\phi_{A,t}, \phi_{B,t}]^\top$ at each site t .

Proposition 17.2. [Godsil and Royle [47]] Given any directed graph G if B is the incidence matrix of G , A is the adjacency matrix of G , and D is the degree matrix such that $D_{ii} = d(v_i)$, then

$$BB^\top = D - A. \quad (13.53)$$

The matrix $L = D - A$ is called the (unnormalized) graph Laplacian of the graph G . BB^\top is independent of the orientation of G and $D-A$ is symmetric, positive, semidefinite; that is, the eigenvalues of D .

Each row of L sums to zero (because $B^\top \mathbf{1} = 0$). Consequently, the vector $\mathbf{1}$ is in the nullspace of L .

The connection between the incidence matrix of a graph and its Laplacian is the well-known equation $L = \partial\partial^\top$.

2021-04-14 Predrag Fan Chung [22] *Spectral Graph Theory* (revised and improved 2006) is the "bible" of spectral graph theory. Should read chapter *Eigenvalues and the Laplacian of a graph*.

See Gabriel Peyré [tweet](#).

Daniel A. Spielman *Spectral and Algebraic Graph Theory* deals with the combinatorial, normalized and random walk version of the Laplacian.

What -I think- is important for us is that any graph Laplacian can be written as

$$\mathcal{L} = SS^\top, \quad (13.54)$$

where S is the matrix whose rows are indexed by the vertices and whose columns are indexed by the edges.

Let $\mathbf{1}$ denote the constant function which assumes the value 1 on each vertex. This is an eigenfunction of \mathcal{L} with eigenvalue 0.

2018-04-05 Predrag There might be a related undirected network model, with a graph Laplacian (13.53). In that case a Lagrangian formulation (in terms of graph Laplacians) might be a more powerful formulation than their Hamiltonian one. “Arrow of time” is perhaps encoded by the orientations of the links in a directed complex network.

2016-10-05 Predrag Zeta functions of infinite graphs are discussed, for example, by

Bryan Clair and Shahriar Mokhtari-Sharghi [26],

Rostislav Grigorchuk and Andrzej Zuk [?46] (that one is about Cayley trees).

Guido, Isola, and Lapidus [51] *Ihara’s zeta function for periodic graphs and its approximation in the amenable case*.

Guido, Isola and Lapidus [52] *A trace on fractal graphs and the Ihara zeta function*

2020-12-18 Predrag Daniele Guido, Tommaso Isola, and Michel Lapidus [50] *Ihara zeta functions for periodic simple graphs* arXiv:math/0605753:

$$Z(G, u) = Z_G(u) = \prod_{[C]} \frac{1}{(1 - u^{[C]})^{1/G_C}}, \quad (13.55)$$

The standard lattice graph $\mathcal{L} = \mathbb{Z}^2$ endowed with the action of the group G which is generated by the rotation by $\frac{\pi}{2}$ around the point P and the translations by elements $(m, n) \in \mathbb{Z}^2$ acting as $(m, n)(v_1, v_2) := (v_1 + 2m, v_2 + 2n)$, for $v = (v_1, v_2) \in V\mathcal{L} = \mathbb{Z}^2$.

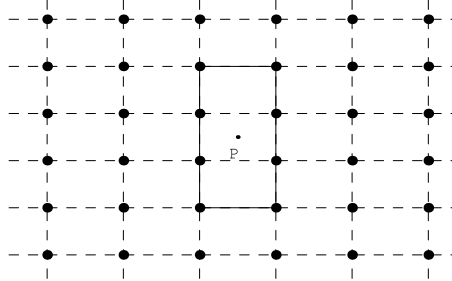
Why face-centered point P ? why $2m$? In their example, the length $[C]$ in (13.55) is the number of group elements that map C into itself (the ‘stabilizer’), see figure 13.4, not what we need.

The main result in the theory of Ihara zeta functions (13.55) says that Z is the reciprocal of a holomorphic function, which, up to a factor, is the determinant of a deformed Laplacian on the graph.

2016-10-05 Predrag Unlike in dynamical systems, Ihara zeta functions are defined on graphs with unoriented (or undirected) edges.

Hashimoto [54] *Zeta functions of finite graphs and representations of p -adic groups*

2020-05-13 Predrag Bass [8] *The Ihara-Selberg zeta function of a tree lattice*. It seems that Ihara zeta function walks carry signs - investigate.


 Figure 13.4: A cycle with $|G_C| = 2$

He also introduces the *edge zeta function* to give a determinant form of Ihara zeta function for undirected graph. This text is from Zhou, Xiao and He [136], arXiv:1502.05771:

- The **edge matrix** W of size $[2m \times 2m]$ for an undirected graph with m undirected edges has entries w_{ij} . The (i, j) -th entry of W , w_{ij} , is a complex variable if the edge e_i is connected with edge e_j with $e_j \neq e_i^{-1}$, and the entry is 0 if otherwise.
- For a closed path C in an undirected graph X written as a sequence of edges $C = e_1 e_2 \cdots e_s$, the **edge norm** of C is

$$N_E(C) = w_{12}w_{23} \cdots w_{s1}.$$

The edge zeta function is defined as follows

$$\zeta_E(W, X) = \prod_{[P] \in \text{Prime Cycles}} (1 - N_E(C))^{-1}.$$

It is clear from this definition that if w_{ij} is set to $z \in \mathbb{C}$, we recover the original Ihara zeta function such that

$$\zeta_G(z) = \zeta_E(W_1, G),$$

where W_1 is the edge matrix when all non-zero entries set to z .

Furthermore, we have the following formula (cf. Chapter 3 of Terras [126])

$$\zeta_E(W, G) = \text{Det}(I - W)^{-1}. \quad (13.56)$$

2016-10-05 Predrag In *A Window Into Zeta and Modular Physics* [80] (that should warm Li Han's heart) Audrey Terras discusses **Ihara zeta function**. She says: "the Ruelle zeta function of a dynamical system, will be shown to be a generalization of the Ihara zeta." Things are looking deep. "It turns out (using the Ihara determinant formula again) that the Riemann

hypothesis means that the graph is Ramanujan”, etc. She also discusses it in ref. [126] *Zeta Functions of Graphs: A Stroll through the Garden*.

To swoon over the multitude of zetas, read Bartholdi [7] *Zeta functions of graphs: a stroll through the garden, by Audrey Terras* [126]. Book review.

Teimoori Faal and M. Loebel [123] Bass' identity and a coin arrangements lemma

Like my topological zeta functions, Loebel's Ihara-Selberg function of G is the infinite product is over the set of the prime reduced cycles of G .

Loebl and Somberg [90] *Discrete Dirac operators, critical embeddings and Ihara-Selberg functions*

da Costa [29] *The Feynman identity for planar graphs:* “ The Feynman identity (FI) of a planar graph relates the Euler polynomial of the graph to an infinite product over the equivalence classes of closed nonperiodic signed cycles in the graph. The main objectives of this paper are to compute the number of equivalence classes of nonperiodic cycles of given length and sign in a planar graph and to interpret the data encoded by the FI in the context of free Lie superalgebras. This solves in the case of planar graphs a problem first raised by Sherman and sets the FI as the denominator identity of a free Lie superalgebra generated from a graph. Other results are obtained on the zeta functions of graphs. ”

da Costa *Graphs and Generalized Witt identities* arXiv:1409.5767

2016-10-05 Predrag Sato [112] *Bartholdi zeta functions of group coverings of digraphs:*

The (Ihara) zeta function of a graph G is defined [63] to be a function of with u sufficiently small, by

$$Z(G, u) = Z_G(u) = \prod_{[C]} \frac{1}{1 - u^{[C]}}, \quad (13.57)$$

where $[C]$ runs over all equivalence classes of prime, reduced cycles of G .

Samuel Cooper and Stratos Prassidis (2010) *Zeta functions of infinite graph bundles*, DOI :

Originally, Ihara defined the zeta function on finite graphs imitating the classical definition of the zeta function, where the product is over all equivalence classes of primitive closed loops C , and $[C]$ denotes the length of C .

2016-10-05 Predrag Horton [60] *Ihara zeta functions of digraphs* considers digraphs whose adjacency matrices are directed edge matrices.

Tarfulea and Perlis [122] An Ihara formula for partially directed graphs: “ In 2001 Mizuno and Sato showed that the Ihara zeta function of a fully directed graph has a similar expression, and in 2005, Sato [112] generalized Ihara's formula to connected, simple, partially directed graphs.

(Sato proved his formula for the more-general two-variable Bartholdi zeta function.) This paper provides a new proof of Ihara's formula for the Ihara zeta function of any finite graph, not necessarily connected or simple, no matter whether it is undirected, fully directed, or partially directed. "

2016-10-30 Predrag I worry a lot about what time-reversibility means - spatiotemporal cat is both time and space reversible, and then there are Ihara zeta functions for undirected graphs. So I find this interesting: Copper-smith, Kadanoff and Zhang [28] *Reversible Boolean networks I: distribution of cycle lengths*. They write: " We [...] consider time-reversible dynamics of N Boolean variables models, with the time evolution of each depending on K of the other variables, which necessarily have the property that every possible point in the state space is an element of one and only one cycle. The orbits can be classified by their behavior under time reversal. The orbits that transform into themselves under time reversal have properties quite different from those that do not; in particular, a significant fraction of latter-type orbits have lengths enormously longer than orbits that are time-reversal symmetric. For large K and moderate N , the vast majority of points in the state space are on one of the time-reversal singlet orbits. However, for any finite K , the random hopping approximation fails qualitatively when N is large enough ($N > 22K$). When K is large, typical orbit lengths grow exponentially with N , whereas for small enough K , typical orbit lengths grow much more slowly with N . The numerical data are consistent with the existence of a phase transition at which the average orbit length grows as a power of N at a value of K between 1.4 and 1.7. However, in the reversible models, the interplay between the discrete symmetry and quenched randomness can lead to enormous fluctuations of orbit lengths and other interesting features that are unique to the reversible case. "

Need to check also

Toffoli and Margolus [127] *Invertible cellular automata: A review*

D'Souza and Margolus [35] *Thermodynamically reversible generalization of diffusion limited aggregation*

2020-05-11 Predrag Deitmar [38] *Ihara zeta functions of infinite weighted graphs*: "The theory of Ihara zeta functions is extended to infinite graphs which are weighted and of finite total weight. In this case one gets meromorphic instead of rational functions and the classical determinant formulas of Bass and Ihara hold true with Fredholm determinants."

Tempesta [124] *A theorem on the existence of trace-form generalized entropies*
Tempesta [125] *Beyond the Shannon-Khinchin formulation: The composability axiom and the universal-group entropy*

2020-05-11 Predrag Supriyo Dutta and Partha Guha *Ihara Zeta Entropy*,
arXiv:1906.02514; *A System of Billiard and Its Application to Information-*

Theoretic Entropy, arXiv:2004.03444: they define Ihara entropy, an information-theoretic entropy based on the Ihara zeta function of a graph. A dynamical system consists of a billiard ball and a set of reflectors correspond to a combinatorial graph. The reflectors are represented by the vertices of the graph. Movement of the billiard ball between two reflectors is represented by the edges. The prime cycles of this graph generate the bi-infinite sequences of the corresponding symbolic dynamical system. The number of different prime cycles of a given length can be expressed in terms of the adjacency matrix of the oriented line graph. It also constructs the formal power series expansion of Ihara zeta function. Therefore, the Ihara entropy has a deep connection with the dynamical system of billiards.

2017-03-08 Predrag Reading Band, Harrison and Joyner [6] *Finite pseudo orbit expansions for spectral quantities of quantum graphs* one expects to run into another rediscovery of Ihara zeta functions, as the links are not directed:

“The *quantum graphs* we consider are metric graphs equipped with a self-adjoint differential operator \mathcal{H} , the Hamiltonian. Here we are particularly interested in the negative Laplace operator,

$$\mathcal{H} : f(x) \mapsto -\frac{d^2 f}{dx^2}, \quad (13.58)$$

or the more general Schrödinger operator,

$$\mathcal{H} : f(x) \mapsto -\frac{d^2 f}{dx^2} + V(x)f(x), \quad (13.59)$$

where $V(x)$ is a *potential*, which we assume to be bounded and piecewise continuous. Note that the value of a function or the second derivative of a function at a point on the bond is well-defined, thus it is not important which coordinate, x_b or $x_{\bar{b}}$ is used. This is in contrast to the first derivative which changes sign according to the direction of the chosen coordinate.”

Indeed, they go through the usual steps of defining oriented graphs and then putting pairs of oriented bonds on each link, etc. This is explored further in

Ren, Aleksić, Emms, Wilson and Hancock [109] *Quantum walks, Ihara zeta functions and cospectrality in regular graphs:* review the literature on the discrete-time quantum walks and the Ihara zeta function.

Setyadi and Stor [113] *Enumeration of graphs with the same Ihara zeta function*

Higuchi, Konno, Sato and Segawa [55] *A remark on zeta functions of finite graphs via quantum walks*

Saito [111] *A proof of Terras' conjecture on the radius of convergence of the Ihara zeta function* has a nice explicit matrix example, and eigenvalues computation.

2020-05-05 Predrag Mizuno and Sato [98] *Zeta functions of digraphs* define a zeta function of a digraph and an L-function of a symmetric digraph. That is the usual Bowen-Ruelle (in ChaosBook topological) zeta function. Tarfulea and Perlis [122] do note: “The formula for the zeta function of a directed graph was proved in 1968, wearing a thin disguise, by Bowen and Lanford [12]. The elementary connection to directed graphs is made explicit in Th.6.4.6 of Lind Marcus [88].”

Various authors, such as Zhou, Xiao and He [136] *Seiberg duality, quiver gauge theories, and Ihara's zeta function*, nevertheless refer to it as “Ihara”, see their Table 2 *Ihara zeta functions for various toric phases of del Pezzo and Hirzebruch quivers*. Apparently, “the toric phases are the most popular.”

“The coefficients of the inverse of Ihara zeta function are related to simple cycles. In gauge theories, this translates to generic super-potentials that can be generated from certain quivers.” This seems to be expansion of a topological zeta function in terms of fundamental cycles.

2020-05-05 Predrag Davey, Hanany and Pasukonis [36] *On the classification of brane tilings*, arXiv:0909.2868. (See also arXiv:hep-th/0503149) has an Appendix A *Tiling catalog*.

A brane tiling (or dimer model) is a periodic bipartite graph on the plane. Alternatively, we may draw it on the surface of a 2-torus by taking the smallest repeating structure(known as the fundamental domain) and identifying opposite edges [1]. The bipartite na-ture of the graph allows us to colour the nodes either white or black such that white nodes only connect to black nodes and vice versa.

2020-05-05 Predrag Sunada [121] *Topological Crystallography*. Have the book ([click here](#)), but do not know how to get useful info for spatiotemporal cat out of it.

“the Ihara zeta function [is] a graph-theoretic analogue of class field theory, discrete Laplacians, and harmonic maps.”

Again, “Abel–Jacobi maps” pop up, and again I have no idea what they are.

2020-05-06 Predrag Ren, Wilson and Hancock [110] *Graph characterization via Ihara coefficients*: For an unweighted graph, the Ihara zeta function is the reciprocal of a quasi characteristic polynomial of the adjacency matrix of the associated oriented line graph.

First, we demonstrate how to characterize unweighted graphs in a per mutation-invariant manner using the polynomial coefficients from the Ihara zeta function, i.e., the Ihara coefficients.

Second, we generalize the definition of the Ihara coefficients to edge-weighted graphs, using the reduced Bartholdi zeta function.

Experimental results reveal that the Ihara coefficients are more effective than methods based on Laplacian spectra.

Bulò, Hancock, Aziz and Pelillo [13] *Efficient computation of Ihara coefficients using the Bell polynomial recursion*: They present a method for computing the Ihara coefficients in terms of complete Bell polynomials and show how the Ihara coefficients can be efficiently computed provided that the eigenvalues of the adjacency matrix are known.

2020-05-05 Predrag Arrigo, Grindrod, Higham and Noferini [4] *On the exponential generating function for non-backtracking walks* do not mention "Ihara", but seem to derive it anyway from a 3-term recurrence relation. They write:

We derive an explicit formula for the exponential generating function associated with non-backtracking walks around both undirected and directed graphs. Eliminating backtracking walks in this context does not significantly increase the computational expense. We show how the new measures may be interpreted in terms of standard exponential centrality computation on a certain multilayer network. Insights from this block matrix interpretation also allow us to characterize centrality measures arising from general matrix functions.

2020-05-11 Predrag Bharatram Rangarajan *A combinatorial proof of Bass's determinant formula for the zeta function of regular graphs*, arXiv:1706.00851: The zeros and poles of the Selberg zeta function appear in the Selberg trace formula, which relates the distribution of primes with the spectrum of the Laplace-Beltrami operator of the surface. The idea of considering closed geodesics as primes inspired the work of Hashimoto [54], Bass [8], Kotani and Sunada [83] to come up with an analogous notion in the discrete setting.

Just like the Selberg zeta function is related to the spectrum of the Laplace-Beltrami operator of the surface, it is natural to ask if its discrete analogue, the Ihara zeta function of a graph, is related to the spectrum of the Laplacian matrix (or the adjacency matrix) of the graph. Bass [8] gives an expression for the Ihara zeta function of a graph $G = (V, E)$ as

$$\zeta_G(t) = \frac{1}{(1 - t^2)^{|E|-|V|} \det(I - tA + (D - I)t^2)}$$

where A is the adjacency matrix of G and D is the diagonal matrix of degrees of the vertices of G , or in other words, $D = \text{diag}(A\vec{1})$. In particular, if G is d -regular, then (see (13.46), derivation (13.67))

$$\zeta_G(t) = \frac{1}{(1 - t^2)^{|E|-|V|} \det(I - tA + (d - 1)t^2 I)} \quad (13.60)$$

gives a way of obtaining the set of poles of $\zeta_G(t)$.

For a general, partially directed graph see Sato [112] and Tarfulea and R. Perlis [122].

Most proofs Bass's determinant formula start by expressing the zeta function in terms of not the adjacency matrix A of G , but the adjacency matrix H of the oriented line graph of G (called the Hashimoto edge-incidence matrix).

In this paper, we shall see a more elementary combinatorial proof of Bass's determinant formula in the case when G is regular. The proof goes as follows:

- The zeta function $\zeta_G(z)$ has an expansion of the form

$$\zeta_G(z) = \exp \left(\sum_{k=1}^{\infty} N_k \frac{z^k}{k} \right)$$

where for $k \in \mathbb{Z}$, N_k is the number of rooted, *non-backtracking* cycles in G of length k .

- An expression for N_k is not immediate, the starting point is the study of non-backtracking walks on G . We can construct the family $\{A_k\}_{k \in \mathbb{Z}_{\geq 0}}$ of $n \times n$ matrices such that for every $k \in \mathbb{Z}_{\geq 0}$ and every $v, w \in V$, $(A_k)_{vw}$ is the number of non-backtracking walks on G of length k from v to w .
- N_k is combinatorially computable from $\text{Tr}(A_k)$.
- $\text{Tr}(A_k)$ is well-understood in terms of the eigenvalues of A and a family of Chebyshev polynomials. These ingredients lead to a proof of Bass's determinant formula.

$(A^k)_{vw}$ counts the total number of walks (with backtrackings) on G from v to w of length k . Let

$$A_0, A_1, A_2, A_3, \dots$$

be $[n \times n]$ matrices over \mathbb{C} such that the value $(A_k)_{vw}$ is the number of *non-backtracking* walks on G from v to w of length k . This family $\{A_k\}_{k \in \mathbb{Z}}$ can be recursively defined using powers of A as follows:

- $A_0 = I$
- $A_1 = A$
- $A_2 = A^2 - dI$
- For $k \geq 3$,

$$A_k = A A_{k-1} - (d-1)A_{k-2}$$

This recurrence relation shows that the ordinary (matrix) generating function for the above sequence is

$$\sum_{k=0}^{\infty} z^k A_k = (1-z^2)I \cdot (I - zA + (d-1)z^2I)^{-1}$$

i.e., generating function

$$\frac{1 - z^2}{1 - Az + (d - 1)z^2}$$

Consider the family of Chebyshev polynomials of the second kind

$$U_0(x), U_1(x), U_2(x), \dots$$

defined by the recurrence

$$U_0(x) = 1$$

$$U_1(x) = 2x$$

and for $k \geq 2$,

$$U_k(x) = U_{k-1}(x)U_1(x) - U_{k-2}(x)$$

and with generating function

$$\sum_{k=0}^{\infty} U_k(x)z^k = \frac{1}{1 - 2xz + z^2}$$

It is easy to see that

$$\sum_{0 \leq j \leq k/2} A_{k-2j} = (d - 1)^{k/2} U_k \left(\frac{A}{2\sqrt{d - 1}} \right)$$

implying that for $k \geq 2$,

$$A_k = (d - 1)^{k/2} U_k \left(\frac{A}{2\sqrt{d - 1}} \right) - (d - 1)^{k/2-1} U_{k-2} \left(\frac{A}{2\sqrt{d - 1}} \right)$$

This holds for $0 \leq k \leq 2$ as well, if

$$U_m(x) = 0$$

for every $m < 0$. This allows us to work with the above expression for A_k for all non-negative integers k .

Taking trace on both sides,

$$\text{Tr}(A_k) = (d - 1)^{k/2} \sum_{j=0}^{n-1} U_k \left(\frac{\mu_i}{2\sqrt{d - 1}} \right) - (d - 1)^{k/2-1} \sum_{i=0}^{n-1} U_{k-2} \left(\frac{\mu_i}{2\sqrt{d - 1}} \right)$$

where

$$d = \mu_0 \geq \mu_1 \geq \dots \geq \mu_{n-1} \geq d$$

are the n eigenvalues of the adjacency matrix A . Thus we have an expression for the trace of A_k as a polynomial in the eigenvalues of A . For a

detailed and elementary exposition of Chebyshev polynomials and non-backtracking walks on regular graphs, the reader is referred to the monograph by Davidoff, Sarnak and Valette [37].

While $(A_k)_{vw}$ counts the number of walks on G from vertex v to vertex w without backtracking, the diagonal element $(A_k)_{vv}$ does *not* count the number of non-backtracking cycles of length k rooted at v . This is because $(A_k)_{vv}$ also counts walks of the form

$$e_1 e_2 \dots e_k$$

where $e_{i+1} \neq \overline{e_i}$ for any $1 \leq i \leq k-1$ but $e_k = \overline{e_1}$. That is, $e_1 e_2 \dots e_k$ is non-backtracking as a walk from v to v , but when considered as a closed walk (or a loop), the two end edges form a backtracking! Such an instance of a backtracking that gets overlooked in $\text{Tr}(A_k)$ shall be referred to as a *tail*.

So $\text{Tr}(A_k)$ counts the number of closed, rooted walks of length k that could have at most 1 tail, and hence does *not* count the rooted, non-backtracking cycles of length k . It is interesting to ask what the number of closed, rooted non-backtracking walks of length k is.

Relation between $M_k = \text{Tr}(A_k)$ and N_k : For every $k \geq 3$,

$$N_k = \begin{cases} M_k - (d-2)(M_{k-2} + M_{k-4} + \dots + M_1) & \text{odd } k \\ M_k - (d-2)(M_{k-2} + M_{k-4} + \dots + M_2) & \text{even } k \end{cases}$$

By linearity of trace,

$$N_k = \begin{cases} \text{Tr}(A_k - (d-2)(A_{k-2} + A_{k-4} + \dots + A_1)) & \text{if } k \text{ is odd} \\ \text{Tr}(A_k - (d-2)(A_{k-2} + A_{k-4} + \dots + A_2)) & \text{if } k \text{ is even} \end{cases}$$

[... after a few steps ... this is related to]

$$U_k(x) - U_{k-2}(x) = 2T_k(x)$$

where $T_k(x)$ is the *Chebyshev polynomial of the first kind* defined by

$$\begin{aligned} T_0(x) &= 1, \quad T_1(x) = x \\ T_k(x) &= 2xT_{k-1}(x) - T_{k-2}(x) \quad \text{for } k \geq 2, \end{aligned} \tag{13.61}$$

with the generating function

$$\sum_{k=0}^{\infty} T_k(x) z^k = \frac{1 - xz}{1 - 2xz + z^2} \tag{13.62}$$

[... after a few probably unnecessary steps, ... taking a derivative ... this

is related to]

$$N_1 z + N_2 \frac{z^2}{2} + N_3 \frac{z^3}{3} + \dots \quad (13.63)$$

$$= -\frac{n(d-2)}{2} \ln(1-z^2) - \sum_{j=0}^{n-1} \ln(1-\mu_j z + (d-1)z^2) \quad (13.64)$$

$$= -\left(\frac{nd}{2} - n\right) \ln(1-z^2) - \ln\left(\prod_{j=0}^{n-1} 1 - \mu_j z + (d-1)z^2\right) \quad (13.65)$$

$$= -(|E| - |V|) \ln(1-z^2) - \ln(\det(I - Az + (d-1)z^2)) \quad (13.66)$$

resulting in (13.43):

Bass's determinant formula Let $G = (V, E)$ be a d -regular graph with adjacency matrix A , and let N_k count the number of rooted, non-backtracking cycles of length k in G . Then

$$\zeta_G(z) = \frac{1}{(1-z^2)^{|E|-|V|} \det(I - zA + (d-1)z^2 I)} \quad (13.67)$$

13.1.5 Maillard

Another scary line of literature. Connecting Baxter to dynamical zetas functions. Maillardinians have a burst at the end of 20th century. Very easy to collect the literature, as only they cite their own articles, and nobody else cites them.

A cute cat map exercise - but I have to bike home, will continue later...

2016-11-16 Predrag Anglès d'Auriac, Boukraa and Maillard [3] *Functional relations in lattice statistical mechanics, enumerative combinatorics, and discrete dynamical systems* write "... non-linear functional relations appearing in [...] lattice statistical mechanics [...] We then consider discrete dynamical systems corresponding to birational transformations. The rational expressions for dynamical zeta functions obtained for a particular two-dimensional birational mapping, depending on two parameters [...] compatible with a chaotic dynamical system.

They obsess about the Arnol'd complexity, which counts the number of intersections between a fixed line and its n th iterate. I do not see why we should care.

I like Bedford and Diller [10] *Real and complex dynamics of a family of birational maps of the plane: The golden mean subshift* better, so I follow their notation here. It's a rather impressive paper.

For reasons known to some people (symmetries of Baxter models?) they

study a birational transformation and its inverse,

$$\begin{aligned} x_{n+1} &= y_n \frac{x_n+a}{x_n-1} & x_{n-1} &= y_n + 1 - a \\ y_{n+1} &= x_n + a - 1 & y_{n-1} &= x_n \frac{y_n-aa}{y_n+1} \end{aligned}, \quad a \in \mathbb{R} \quad (13.68)$$

The map is area-preserving in the sense that it preserves a meromorphic 2-form

$$\frac{dx \wedge dy}{y - x + 1}$$

and is reversible, which means that the map is conjugate to its inverse via involution $(x, y) \rightarrow (-y, -x)$. The inverse transformation amounts to $y_n \leftrightarrow -z_n$, i.e., the time reversal symmetry, and the $x - y = 0$ line is the *time-reversal invariant line*. The topological zeta function for (13.68) is

$$1/\zeta_{\text{top}}(z) = \frac{1 - z - z^2}{1 - z^2}. \quad (13.69)$$

It counts all periodic orbits, real and complex. Interestingly, this zeta satisfies an elegant functional relation relating $\zeta(z)$ and $\zeta(1/z)$.

The zeta function for real roots is complicated and depends on the parameter a .

Bedford and Diller [10] construct a generating partition and the Markov diagram (they call that Graph of Filtration), including the transient nodes. The recurrent part of this graph is just the golden mean graph, with 11 repeats forbidden. They obsess much about their “rectangles.” Show that all periodic orbits are hyperbolic. Discuss pre-periodic orbits. Zeta functions are never mentioned, though topological entropy is computed.

Abarenkova *et al.* [1] *Rational dynamical zeta functions for birational transformations* is not worth reading - the material is better explained in their other papers.

If the dynamical zeta function can be interpreted as the ratio of two characteristic polynomials of two linear operators A and B , namely

$$\frac{1}{\zeta(z)} = \frac{\det(1 - zA)}{\det(1 - zB)}, \quad (13.70)$$

then the number of fixed points is given by

$$\text{Tr}(A^n) - \text{Tr}(B^n). \quad (13.71)$$

In this linear operators framework, the rationality of the ζ function [49, 94], and therefore the algebraicity of the exponential of the topological entropy, amounts to having a finite dimensional representation of the linear operators A and B .

Their only explicit example of a rational zeta dynamical function is the case of the Arnol'd cat map on torus $\mathbb{T}^2 = \mathbb{R}^2 / \mathbb{Z}^2$,

$$A = \begin{pmatrix} 2 & 1 \\ 1 & 1 \end{pmatrix}, \quad B = \begin{pmatrix} 1 & 0 \\ 0 & 1 \end{pmatrix} \quad (13.72)$$

The topological zeta function [64] for Arnol'd cat map is

$$1/\zeta_{\text{top}}(z) = \frac{\det(1-zA)}{\det(1-zB)} = \frac{1-3z+z^2}{(1-z)^2}. \quad (13.73)$$

2016-06-02, 2020-09-24 Predrag From my notes on Isola [64] *ζ -functions and distribution of periodic orbits of toral automorphisms*, see sect. 1.3.7: [...] The topological zeta function for cat-map class of models is (see (4.183))

$$1/\zeta_{\text{top}}(z) = \frac{1-sz+z^2}{(1-z)^2}. \quad (13.74)$$

Define

$$d(s) = z^{-1} - s + z \quad (13.75)$$

then (compare with (13.70))

$$1/\zeta_{\text{top}}(z) = \frac{d(s)}{d(2)} = 1 + \frac{d(s) - d(2)}{d(2)} = 1 - \mu^2 \frac{1}{d(2)} \quad (13.76)$$

I wonder whether the fact that this is quadratic in z has something to do with the time-reversibility, and the unsigned graph's Ihara zeta functions?

The “characteristic function” (5.248) for the 3-point recurrence centered on the s term, $1/z - s + z$ suggests multiplying (13.74) by z^{-1}/z^{-1} . That leads to

$$1/\zeta_{\text{top}}(z) = 1 + \frac{\mu^2}{(1-z)(1-1/z)} = 1 + \left(\frac{z}{1-z} + \frac{1/z}{1-1/z} \right) \mu^2. \quad (13.77)$$

Interpretation: the temporal cat zeta function denominator is the Laplacian, and μ^2 is measuring the deviation from the pure Laplacian case (marginal, no solutions other than the $n = 1$ (line of) fixed point(s)).

Conversely, given the topological zeta function, the generating function for the number of temporal lattice states of period n is given by the logarithmic derivative of the topological zeta function (3.185),

$$\begin{aligned} \sum_{n=0}^{\infty} N_n z^n &= \frac{2-sz}{1-sz+z^2} - \frac{2}{1-z} = \frac{2/z-s}{1/z-s+z} - \frac{2}{1-z} \\ &= \frac{(2/z-s)(1-z)-2(1/z-s+z)}{(1/z-s+z)(1-z)} \\ &= \mu^2 \frac{1+z}{(1/z-s+z)(1-z)} \\ &= \mu^2 [z + (s+2)z^2 + (s+1)^2 z^3 \\ &\quad + (s+2)s^2 z^4 + (s^2+s-1)^2 z^5 + \dots] \end{aligned} \quad (13.78)$$

which is indeed the generating function for $T_T(s/2)$, the Chebyshev polynomial of the first kind.

To me it looks like we should include (time reflection symmetry!) also negative n in the z^n series (Laurent series?), with a negative sign, so I get

$$\begin{aligned} \sum_{n=-\infty}^{\infty} N_n z^n &= \frac{\mu^2}{z^{-1} - s + z} \left(\frac{1+z}{1-z} - \frac{1+z^{-1}}{1-z^{-1}} \right) \\ &= \frac{\mu^2}{z^{-1} - s + z} \frac{(1+z)(1-z^{-1}) - (1-z)(1+z^{-1})}{(1-z)(1-z^{-1})} \\ &= \frac{2\mu^2}{z^{-1} - \mu^2 - 2 + z} \frac{z - z^{-1}}{(1-z)(1-z^{-1})} \\ &= \frac{2\mu^2}{z^{-1} - \mu^2 - 2 + z} \frac{z^{-1} - z}{z^{-1} - 2 + z}. \end{aligned} \quad (13.79)$$

2020-09-30 Predrag The Bernoulli equation rewritten as a first-order difference equation:

$$x_t - sx_{t-1} = -m_t, \quad x_t \in [0, 1]. \quad (13.80)$$

For a Bernoulli system

$$\begin{aligned} 1/\zeta_{\text{top}}(z) &= \exp[\ln(1-sz) - \ln(1-z)] \\ &= \frac{1-sz}{1-z}. \end{aligned} \quad (13.81)$$

Define

$$d(s) = z^{-1} - s \quad (13.82)$$

then (compare with (13.70))

$$1/\zeta_{\text{top}}(z) = \frac{d(s)}{d(2)} = 1 + \frac{d(s) - d(2)}{d(2)} = 1 + (s-1)\frac{1}{d(2)} \quad (13.83)$$

The numerator $(1-sz)$ says that a Bernoulli system is a full shift [33]: there are s fundamental lattice states and every other lattice state is built from their concatenations and repeats.

2020-09-24 Predrag For 2-dimensional spatiotemporal cat the “characteristic function” (5.248) the above musings suggests a guess

$$\begin{aligned} 1/\zeta_{\text{top}}(z_1, z_2) &= \frac{z_1 + z_2 - 2s + z_1^{-1} + z_2^{-1}}{z_1 + z_2 - 4 + z_1^{-1} + z_2^{-1}} \\ &= 1 - \frac{2\mu^2}{z_1 + z_2 - 4 + z_1^{-1} + z_2^{-1}} \\ &= 1 + \frac{2\mu^2}{(1-z_1)(1-1/z_1) + (1-z_2)(1-1/z_2)} \end{aligned} \quad (13.84)$$

If we define

$$d(s) = z_1 + z_2 - 2s + z_1^{-1} + z_2^{-1} \quad (13.85)$$

then (compare with (13.70))

$$1/\zeta_{\text{top}}(z_1, z_2) = \frac{d(s)}{d(2)} \quad (13.86)$$

suggest some derivatives, integrations with respect to the parameter s , resulting in $\ln d(s) - \ln d(2)$ from the ends of the integration domain.

See also (13.73).

2020-05-05 Predrag Kotani and Sunada [83] *Zeta functions of finite graphs* seems cited a lot and perhaps belongs to *ChaosBook.org*.

2020-05-05 Predrag Stark and Terras [118] *Zeta functions of finite graphs and coverings* is cited a lot and perhaps belongs to *ChaosBook.org*.

Stark and Terras [119] *Zeta functions of finite graphs and coverings, Part II*

13.2 Gaussian model

2019-11-04 Predrag Ivashkevich, Izmailian and Hu [65] *Kronecker's double series and exact asymptotic expansions for free models of statistical mechanics on torus:*

Gaussian model is a boson analog of Ising model. Consider square lattice of size $N \times M$ wrapped on a torus. To each site (m, n) of the lattice we assign a continuous variable ϕ_{mn} . The Hamiltonian of the model is

$$H(\phi) = -J \sum_{n=0}^{N-1} \sum_{m=0}^{M-1} (\phi_{mn} \phi_{m+1,n} - 2\phi_{mn}^2 + \phi_{mn} \phi_{m,n+1}) , \quad (13.87)$$

with the partition function

$$Z(J) = \int_{\mathbb{R}^{MN}} e^{-H(\phi)} d\sigma(\phi)$$

If the measure $d\sigma(\phi)$ in the phase space \mathbb{R}^{MN} is Gaussian

$$d\sigma_{\text{Gauss}}(\phi) = \pi^{-MN/2} \prod_{n=0}^{N-1} \prod_{m=0}^{M-1} e^{-\phi_{mn}^2} d\phi_{mn}$$

the integration can be done explicitly and the partition function of the free boson model can be written in terms of the partition function with twisted boundary conditions

$$Z_{\alpha,\beta}(\mu) = \prod_{n=0}^{N-1} 2 \left| \operatorname{sh} \left[M \omega_\mu \left(\frac{\pi(n+\alpha)}{N} \right) + i\pi\beta \right] \right| \quad (13.88)$$

and parameterization $J^{-1} = 4 \operatorname{ch}^2 \mu$ as

$$Z_{\text{Gauss}}(\mu) = \left(\sqrt{2} \operatorname{ch} \mu \right)^{MN} \left[Z_{0,0}(\mu) \right]^{-1} \quad (13.89)$$

where

$$Z_{0,0}^2(\mu) = \prod_{n=0}^{N-1} \prod_{m=0}^{M-1} 4 \left[\sin^2 \left(\frac{\pi n}{N} \right) + \sin^2 \left(\frac{\pi m}{M} \right) + 2 \operatorname{sh}^2 \mu \right] . \quad (13.90)$$

This model exhibit phase transition at the point $\mu_c = 0$ where the partition function is divergent. This is due to the presence of so-called zero mode, i.e. due to the symmetry transformation $\phi_{mn} \rightarrow \phi_{mn} + \text{const}$, which leave the Hamiltonian (13.87) invariant. Correlation functions of disorder operator in this model have been studied by Sato, Miwa and Jimbo.

CHAPTER 13. ISING MODEL IN 2D

The reason why this model is often considered as boson analog of the Ising model is that one can choose another measure in the phase space, which makes this model equivalent to the Ising model considered above

$$d\sigma_{\text{Ising}}(\phi) = 2^{-MN} \prod_{n=0}^{N-1} \prod_{m=0}^{M-1} [\delta(\phi_{mn} - 1) + \delta(\phi_{mn} + 1)] d\phi_{mn}$$

where δ 's are Dirac δ -functions. With such a definition the variables ϕ_{mn} can actually take only two values: +1 or -1, so that $\phi_{mn}^2 = 1$. In this case integration can be replaced by summation over discrete values of $\phi_{mn} = \pm 1$ and the Hamiltonian (13.87) coincides with the Hamiltonian of the Ising model (13.2) up to a constant.

2020-06-19 Predrag Connect to (5.36)?

Recheck [2019-09-25 PC] Levit and Smilansky?

2020-06-19 Predrag P. A. P. Moran [99] *A Gaussian Markovian Process on a Square Lattice* is a very good paper that does all the right stuff with the Gaussian “model,” and ends up with the complete elliptic integral of the first kind (5.251).

2020-06-19 Predrag Eduardo Fradkin [45] *Field Theories of Condensed Matter Physics*, discusses on p. 336 the quantum partition function of the dimer model which is given by the classical partition function of a discrete Gaussian model in three Euclidean dimensions on a cubic lattice. See also p. 332, 345 and 354. Not sure how to connect it to our work.

Shankar [114] *Quantum Field Theory and Condensed Matter* defines the Gaussian model in Eqs. (13.2), (6.219); sect 11.1 *The renormalization group: first pass*;

Marino [95] *Quantum Field Theory Approach to Condensed Matter Physics* (see 5.2 *Gaussian Functional Integrals*) does not seem to refer to the Gaussian model.

Chaikin and Lubensky [17] *Principles of Condensed Matter Physics* see 5.3 *Gaussian integrals*, 5.8.3 *Gaussian model*

Lattice 89: Proceedings of the 1989 Symposium on Lattice Field Theory edited by N. Cabbibo, E. Marinari, G. Parisi

2020-09-06 Predrag Kadanoff [73] on Gaussian model: sect. 3.4 *Lattice Green Function* and many more. The “coefficients matrix” C in Kadanoff eq. (3.9) is the inverse of my ‘propagator’ Δ .

A lattice with one field ϕ_n for each site, then we can define a particularly simple and important problem by giving the coefficient matrix Kadanoff

eq. (3.12)

$$C = \begin{pmatrix} 1 & -K & 0 & 0 & \dots & 0 & -K \\ -K & 1 & -K & 0 & \dots & 0 & 0 \\ 0 & -K & 1 & -K & \dots & 0 & 0 \\ \vdots & \vdots & \vdots & \vdots & \ddots & \vdots & \vdots \\ 0 & 0 & \dots & \dots & \dots & 1 & -K \\ -K & 0 & \dots & \dots & \dots & -K & 1 \end{pmatrix}. \quad (13.91)$$

The on-site interaction normalizes the Gaussian variables, for $K = 0$ one gets the usual multi-dimensional Gaussian. $-K$ is the nearest neighbor coupling strength, related to our case be $-s \rightarrow 1$, off-diagonal $1 \rightarrow -K$, so the conversion is $s = -1/K$ (I believe).

Fourier transform of the d -dimensional Green's function Kadanoff eq. (3.19)

$$G(q) = \frac{1}{1 - 2K \sum_{j=1}^d \cos(2\pi k_j / \ell_j)}, \quad q_j = \quad (13.92)$$

Compare with (5.56) and our Fourier-transformed field for k th discrete d -dimensional Fourier component on $\ell_1, \ell_2, \dots, \ell_d$ torus, no tilt,

$$\hat{\phi}_k = \frac{1}{ds - 2 \sum_{j=1}^d \cos(2\pi k_j / \ell_j)} \hat{m}_k, \quad (13.93)$$

where $k = (k_1, k_2, \dots, k_d)$, so

$$K = \frac{1}{ds}, \quad (13.94)$$

Kadanoff eq. (4.38) shows that the d -dimensional Gaussian model only makes sense when K is in the interval $[-1/2d, 1/2d]$, i.e., if $|s| > 2$. If $|K|$ exceeds this limit (Kadanoff says “dragons live here”), the Gaussian integrals diverge at infinite q -values, and the whole problem stops making sense. When there is any qualitative change in behavior of a many particle system we say that it undergoes a phase transition. The Gaussian model does so at the two points $K = \pm 1/2d$.

I still have some (conceptual) sign problems, as Kadanoff shows that his allowed values K correspond to harmonic oscillator states. I would like that to correspond to $|s| < 2$. I also need to explain why spatiotemporal cat has grammar, while Gaussian model has no restrictions... Still do not understand why all our Hill determinants have an μ^2 prefactor. Inconclusive.

13.3 Tight-binding Hamiltonians

2017-09-11 Predrag Economou [40] *Green's Functions in Quantum Physics* ([click here](#)) contains a vast amount of useful information. Lattice shows up in chap. 5 *Green's Functions for tight-binding Hamiltonians*. Extracted text:

“[...] the Green’s functions for the so-called tight-binding Hamiltonian (TBH) are calculated. The TBH is of central importance for solid-state physics because it is the simplest example of wave propagation in periodic structures. It is also important for quantum physics in general because it is rich in physical phenomena (e.g., negative effective mass, creation of a bound state by a repulsive perturbation) and, at the same time, simple in its mathematical treatment. Thus one can derive simple, exact expressions for scattering cross sections and for bound and resonance levels. The multiple scattering formalism is presented within the framework of the TBH and applied to questions related to the behavior of disordered systems (such as amorphous semiconductors).”

He studies the Green’s functions associated with a class of periodic Hamiltonians, i.e., Hamiltonians remaining invariant under a translation by any vector on a regular d -dimensional lattice.

He also considers the more general case where the lattice can be divided into two interpenetrating sublattices such that each point of sublattice 1 is surrounded by points belonging to sublattice 2; the Hamiltonian remains invariant under translation by vectors of sublattice 1 or sublattice 2.

Periodic Hamiltonians are mathematically equivalent to a system of coupled 1-d harmonic oscillators and, as a result, they describe (by direct generalization to 3-d) the ionic motions in a crystalline solid.

In this approach one views the solids as being made up of atoms brought together from an infinite relative distance. It is then natural (following the usual practice for molecules) to try to express the unknown electronic wave functions as linear combinations of atomic orbitals (LCAO). The simplest version of this approach considers only one atom per primitive crystal cell, only one atomic orbital per atom, nearest-neighbor coupling only, and orthonormality of the atomic orbitals. This oversimplified version of the LCAO is known as the tight-binding model (TBM); the atomic orbital associated with the atom located at site ℓ is symbolized by

$$w(r - \ell) = \langle r|\ell\rangle. \quad (13.95)$$

The matrix elements of the Hamiltonian within this subspace are

$$H = \sum_{\ell} |\ell\rangle \epsilon_{\ell} \langle \ell| + \sum_{\ell m} |\ell\rangle V_{\ell m} \langle m|. \quad (13.96)$$

The diagonal matrix elements are denoted by ϵ_{ℓ} and the off-diagonal matrix elements by $V_{\ell m}$ ($V_{\ell\ell} = 0$). The periodicity of the Hamiltonian, i.e., its invariance under translations by a lattice vector ℓ , implies that

$$\epsilon_{\ell} = \epsilon_0 \quad (13.97)$$

$$V_{\ell m} = V_{\ell-m}. \quad (13.98)$$

For the sake of simplicity one assumes that

$$V_{\ell m} = \begin{cases} V & \text{if } \ell, m \text{ nearest neighbors} \\ 0 & \text{otherwise} \end{cases}. \quad (13.99)$$

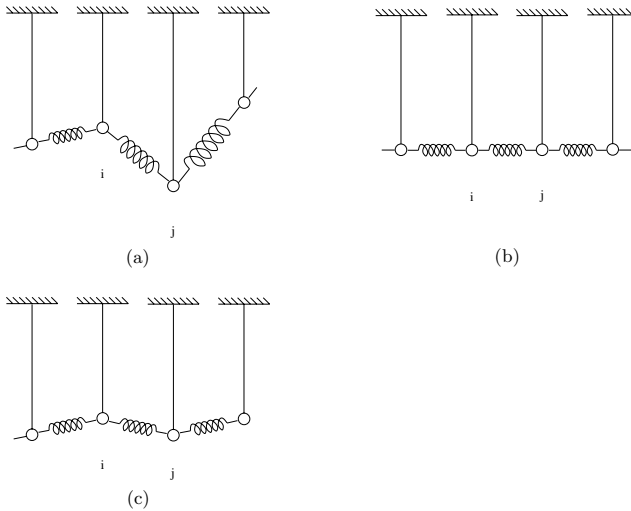


Figure 13.5: One-dimensional coupled pendulum analog of the tight-binding Hamiltonian, nearest-neighbor coupling (a). In the periodic case all pendula and all nearest-neighbor couplings are identical (b). The double spacing periodic case (c). (From Economou [40])

There is only one quantity, V , which, following the usual practice in the literature, can be taken as negative (for s-like orbitals V is indeed negative).

$$H = \begin{pmatrix} \epsilon_0 & V & 0 & 0 & \dots & 0 & V \\ V & \epsilon_0 & V & 0 & \dots & 0 & 0 \\ 0 & V & \epsilon_0 & V & \dots & 0 & 0 \\ \vdots & \vdots & \vdots & \vdots & \ddots & \vdots & \vdots \\ 0 & 0 & \dots & \dots & \dots & \epsilon_0 & V \\ V & 0 & \dots & \dots & \dots & V & \epsilon_0 \end{pmatrix}. \quad (13.100)$$

A negative V , in contrast to a positive V , preserves the well-known property that as the energy of real eigenfunctions increases so does the number of their sign alternation.

The first term on the rhs of (13.96) describes a particle that can be trapped around any particular lattice site ℓ with an eigenenergy ϵ_ℓ . The second term allows the particle to hop from site ℓ to site m with a transfer matrix element $V_{\ell m}$. The quantum motion associated with the Hamiltonian (13.96) is equivalent to the wave motion of the coupled pendula, see figure 13.5.

$$\left(m_i \omega_i^2 + \sum_j \kappa_{ij} - m_i \omega^2 \right) u_j - \sum_j \kappa_{ij} u_j = 0. \quad (13.101)$$

where u_i is the 1-d displacement of the pendulum located at site i , ω_i is its

eigenfrequency in the absence of coupling, and $\sum_j \kappa_{ij}(u_i - u_j)$ is the force exercised on the pendulum at the i site as a result of the couplings with all the other pendula; m_i is the mass at i .

If we generalize to 3-d displacements, the problem of coupled pendula is reduced to that of the ionic (or atomic) motion in solids (by setting $\omega_i = 0$) since each ion (or atom) is indeed performing small oscillations around its equilibrium position with the restoring force being equal to $-\sum_j \kappa_{ij}(u_i - u_j)$. This yields the electronic eigenfunctions and eigenenergies of the TBM. The eigenmodes are propagating waves such that the amplitude at each site is the same and the phase changes in a regular way. For a 2-d square lattice

$$E(\mathbf{k}) = \epsilon_0 + 2V[\cos(k_1 a) + \cos(k_2 a)], \quad (13.102)$$

where a is the lattice constant. In the 1d case, the function $E(\mathbf{k})$ has an absolute maximum (which corresponds to the upper band edge) for $k = \pi/a$ or $-\pi/a$ with a value $E_{max} = \epsilon_0 + 2|V|$; it has an absolute minimum (which corresponds to a lower band edge) for $k = 0$ with a value $E_{min} = \epsilon_0 - 2|V|$. Thus the spectrum is a continuum (a band) extending from $\epsilon_0 - 2|V|$ to $\epsilon_0 + 2|V|$. The bandwidth is $4|V|$.

In his eq. (5.38) the diagonal matrix element of the square lattice Greens function is given by the complete elliptic integral of the first kind [59] (5.251).

2020-10-04 Predrag The reason I went above into detail with TBM is (1) it is spatiotemporal cat for $s < 2$ and (2) has well known elliptic function solutions. According to (13.100), the precise formula relating ϵ_0 and V to spatiotemporal cat stretching factor s is

$$s = -\epsilon_0/V, \quad u_j \rightarrow u_j/\sqrt{-V}.$$

and the spectrum band extends from $\epsilon_0/|V| - 2$ to $\epsilon_0/|V| + 2$, in other words, TBM assumes $|s| < 2$.

I assume the band structure for $s < 2$ has no counterpart in the hyperbolic, $s < 2$ case, but am not sure.

2018-03-18 Predrag to Han - can you have a look at the Group Theory course week 8 exercises, solution 8.3? I should know this, but I do not, and you have thought about it: is spatiotemporal cat in any illuminating sense related to a tight-binding model? We are not doing QM, but if we formulate the problem in the continuous space $x \in \mathbb{R}^d$, rather than the integer lattice $x \in \mathbb{Z}^d$, our Hamiltonian is δ function on each site, and its neighbors.

If there is a relation, we definitely have to explain that in our paper, as many colleagues care about couple spin chains and lattices.

2020-01-27 Predrag to Han - For us there is no field $X(z)$ defined over continuum space $z \in \mathbb{R}^d$, only x_z . Our problems live on the integer lattices $z \in \mathbb{Z}^d$. This might be called ‘tight-binding models’. Please verify whether that’s what ‘tight-binding models’ are.

2019-10-10 Predrag Watanabe [129] *A proof of the Bloch theorem for lattice models:*

“The Bloch theorem states that the expectation value of the U(1) current operator averaged over the entire space vanishes for large quantum systems. The theorem applies as long as all terms in the Hamiltonian are finite ranged. Finite systems are sensitive to the boundary conditions. Under the periodic boundary condition, one can only prove that the current expectation value is inversely proportional to the linear dimension of the system, while the current expectation value completely vanishes before taking the thermodynamic limit when the open boundary condition is imposed. We also provide simple tight-binding models that clarify the limitation of the theorem in dimensions higher than one.”

2020-01-13 Predrag See also Cserti *et al.* [30, 31], in sect. 5.15 *Resistor networks*:

The energy-dependent lattice Green’s function of the tight-binding Hamiltonian for a square lattice, his eq. (30), has energy E playing the role of our stretching parameter s .

2019-07-13 Predrag Kohler and Cubitt [81] *Translationally invariant universal classical Hamiltonians* give an explicit construction of a translationally invariant, 2D, nearest-neighbour, universal classical Hamiltonian with a single free parameter, drawing on techniques from theoretical computer science, in particular complexity-theoretic results on tiling problems. Seems too sophisticated for us.

2020-04-19 Predrag See also chapter 9 *Chronotopic literature*, Politi, Torcini and Lepri [107] *Lyapunov exponents from node-counting arguments*: “That resembles the tight-binding approximation of the 1D Schrödinger equation (with imaginary time) in the presence of a random potential, i.e., the Anderson model.”

13.4 Discrete Schrödinger equation

2020-12-06 Predrag Marius Lemm, Arka Adhikari and Horng-Tzer Yau, *Global eigenvalue distribution of matrices defined by the skew-shift* arXiv:1903.11514 study the following question:

Suppose the entries of the large Hermitian matrices H_N are generated by sampling along the orbits of an ergodic dynamical system. Do their eigenvalues still exhibit random matrix statistics, like the Wigner semicircle law?

We will answer this question in the affirmative for the model of H_N defined below, where the underlying dynamical system is generated from the skew-shift dynamics:

$$\binom{j}{2}\omega + jy + x \mod 1,$$

Here $x, y \in \mathbb{T}$ (with \mathbb{T} being the torus) are the starting positions of the dynamical system and $\omega \in \mathbb{T}$ is a (typically irrational) parameter called the frequency. The skew-shift dynamics possesses only weak ergodicity properties, e.g., it is not even weakly mixing. Nonetheless, it is believed to behave in a quasi-random way (meaning like an i.i.d. sequence of random variables) in various ways reviewed at the end of the introduction. Moreover, the quasi-random behavior of the skew-shift should deviate from that of the more rigid standard shift $j\omega + x \bmod 1$ (the circle rotation by an irrational angle ω). The key difference between the skew-shift and circle rotation is of course the appearance of a quadratic term $j^2\omega$ for the skew-shift. This quadratic term has the effect of increasing the oscillations and thus improving the decay of the exponential sums over skew-shift orbits. This general fact is a central tenet of analytic number theory HL, Mont, W1, W2, and of our analysis here as well.

The model. Let \mathbb{T} be the one-dimensional torus, which we identify with $[0, 1]$ in the usual way. For the skew-shift, the role of the “angle” is played by the frequency $\omega \in [0, 1]$. The skew-shift is then the transformation

$$\begin{aligned} T : \mathbb{T}^2 &\rightarrow \mathbb{T}^2 \\ (x, y) &\mapsto (x + y, y + \omega). \end{aligned}$$

We write T^j for the j -fold iteration of T and $(T^j(x, y))_1$, for the first component of the vector $T^j(x, y) \in \mathbb{T}^2$, i.e.,

$$(T^j(x, y))_1 = \binom{j}{2}\omega + jy + x. \quad (13.103)$$

We consider $2N \times 2N$ Hermitian matrices of the form

$$H = \begin{pmatrix} 0 & X \\ X^* & 0 \end{pmatrix}$$

with X an $[N \times N]$ matrix generated from the skew-shift via

$$X_{i,j} = \frac{1}{\sqrt{N}}e \left[\left(\binom{j}{2}\omega_i + jy_i + x_i \right) \right], \quad e[t] := \exp(2\pi it) \quad (13.104)$$

Here the $\omega_1, \dots, \omega_N$ are chosen deterministically (see the examples below), the y_1, \dots, y_N in (13.104) are sampled uniformly and independently from $[0, 1]$, and the x_1, \dots, x_N are arbitrary. (In particular, one can take $x_1 = x_2 = \dots = x_N = 0$.)

Predrag: (13.104) is an $[N \times N]$ matrix full of complex phases: it is unlike our 3-banded matrices, I think we can ignore these papers.

Marius Lemm GaTech seminar 2020-04-09: “Global eigenvalue distribution of matrices defined by the skew-shift: A central question in ergodic theory is whether sequences obtained by sampling along the orbits of a given

dynamical system behave similarly to sequences of i.i.d. random variables. Here we consider this question from a spectral-theoretic perspective. Specifically, we study large Hermitian matrices whose entries are defined by evaluating the exponential function along orbits of the skew-shift on the 2-torus with irrational frequency. We prove that their global eigenvalue distribution converges to the Wigner semicircle law, a hallmark of random matrix statistics, which evidences the quasi-random nature of the skew-shift dynamics. ”

Kielstra and Lemm *On the finite-size Lyapunov exponent for the Schrödinger operator with skew-shift potential* [arXiv:1904.08871](https://arxiv.org/abs/1904.08871).

A one-dimensional quantum particle living on \mathbb{Z} with energy $E \in \mathbb{R}$ is described by the discrete Schrödinger equation

$$\psi_{n+1} + \lambda v_n \psi_n + \psi_{n-1} = E \psi_n, \quad (13.105)$$

where $\psi = (\psi_n)_{n \in \mathbb{Z}}$ is a sequence in $\ell^2(\mathbb{Z}; \mathbb{C})$. The real-valued potential sequence $v = (v_n)_{n \in \mathbb{Z}}$ represents the environment that the particle is subjected to. (The “coupling constant” $\lambda > 0$ is factored out for convenience.) Physically, one observes a sudden onset of insulating behavior in the presence of a random environment (“Anderson localization”). Mathematically, it is known that for arbitrarily small $\lambda > 0$, the one-dimensional Schrödinger operator

$$(H\psi)_n = \psi_{n+1} + \lambda v_n \psi_n + \psi_{n-1}. \quad (13.106)$$

has pure point spectrum with exponentially decaying eigenfunctions [16, 84].

A natural follow-up question is then: How random does the environment have to localize the quantum particle? Alternative “quasi-random” environments are generated by sampling a nice function along the orbit of an ergodic dynamical system. This question is interesting from a purely mathematical ergodic theory perspective, but it also has practical implications, since computer simulations are mostly based on appropriate pseudo-random number sequences.

A standing conjecture in this direction concerns the case when the potential is generated from the nonlinear skew-shift dynamics $T : \mathbb{T}^2 \rightarrow \mathbb{T}^2$, $T(x, y) = (x + y, y + \omega)$, namely it is of the form

$$v_n = 2 \cos \left(\binom{n}{2} \omega + ny + x \right) \quad (13.107)$$

with ω irrational (say Diophantine). The key difference between (13.107) compared to $v_n = 2 \cos(n\alpha + \theta)$ is the appearance of the nonlinear quadratic term $n^2\omega$. The conjecture states that the associated Schrödinger operator H defined by (13.106) is Anderson localized for arbitrarily small $\lambda > 0$ everywhere in the spectrum. Partial results in this vein are due to Bourgain

and Bourgain-Goldstein-Schlag. Note that the conjecture says in particular that the skew-shift dynamics is appreciably more random-like than the circle rotation where $v_n = 2 \cos(n\alpha + \theta)$. (Recall that the latter is only localized for $\lambda > 1$, for us $s > 2$.) The observation that the skew-shift is more quasi-random than the shift has been made in another context by Rudnick-Sarnak-Zaharescu RSZ and others DR,MY,RS (concerning the spacing distribution) and also recently in ALY (concerning eigenvalues of large Hermitian matrices).

2020-12-06 Predrag Possibly also of interest: Marius Lemm and David Sutter *Quantitative lower bounds on the Lyapunov exponent from multivariate matrix inequalities* arXiv:2001.09115: The Lyapunov exponent characterizes the asymptotic behavior of long matrix products. Recognizing scenarios where the Lyapunov exponent is strictly positive is a fundamental challenge that is relevant in many applications. In this work we establish a novel tool for this task by deriving a quantitative lower bound on the Lyapunov exponent in terms of a matrix sum which is efficiently computable in ergodic situations. Our approach combines two deep results from matrix analysis — the n-matrix extension of the Golden-Thompson inequality and the Avalanche-Principle. We apply these bounds to the Lyapunov exponents of Schrödinger cocycles with certain ergodic potentials of polymer type and arbitrary correlation structure. We also derive related quantitative stability results for the Lyapunov exponent near aligned diagonal matrices and a bound for almost-commuting matrices.

2020-12-06 Predrag Carmona, Klein and Martinelli [16] *Anderson localization for Bernoulli and other singular potentials*:

Bernoulli potentials are potentials that take only two values

$$\mu = p\delta(v - a) + (1 - p)\delta(v - b), \quad 0 < p < 1.$$

Kunz and Souillard [84] *Sur le spectre des opérateurs aux différences finies aléatoires* is presumably similar - models for Anderson localization, we do not need them here.

13.5 Harper's model

2020-12-06 Predrag Kielstra and Lemm *On the finite-size Lyapunov exponent for the Schroedinger operator with skew-shift potential* arXiv:1904.08871 write: “For example, one can consider $v_n = 2 \cos(n\alpha + \theta)$ generated from sampling cosine along an irrational circle rotation; this is the Harper [53] or almost-Mathieu [117] model. It turns out that these linear underlying dynamics only produce localization for sufficiently strong potentials, namely only for $\lambda > 1$ (for us, $s > 2$) [70]. ”

Jitomirskaya [70] *Metal-insulator transition for the almost Mathieu operator*.

Svetlana Jitomirskaya, Lyuben Konstantinov and Igor Krasovsky
On the spectrum of critical almost Mathieu operators in the rational case
arXiv:2007.01005:

The Harper operator, a.k.a. the discrete magnetic Laplacian a tight-binding model of an electron confined to a 2D square lattice in a uniform magnetic field orthogonal to the lattice plane and with flux $2\pi\alpha$ through an elementary cell. It acts on $\ell^2(\mathbb{Z}^2)$ and is usually given in the Landau gauge representation

$$(H(\alpha)\psi)_{m,n} = \psi_{m,n-1} + \psi_{m,n+1} + e^{-i2\pi\alpha n}\psi_{m-1,n} + e^{i2\pi\alpha n}\psi_{m+1,n}, \quad (13.108)$$

first considered by Peierls [104], who noticed that it makes the Hamiltonian separable and turns it into the direct integral in θ of operators on $\ell^2(\mathbb{Z})$ given by:

$$(H_{\alpha,\theta}\phi)_n = \phi_{n-1} + 2\cos(2\pi(\alpha n + \theta))\phi_n + \phi_{n+1}, \quad \alpha, \theta \in [0, 1]. \quad (13.109)$$

In physics literature, it also appears under the names Harper's or the Azbel-Hofstadter model, with both names used also for the discrete magnetic Laplacian $H(\alpha)$. In mathematics, it is universally called the critical almost Mathieu operator [117]. In addition to importance in physics, this model is of special interest, being at the boundary of two reasonably well understood regimes: (almost) localization and (almost) reducibility, and not being amenable to methods of either side.

Simon [117] *Almost periodic Schrödinger operators: A review*
[...] one-dimensional Schrödinger equation, $H = -d^2/dx^2 + V(x)$ with $V(x)$ almost periodic and the discrete (= tight binding) analog, i.e., the doubly infinite Jacobi matrix

$$h_{ij} = \delta_{i,j+1} + V_i\delta_{i,j} + \delta_{i,j-1} \quad (13.110)$$

with V_n almost periodic on the integers.

The Chambers' formula presents the dependence of the determinant of the almost Mathieu operator with $\alpha = p/n$ restricted to the period n with Floquet boundary conditions, on the phase θ and quasimomentum k . In the critical case it is given by

$$\det(\mathcal{J}_{\theta,k,n} - E) = \Delta(E) - 2(-1)^n(\cos(2\pi n\theta) + \cos(kn)), \quad (13.111)$$

where $\ell \in \mathbb{Z}/n$, and in our notation (13.109) is written as (1.118)

$$x_{\ell+1} - s_\ell x_\ell + x_{\ell-1} = -s_\ell, \quad (13.112)$$

with site-dependent stretching s_ℓ (so not a Toeplitz matrix, compare with

(7.7), (18.181), (7.70),(8.24),(8.34), (8.46))

$$\mathcal{J}_{\theta,k,n} := \begin{pmatrix} -s_0 & 1 & 0 & 0 & \cdots & 0 & 0 & e^{-ikn} \\ 1 & -s_1 & 1 & 0 & \cdots & 0 & 0 & 0 \\ 0 & 1 & -s_2 & 1 & \cdots & 0 & 0 & 0 \\ \vdots & \vdots & \vdots & \vdots & \ddots & \vdots & \vdots & \vdots \\ 0 & 0 & 0 & 0 & \cdots & 1 & -s_{n-2} & 1 \\ e^{ikn} & 0 & 0 & 0 & \cdots & 0 & 1 & -s_{n-1} \end{pmatrix}, \quad (13.113)$$

compare with the orbit Jacobian matrix \mathcal{J} (5.83). For Harper model, stretching s_ℓ is given by

$$s_\ell(\theta) = -2 \cos(2\pi \frac{p}{n} \ell + \theta), \quad s(x) = x, \quad (13.114)$$

and the discriminant Δ is independent of θ and k . They obtain a formula of this type for $\det(B_{\theta,k,\ell} - E)$.

2020-12-06 Predrag For $\alpha \in \mathbb{Z}$ this is a Helmholtz problem with stretching parameter $s = 2 \cos 2\pi(\theta)$.

For rational α has periodic s [58], as in (13.114). Note the relative-periodic corner phases $e^{\pm ikq}$ in (13.113)).

Hofstadter [58] *Energy levels and wave functions of Bloch electrons in rational and irrational magnetic fields* writes about rational case: “Algebra reveals the fact that this condition on α is precisely that of rationality: We now proceed, making full use of this somewhat bizarre ansatz.”

He, as everybody else, sooner or later, rewrites (13.112) in the “Percival-Vivaldi” ‘two-configuration representation’ [105] matrix J (1.5),

$$\begin{pmatrix} \Delta\phi_t \\ \Delta\phi_{t+1} \end{pmatrix} = \begin{pmatrix} 0 & 1 \\ -1 & s_t \end{pmatrix} \begin{pmatrix} \Delta\phi_{t-1} \\ \Delta\phi_t \end{pmatrix}. \quad (13.115)$$

(note ‘upside-down’ 2D vector), and concerns himself with the rational, energy $\text{tr } J^m < 2$, oscillatory case.

Note, it’s only about the order of recurrence, nobody says the systems should be Hamiltonian / Lagrangian, works for dissipative systems as well.

The famed butterfly is a plot of the eigenvalues for all rational phases α .

2020-12-06 Predrag I am looking at (13.109) because this is a different way to introduce a nonlinearity than the Hénon CML (9.3) because for irrational α it has a quadratic dependence on the lattice site,

$$2 \cos(2\pi\alpha n) = 2 - (2\pi\alpha n)^2 + \dots$$

Nevertheless, this discrete Schrödinger is very different from temporal cat, so one more Sunday has been wasted (?) on learning other stuff.

2021-06-25 Indubala Satija *Geometry, Number Theory and the Butterfly Spectrum of Two-Dimensional Bloch Electrons* [arXiv:2106.1387](https://arxiv.org/abs/2106.1387):

We take a deeper dive into the geometry and the number theory that underlay the butterfly graphs of the Harper and the generalized Harper models of Bloch electrons in a magnetic field. Root of the number theoretical characteristics of the fractal spectrum is traced to a close relationship between the Farey tree – the hierarchical tree that generates all rationals and the Wannier diagram – a graph that labels all the gaps of the butterfly graph. The resulting Farey-Wannier hierarchical lattice of trapezoids provides geometrical representation of the nested pattern of butterflies in the butterfly graph. Some features of the energy spectrum such as absence of some of the Wannier trajectories in the butterfly graph fall outside the number theoretical framework, can be stated as a simple rule of "minimal violation of mirror symmetry". In a generalized Harper model, Farey-Wannier representation prevails as the lattice regroups to form some hexagonal unit cells creating new *species* of butterflies.

13.6 Frenkel-Kontorova model

2021-02-01 Predrag The equilibria and relative equilibria of Frenkel-Kontorova models [5], widely studied in literature, might be closely related to temporal Hénon and ϕ^4 lattices.

It is difficult stuff, safely ignored, for now:)

Note the text below (8.17) and (13.116).

Search for **2019-12-12 Meisinger and Ogilvie** notes in this blog.

2021-02-01 Anna Vainchtein (U. Pittsburgh)

Traveling waves in a driven Frenkel-Kontorova lattice: Variants of Frenkel-Kontorova model, originally proposed to describe dislocations in crystal lattices, have been widely used to study a variety of physical phenomena, including dynamics of twin boundaries and domain walls, crystal growth, charge-density waves, Josephson junctions and DNA denaturation. I discuss properties and stability of traveling waves in chains of Frenkel-Kontorova type driven by a constant external force. After reviewing some earlier studies for piecewise-smooth variants of the model, where exact and semi-analytical solutions can be constructed, I will describe numerical results for a fully nonlinear damped driven chain from a recent work with J. Cuevas-Maraver (U. of Sevilla), P. Kevrekidis (U. of Mass.) and H. Xu (Huazhong U.). In this setting, **traveling wave solutions are computed as fixed points of a nonlinear map**. [...] Exploring the spectral stability of the obtained waveforms, we identify, at the level of numerical accuracy of our computations, a precise criterion for instability of the traveling wave solutions: monotonically decreasing portions of the kinetic curve always bear an unstable eigendirection.

The recorded talk will be available [here](#). It is a difficult subject, but our case - equilibria and relative equilibria is perhaps a trivial case described in this literature.

2019-06-26 Predrag Mramor and Rink [100] *Ghost circles in lattice Aubry-Mather theory*, [arXiv:1111.5963](#):

“Monotone lattice recurrence relations such as the Frenkel-Kontorova lattice, arise in Hamiltonian lattice mechanics as models for ferromagnetism and as discretization of elliptic PDEs. They are a multidimensional counterpart of monotone twist maps.”

The paper has an appendix of twist maps, refers to Mather and Forni [96] *Action minimizing orbits in Hamiltonian systems*. Example of exact symplectic twist maps are the Chirikov standard map and convex billiards. I think the focus in all this work is on *integrable*, not chaotic: “Under generic conditions, the Poincaré return map of a 2 degree of freedom Hamiltonian system near an elliptic equilibrium point is an exact symplectic twist map. In this case, the corresponding twist map is close to *integrable*, so that it allows for the application of various kinds of perturbation theory [96].” Lectures on *Equidistribution of periodic orbits: An overview of classical VS quantum results* by Degli Esposti, Graffi, and Isola in *Transition to Chaos in Classical and Quantum Mechanics* [11] are also of interest.

Twist maps often admit a variational structure, so that the solutions $x : \mathbb{Z}^d \rightarrow \mathbb{R}$ are the stationary points of a formal action function $W(x)$. Given any rotation vector $\omega \in \mathbb{R}^d$, Aubry-Mather theory establishes the existence of a large collection of solutions of $\nabla W(x) = 0$ of rotation vector ω . For irrational ω , this is the *Aubry-Mather set*. It consists of global minimizers and it may have gaps.

The part relevant to our spatiotemporal cat is the idea of studying globally stationary solutions by means of a formal gradient. We do not really know how to find all invariant 2-tori in 2 or more dimensions, even though we know how to count them, right? They study the parabolic gradient flow $\frac{dx}{dt} = -\nabla W(x)$ and prove that every Aubry-Mather set can be interpolated by a continuous gradient-flow invariant family, the so-called ‘ghost circle’. The existence of these ghost circles is known in dimension $d = 1$, for rational rotation vectors and Morse action functions.

d -dimensional Frenkel-Kontorova lattice: Here, the goal is to find a d -dimensional “lattice configuration” $x : \mathbb{Z}^d \rightarrow \mathbb{R}$ that satisfies

$$V'(x_i) - (\Delta x)_i = 0 \text{ for all } i \in \mathbb{Z}^d. \quad (13.116)$$

The smooth function $V : \mathbb{R} \rightarrow \mathbb{R}$ satisfies $V(\xi + 1) = V(\xi)$ for all $\xi \in \mathbb{R}$. It has the interpretation of a periodic onsite potential.

I like their definition of the discrete Laplace operator $\Delta : \mathbb{R}^{\mathbb{Z}^d} \rightarrow \mathbb{R}^{\mathbb{Z}^d}$, defined as

$$(\Delta x)_i := \frac{1}{2d} \sum_{||j-i||=1} (x_j - x_i) \text{ for all } i \in \mathbb{Z}^d. \quad (13.117)$$

where $||i|| := \sum_{k=1}^d |i_k|$. Thus, $(\Delta x)_i$ is the average of the quantity $x_j - x_i$ computed over the lattice points that are nearest to that with index i , i.e., the graph Laplacian [24, 108] (13.53) for the case of hypercubic lattice, or the “central difference operator” [105].

One can think of (13.116) as a naive discretization of the nonlinear elliptic partial differential equation $V'(u) - \Delta u = 0$ for a function $u : \mathbb{R}^d \rightarrow \mathbb{R}$ and $x_i = u(i)$.

Eq. (13.116) is relevant for statistical mechanics, because it is related to the Frenkel-Kontorova Hamiltonian lattice differential equation

$$\frac{d^2 x_i}{dt^2} + V'(x_i) - (\Delta x)_i = 0 \text{ for all } i \in \mathbb{Z}^d. \quad (13.118)$$

This differential equation describes the motion of particles under the competing influence of an onsite periodic potential field and nearest neighbor attraction. Eq. (13.116) describes its stationary solutions.

In dimension $d = 1$, the solutions of equation (13.116) correspond to orbits of the Chirikov standard map $T_V : \mathbb{A} \rightarrow \mathbb{A}$ of the annulus.

The Frenkel-Kontorova problem (13.116) is an example from a quite general class of lattice recurrence relations to which the results of this paper apply. These are recurrence relations for which there exists, for every $j \in \mathbb{Z}^d$, a real-valued “local potential” function $S_j : \mathbb{R}^{\mathbb{Z}^d} \rightarrow \mathbb{R}$ so that the relation can be written in the form

$$\sum_{j \in \mathbb{Z}^d} \partial_i S_j(x) = 0 \text{ for all } i \in \mathbb{Z}^d. \quad (13.119)$$

It turns out that for the Frenkel-Kontorova problem (13.116), such local potentials exist and it is easy to check that they are given by

$$S_j(x) := V(x_j) + \frac{1}{8d} \sum_{||k-j||=1} (x_k - x_j)^2. \quad (13.120)$$

For the general problem (13.119), the functions $S_j(x)$ will be required to satisfy some rather restrictive hypotheses. Physically, the most important of these hypotheses is the *monotonicity* condition. It is a discrete analogue of ellipticity for a PDE. Among the more technical hypotheses is one that guarantees that the sums in expression (13.119) are finite. For the purpose of this introduction, it probably suffices to say that the potentials (13.120) of Frenkel-Kontorova are prototypical for the $S_j(x)$ that we have in mind.

It is important to observe that the solutions of (13.119) are precisely the stationary points of the formal sum

$$W(x) := \sum_{j \in \mathbb{Z}^d} S_j(x). \quad (13.121)$$

This follows because differentiation of (13.121) with respect to x_i produces exactly equation (13.119) and it explains why solutions to (13.119) are sometimes called *stationary* configurations.

In the case that the periodic onsite potential $V(\xi)$ vanishes, the Frenkel-Kontorova equation (13.116) reduces to the discrete Laplace equation $\Delta x = 0$, for which it is easy to point out solutions. For instance, when $\xi \in \mathbb{R}$ is an arbitrary number and $\omega \in \mathbb{R}^d$ is an arbitrary vector, then the linear functions $x^{\omega, \xi} : \mathbb{Z}^d \rightarrow \mathbb{R}$ defined by

$$x_i^{\omega, \xi} := \xi + \langle \omega, i \rangle$$

obviously satisfy $\Delta x = 0$. It moreover turns out that the $x^{\omega, \xi}$ are *action-minimizers*, in the sense that for every finite subset $B \subset \mathbb{Z}^d$ and every $y : \mathbb{Z}^d \rightarrow \mathbb{R}$ with support in B , it holds that

$$\sum_{j \in \mathbb{Z}^d} (S_j(x^{\omega, \xi} + y) - S_j(x^{\omega, \xi})) \geq 0.$$

Note that this sum is actually finite and can be interpreted as $W(x^{\omega, \xi} + y) - W(x^{\omega, \xi})$.

Definition 13.1. Let $x : \mathbb{Z}^d \rightarrow \mathbb{R}$ be a d -dimensional configuration. We say that $\omega \in \mathbb{R}^d$ is the rotation vector of x if for all $i \in \mathbb{Z}^d$, the limit

$$\lim_{n \rightarrow \infty} \frac{x_{ni}}{n} \text{ exists and is equal to } \langle \omega, i \rangle.$$

Clearly, the rotation vector of $x^{\omega, \xi}$ is equal to ω . On the other hand, in dimension $d \neq 1$, a solution to (13.116) does not necessarily have a rotation vector. An example is the hyperbolic configuration x^h defined by $x_i^h = i_1 i_2 \cdots i_{d-1} i_d$ which solves $\Delta x = 0$.

13.7 Mean field theory for the Ising model

According to E. Brézin and J. Zinn-Justin, finite-size mean field theory for the Ising model is described by the distribution

$$p_{\text{MFT}}(m) \propto \exp(-N f(m)), \quad (13.122)$$

where N is the number of spins and the free energy (the large-deviation potential) at reduced temperature \tilde{t} is

$$f(m) = \frac{1}{2} \tilde{t} m^2 + \frac{1}{4!} m^4, \quad (13.123)$$

to leading order in N .

13.8 Clock model

The [free field solutions](#) of Potts models are most directly related to our dynamical considerations. If all states are allowed the underlying set of states is given by a full shift. If neighboring spins are only allowed in certain specific configurations, then the state space is given by a subshift of finite type. The partition function may then be written as a trace of the adjacency matrix, specifying which neighboring spin values are allowed.

The [wiki](#) says: The Z_N model, a generalization of the Ising model, sometimes known as the *clock model* or the *vector Potts model*, is defined by assigning a spin value at each node r on a graph, with the spins taking values $S_r = \exp \frac{2\pi i q}{N}$, where $q \in \{0, 1, \dots, N-1\}$. The spins therefore take values in the form of complex roots of unity. The spin assigned to each node of the Z_N model is pointing in any one of N directions. The Boltzmann weights for a general edge rr' are:

$$w(r, r') = \sum_{k=0}^{N-1} x_k^{(rr')} (S_r S_{r'}^*)^k$$

where $*$ denotes complex conjugation and the $x_k^{(rr')}$ are related to the interaction strength along the edge rr' . Note that $x_k^{(rr')} = x_{N-k}^{(rr')}$ and x_0 is often set to 1. The (real valued) Boltzmann weights are invariant under the transformations $S_r \rightarrow \omega^k S_r$ and $S_r \rightarrow S_r^*$, the universal rotation and the reflection respectively.

The q -state clock model discretizes the rotor angle $[0, 2\pi]$, so that is not what we need; spatiotemporal cat has discrete winding numbers. It is $X - Y$ model that has our s_n as vortex charges, and interactions between (mod 1) angles, except those are no the nearest neighbor, but logarithmic.

The local magnetic moment or “spin”, a 2D vector dimensionless vector of magnitude one, $S_i = (\cos(2\pi q k), \sin(2\pi q k))$, where $k = 0, 1, \dots, q-1$, at site i can point in any of the q directions in a given plane, with equal probability for all q values. The isotropic Hamiltonian for such a system can be written as:

$$H = -\frac{J}{2} \sum_{\langle ij \rangle} S_i \cdot S_j - B \cdot \sum_i S_i, \quad (13.124)$$

In the q -state clock model on each lattice point there is a vector spin pointing to q different directions, which differ by the angle $2\pi/q$. The 2D q -state clock model is defined by the Hamiltonian

$$H = -J \sum_{\langle ij \rangle} \cos(\theta_i - \theta_j) - h \sum_i \cos \theta_i, \quad (13.125)$$

where J is interaction strength, the summation is over the nearest neighbors, h is the applied weak magnetic field in units of J/μ , where μ is the magnetic moment of each spin usually set to 1, and $\theta_i = 2\pi n_i/q$ with $n_i = 0, \dots, q-1$. Generalized Eq. (13.125) is of form

$$H = \sum_{\langle ij \rangle} V(\theta_i - \theta_j) - h \sum_i \cos \theta_i,$$

where the spin-interaction potential V has the Z_q symmetry. The Villain q -state clock model has

$$V(\phi) = -\frac{J}{\beta} \ln \left\{ \sum_{n=-\infty}^{\infty} \exp [-\beta(\phi - 2\pi n)^2/2] \right\},$$

where $\beta \equiv 1/(k_B T)$ with the Boltzmann constant k_B and temperature T . This potential has been introduced to separate the vortex degrees of freedom from the spin-wave degrees of freedom as an approximate version of the XY model. The Villain clock model on the square lattice possesses self-duality.

The case $q=2$ corresponds to the Ising model, the case $q=3$ is a special case of the Potts model. Already for $q=4$ the phase diagram is more complicated than for the Ising model: there are 3 phases, instead of 2.

Once the partition function is known, the thermodynamic observables, such as internal energy U , specific heat C , and entropy S , can be calculated by employing [101]:

$$U(T) = T^2 \frac{\partial}{\partial T} \ln Z(T, B). \quad (13.126)$$

$$C(T) = \frac{\partial U}{\partial T}, \quad (13.127)$$

$$S(T) = \frac{U}{T} + \ln Z(T, B). \quad (13.128)$$

The lattice average of the spin configuration, equivalent to the magnetization per site M , is given by

$$M = \frac{1}{N} \sum_j S_j. \quad (13.129)$$

They go on to compute the internal energy U and the specific heat C .

In all of the literature the focus is on Berezinskii-Kosterlitz-Thouless (BKT) transition, between a topological phase and the high-temperature paramagnetic (or disordered) phase, and phases possible for $q > 5$. If there is no continuous symmetry, existence of standard ferromagnetic order is allowed at low but finite temperature.

We are focused on the high-temperature paramagnetic (or disordered) phase.

2019-12-12 Predrag Meisinger and Ogilvie *The Sign Problem, PT Symmetry and Abelian Lattice Duality* arXiv:1306.1495: For Abelian models in the class of lattice field theories with the fundamental fields which are elements

section 13.6

$z = \exp(i\theta)$ of $Z(N)$ or $U(1)$, with complex actions, lattice duality maps models with complex actions into dual models with real actions.

Explicit duality relations are given for models for spin and gauge models based on $Z(N)$ and $U(1)$ symmetry groups. The dual forms are generalizations of the $Z(N)$ chiral clock model and the lattice Frenkel-Kontorova model, respectively.

We begin with duality for $d = 2$ $Z(N)$ models with a chemical potential for the Villain, or heat kernel, action. Defining the site-based spin variables as $\exp(2\pi i m(x)/N)$, with $m(x)$ an integer between 0 and N , the partition function is given by

$$Z[J, \mu\delta_{\nu,2}] = \sum_m \sum_{n_\nu} \exp \left[-\frac{J}{2} \sum_{x,\nu} \left(\frac{2\pi}{N} \partial_\nu m(x) - i\mu\delta_{\nu,2} - 2\pi n_\nu(x) \right)^2 \right] \quad (13.130)$$

where $\partial_\nu m(x) \equiv m(x+\hat{\nu}) - m(x)$ and the sum over link variables $n_\nu(x) \in Z$ ensures periodicity. Using the properties of the Villain action, we can write

$$\begin{aligned} Z[J, \mu\delta_{\nu,2}] &= (2\pi J)^{-dV/2} \sum_m \sum_{p_\nu} \exp \left[-\frac{1}{2J} \sum_{x,\nu} p_\nu^2(x) \right. \\ &\quad \left. + i \sum_{x,\nu} p_\nu(x) \left(\frac{2\pi}{N} \partial_\nu m(x) - i\mu\delta_{\nu,2} \right) \right] \end{aligned}$$

where V is the number of sites on the lattice such that dV is the number of links. Summation over the $m(x)$'s give a set of delta function constraints:

$$Z[J, \mu\delta_{\nu,2}] = (2\pi J)^{-dV/2} \sum_{p_\nu} \exp \left[-\frac{1}{2J} \sum_{x,\nu} p_\nu^2(x) + \sum_{x,\nu} p_2(x) \mu \right] \prod_x \delta_{\partial \cdot p, 0(N)}$$

where the notation in the Kronecker delta function indicates $\partial \cdot p = 0$ modulo N . We introduce a dual bond variable $\tilde{p}_\rho(X)$ associated with the dual lattice via $p_\nu(x) = \epsilon_{\nu\rho} \tilde{p}_\rho(X)$ and note that the constraint on p_ν is solved by $\tilde{p}_\rho(X) = \partial_\rho \tilde{q}(X) + N \tilde{r}_\nu(X)$. We have

$$\begin{aligned} Z[J, \mu\delta_{\nu,2}] &= (2\pi J)^{-dV/2} \sum_{\tilde{q}} \sum_{\tilde{r}_\nu} \exp \left[-\frac{1}{2J} \sum_{x,\nu} (\partial_\rho \tilde{q}(X) + N \tilde{r}_\nu(X))^2 \right. \\ &\quad \left. + \mu \sum_{x,\nu} (\partial_1 \tilde{q}(X) + N \tilde{r}_1(X)) \right] \end{aligned}$$

which leads to

$$Z[J, \mu\delta_{\nu,2}] = (2\pi J)^{-dV/2} \exp \left[+\frac{V}{2} J \mu^2 \right] Z \left[\frac{N^2}{4\pi^2 J}, -i \frac{2\pi J \mu}{N} \delta_{\nu,1} \right]$$

The generalized duality here is

$$J \rightarrow \tilde{J} = \frac{N^2}{4\pi^2 J} \quad (13.131)$$

$$\mu\delta_{\nu,2} \rightarrow \tilde{\mu}\delta_{\nu,1} = -i\frac{2\pi J\mu}{N}\delta_{\nu,1}. \quad (13.132)$$

The dual of the original model, which has a complex action, is a chiral $Z(N)$ model with a real action.

2019-12-12 Predrag Jing Chen, Hai-Jun Liao, Hai-Dong Xie, Xing-Jie Han, Rui-Zhen Huang, Song Cheng, Zhong-Chao Wei, Zhi-Yuan Xie, and Tao Xi-ang, *Phase transition of the q -state clock model: duality and tensor renormalization*, [arXiv:1706.03455](https://arxiv.org/abs/1706.03455).

Now, memorize the authors:)

2019-12-22 Predrag

2019-12-22 Predrag

13.9 X - Y model

2019-12-22 Predrag Peter N. Meisinger and Michael C. Ogilvie, *The Sign Problem, PT Symmetry and Abelian Lattice Duality*, [arXiv:1306.1495](https://arxiv.org/abs/1306.1495) (see also Meisinger and Ogilvie *The sign problem and Abelian lattice duality*, [arXiv:1311.5515](https://arxiv.org/abs/1311.5515)): The partition function of the two-dimensional XY model with an imaginary chemical potential term has the form

$$Z[K, \mu\delta_{\nu,2}] = \int_{S^1} [d\theta] \sum_{n_\nu} \exp \left[-\frac{K}{2} \sum_{x,\nu} (\partial_\nu \theta(x) - i\mu\delta_{\nu,2} - 2\pi n_\nu(x))^2 \right].$$

Using the properties of the Villain action, we have

$$Z[K, \mu\delta_{\nu,2}] = \int_{S^1} [d\theta] \prod_{x,\nu} \sum_{p_\nu(x) \in Z} \frac{1}{\sqrt{2\pi K}} e^{-p_\nu^2(x)/2K} e^{ip_\nu(x)(\nabla_\nu \theta(x) - i\delta_{\nu,2}\mu)}.$$

[...] The partition function is now

$$Z = \sum_{\{m(X)\} \in Z} \frac{1}{\sqrt{2\pi K}} e^{-\sum_X [\sum_\nu (\nabla_\nu m(X))^2 / 2K + \mu \nabla_1 m(X)]}.$$

The final step is to introduce a new field $\phi(x) \in R$ using a periodic δ -function, effectively performing a Poisson resummation:

$$Z = \int_R [d\phi(X)] e^{-\sum_X [\sum_\nu (\nabla_\nu \phi(X))^2 / 2K + \mu \nabla_1 \phi(X)]} \sum_{\{m(X)\} \in Z} e^{2\pi i m(X)\phi(X)}.$$

If we keep only the $m = 1$ contributions, we have a lattice sine-Gordon model

$$Z = \int_R [d\phi(X)] \exp \left[- \sum_{X,\mu} \frac{1}{2K} (\nabla_\mu \phi(X))^2 - \sum_X \mu \nabla_1 \phi(X) + \sum_X 2y \cos(2\pi \phi(X)) \right]$$

with $y = 1$. This will be recognized as a two-dimensional lattice version of the Frenkel-Kontorova model, a sine-Gordon model with an additional term proportional to μ . For each fixed value of X_2 , the term $\sum_X \nabla_1 \phi(X)$ counts the number of kinks on that slice: The particles in the original representation manifest as lattice kinks in the dual representation.

2020-06-15 Predrag I do not even know what this is: Mazel, Stuhl and Suhov, *High-density hard-core model on \mathbb{Z}^2 and norm equations in ring $\mathbb{Z}[\sqrt[8]{-1}]$* , arXiv:1909.11648. They study the Gibbs statistics of high-density hard-core configurations on a unit square lattice \mathbb{Z}^2 , for a general Euclidean exclusion distance D , with $D^2 = a^2 + b^2$, $a, b \in \mathbb{Z}$. Pictorially, the problem is to study properties of configurations formed by non-overlapping ‘hard spheres’ of a given diameter (or exclusion distance) D with specified positions of the centers.

They say that a configuration ϕ is periodic if there exist two linearly independent vectors e_1, e_2 such that $\phi(x) = \phi(x + e_1) = \phi(x + e_2)$. If a periodic configuration ϕ contains the origin, we say that ϕ is a *sub-lattice*. The parallelogram with vertices $0, e_1, e_2, e_1 + e_2$ is a *fundamental parallelogram* (FP) for ϕ . We always assume that $e_{1,2}$ are chosen so that the shorter diagonal of the FP divides it into two triangles with non-obtuse angles; one of these triangles, with a vertex at the origin, is referred to as a *fundamental triangle* (FT). They say that a sub-lattice is isosceles or non-isosceles if the FT is isosceles or not.

The term \mathbb{Z}^2 -triangle means a triangle with vertices in \mathbb{Z}^2 . Without loss of generality we will assume that one of the vertices is at the origin $(0, 0)$.

They say that a given value D exhibits *sliding* if exist two or more M-triangles $T^{(1)}, T^{(2)}, \dots$, with (i) a common side called a *sliding base*, with two common vertices, and (ii) distinct third vertices lying in the same half-plane relative to the shared side. Sliding leads to a multitude of periodic and non-periodic ground states characterized by layered or staggered patterns. The point is that under sliding there are countably many periodic and continuum of non-periodic ground states.

References

- [1] N. Abarenkova, J.-C. Anglès d’Auriac, S. Boukraa, S. Hassani, and J.-M. Maillard, “Rational dynamical zeta functions for birational transformations”, *Physica A* **264**, 264–293 (1999).

- [2] M. Aizenman, M. Laínz Valcázar, and S. Warzel, “Pfaffian correlation functions of planar dimer covers”, *J. Stat. Phys.* **166**, 1078–1091 (2017).
- [3] J.-C. Anglès d’Auriac, S. Boukraa, and J.-M. Maillard, “Functional relations in lattice statistical mechanics, enumerative combinatorics, and discrete dynamical systems”, *Ann. Comb.* **3**, 131–158 (1999).
- [4] F. Arrigo, P. Grindrod, D. J. Higham, and V. Noferini, “On the exponential generating function for non-backtracking walks”, *Linear Algebra Appl.* **556**, 381–399 (2018).
- [5] S. Aubry and G. Abramovici, “Chaotic trajectories in the standard map. The concept of anti-integrability”, *Physica D* **43**, 199–219 (1990).
- [6] R. Band, J. M. Harrison, and C. H. Joyner, “Finite pseudo orbit expansions for spectral quantities of quantum graphs”, *J. Phys. A* **45**, 325204 (2012).
- [7] L. Bartholdi, “Zeta functions of graphs: a stroll through the garden, by Audrey Terras. book review”, *Bull. Amer. Math. Soc.* **51**, 177–185 (2014).
- [8] H. Bass, “The Ihara-Selberg zeta function of a tree lattice”, *Int. J. Math.* **3**, 717–797 (1992).
- [9] R. J. Baxter, “The bulk, surface and corner free energies of the square lattice Ising model”, *J. Phys. A* **50**, 014001 (2016).
- [10] E. Bedford and J. Diller, “Real and complex dynamics of a family of birational maps of the plane: The golden mean subshift”, *Amer. J. Math.* **127**, 595–646 (2005).
- [11] J. Bellissard, M. Degli Esposti, G. Forni, S. Graffi, S. Isola, and J. N. Mather, *Transition to Chaos in Classical and Quantum Mechanics*, edited by S. Graffi (Springer, Berlin, 1994).
- [12] R. Bowen and O. Lanford, Zeta functions of restrictions of the shift transformation, in *Global Analysis (Proc. Sympos. Pure Math., Berkeley, CA, 1968)*, Vol. 1, edited by S.-S. Chern and S. Smale (1970), pp. 43–50.
- [13] S. R. Bulò, E. R. Hancock, F. Aziz, and M. Pelillo, “Efficient computation of Ihara coefficients using the Bell polynomial recursion”, *Linear Algebra Appl.* **436**, 1436–1441 (2012).
- [14] P. N. Burgoyne, “Remarks on the combinatorial approach to the Ising problem”, *J. Math. Phys.* **4**, 1320–1326 (1963).
- [15] J. L. Cardy, “Operator content of two-dimensional conformally invariant theories”, *Nucl. Phys. B* **270**, 186–204 (1986).
- [16] R. Carmona, A. Klein, and F. Martinelli, “Anderson localization for Bernoulli and other singular potentials”, *Commun. Math. Phys.* **108**, 41–66 (1987).
- [17] P. M. Chaikin and T. C. Lubensky, *Principles of Condensed Matter Physics* (Cambridge Univ. Press, Cambridge UK, 1995).

- [18] M. Chertkov and V. Y. Chernyak, “Loop calculus in statistical physics and information science”, *Phys. Rev. E* **73**, 065102 (2006).
- [19] M. Chertkov, V. Y. Chernyak, and R. Teodorescu, “Belief propagation and loop series on planar graphs”, *J. Stat. Mech.* **2008**, P05003 (2008).
- [20] G. Chinta, J. Jorgenson, and A. Karlsson, “Zeta functions, heat kernels, and spectral asymptotics on degenerating families of discrete tori”, *Nagoya Math. J.* **198**, 121–172 (2010).
- [21] G. Chinta, J. Jorgenson, and A. Karlsson, “Heat kernels on regular graphs and generalized Ihara zeta function formulas”, *Monatsh. Math.* **178**, 171–190 (2014).
- [22] F. R. K. Chung, *Spectral Graph Theory* (American Math. Soc., 1996).
- [23] D. Cimasoni, “A generalized Kac-Ward formula”, *J. Stat. Mech.* **2010**, P07023 (2010).
- [24] D. Cimasoni, “The critical Ising model via Kac-Ward matrices”, *Commun. Math. Phys.* **316**, 99–126 (2012).
- [25] B. Clair, “The Ihara zeta function of the infinite grid”, *Electron. J. Combin.* **21**, P2–16 (2014).
- [26] B. Clair and S. Mokhtari-Sharghi, “Zeta functions of discrete groups acting on trees”, *J. Algebra* **237**, 591–620 (2001).
- [27] B. Clair and S. Mokhtari-Sharghi, “Convergence of zeta functions of graphs”, *Proc. Amer. Math. Soc.* **130**, 1881–1887 (2002).
- [28] S. N. Coppersmith, L. P. Kadanoff, and Z. Zhang, “Reversible Boolean networks I: distribution of cycle lengths”, *Physica D* **149**, 11–29 (2001).
- [29] G. A. T. F. da Costa, “The Feynman identity for planar graphs”, *Lett. Math. Phys.* **106**, 1089–1107 (2016).
- [30] J. Cserti, “Application of the lattice Green’s function for calculating the resistance of an infinite network of resistors”, *Amer. J. Physics* **68**, 896–906 (2000).
- [31] J. Cserti, G. Széchenyi, and G. Dávid, “Uniform tiling with electrical resistors”, *J. Phys. A* **44**, 215201 (2011).
- [32] P. Cvitanović, “Group theory for Feynman diagrams in non-Abelian gauge theories”, *Phys. Rev. D* **14**, 1536–1553 (1976).
- [33] P. Cvitanović, “Counting”, in *Chaos: Classical and Quantum* (Niels Bohr Inst., Copenhagen, 2020).
- [34] P. Cvitanović and H. Liang, *Spatiotemporal cat: A chaotic field theory*, In preparation, 2021.
- [35] R. M. D’Souza and N. H. Margolus, “Thermodynamically reversible generalization of diffusion limited aggregation”, *Phys. Rev. E* **60**, 264–274 (1999).

- [36] J. Davey, A. Hanany, and J. Pasukonis, “On the classification of brane tilings”, *J. High Energy Phys.* **2010**, 078 (2010).
- [37] G. Davidoff, P. Sarnak, and A. Valette, *Elementary number theory, group theory and Ramanujan graphs* (Cambridge Univ. Press, Cambridge UK, 2001).
- [38] A. Deitmar, “Ihara zeta functions of infinite weighted graphs”, *SIAM J. Discrete Math.* **29**, 2100–2116 (2015).
- [39] J. Dubout, *Zeta functions of graphs, their symmetries and extended Catalan numbers*.
- [40] E. N. Economou, *Green’s Functions in Quantum Physics* (Springer, Berlin, 2006).
- [41] S. Elaydi, *An Introduction to Difference Equations*, 3rd ed. (Springer, Berlin, 2005).
- [42] M. E. Fisher, “Statistical mechanics of dimers on a plane lattice”, *Phys. Rev.* **124**, 1664–1672 (1961).
- [43] M. E. Fisher, “On the dimer solution of planar Ising models”, *J. Math. Phys.* **7**, 1776–1781 (1966).
- [44] C. Fortuin and P. Kasteleyn, “On the random-cluster model: I. Introduction and relation to other models”, *Physica* **57**, 536–564 (1972).
- [45] E. Fradkin, *Field Theories of Condensed Matter Physics* (Cambridge Univ. Press, Cambridge UK, 2013).
- [46] F. Friedli and A. Karlsson, “Spectral zeta functions of graphs and the Riemann zeta function in the critical strip”, *Tohoku Math. J.* **69**, 585–610 (2017).
- [47] C. Godsil and G. . Royle, *Algebraic Graph Theory* (Springer, New York, 2013).
- [48] I. S. Gradshteyn and I. M. Ryzhik, *Tables of Integrals, Series and Products*, 8th ed. (Elsevier LTD, Oxford, New York, 2014).
- [49] J. Guckenheimer, “Axiom A + no cycles $\Rightarrow \zeta_f(t)$ rational”, *Bull. Amer. Math. Soc.* **76**, 592–594 (1970).
- [50] D. Guido, T. Isola, and M. L. Lapidus, “Ihara zeta functions for periodic simple graphs”, in *C^* -algebras and Elliptic Theory II*, edited by D. Burghelea, R. Melrose, A. S. Mishchenko, and E. V. Troitsky (Birkhäuser, Basel, 2008), pp. 103–121.
- [51] D. Guido, T. Isola, and M. L. Lapidus, “Ihara’s zeta function for periodic graphs and its approximation in the amenable case”, *J. Funct. Analysis* **255**, 1339–1361 (2008).
- [52] D. Guido, T. Isola, and M. L. Lapidus, “A trace on fractal graphs and the Ihara zeta function”, *Trans. Amer. Math. Soc.* **361**, 3041–3041 (2009).
- [53] P. G. Harper, “Single band motion of conduction electrons in a uniform magnetic field”, *Proc. Phys. Soc. London, Sect. A* **68**, 874–878 (1955).

- [54] K. Hashimoto, “Zeta functions of finite graphs and representations of p -adic groups”, *Adv. Stud. Pure Math.* **15**, 211–280 (1989).
- [55] Y. Higuchi, N. Konno, I. Sato, and E. Segawa, “A remark on zeta functions of finite graphs via quantum walks”, *Pacific J. Math. Industry* **6**, 1–8 (2014).
- [56] H. Hobrecht and F. Hucht, “Anisotropic scaling of the two-dimensional Ising model I: the torus”, *SciPost Phys.* **7**, 026 (2019).
- [57] H. Hobrecht and F. Hucht, “Anisotropic scaling of the two-dimensional Ising model II: surfaces and boundary fields”, *SciPost Physics* **8**, 032 (2020).
- [58] D. R. Hofstadter, “Energy levels and wave functions of Bloch electrons in rational and irrational magnetic fields”, *Phys. Rev. B* **14**, 2239–2249 (1976).
- [59] T. Horiguchi, “Lattice Green’s functions for the triangular and honeycomb lattices”, *J. Math. Phys.* **13**, 1411–1419 (1972).
- [60] M. D. Horton, “Ihara zeta functions of digraphs”, *Linear Algebra Appl.* **425**, 130–142 (2007).
- [61] A. Hucht, “The square lattice Ising model on the rectangle I: finite systems”, *J. Phys. A* **50**, 065201 (2017).
- [62] C. A. Hurst and H. S. Green, “New solution of the Ising problem for a rectangular lattice”, *J. Chem. Phys.* **33**, 1059–1062 (1960).
- [63] Y. Ihara, “On discrete subgroups of the two by two projective linear group over p -adic fields”, *J. Math. Soc. Japan* **18**, 219–235 (1966).
- [64] S. Isola, “ ζ -functions and distribution of periodic orbits of toral automorphisms”, *Europhys. Lett.* **11**, 517–522 (1990).
- [65] E. V. Ivashkevich, N. S. Izmailian, and C.-K. Hu, “Kronecker’s double series and exact asymptotic expansions for free models of statistical mechanics on torus”, *J. Phys. A* **35**, 5543–5561 (2002).
- [66] N. S. Izmailian, “Finite-size effects for anisotropic 2D Ising model with various boundary conditions”, *J. Phys. A* **45**, 494009 (2012).
- [67] N. S. Izmailian and C.-K. Hu, “Finite-size effects for the Ising model on helical tori”, *Phys. Rev. E* **76**, 041118 (2007).
- [68] N. S. Izmailian, K. B. Oganesyan, and C.-K. Hu, “Exact finite-size corrections for the square-lattice Ising model with Brascamp-Kunz boundary conditions”, *Phys. Rev. E* **65**, 056132 (2002).
- [69] W. Janke and R. Kenna, “Finite-size scaling and corrections in the Ising model with Brascamp-Kunz boundary conditions”, *Phys. Rev. B* **65**, 064110 (2002).
- [70] S. Y. Jitomirskaya, “Metal-insulator transition for the almost Mathieu operator”, *Ann. of Math.* **150**, 1159–1175 (1999).

- [71] J. Jorgenson and S. Lang, “The ubiquitous heat kernel”, in *Mathematics Unlimited - 2001 and Beyond* (Springer, Berlin, 2001), pp. 655–683.
- [72] M. Kac and J. C. Ward, “A combinatorial solution of the two-dimensional Ising model”, *Phys. Rev.* **88**, 1332–1337 (1952).
- [73] L. P. Kadanoff, *Statistical Physics: Statics, Dynamics and Renormalization* (World Scientific, Singapore, 2000).
- [74] W. Kager, M. Lis, and R. Meester, “The signed loop approach to the Ising model: Foundations and critical point”, *J. Stat. Phys.* **152**, 353–387 (2013).
- [75] A. Karlsson and M. Neuhauser, “Heat kernels, theta identities, and zeta functions on cyclic groups”, *Contemp. Math.* **394**, 177–190 (2006).
- [76] P. W. Kasteleyn, “The statistics of dimers on a lattice: I. The number of dimer arrangements on a quadratic lattice”, *Physica* **27**, 1209–1225 (1961).
- [77] P. W. Kasteleyn, “Dimer statistics and phase transitions”, *J. Math. Phys.* **4**, 287–293 (1963).
- [78] B. Kastening, “Simplified transfer matrix approach in the two-dimensional Ising model with various boundary conditions”, *Phys. Rev. E* **66**, 057103 (2002).
- [79] B. Kaufman, “Crystal statistics. II. Partition function evaluated by spinor analysis”, *Phys. Rev.* **76**, 1232–1243 (1949).
- [80] K. Kirsten and F. L. Williams, *A Window Into Zeta and Modular Physics* (Cambridge Univ. Press, 2010).
- [81] T. Kohler and T. Cubitt, “Translationally invariant universal classical Hamiltonians”, *J. Stat. Phys.* **176**, 228–261 (2019).
- [82] E. L. Korotyaev and J. S. Möller, “Weighted estimates for the Laplacian on the cubic lattice”, *Ark. Matematik* **57**, 397–428 (2019).
- [83] M. Kotani and T. Sunada, “Zeta functions of finite graphs”, *J. Math. Sci. Univ. Tokyo* **7**, 7–25 (2000).
- [84] H. Kunz and B. Souillard, “Sur le spectre des opérateurs aux différences finies aléatoires”, *Commun. Math. Phys.* **78**, 201–246 (1980).
- [85] O. M. Lecian, “Reflections on the hyperbolic plane”, *Intern. J. Modern Phys. D* **22**, 1350085 (2013).
- [86] D. Lenz, F. Pogorzelski, and M. Schmidt, “The Ihara zeta function for infinite graphs”, *Trans. Amer. Math. Soc.* **371**, 5687–5729 (2018).
- [87] T. M. Liaw, M. C. Huang, Y. L. Chou, S. C. Lin, and F. Y. Li, “Partition functions and finite-size scalings of Ising model on helical tori”, *Phys. Rev. E* **73**, 041118 (2006).
- [88] D. A. Lind and B. Marcus, *An Introduction to Symbolic Dynamics and Coding* (Cambridge Univ. Press, Cambridge, 1995).

- [89] M. Lis, “A short proof of the Kac-Ward formula”, *Ann. Inst. H. Poincaré D* **3**, 45–53 (2016).
- [90] M. Loebl and P. Somberg, “Discrete Dirac operators, critical embeddings and Ihara-Selberg functions”, *Electron. J. Combin.* **22**, P1–10 (2015).
- [91] I. Lyberg, “Free energy of the anisotropic Ising lattice with Brascamp-Kunz boundary conditions”, *Phys. Rev. E* **87**, 062141 (2013).
- [92] T. Machide, “An elliptic analogue of generalized Dedekind-Rademacher sums”, *J. Number Theory* **128**, 1060–1073 (2008).
- [93] T. Machide, “Sums of products of Kronecker’s double series”, *J. Number Theory* **128**, 820–834 (2008).
- [94] A. Manning, “Axiom A diffeomorphisms have rational zeta function”, *Bull. London Math. Soc.* **3**, 215–220 (1971).
- [95] E. C. Marino, *Quantum Field Theory Approach to Condensed Matter Physics* (Cambridge Univ. Press, Cambridge UK, 2017).
- [96] J. N. Mather and G. Forni, “Action minimizing orbits in Hamiltonian systems”, in *Transition to Chaos in Classical and Quantum Mechanics*, edited by S. Graffi (Springer, Berlin, 1994), pp. 92–186.
- [97] B. M. McCoy and T. T. Wu, *The Two-Dimensional Ising Model*, 2nd ed. (Dover, 1973).
- [98] H. Mizuno and I. Sato, “Zeta functions of digraphs”, *Linear Algebra Appl.* **336**, 181–190 (2001).
- [99] P. A. P. Moran, “A Gaussian Markovian process on a square lattice”, *J. Applied Prob.* **10**, 54–62 (1973).
- [100] B. Mramor and B. Rink, “Ghost circles in lattice Aubry-Mather theory”, *J. Diff. Equ.* **252**, 3163–3208 (2012).
- [101] O. Negrete, P. Vargas, F. Peña, G. Saravia, and E. Vogel, “Entropy and mutability for the q-state clock model in small systems”, *Entropy* **20**, 933 (2018).
- [102] Y. Okabe, K. Kaneda, M. Kikuchi, and C.-K. Hu, “Universal finite-size scaling functions for critical systems with tilted boundary conditions”, *Phys. Rev. E* **59**, 1585–1588 (1999).
- [103] L. Onsager, “Crystal statistics. I. A Two-dimensional model with an order-disorder transition”, *Phys. Rev.* **65**, 117–149 (1944).
- [104] R. Peierls, “Zur Theorie des Diamagnetismus von Leitungselektronen”, *Z. Phys.* **80**, 763–791 (1933).
- [105] I. Percival and F. Vivaldi, “A linear code for the sawtooth and cat maps”, *Physica D* **27**, 373–386 (1987).
- [106] A. Poghosyan, N. Izmailian, and R. Kenna, “Exact solution of the critical Ising model with special toroidal boundary conditions”, *Phys. Rev. E* **96**, 062127 (2017).

- [107] A. Politi, A. Torcini, and S. Lepri, “Lyapunov exponents from node-counting arguments”, *J. Phys. IV* **8**, 263 (1998).
- [108] M. Pollicott, *Dynamical zeta functions*, in *Smooth Ergodic Theory and Its Applications*, Vol. 69, edited by A. Katok, R. de la Llave, Y. Pesin, and H. Weiss (2001), pp. 409–428.
- [109] P. Ren, T. Aleksić, D. Emms, R. C. Wilson, and E. R. Hancock, “Quantum walks, Ihara zeta functions and cospectrality in regular graphs”, *Quantum Inf. Process.* **10**, 405–417 (2010).
- [110] P. Ren, R. C. Wilson, and E. R. Hancock, “Graph characterization via Ihara coefficients”, *IEEE Trans. Neural Networks* **22**, 233–245 (2011).
- [111] S. Saito, “A proof of Terras’ conjecture on the radius of convergence of the Ihara zeta function”, *Discrete Math.* **341**, 990–996 (2018).
- [112] I. Sato, “Bartholdi zeta functions of group coverings of digraphs”, *Far East J. Math. Sci.* **18**, 321–339 (2005).
- [113] A. Setyadi and C. K. Storm, “Enumeration of graphs with the same Ihara zeta function”, *Linear Algebra Appl.* **438**, 564–572 (2013).
- [114] R. Shankar, *Quantum Field Theory and Condensed Matter* (Cambridge Univ. Press, Cambridge UK, 2017).
- [115] O. Shanker, “Exact solution of Ising model in 2d shortcut network”, *Mod. Phys. Lett. B* **23**, 567–573 (2009).
- [116] S. Sherman, “Combinatorial aspects of the Ising model for ferromagnetism. I. A conjecture of Feynman on paths and graphs”, *J. Math. Phys.* **1**, 202–217 (1960).
- [117] B. Simon, “Almost periodic schrödinger operators: A review”, *Adv. Appl. Math.* **3**, 463–490 (1982).
- [118] H. M. Stark and A. A. Terras, “Zeta functions of finite graphs and coverings”, *Adv. Math.* **121**, 124–165 (1996).
- [119] H. M. Stark and A. A. Terras, “Zeta functions of finite graphs and coverings, Part II”, *Adv. Math.* **154**, 132–195 (2000).
- [120] T. Sunada, “Unitary representations of fundamental groups and the spectrum of twisted Laplacians”, *Topology* **28**, 125–132 (1989).
- [121] T. Sunada, *Topological Crystallography* (Springer, Tokyo, 2013).
- [122] A. Tarfulea and R. Perlis, “An Ihara formula for partially directed graphs”, *Linear Algebra Appl.* **431**, 73–85 (2009).
- [123] H. Teimoori Faal and M. Loeb, “Bass’ identity and a coin arrangements lemma”, *Eur. J. Combinatorics* **33**, 736–742 (2012).
- [124] P. Tempesta, “A theorem on the existence of trace-form generalized entropies”, *Proc. Roy. Soc. Ser A* **471**, 20150165 (2015).
- [125] P. Tempesta, “Beyond the Shannon-Khinchin formulation: The compositability axiom and the universal-group entropy”, *Ann. Phys.* **365**, 180–197 (2016).

- [126] A. Terras, *Zeta Functions of Graphs: A Stroll through the Garden* (Cambridge Univ. Press, 2010).
- [127] T. Toffoli and N. H. Margolus, “Invertible cellular automata: A review”, *Physica D* **45**, 229–253 (1990).
- [128] N. V. Vdovichenko, “A calculation of the partition function for a plane dipole lattice”, *Sov. Phys. JETP* **20**, 477–479 (1965).
- [129] H. Watanabe, “A proof of the Bloch theorem for lattice models”, *J. Stat. Phys.* **177**, 717–726 (2019).
- [130] W. Werner, *Percolation et modèle d’Ising* (Société mathématique de France, 2009).
- [131] A. Wipf, T. Heinzl, T. Kaestner, and C. Wozar, “Generalized Potts-models and their relevance for gauge theories”, *SIGMA* **3**, 6–14 (2007).
- [132] C. Wozar, T. Kaestner, A. Wipf, T. Heinzl, and B. Pozsgay, “Phase structure of $\mathbb{Z}(3)$ -Polyakov-loop models”, *Phys. Rev. D* **74**, 114501 (2006).
- [133] M.-C. Wu and C.-K. Hu, “Exact partition functions of the Ising model on $M \times N$ planar lattices with periodic-aperiodic boundary conditions”, *J. Phys. A* **35**, 5189–5206 (2002).
- [134] Y. Yamasaki, “An explicit prime geodesic theorem for discrete tori and the hypergeometric functions”, *Math. Z.* **289**, 361–376 (2017).
- [135] C. N. Yang, “The spontaneous magnetization of a two-dimensional Ising model”, *Phys. Rev.* **85**, 808–816 (1952).
- [136] D. Zhou, Y. Xiao, and Y.-H. He, “Seiberg duality, quiver gauge theories, and Ihara’s zeta function”, *Int. J. Mod. Phys. A* **30**, 1550118 (2015).
- [137] R. M. Ziff, C. D. Lorenz, and P. Kleban, “Shape-dependent universality in percolation”, *Physica A* **266**, 17–26 (1999).

Chapter 14

Checkerboard

14.1 Checkerboard model

2019-03-08 **Zeb** Rodrigues *et al.* [1] looks very interesting.

I'm interested in whether the nonlinearities of these flexible structures can lead to interesting chaotic behavior. The thing foremost on my mind is the structure (not dynamics) of a 1D chain of repeating mechanical elements. A rigid-body mechanism would lead to a nonlinear transfer function between the configuration of one element and its neighbors. That seems like it could lead to something like the logistic equation, and perhaps different structures depending on the shape of the unit cell and the "initial" (i.e., boundary) conditions.

I couldn't get that to work out, but Michael, see figure 14.1 (a), found something that suggests it could work. Specifically, he found a structure that is repeated every three unit cells.

Two-dimensional structures like the origami are also quite interesting, of course, but the 1D chain seems easier to us as a starting point.

2019-03-08 **Adrian** James McInerney work is focused on origami.

2019-03-08 **Michael D. Czajkowski** <michael.czajkowski@physics.gatech.edu>
I have located a configuration of a chain of 1-d rotors which repeats in three cycles, see figure 14.1 (a).

It is not unlike the wheels on a classical steam engine, but with the rod lengths varied around to produce a mismatch. We are thinking, of course, of the sequence of rotors going from left to right (or vice versa) as like time going forward in the iterative cycles of the logistic map. Despite the simplicity it seems promising in identifying a deterministic geometric system, which will never repeat, by varying the intrinsic parameters (like the rotor radius, connector length, etc.).

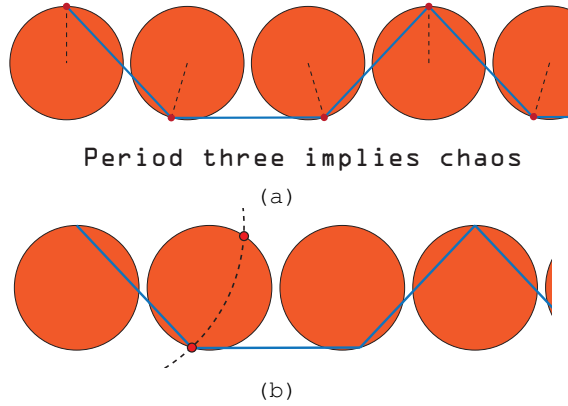


Figure 14.1: (a) The wheels on a steam engine, with the rod lengths varied around to produce a mismatch. (b) Forward-iteration almost always has two solutions, as there are two points at which the two circles intersect.

There is one caveat to this, which is that we are thinking of the (for instance) orientation of the leftmost rotor as the input which (together with the intrinsic length of our blue rod, the radius of the orange circles and the spacing between them) determines the next orientation of the following rod to the right of it. However, this almost always has two solutions, as there are two points at which the two circles intersect, see figure 14.1 (b). So we are not entirely sure yet how to think of determinism in this system. Perhaps that is a bad thing, or perhaps it will be an interesting source of additional richness.

There is a separate perspective on this same mechanical system where there may be an analogue of chaos in a correspondence with topological mechanical polarization, but this is less developed and I will wait to share until I have gathered my thoughts a bit more.

14.1.1 Checkerboard literature

[For the latest entry, go to the bottom of this section](#)

2019-03-08 Predrag Rodrigues, Fonseca, Savi and Paiva [1] *Nonlinear dynamics of an adaptive origami-stent system*

References

- [1] G. V. Rodrigues, L. M. Fonseca, M. A. Savi, and A. Paiva, “[Nonlinear dynamics of an adaptive origami-stent system](#)”, Int. J. Mech. Sci. **133**, 303–318 (2017).

Chapter 15

Sidney's blog

Sidney V. Williams work blog
swilliams425@gatech.edu
sidneywilliams1231@gmail.com
subversion siminos : swilliams425
cell 208 310 3866

The latest entry at the bottom for this blog

15.1 2020 blog

2020-05-20 Predrag to Sidney:

You can write up your narrative in this file. Can clip & paste anything from above sections you want to discuss, that saves you LaTeXing time.

2021-09-09 Predrag The 3rd line of *siminos/spatiotemp/blogCats.tex* says

```
\input{inputs/inclOnlyCats} %process only the files you are editing  
you uncomment a single line in that file to "process only the files you are editing".
```

2021-07-04 Predrag to Sidney Pro tip: compile *blogCats.tex* often, as you write, and fix errors as you write. I had to go all the way back to May to find one of your unbalanced “{” and make the entire blog compile without errors...

2020-08-22 Predrag First task:

Start reading kittens/CL18.tex [3] sect. *Bernoulli map*. Everything up to CL18 sect. s:1D1dLatt *Temporal Bernoulli* you know from the ChaosBook course.

CHAPTER 15. SIDNEY'S BLOG

New stuff starts here. See how much you understand. Write your study notes up here, ask questions - this is your personal blog.

You refer to an equation like this: CL18 eq. tempBern;

to figure like this: CL18 figure fig;BernCyc2Jacob;

to table like this: table 11.1;

to a reference like this: Gutkin and Osipov [9] (*GutOsi15* refers to an article listed in *..bibtex/siminos.bib*).

and to external link like this: "For great wallpapers, see overheads in Engel's course [7]."

2020-08-22 Predrag An example of referring to the main text: Why do you write *orbit Jacobian matrix* CL18 eq. jacobianOrb as a partial derivative, when you already know \mathcal{J} , see CL18 eq. tempFixPoint?

2020-08-24 Sidney Started reading from the beginning as that only adds an additional 4 pages, and it would be beneficial to review.

General Notes: Showing what modern chaos calculations look like. The spatiotemporal cat is the arbitrary dimension generalization of the 1-D Bernoulli map.

(mod 1) subtracts the integer part of $s\phi_t$, this keeps ϕ_{t+1} within the unit interval (group theoretic analogue?). Also partitions the state-space into s sub-intervals.

2020-08-24 Predrag The group theory here compatifies translations on the (infinite) line $\phi \in (-\infty, \infty)$ to translations on the (compact) circle $\phi \in [0, 2\pi]$.

2020-08-24 Sidney Reminder to self: review the symbolic dynamics, and binary operations from chapter 14 of Chaosbook. The unit interval is partitioned into s^n subintervals, each with one unstable period-n point, except the rightmost fixed point is the same as the fixed point at the origin. So there are $s^n - 1$ total period-n periodic points. r in (3.31) is a cyclic permutation that translates forward in time the lattice state by one site. Inverse r because the second term is always one step behind the first term and an inverse r moves the state back one.

Questions 1. I've pretty much never done modular arithmetic before, I understand CL18 eq. BerStretch in the idea that the circle map wraps in on itself and contributes the value of its slope after one go around, but I am unsure on how to use the modular arithmetic to do that, should I look into that?

2020-08-24 Predrag As I do not know what "modular arithmetic" is, don't worry about :)

2020-08-25 Sidney General Notes

CL18 eq. pathBern appears to be a vector of a periodic (or relative periodic orbit) through the Bernoulli map. Review Multishooting. Total number of of periodic points of period n is $N_n = s^n - 1$ but it also equals the magnitude of the determinant of the orbit Jacobian matrix. (got to page 7)

Q1 Is CL18 eq. tempBernFix the evolution function $f^t(y)$ that was referenced throughout ChaosBook?

Q2 What exactly is meant by a "lattice"?

2020-08-24 Predrag .

A1 The whole point of the paper us that ChaosBook is obsolete - in the new formulation, there is no 'time' evolution, no time trajectory $f^t(y)$, there are only sets of fields the live on lattice points that satisfy recurrence relations. CL18 eq. tempBernFix is *orbit Jacobian matrix*, the stability of a lattice state, to be related to stability forward in time in CL18 sect. s:Hill. This is a revolution: there is no more time, there is only spacetime.

A2 Temporal lattice \mathbb{Z} is defined in CL18 eq. pathBern. Spacetime integer lattice \mathbb{Z}^2 , (or more generally \mathbb{Z}^d) in CL18 eq. KanekoCML, CL18 eq. CatMap2d. When you get to it, a 2-dimensional *Bravais lattice* Λ is defined in CL18 eq. 2DBravaisLattice.

If this is unclear, read up on integer lattices, give your own precise definition.

2020-08-26 Sidney Point Lattice (integer lattice is a special case of point lattice) notes from [Wolfram](#): "A point lattice is a regularly spaced array of points." The integer lattice is where all of these points are integers. I will look at the Barvinok lecture tomorrow, I have to finish moving to a different house today. (Stayed on page 7)

Q3 Please correct me if I am wrong, but a lattice seems to be a collection of points where are all regularly spaced, so does "regularly" mean that it is controlled by a deterministic law? If this is the case, the ϕ_n states in a periodic orbit can be grouped as a lattice and ordered by location along the periodic orbit, then the associated "winding" number m_t can be grouped in its own lattice, which in this case is an integer lattice. What is the "regular" spacing for the winding numbers? Have missed the point?

A3 Wolfram is right. When you have a discrete time map, time takes integer values $t = \dots, -1, 0, 1, 2, \dots$. That is called 1-dimensional integer lattice \mathbb{Z} . Once you are in $d = 2$ or higher, the name makes

CHAPTER 15. SIDNEY'S BLOG

sense, as you can visualize \mathbb{Z}^2 as a 'lattice'. It is regular, because all spacings between neighboring points are 1. There is nothing 'deterministic' about this, it just says that time takes its values on integers, rather than on a continuum.

There is only one lattice, but on each lattice site there is a real-valued field ϕ_t and the integer valued 'source' m_t .

2020-08-27 Sidney Thank you for A1, that makes complete sense now. Calculated the orbit Jacobian matrix using equation CL18 eq. tempBernFix, matched with the paper, yay. Orbit Jacobian matrix maps the basis vectors of the unit hyper-cube into a fundamental parallelepiped basis vectors, each of which is given by a column in the orbit Jacobian matrix. $|\text{Det}(s/r)| = s^n$ because r and its inverse are both unitary matrices, and if you multiply every row of an $[n \times n]$ matrix, the determinant is multiplied by the constant raised to the power n . Periodicity $r^n = 1$ accounts for $\bar{0}$ and $\bar{s - 1}$ fixed points being a single periodic point. (got to page 9)

Q4 I was trying to calculate the orbit Jacobian matrix using the r matrix, but the delta function equation CL18 eq. hopMatrix for r doesn't seem to work for the Bernoulli map, I know that $r_{2,1} = 1$ and $r_{1,2} = 1$ which works with the delta function definition. However, $r_{2,1} = \delta_{3,1}$ from CL18 eq. hopMatrix, which should equal zero. Other than just the idea of being cyclic, I don't know why it yields one instead of zero, what am I missing?

A4 Work it out r matrices for $n = 1, 2, 3, \dots$. It will start making sense.

Q5 So, does "lattice state" mean the set of all points (field of all points?) which running through the Bernoulli map requires the specific winding number at that lattice site?

A5 Interesting, grad students too seem to confuse coordinates (for example, $(x, t) = (3.74, -0.02)$ in continuum, $(n, t) = (7, -6)$ on a discretized space) and the fields $\phi(n, t)$. Physical "state" refers to value of field ϕ over every (n, t) - is the grass high or low? rather than the coordinates of spacetime.

How would you state this precisely if you were trying to explain this paper to another student?

2020-08-30 Sidney

A5.1 Sidney: " X_M is the set of all values the field ϕ_z takes over the set of coordinates M ."

A5.2 Predrag: Please reread 2nd paragraph of CL18 sect. s:1D1dLatt and explain what is wrong with your answer A5.1

Notes: For an period- n lattice state X_M the Jacobian matrix is now a function of a $[d \times d]$ matrix J , so the formula for the number of periodic points

of period n (number of lattice states of period n) is now $|\det(1 - J_M)|$ where $J_M = \prod_{t=1}^n J_t$ where J_t is the one-step Jacobian matrix which is assumed to vary in time.

Note to self: look back over the topological zeta function, specifically try to understand derivation of:

$$\frac{1}{\zeta_{top}(z)} = \exp \left(- \sum_{n=1}^{\infty} \frac{z^n}{n} N_n \right)$$

(got to CL18 page s:bernODE)

Predrag: [ChaosBook \(click here\)](#)

Q6 Is “there are s fundamental lattice states, and every other lattice state is built from their concatenations and repeats” is simply a restatement of the fact that the Bernoulli map is a full shift?

A6 For Bernoulli, yes. But search for word ‘fundamental’ in [ChaosBook Counting](#). For example, ‘We refer to the set of all non-self-intersecting loops $\{t_{p_1}, t_{p_2}, \dots, t_{p_f}\}$ as the *fundamental cycles*’. Write up here a more nuanced statement of ‘fundamental’ cycles might be (I do not have firm grip on this either...).

Q7 Is CL18 eq. bernN_n-s=2 a result of expanding in a Taylor the result of the derivative (and product of $1/\zeta_{top}$ and z)? Because the topological zeta function of the Bernoulli map is a closed form function, not an infinite sum.

2020-08-31 Sidney Via a finite difference method, CL18 eq. 1stepDiffEq can be viewed as a first order ODE dynamical system. Back-substituted with (3.31) to show that with $\Delta t = 1$ the velocity field does satisfy the diffeq (7.18). The Bernoulli system can be recast into a discretized ODE whose global linear stability is described by the orbit Jacobian matrix. (Stayed on CL18 page s:bernODE))

2020-09-01 Sidney Started reading CL18 sect. s:kickRot *A kicked rotor*.

(12.2) and (12.1) describe the motion of a rotor being subjected to periodic momentum pulses. The mod is present for the q equation to make sure that the angle varies from 0 to 2π . As in the Bernoulli map case, here mod is also added to the momentum equation to keep it bounded to a unit square. Cat maps with the stretching parameter s are the same up to a similarity transformation. An automorphism is an isomorphism of a system of objects onto itself. An isomorphism is a map that preserves sets and relations among elements.

Q8 Do the kicked rotor equations with Hooke’s law force, and bounded momentum (mod 1 added to CL18 eq. PerViv2.1a) only take the form of CL18 eq. catMap if K is an integer?

- A8 The text states: "The (mod 1) added to CL18 eq. PerViv2.1a makes the map a discontinuous 'sawtooth,' unless K is an integer." How would you make that clearer?
- Q9 How does CL18 eq. catMap have a state space which is a 2-torus? I am having a hard time visualizing how this came about.
- A9 Do you understand how (mod 1) operation turns unbounded stretch CL18 eq. BerStretch into a circle map CL18 eq. n-tuplingMap? Circle map is 1-torus. If both $(q_t, p_t) \in (0, 1] \times (0, 1]$ are wrapped into unit circles, the phase space (q_t, p_t) is not an infinite 2-dimensional plane, but a compact, doubly periodic unit square with opposite edges glued together, i.e., 2-torus.

2020-09-03 Sidney I was typing my description into "summary" textbox above the commit to master button. Obviously I was incorrect, I'll try to type in the "description" for this commit.

2020-09-02 Predrag "Tripping Through Fields" showed up :)

2020-09-03 Sidney

- A5.3 Sidney: I'm not actually quite sure what's wrong with my given definition. From your answer A5 it seems that M is a set of coordinates (the location of the blade of grass) and X_M is the value at that coordinate (the height of the grass at that point). Perhaps I forgot that these lattice states are for periodic orbits, so I forgot the second coordinate (period of length n).
- A5.4 Predrag: The textbook inhomogeneous *Helmoltz equation* is an elliptical equation of form

$$(\square + k^2) \phi(z) = -m(z), \quad z \in \mathbb{R}^d, \quad (15.1)$$

where the *field* $\phi(z)$ is a C^2 functions of *coordinates* z , and $m(z)$ are *sources*. For example, charge density is a *source* of electrostatic *field*.

Suppose you are so poor, your computer lacks infinite memory, you only have miserly only 10 Tb, so you cannot store the infinitely many values that *coordinates* $z \in \mathbb{R}^d$ take. So what do you do?

Perhaps a peak at ChaosBook [ChaosBook A24.1 Lattice derivatives](#) can serve as an inspiration. And once you have done what a person must do, your Helmoltz equation (hopefully) has the form of CL18 eq. OneCat. What is a *field*, a *source*, a *coordinate* then?

2020-09-03 Sidney

- A8.1 The sawtooth statement made sense, what made it unclear for me was the second sentence which started with "in this case" it was (again for me, I might not have been paying enough attention) ambiguous, I didn't know if it was talking about the integer case or the sawtooth case.

A8.2 Predrag: thanks, I rephrased that sentence.

A9.1 I understand, your explanation makes sense, thank you :).

Notes: The discrete time Hamiltonian system induces forward in time evolution on the 2-torus phase space. The orbit Jacobian matrix can take many different forms depending on the map. Despite this the Hill determinant can still count the number of lattice states. (got to page CL18 page s:tempCatCountTEMP)

2020-09-05 Sidney

A5.5 If I was so unlucky to only have 10Tb of memory, I would take a finite interval of points z that I was interested in, and discretize them (evenly, or unevenly) and then evaluate the field (that was probably the wrong wording) at a finite set of points, either of particular interest within the interval, or closely spaced enough so that the values were representative of the values the field took over a continuum. I think that a coordinate is a point in state space specified by specific values of state variables (position, time, momentum etc.). To try to answer source, and field, I'll be thinking of an electric charge, a source is what generates the medium by which other sources are effected, and the field is the medium which acts upon other sources.

A5.6 I did look at [ChaosBook A24.1 Lattice derivatives](#), but it didn't seem to address quite the fundamental confusion I seem to be facing. I'm relatively confident in my coordinate definition, but not at all in my source, and field definition.

2020-09-05 Predrag .

A5.7 Expression 'state space' \mathcal{M} refers to 'states': cats, dancers, i.e., 'fields' X and their names M . 'Coordinates' refer to markings on the floor that they stand on.

Does reading CL18 sect. s:lattState *Lattice states* now helps in distinguish a skater from the skating ring's ice? I rewrote it for your pleasure :)

A5.7 Re. the fundamental confusion of reading [ChaosBook A24.1 Lattice derivatives](#): If you mark every inch on the floor, this is 'discretization'. But the floor is still a floor, no?

2020-09-05 Sidney

A5.8 I read the pink bits of CL18 sect. s:lattState *Lattice states* (as I assume that was the parts that you rewrote specially). From it I (think) I understand. We're looking at two coordinates for most of the Bernoulli and cat map stuff: a spatial one, and a temporal one, the maps only effect the temporal placement, but effect it differently depending on

CHAPTER 15. SIDNEY'S BLOG

where the point was in space when the map acted on it, because the field takes a different value at every point in space (and time). So the coordinates are the field point placement in time and space. The field is the value that is assigned to every lattice point. M keeps getting referred to as an alphabet, so that makes me think that it is similar (perhaps the multidimensional generalization) to the "alphabet" which was used to partition state space in the 1D maps of Chaosbook, such as 0 for the left half of the interval and 1 for the right, and then further partitioning the more the map is applied. Is that close at least?

2020-09-05 Predrag .

- A5.9 Getting hotter. Look at CL18 eq. circ-m and CL18 eq. catMapNewt; ϕ_t and m_t are the same kind of a beast, m_t is just the integer part of the "stretched" field in CL18 eq. BerStretch. In this particular, linear map setting, this integer does double duty, as a letter of an "alphabet". It cannot possibly be a "coordinate", it like saying that a dancer's head is "floor."
- A5.10 In temporal lattice formulation no "map is applied." That is the brilliance of the global spatiotemporal reformulation: there is no stepping forward in time, so there is no map - the only thing that exists is the global fixed point condition that has to be satisfied by field values everywhere on the lattice, simultaneously.

Time is dead.

2020-09-08 Sidney

- Q11 So the temporal cat / spatiotemporal cat equations are moving around points in the lattice instead of through time?
- Q12 Is something of the form of CL18 eq. tempFixPoint an example of the "global fixed point condition"?

2020-09-14 Predrag .

- A11 An equation does not have to be "moving around" anything: think of a quadratic equation $x^2 + bx + c = 0$. Does it "move" anything? No. It's a condition that a single "field" x has to satisfy, and the solution is a root of that equation. The temporal cat / spatiotemporal cat equations are "equations" in the same sense, [bunch of terms involving ϕ_z] = 0.

A12 Yes.

2020-09-09 Sidney Notes: Equations such as CL18 eq. catMapNewt can be solved using similar methods to linear odes: guessing a solution of the form Λ^t and finding the characteristic equation. Then assuming all terms are site independent because the difference of any two solutions of CL18

eq. catMapNewt solve its homogeneous counterpart CL18 eq. diffEqs:CatCharEq.
Got to CL18 page s:tempCatZeta.

Notes: Topological zeta functions count orbits, i.e. time invariant sets of equivalent lattice states related by cyclic permutations. The "search for zeros" CL18 eq. tempCatFixPoint is the "fixed point condition." Which is a global statement which enforces CL18 eq. catMapNewt at every point in the lattice. Got to CL18 page s:catlatt

2020-09-13 Sidney The temporal cat is a special case of the spatiotemporal cat, defined on a one-dimensional lattice \mathbb{Z}^1 . In this case the associated topological zeta function is known in a closed, analytic form.

Coupled map lattices: Starts with a review of finite difference methods for PDEs. The d dimensions in the lattice are d-1 spatial lattice points and 1 temporal one. The PDE is reduced to dynamics of a coupled map lattice, with a set of continuous fields on each site.

A5.11 I have experience with finite difference methods for solving a discretized form of a PDE, but I'm having a hard time visualizing the idea of having a discrete coordinate system in d different directions, but with a continuous field on each site. This may be valuable as it is a specific statement of where I'm getting stuck.

Q13 My current understanding is that at each point in the d-dimensional integer lattice ("point" as in a lattice node with d specified coordinates), but at each point (site) there is a continuous field. What is this field continuous over? It's at one point in a discrete coordinate system. And why is there a continuum at each point? And finally, I assume that these continuous fields are the values of the function being solved for at that point, however, shouldn't that just be a single value? Not a field? I'm sorry if this is a rather silly question, but I'll keep thinking about it and I'll make a note if my understanding (or lack thereof) changes.

A13 Predrag: In CL18 figure 3.2 field x_t or ϕ_t and $f(\phi_t)$ on the discrete site t run over continuous values. For example, at temporal lattice site $t = 7$ the field value is $\phi_7 = 0.374569263952942 \dots$. OK now?

Q13.1 Slight update, it seems that the field is the state of the system and at each discretized point there is a map acting on the state, although that conflicts with the notion that time is dead, so I'm probably still misunderstanding.

A13.1 Predrag: Yes.

Thinking of this as a spring mattress. Often starts out with chaotic on-site dynamics weakly coupled to neighboring sites. In this paper one sets the lattice spacing constant equal to one. Diffusive coupled map lattices introduced by Kaneko:

$$\phi_{n,t+1} = g(\phi_{n,t}) + \epsilon [g(\phi_{n-1,t}) - 2g(\phi_{n,t}) + g(\phi_{n+1,t})] ,$$

where each individual spatial site's dynamical system $g(x)$ is a 1D map, coupled to the nearest neighbors by the discretized second order *spatial* derivative. The form of time-step map $g(\phi_{n,t})$ is the same for all time i.e. invariant under the group of discrete time translations. Spatial stability analysis can be combined with temporal stability analysis, with orbit weights depending exponentially both on the space and the time variables: $t_p \propto e^{-LT\lambda_p}$. r_i translates the field by one lattice spacing in the i^{th} direction.

Q14 What is a lattice period?

A14 Predrag: Does the paragraph above CL18 eq. catlattFix answer your question? I would like to refer to the *set* of numbers $\{\ell_1, \ell_2, \dots, \ell_d\}$ as the *period* of lattice Λ . Would that be confusing?

Q15 Is z in the definition of a lattice state both a temporal and a spatial index? So equivalent to both n and t ?

A15 Predrag: after CL18 eq. CatMap2d I write "a 1-dimensional spatial lattice, with field ϕ_{nt} (the angle of a kicked rotor (12.2) at instant t) at spatiotemporal site $z = (n, t) \in \mathbb{Z}^2$." Should this " $z = (n, t) \in \mathbb{Z}^2$ " be repeated elsewhere. If so, where?

Q16 Often a member of the alphabet can be a negative number, which I assume means that the state is taken out of unity in the negative direction.

A16 Do you understand CL18 figure fig:BernCyc2Jacob and CL18 figure fig:catCycJacob?

The spatiotemporal cat has the point-group symmetries of the square lattice. A lattice state is a set of all field values $X = \{\phi_z\}$ over the d -dimensional lattice that satisfies the spatiotemporal cat equation, with all field values constrained between zero and one. A lattice state X_Λ is a *invariant 2-torus* if it satisfies $X_\Lambda(z + R) = X_\Lambda(z)$ for any discrete translation $R = n_1\mathbf{a}_1 + n_2\mathbf{a}_2 \in \Lambda$. Got to CL18 s:catLatt1x1.

2020-09-14 Sidney

A13.1 I think I'm OK now. I think what I was trying to visualize was a stack of an infinite number of values at each lattice point, which was confusing, but this makes sense.

A14.1 Unfortunately I don't think I quite understand. I understand the idea of the different directions, I understand treating $X_M(\phi_z)$ as a singular fixed point, but I do not understand ℓ_i .

A15.1 I think that I lost that definition of z around CL18 eq. dDCatsT, but I think that may have been a factor of how long it takes me personally to digest this material.

A16.1 After reading the descriptions and staring at it for awhile, I think that I do.

Q17 I tried a couple days back (Thursday or Friday I think, they all blend together) to log in to your bluejeans office. But it must have been one of the times that it had logged you off due to inactivity. There was also another person there I didn't recognize, and I didn't want to step on their toes if they were waiting for you to get back, so I logged off. So, when in general would good times to try hopping into your office?

2020-09-16 Sidney A Bravais lattice can be denoted $\Lambda = [L \times T]_S$ where L is the spatial lattice period, T is the temporal lattice period, S imposes the tilt to the cell. Basis vectors for the Bravais cell can be written as:

$$\mathbf{a}_1 = \begin{pmatrix} L \\ 0 \end{pmatrix}, \quad \mathbf{a}_2 = \begin{pmatrix} S \\ T \end{pmatrix}$$

Q18 If something is written as $850[3 \times 2]_0$ what is the numerical value? More importantly, how is it found? I know it has to do with the cyclic permutations of the prime blocks, but I'm not sure how to get a numerical value.

Got to page CL18 page s:catLattCount

2020-09-17 Sidney For the Bernoulli map its stretching uniformity allows the use of combinatorial methods for lattice points. For temporal (not spatiotemporal) the number of lattice states is the same as the volume of the fundamental parallelepiped, so the magnitude of the determinant of the orbit Jacobian matrix. The block M can be used as a 2D symbolic representation of the lattice system state. For a given admissible source block M , the periodic field can be computed by:

$$\phi_{i_1 j_1} = \sum_{i_2=0}^2 \sum_{j_2=0}^1 \mathbf{g}_{i_1 j_1, i_2 j_2} M_{i_2 j_2}$$

2020-09-19 Predrag Sorry, I've been a bit overwhelmed with lecture preparations, so I will not answer any of the questions quite yet. But I have rewritten the abstract, and the introduction to the paper, up to the start of CL18 sect. s:Bernoulli *Bernoulli map*. Can you have a critical look at the new text, report here if something does not make sense to you?

2020-09-19 Sidney

Update I read through, and aside from some very minor grammar issues (forgetting a "have" after "we") it all makes sense.

2020-09-20 Predrag .

A15.2 I now added the z definition to CL18 eq. dDCatsT, is that clearer?

2020-09-20 Sidney

A15.3 Yes, that makes it clearer.

$$-\sum_{r=1}^{\infty} \frac{1}{r} \text{tr } \hat{\mathbf{J}}_p^r = \text{tr} \left(-\sum_{r=1}^{\infty} \frac{1}{r} \hat{\mathbf{J}}_p^r \right) = \text{tr } \ln \left(\hat{\mathbf{I}}_1 - \hat{\mathbf{J}}_p^r \right) = \ln \det \left(\hat{\mathbf{I}}_1 - \hat{\mathbf{J}}_p^r \right)$$

I liked the text cut from the introduction on page 44, it made the idea of time's death more easily digestible. Finished main paper, will look at the appendices for math.

2020-09-22 Sidney

Math Review Part 1

Updated 9/29/20

Bravais Lattice From [Wikipedia](#): A Bravais lattice is an infinite array of discrete points generated by a set of discrete translation operations described in two dimensional space by:

$$\mathbf{R} = n_1 \mathbf{a}_1 + n_2 \mathbf{a}_2$$

where n_i is any integer and \mathbf{a}_i is a primitive vector, each \mathbf{a}_i lie in different directions, but are not necessarily mutually perpendicular, but they do span the lattice. A fundamental aspect of a Bravais Lattice is that no matter the direction of the primitive vectors, the lattice will look exactly the same from each of the discrete lattice points when looking in that direction. A Lattice is is a periodic array of points where each point is indistinguishable from any other point and has identical surroundings. A unit cell expands the idea of the infinite array of discrete points to include the space inbetween the points, if we are looking at a physical system this includes the atoms in this space. There are two main types of unit cells: primitive unit cells and non-primitive unit cells. A unit cell is the smallest group of atoms of a substance that has the overall symmetry of a crystal of that substance, and from which the entire lattice can be built up by the repetition in three dimensions. A primitive cell must contain only one lattice point, generally, lattice points that are shared by n cells are counted as $\frac{1}{n}$ of the lattice points contained in each of those cells. So traditional primitive cells only contain points at their corners. The most obvious way to form a primitive cell is to use the basis vectors which the lattice is constructed from:

$$C(\mathbf{a}_1, \mathbf{a}_2) = \mathbf{r} = x_1 \mathbf{a}_1 + x_2 \mathbf{a}_2$$

$$0 \leq x_i \leq 1$$

The scaling factors are to ensure that lattice points are placed on the corners of the cell. In the current paper the primitive unit cell of a d-dimensional Bravais lattice tiles the spacetime. $C(\mathbf{a}_1, \mathbf{a}_2)$ is the Bravais cell of a Bravais Lattice spanned by basis vectors $(\mathbf{a}_1, \mathbf{a}_2)$. A

given Bravais Lattice Λ can be defined by an infinity of Bravais cells. Hermite normal form: the analogue of reduced echelon form for matrices over \mathbb{Z}^n . Each family of Bravais cells contains a unique cell of the Hermite normal form, this can be written in terms of L , T , and S , where L , and T are respectively the spatial, and temporal lattice periods, S is the "tilt" of the cell. Hence the lattice can be defined as $[L \times T]_S$.

Prime Bravais Lattices It may be possible to tile a given Bravais lattice Λ by a finer lattice Λ_p . A Bravais lattice is prime if there is no finer Bravais cell, other than the unit volume $[1 \times 1]_0$ that can tile it. If $\det\Lambda$ is a prime number, then Λ is a *prime matrix*. If Λ is neither prime nor unimodular (a square integer matrix having determinant of ± 1), it is composit can be decomposed into a product of two non-unimodular matrices $\Lambda = PQ$. In order to determine all prime lattices Λ_p that tiles a given Bravais lattice Λ :

$$\mathbf{a}_1 = k\mathbf{a}_1^p + l\mathbf{a}_2^p$$

$$\mathbf{a}_2 = m\mathbf{a}_1^p + n\mathbf{a}_2^p$$

observe that a prime tile $(\mathbf{a}_1^p, \mathbf{a}_2^p)$ tiles the large tile only if the larger tile's width L is a multiple of L_p , and the height T is a multiple of T_p , and the two tile "tilts" satisfy:

$$\mathbf{a}_2 = m\mathbf{a}_1^p + \frac{T}{T_p}\mathbf{a}_2^p \rightarrow S = mL_p + \frac{T}{T_p}S_p$$

A prime lattice only tiles the given lattice if the area spanned by the two tilted basis vectors:

$$\mathbf{a}_2 \times \mathbf{a}_2^p = ST_p - TS_p$$

is a multiple of the prime tile area $L_p T_p$. A lattice state is a set of all field values $X = \{\phi_z\}$ over the d-dimensional lattice $z \in \mathbb{Z}$ that satisfies the spatiotemporal cat equation. Lattice state X is a periodic orbit if $X(z + R) = X(z)$ for any discrete translation $R = n_1\mathbf{a}_1 + n_2\mathbf{a}_2$. If a given periodic orbit over lattice Λ is not periodic under translations $R \in \Lambda_p$ for any sublattice Λ_p (except for Λ itself) we shall refer to it as an orbit: a lattice state of smallest periodicity in all spacetime directions.

Shift Operator Shift operator is a matrix: $r_{ij} = \delta_{i+1,j}$, this along with a periodic boundary condition assuming $[n \times n]$ matrix $r^n = I$ yields

$$\begin{pmatrix} 0 & 1 & 0 & 0 \\ 0 & 0 & 1 & 0 \\ 0 & 0 & 0 & 1 \\ 1 & 0 & 0 & 0 \end{pmatrix}$$

A lattice state is a vector with all the values that the field takes on at each point on the lattice. Shift operator is cyclic permutation of a lattice state, changes only the coordinates of the lattice state.

$$r\mathbf{X} = \begin{bmatrix} \phi_1 \\ \phi_2 \\ \vdots \\ \phi_0 \end{bmatrix}$$

$r^T = r^{-1}$ cyclic permutation in the opposite direction, does not destroy anything, only changes the coordinates.

Lattice Derivatives Hypercube in d-dimensions with unit sides. Each side is described by a unit vector in direction $\mu \hat{n}_\mu \in \{\hat{n}_1, \hat{n}_2, \hat{n}_3, \dots, \hat{n}_d\}$ unit lattice cell, points along μ 'th direction.

Forward Lattice Derivative (a is lattice spacing):

$$(\partial_\mu \phi)_l = \frac{\phi(x + a\hat{n}_\mu) - \phi(x)}{a} = \frac{\phi_{l+\hat{n}_\mu} - \phi_l}{a}$$

Backward Lattice Derivative (transpose of forward lattice derivative):

$$(\partial_\mu \phi)^T = \frac{\phi(x - a\hat{n}_\mu) - \phi(x)}{a} = \frac{\phi_{l-\hat{n}_\mu} - \phi_l}{a}$$

Lattice Discretization, Lattice State Divide interval of separation a creating a discrete coordinate system. At each point read off the value of the continuous counterpart. Field has a constant value over the interval. Lattice is a coordinate, set of points, the values of the field at each lattice point is a lattice state.

field $\phi = \phi(x)$ $x = al$ $l \in \mathbb{Z}$

Lattice State $\phi = \{\phi_0, \phi_1, \phi_2, \dots, \phi_{n-1}\}$ "configuration".

N-Site Periodic Lattice After N steps, back

$$r^N = I$$

$$\text{eigenvalues} = \omega = e^{\frac{i2\pi}{N}}$$

$$r^N - I = \prod_{k=0}^{N-1} (r - \omega^k I)$$

N distinct eigenvectors, N-dim space (N irrep)

N projection operators

$$P_k = \prod_{j=k}^{N-1} \frac{r - \omega^j I}{\omega^k - \omega^j}$$

Discrete Fourier Transforms Have a lattice state $\phi = \{\phi_0, \phi_1, \dots, \phi_{N-1}\}$

Kth Fourier Coeff=projection of ϕ onto eigen vector φ

$$\tilde{\phi}_k = \varphi_k^\dagger \cdot \phi = \frac{1}{\sqrt{N}} \sum_{l=0}^{N-1} e^{-\frac{i2\pi}{N} kl} \phi_l$$

Q19 I think I may have gotten to the point where I can go beyond exclusively reading the paper, what should I do beyond? As well, what times would be good for me to drop in on your Bluejeans office during the week?

Q20 I believe I've asked this before, or a form of it, but it seems that the periodic boundary condition is in direct conflict with the definition of the shift operator. Am I missing something?

2020-10-15 Sidney A reread.

The Bernoulli shift map is a circle map due to the mod 1 operation for $[1/s, 1)$ where s is the "stretching parameter" of the general Bernoulli map: $\phi_{t+1} = s\phi_t \pmod{1}$. This subtracts the integer part of $s\phi_t$ yielding the "winding number" m_{t+1} . This keeps ϕ_{t+1} in the unit interval, and divides this interval into s subintervals. The winding number is also the alphabet of the system, denoting at time t , it visits interval m . Brief note from Chaosbook: we can represent a state as a base s decimal of the resulting visitation sequence: $\phi_0 = .m_1 m_2 m_3 \dots$. The Bernoulli map operates on a state by shifting this itinerary over by one: $\phi_0 = .m_1 m_2 m_3 \dots \rightarrow \phi_1 = .m_2 m_3 \dots$. The preimages of critical points (the point which when input into the map yield a maximum value on in the map) partition the map into s^n subintervals, where n is the orbit length. There is no pruning in the Bernoulli map, as its critical points are all unity, however, as it is a circle map the first and last fixed point (rightmost fixed point, and the fixed point at the origin) are the same, so they are counted as one fixed point, and thus the number of periodic orbits is $N_n = s^n - 1$. There can only be one periodic orbit per subinterval because each subinterval is treated as a single point where a certain orbit is possible, thus, there can only be one orbit. For the temporal Bernoulli, 'Temporal' here refers to the state (field) ϕ_t and the winding number m_t (source) taking their values on the lattice sites of a 1-dimensional temporal lattice $t \in \mathbb{Z}$. Over a finite lattice segment they can be written as a state, and a symbol block. The Bernoulli equation can be written as a first order difference equation $\phi_t - s\phi_{t-1} = -m_t$ where ϕ is contained within the unit interval. This is the condition which each point on the lattice must fulfill. This can then be written in terms of the orbit Jacobian matrix, which is a sum of the identity and cyclic permutation matrix which has the condition $r^n = I$. This permutation permutes forward in time the lattice state by one site. The temporal Bernoulli condition can be viewed as a search for zeros of the function involving the orbit Jacobian matrix operating on the lattice state

summed with the symbol block M . This allows the entire lattice state which solves for zero X_M to be treated as a single fixed point. The orbit Jacobian matrix stretches the unit hyper cube such that every periodic point is mapped onto an integer lattice \mathbb{Z}^n site, which is then translated by the winding numbers into the origin to satisfy the fixed point condition. Therefore N_n the number of solutions to the fixed point condition is the number of lattice sites within the fundamental parallelepiped (fp), which is equivalent to the volume of the fp because each unit cell in the lattice only contains one lattice point. So N_n is the magnitude of the determinant of the orbit Jacobian matrix, this is called Hill's Determinant, or the Fundamental Fact. The orbit Jacobian matrix maps the unit hyper cube into the basis vectors of the fundamental parallelepiped which are given by columns of the orbit Jacobian matrix.

2020-10-18 Sidney My notes on Barvinok [1] *Lecture notes*

The theory discussed in these lectures are inspired by a few series formulas, the first being:

$$\sum_{m=1}^n x^m = \frac{1 - x^{n+1}}{1 - x}$$

We take the interval $[0, n]$ and for every integer point in the interval we write the monomial x^m and then take the sum over each integer point on the interval. It gives a polynomial with $n+1$ terms, but can be written in the form given, later we will cover doing the same over a 2D plane (evaluating at each integer point on the plane and summing over every integer point $m = (m_1, m_2)$ with bivariate monomials $x^m = x^{m_1}x^{m_2}$). The second formula is the infinite geometric series:

$$\sum_m^\infty x^m = \frac{1}{1 - x}$$

This makes sense if $|x| < 1$ similarly

$$\sum_{-\infty}^0 x^m = \frac{1}{1 - x^{-1}} = \frac{-x}{1 - x}$$

This converges if $|x| > 1$

$$\sum_{m=-\infty}^\infty x^m$$

This converges for no values, so we will say that it equals zero, this can be reasoned through as every positive integer added to every negative integer is zero, we then subtract zero, as it was double counted:

$$\sum_{m=-\infty}^\infty = \sum_{m=0}^\infty x^m + \sum_{m=-\infty}^0 x^m - x^0 = 0$$

This sugestively agrees with

$$\frac{-x}{1-x} + \frac{1}{1-x} - 1 = 0$$

Geometrically, the real line \mathbb{R}^1 is divided into two unbounded rays intersecting in a point. For every region (the two rays, the line and the point), we construct a rational so that the sum of x^m over the lattice points in the region converges to that rational function, if it converges at all.

2020-10-19 Sidney

Inclusion-exclusion principle

$$|A \cup B| = |A| + |B| - |A \cap B| \quad (15.2)$$

where $|A \cap B|$ is the number of elements which are in both A and B. This avoids double counting.

If we think of a plane of points, we can draw lines which subdivide the plane, each line makes the plane two half planes, and every two lines form four angles, this forms several regions. Among these regions there are regions \mathcal{R} where the sum:

$$\sum_{m \in \mathcal{R} \cap \mathbb{Z}^2} x^m$$

converges for some x , and some regions where the sum will never converge.

We shall show that it is possible to assign a rational function to every region simultaneously so that each series converges to the corresponding rational function, if it converges at all, it will also satisfy the inclusion-exclusion principle.

Definition 1 The scalar product in \mathbb{R}^d is

$$\sum_{i=1}^d x_i y_i$$

for $x = (x_1, \dots, x_d)$ and $y = (y_1, \dots, y_d)$, and the same for $\mathbb{Z}^d \subset \mathbb{R}^d$.

Definition Polyhedron P is the set of solutions to finitely many linear inequalities:

$$P = \left\{ \phi \in \mathbb{R}^d : \sum_{i=1}^d a_{ij} x_j \leq b_i \right\}$$

If all a_{ij} and b_j are integers the polyhedron is rational.

Barvinok notes concern themselves with the set $P \cap \mathbb{Z}^d$ of integer points in a rational polyhedron P . He introduces the algebra of polyhedra to account for all relations among polyhedra.

2020-11-29 Predrag We only need to understand parallelepipeds, not polyhedra in general. Should be easier.

2020-11-30 Sidney I understand your comments. Thank you, I am pretty sure that the general polyhedra stuff can be put in terms of parallelepipeds, so at least it wasn't wasted knowledge, but I'm glad that I don't need to know all of it, it's on the edge of my proof abilities.

2020-11-29 Predrag

Definition 2 For a set $\mathcal{B} \in \mathbb{R}^d$, the function

$$[\mathcal{B}](\phi) = \begin{cases} 1 & \text{if } \phi \in \mathcal{B} \\ 0 & \text{otherwise} \end{cases} \quad (15.3)$$

is called the *indicator* of \mathcal{B} .

2020-10-24 Sidney

The intersection of finitely many (rational) polyhedra is a (rational) polyhedron. The union doesn't have to be, but may be a polyhedron.

Union: The union of a collection of sets is the set of all elements in the collection.

Intersection: $A \cap B$, is the intersection of two sets A and B , i.e., the set containing all elements of A that also belong to B .

The algebra of rational polyhedra is the vector space $\mathcal{P}(\mathbb{Q}^d)$ spanned by the indicators $[P]$ for all rational polyhedra $P \subset \mathbb{R}^d$

2020-11-29 Predrag \mathbb{Q} is the *field of rationals*.

2020-10-24 Sidney

Valuations

Let V be a vector space. A linear transformation $\mathcal{P}(\mathbb{Q}^d) \rightarrow V$ is called a valuation. This course is on the particular valuation $\mathcal{P}(\mathbb{Q}^d) \rightarrow \mathbb{C}(x_1, \dots, x_d)$, where $\mathbb{C}(x_1, \dots, x_d)$ is the space of d -variate rational functions.

Theorem 1 There exists a unique valuation $\chi : \mathcal{P}(\mathbb{R}^d) \rightarrow \mathbb{R}$ called the Euler characteristic, such that $\chi([P]) = 1$ for any non-empty polyhedron $P \subset \mathbb{R}^d$

2020-11-30 Predrag Klain and Rota [11] *Introduction to Geometric Probability*:

A *valuation* on a lattice L of sets is a function μ defined on L that takes real values, and that satisfies the following conditions:

$$\mu(A \cup B) = \mu(A) + \mu(B) - \mu(A \cap B), \quad (15.4)$$

$$\mu(\emptyset) = 0, \quad (15.5)$$

where \emptyset is the empty set. By iterating the identity (18.278) we obtain the inclusion-exclusion principle for a valuation μ on a lattice L, namely

$$\begin{aligned} \mu(A_1 \cup A_2 \cup \dots \cup A_n) &= \sum_i \mu(A_i) - \sum_{i < j} \mu(A_i \cap A_j) \\ &\quad + \sum_{i < j < k} \mu(A_i \cap A_j \cap A_k) + \dots \end{aligned} \quad (15.6)$$

for each positive integer n .

Barvinok [1] Lecture 1, Problem 1 statement of (18.280) is less intelligible: Take sets $A_1, A_2, \dots, A_n \in \mathbb{R}^d$. The inclusion-exclusion formula is

$$\cup A_i = \sum_I (-1)^{|I|-1} [\cap_{i \in I} A_i], \quad (15.7)$$

where the sum is taken over all non-empty subsets $I \subset \{1, \dots, n\}$ and $|I|$ is the cardinality of I .

2020-10-25 Sidney

Identities in the Algebra of Polyhedra

The image of a polyhedron under a linear transformation is a polyhedron.

Theorem 1 Let $P \subset \mathbb{R}^d$ be a polyhedron and let $T: \mathbb{R}^d \rightarrow \mathbb{R}^k$ be a linear transformation. Then $T(P) \subset \mathbb{R}^k$ is a polyhedron. Furthermore, if P is a rational polyhedron and T is a rational linear transformation (that is, the matrix of T is rational), then $T(P)$ is a rational polyhedron.

Linear transformations preserve linear relations among indicators of polyhedra.

Theorem 2 Let $T: \mathbb{R}^d \rightarrow \mathbb{R}^k$ be a linear transformation. Then there exists a linear transformation $T: P(\mathbb{R}^d) \rightarrow P(\mathbb{R}^k)$ such that $T(P) = [T(P)]$ for every polyhedron $P \subset \mathbb{R}^d$.

Most sensible polyhedra have vertices, but some don't.

Definition 1 Let $P \subset \mathbb{R}^d$ be a polyhedron. A point $v \in P$ is called a vertex of P if whenever $v = (x + y)/2$ for some $x, y \in P$, we must have $x = y = v$.

If v is a point in P , we define the tangent cone of P at v as:

$$co(P, v) = \{x \in \mathbb{R}^d : \epsilon x + (1 - \epsilon)v \in P \text{ for all sufficiently small } \epsilon > 0\}$$

Not all polyhedra have vertices. In fact, a non-empty polyhedron has a vertex if and only if it does not contain a line.

Definition 2 We say that a polyhedron P contains a line if there are points x and y such that $y \neq 0$ and $x+ty \in P$ for all $t \in \mathbb{R}$. $P_0(\mathbb{R}^d) \subset P(\mathbb{R}^d)$ is the subspace spanned by the indicators of rational polyhedra that contain lines.

Theorem 3 Let $P \subset \mathbb{R}^d$ be a polyhedron. Then there is a $g \in P_0(\mathbb{R}^d)$ such that

$$[P] = g + \sum_v [co(P, v)],$$

where the sum is taken over all vertices v of P . If P is a rational polytope then we can choose $g \in P_0(\mathbb{Q}^d)$

Definition 3-0 A polytope is a high dimensional generalization of a polyhedron.

Definition 3 Let $A \subset \mathbb{R}^d$ be a non-empty set. the set

$$A^\circ = \{y \in \mathbb{R}^d : \langle x, y \rangle \leq 1 \text{ for all } x \in A\}$$

is called the polar of A , where $\langle x, y \rangle$ is the inner product.

2020-10-27 Sidney

A set S in a vector space over \mathbb{R}^d is convex, if the line segment connecting any two points in S lies entirely within S . If P is a rational polyhedron then P° is also a rational polyhedron.

Theorem 4 There exists a linear transformation $D : P(\mathbb{Q}^d) \rightarrow P(\mathbb{Q}^d)$ such that $D[P] = [P^\circ]$ for every non-empty polyhedron P .

It follows from Theorem 4 that whenever we have a linear identity $\sum_{i=1}^m \alpha_p[P_i] = 0$ among the indicator functions of polyhedra, we have the same identity $\sum_{i=1}^m \alpha_p[P_i^\circ] = 0$ for the indicator functions of their polars.

Barvinok [1] Lecture 3.

For an integer point $\mathbf{m} = (m_1, \dots, m_d)$ we introduce the monomial $\mathbf{x}^\mathbf{m} = x_1^{m_1} \cdots x_d^{m_d}$. Given a set $S \subset \mathbb{R}^d$, we consider the sum

$$f(S, \mathbf{x}) = \sum_{m \in S \cap \mathbb{Z}^d} \mathbf{x}^\mathbf{m} \tag{15.8}$$

Our goal is to find a reasonably short expression for this sum as a rational function in \mathbf{x} .

Example 1 Let \mathcal{R}_+^d be the non-negative orthant, that is the set of all points with all coordinates non-negative. We have

$$\sum_{m \in \mathbb{R}_+^d \cap \mathbb{Z}^d} \mathbf{x}^m = \left(\sum_{m_1=0}^{\infty} x_1^{m_1} \right) \cdots \left(\sum_{m_d=0}^{\infty} x_d^{m_d} \right) = \prod_{i=1}^d \frac{1}{1-x_i}$$

provided that $|x_i| < 1$

Definition Let $u_1, \dots, u_d \in \mathbb{Z}^d$ be linearly independent integer vectors. The simple rational cone generated by u_1, \dots, u_d is the set:

$$K = \left\{ \sum_{i=1}^d \alpha_i u_i : \quad \alpha_i \geq 0 \quad \text{for } i = 1, \dots, d \right\}$$

The fundamental parallelepiped of u_1, \dots, u_d is the set

$$\Pi = \left\{ \sum_{i=1}^d \alpha_i u_i : \quad 1 > \alpha_i \geq 0 \quad \text{for } i = 1, \dots, d \right\}$$

Theorem For a simple rational cone $K = K(u_1, \dots, u_d)$ we have

$$f(K, \mathbf{x}) = \left(\sum_{m \in \Pi \cap \mathbb{Z}^d} \mathbf{x}^m \right) \prod_{i=1}^d \frac{1}{1 - \mathbf{x}^{u_i}}$$

Theorem The number of integer points in the fundamental parallelepiped is equal to its volume.

Sketch of Proof Let Λ be the set of all integer combinations of u_1, \dots, u_d :

$$\Lambda = \left\{ \sum_{i=1}^d \alpha_i u_i : \quad \alpha_i \in \mathbb{Z} \quad \text{for } i = 1, \dots, d \right\}$$

Let us consider all translates $\Pi + u$ with $u \in \Lambda$. We claim that $\Pi + u$ can cover all \mathbb{R}^d without overlapping, this can be extracted from the proof of theorem 1. Let us take a sufficiently large region $X \subset \mathbb{R}^d$ and let us count the number of integer point in X , the set is roughly covered by $\text{vol}X / \text{vol}\Pi$ translations of the parallelepiped, and each translation carries the same number of points hence we must have $|\Pi \cap \mathbb{Z}^d| = \text{vol}\Pi$.

Barvinok [1] Lect. 3, Definition 2. Let $u_1, \dots, u_d \in \mathbb{Z}^d$ be linearly independent vectors and let K be the simple cone generated by u_1, \dots, u_d . We say that K is *unimodular* if the volume of the fundamental parallelepiped Π is 1. Equivalently, K is unimodular if the origin is the unique integer point in Π . Equivalently, (15.8) is of form

$$f(K, \mathbf{x}) = \prod_{i=1}^d \frac{1}{1 - x^{u_i}}. \quad (15.9)$$

2021-01-01 I have been looking at the flow conservation sum rule for the Hénon map, as of today I had my suspicions confirmed that the Hénon map is not flow conserving so, the sum rule will not go to 1. However, I am still investigating the relation between the orbit Jacobian matrix (the Hill matrix) and the local Jacobian J_M . To do this, I have been looking over the proof that was done with the cat map to show that $|\text{Det } \mathcal{J}| = |\det(I - J_M)|$. I am hoping that I can find something similar to this identity for the Hénon map. I have been looking at section five of the cat paper to see if I can adapt anything. I am also going to look at the relaxation method for finding periodic orbits so I can start working within Orbithunter and finding periodic orbits.

Q21 Is XXX?

Q22 What exactly is meant by XXX?

2021-01-02 Sidney Here are my notes from section 5:

Kronecker product $A \otimes B$ A is $[n \times n]$ and B is $[m \times m]$

$$A \otimes B = \begin{pmatrix} a_{11}B & \cdots & a_{1n}B \\ \vdots & \ddots & \vdots \\ a_{n1}B & \cdots & a_{nn}B \end{pmatrix}$$

for A, A' $[n \times n]$ matrices and B,B' $[m \times m]$

$$(A \otimes B)(A' \otimes B') = AA' \otimes BB'$$

$$\text{tr}(A \otimes B) = \text{tr}(A)\text{tr}(B)$$

$$\det(A \otimes B) = \det(A^m)\det(B^n)$$

the two $[mn \times mn]$ block matrices $A \otimes B$ and $A \otimes B$ are equivalent by a similarity transformation

$$B \otimes A = P^T(A \otimes B)P$$

where P is a permutation matrix, as $\det(P) = 1$

$$\det(A \otimes B) = \det(B \otimes A)$$

Consider a rectangular d=2 lattice $[L \times T]_0$ Bravais cell, for this cell, the spatiotemporal orbit Jacobian matrix is

$$\mathcal{J} = r_1 + r_2 - 2sI + r_2^{-1} + r_1^{-1}$$

The index 1 is the spacial direction, and the index 2 is the temporal direction. The $[LT \times LT]$ orbit Jacobian matrix can be rewritten using Kronecker products:

$$\mathcal{J} = I_1 \otimes (r_2 + r_2^{-1}) - sI_1 \otimes I_2 + (r_1 + r_1^{-1}) \otimes I_2$$

$$I_1 = [L \times L] \text{ Identity}$$

$$I_2 = [T \times T] \text{ Identity}$$

Hill determinant: fundamental parallelepiped example Consider the Bravais lattice with basis vectors $\vec{a}_1 = < 3, 0 >$ and $\vec{a}_2 = < 0, 2 >$ a periodic orbit over this Bravais cell has 6 field values, one for each lattice site $z = (n, t)$ on a $[3x2]_0$ rectangle:

$$\begin{bmatrix} \phi_{01} & \phi_{11} & \phi_{21} \\ \phi_{00} & \phi_{10} & \phi_{20} \end{bmatrix}$$

We can stack up the columns of this lattice state and the corresponding sources into 6-dimensional vectors

$$\begin{pmatrix} \phi_{01} \\ \phi_{00} \\ \phi_{11} \\ \phi_{10} \\ \phi_{21} \\ \phi_{20} \end{pmatrix}, \quad \begin{pmatrix} m_{01} \\ m_{00} \\ m_{11} \\ m_{10} \\ m_{21} \\ m_{20} \end{pmatrix}$$

The corresponding orbit Jacobian block-matrix:

$$\mathcal{J}_{[3x2]_0} = \left[\begin{array}{cc|cc|cc} -2s & 2 & 1 & 0 & 1 & 0 \\ 2 & -2s & 0 & 1 & 0 & 1 \\ \hline 1 & 0 & -2s & 2 & 1 & 0 \\ 0 & 1 & 2 & -2s & 0 & 1 \\ \hline 1 & 0 & 1 & 0 & -2s & 2 \\ 0 & 1 & 0 & 1 & 2 & -2s \end{array} \right]$$

The fundamental parallelepiped generated by the action of the orbit Jacobian matrix is spanned by $LT = 6$ basis vectors: the columns of the orbit Jacobian matrix. The fundamental fact now yields the Hill determinant as the number of lattice states

$$N_{[3x2]_0} = |\text{Det}(\mathcal{J}_{[3x2]_0})| = 4(s-2)s(2s-1)^2(2s+3)^2$$

In practice, one often computes the Hill determinant using a Hamiltonian or "transfer matrix" formulation. An example is the temporal cat 3-term recurrence

$$\begin{aligned}\phi_t &= \phi_t \\ \phi_{t+1} &= -\phi_{t-1} + s\phi_t - m_t\end{aligned}$$

In the Percival-Vivaldi "two-configuration" cat map representation

$$\begin{aligned}\hat{\phi}_{t+1} &= \hat{J}_1 \hat{\phi}_t - \hat{m}_t \\ \hat{J}_1 &= \left[\begin{array}{cc} 0 & 1 \\ -1 & s \end{array} \right], \quad \hat{\phi}_t = \left[\begin{array}{c} \phi_{t-1} \\ \phi_t \end{array} \right], \quad \hat{m}_t = \left[\begin{array}{c} 0 \\ m_t \end{array} \right]\end{aligned}$$

Similarly for the d=2 spatiotemporal cat lattice at hand, one can recast into a 5-term recurrence relation:

$$\begin{aligned}\phi_{nt} &= \phi_{nt} \\ \phi_{n,t+1} &= \phi_{n,t-1} - \phi_{n-1,t} + 2s\phi_{nt} - \phi_{n+1,t} - m_{nt} \\ \hat{J}_1 &= \left[\begin{array}{c|c} 0 & I_1 \\ \hline -I_1 & -\mathcal{J} \end{array} \right]\end{aligned}$$

This $[2L \times 2L]$ block matrix generates a "time" orbit by acting on a $2L$ -dimensional "phase space" lattice strip $\hat{\phi}_t$ along the "spatial" direction

2021-01-04 Sidney I am going to take a break from the sum rule proof. However, I do know that the Hénon map is not a closed system so the sum rule does not converge to 1. For this blog entry, I shall take notes on the relaxation method for finding cycles, I will also try to write some code today, if I do, I will post my initial python code here too.

Notes All methods for finding unstable cycles are based on the idea of constructing a new dynamical system such that (i) the position of the cycle is the same for the original system and the transformed one, and (ii) the unstable cycle in the original system is a stable cycle of the transformed system. For example, the Newton-Raphson method replaces iteration of $f(x)$ by iteration of the Newton-Raphson map:

$$x'_i = g_i(x) = x_i - \left(\frac{1}{M(x) - I} \right)_{ij} (f(x) - x)_j$$

A fixed point x_* for a map $f(x)$ is also a fixed point of $g(x)$, indeed a superstable fixed point since $\frac{\partial g_i(x_*)}{\partial x_j} = 0$. The relaxation methods start with a guess of not a few points along an orbit, but a guess of the entire orbit. The relaxation algorithm for finding cycles is based on the observation that a trajectory of a map such as the Hénon map (see the discussion leading up to (2.11)):

$$x_{i+1} = 1 - ax_i^2 + by_i$$

$$y_{i+1} = x_i$$

Is a stationary solution of the relaxation dynamics defined by the flow

$$\frac{dx_i}{d\tau}$$

for any vector field v_i which vanishes on the trajectory. Here τ is a "fictitious time" variable, unrelated to the dynamical time (in this example, the discrete time of map iteration). As the simplest example, take v_i to be the deviation of an approximate trajectory from the exact 2-step recurrence form of the Hénon map:

$$v_i = x_{i+1} - 1 + ax_i^2 - bx_{i-1}$$

For fixed x_{i-1} and x_{i+1} there are two values of x_i satisfying $v_i = 0$. These solutions are the two extremal points of a local "potential" function:

$$v_i = \frac{\partial}{\partial x_i} V_i(x)$$

$$V_i = x_i(x_{i+1} - bx_{i-1} - 1) + \frac{a}{3}x_i^3$$

Assuming that the two extremal points are real, one is a local minimum of $V_i(x)$ and the other is a local maximum. We can modify or vector field differential equation with

$$\begin{aligned} \frac{dx_i}{d\tau} &= r_i v_i \\ r_i &= \pm 1 \end{aligned}$$

The modified flow will be in the direction of the extremal point given by the local maximum of V_i if $r_i = 1$ is chosen, or in the direction of the one corresponding to the local minimum if we take $r_i = -1$. I think that this is because a negative slope seeks to minimize a value, whereas a positive slope seeks to maximize it, therefore, if we can somehow keep the flow from going off into positive or negative infinity, it will go to either a local maximum or local minimum. The goal of the relaxation method is that instead of searching for an unstable periodic orbit of a map, one searches for a stable attractor of a vector field. More generally, consider a d-dimensional map $x' = f(x)$ with a hyperbolic fixed point x_* . Any fixed point x_* is by construction an equilibrium point of the fictitious time flow

$$\frac{dx}{d\tau} = f(x) - x$$

If all eigenvalues of the Jacobian matrix $J(x_*) = Df(x_*)$ have real parts smaller than unity, then x_* is a stable equilibrium point of the flow. If some of the eigenvalues have real parts larger than unity, then one needs to modify the vector field so that the corresponding directions of the flow

are turned into stable directions in a neighborhood of the fixed point. To do this, we can modify the flow by

$$\frac{dx}{d\tau} = \mathbf{C}(f(x) - x),$$

where \mathbf{C} is a $[d \times d]$ invertible matrix. The aim is to turn x_* into a stable equilibrium point of the flow by an appropriate choice of \mathbf{C} . It can be shown that a set of permutation/reflection matrices with one and only one non-vanishing entry ± 1 per row or column (for d -dimensional systems, there are $d!2^d$ such matrices) suffices to stabilize any fixed point. In practice, one chooses a particular matrix \mathbf{C} , and the flow is integrated. For each choice of \mathbf{C} , one or more hyperbolic fixed points of the map may turn into stable equilibria of the flow. We can change the algorithm to a discrete method which solves the issue of lengthy integrations of the fictitious time method. The idea is to construct a very simple map g , a linear transformation of the original f , for which the fixed point is stable. We take the Newton-Raphson map and replace the Jacobian prefactor in it with a constant matrix prefactor:

$$x' = g(x) = x + \Delta\tau \mathbf{C}(f(x) - x),$$

where $\Delta\tau$ is a positive real number, and \mathbf{C} is a $[d \times d]$ permutation and reflection matrix with one and only one non-vanishing entry ± 1 per row or column. A fixed point of f is also a fixed point of g . Since \mathbf{C} is invertible, the inverse is also true. This construction is motivated by the observation that for small $\Delta\tau \rightarrow d\tau$ the map is the Euler method for integrating the modified flow with integration step $\Delta\tau$. The argument why a suitable choice of matrix \mathbf{C} can lead to the stabilization of an unstable periodic orbit is similar to the one used to motivate the construction of the modified vector field. In fact, for very small $\Delta\tau$ this construction just becomes the flow. For a given fixed point of $f(x)$ we again chose a \mathbf{C} such that the flow in the expanding directions of $M(x_*)$ is turned into a contracting flow. The aim is to stabilize x_* by a suitable choice of \mathbf{C} . In the case where the map has multiple fixed points, the set of fixed points is obtained by changing the matrix \mathbf{C} (in general different for each unstable fixed point) and varying initial conditions for the map g . For example, for 2-dimensional dissipative maps it can be shown that the 3 matrices:

$$\begin{pmatrix} 1 & 0 \\ 0 & 1 \end{pmatrix}$$

$$\begin{pmatrix} -1 & 0 \\ 0 & 1 \end{pmatrix}$$

$$\begin{pmatrix} 1 & 0 \\ 0 & -1 \end{pmatrix}$$

suffice to stabilize all kinds of possible hyperbolic fixed points. If $\Delta\tau$ is chosen sufficiently small, the magnitude of the eigenvalues of the fixed point x_* in the transformed system are smaller than one, one has a stable fixed point. However, $\Delta\tau$ should not be chosen too small: since the convergence is geometrical with a ratio $1 - \alpha\Delta\tau$ (where the value of the constant α depends on the stability of the fixed point in the original system), small $\delta\tau$ can slow down the speed of convergence. The critical value of $\Delta\tau$, which just suffices to make the fixed point stable can be read off from the quadratic equations relating the stability coefficients of the original system and those of the transformed system. In practice, one can find the optimal $\Delta\tau$ by iterating the dynamical system stabilized with a given \mathbf{C} and $\Delta\tau$. In general, all starting points converge on the attractor provided $\Delta\tau$ is small enough. If this is not the case, the trajectory either diverges (if $\Delta\tau$ is far too large) or it oscillates in a small section of the state space (if $\Delta\tau$ is close to its stabilizing value). A fixed point can now be found by choosing a starting point in the global neighborhood of the fixed point, and iterating the map g which now converges to the fixed point due to its stability. The basin of attraction is very large. The step size $|g(x) - x|$ decreases exponentially when the trajectory approaches the fixed point. To get the coordinates of the fixed points with a high precision, one therefore needs a large number of iterations for the trajectory which is already in the linear neighborhood of the fixed point. To speed up the convergence of the final part of the approach to a fixed point, it is recommended to do a combination of this approach and the Newton-Raphson method. The fixed points of the n th iterate f^n are periodic points of a cycle of period n . If we consider the map

$$x' = g(x) = x + \Delta\tau\mathbf{C}(f^n - x)$$

the iterates of g converge to a fixed point provided that $\Delta\tau$ is sufficiently small and \mathbf{C} is a $[d \times d]$ constant matrix chosen such that it stabilizes the flow. As n grows, $\Delta\tau$ has to be chosen smaller and smaller.

2021-01-05 Sidney .

Q23 How does one choose what r or \mathbf{C} to use? I know that for sigma, I chose 1 if I want to drive it to converge to a local maximum in the potential, and -1 if I want a local minimum, but how do I know if the fixed point I am dealing with is a maximum or minimum?

2021-01-05 Predrag .

A23

2021-01-05 Sidney I have been hard at work trying to understand relaxation for cyclists. And I have gotten somewhere, not to a solution just yet, but somewhere. I decided that it would be best if I tried to understand the numerical methods employed by OrbitHunter before I started using it, to

this end, I have constructed a crude python code that can find the fixed points of the Hénon map, and the two cycle. My next step is to make the two cycle program more efficient and cleaner, and then to generalize it to n-length orbits. After this has been done I can start work on the exercise that I was set. The code is in

`siminos/williams/python/relax1.py`

2021-01-14 Sidney I have contacted Matt about OrbitHunter and he says that he's working on fixing some things so it's easier for people that are not him to work with. He recommended that I try to work on my own code, so I have been doing that. I was able to get the Two_Cycle working with the modification that it can now determine the sigma itself, but the four_cycle code is still not working, I think I need to change the differential equation solver to a Runge-Kutta algorithm instead of the Euler one I've been using, I'll paste the code under here, please please help if you can.

2021-02-01 Predrag .

Do this Save and svn commit this code as `siminos/williams/python/XXX.py`, then remove the inset from here

```
\#def four_cycle(guesstrajecotry,dt):
\#  henon = Henon(1.4, 0.3)
\#  x0=guesstrajecotry
\#  vi=np.zeros(4)
\#  vi[0]=x0[0]-henon.oneIter(np.roll(x0,2))
\#  vi[1]=x0[1]-henon.oneIter(np.roll(x0,1))
\#  vi[2]=x0[2]-henon.oneIter(np.roll(x0,0))
\#  vi[3]=x0[3]-henon.oneIter(np.roll(x0,-1))
\#  ep=10**(-7)
\#  x=np.zeros(4)
\#  sigma=np.zeros(4)
\#  sigma[:]=1
\#  iglob=0
\#  while np.all(abs(vi))>ep:
\#      iglob+=1
\#      for i in range(0,4):
\#          x[i]=x0[i]-dt*vi[i]
\#          vi[i]=x[i]-henon.oneIter(np.roll(x,(2-i)))
\#          x0[i]=x[i]
\#          print(x[i])
\#          #print(i)
\#          #time.sleep(1)
\#          if abs(x[i])>5 or iglob>100000:
\#              print(x)
```

```
\#             return "Diverged"
\#             sigma[i]=-1
\#             x=np.zeros(4)
\#             x0=np.zeros(4)
\#             vi[0]=x0[0]-henon.oneIter(np.roll(x0,2))
\#             vi[1]=x0[1]-henon.oneIter(np.roll(x0,3))
\#             vi[2]=x0[2]-henon.oneIter(np.roll(x0,4))
\#             vi[3]=x0[3]-henon.oneIter(np.roll(x0,5))
\#             iglob=0
\#             return x
```

For the guess trajectory I put in "np.zeros(4)" and for dt I put in 0.1 to get:
[1.11534978 -0.83649258 0.74365269 -0.33467244] close but no cigar. Also,
this is not intended to be a "best practices" code, I shall work on that once
I have made it work.

2021-01-15 Matt to Sidney **Please comment your code so it is easier to read.**

Comments are lines which start with '#' Pain is a part of the learning process for programming, at least in my experience. Especially for interpreted languages like Python; compiled languages like C, C++, C#, F# etc. are much more explicit and "logical", at the expense of flexibility. You'll be able to look back at old code and be able to write it in a much clearer and nicer way in the future, that I can guarantee.

For now, I'm going to refactor your code; I do not know if it will give the desired results, but hopefully it will get you back on track. You can use this refactored code or simply use it as a guide, but you have to understand its incredibly hard to interpret someone else's code.

The way you have your cycle functions set up is not going to scale, as you'll have to write each component and index separately. Imagine doing this for a thirty two cycle.

Here are some signs that you need to vectorize or refactor your code. I'll explain what this means in the code itself.

1. you start labeling your variables with indices (point1, point2, etc.)
2. You have multiple functions that could be converted into a single function + parameter (two cycle and four cycle can be combined into a "cycle" function)
3. You have functions which are special cases of other functions. A single iteration onelter should be produced by multilter plus parameter that says iteration = 1.

One way of testing if you need a higher order integration scheme is to test large vs. small step sizes. I.e. the step size in Euler can control error, it simply requires a much smaller step size to do so. Also, you might look towards implicit integration schemes which are always stable, for example, backwards Euler would be the simplest.

CHAPTER 15. SIDNEY'S BLOG

2021-01-15 Sidney to Matt Thank you very much for the help, I agree that pain seems to be a necessary ingredient in coding, and it is definitely extremely difficult to interpret another person's code. I can try to rewrite my code to make it more readable, along with references of where I am getting this method if that would be helpful, I shall wait for your response on that as I do not want to take more of your time. Also, I should definitely change the cycle functions, thank you, I will update that in the next iterate of the code. I have made my code all comments (I started each line with #).

2021-01-15 Matt:

Sidney the refactored code is available on an old branch of orbithunter github:

github.com/mgudorf/orbithunter/blob/henon/notebooks/sidney_refactoring.ipynb

The issue was setting sigma to be a constant and not dependent on i . In other words, to need a sigma for each dimension of the cycle.

2021-01-15 Sidney I have been looking at the refactored code, and I see how it works, in fact, I understand it enough to work with it, and have generated a good number of orbits. Unfortunately, the generated periodic points are not the same as they are in [ChaosBook Table 34.2](#) the last 1 to 2 digits are different. I am really unsure as to why this discrepancy exists. The values of the error function v_i get to values below the cutoff of 10^{-7} , and my original Two_Cycle code gave me values equal to those of table 34.2, but with different values of sigma. I am tired, and I have a headache, so I will just take notes on the "Cartesian Product" that I had to use to construct a function to find all possible sigma matrices (C in Chaosbook), and paste in my current working code (the modified one that I took from Matt). My goal over the next few days is to better understand the code, and figure out why there is that small difference between my calculated values and table 34.2.

The Cartesian Product of two sets A and B , denoted by $A \times B$, is the set of all ordered pairs (a, b) where a is an element of set A and b is an element of set B or:

$$A \times B = \{(a, b) \mid a \in A \text{ and } b \in B\}$$

For two sets the Cartesian Product can be computed by constructing a table where one set is the row index and the other is the column index. or $A \times B_{i,j} = (a_i, b_j)$, due to the tabular nature of this product the number of ordered pairs is $L_A L_B$ where L_A is the number of elements in set A and L_B is the number of elements in set B (from [Wikipedia](#)).

2021-02-01 Predrag .

Do this Save and svn commit this code as `siminos/williams/python/XXX.py`,
then remove the inset from here.

Update 2021-05-17: I removed the code here, and put the actual python file in williams/relax

1-17-2021 Sidney I was able to get the code to match the table in Chaosbook, I did this by changing the while loop condition to `# np.any(abs(cycle.deviation()) > ep)`

Will discuss whether this is better or not at the next meeting

1-28-2021 Sidney Lots of coding issues later I finally have a working algorithm for calculating the periodic points and expanding eigenvalues for the Hamiltonian Hénon map ($b = -1, a = 6$). It is messy, and I have not written the loop to calculate, and then write to an external document all cycles up to length n, but that should not be difficult, I also need to write this loop for my (still working) non-Hamiltonian code. Matt has been helping me clean up my code, I have been finding that my skills in matrix manipulation within Python are sorely lacking, and I hope that I can fix this. Once I have cleaned up the code, added the last few loops, and added comments and other such things to make it more readable, I shall upload it to the repository. After that point I hope to read at least some of Han's blog and take notes on it so that I can better understand what the rest of the group is doing.

15.2 2021 blog

2021-02-01 Predrag to Sidney - sorry about the Frenkel-Kontorova interruption, not worth your time right now, but Han and I might profit from being the first to read it. We'll keep it here until then.

2021-02-07 Sidney No issues with the interruption. I have been working towards understanding the next step, which is applying a Fourier transform on my states (cycles) to get them into Fourier space. From Han and other resources (Strang Linear Algebra), I know that all I have to do is apply a discrete Fourier transform on the periodic cycle vector, so it boils down to matrix vector multiplication where the elements are $F_{jk} = w^{jk}$ where w is a complex root of unity. I think I could easily code this myself, however, I feel like I could use a prebuilt package to go much faster, so I will use the numpy fft package, and from there figure out how to create plots like Han did. I will hopefully soon have a full functional nice code to put into the repository.

Q24 Sidney I know that the Fourier modes make it a lot easier to see the symmetries, but is there a reason for that? Or is it just coincidence? Or, is it too far beyond my level of pure math to appreciate?

2021-02-09 Sidney I have modified my code and made it so I can generate the symbol sequences for all orbits (001101 etc.) up to a certain length n and

store them in a list. I can then take this list and find the actual points of the cycle using my inverse iteration code, but for some reason the code diverges if I put the symbol sequence in the "wrong" order. For example, it gets the correct points if I put in 10 but not if I put in 01 which is weird. I still need to fix it. I have also used the fast Fourier transform from numpy to get the cycles into Fourier space. Now all I need to do is figure out why the code doesn't like some orders, and then figure out how to plot the points in Fourier space.

2021-02-24 Sidney I have officially completed my code, I will ask about how to upload my data and images here, I will also work on cleaning my code up a bit, and perhaps adding in the Fourier bit to the non-Hamiltonian Hénon map. Until that point though, it has become extremely obvious that I need to look at the theory about WHY I am doing Fourier transforms, so I am going to turn [Michael Engel's course \[7\]](#), based on Sands [13] *Introduction to crystallography* (1969) ([click here](#)). My notes:

Point Symmetry **Definition 1:** An Euclidean move $\mathcal{T} = \{A, b\}$ is a linear transformation that leaves space invariant:

$$x \mapsto \mathcal{T}(x) = Ax + b$$

Here, x is a vector, A a $[3 \times 3]$ orthogonal matrix and b a 3-vector.

Definition 2: The product of two transformations $\mathcal{T}_2 = \{A_1, b_1\}$ and $\mathcal{T}_2 = \{A_2, b_2\}$ is: $\mathcal{T}_2 \circ \mathcal{T}_1 = \{A_2 A_1, A_2 b_1 + b_2\}$ (\mathcal{T}_1 is applied first)

Definition 3: The order of a transformation \mathcal{T} is the smallest integer n such that $\mathcal{T}^n(x) = x$ one can also say this transformation is n -fold.

Observations:

1. The inverse is: $\mathcal{T}^{-1} = \{A^{-1}, -A^{-1}b\}$
2. Every transformation of finite order n (ie $\mathcal{T}^n = 1$) leaves at least one point invariant.

2021-02-27 Sidney Notes from Engel's course [7].

A group G , together with an operation, that combines any two elements a and b to form another element $a \cdot b$. To qualify as a group, the set and the operation must satisfy the group axioms:

Closure For all a and b in G , the result of the operation $a \cdot b$ is also in G

Associativity For all a, b , and c in G , $(a \cdot b) \cdot c = a \cdot (b \cdot c)$

Identity Element There must exist an identity element in G

Inverse Element For each a in G there must exist an inverse which yields the identity element when the group operation is applied between the two elements.

A symmetry of an object in space is an Euclidean move which leaves the object indistinguishable. The order of the group is equal to the number of elements in that group.

2021-02-27 Sidney Figure 15.1 shows all Hamiltonian Hénon (2.11), $a = 6$ lattice states of period $n = 6$, in the C_6 reciprocal lattice.

2021-02-27 Sidney Notes from Engel's course [7].

If G is a group and X is a set, then a left group action of G on X is a binary function:

$$GX \rightarrow X$$

denoted

$$(g, x) \mapsto g \cdot x$$

Which satisfies the following two axioms:

$$1. (gh)x = g(hx)$$

$$2. ex = x$$

The set X is called a left G -set. The group G is said to act on X on the left. When a group G acts on a set X the orbit of a point x in X is the set of elements of X to which x can be moved by the elements of G . The orbit of x is denoted as Gx :

$$Gx = \{g \cdot x | g \in G\}$$

The properties of a group guarantee that the set of orbits of X under the action of G form a partition of X . The associated equivalence relation is $x \sim y$ if and only if there exists a g in G with $gx = y$. The orbits are then the equivalence classes under this relation, two elements x and y are equivalent if and only if their orbits are the same ie $Gx = Gy$. For every x in X , we define the stabilizer subgroup of x (also called the isotropy group or little group) as the set of all elements in G that fix x :

$$G_x = \{g \in G | g \cdot x = x\}$$

In short: the orbit consists of all points that are equivalent under symmetry. And the stabilizer consists of all symmetries that leave a point invariant.

Definition 6: A point symmetry is a symmetry which leaves a point x_0 invariant: $\mathcal{T}(x_0) = x_0$

So, we can see that translations cannot be point symmetries, symmetries with finite order are point symmetries, symmetries with infinite order cannot be point symmetries.

Definition 7: A point group is a group of point symmetries which leave a common point x_0 invariant.

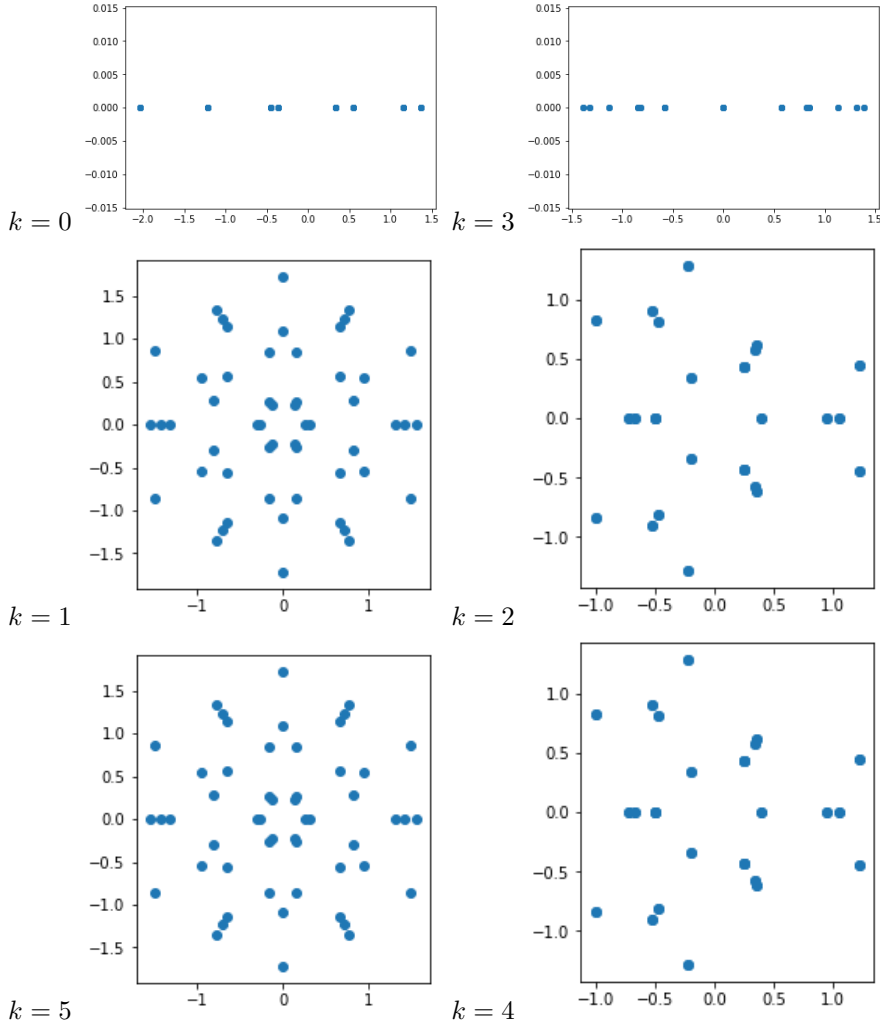


Figure 15.1: Hamiltonian Hénon (2.11), $a = 6$ lattice states of period $n = 6$, in the C_6 reciprocal lattice, $k = 0, 1, 2, 3, 4, 5$. $k = 0, 3$ are purely real. $k = 5, 4$ are the same as $k = 1, 2$, respectively, up to time reversal. Compare with Han's figure 18.60, for example.

So, we can see that a point group is a finite subgroup of $O(3)$, this space of three dimensional orthogonal matrices.

$$\text{Note: } O(3) = \{A \in \mathcal{R}^{3 \times 3} : A^T A = 1\}$$

$$SO(3) = \{A \in \mathcal{R}^{3 \times 3} : A^T A = 1, \det(A) = 1\}$$

Definition 8: Two subgroups H_1 and H_2 of a group G are conjugated if there exists a $g \in G$, such that:

$$H_2 = g^{-1} H_1 g$$

Example: $G = O(3)$. Two point groups are conjugated, if there is a change of basis that maps them into each other.

Cyclic groups: C_1, C_2, C_3, \dots where C_n consists of all rotations about a fixed point by multiples of $360/n$

Dihedral groups: $D_1, D_2, D_3, D_4, \dots$ where D_n (of order $2n$) consists of the rotations in C_n together with reflections in n axes that pass through the fixed point.

2021-03-07 Predrag For the current project, we need to understand D_n symmetry: see [Ding thesis example 2.9](#).

pdflatex *siminos/lyapunov/blog.tex*, read sect. 7.11.2 *Factorization of C_n and D_n* .

See also sect. [24.3 Pow wow 2021-01-08](#).

2021-03-07 Sidney I shall now attempt some of the exercises in Engel's [[7](#)] *Point Groups* lecture.

[exercise 2](#) Exercise 1

[exercise 3](#) Exercise 3

Determination of the point group of an object in space

1. Object linear: $C_{\infty v}$ or $D_{\infty h}$
2. High symmetry, non-axial: $T, T_h, T_d, O, O_h, I, I_h$
3. No rotation axis: C_1, C_i, C_s .

Carolyn's packings of small spheres on a big sphere

The point groups are for the sphere on the left: C_{2v} because it has 3 axes that it can rotate 180° around, and for each one it can then perform a flip and remain unchanged, I am unsure about the second sphere.

2021-03-07 Predrag For the current project, it will suffice to focus on 1-dimensional and 2-dimensional crystals (wallpaper groups). Engel is a chemist, so 3-dimensional symmetries are the most important thing, but we are good enough keeping to 2 dimensions.

CHAPTER 15. SIDNEY'S BLOG

2021-03-13 Sidney Here are my notes on Xiong Ding's example 2.9 and 2.8 in his thesis which is referenced above.

Example 2.8 Character table of dihedral group $D_n = C_{nv}$ n odd

$$D_n = \{e, C_n, C_n^2, \dots, C_n^{n-1}, r, C_nr, \dots, C_n^{n-1}r\}$$

D_n has n rotation elements and n reflections. Group elements satisfy $C_n^i C_n^j r = C_n^j r C_n^{n-i}$, so C_n^i and C_n^{n-i} form a class. Also, $C_n^{n-i} C_n^{2i+j} r = C_n^j r C_n^{n-i}$ implies that $C_n^j r$ and $C_n^{2i+j} r$ are in the same class. Therefore, there are only three different types of classes:

$\{e\}$, $\{C_n^k, C_n^{n-k}\}$, $\{r, C_nr, \dots, C_n^{n-1}r\}$. The total number of classes is $(n+3)/2$. In this case, there are 2 one dimensional irreducible representations (symmetric A_1 and antisymmetric A_2) and $(n-1)/2$ two-dimensional irreducible representations. In the j^{th} two-dimensional irreducible representation, class $\{e\}$ has form $\begin{pmatrix} 1 & 0 \\ 0 & 1 \end{pmatrix}$, class $\{C_n^k, C_n^{n-k}\}$ has form $\begin{pmatrix} \exp(\frac{i2\pi ki}{n}) & 0 \\ 0 & \exp(-\frac{i2\pi ki}{n}) \end{pmatrix}$, and class $\{r, C_nr, \dots, C_n^{n-1}r\}$ has form $\begin{pmatrix} 0 & 1 \\ 1 & 0 \end{pmatrix}$

Definition of Irreducible Representation (and Representation): Will be using the Dresselhaus lecture notes from 2002 downloaded from the [Chaosbook website](#):

Representation: A representation of an abstract group is a substitution group (matrix group with square matrices) such that the substitution group is homomorphic (or isomorphic) to the abstract group. We assign a matrix $D(A)$ to each element A of the abstract group such that $D(AB) = D(A)D(B)$.

Homomorphic/Isomorphic: Two groups are isomorphic or homomorphic if there exists a correspondence between their elements such that each

$$A \rightarrow \hat{A}$$

$$B \rightarrow \hat{B}$$

$$AB \rightarrow \hat{A}\hat{B}$$

If the two groups have the same order, then they are isomorphic.

Irreducible Representation: If by one and the same equivalence transformation, all the matrices in the representation of a group can be made to acquire the same block form, then the representation is said to be reducible, otherwise it is irreducible. Thus, an irreducible representation cannot be expressed in terms of representations of lower dimensionality.

Aside: how to find a character table of a group. See [here](#) for the source, symbol A denotes symmetric with C_n so yields a 1 in the

character table for all C. The subscripts 1, and 2 are symmetric (1) and antisymmetric (-1) respectively with respect to flips r . I am unsure about how the E_j column got its entries, it looks like it was a trace of the matrix representations, but I don't know the rule for that.

Q Sidney Conventionally, the irreps are the rows, and the symmetry operations are the columns, why are they transposed here?

2021-03-18 Sidney A review of the Group theory from Chaosbook, especially the irreps, and character tables. The goal of this is so that I can actually understand the character tables presented in the examples of Xiong Ding's thesis.

Q2 Sidney I am a little unsure about the statement in example 2.8 of Ding's thesis "in the j th two-dimensional irreducible representation class $\{r, rC_n, \dots, rC_n^{n-1}\}$ has the form $\begin{pmatrix} 0 & 1 \\ 1 & 0 \end{pmatrix}$. Shouldn't there a contribution from the rotation group C_n ? This looks just like the inversion (reflection?) group r .

From Dresselhaus again.

The Unitary of Representations: This theorem which shows that in most physical cases, the elements of a group can be represented by unitary matrices.

Theorem: Every representation with matrices having non-vanishing determinants can be brought into unitary form by an equivalence transformation. Skipping writing out the nitty gritty of the proof, we can first form a hermitian matrix using the representations of the group. We can then take advantage of the fact that any Hermitian matrix can be diagonalized by a suitable unitary transformation. We can construct this by doing a similarity transformation with some U from there we can redefine $\hat{A}_x = d^{-1/2}U^{-1}A_xUd^{1/2}$ where d is the diagonal matrix. We can then show that \hat{A}_x is unitary by simple calculation, thus we have proved the theorem.

We can use this theorem to prove Schur's Lemma which is: A matrix which commutes with all matrices of an irreducible representation is a constant matrix (a constant times the unit matrix). Therefore, if a non-constant commuting matrix exists, the representation is reducible.

Proof: Let M be a matrix which commutes with all matrices of the representation A_1, A_2, \dots, A_h :

$$MA_x = A_xM$$

Take the adjoint of both sides:

$$A_x^\dagger M^\dagger = M^\dagger A_x^\dagger$$

CHAPTER 15. SIDNEY'S BLOG

From the Unitary Representations theorem, with no loss of generality we can assume that A_x is unitary, so we can multiply on the left and right to obtain:

$$M^\dagger A_x = A_x M^\dagger$$

So, if M commutes with A_x then so does M^\dagger .

2021-03-22 Sidney I read through the rest of the proof, and I will continue Dresselhaus notes later, but now, I will review some [Chaosbook](#) material. I also looked at the decomposition of the cat map done by Predrag, but I do not understand it enough to see if it works with the Hénon map, so I will discuss in tomorrow's meeting. Anyway, here are notes for Week 13.

Video 1: Hard Work Builds Character Elementary examples of discrete groups: the character table characterizes the finite group.

2-element group: $\{e, g\} \quad g^2 = e. \quad S_2, D_1, C_2, \dots$ used to tile our space. Imagine butterfly, symmetry axis across the middle. Can separate the space into two spaces $\tilde{\mathcal{M}} \in \{\tilde{x}\}$ and $\tilde{\mathcal{M}}_2 = \{-\tilde{x}\}$ (top view of butterfly space). On the side, it is just a line, half of the line can be the fundamental domain, everything else is a copy of the fundamental domain. (Order of the group is the number of elements in it). Think of scalar functions defined on this domain $\rho(x)$. Can divide it into two functions $\rho_1(\tilde{x})$ (defined on fundamental domain) and $\rho_2 = \rho(-\tilde{x})$. Can decompose this function into a vector of functions evaluated on the fundamental domain, the vector will have a length equal to the order of the group. Can write the original function on the fundamental domain as $\rho(\tilde{x}) = \frac{1}{2}(\rho(\tilde{x}) + \rho(-\tilde{x})) + \frac{1}{2}(\rho(\tilde{x}) - \rho(-\tilde{x}))$ (decompose into symmetric, and antisymmetric components). $\rho(\tilde{x}) = \rho_+(\tilde{x}) + \rho_-(\tilde{x}). \quad \rho_\alpha = \frac{1}{|G|} \sum_g \chi_\alpha(g) \rho$. Where χ is the characters from the character table.

2: The Symmetry Group of a Propeller 3 elements. $G = \{e, g_2, g_3\} \quad g^3 = e$, rotation by $2\pi/3$ C_3 cyclic group with three elements. Can look at this as an abstract group (no physical, or geometrical realization): $g_2 = \omega \quad g_3 = \omega^3 \quad \omega^3 = e$. Can write a multiplication table from these relationships with the inverses, there is the identity along the diagonal. Matrix representation: in 2D plane the identity is just the unit matrix, and the other elements are just the rotation matrices.

I shall end my notes here for today (it is getting late).

2021-04-19 Sidney I have been working through the chapter 10 [ChaosBook problems](#) and I'm pretty confident with all but problem 10.2, could I possibly have a hint on where to start?

2021-03-07 Predrag I put all solutions that I have [here](#). They are pretty incomplete. If you have solutions that I do not have, or better / comparable solutions to those that I do have, let me know.

2021-04-24 Sidney Here I will attempt to derive the orbit Jacobian matrix, so that I can later find the eigenvalues and eigenvectors. I will start with analytically finding lattice states, and eigen-things. We will see how well that goes. First, the temporal Hénon is $x_{n+1} + ax_n^2 + x_{n-1} - 1 = 0$ this was drawn from the beginning of chapter 2 *Temporal Hénon*. Following the formalism of the CL18 paper, I can rewrite the map as $r + 2a\mathbb{X} + r^{-1} - I = 0$ where the 2 has come from the fact that finding the orbit Jacobian matrix is in effect taking a derivative, now the orbit Jacobian matrix is
[2021-05-01 Sidney: *this has wrong entries on the diagonal, (15.10), (3.85) is the correct formula.*]

$$\mathcal{J} = r + 2a\mathbb{X} + r^{-1} = \begin{bmatrix} 2ax_n & 1 & 0 & 0 & \dots & 0 & 1 \\ 1 & 2ax_n & 1 & 0 & \dots & 0 & 0 \\ 0 & 1 & 2ax_n & 1 & \dots & 0 & 0 \\ \vdots & \vdots & \vdots & \vdots & \ddots & \vdots & \vdots \\ 0 & 0 & \dots & \dots & \dots & 2ax_n & 1 \\ 1 & 0 & \dots & \dots & \dots & 1 & 2ax_n \end{bmatrix},$$

where the ones on the upper right and lower left corners, are a result of the periodic boundary conditions. The goal is to adapt this so that we can apply the time reversal boundary conditions, and thus construct time-symmetric lattice states.

2021-05-01 Sidney Here is the correct orbit Jacobian matrix (in the above I made a mistake):

$$\begin{aligned} \mathcal{J} &= \sigma + 2a\mathbb{X} + \sigma^{-1} \\ &= \begin{bmatrix} 2ax_0 & 1 & 0 & 0 & \dots & 0 & 1 \\ 1 & 2ax_1 & 1 & 0 & \dots & 0 & 0 \\ 0 & 1 & 2ax_2 & 1 & \dots & 0 & 0 \\ \vdots & \vdots & \vdots & \vdots & \ddots & \vdots & \vdots \\ 0 & 0 & \dots & \dots & \dots & 2ax_{n-2} & 1 \\ 1 & 0 & \dots & \dots & \dots & 1 & 2ax_{n-1} \end{bmatrix} \end{aligned} \quad (15.10)$$

I'll look at (and try to understand) the proof of the Hill's formula.

2021-05-05 Predrag Please modify your code so you are computing the (rescaled) temporal Hénon (2.44), orbit Jacobian matrix (3.85).

2021-05-05 Sidney I shall modify my code to do that, first, I will look at the rescaled temporal Hénon (2.44). Just for my own satisfaction, I shall rederive (2.44) and (3.85). The Hamiltonian Hénon map is given by

$$x_{n+1} = 1 - ax_n^2 - x_{n-1}$$

We note that an n-step recurrence relation is the discrete analogue to an order-n differential equation. We can now introduce the change of vari-

ables $\phi_n \equiv ax_n$ this turns our map into:

$$\frac{1}{a}\phi_{n+1} = 1 - \frac{1}{a}\phi_n^2 - \frac{1}{a}\phi_{n-1}$$

Rearranging, we get

$$a = \phi_{n+1} + \phi_n^2 + \phi_{n-1}. \quad (15.11)$$

The derivative of this map yields its orbit Jacobian matrix:

$$\mathcal{J}_p = r + 2\mathbb{X} + r^{-1}$$

Thus, we have rederived (2.44) and (3.85). I can now put it into my code. I am currently trying to understand the derivation of:

$$\hat{\mathcal{J}}_p = \begin{bmatrix} \mathbf{1} & & & -J(\phi_0) \\ -J(\phi_1) & \mathbf{1} & & \\ & \ddots & \ddots & \\ & & -J(\phi_{n-2}) & \mathbf{1} \\ & & & -J(\phi_{n-1}) & \mathbf{1} \end{bmatrix},$$

Any hints would be much appreciated.

2021-05-10 Predrag It's all in the blog, and the *siminos* repo. But why don't you go back where you started, and reread CL18 [3]:

sect. 1.5 Stability of an orbit vs. its time-evolution stability

appendix C Spatiotemporal stability

2021-05-10 Predrag One thing you can maybe help Han and me with; we find the block matrix formulation of sect. 8.5 *Spatiotemporal cat Hill's formula* quite reader-unfriendly. I like the latest version, sect. 8.9 *Han's Hénon map Hill's formula* better. Any suggestions how to make this easier to read are welcome!

2021-05-06 Matt to Sidney It's not clear to me what you need help with, but the origin of the derivation of the aforementioned matrix is the Jacobian of a multipoint shooting method (see *ChaosBook* sec. 16.2 *Multipoint shooting method* and *ChaosBook example 16.2*) vector $x_n - f(x_{n-1})$, $n \in 0, \dots, N$ (indices may be off depending on how matrix is ordered), which finds cycles of length n by solving a system of single steps. If the vector equals 0 then this means that we have found a cycle/orbit as we have found a set of points which is closed under evolution (we can take N steps and return to our original position, starting from any of the N points defining the cycle). The actual matrix, as with all Jacobians, tells us how the tangent space evolves. In terms of the multipoint shooting, this is the combination of N single step Jacobians. If you are on the cycle (i.e. no deviations, or components in the tangent space) which evolve

other than the velocity, which is mapped into the velocity at the new point. This is a quick and dirty explanation which is probably over simplifying, but the near-tautological explanation is: if you're on the cycle, then you don't get pushed away from the cycle due to your deviation from the cycle.

tl;dr It's the Jacobian of the multipoint shooting equation $x_n - f^t(x_{n-1})$.

2021-05-10 Predrag Talking about multishooting, the material around eq. (7.70) might be worth revisiting.

2021-05-09 Sidney Thank you Matt, it makes sense now, given the definition of the single step Jacobian it just sort of pops out. So, at this point I know how to get both the traditional orbit Jacobian matrix (which I am currently working on coding in) and the orbit Jacobian matrix in terms of the single step Jacobian (which I also know how to derive).

2021-05-09 Sidney At this point, I am trying to understand the block matrix form that can be generated by applying a permutation matrix defined by the circular Kronecker delta. What I do not understand, is:

What is the difference between the circular Kronecker delta, and the regular one?

2021-05-10 Predrag Regular one is defined on \mathbb{Z} (no restrictions), the circular one on C_n (periodic chain, so $\mod n$). (Re)read [ChaosBook appendix X.3 Discrete Fourier transforms](#).

2021-05-09 Sidney And I am also having difficulty deriving the appropriate permutation matrix. I want to try turning the two-cycle orbit Jacobian matrix (in terms of single-step Jacobians) into the block matrix form. The following is my (incorrect) derivation of the 4x4 permutation matrix. I have assumed that when the index for the circular Kronecker delta reads something like $4, j$ it is equivalent to $0, j$, as that would be equivalent to going to the end of the columns (index j) and then starting back at the beginning. By doing this I get: P is a $[2n \times 2n]$ permutation matrix. Defined through the circular Kronecker delta: $P_{k,j} = \delta_{2k-1,j}$, for a periodic orbit of length $n = 2$ P is

$$P = \begin{bmatrix} 1 & 0 & 0 & 0 \\ 0 & 0 & 1 & 0 \\ 1 & 0 & 0 & 0 \\ 0 & 0 & 1 & 0 \end{bmatrix}$$

(This is wrong)

What did I do wrong?

2021-05-10 Predrag By 'permutation matrix' you mean the one-step cyclic permutation r , or the shift matrix (7.7)? The circular Kronecker delta is just the $[n \times n]$ identity matrix. I leave it to Han and you to figure out what went wrong :)

2021-05-13 Han My Kronecker delta representation was wrong... (8.54) should be correct. I don't have a more compact way to write this permutation matrix. The permutation matrix for $n = 2$ is:

$$\begin{bmatrix} 1 & 0 & 0 & 0 \\ 0 & 0 & 1 & 0 \\ 0 & 1 & 0 & 0 \\ 0 & 0 & 0 & 1 \end{bmatrix}.$$

2021-05-10 Predrag To everybody - always number sites of length- n periodic chains (necklaces) as

$$\{0, 1, 2, \dots, n - 1\},$$

otherwise discrete Fourier transforms will go awkward on you.

2021-05-10 Predrag Regarding sect. 2.2 "Center of mass" puzzle:

Relevant Gallas papers are all in ChaosBook.org/library, for example ([click here](#)), with their names (always!) given by their BibTeX ID.

Predrag's unpublished 2004 drafts and calculations can be accessed by clicking on the link given there:

ChaosBook.org/projects/revHenon

There is no need to look at old drafts of papers, as the most of the relevant stuff is already included in that section, but the link includes some data files, orbit plots and programs that might be useful to Sidney as cross-checks on his calculations.

2021-05-12 Sidney Here are some notes from the last meeting: Any matrix can be written as a sum of projections into the different eigendirections. An anti-diagonal matrix, as well as the anti-diagonal matrix multiplied by sigma and its powers give the reflection matrix, and the reflection matrix across all axes.

Q What are these axes? A reflection matrix has two eigenvalues ± 1 (corresponding to either the symmetric, or antisymmetric subspace), and a projection operator can be constructed by subtracting out the opposite of the subspace you want to project onto. This projection operator can be applied to the left of the orbit Jacobian matrix to project it onto either the symmetric, or antisymmetric space. In this way, the orbit Jacobian matrix can be written as $\mathcal{J} = \mathcal{J}_- + \mathcal{J}_+$, it is worth noting that $\det(A + B) \neq \det(A) + \det(B)$. In the case of a linear map (where the fundamental fact still applies) the determinant of \mathcal{J}_{\pm} counts the number of time symmetric/antisymmetric orbits. Note that we need to apply the time symmetric boundary conditions in order to enforce time symmetric orbits.

Q2 Is this last statement correct? I have now updated my code to work with the scaled Hénon map. Actually, I just did the lazy thing of dividing all

values in all orbits by a . I also added a function to generate the (scaled) orbit Jacobian matrix, and I tried calculating its eigenvalues and vectors, it all seems to work, but I'm really not sure what I should be seeing for eigenvalues and vectors, I will paste my code below (I will past all of it, but it's mostly the same as before, just with a little added on the end): There is probably some extra code in there that just isn't being used, but hey, it's a work in progress. Update 2021-05-17: I have added this code to the williams/relax folder in the subversion, so I have now deleted the code here.

2021-05-13 Sidney With Han's help I was able to see the permutation matrix, and I was able to reproduce the Hill's formula "proof" for the specific case of $n=2$ (I use quotation marks because I only proved it for one case, and not all cases) I will probably keep thinking about how to generalize it, but I now feel better about applying Hill's formula to my orbit Jacobian matrix. I have been trying to work through the algebra with the reflection, and the corresponding projection matrices described in Han's most recent blog post. I understand qualitatively what's happening, effectively the projection operator is just the reflection operator with one of the eigenspaces subtracted out, with an additional weight that forces the identity $\mathbb{1} = \sum_i P_{A_i}$, this is a formula for a generic matrix. I cannot find anywhere in lectures, or textbooks where this is formalized, so I am not sure how the weights are constructed, but I'll keep looking at it.

2021-05-15 Matt I'll put a couple of responses here to hopefully help Sidney out. Response to questions in 2021-05-12 Sidney. It seems like the questions are with respect to the proceeding sentences but they are in different paragraphs so it is unclear to me if that is what you meant.

Q What are these axes? Is the question with respect to a specific system or just in general? If we're talking about reflection in D dimensional euclidean space then we can reflect over any $D - 1$ dimensional hyperplane, so I'm assuming it's talking about reflection where the eigenvectors are the normal vectors to these planes, so the hyperplane which is normal to each eigenvector can define a reflection so maybe this is what you're referring to?

Q2 Is this last statement correct? What is "the last statement"? The last statement before the question, the last statement of the previous paragraph...? Is it the following?

Note that we need to apply the time symmetric boundary conditions in order to enforce time symmetric orbits

To ensure that you get a time symmetric orbit then yes you have to impose boundary conditions which constrain you to that subspace. The unconstrained method (if variational in formulation) could possibly find these orbits, but there would be no guarantee.

Response to 2021-05-13 Sidney.

I understand qualitatively what's happening, effectively the projection operator is just the reflection operator with one of the eigenspaces subtracted out, with an additional weight that forces the identity $\mathbb{I} = \sum_i P_{A_i}$, this is a formula for a generic matrix. I cannot find anywhere in lectures, or textbooks where this is formalized, so I am not sure how the weights are constructed, but I'll keep looking at it.

Where "this" is formalized: The "weights" are simply normalization coefficients. The sum of the projection operators equaling the identity essentially says that the "full" space can be decomposed into projection subspaces, each of which has its own projection operator. I.e. each subspace is a component of the full space. Predrag formalizes the projection operators *a lot*; especially in his group theory stuff which this is directly related to.

For a reflection operator we can decompose

$$\sum P_{\pm} = \frac{1}{2}(\mathbb{I} \pm R) = 1/2(\mathbb{I} + \mathbb{I} + R - R) = 1/2(2\mathbb{I}) = \mathbb{I}.$$

For a symmetry subspace that can be broken into 4 subspaces, the normalization would be $1/4$, etc.

2021-05-23 Sidney Thank you to Matt for the explanation, I also have now attended the group theory lecture on projection operators (I've actually been thinking about this a good bit, but taking the time to condense my thoughts onto my blog is not one of my strong suits). Anyway, the projection operator formalism for matrices can be derived from the Hamilton-Cayley theorem:

$$\prod_i (\mathbb{M} - \lambda_i \mathbb{I}) = 0$$

In words, this is just the statement that a matrix satisfies its own characteristic equation. However, if we take one element out of the product, the RHS will no longer be zero:

$$\prod_{i \neq j} (M - \lambda_i \mathbb{I}) = \prod_{i \neq j} (\lambda_j - \lambda_i) \mathbf{e}_i$$

We can rearrange to get:

$$\mathbb{P}_j = \prod_{i \neq j} \frac{\mathbb{M} - \lambda_i \mathbb{I}}{\lambda_j - \lambda_i}$$

Which is the definition of the projection operators that Han used, I was also able to reproduce his results. I also found out an issue with my code for finding time-reversal symmetric orbits. I was not taking into account permutations, but that is an easy fix, that I hope to fix quickly.

When I have, I can create a bank of orbits appropriate to use with the orbit Jacobian matrix projected into the symmetric subspace using projection operators, I know how to construct this both by hand, and by code, I just need to implement it. I also need to go through chapter 15 in Chaos-book, as it gives good visualization of what the Hamiltonian Hénon map does. I will add my notes here when I have a chance, hopefully tonight, or tomorrow. I also think that I should explore the volume of the parallelepiped represented by the orbit Jacobian matrix. I could probably use a package for that, but what I'll most likely do is just use the fact that the determinant of a matrix is just the product of its eigenvalues:

$$\det A = \prod_i \lambda_i$$

Then take the absolute value. I can then check the volumes generated by different orbits.

2021-05-26 Sidney I reviewed the spatiotemporal cat derivation to see if I could extend the idea to the Hénon map, I think I have.

If we enforce the following restrictions, we can qualitatively derive the spatiotemporal Hénon map:

- Each site couples to its nearest neighbors
- Spatial and temporal coupling is of the same strength
- Invariant under spatial translations
- Invariant under spatial reflections
- Invariant under space time exchange

With these conditions our temporal Hénon (2.44), (15.11)

$$a = \phi_{t+1} + \phi_t^2 + \phi_t$$

generalizes to my proposal for the spatiotemporal Hénon

$$\phi_{n,t+1} + \phi_{n,t-1} + 2\phi_{n,t}^2 + \phi_{n+1,t} + \phi_{n-1,t} = a. \quad (15.12)$$

The factor of two comes from adding together two Hénon maps (one spatial and one temporal), following the derivation of the spatiotemporal cat. I need to try to read Gutkin and Osipov [9] [arXiv:1503.02676](#) to get a better idea of the derivation.

2021-05-28 Predrag I doubt you will find it in Gutkin and Osipov [9] - if you do, cite their words in detail here. The above argument is mine, from Gutkin *et al.* [8] and CL18 (kittens/ folder in this repository).

2021-05-28 Predrag Your spatiotemporal Hénon (15.12) looks OK to me, except maybe adding the maps for each direction of a d -dimensional lattice results in da on the RHS? In the spirit of [eq. \(80\)](#) in CL18.pdf?

How does your spatiotemporal Hénon compare to Politi and Torcini [12], sect. 9.3 Periodic orbits in coupled Hénon maps?

2021-05-27 Sidney Here is my attempt at looking at the eigenvalues, eigenvectors, and the determinants of the orbit Jacobian matrix. My orbit Jacobian matrix constructor only works with orbits of length 3 and above, this is because is row has three values in it that permute, and I'm not sure how to scale it down, will discuss this at the next meeting. I cannot tell anything about the eigen stuff so far, it seems almost random, however, the determinant values are each approaching an integer value, so maybe that is something.

Note: I removed the table here because it was wrong

I will hopefully rearrange some of these tables to group them by orbit in a later post, but for now, here is the "raw" data, let me know if anything appears.

2021-05-31 Sidney I'm not sure why, but the large table with all of the eigenvalues does not appear in the pdf version of the blog. I am not sure how to fix that, if anyone could let me know, that would be great. I still need to put it into a more readable format anyway. I also looked at [eq. \(80\)](#) in `CL18.pdf`, and it is the reason that I did not have $d * a$ on the RHS, the form of the spatiotemporal cat [eq. \(79\)](#), has only M not $2M$, which it would have if both sides were added (right?), I need to read up on the coupled maps, that will be something I do next (along with the better tables).

That would also say that '1100' is symmetric under time inversion.

2021-06-03 Sidney I want to try to take advantage of Hill's formula:

$$\text{Det}(\mathcal{J}_p) = \det(\mathbf{1} - \mathbb{J}_p) = (1 - \Lambda_p) \left(1 - \frac{1}{\Lambda_p}\right) = 2 - \Lambda_p - 1/\Lambda_p. \quad (15.13)$$

So, I need to calculate the eigenvalues for the scaled time-step Jacobian matrix, but first I need to find the form of the scaled time-step Hénon map [\(15.14\)](#)

$$\begin{aligned} x_{n+1} &= 1 - ax_n^2 + by_n \\ y_{n+1} &= x_n \end{aligned} \quad (15.14)$$

We scale $x \rightarrow \frac{1}{a}\phi$, $y \rightarrow \frac{1}{a}\varphi$, and the Hénon map becomes:

$$\begin{aligned} \phi_{n+1} &= a - \phi_n^2 + b\varphi_n \\ \varphi_{n+1} &= \phi_n \end{aligned} \quad (15.15)$$

Temporal stability of the n th iterate of the Hamiltonian Hénon map is ¹

$$M^n(\phi_0) = \prod_{m=n}^1 \begin{bmatrix} -2\phi_m & -1 \\ 1 & 0 \end{bmatrix}, \quad \phi_m = f_1^m(\phi_0, \varphi_0). \quad (15.16)$$

It is very important to understand the Floquet multipliers are invariant under all smooth coordinate changes, see [ChaosBook sect. 5.4](#), so they are not affected by this rescaling.. When we find the eigenvalues of this matrix they give contracting and expanding, we are interested in the expanding stability multiplier. There are three period 4 orbits: 1110, 1100, 1000, they have the following expanding Floquet multipliers:

2021-06-04 Predrag I do not seem to have handy list of the Hamiltonian $a = 6$ Hénon map Floquet multipliers. Floquet exponents for many $a = 1.4, b = 0.3$ orbits are listed in [ChaosBook table 34.2](#). I believe that [sect. 8.9 Han's Hénon map Hill's formula](#) also applies to the dissipative case, might be worth by repeating the derivation with $b \neq -1$, or at least checking it for a few short periodic orbits.

2021-06-11 Sidney I have read some of Wen's 2014 project [ChaosBook.org/projects/Wen14.pdf](#), I should take some notes and put them here.

2021-06-11 Sidney The Hill determinant should equal $2 - \Lambda_p - 1/\Lambda_p$ by Hill's formula (15.13), where Λ_p is the expanding eigenvalue of the time-step Jacobian for that orbit, see table 15.1.

2021-06-11, 2021-06-23 Sidney Table 15.2 lists the Hill determinants computed from the orbit Jacobian matrices. Comparing with table 15.1 period-4 Hill determinants, we see that the Hill's formula (15.13) is satisfied to high precision.

2021-06-12 Predrag It looks like you now have the correct Hill determinants. Their numbers agree with [ChaosBook Table 18.1](#); there are 6 period-5 orbits, and 9 period-6 orbits. The period-6 itineraries are not yet correctly assigned, fix that. The ones with even #'s of '1's are presumably the positive ones.

2021-06-12 Sidney I shall fix the itineraries for 6 cycles, and I'll add the itineraries of the other, shorter cycles later. Some were correct, and the negative determinants were in fact the odd number of 1s.

2021-06-13 Predrag Do include fixed points and the period 2 in table 15.2; might be helpful for understanding magnitudes of longer period Hill determinants.

¹Predrag 2021-06-04: Was

$$\begin{bmatrix} -2\phi_n & b \\ 1 & 0 \end{bmatrix}$$

The correct form is (2.27). Hence, with Sidney's "scaled Jacobian," the four cycle Floquet multipliers were all wrong.

2021-06-13 Predrag to Han and Sidney If you think of the Hénon map as a fat-tened parabola, then 0 fixed point has large positive slope (4 for the Ulam map), and 1 fixed point has small negative slope (-2 for the Ulam map). This explains the magnitudes, and should also determine the signs of Hill determinants in table 15.2.

However, either there is a - sign specific to Sidney's definition of the Hénon orbit Jacobian matrix, or Han and Predrag have to redefine both temporal cat and temporal Hénon orbit Jacobian matrix, so we do not pick up an extraneous '-' sign for odd period lattice states.

See also (5.284).

Fixing this is not essential, as we use only the absolute values of determinants in periodic orbit formulas.

2021-06-13 Sidney In the 2014 project paper by Haoran Wen, it is stated that for a range of a and b , the Hénon map is "structurally stable" and that means that the transport properties of the system have a smooth dependence on the parameters. And then it states that the lack of structural stability will result in the creation and destruction of infinitely many periodic orbits for any parameter change. Does that mean that a structurally stable system has relatively few bifurcations?

2021-06-13 Predrag It's a long story, starting with a wrong conjecture by Smale, but the answer is NO bifurcations for open intervals of system parameter values. Tends to be possible only for repellers, that is why you are working with Hénon $a > 6$ which has all possible binary symbolic dynamics cycles, and no bifurcations as you increase the parameter a .

Cat map has a finite grammar (is a "generating partition") for precisely $s=\text{integer} > 2$, but change s to an open interval of real values around -let's say- $s=3$, and infinity of cycle get created and destroyed for any finite change in s .

2021-06-13 Sidney So, at $a=6$ we achieve all binary symbolic dynamics, and anything more than that we still have all binary symbols? No creation or destruction? Is there a proof for this in the blog or somewhere else easily linkable to, that wouldn't take me days to digest?

2021-06-13 Predrag No, not $a = 6$ - that's just the closest integer value. Chaos-Book sect. 15.2 *Horseshoes* explains it, and -for example- Endler and Galas [6] say "This classification is independent of the control parameters. Orbits are specially interesting for $a > 5.69931\dots$, since beyond this value there is a complete Smale horseshoe [14] and all orbits are real."

2021-06-14 Sidney blogCats is being weird for me, it is only showing the most recently added parts, plus the table of contents, so right now when I build it, it only gives the dihedral groups chapter, even though all the include commands are not commented out.

2021-06-14 Predrag In `inclOnlyCats.tex` the uncommented line was

```
\includeonly{chapter/groups}
```

so `blogCats.tex` was doing what it should.

2021-06-14 Sidney to Predrag and Han I am having trouble defining the orbit Jacobian matrix for orbit length 1 and 2, this is because my code is designed to have a minimum width of 3 for the matrix, because there needs to be the terms for $\phi_{n+1}, \phi_{n-1}, \phi_n$, and I am not sure how to do that for 1 and 2 orbit lengths, should I just have the orbit repeat?

2021-06-14 Predrag The fixed points and period-2 lattices you can evaluate by hand, I believe. CL18 [sect. 1.4 Fundamental fact](#) and [sect. 2.4 Fundamental fact](#) evaluate the period-2 lattice orbit Jacobian matrices. If you understand how (18.150), (18.151), and CL18 (103) were derived, you will understand all such special cases.

2021-06-14 Sidney to Predrag and Han Is 6 digits of accuracy good enough? Is there a different method I should use? I am using the one from [Chaos-Book chapter 7 Fixed points](#) (the link is right here, I'll use that style of referencing in the future).

2021-06-18 Sidney to Predrag and Han I am trying to reproduce the projection operator analysis for D_6 symmetric lattice states and I am not really sure how to do that, which of Han's posts talks about the lattice states? As well, doesn't the projection analysis apply for D_n in general, not just specific lattice states?

2021-06-19 Sidney to Predrag and Han I tried to read Endler and Gallas [5] [2006 paper](#) (not the Endler and Gallas paper [6] that Predrag mentioned) because Predrag said that it explained two period 3, one period 4, and two period 6 values in my table 15.2, but I am not quite sure how the authors are getting their P polynomials, or their S polynomials, specifically, I am not sure where the a value comes in, because when I just try to expand their eq. (3) and regroup it into eq. (6), I could not, so I am very confused. What obvious thing am I missing?

2021-06-19 Predrag To "expand their eq. (3) and regroup it into eq. (6)" you need to know analytically all period-4 periodic points, do you know them? They claim that "the solution of this problem is trivial because ref. [4] contains the solution for arbitrary a and b."

However, I was referring to the Endler and Gallas [6] Table 1. The invariant quantity that they associate with a periodic orbit is the orbital sum (2.14), the sum over the periodic points, while the Hill determinant involves various sums over values of fields raised to various powers. You will immediately note that the cases that have integer orbit sums correspond to your integer-valued Hill determinants. They had no reason to

think of Hill determinants, so that would be a major reworking of their paper(s); I do not think you want to do that.

2021-06-20 Sidney to Predrag and Han Oops

I agree that a major reworking is probably not in the cards, I will go back to trying to understand orbit Jacobian matrices for the fixed point, and period 2 orbits. Endler and Gallas [4, 5] look exceptionally cool, I'll give them a whirl.

2021-06-23 Sidney I worked through both Endler and Gallas papers [4, 5], as much as I could. Here is what I came up with: in ref. [5] the two important equations are $P_k(x)$ and $S_k(\sigma)$, where $S_k(\sigma)$ is found through manipulating the (scaled) Hénon map and σ is the sum of all points in the cycle, $P_k(x)$ is defined as

$$P_k = \prod_{\ell=1}^k (x - x_\ell),$$

where x_ℓ is the ℓ th orbit point. The algorithm is simple: construct $P_k(x)$ by expanding the product and putting each coefficient in terms of σ , then use $S_k(\sigma) = 0$ to determine how many unique orbits of length k and 2. what values σ can take, then combine with $P_k(x)$ to solve for each orbit point. I will work two examples, first an orbit of length 1:

$$\sigma = x_1$$

$$P_1 = x - \sigma$$

$$x_{t+1} = a - x_t^2 - x_{t-1} = x_1 = a - x_1^2 - x_1$$

Or

$$2\sigma + \sigma^2 - a = 0 = S_1(\sigma)$$

As this is a quadratic equation, we know that there are two different fixed points, and we can solve for them directly via $S_1(\sigma) = 0$, now for an orbit of length 2:

It is useful to first state that $a = 2x_2 + x_1^2 = 2x_1 + x_2^2$ by the Hénon map, and $\sigma = x_1 + x_2$

$$P_2(x) = (x - x_1)(x - x_2) = x^2 - \sigma x + x_1 x_2 = x^2 - \sigma x + \frac{1}{2}a - \frac{1}{2}\sigma^2 - \sigma$$

If we subtract the two a equations we get

$$0 = 2x_2 - 2x_1 + x_1^2 - x_2^2 = 2(x_2 - x_1) + (x_1 + x_2)(x_1 - x_2)$$

so

$$S_2(\sigma) = \sigma - 2 = 0$$

From this we know that there is one 2 cycle and this can be solved by solving for σ and solving for the roots of $P_2(x)$. There's a lot of algebra here, but I am sure there is some number theory trick that can be used that I am unaware of. I am also a little confused by the factorization (2.16)

$$S_k(\sigma) = C_k^2(\sigma)D_k(\sigma)N_k(\sigma),$$

I think that it is a statement that the polynomial $S_k(\sigma)$ can be decomposed into polynomials that each give roots for the Chiral, Diagonal, and Non-diagonal orbits respectively. So it should be a way to count the number of each type of orbit. However, I am not sure how to tell the difference between any of them, I sort of understand that C_k has to be squared, and that could distinguish it, but I'm really not sure how to tell them apart.

Q16.1 Any suggestions for this?

A16.1 **Predrag 2021-07-04** Work through papers, they are clear and pedagogical

I have also figured out how to get the determinants of period 1 and period 2 cycles, I updated table 15.2 to include them. You'll notice that the determinant for $\bar{0}$ and $\bar{1}$ were negatives of each other up to six decimal places, neat. 10 was the integer -12 up to six decimal places, again, neat.

Q16.2 How do I calculate eigenvalues for periods 1 and 2?

A16.2 Here is how:

Period 1: For the fixed points, I get

$$\phi_{0,1} = -1 \pm \sqrt{1+a} \rightarrow -1 \pm \sqrt{7} \quad (15.17)$$

$\mathcal{J}_{0,1}$ are $[1 \times 1]$ matrices

$$\phi_{t+1} + \phi_t^2 + \phi_{t-1} = a$$

$$F[\phi] = 2\phi + \phi^2 - a = 0,$$

Evaluating the Hill determinants (7.6) for both fixed points:

$$\mathcal{J}_{0,1} = 2(1+\phi), \quad \text{Det } \mathcal{J}_{0,1} = \pm 2\sqrt{1+a} \rightarrow \pm 5.2915026, \quad (15.18)$$

in agreement with the numerical estimates of table 15.2. The Hill determinants of the two fixed points are negatives of each other.

Period 2: The periodic points in the 10 orbit are (I did it on paper, do not want to reproduce it here):

$$\phi_{1,2} = 1 \pm \sqrt{a-3} \rightarrow 1 \pm \sqrt{3} \quad (15.19)$$

Table 15.1: Hill determinants for the Hamiltonian $a = 6$ Hénon map, period-4 lattice states, computed from time-evolution side of the Hill's formula (15.13). The pesky overall 'sign' presumably means we have to change the overall sign in the **definition of orbit Jacobian matrix \mathcal{J} everywhere**.

Orbit	Hill determinant
1110	105.697960425014
1100	-576.000010077746
1000	1046.301985671792

\mathcal{J}_{10} follows

$$\begin{aligned} F[\phi]_1 &= 2\phi_2 + \phi_1^2 - a = 0 \\ F[\phi]_2 &= 2\phi_1 + \phi_2^2 - a = 0, \\ \mathcal{J}_{10} &= \begin{bmatrix} 2\phi_{01} & 2 \\ 2 & 2\phi_{10} \end{bmatrix}. \end{aligned} \quad (15.20)$$

Hill determinants are *symmetric polynomials* in lattice fields $\{\phi_1, \phi_2, \dots, \phi_n\}$, which are, by construction, all *prime cycle p invariants*. The orbital sum (2.14) is one example. Another one is (15.21).

In case at hand,

$$\text{Det } \mathcal{J} = 4(\phi_{01}\phi_{10} - 1) = 4(3 - a) \rightarrow -12. \quad (15.21)$$

The Hill determinant is *exactly* 12, up to the annoying overall sign that **cries out** for a *redefinition* of orbit Jacobian matrix.

2021-06-25 Sidney With the above analytic calculations, I feel very confident in stating that my code is accurate up to 6 decimal places.

Q16.3 Is there a way to rigorously prove that the code is accurate up to 6 decimal places?

Q16.4 Is this worth doing if it exists?

A16.4 **Predrag 2021-07-04** No.

Q16.5 What do these values mean? An integer Hill determinant should mean something right?

A16.4 **Predrag 2021-07-04** It is well explained in papers you have been reading. Integer Hill determinant is a historical accident, due to our (arbitrary) choice $a = 6$. But it gave Gallas and collaborators a clue that something is going on. As does (15.26). Be Gallas.

And finally, I was thinking about the multidimensional Hénon map. Since this is not a physical problem, there is no "physical" definition about what makes a map "Hénon map" like, so it would be good to stick to the mathematical requirement of the folding being linearly related to b , so I was

Table 15.2: Hill determinants for the Hamiltonian $a = 6$ Hénon map, with correct symbolic dynamics. Indicated in red are values presumably explained by Endler and Gallas [6].

Period 1	
0	5.291502844
1	-5.291502494
Period 2	
10	-12.000000720
Period 3	
110	-53.914854639
100	133.914853323
Period 4	
1110	-105.697960425
1100	576.000010077
1000	-1046.301985671
Period 5	
11110	-388.996791481
11100	591.500599893
11010	712.689732105
00101	-768.203977660
00011	-4443.524089969
00001	7608.534459743
Period 6	
111110	-1045.3849327
111100	3899.9387739
111010	1092.9103354
111000	-4786.6149478
101000	5135.6190985
110100	-6396.0000670
001011	-6395.9999673
110000	32220.0609406
100000	-54576.5295457

thinking that for the multidimensional map, the Hénon-ness could be satisfied if the appropriate time Jacobian matrix determinant would be $-b^d$, unfortunately, I don't know how to define the correct time Jacobian.

2021-07-03 Sidney I have not had much time outside of my internship lately, so I haven't done much. However, I did make an attempt at showing that the eigenvalues of the orbit Jacobian matrix are coordinate-choice independent. It did not go well. First, I must remember that

$$\mathcal{J}_{ij} = \frac{\delta F[\phi]_i}{\delta \phi_j},$$

evaluated at a lattice state ϕ_M

$$F[\phi_M] = 0.$$

This gives a problem when I try to repeat the proof done for time-step Jacobians, because I get

$$\mathcal{J}'(\phi'_M)_{ij} = \Gamma(0)_{ik} \mathcal{J}_{kl} \Gamma^{-1}(\phi_M)_{lj}, \quad (15.22)$$

which means that I cannot cancel the Γ s in the determinant. So, I have failed to prove anything.

2021-06-24 Predrag Wow, I did not expect $\text{Det } \mathcal{J}_0 = -\text{Det } \mathcal{J}_1$! But Sidney's (15.17) nails it.

2021-06-13 Predrag Note the '[.91485](#)' decimal digits for period 3. Those are presumably explained by Endler and Gallas [6] analytic expressions, see their Table 1. For us they mean that Sidney's code is accurate to ca. 6 significant digits.

The 1100 Hill determinant is integer $576 = (6 \times 4)(-6 \times -4)$, (see (15.26)). Explain this factorization.

(15.20) explains 01 Hill determinant=12, but do you have an argument that this is the symmetry reduced Hill determinant= $2\sqrt{3}$ squared?

Show that 001011 and 001101 Hill determinants are $(\text{integer})^2$ (are they?).

This is also a helpful check on the time-inversion factorization formulas Han and I are trying to establish.

2021-07-06 Predrag Regarding Sidney's attempt (15.22) to prove that the eigenvalues of the orbit Jacobian matrix \mathcal{J} are coordinate-choice independent:

The time-evolution Jacobian matrix in general has a different left $\Gamma(\phi_t)_{ik}$ and right $\Gamma^{-1}(\phi_0)_{lj}$ [$d \times d$] matrices, they line up only for the period value $t = n$, so the periodic boundary condition will have to be a part of your proof.

How the time-periodicity is built into orbit Jacobian matrices is explained by (18.341). From that you can perhaps see how the periodicity is imposed on the coordinate-change Jacobian [$nd \times nd$] matrices $\Gamma(X)_{lj} \dots$

See whether you can prove it first for the Hill determinant $\det \mathcal{J}$?

To get it for individual eigenvalues, you'll have to write the eigenvalue, eigenvector equation for the orbit Jacobian matrix \mathcal{J} , then apply coordinate transformation $\Gamma(X)_{lj}$.

2021-07-06 Sidney I have considered showing that the Hill determinant is coordinate invariant, but I think that's just a matter of mentioning that Jacobian matrix has coordinate invariant eigenvalues. I'll formalize that in a later post (most likely the next one).

I have also come up with a proof that the \mathcal{J} has the same set of eigenvalues evaluated at every point in the orbit, I suspect that there is a proof for the eigenvectors, but I don't know how to do it, again, will formalize on my next post.

2021-07-07 Predrag The orbit Jacobian matrix \mathcal{J} is global, a property of the entire lattice state, so I do not understand " \mathcal{J} has the same set of eigenvalues evaluated at every point in the orbit."

2021-07-06 Sidney I am not sure what was meant by "do you have an argument that this is the symmetry reduced Hill determinant= $2\sqrt{3}$ squared?". I assume this is something either from the group theory course, or blog which I have not yet gone over, but does this mean that I should look for some symmetry reduction of a matrix whose Hill determinant has the value $2\sqrt{3}$?

2021-07-07 Predrag Basically, yes. I'm referring to C_n^2 term in (2.15), $\sqrt{\zeta_{top}(t^2)}$ in (4.149), etc., throughout the time-reversal discussions in the blog.

Endler and Gallas [5] eq. (9) and Table 1 has

$$D_{0011} = \sigma, \quad P_{0011} = (x^2 - a)^2, \quad (15.23)$$

There are two period 6 diagonal orbits

$$D_6 = \sigma^2 + 4\sigma - 4a, \quad \text{orbits } 000111 \text{ and ??}, \quad (15.24)$$

but 000111 of figure 2.1 (c) belongs to N_6 messy polynomial eq. (14).

My reasoning is that due to the $\{1, s\}$ time-reversal symmetry, any $t < 0$ temporal lattice site can be mapped into $t > 0$ by time reversal s , so the D_∞ 'configuration' fundamental domain is the $t \geq 0$ temporal half-lattice. Full lattice periodic states Hill determinants for orbits such as 01, 0011 in table 15.2 are then (that's not quite right) squares (twice the relative periodic orbit period) of the fundamental domain orbit Hill determinants, as in example 4.11 D_1 factorization.

But there no reason why you should know that, Han and I are still working it out, will have more concrete suggestions for the Hénon case once we understand it better.

2021-06-13 Predrag If you think of the Hénon map as a fattened parabola, then 0 fixed point has large positive slope (4 for the Ulam map), and 1 fixed point has small negative slope (-2 for the Ulam map). This explains the magnitudes, and should also determine the signs of Hill determinants in table 15.2.

2021-07-07 Predrag Endler and Gallas [5] eq. (13) presumably explains the integer valued pair of period-6 orbits in table 15.2:

$$C_6 = \sigma - 2, \quad \text{orbits } 110100, 001011, \quad (15.25)$$

2021-06-25 Sidney My numerical values for period 4 eigenvalues:

1000	6.77624515, -7.4374406, -4.23778399, $-\sigma$,
1110	-2.39080489, 1.58070478, 5.70907942, σ ,
1100	6, 4, -6, -4

(15.26)

2021-07-04 Predrag to Sidney and Han What's up with two distinct orbits $\overline{1000}$ and $\overline{1110}$ in (15.26), with different Hill determinants in table 15.2, sharing the eigenvalue $\sigma = 2\sqrt{6} = 4.89897947$ (see (15.27))? Well... when two numbers agree to 9 significant digits, it's usually a mere numerical coincidence. Happens 1/1 000 000 000 of time :)

2021-07-25 Predrag Endler and Gallas [4] have all period-4 periodic points:

$$S_4(\sigma) = \sigma(\sigma^2 - 4a) \quad (15.27)$$

The the 2-points on diagonal $\overline{0011}$ of figure 2.1 (b) has $\sigma = 0$. For $a = 6$ the $\overline{1000}$ has $\sigma = -2\sqrt{6} = -4.898979485566356$ and $\overline{1110}$ has $\sigma = 2\sqrt{6}$, which happens to be their common eigenvalue in (15.26). Endler and Gallas [5] also define

$$\begin{aligned} \alpha &= \sqrt{6 + 2\sqrt{6}} = 3.3013602478 \\ \beta &= \sqrt{6 - 2\sqrt{6}} = 1.04929524655. \end{aligned} \quad (15.28)$$

and the corresponding orbital equations

$$\begin{aligned} P_{1000}(x) &= (x^2 - \alpha^2)(x + \sqrt{6})^2 \\ P_{0111}(x) &= (x^2 - \beta^2)(x - \sqrt{6})^2 \\ P_{0011}(x) &= (x^2 - 6)^2. \end{aligned} \quad (15.29)$$

2021-07-25 Predrag For a 4-cycle p , the Hill determinant of the orbit Jacobian matrix (3.85) is the polynomial

$$\text{Det}(\mathcal{J}_p) = 2^2 [2^2 x_0 x_1 x_2 x_3 - x_0 x_3 - x_1 x_2 - x_2 x_3 - x_1 x_0], \quad (15.30)$$

not involving the orbit sum σ , not in the form currently written. Looks like one should rescale ϕ_i (again?).

The quadratic part is a sum of sequential pairs. There are two kinds of ways in which it can be time-reversal invariant:

- 2 on diagonal x_0x_2 fixed, $x_1 = -x_3$

$$\text{Det}(\mathcal{J}_p) = 2^2 [-2^2 x_0 x_1^2 x_2], \quad (15.31)$$

- none on diagonal, $x_0 = -x_1, x_2 = -x_3$

$$\begin{aligned} \text{Det}(\mathcal{J}_p) &= 2^2 [2^2 x_0^2 x_2^2 + 2x_0 x_2 + x_2^2 + x_0^2] \\ &= 2^2 [(2x_0 x_2)^2 + (x_0 + x_2)^2], \end{aligned} \quad (15.32)$$

At the first glance, Hill determinants do not seem to factorize, but the time reversal symmetry assumptions (and signs) have to be checked.

2021-07-25 Predrag Some while-falling-asleep reflections on orbits $\overline{1000}$ and $\overline{1110}$ in (15.26), sharing the eigenvalue $\sigma = 2\sqrt{6}$:

If an orbit has a symmetry H , all of its lattice states (periodic points) presumably live in an invariant subspace \mathcal{M}_H . An example is Kuramoto-Sivashinsky, where orbits that start in the antisymmetric subspace stay in this lower dimensional subspace.

Example 4.11 possibly explains this for binary symbolic dynamics (note: there our '0, 1' are denoted '−, +'). In table 4.5 the pair $\{-+++,\text{+---}\} \rightarrow$ fundamental domain $\overline{0011}$, i.e., we are back to our perennial problem of mistaking internal dynamical symmetries for time reversal, not sure this symmetry reduction is the one we need.

My hunch is that *all* short orbits live in invariant subspace(s), with $\overline{110100}$ and $\overline{001011}$ being the first exceptions.

Orbit $\overline{1000}$ is like figure 2.1 (c), placed in the upper right corner, with no points on the diagonal. Orbit $\overline{1110}$ is in the lower left, also symmetric across the diagonal. Endler and Gallas [5] plot them in their fig. 2. According to J. Montaldi table 4.4, the D_4 permutation representation irreps are $A_0 + B_1 + E$.

In the 2-dimensional invariant subspace E (?) orbits $\overline{1000}$ and $\overline{1110}$ are period-2 orbits (I'm guessing, have not checked) and their eigenvalues might be related, like, for example, $\bar{0}$ and $\bar{1}$ in table 15.1. Or there is shared eigenvalue in one of the 1-dimensional subspaces. Remember the z -axis dynamics for the Lorenz flow? Read [ChaosBook Desymmetrization of Lorenz flow](#) (here example 4.4) to understand that not every linearly independent space is invariant under time dynamics.

However, the orbit Jacobian matrix \mathcal{J} is always a perturbation in the full \mathcal{M} , thus 3 other eigenvalues, all different. I would be happier if there

were only 2 distinct eigenvalues per each cycle, but you cannot have everything. At least, not if you don't try.



example 4.28
p. 285



example 4.4
p. 272

Basically, also for nonlinear systems orbit Jacobian matrix is linear, so irreps of the symmetry group do block-diagonalize it. A stronger claim; symmetry can restrict entire orbits to flow-invariant subspaces of the phase space \mathcal{M} , even for nonlinear flows. Then some of the orbit Jacobian matrix eigenvectors point into that subspace.

2021-07-25 Predrag Combination $r + r^{-1}$ in (15.10) commutes with σ , and σ conjugacy reverses \mathbb{X}

$$\begin{aligned} \sigma \mathcal{J} \sigma &= r + 2\sigma \mathbb{X} \sigma + r^{-1} \\ &= \begin{bmatrix} 2x_{n-1} & 1 & 0 & 0 & \dots & 0 & 1 \\ 1 & 2x_{n-2} & 1 & 0 & \dots & 0 & 0 \\ 0 & 1 & 2x_2 & 1 & \dots & 0 & 0 \\ \vdots & \vdots & \vdots & \vdots & \ddots & \vdots & \vdots \\ 0 & 0 & \dots & \dots & \dots & 2x_1 & 1 \\ 1 & 0 & \dots & \dots & \dots & 1 & 2x_0 \end{bmatrix} \quad (15.33) \end{aligned}$$

Next, evaluate Hill determinant with a projection operator inserted. Should factorize?

$$\begin{aligned} \text{Det } \mathcal{J} &= \text{Det}(r + 2\sigma \mathbb{X} \sigma + r^{-1}) \\ &= \text{Det}(r + 2\mathbb{X} + r^{-1})(P_+ + P_-) \\ &= \text{Det}(P_+ \mathcal{J}) \text{Det}(P_- \mathcal{J}) \quad (15.34) \end{aligned}$$

2021-08-04 Han Yes! Read the text starting about (18.364) to see how that works.

2021-08-08 Sidney I have been out of the loop for awhile, so what I'm going to try to do is read up on what I missed, and take notes on that, and write it up in my blog, and then continue on with the work here, hopefully that can all happen in a timely fashion.

2021-08-20 Sidney I have been reading LC21 and other parts of Han's blog and taking notes as appropriate, as this already exists in this blog, I'll only talk about it when I can add something. Anyway, I've been thinking about the time reversal pairs in the temporal Hénon. In the case of 110100 and 001011, the determinants of the orbit Jacobian matrices were equal and they are a time reversal pair. I think that maybe we can try to make a global statement about the relative weights of time reversal pairs. So, here is the first step in trying to see that.

First, I will remind everyone of the definition of the orbit Jacobian matrix:

$$\mathcal{J}_{ij} = \frac{\partial F[\mathbf{X}]_i}{\partial \phi_j}$$

This is defined for any lattice state: $\mathbf{X} = [\phi_1, \phi_2, \dots, \phi_n]$, i defines the lattice point which is considered the "current" location, ie. for the temporal Hénon, $i = 1$ says that the first lattice state is what we should use for n^{th} in time, instead of $n + 1$ or $n - 1$. j defines the lattice point which the defining equation will be differentiated with respect to. By definition, any periodic orbit can be cyclically permuted and still be the same periodic orbit. When this happens the indices in the lattice state get shifted, say $1 \rightarrow 3$. In this case, the indices in the orbit Jacobian matrix must be redefined in accordance to the shift, if we want to know how the "original" orbit and the "permuted" Jacobians relate. As both indices in the definitions of the orbit Jacobian matrix depend on the same index definition for the lattice state, when the lattice state is permuted by some number of steps p the indices in the definition for orbit Jacobian matrix change as follows

$$i \rightarrow \alpha \equiv i + r, \quad j \rightarrow \gamma \equiv j + r. \quad (15.35)$$

In fact, if we ignore the rules for "sameness" of orbit and say that the order of the lattice state can be arranged arbitrarily, the indices in the orbit Jacobian matrix definition are mapped as follows: $i \rightarrow \alpha \equiv f(i)$ and $j \rightarrow \gamma \equiv f(j)$, where $f(x)$ is some one-to-one map appropriate for the rearrangement applied to the lattice state. If we define a "diagonal entry" of the orbit Jacobian matrix as when the difference between the indices is zero, we can construct two indicator functions:

$$\Delta_{ij} = i - j$$

$$\Delta'_{\alpha\gamma} = \alpha - \gamma = f(i) - f(j)$$

As can be seen, when $i = j$ both indicator functions are zero, indicating that a diagonal entry in one index space, is a diagonal entry in the other index space. In fact, as $f(x)$ is one-to-one by definition there are an equal number of diagonal entries in each index space. And finally, as the definitions of the orbit Jacobian matrix in either index space are isomorphic:

$$\frac{\partial F[\mathbf{X}]_i}{\partial \phi_j} \simeq \frac{\partial F[\mathbf{X}]_\alpha}{\partial \phi_\gamma}$$

and as the individual lattice values are unchanged by the rearranging, not only are there an equal number of diagonal entries in each index space, but the same values exist in each. Thus, the (unordered) set of diagonal orbit Jacobian matrix entries is invariant under one-to-one index mappings, ie. arbitrary rearrangements of lattice state order.

This shows that under time reversal, the diagonal entries of an orbit Jacobian matrix are preserved, even if the orbit is not time reversal symmetric.

CHAPTER 15. SIDNEY'S BLOG

I may have made a mistake here, either in the math, or just basic notation, please let me know!

2021-08-23 Predrag I am not sure about this proof, discuss it with Matt and Han first.

Here how I think about (as always, I might be wrong): The beauty of our spatiotemporal, global approach is that every lattice state (ie, a solution of the defining equations of a particular problem) is a fixed point in its high-dimensional phase space. So, if you can show that the eigenvalues of a fixed point problem in $1, 2, 3, \dots, 63\,873, \dots$, dimensions do not change under a smooth nonlinear change of fields, you have proven what we need to prove.

If you understand it 1 or 2 dimensions, you probably understand it any number of dimensions.

Reflection symmetry (sometime known as time reversal) comes in (see [ChaosBook sect. 8.3](#)) as an additional set of relations between the stability eigenvalues.

2021-08-23 Sidney At this point, I have pretty much settled on wanting to work on the mathematical physics end of plasma physics. Specifically with turbulence, and nonlinear aspects of fusion and astrophysics. But I quite frequently worry that I will miss out a great deal by not working with quantum, especially path integrals and field theories. I know that you transitioned from high energy to nonlinear dynamics and turbulence. How did you find that? And how analogous is the math? I know that for awhile there was quite a bit of overlap between turbulence and QFT methods, but that seems to have fallen by the wayside.

2021-08-23 Predrag Mhm. My impression is that [much is going on](#), for example [here](#), and you just happen to be on the most fearless and inventive team in the field.

Don't be [Fritz Haake](#) (who accepted the invitation on 30 May 2011). He, who hesitates, is lost.

2021-08-25 Predrag I keep saying that the proof of the invariance of orbit Jacobian matrix \mathcal{J} eigenvalues for a nonlinear but nonsingular redefinition of fields ϕ_i is a variant of [ChaosBook sect. 5.4 Floquet multipliers are metric invariants](#), but I'm not getting traction on that from anyone.

In today's group meeting, I interpreted Sidney's proof of the invariance of orbit Jacobian matrix \mathcal{J} eigenvalues (15.35) as a permutation matrix on site labels, made a claim that any other permutation than D_n cyclic ones or their reversals will change the value of temporal Hénon Hill determinant, and challenged Sidney to compute Hill determinant for other permutations, see that the resulting determinant is different.

But for temporal Hénon I am probably wrong, as Endler and Gallas [5] prove that all their polynomials depend only on the orbital sum (2.14).

I believe that will not be true for the ϕ^4 theory (3.21) on d -dimensional lattice (5.115), with the Hill determinant of the same form (2.9), see sect. 5.7.3 *Classical ϕ^4 lattice field theory*, because in that case bilinear terms in lattice fields arising from (18.364) cannot be eliminated.

Sidney could easily write the program to find all of its 3^n lattice states for small n ; it is mostly a replacement of the quadratic function in his temporal Hénon Biham-Wentzel program by a cubic one.

2021-08-26 Sidney I mostly tried to write the proof to see if I could show that the diagonal values were an invariant set for rearrangements of the orbits, because if I could, I could say something about the equal determinants of the length 6 time reversal pairs I calculated for the temporal Hénon. I need to look more at other cases.

As well, I tried again to look at varying the proof from [ChaosBook](#) sect. 5.4 *Floquet multipliers are metric invariants*. But I run into the issue that the fixed point condition for the map which is having its derivative taken for the orbit Jacobian matrix, is different than the fixed point condition for the map having its derivative taken for the time-step Jacobian. Namely, from CL18 eqn 13, it is stated that $F[\Phi] = 0$ is the fixed point condition, NOT $F[\Phi] = \Phi$ which would be required for the proof from Chaosbook to be carried out in the same way. I also tried to take Predrag's suggestion of looking directly at permutation matrices, and then taking the determinant to show that everything is invariant around an orbit. I tried the shift, i.e., the permutation matrix (3.32)

$$r_{ij}^s = \delta_{i,j+s},$$

shifting each entry backwards by s steps. Shifting the n -dimensional vector $F[X]$

$$f[\varphi] = F[r^{-s}X]$$

a function of the n -dimensional lattice state vector X , such that the orbit Jacobian matrix

$$\mathcal{J} = \frac{\partial f[\varphi]}{\partial \varphi} = \frac{\partial r^s F[r^{-s}X]}{\partial r^{-s}X}.$$

And after this point I am stuck, mostly because I am not sure if this is right, and it's weird dividing by a matrix, although, I probably need to take the derivative of the change of coordinates that I defined.

2021-08-26 Sidney For the one-dimensional case (eqn 5.15 in Chaosbook) the final conclusion relies on the fixed point condition being $f(x) = x$. However, $F[X]$ is effectively defined as $f(x) - x$. This causes a problem whether we're looking at scalars or vectors.

I thought a little more about the permutation proof, r^s is not position dependent, so there is no weird Jacobian shenanigans, using the chain

rule we should just get

$$\mathcal{J} = \frac{\partial f[\varphi]}{\partial \varphi} = r^s \frac{\partial F[X]}{\partial X} r^{-s}.$$

I think that this is right, then we can just move around the determinant by the permutation property. I should think more how to relate this to eigenvalues.

2021-08-27 Sidney What is this “square root” thereof thou speaketh?

2021-08-05, 2021-08-28 Predrag It's been fuzzy all along, but roughly speaking it is this: Stability (at least, temporal evolution stability) is multiplicative along an orbit, so if you go twice as many time steps (lattice sites in our perspective), the stability gets squared.

Conversely, in going from period $n = 2m$ (18.356) D_8 symmetric orbit $\phi_1\phi_2\phi_3\phi_4|\phi_4\phi_3\phi_2\phi_1|$ to the orbit Jacobian matrices evaluated on the m -dimensional $\phi_1\phi_2\phi_3 \cdots \phi_m$ subspaces (18.359), the stability gets square-rooted. There are many little things that I do not understand about how this works in detail that you could easily work out

1. What type from the list (4.19)-(4.22) is each of the short temporal Hénon orbits that you have? Han tells me my guesses (15.36) to (15.38) are wrong.
2. What is its Hill determinant? Which block of orbit Jacobian matrices (18.359) goes with which orbit? What are its eigenvalues, the symmetries of eigenvectors?
3. What is the relation between our (4.19)-(4.22) and Endler and Gallas [5] symmetry classifications?

Inspecting Endler and Gallas [5] fig. 2: the Hénon period-4 orbits, $n = 2m$, are of form

$$\overline{1000} : \quad \boxed{\phi_0} \underline{\phi_1} \boxed{\phi_0} \phi_1, \quad (15.36)$$

and

$$\overline{1110} : \quad \boxed{\phi_0} \underline{\phi_1} \boxed{\phi_2} \phi_1, \quad (15.37)$$

with symmetric-antisymmetric subspace dimensions $d_+ = 3$, $d_- = 1$, and

$$\overline{1100} : \quad \underline{\phi_2} \underline{\phi_1} |\phi_1 \phi_2|, \quad (15.38)$$

with symmetric-antisymmetric subspace dimensions $d_+ = 2$, $d_- = 2$.

I leave it to the gentlepersons of this blog to compute the $[1 \times 1]$ Hill determinants $\text{Det}(\mathcal{J}_-)$ for $\overline{1000}$ and $\overline{1110}$ in (15.26), show their sole eigenvalue is $\pm\sigma = 2\sqrt{6}$.

8/29/2021 Sidney I am very confused. First off, I found out that I don't know how to block-diagonalize matrices using symmetry operators, I tried to recreate the CO_2 example in the group theory notes, but to no avail. So I turned to trying to show Hill determinants $\text{Det}(\mathcal{J}_-)$ for $\overline{1000}$ and $\overline{1110}$ in (15.26) is, $\pm\sigma = 2\sqrt{6}$. But I am missing a factor of two, and I don't know why. I did the following:

The symmetry is an "even" reflection as defined in (3.174), so the symmetry matrix is

$$\sigma = \begin{bmatrix} 1 & 0 & 0 & 0 \\ 0 & 0 & 0 & 1 \\ 0 & 0 & 1 & 0 \\ 0 & 1 & 0 & 0 \end{bmatrix}$$

From here, I can construct projection operators for the symmetric and anti-symmetric subspaces of this operator:

$$P_+ = \frac{1}{2}(I - \sigma) \quad P_- = \frac{1}{2}(I + \sigma)$$

Taking the trace of each of these operators gives me the dimension of each of these subspaces: $d_+ = 3$, $d_- = 1$. Now, let's look at $\overline{1000} \phi_0, \phi_1, -\phi_0, \phi_1$. In this case the (incorrect! - see (15.40)) orbit Jacobian matrix is

$$\mathcal{J} = \begin{bmatrix} \phi_0 & 1 & 0 & 1 \\ 1 & \phi_1 & 1 & 0 \\ 0 & 1 & -\phi_0 & 1 \\ 1 & 0 & 1 & \phi_1 \end{bmatrix} \quad (15.39)$$

$$\sigma\mathcal{J} = \begin{bmatrix} \phi_0 & 1 & 0 & 1 \\ 1 & 0 & 1 & \phi_1 \\ 0 & 1 & -\phi_0 & 1 \\ 1 & \phi_1 & 1 & 0 \end{bmatrix}$$

The trace of $P_- \mathcal{J} = \frac{1}{2}(\mathcal{J} - \sigma\mathcal{J})$ should give me the eigenvalue for the asymmetric subspace, this gives ϕ_1 which equals $\sqrt{6}$ from Endler and Gallas [5], which is missing a factor of -2, I have no idea what's wrong (since corrected in (15.40)).

2021-08-29 Predrag Getting it up to factor of 2 is a triumph! The rest is work :) Have you tried cross-checking formulas? One cannot trust anyone, one always makes sure that the formulas are as you yourself have derived them. I would not be surprised if there should be $2\phi_j$ along the diagonal...

In this context: (3.20) and the footnote next to it will amuse you.

A small aside - when you refer to an equation, like (3.174), refer to it, rather than having the reader try to figure out where it came from. It's much faster for everyone if you just do it.

A much less important thing at this stage: The macros such as σ [backslash Refl] are here for a reason - as the research progresses we often find that a better notation exists in literature. That can be fixed by editing a few characters in *siminos/inputs/defsSpatiotemp.tex*.

2021-08-29 Predrag to Sidney Here is a request that requires minimal work - you have it in your code or data sets: Plot the values of lattice state fields for the 6 lattice states of table 2.3 and figure 2.3 in the same format as figure 3.13 (b).

Note - temporal Hénon fields can be positive or negative. I'm particularly interested to see if any of your lattice states are antisymmetric under reflection across ϕ_0 .

2021-09-01 Sidney In my last post I used the incorrect definition (15.39) of \mathcal{J} , the correct definition is

$$\mathcal{J} = \begin{bmatrix} 2\phi_0 & 1 & 0 & 1 \\ 1 & 2\phi_1 & 1 & 0 \\ 0 & 1 & -2\phi_0 & 1 \\ 1 & 0 & 1 & 2\phi_1 \end{bmatrix} \quad (15.40)$$

This, along with remembering that ϕ_1 is negative for the 1000 orbit, fixes the factor of negative 2 I was missing. I have also figured out my block diagonalization issue from before. Now the question is, why would $\overline{1000}$ and $\overline{0111}$ have equal but opposite eigenvalues for the asymmetric subspace of the reflection operator (is this the correct vocab?). I also think I know what is wanted for the plots, I will do that.

Back to an earlier project: eigenvalues of \mathcal{J} in different coordinates. \mathcal{J} is not a derivative on space (like the one time step Jacobian is), it is instead a derivative on periodic lattice points (again, could be incorrect vocab, will work on this). So, maybe instead of using a regular coordinate transform, we should a transform specifically on the periodic orbit? Maybe that would help with the issue of the fixed point condition being $F[X] = 0$ instead of $F[X] = X$.

2021-09-01 Sidney to Predrag What colors should I use for the bars when I do your plotting suggestion for temporal Hénon, the colors mattered in the other bar graphs.

2021-09-01 Predrag Quality of a plot does not matter much at the exploratory stage, I know by plotting by hand the shapes of the 6 lattice states - they follow from their symbolic dynamics. However, if you have accurate numbers for fields and eigenvalues, you could discover the symmetries that I am missing in hand-sketches. Or you can put intelligible data files in you computing folder *siminos/williams/* and make Predrag do your work, as in (15.26):

Plot the values of lattice state fields for the 6 lattice states of table 2.3 and figure 2.3 in the same format as figure 3.13 (b), using the same color scheme. When I plot them, I place the yellow bar at 0, then two red bars to the left and two blue to the right. You can also superimpose symbol dynamics code upon it - you will immediately understand '0's are negative and '1's are positive.

2021-09-03 Predrag To determine C_5 period-5 states of table 2.3 you only need to determine the D_5 length-3 block lattice state defined by boundary conditions of (3.168) - you might want to check whether the lattice states so obtained agree with the ones you already have.

Their Hill determinants are the determinants of the 3-dimensional orbit Jacobian matrix (3.169).

To determine C_6 period-6 states of table 2.3 you only need to determine the corresponding D_6 length-4 or -3 block lattice state defined by boundary conditions analogous to (3.168). Their Hill determinants are the determinants of 4- or 3-dimensional orbit Jacobian matrix (3.171) or (3.172).

2021-09-03 Predrag 2 Andrew afugett3 = fuggedaboutit

2021-09-06 Sidney 2 Everyone Sorry for the long silence, just settling back into everything. I will be working on the plots today, and will update as I go along, as well, I will show Andrew how to get the repository on his laptop.

Period $n = 5$ lattice states of table 2.3 plotted as in figure 3.13. They are all reflection symmetric, with fixed lattice field ϕ_0 colored gold. Note that the symbolic dynamics is given by the signs of lattice site fields. **This plot is now superseded by figure 2.2.** (right)

2021-09-06 Sidney I completed the plots for both lattice field values, and the associated eigenvalues. The formatting is not finished yet, but I will change that later. Currently, I have the lattice state that remains fixed colored gold, and the ones that flip colored maroon.

2021-09-07 Predrag .

1. Figure 15.2(a) agrees with my own sketch, but only examination of the actual ϕ_j values can reveal further symmetries and factorizations.
2. Figure 15.2(b) currently does not make much sense to me. 3 of the eigenvalues should belong to the symmetric subspace (15.41), (4.27), 2 to the antisymmetric subspace (4.29).
3. 2021-09-27: Figure 15.2(a) is now superseded by figure 2.2.

2021-09-06 Sidney For a D_5 lattice state, the following boundary conditions are respected: $\phi_i = \phi_{i+5}$ and $\phi_{-i} = \phi_i$, if we follow (3.168), we find the

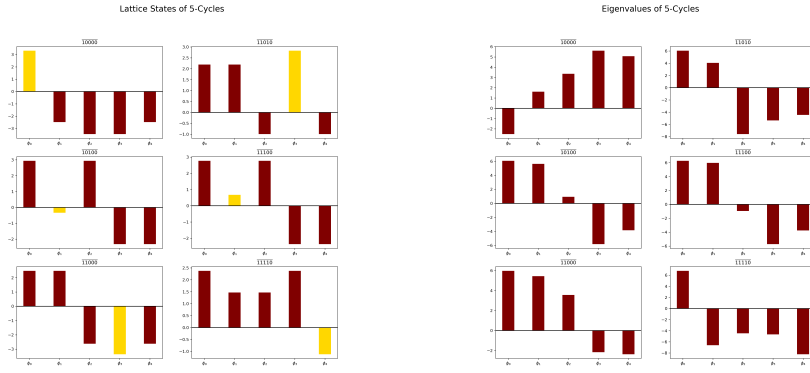


Figure 15.2: Temporal Hénon (2.44), $a = 6$: (left) The associated orbit Jacobian matrix eigenvalues (?). Currently we have no interpretation. Should't the corresponding eigenvectors be (anti)symmetric?

temporal Hénon orbit Jacobian matrix in the symmetric subspace is

$$\mathcal{J}_+ = \begin{pmatrix} 2\phi_0 & 2 & 0 \\ 1 & 2\phi_1 & 1 \\ 0 & 1 & 2\phi_2 + 1 \end{pmatrix} \quad (15.41)$$

As well, from (3.168), I can find the 3 equations that define this sort of orbit for temporal Hénon

$$\begin{aligned} \phi_0^2 + 2\phi_1 &= a \\ \phi_0 + \phi_1^2 + \phi_2 &= a \\ \phi_1 + \phi_2^2 + \phi_2 &= a \end{aligned} \quad (15.42)$$

Is there a good way of solving this system analytically? Otherwise, should I just check it by numerically finding solutions?

2021-09-07 Predrag No, for us getting into the Endler-Gallas annalytic solutions is getting too deep into the weeds. Use the same Biham-Wentzel program you have already written, with the boundary conditions added. The wonderful thing is that you are looking for the roots of an order 2^3 polynomial rather than 2^5 .

To compute the Hill determinant $\text{Det } \mathcal{J}_+$, Han would recommend doing the discrete Fourier transform first.

2021-09-07 Predrag Currently I prefer the (3.20) form of the temporal Hénon to (2.44), but that is not very important at this stage.

2021-09-07 Sidney The full orbit Jacobian matrix for the D_5 cycles of the temporal Hénon commutes with reflection about the center lattice state (3.164).

Therefore, we can block diagonalize to find the orbit Jacobian matrices of the symmetric and antisymmetric subspaces:

$$\mathcal{J}_{D_5} = \begin{pmatrix} 2\phi_2 - 1 & 1 & 0 & 0 & 0 \\ 1 & 2\phi_1 & 0 & 0 & 0 \\ 0 & 0 & 2\phi_0 & 2 & 0 \\ 0 & 0 & 1 & 2\phi_1 & 1 \\ 0 & 0 & 0 & 1 & 2\phi_2 + 1 \end{pmatrix} \quad (15.43)$$

Which gives the same matrix for the symmetric subspace as (15.41), therefore either boundary conditions or projection operators are effective for these sort of calculations.

I took a look at my code, and it seems that I wrote it with no ability to scale a , I will fix that, and add in the functionality of using the traditional field theory formulation and the rescaled "Gallas" notation that I have been using for awhile.

2021-09-09 Predrag You sure about (15.43)? It might be correct, but how did you derive it?

2021-09-13 Sidney I am quite sure of (15.43). I noticed that the orbit Jacobian matrix for a time reversal invariant orbit commutes with the $[5 \times 5]$ reflection matrix

$$\sigma = \begin{pmatrix} 0 & 0 & 0 & 0 & 1 \\ 0 & 0 & 0 & 1 & 0 \\ 0 & 0 & 1 & 0 & 0 \\ 0 & 1 & 0 & 0 & 0 \\ 1 & 0 & 0 & 0 & 0 \end{pmatrix} \quad (15.44)$$

So, I found all the eigenvectors associated with (15.44) by an online calculator and arranged them so that the ones associated with -1 (antisymmetric) and 1 (symmetric) were grouped together in a matrix S , I then used an online calculator to perform

$$S^{-1} \mathcal{J} S = \mathcal{J}_{BD}$$

And after shuffling around the columns of S (which is allowed for diagonalization), I got (15.43).

2021-09-07 Sidney This brings me to what Predrag has asked me to do:

Predrag check list

1. I will need to reformulate everything back into the unscaled field values so that a multiplies the quadratic term.
2. Find eigenvalues of D_5 lattice states in the symmetric subspace to explain figure 15.2 (right).

3. Prove that the eigenvalues of the orbit Jacobian matrix are metric invariants. I am stuck here.
4. Implement Han's boundary conditions into my code so that I can directly find orbits with specific symmetries.

2021-09-12 Sidney I will start working on adding boundary conditions to find different symmetries (a task I have added to the list) after I clean up my code, and make it easy to switch between Gallas form, and Field Theory form.

2021-09-13 Sidney I have changed my code so that it can be easily switched between the Hénon [10] (2.4), and Endler and Gallas [6] rescaled (2.20), I have added this updated code *Relaxation Method Henon with Orbit Jacobian.py* to *siminos/williams/python/relax*.

2021-09-14 Predrag 2 Sidney Added exercise 4 *The matrix square root*.

2021-09-14 Sidney 2 Predrag and Han I looked at exercise 4 *The matrix square root*. I feel confident in being able to do that. However, I am not sure why I am looking at the square root here. From what I gathered during today's meeting, taking the square root of the time-step Jacobian at the boundary point did not give equality to the hill determinant of the symmetry reduced orbit Jacobian matrix. My impression was that I would instead need to look for a "square root" of the temporal Hénon is that incorrect?

2021-09-17 Sidney 2 Anyone Just for clarification, I should be looking at (18.392) for time symmetric orbits of the temporal Hénon. I was thinking that since this is an identity for the forward in time 2×2 Jacobian, for orbits symmetric with respect to time reversal, I would look at the Hill determinant $\text{Det } \mathcal{J} = \det(1 - J)$ and check to see that the equality holds for when I take the half orbit of time-step J , compare to the symmetric part of (15.43). Is that a good strategy?

2021-09-17 Sidney I have completed exercise 4, the solution I got on pen and paper matches the solution that Predrag provided. I will take Andrew through it tomorrow.

2021-09-17 Sidney With respect to adding boundary conditions to my code: I do not know how to do it as I am not using the Biham-Wentzel method for the temporal Hénon, instead (a detail nowhere described in the blog) I invert it and feed the code a symbol sequence, see Vattay's *ChaosBook exercise 7.2*, copied to here as exercise 2.1.

2021-09-17 Sidney I do not know how to change the boundary conditions.

2021-09-30 Sidney The above statement is still true, although, around studying for tests, and other homework, I been working on testing the formula (18.392) numerically. I have also been review some of the group theory

lectures from over the summer. What I did, was say that the "factored" time-step Jacobian for a time symmetric period-5 is

$$\tilde{J} = J_2 J_1 \sqrt{J_0} \quad (15.45)$$

Where $\sqrt{J_0}$ can be calculated through the methods worked through in exercise 4. I then did the following calculation for every $\sqrt{J_0}$

$$|\text{Det } \mathcal{J}_+| - |\det(I - \tilde{J})|(should) = 0, \quad (15.46)$$

where \mathcal{J}_+ is the $[3 \times 3]$ block in (15.43). This did not work. The closest I got to getting zero was 3.4, which isn't even an integer. So, I turned to Mathematica, and found that $\text{Det } \mathcal{J}_+$ has a fundamentally different form from $\det(I - \tilde{J})$ for the temporal Hénon with a time symmetric five cycle, so, I went back to the drawing board. In the meeting at the beginning of the week, it was mentioned that the time-step Jacobians had to satisfy the time symmetry boundary conditions, and my thought was to try to force this by finding the Jacobian for each equation along a time symmetric period-5 which, with boundary conditions, yields a 3 equations:

$$2\phi_1 + \phi_0^2 = a \quad (15.47)$$

$$\phi_2 + \phi_1^2 + \phi_0 = a \quad (15.48)$$

$$\phi_2 + \phi_2^2 + \phi_1 = a \quad (15.49)$$

The time step Jacobian from (15.47) is $J_0 = -\phi_0$, and the time step Jacobian from (15.48) is just the normal one for the temporal Hénon. I am not sure how to get a Jacobian out of (15.49), perhaps the quadratic equation? If anyone has suggestions, that would be lovely.

2021-10-05 Sidney In this blog entry I describe Vattay's method of determining the periodic orbits of the Hamiltonian (phase space volume preserving) temporal Hénon (2.71), exercise 2.1 *Inverse iteration method for a Hénon repeller*, solution on page 122.

First, I generate a list of all possible binary itineraries of a given length. This is a coding exercise, so I will not discuss that here. To determine the periodic orbits, Vattay inverts the temporal Hénon (2.71) as in (2.72):

$$\phi_i^{(m+1)} = \sigma_i \sqrt{\frac{1 - \phi_{i+1}^{(m)} - \phi_{i-1}^{(m)}}{a}}, \quad (15.50)$$

where S_i is a sign generated by the symbol sequence. I start the iteration by setting the initial guess orbit to

$$\phi_i^{(0)} = \sigma_i a^{-1/2}$$

(remember you $a \rightarrow \infty$ lattice states estimates?) and then evaluating (15.50). I then subtract the RHS from the LHS of the temporal Hénon for

each point on the cycle and if it is smaller than a certain predetermined tolerance, the loop terminates, and the cycle is found. The meat of the method is contained in these two loops:

```
for i in range(0,len(symbols)):
    cycle[i]=signs[i]*np.sqrt(abs(1-np.roll(cycle,1)[i]-np.roll(cycle,-1)[i])/a)
for i in range(0,len(symbols)):
    deviation[i]=np.roll(cycle,-1)[i]-(1-a*(cycle[i])**2-np.roll(cycle,1)[i])
```

I could probably set time symmetric boundary conditions in the second loop, perhaps through an if statement.

I tried stating that (15.49) could be written as $\phi_3 = a - \phi_2^2 - \phi_1$, which would give just the normal temporal Hénon Jacobian, but it did not match with the determinant of the $[3 \times 3]$ block in (15.43). So my hunch was wrong. Not quite sure where to go from here in that area.

2021-10-12 Sidney I am currently trying to address "Find eigenvalues of D_5 lattice states in the symmetric subspace to explain figure 15.2 (right)." from 15.2. I found a equation for the symmetric part of the orbit Jacobian matrix \mathcal{J}_+ (15.43), it is of the form $a\lambda^3 + b\lambda^2 + c\lambda + d$ where the coefficients are all inelegant sums of the lattice field values of a given orbit, it is not particularly helpful.

2021-10-15 Predrag You have to check that the "inelegant sums" are invariant under D_n symmetries. Han knows and explains how to compute the eigenvalues and eigenvectors (irreps of D_n) on the reciprocal lattice.

I think you will eventually end up with evrything being expressible in terms of traces of powers of $\text{Tr } \mathcal{J}_+^k$.

I am curious how many orbit Jacobian matrix \mathcal{J} eigen-directions are expanding, what do they look like, stuff like that.

2021-10-12 Sidney I think that part of the confusion of the right hand side of figure 15.2 is that I tried to assign eigenvalues to individual lattice sites, which is just incorrect, right?

2021-10-15 Predrag Eigenvalues are properties of the whole matrix, not a single site. Only if the matrix is diagonalized are they associates with eigenstates ('lattice sites' of the reciprocal lattice).

2021-10-12 Sidney I am going to look at (15.28) again to see if I can see some pattern. But as of right now, I think the main conclusion is that the eigenvalues do not necessarily have the same symmetries as the orbit they belong to.

2021-10-15 Predrag Eigenvectors have symmetries, not the eigenvalues.

2021-10-25 Sidney I have generated some good data for the eigenstuff, see figure ???. I need to do further analysis to see which eigenstate(s) is most

important. As well, I think I have some insight into why (18.392) does not work. The orbit Jacobian matrix can be block diagonalized into symmetric and antisymmetric blocks. As this is the case, Hill's formula can be written as

$$\text{Det}(\mathcal{J}_-) \text{Det}(\mathcal{J}_+) = \det |I - J|$$

If we assume we can write J as $(J')^2$ (which is what (18.392) assumed), we can then write Hill's formula as

$$\text{Det}(\mathcal{J}_-) \text{Det}(\mathcal{J}_+) = \det |I - J'| \det |I + J'|$$

Which does not imply that $\text{Det}(\mathcal{J}_+) = \det |I - J'|$ which I numerically showed to be incorrect a few weeks ago. This does not necessarily help find a correct factorization, but it at least shows us what is wrong.

2021-11-11 Sidney I added the plots of the eigenstates for every 5-cycle, as well as the decomposition for each period lattice state. Unfortunately, there seems to be no correlation between the important eigenstates and the size of the eigenvalues.

2021-11-11 Predrag to Sidney .

The figures currently in *siminos/williams/python/* are not *.svg vector graphics - they are bit images. To see them, download [Inkscape](#) and try to edit them.

2021-11-11 Sidney I suppose that almost makes sense because treating the whole cycle as a fixed point removes iteration from our calculations, perhaps they will be useful for global stability analysis?

2021-11-11 Predrag to Sidney I think so too. Note that as the orbit Jacobian matrix is symmetric (at least for the full Bravais cell - you have to show it also works for the symmetry-reduced case and $b \neq -1$) all multipliers Λ_j are real. Their signs might mean something.

2021-11-11 Predrag to Han .

1. Before Sidney automatizes looking at eigenvectors, what output format do you prefer? Sidney's narrow bars as field values, as in figure 15.2, or Han's fat bars, as in figure 2.2?
2. The problem with temporal Hénon is that due to all period-5 lattice states being symmetric, we are getting only 3-dimensional examples. For temporal cat you have asymmetric period-5 lattice states, there is more information in them.
3. Can you take your beloved temporal cat products of $[s - 2 \cos(\frac{2\pi j}{n})]$ and do the corresponding eigenvector plots as *siminos/williams/python/* for (some of) illustrative temporal cat period-5 lattice states? Any striking similarities?

2021-11-11 Predrag .

I find the eigenvectors currently in *siminos/williams/python/*Figures/ utterly fascinating.

The n multipliers Λ_j , $j = 1, 2, \dots, n$ (ChaosBook reserves the lower case λ_j to exponents, but we might change that for the spatiotemporal theory) seem all to be of the same order of magnitude - that will be more apparent when we see their lists for examples of lattice states of periods $n = 6, 7, 8, \dots$.

2021-12-06 Sidney I am still a little unsure how to get the files saved as *.svg vector graphics, the line which saves the pictures is given by

```
plt.savefig(name+'.svg',dpi=300)
```

where name is defined earlier in the code. I am not sure why that does not work. I am also quite close to automating the cycle finding process with nice looking, and useful figures, I will do that after finals.

I am still stuck on proving that the eigenvalues of the orbit Jacobian matrix are invariant under nonlinear coordinate transforms, the fixed point condition under the field theory just does not seem to allow for it.

I now understand how Han was able to find $2\cos(k) - s$ for the eigenvalues, but I am currently having a hard time generalizing that to temporal Hénon I will keep working.

Finally, I have found a (probably useless) tensorial formulation of our theory which allows for the analysis of multiple equation systems (think the Lorenz equations discretized, or temporal Hénon before being compressed into a single equation). It is as follows

$$G^{kl} [\Phi] = \Gamma_{ij}^{kl} \Phi^{ij} + M^{kl} = 0^{kl}, \quad (15.51)$$

Where the index k is for the k^{th} equation, and index l is for the l^{th} lattice point. The index i ranges from 1 to n for a length n orbit, it is the field value on the l^{th} lattice point for the j^{th} variable (think x and y for Hénon).

$$\Gamma_{ij}^{kl} \equiv \frac{\delta G^{kl} [\Phi]}{\delta \Phi_{ij}}, \quad (15.52)$$

Several caveats here, I am sure that I could condense this, perhaps combining the i and l index, I am also pretty sure that I messed up the Einstein notation with the co and contravariant indices. And finally, this is likely completely useless as I am pretty sure that given a system of k first order difference equations, it can be combined into a single higher order equation like what was done with temporal Hénon

2021-12-17 Sidney I have been trying to get an equation which shows the bounds of the eigenvalues of the temporal Hénon but the method of just guessing $e^{\omega^n z}$ doesn't work for the orbit Jacobian matrix for Hénon because it does

not commute with the shift operator ($\delta_{j+1,k}$), so there is probably some other $u(z)$ that I need to use, I am not sure though.

2021-12-18 Sidney I am trying to establish bounds for the temporal Hénon. I can do this numerically, with the minimum value being -0.607625218511 etc. and the maximum still to be calculated with the code provided for ChaosBook.org/course1 [homework 7](#). The stable and unstable manifolds trace out the region that is bounded (Ω), and the maxima and minima are determined by their intersections, and I know that these manifolds can be calculated numerically through forward and backward iteration, but I feel like I should be able to find these intersections analytically. Is there something else that I could do? Or do I have to resort to numerics?

2021-12-20 Predrag I do not believe I have ever seen an analytic expression for a non-trivial intersection of stable / unstable manifolds. The lower left corner of [ChaosBook fig. 15.5](#) you know analytically: it is the stability of fixed point $\bar{0}$. The upper right corner of the Smale horseshoe non-wandering set is the heteroclinic point - lacking something more clever, one might approximate it by the longest nearby periodic orbit, of form $\overline{100\cdots 0}$. You only need an lower bound on the magnitude of the multiplier, it's OK to be crude about such a bound.

An example of $\overline{100\cdots 0}$ sequence of periodic orbits is given in Artuso, Aurell and Cvitanović *Recycling of strange sets: II. Applications*, see their [fig. 2](#). That would correspond to the tangency stretching parameter a value (3.56); you are looking at a larger stretching so there is no funny $\sqrt{\cdots}$ limit in your case, your limit is cleanly hyperbolic, see figure 2.2.

2021-09-12 to 2021-09-14, 2021-12-22 Sidney, Predrag It looked like a wild goose chase, so not to distract Sidney further I had moved the discussion of anti-integrable "perturbation theory" to sect. 2.1.1 *Temporal Hénon*. But it remains of interest: many new references there in sect. 2.1.1 *Temporal Hénon in anti-integrable limit*.

I have added my guess (5.123) for the infinite coupling g anti-integrable limit of ϕ^4 theory. That gives a 3-letter alphabet $\mathcal{A} = \{-1, 0, 1\}$. One can use it to find by continuation any lattice state, at g as low as possible. 'Generalized Hénon maps' AKA ϕ^4 field theory posts are in sect. 5.7.3 *Classical ϕ^4 lattice field theory*.

15.3 Sidney exercises

1. Hénon temporal lattice.

1-dimensional temporal Hénon lattice (see [ChaosBook Example 3.5](#)) is given by a 3-term recurrence

$$\phi_{n+1} + a\phi_n^2 - b\phi_{n-1} = 1.$$

The parameter a quantifies the “stretching” and b quantifies the “contraction”.

The single Hénon map is nice because the system is a nonlinear generalization of temporal cat 3-term recurrence CL18 eq. catMapNewt, with no restriction to the unit hypercube XXX, but has binary dynamics.

There is still a tri-diagonal orbit Jacobian matrix \mathcal{J} CL18 eq. tempCatFixPoint, but CL18 eq. (Hessian) is now lattice state dependent. Also, I believe Han told me that CL18 sect. s:Hill *Hill determinant: stability of an orbit vs. its time-evolution stability* block matrices derivation of Hill’s formula does not work any more. Neither does the ‘fundamental fact’, as each lattice state’s orbit Jacobian matrix is different, and presumably does not count periodic states, as there is no integer lattice within the Hill determinant volume.

Does the [ChaosBook flow conservation](#) sum rule [ChaosBook ed. \(27.15\)](#) (or CL18.tex eq. Det(jMorb)eights) still work?

The assignment: Implement the variational searches for periodic states in Matt’s [OrbitHunter](#), find all lattice states up to $n = 6$.

(a) $a = 1.4$ $b = 0.3$, compare with [ChaosBook Table 34.2](#).

(b) For $b = -1$ the system is time-reversible or ‘Hamiltonian’, see [ChaosBook Example 8.5](#). For definitiveness, in numerical calculations in examples to follow we fix (arbitrarily) the stretching parameter value to $a = 6$, a value large enough to guarantee that all roots of the periodic point condition $0 = f^n(x) - x$ are real.

Note also [ChaosBook sect A10.3 Hénon map symmetries](#) and [ChaosBook Exer. 7.2 Inverse iteration method](#).

The deviation of an approximate trajectory from the 3-term recurrence is

$$v_n = \phi_{n+1} - (1 - a\phi_n^2 + b\phi_{n-1})$$

In classical mechanics force is the gradient of a potential, which Biham-Wenzel [2] construct as a cubic potential

$$V_n = \phi_{n+1}\phi_n - b\phi_n\phi_{n-1} + (a\phi_n^3 - \phi_n). \quad (15.53)$$

With the cubic potential at lattice site n we can start to look for orbits variationally. Note that the potential is time-reversal invariant for $b = 1$.

Compare with XXX

2. **Engel Point Groups 1.** (Engel's [7] Point Groups Exercise 1): The molecule on the left has C_{1s} which signifies that it has reflection symmetry over one axis. The molecule on the right has C_3 symmetry, signifying that it is symmetric by rotations of $\frac{2\pi}{3}$ or one third of a full circle.

M. Engel

3. **Engel Point Groups 3.** (Engel's [7] Point Groups Exercise 3): Three point groups for C_2H_6 : a. C_{3v} because rotating it by 1/3 of a circle leaves it invariant, and one can cut the molecules into three identical pieces. b. C_s because the top and bottom have the same orientation, it is like looking in a mirror, so can apply reflection symmetry. c. Unsure, perhaps inversion symmetry C_i .

M. Engel

4. **The matrix square root.** Consider matrix

$$A = \begin{bmatrix} 4 & 10 \\ 0 & 9 \end{bmatrix}.$$

Generalize the square root function $f(x) = x^{1/2}$ to a square root $f(A) = A^{1/2}$ of a matrix A .

- a) Which one(s) of these is/are the square root of A

$$\begin{bmatrix} 2 & 2 \\ 0 & 3 \end{bmatrix}, \begin{bmatrix} -2 & 10 \\ 0 & 3 \end{bmatrix}, \begin{bmatrix} -2 & -2 \\ 0 & -3 \end{bmatrix}, \begin{bmatrix} 2 & -10 \\ 0 & -3 \end{bmatrix} ?$$

- b) Assume that the eigenvalues of a $[d \times d]$ matrix are all distinct. How many square root matrices does such matrix have?

- c) Given a $[2 \times 2]$ matrix A with a distinct pair of eigenvalues $\{\lambda_1, \lambda_2\}$, write down a formula that generates all square root matrices $A^{1/2}$. Hint: one can do this using the 2 projection operators associated with the matrix A .
points

Solution 1 - Hénon temporal lattice.

- (a) Here's my initial attempt, I'm trying to see if the flow conservation law CL18 eq. $\text{Det}(jM\sigma)$ still works for the Hénon map:

$$\phi_{n+1} + a\phi_n^2 - b\phi_{n-1} = 1$$

The first step seems to be to construct the orbit Jacobian matrix \mathcal{J} :

$$F[\Phi] = \mathcal{J}\Phi - I \quad (15.54)$$

Where I is the identity matrix, and F is the function where we want to find the zeros for (the orbits). We can rewrite this as:

$$(\sigma + aI\Phi - b\sigma^{-1})\Phi = I \quad (15.55)$$

CHAPTER 15. SIDNEY'S BLOG

Therefore, \mathcal{J} is

$$\mathcal{J} = \sigma + aI\Phi - b\sigma^{-1} = \begin{bmatrix} a\phi_1 & 1 & 0 & \cdots & -b \\ -b & a\phi_2 & 1 & \cdots & 0 \\ 0 & \ddots & \ddots & \ddots & \vdots \\ \vdots & \cdots & -b & a\phi_{n-1} & 1 \\ 1 & 0 & \cdots & -b & a\phi_n \end{bmatrix} \quad (15.56)$$

Before I take a crack at seeing if this flow conservation still holds, I do have some questions:

Q1 Sidney It appears that the derivation from chapter 23 (eqn 23.17, I don't know how to cite that specifically) the denominator of the sum rule is a product of the eigenvalues Λ_{pi} , which (if I remember correctly) are just the eigenvalues of the orbit Jacobian matrix of the flow or map, which from basic linear algebra I know to be just the determinant of the orbit Jacobian matrix. It cannot be that straightforward, where is the flaw in my logic?

Q2 Sidney How do I go from the periodic orbit formulation of the sum rule from Ch 23 to the lattice formulation? My initial thought is that since lattice states are akin to a periodic orbit (right?) that the sum can just be immediately changed from a sum over all periodic orbits, to a sum over all lattice states. Is this reasoning correct?

Comment Sidney I now realize that the flow sum rule involving the orbit Jacobian matrix (NOT the Hill matrix) is a fundamental property that applies to all systems (at least all closed systems), what I now know is that I need to work out if I can convert between the determinant of the orbit Jacobian matrix and the determinant of the Hill matrix.

Plan Sidney I am going to try to see what I can do with the block matrix proof, and I will get back to everyone on Friday

Update Sidney I tried working out the proof with the block matrices for just the regular Bernoulli map, I understand everything except the sentence "For a period- n lattice state Φ_M , the orbit Jacobian matrix (15) is now a $[nd \times nd]$ matrix function of the $[d \times d]$ block matrix J ." It sort of seemed like it was much like "poof! And then a miracle happens!" I will keep exploring.

I shall now correct my mistake with the derivation of the orbit Jacobian matrix/Hill matrix \mathcal{J} I shall use the differential definition:

$$\mathcal{J}_{ij} = \frac{\delta F[\Phi]_j}{\delta \phi_i}$$

Which gives us that $\mathcal{J} = \sigma + 2aI\Phi_n - b\sigma^{-1}$. Now I will use the differential definition of the local Jacobian, where f is a functions such that $f(\phi_n) = \phi_{n+1}$

$$J_{ij} = \frac{\partial f(\phi_n)_i}{\partial \phi_{n,j}}$$

Which gives us that $J(\phi_n) = -2a\phi_n$. So we can rewrite $\mathcal{J} = \sigma - J(\phi_{in})I - b\sigma^{-1}$, with the understanding that J changes along the diagonal. I am not quite sure how to bring this to the sum rule, but I will soon (hopefully), how do I math things like ϕ and Φ bold?

Update Sidney I need to do a proper mathematical look at the flow conservation, but the Hénon map is not flow conserving (some trajectories are inadmissible) so the sum rule does not equal 1, I will try later to look at what it does equal analytically, but until then I will tackle the computation. I have made great progress with that, with help from Matt I was able to create a working code that gave me the correct orbits up to length 10 (I could not check past that). The code is in my blog. Once Matt has completed the current round of OrbitHunter updates I shall try to use that to reproduce my results.

Solution Sidney (a) The flow conservation sum rule does not sum to 1 so it does not work as before, I still need to try to relate the global Hill matrix to the local Jacobian matrix, I think I may be close to reworking the block matrix proof. Anyway, here are the periodic points I found (please note that the code cannot be used to find fixed points ($n=1$) so I just did it analytically, I will try to add that to the code later):

$$n = 1 \quad -1.13135447$$

$$n = 1 \quad 0.63135447$$

$$n = 2 \quad [0.97580005, -0.47580005]$$

$$n = 4 \quad [1.12506994, -0.70676678, 0.63819399, 0.21776177]$$

$$n = 6 \quad [1.03805954, -0.41515894, 1.07011813, -0.72776163, 0.57954366, 0.31145232]$$

$$n = 6 \quad [1.1579582, -0.8042199, 0.44190995, 0.48533586, 0.80280173, 0.2433139]$$

When I tried to find $n = 3$ and $n = 5$ the code returned nothing, this matches with what is tabulated in table 34.2. I will try using some of the analytical pruning techniques to prove that $n = 3$ and $n = 5$ are not allowed.

(Sidney Williams 2021-01-20)

Solution 2 - Engel Point Groups 1. *The molecule on the left has C_i symmetry which is inversion symmetry NOT reflection symmetry because the top and bottom arrangements are not like they would be if placed in front of a mirror. The molecule on the right has C_{3v} symmetry, which is pyramidal symmetry which corresponds to the fact that one could take three slices of the molecule and they would each be identical, not just the configuration would be preserved by a rotation.*

(Sidney Williams 2021-03-07)

Solution 3 - Engel Point Groups 3. *Apparently, it depends based on whether we are dealing with staggered Ethane or not. If it is staggered, then it has inversion symmetry, if it is not, it has reflection symmetry, it should have C_3 symmetry instead of C_{3v} which confuses me a great deal. If I remember correctly it should correspond to a reflection vertical plane, which it should have, so I do not understand. The third one is C_2 which I do not understand how it is different from the inversion symmetry. Although, looking at simulations from [here](#), it looks like the C_2 group can be used to rotate about axes that are different in orientation from just right through the middle.* (Sidney Williams)

2021-03-07

Solution 4 - The matrix square root. .

a) It is easy to check that

$$A = \begin{bmatrix} 4 & 10 \\ 0 & 9 \end{bmatrix} = \left(A_{ij}^{1/2} \right)^2$$

for the matrices

$$\begin{aligned} A_{++}^{1/2} &= \begin{bmatrix} 2 & 2 \\ 0 & 3 \end{bmatrix}, & A_{+-}^{1/2} &= \begin{bmatrix} -2 & 10 \\ 0 & 3 \end{bmatrix} \\ A_{--}^{1/2} &= \begin{bmatrix} -2 & -2 \\ 0 & -3 \end{bmatrix}, & A_{-+}^{1/2} &= \begin{bmatrix} 2 & -10 \\ 0 & -3 \end{bmatrix} \end{aligned} \quad (15.57)$$

Being upper-triangular, the eigenvalues of the four matrices can be read off their diagonals: there are four square root \pm eigenvalue combinations $\{3,2\}$, $\{-3,2\}$, $\{3,-2\}$, and $\{-3,-2\}$.

Associated with each set $\lambda_i \in \{\lambda_1, \lambda_2\}$ is the projection operator

$$P_{ij}^{(1)} = \frac{1}{\lambda_1 - \lambda_2} (A_{ij}^{1/2} - \lambda_2 \mathbf{1}) = \begin{bmatrix} 0 & 2 \\ 0 & 1 \end{bmatrix} \quad (15.58)$$

$$P_{ij}^{(2)} = \frac{1}{\lambda_2 - \lambda_1} (A_{ij}^{1/2} - \lambda_1 \mathbf{1}) = \begin{bmatrix} 1 & -2 \\ 0 & 0 \end{bmatrix}. \quad (15.59)$$

Note that all ‘square root’ matrices have the same projection operators / eigenvectors as the matrix A itself, so one can drop the ij subscripts on $P^{(1)}$, $P^{(2)}$.

b) If the eigenvalues of a $[d \times d]$ matrix are all distinct, the matrix is diagonalizable, so the number of square root \pm combinations is 2^d . However, for general matrices things can get crazy - there can be no, or some, or ∞ of ‘square root’ matrices.

c) We know $\{\lambda_1, \lambda_2\}$ and $P^{(\alpha)}$ for A , and the four ‘square root’ eigenvalues are clearly $\{\pm\lambda_1^{1/2}, \pm\lambda_2^{1/2}\}$. That suggest finding the ‘square root’ matrices (15.57) by reverse-engineering (15.58), (15.59):

$$A_{ij}^{1/2} = (\lambda_1 - \lambda_2) P^{(1)} + \lambda_2 \mathbf{1},$$

which is, of course, how the problem was cooked up. For example,

$$A_{+-}^{1/2} = (+3 - (-2)) \begin{bmatrix} 0 & 2 \\ 0 & 1 \end{bmatrix} + (-2) \begin{bmatrix} 1 & 0 \\ 0 & 1 \end{bmatrix}.$$

References

- [1] A. Barvinok, *Lattice Points, Polyhedra, and Complexity*, tech. rep. (Univ. of Michigan, Ann Arbor MI, 2004).
- [2] O. Biham and W. Wenzel, “Characterization of unstable periodic orbits in chaotic attractors and repellers”, Phys. Rev. Lett. **63**, 819 (1989).
- [3] P. Cvitanović and H. Liang, Spatiotemporal cat: A chaotic field theory, In preparation, 2021.
- [4] A. Endler and J. A. C. Gallas, “Arithmetical signatures of the dynamics of the Hénon map”, Phys. Rev. E **65**, 036231 (2002).
- [5] A. Endler and J. A. C. Gallas, “Conjugacy classes and chiral doublets in the Hénon Hamiltonian repeller”, Phys. Lett. A **356**, 1–7 (2006).

- [6] A. Endler and J. A. C. Gallas, “Reductions and simplifications of orbital sums in a Hamiltonian repeller”, *Phys. Lett. A* **352**, 124–128 (2006).
- [7] M. J. Engel, *Short-Course on Symmetry and Crystallography*, 2011.
- [8] B. Gutkin, L. Han, R. Jafari, A. K. Saremi, and P. Cvitanović, “Linear encoding of the spatiotemporal cat map”, *Nonlinearity* **34**, 2800–2836 (2021).
- [9] B. Gutkin and V. Osipov, “Classical foundations of many-particle quantum chaos”, *Nonlinearity* **29**, 325–356 (2016).
- [10] M. Hénon, “A two-dimensional mapping with a strange attractor”, *Commun. Math. Phys.* **50**, 94–102 (1976).
- [11] D. A. Klain and G.-C. Rota, *Introduction to Geometric Probability* (Cambridge Univ. Press, 2006).
- [12] A. Politi and A. Torcini, “Periodic orbits in coupled Hénon maps: Lyapunov and multifractal analysis”, *Chaos* **2**, 293–300 (1992).
- [13] D. E. Sands, *Introduction to Crystallography* (Dover, 1969).
- [14] D. G. Sterling, H. R. Dullin, and J. D. Meiss, “Homoclinic bifurcations for the Hénon map”, *Physica D* **134**, 153–184 (1999).

Chapter 16

Ibrahim's blog

Ibrahim Abu-hijeh
iabuhijleh3@gatech.edu
subversion siminos : iabuhijleh3
cell +1 714 488 8926

The latest entry at the bottom for this blog

2021-12-07 Predrag to Ibrahim:

As you go along, write up your narrative in this file, ask questions - this is your personal blog, like an experimentalist's log - everything that you learn and want to share goes in here. Clip & paste anything from other sections you want to discuss, that saves you LaTeXing time.

2021-12-07 Predrag The 3rd line of *siminos/spatiotemp/blogCats.tex* says "process only the files you are editing",

```
\input{inputs/inclOnlyCats}
```

you uncomment a single line in that file to "process only the files you are editing".

2021-12-07 Predrag to Ibrahim :

You refer to a reference like this: Gutkin and Osipov [2] (*GutOsi15* refers to an article listed in *..bibtex/siminos.bib*).

and to external link like this: "For great wallpapers, see overheads in Engel's course [1]."

Pro tip: compile *blogCats.tex* often, as you write, and fix errors as you write. I had to go all the way back to May to find one of Sidney's unbalanced "{" and make the entire blog compile without errors...

16.1 Spring 2021 blog

2021-12-07 Predrag My notes are in sect. 5.7.3 *Classical ϕ^4 lattice field theory*.
Harrison and you should form a study group to understand this - it's
absolutely essential.

2021-12-08 Predrag The Hénon map/ ϕ^3 approaches should be safe for multi-modal maps with complete repelling sets, and it should work for finite-grammar Smale horseshoe repellers. Smale's original horseshoe [3], his fig. 1 was unimodal, but he also explicitly gives our ϕ^4 bimodal repeller, his fig. 5.

2021-01-27 Predrag For some background on D_∞ symmetry of the temporal cat and ϕ^4 1d lattice field theory, sect. 3.10 *Translations and reflections*, see remark 4.1 Time reversal; not a priority as yet.

2021-12-07 Predrag The quick & dirty calculation of short period lattice states is outlined by Sidney in (15.50), see Vattay's *ChaosBook exercise 7.2*, copied to here as exercise 2.1. We need something like that for ϕ^4 .

The Biham-Wentzel method (3.55) (search throught this blog) might be better. We'll need better methods, but not yet.

2021-12-07 Ibrahim I do not understand sources m_t in (3.20) and (3.21). In temporal cat (3.19) they are a finite integer-valued alphabet that translates the field to the right fixed point, but for the nonlinear field theories they are simply a constant? A constant that can be changed by shifting fields?

2021-12-08, 2021-12-10 Predrag You are right - we should think of m_t is a (possibly noninteger) shift that centers the map on a given nonlinear segment. Read sect. 5.9.1 and footnote after (3.59), see whether you have a good formulation that cover all three cases.

2021-12-07 Predrag First task:

Start reading chapter 3 LC21: *Time reversal for lattice field theories*.

Write your study notes up here. And now it's done.

2021-09-12 to 2021-12-22 Predrag I have added my guess (5.123) for the infinite coupling g anti-integrable limit of ϕ^4 theory. That gives a 3-letter alphabet $\mathcal{A} = \{-1, 0, 1\}$. One can use it to find by continuation any lattice state, at g as low as possible. 'Generalized Hénon maps' AKA ϕ^4 field theory posts are in sect. 5.7.3 *Classical ϕ^4 lattice field theory*.

References

- [1] M. J. Engel, *Short-Course on Symmetry and Crystallography*, 2011.
- [2] B. Gutkin and V. Osipov, “Classical foundations of many-particle quantum chaos”, *Nonlinearity* **29**, 325–356 (2016).
- [3] S. Smale, “Differentiable dynamical systems”, *Bull. Amer. Math. Soc.* **73**, 747–817 (1967).

Chapter 17

Xuanqi's blog

Xuanqi Wang
xwang3021@gatech.edu
subversion siminos : xwang3021
cell +86 177-2115-8435
WeChat y2528742620

The latest entry at the bottom for this blog

2021-12-07 Predrag to Xuanqi:

As you go along, write up your narrative in this file, ask questions - this is your personal blog, like an experimentalist's log - everything that you learn and want to share goes in here. Clip & paste anything from other sections you want to discuss, that saves you LaTeXing time.

2021-09-09 Predrag The 3rd line of *siminos/spatiotemp/blogCats.tex* says "process only the files you are editing",

```
\input{inputs/inclOnlyCats}
```

you uncomment a single line in that file to "process only the files you are editing".

2021-12-07 Predrag to Xuanqi .

You refer to a reference like this: Gutkin and Osipov [2] (*GutOsi15* refers to an article listed in *..bibtex/siminos.bib*).

and to external link like this: "For great wallpapers, see overheads in *Engel's* course [1]."

Pro tip: compile *blogCats.tex* often, as you write, and fix errors as you write. I had to go all the way back to May to find one of Sidney's unbalanced "{" and make the entire blog compile without errors...

17.1 Spring 2021 blog

2021-12-08 Predrag I believe that the ϕ^4 is not very different from the ϕ^3 theory for sufficiently strong stretching parameter. Here are proposed exercises for you to develop intuition about that:

1. Plot the 3^n Smale horseshoe for ϕ^4 1-d forward-in time map, in the (ϕ_t, ϕ_{t+1}) plane, paralleling [ChaosBook fig. 15.5](#) for ϕ^3 , i.e., Hénon map [\(3.55\)](#), [\(2.8\)](#), [\(9.2\)](#).
The intuition is topological; 1-d parabola repeller (with parabola height larger than 1) has the same kind of Cantor set as the complete Smale horseshoe repeller for the Hénon map. Similarly, I expect [ChaosBook fig. 11.4](#), here [\(4.209\)](#), to capture the topology of the ϕ^4 repeller.
2. For the Hénon map stretching parameter values a larger than [\(2.39\)](#), the ‘critical’ value $a_h = 5.69931 \dots$ guarantee a complete horseshoe. What is (very roughly) a corresponding value for the ϕ^4 theory?
3. (harder, not essential as yet) Quotient the D_1 symmetry for ϕ^4 , as in [ChaosBook fig. 11.5](#).

Ibrahim and you should form a study group to understand this - it’s absolutely essential.

2021-12-08 Predrag The above approaches should be safe for multimodal maps with complete repelling sets, and it should work for finite-grammar Smale horseshoe repellers. Smale’s original horseshoe [3], his fig. 1 was unimodal, but he also explicitly gives our ϕ^4 bimodal repeller, his fig. 5.

2021-12-07 Predrag Parallel reading, while you work on the above: chapter 3 LC21: *Time reversal for lattice field theories*.

Write your study notes up here.

2021-09-12 to 2021-12-22 Predrag I have added my guess [\(5.123\)](#) for the infinite coupling g anti-integrable limit of ϕ^4 theory. That gives a 3-letter alphabet $\mathcal{A} = \{-1, 0, 1\}$. One can use it to find by continuation any lattice state, at g as low as possible. ‘Generalized Hénon maps’ AKA ϕ^4 field theory posts are in sect. [5.7.3 Classical \$\phi^4\$ lattice field theory](#).

2021-12-?? Xuanqi

References

- [1] M. J. Engel, [Short-Course on Symmetry and Crystallography](#), 2011.

- [2] B. Gutkin and V. Osipov, “Classical foundations of many-particle quantum chaos”, *Nonlinearity* **29**, 325–356 (2016).
- [3] S. Smale, “Differentiable dynamical systems”, *Bull. Amer. Math. Soc.* **73**, 747–817 (1967).

Chapter 18

Han's blog

Don't be [Fritz Haake](#). He, who hesitates, is lost.

Han Liang <han_liang@gatech.edu> work blog
WeChat lhan118

[The latest entry at the bottom for this blog](#)

2018-03-18 Predrag Our blog posts are divided into sect. [18.1 Rhomboid corner partition](#), sect. [18.2 Rhomboid center partition](#), sect. [18.4 Reduction to the fundamental domain](#), and sect. [18.5 Spatiotemporal cat partition](#)

2018-01-19 Han Here is an example of [text edit by me](#), and here one of a footnote by me¹.

2018-01-19 Han (Discussion with Predrag, cat maps project Spring 2018:

- blog the project progress here
- blog whatever I'm reading and learning about dynamical systems here

2018-06-05 to 06-11 Predrag Read chapter ?, part of ?, and ? of Chaosbook. Do homework of online Course 1, Weeks ? and ?.

2018-01-19 to 02-11 Han Read Chapters ?, ?, part of ?, and ? of Chaosbook. Did homework of Weeks ? and ?.

2018-01-11 Predrag to Han: Caution - my posts can be erased your edits, if you omit to *svn up* before starting your edit.

Regarding new figures: always save *HL*.png* (or *HL*.pdf*) in *siminos/figs/*, then *svn add HL*.png* (where * is a name of the figure).

¹Han 2018-01-19: Han test footnote

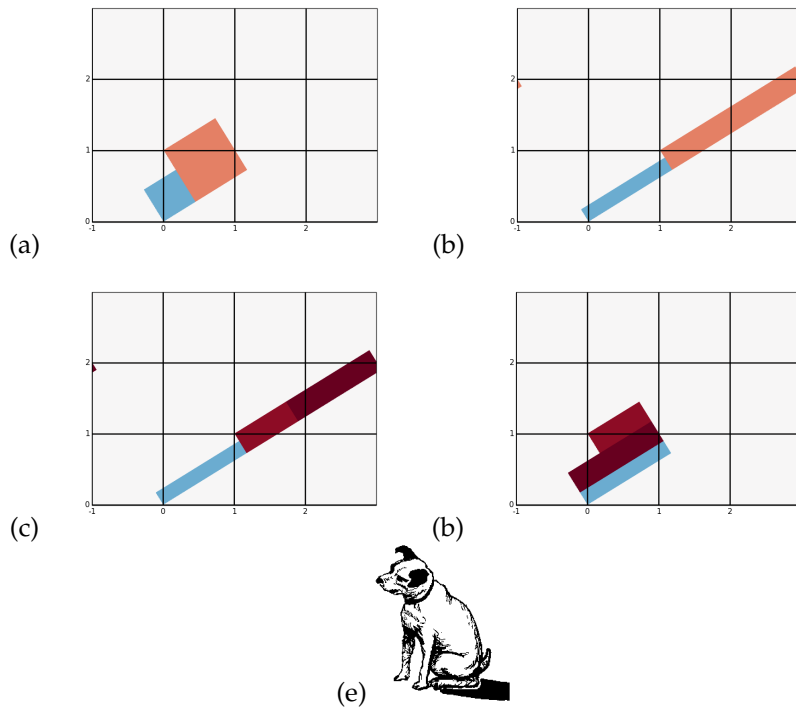


Figure 18.1: Figure 1.1 recomputed with my python code. (a) Two-squares Adler-Weiss generating partition for the canonical Thom-Arnol'd cat map (1.1), with borders given by stable-unstable manifolds of the unfolded cat map lattice points near to the origin. (b) The first iterate of the partition. (c) The first iterate of the partition intersections, (d) The iterate pulled back into the generating partition, and (e) the corresponding 5-letter transition graph. In (b) and (c) we still have to relabel Crutchfield's arbitrary partition labels with our shift code. This is a "linear code," in the sense that for each square one can count how many side-lengths are needed to pull the overhanging part of (c) back into the two defining squares.

Remember, always, before starting your work session with
svn up and concluding it with
svn ci -m "added entropy figures" you have to go to the root directory, *cd [...]siminos*. Otherwise you are not refreshing all bibtex, figures and other files in the repository.

2018-01-12 Predrag to Han

On *zero.physics.gatech.edu*, or Matt's *light.physics.gatech.edu*, or
your and Andy's *hard.physics.gatech.edu*, or visitor office *love.physics.gatech.edu*,
or any other CNS linux workstation your userid is

XXXX? (the same passwd as for svn - please change it once you log in)

Do not do calculations on the server *zero.physics.gatech.edu* - from any
CNS machine

ssh XXXX?@hard.physics.gatech.edu

save all data on the local hard disk */usr/local/home/han/*. I should make a
link in your CNS home directory:

cd homeHard

Help for CNS system, and all our documentation is on
www.cns.gatech.edu/CNS-only cnsuser cnsweb

but current crop of grad students, as a matter of principle, never look at
any info, or add to these homepages.

Good luck - Matt knows linux best, also Simon Berman, Xiong Ding
and Burak Budanur (via Skype) know a lot.

18.1 Rhomboid corner partition

Partitions, alphabets. A division of phase space \mathcal{M} into a disjoint union of distinct regions $\mathcal{M}_A, \mathcal{M}_B, \dots, \mathcal{M}_Z$ constitutes a *partition*. Label each region by a symbol m from an N -letter *alphabet* $\mathcal{A} = \{A, B, C, \dots, Z\}$, where $N = n_{\mathcal{A}}$ is the number of such regions. Alternatively, one can distinguish different regions by coloring them, with colors serving as the "letters" of the alphabet. For notational convenience, in alphabets we sometimes denote negative integer m by underlining them, as in $\mathcal{A} = \{-2, -1, 0, 1, 2\} = \{\underline{2}, \underline{1}, 0, 1, 2\}$.

A generating partition must map borders onto borders under dynamics (Adler-Weiss).

2018-01-18 Han `figSrc/han/python/HLcatmapArnold.py` reproduces the standard Arnol'd map partition, figure 18.1. The plots are in `siminos/figs/`.

`figSrc/han/python/HLcatmapPV.py` reproduces Predrag's hand-sketch of the Percival-Vivaldi [51] "two-configuration representation" cat map partition, figure 18.2.

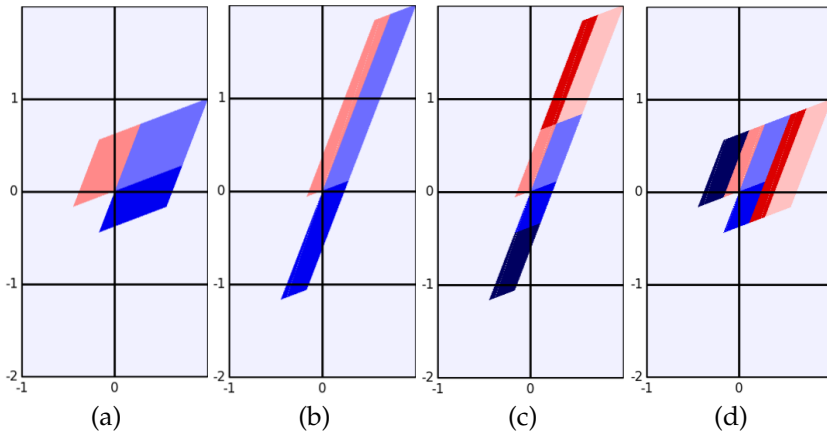


Figure 18.2: Figure 1.6 recomputed with my python code. (a) 3-rectangle, time-reversal symmetric Percival-Vivaldi cat map (1.5) partition. (b) The first forward iterate of the partition. (c) The first forward iterate of the partition, with the stable manifold intersections dividing it into 6 regions. (d) The 6 rhomboids (5 when the two blue regions are treated as one) are translated back into the generating partition, with the subscript label indicating the square-lattice vertical translation group elements: $\{T_{AA} = g_0^{A \rightarrow A}, T_{BB} = g_0^{B \rightarrow B}, T_{BA} = g_{-1}^{A \rightarrow B}, T'_{AA} = g_1^{A \rightarrow A}, T_{AB} = g_1^{B \rightarrow A}\}$. If the two blue regions are considered as a single partition, one obtains the standard Adler-Weiss 2-partition, with 5 distinct return maps one step forward in time, and the corresponding 5-letter transition graph of figure 1.1 (e). Together, these transitions make up the transition graph of figure 1.1 (c). The partition is generating, in the sense that the walks on this transition graph generate all admissible sequences.

2018-01-19 Predrag In the Percival-Vivaldi partition, (1.5) there is only one partition, the $[\phi_0, \phi_1]$ unit square. In the Adler-Weiss partition of figure 18.2(a) there are two rhomboid partitions, each with its own coordinates, lets say the big rhomboid $[\phi_0^A, \phi_1^A]$ and the small rhomboid $[\phi_0^B, \phi_1^B]$ (and perhaps also its time-reversal partner $[\phi_0^{B'}, \phi_1^{B'}]$), each bounded not by a unit square, but by the vectors (S^A, U^A) , (S^B, U^B) of the stable/unstable manifold segments that border the rhomboids. As this is a symplectic mapping, the important property of these rhomboids is their (oriented) area, for 1D dof given by the wedge or skew-symmetric product

$$A^\alpha = U^\alpha \wedge S^\alpha = U_i^\alpha \epsilon^{ij} S_j^\alpha, \quad \alpha \in \{A, B\}. \quad (18.1)$$

The figure 18.1 and figure 18.2 partitions are related by canonical (in 1D dof area-preserving) transformations, so for given stretching s , the small and the large rectangle/rhomboid areas are the same in any partition. Likewise, topologically the dynamics should be the same, i.e., have the same transition graph figure 1.1 (c).

That should naturally follow from the generator (Lagrangian) formulation sect. 8.2 in any choice of symplectically-paired coordinates.

Having several coordinate systems, one for each partition, is standard; a typical example are the three Poincaré sections of the 3-disk pinball, Fig. 15.15: *Poincaré section coordinates for the 3-disk game of pinball*, ChaosBook chapter *Charting the state space* [17].

2018-01-25 Predrag Figure out Toeplitz matrix for the simplest cycle(s) of period two (for Toeplitz matrices, see the post of 2017-09-09 on page 326, and the posts in sect. 1.5).

Hopefully only a $[2 \times 2]$ matrix. Understand its stability multipliers, eigenvectors.

2018-01-19 Han I've been working on reading the ChaosBook materials and doing the online Course 1.

2018-01-26 Predrag to Han: Can you compute analytically areas of partitions in figure 18.2, show that they are the same as those in figure 1.1 and figure 18.1? I expect them to be simple formulas in terms of stability multipliers (1.6).

2018-01-27 Han I have computed the area of the small partition B in figure 18.2 and figure 18.1. The areas of the small partitions are the same, for $s = 3$ they are $A_B = \frac{1}{2}(1 - \frac{1}{\sqrt{5}})$. If the stability multipliers are $(\Lambda, 1/\Lambda)$, where $\Lambda > 1$, as in (1.6), the area of the small partition B in figure 18.1 is given by

$$A_B = \frac{1 - 1/\Lambda}{\sqrt{D}} = \frac{1}{\Lambda + 1}. \quad (18.2)$$

The area of figure 18.2 is $A_B = \frac{(\Lambda-1)/\Lambda}{\sqrt{D}}$, i.e., the same.

2018-02-16 Predrag Is $|\mathcal{M}_B| = (\Lambda - 2)/\sqrt{D}$ in (1.109), for $s = 3$, the same as $|\mathcal{M}_B| = \frac{1-1/\Lambda}{\sqrt{D}} = \frac{1}{\Lambda+1}$ of (18.2)? Indeed, that follows from (??) by inspection.

2018-01-27 Predrag Thanks! Did you use (18.1) to compute them? I think we need that formalism to harmonize the discussion with sect. 8.2 generating functions.

Did you also check that the area of the big partition is $A_A = (1+1/\Lambda)/\sqrt{D}$?

2018-01-27 Predrag Maybe you do not see what has happened in the blog - I always use `svn diff` (it works nicely in the Windows GUI) to see what has changed.

Anyway, I stared the explicit construction of the Perron-Frobenius operator in example 1.4, so we also need the sub-partitions areas to check that.

2018-01-31 Han I have checked the area of the big partition. Adding the areas of each partition together we will get 1, so it should be correct. I didn't use (18.1) to compute the area. I found the coordinates of all the vertices on the edges of the parallelograms and got the vectors that border the partition then did the cross product (kind of tedious...). Using (18.1) to compute the areas should be very easy.

2018-02-10 Predrag computed them in (1.109).

2018-01-19 Predrag Read chapter *Walkabout: Transition graphs* [18]. Always try to work through examples. Eventually we want to try to solve Exercise 17.1 *Time reversibility*. The solution might be someplace here, in sect. 13.1 *Ihara zeta functions*.

2018-01-31 Han I have read chapter *Walkabout: Transition graphs*.

2018-02-01 Predrag I think a good partition is given in figure 18.3. The symbolic dynamics notation should probably be a 7-letter alphabet, something like

$$\begin{aligned} A &\rightarrow A_{(0,0)}, & B_2 \rightarrow B_{(0,0)}, & B'_2 \rightarrow B'_{(0,0)} \\ B_1 &\rightarrow B_{(-1,0)}, & B'_1 \rightarrow B_{(0,-1)} \\ B_3 &\rightarrow B_{(-1,-1)}, & B'_3 \rightarrow B'_{(-1,-1)}. \end{aligned} \tag{18.3}$$

2018-02-01 Predrag [2018-02-11 accomplished for the two-rectangle partition]

Han points out that the unit square borders, have no physical meaning, and that the partition still has only three regions A, B, B' , as in figure 1.8. The time forward partition is given in figure 1.7 (b).

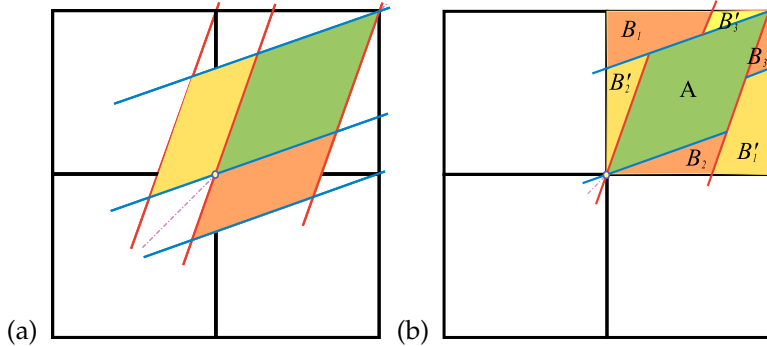


Figure 18.3: Abandoned attempt: (a) The three-rectangle, time reversal symmetric generating partition for the Percival-Vivaldi cat map (1.5), with borders given by cat map stable-unstable manifolds. (b) The three-rectangle partition of the unit square. In this partition A, B_2, B'_2 already lie within the unit square, while B_1 is shifted by $(-1, 0)$, B_3 is shifted by $(-1, -1)$, and B'_1 is shifted by $(0, -1)$, B'_3 is shifted by $(-1, -1)$. It is more partitions than going forward in time, but I hope it will be the right thing for the Lagrangian formulation.

2018-02-11 Han I have verified some admissible and inadmissible orbits by the Green's function. The Percival-Vivaldi cat map matrix with $s = 3$ is:

$$\mathbf{A} = \begin{bmatrix} 0 & 1 \\ -1 & 3 \end{bmatrix} \quad (18.4)$$

For the period $T = 4$ we can represent the orbit Jacobian matrix \mathcal{J} with periodic boundary conditions by a $[4 \times 4]$ circulant matrix

$$-\mathcal{J} = \begin{bmatrix} 3 & -1 & 0 & -1 \\ -1 & 3 & -1 & 0 \\ 0 & -1 & 3 & -1 \\ -1 & 0 & -1 & 3 \end{bmatrix} \quad (18.5)$$

The corresponding Green's function is the inverse of matrix of orbit Jacobian matrix $-\mathcal{J}$

$$\mathbf{g} = \begin{bmatrix} \frac{7}{15} & \frac{1}{5} & \frac{2}{15} & \frac{1}{5} \\ \frac{1}{5} & \frac{7}{15} & \frac{1}{5} & \frac{2}{15} \\ \frac{2}{15} & \frac{1}{5} & \frac{7}{15} & \frac{1}{5} \\ \frac{1}{5} & \frac{2}{15} & \frac{1}{5} & \frac{7}{15} \end{bmatrix} \quad (18.6)$$

Then given symbol block $M = m_0m_1m_2m_3$, we can calculate the corresponding orbit $X_M = (x_1, x_2, x_3, x_4)$. For example, if

$$M = \begin{bmatrix} 0 \\ 2 \\ 2 \\ 0 \end{bmatrix} \quad \Rightarrow \quad X = \frac{1}{3} \begin{bmatrix} 2 \\ 4 \\ 4 \\ 2 \end{bmatrix}. \quad (18.7)$$

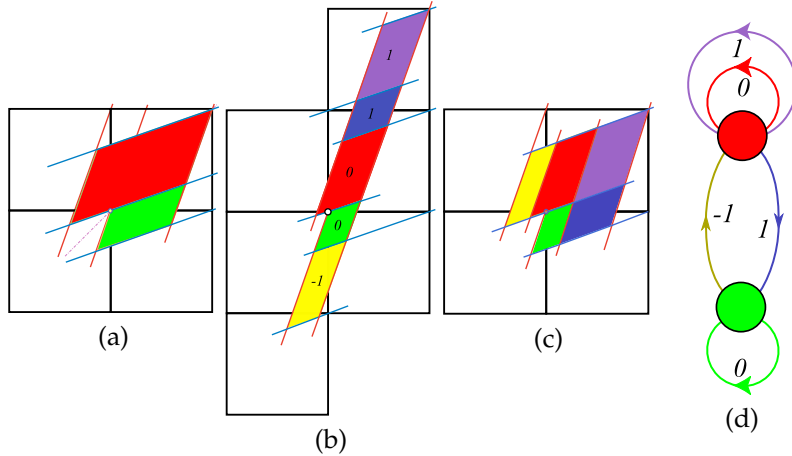


Figure 18.4: (Color online) (a) An Adler-Weiss generating partition of the unit torus into rectangles \mathcal{M}_A (red) and \mathcal{M}_B (green) for the Percival-Vivaldi cat map (1.5), with borders given by the cat map stable (blue) and unstable (red) manifolds. (b) Mapped one step forward in time, the rectangles are stretched along the unstable direction and shrunk along the stable direction. Sub-rectangles \mathcal{M}_j that have to be translated back into the partition are indicated by color and labeled by their lattice translation $m_j \in \{-1, 0, 1\}$. (c) The sub-rectangles \mathcal{M}_j translated back into the unit square yield a generating partition labelled by the 5-letter alphabet (18.10), with (d) the finite grammar given by the transition graph for this partition. The nodes refer to the rectangles A and B , and the five links correspond to the five sub-rectangles induced by one step forward-time dynamics. (Compare with figure 1.2. For details, see ChaosBook [19]).

This orbit should be inadmissible since it contains the pruned block 22, and indeed the corresponding periodic points fall outside the unit interval, $\{x_1, x_2\} > 1$. Examples of two admissible 4-cycles:

$$\begin{bmatrix} 0 \\ 2 \\ 0 \\ 0 \end{bmatrix} \Rightarrow X = \frac{1}{15} \begin{bmatrix} 6 \\ 14 \\ 6 \\ 4 \end{bmatrix}; \quad \begin{bmatrix} 0 \\ 1 \\ 1 \\ 0 \end{bmatrix} \Rightarrow X = \frac{1}{3} \begin{bmatrix} 1 \\ 2 \\ 2 \\ 1 \end{bmatrix}$$

We can verify that these are periodic orbits by iterating

$$\mathbf{A} \begin{bmatrix} x_{t-1} \\ x_t \end{bmatrix} = \begin{bmatrix} x_t \\ x_{t+1} \end{bmatrix} + \begin{bmatrix} 0 \\ m_t \end{bmatrix}. \quad (18.8)$$

2018-02-11 Predrag Very nice! Let's take your Green's function (18.6) for 4-cycles

$$g = \frac{1}{15} \begin{bmatrix} 7 & 3 & 2 & 3 \\ 3 & 7 & 3 & 2 \\ 2 & 3 & 7 & 3 \\ 3 & 2 & 3 & 7 \end{bmatrix} \quad (18.9)$$

but now test whether all period 4 closed walks on the transition graph of figure 18.7(d) yield admissible 4-cycles.

The partition figure 18.4(c) is labeled / colored by a 5-symbol alphabet (1.9):

$$\mathcal{A} = \{1, 2, 3, 4, 5\} = \{A^0 A, B^1 A, A^1 A, B^0 B, A^1 B\}, \quad (18.10)$$

that labels the five sub-rectangles \mathcal{M}_{m_j} of the cat map phase space, $\mathcal{M} = \cup \mathcal{M}_{m_j}$, by the links of the transition graph of figure 1.9(d), with all admissible itineraries generated by all walks on the transition graph. Rational values correspond to periodic orbits, with the phase space periodic points uniquely labeled by the admissible itineraries of symbols from \mathcal{A} .

Bird and Vivaldi [12] tabulate the numbers of orbits (they call that $N_T(\lambda)$ in their Table 1, with $s = K = 3$ and 4),

$$\sum_{T=1}^{\infty} z^T N_T = z + 2z^2 + 5z^3 + 10z^4 + 24z^5 \dots \quad (18.11)$$

They say that there are $N_4(\lambda) = 10$ admissible period 4 orbits. They can be read off as walks on figure 18.4(d):

$$\begin{array}{ccccc} \overline{1113} & \overline{1125} & \overline{1245} & \overline{1253} & \overline{1325} \\ 0001 & 001\underline{1} & 010\underline{1} & 01\underline{11} & 011\underline{1} \\ \overline{1133} & \overline{3325} & \overline{3331} & \overline{3245} & \overline{4452} \\ 0011 & 111\underline{1} & 1110 & 110\underline{1} & 00\underline{11} \end{array} \quad (18.12)$$

with the corresponding translations read off the superscripts in (18.10). My sub-rectangles alphabet (18.10) is superfluous; the translations

$$m_t \in \{\underline{1}, 0, 1\} \quad (18.13)$$

from (18.10) alone label uniquely the admissible orbits, as they should, as the relation is linear. We have to figure out how to argue that reading $\{m_t\}$ off the graph alone suffices to label the orbit. Not obvious, as links 0 and 1 occur twice. Green 0 has to be followed by $\underline{1}$, the red 0 has to be followed by 3 or 2, so they are distinct. The blue 1 must eventually be followed by $\underline{1}$, but how is that different from the purple 1?

Some clever recoding idea is called for.

2018-02-11 Han I have computed all ten 4-cycles using Green's function (18.9) and plotted all their periodic points in figures 18.5 and 18.6.

$$M = \begin{bmatrix} 0 \\ 0 \\ 0 \\ 1 \end{bmatrix} \Rightarrow X_{0001} = \frac{1}{15} \begin{bmatrix} 3 \\ 2 \\ 3 \\ 7 \end{bmatrix}.$$

Likewise,

$$\begin{aligned} X_{001\underline{1}} &= \frac{1}{15} [-1 \ 1 \ 4 \ -4], & X_{010\underline{1}} &= \frac{1}{15} [0 \ 5 \ 0 \ -5] \\ X_{01\underline{1}\underline{1}} &= \frac{1}{15} [4 \ 6 \ -1 \ 6], & X_{011\underline{1}} &= \frac{1}{15} [2 \ 8 \ 7 \ -2] \\ X_{0011} &= \frac{1}{15} [5 \ 5 \ 10 \ 10], & X_{111\underline{1}} &= \frac{1}{15} [9 \ 11 \ 9 \ 1] \\ X_{1110} &= \frac{1}{15} [12 \ 13 \ 12 \ 8], & X_{110\underline{1}} &= \frac{1}{15} [7 \ 8 \ 2 \ -2] \\ X_{00\underline{1}\underline{1}} &= \frac{1}{15} [1 \ -1 \ -4 \ 4] \end{aligned} \quad (18.14)$$

I verified these orbits by finding the position of each point (ϕ_t, ϕ_{t+1}) on the partition \mathcal{M}_A or \mathcal{M}_B . They are all admissible. The count agrees with table 4.1.

2018-02-11 Predrag It feels like magic; we know that what the 2-rectangle partition is, and we have derived the transition graph of figure 18.4(d), and that by similarity transformation this is the same for any $s = 3$ cat map, but it is still not obvious that the 3-letter alphabet (18.13) does the job. I assume you have not checked any of the original literature, but I do not recall seeing such alphabet...

2018-02-11 Predrag Next: I have mostly solved and moved example 1.4 *Perron-Frobenius operator for the Arnol'd cat map* to section sect. 1.10 Examples. It would be good if you worked through it and understood the transfer

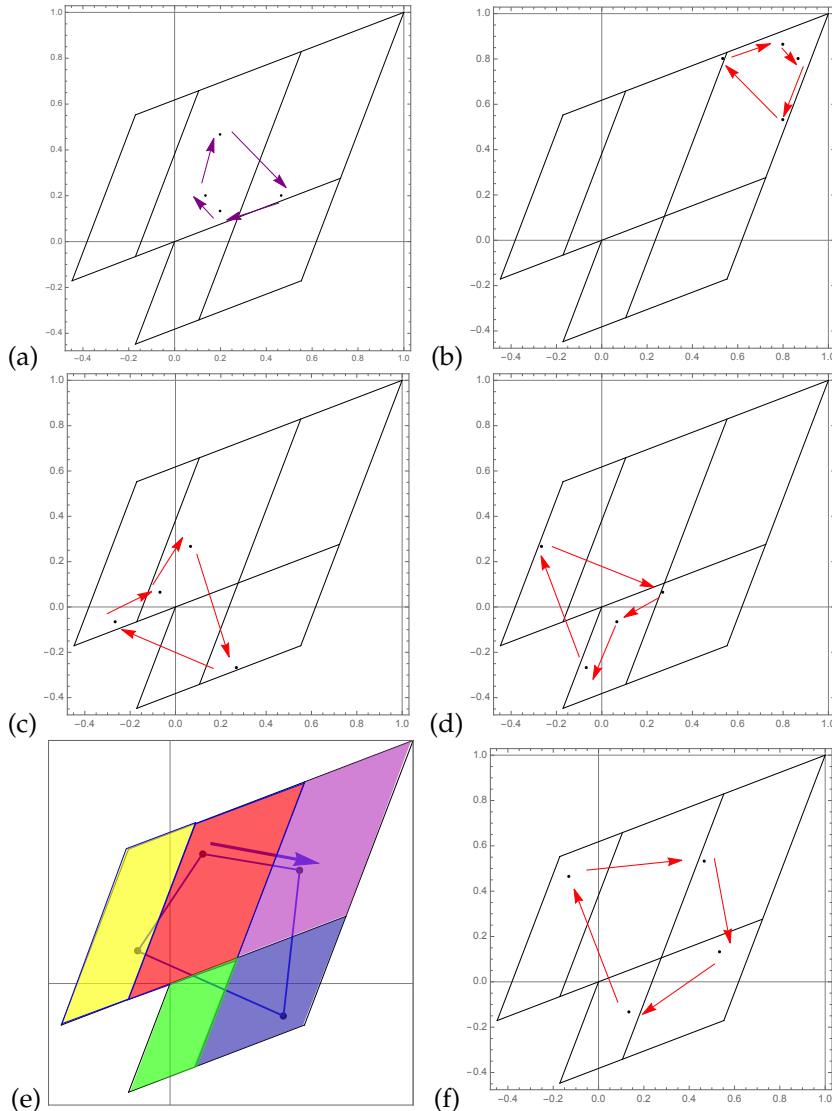


Figure 18.5: Abandoned attempt: All 4-cycles from (18.14): (a) $X_{0001} = X_{1113}$, (b) X_{1110} , (c) X_{0011} , (d) X_{0011} , (e) X_{0111} , (f) X_{1101} , (g) to (j) continued in figure 18.6.

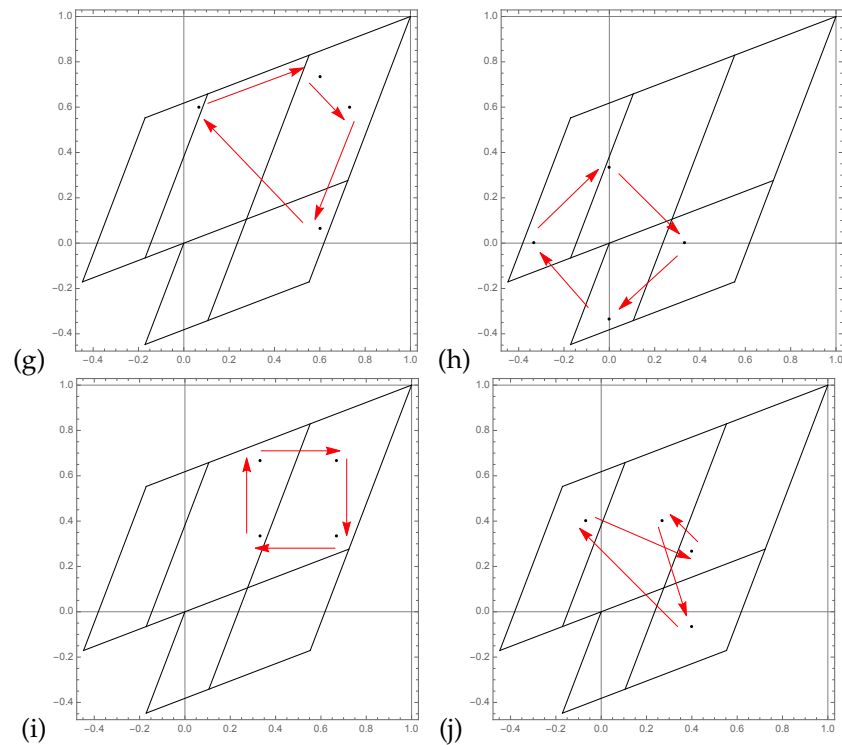


Figure 18.6: Continuation of figure 18.5: (g) X_{1111} , (h) X_{0011} , (i) X_{0011} , and (j) X_{0111} ,

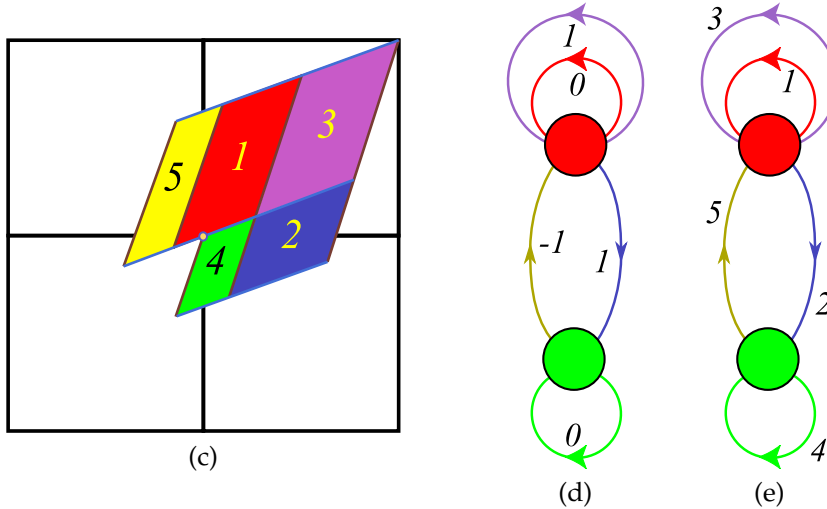


Figure 18.7: (Figure 18.4 continued) (c) The sub-rectangles \mathcal{M}_j , indicated by the compact 5-letter alphabet (18.10). (d) Admissible orbits correspond to walks on the transition graph for this partition. The nodes refer to the rectangles A and B , and the five colored links, labeled by their lattice translation $m_j \in \{\underline{1}, 0, 1\}$, correspond to the five sub-rectangles reached in one step forward-time dynamics. (e) Compact labeling, see (18.10).

matrix L (1.110), which I am reading off figure 18.7, in particular computed its eigenvalues (interpret the $\lambda = 1$ eigenvalue) and eigenvectors (the leading one should be the natural measure). Here

$$s = 3, \text{ so } \Lambda = \frac{3 + \sqrt{5}}{2} = 2.6180, \text{ and } D = 5.$$

2018-02-12 Predrag Can you plot the stretched domains corresponding to figure 18.4(b) for one step back in time (inverse map)? Should look something like figure 18.8.

2018-03-01 Han I have calculated the stretched domains corresponding to figure 18.4(b) for one step back in time. The result is in figure 18.9(c) which is not the same as figure 18.8(b). I guess this is because I start from partition in figure 18.9(a). If I start from the partition flipped from figure 18.9(a) across the $\phi_1 = \phi_0$ I will get figure 18.8(b). The overlap 2 partition is also different from figure 18.8(c). I'm not sure...

2018-03-01 Predrag My figure 18.8 was just a quick sloppy sketch. I'm confident that your figure 18.9 is right.

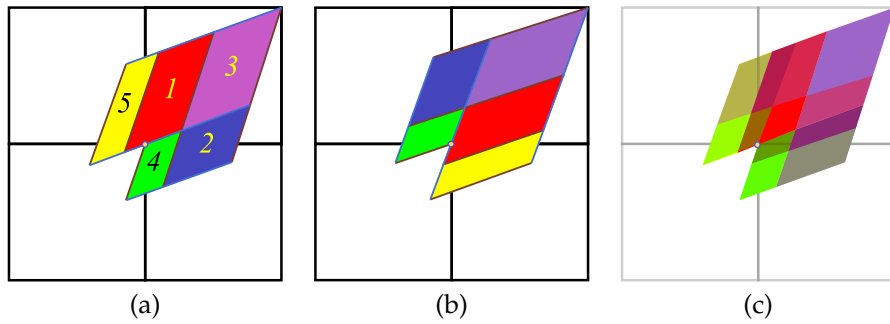


Figure 18.8: (From figure 18.4) (a) The forward in time sub-rectangles \mathcal{M}_j , indicated by color / 5-letter alphabet (18.10). (b) The corresponding partition defined for one step backward in time (not the partition (a) iterated back). (c) The overlap 2-step partition. Not sure this is right.

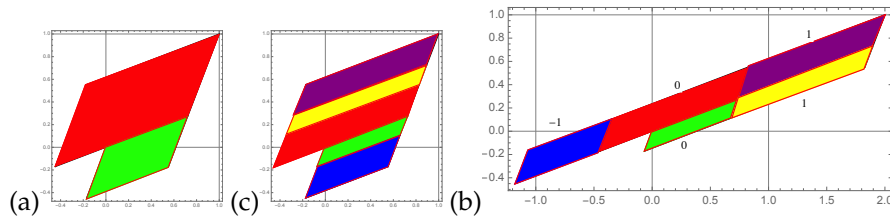


Figure 18.9: (a) The two rectangles partition of the Percival-Vivaldi cat map. (b) Mapped one step backward in time. (c) The stretched partition has been translated back to the original shape.

2018-02-15 Han I have read the section *Markov Partitions for Hyperbolic Toral Automorphisms* of Robinson's book. I'm currently working on example 1.4. The (1.110) seems not correct. I'm working on it.

2018-02-16 Predrag I'm complicating this unnecessarily - it would be nice to get the correct 5-rectangles transfer matrix (1.110), but it is unnecessary for our purposes: the two-rectangle partition $[2 \times 2]$ Markov matrix, where one sums over all admissible transitions, should suffice (for notation, see (18.10) and ref. [20]):

$$\begin{bmatrix} \phi'_A \\ \phi'_B \end{bmatrix} = L\phi = \begin{bmatrix} L_{A^0A} + L_{A^1A} & L_{A^1B} \\ L_{B^1A} & L_{B^0B} \end{bmatrix} \begin{bmatrix} \phi_A \\ \phi_B \end{bmatrix} \quad (18.15)$$

$$\begin{aligned} L &= \begin{bmatrix} L_{A^0A} + L_{A^1A} & L_{A^1B} \\ L_{B^1A} & L_{B^0B} \end{bmatrix} = \begin{bmatrix} \frac{|\mathcal{M}_1|+|\mathcal{M}_3|}{|\mathcal{M}_A|} & \frac{|\mathcal{M}_5|}{|\mathcal{M}_A|} \\ \frac{|\mathcal{M}_2|}{|\mathcal{M}_B|} & \frac{|\mathcal{M}_4|}{|\mathcal{M}_B|} \end{bmatrix} \\ &= \frac{1}{\Lambda} \begin{bmatrix} 2 & \Lambda - 2 \\ \Lambda - 1 & 1 \end{bmatrix}. \end{aligned} \quad (18.16)$$

in compact notation $\{A^0A, B^1A, A^1A, B^0B, A^1B\} = \{1, 2, 3, 4, 5\}$. Then

$$\begin{aligned} \text{Det}(1 - zL) &= \begin{vmatrix} 1 - 2z/\Lambda & -z(\Lambda - 2)/\Lambda \\ -z(\Lambda - 1)/\Lambda & 1 - z/\Lambda \end{vmatrix} \\ &= 1 - 3\frac{z}{\Lambda} + 2\frac{z^2}{\Lambda^2} - \frac{z^2}{\Lambda^2}(\Lambda - 1)(\Lambda - 2) \\ &= 1 - 3\frac{z}{\Lambda} - \frac{z^2}{\Lambda}(\Lambda - 3), \end{aligned} \quad (18.17)$$

in agreement with the loop expansion (1.112).

2018-02-16 Predrag For $s \geq 3$, the 3-letter alphabet (1.9) generalizes to

$$\mathcal{A} = \{\underline{1}, 0, 1, \dots, s-2\}. \quad (18.18)$$

What keeps the forward iterates of the small rectangle in check is the way this area shrinks with large Λ in (1.109).

2018-02-18 Han For $s \geq 3$ the alphabet for the 2- (and 3-) rectangle partition is (18.18): see the 3-rectangle stable and unstable manifolds borders partition for $s = 5$ in figure 18.10.

2018-02-18 Predrag Great. It should lead to more sensible labelling of figure 18.7 (e) transition graph, for arbitrary s . You can see that, much like in the Percival-Vivaldi figure 1.2, there is an *interior* $(s-1)$ -letter alphabet \mathcal{A}_0 which is a full shift ($(s-1)$ loops attached to node A), and some kind of 2-letter *exterior* alphabet \mathcal{A}_1 that has to do with node B .

A well-understood alphabet can help us with solving the 2-dimensional spatiotemporal cat - there the interior alphabet \mathcal{A}_0 is still a full shift, while the exterior alphabet \mathcal{A}_1 is a bit bigger.

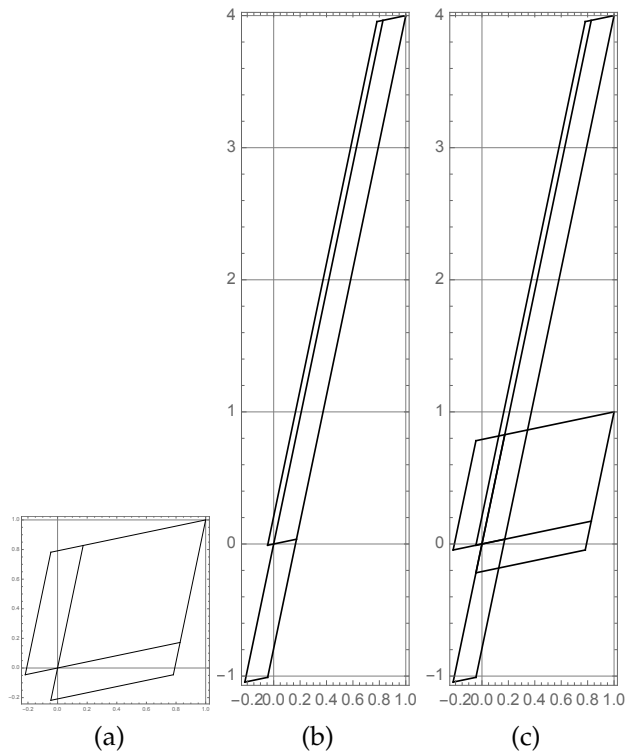


Figure 18.10: (a) The 3-rectangle partition for $s = 5$. (b) The first forward iterate of the partition. (c) I put (a) and (b) together so it obvious that the alphabet is from -1 to 4 .

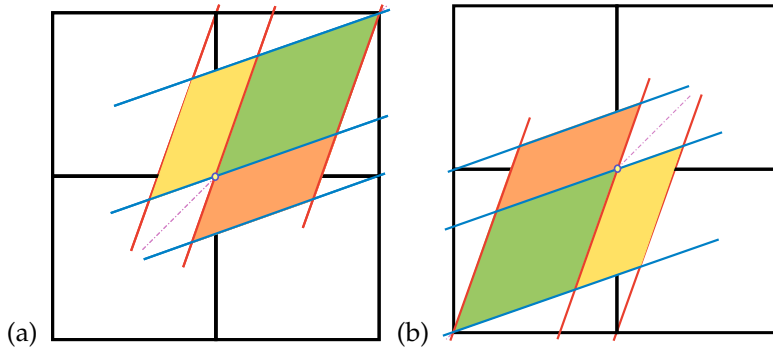


Figure 18.11: Abandoned attempt: (a) The three-rectangle, time reversal symmetric generating partition for the Percival-Vivaldi cat map (1.5), with borders given by cat map stable-unstable manifolds. (b) The three-rectangle partition obtained by space reversal (reflection across the anti-diagonal) is also a valid generating partition, but the distinct from (a). Thus this partition does not exhibit in a simple way the space reflection symmetry that is evident in figure 1.2.

2018-02-19 Predrag The alphabet (18.13), $m_t \in \{\underline{1}, 0, 1\}$ is not good, as it seems not to encode any of the symmetries of orbits in figures 18.5 and 18.6.

2018-02-19 Predrag I wonder why all cycles (except for a small kink in X_{0111}) turn clockwise? Reminds me of harmonic oscillator, that also has a unique rotation direction - might be a consequence of symplectic dynamics.

2018-02-27 Han I have read the Chapter 15 *Counting* of Chaosbook. It's not easy. Finally have some general ideas about the topological zeta function.

2018-01-31 Han Matrices (1.8) can diagonalize (1.5) (I may be wrong).

2018-02-13 Predrag Your Green's function is symmetric. Diagonalize?

2018-02-13 Han The eigenvalues of this Green's function are $1, 1/3, 1/3, 1/5$. These are also the diagonal elements of the diagonalized matrix.

2018-02-13 Predrag Mhm - you sure? I was expecting $\sqrt{5}$'s. What about eigenvectors? Try period-5. 5 is a prime.

2018-02-13 Han When the circulant matrix and the Green's function are $[5 \times 5]$ matrices, the eigenvalues of the Green's function are

$$1, (7 + \sqrt{5})/2, (7 + \sqrt{5})/2, (7 - \sqrt{5})/2, (7 - \sqrt{5})/2, \quad (18.19)$$

corresponding to eigenvectors:

$$(1, 1, 1, 1, 1), \\ ((-1 + \sqrt{5})/2, (1 - \sqrt{5})/2, -1, 0, 1),$$

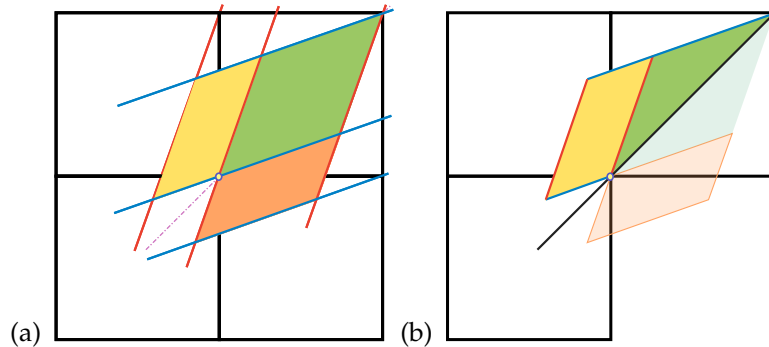


Figure 18.12: Abandoned attempt: (a) The three-rectangle, time reversal symmetric generating partition for the Percival-Vivaldi cat map (1.5), with borders given by cat map stable-unstable manifolds. Large rectangle is self-dual under time reversal (reflection across the diagonal), while the two small rectangles are mapped into each other. This implies that we should go to a fundamental domain (positive time only), and recode the dynamics according to example 4.11 D_1 factorization: (b) The three-rectangle partition time reversal fundamental domain (the half of the full partition, cut in two by the time reflection diagonal). Need to check whether we can handle the reflection of m_n as well.

$$\begin{aligned} & (-1, (1 - \sqrt{5})/2, (-1 + \sqrt{5})/2, 1, 0), \\ & ((-1 - \sqrt{5})/2, (1 + \sqrt{5})/2, -1, 0, 1), \\ & (-1, (1 + \sqrt{5})/2, (-1 - \sqrt{5})/2, 1, 0). \end{aligned}$$

2018-02-13 Predrag Mhm - surprised again. I was motivated by (1.38) and (1.94), and expected you to (re)discover sort of a [discrete Fourier transform](#), but with hyperbolic functions. Back to drawing board.

2018-04-22 Predrag Fourier-transformed cycle points \hat{M} for the periodic points

of figure 18.5:

$$\begin{aligned}
 \hat{M}_{0001} &= \frac{1}{2} [1, -i, -1, i] \Rightarrow \hat{\phi} = [0, , 0,] \\
 \hat{M}_{1110} &= \frac{1}{2} [3, i, 1, -i] \Rightarrow \hat{\phi} = [0, , 0,] \\
 \hat{M}_{001\underline{1}} &= \frac{1}{2} [0, -1 + i, 2, -1 - i] \Rightarrow \hat{\phi} = [0, , ,] \\
 \hat{M}_{00\underline{1}1} &= \frac{1}{2} [0, 1 - i, -2, 1 + i] \Rightarrow \hat{\phi} = [0, , ,] \\
 \hat{M}_{011\underline{1}} &= \frac{1}{2} [1, -1 + 2i, 1, -1 - 2i] \Rightarrow \hat{\phi} = [0, , ,] \\
 \hat{M}_{110\underline{1}} &= \frac{1}{2} [1, 1 + 2i, 1, 1 - 2i] \Rightarrow \hat{\phi} = [0, , ,] \\
 \hat{M}_{111\underline{1}} &= \frac{1}{2} [2, 2i, 2, -2i] \Rightarrow \hat{\phi} = [, , ,] \\
 \hat{M}_{001\underline{1}} &= \frac{1}{2} [0, -1 + i, 2, -1 - i] \Rightarrow \hat{\phi} = [, , ,] \\
 \hat{M}_{0011} &= \frac{1}{2} [2, -1 - i, 0, -1 + i] \Rightarrow \hat{\phi} = [0, , ,] \\
 \hat{M}_{01\underline{1}1} &= \frac{1}{2} [1, 1, -3, 1] \Rightarrow \hat{\phi} = [0, , ,]
 \end{aligned}
 \tag{18.20}$$

Each cycle has 3 further cycle points, not computed here (but that should be plotted in the Brillouin zone). I did not compute $\hat{\phi}_k$, as that is a trivial multiplication by the diagonalized Green's function (18.33).

Take home messages; writing Fourier transforms of periodic points analytically is not useful. Only cycle-4 orbits are related to Gaussian integers, for other orbits there will be no nice analytic formulas. And already for 4-cycles, the phases are not rational fractions of 2π . For example for $1+2i$ the polar form phase in radians is $\arctan 2 = 1.10715$.

2018-02-21 Predrag The Green's function (18.9) and eigenvalues and eigenvectors (18.19) all have Toeplitz matrix structure. In case like this, when the problem has been around for centuries, reading literature is a great time saver, especially if someone has already done the dive into literature for you. You can understand your Mathematica results by the analytic solution for any cycle lengths and any s , for example (1.52) and (1.55). Here you learn, explicitly, that for $s > 2$, the lattice should not be expanded in Fourier modes, but in sinh and cosh's. There are some other cute formulas in literatures, for example (1.94) and (1.95).

2018-04-25 Predrag Reciprocal lattice is standard. I think you need to use stable / unstable eigenvectors in configuration space, compute reciprocal lattice with respect to them. Will continue writeup (unless you beat me to it:)

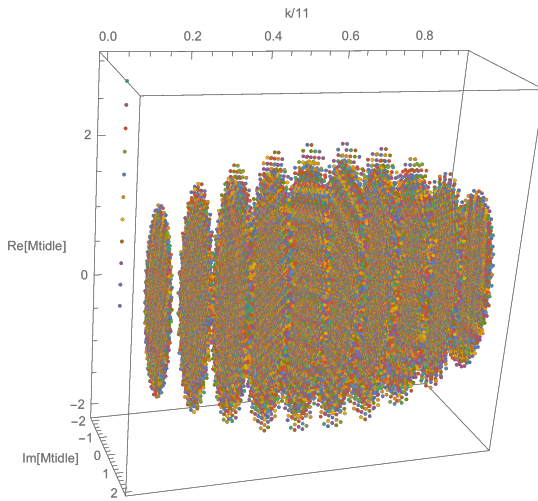


Figure 18.13: The Fourier transform of the 39601 period $n = 11$ lattice states (see (1.14)) of the rhomboid corner partition in the complex plane.

2018-04-25 Predrag Scratch stable / unstable eigenvectors - there is no integer-multiple tiling along those directions (I guess it is a antiperiodic tiling), the only configuration space vector is 1-dimensional, pointing for Percival-Vivaldi cat map along the vertical direction.

2018-04-22 Predrag Trying to get some feeling for the Fourier space representation, by computing the rhomboid corner partition 4-cycles (18.20), to see how they differ from the rhomboid center partition 4-cycles (18.32). The main take home message; analytic form of these Fourier transforms does not seem helpful, seems best to plot them numerically, in complex plane for the reciprocal lattice / Brillouin zone (not attempted yet).

2018-04-25 Han I plotted all of the admissible 11-cycles of the rhomboid corner partition in complex plane in figure 18.13. It looks like if I plot the figure with k from -5 to 5 instead of from 0 to 10 (which is to move the part with $k > 5$ to the left side of the origin), this figure will be symmetric about $k = 0$ plane. I tried to make some changes to the figure but the program keep getting frozen when I plot the figure. I will try again later on a desktop.

2018-04-25 Predrag Fascinating. Is it possible to generate a version that is 3D live (can be rotated)? Also, we need to plot these in the Brillouin zone, not just raw Fourier...

18.2 Rhomboid center partition

A generating partition must map borders onto borders under dynamics (Adler-Weiss), but a really nice partition should also embody all symmetries of the dynamics; invariance under spatial reflections and the time reversal.

For the Percival-Vivaldi cat map the dynamics commutes with the spatial reflection σ (across anti-diagonal), while time reversal will require extra thinking.

For the Percival-Vivaldi cat map the flip across the $\phi_1 = \phi_0$ diagonal together with the reversal of the direction of evolution is the D_1 symmetry that corresponds to the invariance of cat map under time reversal.

2018-04-20 Predrag Currently figure 18.16 (b) does not map a border onto a border within region D of figure 18.17 (a); sadly, the partition studied in this section is not generating.

2018-02-18 Predrag Percival-Vivaldi alphabet can be made symmetric under spatial reflection by picking the origin in the middle of the unit interval, see sect. ???. The tiling figure 1.4 (b) and the partition figure 18.3 (b) suggests that partition should be centered differently to fully exploit the symmetries of the tiling - perhaps with the fixed point in the center of the square, rather with the fixed point in the corner.

2018-02-28 Predrag A proposal for a space and time symmetric partition in figure 18.14. Do you see how to fix it?

2018-02-28, 018-03-18 Han Yes! A space reflection symmetric partition in figure 18.14 is obtained by cutting the yellow and orange rectangles into halves, as shown in figure 18.15. That is natural in the centered unit square tiling of the plane, i.e., the grid going through multiples of $(1/2, 1/2)$. Figure 18.15(c) shows that this partition tiles the whole space. The forward image of the partition of figure 18.15 (b) figure 18.16. Figure 18.16 is the labeled 7-rectangle partition, together with the transition graph. The alphabet is

$$m_t \in \{\underline{2}, \underline{1}, 0, 1, 2\} . \quad (18.21)$$

2018-03-18 Predrag Staring at the partition of figure 18.16: no wander I failed to draw it by hand. In figure 18.16 (b) there are little holes next to D and G and the weird overlaps $\mathcal{M}_D \cap f(\mathcal{M}_E)$, $\mathcal{M}_G \cap f(\mathcal{M}_F)$, it's a miracle that the partition works. You might want to check it for longer period orbits in \mathcal{M}_D .

2018-03-05 Han All period 4 orbits in the symmetric partition figure 18.15 (b)

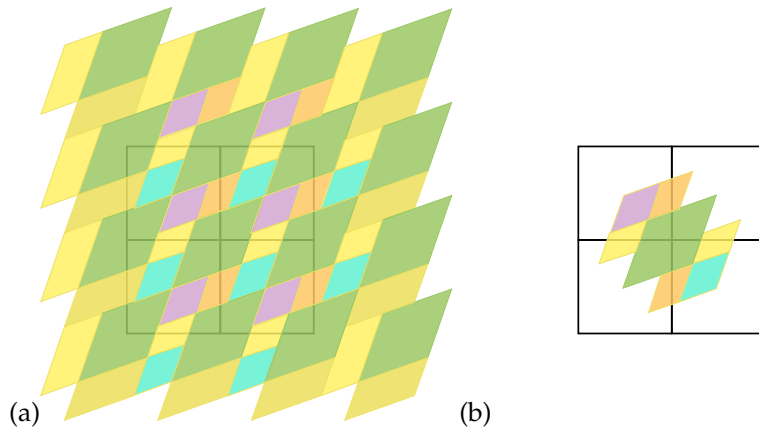


Figure 18.14: Abandoned attempt: (a) Tiling of the square lattice by a five-rectangle, time reversal and space reflection symmetric partition. Note that we have used the continuous translation invariance to place the center of the large tile A at the origin. (b) An almost generating five-rectangle, time reversal and space reflection symmetric partition, except that the yellow / orange rectangles appear twice, so the area this covers exceeds the unit area.

are

$$\begin{aligned}
 X_{1111} &= \frac{1}{15} [5 \ 5 \ -5 \ -5] , & X_{0202} &= \frac{1}{15} [0 \ -10 \ 0 \ 10] \\
 X_{0011} &= \frac{1}{15} [-1 \ 1 \ 4 \ -4] , & X_{0011} &= \frac{1}{15} [1 \ -1 \ -4 \ 4] \\
 X_{1221} &= \frac{1}{15} [2 \ -7 \ 7 \ -2] , & X_{2211} &= \frac{1}{15} [7 \ -7 \ 2 \ -2] \\
 X_{0111} &= \frac{1}{15} [4 \ 6 \ -1 \ 6] , & X_{1011} &= \frac{1}{15} [-6 \ -4 \ -6 \ 1] \\
 X_{1012} &= \frac{1}{15} [3 \ 2 \ 3 \ -8] , & X_{1012} &= \frac{1}{15} [-3 \ -2 \ -3 \ 8]
 \end{aligned} \tag{18.22}$$

The orbits are in figures 18.18 and 18.20. All orbits are symmetric about both $\phi_1 = \phi_0$ and $\phi_1 = -\phi_0$, either self-dual or come in pairs.

2018-03-05 Predrag Beautiful! We have the doubly symmetric partition nailed. I do not think this is anywhere in the literature. Can you connect to symmetries to cycle itineraries?

2018-04-08 Han I have recomputed the 4-cycles of (18.22) in the face-centered Percival-Vivaldi unit square non-partition. That screws up the above

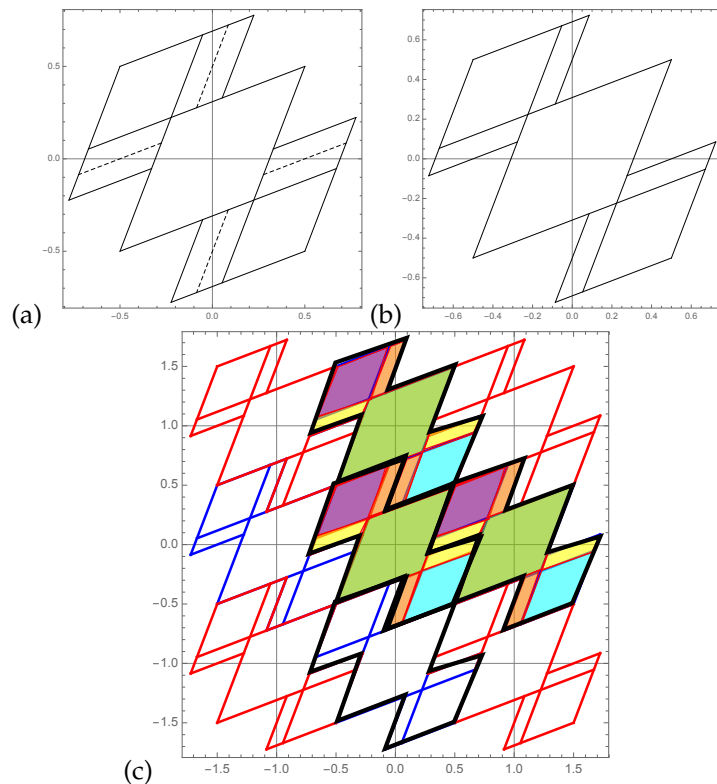


Figure 18.15: (a) Start with the partition of figure 18.14 (b). The dashed lines in the directions of stable and unstable manifolds cut the yellow and orange rectangles into halves. (b) The symmetric partition obtained by removing halves of yellow and orange rectangles has area 1. (c) The partition tiles the square lattice.

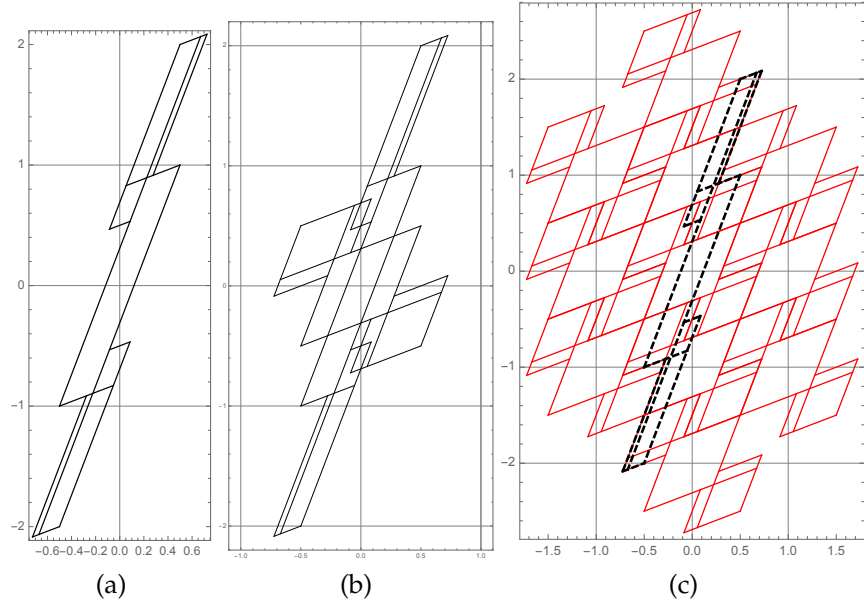


Figure 18.16: (a) The forward image of the 7-rectangle partition figure 18.15 (b). (b) The stretched partition overlaid over the original partition. (c) The stretched partition overlaid over the tiled lattice. The x and y axes are not plotted to the same scale.

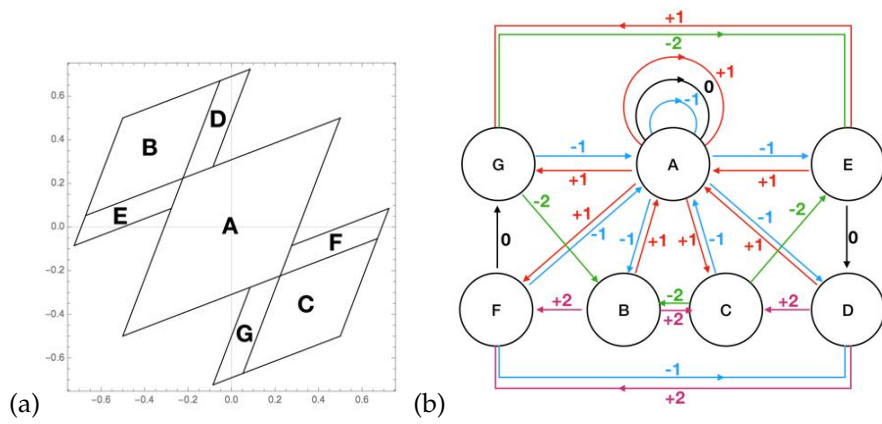


Figure 18.17: (a) The labeled 7-rectangle partition, and (b) the corresponding 7-node transition graph.

X_{1012} , X_{0202} , and $X_{\underline{1}012}$:

$$\begin{aligned}
 X_{\underline{1}111} &= \frac{1}{15} \begin{bmatrix} -5 & -5 & 5 & 5 \end{bmatrix}, & X_{\underline{1}010} &= \frac{1}{15} \begin{bmatrix} -5 & 0 & 5 & 0 \end{bmatrix} \\
 X_{00\underline{1}1} &= \frac{1}{15} \begin{bmatrix} -1 & 1 & 4 & -4 \end{bmatrix}, & X_{00\underline{1}1} &= \frac{1}{15} \begin{bmatrix} 1 & -1 & -4 & 4 \end{bmatrix} \\
 X_{1\underline{2}21} &= \frac{1}{15} \begin{bmatrix} 2 & -7 & 7 & -2 \end{bmatrix}, & X_{2\underline{2}11} &= \frac{1}{15} \begin{bmatrix} 7 & -7 & 2 & -2 \end{bmatrix} \\
 X_{01\underline{1}1} &= \frac{1}{15} \begin{bmatrix} 4 & 6 & -1 & 6 \end{bmatrix}, & X_{\underline{1}011} &= \frac{1}{15} \begin{bmatrix} -6 & -4 & -6 & 1 \end{bmatrix} \\
 X_{0001} &= \frac{1}{15} \begin{bmatrix} 3 & 2 & 3 & 7 \end{bmatrix}, & X_{\underline{1}000} &= \frac{1}{15} \begin{bmatrix} -7 & -3 & -2 & -3 \end{bmatrix}
 \end{aligned} \tag{18.23}$$

2018-03-05 Predrag I still think that if one day you plot all cycle *points* (no lines connecting them) on a single copy of the generating partition, you'll find the resulting picture very cute:

A hint from literature: Percival and Vivaldi [51] write: "For the cat maps the periodic orbits lie on a rational lattice, so all surds cancel, as shown in the companion paper [52] on the number theory of the periodic orbits of the automorphisms of the torus."

Sect. 19.2 *Numbers of periodic orbits* and sect. 20.2.1 *Periodic orbits - first approach* might also help with developing some intuition about figure 18.22.

2018-03-07 Predrag The alphabet (18.21) seems to make sense. Space reflection acts as

$$j \leftrightarrow \underline{j}. \tag{18.24}$$

The total translation (the sum of symbols) is zero (the orbit is periodic, standing) for all, except for figure 18.20(i) and (j) which translate by ± 1 (the orbit is relative periodic, running).

The time reversal should reverse the order of symbols, which it seems to do, at least for figures 18.18 and 18.20:

$$(c, d) \ 001\underline{1} \leftrightarrow 00\underline{1}1, \quad (e, f) \ \underline{1}1\underline{2}2 \leftrightarrow 2\underline{2}11, \tag{18.25}$$

rest self-dual.

2018-03-15 Han In figure 18.22 I plotted all the cycle points on a single copy of the partition for both partitions of figures 18.4 and 18.15.

2018-03-22 Han I have added the period 1, 2 and 3 orbits to figure 18.23. The period 1 and 2 orbits fill the holes of figure 18.22(b). Each of the period 3 orbits has only one symmetry, and they have the other symmetry in pairs.

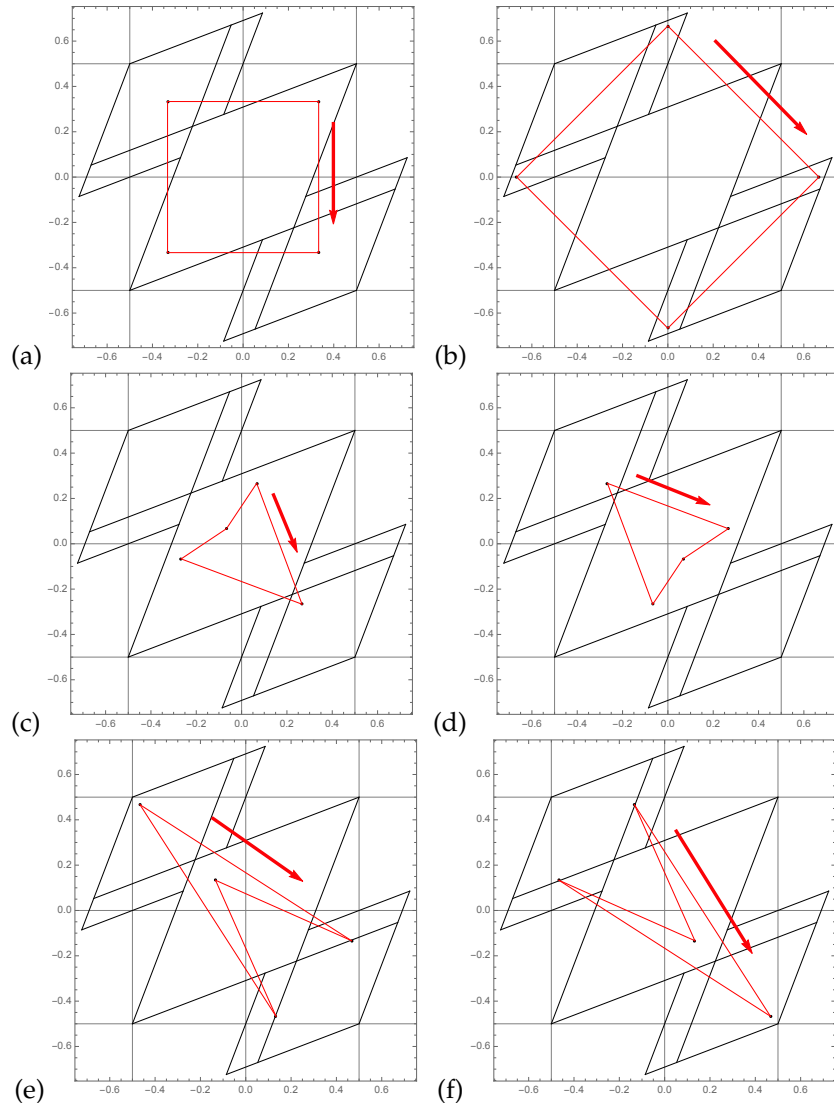


Figure 18.18: All 4-cycles from (18.22): (a) $X_{11\bar{1}\bar{1}}$ (b) $X_{02\bar{0}2}$, (c) $X_{00\bar{1}\bar{1}}$, (d) $X_{00\bar{1}1}$, (e) $X_{1\bar{1}2\bar{2}}$, (f) $X_{2\bar{2}1\bar{1}}$, (g) to (j) continued in figure 18.20.

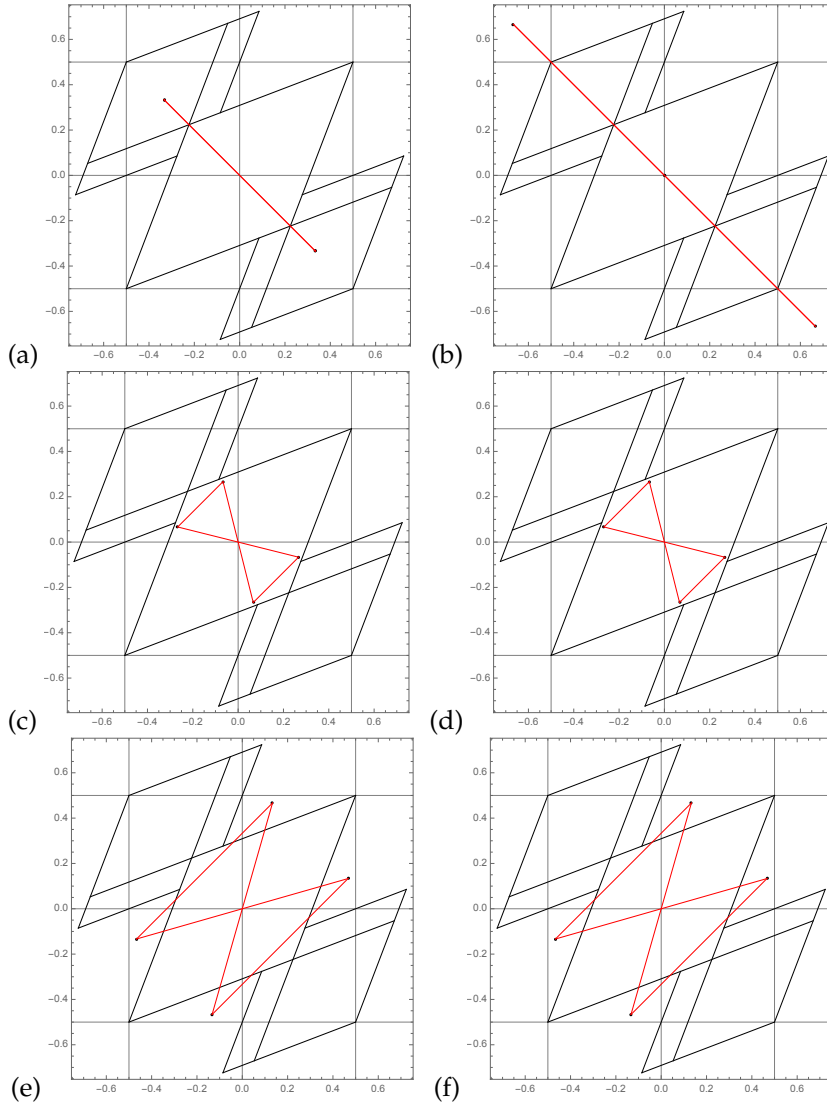


Figure 18.19: All 4-cycles from (18.22) plotted in “Lagrangian” coordinates $\{\phi_{t-1}, \phi_{t+1}\}$, in the order of figure 18.18. The 7-rectangle partition figure 18.15(b), appropriate to $\{\phi_t, \phi_{t+1}\}$ plots, is included only to guide the eye. (a) $X_{1\underline{1}11}$ is a “Laplacian” self-retracing 2-cycle (18.37). (b) $X_{0\underline{2}02}$ is a “Laplacian” self-retracing 2-cycle (18.38). (c) $X_{001\underline{1}}$ and its time reversal (d) $X_{001\underline{1}}$ map into one cycle; (e) $X_{1\underline{2}21}$ and its time reversal (f) $X_{2\underline{2}11}$ map into one cycle; (g) to (j) continued in figure 18.21.

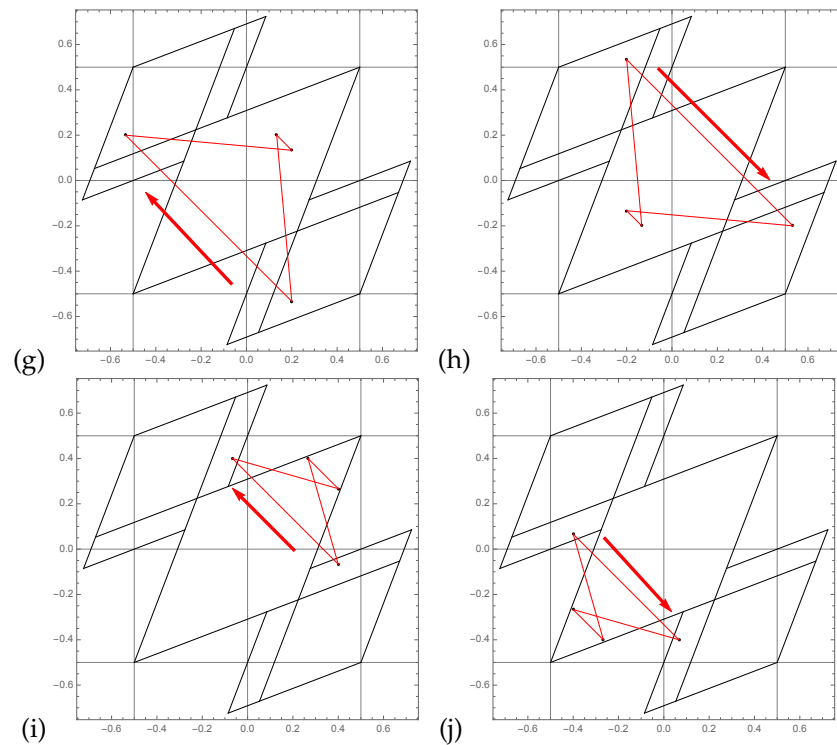


Figure 18.20: Continuation of figure 18.18: (g) X_{1012} , (h) $X_{10\underline{1}2}$ (i) X_{0111} , and (j) $X_{011\underline{1}}$,

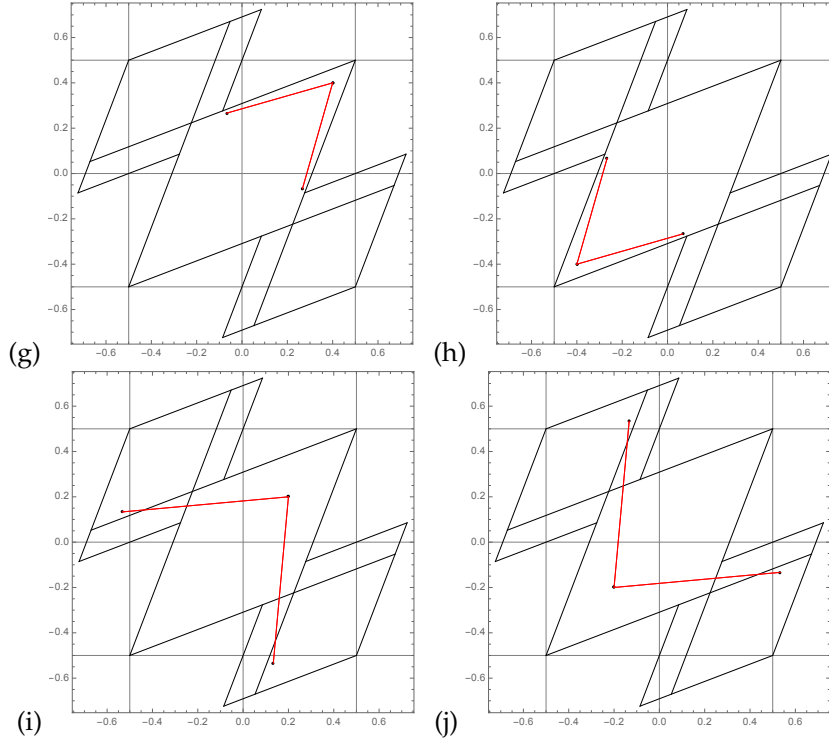


Figure 18.21: Continuation of figure 18.19 - the space reflection dual pairs: (g) X_{0111} and its time reversal (h) X_{1011} map into space-reflection dual 4-cycles; (i) X_{1012} and (j) X_{1021} map into space-reflection dual 4-cycles.

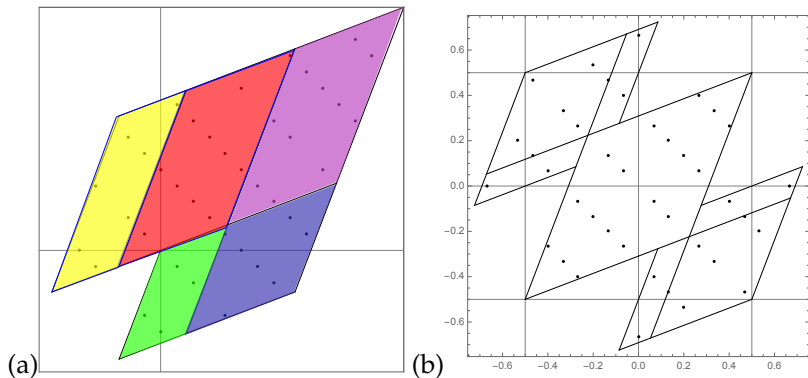


Figure 18.22: All period 4 orbits in the partition of (a) figure 18.4, and (b) figure 18.15. The holes correspond to missing cycle-1 and cycle-2 points.

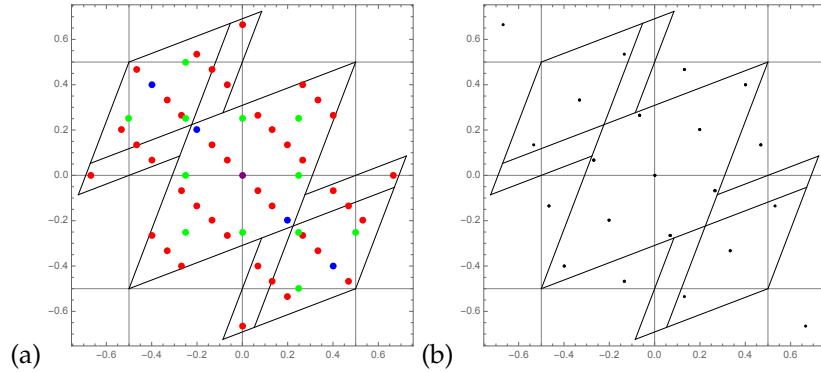


Figure 18.23: (a) All periodic points that belong to the 1 (purple), 2 (blue) and 4 (red) orbits, plotted in “Hamiltonian” coordinates $\{\phi_t, \phi_{t+1}\}$. The period 1- and 2-orbits fill the holes between period 4 orbits in the figure 18.22 (b). The 3 (green) orbits start a new grid, to be filled out by the period 6, 9, etc orbits. (b) All periodic points that belong to the period 4 orbits of figure 18.23 plotted in “Lagrangian” coordinates $\{\phi_{t-1}, \phi_{t+1}\}$. The 7-rectangle partition figure 18.15 (b), appropriate to $\{\phi_t, \phi_{t+1}\}$ plots, is included only to guide the eye. The numbers of orbits are listed in (18.11).

2018-03-13 Predrag An aside, not even right, a failed attempt kept here only for the record: going from the partition of figure 18.4 to the partition of figure 18.15 we have translated the origin to $\hat{\phi}_t = \phi_t - 1/2$, so the map (1.5) is now

$$\begin{bmatrix} \hat{\phi}'_{t+1} \\ \hat{\phi}'_t \end{bmatrix} = \mathbf{A} \begin{bmatrix} \hat{\phi}_t \\ \hat{\phi}_{t-1} \end{bmatrix} - \frac{1}{2} \begin{bmatrix} 0 \\ s-2 \end{bmatrix}. \quad (18.26)$$

I'm not sure why we would be allowed to drop such translational terms. A cute fact is that Percival and Vivaldi [51] actually define the map (1.5) on $\phi_t \in [-1/2, 1/2]$ interval, i.e., without the translation term in (18.26). Such translations should not affect the map (it's the same automorphism of the torus, just in different coordinates) but I do not have a clean argument that they do not matter.

2018-03-15 Han We didn't change the origin when the partition changed from figure 18.4 to figure 18.15. The map is also not changed. What we did is changing the boundary of the partition. So the map is still:

$$\begin{bmatrix} \phi_{t+1} \\ \phi_t \end{bmatrix} = \mathbf{A} \begin{bmatrix} \phi_t \\ \phi_{t-1} \end{bmatrix}. \quad (18.27)$$

2018-04-20 Predrag Currently figure 18.16(b) does not map a border onto a border within region D of figure 18.17(a); it looks as though D would

have to be cut horizontally into two halves, and even that does not complete the task. So, sadly, the partition studied in this section is not generating, and (for time being?) we have to give up on the whole section.

18.2.1 Reduction to the reciprocal lattice

2018-03-18 Predrag Check in $d = 1$ whether (18.59) together with the inverse Fourier transform (18.63) recovers any of your periodic orbits?

Does the circulant eigenvalue formula (18.51) explain your (18.19)?

2018-03-19 Predrag Does the inverse Fourier transform of the propagator in (18.59) reproduce the usual $d = 1$ configuration Green's function (1.136)?

2018-03-22 Han In $d = 1$, (18.59) can recover the periodic orbits. (18.59) can be written as:

$$\hat{\phi} = \text{diag}(\lambda)^{-1} \hat{m}, \quad (18.28)$$

where λ is the eigenvalue of the damped Poisson matrix (18.49). Then we have:

$$\phi = U^\dagger \text{diag}(\lambda)^{-1} U m, \quad (18.29)$$

When $d = 1$, $s = 3$ and $n = 4$ (4-cycles),

$$\text{diag}(\lambda)^{-1} = \begin{pmatrix} 1 & 0 & 0 & 0 \\ 0 & 3 & 0 & 0 \\ 0 & 0 & 5 & 0 \\ 0 & 0 & 0 & 3 \end{pmatrix} \quad (18.30)$$

Then the Green's function for 4-cycle is:

$$g = U^\dagger \text{diag}(\lambda)^{-1} U = \frac{1}{15} \begin{pmatrix} 7 & 3 & 2 & 3 \\ 3 & 7 & 3 & 2 \\ 2 & 3 & 7 & 3 \\ 3 & 2 & 3 & 7 \end{pmatrix} \quad (18.31)$$

which is same as (18.9).

Using (18.51) we can also get the result of (18.19).

2018-04-18 Predrag Can you plot the Fourier space (18.59) points $\hat{\phi}_k$, \hat{m}_k corresponding to your periodic orbits of figure 18.23 (a)? Interpret what you get?

2018-04-18 Han $\hat{\phi}_k, \hat{m}_k$ for the periodic points of figure 18.23 (a):

$$\begin{aligned}
 \hat{M}_{1111} &= \begin{bmatrix} 0 & \sqrt{2}e^{i\pi/4} & 0 & \sqrt{2}e^{-i\pi/4} \end{bmatrix} \Rightarrow \hat{X} = \begin{bmatrix} 0 & \frac{\sqrt{2}e^{i\pi/4}}{3} & 0 & \frac{\sqrt{2}e^{-i\pi/4}}{3} \end{bmatrix} \\
 \hat{M}_{0202} &= \begin{bmatrix} 0 & -2e^{i\pi/2} & 0 & -2e^{-i\pi/2} \end{bmatrix} \Rightarrow \hat{X} = \begin{bmatrix} 0 & -\frac{2}{3}e^{i\pi/2} & 0 & -\frac{2}{3}e^{-i\pi/2} \end{bmatrix} \\
 \hat{M}_{0011} &= \begin{bmatrix} 0 & -\frac{e^{-i\pi/4}}{\sqrt{2}} & 1 & -\frac{e^{i\pi/4}}{\sqrt{2}} \end{bmatrix} \Rightarrow \hat{X} = \begin{bmatrix} 0 & -\frac{e^{-i\pi/4}}{3\sqrt{2}} & \frac{1}{5} & -\frac{e^{i\pi/4}}{3\sqrt{2}} \end{bmatrix} \\
 \hat{M}_{0011} &= \begin{bmatrix} 0 & \frac{e^{-i\pi/4}}{\sqrt{2}} & -1 & \frac{e^{i\pi/4}}{\sqrt{2}} \end{bmatrix} \Rightarrow \hat{X} = \begin{bmatrix} 0 & \frac{e^{-i\pi/4}}{3\sqrt{2}} & -\frac{1}{5} & \frac{e^{i\pi/4}}{3\sqrt{2}} \end{bmatrix} \\
 \hat{M}_{1221} &= \begin{bmatrix} 0 & -\frac{e^{i\pi/4}}{\sqrt{2}} & 3 & -\frac{e^{-i\pi/4}}{\sqrt{2}} \end{bmatrix} \Rightarrow \hat{X} = \begin{bmatrix} 0 & -\frac{e^{i\pi/4}}{3\sqrt{2}} & \frac{3}{5} & -\frac{e^{-i\pi/4}}{3\sqrt{2}} \end{bmatrix} \\
 \hat{M}_{2211} &= \begin{bmatrix} 0 & \frac{e^{-i\pi/4}}{\sqrt{2}} & 3 & \frac{e^{i\pi/4}}{\sqrt{2}} \end{bmatrix} \Rightarrow \hat{X} = \begin{bmatrix} 0 & \frac{e^{-i\pi/4}}{3\sqrt{2}} & \frac{3}{5} & \frac{e^{i\pi/4}}{3\sqrt{2}} \end{bmatrix} \\
 \hat{M}_{0111} &= \begin{bmatrix} 1/2 & 1/2 & -3/2 & 1/2 \end{bmatrix} \Rightarrow \hat{X} = \begin{bmatrix} 1/2 & 1/6 & -3/10 & 1/6 \end{bmatrix} \\
 \hat{M}_{0111} &= \begin{bmatrix} -1/2 & -1/2 & 3/2 & -1/2 \end{bmatrix} \Rightarrow \hat{X} = \begin{bmatrix} -1/2 & -1/6 & 3/10 & -1/6 \end{bmatrix} \\
 \hat{M}_{1012} &= \begin{bmatrix} 0 & e^{i\pi/2} & 2 & -e^{i\pi/2} \end{bmatrix} \Rightarrow \hat{X} = \begin{bmatrix} 0 & \frac{e^{i\pi/2}}{3} & 2/5 & -\frac{e^{i\pi/2}}{3} \end{bmatrix} \\
 \hat{M}_{1012} &= \begin{bmatrix} 0 & -e^{i\pi/2} & -2 & e^{i\pi/2} \end{bmatrix} \Rightarrow \hat{X} = \begin{bmatrix} 0 & -\frac{e^{i\pi/2}}{3} & -2/5 & \frac{e^{i\pi/2}}{3} \end{bmatrix}
 \end{aligned} \tag{18.32}$$

2018-04-18 Predrag The 0th Fourier component of $M = 0111$ equals $\hat{m}_0 = 1/2$, as it should.

I would expect the time-reversal pairs to be the complex-conjugate pairs in Fourier space, as C_4 shift moves them in opposite directions.

2018-04-18 Han The Green's function (18.59) that relates $\hat{\phi}_k$ to \hat{m}_k is:

$$\hat{\phi} = \begin{pmatrix} 1 & 0 & 0 & 0 \\ 0 & \frac{1}{3} & 0 & 0 \\ 0 & 0 & \frac{1}{5} & 0 \\ 0 & 0 & 0 & \frac{1}{3} \end{pmatrix} \hat{m} \tag{18.33}$$

If we shift the orbit to the left by one time step, each component of the Fourier transform will be multiplied by the C_4 cyclic group phase factor. For a 4-cycle the phase factors are

$$e^{-i2\pi k/4} = (1, e^{-i\pi/2}, -1, e^{-i3\pi/2}) = (1, i, -1, -i). \tag{18.34}$$

2018-04-18 Han The \hat{m} in (18.35) are transforming under the C_4 shift by phase factors (18.34). For example, the $1\underline{221}$ and $2\underline{211}$ which correspond to successive periodic points in the same 4-cycle, have the correct Fourier trans-

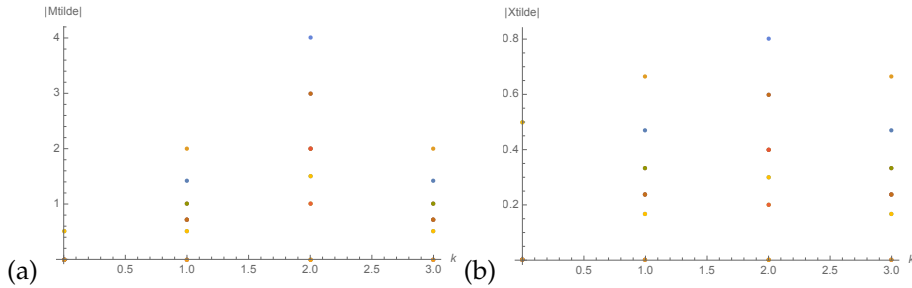


Figure 18.24: (a) The Fourier space points \hat{m}_k of all the periodic orbits with period 1, 2 and 4. The x-axis is k and y-axis is the absolute value of \hat{m}_k . (b) The Fourier space points $\hat{\phi}_k$.

forms,

$$\begin{aligned} m = \begin{bmatrix} 1 & -2 & 2 & -1 \end{bmatrix} &\Rightarrow \hat{m} = \begin{bmatrix} 0 & -\frac{e^{i\pi/4}}{\sqrt{2}} & 3 & -\frac{e^{-i\pi/4}}{\sqrt{2}} \end{bmatrix} \\ m = \begin{bmatrix} -2 & 2 & -1 & 1 \end{bmatrix} &\Rightarrow \hat{m} = \begin{bmatrix} 0 & -\frac{e^{-i\pi/4}}{\sqrt{2}} & -3 & -\frac{e^{i\pi/4}}{\sqrt{2}} \end{bmatrix} \end{aligned} \quad (18.35)$$

2018-04-18 Han I plot the Fourier space points of all of the orbits of period 1, 2 and 4 in figure 18.24 using the absolute value of $\hat{\phi}_k$ and \hat{m}_k .

2018-04-18 Predrag My hunch is that we do not want to plot the absolute values of $\hat{\phi}_k$. You might want to plot in the complex plane instead. We have to review what Brillouin zone means for 1D crystals. Mourigal, DeHeer and Berger students presumably understand that...

18.3 Time reversal

For our main thrust on understanding both the forward and backward in time, and the global temporal cat time-reversal symmetry, see sect. 4.2 *Temporal cat reversibility factorization*.

2018-02-12 Predrag Can you plot the stretched domains for one step back in time (inverse map)? The intersections of the past and future might help you intuition, in the way staring at the figure following figure 1.2 in Gutkin *et al.* [31] reveals the Smale-horseshoe structure.

Remember, our goal is to reformulate the problem in a global, Lagrangian way that is explicitly invariant under time reversal.

2018-02-19 Predrag The flip across the $\phi_1 = \phi_0$ diagonal together with the reversal of the direction of evolution is the D_1 symmetry that corresponds

to the invariance of cat map under time reversal. There are at least two kinds of orbits:

1. self-dual, here figure 18.5 (a) and (b), figure 18.6 (g), (h), (i) and (j)
 - even period cycles have $0, 2, 4, \dots$ points on the diagonal
 - odd period cycles have $1, 3, 5, \dots$ points on the diagonal (need to plot odd period cycles to see that they always have at least one point on the diagonal)
2. orbits that come in pairs, here figure 18.5 (c) \leftrightarrow (d), (e) \leftrightarrow (f)
3. There is also invariance of the cat map dynamics (1.118) spatial reflection flip across the $\phi_1 = -\phi_0$ anti-diagonal, together with $m_n \rightarrow -m_n$ so the full symmetry is in some sense $D_1 \times D_1$.
 - 1 copy, self-dual under both symmetries: figure 18.6 (h)
 - Figure 18.5 (a) \leftrightarrow (b), self-dual under time reversal
 - Figure 18.5 (c) \leftrightarrow (d) is self-dual under the second reflection
 - 4 copies (need to get longer cycles to see examples)
4. However, as figure 18.11 illustrates, the partition is only in part invariant under the spatial reflection, resulting in some cycles missing their spatial-reflection sisters:
 - Figure 18.5 (e) and (f)
 - Figure 18.6 (g) and (j)

2018-02-21 Predrag The time reversal symmetry fundamental domain is given in figure 18.12 (b). One needs to describe the symmetry reduced dynamics on the fundamental domain, as in ChaosBook.org *Figure 11.7*: “The bimodal Ulam sawtooth map restricted to the fundamental domain.”

2018-04-08 Han I have plotted in figures 18.19 and 18.21. all 4-cycles in ‘Lagrangian’ coordinates $\{\phi_{t-1}, \phi_{t+1}\}$, in the unit-square face centered partition of figure 18.17. The periodic orbits in this partition are given by (18.23) (which seems to be (18.22) modulo some cyclic permutations). Note that sometimes different solutions appear to have the same orbit, and that sometimes points belonging to different solutions appear in the same position. The reason is that given the field values ϕ_{t-1} and ϕ_{t+1} we cannot decide ϕ_t without knowing the m_t . For example, the points $\{\phi_1, \phi_3\}$ for the first two solutions X_{1111} and X_{1010} are the same.

I also plotted all of the solutions in figure 18.23 (b). There are fewer points than figure 18.23 (a), because some of the points coincide. The 2-cycle and the fixed point solutions

$$\begin{aligned} X_{11} &= \frac{1}{15} \begin{bmatrix} -3 & 3 \end{bmatrix}, & X_{22} &= \frac{1}{15} \begin{bmatrix} -6 & 6 \end{bmatrix} \\ X_0 &= \begin{bmatrix} 0 \end{bmatrix} \end{aligned} \tag{18.36}$$

also coincide with points of the 4-cycle solutions.

2018-04-05 Predrag In the “Lagrangian” coordinates $\{\phi_{t-1}, \phi_{t+1}\}$ formulation the 2-cycles are self-dual, as in (18.37), and the fixed point is very special, as it sits in the maximally invariant subspace.

2018-04-05 Predrag Everything works like charm in the “Lagrangian” coordinates $\{\phi_{t-1}, \phi_{t+1}\}$ formulation, except that you should fix a few cycles in figure 18.23 (b), figures 18.19 and 18.21: so far you are plotting periodic points in Percival-Vivaldi face centered unit square non-partition, rather than our 7-region partition. Please replace all plots by plots with the 7-rectangle partition of figure 18.15 (b) indicated, as in figure 18.18.

If

$$X_{11\underline{11}} = \frac{1}{15} [\begin{array}{cccc} 5 & 5 & -5 & -5 \end{array}]$$

then points on the orbit are (ignoring the 1/15 factor) a self-retracing 2-cycle

$$(\phi_{t-1}, \phi_{t+1}) = \{(-5, 5), (5, -5), (5, -5), (-5, 5)\} = X_{1\underline{1}} + X_{1\underline{1}}^\top. \quad (18.37)$$

If

$$X_{0\underline{2}02} = \frac{1}{15} [\begin{array}{cccc} 0 & -10 & 0 & 10 \end{array}]$$

then points on the orbit are (ignoring the 1/15 factor) a self-retracing 2-cycle

$$(\phi_{t-1}, \phi_{t+1}) = \{(10, -10), (0, 0), (-10, 10), (0, 0)\} = X_{0\underline{2}} + X_{0\underline{2}}^\top, \quad (18.38)$$

where ‘+’ stands for string concatenation.

All this is very instructive about how “Laplacian” graphs implement time-reversal invariance. My hunch is that the correct formulation is a “Laplacian” representation such as (13.53). Briefly, B is the (directed) incidence matrix of our directed graph G transition graph, giving us our 7-rectangles partition, and A is the adjacency matrix of (undirected) G .

(Read also sect. 13.1.3.)

That gives us a reformulation of directed graphs as undirected graphs, and maybe we will know how to do it directly, rather than via (to me unappealing) Ihara zeta functions route.

We still have to take care of space-reversal invariance. I think we need to go to the fundamental domain figure 18.26 (a).

2018-04-10 Predrag My hunch is that we need a simpler transition graph than figure 18.17 (b), hopefully an undirected graph. Maybe we do not need a transition graph at all, or we need to formulate the graph is the 2-step “Lagrangian” coordinates $\{\phi_{t-1}, \phi_{t+1}\}$.

Can you list the pruned (inadmissible, forbidden) strings in the alphabet (18.21)? Presumably only blocks of period-2 and 3 are needed, and they are hopefully explicitly time-reversal invariant.

2018-04-12 Han I tried to get the pruned string from the transition graph figure 18.17. The pruned strings for blocks of period-2 are of two types:

$$12, 21, \underline{12}, \underline{21}, 22, \underline{22}, \quad (18.39)$$

but I'm not so sure...

Compare with (18.36); of the $5 \times 4 - 6 = 14$ remaining non-repeating admissible 2-blocks, the period-2 periodic points $\underline{11}, \underline{11}, \underline{22}, \underline{22}$, are realized, but not the $\underline{12}, \underline{21}, \underline{12}, \underline{21}, \underline{01}, \underline{10}, \underline{01}, \underline{10}$ and $\underline{02}, \underline{20}, \underline{02}, \underline{20}$ 2-cycles.

2018-04-18 Han The three types of *new* period-3 pruned blocks from transition graph figure 18.17 are:

$$\begin{aligned} &002, 200, 00\underline{2}, \underline{2}00, \\ &102, 201, \underline{10}\underline{2}, \underline{2}0\underline{1}, \\ &202, \underline{2}0\underline{2}, \end{aligned} \quad (18.40)$$

new in the sense that the remaining blocks contain (18.39) blocks of period-2, which are pruned 2-blocks:

$$\begin{aligned} &122, 12\underline{1}, 120, 121, 122, 112, \underline{11}\underline{2}, \underline{12}\underline{1}, \underline{12}\underline{2} \\ &\underline{12}\underline{2}, \underline{12}\underline{1}, \underline{12}0, \underline{12}1, \underline{12}2, \underline{11}\underline{2}, \underline{11}\underline{2}, \underline{12}\underline{1}, \underline{12}\underline{2} \\ &\underline{21}\underline{2}, \underline{22}\underline{1}, \underline{22}\underline{2}, \underline{21}\underline{2}, \underline{21}\underline{1}, \underline{21}0, \underline{21}1, \underline{21}2, \underline{22}\underline{2}, \underline{22}\underline{1}, \underline{22}0, \underline{22}1, \underline{22}2 \\ &\underline{21}\underline{2}, \underline{22}\underline{1}, \underline{22}\underline{2}, \underline{22}\underline{1}, \underline{22}0, \underline{22}\underline{1}, \underline{22}\underline{2}, \underline{21}\underline{2}, \underline{21}\underline{1}, \underline{21}0, \underline{21}\underline{1}, \underline{21}\underline{2} \\ &021, 022, \underline{02}\underline{1}, \underline{02}2, 012, 01\underline{2}. \end{aligned} \quad (18.41)$$

Length-2 and -3 pruned blocks form space-reflection and time-reversal invariant sets. We expect that each such sets gets replaced by one pruning block in the fundamental domain of figure 18.25 (b).

2018-04-12 Predrag Lets hope that there are no *new* period-4 pruned block's.

2018-04-11 Predrag Maybe in the "Lagrangian" coordinates $\{\phi_{t-1}, \phi_{t+1}\}$ we need to recode (18.22) 4-cycles, so I tried summing the pairs of successive shifts:

$$\begin{aligned} X_{1111} &\Rightarrow 2020, & X_{0202} &\Rightarrow \underline{2}222 \\ X_{0011} &\Rightarrow 010\underline{1} = X_{00\underline{1}1} \Rightarrow 01\underline{0}1 \\ X_{1\underline{2}2\underline{1}} &\Rightarrow \underline{10}10 = X_{2\underline{2}1\underline{1}} \Rightarrow 01\underline{0}1 \\ X_{0111} &\Rightarrow 1001, & X_{1011} &\Rightarrow \underline{11}00 \\ X_{1012} &\Rightarrow \underline{11}\underline{11}, & X_{\underline{10}12} &\Rightarrow \underline{11}\underline{11}. \end{aligned} \quad (18.42)$$

What that does is to replace the shifts coded by alphabet (18.21) by averages (modulo factor 1/2) of pairs of successive shifts. Everybody is self-dual under time, and the last two pairs are related by space reflections, as it should be. However (c,d) should not be the same as (e,f), and (i,j) is already self-dual under both reflections, so this is recorded here just as **another failed attempt** to understand undirected graphs.

2018-04-12 Han I have replaced the plots in figure 18.23 (b), figures 18.19 and 18.21.

The solutions I used are in (18.22). Note that for this partition, in order to decide whether a solution is admissible we only need to check whether $\{\phi_{t-1}, \phi_t\}$ (**not** the Lagrangian coordinates $\{\phi_{t-1}, \phi_{t+1}\}$) is in the partition. So we can see that some of the points are out of the partition. Actually, since we don't check if the Lagrangian coordinates are in the partition, I probably shouldn't put the partition in the figure. If we want to let the Lagrangian coordinates to be in the 7-region partition, we will be using another partition in which the solutions are different from (18.22).

2018-03-22 Predrag I think you have the spatial inversion fundamentally nailed. What about the transition graph?

2018-04-27 Predrag Continuing on the (13.51) theme, we also transform the identity (1.2), noted by string people, to Percival-Vivaldi coordinates:

$$\begin{aligned} \mathbf{L}' &= \begin{bmatrix} -1 & 2 \\ 1 & 0 \end{bmatrix} \begin{bmatrix} 1 & 1 \\ 0 & 1 \end{bmatrix} \begin{bmatrix} -1 & 2 \\ 1 & 0 \end{bmatrix} = \begin{bmatrix} 1 & -1 \\ 0 & 1 \end{bmatrix} \\ \mathbf{L}'^\top &= \begin{bmatrix} -1 & 2 \\ 1 & 0 \end{bmatrix} \begin{bmatrix} 1 & 0 \\ 1 & 1 \end{bmatrix} \begin{bmatrix} -1 & 2 \\ 1 & 0 \end{bmatrix} = \begin{bmatrix} -1 & 4 \\ -1 & 3 \end{bmatrix}, \end{aligned} \quad (18.43)$$

so

$$\mathbf{L}' \mathbf{L}'^\top = \begin{bmatrix} 1 & -1 \\ 0 & 1 \end{bmatrix} \begin{bmatrix} -1 & 4 \\ -1 & 3 \end{bmatrix} = \begin{bmatrix} 0 & 1 \\ -1 & 3 \end{bmatrix}.$$

Under the similarity transformation, the transpose (time reversal?) structure of (1.2) is lost, so this transpose structure (13.53) does not seem to play nice with symplectic transformations.

2018-02-11 Predrag In (the current draft of) Gutkin *et al.* [31] I wrote "The Adler-Weiss Markov partition for the Arnol'd cat map [1–3] utilizes the stable / unstable manifold of the fixed point at the origin to partition the torus into a 3-rectangles generating partition (see, for example, Devaney [14, 25]). It is a subshift of finite type (3 symbols alphabet $\bar{\mathcal{A}}$, with a finite grammar), or a 5 symbols full shift."

This is discussed in 2016-06-02 sect. 1.3.8 notes on Creagh [14], *Quantum zeta function for perturbed cat maps*. Creagh explains both the 3-letter and the 5-letter alphabet in ref. [14] Sect. III. A. *The classical map*. Robinson [55] goes through the construction clearly, step by step. The 3-rectangles generating partition is constructed for the antisymplectic map C given in (5.192) and (4.170), whose double iteration is the Arnold cat map - orbits of the cat map are then coded by sequences whose period is even. I do not see how this would result in our pretty shifts 3-letter alphabet (18.13).

2018-03-26 Predrag I have a hunch that the partition can be related to the Lagrangian (the generating function).

Area-preserving maps that describe kicked rotors subject to a discrete time sequence of angle-dependent impulses $P(x_n)$ of form (7.54), (7.55)

have a *generating function* (5.84)

$$F(q_n, q_{n+1}) = \frac{1}{2}(q_n - q_{n+1})^2 - V(q_n)^2, \quad P(q) = -\frac{dV(q)}{dq}. \quad (18.44)$$

This generating function is the discrete time Lagrangian for a particle moving in potential $V(x)$. Eq. (7.54) says that in one time step Δt the configuration trajectory starting at ϕ_n reaches $\phi_{n+1} = \phi_n + p_{n+1}\Delta t$, and (7.55) says that at each kick the angular momentum p_n is accelerated to p_{n+1} by the force pulse $P(x_n)\Delta t$.

2018-04-12 Predrag My hunch is that to go from the time evolution (Hamiltonian), initial point formulation to the Lagrangian, end points formulation, we will have to do it not by groping blindly, but by the standard Hamiltonian \rightarrow Lagrangian transformation. The Legendre transforms between Hamiltonian and Lagrangian generating functions of sect. 8.2 are of form (this formula might be wrong in detail!)

$$H(q_k, p_k) = p_k q_{k+1} - L(q_k, q_{k+1}), \quad (18.45)$$

where q_{k+1} is implicitly defined by $p_k = \partial_{q_k} L(q_k, q_{k+1})$.

18.4 Reduction to the fundamental domain

2018-03-07 Predrag While the original cell has edges of length 1, the quarter cells with edges of length 1/2 are already set up for a reduction to 1/4 fundamental domain, whose sides are the diagonal and the anti-diagonal. That might be the justification for halving the side-strips as you have done: the cutting line goes through the length 1/2 lattice.

2018-03-11 Predrag Figure 18.25 (b) is cute. To me it suggests a 3-node (A, B, C) transition graph, with alphabet to be figured out.
 (a) $\underline{\underline{1111}} \rightarrow A$? (on both space and time symmetry lines) and
 (b) $\underline{\underline{0202}} \rightarrow \underline{\underline{C}}$ (space, time flip symmetric) are now fixed points.
 (c) $\underline{\underline{0011}}$ and (d) $\underline{\underline{0011}}$ (2 points on space symmetry line) are now one 2-cycle $\rightarrow \underline{\underline{AB}}$,
 (e) $\underline{\underline{1122}}$ and (f) $\underline{\underline{2211}}$ (on space symmetry line) are now one 2-cycle $\rightarrow \underline{\underline{A?B?}}$,
 (g) $\underline{\underline{1012}}$ and (h) $\underline{\underline{1012}}$ (time flip symmetric) are now one 2-cycle $\rightarrow \underline{\underline{A?B?}}$,
 (i) $\underline{\underline{0111}}$, and (j) $\underline{\underline{0111}}$ (time flip symmetric) are now one 2-cycle $\rightarrow \underline{\underline{AC}}$.
 This 3-partitions alphabet is not the right alphabet - still need to work out the the corresponding 5-letter transition graph links alphabet.

2018-03-15 Han The fundamental domain figure 18.25 (b) symbolic dynamics
 (a) $\underline{\underline{1111}} \rightarrow \underline{\underline{AB}}$ (on both space and time symmetry lines, see figure 18.28 (a))
 and
 (b) $\underline{\underline{0202}} \rightarrow \underline{\underline{C}}$ (space, time flip symmetric) are now fixed points.

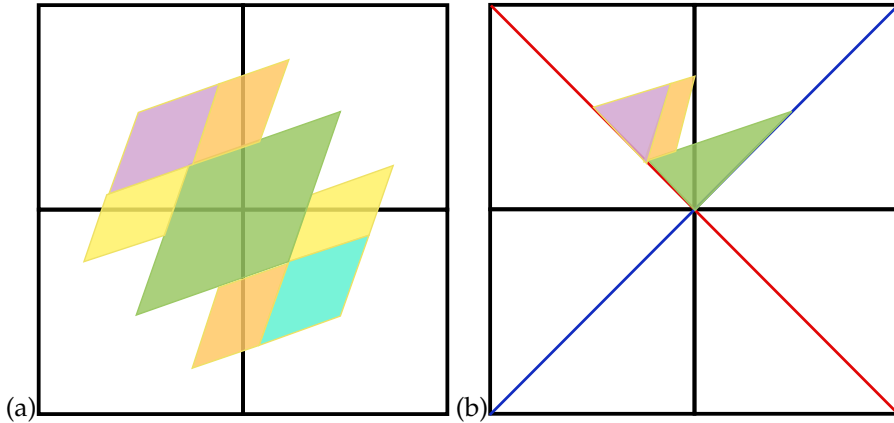


Figure 18.25: Figure 18.14 (b) continued. (a) Almost correct time reversal and space reflection symmetric partition - the correct one is figure 18.15 (b). (b) Three triangles/rectangles fundamental domain partition. Could it be cuter?

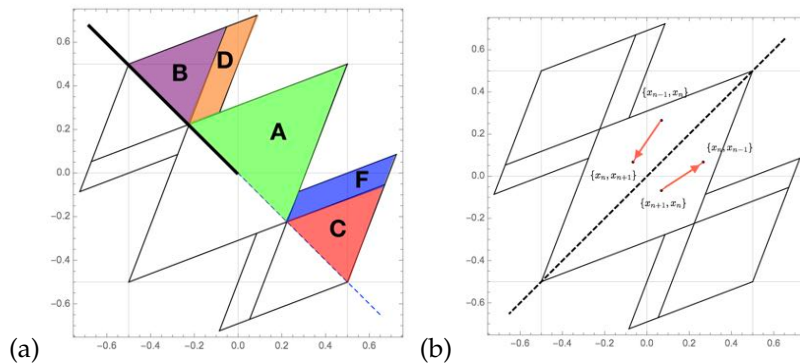


Figure 18.26: (a) The labeled space inversion fundamental domain partition.
(b) The 1-step orbit after *time reversal*.

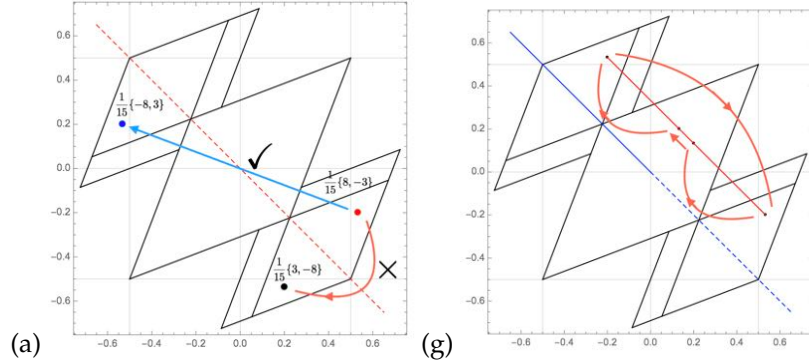


Figure 18.27: (a) The *space inversion* operation. Point $(-8/15, 3/15)$ happens to be a periodic point of period 4, cycle $\underline{1012} \rightarrow \overline{CAAB}$, see (18.18)(g,h). Actually, any fractional coordinate belongs to a periodic orbit. The orange line is here just to confuse you; under inversion $(3/15, -8/15)$ maps into $(-3/15, 8/15)$ (not drawn). (g) The two corresponding 4-cycles reduced to a single 4-cycle in the space inversion fundamental domain, $\underline{1012}$ and $\underline{1012} \rightarrow \overline{CAAB}$.

- (c) $\overline{00\underline{11}}$ and (d) $\overline{00\underline{11}} \rightarrow \overline{AAAB}$,
- (e) $\underline{11}\overline{22}$ and (f) $\underline{22}\overline{11} \rightarrow \overline{ABBB}$,
- (g) $\underline{1012}$ and (h) $\underline{1012}$ (time flip symmetric) $\rightarrow \overline{AABB}$,
- (i) $\underline{0111}$, and (j) $\underline{0111}$ (time flip symmetric) $\rightarrow \overline{AACC}$.

2018-03-22 Han If we reduce the partition by the spatial inversion symmetry, the fundamental domain is shown in figure 18.26(a). Note that the boundary $\{0, 0\} \rightarrow \{\infty, -\infty\}$ goes to $\{0, 0\} \rightarrow \{-\infty, \infty\}$ after inversion. So for the boundary I only keep the points on $(\{0, 0\}, \{-\infty, \infty\})$ half-diagonal (the thick black line in figure 18.26(a)). For example, consider the orbit of $\underline{1111}$. This orbit is shown in figure 18.28(a). The inversion will move the point $\frac{1}{3}\{1, -1\}$ to $\frac{1}{3}\{-1, 1\}$, so I only keep the $\frac{1}{3}\{1, -1\}$ and discard $\frac{1}{3}\{-1, 1\}$ which is on the dashed line. Then this orbit become a 2-cycle \overline{AB} .

From figure 18.28 we can see that the rest of the cycles in figures 18.18 and 18.20 are:

- (a) $\overline{11\underline{11}} \rightarrow \overline{AB}$
- (b) $\overline{0202} \rightarrow \overline{DF}$,
- (c) $\overline{00\underline{11}}$ and (d) $\overline{00\underline{11}} \rightarrow \overline{AAAB}$,
- (e) $\underline{11}\overline{22}$ and (f) $\underline{22}\overline{11} \rightarrow \overline{BBCA}$,
- (g) $\underline{1012}$ and (h) $\underline{1012} \rightarrow \overline{CAAB}$,
- (i) $\underline{0111}$, and (j) $\underline{0111} \rightarrow \overline{AAFD}$.

Now we have two 2-cycles but the rest of the 4-cycles are still 4-cycles. The two 2-cycles (blue points in figure 18.23) in the full domain are now fixed points.

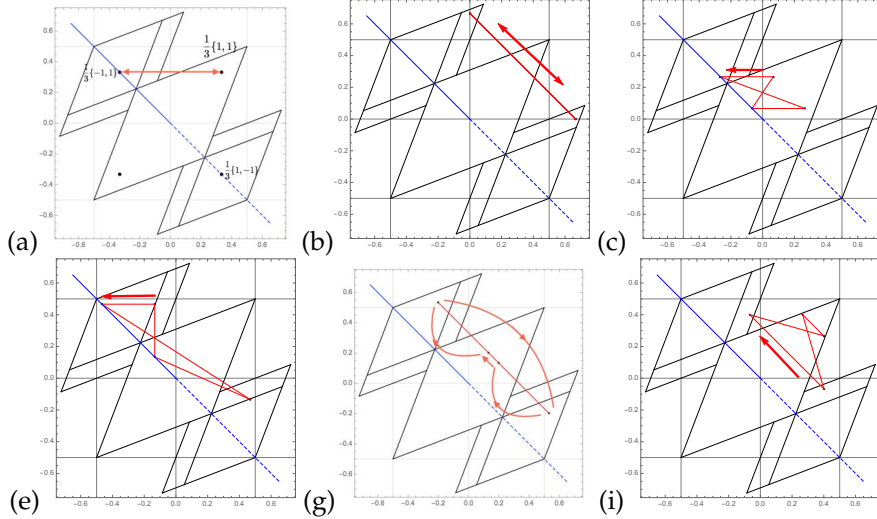


Figure 18.28: The orbits in the fundamental domain of 4-cycles (a) $\overline{1111} \rightarrow \overline{AB}$ in the fundamental domain. (b) $\overline{0202} \rightarrow \overline{DF}$, (c) $\overline{0011}$ and $\overline{0011} \rightarrow \overline{AAAB}$, (e) $\overline{1122}$ and $\overline{2211} \rightarrow \overline{BBCA}$, (g) $\overline{1012}$ and $\overline{1012} \rightarrow \overline{CAAB}$, (i) $\overline{0111}$, and $\overline{0111} \rightarrow \overline{AAFD}$. Compare with figures 18.18 and 18.20.

2018-03-22 Han If we have a orbit $\{\phi_{n-1}, \phi_n\} \rightarrow \{\phi_n, \phi_{n+1}\}$, the time reversal will change this orbit to $\{\phi_{n+1}, \phi_n\} \rightarrow \{\phi_n, \phi_{n-1}\}$. Do a flip across the diagonal we will get the orbit after time reversal but the direction of the orbit also changed, as shown in figure 18.26(b). I guess this is why the time reversal is more tricky...

2020-01-10 Predrag Stewart and Gökaydin [56] *Symmetries of quotient networks for doubly periodic patterns on the square lattice*, ([click here](#)).

18.5 Spatiotemporal cat partition

Consider a d -dimensional hypercubic lattice, infinite in extent, with each site labeled by d integers $z \in \mathbb{Z}^d$. The d -dimensional *spatiotemporal cat* is defined by the discrete screened Poisson equation

$$(-\square + s - 2d) \phi_z = m_z, \quad m_z \in \mathcal{A}, \quad (18.46)$$

$$\mathcal{A} = \{-(s+1)/2, \dots, -1, 0, 1, 2, \dots, (s+1)/2\},$$

where $\phi_z \in [-1/2, 1/2]^2$ (compare with (18.157)). It is a convention that we do not use, as that is not defined on the integer lattice). The map is smooth and fully hyperbolic for integer $s > 2d$.

For a discrete d -dimensional Euclidean spacetime the Laplacian is given by

$$\square \phi_n \equiv \phi_{n+1} - 2\phi_n + \phi_{n-1} \quad (18.47)$$

$$\square \phi_{n_1 n_2} \equiv (\square_1 + \square_2) \phi_{n_1 n_2} \quad (18.48)$$

$$\begin{aligned} \square_1 \phi_{n_1 n_2} &= \phi_{n_1+1, n_2} - 2\phi_{n_1 n_2} + \phi_{n_1-1, n_2} \\ \square_2 \phi_{n_1 n_2} &= \phi_{n_1, n_2+1} - 2\phi_{n_1 n_2} + \phi_{n_1, n_2-1} \end{aligned}$$

in $d = 1, 2, \dots$ dimensions.

What role do the spatiotemporal neighbors play? The local strength of "turbulence" at each site is parameterized by the stretching parameter s . The effect of neighbors is to "calm down" the local turbulence by distributing the stretching parameter $s - 2$ along the d directions in (18.46), effectively decreasing it as $s - 2 \rightarrow s/d - 2$,

$$\sum_{j=1}^d (-\square_j + s/d - 2) \phi_z = m_z. \quad (18.49)$$

An $[L \times L]$ circulant matrix

$$C = \begin{bmatrix} c_0 & c_{L-1} & \dots & c_2 & c_1 \\ c_1 & c_0 & c_{L-1} & & c_2 \\ \vdots & c_1 & c_0 & \ddots & \vdots \\ c_{L-2} & & \ddots & \ddots & c_{L-1} \\ c_{L-1} & c_{L-2} & \dots & c_1 & c_0 \end{bmatrix}, \quad (18.50)$$

has eigenvectors (discrete Fourier modes) and eigenvalues $Cv_k = \lambda_k v_k$

$$\begin{aligned} v_k &= \frac{1}{\sqrt{L}}(1, \epsilon^k, \epsilon^{2k}, \dots, \epsilon^{k(L-1)})^T, \quad k = 0, 1, \dots, L-1 \\ \lambda_k &= c_0 + c_{L-1}\epsilon^k + c_{L-2}\epsilon^{2k} + \dots + c_1\epsilon^{k(L-1)}, \end{aligned} \quad (18.51)$$

where

$$\epsilon = e^{2\pi i/L} \quad (18.52)$$

is a root of unity.

For the determinant of a circulant matrix, see [here](#). For the "definitive book on circulants," see [Alun Wyn-jones](#). It is long - I have not checked whether it is good.

The unitary matrix U obtained by stacking eigenvectors (18.51) into a Van-dermonde matrix is the discrete Fourier transform

$$U_{kj} = \frac{1}{\sqrt{L}} e^{2\pi i k j / L}, \quad (18.53)$$

which diagonalizes any circulant matrix C ,

$$U^\dagger C U = \text{diag}(\lambda).$$

The eigenvalues of the $[L \times L]$ left-shift matrix

$$C = \begin{bmatrix} 0 & 1 & 0 & 0 & 0 \\ 0 & 0 & 1 & 0 & 0 \\ 0 & 0 & 0 & \ddots & 0 \\ 0 & 0 & 0 & 0 & 1 \\ 1 & 0 & 0 & 0 & 0 \end{bmatrix} \quad (18.54)$$

that shifts the orbit of an L -cycle to the left by one step and generates the cyclic group C_L are

$$(\lambda_k) = (e^{-i2\pi k/L}) = (1, e^{-i2\pi/L}, e^{-i3\pi/2}, \dots, e^{-i2\pi(L-1)/L}). \quad (18.55)$$

Thus, if the orbit is shifted to the left by one step, each component of its Fourier transform will be multiplied by the C_L cyclic group phase factor. That implies that for any cyclic-permutation invariant set, such as (11.10), the set of periodic points \mathcal{M}_p that belong to a given p -cycle, one only needs to specify the magnitude of k th Fourier component, the rest is generated by cyclic transformations ²

Take a cycle point block $M = \underline{1221}$ and stack its cyclic permutations (the successive periodic points in its 4-cycle) $M = \underline{2211}, \dots$, into the circulant matrix (18.50),

$$[M]_{\underline{1221}} = \begin{bmatrix} 1 & -2 & 2 & -1 \\ -2 & 2 & -1 & 1 \\ 2 & -1 & 1 & -2 \\ -1 & 1 & -2 & 2 \end{bmatrix}. \quad (18.56)$$

Its discrete Fourier transform is given by circulant matrix eigenvalues (18.51):

$$\hat{M}_{\underline{1221}} = \frac{1}{2} \begin{bmatrix} 1 - 2 + 2 - 1 \\ 1 - 2\epsilon + 2\epsilon^2 - 1\epsilon^3 \\ 1 - 2\epsilon^2 + 2 - 1\epsilon^2 \\ 1 - 2\epsilon^3 + 2\epsilon^2 - 1\epsilon \end{bmatrix} = \frac{1}{2} \begin{bmatrix} 0 \\ -(1+i) \\ 6 \\ -(1-i) \end{bmatrix} = \begin{bmatrix} 0 \\ -\frac{1}{\sqrt{2}}\epsilon^{1/2} \\ 3 \\ -\frac{1}{\sqrt{2}}\epsilon^{-1/2} \end{bmatrix}.$$

It suffices to compute the Fourier transform of a single periodic point, as the rest, obtained by the C_L shifts, is generated by multiplicaton by phase factors (18.55).

For example, the Fourier transformed cycle points $\hat{M}_{\underline{1221}}$ and $\hat{M}_{\underline{2211}}$,

$$\hat{M}_{\underline{2211}} = \frac{1}{2} \begin{bmatrix} -2 + 2 - 1 + 1 \\ -2 + 2\epsilon - 1\epsilon^2 + 1\epsilon^3 \\ -2 + 2\epsilon^2 - 1 + 1\epsilon^2 \\ -2 + 2\epsilon^3 - 1\epsilon^2 + 1\epsilon \end{bmatrix} = \frac{1}{2} \begin{bmatrix} 0 \\ -(1-i) \\ -6 \\ -(1+i) \end{bmatrix} = \begin{bmatrix} 0 \\ -\frac{1}{\sqrt{2}}\epsilon^{-1/2} \\ -3 \\ -\frac{1}{\sqrt{2}}\epsilon^{1/2} \end{bmatrix}.$$

²Predrag 2018-04-21: Not true - need to specify the relative phases between successive Fourier components, unless we can prove that each cycles has unique set of Fourier component magnitudes.

which correspond to successive periodic points in a 4-cycle, have the correct Fourier transforms,

$$\begin{aligned} M_{122\underline{1}} \Rightarrow \hat{M}_{122\underline{1}} &= \begin{bmatrix} 0 & -\frac{1}{\sqrt{2}}\epsilon^{1/2} & 3 & -\frac{1}{\sqrt{2}}\epsilon^{-1/2} \end{bmatrix} \\ CM_{122\underline{1}} = M_{221\underline{1}} \Rightarrow e^{-i2\pi k/4} \hat{M}_{122\underline{1},k} = \hat{M}_{221\underline{1}} &= \begin{bmatrix} 0 & -\frac{1}{\sqrt{2}}\epsilon^{-1/2} & -3 & -\frac{1}{\sqrt{2}}\epsilon^{1/2} \end{bmatrix}. \end{aligned}$$

The eigenvalues of the damped Poisson matrix (18.49) in $d = 1$ are

$$\lambda_k = s - \epsilon^k - \epsilon^{-k} = s - 2 \cos(2\pi k/L). \quad (18.57)$$

In d dimensions the discrete Fourier transform is no longer a 2-index matrix, but it acts tensorially,

$$U_{kz} = U_{k_1 k_2 \dots k_d, n_d \dots n_2 n_1} = \frac{1}{\sqrt{L_1 \dots L_d}} e^{2\pi i \sum_{j=1}^d k'_j n_j / L_j}. \quad (18.58)$$

As the d translations commute, U diagonalizes the d -dimensional (damped) screened Poisson equation (18.49) yielding the Fourier-transformed field for each discrete d -dimensional Fourier component

$$\hat{\phi}_k = \frac{1}{2d - s + 2 \sum_{j=1}^d \cos(2\pi k_j / L_j)} \hat{m}_k, \quad (18.59)$$

where $k = (k_1, k_2), \hat{\phi} = U\phi, \hat{m} = Um$, and U is the discrete Fourier transformation (18.58).

2018-03-05 Predrag Not sure you have ever worked through these formulas, so here they are as exercise 1.1 and exercise 1.2. Can you go through them, and fix both the formulation of the problems, and current sketches of the solutions?

2018-03-08 Han Wrote up solution 1.1 and solution 1.2. I have compared (1.149) with the Green's function of 4-cycles (18.9) for $s = 3$, but prefer to keep the actual calculations secret. Trust me: each cycle point matches.

Disposed of Predrag's wild guess (1.139) for the $d = 2$ Green's function. Wrote up solution 1.3.

2018-03-11 Predrag In $d = 2$ dimensions any solution \mathbf{X} uniquely recovered from its symbolic representation M ,

$$\phi_z = \sum_{z' \in \mathbb{Z}^2} g_{zz'} m_{z'}, \quad g_{zz'} = \left(\frac{1}{-\square + s - 4} \right)_{zz'}, \quad (18.60)$$

where $g_{zz'} = g_{nt, n't'}, z = (nt), z' = (n't') \in T^2_{[L_1 \times L_2]},$ is the Green's function for the 2-dimensional (damped) screened Poisson equation. A lattice state M is admissible if and only if all ϕ_z given by (18.60) fall into the generating partition.

Take $\mathcal{R} = \mathcal{R}^{[L_1 \times L_2]}$ to be a rectangular region. Any $L \times T$ block of interior symbols $M = \{m_z \in \mathcal{A}_0 | z \in \mathbb{Z}_{LT}^2\}$,

$$\mathbb{Z}_{LT}^2 = \{z = (n, t) | n = 1, \dots, L, t = 1, \dots, T\},$$

is admissible and generates a invariant 2-torus solution. Its coordinate representation $\Gamma = \{\phi_z, z \in \mathbb{Z}_{LT}^2\}$, is obtained by taking inverse of (18.46):

$$\phi_z = \sum_{z' \in \mathbb{Z}_{LT}^2} g_{zz'}^0 m_{z'}, \quad m_{z'} \in \mathcal{A}_0, \quad (18.61)$$

where $g_{zz'}^0$ is the corresponding Green's function with periodic boundary conditions. The block $M = \{m_{nt} \in \mathcal{A}, (n, t) \in \mathbb{Z}^2\}$ can be used as a 2-dimensional symbolic representation of the lattice system state.

2018-03-15 Han I have found a solution of the Green's function in 2-dimensional lattice in Morita [50] *Useful procedure for computing the lattice Green's function - square, tetragonal, and bcc lattices*. Our Green's function should be:

$$g_{l't',lt} = \frac{1}{\pi^2} \int_0^\pi dy \int_0^\pi dz \frac{\cos[(l-l')y] \cos[(t-t')z]}{s - \cos y - \cos z}. \quad (18.62)$$

I threw this to Mathematica and it told me it's a hypergeometric function. Maybe it can be written in a easier form... I'm still trying.

2018-03-15 Predrag I had read Morita [50], and a number of similar papers, see sect. 5.5 Green's blog. We had used (18.62) in our paper [31], see (5.46). I would be very impressed if Mathematica fetched this bone you threw at it, and brought back anything intelligent. When you read this literature, be alert for what boundary conditions they use. We only need the periodic bc. Any other bc, such as Dirichlet, breaks translation invariance, and makes evaluation of Green's functions a very difficult problem.

I'm hoping we can simply verify a simple guess (the wrong guess (1.139) was not it), for any d , that would be so much simpler to write up.

2018-03-16 Predrag The bold and reckless proposal of 2018-03-05, 2018-03-11 Predrag continued: I believe we have the lattice Green's functions in d dimensions nailed.

- consider a d -dimensional discretized torus, with (n_1, n_2, \dots, n_d) points along each direction
- for each lattice site z pick admissible block $\{m_z\}$ allowed by our generating partition for given s
- Do the d -dimensional discrete Fourier transform of our (damped) screened Poisson equation. This yields the Fourier-transformed field for each discrete d -dimensional Fourier component, where $\hat{\phi} = U\phi$, $\hat{m} = Um$, and U is the discrete Fourier transformation (a stack of Fourier eigenfunctions).

- Then get the field in the original configuration space by the inverse Fourier transform (relax - it is just a matrix multiplication)

$$\phi = U^\dagger \hat{\phi}. \quad (18.63)$$

I've been always asking myself what would a Fourier transform of a periodic orbit look like, and what it would mean. Well, now we can plot $(\hat{\phi}_k, \hat{\phi}_{k+1})$ for each periodic orbit p , and ponder it.

(Han, continue at your leisure:)

2018-03-05 Predrag With period-5 I expect that you will find orbits that have only one or no symmetries.

2018-03-18 Predrag As illustrated in figure 18.16 (a), dynamics commutes with the spatial reflection σ (across anti-diagonal), while time reversal will require extra thinking. Why don't you first implement symmetry reduction for the spatial reflection σ , with the fundamental domain the partition being half above the anti-diagonal in figure 18.25 (a), and we postpone figure 18.25 (b) for later?

2018-03-05,2018-03-18 Predrag I have flashed out in the above the bold and reckless proposal for symbolic dynamics in d dimensions. We probably do not need the $d = 2$ Green's function in configurations space, as all periodic orbits can be computed directly in the momentum space, then Fourier transformed.

2018-03-22 Han I think the operation corresponding to the spatial reflection $\{\phi_{n-1}, \phi_n\} \rightarrow \{-\phi_{n-1}, -\phi_n\}$ is not the reflection σ across the anti-diagonal but the rotation of π about the origin as shown in figure 18.27 (a).

2018-03-22 Predrag I might be wrong, but I would not go for a rotation interpretation - I think it is identical to the parity operation in case at hand. $\phi_t \in T^1$ is the only phase space coordinate at lattice site t . Parity sends $\phi_t \rightarrow -\phi_t$, $m_t \rightarrow -m_t$. It is a symmetry of the equations of motion, see (18.8) for the time-forward 2D version, or (18.46) for the $d = 1$ lattice formulation. To be able to rotate, you need to think of $\phi_t \in (-\infty, \infty)$ as embedded in 2 or 3 dimensions. That is motivated by our 2D plots, but not necessary.

I replaced "rotation" by "inversion" in your notes - if I am wrong, we can easily revert the commented-out parts.

2018-03-05 Predrag In $d = 2$ case compute the eigenvalues, eigenvectors for $s = 5$ and the transition graph (I think you already have them). Then you can test it by generating a bunch of admissible $[2 \times 2]$ or $[3 \times 2]$ or $[4 \times 2]$ blocks. The number of distinct ones can be reduced by reflection symmetries. It is not clear to me which ones are admissible, as yet, so you

can generate all, solve by inverting corresponding the doubly-periodic 2-tori Toeplitz (tensor) matrix → Green's function which gives you doubly-periodic lattice states. Then you can check which ones are within your Adler-Weiss partition.

2018-03-29 Han In $d = 2$ dimensions the Green's function $g_{zz'} = g_{\ell t, \ell' t'}$, $z = (\ell t), z' = (\ell' t') \in T^2_{(n_1, n_2)}$ is a $[3 \times 3] \times [3 \times 3]$ tensor. Using the tensor Fourier transform (18.58), I calculated several periodic $[3 \times 3]$ blocks, with $z = (\ell t), z' = (\ell' t') \in T^2_{(3,3)}$. For example, the symbol blocks and the corresponding 9 field values of two admissible 2-torus states are, in the notation of (11.11),

$$M_1 = \begin{pmatrix} 1 & 0 & 0 \\ 0 & 1 & 0 \\ 0 & 0 & 1 \end{pmatrix} \Rightarrow X_1 = \frac{1}{14} \begin{pmatrix} 6 & 4 & 4 \\ 4 & 6 & 4 \\ 4 & 4 & 6 \end{pmatrix} \quad (18.64)$$

$$M_2 = \begin{pmatrix} 1 & 0 & 0 \\ 0 & 1 & 2 \\ 0 & 0 & 1 \end{pmatrix} \Rightarrow X_2 = \frac{1}{14} \begin{pmatrix} 8 & 6 & 7 \\ 7 & 9 & 12 \\ 6 & 6 & 9 \end{pmatrix} \quad (18.65)$$

In this calculation I used the Percival-Vivaldi partition of figure 1.2, with $0 \leq x < 1$, and $s = 5$.

As the blocks are doubly periodic, a single prime 2-torus p represents all vertical and horizontal cyclic permutations of the corresponding symbol block M_p . Furthermore, by lattice symmetries, M_p related by reflection and axes interchange symmetries are equivalent, (and -not sure of this- by the site symmetries, also internally space and time reversed) states are equivalent.

In $d = 1$ dimension, the Percival-Vivaldi partition alphabet is an $s = (s - 2) + 2$ letter alphabet (18.18). It has been shown in Gutkin *et al.* [31] that in $d = 2$ dimensions the Percival-Vivaldi partition $s + 3 = (s - 4) + 7$ letter alphabet $\mathcal{A} = \mathcal{A}_0 \cup \mathcal{A}_1$ can be split into the interior \mathcal{A}_0 and exterior \mathcal{A}_1 alphabets

$$\mathcal{A}_0 = \{0, \dots, s - 4\}, \quad \mathcal{A}_1 = \{\underline{3}, \underline{2}, \underline{1}\} \cup \{s - 3, s - 2, s - 1\}. \quad (18.66)$$

For example, for $s = 5$ the interior, respectively exterior alphabets are

$$\mathcal{A}_0 = \{0, 1\}, \quad \mathcal{A}_1 = \{\underline{3}, \underline{2}, \underline{1}\} \cup \{2, 3, 4\}. \quad (18.67)$$

If all m_z belong to \mathcal{A}_0 then $M = \{m_z | z \in \mathbb{Z}^2\}$ is a full shift (11.6). In particular, the above M_1 is admissible, while M_2 could have been pruned (in this case the explicit calculation shows it is admissible).

2018-03-29 Predrag Make sure you understand the alphabet (18.193). My alphabet (18.46) might be wrong; for s large the number of letters does grow as s , but I do not quite see what corresponds to the \mathcal{A}_1 letters. It has something to do with distributing s between d dimensions, as in (18.49).

2018-03-29 Predrag We'll have to think of how to visualize the states X , something analogous to figure 18.18. There is no preferred time evolution direction, so it does not make sense to connect them by lines. But the states will align on lattices, as in figure 18.23.

2018-03-29 Predrag Keeping in mind where we want to go with this, might be better to use spatially-symmetric, unit-square face centered partition (18.46), rather than the unit-square corner (vertex?) partition of figure 1.2.

2018-03-30 Predrag regarding your Tuesday, April 3 **Diffusion confusion** presentation: use it as a motivation for learning some theory applicable to your spatiotemporal cat project. Do not do too much in the class, just work out a few things in full detail (otherwise nobody learns anything).

Read [ChaosBook Chapter 24 Deterministic diffusion](#). You also might find my online lectures, [Week 13](#) helpful. Maybe also have a glance at [ChaosBook Appendix A24 Deterministic diffusion](#). As Dan has already covered everything, you can pick and chose: maybe redo the 1-dimensional example sect. 24.2 *Diffusion induced by chains of 1-dimensional maps* using the discrete Fourier that you are using for cat maps? Doing some nontrivial partitions, as in figure 24.4 of example 24.4?

My Group Theory course birdtracks.eu/courses/PHYS-7143-17 might be of interest. Cyclic group C_n shows up in [week 2](#) Examples 2.3 and 2.4.

Because of the reflection symmetries, the cat map and spatiotemporal cat symmetry is actually not C_n , but the dihedral group D_n , whose irreducible representations are not the complex 1-dimensional $\exp(2\pi i k j / \ell)$, but the real 2-dimensional $(\cos(2\pi i k j / \ell), \sin(2\pi i k j / \ell))$, see [week 4](#) Exercises 4.3 and 4.4.

The most important for you is [week 8 Space groups](#). The symmetries of our spatiotemporal cat are summarized by figure 8.1 and in the exercise 8.1. *Band structure of a square lattice*. The elastic (not chaotic) cousin of spatiotemporal cat is described in sect. 8.2 *Elastodynamic equilibria of 2D solids*.

The whole course is a subversion repository that I can give you access to, if you want to reuse any of the LaTeX, or see the solution sets.

2018-04-05 Han I have calculated all admissible $[2 \times 2]$ periodic blocks in the unit-square face centered partition, $-\frac{1}{2} \leq \phi_{n_1 n_2} < \frac{1}{2}$, for $s = 5$. The alphabet is:

$$\mathcal{A} = \{-4, -3, -2, -1, 0, 1, 2, 3, 4\} \quad (18.68)$$

Using the coordinates $\{\phi_{l-1,t}, \phi_{l,t-1}, \phi_{l,t}\}$ to represent a point in the block, I plot all periodic points of the admissible blocks in a 3-dimensional unit cube, as shown in figure 18.29.

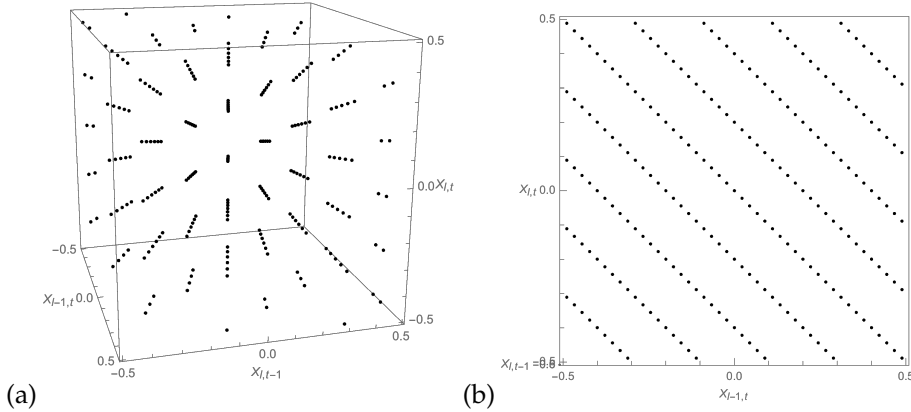


Figure 18.29: (a) All of the points in the periodic $[2 \times 2]$ blocks. The coordinates of each points are $\phi_{l-1,t}$, $\phi_{l,t-1}$ and ϕ_{lt} . (b) The front view of (a). Clearly these points are arranged in lines.

2018-04-05 Predrag Were there any inadmissible blocks in the unit-square face centered partition? Or are you using the transition graph for $s = 5$ to generate only admissible blocks?

2018-04-05 Predrag The visualization of figure 18.29 is quite interesting. All periodic points $\phi_{n_1 n_2}$ have the same denominator?

2018-04-05 Predrag If you want to have a 2-dimensional visualisation for each block analogous to (18.64), color the symbol M_j $[L_1 \times L_2]$ block with 9 discrete color alphabet \mathcal{A} from (18.68), and the corresponding state X_j $[L_1 \times L_2]$ block with colors chosen from a continuum color strip.

2018-04-05 Predrag As this is a linear problem, you can also represent closeness of two $[L_1 \times L_2]$ blocks by using this coloring scheme for $M_2 - M_1$ and $X_2 - X_1$. To find the closest “distance” between 2-tori, you will have to go through all cyclic permutations of the second one to align it optimally (or, if you understand ChaosBook course, you’ll have to ‘slice’).

For pairs of distinct 2-tori which share the same region of m_z ’s, or a single 2-torus in which the same region of m_z ’s appears twice, the states ϕ_z in the center of the region should be exponentially close, in order to argue that they shadow each other.

This is illustrated in ref. [31], but there we do not use the linearity to actually subtract $X_2 - X_1$.

2018-04-05 Predrag Mark the lattice point z with the minimal value of $|x_z^{(2)} - x_z^{(1)}|$ on above graphs, and in the text state the minimal value of $|x_z^{(2)} - x_z^{(1)}|$.

You can also state the mean Euclidean (or L2) distance between the two invariant 2-tori:

$$d_{X_2-X_1} = \left(\frac{1}{LT} \sum_z (x_z^{(2)} - x_z^{(1)})^2 \right)^{1/2}, \quad (18.69)$$

or distance averaged over the lattice points restricted a region \mathcal{R} .

An aside: not sure that the Euclidean distance is the correct one. A better one might be the overlap, with the Green's function sandwiched something like

$$\frac{X_2^\top g X_1}{X_2^\top X_1} \quad (18.70)$$

correctly normalized (as it stands, it is dimensionally wrong - is this "fidelity"?), and maximized by going through all cyclic permutations of X_2 (to align it optimally, or by 'slicing'). The overlap is maximal for $X_2 = X_1$, and falls off exponentially, depending on how much of the two invariant 2-tori differ.

The correct distance really should be the difference between two actions - that is symplectically invariant.

2018-04-05 Han This problem probably is not important. And I might be wrong. In the $[2 \times 2]$ blocks if we use the unit-square corner partition, we have the symbol block and the corresponding 4 field values:

$$M = \begin{pmatrix} 1 & 1 \\ 1 & 1 \end{pmatrix} \Rightarrow X = \begin{pmatrix} 1 & 1 \\ 1 & 1 \end{pmatrix} \quad (18.71)$$

which is not admissible, since for the unit-square corner partition the range of the field values is $0 \leq \phi_{lt} < 1$. But if all m_z belong to $\mathcal{A}_0 = \{0, 1\}$ then $M = \{m_z | z \in \mathbb{Z}^2\}$ should be a full shift (according to (18.193)).

2018-04-05 Predrag This, I think, is important (search for 'Manning' in this blog), and we have to understand it. I think you have to define *all* partition regions *including* the borders, in this example as $0 \leq \phi_{lt} \leq 1$, and then take care of over-counting the border points, such as (18.71) by quotienting the zeta function as in (3.190).

18.6 Running blog

This section contains recent entries, before they are moved to the appropriate specific section above.

2018-04-25 Predrag Moved all our time-reversal invariant formulation musings into sect. 18.3 *Time reversal*.

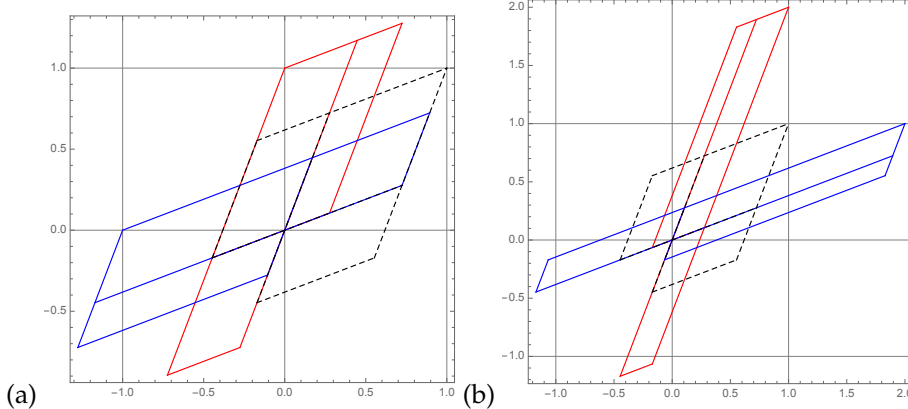


Figure 18.30: (a) The 3-rectangle rhomboid corner partition mapped half a step forward and half a step backward in time. (b) The partition mapped one step forward and one step backward in time. The black dashed lines are the 3-rectangle partition. The red lines are the partition mapped half a step or one step forward in time. The blue lines are the partition mapped half a step or one step backward in time.

2018-05-10 Han The Percival-Vivaldi cat map and the corresponding "square root" matrix are:

$$\mathbf{B} = \tilde{\mathbf{C}}^2 = \begin{bmatrix} 0 & 1 \\ -1 & 3 \end{bmatrix}, \quad \tilde{\mathbf{C}} = \mathbf{S}^{-1} \mathbf{C} \mathbf{S} = \begin{bmatrix} -1 & 1 \\ -1 & 2 \end{bmatrix}. \quad (18.72)$$

I plotted the 3-rectangle partition that mapped one step forward and one step backward using the matrix $\tilde{\mathbf{C}}$ (which can be seen as half a step forward and backward with Percival-Vivaldi cat map). Figure 18.31 is the partition mapped half a step forward in time. And figure 18.32 is the partition for half a step backward in time. Figure 18.33 is the overlap of the two partitions.

2018-05-10 Predrag Is it interesting to see the explicit form of the unimodular transformation \mathbf{S} in (18.72)?

Figure 18.31, figure 18.32 and Figure 18.33 are presumably partitioned in too many subregions.

2018-05-10 Han From figure 18.33 we can see that the overlap of the figure that mapped half a step forward and backward is not symmetric about the diagonal $x_1 = x_0$. Actually in figure 18.30 we can see that the partition that mapped half a step forward and backward are symmetric about the antidiagonal $x_1 = -x_0$ while the partition that mapped one step forward and backward in figure 18.30 (b) are symmetric about the diagonal $x_1 = x_0$. The reason is that the map $\tilde{\mathbf{C}}$ has a negative eigenvalue that flips the

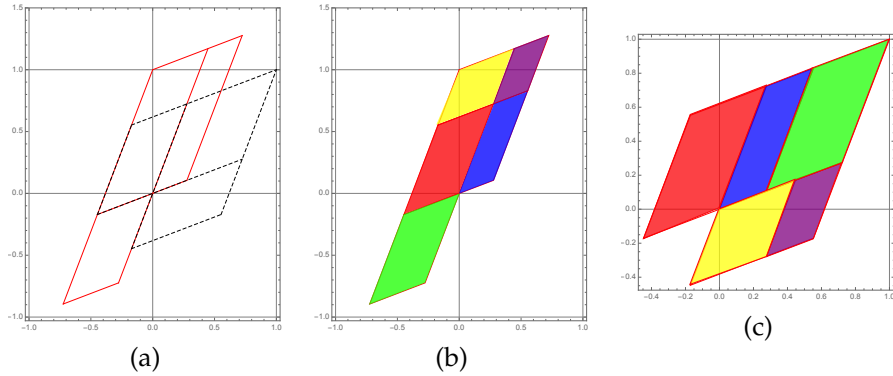


Figure 18.31: (a) and (b) are the partition that mapped half a step forward in time. (c) The mapped partition translated back to the original unit area.

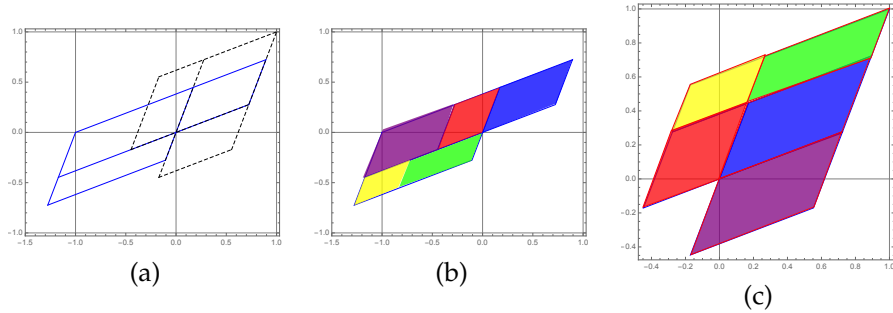


Figure 18.32: (a) and (b) are the partition that mapped half a step backward in time. (c) The mapped partition translated back to the original unit area.

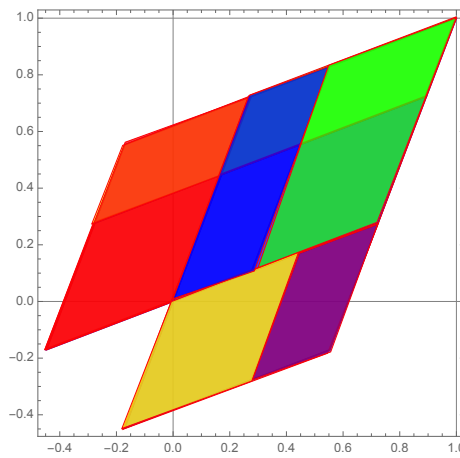


Figure 18.33: The overlap of figure 18.31(c) and figure 18.32(c).

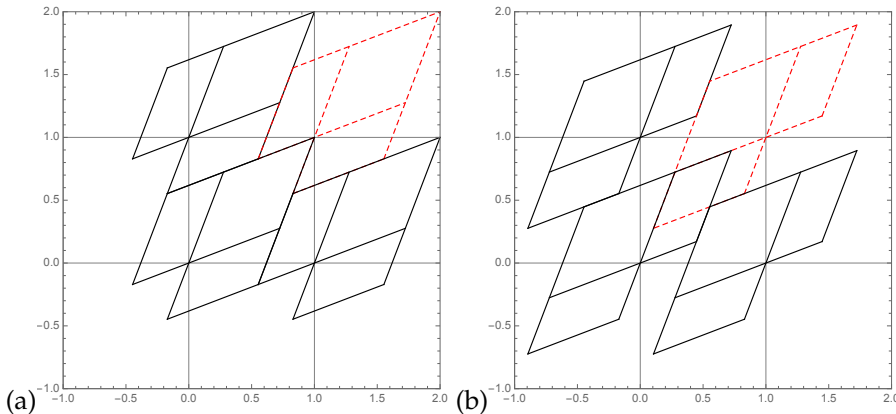


Figure 18.34: (a) The generating partition tiling the square lattice. (b) The flipped partition.

partition in the direction of stable manifold. If we use a partition that is symmetric about antidiagonal $x_1 = -x_0$, perhaps the overlap of the half a step forward and backward will be symmetric about antidiagonal $x_1 = -x_0$. But I'm not sure if this is what we want...

2018-05-10 Predrag You are starting from figure 18.32 (a) dotted lines partition (ie, figure 1.9 (a) that I had pulled out of a hat). But the literature suggests that for the golden cat map (5.192) Adler-Weiss partition might look something like Exercise 8.4 and Fig. 37. *Partition from the “behold” proof of the Pythagorean theorem*. That looks very space- and time-reflection symmetric, in contrast to figure 1.8 (b). Does it become something interesting for the Percival-Vivaldi golden cat map?

2018-05-13 Han Flipping the partition along the stable direction doesn't work. As shown in figure 18.34, the flipped partition cannot tile the square lattice.

2018-05-22 Han I plotted the Fourier transform of all the admissible period-5 of the rhomboid corner partition in the Brillouin zone in figure 18.35. For a 1-dimensional lattice with lattice spacing 1, the reciprocal lattice has spacing $2\pi/1 = 2\pi$, with the (first) Brillouin zone from $k = -\pi$ to $k = \pi$. From figure 18.35 we can see that the Fourier transform in the Brillouin zone is symmetric about the $k = 0$. And if we rotate this figure, we can see that some points lie on a straight line. Figure 18.35 (b) is all irreps overlaid. Due to the time reversal, all $k = 2\pi/5$ irrep states are the same as the $k = 4\pi/5$ irrep states.

I have put the Mathematica notebook in
`siminos/figSrc/han/Mathematica/HLFourierTranform5Cycles.nb`
so one can rotate the figure.

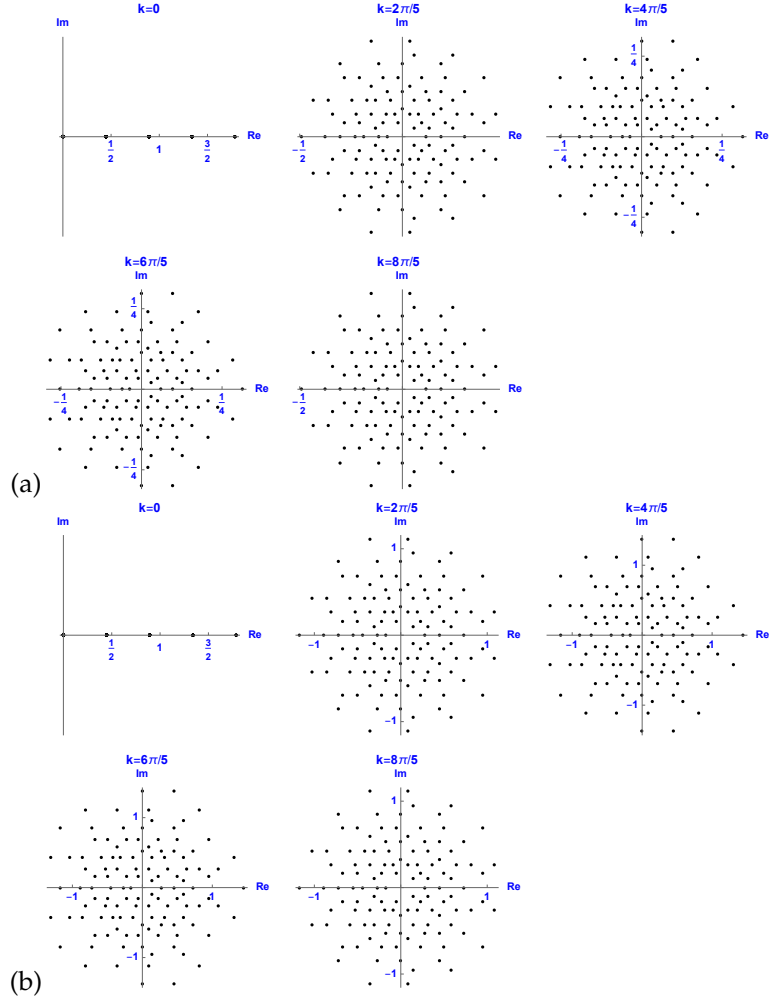


Figure 18.35: (a) The 121 period $n = 5$ reciprocal lattice states \hat{X} (see table 4.1) of the $s = 3$ temporal cat, obtained by C_5 discrete Fourier transform diagonalization, plotted in the Brillouin zone for the rhomboid corner partition. (b) The 121 period $n = 5$ reciprocal lattice admissible symbol blocks \hat{M} of the $s = 3$ temporal cat, obtained by C_5 discrete Fourier transform diagonalization, plotted in the Brillouin zone for the rhomboid corner partition. (Continued in figure 18.52.)

2021-01-27 Han Figure 18.35 (c,d) is the C_5 discrete Fourier transform of symbol blocks M . Note that on the reciprocal lattice symbol blocks \hat{M} lie on the straight lines.

2018-06-11 Han I have finished reading that introduction to group theory. I knew some basic concept of group theory before but never learned it systematically. It is interesting.

2018-06-11 Han This is one possible way to get the generating partition for a 2-dimensional lattice, but I'm not sure if this is useful.

I understand on each lattice site there is a two-torus. In our case the x and y coordinates are $x_{\ell,t-1}$ and $x_{\ell,t}$ separately (Is this right?). But I don't know how can we have the generating partition in this torus, since the evolution of the field value is affected by the neighboring sites.

2018-06-21 Predrag Your difficulty is that you keep on thinking in Hamiltonian way, where one steps in time, using the Hamilton's equations for (q_t, p_t) , where we had replaced the momentum p_t (at spatial position ℓ) by velocity $p_t = (x_{\ell t} - x_{\ell,t-1})/\Delta t$, and thus initializing the Hamiltonian, a second-order difference equation for *evolution in time* by two horizontal rows $(x_{\ell t}, x_{\ell,t-1})$, $\ell \in \mathbb{Z}$ in the spacetime plane.

You have to think in the spacetime, Lagrangian way instead. On each lattice site $z = (\ell, t)$ there is a scalar field $x_{\ell t}$, not a two-torus. The field $x_{\ell,t-1}$ belongs to a neighboring site $z = (\ell, t-1)$. The two fields do not form a dynamical system on a two-torus, as the dynamics is also influenced by spatial neighbors $x_{\ell \pm 1, t}$.

2018-06-11 Han In order to integrate a 2nd order differential equation with only one variable, we need a 2-points initial condition. This the case in the time evolution 1-dimensional problem, where the equation (18.47) is a discrete "differential equation" in one-dimension. When we solve a 2-dimensional partial differential equation, we need the boundary condition. In the Dirichlet case, these are the field values on the boundary of the two-dimensional domain.

So if we use the similar way as one-dimension to treat the two-dimensional problem, we probably should start with not a single point, but the field values on all lattice sites at a certain time. In other words, the partition is defined by x_{t-1} and x_t in one-dimension, where in two-dimension it is defined in a higher dimensional torus with coordinates $x_{\ell,t-1}$ and $x_{\ell,t}$, and ℓ is an integer from $-\infty$ to ∞ . When we have a periodic boundary in ℓ , the number of coordinates will be reduced.

2018-06-21 Predrag You keep on thinking in Hamiltonian way. "The field values on all lattice sites at a certain time" is a horizontal line in the space-time plane. Yes, you need two successive lines to initiate Hamiltonian time evolution. Those equations are ugly (see this blog, for example (5.2),

Gutkin and Osipov [32], and Gutkin *et al.* [31]) and we only know how to solve them for small “number of particles” L , not for $\ell \in \mathbb{Z}$.

2018-06-21 Predrag The problem you are solving is a Helmholtz equation. You do not do that by specifying initial conditions. With Dirichlet b.c.’s that is the equation for a drum, with a specified boundary, a hard problem to solve in general. However, with periodic b.c.’s, on a spatiotemporal 2-torus it is much easier, as it is an algebraic equation for the spatiotemporal discrete Fourier coefficients.

2018-06-21 Predrag Can we get “the generating partition” which is a 4-torus?
Not obvious...

2018-06-11 Han If the spatial period is larger than 2, the dimension of the partition will be also larger.

2018-06-21 Predrag Can we get “the generating partition” which is a $2L$ -torus?
Not obvious, and it probably gets uglier and uglier...

2018-06-11 Han Using the method in Robinson’s book, I think we will get the generating partition from these eigenvectors. But these are at least in 4-dimensions. It is not obvious what the partition looks like. And I think this is not Lagrangian... More important thing is, if we decide the period in space, can we still see the spatiotemporal symmetry?

2018-06-21 Predrag My experience from Kuramoto-Sivashinsky is that every small spatial length torus (really a cylinder, as the time is infinite) has its own grammar, and I expect the grammar for the $t \in \mathbb{Z}$ be simpler than all these small spatial domains.

2018-06-27 Predrag Just that we are on the same page: In d -dimensional phase space, a partition is a d -dimensional volume, and its borders are co-dimension 1, i.e., $(d - 1)$ -dimensional. In case at hand, the partition borders are 3-dimensional hyper-planes, not 2-dimensional planes. By “the planes given by 3 of the eigenvectors” you mean a 3-dimensional hyper-plane, I assume.

2018-06-26 Han To find the planes given by 3 of the eigenvectors, we simply find the normal vector that is perpendicular to the 3 eigenvectors. The 4 normal vectors we have are:

$$\begin{aligned} L_{123} &= (-\Lambda_3, -\Lambda_3, 1, 1) \\ L_{124} &= (1, 1, -\Lambda_3, -\Lambda_3) \\ L_{134} &= (\Lambda_1, -\Lambda_1, -1, 1) \\ L_{234} &= (-1, 1, \Lambda_1, -\Lambda_1) \end{aligned} \tag{18.73}$$

L_{123} means this is the normal vector that is perpendicular to the eigenvectors e_1 , e_2 and e_3 . Using these normal vectors we can easily get the

expression of the planes. The 4 planes passing through the origin are:

$$\begin{aligned} -\Lambda_3x - \Lambda_3y + z + w &= 0 \\ x + y - \Lambda_3z - \Lambda_3w &= 0 \\ \Lambda_1x - \Lambda_1y - z + w &= 0 \\ -x + y + \Lambda_1z - \Lambda_1w &= 0 \end{aligned} \tag{18.74}$$

The first problem is: the last two planes in (18.74) pass through both the origin and the point $(1, 1, 1, 1)$.

2018-06-27 Predrag After you take mod 1? Otherwise the hyperplanes are distinct, right?

2018-06-26 Han So if we follow the same method we used in the one-dimensional case as I state above, the partition won't exist... But I guess my method is not correct anyway. To find the correct partition we will have to understand the structure of these vectors in this 4-dimensional space. And as you see from (18.261–18.74), there are many symmetries. I expect the partition will still be very similar to the one-dimensional case of figure 18.3. I'm still working on this.

2018-06-28 Han The four hyperplanes in (18.74) are distinct. The last two hyperplanes pass through both the origin and the point $(1, 1, 1, 1)$.

2018-06-28 Han I just realize that using the hyperplane passing through the origin and the point $(1, 1, 1, 1), (1, 0, 0, 0), (0, 1, 0, 0), (0, 0, 1, 0)$ and $(0, 0, 0, 1)$ won't give us the correct partition.

Now I'm thinking given 3 distinct planes in 3-dimensions, how to construct a region whose volume is 1 enclosed by planes that are parallel to these 3 planes. And the origin and the point $(1, 1, 1)$ should be on the borders. And this region should "tile" the 3-dimensional space. Intuitively this region should be enclosed by the planes passing through the points with integer coordinates (like $(1, 1, 0), (1, 0, 0)$). I have tried many ways to enclose the region but I can't get the correct volume. The most straightforward way should be cutting a unit cube with one of the planes and move the cut off part to the other end of the cube. But it is still hard to imagine. Currently I think there may be more subregions than just 1 large cube and 3 small cubes.

2018-06-29 Han I have solved the 3-dimensional tiling problem. It's not too complicated. The most important idea is: since the region will tile the whole 3-dimensional space, when we move the region along the direction of an axis by 1 unit of length, the borders of the new region must touch the borders of the old region. So if the planes passing through the origin and point $(1, 1, 1)$ are the borders, the planes passing through the points $(1, 0, 0), (0, 1, 0), (0, 0, 1), (1, 1, 0), (1, 0, 1)$, and $(0, 1, 1)$ must also be

the borders (because these planes can be moved from the planes passing through the origin and $(1, 1, 1)$ by 1 unit length).

Now I'm able to find the tiling region given 3 distinct planes and get the correct result. Hopefully this will help me to get the correct partition in 4-dimensions.

2018-07-09 Han I will start with the result: I already have the partition (which I think is a generating partition) of the two-dimensional problem with spatial length of two, and use this partition to calculate the solutions of all admissible 2×2 blocks. From the solutions I find that the alphabet is reduced, but not in a perfect way. The left site and right site have different alphabet.

The partition is defined in a four-dimensional space $\{x_{1,t-1}, x_{2,t-1}, x_{1,t}, x_{2,t}\}$. It has the time reversal symmetry, i.e., if you swap $x_{1,t-1}, x_{2,t-1}$ with $x_{1,t}, x_{2,t}$, the partition is unchanged. Because of the periodic spatial boundary, it should also have the space reflection symmetry (the partition should be invariant when we swap $x_{1,t-1}, x_{1,t}$ with $x_{2,t-1}, x_{2,t}$). But I can't find such a symmetric generating partition. So the result is if we have a solution $\{x_{1,t-1}, x_{2,t-1}, x_{1,t}, x_{2,t}\}$, $\{x_{2,t-1}, x_{1,t-1}, x_{2,t}, x_{1,t}\}$ is not necessarily an admissible solution. Another result is the alphabet of the left site (corresponding to $x_{1,t}$) has different alphabet from the right site (corresponding to $x_{2,t}$).

Remember that when we use the "square cube" partition for two-dimensional problem, the letters of the alphabet are from -4 to 4 if the field values are $-\frac{1}{2} \leq x \leq \frac{1}{2}$. And if the field values are $0 \leq x \leq 1$, the alphabet is from -3 to 4. Using my new partition to calculate all admissible 2×2 blocks, the alphabet for the left site is from -1 to 5, and the alphabet for the right site is from -4 to 1. There is only one solution with left site $m = -1$. So I think if we use a longer block, the complete alphabet of the right site should be from -5 to 1 (because they should have same number of letters). Anyway, I think this shows that this new partition is very likely to be a generating partition.

2018-07-13 Predrag That's scary: "The left site and right site have different alphabet." But already had the unwelcome asymmetry in the forward / backward in time generating partition, that we could never resolve, so that might be a disease of the concept of generating partitions.

Mention that $s = 5$?

2018-07-09 Han The next part is the tedious detailed method that find the partition in four-dimensions. In fact I should call it the method of finding the tiling region in four-dimensions enclosed by boundaries with given directions passing through the points with integer coordinates. Like I said one week ago, the boundaries must consist of hyperplanes that passing through all of the neighboring points, not just $(1, 1, 1, 1)$, $(1, 0, 0, 0)$, $(0, 1, 0, 0)$, $(0, 0, 1, 0)$ and $(0, 0, 0, 1)$, but also $(0, 1, 1, 1)$, $(1, 0, 1, 1)$, $(1, 1, 0, 1)$,

$(1, 1, 1, 0), (1, 1, 0, 0), (1, 0, 1, 0), (1, 0, 0, 1), (0, 1, 1, 0), (0, 1, 0, 1)$ and $(0, 0, 1, 1)$. So the structure is actually very complex. I figured out a easy way to get the correct partition.

We know that these points listed above are fixed points if included in our partition. So we want some of these points to be on the boundary or on the cross section of several different boundaries, but not necessarily on the vertex of our partition. But to make the partition simpler and similar to the figure 18.2, I choose the point $(1, 1, 1, 1)$ to be a vertex of our partition, which is a cross point of four hyperplanes. The expression of these four hyperplanes are:

$$\begin{aligned} -\Lambda_3 x - \Lambda_3 y + z + w &= 2 - 2\Lambda_3 \\ x + y - \Lambda_3 z - \Lambda_3 w &= 2 - 2\Lambda_3 \\ \Lambda_1 x - \Lambda_1 y - z + w &= 0 \\ -x + y + \Lambda_1 z - \Lambda_1 w &= 0 \end{aligned} \tag{18.75}$$

So these four hyperplanes will be the boundaries of our partition. The next step is to write down all of the hyperplanes passing through all of the neighboring points listed above. For each of these points, there will be four hyperplanes that are similar to the (18.74–18.75) but have different constants at the right hand side. Then we find four hyperplanes that are parallel to the four hyperplanes in (18.75) respectively that we can enclose the largest possible volume with these eight hyperplanes. For example, if we look at all of the hyperplanes that are parallel to the third hyperplane in (18.75), we find that the possible constants on the right hand side are $\Lambda_1, -\Lambda_1, 1, -1, 0, \Lambda_1 - 1, \Lambda_1 + 1, 1 - \Lambda_1$ and $-1 - \Lambda_1$. So to enclose the largest possible volume we will pick the hyperplane with right hand side of $\Lambda_1 + 1$ or $-1 - \Lambda_1$. We have two options, and I think this is why the rules for the left site and right site are different. I chose $\Lambda_1 + 1$ when I get the partition. If I use $-1 - \Lambda_1$ I think the rule of the left site and the right site will be swapped.

Now we have a very large and simple region in four-dimensions. And we know that the point $(1, 1, 1, 1)$ will be on a vertex of our partition. And the four hyperplanes passing through it will be the boundaries, but only the parts that are close to the vertex is guaranteed. The next step is to move this large region by one unit length along the coordinate axes. Our original region has a vertex on $(1, 1, 1, 1)$. And now we have 15 new regions that have vertices on $(1, 0, 0, 0), (0, 1, 0, 0), (0, 0, 1, 0), (0, 0, 0, 1), (0, 1, 1, 1), (1, 0, 1, 1), (1, 1, 0, 1), (1, 1, 1, 0), (1, 1, 0, 0), (1, 0, 1, 0), (1, 0, 0, 1), (0, 1, 1, 0), (0, 1, 0, 1), (0, 0, 1, 1)$ and $(0, 0, 0, 0)$. Our partition should be a region that has one unit volume, and tiles the whole space. So if we move the partition to these positions they should have no overlaps. But using this large region we will have overlaps for sure. So we just need to find the overlaps between these 15 new regions and our original region, and cut off these overlapped region from the original region. Then what we

get is the correct partition. It has no overlap with the neighboring region, and I have calculate that the volume of this partition is one.

2018-07-10 Han I have the hyperplanes passing through the origin and the point $(1, 1, 1, 1)$ in (18.74–18.75). Other hyperplanes are:

Hyperplanes passing through $(1, 0, 0, 0)$:

$$\begin{aligned} -\Lambda_3x - \Lambda_3y + z + w &= -\Lambda_3 \\ x + y - \Lambda_3z - \Lambda_3w &= 1 \\ \Lambda_1x - \Lambda_1y - z + w &= \Lambda_1 \\ -x + y + \Lambda_1z - \Lambda_1w &= -1 \end{aligned} \tag{18.76}$$

Hyperplanes passing through $(0, 1, 0, 0)$:

$$\begin{aligned} -\Lambda_3x - \Lambda_3y + z + w &= -\Lambda_3 \\ x + y - \Lambda_3z - \Lambda_3w &= 1 \\ \Lambda_1x - \Lambda_1y - z + w &= -\Lambda_1 \\ -x + y + \Lambda_1z - \Lambda_1w &= 1 \end{aligned} \tag{18.77}$$

Hyperplanes passing through $(0, 0, 1, 0)$:

$$\begin{aligned} -\Lambda_3x - \Lambda_3y + z + w &= 1 \\ x + y - \Lambda_3z - \Lambda_3w &= -\Lambda_3 \\ \Lambda_1x - \Lambda_1y - z + w &= -1 \\ -x + y + \Lambda_1z - \Lambda_1w &= \Lambda_1 \end{aligned} \tag{18.78}$$

Hyperplanes passing through $(0, 0, 0, 1)$:

$$\begin{aligned} -\Lambda_3x - \Lambda_3y + z + w &= 1 \\ x + y - \Lambda_3z - \Lambda_3w &= -\Lambda_3 \\ \Lambda_1x - \Lambda_1y - z + w &= 1 \\ -x + y + \Lambda_1z - \Lambda_1w &= -\Lambda_1 \end{aligned} \tag{18.79}$$

Hyperplanes passing through $(0, 1, 1, 1)$:

$$\begin{aligned} -\Lambda_3x - \Lambda_3y + z + w &= 2 - \Lambda_3 \\ x + y - \Lambda_3z - \Lambda_3w &= 1 - 2\Lambda_3 \\ \Lambda_1x - \Lambda_1y - z + w &= -\Lambda_1 \\ -x + y + \Lambda_1z - \Lambda_1w &= 1 \end{aligned} \tag{18.80}$$

Hyperplanes passing through $(1, 0, 1, 1)$:

$$\begin{aligned} -\Lambda_3x - \Lambda_3y + z + w &= 2 - \Lambda_3 \\ x + y - \Lambda_3z - \Lambda_3w &= 1 - 2\Lambda_3 \\ \Lambda_1x - \Lambda_1y - z + w &= \Lambda_1 \\ -x + y + \Lambda_1z - \Lambda_1w &= -1 \end{aligned} \tag{18.81}$$

Hyperplanes passing through $(1, 1, 0, 1)$:

$$\begin{aligned} -\Lambda_3x - \Lambda_3y + z + w &= 1 - 2\Lambda_3 \\ x + y - \Lambda_3z - \Lambda_3w &= 2 - \Lambda_3 \\ \Lambda_1x - \Lambda_1y - z + w &= 1 \\ -x + y + \Lambda_1z - \Lambda_1w &= -\Lambda_1 \end{aligned} \tag{18.82}$$

Hyperplanes passing through $(1, 1, 1, 0)$:

$$\begin{aligned} -\Lambda_3x - \Lambda_3y + z + w &= 1 - 2\Lambda_3 \\ x + y - \Lambda_3z - \Lambda_3w &= 2 - \Lambda_3 \\ \Lambda_1x - \Lambda_1y - z + w &= -1 \\ -x + y + \Lambda_1z - \Lambda_1w &= \Lambda_1 \end{aligned} \tag{18.83}$$

Hyperplanes passing through $(1, 1, 0, 0)$:

$$\begin{aligned} -\Lambda_3x - \Lambda_3y + z + w &= -2\Lambda_3 \\ x + y - \Lambda_3z - \Lambda_3w &= 2 \\ \Lambda_1x - \Lambda_1y - z + w &= 0 \\ -x + y + \Lambda_1z - \Lambda_1w &= 0 \end{aligned} \tag{18.84}$$

Hyperplanes passing through $(1, 0, 1, 0)$:

$$\begin{aligned} -\Lambda_3x - \Lambda_3y + z + w &= 1 - \Lambda_3 \\ x + y - \Lambda_3z - \Lambda_3w &= 1 - \Lambda_3 \\ \Lambda_1x - \Lambda_1y - z + w &= \Lambda_1 - 1 \\ -x + y + \Lambda_1z - \Lambda_1w &= \Lambda_1 - 1 \end{aligned} \tag{18.85}$$

Hyperplanes passing through $(1, 0, 0, 1)$:

$$\begin{aligned} -\Lambda_3x - \Lambda_3y + z + w &= 1 - \Lambda_3 \\ x + y - \Lambda_3z - \Lambda_3w &= 1 - \Lambda_3 \\ \Lambda_1x - \Lambda_1y - z + w &= \Lambda_1 + 1 \\ -x + y + \Lambda_1z - \Lambda_1w &= -\Lambda_1 - 1 \end{aligned} \tag{18.86}$$

Hyperplanes passing through $(0, 1, 1, 0)$:

$$\begin{aligned} -\Lambda_3x - \Lambda_3y + z + w &= 1 - \Lambda_3 \\ x + y - \Lambda_3z - \Lambda_3w &= 1 - \Lambda_3 \\ \Lambda_1x - \Lambda_1y - z + w &= -\Lambda_1 - 1 \\ -x + y + \Lambda_1z - \Lambda_1w &= \Lambda_1 + 1 \end{aligned} \tag{18.87}$$

Hyperplanes passing through $(0, 1, 0, 1)$:

$$\begin{aligned} -\Lambda_3x - \Lambda_3y + z + w &= 1 - \Lambda_3 \\ x + y - \Lambda_3z - \Lambda_3w &= 1 - \Lambda_3 \\ \Lambda_1x - \Lambda_1y - z + w &= 1 - \Lambda_1 \\ -x + y + \Lambda_1z - \Lambda_1w &= 1 - \Lambda_1 \end{aligned} \quad (18.88)$$

Hyperplanes passing through $(0, 0, 1, 1)$:

$$\begin{aligned} -\Lambda_3x - \Lambda_3y + z + w &= 2 \\ x + y - \Lambda_3z - \Lambda_3w &= -2\Lambda_3 \\ \Lambda_1x - \Lambda_1y - z + w &= 0 \\ -x + y + \Lambda_1z - \Lambda_1w &= 0 \end{aligned} \quad (18.89)$$

So all of these hyperplanes are perpendicular to one of the four vectors in (18.73). When I get the large original region, I use the boundaries:

$$\begin{aligned} \Lambda_1x - \Lambda_1y - z + w &= 0 \\ -x + y + \Lambda_1z - \Lambda_1w &= 0 \\ \Lambda_1x - \Lambda_1y - z + w &= \Lambda_1 + 1 \\ -x + y + \Lambda_1z - \Lambda_1w &= \Lambda_1 + 1 \end{aligned} \quad (18.90)$$

These are four of the eight boundaries that enclose the large region. These four hyperplanes are perpendicular to the last two vectors in (18.73). And you can see why we have different rules for the left site and right site. If I use :

$$\begin{aligned} \Lambda_1x - \Lambda_1y - z + w &= \frac{\Lambda_1 + 1}{2} \\ -x + y + \Lambda_1z - \Lambda_1w &= \frac{\Lambda_1 + 1}{2} \\ \Lambda_1x - \Lambda_1y - z + w &= \frac{\Lambda_1 + 1}{2} \\ -x + y + \Lambda_1z - \Lambda_1w &= \frac{\Lambda_1 + 1}{2}, \end{aligned} \quad (18.91)$$

instead of (18.90) I will have a partition that is invariant under the swap of $x_{1,t-1}, x_{1,t}$ and $x_{2,t-1}, x_{2,t}$ (in the equation of the planes it is a swap of x, z and y, w). Then we will have the same rule for both the left site and right site. But unfortunately these hyperplanes don't pass through the fixed points (points with integer coordinates). From the experience of the one-dimensional problem I don't think this will give us the generating partition.

2018-07-10 Han This part is not important. The problem of finding a tiling region in three-dimensions is very instructive when we find the generating partition in four-dimensions. Assuming we are given 3 independent

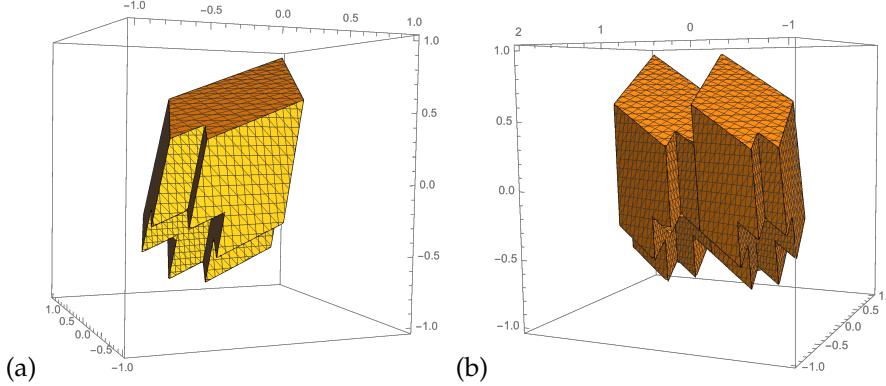


Figure 18.36: (a) A tiling region in three-dimensions. (b) The tiling region and one nearest neighboring region. You can see the boundaries exactly matched.

planes in three-dimensions. We want to find a region that can be used to tile the whole space by moving integer number of unit length along the coordinate axes. This region has unit volume. And we want to use the planes passing through the points with integer coordinates to enclose this region. Figure 18.36 is the tiling region that I get. It's not unique. From this figure you can imagine the structure of the four-dimensional partition. I have a Mathematica notebook in [siminos/figSrc/han/Mathematica/HL3-dimensional_tiling.nb](#) so you can rotate the figure.

2018-07-13 Predrag If you are very lucky, 1-step in space direction might suffice to understand all steps in space, just like for time evolution one step in time gave partition for times. However, you are not using the symplectic structure of the Hamiltonian formulation you are exploring. The Hamiltonian phase space for this problem are the four 4-vectors, something like

$$(\vec{x}_{1,t}, \vec{p}_{1,t}, \vec{x}_{2,t}, \vec{p}_{2,t}),$$

where the symplectic 2- and 4-volumes

$$\vec{x}_{1,t}^\top \omega \vec{p}_{1,t}, + \vec{x}_{2,t}^\top \omega \vec{p}_{2,t},$$

and $\det(\vec{x}_{1,t}, \vec{p}_{1,t}, \vec{x}_{2,t}, \vec{p}_{2,t}) = 4\text{-volume}$. where you can choose $\vec{x}_{1,t}^\top \cdot \vec{x}_{2,t} = 0$.

2018-08-02 Han I have been trying to get a general formula of the number of periodic orbits. In fact given (18.264–18.266) we can write down the gen-

eral formula explicitly:

$$N_{[L \times T]} = \prod_{i=1}^L \left[\sum_{n=0}^{T/2} \sum_{m=0}^n \sum_{q=0}^{T-2m} \binom{T}{2n} \binom{n}{m} \binom{T-2m}{q} (-1)^{m+q} 2^{-T+2m+q+1} s^{T-2m-q} \cos^q\left(\frac{2\pi i}{L}\right) - 2 \right] \quad (18.92)$$

when T is an even number (if T is odd we only need to change the $T/2$ to $(T+1)/2$). But I cannot find a easier form where T and L are interchangeable. I'm trying to simplify (18.92) and thinking that using the **multiple-angle formulas** and some identities of the combinations we can cancel the cosine terms. Because generally they are irrational numbers but the results of (18.92) are always integers.

I was hoping that each term of the product in (18.92) is an integer but this is not true. One example is when $L = 5$ and $T = 1$, one of the eigenvalues of the evolution matrix is $\Lambda(L)_1 = 1/2(s - 2 \cos(2\pi/5) + \sqrt{(s - 2 \cos(2\pi/5))^2 - 4})$. The corresponding term in the product is:

$$(\Lambda_1 + \Lambda_1^{-1} - 2) = s - 2 - 2 \cos\left(\frac{2\pi}{5}\right) = \frac{1}{2}(7 - \sqrt{5}) \quad (18.93)$$

which is not an integer. The term corresponding to the eigenvalue containing $\cos(4\pi/5)$ is equal to $\frac{1}{2}(7 + \sqrt{5})$. Multiplying these two terms together gives us an integer. This means that each term in the product is not necessarily an integer and I will need to evaluate the product explicitly to cancel the trigonometric functions.

I also tried to evaluate (18.264) for several different L and T s, hoping to find the expression directly. But I didn't find any valid expression. I guess the general formula cannot be trivial. I observed something but they are not helpful... Rana already stated this in her report, see (19.4). When the spatial length is 1, the number of periodic orbits can be expressed with Fibonacci numbers. And when $L = 2$ or $L = 3$, we can also express the number of periodic orbits by Fibonacci numbers but in very different forms.

2018-08-03 Han I think I remember everything in the online meeting, but not necessarily understand everything. Here is my best attempt at a summary:

- (1) Understand the eigenvalues of Toeplitz tensors. When we calculated the Green's function of the 2-dimensional spatiotemporal cat we used the tensor Fourier transform (18.58) to diagonalize the circulant tensor (1.155). And the diagonal elements are the eigenvalues of the circulant tensor?
- (2) Go from the Hamiltonian formulation (18.259) to the Lagrangian formulation (5.3), as in sect. 8.2. Use symplectic transformations.

- (3) Use the symmetries of the system, see sect. ???. We have time reversal symmetry and space inversion symmetry, and more.
- (4) By Noether's theorem, sect. 7.3, for each symmetry there should exist a conserved quantity, such as energy, the discrete momentum, discrete rotations; it's a research active subject, here is a recent [conference](#). For field theory one expects infinitely many conserved quantities. Crazy idea, but very satisfying if true: could the conserved quantities be the numbers of periodic orbits?
- (5) I'm not sure about this last thing. By similarity transformation we can interchange change the L and T ?

2018-08-03 Han I just realized that I can also use the "determinant" of the circulant tensor to get the number of the periodic orbits directly... I believe you already know this and this is why you told me to look at the Toeplitz tensors...³

For the $d = 1$ case, the number of the periodic orbits is the determinant of the circulant matrix (1.144). When the dimension is larger than 1, we have a circulant tensor instead of the circulant matrix. And the determinant can be given by the product of all the eigenvalues. (I guess I need to think more before we can call it determinant...) When we calculate the Green's function, we use the tensorial Fourier transform to diagonalize the tensor. For a tensor $\mathcal{D}_{lt,l't'}$ the diagonal elements are $\mathcal{D}'_{lt,lt}$. Then the determinant is given by:

$$\det(\mathcal{D}) = \prod_{t=1}^T \prod_{l=1}^L \mathcal{D}'_{lt,lt} \quad (18.94)$$

where the \mathcal{D}' is the diagonalized \mathcal{D} . I have tried a few blocks and this gives me correct number of periodic orbits. Everything is clear now. I will get the general form as soon as possible.

2018-08-06 Han The number of periodic points of the discrete 2-torus is:⁴

$$N_{[L \times T]} = \prod_{t=1}^T \prod_{l=1}^L \left(s - 2 \cos\left(\frac{2\pi l}{L}\right) - 2 \cos\left(\frac{2\pi t}{T}\right) \right) \quad (18.95)$$

In all $d = 2$ examples we take $s = 5$.⁵

³Predrag 2018-08-010: Is the "determinant" of the circulant tensor defined anywhere in the literature?

⁴Predrag 2018-08-25: My conceptual problem is totally elementary, and I probably have seen the answer and forgotten it: how does this product of various cos's yield integers? It has to, as we started with integers and then went through Fourier transforms to get this diagonalized formula. Wonder whether there is a more direct way of seeing it... Also, why is everything cos's, whereas we know that for sufficiently large s everything is cosh's? For $d = 1$ the eigenvalues, eigenvectors [49] are cos's for $-2 < s < 2$, but cosh's for $s > 2$, see (1.52). Note also that there is one trivial eigenvalue (rotational invariance?) and $T - 1$ non-trivial ones.

⁵Predrag 2018-08-25: Notation $N_{[L \times T]}$ is experimental.

2018-08-06 Han I have calculated the topological entropy using (18.264). The topological entropy of spatially periodic discrete domain of period L is

$$h(L) = \lim_{T \rightarrow \infty} \frac{1}{T} \ln N_{LT} \quad (18.96)$$

Using (18.264) we have:

$$\begin{aligned} h(L) &= \lim_{T \rightarrow \infty} \frac{1}{T} \ln \prod_{i=1}^L (\Lambda_i^T + \Lambda_i^{-T} - 2) \\ &= \sum_{i=1}^L \ln \Lambda_i = \sum_{i=1}^L \ln \frac{\lambda_i + \sqrt{\lambda_i^2 - 4}}{2} \end{aligned} \quad (18.97)$$

where λ_i is given by (18.265).

Using (18.95) we can get the same result. Substituting (18.95) into (18.96) we have:

$$\begin{aligned} h(L) &= \lim_{T \rightarrow \infty} \frac{1}{T} \ln \prod_{t=1}^T \prod_{l=1}^L [5 - 2 \cos(\frac{2\pi l}{L}) - 2 \cos(\frac{2\pi t}{T})] \\ &= \sum_{l=1}^L \lim_{T \rightarrow \infty} \frac{1}{T} \sum_{t=1}^T \ln [5 - 2 \cos(\frac{2\pi l}{L}) - 2 \cos(\frac{2\pi t}{T})] \end{aligned} \quad (18.98)$$

When T goes to infinity, we can change the sum over t to an integral. Let $a_l = 5 - 2 \cos(2\pi l/L)$. Then (18.99) becomes:

$$\begin{aligned} h(L) &= \sum_{l=1}^L \int_0^1 \ln [5 - 2 \cos(\frac{2\pi l}{L}) - 2 \cos(2\pi t)] dt \\ &= \sum_{l=1}^L \int_0^1 \ln [a_l - 2 \cos(2\pi t)] dt \\ &= \sum_{l=1}^L \ln \frac{a_l + \sqrt{a_l^2 - 4}}{2}, \end{aligned} \quad (18.99)$$

which is same as (18.97).

2018-08-06 Han The rate of growth of the number of periodic orbits per unit

spatial length is $h(L)/L$. As L goes to infinity, we have

$$\begin{aligned}
 h &= \lim_{L \rightarrow \infty} \frac{h(L)}{L} = \lim_{\substack{L \rightarrow \infty \\ T \rightarrow \infty}} \frac{1}{L} \frac{1}{T} \ln N_{[L \times T]} \\
 &= \lim_{L \rightarrow \infty} \frac{1}{L} \sum_{l=1}^L \lim_{T \rightarrow \infty} \frac{1}{T} \sum_{t=1}^T \ln \left(5 - 2 \cos\left(\frac{2\pi l}{L}\right) - 2 \cos\left(\frac{2\pi t}{T}\right) \right) \\
 &= \int_0^1 \int_0^1 \ln[5 - 2 \cos(2\pi x) - 2 \cos(2\pi t)] dt dx \\
 &= \int_0^1 \ln \frac{[5 - 2 \cos(2\pi x)] + \sqrt{[5 - 2 \cos(2\pi x)]^2 - 4}}{2} dx \quad (18.100)
 \end{aligned}$$

Evaluating this numerically we get that the topological entropy density per unit length and unit time is $h \approx 1.508$.

2018-08-010 Predrag The number of periodic orbits (18.95) seems to be the product of Harshaw (5.56) eigenvalues for a doubly-periodic torus, just have to get the s dependence right.⁶ The eigenvalues of the damped Poisson matrix (18.49) in $d = 1$ are given by (18.57) or (18.265)

$$\lambda(L)_k = s - 2 \cos(2\pi k/L) . \quad (18.101)$$

2018-08-010 Predrag I'm optimistic about the drift of our argument. We are almost home. We should be able to relegate the Hamiltonian derivation to a tedious exercise in ChaosBook. Laplacian, or more precisely, the Green's function counts all paths. The trace of Green's function (i) counts all periodic points $N_{[L \times T]}$, and (ii) is given by the sum of eigenvalues (18.95). As explained in ChaosBook, the trace is a derivative of the determinant (topological zeta function), and thus we should be able to write down the spatiotemporal cat topological zeta function.

The classical trace formula and zeta function follow from the Green's function evaluated on all doubly periodic invariant 2-tori.

2018-08-15 Han By Green's function I guess you don't mean the inverse of the matrix at the left hand side of the (damped) screened Poisson equation (5.3) (We used to call it Green's function)? Because the trace of this matrix doesn't give us the number of the periodic orbits.

The trace of the Green's function is:

$$\text{Tr}(\Delta) = \sum_{T=1}^{\infty} \sum_{L=1}^{\infty} z^{L+T} \prod_{t=1}^T \prod_{l=1}^L \left(s - 2 \cos\left(\frac{2\pi l}{L}\right) - 2 \cos\left(\frac{2\pi t}{T}\right) \right) \quad (18.102)$$

⁶Predrag 2018-12-01: Do not remember where I got these Harshaw eigenvalues?

I'm not sure about the z^{L+T} (maybe it should be z^{LT} ?). The topological zeta function can be gotten from:

$$\text{Tr}(\Delta) = -z \frac{d}{dz} \ln \frac{1}{\zeta(z)} \quad (18.103)$$

So now the problems are how to evaluate the sum of the number of periodic orbits, and what is the correct form of z^{L+T} .

2018-08-15 Han From the definition of the topological zeta function:

$$1/\zeta_{\text{top}}(z) = \exp\left(-\sum_{n=1}^{\infty} \frac{z^n}{n} N_n\right) \quad (18.104)$$

we can get the topological zeta function by substituting the number of periodic points to (18.104). But now we have number of points in the doubly periodic invariant 2-tori $N_{[L \times T]}$ instead of 1-dimensional loops N_n . So I'm not sure what is the correct form of the topological zeta function of our problem.

2018-08-23 Han I haven't figured out how to evaluate the sum of the number of the periodic blocks. Assume the topological zeta function of the 2-torus is:

$$\zeta(z_1, z_2) = \exp\left(\sum_{T=1}^{\infty} \sum_{L=1}^{\infty} \frac{z_1^L z_2^T}{LT} N_{[L \times T]}\right) \quad (18.105)$$

We will need to evaluate the sum:

$$\sum_{T=1}^{\infty} \sum_{L=1}^{\infty} \frac{z_1^L z_2^T}{LT} N_{[L \times T]} = \sum_{L=1}^{\infty} \frac{z_1^L}{L} \sum_{T=1}^{\infty} \frac{z_2^T}{T} N_{[L \times T]} \quad (18.106)$$

The second sum can be evaluated using (18.264). (we don't like this formula because this expression is not compact and it's not symmetric about L and T , but it has the time period T in the exponent which makes it easier to calculate the sum) Expanding (18.264) each term is a constant times a combination of eigenvalues to the power of T , and the sum over all time period T will give us a logarithm of a product of eigenvalues, similar to (18.267). Then we evaluate the sum over L , which is a sum of logarithms. I haven't figured out how to evaluate this.

2018-08-23 Han I spent some time trying to understand the meaning of this experimental topological zeta function of 2-torus (18.105). If we write the local trace of a periodic block as t_p , then we have:

$$\begin{aligned} z_1^L z_2^T N_{[L \times T]} &= \sum_{\substack{L_p|L \\ T_p|T}} L_p T_p t_p^{\left(\frac{L}{L_p} \frac{T}{T_p}\right)} \\ &= \sum_p L_p T_p \sum_{r_1=1}^{\infty} \sum_{r_2=1}^{\infty} \delta_{L, L_p r_1} \delta_{T, T_p r_2} t_p^{r_1 r_2} \end{aligned} \quad (18.107)$$

Substitute (18.107) into (18.105):

$$\begin{aligned}
 1/\zeta_{\text{top}}(z_1, z_2) &= \exp \left(- \sum_{T=1}^{\infty} \sum_{L=1}^{\infty} \frac{z_1^L z_2^T}{LT} N_{[L \times T]} \right) \\
 &= \exp \left(- \sum_p \sum_{\substack{r_1 \\ r_2}} \frac{t_p^{r_1 r_2}}{r_1 r_2} \right) \\
 &= \exp \left(\sum_p \sum_{r_1} \frac{1}{r_1} \sum_{r_2} -\frac{1}{r_2} (t_p^{r_1})^{r_2} \right) \\
 &= \exp \left(\sum_p \sum_{r_1} \frac{1}{r_1} \ln(1 - t_p^{r_1}) \right)
 \end{aligned} \tag{18.108}$$

This sum over r_1 is convergent for small t_p but I can't get a simpler formula. Let:

$$f(t_p) = \exp \left(\sum_{r_1} \frac{1}{r_1} \ln(1 - t_p^{r_1}) \right) \tag{18.109}$$

Then the topological zeta function becomes:

$$1/\zeta_{\text{top}}(z_1, z_2) = \prod_p f(t_p) \tag{18.110}$$

This is not a product of $(1 - t_p)$ as I was hoping. But it is still a product of all the prime periodic blocks.

I also found Ban, Hu, Lin, and Lin [7], *Zeta functions for two-dimensional shifts of finite type*, see post 2016-05-04 **Predrag** above. I'm not sure if that is applicable to our problem.

2018-08-23 Han Here I will explain why (18.95) gives us the number of periodic blocks.

Consider first a 1-dimensional discrete time lattice of period T . The admissible periodic orbits are the solutions of the (damped) screened Poisson equation

$$\mathcal{D}\phi = m, \tag{18.111}$$

where ϕ is a vector in T -dimensional space, and \mathcal{D} is the circulant matrix given by (1.40). If we set each element of ϕ to be larger or equal to 0 and smaller than 1 (the shape of the partition does not affect the number of solutions), all admissible ϕ are in a T -dimensional hypercube of unit volume. The block m is also a T -dimensional vector but with integer coordinates. The matrix \mathcal{D} acting on a unit hypercube stretches it into a hyper-parallelepiped in T -dimensional space. Within each unit

volume of the stretched region there is a unique point with integer coordinates, corresponding to one periodic solution. Hence the volume of the stretched region, which is equal to the absolute value of the determinant of the matrix \mathcal{D} , is the number of periodic solutions of the given time period T .

For 2 or more spacetime dimensions the (damped) screened Poisson equation is always of the form (18.111). As the rank of tensors ϕ and m is d , one can always relabel the d indices as one vector index. For a 2-dimensional lattice, ϕ and m are 2-index tensors which can be relabelled as LT -dimensional vectors, and \mathcal{D} is a (tensor) matrix with its two pairs of indices ranging over (LT, LT) . The initial vector x is in a unit volume LT -dimensional hypercube, which is stretched by the (tensor) matrix \mathcal{D} into a hyper-parallelepiped whose volume is given by the determinant (18.94) of the (tensor) matrix \mathcal{D} .

The $[L \times T \times L \times T]$ tensor \mathcal{D} can be viewed as a (LT, LT) matrix, with the same number of elements. This rank 4 tensor, written as matrix, is in general not a circulant matrix. But the eigenvalues are same as the eigenvalues of the tensor; it is a block matrix which has a similar pattern as a circulant matrix. The determinant of this matrix is given by (18.94), and it indeed gives us the volume of the stretched region, i.e., the number of invariant 2-tori.

The determinant of \mathcal{D} (18.95) is the product of all the eigenvalues calculated by the discrete Fourier transform diagonalization of \mathcal{D} .

2018-08-30 Han The above attempt at a definition of the topological zeta function of the two-torus (18.105) is wrong because I only count the periodic blocks that tile the space (and time) by moving in the direction of space or time. A more appropriate definition of the topological zeta function of two-dimensional torus is given in Lind [38] *A Zeta function for \mathbb{Z}^d -actions* (Predrag found the paper [here](#)). If needed, his book [39] is in the CNS library).

Lind [38] defines the topological zeta function as⁷

$$\zeta_\alpha(s) = \exp \left(\sum_{J \in \mathcal{J}_d} \frac{p_J(\alpha)}{|J|} s^{|J|} \right) \quad (18.112)$$

where $\alpha : X \rightarrow X$ is a \mathbb{Z}^d -action. \mathcal{J}_d is the collection of finite-index subgroups in \mathbb{Z}^d . For $J \in \mathcal{J}_d$ put $|J| = |\mathbb{Z}^d/J|$, and

$$p_J(\alpha) = |\{x \in X : \alpha^\mathbf{n} x = x \text{ for all } \mathbf{n} \in J\}|. \quad (18.113)$$

For 2-dimensional lattice, a convenient general form of \mathcal{J}_2 is:

$$\mathcal{J}_2 = \left\{ \begin{bmatrix} a & b \\ 0 & c \end{bmatrix} \in \mathbb{Z}^2 : a \geq 1, c \geq 1, 0 \leq b \leq a-1 \right\} \quad (18.114)$$

⁷Han 2018-08-31: In Lind's article the subgroup of \mathbb{Z}^d is written as L . To avoid confusion with our spatial length L , I change it to J in this blog.

which gives us a complete collection of the tiling patterns, with each pattern only listed once. Each J is corresponding to one given tiling pattern, and

$$\mathbb{Z}^2/J = \begin{bmatrix} a & b \\ 0 & c \end{bmatrix}. \quad (18.115)$$

2018-10-09 Predrag Lind and Schmidt [40] *Symbolic and algebraic dynamical systems*, ([click here](#)) studies zeta functions for \mathbb{Z}^d actions.

2018-08-31 Han For each J , the corresponding periodic solutions satisfy:

$$x\left(\begin{bmatrix} l \\ t \end{bmatrix}\right) = x\left(\begin{bmatrix} l \\ t \end{bmatrix} + \begin{bmatrix} a & b \\ 0 & c \end{bmatrix} \begin{bmatrix} i \\ j \end{bmatrix}\right), \begin{bmatrix} i \\ j \end{bmatrix} \in \mathbb{Z}^2 \quad (18.116)$$

When $b = 0$, we are tiling the area by moving the block (the smallest repeating unit) along the time direction and along the space direction. The number of points in these solutions is given by (18.95).

To find the solution satisfies the relation (18.116), we need to modify the boundary of the tensor (1.40). I haven't figured out how to imagine the modified tensor. A easier way is to expand the tensor into a $LT \times LT$ matrix then modify it. Using the inverse of this matrix (the Green's function) we can solve for the periodic block that satisfies (18.116). And the determinant of the modified matrix is the number of periodic points.

I already found the general formula counting the number of periodic points, though I don't know why this works. Define:

$$B = \mathbb{Z}^2/J = \begin{bmatrix} a & b \\ 0 & c \end{bmatrix} \quad (18.117)$$

which is uniquely corresponding to a tiling pattern. Then the number of periodic points is:

$$N_J = \prod_{t=1}^T \prod_{l=1}^L \left(s - 2 \cos\left(\frac{2\pi l'}{\det(B)}\right) - 2 \cos\left(\frac{2\pi t'}{\det(B)}\right) \right) \quad (18.118)$$

where l' and t' are given by:

$$\begin{bmatrix} t' \\ l' \end{bmatrix} = B \begin{bmatrix} t \\ l \end{bmatrix} = \begin{bmatrix} a & b \\ 0 & c \end{bmatrix} \begin{bmatrix} t \\ l \end{bmatrix} \quad (18.119)$$

The L and T in (18.118) are the spatial and the time periods, and from (18.116) we know that $L = a$ and $T = c$. N_J is the determinant of the modified matrix, and each terms in (18.118) is an eigenvalue of the modified matrix.

I haven't understood why (18.118) works. And I'm sure (18.118) is not a good way to write the formula, because in (18.116) l is first component in the column vector but in (18.118) it becomes the second component. We can't generalize this formula to three-dimensions. Perhaps a better way is to let:

$$\begin{bmatrix} l'' \\ t'' \end{bmatrix} = C \begin{bmatrix} l \\ t \end{bmatrix} = \frac{1}{ac} \begin{bmatrix} c & 0 \\ -b & a \end{bmatrix} \begin{bmatrix} l \\ t \end{bmatrix}, \quad (18.120)$$

where C is the cofactor matrix of B . The number of periodic points is:

$$N_J = \prod_{t=1}^T \prod_{l=1}^L (s - 2 \cos(2\pi l'') - 2 \cos(2\pi t'')) \quad (18.121)$$

(18.118) and (18.121) give the same result. The eigenvalues are also the same.

I don't understand these formulas. But good thing is these formulas are modified from (18.95) using the matrix $B = \mathbb{Z}^2/J$, so given a translation pattern we can count the number of periodic points directly.

2018-02-16 Predrag We need a simple explanation for why the 2-dimensional A^n and the linearization of the $2n$ -dimensional matrix give the same multipliers, so I am re-reading Mackay and Meiss [42], *Linear stability of periodic orbits in Lagrangian systems* and incrementally editing the discussion of sect. 8.1.

2018-09-25 Predrag The 2018-09-27 math seminar by Igor Pak, UCLA, might be related to our invariant 2-tori counting: " Given a convex polytope P , what is the number of integer points in P ? This problem is of great interest in combinatorics and discrete geometry, with many important applications ranging from integer programming to statistics. From computational point of view it is hopeless in any dimensions, as the knapsack problem is a special case. Perhaps surprisingly, in bounded dimension the problem becomes tractable. How far can one go? Can one count points in projections of P , finite intersections of such projections, etc? We will survey both classical and recent results on the problem, emphasizing both algorithmic and complexity aspects. Some elegant hardness results will make an appearance in dimension as small as three. If time permits, we will discuss connections to Presburger Arithmetic and decidability problems for irrational polyhedra. Joint work with Danny Nguyen. "

We went, were dazzled and understood very little of it all.

2018-10-02 Han I tried to use (7.57) as the Lagrangian. It will give a result (7.61) different from (7.64). But I think this is not correct. The first reason is: using (7.53) we can eliminate all of the p 's, and get an equation of q_{n+1} , q_n , and q_{n-1} . The equation we get is (7.64).

The second reason is: we should be able to use the Lagrangian to get the momentum by (5.73). But using Lagrangian (7.57) we can't get the correct momentum. Using (7.62) we can get the correct momentum for both p_{n+1} and p_n .

I haven't read through Percival and Vivaldi [51]. But in their definition of Lagrangian they used X_t instead of x_t . It seems like this capital X is not constrained by modulo 1? I might be wrong. I'm still reading this article.

2018-10-19 Han Note: this entry is superseded by the derivation 2019-03-20 Han below, starting with eq. (18.160).

I have found a way to prove that (18.121) gives the determinant of the orbit Jacobian matrix for the two-dimensional lattice, for both the periodic boundary and relative periodic (twisted) boundary.

The orbit Jacobian matrix can always be written as:

$$\mathcal{J} = \sum_{j=1}^d (-s\mathbf{1} + r_j + r_j^\top) . \quad (18.122)$$

But for blocks with different size or different boundary, the shift matrices r_j satisfy different conditions. For example, consider the periodic blocks satisfying (18.116). The shift matrices satisfy:

$$\begin{aligned} r_l^a r_t^0 &= \mathbf{1} \\ r_l^b r_t^c &= \mathbf{1} . \end{aligned} \quad (18.123)$$

If $b = 0$, this is a regular periodic block. From (18.123) we can see that:

$$\begin{aligned} r_l^a &= \mathbf{1} \\ r_l^{ab} r_t^{ac} &= r_t^{ac} = \mathbf{1} . \end{aligned} \quad (18.124)$$

So the eigenvectors of r_l and r_t are also the eigenvectors of the shift matrices in a $a \times ac$ regular periodic block (The size of the eigenvector of the shift matrix with relative periodic (twisted) boundary is $a \times c$, but we can repeat this eigenvector to fill a $a \times ac$ block). The eigenvector of this large block can be written as:

$$\mathbf{e}_{lt} = e^{2\pi i(\frac{l'}{a} + \frac{t}{ac})} , \quad (18.125)$$

where $l' = 1, 2, \dots, a$ and $t' = 1, 2, \dots, ac$. Here the subscripts l and t are the indices of the elements. For this large block, the number of eigenvectors is $a \times ac$. But only ac of these eigenvectors satisfy (18.123):

$$\begin{aligned} r_l^b r_t^c \mathbf{e} &= \mathbf{e} \\ \implies e^{2\pi i[(\frac{(l+b)}{a} + \frac{(t+c)}{ac}) t']} &= e^{2\pi i(\frac{l'}{a} + \frac{t}{ac})} . \end{aligned} \quad (18.126)$$

So to make the eigenvectors satisfy (18.123), we must have:

$$\begin{aligned} \frac{(l+b)l'}{a} + \frac{(t+c)t'}{ac} &= \frac{ll'}{a} + \frac{tt'}{ac} + n \\ t' &= -bl' + na, \quad n \in \mathbb{Z} \end{aligned} \quad (18.127)$$

Let $l' = 1, 2, \dots, a$, and let $n = 1, 2, \dots, c$, we will get ac sets of l' and t' s. Write the elements of the eigenvectors as:

$$\begin{aligned} \mathbf{e}_{lt} &= e^{2\pi i [\frac{lcl'}{ac} + \frac{t(-bt' + na)}{ac}]} \\ &= e^{2\pi i [ll^* + tt^*]} \end{aligned} \quad (18.128)$$

where:

$$\begin{bmatrix} l^* \\ t^* \end{bmatrix} = \frac{1}{ac} \begin{bmatrix} c & 0 \\ -b & a \end{bmatrix} \begin{bmatrix} l' \\ n \end{bmatrix} = C \begin{bmatrix} l' \\ n \end{bmatrix}, \quad (18.129)$$

The matrix C is the cofactor matrix of the matrix in (18.116) divided by the determinant of this matrix (which is also the transpose of the inverse matrix). So for a given set of l' and n , we have a specific eigenvector that has:

$$\begin{aligned} (\sigma_l + r_l^\top) \mathbf{e}_{l',n} &= 2 \cos(2\pi l^*) \mathbf{e}_{l',n} \\ (r_t + r_t^\top) \mathbf{e}_{l',n} &= 2 \cos(2\pi t^*) \mathbf{e}_{l',n}. \end{aligned} \quad (18.130)$$

The subscripts l' and n mean that this is the eigenvector that given by a certain set of l' and n (So $\mathbf{e}_{l',n}$ here is a vector, not the l' 'th and n th component.). l^* and t^* are determined by l' and n using (18.129).

So the eigenvalues of the orbit Jacobian matrix are:

$$\sum_{j=1}^2 (-s\mathbf{1} + r_j + r_j^\top) \mathbf{e}_{l',n} = [-2s + 2 \cos(2\pi t^*) + 2 \cos(2\pi l^*)] \mathbf{e}_{l',n}, \quad (18.131)$$

and the determinant is the product of all eigenvalues is

$$\det \sum_{j=1}^2 (-s\mathbf{1} + r_j + r_j^\top) = \prod_{l'=1}^a \prod_{n=1}^c [-2s + 2 \cos(2\pi t^*) + 2 \cos(2\pi l^*)], \quad (18.132)$$

the same as (18.121). ⁸

Now a problem is: I don't know why in (18.129) the matrix is a transpose of the inverse of the matrix in (18.116). I just calculate the eigenvectors explicitly and the result I get is a cofactor matrix. I don't know if this is correct for higher dimensional lattice.

⁸Predrag 2019-07-11: to Han - correct the notation l', n, t^*, l^*

Another possible problem is: in (18.127), choose l' from $1, 2, \dots, a$ and n from $1, 2, \dots, c$ will give us a set of eigenvectors. But are these eigenvectors always independent? If we choose l' and n in this way, the t' we get is not always in $1, 2, \dots, ac$. But as long as the t' 's we get can form different eigenvectors we should be fine. I'm sure the eigenvectors are independent, but I'm still thinking how to prove it.

2018-10-26 Han Using the reciprocal lattice I found that using the transpose of inverse matrix as (18.129) is correct for three-dimensional lattice. I tried to prove that this method is correct for any dimensions.

For d -dimensional lattice, the size and the way of tiling of a periodic block can be given by:

$$x\left(\begin{bmatrix} l_1 \\ l_2 \\ \vdots \\ l_d \end{bmatrix}\right) = x\left(\begin{bmatrix} l_1 \\ l_2 \\ \vdots \\ l_d \end{bmatrix} + \mathbf{A} \begin{bmatrix} j_1 \\ j_2 \\ \vdots \\ j_d \end{bmatrix}\right), \quad \begin{bmatrix} j_1 \\ j_2 \\ \vdots \\ j_d \end{bmatrix} \in \mathbb{Z}^d, \quad (18.133)$$

where:

$$\mathbf{A} = \begin{bmatrix} a_{11} & a_{12} & a_{13} & \dots & a_{1d} \\ 0 & a_{22} & a_{23} & \dots & a_{2d} \\ 0 & 0 & a_{33} & \dots & a_{3d} \\ \vdots & \vdots & \vdots & \ddots & \vdots \\ 0 & 0 & 0 & \dots & a_{dd} \end{bmatrix}, \quad (18.134)$$

where $a_{ii} \geq 1$ and for $j \neq i, 0 \leq a_{ij} \leq a_{ii} - 1$. All elements are integers.

Follow the same procedure as above, we know that the eigenvectors of the shift matrices with the periodic boundary conditions defined in (18.133) have the form:

$$\vec{e}_{\vec{l}} = e^{2\pi i [l_1 l_1^* + l_2 l_2^* + \dots + l_d l_d^*]}. \quad (18.135)$$

This is an element of the eigenvector for a given set of \vec{l}^* .

The shift matrices need to satisfy the relations:

$$\begin{aligned} r_{l_1}^{a_{11}} &= \mathbf{1} \\ r_{l_1}^{a_{12}} r_{l_2}^{a_{22}} &= \mathbf{1} \\ r_{l_1}^{a_{13}} r_{l_2}^{a_{23}} r_{l_3}^{a_{33}} &= \mathbf{1} \\ &\vdots \end{aligned} \quad . \quad (18.136)$$

Using these operators acting on the eigenvectors (18.135), we have:

$$\begin{bmatrix} a_{11} & 0 & 0 & \dots & 0 \\ a_{12} & a_{22} & 0 & \dots & 0 \\ a_{13} & a_{23} & a_{33} & \dots & 0 \\ \vdots & \vdots & \vdots & \ddots & \vdots \\ a_{1d} & a_{2d} & a_{3d} & \dots & a_{dd} \end{bmatrix} \begin{bmatrix} l_1^* \\ l_2^* \\ l_3^* \\ \vdots \\ l_d^* \end{bmatrix} = \mathbf{A}^\top \begin{bmatrix} l_1^* \\ l_2^* \\ l_3^* \\ \vdots \\ l_d^* \end{bmatrix} = \begin{bmatrix} q_1 \\ q_2 \\ q_3 \\ \vdots \\ q_d \end{bmatrix}, \begin{bmatrix} q_1 \\ q_2 \\ q_3 \\ \vdots \\ q_d \end{bmatrix} \in \mathbb{Z}^d. \quad (18.137)$$

So \vec{l}^* satisfies:

$$\begin{bmatrix} l_1^* \\ l_2^* \\ l_3^* \\ \vdots \\ l_d^* \end{bmatrix} = (\mathbf{A}^{-1})^\top \begin{bmatrix} q_1 \\ q_2 \\ q_3 \\ \vdots \\ q_d \end{bmatrix}, \quad (18.138)$$

which is the general form of (18.129).

Given these eigenvectors, the determinant of the orbit Jacobian matrix is:

$$\text{Det} \left[\sum_{j=1}^d (-s\mathbf{1} + r_j + r_j^T) \right] = \prod_{q_1=1}^{a_{11}} \prod_{q_2=1}^{a_{22}} \cdots \prod_{q_d=1}^{a_{dd}} \left[-ds + \sum_{j=1}^d 2 \cos(2\pi l_j^*) \right], \quad (18.139)$$

where the l_j^* is given by (18.138). This is the general form of the determinant of the orbit Jacobian matrix, for any given dimensions, for both regular and relative periodic (twisted) boundary.

But there is one last thing that I haven't figure out... How do I know the indexes of the product in (18.139) is q_d from 1 to a_{dd} ? It's obvious in low dimensions. But I don't know how to prove this in any dimensions. I'm still working on this.

2018-11-29 Han Here I will summarize how do we count the number of periodic solutions and what do we still need to prove.

For a d -dimensional hypercubic lattice with each site labeled by d integers $z \in \mathbb{Z}^d$, we already know that the field value on each lattice site can be solved from:

$$(-\square + s - 2d) \phi_z = m_z, \quad (18.140)$$

where m_z is a given integer. If we want to solve for the periodic solutions, we will need to use the Laplacian \square with periodic boundaries. Eq. (18.140) holds for all kinds of periodic solutions. All properties of the periodic blocks are embedded in the Laplacian, including the spatial

length, time period and the way in which the block is twisted when it tiles the space.

ϕ_z is on a torus with length 1. The range of this torus can be simply as from 0 to 1, or a very complicated form as what we do in figure 18.2. But the range and partition of the torus will not affect the number of periodic solutions. The range of m_z depends on the range of the torus.

So the counting problem becomes solving:

$$(-\square + s - 2d) \phi = \mathbf{m}, \quad (18.141)$$

and count how many sets of integers \mathbf{m} can be given to (18.141) that have solutions X enclosed in the unit volume torus. Here X and \mathbf{m} have d indices. The range of these indices are from 1 to the length of the periodic block in the corresponding directions. Equation (18.141) is a set of linear equations. Even though X and \mathbf{m} are rank d tensors and $(-\square + s - 2d)$ is a rank $2d$ tensor, they are calculated as vectors and matrix.

Since the range of the torus will not affect the number of solutions, here we will choose the simplest torus: $0 \leq \phi_z < 1$. Then the admissible region of the vector x is a high dimensional hypercube with all coordinates larger or equal to 0 and smaller than 1. The dimension of vector X and \mathbf{m} is $\prod_{i=1}^d L_i$, where L_i is the length of periodic block in the i th directions. To count the number of solutions, imagine the admissible unit volume hypercube is mapped by matrix $(-\square + s - 2d)$ into a larger region. And each integer point enclosed in this region is corresponding to a periodic solution. (Unfinished)

2018-12-06 Han I checked that using the Chebyshev polynomial of the first kind we can calculate determinant of the circulant matrix (the orbit Jacobian matrix).

We already know that the determinant of the $[n \times n]$ Toeplitz matrix:

$$\mathcal{D}_n = \begin{pmatrix} s & -1 & 0 & 0 & \dots & 0 & 0 \\ -1 & s & -1 & 0 & \dots & 0 & 0 \\ 0 & -1 & s & -1 & \dots & 0 & 0 \\ \vdots & \vdots & \vdots & \vdots & \ddots & \vdots & \vdots \\ 0 & 0 & \dots & \dots & \dots & s & -1 \\ 0 & 0 & \dots & \dots & \dots & -1 & s \end{pmatrix} \quad (18.142)$$

can be calculated using the Chebyshev polynomial of the second kind:

$$\det(\mathcal{D}_n) = U_n(s/2). \quad (18.143)$$

Now we want to calculate the determinant of the $n \times n$ circulant matrix:

$$-\mathcal{J} = H_n = \begin{pmatrix} s & -1 & 0 & 0 & \dots & 0 & -1 \\ -1 & s & -1 & 0 & \dots & 0 & 0 \\ 0 & -1 & s & -1 & \dots & 0 & 0 \\ \vdots & \vdots & \vdots & \vdots & \ddots & \vdots & \vdots \\ 0 & 0 & \dots & \dots & \dots & s & -1 \\ -1 & 0 & \dots & \dots & \dots & -1 & s \end{pmatrix}. \quad (18.144)$$

Expand the determinant of H_n by minors at the first row:

$$\begin{aligned} \det(H_n) &= \sum_{j=1}^n (-1)^{j+1} (H_n)_{1,j} M_{1j}(H_n) \\ &= s M_{11}(H_n) + (-1)(-1) M_{12}(H_n) + (-1)^{n+1} (-1) M_{1n}(H_n). \end{aligned} \quad (18.145)$$

The $M_{ij}(H_n)$ is a minor of matrix H_n , obtained by taking the determinant of H_n with row i and column j removed. The three minors in (18.145) are:

$$M_{11}(H_n) = \det(\mathcal{D}_{n-1}), \quad (18.146)$$

$$\begin{aligned} M_{12}(H_n) &= \det \begin{pmatrix} -1 & -1 & 0 & 0 & \dots & 0 & 0 \\ 0 & s & -1 & 0 & \dots & 0 & 0 \\ 0 & -1 & s & -1 & \dots & 0 & 0 \\ \vdots & \vdots & \vdots & \vdots & \ddots & \vdots & \vdots \\ 0 & 0 & \dots & \dots & \dots & s & -1 \\ -1 & 0 & \dots & \dots & \dots & -1 & s \end{pmatrix} \\ &= (-1) \det(\mathcal{D}_{n-2}) \\ &\quad + (-1)^n (-1) \det \begin{pmatrix} -1 & 0 & 0 & \dots & 0 & 0 \\ s & -1 & 0 & \dots & 0 & 0 \\ -1 & s & -1 & \dots & 0 & 0 \\ \vdots & \vdots & \vdots & \ddots & \vdots & \vdots \\ 0 & \dots & \dots & \dots & s & -1 \end{pmatrix} \\ &\quad \text{(expand by minor at the first column)} \\ &= (-1) \det(\mathcal{D}_{n-2}) + (-1)^n (-1)(-1)^{n-2} \\ &\quad \text{(the last matrix is a lower triangular matrix)} \\ &= -\det(\mathcal{D}_{n-2}) - 1, \end{aligned} \quad (18.147)$$

$$\begin{aligned}
 M_{1n}(H_n) &= \det \begin{pmatrix} -1 & s & -1 & 0 & \dots & 0 \\ 0 & -1 & s & -1 & \dots & 0 \\ \vdots & \vdots & \vdots & \vdots & \ddots & \vdots \\ 0 & 0 & \dots & \dots & \dots & s \\ -1 & 0 & \dots & \dots & \dots & -1 \end{pmatrix} \\
 &= (-1) \det \begin{pmatrix} -1 & s & -1 & 0 & \dots & 0 \\ 0 & -1 & s & -1 & \dots & 0 \\ \vdots & \vdots & \vdots & \vdots & \ddots & \vdots \\ 0 & 0 & \dots & \dots & \dots & s \\ 0 & 0 & \dots & \dots & \dots & -1 \end{pmatrix} \\
 &\quad + (-1)^{n-2} (-1) \det \begin{pmatrix} s & -1 & 0 & \dots & 0 & 0 \\ -1 & s & -1 & \dots & 0 & 0 \\ \vdots & \vdots & \vdots & \ddots & \vdots & \vdots \\ 0 & 0 & \dots & \dots & s & -1 \\ 0 & 0 & \dots & \dots & -1 & s \end{pmatrix} \\
 &\quad (\text{expand by minor at the first column}) \\
 &= (-1)(-1)^{n-2} + (-1)^{n-2} (-1) \det \mathcal{D}_{n-2}. \tag{18.148}
 \end{aligned}$$

So the determinant of the $n \times n$ circulant orbit Jacobian matrix is:

$$\begin{aligned}
 \text{Det}(-\mathcal{J}) &= \det(H_n) \\
 &= s M_{11}(H_n) + (-1)(-1) M_{12}(H_n) + (-1)^{n+1} (-1) M_{1n}(H_n) \\
 &= s \det(\mathcal{D}_{n-1}) + (-1)(-1)(-\det(\mathcal{D}_{n-2}) - 1) \\
 &\quad + (-1)^{n+1} (-1)[(-1)(-1)^{n-2} + (-1)^{n-2} (-1) \det \mathcal{D}_{n-2}] \\
 &= s U_{n-1}(s/2) - 2 U_{n-2}(s/2) - 2 \\
 &= U_n(s/2) - U_{n-2}(s/2) - 2 \\
 &\quad (\text{use recurrence relation } U_{n+1}(x) = 2xU_n(x) - U_{n-1}(x)) \\
 &= 2T_n(s/2) - 2 \\
 &\quad (\text{use relation } T_n(x) = \frac{1}{2}(U_n(x) - U_{n-2}(x))), \tag{18.149}
 \end{aligned}$$

In agreement with (??).

When the time period n is 1 and 2, the orbit Jacobian matrix will be special:

$$-\mathcal{J} = \begin{pmatrix} s-2 \end{pmatrix}, \tag{18.150}$$

$$-\mathcal{J} = \begin{pmatrix} s & -2 \\ -2 & s \end{pmatrix}. \tag{18.151}$$

These determinants still satisfy (??).

2018-12-06 Predrag Wow - very impressive! I remember the proof of (18.143) being very quick, basically a 3-term recurrence relation (second-order difference equation [26]), in a reference cited someplace close to (1.43). Maybe you can show it by induction, assuming that if (??) is true for $n - 1$, then it is true for n . Then you start the recursion with (18.150) and (18.151).

2018-12-11 Han I have read Kook and Meiss [37] *Application of Newton's method to Lagrangian mappings*. The Newton's method here is a computational algorithm.

In this article the orbit Jacobian matrix is written as a block matrix and they invert the orbit Jacobian matrix via block-diagonalization. A block matrix is a matrix defined by smaller matrices, called blocks. I tried to write the orbit Jacobian matrix of 2-dimensional cat map (a rank 4 tensor) explicitly as a matrix (write the $L \times T \times L \times T$ tensor as a $LT \times LT$ matrix). The matrix can be written as a block matrix. For example, the orbit Jacobian matrix of a $[3 \times 3]$ periodic block (not relative periodic) is:

$$-\mathcal{J}_{[3 \times 3]_0} = \begin{pmatrix} \mathbf{S} & -\mathbf{I} & -\mathbf{I} \\ -\mathbf{I} & \mathbf{S} & -\mathbf{I} \\ -\mathbf{I} & -\mathbf{I} & \mathbf{S} \end{pmatrix}, \quad (18.152)$$

which is a circulant block matrix. The \mathbf{S} and \mathbf{I} are 3×3 matrices:

$$\mathbf{S} = \begin{pmatrix} s & -1 & -1 \\ -1 & s & -1 \\ -1 & -1 & s \end{pmatrix}, \quad \mathbf{I} = \begin{pmatrix} 1 & 0 & 0 \\ 0 & 1 & 0 \\ 0 & 0 & 1 \end{pmatrix}. \quad (18.153)$$

So perhaps using the Fourier transform to diagonalize the orbit Jacobian matrix tensor in each direction can be interpreted as doing the block-diagonalization to the block matrix and diagonalizing the block.

But for blocks with relative periodic (twisted) boundaries, the orbit Jacobian matrix will become more complicated...

2019-01-08 Han I made figure 18.37 to show how the volume (area) of the stretched torus counts the number of periodic points. Consider the cat map with $s = 3$. The periodic solutions satisfy:

$$\mathcal{J} \mathbf{X} = -\mathbf{M}, \quad (18.154)$$

where \mathcal{J} is the orbit Jacobian matrix of the periodic orbit with period n . If any ϕ on the torus satisfies (18.154), this ϕ is a periodic solution. So we can count the periodic points using H_n to stretch the torus and counting the number of integer points enclosed in the stretched region. I plotted the stretched region of periodic solutions with $n = 2$ and $n = 3$. The orbit Jacobian matrix for $n = 2$ and $n = 3$ are:

$$-\mathcal{J} = \begin{pmatrix} 3 & -2 \\ -2 & 3 \end{pmatrix} \quad (18.155)$$

$$-\mathcal{J} = \begin{pmatrix} 3 & -1 & -1 \\ -1 & 3 & -1 \\ -1 & -1 & 3 \end{pmatrix} \quad (18.156)$$

Let the range of the field value ϕ be $0 \leq \phi < 1$. Figure 18.37 (a) shows the number of periodic points with length 2. The unit square enclosed by black lines is the available region of (ϕ_n, ϕ_{n+1}) . The parallelogram with red borders are the region of the unit square stretched by the orbit Jacobian matrix \mathcal{J} . There are 4 blue dots which are the integer points in the parallelogram. Each one of these blue dots corresponds to a periodic point. The 4 green dots are integer points on the vertices of the parallelogram. These 4 points contribute to 1 periodic point. So there are 5 periodic points with period 2, corresponding to 3 periodic solutions (1 fixed point and 2 2-cycles). The area of this parallelogram is 5.

Figure 18.37 (b) shows the periodic points with length 3. The square cube with black border is the available region of torus $(\phi_n, \phi_{n+1}, \phi_{n+2})$. After stretched by orbit Jacobian matrix \mathcal{J} it becomes the parallelepiped with red border. There are 6 blue dots which are the integer points completely enclosed in the parallelepiped. The 8 green dots are integer points on the vertices of the parallelepiped, which contribute to 1 periodic points. There are 18 pink points which are integer points on the surface of the parallelepiped. These 18 points contribute to 9 periodic points. So the number of periodic points is 16 which is also the volume of the parallelepiped. I have a Mathematica notebook with this 3d plot in [siminos/figSrc/han/Mathematica /HLCountingFigures.nb](#) so you can rotate it.

2019-01-16 Han According to (18.46), the covering alphabet for the $s = 5$ spatiotemporal cat is

$$\mathcal{A} = \{3, 2, 1, 0, 1, 2, 3\}.$$

I plotted two $[12 \times 12]$ blocks of $d = 2, s = 5$ spatiotemporal cat. I choose the field to be in the range $\phi_z \in [-1/2, 1/2]$. Figure 18.38 are blocks corresponding to two admissible invariant 2-tori of figure 18.39. The m_z within the black borders are the same. Figure 18.40 shows the distance and the logarithm of the absolute value of the distance between these two invariant 2-tori.

The covering alphabet for this $\phi_z \in [-1/2, 1/2]$ spatiotemporal cat is

$$m_z \in \{-4, -3, -2, -1, 0, 1, 2, 3, 4\}. \quad (18.157)$$

⁹ To make it easier to find an admissible field here I only used $m_z \in \{-2, -1, 0, 1, 2\}$. But using m_z in this range does not guarantee that corresponding field is admissible. The starting random block of m_z usu-

⁹Predrag 2019-01-16: Is (18.46) wrong?

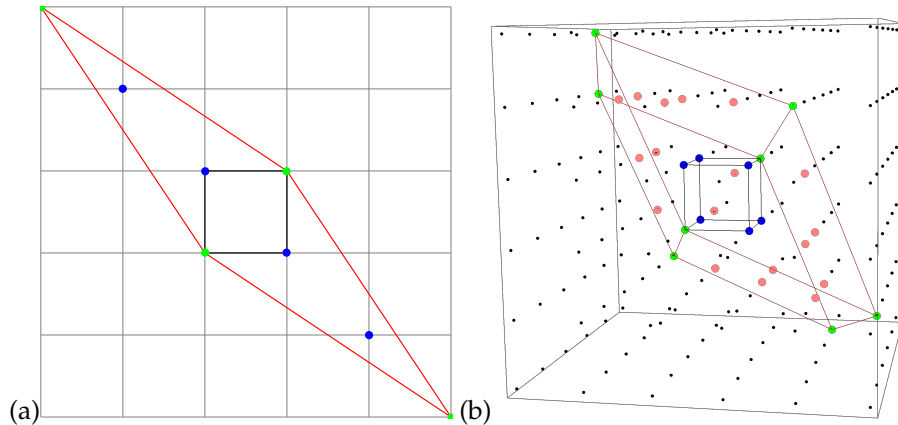


Figure 18.37: (a) A 2-dimensional torus (with black border) stretched by $-J$. The blue dots are internal integer points in the stretched parallelogram (with red border). The green dots are on the vertices of the parallelogram. (b) A 3-dimensional torus (with black border) stretched by $-J$. The blue dots are internal integer points in the stretched parallelepiped (with red border). The green dots are on the vertices of the parallelepiped. The pink dots are on the surface of the parallelepiped.

ally yields some ϕ_z outside $[-1/2, 1/2]$, so we keep changing the corresponding m_z until we find an admissible block. I can also redo this using (18.157).

The $[12 \times 12]$ blocks might be too small. As this block is periodic we might need a larger block to observe fields that differ exponentially. Adrien used $[18 \times 18]$ blocks.

2019-01-16 Predrag Shadowing looks promising. The Gutkin version has an argument about exponentially close shadowing using Green's functions.

You have to be very precise in explaining the algorithm that gets you from the initial random $[L_1 \times L_2]$ block to an admissible block. You know the number of distinct invariant 2-tori from your orbit Jacobian matrix determinant counting formula. If you have a systematic way of generating blocks for all admissible invariant 2-tori, that would be satisfying, even if we do not have a walks-on-Markov graph interpretation.

2019-01-16 Predrag As ϕ_z are rational numbers (presumably with large denominators, you can have a look), some distances in figure 18.40 (a) could be exactly zero.

2019-01-18 Han Figure 18.41 is an example of admissible symbol block M and the corresponding state X for a $[12 \times 12]$ 2-torus of the $d = 2, s = 5$ spatiotemporal cat. Here I started with random symbol block M with m_z from -4 to 4. The algorithm:

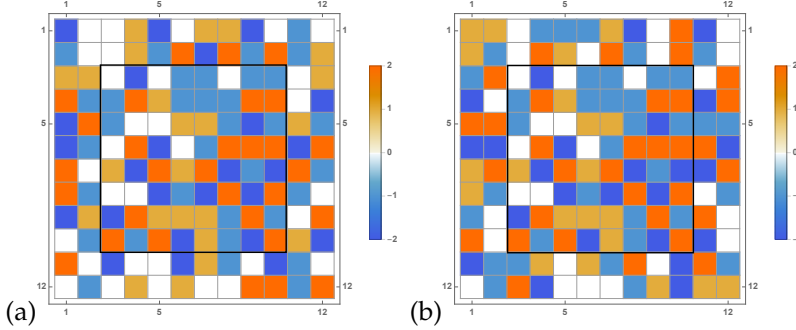


Figure 18.38: (a) and (b) are two admissible $[12 \times 12]$ blocks corresponding to the two distinct invariant 2-tori of figure 18.39. They coincide within the shared $[8 \times 8]$ block M_R , region R indicated by the black border.

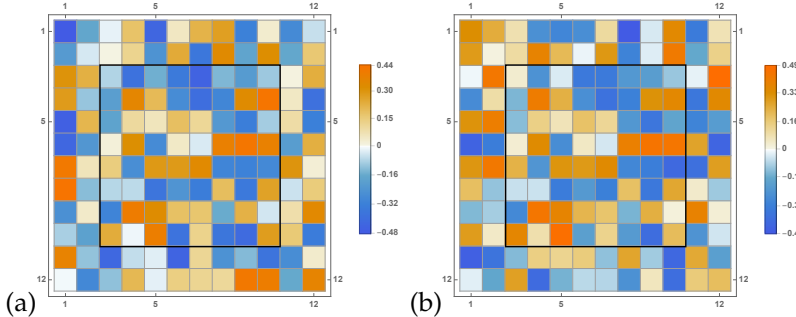


Figure 18.39: The two invariant 2-tori whose symbol arrays are given by the admissible $[12 \times 12]$ blocks of figure 18.38.

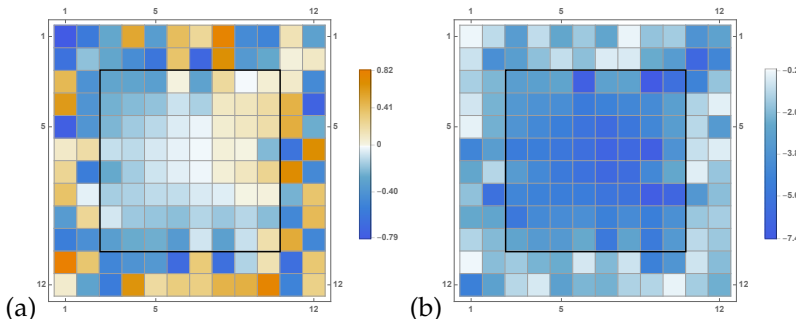


Figure 18.40: (a) The pointwise distance between the invariant 2-tori of figure 18.39. (b) The logarithm of the absolute value of the distance between the two invariant 2-tori indicate exponential shadowing close to the center of the shared M_R .

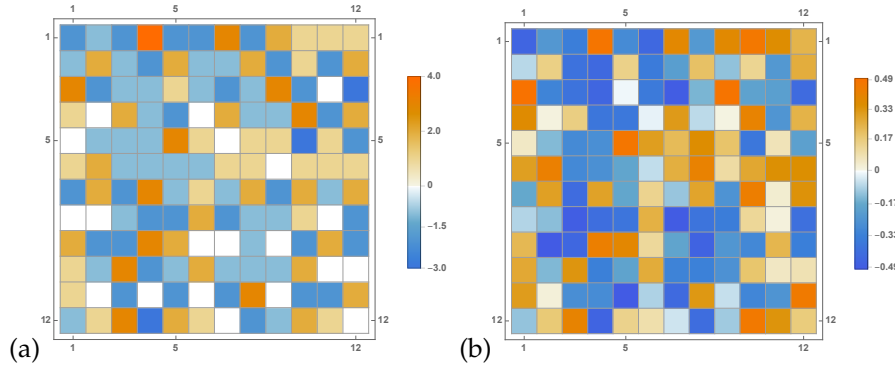


Figure 18.41: (a) An example of an admissible block M , initiated by a guess block with many $m_z = 4$. Row 1, column 3 site is the only one with $m_{(3,12)} = 4$.
 (b) The corresponding invariant 2-torus.

Use the Green's function to calculate the state X given the random symbol block M . If the maximum ϕ_z is larger or equal to $1/2$, find the position z of this maximum and change the corresponding symbol m_{max} to $m_{max} - 1$. If the minimum of this field is smaller than $-1/2$, find the position of the minimum and change the corresponding symbol m_{min} by $m_{min} + 1$. Then use the new block M to calculate the state X , and repeat this procedure until the state ϕ_z at every site is larger or equal to $-1/2$, and smaller than $1/2$. Generally it takes 70 to 100 iterations to reach an admissible block M .

As we expected, the symbol 4 and -4 are not very likely to exist in the admissible field. Because the maximum (minimum) of the field are likely to have 4 (-4) on its site (but not always). Figure 18.41 is a very rare case which still has a symbol equal to 4. In most of my runs I end up with all symbol from -3 to 3.

2019-01-19 Predrag Why go in steps of one? Symbol m_z is the integer part of ϕ_z that implements the translation to the desired unit interval (modulo 1 operation). So do not change $m_z \rightarrow m_z \pm 1$, but replace m_z by the integer translation that places ϕ_z into the admissible range. Also, start at one point z , and do this along a rectangular “out-spiral” around it. That will ensure that the center is exponentially well determined, and I expect that all inadmissible site values will sit outside the spiral.

2019-01-19 Predrag Matt, Han and I are using different words for the same things, so I keep editing everybody notes into the ‘standard’ notation. Probably best to read chapter 11 *Symbolic dynamics: a glossary*, and we discuss if something has to be changed.

2019-01-19 Predrag In our convention, the first lattice index is ‘space’, increasing from left to right, and the second index is ‘time’, increasing from bot-

tom up, see for example (11.8), so the y -axis labels in figure 18.41 (a) and all other figures of symbol blocks M should be increasing as one goes up. For symbol blocks the alphabet / number of colors is a discrete set, so the color bar on the right should be a set of colored squares. The states X , however, do need a continuous color bar.

2019-01-24 Han I redid the shadowing using symbol block M with m_z from -4 to 4. Figure 18.42 are blocks corresponding to two admissible invariant 2-tori of figure 18.43. The m_z within the black borders are the same. Figure 18.44 shows the distance and the logarithm of the absolute value of the distance between these two invariant 2-tori.

The algorithm I used is:

(1) Start with a random admissible state X^0 with $-1/2 \leq \phi_z < 1/2$. Calculate the corresponding symbol block M^0 . The m_z s in this symbol block are not integers. So we need to round these m_z s to the nearest integers and get symbol block M^1

(2) Use the Green's function and the integer symbol block M^1 to calculate the state X^1 . If the maximum ϕ_{max} is larger or equal to $1/2$, calculate the distance $\delta\phi_{max} = \phi_{max} - 1/2$. Round up $5\delta\phi_{max}$ (and call it δm_{max}). Then change the corresponding symbol m_{max} to $m_{max} - \delta m_{max}$. If the minimum ϕ_{min} is smaller than $1/2$, calculate the distance $\delta\phi_{min} = -\phi_{min} - 1/2$. Round up $5\delta\phi_{min}$ (and call it δm_{min}). Then change the corresponding symbol m_{min} to $m_{min} + \delta m_{min}$.

(3) Now we get a new symbol block M^2 . Repeat step (2) until all ϕ_z in X are in the admissible range.

Since we start with a state X with only admissible ϕ_z , now we only need no more than 10 iterations to reach an admissible block. Here we have to round up δm_{max} and δm_{min} so we always make a non-zero change. If we don't do this the program will very likely run into an endless loop.

The color bar of the symbol block should be colored squares. I haven't fixed this and the awkward axes due to "technical reasons"... Will fix that soon.

2019-03-01 Han To summarize why can we use the determinant of orbit Jacobian matrix to count the number of periodic solutions: For one-dimensional cat map, the problem of solving for a periodic string eventually becomes solving the linear equations

$$\begin{bmatrix} s & -1 & 0 & \dots & -1 \\ -1 & s & -1 & \dots & 0 \\ 0 & -1 & s & \dots & 0 \\ \vdots & \vdots & \vdots & \ddots & \vdots \\ -1 & 0 & 0 & \dots & s \end{bmatrix} \begin{bmatrix} x_1 \\ x_2 \\ x_3 \\ \vdots \\ x_T \end{bmatrix} = \begin{bmatrix} m_1 \\ m_2 \\ m_3 \\ \vdots \\ m_T \end{bmatrix}, \begin{bmatrix} m_1 \\ m_2 \\ m_3 \\ \vdots \\ m_T \end{bmatrix} \in \mathbb{Z}^T. \quad (18.158)$$

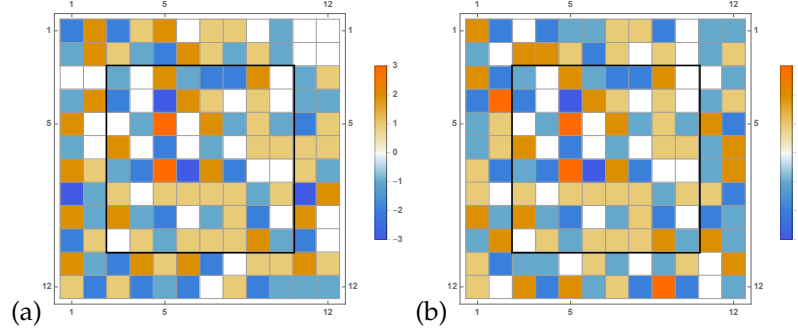


Figure 18.42: (a) and (b) are two admissible $[12 \times 12]$ blocks corresponding to the two distinct invariant 2-tori of figure 18.43. They coincide within the shared $[8 \times 8]$ block M_R , region R indicated by the black border.

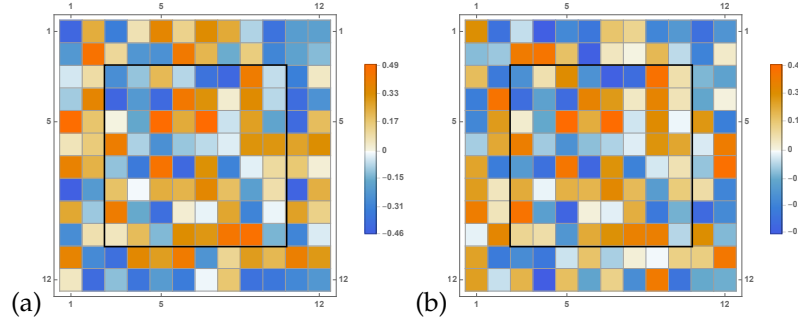


Figure 18.43: The two invariant 2-tori whose symbol arrays are given by the admissible $[12 \times 12]$ blocks of figure 18.42.

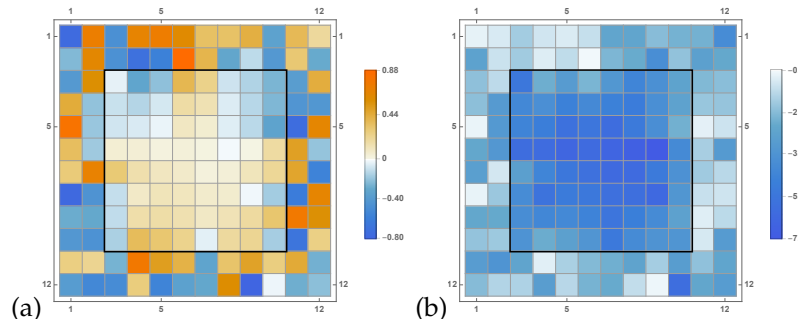


Figure 18.44: (a) The pointwise distance between the invariant 2-tori of figure 18.43. (b) The logarithm of the absolute value of the distance between the two invariant 2-tori indicate exponential shadowing close to the center of the shared M_R .

for x 's.

For any set of integers m_z , there is a solution x_z . But the solution is admissible only when each one of the field values x_z 's is larger or equal to 0 and smaller than 1. So all admissible solutions of period T are constrained to a T -dimensional hypercube with unit volume (all the field values within $0 \leq x_z < 1$). This hypercube will be stretched to a n -dependent parallelepiped by the orbit Jacobian matrix in (18.158). And each of the integer points inclosed within stretched parallelepiped will correspond to a periodic solution with period n . So the problem of counting the number of period solutions becomes counting the number of integer points enclosed in a parallelepiped.

Since all the field values can be equal to 0 but not equal to 1, when counting the integer points we must not count the points on the boundaries which correspond to field values 1. So counting the number of integer points in the parallelepiped is like counting the number of atoms in a unit cell. The parallelepiped can tile the space like the unit cell of a crystal lattice. And when the parallelepipeds tile the space, each of them is a cell of integer points, i.e., each of them is a repeating unit of integer points. The number of points in a large space is equal to the number of parallelepiped times the number of integer points within one parallelepiped. The density of integer points in the space is 1 per unit volume. So for an infinitely large space the number of integer points in it is equal to its volume. The number of the tiling parallelepipeds is equal to the space's volume divided by the volume of one parallelepiped. So the number of points in one parallelepiped is equal to the volume of the parallelepiped, which is given by the determinant of the orbit Jacobian matrix in (18.158).

To summarize, the reason that we can use the volume to count integer points is:

1. The region is a parallelepiped (so it can tile the space).
2. All vertices of the parallelepiped are integer points (so when tiling the space, each of these parallelepipeds is a repeating unit of integer points).
3. The density of integer points is one per unit volume.

2019-03-02 Han In order to count the cat map periodic solutions, and compute the field configuration given a symbol string, we diagonalize the orbit Jacobian matrix by a Fourier transform and compute its inverse, i.e., the Green's function. For the d -dimensional spatiotemporal cat, fields and symbol arrays are rank d tensors, related by the orbit Jacobian matrix in (18.158) which is a rank $2d$ tensor. This is still a linear equation, so the above method of counting and computing d -periodic solutions still applies. For a d -periodic block we now use the d -dimensional Fourier transform to invert the orbit Jacobian matrix and compute the d -periodic field configuration.

For a relative periodic block, with relative periodic (twisted) boundary, we cannot use Fourier transform.¹⁰ In this case we are still solving (18.158) except the rank $2d$ tensor is no longer a circulant tensor.¹¹ But we can still solve for the eigenvectors. I have shown how to compute the eigenvectors and eigenvalues in (18.122–18.132) and verified this is correct for small blocks. In (18.133–18.139) I proved this is correct in any dimension. Using these eigenvectors we can diagonalize the orbit Jacobian matrix and get the inverse (Green's function). The only problem is even though the counting formula is very compact, it seems to me that now it is hard to simplify the topological zeta function.¹²

I have explained everything clearly to Glen. He doesn't think there is any problem in these computations.

2019-02-04 Predrag What follows are some raggedly thoughts, you have already thought through all of them... My problem is I do not understand Lind [38] and your notes starting with **2018-08-30 Han** above.

We need to count all periodic and relative periodic orbits. In ChaosBook this is no harder than counting periodic orbits, but one has to quotient the symmetries first: for 2-dimensional spatiotemporal cat those are first the time and space translations, then the point group. The goal is to enumerate all distinct tilings of a square (hypercubic) lattice. I believe they have to be doubly (in general, d -periodic, but we have not proven it. Is it obvious that a -let's say- L -shaped region is not a legal tile? A quick sketch shows that a 3-sites L -shaped tile is equivalent to both $[1 \times 3]$ and $[3 \times 1]$ relative-periodic tilings, but is such a thing true in general?

Consider a finite block of symbols $M_{\mathcal{R}} \subset M$, over a finite $[L_1 \times L_2 \times \cdots \times L_d]$ hyper-parallelopiped region $\mathcal{R} \subset \mathbb{Z}^d$. In particular, let M_p over a finite rectangular $[L_1 \times L_2 \times \cdots \times L_d]$ lattice region be the $[L_1 \times L_2 \times \cdots \times L_d]$ d -periodic block of M whose repeats tile \mathbb{Z}^d .

Rectangles $[L_1 \times L_2]$ are obviously tiles, however the shape of a general tile does not have to be rectangular, or even connected - one is allowed to shift j th column $[1 \times L_2]$ by an arbitrary vertical shift $r_2^{s_j}$, $0 \leq s_j < L_2$, and k th row $[L_1 \times 1]$ by an arbitrary horizontal shift $r_1^{s_k}$, and any such raggedly 'tile' tiles the (hyper-)lattice.

Here I'm visualizing fields as residing on face-centered lattice, and translation shifts as acting across the vertical / horizontal boundary lines. Each solution finite block $X_{\mathcal{R}} \subset M$ breaks translational invariances, but

¹⁰Predrag 2019-02-04: A relative periodic block \hat{p} is always preperiodic to a periodic block whose period $T_p = rT_{\hat{p}}$, so you can always Fourier-transform this larger torus. But the right way of doing is acting relative periodic block \hat{p} with the translation r^r that makes it periodic, and then Fourier-transforming the minimal d -torus.

¹¹Predrag 2019-02-04: The orbit Jacobian matrix times the translation r^r is circulant, I believe. That is how we compute the Jacobian matrices of relative periodic orbits in ChaosBook.

¹²Predrag 2019-02-04: I doubt it. In ChaosBook we show that after symmetry reduction, counting relative periodic orbits is not any harder than counting periodic orbits.

the quotient (lattice)/ \mathcal{R} is still translationally invariant for \mathcal{R} a rectangle. But what if X is relative-periodic?

The reason I'm sketching such raggedly tiles is to try to visualize a 'natural' tile for a relative periodic tiling. In continuum dynamics one can go to a co-moving frame, where the trajectory on average looks stationary (no phase drift) but on a lattice there is no way of drawing a parallelopiped with straight sides - they must be raggedly...

Be it as it may, I define a relative (relative) periodic field by demanding that it satisfy

$$x_{jk} = r_1^{S_1} r_2^{S_2} x_{j+L_1, k+L_2} \text{ on every } z = (j, k) \text{ lattice site} \quad (18.159)$$

$0 \leq S_1 < L_1$, $0 \leq S_2 < L_2$. i.e., field value x_{jk} reappears spatiotemporally after periods (L_1, L_2) (in that case, we can draw a rectangle tile), and, in general, translated by shifts $(r_1^{S_1}, r_2^{S_2})$ bounded by corresponding periods.

Field configuration (18.159) is a legal (though not yet necessarily admissible) field configuration. One first has to enumerate such configurations distinct under the d -translations. There are clearly many equivalent relative tilings, for example easy to sketch vertical $[1 \times 3]$ and horizontal $[3 \times 1]$ relative-periodic tilings...

Next one has to quotient the point-group, for example the D_4 symmetry for the square lattice.

2019-03-20 Han Using the reciprocal lattice to determine the eigenvalues turns out to be much simpler than my previous method to find the eigenvectors for a relative periodic (twisted) boundary, leading to my formula (18.121) for the number of periodic points.

The idea is: a periodic tiling pattern is given by a Bravais lattice. All possible eigenmodes (eigenvalues, eigenvector pairs) are given by the reciprocal lattice wave vectors.

Imagine we have an infinite d -dimensional space with a field on it. There are translation operators in d independent directions. The eigenvectors (eigenstates) of these translation operators are plane waves:

$$f_{\mathbf{k}}(\mathbf{X}) = e^{i\mathbf{k} \cdot \mathbf{X}}, \quad (18.160)$$

where \mathbf{k} is any d -dimensional vector. Now we put a Bravais lattice in it, with lattice points given by

$$\mathbf{R} = \sum_{i=1}^d n_i \mathbf{a}_i, \quad (18.161)$$

with \mathbf{a}_i are the d independent Bravais cell vectors, and $n_i \in \mathbb{Z}$. In order that wave vectors \mathbf{k} in (18.160) have the periodicity of the Bravais lattice,

they must satisfy

$$f_{\mathbf{k}}(\mathbf{X} + \mathbf{R}) = e^{i\mathbf{k}\cdot\mathbf{X}} e^{i\mathbf{k}\cdot\mathbf{R}} = e^{i\mathbf{k}\cdot\mathbf{X}} = f_{\mathbf{k}}(\mathbf{X}), \quad (18.162)$$

so $\mathbf{k} \cdot \mathbf{R}$ must equal to an integer times 2π . The admissible \mathbf{k} lie on the reciprocal lattice if

$$\mathbf{K} = \sum_{i=1}^d k_i \mathbf{b}_i, \quad (18.163)$$

where the k_i are integers, and \mathbf{b}_i satisfy

$$\mathbf{b}_i \cdot \mathbf{a}_j = 2\pi \delta_{ij}. \quad (18.164)$$

Each lattice site in this reciprocal lattice corresponds to one eigenmode (eigenvalues, eigenvector pair), so there are still an infinity of them. But this is only true when we have a continuous periodic field in the space. For the cat map, the field has support only on the lattice sites. So the coordinates \mathbf{X} of this field are not continuous numbers but integer indices. In this case we only need wave vectors in a small region. This region is given by the first Brillouin zone of the reciprocal lattice.

For example, consider the 2D spatiotemporal cat. We want to find solutions with periodicity given by Bravais lattice:

$$\mathcal{L} = \{n_1 \mathbf{a}_1 + n_2 \mathbf{a}_2 | n_i \in \mathbb{Z}\}. \quad (18.165)$$

If these two basis vectors \mathbf{a}_1 and \mathbf{a}_2 are in the directions of the basis of the integer lattice, this is a regular periodic condition. A general periodic condition is $\mathbf{a}_1 = (l_1, l_2)$ and $\mathbf{a}_2 = (0, l_3)$.¹³ In Lind's paper this periodicity is written as a matrix, in the Hermite normal form (5.205).

$$[\mathbf{a}_1 \quad \mathbf{a}_2] = \begin{bmatrix} l_1 & l_2 \\ 0 & l_3 \end{bmatrix}. \quad (18.166)$$

The reciprocal lattice of this Bravais lattice is:

$$\bar{\mathcal{L}} = \{n_1 \mathbf{b}_1 + n_2 \mathbf{b}_2 | n_i \in \mathbb{Z}\}. \quad (18.167)$$

These two basis vectors satisfy (18.164). In this example they are

$$[\mathbf{b}_1 \quad \mathbf{b}_2] = \frac{2\pi}{l_1 l_3} \begin{bmatrix} l_3 & 0 \\ -l_2 & l_1 \end{bmatrix}, \quad (18.168)$$

which is the transpose of the inverse matrix of (18.166) times 2π . This is true in any dimension, as to satisfy (18.164), we must have

$$\begin{bmatrix} \mathbf{a}_1 \\ \mathbf{a}_2 \\ \vdots \\ \mathbf{a}_d \end{bmatrix} [\mathbf{b}_1 \mathbf{b}_2 \cdots \mathbf{b}_d] = 2\pi \mathbf{1}. \quad (18.169)$$

¹³Han 2019-06-25: (Should be $\mathbf{a}_1 = (l_1, 0)$ and $\mathbf{a}_2 = (l_2, l_3)$?)

Predrag 2019-06-26: Sorry, at the moment I'm not thinking about this, can you derive the correct \mathbf{a}_j for me?

So for any wave vector on the reciprocal lattice $\mathbf{k} = n_1 \mathbf{b}_1 + n_2 \mathbf{b}_2$, there is an eigenvector that satisfies the periodicity of the Bravais lattice:

$$f_{\mathbf{k}}(\mathbf{X}) = e^{i\mathbf{k}\cdot\mathbf{X}} = e^{i(n_1 \mathbf{b}_1 \cdot \mathbf{X} + n_2 \mathbf{b}_2 \cdot \mathbf{X})}, \quad (18.170)$$

where $\mathbf{X} = \{x_1, x_2\}$ are a lattice site vector. This is the same as my relative periodic (twisted) boundary eigenvectors (18.128).

But I have concern for the range of n_1 and n_2 in (18.170). n_1 and n_2 give us the position of the wave vector. The range of these two should make sure the wave vector in the Brillouin zone of the integer lattice. Consider a very specific example: let the basis of the Bravais lattice be:

$$[\mathbf{a}_1 \quad \mathbf{a}_2] = \begin{bmatrix} l_1 & l_2 \\ 0 & l_3 \end{bmatrix} = \begin{bmatrix} 3 & 1 \\ 0 & 2 \end{bmatrix}. \quad (18.171)$$

We can find the reciprocal lattice by compute the inverse of matrix in (18.171). The Bravais lattice and the reciprocal lattice are shown in figure 18.45. Figure 18.45(a) is the Bravais lattice which gives us the periodicity. Each parallelogram is a repeating unit of the field. The red and blue arrows are the two basis vectors \mathbf{a}_1 and \mathbf{a}_2 . Figure 18.45(b) is the reciprocal lattice. Each lattice site is a wave vector of the eigenvalue of the translation operator that satisfies the periodicity given by the Bravais lattice. The square enclosed by green dashed lines is the first Brillouin zone of the integer lattice. The field of spatiotemporal cat is a discrete field only defined on the integer points. Any field defined only on the discrete lattice can be transformed to a continuous field in the first Brillouin zone of the discrete lattice by Fourier transform. So all of the eigenvectors of this discrete field can be expressed with wave vectors in this Brillouin zone. This periodic block has 6 lattice sites in it, so each state is a 6-dimensional vector. There should be 6 eigenvectors. In figure 18.45(b) we do have 6 points in the green square (the two points on the boundary should be counted as one).

The problem is: the reciprocal lattice is not a square lattice as the Brillouin zone of the integer lattice. We cannot give a range of n_1 and n_2 in (18.170) separately. In my previous method I just used $n_1 = 0, 1, 2$ and $n_2 = 0, 1$. These are corresponding to the wave vectors enclosed in the square with green dashed boundaries in figure 18.46. In figure 18.46 the blue gridlines are reciprocal lattice of the integer lattice. We don't really need to use the wave vectors in the first Brillouin zone to express the eigenvectors. Any two wave vectors that differ by a vector in the reciprocal lattice of the integer lattice (in figure 18.46 it's the lattice of blue lines) should give us equivalent eigenvectors. So can we use the green square in figure 18.46 to enclose the wave vectors instead of the green square in figure 18.45(b), and have n_1 and n_2 go over a set of integers independently? I think the answer is yes. I just need to think a bit more about this...

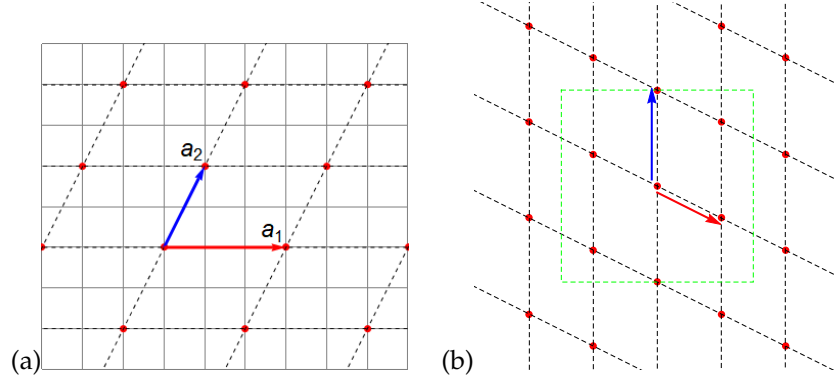


Figure 18.45: (a) The Bravais lattice defines the periodicity of the field. The red arrow is $a_1 = (3, 0)$ and the blue arrow is $a_2 = (1, 2)$. (b) The reciprocal lattice of the Bravais lattice (a). Each reciprocal lattice point is a wave vector of the eigenvector of the translation operator with periodicity given by the Bravais lattice (a). The green dashed lines enclose the first Brillouin zone of the **integer lattice** (not the Bravais lattice (a)). The wave vectors in this first Brillouin zone give us all the eigenvectors of the translation operator. The wave vectors outside of this region (**the first Brillouin zone enclosed by the green dashed lines**) are equivalent to a wave vector in the region (**2019-03-20 PC: what regions?**).

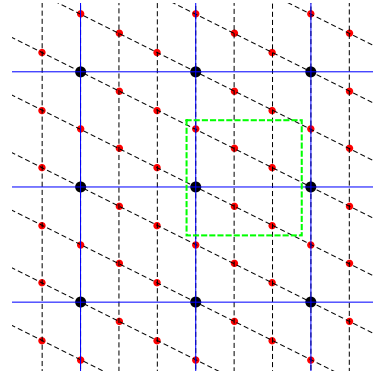


Figure 18.46: The reciprocal lattice of both the original direct lattice and the integer lattice. The red points are the reciprocal lattice of the Bravais lattice in figure 18.45(a). The black points are the reciprocal lattice of the integer lattice. Each of these squares enclosed by the blue lines has edge length 2π . And these squares are also repeating unit of the wave vectors (the red dots in this figure). Two wave vectors are equivalent if they are different by a vector on the reciprocal lattice of the integer lattice.

2019-04-12 Han After we get the eigenvectors of the translation operator, we can compute the eigenvalues of the orbit Jacobian matrix. For a d -dimensional cat map, the orbit Jacobian matrix is:

$$H = \sum_{j=1}^d \frac{s}{d} - r_j - r_j^\top. \quad (18.172)$$

The eigenvectors of the translation operators are eigenvectors of this orbit Jacobian matrix. All the eigenvectors have the form $f_{\mathbf{k}}(\mathbf{X}) = e^{i\mathbf{k}\cdot\mathbf{X}}$, where the wave vector \mathbf{k} is a vector on the reciprocal lattice of the direct lattice which gives the periodic tiling pattern. Let

$$\mathbf{k} = \begin{bmatrix} k_1 \\ k_2 \\ \vdots \\ k_d \end{bmatrix}, \quad \mathbf{X} = \begin{bmatrix} x_1 \\ x_2 \\ \vdots \\ x_d \end{bmatrix}. \quad (18.173)$$

Then we have:

$$(r_j + r_j^\top) f_{\mathbf{k}}(\mathbf{X}) = e^{i(\mathbf{k}\cdot\mathbf{X}-k_j)} + e^{i(\mathbf{k}\cdot\mathbf{X}+k_j)} = 2 \cos k_j e^{i\mathbf{k}\cdot\mathbf{X}} = 2 \cos k_j f_{\mathbf{k}}(\mathbf{X}). \quad (18.174)$$

The eigenvalue of the orbit Jacobian matrix corresponding to the eigenvector labeled by \mathbf{k} is:

$$\lambda_{\mathbf{k}} = \sum_{j=1}^d \frac{s}{d} - 2 \cos k_j. \quad (18.175)$$

Then the problem becomes finding k_j . \mathbf{k} can be written as:

$$\mathbf{k} = \begin{bmatrix} k_1 \\ k_2 \\ \vdots \\ k_d \end{bmatrix} = [\mathbf{b}_1 \ \mathbf{b}_2 \ \dots \ \mathbf{b}_d] \begin{bmatrix} n_1 \\ n_2 \\ \vdots \\ n_d \end{bmatrix} = n_1 \mathbf{b}_1 + n_2 \mathbf{b}_2 + \dots + n_d \mathbf{b}_d. \quad (18.176)$$

\mathbf{b}_i s are the vertical primitive vectors of the reciprocal lattice that satisfy (18.164). $[\mathbf{b}_1 \ \mathbf{b}_2 \ \dots \ \mathbf{b}_d]$ is a $d \times d$ matrix. n_i s are integers. Each wave vector \mathbf{k} is corresponding to a set of integers n_i .

A simple example is a two-dimensional cat map with the periodic pattern described by direct lattice with primitive vectors given in (18.166). The matrix of the primitive vectors of the reciprocal lattice is 2π times the transpose of the inverse of matrix in (18.166), given by (18.168). Then wave vector is:

$$\mathbf{k} = \begin{bmatrix} k_1 \\ k_2 \end{bmatrix} = [\mathbf{b}_1 \ \mathbf{b}_2] \begin{bmatrix} n_1 \\ n_2 \end{bmatrix} = \begin{bmatrix} \frac{2\pi n_1}{l_1} \\ \frac{2\pi n_2}{l_3} - \frac{2\pi l_2 n_1}{l_1 l_3} \end{bmatrix}. \quad (18.177)$$

Substitute into (18.175):

$$\begin{aligned}\lambda_{\mathbf{k}} &= \sum_{j=1}^2 \frac{s}{2} - 2 \cos k_j \\ &= s - 2 \cos k_1 - 2 \cos k_2 \\ &= s - 2 \cos\left(\frac{2\pi n_1}{l_1}\right) - 2 \cos\left(\frac{2\pi n_2}{l_3} - \frac{2\pi l_2 n_1}{l_1 l_3}\right).\end{aligned}\quad (18.178)$$

And this is the eigenvalue of the orbit Jacobian matrix corresponding to the eigenvector with wave vector $\mathbf{k} = n_1 \mathbf{b}_1 + n_2 \mathbf{b}_2$.

The determinant of the orbit Jacobian matrix is the product of all the eigenvalues:

$$\det H = \prod_{\mathbf{k}} \lambda_{\mathbf{k}} = \prod_{n_1=0}^{l_1-1} \prod_{n_2=0}^{l_3-1} s - 2 \cos\left(\frac{2\pi n_1}{l_1}\right) - 2 \cos\left(\frac{2\pi n_2}{l_3} - \frac{2\pi l_2 n_1}{l_1 l_3}\right). \quad (18.179)$$

I haven't found an elegant way to prove the product after the second equals sign is correct, that n_1 is from 0 to $l_1 - 1$ and n_2 is from 0 to $l_3 - 1$. One way to understand this is by looking at figure 18.46. The red points are the reciprocal lattice of the original direct lattice given by (18.171). The black points are the reciprocal lattice of the integer lattice. Since the field value only appears on the integer points, any two Fourier modes with wave vectors that are different by a vector on the reciprocal lattice of the integer lattice (in figure 18.46 they are different by a vector on the black points) are equivalent. So we only need wave vectors in a primitive cell of the reciprocal lattice of the integer lattice. When we choose n_1 from 0 to $l_1 - 1$ and n_2 from 0 to $l_3 - 1$ we find all the wave vectors in the primitive cell enclosed by the green dashed line in figure 18.46. The l_1 and l_3 here are two elements on the diagonal of the matrix (18.171). And choosing n_1 and n_2 using the numbers on the diagonal of the matrix of the primitive vectors is only correct when the matrix is an upper triangular matrix. For a more general matrix we are not able to let n_1 and n_2 go through a set of numbers independently. But if Lind is correct then all periodic patterns on an integer lattice can be described by a set of primitive vectors which can form an upper triangular matrix.

The number of periodic solutions with periodic pattern given by (18.171) is equal to the determinant of the orbit Jacobian matrix given by (18.179).

2019-10-04 Han I haven't found the proof of (7.45), so I will prove it here.

Assuming we have a d -dimensional map. The state of the system at time t is given by a d -dimensional vector $\mathbf{X}(t) = \{x_1(t), x_2(t), \dots, x_d(t)\}$. The forward-time Jacobian matrix is:

$$J(t)_{ij} = \frac{\partial x_i(t+1)}{\partial x_j(t)}. \quad (18.180)$$

A block matrix is a matrix defined by smaller matrices, called blocks. The matrix H (7.33) is now an $[n_p d \times n_p d]$ block matrix:

$$H(\phi_p) = \begin{pmatrix} \mathbf{1} & & & -\mathbf{J}(n_p) \\ -\mathbf{J}(1) & \mathbf{1} & & \\ & \cdots & \mathbf{1} & \\ & & \cdots & \\ & & & \mathbf{1} \\ & & & -\mathbf{J}(n_p-1) & \mathbf{1} \end{pmatrix}, \quad (18.181)$$

where $\mathbf{1}$ is a d -dimensional identity matrix and $\mathbf{J}(t)$ is the $[d \times d]$ forward-time Jacobian matrix. To evaluate the determinant of the matrix H , we will eliminate the off diagonal elements in the lower triangular region start from the second row. Eventually the matrix H becomes:

$$\tilde{H}(\phi_p) = \begin{pmatrix} \mathbf{1} & & & -\mathbf{J}(n_p) \\ 0 & \mathbf{1} & & -\mathbf{J}(1)\mathbf{J}(n_p) \\ 0 & 0 & \mathbf{1} & -\mathbf{J}(2)\mathbf{J}(1)\mathbf{J}(n_p) \\ 0 & 0 & 1 & \cdots \\ 0 & 0 & & \mathbf{1} - \mathbf{J} \end{pmatrix}, \quad (18.182)$$

where $\mathbf{J} = \mathbf{J}(n_p-1)\mathbf{J}(n_p-2)\dots\mathbf{J}(2)\mathbf{J}(1)\mathbf{J}(n_p)$. The determinant of the block matrix \tilde{H} is equal to the product of the determinant of the matrices on the diagonal, which is the determinant of $\mathbf{1} - \mathbf{J}$.

The cat map is a 2-dimensional map that can be written as 1-dimensional time delay map. A general form of this map is ¹⁴

$$x_{t+1} = f(x_t, x_{t-1}). \quad (18.183)$$

The forward-time Jacobian matrix can be written as:

$$\mathbf{J}(t) = \frac{\partial(x_t, x_{t+1})}{\partial(x_{t-1}, x_t)} = \begin{pmatrix} 0 & 1 \\ f_2(x_t, x_{t-1}) & f_1(x_t, x_{t-1}) \end{pmatrix}, \quad (18.184)$$

where the subscript of f_k refers to the derivative with respect to the k th argument of f . For a periodic orbit p , the matrix H is:

$$H(\phi_p) = \begin{pmatrix} 1 & & & -f_2(x_{n_p}, x_{n_p-1}) & -f_1(x_{n_p}, x_{n_p-1}) \\ -f_1(x_1, x_{n_p}) & 1 & & & -f_1(x_{n_p}, x_{n_p-1}) \\ -f_2(x_2, x_1) & -f_1(x_2, x_1) & 1 & & -f_2(x_1, x_{n_p}) \\ & & \cdots & & \\ & & -f_2(x_{n_p-1}, x_{n_p-2}) & -f_1(x_{n_p-1}, x_{n_p-2}) & 1 \end{pmatrix}. \quad (18.185)$$

¹⁴Predrag 2019-10-11: Note to myself: Reference the cat map equation in the text. Explain how imposing "direction" of time is in the case arbitrary, but related to Hamiltonian formulation (which this is not)

To change this matrix to upper triangular form,¹⁵

first add $f_1(x_1, x_{n_p})$ times the first row to the second row:

$$\left(\begin{array}{cccc} 1 & & & -f_2(x_{n_p}, x_{n_p-1}) \\ 0 & 1 & & -f_2(x_{n_p}, x_{n_p-1})f_1(x_1, x_{n_p}) \\ -f_2(x_2, x_1) & -f_1(x_2, x_1) & 1 & -f_2(x_1, x_{n_p}) - f_1(x_2, x_1)f_1(x_1, x_{n_p}) \\ \vdots & & & 1 \\ -f_2(x_{n_p-1}, x_{n_p-2}) & & -f_1(x_{n_p-1}, x_{n_p-2}) & \end{array} \right)$$

Note that the $[2 \times 2]$ block on the upper-right corner is $-\mathbf{J}(1)\mathbf{J}(n_p)$. After we finish the first two rows, when we eliminate the elements on the t th row in the lower triangular region, we will add $f_2(x_{t-1}, x_{t-2})$ times the $(t-2)$ th row plus $f_1(x_{t-1}, x_{t-2})$ times the $(t-1)$ th row to the t th row. If the $[2 \times 2]$ block on the right end of the $(t-2)$ th and $(t-1)$ th row is $-\mathbf{J}_{t-1}$, after we eliminate the sub-diagonal elements on the t th row the $[2 \times 2]$ block on the right end of the $(t-1)$ th and t th row is $-\mathbf{J}(t-1)\mathbf{J}_{t-1}$.

Repeat this procedure until we reach the $(n_p - 1)$ row. The $[2 \times 2]$ block on the right end of the $(n_p - 2)$ th and $(n_p - 1)$ th row is:

$$\begin{pmatrix} 0 & 0 \\ 1 & 0 \end{pmatrix} - \mathbf{J}_{n_p-1},$$

where $\mathbf{J}_{n_p-1} = \mathbf{J}(n_p - 2) \dots \mathbf{J}(1)\mathbf{J}(n_p)$. The next step is eliminating the off-diagonal elements in the last row. We will only eliminate the element on the $(n_p - 2)$ th column by adding $f_2(n_p - 1, n_p - 2)$ times the $(n_p - 2)$ th row plus $f_1(n_p - 1, n_p - 2)$ times the $(n_p - 1)$ th row to the last row. The $[2 \times 2]$ block on the lower-right corner is now:

$$\mathbf{1} - \mathbf{J}(n_p - 1)\mathbf{J}_{n_p-1}.$$

Now the matrix H becomes an upper-triangular block matrix:

$$\tilde{H}(\phi_p) = \begin{pmatrix} \mathbf{1} & & -\mathbf{J}(1)\mathbf{J}(n_p) \\ & 1 & \dots \\ & & 1 & \dots \\ & & & 1 \\ & & & & \mathbf{1} - \mathbf{J} \end{pmatrix}, \quad (18.187)$$

where $\mathbf{1}$ is a 2-dimensional identity matrix and $\mathbf{J} = \mathbf{J}(n_p - 1)\mathbf{J}(n_p - 2) \dots \mathbf{J}(1)\mathbf{J}(n_p)$. The determinant of matrix H is equal to the product of the determinant of the matrices on the diagonal, which is equal to the determinant of $\mathbf{1} - \mathbf{J}$.

¹⁵Predrag 2019-10-11: to Han - can you derive this more elegantly using the C_N formulation of (7.7)?

2019-10-13 Predrag to Han - can you have a look at my Guckenheimer and Meloon [30] “symmetric multiple shooting algorithm” notes, sect. 7.5? First verify and understand that their argument that the orbit Jacobian matrix for their (7.70) is equivalent to the orbit Jacobian matrix for the ‘forward shooting’ case.

Then do the same for the time-reversible ‘error’ field (7.70) with self-adjoint (symmetric orbit Jacobian matrix) orbit Jacobian matrix (7.72). We have to show that its determinant is the Hill’s formula.

2019-11-11 Han One possible way to evaluate determinant (18.95) is to compute the sum:

$$\sum_{n=0}^{N-1} \sum_{m=0}^{M-1} \frac{1}{s - 2 \cos(2\pi n/N) - 2 \cos(2\pi m/M)}. \quad (18.188)$$

Let $s = \cosh \lambda$, multiply (18.188) by $\sinh \lambda$, and integrate over λ , we have:

$$\begin{aligned} & \sum_{n=0}^{N-1} \sum_{m=0}^{M-1} \int d\lambda \frac{\sinh \lambda}{\cosh \lambda - 2 \cos(2\pi n/N) - 2 \cos(2\pi m/M)} \\ &= \sum_{n=0}^{N-1} \sum_{m=0}^{M-1} \ln[\cosh \lambda - 2 \cos(2\pi n/N) - 2 \cos(2\pi m/M)] \\ &= \ln \prod_{n=0}^{N-1} \prod_{m=0}^{M-1} [\cosh \lambda - 2 \cos(2\pi n/N) - 2 \cos(2\pi m/M)], \end{aligned} \quad (18.189)$$

which is logarithm of the determinant.

This method is used by Wu in *Theory of resistor networks: the two-point resistance* [57]. He defines

$$I_\alpha(\ell) = \frac{1}{N} \sum_{n=0}^{N-1} \frac{\cos(\alpha \ell \frac{n\pi}{N})}{\cosh \lambda - \cos(\alpha \frac{n\pi}{N})}, \quad \alpha = 1, 2,$$

and proves for $\alpha = 2$:

$$I_2(\ell) = \frac{\cosh(N/2 - \ell)\lambda}{(\sinh \lambda) \sinh(N\lambda/2)}, \quad 0 \leq \ell < N.$$

Setting $\ell = 0$, multiplying $I_2(\ell)$ by $\sinh \lambda$ and integrating over λ , he proves that:

$$\prod_{n=0}^{N-1} \left(\cosh \lambda - \cos \frac{2n\pi}{N} \right) = \sinh^2(N\lambda/2), \quad (18.190)$$

and this is also applicable to our counting formula of the cat map.

To evaluate the determinant one first evaluates the sum (18.188). Wu introduces $S_\alpha(\ell)$ (5.260) and evaluates it by carrying out the summation:

$$\mathcal{R}e \frac{1}{N} \sum_{n=0}^{N-1} \frac{1}{1 - a e^{i2\theta_n}}, \quad a < 1$$

in different ways. This method works out because:

$$\mathcal{R}e \frac{1}{1 - a e^{i2\theta_n}} = \frac{1 - a \cos(2\theta_n)}{1 + a^2 - 2a \cos(2\theta_n)},$$

which gives the constant term minus $\cos \theta_n$ in the denominator that one needs. But the method does not work for (18.188). The denominator one wants to evaluate is a constant term minus $\cos \theta_n$ minus $\cos \phi_m$. Intuitively one wants to evaluate:

$$\mathcal{R}e \frac{1}{NM} \sum_{n=0}^{N-1} \sum_{m=0}^{M-1} \frac{1}{1 - a e^{i2\theta_n} - a e^{i2\phi_m}}.$$

But

$$\mathcal{R}e \frac{1}{1 - a e^{i2\theta_n} - a e^{i2\phi_m}} = \frac{1 - a \cos(2\theta_n) - a \cos(2\phi_m)}{1 + 2a^2 - 2a \cos(2\theta_n) - 2a \cos(2\phi_m) + 2a^2 \cos(2\theta_n - 2\phi_m)}.$$

There is a $\cos(2\theta_n - 2\phi_m)$ in the denominator that we don't want. We will need use a different way to evaluate (18.188). I'm still trying other ways. I think this may work out.

2019-11-11 Han Ivashkevich, Izmailian and Hu [34] Kronecker's double series and exact asymptotic expansions for free models of statistical mechanics on torus partition function with twisted boundary conditions

$$Z_{\alpha,\beta}^2(\mu) = \prod_{n=0}^{N-1} \prod_{m=0}^{M-1} 4 \left[\sin^2 \left(\frac{\pi(n+\alpha)}{N} \right) + \sin^2 \left(\frac{\pi(m+\beta)}{M} \right) + 2 \sinh^2 \mu \right]$$

is exactly what is needed. Note that setting $\alpha = \beta = 0$:

$$\sin^2 \left(\frac{\pi(n+\alpha)}{N} \right) + \sin^2 \left(\frac{\pi(m+\beta)}{M} \right) + 2 \sinh^2 \mu = 4 \cosh(2\mu) - 2 \cos \left(\frac{2\pi n}{N} \right) - 2 \cos \left(\frac{2\pi m}{M} \right).$$

They use the identity

$$4 |\sinh(M\omega + i\pi\beta)|^2 = \prod_{m=0}^{M-1} 4 \left[\sinh^2 \omega + \sin^2 \left(\frac{\pi(m+\beta)}{M} \right) \right]$$

to get rid of one product, and obtain

$$Z_{\alpha,\beta}^2(\mu) = \prod_{n=0}^{N-1} 4 |\sinh \left[M\omega_\mu \left(\frac{\pi(n+\alpha)}{M} \right) + i\pi\beta \right]|^2 \quad (18.191)$$

where $\omega_\mu(k) = \operatorname{arc sinh} \sqrt{\sin^2 k + 2 \sinh^2 \mu}$. Then they use a formula in the appendix that I haven't gone through yet.

To be continued...

2019-11-23 Predrag Moved to sect. ?? *Prime invariant 2-tori* / ref. [23].

Restrict the admissible field values ϕ_z at lattice site $z = (n_1, n_2)$ to the now in CL symmetric unit interval $\phi \in [-1/2, 1/2]$, with 9-letter alphabet

$$\mathcal{A} = \{\underline{4}, \underline{3}, \underline{2}, \underline{1}, 0, 1, 2, 3, 4\}. \quad (18.192)$$

now in CL

2019-11-22 Han The algorithm for generating all $[2 \times 2]$ and $[3 \times 2]$ Bravais lattices prime blocks moved to sect. ?? *Prime invariant 2-tori* / ref. [23].

2019-11-23 Predrag For $d = 2, s = 5$ spatiotemporal cat with Dirichlet b.c.'s, ref. [31] splits the $s + 3$ letter alphabet $\mathcal{A} = \mathcal{A}_0 \cup \mathcal{A}_1$ into the interior \mathcal{A}_0 and exterior \mathcal{A}_1 alphabets

$$\mathcal{A}_0 = \{0, 1\}, \quad \mathcal{A}_1 = \{\underline{3}, \underline{2}, \underline{1}\} \cup \{2, 3, 4\}. \quad (18.193)$$

If all $m_z \in M$ belong to \mathcal{A}_0 , M is admissible, i.e., $\mathcal{A}_0^{\mathbb{Z}^2}$ is a full shift.

If you look at your $[2 \times 2]$ inadmissible blocks do you see any indication that invariant 2-tori alphabets also split into the interior \mathcal{A}_0 and exterior \mathcal{A}_1 alphabets?

2019-11-23 Predrag I forgot to mention the most important thing - when studying pruning, we focus on the inadmissible blocks; often they give us the grammar of the admissible blocks.

2019-11-23 Predrag For uses of the lexical ordering, table [ChaosBook 18.1: Orbits for the binary symbolic dynamics up to length 9](#), and appendix [ChaosBook A18.2 Prime factorization for dynamical itineraries](#) might be of interest.

[Kai Hansen](#) and I found it very useful to plot periodic points as 'Danish pastry', see [ChaosBook Sect. 15.3 Symbol plane](#), which gave us very clean illustration of pruning rules. For that, one has to recode symbolic dynamics, the symbols m_z shifted into nonnegative integers,

$$\gamma_z = m_z + 4.$$

A way to map the array such as (11.17) onto a 'Danish pastry' unit square is to write it as something like (wrong as it stands)

$$(\gamma_1, \gamma_2)_{(M_R)} = (0.\gamma_{11}\gamma_{21}\gamma_{31}\gamma_{41} \cdots \gamma_{L1}, 0.\gamma_{11}\gamma_{12}\gamma_{13}\gamma_{14} \cdots \gamma_{1T}) \quad (18.194)$$

in base $s + 3$, where $\gamma_k \in \{0, 1, \dots, s + 3\}$

2019-11-24 Predrag Thanks for (11.24) and (11.25) counts! It is wonderful to have several independent confirmations of the invariant 2-tori count volume formula (5.298). Clearly my suggestion of constructing covering prime blocks wildly overcounts the candidates for admissible prime invariant 2-tori, so we should give up this avenue of constructing them - no need to count any larger Bravais lattices.

2020-01-11 Predrag Pondering figure 5.7; for both temporal cat and spatiotemporal cat, we should order the ‘spring mattress’ normal modes like we always do. For example, we have from **2018-02-13 Han** (18.19) (that should have been written in terms of $\Lambda = (3 + \sqrt{5})/2 = 2.6180$ for $s = 3$) the eigenvalues of the $[5 \times 5]$ Green’s function,

$$(\lambda_0, \lambda_1 = \lambda_2, \lambda_3 = \lambda_4) = (1, 2.38, 2.38, 4.62, 4.62) \quad (18.195)$$

and the corresponding (normalized) eigenvectors:

$$\begin{aligned} \mathbf{e}^{(0)} &= \frac{1}{\sqrt{5}}(1, 1, 1, 1, 1) \\ \mathbf{e}^{(1)} &= \frac{1}{2.689}(-1.618, 1.618, -1, 0, 1) \\ \mathbf{e}^{(2)} &= \frac{1}{2.689}(-1, 1.618, -1.618, 1, 0) \\ \mathbf{e}^{(3)} &= \frac{1}{1.662}(0.618, -0.618, -1, 0, 1) \\ \mathbf{e}^{(4)} &= \frac{1}{1.662}(-1, -0.618, 0.618, 1, 0). \end{aligned} \quad (18.196)$$

By orthogonality to the ground state $\mathbf{e}^{(0)}$, the mean values of other eigenvectors are 0. $\mathbf{e}^{(1)} \rightarrow \mathbf{e}^{(2)}$ and $\mathbf{e}^{(3)} \rightarrow \mathbf{e}^{(4)}$ have the same energy by time-reversal invariance.

As the action has form

$$S[\mathbf{X}] = \frac{1}{2} \sum_{t=1}^n \left\{ (\partial \phi_t)^2 + \frac{1}{2}(2-s) \phi_t^2 \right\} + \sum_{t=1}^n m_t \phi_t. \quad (18.197)$$

For $0 \leq s < 2$ this is the action for a 1-dimensional chain of nearest-neighbor coupled harmonic oscillators. Here we are, however, interested in the everywhere hyperbolic, unstable, anti-harmonic or inverted parabolic potential, $s \geq 2$ case. The energy of a normalized eigenmode $\mathbf{e}_{(j)} \cdot \mathbf{e}^{(j)} = 1$ is obtained by flipping the sign of the potential term.

$$E_j = \frac{1}{2} \sum_{t=1}^n \mathbf{e}_{(j)}^t \square \mathbf{e}^{(j)}_t + \frac{n}{2}(s-1) = \frac{n}{2} \left(\frac{\omega_j^2}{n} + (s-1) \right), \quad (18.198)$$

for temporal cat, and

$$E_j = \frac{LT}{2} \left(\frac{\omega_j^2}{LT} + (s-1) \right), \quad (18.199)$$

for spatiotemporal cat, where ω_j^2 are the Laplacian eigenvalues. This spatiotemporal cat energy is wrong, in the sense that I have not picked out a time direction - it's really an Euclidean, 'elasticity' mode.

Not sure whether we should be looking at normalized eigenmodes, but at least the energy density $E_j/(LT)$ looks sensible in this definition, extensive with the system size. However, looking at the eigenvector signs, to me it looks like $e^{(1)}$ should have a higher energy than $e^{(3)}$ (more wiggles).

2020-01-11 Predrag So you are saved by the bell again: Have to compute and plot the lowest energies eigenmodes for large n temporal cat, and for as large $[L \times T]$ spatiotemporal cat. So you can avoid actual paper writing while you do that.

The point is to demonstrate that even though the microscopic, site dynamics is chaotic, the most important lattice modes are 'hydrodynamic', i.e., long wavelength in units of the lattice spacing.

Once you see the eigenfunctions, it will be very hard to explain why would not one exploit the D_4 and spacetime reflection symmetries.

2CB

2020-01-16 Han I computed the 5776 lattice states X of period $n = 9$ for the $s = 3$ temporal cat (see (1.14); corresponding to 960 prime lattice states, see (1.17)) with the with the 3-letter alphabet A (1.9) defined in figure 1.9. The action, according to ref. [23], is

$$S[X] = \frac{1}{2} X^\top J X + X^\top M = \frac{1}{2} \sum_{t,t'=1}^T \phi_{t'} J_{t't} \phi_t + \sum_{t=1}^T m_t \phi_t. \quad (18.200)$$

I omitted the sources M , and computed $2S[X] = X^\top J X$ for these solutions. The (twice the) action ranges between 0 and $239/76 = 3.1447 = \pi + 0.0031$. The lowest action 0 comes from the solution which has 0 field X everywhere.

The second lowest action is $17/76 = 0.224$. This action comes from the single source lattice state

$$\begin{aligned} M_1 &= (1, 0, 0, 0, 0, 0, 0, 0, 0) \\ X_1 &= \frac{1}{76} (-34, -13, -5, -2, -1, -1, -2, -5, -13) \\ &\approx -\frac{1}{4} (1 + \cos 2\pi t/n), \end{aligned} \quad (18.201)$$

its $m_t \rightarrow -m_t$ reflection

$$\begin{aligned} M_2 &= (1, 0, 0, 0, 0, 0, 0, 0, 0) \\ X_2 &= \frac{1}{76} (34, 13, 5, 2, 1, 1, 2, 5, 13), \end{aligned} \quad (18.202)$$

and their translations. The state (and its reflection) with the third lowest action has source:

$$\begin{aligned} M_3 &= (\underline{1}, 1, 0, 0, 0, 0, 0, 0, 0) \\ M_4 &= (1, \underline{1}, 0, 0, 0, 0, 0, 0, 0). \end{aligned} \quad (18.203)$$

So the lowest actions correspond to the states disturbed by the smallest sources.

Then I computed the energy (18.198) of these solutions. If I neglect the sources, the energy is given by $E = 1/2 X^\top (-\square + 2 - s)X$. The energy of these solutions range from $-3/8$ to $5233/2888$. The solution with lowest energy is the period-3 lattice state $X_{\underline{1}00}$

$$\begin{aligned} X &= \frac{1}{4}(-2, -1, -1, -2, -1, -1, -2, -1, -1) \\ M &= (\underline{1}, 0, 0, \underline{1}, 0, 0, \underline{1}, 0, 0), \end{aligned} \quad (18.204)$$

its reflection, and its translations.

But if we compute the energy with source, $E = 1/2 X^\top (-\square + 2 - s)X + M^\top X$, the energy of these solutions will range from 0 to $23397/2888$. The 0 energy again comes from the fixed point solution with 0 field. And the second lowest energy, $1161/2888$, comes from solutions with second lowest action, (18.202–18.203) and their translations.

2020-01-17 Predrag I have no idea how you count lattice states, so I included the official, ChaosBook style census in (1.14), and the prime lattice states (1.17), in sect. 1.3.2.

I think it is worth your time understanding that, as we hope to generalize it to spatiotemporal cat counting, see sect. ??.

2020-01-21 Han Moved the proof of not-Hill's formula using LU decomposition to here:

18.6.1 Stability of a periodic point vs. stability of the orbit

Consider a d -dimensional map $\phi_{t+1} = f(\phi_t)$, where $\phi_t = \{\phi_{t,1}, \phi_{t,2}, \dots, \phi_{t,d}\}$ is the state of the system at time t . In case at hand, the one time step Jacobian matrix

$$J(\phi_t)_{ij} = \left. \frac{\partial f(\phi)_i}{\partial \phi_j} \right|_{\phi_i = \phi_{i,t}} \quad (18.205)$$

stretches uniformly, so the Jacobian matrix does not depend on the field value ϕ_t or time t , $J(\phi_t) = J$.

For a lattice state X_p with period n_p , the orbit Jacobian matrix is a $[n_p d \times n_p d]$ block matrix

$$\mathcal{J}_p = \begin{pmatrix} \mathbf{1} & & & -J \\ -J & \mathbf{1} & & \\ & \cdots & \mathbf{1} & \\ & & \cdots & \mathbf{1} \\ & & & -J & \mathbf{1} \end{pmatrix} = \mathbf{1} - J r^{-1}, \quad (18.206)$$

where $\mathbf{1}$ is a d -dimensional identity matrix, and J is the one time step $[d \times d]$ Jacobian matrix (18.205).

To evaluate the determinant of the orbit Jacobian matrix, let L be a $[n_p d \times n_p d]$ block lower-triangular matrix:

$$L = \begin{pmatrix} \mathbf{1} & & & & \\ J & \mathbf{1} & & & \\ \vdots & J & \mathbf{1} & & \\ J^{n_p-2} & & \ddots & \mathbf{1} & \\ J^{n_p-1} & J^{n_p-2} & \cdots & J & \mathbf{1} \end{pmatrix}, \quad (18.207)$$

and U be a $[n_p d \times n_p d]$ block upper-triangular matrix:

$$U = \begin{pmatrix} \mathbf{1} & & & -J & \\ & \mathbf{1} & & -J^2 & \\ & & \mathbf{1} & -J^3 & \\ & & & \ddots & \\ & & & & \mathbf{1} - J^{n_p} \end{pmatrix}. \quad (18.208)$$

Note that:

$$L\mathcal{J}_p = U, \quad (18.209)$$

and the determinant of L is 1. The determinant of orbit Jacobian matrix is:

$$\det \mathcal{J}_p = \det(L\mathcal{J}_p) = \det U = \det(\mathbf{1} - J^{n_p}). \quad (18.210)$$

18.6.2 2020-06-12 Han : Temporal cat derivation using determinant recursion

From (1.113) to (1.119) we solved an inhomogeneous difference equation

$$\phi_{t+2} - s\phi_{t+1} + \phi_t = -2(s-2),$$

and the general solution is (1.119) with $m = -2(s-2)$. But then we use this general solution to find the number of solutions, which assumes that the number of solutions N_n satisfies the difference equation:

$$N_{t+2} - sN_{t+1} + N_t = -2(s-2).$$

And this is the recurrence relation that we need to prove.

I can only prove this recurrence relation by expanding the determinant of the orbit Jacobian matrix. Here is a method that is slightly simpler than the old one:

$$N_n = |\text{Det } \mathcal{J}_n| = \begin{vmatrix} s & -1 & 0 & 0 & \dots & 0 & -1 \\ -1 & s & -1 & 0 & \dots & 0 & 0 \\ 0 & -1 & s & -1 & \dots & 0 & 0 \\ \vdots & \vdots & \vdots & \vdots & \ddots & \vdots & \vdots \\ 0 & 0 & \dots & \dots & \dots & s & -1 \\ -1 & 0 & \dots & \dots & \dots & -1 & s \end{vmatrix}_{[n \times n]} \quad (18.211)$$

$$= \begin{vmatrix} s & -1 & 0 & 0 & \dots & 0 & 0 \\ -1 & s & -1 & 0 & \dots & 0 & 0 \\ 0 & -1 & s & -1 & \dots & 0 & 0 \\ \vdots & \vdots & \vdots & \vdots & \ddots & \vdots & \vdots \\ 0 & 0 & \dots & \dots & \dots & s & -1 \\ -1 & 0 & \dots & \dots & \dots & -1 & s \end{vmatrix}_{[n \times n]} \quad (18.212)$$

$$+(-1)^{n+1}(-1) \begin{vmatrix} -1 & s & -1 & 0 & \dots & 0 \\ 0 & -1 & s & -1 & \dots & 0 \\ \vdots & \vdots & \vdots & \ddots & \vdots & \vdots \\ 0 & 0 & \dots & \dots & -1 & s \\ -1 & 0 & \dots & \dots & \dots & -1 \end{vmatrix}_{[(n-1) \times (n-1)]} \quad (18.213)$$

$$= \begin{vmatrix} s & -1 & 0 & 0 & \dots & 0 & 0 \\ -1 & s & -1 & 0 & \dots & 0 & 0 \\ 0 & -1 & s & -1 & \dots & 0 & 0 \\ \vdots & \vdots & \vdots & \vdots & \ddots & \vdots & \vdots \\ 0 & 0 & \dots & \dots & \dots & s & -1 \\ 0 & 0 & \dots & \dots & \dots & -1 & s \end{vmatrix}_{[n \times n]} \quad (18.214)$$

$$+(-1)^{n+1}(-1) \begin{vmatrix} -1 & 0 & 0 & \dots & 0 & 0 \\ s & -1 & 0 & \dots & 0 & 0 \\ -1 & s & -1 & \dots & 0 & 0 \\ \vdots & \vdots & \vdots & \dots & \ddots & \vdots \\ 0 & \dots & \dots & -1 & s & -1 \end{vmatrix}_{[(n-1) \times (n-1)]} \quad (18.215)$$

$$+(-1)^{n+1}(-1)^n(-1) \left| \begin{array}{cccccc} s & -1 & 0 & 0 & \dots & 0 \\ -1 & s & -1 & 0 & \dots & 0 \\ 0 & -1 & s & -1 & \dots & 0 \\ \vdots & \vdots & \vdots & \vdots & \ddots & \vdots \\ 0 & 0 & \dots & \dots & \dots & s \end{array} \right|^{[(n-2) \times (n-2)]} \quad (18.216)$$

$$+(-1)^{n+1}(-1) \begin{vmatrix} -1 & s & -1 & 0 & \dots & 0 \\ 0 & -1 & s & -1 & \dots & 0 \\ \vdots & \vdots & \vdots & \ddots & \vdots & \vdots \\ 0 & 0 & \dots & \dots & -1 & s \\ 0 & 0 & \dots & \dots & \dots & -1 \end{vmatrix}_{[(n-1) \times (n-1)]} \quad (18.217)$$

where $-\mathcal{J}_n$ is the $[n \times n]$ tridiagonal matrix:

$$-\mathcal{J}_n = \begin{pmatrix} s & -1 & 0 & 0 & \dots & 0 & 0 \\ -1 & s & -1 & 0 & \dots & 0 & 0 \\ 0 & -1 & s & -1 & \dots & 0 & 0 \\ \vdots & \vdots & \vdots & \vdots & \ddots & \vdots & \vdots \\ 0 & 0 & \dots & \dots & \dots & s & -1 \\ 0 & 0 & \dots & \dots & \dots & -1 & s \end{pmatrix}. \quad (18.219)$$

The determinant of $-\mathcal{J}_n$ satisfy the recurrence relation:

$$-\det(-\mathcal{J}_n) + s \det(-\mathcal{J}_{n-1}) - \det(-\mathcal{J}_{n-2}) = 0. \quad (18.220)$$

So the determinant of the orbit Jacobian matrix satisfies:

$$\begin{aligned} & N_{n+2} - sN_{n+1} + N_n \\ = & [-\det(-\mathcal{J}_{n+2}) + s\det(-\mathcal{J}_{n+1}) - \det(-\mathcal{J}_n)] \\ & + [-\det(-\mathcal{J}_n) + s\det(-\mathcal{J}_{n-1}) - \det(-\mathcal{J}_{n-2})] - 2(2-s) \\ = & 2(s-2), \end{aligned} \quad (18.221)$$

which is the difference equation that we use to solve for N_n .

2020-01-28 Predrag Is (4.116) or (1.46) the recursion we need for Chebyshevs?
Or 2017-09-09 Predrag post?

2020-01-31 Predrag Here is a [stackexchange](#) recurrence relation for $U_n(s/2)$ determinants of a circulant matrix. Can you do the same for $T_n(s/2)$. Then we are done with the spatiotemporal cat zeta function.

2019-09-27, 2020-01-31 Predrag Write this up here, then distill into a paragraph, insert into the *kittens/CL18.tex*:

Littlejohn [notes](#) are simple and clear on how one evaluates determinants of 3-diagonal matrices, via 3-term recurrence (second-order difference equation [26]), see his eq. (74). For temporal cat substitute $2 - c_j \rightarrow s$, specify the boundary condition, identify it as the recursive definition of the appropriate Chebyshev polynomials:

This is an $[(n-1) \times (n-1)]$ tridiagonal matrix (see $-\mathcal{J}_n = \mathcal{D}_n$ in (1.47)). To prove that $\text{Det}(-\mathcal{J}_n) = 2T_n(s/2) - 2$, $T_n(s/2)$ Chebyshev polynomial of the first kind, define $\text{Det}(-\mathcal{J}_k)$ as the determinant of the upper $[k \times k]$ diagonal block, and set $\text{Det}(-\mathcal{J}_0) = 1$. Then by Cramer's rule, we find the recursion relation (something like (18.149), but make it more compact),

$$T_{k+1}(s/2) - sT_k(s/2) + T_{k-1}(s/2) = 0. \quad (18.222)$$

Littlejohn then rescales the equation in the form appropriate to taking a continuum limit - we do not have to do that here.

2019-09-27 PC Question: Is there such recurrence relation for the 2-dimensional spatiotemporal cat? I suspect that at the worst it is two 3-term recurrences (second-order difference equations [26]), one for each index. Because of the space \Leftrightarrow time symmetry they might turn into something simple for square domains.

2020-03-03 Predrag For spatiotemporal cat the block circulant matrix with circulant blocks has for $[3 \times 2]_0$ form

$$\mathcal{J}_{[3 \times 2]_0} = \left(\begin{array}{cc|cc|cc} -2s & 2 & 1 & 0 & 1 & 0 \\ 2 & -2s & 0 & 1 & 0 & 1 \\ \hline 1 & 0 & -2s & 2 & 1 & 0 \\ 0 & 1 & 2 & -2s & 0 & 1 \\ \hline 1 & 0 & 1 & 0 & -2s & 2 \\ 0 & 1 & 0 & 1 & 2 & -2s \end{array} \right). \quad (18.223)$$

of $[L \times L]$ block form, $L = 3$, with $[T \times T]$ blocks, $T = 2$.

2020-03-03 Han For $\mathcal{J}_{[3 \times 3]_0}$ the block circulant matrix is:

$$\left(\begin{array}{ccc|ccc|ccc} -2s & 1 & 1 & 1 & 0 & 0 & 1 & 0 & 0 \\ 1 & -2s & 1 & 0 & 1 & 0 & 0 & 1 & 0 \\ 1 & 1 & -2s & 0 & 0 & 1 & 0 & 0 & 1 \\ \hline 1 & 0 & 0 & -2s & 1 & 1 & 1 & 0 & 0 \\ 0 & 1 & 0 & 1 & -2s & 1 & 0 & 1 & 0 \\ 0 & 0 & 1 & 1 & 1 & -2s & 0 & 0 & 1 \\ \hline 1 & 0 & 0 & 1 & 0 & 0 & -2s & 1 & 1 \\ 0 & 1 & 0 & 0 & 1 & 0 & 1 & -2s & 1 \\ 0 & 0 & 1 & 0 & 0 & 1 & 1 & 1 & -2s \end{array} \right), \quad (18.224)$$

in agreement with *Tensors.nb*.

2020-03-03 Predrag Can you compare $[3 \times 1]_0$ with the temporal cat $n = 3$ case,

$$\mathcal{J}_3 = \left(\begin{array}{c|c|c} -s & 1 & 1 \\ \hline 1 & -s & 1 \\ \hline 1 & 1 & -s \end{array} \right). \quad (18.225)$$

2020-03-03 Han The correct form is:

$$\mathcal{J}_{[3 \times 1]_0} = \left(\begin{array}{c|c|c} -2s + 2 & 1 & 1 \\ \hline 1 & -2s + 2 & 1 \\ \hline 1 & 1 & -2s + 2 \end{array} \right). \quad (18.226)$$

The block on the diagonal has a form similar to the orbit Jacobian matrix of the temporal cat. For $n = 2$ the orbit Jacobian matrix has the form (18.151), and for $n = 1$ the orbit Jacobian matrix has the form (18.150), because for a fixed point (1-cycle) in temporal cat, the field value and source satisfy:

$$(-s + 2)\phi_t = -m_t.$$

2020-03-17 Han In order to determine all prime tiles

$$\mathbf{b}_1 = \begin{pmatrix} L_p \\ 0 \end{pmatrix}, \quad \mathbf{b}_2 = \begin{pmatrix} S_p \\ T_p \end{pmatrix}, \quad (18.227)$$

that tile a larger tile

$$\mathbf{a}_1 = \begin{pmatrix} L \\ 0 \end{pmatrix}, \quad \mathbf{a}_2 = \begin{pmatrix} S \\ T \end{pmatrix}, \quad (18.228)$$

observe that a prime tile tiles the larger tile only if its width L is a multiple of L_p , its height T is a multiple of T_p , and the tile ‘tilts’ are related by

$$\mathbf{a}_2 = n\mathbf{b}_1 + \frac{T}{T_p}\mathbf{b}_2 \quad \rightarrow \quad S = nL_p + \frac{T}{T_p}S_p \quad (18.229)$$

i.e., the area spanned by the two ‘tilted’ basis vectors $\mathbf{a}_2 \times \mathbf{b}_2 = ST_p - TS_p$ must be a multiple of the prime tile area $L_p T_p$.

Another way to understand the prime tile condition is illustrated in figure 18.47. The gray parallelogram is the Bravais cell of the larger tile and the blue parallelogram is the Bravais cell of the prime tile. In this figure we assume that the first two relations, L_p divides L and T_p divides T are already satisfied. In the periodic field over the larger tile, the field value at the tip of \mathbf{a}_2 (marked A) is the same as the field value at the origin O. And for the periodic field of the prime tile, the field value at the tip of $(T/T_p)\mathbf{b}_2$ (marked B) is same as the field value on the origin, hence the field values at points A and B are the same, $\mathbf{a}_2 = (T/T_p)\mathbf{b}_2$ which requires that $A - B$ can be divided by L_p . So $S - (T/T_p)S_p$ must be divisible by L_p .

2020-06-05 Han Suppose a Bravais lattice \mathcal{L} with basis

$$\begin{aligned} \Lambda &= [\mathbf{a}_1 \mid \mathbf{a}_2] = \begin{bmatrix} a_{11} & a_{12} \\ a_{21} & a_{22} \end{bmatrix} \\ \det \mathcal{L} &= a_{11}a_{22} - a_{12}a_{21}. \end{aligned} \quad (18.230)$$

is tiled by a finer lattice \mathcal{L}_p with a basis

$$\begin{aligned} \Lambda_p &= [\mathbf{a}_1^p \mid \mathbf{a}_2^p] = \begin{bmatrix} a_{11}^p & a_{12}^p \\ a_{21}^p & a_{22}^p \end{bmatrix} \\ \det \mathcal{L}_p &= a_{11}^p a_{22}^p - a_{12}^p a_{21}^p. \end{aligned} \quad (18.231)$$

As \mathcal{L} is a sublattice of \mathcal{L}_p , the basis must satisfy

$$\Lambda = [k\mathbf{a}_1^p + l\mathbf{a}_2^p \mid m\mathbf{a}_1^p + n\mathbf{a}_2^p] = \Lambda_p \begin{bmatrix} k & m \\ l & n \end{bmatrix}, \quad (18.232)$$

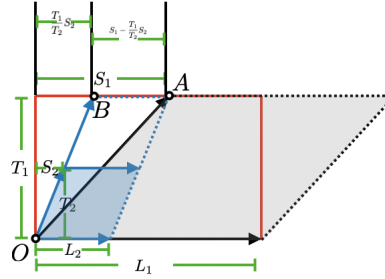


Figure 18.47: The gray parallelogram is the Bravais cell of the large tile and the blue parallelogram is the Bravais cell of the prime tile p , $T = 2T_p$ and $L = 3L_p$. The repeat the prime tile in the temporal direction reaches the upper boundary of the large tile at point B . If the prime tile can tile the large tile then the periodic boundary of the prime tile should satisfy the periodic boundary of the large tile. So the field value at point B should be same as the field value at point A . The distance between point B and point A should be equal to L_p multiplied by an integer.

where k, l, m and n are integers. Solving this equation we have

$$\begin{aligned} k &= \frac{a_{11}a_{22}^p - a_{21}a_{12}^p}{\det \mathcal{L}_p}, & l &= \frac{a_{21}a_{11}^p - a_{11}a_{21}^p}{\det \mathcal{L}_p} \\ m &= \frac{a_{12}a_{22}^p - a_{22}a_{12}^p}{\det \mathcal{L}_p}, & n &= \frac{a_{22}a_{11}^p - a_{12}a_{21}^p}{\det \mathcal{L}_p}, \end{aligned} \quad (18.233)$$

and

$$\frac{\det \mathcal{L}}{\det \mathcal{L}_p} = \det \begin{bmatrix} k & m \\ l & n \end{bmatrix} = kn - lm. \quad (18.234)$$

To satisfy these relations, $|\mathbf{a}_1 \times \mathbf{a}_1^p|$, $|\mathbf{a}_1 \times \mathbf{a}_2^p|$, $|\mathbf{a}_2 \times \mathbf{a}_1^p|$ and $|\mathbf{a}_2 \times \mathbf{a}_2^p|$ need to be multiples of the prime tile area $\det \mathcal{L}_p$, with one relation on these integers imposed by the volume ratio (18.234) also being an integer.

2020-08-15 Predrag Is

$$\text{tr} \begin{bmatrix} k & m \\ l & n \end{bmatrix} = \text{tr} (\Lambda_p^{-1} \Lambda) \quad (18.235)$$

an important invariant?

2020-08-15 Predrag Any integer $[2 \times 2]$ matrix with nonvanishing determinant defines a Bravais cell, so we can turn the above argument around. The form of (18.232) suggests that if we have two prime lattices, we can construct a ‘non-prime’ (?) Bravais lattice by multiplication

$$\Lambda_{pp'} = \Lambda_p \Lambda_{p'}. \quad (18.236)$$

Can we construct all Bravais lattices this way? Not clear, as the two Bravais cells do not commute, $\Lambda_p \Lambda_{p'} \neq \Lambda_{p'} \Lambda_p$. Their volumes do multiply

$\det \Lambda_{pp'} = \det \Lambda_p \det \Lambda_{p'}$ so it is still possible they generate the same Bravais lattice, or two within an relative periodic orbit family of the same volume, but different tilt.

The ordered concatenations of primes, [ChaosBook Appendix A18.2 Prime factorization for dynamical itineraries](#) might do the trick. See also the factorization algorithm ([5.197](#)).

2020-08-15 Predrag This checks with the Hermite normal form basis ([18.227](#)), where $a_{21} = a_{21}^p = 0$:

$$k = \frac{LT_p}{\det \mathcal{L}_p} = \frac{L}{L_p}, \quad l = 0,$$

$$m \det \mathcal{L}_p = ST_p - TS_p, \quad n = \frac{TL_p}{\det \mathcal{L}_p} = \frac{T}{T_p},$$

The volume relation

$$\frac{\det \mathcal{L}}{\det \mathcal{L}_p} = \det \begin{bmatrix} k & m \\ 0 & n \end{bmatrix} = kn \quad (18.237)$$

is trivially true. The trace ([18.238](#))

$$\text{tr} \begin{bmatrix} k & m \\ l & n \end{bmatrix} = \frac{L}{L_p} + \frac{T}{T_p} \quad (18.238)$$

does not depend on S , so it is not an invariant that we are looking for.

2020-08-15 Predrag Consider now the prime Bravais cell whose volume is a prime number,

$$\det \mathcal{L}_p = p.$$

Its only divisor is the unit cell of \mathbb{Z}^2 , so ([18.233](#)) becomes

$$\begin{bmatrix} k & m \\ l & n \end{bmatrix} = \begin{bmatrix} a_{11} & a_{12} \\ a_{21} & a_{22} \end{bmatrix}. \quad (18.239)$$

In the Hermite normal form basis ([18.227](#)) we chose $L = p$, $T = 1$, so

$$\begin{bmatrix} k & m \\ l & n \end{bmatrix} = \begin{bmatrix} L & S \\ 0 & T \end{bmatrix}, \quad S = 0, 1, \dots, p-1. \quad (18.240)$$

According to ([18.233](#)) the unimodular-transformation invariant formula (is it?) for S is

$$S = \mathbf{a}_2 \times \mathbf{a}_2^p = a_{12}a_{22}^p - a_{22}a_{12}^p, \quad (18.241)$$

where Λ_p is an unit area Bravais cell (not necessarily the unit square) that tiles \mathcal{L} .

Some of discussion in the [2020-07-11 Predrag](#) post, around eq. ([5.197](#)), might be relevant.

2020-08-15 Predrag As an example of an arbitrary Bravais cell Λ , consider the prime Bravais lattice figure 5.3, with the ‘integral basis’ vectors (5.178) and $\det \mathcal{L} = 7$

$$\begin{bmatrix} a_{11} & a_{12} \\ a_{21} & a_{22} \end{bmatrix} = \begin{bmatrix} 3 & 2 \\ 1 & 3 \end{bmatrix}. \quad (18.242)$$

2020-08-16 Predrag to Han: Figure 5.5 is an example to rethink. It shows four parallelograms of area 10. The two blue parallelograms are claimed to be ‘primitive’. The two red parallelograms can clearly be tiled by either 2 or 5 smaller tiles. I do not trust Holmin [33] on this. Bravais *lattices* clearly must be tiled by 1/2 or 1/5th prime Bravais lattices in all four cases.

1. Can you bring the first 3 parallelograms into the Hermite normal form basis (18.227)?
2. Are they distinct?
3. Are they $[5 \times 2]_S$ or $[10 \times 1]_S$?

Note, $[10 \times 1]_S$ does not make 10 a ‘prime’, as that can be tiled by $[5 \times 1]_{S_p}$ and $[2 \times 1]_{S_p}$.

2020-08-18 Han The the first 3 Bravais cells in figure 5.5 are:

$$\Lambda'_1 = \begin{bmatrix} 3 & 1 \\ 2 & 4 \end{bmatrix}, \quad \Lambda'_2 = \begin{bmatrix} 3 & 1 \\ -1 & 3 \end{bmatrix}, \quad \Lambda'_3 = \begin{bmatrix} 3 & 2 \\ 1 & 4 \end{bmatrix}.$$

Unimodular matrices ($U_j \in \text{SL}_2(\mathbb{Z})$, special linear group over integers of degree 2)¹⁶

$$U_1 = \begin{bmatrix} 2 & 1 \\ -1 & 0 \end{bmatrix}, \quad U_2 = \begin{bmatrix} 3 & 2 \\ 1 & 1 \end{bmatrix}, \quad U_3 = \begin{bmatrix} 4 & 1 \\ -1 & 0 \end{bmatrix},$$

bring these to the Hermite normal form:

$$\begin{aligned} \Lambda_1 &= \Lambda'_1 U_1 = \begin{bmatrix} 5 & 3 \\ 0 & 2 \end{bmatrix}, \quad \Lambda_2 = \Lambda'_2 U_2 = \begin{bmatrix} 10 & 7 \\ 0 & 1 \end{bmatrix} \\ \Lambda_3 &= \Lambda'_3 U_3 = \begin{bmatrix} 10 & 3 \\ 0 & 1 \end{bmatrix}. \end{aligned} \quad (18.243)$$

So these 3 basis span 3 different lattices. None of them is a prime lattice. $[5 \times 2]_3$ is a sublattice of $[5 \times 1]_4$ and $[1 \times 2]_0$, $[10 \times 1]_7$ is a sublattice of $[5 \times 1]_2$ and $[2 \times 1]_1$, and $[10 \times 1]_3$ is a sublattice of $[5 \times 1]_3$ and $[2 \times 1]_1$.

2020-08-21 Han In this paper, we are able to systematically enumerate all possible solutions of the spatiotemporal cat in two steps. The first step is to generate the Bravais lattices which describe the periodicities of the solutions. The second step is to compute the solutions with the given periodicities and to count the number of the solutions, which can be done

¹⁶Predrag 2020-08-18: where do your U_j 's come from?

in two ways: using the Fourier transform to diagonalize the orbit Jacobian matrix, or computing the determinant of the orbit Jacobian matrix directly.

2020-08-28 Han Periodicity: The field is invariant under a discrete translation group, which is isomorphic to a Bravais lattice.

2020-09-08 Predrag I do not know whether you have read any literature that defines precisely our lattices, but if you have, use that knowledge now. Clearly, we have to give up on “Bravais” lattices as all references say there are only 5 Bravais lattices in $d = 2$, so we are misusing the term - my bad. Keep on reading.

2020-09-24 Predrag While writing up tomorrow’s talk, I came up with a simple guess (13.84) for spatiotemporal cat zeta function. The factor $2(s - 2)$ the we see in every $N_{[L \times T]_S}$ is automatic. Can you check whether it agrees with our lattice state counts? It has no tilt S anywhere, so if it works, it should generate the sums of all states whose tile has area $[L \times T]$. To recover lattice state counts $N_{[L \times T]}$ you probably have to take derivatives of $\ln \det$ in both z_1 and z_2 , something like

$$\sum_{L=1} \sum_{T=1} z_1^L z_2^T N_{[L \times T]} = -\frac{1}{1/\zeta_{\text{top}}} z_1 z_2 \frac{d}{dz_1} \frac{d}{dz_2} (1/\zeta_{\text{top}}). \quad (18.244)$$

Have not checked any of that. For once, the real time pressure is on - if true, I can announce it at 10am Friday. Who knows when I get to give another talk on spatiotemporal cat? :)

2020-09-24 Han It does not work. If zeta function we have is:

$$1/\zeta_{\text{top}} = \exp \left(\sum_{L=1} \sum_{T=1} \frac{z_1^L z_2^T}{LT} N_{[L \times T]} \right), \quad (18.245)$$

then we have

$$f(z_1, z_2) = \sum_{L=1} \sum_{T=1} z_1^L z_2^T N_{[L \times T]} = z_1 z_2 \frac{\partial^2}{\partial z_1 \partial z_2} \ln(1/\zeta_{\text{top}}). \quad (18.246)$$

From the guess “zeta” function (13.84)

$$1/\zeta_{\text{top}}(z_1, z_2) = 1 - \frac{2(s - 2)}{z_1 + z_2 - 4 + z_1^{-1} + z_2^{-1}} \quad (18.247)$$

I get

$$\begin{aligned} f(z_1, z_2)/4(s - 2) &= \\ &\frac{(z_1 - z_1^{-1})(z_2 - z_2^{-1}) (z_1 + z_2 - s - 2 + z_1^{-1} + z_2^{-1})}{(z_1 + z_2 - 4 + z_1^{-1} + z_2^{-1})^2 (z_1 + z_2 - 2s + z_1^{-1} + z_2^{-1})^2}, \end{aligned} \quad (18.248)$$

which changes sign separately under each spacetime reflection (reversal) $z_1 \rightarrow z_1^{-1}$, and is invariant under the space \leftrightarrow time diagonal reflection $z_1 \leftrightarrow z_2$. Doing the same for the 1-dimensional temporal cat, I rederive (13.78):

$$f(z) = (s-2) \frac{1}{z^{-1} - s + z} \frac{1+z}{1-z} = \frac{2-sz}{z^2 - sz + 1} - \frac{2}{1-z}.$$

I rechecked that this, expended as a power series, gives the correct periodic points count.

To count $N_{[L \times T]}$, we can either compute:

$$N_{[L \times T]} = \frac{1}{L!T!} \lim_{z_1, z_2 \rightarrow 0} \frac{\partial^L}{\partial z_1^L} \frac{\partial^T}{\partial z_2^T} f(z_1, z_2), \quad (18.249)$$

or:

$$N_{[L \times T]} = \frac{1}{(L-1)!(T-1)!} \lim_{z_1, z_2 \rightarrow 0} \frac{\partial^L}{\partial z_1^L} \frac{\partial^T}{\partial z_2^T} \ln(1/\zeta_{\text{top}}). \quad (18.250)$$

I have tried both (18.249) and (18.250). The results for small L and T are either 0 or not converge. And this happens in most of the spatiotemporal cat zeta functions that we guessed.

2020-09-24 Predrag f (18.248) is pretty close in form to (13.79), but why are denominators squared? It's almost like our derivatives are not right, might be something like

$$\frac{1}{2} \left(z \frac{\partial}{\partial z} - z^{-1} \frac{\partial}{\partial(z^{-1})} \right)$$

would be better. In $d=2$ there might be some conformal, complex plane, Cauchy-Riemann magic going on, compare with use of 'time reversal' in (13.9), (13.11) and figure 13.2.

2020-10-06 Han Revisiting my attempt of 2 years ago, see (18.107): We need a definition of the topological zeta function of fields on the 2-dimensional lattice. (18.245) is incorrect. We want to find a topological zeta function that can be written into the product formula of prime orbits.

I tried to prove that (18.245) gives us a topological zeta function in (18.107–18.110). But there is a mistake in the beginning. If the $N_{[L \times T]}$ means number of fixed points on $[L \times T]_0$, we will let each of the prime orbits $[L_p \times T_p]_{S_p}$ with non-zero S_p that tiles $[L \times T]_0$ contributes LT times in the $N_{[L \times T]_0}$, where they actually only contribute $L_p T_p$ times.

If the $N_{[L \times T]}$ is the sum of all states whose tile is $[L \times T]$, then this is intuitively wrong since we will overcount some solutions. For example, the trivial solution, fixed point on $[1 \times 1]_0$, is counted in all states whose tile is $[L \times T]$ with different S .

Assume the weight assigned to a prime orbit p is:

$$t_p = t_{p1} t_{p2}, \quad \text{where } t_{p1} = z_1^{L_p}, \quad t_{p2} = z_2^{T_p}. \quad (18.251)$$

Rewrite the number of lattice states as:

$$\begin{aligned} z_1^L z_2^T N_{[L \times T]_S} &= \sum_{L_p | L} L_p t_{p1}^{\frac{L}{L_p}} \sum_{T_p | T} T_p t_{p2}^{\frac{T}{T_p}} \sum_{L_p T_p | ST_p - TS_p} 1 \quad (18.252) \\ &= \sum_p L_p T_p \sum_{r_1=1}^{\infty} \sum_{r_2=1}^{\infty} t_{p1}^{r_1} t_{p2}^{r_2} \delta_{r_1 L_p, L} \delta_{r_2 T_p, T} \\ &\quad \sum_{r_S=-\infty}^{\infty} \delta_{r_S L_p, S - r_2 S_p}, \end{aligned}$$

where

$$\begin{aligned} L &= r_1 L_p, \quad T = r_2 T_p \\ ST_p - TS_p &= r_S L_p T_p \\ \Rightarrow S &= r_S L_p + r_2 S_p \quad \text{mod } L. \end{aligned} \quad (18.253)$$

The next step is to sum over L , T and S . Taking sum of (18.252) over L and T from 1 to ∞ , we will get rid of the Kronecker deltas, as in (18.108). The geometric series in powers of L_p sums up as in the $d = 1$ case, but T and S sums are entangled through r_2 . The generating function for the numbers of lattice states is

$$\begin{aligned} \Gamma(z_1, z_2) &= \sum_{L=1}^{\infty} \sum_{T=1}^{\infty} z_1^L z_2^T \sum_{S=0}^{L-1} N_{[L \times T]_S} \\ &= \sum_p \frac{L_p t_{p1}}{1 - t_{p1}} T_p \sum_{r_2=1}^{\infty} t_{p2}^{r_2} \\ &\quad \sum_{S=0}^{L-1} \sum_{r_S=-\infty}^{\infty} \delta_{r_S L_p + r_2 S_p, S} \end{aligned} \quad (18.254)$$

The sum over S is tricky. For $S = 0$,

$$r_S L_p = -r_2 S_p$$

and as $0 \leq S_p / L_p < 1$, so $-r_2 < r_S \leq 0$ is non-positive. For $S = L - 1$,

$$r_S = r_1 - \frac{1 + r_2 S_p}{L_p}.$$

r_S is strictly positive.

But if we take r_S from $-\infty$ to ∞ , for some of the r_S there will not be a $S \in [0, L - 1]$ such that $ST_p - TS_p = L_p T_p r_S$. Maybe we need to find a

range of r_S in the sum in (18.252) such that for any r_S there exists one S that have $\delta_{r_S L_p + r_2 S_p, S} = 1$.

The weight (18.251) is likely incorrect, and it will determine the factor in front of $N_{[L \times T]_S}$ in the zeta function. But I think we need to first know how to write the zeta function into the product form, then we will be able to interpret and construct the zeta function.

2020-10-09 Han We need to reduce the range of the sum of r_S such that for any r_S in the range there is one $S \in [0, L)$ that satisfy:

$$r_S = \frac{S - r_2 S_p}{L_p}.$$

Known the range of S and the relation between S and r_S , the reduced range of r_S is:

$$r_S \in \left[-\frac{r_2 S_p}{L_p}, r_1 - \frac{r_2 S_p}{L_p} \right].$$

Sum the separated term with S in (18.252) over S :

$$\sum_{S=0}^{L-1} \sum_{r_S=\lceil -\frac{r_2 S_p}{L_p} \rceil}^{\lceil r_1 - \frac{r_2 S_p}{L_p} - 1 \rceil} \delta_{r_S L_p + r_2 S_p, S} = \sum_{r_S=\lceil -\frac{r_2 S_p}{L_p} \rceil}^{\lceil r_1 - \frac{r_2 S_p}{L_p} - 1 \rceil} 1 = r_1. \quad (18.255)$$

The $\lceil x \rceil$ is the least integer greater than or equal to x .

The zeta function (18.245) can be written into product formula:

$$\begin{aligned} 1/\zeta_{\text{top}} &= \exp \left(- \sum_{L=1} \sum_{T=1}^{L-1} \sum_{S=0}^L \frac{z_1^L z_2^T}{LT} N_{[L \times T]_S} \right) \\ &= \exp \left(- \sum_p \sum_{r_1=1}^{\infty} \sum_{r_2=1}^{\infty} \frac{t_p^{r_1 r_2} r_1}{r_1 r_2} \right) \\ &= \exp \left(\sum_p \sum_{r_1=1}^{\infty} \ln(1 - t_p^{r_1}) \right) \\ &= \prod_p \left[\prod_{r_1=1}^{\infty} (1 - t_p^{r_1}) \right]. \end{aligned} \quad (18.256)$$

This result is very similar to the zeta functions in Lind [38]. In Lind [38], the function

$$\prod_{r_1=1}^{\infty} \frac{1}{1 - t_p^{r_1}}$$

is called the generating function for the partition function.

2020-10-07 Predrag The Kronecker (circular) delta function for a periodic lattice

$$\delta_{kj} = \frac{1}{L} \sum_{\ell=0}^{L-1} e^{i \frac{2\pi}{L} (k-j)\ell}. \quad (18.257)$$

takes care of $\mod L$ and $\mod T$ in (18.252), but what is Kronecker delta for S ? What is the periodicity there? I suspect one has to average over the unimodular group there, with a double sum over 2 generators, as in (13.10), (13.11) and figure 13.2. The eigenfunctions might be some fancy 19th century special functions.

2020-10-07 Predrag As far as I can see, S sum can be separated as in my rewritten version of (18.252). That looks strange.

2020-10-07 Han Counting formulas like (11.19), for the number of prime $[2 \times 2]_0$ lattice states is

$$M_{[2 \times 2]_0} = \frac{1}{2 \cdot 2} (N_{[2 \times 2]_0} - 2M_{[2 \times 1]_0} - 2M_{[1 \times 2]_0} - 2M_{[2 \times 1]_1} - M_{[1 \times 1]_0}),$$

relate numbers $N_{[L \times T]_S}$ and $M_{[L \times T]_S}$. Numbers such as the number of orbits M_p do not appear in formula (18.252) because when we compute the sum over all the prime orbits, labeled by p , each prime orbit will contribute once to the sum. If the number of prime $[2 \times 2]_0$ lattice states is $M_{[2 \times 2]_0}$, there will be $M_{[2 \times 2]_0}$ orbits with $[L_p \times T_p]_{S_p} = [2 \times 2]_0$ that will be summed.

2020-10-07 Predrag Not getting a simpler formula than (18.109) is OK; looks like you are dealing with polylogs ([wiki](#)), and specifically with dilogs ([wiki](#)), and/or Spence's function ([wiki](#)).

Some random references, hopefully we do not need them:

Zagier (Predrag's MIT wunderkid) [*The Dilogarithm Function*](#).

[*Dilogarithm identities in conformal field theory and group homology*](#).

18.6.3 Lattices and periodicities

2020-12-21 Predrag Moved this section written by Han to CL18.tex, chapter catlatt.tex

2018-06-11 Han For example, consider the simplest case in two-dimensions, with the period of ℓ is $L = 2$. In this case, we will need to know $x_{1,t-1}$, $x_{2,t-1}, x_{1,t}$ and $x_{2,t}$ to solve for the field values on all of the lattice sites, $t \in \mathbb{Z}$. And we can also define the generating partition in the space spanned

by these four values. If the field value satisfies (18.46) where $d = 2$, the state evolves with time as:

$$A \begin{bmatrix} \phi_{1,t-1} \\ \phi_{2,t-1} \\ \phi_{1,t} \\ \phi_{2,t} \end{bmatrix} = \begin{bmatrix} 0 & 0 & 1 & 0 \\ 0 & 0 & 0 & 1 \\ -1 & 0 & s & -2 \\ 0 & -1 & -2 & s \end{bmatrix} \begin{bmatrix} \phi_{1,t-1} \\ \phi_{2,t-1} \\ \phi_{1,t} \\ \phi_{2,t} \end{bmatrix} = \begin{bmatrix} \phi_{1,t} \\ \phi_{2,t} \\ \phi_{1,t+1} \\ \phi_{2,t+1} \end{bmatrix} + \begin{bmatrix} 0 \\ 0 \\ m_{1,t} \\ m_{2,t} \end{bmatrix} \quad (18.258)$$

The matrix A gives us the cat map for the lattice with spatial period of 2. If the spatial period is longer, the general matrix A will be:

$$A = \left[\begin{array}{cccc|cccccc} 0 & \dots & 0 & | & 1 & 0 & \dots & 0 & 0 \\ \vdots & \ddots & \vdots & | & \vdots & \ddots & & \vdots \\ 0 & \dots & 0 & | & 0 & 0 & \dots & 1 & 0 \\ \hline -1 & 0 & \dots & 0 & | & s & -1 & \dots & 0 & -1 \\ 0 & -1 & \dots & 0 & | & -1 & s & -1 & & 0 \\ \vdots & \ddots & \vdots & | & \vdots & \ddots & \ddots & \ddots & \vdots \\ 0 & 0 & \dots & -1 & 0 & | & 0 & -1 & s & -1 \\ 0 & 0 & \dots & 0 & -1 & | & -1 & 0 & \dots & -1 & s \end{array} \right] \quad (18.259)$$

which is very similar to the cat map matrix in one-dimension.

2020-07-12 Predrag See (8.8) for a compact rewrite.

2018-06-21 Predrag This is nice. In principle it should be already in this blog, for example (5.2), and in Gutkin and Osipov [32], and Gutkin *et al.* [31], but I do not recognize the equations. My impression is that the spectrum of A for going forward in time is hard to interpret, but I have not tried.

2018-06-11 Han After we get the matrix A , we can get the eigenvalues and eigenvectors. There will be 4 eigenvectors for the case (18.258) where the spatial period is 2. With these four eigenvectors we can define the generating partition in the space spanned by $x_{1,t-1}, x_{2,t-1}, x_{1,t}$ and $x_{2,t}$ which is a 4-torus.

2018-06-26 Han I have tried to get the partition for spatiotemporal cat with spatial period $L = 2$. But this is more complex than I thought. I thought the partition will be same as the one-dimensional case. So using the 4 eigenvectors we will have 4 planes, and each of them is parallel to 3 of the eigenvectors. The 4 planes passing through the origin and the 4 planes passing through the point $(1, 1, 1, 1)$ will enclose a four-dimensional "cube" which is corresponding to the large rectangle in the figure 18.3 (a). And using 4 planes passing through the points $(1, 0, 0, 0)$, $(0, 1, 0, 0)$, $(0, 0, 1, 0)$ and $(0, 0, 0, 1)$ separately we will have 4 small region corresponding to

the 2 small rectangle in figure 18.3. This is the simplest case, but it doesn't work out.

The eigenvalues of the matrix in (18.258) where $s = 5$ are:

$$\begin{aligned}\Lambda_1 &= \frac{1}{2}(7 + 3\sqrt{5}) \\ \Lambda_2 &= \frac{1}{2}(7 - 3\sqrt{5}) = \Lambda_1^{-1} \\ \Lambda_3 &= \frac{1}{2}(3 + \sqrt{5}) \\ \Lambda_4 &= \frac{1}{2}(3 - \sqrt{5}) = \Lambda_3^{-1}\end{aligned}\tag{18.260}$$

The corresponding eigenvectors are:

$$\begin{aligned}e_1 &= (-1, 1, -\Lambda_1, \Lambda_1) \\ e_2 &= (-\Lambda_1, \Lambda_1, -1, 1) \\ e_3 &= (1, 1, \Lambda_3, \Lambda_3) \\ e_4 &= (\Lambda_3, \Lambda_3, 1, 1)\end{aligned}\tag{18.261}$$

Note that Λ_3 and Λ_4 are the eigenvalues of the Percival-Vivaldi cat map with $s = 3$. These two eigenvectors are corresponding to the case when all of the sites are having a same value at a given time.

2018-06-27 Predrag Looks like the configuration eigenvectors,

$$e_{2i+1}^\top \cdot e_{2j+1} = 0, \quad i \neq j,$$

and the momentum eigenvectors,

$$e_{2i}^\top \cdot e_{2j} = 0, \quad i \neq j,$$

will be separately orthogonal for the L -“particles” lattice. If we are lucky, the j th phase-space area $e_{2j}^\top \cdot e_{2j+1} = A_j$ is preserved by the (symplectic?) map (18.259); generically I think only the sum of areas is preserved.

2018-07-13 Predrag discussion with Han: think how to generalize the number of periodic orbits (19.3) to the $L = 2$ case. Your arbitrary L evolution matrix (18.259) has a very nice form, which might lead to some nice generalization of eigenvalue formulas (18.260) to arbitrary L . We do not really need explicit alphabets; to get topological zeta functions for this problem, we only need formulas like (19.3) that only need eigenvalues (coordinate choice invariant properties of dynamics). For $L = 1$ case the object of interest is the topological entropy $\ln \Lambda$ (the rate of growth of the number of periodic orbits with $T \rightarrow \infty$). For large L you need the rate of growth of the number of periodic orbits per unit length, i.e., $(\ln \Lambda_j)/L$, where Λ_j is the leading eigenvalue in the generalized (18.260).

2018-07-27 Predrag That suggests computing analytic expressions for eigenvalues for invariant 2-tori $\mathcal{R} = [2 \times 2]$, $\mathcal{R} = [3 \times 3]$, $\mathcal{R} = [4 \times 4], \dots$, try to divine $T \leftrightarrow L$ interchange symmetry from those...

2018-08-02 Predrag Have you had a look at sect. 5.4 *Toeplitz tensors*? References cited there might offer efficient ways of computing spectra of your doubly cyclic tensorial matrices.

2018-07-24 Han The number of periodic points for the $L = 2$ case is easy to get. The number of periodic points with time period T is:

$$N_{[L \times T]} = |\det(\mathbf{A}(L)^T - \mathbf{I})| \quad (18.262)$$

In all examples we take $s = 5$. Since the matrices \mathbf{A} and \mathbf{I} can be diagonalized simultaneously, the number of periodic points for the $L = 2$ case is:

$$\begin{aligned} N_{[2 \times T]} &= |(\Lambda_1^T - 1)(\Lambda_1^{-T} - 1)(\Lambda_3^T - 1)(\Lambda_3^{-T} - 1)| \\ &= |[2 - (\Lambda_1^T + \Lambda_1^{-T})][2 - (\Lambda_3^T + \Lambda_3^{-T})]| \end{aligned} \quad (18.263)$$

As the Hamiltonian evolution matrix (18.259) is symplectic, its eigenvalues come in pairs for any L (for any eigenvalue Λ_j , Λ_j^{-1} is also an eigenvalue). So the number of periodic orbits with time period T and spatial period L is

$$\begin{aligned} N_{[L \times T]} &= \prod_{i=1}^L |(\Lambda_i^T - 1)(\Lambda_i^{-T} - 1)| \\ &= \prod_{i=1}^L (\Lambda_i^T + \Lambda_i^{-T} - 2) = N_{[T \times L]}. \end{aligned} \quad (18.264)$$

The problem is how to get a general form of the eigenvalues. We have the same number of orbits for the $[T \times L]$ block and the $[L \times T]$ block, so (18.264) must be a function of L and T invariant under the $T \leftrightarrow L$ exchange.

2018-07-24 Han Perhaps there is a better way to get the general formulas of the eigenvalues of (18.259), I just haven't figured it out. It seems like the eigenvalues of (18.259) are completely determined by the eigenvalues of the small Toeplitz matrix at the bottom right corner of this matrix (The large evolution matrix itself is not a Toeplitz matrix). For example, when $L = 2$ and $s = 5$ the eigenvalues of the Toeplitz matrix are 7 and 3. The eigenvalues of the evolution matrix are $\frac{1}{2}(7+3\sqrt{5})$, $\frac{1}{2}(7-3\sqrt{5})$, $\frac{1}{2}(3+\sqrt{5})$ and $\frac{1}{2}(3-\sqrt{5})$. When $L = 3$, the eigenvalues of the Toeplitz matrix are 6, 6 and 3, while the eigenvalues of the evolution matrix are $\frac{1}{2}(6+4\sqrt{2})$, $\frac{1}{2}(6+4\sqrt{2})$, $\frac{1}{2}(6-4\sqrt{2})$, $\frac{1}{2}(6-4\sqrt{2})$, $\frac{1}{2}(3+\sqrt{5})$ and $\frac{1}{2}(3-\sqrt{5})$.

So generally, the eigenvalues of (18.259) can be expressed as $\frac{1}{2}(a+b)$ and $\frac{1}{2}(a-b)$. And we know that $\frac{1}{2}(a+b) \times \frac{1}{2}(a-b) = \frac{1}{4}(a^2 - b^2) = 1$. And we

know that a is an eigenvalue of the small Toeplitz matrix at the bottom right corner of (18.259). The general expression for the Toeplitz matrix is (from (18.51)):

$$\lambda(L)_i = s - 2 \cos\left(\frac{2\pi i}{L}\right), \quad i = 1, 2, \dots, L \quad (18.265)$$

where L is the spatial period of the lattice and the rank of the Toeplitz matrix. The eigenvalues of (18.259) are:

$$\Lambda(L)_i^{\pm} = \frac{1}{2}(\lambda_i \pm \sqrt{\lambda_i^2 - 4}), \quad i = 1, 2, \dots, L. \quad (18.266)$$

From (18.265) you can see that for any L , when $i = L$ we will get the eigenvalue $\lambda(L)_L = s - 2$. That is why when $s = 5$ the Toeplitz matrix will always have eigenvalue 3. And this will give us the eigenvalues of the large evolution matrix $\frac{1}{2}(3 + \sqrt{5})$ and $\frac{1}{2}(3 - \sqrt{5})$, which are corresponding to the case when all of the sites have a same field value at a given time (same as the one-dimensional case).

Now we have the general formula of the matrix (18.259). In principle I can get a general expression of number of periodic orbits with a given length L and period T . The number of periodic orbits will be a function of s , L and T . But as you can see my formula of eigenvalues of arbitrary L evolution matrix (18.259) is not pretty. When $L < 5$, (18.265) will be an integer but when $L = 5$ the eigenvalue in (18.265) starts to become an irrational number and the eigenvalue of (18.259) also becomes uglier. So I'm still trying to find an elegant expression.

I haven't figured out how to prove that the eigenvalues of (18.259) are $\frac{1}{2}(a + b)$ and $\frac{1}{2}(a - b)$ where a is eigenvalue of the small Toeplitz matrix and $b = \sqrt{a^2 - 4}$. I just calculated all of the eigenvalues of the (18.259) and the small Toeplitz matrix from $L = 1$ to $L = 5$. And they are all matched. I will think about how to prove this.

2018-08-15 Han This part is not important. It's just a practice for myself. Given a spatial length L , the topological zeta function can be calculated from (18.264). For example, if $L = 2$, we will have four eigenvalues from matrix (18.259). Let these four eigenvalues be Λ_1^+ , Λ_1^- , Λ_2^+ and Λ_2^- . Expand (18.264) we can see that each term is a constant times a combination of eigenvalues to the power of n . Substitute (18.264) into (18.104) we have the topological zeta function:

$$\zeta(z) = \frac{(1 - z\Lambda_1^+)^2(1 - z\Lambda_1^-)^2(1 - z\Lambda_2^+)^2(1 - z\Lambda_2^-)^2}{(1 - z\Lambda_1^+\Lambda_2^+)(1 - z\Lambda_1^-\Lambda_2^+)(1 - z\Lambda_1^+\Lambda_2^-)(1 - z\Lambda_1^-\Lambda_2^-)(1 - z)^4} \quad (18.267)$$

As L becomes larger, the topological zeta function becomes more complicated but it can still be written in a similar form.

2020-10-20 Predrag We have temporal cat relations (1.6), (1.7), (1.39), (1.42),
 $s = 2 \cosh(\lambda)$,

$$2T_T(s/2) = \Lambda^T + \Lambda^{-T} = 2 \cosh(T\lambda),$$

and the Hill determinant formula

$$N_T = |\text{Det } \mathcal{J}| = \prod_{k=0}^{T-1} [s - 2 \cos(2\pi k/T)] = 2 \cosh(T\lambda) - 2. \quad (18.268)$$

Consider the Hermitian orbit Jacobian matrix:

$$\mathcal{J}_T(\theta) = \begin{pmatrix} s & -e^{i\theta} & 0 & 0 & \dots & 0 & -e^{-i\theta} \\ -e^{-i\theta} & s & -e^{i\theta} & 0 & \dots & 0 & 0 \\ 0 & -e^{-i\theta} & s & -e^{i\theta} & \dots & 0 & 0 \\ \vdots & \vdots & \vdots & \vdots & \ddots & \vdots & \vdots \\ 0 & 0 & \dots & \dots & \dots & s & -e^{i\theta} \\ -e^{i\theta} & 0 & \dots & \dots & \dots & -e^{-i\theta} & s \end{pmatrix} \quad (18.269)$$

The usual Toeplitz eigenvalues formula yields the right-hand side of the identity:

$$\det \mathcal{J}_T(\theta) = 2 \cosh(T\lambda) - 2 \cos(T\theta) = \prod_{t=0}^{T-1} \left[s - 2 \cos\left(\theta + \frac{2\pi t}{T}\right) \right].$$

The left-hand side presumably comes from the Hill's formula - have not checked.

What are these θ phases? Remember that $[L \times 1]_0$ could be thought of 1-dimensional lattice, but with s appropriately redefined. When on considers $[L \times 1]_S$, the tilt S can be distributed uniformly over the lattice by picking $\theta = 2\pi S/L$.

Taking $\theta = 2\pi S/T$ does not do anything - $\det \mathcal{J}_T(\theta)$ is the same for all S .

2020-10-20 Han Using identity (10.51)

$$\cosh(nx) - \cos(ny) = 2^{n-1} \prod_{k=0}^{n-1} \left[\cosh x - \cos\left(y + \frac{2k\pi}{n}\right) \right],$$

the counting formula (18.179) can be rewritten as:

$$\begin{aligned} N_{[L \times T]_S} &= \left| \prod_k \lambda_k \right| \\ &= \prod_{n_1=0}^{L-1} \prod_{n_2=0}^{T-1} \left[2s - 2 \cos\left(\frac{2\pi n_1}{L}\right) - 2 \cos\left(-\frac{2\pi n_1 S}{LT} + \frac{2\pi n_2}{T}\right) \right] \\ &= \prod_{n_1=0}^{L-1} \left[\prod_{n_2=0}^{T-1} \left(2s - 2 \cos\frac{2\pi n_1}{L} - 2 \cos\frac{2\pi n_2}{T} \right) - \left(2 \cos\frac{2\pi n_1 S}{L} - 2 \right) \right]. \end{aligned} \quad (18.270)$$

Let

$$\tilde{N}_{[L \times T]}(n_1) = \prod_{n_2=0}^{T-1} \left(2s - 2 \cos \frac{2\pi n_1}{L} - 2 \cos \frac{2\pi n_2}{T} \right).$$

Then

$$N_{[L \times T]_S} = \prod_{n_1=0}^{L-1} \left[\tilde{N}_{[L \times T]}(n_1) - \left(2 \cos \frac{2\pi n_1 S}{L} - 2 \right) \right].$$

For a L sites 1-dimensional chain involves with time, the number of fixed points that are invariant after T time steps with a tilt S is:

$$\begin{aligned} N_{[L \times T]_S} &= \prod_{n_1=0}^{L-1} \left(\Lambda_{n_1}^T + \Lambda_{n_1}^{-T} - 2 \cos \frac{2\pi n_1 S}{L} \right) \\ &= \prod_{n_1=0}^{L-1} \left[2 \cosh(T\lambda_{n_1}) - 2 \cos \frac{2\pi n_1 S}{L} \right], \end{aligned} \quad (18.271)$$

where

$$\lambda_{n_1} = \cosh^{-1} \left(s - \cos \frac{2\pi n_1}{L} \right).$$

When $S = 0$, (18.271) becomes (18.264).

2020-12-23 Predrag Looks like (13.4), where one allows tilts in both time and space directions, no? There one uses $4 \sin^2 \theta/2$ instead of $2 \cos \theta$, as in (4.43).

2020-10-30 Han The determinant of the orbit Jacobian matrix (18.269) is:

$$\det \mathcal{J}_T(\theta) = \prod_{t=0}^{T-1} \left[s - 2 \cos \left(\theta + \frac{2\pi t}{T} \right) \right] = 2 \cos(T\lambda) - 2 \cos(T\theta), \quad (18.272)$$

where $\lambda = \arccos(s/2)$, if the stretching parameter $s < 2$. Here I used the oscillatory counterpart (in the sense of (5.29) and (5.30)) of the identity (10.51)

$$2 \cos(nx) - 2 \cos(ny) = \prod_{k=0}^{n-1} \left[2 \cos x - 2 \cos \left(y + \frac{2k\pi}{n} \right) \right], \quad (18.273)$$

from [Gradshteyn and Ryzhik \[28\]](#) (1965) *Table of Integrals, Summations and Products* 1.395.2. It can also be proved by using the Chebyshev polynomial identity of [Wikipedia](#):

$$T_n(x) = \begin{cases} \cos(n \arccos x) & \text{if } |x| \leq 1 \\ \cosh(n \operatorname{arcosh} x) & \text{if } x \geq 1 \\ (-1)^n \cosh(n \operatorname{arcosh}(-x)) & \text{if } x \leq -1 \end{cases}.$$

In the continuous limit of the spatiotemporal cat equation becomes Helmholtz equation, whose solutions are also cosines and sines.

2020-10-31 Predrag Please read and correct/improve my attempt to consolidate this material in a single sect. 5.2 Helmholtz type equations.

2020-10-31 Predrag I think of Helmholtz → screened Poisson equation relation as the Helmholtz wavenumber $ik = m$ conversion, where m is the mass of the scalar Yukawa particle. The relations (1.52), (1.54), and (1.55) are then “trivial”, in the sense that they are just examples of (5.29) and (5.30) conversion of oscillating solutions to exponentials.

2020-10-31 Predrag Perhaps of interest to Han: Wu [57] (5.258), (5.259).

2020-10-31 Predrag Shouldn't we abandon the stretching parameter s , and rewrite everything physically, in terms of the mass $\mu^2 = d(s - 2) > 0$?

Chebyshev polynomials such as (18.268) are written in terms of s , but all our Hill determinants / periodic orbit counts might look more natural as polynomials in μ^2 .

2020-11-13 Han Using the counting formula (18.264) the topological zeta function of 2-dimensional spatiotemporal cat with $L = 3$ I get:

$$\begin{aligned} \frac{1}{\zeta(z)} &= \exp \left(- \sum_{T=1}^{\infty} \frac{z^T}{T} N_{[3 \times T]} \right) \\ &= \frac{N(z)}{D(z)}, \end{aligned} \quad (18.274)$$

where the numerator and denominator of the zeta function are:

$$\begin{aligned} N(z) &= (1 - \Lambda_1^{-1}z)^4 (1 - \Lambda_1 z)^4 (1 - \Lambda_2^{-1}z)^4 \\ &\quad (1 - \Lambda_2 z)^4 (1 - \Lambda_3^{-1}z)^4 (1 - \Lambda_3 z)^4 \\ &\quad (1 - \Lambda_1 \Lambda_2 \Lambda_3^{-1}z) (1 - \Lambda_1^{-1} \Lambda_2^{-1} \Lambda_3 z) (1 - \Lambda_1^{-1} \Lambda_2 \Lambda_3^{-1}z) \\ &\quad (1 - \Lambda_1 \Lambda_2^{-1} \Lambda_3 z) (1 - \Lambda_1 \Lambda_2^{-1} \Lambda_3^{-1}z) (1 - \Lambda_1^{-1} \Lambda_2 \Lambda_3 z) \\ &\quad (1 - \Lambda_1^{-1} \Lambda_2^{-1} \Lambda_3^{-1}z) (1 - \Lambda_1 \Lambda_2 \Lambda_3 z), \end{aligned} \quad (18.275)$$

and

$$\begin{aligned} D(z) &= (1 - \Lambda_1 \Lambda_2^{-1}z)^2 (1 - \Lambda_1^{-1} \Lambda_2 z)^2 (1 - \Lambda_1^{-1} \Lambda_2^{-1}z)^2 (1 - \Lambda_1 \Lambda_2 z)^2 \\ &\quad (1 - \Lambda_1 \Lambda_3^{-1}z)^2 (1 - \Lambda_2 \Lambda_3^{-1}z)^2 (1 - \Lambda_1^{-1} \Lambda_3 z)^2 (1 - \Lambda_2^{-1} \Lambda_3 z)^2 \\ &\quad (1 - \Lambda_1^{-1} \Lambda_3^{-1}z)^2 (1 - \Lambda_1 \Lambda_3 z)^2 (1 - \Lambda_2^{-1} \Lambda_3^{-1}z)^2 (1 - \Lambda_2 \Lambda_3 z)^2 \\ &\quad (1 - z)^8 \end{aligned} \quad (18.276)$$

2020-11-29 Predrag For a set $\mathcal{B} \in \mathbb{R}^d$, the function

$$[\mathcal{B}](\phi) = \begin{cases} 1 & \text{if } \phi \in \mathcal{B} \\ 0 & \text{otherwise} \end{cases} \quad (18.277)$$

is called the *indicator* of \mathcal{B} .

2020-11-30 Predrag Klain and Rota [36] *Introduction to Geometric Probability*:

A *valuation* on a lattice L of sets is a function μ defined on L that takes real values, and that satisfies the following conditions:

$$\mu(A \cup B) = \mu(A) + \mu(B) - \mu(A \cap B), \quad (18.278)$$

$$\mu(\emptyset) = 0, \quad (18.279)$$

where \emptyset is the empty set. By iterating the identity (18.278) we obtain the inclusion-exclusion principle for a valuation μ on a lattice L , namely

$$\begin{aligned} \mu(A_1 \cup A_2 \cup \dots \cup A_n) &= \sum_i \mu(A_i) - \sum_{i < j} \mu(A_i \cap A_j) \\ &\quad + \sum_{i < j < k} \mu(A_i \cap A_j \cap A_k) + \dots \end{aligned} \quad (18.280)$$

for each positive integer n .

Barvinok [9] Lecture 1, Problem 1 statement of (18.280) is less intelligible: Take sets $A_1, A_2, \dots, A_n \in \mathbb{R}^d$. The inclusion-exclusion formula is

$$\cup A_i = \sum_I (-1)^{|I|-1} [\cap_{i \in I} A_i], \quad (18.281)$$

where the sum is taken over all non-empty subsets $I \subset \{1, \dots, n\}$ and $|I|$ is the cardinality of I .

2020-12-15 Han Figure 18.48 is the fundamental parallelepiped of the symmetry reduced temporal Bernoulli system with $s = 2$. The fundamental domain hypercube $\hat{X} \in [0, 1/2]^n$ is divided into 2^n smaller hypercubes by the symbolic dynamics $\hat{\mathcal{A}}$. Each one of the smaller hypercubes is subject to different orbit Jacobian matrix, so the orbit Jacobian matrix maps these hypercubes into different positions.

Each integer point in the fundamental parallelepiped is corresponding to one lattice state of the symmetry reduced temporal Bernoulli system. But now the number of integer points is no longer equal to the volume of the fundamental parallelogram. So we need a smart way to count the number of lattice states. It's possible that the volume of the fundamental parallelogram mapped from the unit hypercube $[0, 1]^n$ gives the correct number of fixed points. Still need to understand why can we count in this way...

2020-12-16 Predrag Figure 18.48 is cool, and you are right, now orbit Jacobian matrices differ because of $\pm s$ on the diagonal, so different fundamental parallelepipeds go different places.

Do prove that the $|\text{Hill determinant}|$ is the same for all of them.

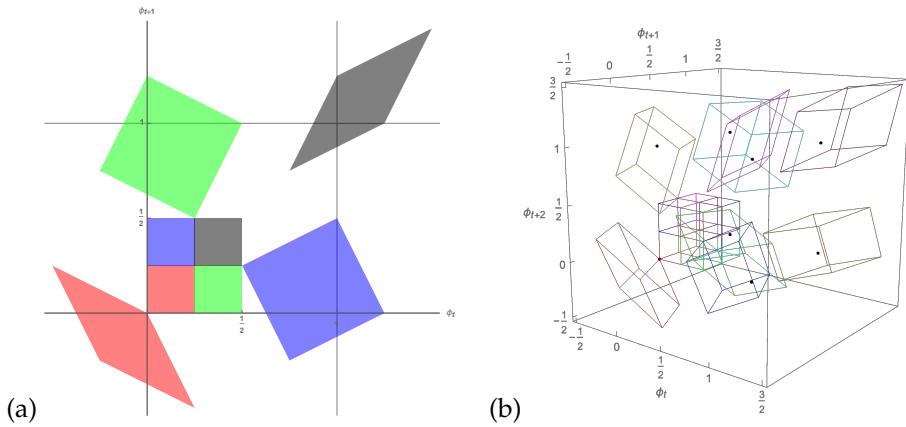


Figure 18.48: The fundamental parallelepiped of the symmetry reduced temporal Bernoulli system with $s = 2$. (a) The fundamental parallelogram of length 2 lattice state. The fundamental domain hypercube $\hat{X} \in [0, 1/2]^2$ is mapped into four fundamental parallelograms by the orbit Jacobian matrix. Each one of them contains one integer point, which is corresponding to a lattice state with length 2. The total area of the four fundamental parallelograms is $4 \times 1/4$. (b) The fundamental parallelepiped of length 3 lattice state. The fundamental domain hypercube $\hat{X} \in [0, 1/2]^3$ is divided into 2^3 hypercubes, and each one of them is mapped to a fundamental parallelepiped. The black dots are integer points. Each one of the fundamental parallelepipeds contains one integer point. So the number of the lattice states with length 3 is 8. The total volume of the 8 fundamental parallelepipeds is $8 \times 1/8$.

I expect $\det(\mathcal{J}\mathcal{L})/\det\mathcal{L}$ from (5.185) to be the correct formula, so we have to divide the volumes you get by 2^{-n} . Or maybe rescale fields ϕ_t as we discussed, so you apply the fundamental fact to unit hypercube.

Sidney has gone through the lattice points enumeration [8, 10, 11, 24] proof, ask him to explain it to you.

2020-12-22 Han Expand the antisymmetric contribution of an orbit into the trace form:

$$H_p = \{e\} : (1 - t_{\hat{p}}) = \exp[\ln(1 - t_{\hat{p}})] = \exp\left[-\sum_{n=1} t_{\hat{p}}^n\right]$$

$$H_p = \{e, \sigma\} : (1 + t_{\hat{p}}) = \exp\left[-\sum_{n=1} \frac{(-1)^n t_{\hat{p}}^n}{n}\right]$$

2020-12-24 Han The attempt described in this post failed, as the fundamental domain is not $\hat{\phi}_t \in [0, 1/2]$:

Quotient the cat map

$$\phi_{t+1} - s\phi_t + \phi_{t-1} = -m_t \quad \phi_t \in [0, 1)$$

to the fundamental domain by the dynamical $D_1 = \{e, \sigma\}$ symmetry. The fundamental domain is $\hat{\phi}_t \in [0, 1/2]$. The map in the fundamental domain is:

$$\begin{aligned} \hat{\phi}_{t+1} - s\hat{\phi}_t + \hat{\phi}_{t-1} &= -m_t, & -\hat{\phi}_{t-1} + s\hat{\phi}_t - m_t &\leq 1/2 \\ 1 - \hat{\phi}_{t+1} - s\hat{\phi}_t + \hat{\phi}_{t-1} &= -m_t, & -\hat{\phi}_{t-1} + s\hat{\phi}_t - m_t &> 1/2. \end{aligned} \tag{18.282}$$

Figure 18.49 (a) is the 3 points recurrence relation of the cat map with $s = 3$, and (b) is the recurrence relation in the fundamental domain.

2020-12-24 Han The cat map is a map: $[0, 1]^2 \rightarrow [0, 1]^2$. So using the reflection symmetry we can only reduce the state space to the fundamental domain which is a half of the full phase space, not a quarter. In the figure 18.49 (a) we can see that by using the symmetry $\{\phi_{t+1}, \phi_t, \phi_{t-1}\} \rightarrow \{\sigma\phi_{t+1}, \sigma\phi_t, \sigma\phi_{t-1}\}$ we reduce the phase space volume by half.

Another way to see why the $\hat{\phi}_t \in [0, 1/2]$ fundamental domain is incorrect: Assuming that $\phi_t \in [0, 1/2]$ and $\phi_{t-1} \in (1/2, 1)$, we can compute

$$\phi_{t+1} = +s\phi_t - \phi_{t-1} \pmod{1}. \tag{18.283}$$

But in the fundamental domain we have $\hat{\phi}_t = \phi_t$, $\hat{\phi}_{t-1} = 1 - \phi_{t-1}$ and using the map (18.282)

$$\hat{\phi}_{t+1} = \begin{cases} -1 + \phi_{t-1} + s\phi_t \pmod{1}, & -\hat{\phi}_{t-1} + s\hat{\phi}_t - m_t \leq 1/2, \\ 2 - \phi_{t-1} - s\phi_t \pmod{1}, & -\hat{\phi}_{t-1} + s\hat{\phi}_t - m_t > 1/2. \end{cases}$$

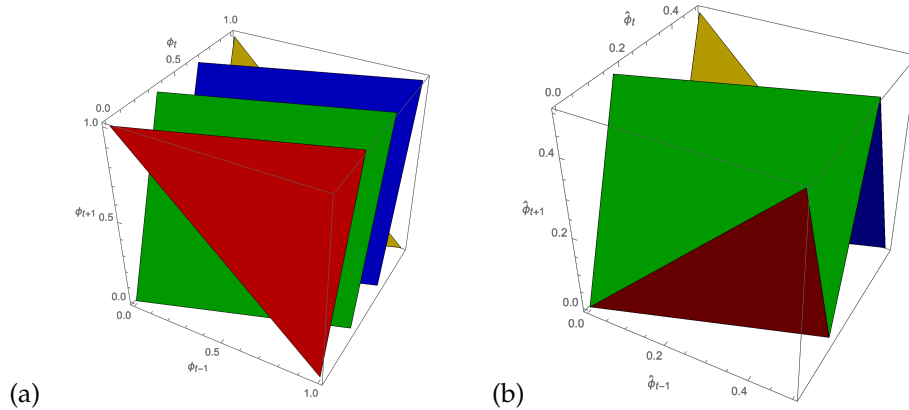


Figure 18.49: (a) A 3D visualization of the forward-in-time figure 1.2 cat map 3-term recurrence condition for the $s = 3$ cat map (18.283) of, $\{\phi_t\} \in [0, 1)$. (b) **Incorrect:** The 3 points recurrence relation in the fundamental domain $\{\hat{\phi}_{t-1}, \hat{\phi}_t, \hat{\phi}_{t+1}\} \in [0, 1/2]^3$. To rotate the figures, use the notebook [siminos/figSrc/han/Mathematica/HLSymmReducedCat.nb](#).

And neither of them is equal to ϕ_{t+1} or $1 - \phi_{t+1}$. So this lattice state in the full space $\{\phi_{t-1}, \phi_t, \phi_{t+1}\}$ does not have a corresponding lattice state in the fundamental domain. The correct fundamental domain should be $\{\hat{\phi}_{t-1}, \hat{\phi}_t\} \in [0, 1)^2 / D_1$ which is not $[0, 1/2]^2$.

2020-12-24 Predrag I think you are right - the fundamental domain $\hat{\mathcal{M}} = \mathcal{M}/D_1$, should be $1/2$ of \mathcal{M} , but my previous attempts (above in the blog) to quotient that have failed...

Thinking forward in time is a human condition, difficult to cure. Figure 18.49(a) is a nice 3D visualization of the forward-in-time figure 1.2 cat map which leads to the total mess described in Gutkin *et al.* [31]. That is why I included [figure 2](#) and [table 2](#) in that paper – an impossible number-theoretic problem created by ignoring the well-known generating partition construction.

Try plotting instead the temporal cat condition

$$\phi_t = \frac{1}{s}(\phi_{t+1} + \phi_{t-1} + m_t) \pmod{1}. \quad (18.284)$$

As illustrated by figure 1.2, there are the two kinds of pieces within the state space partition: the rectangles $\mathcal{M}_0, \dots, \mathcal{M}_{s-2}$, and the two exterior half sized triangles $\mathcal{M}_1, \mathcal{M}_{\mu^2}$, labeled by the $(\mu^2 + 1)$ -letter *interior* alphabet \mathcal{A}_0 , and the two-letter *exterior* alphabet \mathcal{A}_1 , respectively. For integer $s \geq 2$ these alphabets are

$$\mathcal{A} = \mathcal{A}_0 \cup \mathcal{A}_1, \quad \mathcal{A}_0 = \{0, \dots, \mu^2\}, \quad \mathcal{A}_1 = \{-1, \mu^2 + 1\}. \quad (18.285)$$

For the interior alphabet \mathcal{A}_0 there will be two complete rectangles in the plot corresponding to figure 18.49(a); for the alphabet \mathcal{A}_1 two triangles. You can plot the (exponentially many) admissible intermediate $\{\phi_t\}$ planes; you'll see that $1/s$ prefactor is $1/|\text{Det } \mathcal{J}_T|$. We still do not know a simple grammar rule for spatiotemporal cat, so understanding these plots might help, but we had already gone that way [31], and failed. My hunch is that understanding D_1 quotiented orbit Jacobian matrix $\hat{\mathcal{J}}$ is our best chance.

2020-12-29 Predrag Temporal cat dynamical $D_1 = \{e, \sigma\}$ symmetry is

$$\sigma\phi_t = 1 - \phi_t, \quad \sigma m_t = \mu^2 - m_t, \quad \text{for all } t \in \mathbb{Z}, \quad (18.286)$$

where m_t takes values in the s -letter alphabet (18.285).

Any codimension-1 hyperplane going through the center of mass point $\phi_t^* = 1/2$ divides the unit hypercube phase space $\mathcal{M} = \{\phi_t\} \in [0, 1]^n$ into two equal parts related by inversion through center (18.286) and can thus serve as a boundary $\hat{\mathcal{M}} \cap (\sigma\hat{\mathcal{M}})$ of a fundamental domain $\hat{\mathcal{M}}$, and its copy $\sigma\hat{\mathcal{M}}$. By the inclusion-exclusion principle (18.278)

$$\mathcal{M} = \hat{\mathcal{M}} + \sigma\hat{\mathcal{M}} - \hat{\mathcal{M}} \cap (\sigma\hat{\mathcal{M}}). \quad (18.287)$$

The natural fundamental domain $\hat{\mathcal{M}} = \{\hat{\phi}_t\} \in [0, 1]^n / D_1$ for a period-3 lattice state that satisfies the half-phase space condition and fits into the unit hypercube is given by the plane that goes through all the $1/2$ edges, i.e., a hexagon. In 4 dimensions the intersection is 2-dimensional, an octahedron.

A hyperplane:

$$\sum_{k=1}^n \alpha_k \phi_k = 1, \quad \alpha_k \geq 0.$$

There are $n2^n$ edges in a hypercube. The simplest choice would be vector α connecting two opposite corners of a hypercube. The bisecting hyperplane has to cut $2n$ edges (?) in a symmetric way under C_n rotations about the vector α .

I'm starting to feel that construction explicit fundamental domain in this case is a bad idea...

(what follows is currently **incorrect**:

$$\text{if } \sum_t \phi_t \begin{cases} < 1, & \hat{\phi}_t = \phi_t \text{ is in the fundamental domain} \\ = 1, & \hat{\phi}_t = \phi_t = \sigma\phi_t \text{ is in the border} \\ > 1, & \hat{\phi}_t = \sigma\phi_t = 1 - \phi_t. \end{cases} \quad (18.288)$$

The temporal cat condition in/out of the fundamental domain is:

$$\begin{aligned} \hat{\phi}_{t+1} - s\hat{\phi}_t + \hat{\phi}_{t-1} &= -m_t, \\ 1 - \hat{\phi}_{t+1} - s\hat{\phi}_t + \hat{\phi}_{t-1} &= -m_t, \end{aligned} \quad . \quad (18.289)$$

Can you figure out how does the \hat{m}_t s -letter alphabet come out of the full alphabet (18.285)?

2021-01-13 Han The factorization of (4.183) can be interpreted as the product of the topological zeta function of a half time step cat map. The topological zeta function of the cat map has a rational form:

$$\frac{1}{\zeta(z)} = \frac{\det(1 - zA)}{\det(1 - zB)}, \quad A = \begin{pmatrix} 2 & 1 \\ 1 & 1 \end{pmatrix}, \quad B = \begin{pmatrix} 1 & 0 \\ 0 & 1 \end{pmatrix}. \quad (18.290)$$

where the matrix A and B are the transition matrices of the Markov diagrams in figure 4.2 (a) and (b). When the topological zeta function has a fractional form (18.290), the number of the periodic points with period n is given by

$$\text{Tr } A^n - \text{Tr } B^n.$$

Using the Markov diagram, the number of periodic points is given by the number of the closed walks in the graph of matrix A , with the closed walks in the graph of matrix B eliminated.

The topological zeta function of the half time step map is

$$\frac{1}{\tilde{\zeta}(t)} = \frac{\det(1 - tA')}{\det(1 - tB')}, \quad A' = \begin{pmatrix} 1 & 1 \\ 1 & 0 \end{pmatrix}, \quad B' = \begin{pmatrix} 0 & 1 \\ 1 & 0 \end{pmatrix}, \quad (18.291)$$

where

$$A'^2 = A, B'^2 = B.$$

Let $t^2 = z$, we can factorize the topological zeta function of cat map:

$$\frac{1}{\zeta(z)} = \frac{1}{\tilde{\zeta}(t)} \frac{1}{\tilde{\zeta}(-t)}.$$

And the Markov diagram of the transition matrix A' and B' are shown in figure 4.2 (c) and (d). If we map the figure (c) and (d) two times forward in time we will get the figure (a) and (b).

So in (4.183) we factorized the topological zeta function using the "half map". To use the symmetries we probably need a different factorization...

2018-02-11 Han Bird and Vivaldi [12] say that for $s = 3$ there are $N_4(\lambda) = 10$ admissible period 4 orbits. They can be read off as walks on figure 18.4 (d), see (18.12). We have also computed them in sect. 18.2 *Rhomboid center partition*, see (18.22), as well as (18.23).

2018-04-22 Predrag The discrete Fourier-transformed cycle points \hat{M} for the periodic points of figure 18.5 are complex vectors (18.20). Similarly for (18.32). [...] Take-home messages is that writing Fourier transforms of periodic points analytically is not useful. Only cycle-4 orbits are related to Gaussian integers, for other orbits there will be no nice analytic formulas. And already for 4-cycles, the phases are not rational fractions of 2π .

2021-01-16 Han The state space of the 1-dimensional lattice state can be divided into subspaces by the irreps of the dihedral group. For example, when the period of the lattice state is 4, the dihedral group has a $[4 \times 4]$ matrix representation which act on the 4-dimensional state space of the lattice state. This representation can be generated by the reflection operator: ¹⁷

$$\sigma = \begin{pmatrix} 0 & 0 & 0 & 1 \\ 0 & 0 & 1 & 0 \\ 0 & 1 & 0 & 0 \\ 1 & 0 & 0 & 0 \end{pmatrix},$$

and the shift operator:

$$r = \begin{pmatrix} 0 & 1 & 0 & 0 \\ 0 & 0 & 1 & 0 \\ 0 & 0 & 0 & 1 \\ 1 & 0 & 0 & 0 \end{pmatrix}.$$

They both commute with the orbit Jacobian matrix. Using the sine and cosine basis we can block diagonalize this representation such that each block on the diagonal is an irrep of the D_4 group, using the orthogonal matrix:

$$T = \begin{pmatrix} \mathbf{e}_1 \\ \mathbf{e}_2 \\ \mathbf{e}_3 \\ \mathbf{e}_4 \end{pmatrix} = \begin{pmatrix} \frac{1}{2} & \frac{1}{2} & \frac{1}{2} & \frac{1}{2} \\ -\frac{1}{2} & \frac{1}{2} & -\frac{1}{2} & \frac{1}{2} \\ 0 & -\frac{1}{\sqrt{2}} & 0 & \frac{1}{\sqrt{2}} \\ \frac{1}{\sqrt{2}} & 0 & -\frac{1}{\sqrt{2}} & 0 \end{pmatrix},$$

each row of which is a basis vector. The k th components of these basis vectors are:

$$\mathbf{e}_{1k} = \frac{1}{2} e^{\frac{2\pi i 0k}{4}}, \mathbf{e}_{2k} = \frac{1}{2} e^{\frac{2\pi i 2k}{4}}, \mathbf{e}_{3k} = \frac{1}{\sqrt{2}} \cos\left(\frac{2\pi k}{4}\right), \mathbf{e}_{4k} = \frac{1}{\sqrt{2}} \sin\left(\frac{2\pi k}{4}\right).$$

Using this set of basis we can block diagonalize the reflection and shift operators:

$$T\sigma T^\top = \begin{pmatrix} 1 & 0 & 0 & 0 \\ 0 & -1 & 0 & 0 \\ 0 & 0 & 0 & 1 \\ 0 & 0 & 1 & 0 \end{pmatrix},$$

$$TrT^\top = \begin{pmatrix} 1 & 0 & 0 & 0 \\ 0 & -1 & 0 & 0 \\ 0 & 0 & 0 & 1 \\ 0 & 0 & -1 & 0 \end{pmatrix},$$

¹⁷Predrag 2021-06-13: You could not have chosen more devious notation: pretty much everywhere I (and some sophisticated wiki's) write r for the $2\pi/n$ rotation (translation), and s_j for reflection across j th symmetry axis, see table ???. I'm experimenting with writing this up as in sect. 4.5.

which contain 3 irreps along the diagonal. The first one is the 1-dimensional symmetric irrep. The second one is antisymmetric under shift by one lattice site and one type of reflections, symmetric under other group operations. This representation is called B_1 or B_2 . The third one is the 2-dimensional irrep.

Using the orthogonal matrix T we can rewrite a lattice state into the space with sine and cosine basis. For example, a lattice state $\{a, b, c, d\}$ becomes:

$$T \begin{pmatrix} a \\ b \\ c \\ d \end{pmatrix} = \begin{pmatrix} \frac{a}{2} + \frac{b}{2} + \frac{c}{2} + \frac{d}{2} \\ -\frac{a}{2} + \frac{b}{2} - \frac{c}{2} + \frac{d}{2} \\ \frac{d}{\sqrt{2}} - \frac{b}{\sqrt{2}} \\ \frac{a}{\sqrt{2}} - \frac{c}{\sqrt{2}} \end{pmatrix}.$$

The shifted and reversed lattice states $\{d, a, b, c\}$ and $\{d, c, b, a\}$ become:

$$T \begin{pmatrix} d \\ a \\ b \\ c \end{pmatrix} = \begin{pmatrix} \frac{a}{2} + \frac{b}{2} + \frac{c}{2} + \frac{d}{2} \\ \frac{a}{2} - \frac{b}{2} + \frac{c}{2} - \frac{d}{2} \\ \frac{c}{\sqrt{2}} - \frac{a}{\sqrt{2}} \\ \frac{d}{\sqrt{2}} - \frac{b}{\sqrt{2}} \end{pmatrix}, \quad T \begin{pmatrix} d \\ c \\ b \\ a \end{pmatrix} = \begin{pmatrix} \frac{a}{2} + \frac{b}{2} + \frac{c}{2} + \frac{d}{2} \\ \frac{a}{2} - \frac{b}{2} + \frac{c}{2} - \frac{d}{2} \\ \frac{a}{\sqrt{2}} - \frac{c}{\sqrt{2}} \\ \frac{d}{\sqrt{2}} - \frac{b}{\sqrt{2}} \end{pmatrix}.$$

So in the subspace of the last two components in the new basis, the shift and time reflection act as rotation and reflection in 2-dimensional space. The sign of the second component is changed because the second irrep contained in the reducible representation is -1 for the reflection σ and shift r .

To find the fundamental domain of the cyclic permutation symmetry and time reversal symmetry in this new state space, we need to quotient the subspace of the last two components to $1/8$ of the full subspace.

But I still need to think about how does the second 1-dimensional irrep affect the fundamental domain. Moreover, the boundary of the fundamental domain is a 3-dimensional space, which can have a complicated structure. I assume we will reach the boundary when some of the field values are equal. For example, the lattice states $\{a, b, a, b\}$ and $\{b, a, b, a\}$ are:

$$T \begin{pmatrix} a \\ b \\ a \\ b \end{pmatrix} = \begin{pmatrix} a+b \\ b-a \\ 0 \\ 0 \end{pmatrix}, \quad T \begin{pmatrix} b \\ a \\ b \\ a \end{pmatrix} = \begin{pmatrix} a+b \\ a-b \\ 0 \\ 0 \end{pmatrix}.$$

The last two components are on the origin, which is on the boundary of the fundamental domain. The lattice state $\{a, b, a, b\}$ is a repeat of a shorter lattice, so perhaps the position in the subspace and the second component (subspace of the second 1-dimensional irrep) tell us information about whether the lattice state can be reduced to shorter prime state.

2021-01-22 Han It's easier to see the discrete Fourier transform (sine and cosine transform) of the lattice state space in 3-dimensional space. In the state

space of the lattice state with period-3, the reflection and shift operators are:

$$\sigma = \begin{pmatrix} 0 & 0 & 1 \\ 0 & 1 & 0 \\ 1 & 0 & 0 \end{pmatrix}, \quad r = \begin{pmatrix} 0 & 1 & 0 \\ 0 & 0 & 1 \\ 1 & 0 & 0 \end{pmatrix}.$$

Using the sine and cosine basis:

$$T = \begin{pmatrix} \frac{1}{\sqrt{3}} & \frac{1}{\sqrt{3}} & \frac{1}{\sqrt{3}} \\ -\frac{1}{\sqrt{6}} & -\frac{1}{\sqrt{6}} & \sqrt{\frac{2}{3}} \\ \frac{1}{\sqrt{2}} & -\frac{1}{\sqrt{2}} & 0 \end{pmatrix},$$

the reflection and shift operators are block diagonalized:

$$T\sigma T^\top = \begin{pmatrix} 1 & 0 & 0 \\ 0 & -\frac{1}{2} & \frac{\sqrt{3}}{2} \\ 0 & \frac{\sqrt{3}}{2} & \frac{1}{2} \end{pmatrix}, \quad TrT^\top = \begin{pmatrix} 1 & 0 & 0 \\ 0 & -\frac{1}{2} & \frac{\sqrt{3}}{2} \\ 0 & -\frac{\sqrt{3}}{2} & -\frac{1}{2} \end{pmatrix},$$

which contain a symmetric 1-dimensional irrep and a 2-dimensional irrep. The orbit Jacobian matrix is diagonalized in this basis:

$$T\mathcal{J}T^\top = \begin{pmatrix} -1 & 0 & 0 \\ 0 & -4 & 0 \\ 0 & 0 & -4 \end{pmatrix}.$$

Note that in the subspace of 2-dimensional irrep the orbit Jacobian matrix is $-4 \times$ identity matrix.

Figure 18.50 shows the fundamental parallelepipeds of the period 3 lattice states in the configuration space and the "Fourier space". The shapes of the unit cube and the fundamental parallelepiped are not changed.

Figure 18.51 shows the fundamental parallelepipeds of the period 3 lattice states observed from the direction of the symmetric eigenvector of the reflection and shift operators. In the configuration space this eigenvector is $\{1, 1, 1\}$ and in the "Fourier space" this eigenvector is $\{1, 0, 0\}$. These 2 figures are projections of the fundamental parallelepipeds in the subspace of the 2-dimensional irrep. The red and blue dots are the periodic points mapped by the orbit Jacobian matrix. In this figure we see that the periodic points exist on the same positions in the 2-dimensional subspace.

In the [wikipedia of the orthogonal transformation](#), the orthogonal transformation is a linear transformation that preserves length of vectors and the angles between them.

2021-01-25 Predrag Just so we do not forget: this eventually goes into our main thrust on understanding both the forward and backward in time, and

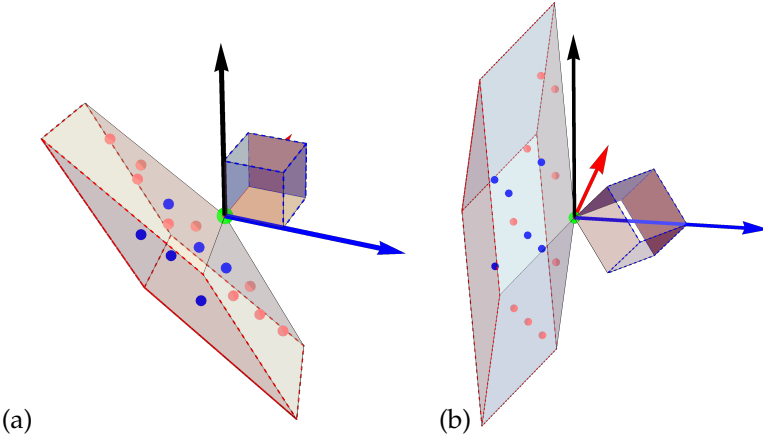


Figure 18.50: (a) The fundamental parallelepiped and the unit cube of the lattice state with period 3 in the configuration space. (b) The fundamental parallelepiped and the unit cube of the lattice state with period 3 in the “Fourier space”. The 3 arrows are the axes of the space. The fundamental parallelepiped in the “Fourier space” is different from the fundamental parallelepiped in the configuration space by a rotation. To rotate the figures, use the notebook [siminos/figSrc/han/Mathematica/HIirrepsBlockLength3.nb](#).

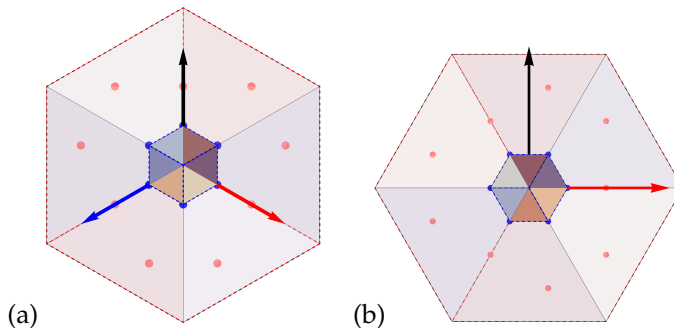


Figure 18.51: (a) The fundamental parallelepiped and the unit cube of the lattice state with period 3 in the configuration space observed from the direction of $\{1, 1, 1\}$. (b) The fundamental parallelepiped and the unit cube of the lattice state with period 3 in the “Fourier space” observed from the direction of $\{1, 0, 0\}$. In the figure (a) the blue and red dots are integer points enclosed by the fundamental parallelepiped. Each one of the integer points is related to one periodic point. In the “Fourier space”, the blue and red dots are integer points transformed by the matrix T . They still form a cubic lattice, but the coordinates are no longer integers.

the global temporal cat time-reversal symmetry, see sect. 4.2 *Temporal cat reversibility factorization*.

For our many (mostly failed) attempts to find an Adler-Weiss forward and backward in time symmetric partition, see sect. 18.3 *Time reversal*.

[Birdtracks.eu Sect. 8.2.3 Time reversal symmetry](#) might be relevant to spatiotemporal cat: when the Hamiltonian is invariant under time reversal, the symmetry group is enlarged.

Not to reinvent the wheel: sect. 4.6 *Reduction to the reciprocal lattice* has various references to the standard space groups theory. It proceeds in two steps

1. Discrete Fourier transform diagonalizes the translational symmetry C_T ; that is the “reduction to the reciprocal lattice,” with complex eigenvectors.

My problem with figure 18.50 (b) and figure 18.51 (b) is that I expected to see the infinite lattice \mathbb{Z} eigenstates represented by a *unit interval* on the reciprocal lattice.

2. Point group D_1 irreps ‘diagonalization’ reduces this to D_T , with real 1- and 2-dimensional irreps.

My problem with figure 18.50 (b) and figure 18.51 (b) is that I expected to see the infinite lattice \mathbb{Z} with reflection represented by a $1/2$ *unit interval* fundamental domain on the reciprocal lattice.

For D_n symmetry: see [Ding thesis example 2.9](#).

Also, change to *siminos/lyapunov* subdirectory,
`pdflatex blog`
 read sect. 7.11.2 *Factorization of C_n and D_n* .

2021-01-26 Han Figure 18.52 (a) shows the period-5 reciprocal lattice states the temporal cat for $s = 3$. The total number of the lattice states is given by $N_5 = |\text{Det } \mathcal{J}| = 121$.

See also the discussion in blog post **2018-05-22 Han** above, a few pages after (18.72).

Figure 18.52 (b) shows the lattice states in the fundamental domain. The fundamental domain contains lattice states with the argument of the second component of the Fourier transform of the lattice states greater or equal to $-2\pi/10$, less than $2\pi/10$.

The number of lattice states in the fundamental domain is 25. One of them is the constant $\{0, 0, 0, 0, 0\}$ state. Each one of the other, prime solutions contributes 5 times to N_5 , the total number of lattice states belong to the same time orbit. So we have the total number of solutions: $N_5 = 121 = 1 + M_5 \times 5 = 1 + 24 \times 5$, see table 4.1.

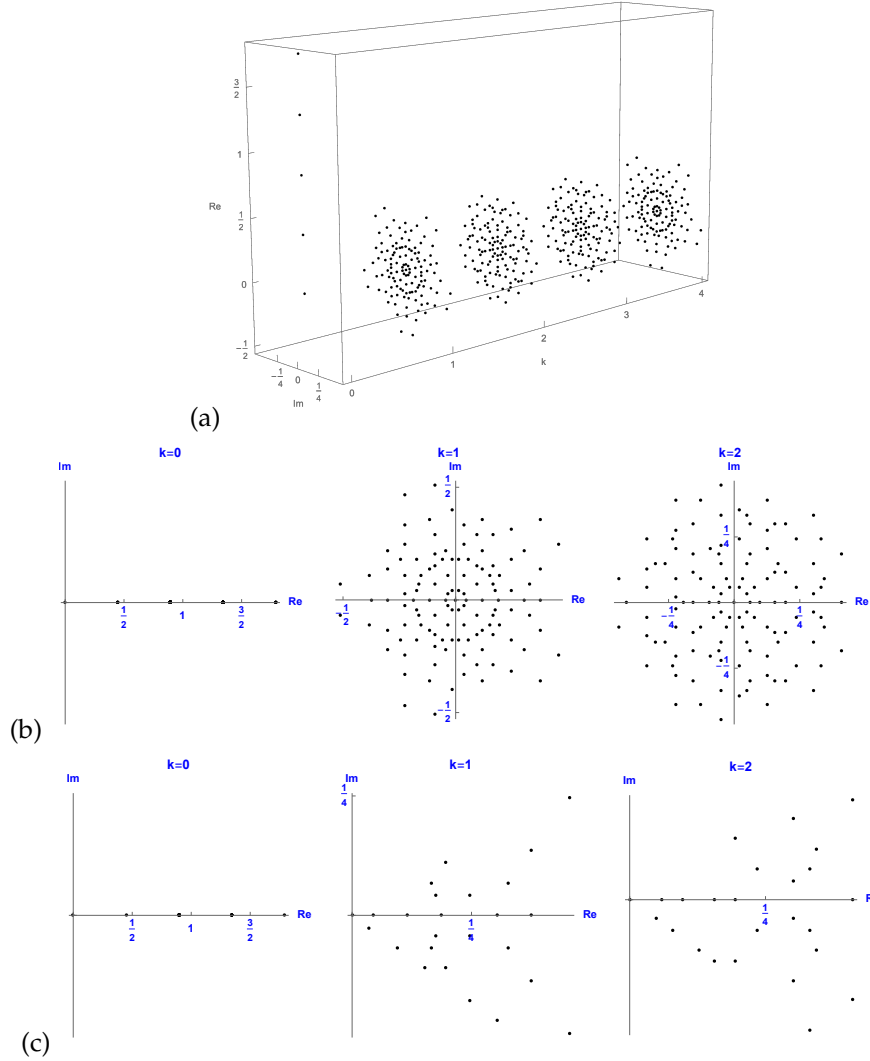


Figure 18.52: (Continuation of figure 18.35.) The 121 period $n = 5$ reciprocal lattice states (see table 4.1) of the $s = 3$ temporal cat, obtained by discrete C_5 Fourier transform diagonalization. (a) A perspective view. (b) $k = 0, 1, 2$ irreps of C_5 . By time reversal $k = 3$ has the same prime orbits as $k = 2$, and $k = 4$ as $k = 1$. (c) The C_5 symmetry reduced fundamental domain contains reciprocal lattice states whose phases lie in $[-2\pi/10, 2\pi/10]$, one reciprocal lattice state for each C_5 group orbit. The constant lattice state $\{0, 0, 0, 0, 0\}$ lives in a boundary, the intersection of the fundamental domain and all its images, with each reciprocal lattice state a $k = 0$ average over corresponding lattice states, hence real. For C_{11} reciprocal lattice states, see figure 18.13. (Continued in figure 18.53.)

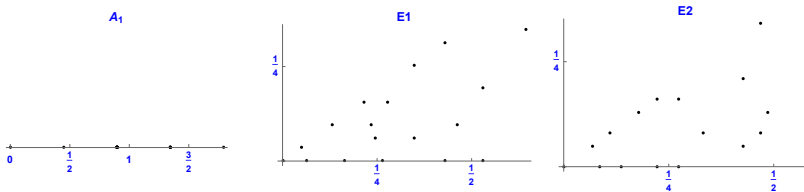


Figure 18.53: The C_5 $k = 0, 1, 2$ fundamental domains $[-2\pi/10, 2\pi/10]$ of figure 18.52(c) are complex conjugation symmetric, so they can be tiled by a $1/2$ domain $[0, 2\pi/10]$ and its complex-conjugate image. In the $[0, 2\pi/10]$ domain there are 18 reciprocal lattice states. One of them is the origin. Excluding origin, there are 10 points on the $1/2$ domain boundaries, 5 points on the real axis (with phase 0), and 5 points with phase $2\pi/10$ belonging to the same set of states in the time orbit, but with reverse rotation in time. The remaining 7 points lie inside the $1/2$ domain. Their group orbits, generated by rotations and reflections include 10 lattice states. So the total number of the C_5 lattice states is $1 \times \bar{1} + 10 \times \bar{5} + 7 \times \bar{10} = 121$, where 121 is the coefficient of the z^5 term in the number of states generating function $F(z)$ of (1.14). This is *not* a D_5 symmetry-reduction, as self-dual orbits are not represented as repeats of prime orbits of $1/2$ period (coefficients of the D_5 generating function $F'(t)$, $t^2 = z$) and time-reversal pairs are counted as distinct orbits, whereas under D_5 each such pair is a single prime orbit, see the D_3 example figure 3.5. (Continued in figure 18.54.)

2021-01-26 Predrag I think a very nice picture is emerging of fundamental domains and prime orbits for temporal cat, and hopefully eventually for spatiotemporal cat.

You need to explain what every periodic lattice concept becomes on reciprocal lattice, in particular how prime periodic states in the reciprocal lattice fundamental domain relate to the lattice states.

If one reduces only the C_n symmetry, the numbers of reciprocal lattice states in the fundamental domain are presumably given by M_n in table 4.1. Note that for non-prime n there will be more prime orbits, and more points in invariant subspaces (borders).

Once one also reduces the reflection symmetry, the numbers of reciprocal lattice states in the D_n fundamental domain are given by \tilde{M}_n in the golden (Fibonacci [5]) cat map table 4.2 and (4.182). This should be the same as counting walks on the “half time-step” Markov graph figure 4.2.

Is figure 18.52 (b) for $k = 4\pi/5$ correct? I think you have to rotate by the appropriate $2\pi\ell/5$ the points that are outside the fundamental domain.

2021-01-27 Han I believe figure 18.52 (b) for $k = 4\pi/5$ and $k = 6\pi/5$ is correct.

To make this figure, I plotted all of the solutions then only kept the solutions with the $k = 2\pi/5$ component in $[-2\pi/10, 2\pi/10]$. If you rotate the solutions to move the $k = 4\pi/5$ component into the fundamental domain, the $k = 2\pi/5$ component will come out of the fundamental domain.

Figure 18.35 shows the solutions in the generating partition (the rhomboid corner partition), while figure 18.52 are solutions with field values in $[0, 1]$.

For the Fourier transform of the field of figure 18.35, see figure 18.52 (a,b).

2021-01-27 Han Apparently I was wrong assuming the Fourier transforms of the symbol blocks appear on straight lines when the Fourier transforms of the fields are not... The figure 18.35 (a) and (b) are almost identical. The only difference is the scale. The reason is that in the Fourier space, orbit Jacobian matrix is diagonalized so the source terms are equal to the fields times the eigenvalues.

2021-01-27 Predrag I think this all is falling into place in a very nice way. This is all about the symmetry reduction of the space lattice (the “floor”), we still have to do the dynamical D_1 temporal cat (the “cat”) symmetry separately.

A system other than the temporal cat organized by D_{nn} irreps is a convex regular polygon (a polygon that is equiangular and equilateral) n -disk scatterer. In ChaosBook we work out the $n = 2, 3, 4$ cases. Unlike the temporal cat, if disks are sufficiently thin, all symbol blocks are admissible (full grammar, no pruning).

Temporal cat lattice states correspond to all n at one go.

(a)

(b)

Figure 18.54: (Continuation of figure 18.52.) The 9 period $n = 5$ reciprocal lattice states (hopefully given by (4.182)) of the $s = 3$ temporal cat, obtained by discrete D_5 irreps $A_1 \otimes E_2 \otimes E_2$ diagonalization of the $1/2$ time step or the temporal golden (Fibonacci [5]) cat lattice (generating functions in powers of t^n). (a) A_1, E_2 and E_2 irreps of D_5 . For D_5 all reciprocal lattice states are real. (b) The D_5 symmetry-reduced fundamental domain contains reciprocal lattice states whose phases lie in $[0, 2\pi/10]$, one reciprocal lattice state for each D_5 group orbit. The constant lattice state $\{0, 0, 0, 0, 0\}$ lives in the intersection of the fundamental domain and all its images. The time reversal symmetry corresponds to complex conjugation, with opposite direction orbits identified. The phase $=0$ states are self-dual, reciprocal lattice states on the real axis that is a fundamental domain boundary, and are correctly counted by the inclusion-exclusion principle (18.278). See 2021-01-27 Predrag above to see how this is done correctly for D_3 and D_4 .

2021-01-27 Predrag For some background on D_∞ symmetry of the temporal cat and ϕ^4 1d lattice field theory, sect. 3.10 *Translations and reflections*, see remark 4.1 Time reversal; not a priority as yet.

2021-01-27 Predrag The brilliant thing about my fellow Dane Caspar Wessel's great invention is that in the complex plane the unit circle is a *circle*, not squashed into an ellipse :) Can you replot figure 18.35 and figure 18.52, so Re and Im axes have the same scale? Label them as Re and Im , instead of the awkward long labels you have now - you can explain axes in the figure caption. Also, in this C_5 example, plot the 5 irreps (Fourier components in the C_5 case) side by side, rather than a perspective drawing of 5 planes cutting across a parallelepiped. Use the same names for the figure files, just plot them Wessel's way.

I think you might want to repeat this for C_6 , as there you get two extra sets of boundaries between 2-state and 3-state repeats, that's more like the case of general C_n reciprocal lattice state.

2021-01-27 Predrag The brilliant thing about D_n irreps is that they are all real, so you don't have to plot Wessel's 2D complex plane. However they all (except the two or 4 1-dimensional irreps) are 2-dimensional, so you still have to plot $\cos 2\pi k/n, \sin 2\pi k/n$ planes. How do your reciprocal lattice states look in these 2-dimensional irreps for the C_5 and C_6 examples?

2021-01-29 Predrag 2 Han Can you plot the D_5 -symmetry reduced figure 18.54? If the caption is not clear, call me, let's discuss.

2021-02-01 Predrag 2 Han About plotting the D_n -symmetry reduced figure 18.54: not sure what the good way is plotting the 2-dimensional representations.

Maybe complex regular irreps [ChaosBook example 25.7 Basis for irreps of \$D_3\$](#) suggest the way to plot?

I find [Harter's Sect. 3.3 Second stage of non-Abelian symmetry analysis](#) particularly illuminating. It shows how physically different (but mathematically isomorphic) higher-dimensional irreps are constructed corresponding to different subgroup embeddings. One chooses the irrep that corresponds to a particular sequence of physical symmetry breakings.

2021-02-02 Han In figure 18.53, there are 18 lattice states in the fundamental domain. The lattice state on the origin is $\{0, 0, 0, 0, 0\}$.

The 5 lattice states X on the boundary with phase 0 are:

$$\begin{aligned} \frac{1}{11}\{2, 1, 1, 2, 5\}, \quad \frac{1}{11}\{4, 2, 2, 4, 10\}, \quad \frac{1}{11}\{6, 3, 3, 6, 4\}, \\ \frac{1}{11}\{8, 4, 4, 8, 9\}, \quad \frac{1}{11}\{10, 5, 5, 10, 3\}. \end{aligned} \quad (18.292)$$

The 5 periodic orbits on the boundary with phase $2\pi/10$ are:

$$\begin{aligned} \frac{1}{11}\{6, 1, 8, 1, 6\}, \quad \frac{1}{11}\{7, 3, 2, 3, 7\}, \quad \frac{1}{11}\{8, 5, 7, 5, 8\}, \\ \frac{1}{11}\{9, 7, 1, 7, 9\}, \quad \frac{1}{11}\{10, 9, 6, 9, 10\}. \end{aligned} \quad (18.293)$$

Orbits on the boundaries are invariant under reflection.

The 7 periodic orbits in the fundamental domain are:

$$\begin{aligned} \frac{1}{11}\{4, 3, 5, 1, 9\}, \quad \frac{1}{11}\{4, 5, 0, 6, 7\}, \quad \frac{1}{11}\{7, 0, 4, 1, 10\}, \\ \frac{1}{11}\{8, 7, 2, 10, 6\}, \quad \frac{1}{11}\{10, 0, 1, 3, 8\}, \quad \frac{1}{11}\{9, 0, 2, 6, 5\}, \\ \frac{1}{11}\{9, 3, 0, 8, 2\}. \end{aligned} \quad (18.294)$$

2021-02-09 Han Also note that the orbits with time reversal symmetry ([18.292–18.293](#)) have phase $2\pi/10$ in the subspace of E_1 and $4\pi/10$ in the subspace of E_2 , or phase 0 in both E_1 and E_2 subspaces. So when a lattice state has time reversal symmetry, this lattice state exists in the 3-dimensional subspace. The dimension of the subspace is probably the period of the orbit after quotientienting by the symmetry.

2021-02-02 Han The transition matrix of the half step map is given by the matrix A' in ([18.291](#)). The map

$$\left(\begin{array}{c} q_{t+1} \\ p_{t+1} \end{array} \right) = A' \left(\begin{array}{c} q_t \\ p_t \end{array} \right) \pmod{1} \quad (18.295)$$

can be rewritten as:

$$\begin{pmatrix} q_t \\ q_{t+1} \end{pmatrix} = \begin{pmatrix} 0 & 1 \\ 1 & 1 \end{pmatrix} \begin{pmatrix} q_{t-1} \\ q_t \end{pmatrix} \pmod{1}. \quad (18.296)$$

(Predrag: see (4.170), (4.173). This is not the Percival-Vivaldi two configuration representation.)

For $s = 3$, $\mathcal{J} = \tilde{\mathcal{J}}^\top \tilde{\mathcal{J}}$, where the inversion-reduced orbit Jacobian matrix is:

$$\tilde{\mathcal{J}} = \begin{pmatrix} 1 & -1 & 0 & 0 & \dots & 0 & 1 \\ 1 & 1 & -1 & 0 & \dots & 0 & 0 \\ 0 & 1 & 1 & -1 & \dots & 0 & 0 \\ \vdots & \vdots & \vdots & \vdots & \ddots & \vdots & \vdots \\ 0 & 0 & \dots & \dots & \dots & 1 & -1 \\ -1 & 0 & \dots & \dots & \dots & 1 & 1 \end{pmatrix}, \quad (18.297)$$

as in (4.55).

This map has $\tilde{N}_5 = 11$ period $n = 5$ lattice states. One of them is the fixed point $\{0, 0, 0, 0, 0\}$. The other 10 lattice states are the $\tilde{M}_5 = 2$ prime orbits:

$$\frac{1}{11}\{9, 3, 1, 4, 5\}, \quad \frac{1}{11}\{10, 7, 6, 2, 8\}, \quad (18.298)$$

and the cyclic permutations, in agreement the golden cat map counts table 4.2 and (4.182). The repeats of these two orbits are the orbits

$$\frac{1}{11}\{4, 3, 5, 1, 9\}, \quad \frac{1}{11}\{8, 7, 2, 10, 6\} \quad (18.299)$$

in the (18.294).

The half step lattice has 121 period $n = 10$ lattice states. Some of the orbits are:

$$\begin{aligned} \frac{1}{11}\{7, 8, 4, 1, 5, 6, 0, 6, 6, 1\}, & \quad \frac{1}{11}\{7, 9, 5, 3, 8, 0, 8, 8, 5, 2\}, \\ \frac{1}{11}\{7, 10, 6, 5, 0, 5, 5, 10, 4, 3\}, & \quad \frac{1}{11}\{4, 2, 6, 8, 3, 0, 3, 3, 6, 9\}, \\ \frac{1}{11}\{8, 2, 10, 1, 0, 1, 1, 2, 3, 5\}, & \quad \frac{1}{11}\{5, 4, 9, 2, 0, 2, 2, 4, 6, 10\}, \\ \frac{1}{11}\{7, 3, 10, 2, 1, 3, 4, 7, 0, 7\}, & \quad \frac{1}{11}\{6, 4, 10, 3, 2, 5, 7, 1, 8, 9\}, \\ \frac{1}{11}\{9, 7, 5, 1, 6, 7, 2, 9, 0, 0\}, & \quad \frac{1}{11}\{9, 8, 6, 3, 9, 1, 10, 0, 10, 10\}, \\ \frac{1}{11}\{10, 8, 7, 4, 0, 4, 4, 8, 1, 9\}. & \end{aligned} \quad (18.300)$$

Each one of these orbits is corresponding to two orbits in (18.292–18.294)

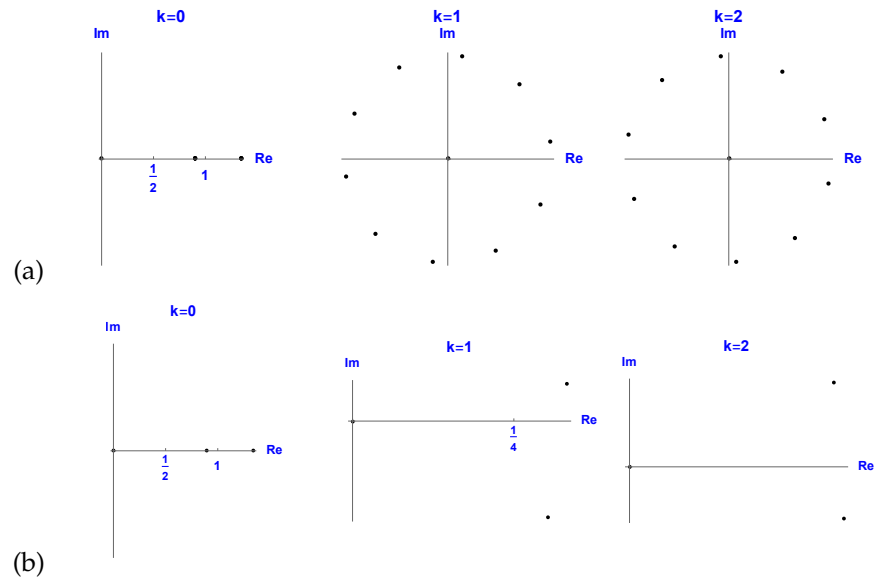


Figure 18.55: (a) The $\tilde{N}_5 = 11$ period $n = 5$ reciprocal lattice states of the $1/2$ time step lattice (temporal golden cat) of the $s = 3$ temporal cat, obtained by discrete C_5 irreps diagonalization. (b) The C_5 symmetry-reduced fundamental domain contains $\tilde{M}_5 = 2$ prime reciprocal lattice states whose phases lie in $[-2\pi/10, 2\pi/10]$, one prime reciprocal lattice state for each C_5 group orbit. The constant lattice state $\{0, 0, 0, 0, 0\}$ lives in the intersection of the fundamental domain and its images.

2021-02-04 Predrag Sect. 4.3.2 contains my 2008 Baake, Roberts and Weiss [6] *Periodic orbits of linear endomorphisms on the 2-torus and its lattices* arXiv:0808.3489 reading notes. Please improve them, if you read the paper. In any case, we must read 1997 sect. 4.3.3 Baake, Hermisson and Pleasants [4] *The torus parametrization of quasiperiodic LI-classes*, add your notes to the subsection there.

2021-02-06 Han Added figure 18.56, the generating partition of the golden cat map (1/2 time step map) (4.170), (4.173), (18.296), the time-reversal reduction of the $s = 3$ Thom-Arnol'd cat map (1.1) and figure 1.1.

2021-02-06 Predrag Note: this is *not* the time-reversal reduction (5.193) of the Percival-Vivaldi cat map figure 1.9 and (18.72), that is done in figure 18.57. I would prefer such Percival-Vivaldi golden cat map figure for inclusion into ChaosBook.

The colors in figure 18.56 (a) and (b) should be consistent, as in figure 1.9. But do not waste time on fixing that, draw the Percival-Vivaldi golden cat map instead.

In despair, I had drawn the original by hand, see *PVAdlerWeissB-a.svg*, *PVAdlerWeissB-b.svg*, *PVAdlerWeissB-c.svg* and *PVAWMarkovCol.svg*. How do I know that? Every figure I draw has the source program indicated as a comment. You can edit *.svg files using Inkscape, all you have to do is to replace $\Lambda \rightarrow \tilde{\Lambda}$ in figure 1.9 (b), remove the extra sub-partitions. Almost done in figure 18.32 (c).

2021-02-08 Han Using (18.72), the generating partition of the half-step $\mu = 1$ Percival-Vivaldi cat map is shown in figure 18.57.

2021-02-06 Predrag Very nice, thank you. Still, it would be nice to also have the $\mu > 1$ generating partition, no necessarily as a drawing.

2021-02-06 Predrag OK, we are done. You know what to do next. We now have the golden cat orbit Jacobian matrix (4.55) on the half-time step lattice for any μ . We had it all along, but I made a few trivial errors, and you did not check those calculations, so it took a bit too long...

1. You can now compute

$$\begin{aligned} \sum_{n=1} \tilde{N}_n(\mu) t^n &= -\tilde{\zeta} t \frac{d}{dt} \frac{1}{\tilde{\zeta}} \\ &= ??t + ??t^2 + \mu(\mu^2 + 3)t^3 + ??t^4 + ??t^5 + ??t^6 + ??t^7 \\ &\quad + ??t^8 + ??t^9 + \dots . \end{aligned} \tag{18.301}$$

2. Does it agree with (4.182)?
3. Does your $N(s)_n = \tilde{N}(\mu)_n^2$ agree with (4.66) for $n = 3$?

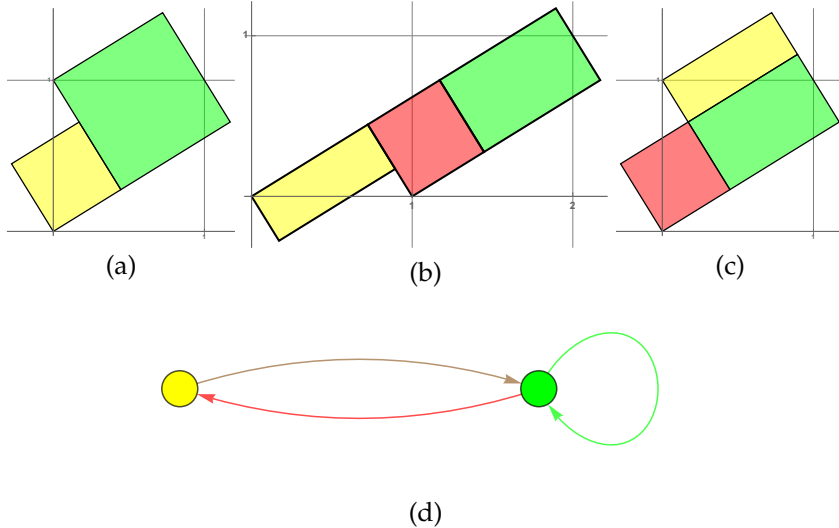


Figure 18.56: (a) An Adler-Weiss generating partition of the unit torus for the golden cat map (1/2 time step map) (4.170), (4.173), (18.296), the time-reversal reduction of the $s = 3$ Thom-Arnol'd cat map (1.1) and figure 1.1, with rectangle \mathcal{M}_A (green) and \mathcal{M}_B (yellow) borders given by the stable and unstable manifolds, i.e., along the two eigenvectors corresponding to the eigenvalues of the matrix A' in (18.295). (b) Mapped one step forward in time, the rectangles are stretched along the unstable direction and shrunk along the stable direction. The eigenvectors are the same as for the Arnol'd cat map, but eigenvalue $\tilde{\Lambda}$ (5.194) is a square root of the Arnol'd cat map eigenvalue (1.6), $\Lambda = \tilde{\Lambda}^2$, hence less stretching. As always, sub-rectangles have to be translated back into the initial partition. (c) The sub-rectangles translated back into the initial partition yield a generating partition, with the finite grammar given by the transition graph (d) of figure 4.2. The nodes refer to the rectangles A and B , and the three links correspond to the three sub-rectangles induced by one step forward-time dynamics. The generating partition of the half-step $\mu = 1$ Percival-Vivaldi cat map is shown in figure 18.57.

4. Does it agree with our temporal cat $N(s)_n$ series? For example, with (5.242).
5. Derive $1/\tilde{\zeta}(t)$
6. Does it agree with (4.45)? with (4.181)?

You'll be glad to hear that have named "golden" cats for $\mu > 1$ "metal cats" in a paper that was published, so that will be the official name for those zeta's :)

2021-02-06 Predrag Started drafting sect. 4.2 *Time reversal symmetry reduction* for CL18.

2021-02-08 Han We are not done yet... While in the above we here use Percival-Vivaldi [51] "two-configuration representation" cat map (1.5)

$$\mathbf{A} = \begin{bmatrix} 0 & 1 \\ -1 & s \end{bmatrix} \quad (18.302)$$

Gutkin *et al.* [31] cat map (derived as a piece of the standard map, see (2.66)) is of form:

$$A = \begin{pmatrix} s-1 & 1 \\ s-2 & 1 \end{pmatrix}. \quad (18.303)$$

The square root of this matrix is not an integer matrix if $s \neq 3$.

\tilde{A} and A can be diagonalized simultaneously if $\tilde{A}^2 = A$ (*Predrag feels a bit unconformable taking a square root of an asymmetric matrix, even though you diagonalize it first...*). We can always use matrix:

$$\mathbf{S} = \begin{pmatrix} e^{(+)} & e^{(-)} \end{pmatrix}$$

to diagonalize the matrix A , where $e^{(+)}$ and $e^{(-)}$ are the two eigenvectors of the matrix A :

$$\mathbf{S}^{-1} A \mathbf{S} = \begin{pmatrix} \Lambda & 0 \\ 0 & \Lambda^{-1} \end{pmatrix}.$$

Then there are four possible \tilde{A} s:

$$\begin{aligned} \mathbf{S} \begin{pmatrix} \sqrt{\Lambda} & 0 \\ 0 & \sqrt{\Lambda^{-1}} \end{pmatrix} \mathbf{S}^{-1}, \quad & \mathbf{S} \begin{pmatrix} \sqrt{\Lambda} & 0 \\ 0 & -\sqrt{\Lambda^{-1}} \end{pmatrix} \mathbf{S}^{-1}, \quad (18.304) \\ \mathbf{S} \begin{pmatrix} -\sqrt{\Lambda} & 0 \\ 0 & \sqrt{\Lambda^{-1}} \end{pmatrix} \mathbf{S}^{-1}, \quad & \mathbf{S} \begin{pmatrix} -\sqrt{\Lambda} & 0 \\ 0 & -\sqrt{\Lambda^{-1}} \end{pmatrix} \mathbf{S}^{-1}. \end{aligned}$$

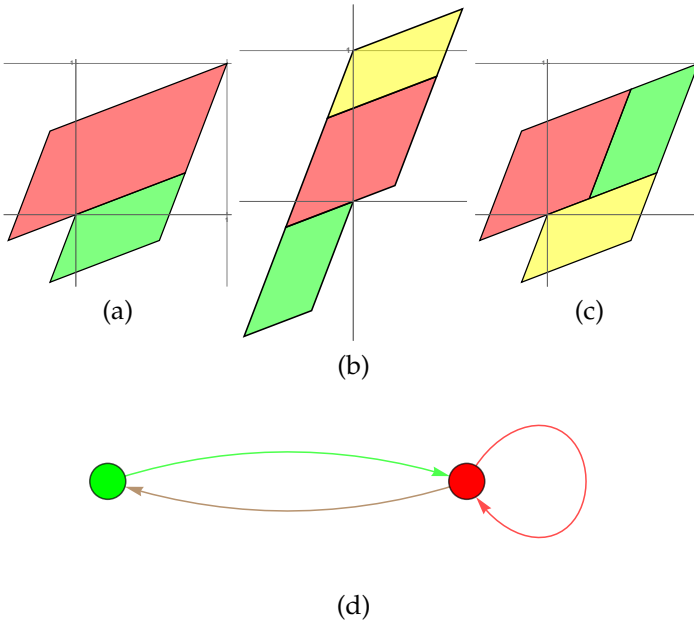


Figure 18.57: (a) An Adler-Weiss generating partition of the unit torus for the golden cat map (1/2 time step map) (5.193), (18.72), the time-reversal reduction of the $s = 3$ or $\mu = 1$ Percival-Vivaldi cat map (1.5) and figure 1.9, with rectangle \mathcal{M}_A (red) and \mathcal{M}_B (green) borders given by the stable and unstable manifolds, i.e., along the two eigenvectors corresponding to the eigenvalues of the matrix $\tilde{\mathbf{C}}$ in (18.72). (b) Mapped one half time-step forward in time, the rectangles are stretched along the unstable direction and shrunk along the stable direction. The eigenvectors are the same as for the Percival-Vivaldi cat map, but eigenvalue $\tilde{\Lambda}$ (5.194) is a square root of the Percival-Vivaldi cat map eigenvalue (1.6), $\Lambda = \tilde{\Lambda}^2$, hence less stretching. (c) As always, the sub-rectangles translated back into the initial partition yield a generating partition, with the finite grammar given by the transition graph (d) of figure 4.2. The nodes refer to the green and red rectangles, and the three links correspond to the three sub-rectangles induced by one forward half time-step.

I found these four solutions for general $s - 2 = \mu^2$:

$$\begin{aligned}
 \tilde{A} &= \begin{pmatrix} a & b \\ c & d \end{pmatrix}, \quad \text{where} \\
 &= \begin{pmatrix} -\mu & -\mu^{-1} \\ -\mu & 0 \end{pmatrix}, \quad \text{negative trace, usually not a solution} \\
 &= \begin{pmatrix} \mu & \mu^{-1} \\ \mu & 0 \end{pmatrix}, \quad \text{and also solutions for which trace } \neq \mu: \\
 a &= -\frac{\mu^2 + 2}{\sqrt{\mu^2 + 4}}, b = -\frac{1}{\sqrt{\mu^2 + 4}}, c = -\frac{\mu^2}{\sqrt{\mu^2 + 4}}, d = -\frac{2}{\mu^2 + 4} \\
 a &= \frac{\mu^2 + 2}{\sqrt{\mu^2 + 4}}, b = \frac{1}{\sqrt{\mu^2 + 4}}, c = \frac{\mu^2}{\sqrt{\mu^2 + 4}}, d = \frac{2}{\mu^2 + 4} \quad (18.305)
 \end{aligned}$$

So only when $s = 3$ or $\mu = 1$ Thom-Arnol'd cat map we can find an integer matrix \tilde{A} .

And we cannot find square root of the Percival-Vivaldi cat map. Solving (18.72):

$$\mathbf{B} = \tilde{\mathbf{C}}^2 = \begin{pmatrix} 0 & 1 \\ -1 & s \end{pmatrix},$$

the four solutions are

$$\begin{aligned}
 \tilde{\mathbf{C}} &= \begin{pmatrix} a & b \\ c & d \end{pmatrix}, \quad \text{where} \\
 a &= \mu^{-1}, b = -\mu^{-1}, c = \mu^{-1}, d = \frac{1-s}{\mu}, \quad \text{negative trace } \mu \\
 a &= -\mu^{-1}, b = \mu^{-1}, c = -\mu^{-1}, d = \frac{s-1}{\mu} \\
 a &= -\frac{1}{\sqrt{\mu^2 + 4}}, b = -\frac{1}{\sqrt{\mu^2 + 4}}, c = \frac{1}{\sqrt{\mu^2 + 4}}, d = \frac{-1-s}{\mu} \\
 a &= \frac{1}{\sqrt{\mu^2 + 4}}, b = \frac{1}{\sqrt{\mu^2 + 4}}, c = -\frac{1}{\sqrt{\mu^2 + 4}}, d = \frac{s+1}{\sqrt{\mu^2 + 4}} \quad (18.306)
 \end{aligned}$$

2021-02-08 Han For me $\mathcal{J} \neq \tilde{\mathcal{J}}^\top \tilde{\mathcal{J}}$. Let

$$\tilde{\mathcal{J}} = \begin{pmatrix} \mu & -1 & 0 & 0 & \dots & 0 & 1 \\ 1 & \mu & -1 & 0 & \dots & 0 & 0 \\ 0 & 1 & \mu & -1 & \dots & 0 & 0 \\ \vdots & \vdots & \vdots & \vdots & \ddots & \vdots & \vdots \\ 0 & 0 & \dots & \dots & \dots & \mu & -1 \\ -1 & 0 & \dots & \dots & \dots & 1 & \mu \end{pmatrix}.$$

Then we have (4.40), and I believe that the determinant $\det \mathcal{J}$ and $\det (\tilde{\mathcal{J}}^\top \tilde{\mathcal{J}})$ are only equal when the period of the lattice state is an odd number.

2021-02-09 Predrag I expect the forward-in-time Jacobian \tilde{J} to be related to the orbit Jacobian matrix $\tilde{\mathcal{J}}$ as in sect. 8.5 *Spatiotemporal cat Hill's formula*. You have explicit orbit Jacobian matrix $\tilde{\mathcal{J}}$ (4.55), so write down the corresponding \tilde{J} acting on 1/2 time-step lattice.

2021-02-12 Han [2021-02-15 Predrag moved this post to the draft of *reversal.tex*, see (4.46).]

2021-02-13 Predrag I think it might be perhaps more informative and easier to survey the symmetries if one lists lattice states by their symbol blocks rather than lattice fields in listings such as (18.292), (18.293), (18.294) and (18.300), as you did for period-4 lattice states (18.14), (18.20) and (18.32).

Note that golden/metal cat number of alphabet letters $\tilde{\mathcal{A}}$ is about \sqrt{c} of the cat map alphabet \mathcal{A} .

2021-02-24 Han I computed the period-6 lattice states of the temporal cat with $s = 3$. Figures 18.58 and 18.59 are the reciprocal lattice states obtained by discrete C_6 irreps diagonalization.

The C_6 group has 4 subgroups, which are **1**, C_2 , C_3 and C_6 . In the space of the irreps of C_6 , the subspace spanned by the $k = 0$ Fourier mode is the subspace of the **1** subgroup. $k = 0$ and $k = 3$ Fourier modes span the subspace of the C_2 subgroup. $k = 0, k = 2$ and $k = 4$ Fourier modes span the subspace of the C_3 subgroup. Using the subspaces of these subgroups, we can divide the lattice states into 4 categories.

The first category includes lattice states that are in the subspace of **1**. We only have 1 lattice state in this category, which is the $\{0, 0, 0, 0, 0, 0\}$.

The second category includes lattice states that are in the subspace of C_2 but not in the subspace of **1**. These lattice states have non-zero components only in the subspace spanned by $k = 0$ and $k = 3$ Fourier modes, as shown in figure 18.58 (a). There are 4 lattice states in this subspace, which are the 2 period-2 orbits and their cyclic permutations.

The third category includes lattice states that are in the subspace of C_3 but not in the subspace of **1**. These lattice states have non-zero components only in the subspace spanned by $k = 0, k = 2$ and $k = 4$ Fourier modes, as shown in figure 18.58 (b). There are 15 lattice states in this category, which are the 5 period-3 orbits and their cyclic permutations.

The last category includes lattice states that are not in the subspace of **1**, C_2 or C_3 . These lattice states are the prime period-6 lattice states, which are not repeats of shorter lattice states. Note that some of these lattice states have 0 component in the $k = 1$ subspace, but they have non-zero components in both the $k = 2$ and $k = 3$ subspaces, so they are not in the subspace of C_2 or C_3 . Figure 18.59 (a) shows the reciprocal lattice states with non-zero $k = 1$ component. Figure 18.59 (b) shows the reciprocal lattice states with zero $k = 1$ component but non-zero $k = 2$ and $k = 3$

components. There are 276 reciprocal lattice states in the Figure 18.59 (a) and 24 lattice states in the Figure 18.59 (b).

To get the number of orbits, we need to count the number of reciprocal lattice states in the fundamental domain. For the reciprocal lattice states with non-zero $k = 1$ component, the fundamental domain contains reciprocal lattice states whose phase of the $k = 1$ component lies in $(-\pi/6, \pi/6]$. For the reciprocal lattice states with zero $k = 1$ component and non-zero $k = 2$ and $k = 3$ components, the fundamental domain contains reciprocal lattice states whose phase of the $k = 2$ component lies in $(-\pi/3, \pi/3]$ and $k = 3$ component lies in $(-\pi/2, \pi/2]$. The reciprocal lattice states in the fundamental domain are shown in figure 18.60. There are 46 reciprocal lattice states in figure 18.60 (a) and 4 reciprocal lattice states in (b). Each one of the them is corresponding to a prime period-6 periodic orbit.

2021-02-24 Han Now we want to find the lattice states that are invariant under reflection. For D_6 there are 6 group elements with reflection. Reflection operators will reflect the reciprocal lattice states over an axis in each one of the subspaces (except for the $k = 0$ subspace, which is the symmetric irrep). Let θ_n be the polar angle of the reflection axis in the subspace of $k = n$. The 6 reflection operators will reflect the subspaces over the axes:

- (1). $\theta_1 = 0, \theta_2 = 0, \theta_3 = 0$.
- (2). $\theta_1 = \pi/6, \theta_2 = \pi/3, \theta_3 = \pi/2$.
- (3). $\theta_1 = \pi/3, \theta_2 = 2\pi/3, \theta_3 = 0$.
- (4). $\theta_1 = \pi/2, \theta_2 = 0, \theta_3 = \pi/2$.
- (5). $\theta_1 = 2\pi/3, \theta_2 = \pi/3, \theta_3 = 0$.
- (6). $\theta_1 = 5\pi/6, \theta_2 = 2\pi/3, \theta_3 = \pi/2$.

If a reciprocal lattice state lies on one set of these axes, then the lattice state is invariant under one of the reflections.

Now check the figure 18.60 (a). The points in $k = 1$ subspace are in the fundamental domain. So we can only have reciprocal lattice states on the first two sets of axes, which are plotted by the green and red lines in the figure.

Figure 18.61 (a) are the reciprocal lattice states that lie on the red axes, $\theta_1 = \pi/6, \theta_2 = \pi/3, \theta_3 = \pi/2$. There are only two orbitss:

$$\frac{1}{8}\{5, 5, 2, 1, 1, 2\}, \quad \frac{1}{8}\{7, 7, 6, 3, 3, 6\}. \quad (18.307)$$

Figure 18.61 (b) are the reciprocal lattice states that lie on the green axes,

$\theta_1 = 0, \theta_2 = 0, \theta_3 = 0$. There are 14 lattice states:

$$\begin{aligned} & \frac{1}{40}\{6, 29, 1, 14, 1, 29\}, \quad \frac{1}{40}\{10, 35, 15, 10, 15, 35\}, \\ & \frac{1}{40}\{14, 21, 9, 6, 9, 21\}, \quad \frac{1}{40}\{18, 27, 23, 2, 23, 27\}, \\ & \frac{1}{40}\{24, 36, 4, 16, 4, 36\}, \quad \frac{1}{40}\{26, 39, 11, 34, 11, 39\}, \\ & \frac{1}{40}\{18, 7, 3, 2, 3, 7\}, \quad \frac{1}{40}\{30, 25, 5, 30, 5, 25\}, \\ & \frac{1}{40}\{32, 28, 12, 8, 12, 28\}, \quad \frac{1}{40}\{34, 31, 19, 26, 19, 31\}, \\ & \frac{1}{40}\{36, 34, 26, 4, 26, 34\}, \quad \frac{1}{40}\{38, 37, 33, 22, 33, 37\}, \\ & \frac{1}{40}\{36, 14, 6, 4, 6, 14\}, \quad \frac{1}{40}\{38, 17, 13, 22, 13, 17\}. \end{aligned} \quad (18.308)$$

The rest 30 reciprocal lattice states are not invariant under time reflection.
There are 15 lattice states:

$$\begin{aligned} & \frac{1}{40}\{18, 17, 33, 2, 13, 37\}, \quad \frac{1}{40}\{20, 25, 15, 20, 5, 35\}, \\ & \frac{1}{40}\{21, 29, 26, 9, 1, 34\}, \quad \frac{1}{40}\{36, 9, 31, 4, 21, 19\}, \\ & \frac{1}{40}\{21, 39, 16, 9, 11, 24\}, \quad \frac{1}{40}\{28, 7, 33, 12, 3, 37\}, \\ & \frac{1}{40}\{32, 18, 22, 8, 2, 38\}, \quad \frac{1}{40}\{28, 17, 23, 12, 13, 27\}, \\ & \frac{1}{40}\{32, 23, 37, 8, 27, 33\}, \quad \frac{1}{40}\{36, 29, 11, 4, 1, 39\}, \\ & \frac{1}{40}\{31, 29, 16, 19, 1, 24\}, \quad \frac{1}{40}\{25, 35, 0, 5, 15, 0\}, \\ & \frac{1}{40}\{31, 39, 6, 19, 11, 14\}, \quad \frac{1}{40}\{32, 3, 17, 8, 7, 13\}, \\ & \frac{1}{40}\{38, 7, 23, 22, 3, 27\}, \end{aligned} \quad (18.309)$$

and their reflections.

In the figure 18.60 (b) there are only 4 reciprocal lattice states. Two of them are on the red and green axes:

$$\frac{1}{20}\{14, 1, 9, 6, 9, 1\}, \quad \frac{1}{20}\{19, 11, 14, 11, 19, 6\}. \quad (18.310)$$

The rest two are:

$$\frac{1}{20}\{17, 3, 12, 13, 7, 8\}, \quad (18.311)$$

and its reflection.

Note that in the figure 18.60 (b), the red axes are $\theta_1 = 2\pi/3$, $\theta_2 = \pi/3$, $\theta_3 = 0$, which are different from the red axes in the figure 18.60 (a).

2021-02-26 Matt They are palindromes.

2021-03-09 Han When we found the lattice states of the golden cat (Fibonacci [5]) in (18.298–18.300), we did not use the time reflection symmetry. That is why lattice states in (18.298) are corresponding to the cat map's lattice states without reflection symmetry. The boundary of the lattice states of golden cat in (18.298) is periodic, not periodic with reflection.

2021-03-10 Predrag Correct. When you quotient a symmetry, the symmetry-reduced map does not have that symmetry. Golden cat is clearly not time-reversal invariant.

2021-03-09 Han We can find the lattice states with reflection symmetry by finding short lattice state with periodic reflection boundary conditions.

Odd period example: a period-5 reflection symmetric lattice states tiles the infinite lattice \mathcal{L} with a reflection-fixed $\boxed{\phi_0}$ and a length-2 block (ϕ_1, ϕ_2) ,

$$\cdots \phi_2 \phi_1 \boxed{\phi_0} \phi_1 \phi_2 | \phi_2 \phi_1 \boxed{\phi_0} \phi_1 \phi_2 | \cdots . \quad (18.312)$$

The boundary conditions are the index 5-periodicity mod 5, and the even reflection across $\boxed{\phi_0}$, or odd reflection after ϕ_2 :

$$\phi_i = \phi_{i+5}, \quad \phi_{-i} = \phi_i.$$

The temporal cat defining equation (3.45)

$$\phi_{t+1} - s_t \phi_t + \phi_{t-1} = -m_t, \quad (18.313)$$

is a length 3 block lattice state condition of form

$$\begin{aligned} -s_0 \phi_0 + 2\phi_1 &= -m_0 \\ \phi_0 - s_2 \phi_1 + \phi_2 &= -m_1, \\ \phi_1 - (s_3 - 1)\phi_2 &= -m_2 \end{aligned} \quad (18.314)$$

Starting with $\boxed{\phi_0}$, followed by the block (ϕ_1, ϕ_2) , yields a 3-dimensional orbit Jacobian matrix \mathcal{J}_+

$$\begin{pmatrix} -s_0 & 2 & 0 \\ 1 & -s_1 & 1 \\ 0 & 1 & -s_2 + 1 \end{pmatrix} = \begin{pmatrix} -s_0 & 1 & 1 \\ 1 & -s_1 & 1 \\ 1 & 1 & -s_2 \end{pmatrix} + \begin{pmatrix} 0 & 1 & -1 \\ 0 & 0 & 0 \\ -1 & 0 & 1 \end{pmatrix} \quad (18.315)$$

where the last matrix is displayed just to indicate the form of the even \square and odd $|$ bc's, and that they only affect the top and the bottom rows. The translational symmetry is broken.

For $s_j = 3$ the determinant of this orbit Jacobian matrix is 11, which counts the number of lattice states that satisfy the reflection symmetry (18.312). There are 10 period-5 lattice state with time reflection symmetry (18.292–18.293), and 1 period-1 lattice state, see table 18.3.

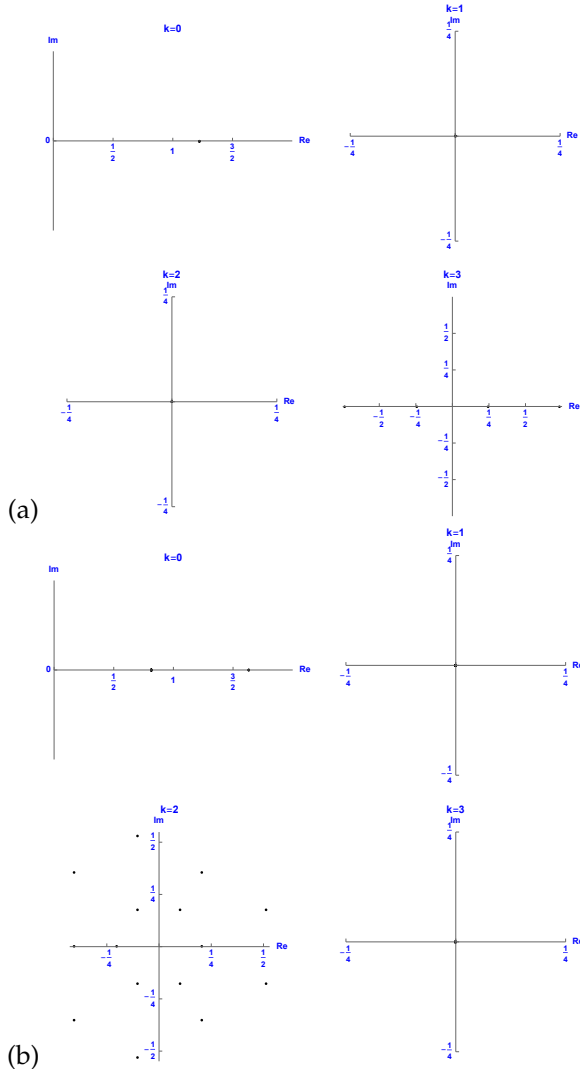


Figure 18.58: The period-6 reciprocal lattice states of the temporal cat with $s = 3$, obtained by discrete C_6 irreps diagonalization. (a) The reciprocal lattice states in the subspace of C_2 , whose components are non-zero only in the $k = 0$ and $k = 3$ subspace. These lattice states are repeats of period-2 lattice states. (b) The reciprocal lattice states in the subspace of C_3 , whose components are non-zero only in the $k = 0$, $k = 2$ and $k = 4$ subspace. These lattice states are repeats of period-3 lattice states.

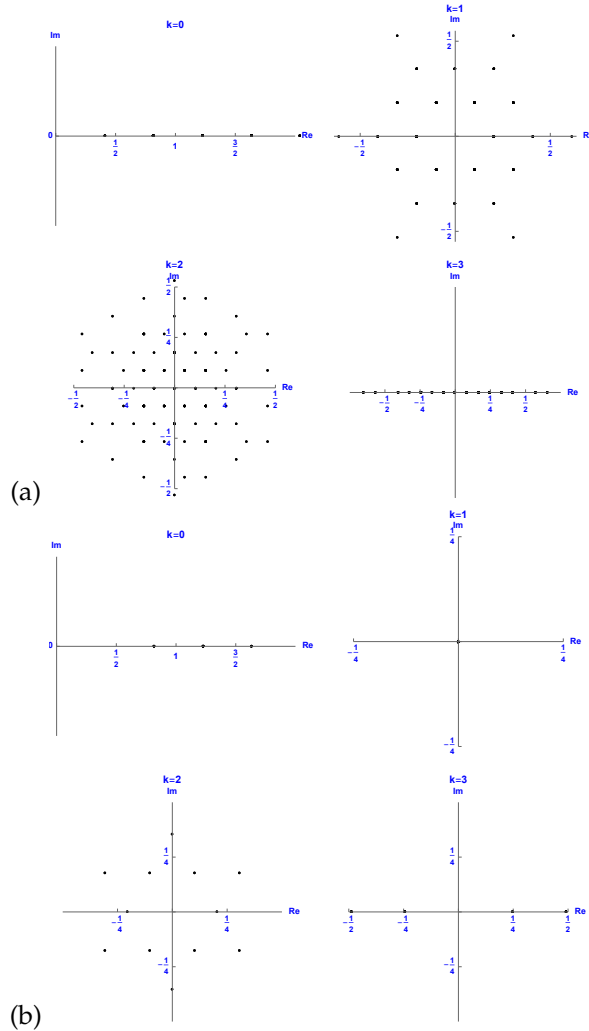


Figure 18.59: The period-6 reciprocal lattice states of the temporal cat with $s = 3$, obtained by discrete C_6 irreps diagonalization. (a) The reciprocal lattice states that are not in the subspace of C_2 or C_3 , which have non-zero component in the $k = 1$ subspace. (b) The reciprocal lattice states that are not in the subspace of C_2 or C_3 , which have zero component in the $k = 1$ subspace and non-zero components in the $k = 2$ and $k = 3$ subspaces.

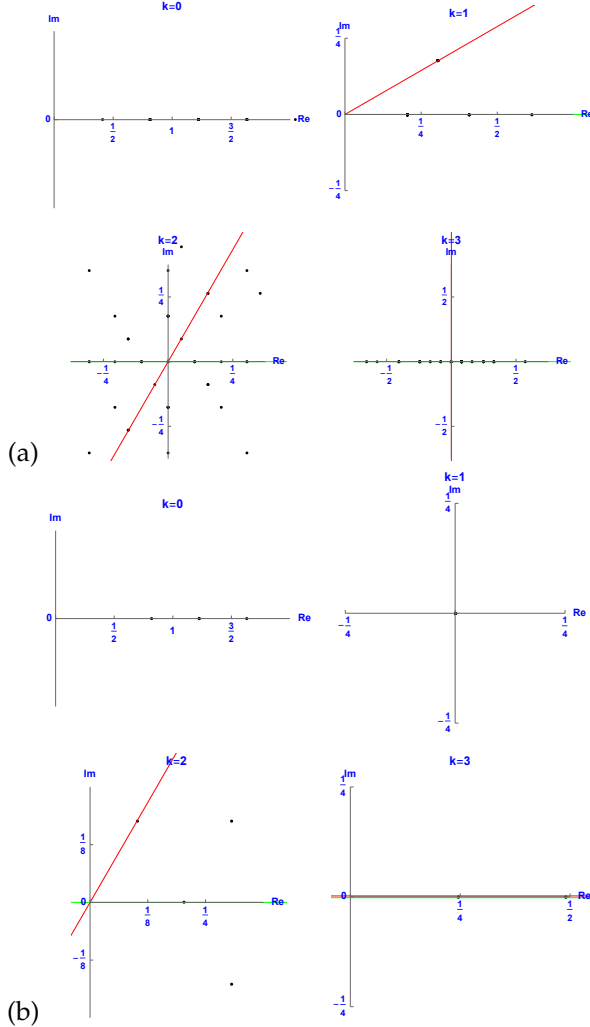


Figure 18.60: The period-6 reciprocal lattice states of the temporal cat with $s = 3$, obtained by discrete C_6 irreps diagonalization. (a) The reciprocal lattice states that are not in the subspace of C_2 or C_3 , which have non-zero component in the $k = 1$ subspace. The symmetry-reduced fundamental domain contain reciprocal lattice states whose phase of the $k = 1$ component lies in $(-\pi/6, \pi/6]$. (b) The reciprocal lattice states that are not in the subspace of C_2 or C_3 , which have zero component in the $k = 1$ subspace and non-zero components in the $k = 2$ and $k = 3$ subspaces. The symmetry-reduced fundamental domain contain reciprocal lattice states whose phase of the $k = 2$ component lies in $(-\pi/3, \pi/3]$, and phase of the $k = 3$ component lies in $(-\pi/2, \pi/2]$. The red and green lines are axes of reflections. For D_n irreps, see the D_3 example figure 3.5.

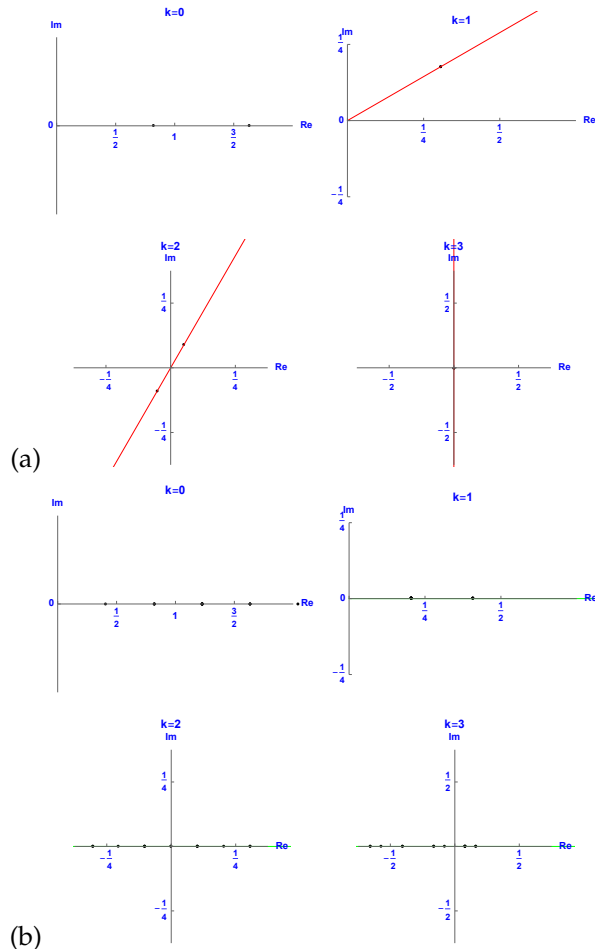


Figure 18.61: (a) The period-6 reciprocal lattice states with non-zero $k = 1$ components, which are in the fundamental domain and on the axes of reflection $\theta_1 = \pi/6, \theta_2 = \pi/3, \theta_3 = \pi/2$ (the red lines). (b) The reciprocal lattice states with non-zero $k = 1$ components, which are in the fundamental domain and on the axes of reflection $\theta_1 = 0, \theta_2 = 0, \theta_3 = 0$ (the green lines). These two sets of reciprocal lattice states are invariant under time reflection.

2021-03-09 Han *Even period, odd reflection* example: the period-6 lattice states with odd reflection symmetry, are tiled by length-3 blocks $\{\phi_0, \phi_2, \phi_2\}$ that tile the infinite lattice as:

$$\dots \phi_2 \phi_2 \phi_0 | \phi_0 \phi_2 \phi_2 | \phi_2 \phi_2 \phi_0 | \phi_0 \phi_2 \phi_2 | \dots , \quad (18.316)$$

Even period, even reflection example: length-4 blocks $\{\phi_0, \phi_2, \phi_3, \phi_4\}$ that tile the infinite lattice as:

$$\dots \phi_3 \phi_2 \boxed{\phi_0} \phi_2 \phi_3 \boxed{\phi_4} \phi_3 \phi_2 \boxed{\phi_0} \phi_2 \phi_3 \boxed{\phi_4} \dots . \quad (18.317)$$

The orbit Jacobian matrix of the period-3 lattice states is:

$$-\mathcal{J} = \begin{pmatrix} s-1 & -1 & 0 \\ -1 & s & -1 \\ 0 & -1 & s-1 \end{pmatrix}. \quad (18.318)$$

The determinant of this orbit Jacobian matrix is 8. The 8 orbits are:

$$\begin{aligned} \phi_{000} &= \{0, 0, 0\}, \\ \phi_{010} &= \frac{1}{4}\{1, 2, 1\}, \phi_{1\underline{1}1} = \frac{1}{2}\{1, 0, 1\}, \phi_{101} = \frac{1}{4}\{3, 2, 3\}, \end{aligned}$$

and

$$\phi_{001} = \frac{1}{8}\{1, 2, 5\}, \phi_{011} = \frac{1}{8}\{3, 6, 7\}, \phi_{100} = \frac{1}{8}\{5, 2, 1\}, \phi_{110} = \frac{1}{8}\{7, 6, 3\}.$$

The 8 lattice states consist of 1 period-1 orbit, 3 period-3 orbits and 4 period-6 lattice states from (18.307). Each invariant lattice state in (18.307) appears twice because we haven't quotiented the time translation symmetry.

The orbit Jacobian matrix of the period-4 lattice states is:

$$-\mathcal{J} = \begin{pmatrix} s & -2 & 0 & 0 \\ -1 & s & -1 & 0 \\ 0 & -1 & s & -1 \\ 0 & 0 & -2 & s \end{pmatrix}. \quad (18.319)$$

For $s = 3$ the determinant of this orbit Jacobian matrix is 40. The 40 lattice states include: 1 period-1 orbit,

$$\phi_0 = \{0\},$$

2 period-2 orbits, corresponding to 4 lattice states:

$$\phi_{\underline{1}2} = \frac{1}{5}\{1, 4\}, \phi_{01} = \frac{1}{5}\{2, 3\},$$

3 period-3 orbits, 9 lattice states in all ¹⁸

$$\phi_{\underline{1}11} = \frac{1}{2}\{0, 1, 1\}, \phi_{011} = \frac{1}{4}\{2, 3, 3\}, \phi_{100} = \frac{1}{4}\{2, 1, 1\},$$

and 16 period-6 orbits from (18.308) and (18.310), each one of which appears twice.

2021-03-09 Han Finding the lattice states with reflection symmetry by setting the boundary conditions with reflection is not efficient, because it becomes harder to separate shorter orbits from the long prime orbits.

Perhaps the smarter way is to still use the periodic boundary conditions and only use the Fourier modes with the reflection symmetries that we need.

The eigenvectors of the orbit Jacobian matrix (18.319) are:

$$\begin{aligned} \mathbf{e}_0 &= (1, 1, 1, 1), \mathbf{e}_1 = (1, 1/2, -1/2, -1), \\ \mathbf{e}_2 &= (1, -1/2, -1/2, 1), \mathbf{e}_3 = (1, -1, 1, -1), \end{aligned} \quad (18.320)$$

with eigenvalues:

$$\lambda_0 = 1, \lambda_1 = 2, \lambda_2 = 4, \lambda_3 = 5.$$

The k th component of the j th eigenvector is:

$$\mathbf{e}_{jk} = \cos\left(\frac{\pi}{3}jk\right). \quad (18.321)$$

Compare with [ChaosBook eq. \(A24.25\)](#) notation; for period-6

$$\mathbf{e}_k^{(j)} = \cos\left(\frac{2\pi}{6}jk\right). \quad (18.322)$$

The eigenvalue of the j th eigenvector is:

$$\lambda_j = s - 2 \cos\left[\frac{2\pi}{6}(j-1)\right]. \quad (18.323)$$

Comparing the eigenvectors of the orbit Jacobian matrix of the period-6 cat map with periodic boundary condition, with the eigenvectors in (18.320), we can see that the eigenvectors in (18.320) are given by the first 4 components of the cosine basis vectors, which are the eigenvectors of the period-6 orbit Jacobian matrix with periodic boundary condition and reflection symmetry.

2021-03-10 Predrag This discussion reminds me of Baake *et al.* 1997 paper [4] *The torus parametrization of quasiperiodic LI-classes* ([click here](#)), sect. 2.3 *Symmetry*. Note the factorization of orbit Jacobian matrix, their eq. (11) (enter what you learn from that paper into sect. 4.3.3 - remember, it's the only one we found that introduces 1/2 unit length lattice). Have no feeling whether we are to worry about their 'inflation'.

¹⁸Predrag 2021-03-10: I shortened these to period 3

2021-03-10 Predrag Boring remarks, but easiest to be consistent in the notation early on, so do not have to fix these later:

Remember, discrete Fourier modes are always counted starting with zero, $k = 0, 1, \dots, n-1$, see [ChaosBook eq. \(A24.32\)](#). The constant eigenvector in (18.320) is always $\mathbf{e}^{(0)} = (1, 1, 1, 1)$ (why have you gone to curly vector $= \{\dots\}$ notation?), and you avoid the awkward $(j-1)(k-1)$ in (18.321), (18.323).

Please fix that throughout your blog, so I do not have to waste time on that.

2021-03-10 Predrag For D_n irreps, I think we should use the (4.43) form of eigenvalues, and Klein-Gordon mass μ

$$\begin{aligned}\lambda_m &= \mu^2 + 4 \sin^2(\alpha_m/2) \\ &= \left(\mu - i 2 \sin\left(\frac{\alpha_m}{2}\right)\right) \left(\mu + i 2 \sin\left(\frac{\alpha_m}{2}\right)\right) \\ \alpha_m &= 2\pi m/n,\end{aligned}\tag{18.324}$$

rather than (18.323) and stretching s , which is appropriate to C_n irreps. Identities like (13.5), (18.191), (13.90) and Gradshteyn and Ryzhik [28] Eq. 1.317.1 ([click here](#))

$$2 \sin^2(\theta/2) = 1 - \cos(\theta)\tag{18.325}$$

are also suggestive in this context.

2021-03-10 Predrag In time evolution setting, it's important for me to distinguish Floquet multipliers Λ , see [ChaosBook eq. \(4.8\)](#) from Floquet exponents λ , see [ChaosBook eq. \(5.4\)](#). So I suspect for orbit Jacobian matrix we want to use Λ_j in formulas such as (18.323). But I'm not sure, have not thought that through yet...

2021-03-10 Predrag to Han Grava, Kriecherbauer, Mazzuca and McLaughlin [29] *Correlation functions for a chain of short range oscillators*, [arXiv:2010.09612](#) (enter your notes into sect. 4.3.1) is interesting for us. The setting is N -body, coupled harmonically to neighbors up to a finite distance m away, i.e., period N 1-dimensional discrete spatial lattice, continuous in time, see (4.92). Our problem corresponds essentially their spatial eigenstates (we still seem to be only ones that are thinking of this for a temporal lattice).

1. Like us in (4.40), they construct a '*localized square root*' (4.95)
2. Trigonometric relations like (4.43) and functional factorizations are a result from 1915, known as Fejér and Riesz [54, pg. 117 f] lemma (4.102), (4.105).
3. Do you understand what to they gain by (4.98) going from half- m -physical vector to m -physical vector?

4. They seem to separate the symmetric and antisymmetric subspaces in the Hamiltonian formulation (4.110).
5. Hénon system must be some version of their nonlinear system (4.111), with the cubic nonlinearity $\chi \neq 0$.
6. They only do the harmonic $s = 2, \mu = 1$ case.
7. I have not yet seen any papers that do this for the discrete temporal lattice.

2021-03-23 Han Following the method used in Grava, Kriecherbauer, Mazzuca and McLaughlin [29], we first write the "Hamiltonian" form of the cat map:

$$\begin{bmatrix} q_{t+1} \\ p_{t+1} \end{bmatrix} = \begin{bmatrix} s-1 & 1 \\ s-2 & 1 \end{bmatrix} \begin{bmatrix} q_t \\ p_t \end{bmatrix} \pmod{1}.$$

Define $\dot{q}_t \equiv q_t - q_{t-1}$ and $\dot{p}_t \equiv p_{t+1} - p_t$. We have:

$$\begin{cases} \dot{q}_t = p_t = \frac{\partial H}{\partial p_t}, \\ \dot{p}_t = (s-2)q_t = -\frac{\partial H}{\partial q_t}, \end{cases} \quad (18.326)$$

then the Hamiltonian of cat map is:

$$H_t = \frac{1}{2}p_t^2 - \frac{1}{2}(s-2)q_t^2. \quad (18.327)$$

The coefficient of the q_t^2 term is negative because this is a kicked rotor. If the coefficient of the q_t^2 term is positive then this will become a harmonic oscillator.

2021-03-24 Han Note that I defined $\dot{p}_t \equiv p_{t+1} - p_t$ instead of $p_t - p_{t-1}$, because otherwise I cannot find a Hamiltonian that satisfies the Hamilton's equations (18.326).

2021-03-24 Han By factorizing the matrix generated by the m -physical vector (4.91) into the matrix generated by the half- m -physical vector (4.95), they rewrote the Hamiltonian into a sum of a set of local Hamiltonian:

$$e_j = \frac{1}{2}p_j^2 + \frac{1}{2}r_j^2.$$

2021-03-24 Han To reverse time in the phase space $\{q_t, p_t\}$, we need to use the time-reversal operator:

$$T = \begin{bmatrix} 1 & 0 \\ 2-s & -1 \end{bmatrix}. \quad (18.328)$$

This operator satisfies:

$$TT = \begin{bmatrix} 1 & 0 \\ 0 & 1 \end{bmatrix},$$

and

$$T A T = A^{-1},$$

where

$$A = \begin{bmatrix} s-1 & 1 \\ s-2 & 1 \end{bmatrix}.$$

But if we write the Hamiltonian as:

$$H_t = \frac{1}{2} \mathbf{x}^\top H \mathbf{x},$$

where

$$\mathbf{x} = \begin{bmatrix} q_t \\ p_t \end{bmatrix}$$

and

$$H = \begin{bmatrix} -(s-2) & 0 \\ 0 & 1 \end{bmatrix},$$

we will find that $[T, H] \neq 0\dots$

2021-03-25 Predrag This T is one of the two involutions but you are right, they do not commute.

2021-03-25 Predrag Re. $\dot{p}_t \equiv p_{t+1} - p_t$ convention you mention above, I understand. One always has to be explicit about how you define lattice derivatives: forward/backward difference operators, see (5.103), (5.104) or centered, reflection (anti)symmetric difference operators (5.106), that we use in (4.38). Bolotin and Treschev [13] eq. (2.5) discuss this at length, see their symmetric generating function $L(q_t, q_{t+1})$ defined in (5.84), and the discussion and references in that part of the blog. These just coordinate changes, should not effect any invariant quantities, like what solutions exist, of what stabilities they have.

2021-03-26 Predrag I'm frustrated not to see a clear connection between the discrete time-reflection symmetry and zeta function factorization (4.177), if there is any.¹⁹ How about this: You have verified factorizations such as (4.44). You know $|\det \mathcal{J}| = |\det (\hat{\mathbf{1}}_1 - \hat{\mathbf{J}}_p)|$ from (8.38).

Can you use $|\det \mathcal{J}_\pm| = |\det (\hat{\mathbf{1}}_1 - \hat{\mathbf{J}}_{\pm,p})|$ to reverse engineer the Hamiltonian for each subspace, and explain how the time reversal relates the two (three) Hamiltonians?

2021-03-26 Han We can use the product formula (4.268) to check if the factorization (4.183) is given by the time-reversal symmetry.

An orbit p with length n_p will contribute to the zeta function as:

$$\begin{aligned} \mathcal{H}_p = \{e\} : \quad (1 - z^{n_p})^2 &= (1 - z^{n_p})(1 - z^{n_p}) \\ \mathcal{H}_p = \{e, r\} : \quad (1 - z^{n_p}) &= (1 - z^{n_p/2})(1 + z^{n_p/2}). \end{aligned} \quad (18.329)$$

¹⁹Predrag 2021-03-25: Have you ever checked whether my factorization (4.177) is correct?

n	1	2	3	4	5	6
N_n	1	5	16	45	121	320
M_n	1	2	5	10	24	50
\tilde{M}_n	1	2	3	6	10	18

Table 18.1: Lattice states and orbit counts for the $s = 3$ cat map. \tilde{M}_n is the number of prime orbits with length n that are invariant under time reflection.

We know the number of prime orbits of the cat map with $s = 3$, and the number of prime orbits that are invariant under time reflection up to length 6 (table 18.1).

Let $z = t^2$. The zeta functions factorized by the time-reversal symmetry are:

$$\begin{aligned} 1/\zeta_{A_1} &= (1-t)(1-t^2)^2(1-t^3)^3(1-t^6)(1-t^4)^6(1-t^8)^2 \\ &\quad (1-t^5)^{10}(1-t^{10})^7(1-t^6)^{18}(1-t^{12})^{16}\dots \\ &= 1 - t - 2t^2 - t^3 - 2t^4 + t^5 + 39t^7 + 34t^8 + t^9 - 38t^{10} + O(t^{11}), \end{aligned} \quad (18.330)$$

$$\begin{aligned} 1/\zeta_{A_2} &= (1+t)(1+t^2)^2(1+t^3)^3(1-t^6)(1+t^4)^6(1-t^8)^2 \\ &\quad (1+t^5)^{10}(1-t^{10})^7(1+t^6)^{18}(1-t^{12})^{16}\dots \\ &= 1 + t + 2t^2 + 5t^3 + 10t^4 + 23t^5 + 48t^6 \\ &\quad + 73t^7 + 130t^8 + 247t^9 + 422t^{10} + O(t^{11}). \end{aligned} \quad (18.331)$$

And the zeta functions from (4.183) are:

$$\begin{aligned} 1/\zeta_- &= \frac{1-t-t^2}{1-t^2} \\ &= 1 - t - t^3 - t^5 - t^7 - t^9 + O(t^{11}), \end{aligned} \quad (18.332)$$

$$\begin{aligned} 1/\zeta_+ &= \frac{1+t-t^2}{1-t^2} \\ &= 1 + t + t^3 + t^5 + t^7 + t^9 + O(t^{11}). \end{aligned} \quad (18.333)$$

These two factorizations are both correct if we expand their product:

$$\frac{1}{\zeta_{A_1}} \frac{1}{\zeta_{A_2}} = 1 - t^2 - 2t^4 - 3t^6 - 4t^8 - 5t^{10} + O(t^{11}),$$

$$\frac{1}{\zeta_-} \frac{1}{\zeta_+} = 1 - t^2 - 2t^4 - 3t^6 - 4t^8 - 5t^{10} + O(t^{11}).$$

So the factorization of (4.183) is correct but it is not factorized by the time reversal symmetry. But the factorization (18.329) may be wrong because I did not treat the boundary orbits correctly...

2021-04-09 Han (Continuation of (18.315), (18.318) and (18.319).)

The numbers of lattice states self-dual under time reversal are given by the Hill determinants of the orbit Jacobian matrix with the reflection-symmetric boundary conditions (18.336), (18.335), and (18.334), corresponding to (2.32), (2.33) and (2.36).

When the period $n = 2m - 1$ of the orbit is odd, there is only one kind of reflection boundary condition:

$$\overline{|\phi_0| \phi_1 \phi_2 \cdots \phi_m | \phi_m \cdots \phi_2 \phi_1|}. \quad (18.334)$$

This period $2m - 1$ lattice state has the $[n \times n]$ orbit Jacobian matrix:

$$\mathcal{J} = \begin{pmatrix} s & -2 & 0 & 0 & \dots & 0 & 0 \\ -1 & s & -1 & 0 & \dots & 0 & 0 \\ 0 & -1 & s & -1 & \dots & 0 & 0 \\ \vdots & \vdots & \vdots & \vdots & \ddots & \vdots & \vdots \\ 0 & 0 & \dots & \dots & \dots & s & -1 \\ 0 & 0 & \dots & \dots & \dots & -1 & s-1 \end{pmatrix}.$$

The Hill determinant of this orbit Jacobian matrix is:

$$|\det \mathcal{J}| = \prod_{j=0}^{n-1} \left[s - 2 \cos\left(\frac{2\pi j}{2n-1}\right) \right].$$

An example is period-5 orbit (18.315).

When the period of the orbit is even, $n = 2m$ there are two kinds of boundary conditions with reflection symmetry.

The first kind of boundary condition is:

$$\overline{\phi_1 \phi_2 \phi_3 \cdots \phi_m | \phi_m \cdots \phi_2 \phi_1|}. \quad (18.335)$$

The $[n \times n]$ orbit Jacobian matrix is:

$$\mathcal{J} = \begin{pmatrix} s-1 & -1 & 0 & 0 & \dots & 0 & 0 \\ -1 & s & -1 & 0 & \dots & 0 & 0 \\ 0 & -1 & s & -1 & \dots & 0 & 0 \\ \vdots & \vdots & \vdots & \vdots & \ddots & \vdots & \vdots \\ 0 & 0 & \dots & \dots & \dots & s & -1 \\ 0 & 0 & \dots & \dots & \dots & -1 & s-1 \end{pmatrix}.$$

The determinant of this orbit Jacobian matrix is:

$$|\det \mathcal{J}| = \prod_{j=0}^{n-1} \left[s - 2 \cos\left(\frac{2\pi j}{2n}\right) \right].$$

The second kind of boundary condition is:

$$\overline{\phi_0\phi_1\phi_2 \cdots \phi_{m-1}\phi_m\phi_{m-1} \cdots \phi_2\phi_1}. \quad (18.336)$$

Each $\overline{\phi_1\phi_2 \cdots \phi_{n-1}\phi_n\phi_{n+1}}$ corresponds to a period- $2n$ lattice state. The $[(n+1) \times (n+1)]$ orbit Jacobian matrix is:

$$\mathcal{J} = \begin{pmatrix} s & -2 & 0 & 0 & \dots & 0 & 0 \\ -1 & s & -1 & 0 & \dots & 0 & 0 \\ 0 & -1 & s & -1 & \dots & 0 & 0 \\ \vdots & \vdots & \vdots & \vdots & \ddots & \vdots & \vdots \\ 0 & 0 & \dots & \dots & \dots & s & -1 \\ 0 & 0 & \dots & \dots & \dots & -2 & s \end{pmatrix},$$

with Hill determinant

$$\begin{aligned} |\det \mathcal{J}| &= \prod_{j=0}^n [s - 2 \cos \alpha_j], \quad \alpha_j = 2\pi j / 2n \quad (18.337) \\ &= \prod_{j=0}^n (\mu + e^{i\alpha_j/2} - e^{-i\alpha_j/2}) (\mu + e^{i\alpha_j/2} - e^{-i\alpha_j/2})^*. \end{aligned}$$

where we have replaced $(s - 2 \cos \alpha)$ by $(\mu^2 + 4 \sin^2(\alpha/2))$, in the (4.43) time-reversal spirit.

The above Hill determinants count the number of lattice states that have time reversal symmetry.

In order to compare with Gallas [27] (a step not needed for our calculations): his orbits with time reversal symmetry are categorized into two classes: diagonal class and non-diagonal class. For orbits with even period, the diagonal class orbits satisfy the boundary condition (18.335), and the non-diagonal class orbits satisfy the boundary condition (18.336).

Let A_n be the number of lattice states with period n that satisfy the boundary condition (18.334) if n is odd and the boundary condition (18.335) if n is even. And let Q_n be the number of lattice states with period n that satisfy the boundary condition (18.334) if n is odd and the boundary condition (18.336) if n is even.

$$A_n = \begin{cases} \prod_{j=0}^{\frac{n-1}{2}} \left[s - 2 \cos \left(\frac{2\pi j}{n} \right) \right], & n \text{ is odd,} \\ \prod_{j=0}^{\frac{n}{2}-1} \left[s - 2 \cos \left(\frac{2\pi j}{n} \right) \right], & n \text{ is even.} \end{cases}$$

n	1	2	3	4	5	6	7	8	9	10	11
D_n	1	0	3	1	10	2	28	9	72	22	198
N_n	0	2	0	5	0	16	0	45	0	130	0

Table 18.2: Time reversal symmetric prime orbit counts for the $s = 3$ cat map. D_n is the number of symmetric orbits with points on the diagonal in the state space. N_n is the number of symmetric orbits without points on the diagonal.

$$Q_n = \begin{cases} \prod_{j=0}^{\frac{n-1}{2}} \left[s - 2 \cos\left(\frac{2\pi j}{n}\right) \right], & n \text{ is odd}, \\ \prod_{j=0}^{\frac{n}{2}} \left[s - 2 \cos\left(\frac{2\pi j}{n}\right) \right], & n \text{ is even}. \end{cases}$$

Now let D_n be the number of orbits with period n that satisfy the boundary condition (18.334) if n is odd and (18.335) if n is even. And N_n is the number of orbits with period n that satisfy the boundary condition (18.334) if n is odd and (18.336) if n is even. Then we have the relation:

$$A_n = \sum_{d|n} a_n D_n,$$

$$Q_n = \sum_{d|n} a_n N_n,$$

where

$$a_n = \begin{cases} 1, & n \text{ is odd}, \\ 2, & n \text{ is even}. \end{cases}$$

We can use the Möbius inversion formula to compute the number of the orbits with the time reversal symmetry:

$$D_n = \frac{1}{a_n} \sum_{d|n} \mu\left(\frac{n}{d}\right) A_n,$$

$$N_n = \frac{1}{a_n} \sum_{d|n} \mu\left(\frac{n}{d}\right) Q_n,$$

where $\mu(n)$ is the Möbius function. Note that using these formulas we will have $D_n = N_n$ if n is odd. In Gallas [27], by definition $N_n = 0$ if n is odd. Set $N_n = 0$ for odd n . The number of orbits with time reversal symmetry is shown in table 18.2.

2021-04-13 Han Let $A : (x, y) \rightarrow (x', y')$ be the cat map with $s = 3$:

$$A \begin{bmatrix} x \\ y \end{bmatrix} = \begin{bmatrix} 0 & 1 \\ -1 & 3 \end{bmatrix} \begin{bmatrix} x \\ y \end{bmatrix} \pmod{1}.$$

And T is the time reflection:

$$T \begin{bmatrix} x \\ y \end{bmatrix} = \begin{bmatrix} 0 & 1 \\ 1 & 0 \end{bmatrix} \begin{bmatrix} x \\ y \end{bmatrix}.$$

Fixed points of T satisfy:

$$x = y.$$

Fixed points of $A \circ T$ satisfy:

$$A \circ T \begin{bmatrix} x \\ y \end{bmatrix} = \begin{bmatrix} 1 & 0 \\ 3 & -1 \end{bmatrix} \begin{bmatrix} x \\ y \end{bmatrix} \pmod{1} = \begin{bmatrix} x \\ y \end{bmatrix},$$

which can be written as:

$$3x - 2y \pmod{1} = 0.$$

For time reversal symmetric periodic orbits with odd period, each orbit has one point on the $\text{Fix}(AT)$ and one point on the $\text{Fix}(T)$. If the period is $2n + 1$ and (ϕ_0, ϕ_1) is on $\text{Fix}(AT)$, then (ϕ_n, ϕ_{n+1}) is on $\text{Fix}(T)$. So we have:

$$3\phi_0 - 2\phi_1 \pmod{1} = 0,$$

and

$$A^n \begin{bmatrix} \phi_0 \\ \phi_1 \end{bmatrix} = \begin{bmatrix} \phi_n \\ \phi_{n+1} \end{bmatrix}.$$

A^n is:

$$A^n \begin{bmatrix} x \\ y \end{bmatrix} = \begin{bmatrix} \frac{2^{-n+1}[(3-\sqrt{5})^{n-1}-(3+\sqrt{5})^{n-1}]}{\sqrt{5}} & \frac{2^{-n}[-(3-\sqrt{5})^n+(3+\sqrt{5})^n]}{\sqrt{5}} \\ \frac{2^{-n}[(3-\sqrt{5})^n-(3+\sqrt{5})^n]}{\sqrt{5}} & \frac{2^{-n-1}[-(3-\sqrt{5})^{n+1}+(3+\sqrt{5})^{n+1}]}{\sqrt{5}} \end{bmatrix} \begin{bmatrix} x \\ y \end{bmatrix} \pmod{1}.$$

For example, if $n = 4$ and the period of the orbit is $2n + 1 = 9$, we have:

$$A^4 \begin{bmatrix} \phi_0 \\ \phi_1 \end{bmatrix} = \begin{bmatrix} -8 & 21 \\ -21 & 55 \end{bmatrix} \begin{bmatrix} \phi_0 \\ \phi_1 \end{bmatrix} \pmod{1} = \begin{bmatrix} \phi_n \\ \phi_{n+1} \end{bmatrix},$$

which can be written as:

$$-13\phi_0 + 34\phi_1 \pmod{1} = 0.$$

So we have:

$$\begin{bmatrix} 3 & -2 \\ -13 & 34 \end{bmatrix} \begin{bmatrix} \phi_0 \\ \phi_1 \end{bmatrix} \pmod{1} = 0.$$

Then the number of periodic points on the $\text{Fix}(AT)$ is given by the determinant:

$$\left| \det \begin{bmatrix} 3 & -2 \\ -13 & 34 \end{bmatrix} \right| = 76.$$

When the period of the orbit is even, each orbit has two points on $\text{Fix}(AT)$ and none on $\text{Fix}(T)$, or two points on $\text{Fix}(T)$ and none on $\text{Fix}(AT)$. For example, if the period is 10, when the orbits have no point on $\text{Fix}(AT)$, we have:

$$\phi_0 = \phi_1,$$

and

$$A^5 \begin{bmatrix} \phi_0 \\ \phi_1 \end{bmatrix} \pmod{1} = \begin{bmatrix} -21 & 55 \\ -55 & 144 \end{bmatrix} \begin{bmatrix} \phi_0 \\ \phi_1 \end{bmatrix} \pmod{1} = \begin{bmatrix} \phi_n \\ \phi_n \end{bmatrix}.$$

Then the periodic point (ϕ_0, ϕ_1) satisfies:

$$\begin{bmatrix} 1 & -1 \\ -34 & 89 \end{bmatrix} \begin{bmatrix} \phi_0 \\ \phi_1 \end{bmatrix} \pmod{1} = 0.$$

So the number of points on the $\text{Fix}(T)$ is:

$$\left| \det \begin{bmatrix} 1 & -1 \\ -34 & 89 \end{bmatrix} \right| = 55.$$

When the orbits have no periodic point on $\text{Fix}(T)$, we have:

$$3\phi_0 - 2\phi_1 \pmod{1} = 0,$$

and

$$A^5 \begin{bmatrix} \phi_0 \\ \phi_1 \end{bmatrix} \pmod{1} = \begin{bmatrix} -21 & 55 \\ -55 & 144 \end{bmatrix} \begin{bmatrix} \phi_0 \\ \phi_1 \end{bmatrix} \pmod{1} = \begin{bmatrix} \phi_n \\ \phi_{n+1} \end{bmatrix},$$

where

$$3\phi_n - 2\phi_{n+1} \pmod{1} = 0.$$

So we have:

$$\begin{bmatrix} 3 & -2 \\ 47 & -123 \end{bmatrix} \begin{bmatrix} \phi_0 \\ \phi_1 \end{bmatrix} \pmod{1} = 0.$$

$$\left| \det \begin{bmatrix} 3 & -2 \\ 47 & -123 \end{bmatrix} \right| = 275.$$

Using the number of periodic points on $\text{Fix}(T)$ and $\text{Fix}(AT)$ we can count the number of orbits. The result is shown in table 18.3.

2021-04-13 Predrag Pozrikidis [53] *An introduction to grids, graphs, and networks*, ([click here](#)) has a clear discussion of various boundary conditions, (see some of my clippings around (5.286), but it is better to check out the book). For an example of *Dirichlet boundary conditions* orbit Jacobian matrix $-\mathcal{J}$ (1.40). See also antiperiodic sum (1.51).

2021-04-13 Predrag My problems with bc's approaches is they are a natural starting point, but they do not scale up. At all. Even for the 3-disk pinball you start by thinking of symmetry axes as mirrors, but then what do you do with the 2-dimensional irreps? Hill's formula $\det H = \det(1 - J_p)$ for the periodic case.

n	F_n	C_n	SF_n	SC_n
1	1	1	1	1
2	5	2	1 5	0 2
3	16	5	4	3
4	45	10	3 15	1 5
5	121	24	11	10
6	320	50	8 40	2 16
7	841	120	29	28
8	2205	270	21 105	9 45
9	5776	640	76	72
10	15125	1500	55 275	22 130

Table 18.3: F_n is the number of lattice states with period n . C_n is the number of periodic orbits with period n . SF_n is the number of symmetric fixed points of A^n on $\text{Fix}(T)$ for odd n , and on $\text{Fix}(T)$, $\text{Fix}(AT)$ for even n . SC_n is the number of symmetric orbits with periodic points on $\text{Fix}(T)$ for odd n , and on $\text{Fix}(T)$, $\text{Fix}(AT)$ for even n . The notations are same as the notations used in Table 1.2.3.5.1 of MacKay's thesis [41].

2021-05-11 Han The product of eigenvalues of the antisymmetric eigenvectors of the orbit Jacobian matrix does count the number of antisymmetric lattice states.

For example, if the period of the lattice states is 6, we have two kinds of reflections. If the lattice state is antisymmetric under reflection over half lattice sites, the antisymmetric subspace is 3-dimensional. And the lattice state tiles the infinite lattice as:

$$\overline{\phi_1 \phi_2 \phi_3 | \underline{\phi_3} \underline{\phi_2} \underline{\phi_1}} = \dots \underline{\phi_3} \underline{\phi_2} \underline{\phi_1} | \phi_1 \phi_2 \phi_3 | \underline{\phi_3} \underline{\phi_2} \underline{\phi_1} | \phi_1 \phi_2 \phi_3 \dots , \quad (18.338)$$

where the underline means negative.

The orbit Jacobian matrix in the 3-dimensional antisymmetric subspace is:

$$\mathcal{J} = \begin{bmatrix} s+1 & -1 & 0 \\ -1 & s & -1 \\ 0 & -1 & s+1 \end{bmatrix} .$$

The eigenvalues of this orbit Jacobian matrix in the 3-dimensional anti-symmetric subspace are $s-1$, $s+1$ and $s+2$, which are the eigenvalues of the antisymmetric eigenvectors of the orbit Jacobian matrix in the full space.

If the lattice state is antisymmetric under reflection over integer lattice sites, the antisymmetric subspace is 2-dimensional. The lattice state tiles the infinite lattice as:

$$\overline{0 | \phi_1 \phi_2 | \underline{\phi_3} \underline{\phi_2} \overline{0}} = \dots \underline{\phi_2} \underline{\phi_1} \overline{0} | \phi_1 \phi_2 \overline{0} | \underline{\phi_2} \underline{\phi_1} \overline{0} | \phi_1 \phi_2 \dots , \quad (18.339)$$

The orbit Jacobian matrix in the 2-dimensional antisymmetric subspace is:

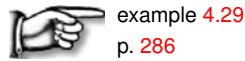
$$\mathcal{J} = \begin{bmatrix} s & -1 \\ -1 & s \end{bmatrix}.$$

The eigenvalues of this orbit Jacobian matrix in the 2-dimensional anti-symmetric subspace are $s - 1, s + 1$, which are the eigenvalues of the antisymmetric eigenvectors of the orbit Jacobian matrix in the full space.

2021-06-13 Predrag I think I'm starting to understand *Máo Zhǔxí Yǔlù*. The 3 types of D_∞ symmetric states X are -well- symmetric, and that means that the number $\sim m$ of distinct fields that describe the corresponding period- n Bravais cell is $\sim n/2$. They satisfy non-periodic bc's equations such as (3.168).

2021-06-13 Predrag That block-diagonalizes into eigenvectors that *point within* the symmetry subspace of the same symmetry as the lattice state, and the (antisymmetric) rest, that *point out of* it. That's all as it should be for a fixed point with a symmetry.

2021-05-11 Han To write the orbit Jacobian matrix in the reflection symmetric or antisymmetric subspace, we can use the projection operators.



To get the orbit Jacobian matrix in the antisymmetric subspace, we can project the orbit Jacobian matrix of the full space into the antisymmetric subspace:

$$\mathcal{J}P_{R^-} = \frac{1}{2} \begin{bmatrix} s+1 & -1 & 0 & 0 & 1 & -s-1 \\ -1 & s & -1 & 1 & -s & 1 \\ 0 & -1 & s+1 & -s-1 & 1 & 0 \\ 0 & 1 & -s-1 & s+1 & -1 & 0 \\ 1 & -s & 1 & -1 & s & -1 \\ -s-1 & 1 & 0 & 0 & -1 & s+1 \end{bmatrix},$$

$$\mathcal{J}P_{rR^-} = \frac{1}{2} \begin{bmatrix} 0 & 0 & 0 & 0 & 0 & 0 \\ 0 & s & -1 & 0 & 1 & -s \\ 0 & -1 & s & 0 & -s & 1 \\ 0 & 0 & 0 & 0 & 0 & 0 \\ 0 & 1 & -s & 0 & s & -1 \\ 0 & -s & 1 & 0 & -1 & s \end{bmatrix}.$$

And the orbit Jacobian matrix of the antisymmetric subspace can be found in the top left blocks of $\mathcal{J}P_{R^-}$ and $\mathcal{J}P_{rR^-}$.

2021-06-01 Han I'm still not able to use the number of symmetric lattice states from table 18.3 to compute the factor of the topological zeta function which is corresponding to the symmetric orbits.

Remember that for the number of the periodic points N_n , we have:

$$z^n N_n = \sum_{n_p|n} n_p t_p^{\frac{n}{n_p}} = \sum_p n_p \sum_{r=1}^{\infty} \delta_{n,rn_p} t_p^r.$$

Then the topological zeta function is:

$$\begin{aligned} \frac{1}{\zeta(z)} &= \exp \left(- \sum_{n=1}^{\infty} \frac{z^n N_n}{n} \right) \\ &= \exp \left(- \sum_{n=1}^{\infty} \frac{1}{n} \sum_p n_p \sum_{r=1}^{\infty} \delta_{n,rn_p} t_p^r \right) \\ &= \exp \left(- \sum_p \sum_{r=1}^{\infty} \frac{1}{r} t_p^r \right) \\ &= \prod_p (1 - t_p). \end{aligned} \tag{18.340}$$

Now let D_n be the number of symmetric lattice states with points on the diagonal. we have

$$z^n D_n = \sum_{n_p|n} a_p t_p^{\frac{n}{n_p}} = \sum_p a_p \sum_{r=1}^{\infty} \delta_{n,rn_p} t_p^r,$$

where

$$a_p = \begin{cases} 1, & n_p \text{ is odd}, \\ 2, & n_p \text{ is even}. \end{cases}$$

And

$$\sum_{n=1}^{\infty} z^n D_n = \sum_p a_p \sum_{r=1}^{\infty} t_p^r.$$

To find the topological zeta function that count the number of orbits with symmetry, I need to find a function $f(n)$ such that:

$$f(rn_p) = r a_p.$$

So

$$\sum_{n=1}^{\infty} \frac{1}{f(n)} z^n D_n = \sum_p \sum_{r=1}^{\infty} \frac{a_p}{r a_p} t_p^r.$$

2021-06-11 Han The orbit Jacobian matrix of a long lattice state which is a repeat of short lattice state of period n can be written as a tri-diagonal block

matrix:

$$\mathcal{J} = \left[\begin{array}{c|c|c|c|c} \mathbf{S} & \mathbf{R} & \mathbf{0} & \cdots & \mathbf{L} \\ \mathbf{L} & \mathbf{S} & \mathbf{R} & \cdots & \mathbf{0} \\ \vdots & \vdots & \ddots & \ddots & \vdots \\ \mathbf{0} & \mathbf{0} & \cdots & \mathbf{S} & \mathbf{R} \\ \mathbf{R} & \mathbf{0} & \cdots & \mathbf{L} & \mathbf{S} \end{array} \right], \quad (18.341)$$

where \mathbf{S} , \mathbf{R} and \mathbf{L} are $[n \times n]$ matrix blocks:

$$\begin{aligned} \mathbf{S} &= \begin{bmatrix} -s & 1 & & & 0 \\ 1 & -s & 1 & & \\ & \ddots & \ddots & \ddots & \\ & & 1 & -s & 1 \\ 0 & & & 1 & -s \end{bmatrix}, \\ \mathbf{R} &= \begin{bmatrix} 0 & \cdots & 0 \\ & \ddots & \vdots \\ 1 & & 0 \end{bmatrix}, \quad \mathbf{L} = \begin{bmatrix} 0 & & 1 \\ \vdots & \ddots & \\ 0 & \cdots & 0 \end{bmatrix}. \end{aligned} \quad (18.342)$$

The tri-diagonal block matrix can be projected into the symmetric subspace of the shorter lattice state. As an example, take the shorter lattice state of period $n = 4$, and the long lattice state given by the shorter lattice state repeated 4 times. Then the reflection operator can also be written

into the 16-dimensional space of the long lattice state:

$$\begin{aligned}
 R &= \left[\begin{array}{cccc|cccc|cccc|cccc} 0 & 0 & 0 & 1 & 0 & 0 & 0 & 0 & 0 & 0 & 0 & 0 & 0 & 0 & 0 & 0 & 0 \\ 0 & 0 & 1 & 0 & 0 & 0 & 0 & 0 & 0 & 0 & 0 & 0 & 0 & 0 & 0 & 0 & 0 \\ 0 & 1 & 0 & 0 & 0 & 0 & 0 & 0 & 0 & 0 & 0 & 0 & 0 & 0 & 0 & 0 & 0 \\ 1 & 0 & 0 & 0 & 0 & 0 & 0 & 0 & 0 & 0 & 0 & 0 & 0 & 0 & 0 & 0 & 0 \\ \hline 0 & 0 & 0 & 0 & 0 & 0 & 0 & 1 & 0 & 0 & 0 & 0 & 0 & 0 & 0 & 0 & 0 \\ 0 & 0 & 0 & 0 & 0 & 0 & 1 & 0 & 0 & 0 & 0 & 0 & 0 & 0 & 0 & 0 & 0 \\ 0 & 0 & 0 & 0 & 0 & 1 & 0 & 0 & 0 & 0 & 0 & 0 & 0 & 0 & 0 & 0 & 0 \\ 0 & 0 & 0 & 0 & 1 & 0 & 0 & 0 & 0 & 0 & 0 & 0 & 0 & 0 & 0 & 0 & 0 \\ \hline 0 & 0 & 0 & 0 & 1 & 0 & 0 & 0 & 0 & 0 & 0 & 0 & 0 & 0 & 0 & 0 & 0 \\ 0 & 0 & 0 & 0 & 0 & 1 & 0 & 0 & 0 & 0 & 0 & 0 & 0 & 0 & 0 & 0 & 0 \\ 0 & 0 & 0 & 0 & 0 & 0 & 1 & 0 & 0 & 0 & 0 & 0 & 0 & 0 & 0 & 0 & 0 \\ 0 & 0 & 0 & 0 & 0 & 0 & 0 & 1 & 0 & 0 & 0 & 0 & 0 & 0 & 0 & 0 & 0 \\ \hline 0 & 0 & 0 & 0 & 0 & 0 & 0 & 0 & 0 & 0 & 0 & 0 & 0 & 0 & 0 & 0 & 1 \\ 0 & 0 & 0 & 0 & 0 & 0 & 0 & 0 & 0 & 0 & 0 & 0 & 0 & 0 & 0 & 1 & 0 \\ 0 & 0 & 0 & 0 & 0 & 0 & 0 & 0 & 0 & 0 & 0 & 0 & 0 & 0 & 1 & 0 & 0 \\ 0 & 0 & 0 & 0 & 0 & 0 & 0 & 0 & 0 & 0 & 0 & 0 & 0 & 1 & 0 & 0 & 0 \\ \end{array} \right] \\
 &= \left[\begin{array}{c|c|c|c} \hat{R} & 0 & 0 & 0 \\ \hline 0 & \hat{R} & 0 & 0 \\ \hline 0 & 0 & \hat{R} & 0 \\ \hline 0 & 0 & 0 & \hat{R} \end{array} \right], \tag{18.343}
 \end{aligned}$$

where \hat{R} is the reflection operator in the 4-dimensional space of the shorter lattice state. Using the projection operator of this reflection matrix R :

$$\begin{aligned}
 P_{R^+} &= \frac{1}{2} \left[\begin{array}{cccc|cccc|cccc|cccc} 1 & 0 & 0 & 1 & 0 & 0 & 0 & 0 & 0 & 0 & 0 & 0 & 0 & 0 & 0 & 0 & 0 \\ 0 & 1 & 1 & 0 & 0 & 0 & 0 & 0 & 0 & 0 & 0 & 0 & 0 & 0 & 0 & 0 & 0 \\ 0 & 1 & 1 & 0 & 0 & 0 & 0 & 0 & 0 & 0 & 0 & 0 & 0 & 0 & 0 & 0 & 0 \\ 1 & 0 & 0 & 1 & 0 & 0 & 0 & 0 & 0 & 0 & 0 & 0 & 0 & 0 & 0 & 0 & 0 \\ \hline 0 & 0 & 0 & 0 & 1 & 0 & 0 & 1 & 0 & 0 & 0 & 0 & 0 & 0 & 0 & 0 & 0 \\ 0 & 0 & 0 & 0 & 0 & 1 & 1 & 0 & 0 & 0 & 0 & 0 & 0 & 0 & 0 & 0 & 0 \\ 0 & 0 & 0 & 0 & 0 & 0 & 1 & 1 & 0 & 0 & 0 & 0 & 0 & 0 & 0 & 0 & 0 \\ 0 & 0 & 0 & 0 & 0 & 1 & 0 & 0 & 1 & 0 & 0 & 0 & 0 & 0 & 0 & 0 & 0 \\ \hline 0 & 0 & 0 & 0 & 0 & 0 & 0 & 0 & 1 & 0 & 0 & 1 & 0 & 0 & 0 & 0 & 0 \\ 0 & 0 & 0 & 0 & 0 & 0 & 0 & 0 & 0 & 1 & 1 & 0 & 0 & 0 & 0 & 0 & 0 \\ 0 & 0 & 0 & 0 & 0 & 0 & 0 & 0 & 0 & 0 & 1 & 1 & 0 & 0 & 0 & 0 & 0 \\ 0 & 0 & 0 & 0 & 0 & 0 & 0 & 0 & 1 & 0 & 0 & 1 & 0 & 0 & 0 & 0 & 0 \\ \hline 0 & 0 & 0 & 0 & 0 & 0 & 0 & 0 & 0 & 0 & 0 & 0 & 1 & 0 & 0 & 0 & 1 \\ 0 & 0 & 0 & 0 & 0 & 0 & 0 & 0 & 0 & 0 & 0 & 0 & 0 & 1 & 1 & 0 & 0 \\ 0 & 0 & 0 & 0 & 0 & 0 & 0 & 0 & 0 & 0 & 0 & 0 & 0 & 1 & 1 & 0 & 0 \\ 0 & 0 & 0 & 0 & 0 & 0 & 0 & 0 & 0 & 0 & 0 & 0 & 1 & 0 & 0 & 0 & 1 \\ \end{array} \right] \\
 &= \left[\begin{array}{c|c|c|c} P_{\hat{R}^+} & 0 & 0 & 0 \\ \hline 0 & P_{\hat{R}^+} & 0 & 0 \\ \hline 0 & 0 & P_{\hat{R}^+} & 0 \\ \hline 0 & 0 & 0 & P_{\hat{R}^+} \end{array} \right] \tag{18.344}
 \end{aligned}$$

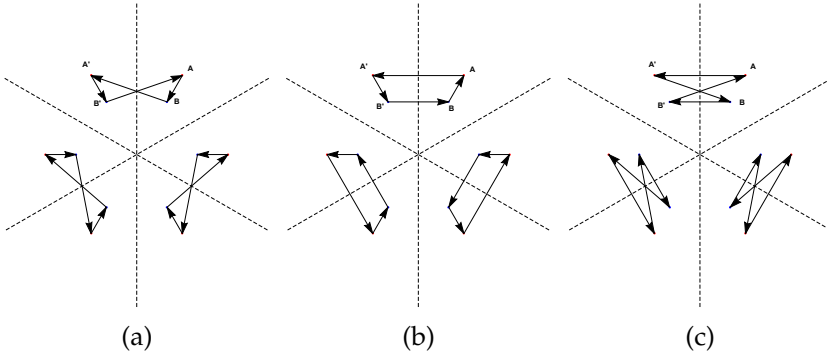


Figure 18.62: (a): Reflection invariant orbits of system with D_3 symmetry. The orbit $ABA'B'$ will be changed to $A'B'AB$ after reflection. (b) and (c): Orbits that cannot exist for system with D_3 symmetry. Although the sets of periodic points in these orbits are invariant under reflection, the order of the periodic points in these orbits will be changed to the opposite direction. $AA'B'B$ will be changed to $A'ABB'$ and $AA'BB'$ will be changed to $A'AB'B$.

the orbit Jacobian matrix is projected into the symmetric subspace and it still has the tri-diagonal form:

$$\mathcal{J}P_{R^+} = \begin{bmatrix} SP_{\hat{R}^+} & RP_{\hat{R}^+} & 0 & LP_{\hat{R}^+} \\ LP_{\hat{R}^+} & SP_{\hat{R}^+} & RP_{\hat{R}^+} & 0 \\ 0 & LP_{\hat{R}^+} & SP_{\hat{R}^+} & RP_{\hat{R}^+} \\ RP_{\hat{R}^+} & 0 & LP_{\hat{R}^+} & SP_{\hat{R}^+} \end{bmatrix}. \quad (18.345)$$

2021-06-25 Han I realized why figure 4.11 (b) is unnatural to me. If the time is continuous, we cannot have an orbit with reflection symmetry like figure 4.11 (b), because if the system has reflection symmetry, then the reflection axis (the boundary) is an invariant set, and orbit cannot cross it. So orbit with reflection symmetry can only exist on the boundary.

If the time is discrete then orbit with reflection symmetry can exist as shown in figure 18.62 (a). Note that figure 18.62 (b) and (c) cannot exist because these two orbits will change direction after reflection, i.e., the orbit will go opposite direction in the flipped fundamental domain. Even though these two kinds of orbits will not exist for system with reflection symmetry, these are the orbits that will exist for system with time reversal symmetry.

2021-07-04 Predrag to Han I think I have finally found the ‘dihedral’ zeta function in the literature. The much desired -see (2.16)- square root and dependence on t^2 makes an appearance in the Lind zeta function (4.149)!

Please drop everything, and check and correct my draft sect. 4.4 *A Lind*

zeta function for flip systems. I hope this finally leads to a paper on zeta-function factorization in time-reversal invariant temporal lattices.

2021-07-09 Han Figure 3.5 shows period-3 lattice states of $s = 3$ temporal cat, plotted in the subspace of the irreps (4.164) of the permutation representation. Using these 16 lattice states as a set on which the D_3 group acts, we can apply the Burnside theorem (18.348), using the D_3 table of marks table 4.3 to compute the number of lattice states that are invariant under the action of each subgroup.

Since irrep A_1 is a symmetric irrep, we only need to study the orbits in the subspace of irrep E_1 . Lattice states related by cyclic permutations are connected by blue lines in the figure 3.6(a). The two biggest triangles are two orbits without time reflection symmetry. There are three smaller triangles which are orbits with time reflection symmetry. And the point on the center is invariant under all group actions. This set of lattice states is corresponding to an element of the *Burnside ring* $\Omega(D_3)$:

$$a_{[D_3/1]} \left[\frac{D_3}{1} \right] + a_{[D_3/D_1]} \left[\frac{D_3}{D_1} \right] + a_{[D_3/C_3]} \left[\frac{D_3}{C_3} \right] + a_{[D_3/D_3]} \left[\frac{D_3}{D_3} \right]. \quad (18.346)$$

In this expression, $[D_3/H]$ is a kind of group orbits that are generate by factor group D_3 on a point x in the orbit, and x is invariant under the action of subgroup H . And $a_{[D_3/H]}$ is the number of this kind of group orbits.

For the period 3 lattice states of cat map, $a_{[D_3/1]}$ is the number of group orbits that is only invariant under the identity subgroup 1 , which is 1. Note that the two biggest triangles are one group orbit. $a_{[D_3/D_1]}$ is 3, since there are 3 smaller triangles that are invariant under reflection subgroup D_1 . $a_{[D_3/C_3]}$ is 0. Although there is one point on the center that is invariant under C_3 , the stabilizer (isotropy) subgroup is D_3 itself. So this point will contribute to $a_{[D_3/D_3]}$ instead of $a_{[D_3/C_3]}$.

The expression of the ring element of this set of orbits is

$$1 \left[\frac{D_3}{1} \right] + 3 \left[\frac{D_3}{D_1} \right] + 0 \left[\frac{D_3}{C_3} \right] + 1 \left[\frac{D_3}{D_3} \right].$$

Let

$$\mathbf{a} = (a_{[D_3/1]}, a_{[D_3/D_1]}, a_{[D_3/C_3]}, a_{[D_3/D_3]}) = (1, 3, 0, 1), \quad (18.347)$$

we can use the Burnside theorem (4.163)

$$\mathbf{a}M = \mathbf{u}, \quad (18.348)$$

to compute the \mathbf{u} which are the numbers of states fixed by the subgroups. M is the matrix of the table of marks of D_3 table 4.3. The result is:

$$\mathbf{u} = (16, 4, 1, 1).$$

16 is the number of states that are invariant under the identity group $\mathbf{1}$, which is the total number of states. 4 is the number of states that are invariant under a reflection subgroup D_1 . As shown in figure 3.6 (b), there are 4 points on each one of the reflection axis (red dashed lines). The number of states that are invariant under D_3 and C_3 subgroups is 1, which is the fixed point state, or the center.

It is easy for me to find the number of states invariant under the action of a group. So to make a good use of (18.348) we should find the number of lattice states that are invariant under subgroup actions, then use the inverse of the table of marks to find the numbers of each kind of orbit.

2021-07-10 Han The dihedral group

$$D_6 = \langle r, s \mid srs = r^5, r^6 = s^2 = 1 \rangle.$$

has 10 subgroup conjugacy classes (see (4.141) for notation):

- The identity subgroup $\mathbf{1} = \{1\}$.
- Dihedral subgroup $D_{1,0} = \{1, s\} = \langle s \rangle$ and its conjugate subgroups.
- Dihedral subgroup $D_{1,1} = \{1, rs\} = \langle rs \rangle$ and its conjugate subgroups.
- Cyclic subgroup $C_2 = \{1, r^3\} = \langle r^3 \rangle$.
- Dihedral subgroup $D_2 = \{1, r^3, s, r^3s\} = \langle r^3, s \rangle$ and its conjugate subgroups.
- Cyclic subgroup $C_3 = \{1, r^2, r^4\} = \langle r^2 \rangle$.
- Dihedral subgroup $D_{3,0} = \{1, r^2, r^4, s, r^2s, r^4s\} = \langle r^2, s \rangle$.
- Dihedral subgroup $D_{3,1} = \{1, r^2, r^4, rs, r^3s, r^5s\} = \langle r^2, rs \rangle$.
- Cyclic subgroup $C_6 = \{1, r, r^2, r^3, r^4, r^5\} = \langle r^5 \rangle$.
- D_6 group.

The table of marks of these subgroups is give in table 18.4.

2021-07-10 Han For the temporal cat with $s = 3$, we have 320 lattice states with period 6. Let u_H be the number of states that are invariant under the action of the subgroup H . Then

$$\begin{aligned} \mathbf{u} &= (u_{\mathbf{1}}, u_{C_2}, u_{D_{1,0}}, u_{D_{1,1}}, u_{C_3}, u_{D_2}, u_{C_6}, u_{D_{3,0}}, u_{D_{3,1}}, u_{D_6}) \\ &= (320, 16, 8, 40, 5, 4, 1, 1, 5, 1). \end{aligned} \quad (18.349)$$

Using the Burnside theorem (4.163) we have the corresponding Burnside ring:

$$\begin{aligned} \mathbf{a} &= \mathbf{u}M^{-1} \\ &= (16, 1, 2, 16, 0, 3, 0, 0, 2, 1). \end{aligned} \quad (18.350)$$

The interpretation of these numbers (see also (18.347)):

Table 18.4: D_6 table of marks, taken from [GAP sect. 70.12-2 Table of marks dihedral](#). For D_3 , see table 4.3.

D_6	$\mathbf{1}$	C_2	$D_{1,0}$	$D_{1,1}$	C_3	D_2	C_6	$D_{3,0}$	$D_{3,1}$	D_6
$D_6/\mathbf{1}$	12									
D_6/C_2	6	6								
$D_6/D_{1,0}$	6	0	2							
$D_6/D_{1,1}$	6	0	0	2						
D_6/C_3	4	0	0	0	4					
D_6/D_2	3	3	1	1	0	1				
D_6/C_6	2	2	0	0	2	0	2			
$D_6/D_{3,0}$	2	0	2	0	2	0	0	2		
$D_6/D_{3,1}$	2	0	0	2	2	0	0	0	2	
D_6/D_6	1	1	1	1	1	1	1	1	1	1

- $a_{[D_6/\mathbf{1}]} = 16$: there are 16 pairs of C_6 orbits without any symmetry.
- $a_{[D_6/C_2]} = 1$: there is 1 pair of C_3 period 3 orbits without any symmetry, see figure 3.6.
- $a_{[D_6/D_{1,0}]} = 2$ and $a_{[D_6/D_{1,1}]} = 16$ are the numbers of C_6 period 6 orbits that are invariant under two types of reflections, in agreement with table 18.3 SC_6 .
- $a_{[D_6/C_3]} = 0$: there is no orbit of C_2 period 2 without reflection symmetry.
- $a_{[D_6/D_2]} = 3$: there are 3 C_3 period 3 orbits with reflection symmetry, in agreement with table 18.3 SC_3 .
- $a_{[D_6/C_6]} = 0$: there is no fixed point lattice state without reflection symmetry.
- $a_{[D_6/D_{3,0}]} = 0$ and $a_{[D_6/D_{3,1}]} = 2$ are the numbers of C_2 period 2 orbits invariant under both types of reflections, in agreement with table 18.3 SC_2 .
- $a_{[D_6/D_6]} = 1$: there is one fixed point lattice state with reflection symmetry.

2021-07-11 Predrag To me indicating D_6 in $a_{[D_6/D_{1,0}]}$, etc, in (18.347) and (18.350) seems redundant. Is that a notation literature uses? Otherwise indicating just the subgroup, as in $a_{D_{1,0}}$, should suffice?

2021-07-11 Predrag A remark on the level of ChaosBook generality: Looks like one should abandon the notion of ‘prime’, ‘relative prime’ orbit. The notion of ‘orbit’ covers all that, so the distinction is only between ‘lattice state’ and ‘orbit’, there is no ‘non-prime’ orbit.

2021-07-11 Predrag Very nice - I have changed the notation following (4.141), and tentatively reordered the list (but not in the table, there we follow GAP) by grouping C_n 's, D_n 's together, and putting D_1 's ahead of C_2 's, though ordering by the order of the group might be more logical.

A beautiful thing is that the Lind zeta function (4.149), (4.153) does not seem to depend on all these subgroup lattice details. That might be the genius of zeta functions; the 'prime' orbits are only defined in terms of C_n 's, D_n 's, and all these subgroup complications arise only when one insists on counting the lattice states. Which is what is fundamentally not needed, that should be emphasized in the putative paper.

2021-07-17 Predrag to Han Before we can hope that sect. 4.4 *A Lind zeta function for flip systems* is publishable, we have to explain clearly that the quotient taken is a lattice/sublattice quotient, isomorphic to a point group. I've used the *CL18.tex* spatiotemporal cat text as a starting point for sect. ?? *1-dimensional lattices and sublattices* - please shorten it to a few paragraphs? To make that understandable, I believe we need to draw some 1-dimensional lattice, line group figures, illustrating

1. the unit tile has no symmetry (and arrow? a fish? drawn in it, pointing to the right?) for a generic dynamical system, such as the usual Hénon map.
2. Reversible dynamical system's unit tile has a midpoint and edge-flip reflection symmetry (draw left-right arrow? moustache?)
3. Draw a figure illustrating that $rH(n, k)r^{-1} = H(n, k + 2)$.
4. draw (for example?) a 1-dimensional, period 4 Bravais cell, and draw the (4.141) $k = 0, 1, 2, 3$ flips of it.

2021-07-17 Predrag to Han and Sidney Looking at figure 3.6: The temporal cat (but not the temporal Hénon) has a *dynamical symmetry* under the simultaneous inversion S through the center of the $0 \leq \phi_j < 1$ unit interval, see (4.23). Can you check whether the (4.183), (4.177) Isola zeta function factorization is a consequence of this dynamical inversion symmetry? $S^2 = 1$ should give you the projection operators.

2021-07-21 Han In the Lind zeta function (4.137), each subgroup H is a symmetric group of a set of lattice states. For the flip system (dynamical system with time reversal symmetry), there are two kinds of subgroups of D_∞ (4.7): $H(n)$ and $H(n, k)$ (4.141). These two subgroups act on infinite lattice states. N_n and $N_{n,k}^\sigma$ are the numbers of lattice states that are invariant under the $H(n)$ and $H(n, k)$.

We need to define the action of the D_∞ on the lattice state. Let the generator r shift the lattice state one step to the left, and the generator σ reflect the lattice state over the 0th lattice point. Then figure 18.63 shows lattice states that are invariant under subgroups of D_∞ .

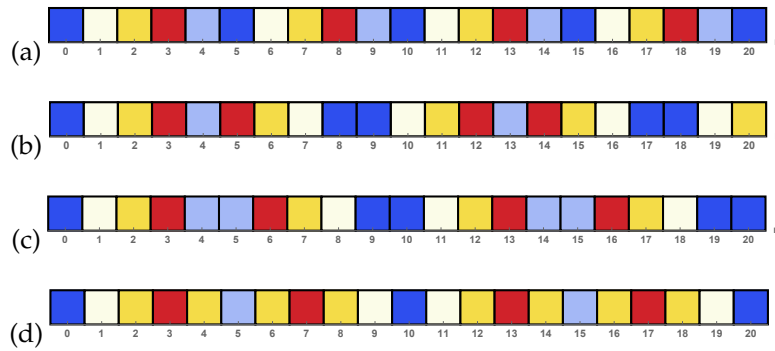


Figure 18.63: Lattice states same as figure 3.13 but the field values are color coded (we have since abandoned this approach), rather than plotted as $\phi_t \in [0, 1]$. Horizontal: lattice sites labelled by $t \in \mathbb{Z}$. Vertical: value of field ϕ_t , plotted as a bar centred at lattice site t . A period n lattice state X has one of the 4 possible symmetries, illustrated by: (a) A period-5 lattice state X invariant under the translation group $H(5)$, with no reflection symmetry. Its D_5 orbit are $2n = 10$ distinct lattice states, $5 C_\infty$ translations and $5 D_\infty$ translate-reflections. (b) A period 9, odd-period lattice state (3.158), invariant under the space group $H(9, 8)$. This lattice state has reflection symmetry over the 4th lattice point (as in figure 3.10(a)), and the midpoint between 8th and 9th lattice points (as in figure 3.10(b)). (c) A period 10, even-period lattice state (3.159), invariant under the space group $H(10, 9)$. This lattice state has reflection symmetry over the midpoint between the 4th and 5th lattice points and the midpoint between 9th and 10th lattice points. (d) A period 10, even-period lattice state (3.160), invariant under the space group $H(10, 0)$. This lattice state has reflection symmetry over the 0th lattice point and the 5th lattice point. Note that $H(10, 9)$ and $H(10, 0)$ are not conjugate subgroups, so we cannot use translations or reflections to make the lattice state (c) satisfy the symmetry of lattice state (d). The D_n orbits of reflection-symmetric lattice states (b-c) contain only n lattice state C_n translations, as any reflection results in a translation of the initial lattice state.

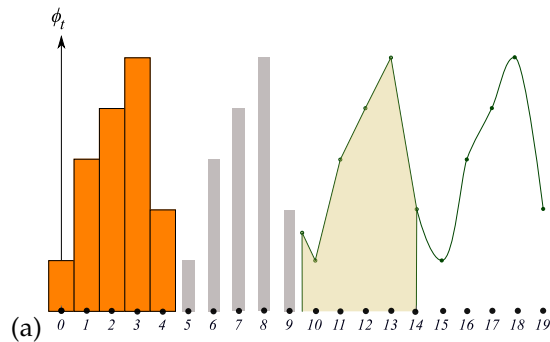


Figure 18.64: For a time-reversal invariant system, a period n lattice state X , plotted here as the field values ϕ_t , each bar centred at lattice site t , has one of the 4 possible symmetries, illustrated by: (a) A period-5 lattice state X invariant under the translation group $H(5)$, with no time reversal symmetry.

2021-07-22 Predrag I was wrong: color-coded figure 18.63 is useless, while the field figure 3.13 is much easier to understand.

2021-07-27 Han The two small triangles in figure 3.6 are related by the D_1 : $S\phi_i = 1 - \phi_i$ symmetry. Let T be the irreps transformation, ϕ_1 and ϕ_2 be two lattice states related by $\phi_1 = 1 - \phi_2$. Then we have :

$$T\phi_1 = T\mathbf{1} - T\phi_2 = (1, 0, 0, \dots) - T\phi_2, \quad (18.351)$$

where $(1, 0, 0, \dots)$ is a vector with the first component 1 and other components 0. The first component in the space of irreps is the component in the subspace of the 1-dimensional symmetric irrep, which is the average value of the lattice state. The effect of the action of S is to inverse the sign of the lattice state in the space of irreps except for the subspace of the 1-dimensional symmetric irrep.

But why the two big triangles and the one medium size triangle do not have inversions? The orbit of these triangles are $1/4(0, 1, 3)$ and $1/2(1, 1, 0)$. When we apply the inversion S , 0 is mapped to 0 instead of 1. So these two orbits are mapped to $1/4(0, 3, 1)$ and $1/2(1, 1, 0)$, which are themselves.

2021-07-28 Predrag Moved the two “ $H(n, k)$ is not a normal subgroup” posts to example 4.18. I agree with both.

2021-07-28 Predrag I feel that the coset count is easiest to understand looking at the 3-disk billiard, [ChaosBook example 11.6](#). I find the notion of “isotropy” group too restrictive, and prefer “symmetry of a solution”, see [ChaosBook eq. \(11.2\)](#). Let me know if you agree, and if not, suggest rewrites for the ChaosBook text.

2021-07-28 Predrag Rather than Lind's nebulous 'index' [38], for $|G/H|$ in (4.137)

I would like to use [ChaosBook p. 166](#):

Definition: Multiplicity. For a finite discrete group, the multiplicity of orbit p is $m_p = |G|/|G_p|$.

2021-07-28 Predrag Checked: [Douglas Lind](#) does have a Lind zeta function (4.137) in Lind [38]. His Theorem 5.4 presumably is the product formula for his zeta.

More important for us, going forward to spatiotemporal cat, he knows how to count prime tiles in any \mathbb{Z}^d lattice, see his Table 1.

2021-08-04 Han To block diagonalize the orbit Jacobian matrix by the symmetric and antisymmetric subspace of the reflection operator as in (15.34), we need to use the eigenvectors of the reflection operator. For example, generally the orbit Jacobian matrix of the Henon map (3.85) is not invariant under reflection and translation. But if the orbit has the reflection symmetry, we can use the reflection operator, under the action of which the orbit is invariant, to project the orbit Jacobian matrix into symmetric and antisymmetric subspace, or block diagonalize the orbit Jacobian matrix.

If the period of the orbit is odd, there is only one kind of reflections. For example, if the period is 9, the orbit can be written as a vector in the 9 dimensional space of lattice state:

$$\overline{\phi_1\phi_2\phi_3\phi_4\phi_5\phi_4\phi_3\phi_2\phi_1}. \quad (18.352)$$

This orbit is invariant under the reflection operator:

$$\sigma = \begin{bmatrix} 0 & 0 & 0 & 0 & 0 & 0 & 0 & 0 & 1 \\ 0 & 0 & 0 & 0 & 0 & 0 & 0 & 1 & 0 \\ 0 & 0 & 0 & 0 & 0 & 0 & 1 & 0 & 0 \\ 0 & 0 & 0 & 0 & 0 & 1 & 0 & 0 & 0 \\ 0 & 0 & 0 & 0 & 1 & 0 & 0 & 0 & 0 \\ 0 & 0 & 0 & 1 & 0 & 0 & 0 & 0 & 0 \\ 0 & 0 & 1 & 0 & 0 & 0 & 0 & 0 & 0 \\ 0 & 1 & 0 & 0 & 0 & 0 & 0 & 0 & 0 \\ 1 & 0 & 0 & 0 & 0 & 0 & 0 & 0 & 0 \end{bmatrix}. \quad (18.353)$$

Let the diagonalizing matrix V be:

$$V = \begin{bmatrix} 1 & 0 & 0 & 0 & 0 & -1 & 0 & 0 & 0 \\ 0 & 1 & 0 & 0 & 0 & 0 & -1 & 0 & 0 \\ 0 & 0 & 1 & 0 & 0 & 0 & 0 & -1 & 0 \\ 0 & 0 & 0 & 1 & 0 & 0 & 0 & 0 & -1 \\ 0 & 0 & 0 & 0 & 1 & 0 & 0 & 0 & 0 \\ 0 & 0 & 0 & 1 & 0 & 0 & 0 & 0 & 1 \\ 0 & 0 & 1 & 0 & 0 & 0 & 0 & 1 & 0 \\ 0 & 1 & 0 & 0 & 0 & 0 & 1 & 0 & 0 \\ 1 & 0 & 0 & 0 & 0 & 1 & 0 & 0 & 0 \end{bmatrix}, \quad (18.354)$$

each column of which is an eigenvector of the reflection operator. The first 5 vectors span the symmetric subspace of reflection and the last 4 vectors span the antisymmetric subspace. Using the eigenvectors the orbit Jacobian matrix can be block diagonalized as:

$$V^{-1} \mathcal{J} V = \left[\begin{array}{cc|cc|cc} 2\phi_1 + 1 & 1 & 0 & 0 & 0 & 0 & 0 & 0 \\ 1 & 2\phi_2 & 1 & 0 & 0 & 0 & 0 & 0 \\ 0 & 1 & 2\phi_3 & 1 & 0 & 0 & 0 & 0 \\ 0 & 0 & 1 & 2\phi_4 & 1 & 0 & 0 & 0 \\ 0 & 0 & 0 & 2 & 2\phi_5 & 0 & 0 & 0 \\ \hline 0 & 0 & 0 & 0 & 0 & 2\phi_1 - 1 & 1 & 0 \\ 0 & 0 & 0 & 0 & 0 & 1 & 2\phi_2 & 1 \\ 0 & 0 & 0 & 0 & 0 & 0 & 1 & 2\phi_3 \\ 0 & 0 & 0 & 0 & 0 & 0 & 0 & 1 \end{array} \right] \quad (18.355)$$

If the period of the orbit is even, there are two kinds of reflections. For example, the orbit

$$\overline{\phi_1 \phi_2 \phi_3 \phi_4 | \phi_4 \phi_3 \phi_2 \phi_1} \quad (18.356)$$

is invariant under the 1/2 lattice spacing reflection:

$$\sigma = \left[\begin{array}{cccccccc} 0 & 0 & 0 & 0 & 0 & 0 & 0 & 1 \\ 0 & 0 & 0 & 0 & 0 & 0 & 1 & 0 \\ 0 & 0 & 0 & 0 & 0 & 1 & 0 & 0 \\ 0 & 0 & 0 & 0 & 1 & 0 & 0 & 0 \\ 0 & 0 & 0 & 1 & 0 & 0 & 0 & 0 \\ 0 & 0 & 1 & 0 & 0 & 0 & 0 & 0 \\ 0 & 1 & 0 & 0 & 0 & 0 & 0 & 0 \\ 1 & 0 & 0 & 0 & 0 & 0 & 0 & 0 \end{array} \right]. \quad (18.357)$$

Using the eigenvector matrix:

$$V = \left[\begin{array}{cccccccc} 1 & 0 & 0 & 0 & -1 & 0 & 0 & 0 \\ 0 & 1 & 0 & 0 & 0 & -1 & 0 & 0 \\ 0 & 0 & 1 & 0 & 0 & 0 & -1 & 0 \\ 0 & 0 & 0 & 1 & 0 & 0 & 0 & -1 \\ 0 & 0 & 0 & 1 & 0 & 0 & 0 & 1 \\ 0 & 0 & 1 & 0 & 0 & 0 & 1 & 0 \\ 0 & 1 & 0 & 0 & 0 & 1 & 0 & 0 \\ 1 & 0 & 0 & 0 & 1 & 0 & 0 & 0 \end{array} \right], \quad (18.358)$$

we can block diagonalize the orbit Jacobian matrix as:

$$V^{-1} \mathcal{J} V = \left[\begin{array}{cccc|cccc} 2\phi_1 + 1 & 1 & 0 & 0 & 0 & 0 & 0 & 0 \\ 1 & 2\phi_2 & 1 & 0 & 0 & 0 & 0 & 0 \\ 0 & 1 & 2\phi_3 & 1 & 0 & 0 & 0 & 0 \\ 0 & 0 & 1 & 2\phi_4 + 1 & 0 & 0 & 0 & 0 \\ \hline 0 & 0 & 0 & 0 & 2\phi_1 - 1 & 1 & 0 & 0 \\ 0 & 0 & 0 & 0 & 1 & 2\phi_2 & 1 & 0 \\ 0 & 0 & 0 & 0 & 0 & 1 & 2\phi_3 & 1 \\ 0 & 0 & 0 & 0 & 0 & 0 & 1 & 2\phi_4 - 1 \end{array} \right] \quad (18.359)$$

If the orbit is

$$\overline{\phi_1 \phi_2 \phi_3 \phi_4 \phi_5 \phi_4 \phi_3 \phi_2}, \quad (18.360)$$

the corresponding reflection operator leaves sites 1 and 4 invariant:

$$\sigma_1 = \left[\begin{array}{cccccccc} 1 & 0 & 0 & 0 & 0 & 0 & 0 & 0 \\ 0 & 0 & 0 & 0 & 0 & 0 & 0 & 1 \\ 0 & 0 & 0 & 0 & 0 & 0 & 1 & 0 \\ 0 & 0 & 0 & 0 & 0 & 1 & 0 & 0 \\ 0 & 0 & 0 & 0 & 1 & 0 & 0 & 0 \\ 0 & 0 & 0 & 1 & 0 & 0 & 0 & 0 \\ 0 & 0 & 1 & 0 & 0 & 0 & 0 & 0 \\ 0 & 1 & 0 & 0 & 0 & 0 & 0 & 0 \end{array} \right]. \quad (18.361)$$

Using the eigenvector matrix:

$$V = \left[\begin{array}{cccccccc} 1 & 0 & 0 & 0 & 0 & 0 & 0 & 0 \\ 0 & 1 & 0 & 0 & 0 & -1 & 0 & 0 \\ 0 & 0 & 1 & 0 & 0 & 0 & -1 & 0 \\ 0 & 0 & 0 & 1 & 0 & 0 & 0 & -1 \\ 0 & 0 & 0 & 0 & 1 & 0 & 0 & 0 \\ 0 & 0 & 0 & 1 & 0 & 0 & 0 & 1 \\ 0 & 0 & 1 & 0 & 0 & 0 & 1 & 0 \\ 0 & 1 & 0 & 0 & 0 & 1 & 0 & 0 \end{array} \right], \quad (18.362)$$

the orbit Jacobian matrix can be block diagonalized as:

$$V^{-1} \mathcal{J} V = \left[\begin{array}{ccccc|ccc} 2\phi_1 & 2 & 0 & 0 & 0 & 0 & 0 & 0 \\ 1 & 2\phi_2 & 1 & 0 & 0 & 0 & 0 & 0 \\ 0 & 1 & 2\phi_3 & 1 & 0 & 0 & 0 & 0 \\ 0 & 0 & 1 & 2\phi_4 & 1 & 0 & 0 & 0 \\ 0 & 0 & 0 & 2 & 2\phi_5 & 0 & 0 & 0 \\ \hline 0 & 0 & 0 & 0 & 0 & 2\phi_2 & 1 & 0 \\ 0 & 0 & 0 & 0 & 0 & 1 & 2\phi_3 & 1 \\ 0 & 0 & 0 & 0 & 0 & 0 & 1 & 2\phi_4 \end{array} \right]. \quad (18.363)$$

2021-08-04 Han The choice of eigenvectors in the symmetric and antisymmetric subspaces is not unique, and it will not affect the determinant of the

orbit Jacobian matrix in the subspaces. So we can compute the determinant of the orbit Jacobian matrix in the subspaces without using any eigenvector.

The determinant of a matrix can be written as the antisymmetrized trace of the matrix [16]:

$$\text{Det } M = \text{Tr}_p AM = \frac{1}{p} \sum_{k=1}^p (-1)^{k-1} (\text{Tr}_{p-k} AM) \text{Tr} M^k, \quad (18.364)$$

where A is the antisymmetrization projection operator, p is the dimension of the matrix M . To compute the determinant of the orbit Jacobian matrix in the subspace, we need to first project the matrix into the subspace, then compute the antisymmetrized trace with the dimension of the subspace.

For example, consider (18.356) symmetric orbit $\overline{\phi_1\phi_2\phi_3\phi_4|\phi_4\phi_3\phi_2\phi_1|}$. The determinant of the orbit Jacobian matrix \mathcal{J}_+ in the symmetric subspace is:

$$\begin{aligned} \text{Det}(P_+ \mathcal{J}) &= \left\| \begin{array}{ccccccccc} -s_1 + 1 & 1 & \cdot & \cdot & \cdot \\ 1 & -s_2 & 1 & \cdot & \cdot \\ \cdot & 1 & -s_3 & 1 & \cdot \\ \cdot & \cdot & 1 & -s_4 + 1 & \cdot \\ s_1 s_2 s_3 s_4 + s_1 s_2 s_3 + s_2 s_3 s_4 & & & & & & & & \\ +s_1 s_2 + s_2 s_3 + s_1 s_4 + s_3 s_4 + s_1 + s_2 + s_3 + s_4 & & & & & & & & \end{array} \right\| \\ &= s_1 s_2 s_3 s_4 + s_1 s_2 s_3 + s_2 s_3 s_4 \\ &\quad + s_1 s_2 + s_2 s_3 + s_1 s_4 + s_3 s_4 + s_1 + s_2 + s_3 + s_4. \end{aligned} \quad (18.365)$$

Alternatively, using the projection operator to project the orbit Jacobian matrix into the symmetric subspace $P_+ \mathcal{J} = \mathcal{J}_+$:

$$\mathcal{J}_+ = \frac{1}{2} \begin{bmatrix} 2\phi_1 + 1 & 1 & 0 & 0 & 0 & 0 & 1 & 2\phi_1 + 1 \\ 1 & 2\phi_2 & 1 & 0 & 0 & 1 & 2\phi_2 & 1 \\ 0 & 1 & 2\phi_3 & 1 & 1 & 2\phi_3 & 1 & 0 \\ 0 & 0 & 1 & 2\phi_4 + 1 & 2\phi_4 + 1 & 1 & 0 & 0 \\ 0 & 0 & 1 & 2\phi_4 + 1 & 2\phi_4 + 1 & 1 & 0 & 0 \\ 0 & 1 & 2\phi_3 & 1 & 1 & 2\phi_3 & 1 & 0 \\ 1 & 2\phi_2 & 1 & 0 & 0 & 1 & 2\phi_2 & 1 \\ 2\phi_1 + 1 & 1 & 0 & 0 & 0 & 0 & 1 & 2\phi_1 + 1 \end{bmatrix} \quad (18.366)$$

and using (18.364) we have:

$$\begin{aligned} \text{Det}(\mathcal{J}_+) &= \text{Tr}_4(A \mathcal{J}_+) \\ &= \frac{1}{4!} \{ (\text{Tr} \mathcal{J}_+)^4 - 6(\text{Tr} \mathcal{J}_+)^2 \text{Tr} \mathcal{J}_+^2 + 3(\text{Tr} \mathcal{J}_+^2)^2 \\ &\quad + 8\text{Tr} \mathcal{J}_+^3 \text{Tr} \mathcal{J}_+ - 6\text{Tr} \mathcal{J}_+^4 \} \\ &= 16\phi_1\phi_2\phi_3\phi_4 + 8\phi_1\phi_2\phi_3 + 8\phi_2\phi_3\phi_4 - 4\phi_1\phi_2 + 4\phi_2\phi_3 \\ &\quad - 4\phi_1\phi_4 - 4\phi_3\phi_4 - 2\phi_1 - 2\phi_2 - 2\phi_3 - 2\phi_4, \end{aligned} \quad (18.367)$$

the same result as computing the determinant of the $[4 \times 4]$ matrix.

If the orbit is $\overline{\phi_1\phi_2\phi_3\phi_4\phi_5\phi_4\phi_3\phi_2}$, see (18.360), the determinant of the orbit Jacobian matrix in the symmetric subspace is:

$$\begin{aligned} \text{Det}(\mathcal{J}_+) &= \text{Det} \begin{bmatrix} 2\phi_1 & 2 & 0 & 0 & 0 \\ 1 & 2\phi_2 & 1 & 0 & 0 \\ 0 & 1 & 2\phi_3 & 1 & 0 \\ 0 & 0 & 1 & 2\phi_4 & 1 \\ 0 & 0 & 0 & 2 & 2\phi_5 \end{bmatrix} \\ &= 32\phi_1\phi_2\phi_3\phi_4\phi_5 - 16\phi_1\phi_2\phi_3 - 8\phi_1\phi_2\phi_5 \\ &\quad - 8\phi_1\phi_4\phi_5 - 16\phi_3\phi_4\phi_5 + 4\phi_1 + 8\phi_3 + 4\phi_5. \end{aligned} \tag{18.368}$$

We can get the same result from the orbit Jacobian matrix projected into the symmetric subspace:

$$P_+\mathcal{J} = \frac{1}{2} \begin{bmatrix} 4\phi_1 & 2 & 0 & 0 & 0 & 0 & 0 & 2 \\ 2 & 2\phi_2 & 1 & 0 & 0 & 0 & 1 & 2\phi_2 \\ 0 & 1 & 2\phi_3 & 1 & 0 & 1 & 2\phi_3 & 1 \\ 0 & 0 & 1 & 2\phi_4 & 2 & 2\phi_4 & 1 & 0 \\ 0 & 0 & 0 & 2 & 4\phi_5 & 2 & 0 & 0 \\ 0 & 0 & 1 & 2\phi_4 & 2 & 2\phi_4 & 1 & 0 \\ 0 & 1 & 2\phi_3 & 1 & 0 & 1 & 2\phi_3 & 1 \\ 2 & 2\phi_2 & 1 & 0 & 0 & 0 & 1 & 2\phi_2 \end{bmatrix}. \tag{18.369}$$

The determinant is:

$$\begin{aligned} \text{Det}(\mathcal{J}_+) &= \text{Tr}_5(A\mathcal{J}_+) \\ &= \frac{1}{5!} \left\{ (\text{Tr } \mathcal{J}_+)^5 - 10(\text{Tr } \mathcal{J}_+)^3 \text{Tr } \mathcal{J}_+^2 + 15(\text{Tr } \mathcal{J}_+)(\text{Tr } \mathcal{J}_+^2)^2 \right. \\ &\quad + 20\text{Tr } \mathcal{J}_+^3(\text{Tr } \mathcal{J}_+)^2 - 20\text{Tr } \mathcal{J}_+^2 \text{Tr } \mathcal{J}_+^3 \\ &\quad \left. - 30\text{Tr } \mathcal{J}_+^4 \text{Tr } \mathcal{J}_+ + 24\text{Tr } \mathcal{J}_+^5 \right\} \\ &= 32\phi_1\phi_2\phi_3\phi_4\phi_5 - 16\phi_1\phi_2\phi_3 \\ &\quad - 8\phi_1\phi_2\phi_5 - 8\phi_1\phi_4\phi_5 - 16\phi_3\phi_4\phi_5 \\ &\quad + 4\phi_1 + 8\phi_3 + 4\phi_5. \end{aligned} \tag{18.370}$$

2021-08-04 Han Using the antisymmetrized trace formula (18.364) we can compute the determinant of a matrix in the subspace. The reason is simple: when the matrix is diagonalized, some elements on the diagonal will be zero. These zeros will not contribute to the trace of the matrix. So if we use the antisymmetrized trace formula with the correct dimension, the determinant we get is the determinant of the matrix in the subspace with non-zero eigenvalues.

2021-08-04 Predrag Very nice!

2021-08-04 Predrag It might that the above symmetric polynomials in ϕ_i are all reducible to powers of the orbital sum r_p defined in (2.14), a orbit p invariant. For an example, see (2.24). But probably specific to Hénon only...

2021-08-05 Predrag Added

\newcommand{\sitebox}[1]

that enables you to control the margin around $\boxed{\phi_{n-1}}$. Gave up on playing with $\boxed{\phi_n}$ and $\boxed{\phi_n}$.

2021-08-04 Predrag You are using the wrong definition of Hénon orbit Jacobian matrix, there are no factors of a in (3.85). Please fix throughout. We prefer Gallas *et al.* convention (3.85).

2021-08-04, 2021-08-11 Predrag I have -an experiment- sat $2\phi_j = -s_j$, temporal cat style in (18.366) and (5.117), just to see how we like that. The signs might be wrong, please recheck.

This also connect to the one-dimensional Schrödinger operator (13.106), where $\lambda v_n = -s_j$. “The real-valued potential sequence $v = (v_n)_{n \in \mathbb{Z}}$ represents the environment that the particle is subjected to, with the “coupling constant” $\lambda > 0$ is factored out for convenience.”

2021-08-04 Predrag It seems better to number lattice sites as $\phi_0\phi_1\phi_2 \cdots \phi_{n-1}$, at least when one or two lattice sites are invariant under the reflection, see (18.372) and (18.373).

2021-08-04 Predrag Let us try to explicitly connect and generalize Kim *et al.* [35] orbit-counting “generating function” (4.150) counts

$$N_{2m-1,0}, N_{2m,0}, N_{2m,1} \quad (18.371)$$

as well as MacKay’s thesis [41] table 18.3, and Gallas *et al.* (2.15), to the Hill determinant-weighted, symmetry reduced and factorized periodic orbit weights t_p , by connecting

period $n = 2m - 1$ odd ($N_{2m-1,k}, SC_n$) n cyclicly related lattice states

$$\overline{\phi_0|\phi_1\phi_2 \cdots \phi_m|\phi_m \cdots \phi_2\phi_1}. \quad (18.372)$$

to 1 boundary point ‘diagonal’ class **D** (2.36), (18.312), (18.334), (18.352); m -dimensional symmetric, $(m-1)$ -dimensional antisymmetric subspace (18.355).

period $n = 2m$ even, $k = \text{even}$ ($N_{2m,k}, SF_n$ (?)) $m = n/2$ cyclicly related lattice states

$$\overline{\phi_0|\phi_1\phi_2 \cdots \phi_{m-1}|\phi_m|\phi_{m-1} \cdots \phi_2\phi_1}. \quad (18.373)$$

to no boundary point ‘non-diagonal’ class N (2.31), (18.317), (18.336), antisymmetric (18.339), (18.360); $(m+1)$ -dimensional symmetric, $(m-1)$ -dimensional antisymmetric subspace (18.363).

period $n = 2m$ even, $k = \text{odd}$ ($N_{2m,k}$, SF_n (?)) $m = n/2$ cyclicly related lattice states

$$\overline{\phi_1\phi_2\phi_3 \cdots \phi_m|\phi_m \cdots \phi_2\phi_1|}. \quad (18.374)$$

to 2 boundary points ‘diagonal’ class D (2.35), (18.316), (18.335), antisymmetric (18.338), (18.356), (18.366); m -dimensional symmetric, m -dimensional antisymmetric subspace (18.359). Also and (5.117).

I have almost certainly mixed up the two even-period classes, please correct.

2021-08-05 Predrag We have to distinguish the symmetric (18.335) from the antisymmetric (18.338), (18.339) throughout.

I started writing this up in sect. 4.1.4 *Reflection-symmetric lattice states*.

Orbit Jacobian matrix \mathcal{J} is linear, so the antisymmetric-symmetric factorization will always apply to it. However, I expect the antisymmetric subspace to be flow-invariant for nonlinear systems (such as temporal Hénon; but also temporal cat should have an interesting space of antisymmetric solutions), with lattice states within that lower-dimensional subspace. That would explain shared eigenvalues such as (15.26): do the two distinct Hénon orbits $\overline{1000}$ and $\overline{1110}$ both live in the lower-dimensional antisymmetric subspace, and because of that share the eigenvalue r ?

See my post that includes (15.36).

My hunch based on the experience with Kuramoto-Sivashinsky antisymmetric subspace being flow-invariant, see example 4.4 *Desymmetrization of Lorenz flow*, ChaosBook example 30.1 *Kuramoto-Sivashinsky antisymmetric subspace* and ChaosBook example 30.2 *Cyclic subgroups of SO(2)*.

2021-08-11 Predrag I have -an experiment- sat $2\phi_j = -s_j$, temporal cat style in (18.366) and (5.117), just to see how we like that. The signs might be wrong, please recheck.

This also connects to the Harper’s model (13.112), tight-binding model (13.96), and one-dimensional Schrödinger operator (13.110), (13.59) and (13.106), where $\lambda v_n = -s_j$. “The real-valued potential sequence $v = (v_n)_{n \in \mathbb{Z}}$ represents the environment that the particle is subjected to, with the ‘coupling constant’ $\lambda > 0$ is factored out for convenience.”

2021-08-11 Predrag Let’s get Hamiltonian Hénon system (2.11) even closer to the temporal cat, by multiplying both sides by $-2a$ and taking $\phi_j = -2ax_j$. The rescaled temporal Hénon is (2.5). Now the orbit Jacobian matrix is of the desired temporal cat form (2.9), with $s_j = \phi_j$, and once you have an expression for Hill determinant $\|\mathcal{J}[X]\|$ in terms of traces

$\text{Tr } \mathcal{J}^k$, i.e., the D_n invariant orbital sums for products of fields on consecutive lattice sites, they will be the same for the temporal cat and the temporal Hénon.

Not only that, but we should be able to write (5.119) action $S[X]$ such that the derivative of the quartic term yields classical ϕ^4 theory (5.118) on d -dimensional lattice (5.115), with the Hill determinant of the same form (2.9).

2021-08-11 Predrag It would be good to evaluate small Hill determinants both in terms of traces (18.364), and on the C_n and D_n reciprocal lattices. Reciprocal lattice is diagonalized, and eigenvectors are presumably explicit.

2021-08-11 Predrag If you use birdtracks, determinant is the full antisymmetrizer, and time reversal is a permutation with all lines crossed. The contraction with antisymmetrizer might simplify some calculations.

2021-08-11 Predrag I have a hunch why for Hénon only the orbital sum $\text{Tr } \mathcal{J}$ matters. For $\text{Tr } \mathcal{J}^2$ you can use the temporal Hénon recurrence (2.5) to eliminate ϕ_t^2 in terms of terms linear in $\phi_{t\pm 1}$. The same, but for $\text{Tr } \mathcal{J}^3$, might apply to the ϕ^4 theory ϕ_t^3 terms in (5.115).

2021-08-14 Predrag About ‘right’ and ‘left’. We have to distinguish the action of the translation operator r on coordinates (lattice site label i in discretizing $x \rightarrow x_i$):

r_j is a counterclockwise rotation of a polygon by j vertices, or right translation of a \mathbb{Z} lattice by j sites (we follow [Dihedral group wiki](#)).

vs. its action on *fields*, i.e., functions $\phi_i = \phi(x_i)$, given by the Wigner definition of the effect of transformations on functions, [ChaosBook eq. \(25.2\)](#). I hope our introduction of translations (3.32) is in agreement for the convention for fields.

Time evolution clearly increases the field’s site index, $\phi_t \rightarrow \phi_{t+1}, \dots$, and thus shift the lattice state to the left; if I sit at the origin, lattice site ‘0’, I should be seeing ϕ_0 , then the one time-step r ‘later’ ϕ_1 , and so on.

We also have to make sure that the direction of shift [ChaosBook eq. \(14.12\)](#) is consistent with our usage here.

Am I correct?

2021-08-14 Predrag Experimenting with lattice state plots of figure 3.13 see figure 18.64 and figure 18.65. I still find bar graph figure 3.13 the best.

If a Mathematica figure
`siminos/figs/*.pdf`

is getting into almost publishable shape, please save it also as a
`siminos/figSrc/inkscape/*.svg`.

Makes easier for me to fine-tune it for the publication.

2021-08-14 Predrag I hope figure 18.65 settles for once and all the ‘odd’ and ‘even’ reflections.

2021-08-17 Han I redid figure 18.65 in figure 3.10 using Mathematica, so the style of the figure is similar to figure 3.13. The lattice states in figure 3.10 and figure 3.13 are actual solutions of temporal cat with $s = 3$.

2021-08-17 Predrag Experimenting with colors in figure 3.10 (a) and figure 3.13 (b). There is no need to change your Mathematica code, this is best done for the publication version in Inkscape LaTeX labeled svg.

2021-08-22 Predrag I believe was wrong in asking that we look at the stability of repeats of a shorter period block, the 2021-06-11 Han, (18.341) post above. That does not arise in the new formulation of periodic orbit theory; the Hill determinant is computed on any lattice state X in the orbit \mathcal{M}_X (3.151) of a lattice state X . There are only orbits, nothing is computed on repeats. There should be no repeats summation in the derivation of zeta functions.

2021-05-11, 2021-08-05, 2021-08-22 Predrag zu Sam Spielen Sie es noch einmal, bitte:

What I do not understand is the relation between the symmetry of a lattice state (4.19) - (4.22), and the Hill determinant factorization of it. Am I supposed to extend this list to include the antisymmetric lattice states (4.25), (4.33)? Does each carry only the Hill determinant of the orbit Jacobian matrix $\text{Det}(\mathcal{J}_{\pm})$ with the same symmetry as the corresponding lattice state? If so, how do we get rid of the other $\text{Det}(\mathcal{J}_{\pm})$ in the factorized $\text{Det}(\mathcal{J})$?

Can you plot the appropriate lattice states, for temporal cat, but preferably for temporal Hénon, with analytic formulas for $\text{Det}(\mathcal{J}_{\pm})$?

2021-08-26 Han We already know how to count the number of periodic lattice states for temporal cat:

$$N_n = \prod_{j=0}^{n-1} \left(s - 2 \cos \frac{2\pi j}{n} \right) = 2T_n(s/2) - 2 = \Lambda^n + \Lambda^{-n} - 2, \quad (18.375)$$

where $\Lambda = \frac{1}{2}(s + \sqrt{(s-2)(s+2)})$. For $n = 2m - 1$,

$$N_{n,0} = \prod_{j=0}^{m-1} \left(s - 2 \cos \frac{2\pi j}{n} \right) = \sqrt{(\Lambda^n + \Lambda^{-n} - 2)(s-2)}. \quad (18.376)$$

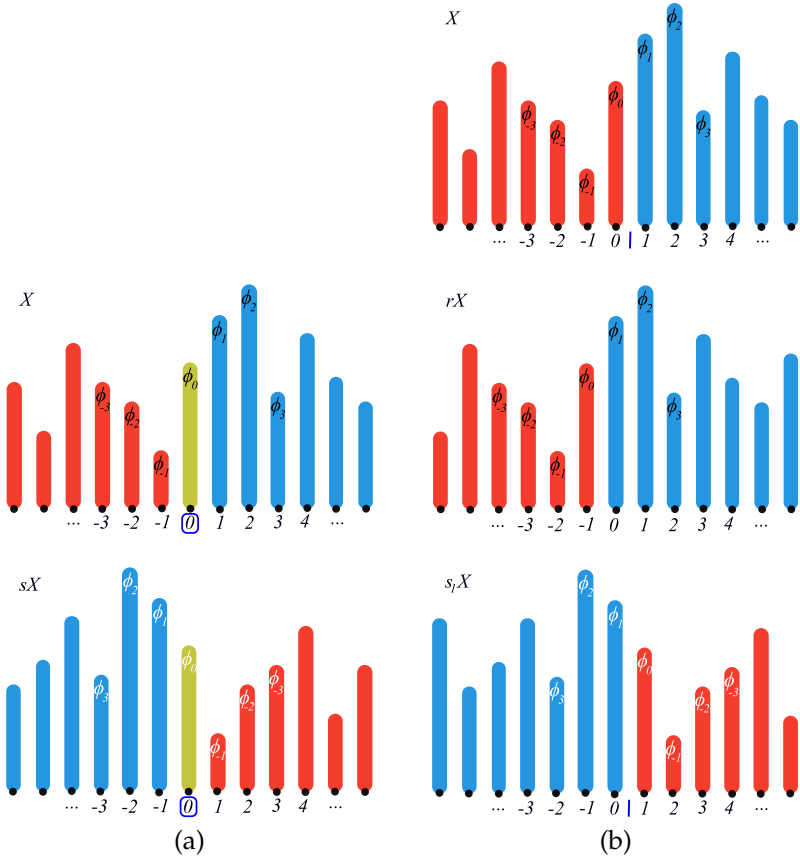


Figure 18.65: There are two classes (3.144) of lattice state reflections: even, across a lattice site, and odd, across the mid-point between a pair of adjacent lattice sites. (a) In example (3.146) even reflection σ exchanges (blue ϕ_j) \leftrightarrow (red ϕ_{-j}) while leaving the field ϕ_0 at lattice site $\boxed{0}$ fixed. (b) In example (3.147) odd $\sigma_1 = \sigma r$ swaps the ‘blues’ and the ‘reds’ by a lattice translation $X \rightarrow rX$, followed by a reflection σ . The result is a reflection across the midpoint of the $[01]$ interval, marked ‘|’. Horizontal: lattice sites $j \in \mathbb{Z}$. Vertical: lattice site fields ϕ_j , labeled by their values before the reflection.

For $n = 2m$,

$$\begin{aligned} N_{n,0} &= \prod_{j=0}^m \left(s - 2 \cos \frac{2\pi j}{n} \right) \\ N_{n,1} &= \prod_{j=0}^{m-1} \left(s - 2 \cos \frac{2\pi j}{n} \right), \end{aligned} \quad (18.377)$$

and

$$\frac{1}{2} (N_{n,0} + N_{n,1}) = \frac{s+3}{2} \prod_{j=0}^{m-1} \left(s - 2 \cos \frac{2\pi j}{n} \right) = \frac{s+3}{2} \sqrt{\frac{(\Lambda^n + \Lambda^{-n} - 2)(s-2)}{(s+2)}} \quad (18.378)$$

Note that:

$$\sqrt{\Lambda^n + \Lambda^{-n} - 2} = \sqrt{\Lambda^n (1 - \Lambda^{-n})^2} = |\Lambda^{n/2} - \Lambda^{-n/2}|. \quad (18.379)$$

Using this identity, the number of lattice states can be written as polynomials: For $n = 2m - 1$:

$$\begin{aligned} N_{n,0} &= \sqrt{s-2} \left| \Lambda^{n/2} - \Lambda^{-n/2} \right| \\ &= \sqrt{\frac{s-2}{\Lambda}} \left| \Lambda^m - \Lambda^{-m+1} \right|. \end{aligned} \quad (18.380)$$

For $n = 2m$:

$$\begin{aligned} \frac{1}{2} (N_{n,0} + N_{n,1}) &= \frac{s+3}{2} \sqrt{\frac{s-2}{s+2}} \left| \Lambda^{n/2} - \Lambda^{-n/2} \right| \\ &= \frac{s+3}{2} \sqrt{\frac{s-2}{s+2}} \left| \Lambda^m - \Lambda^{-m} \right|. \end{aligned} \quad (18.381)$$

Now we can compute the $h(t)$ from (3.207)

$$\begin{aligned} h(t) &= \sum_{m=1}^{\infty} \left[N_{2m-1,0} t^{2m-1} + (N_{2m,0} + N_{2m,1}) \frac{t^{2m}}{2} \right] \\ &= \sqrt{s-2} \frac{\Lambda^{1/2} t}{1 - \Lambda t^2} - \sqrt{s-2} \frac{\Lambda^{-1/2} t}{1 - \Lambda^{-1} t^2} \\ &\quad + \frac{s+3}{2} \sqrt{\frac{s-2}{s+2}} \frac{\Lambda t^2}{1 - \Lambda t^2} - \frac{s+3}{2} \sqrt{\frac{s-2}{s+2}} \frac{\Lambda^{-1} t^2}{1 - \Lambda^{-1} t^2}. \end{aligned} \quad (18.382)$$

Using (3.206) we have the "flip" part of the zeta function. Testing this zeta function using (3.233), we have:

$$\begin{aligned} -t \frac{\partial}{\partial t} (\ln e^{-h(t)}) &= t + 6t^2 + 12t^3 + 36t^4 + 55t^5 + 144t^6 \\ &\quad + 203t^7 + 504t^8 + 684t^9 + 1650t^{10} + \dots \end{aligned} \quad (18.383)$$

which is in agreement with (3.233) and table 18.3.

2021-08-29, 2021-08-30 Predrag I have been struggling with antisymmetric lattice states - see around eq. (4.34) - the Hill determinant that I got is wrong, will remove it from your blog.

Antisymmetric lattice states do not exist. I sketched - by hand, not posted here - the values of lattice state fields for the 6 temporal Hénon lattice states of table 2.3 and figure 2.3 in the same format as figure 3.13 (b). They are all nicely symmetric.

2021-08-30 Predrag I think I'm starting to understand *Máo Zhǔxí Yǔlù*. The 3 types of D_∞ symmetric states X are -well- symmetric, and that means that the number $\sim m$ of distinct fields that describe the corresponding period- n Bravais cell is $\sim n/2$. They satisfy non-periodic bc's equations such as (18.314).

The orbit Jacobian matrix $\mathcal{J}[X]$ is best understood by starting with the period- n Bravais cell stability. That block-diagonalizes into eigenvectors that *point within* the symmetry subspace of the same symmetry as the lattice state, and the (antisymmetric) rest, that *point out of* it. That's all as it should be for a fixed point with a symmetry.

It is all breathtakingly simple on the reciprocal lattice. Period- n Bravais cell maps onto a regular n -gon in the reciprocal lattice, with the usual D_n symmetry axes. Time reversal amounts to complex conjugation, and the symmetric solutions sit on the symmetry axes, which are also the boundaries of the fundamental domain. Lattice shift r_j maps out the G -orbit by running on circles, and orbits visit the $1/2n$ wedge only once, so the points in the fundamental domain represent an orbit each.

2021-08-30 Predrag Back to fuzzy thinking...

Q. can one construct invariant, lower dimensional subspace like (18.314), such that all 'dynamics' is restricted to it? In reciprocal space, only the orbits that sit on symmetry axes? What I call a 'flow-invariant subspace.'

That would be the famed 'square root' or 'golden' temporal Hénon.

2021-09-03 Predrag *Slicing the reciprocal lattice; stretching out the pizza slice into a full pizza per each Fourier mode.*

Inspect figure 3.5, 18.35, 18.52, 18.53, 18.58, 18.59, 18.60, ...: for C_n , wavenumbers $k > 1$ they have k -fold symmetry; for D_n , the $2k$ -fold symmetry. Why? If you plot all period- n lattice states at one go, you plot all their group orbits at one go. In k th mode, they rotate k times faster than the $k = 1$ irrep. It will amount to a Bernoulli map with slope k per each Fourier mode, with phase written as an integer (integer part of the phase $k\theta_k$ in units of 2π) + reminder representing angle across the fundamental pizza slice, scaled to 2π for C_n , and to π for D_n . There each orbit is represented by a single reciprocal lattice state.

That is illustrated by the C_5 figure 18.52(c) and D_5 figure 18.53(c) $k = 0, 1, 2$ fundamental domains $[-2\pi/(2nk), 2\pi/(2nk))$. Multiplied by $n k$ they fill out the whole (semi)circle for all n .

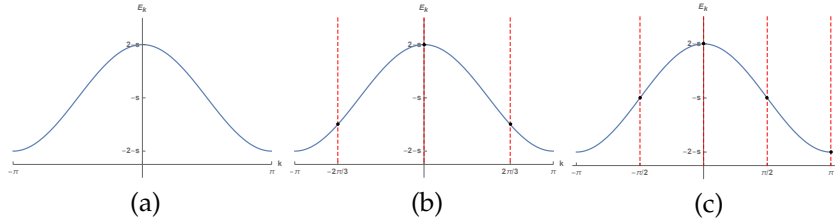


Figure 18.66: (a) The eigenvalue E_k of the orbit Jacobian matrix on the infinite lattice as a function of the wave vector k in the first Brillouin zone. The orbit Jacobian matrix has the reflection symmetry so the eigenvalue is also invariant under the reflection $k \rightarrow -k$. (b) For period 3 lattice states, the wave vectors of the eigenstates exist on the reciprocal lattice spanned by $2\pi/3$. These lattice sites are labeled by the red dashed lines. There are only 3 period 3 eigenstates, with eigenvalues $-1 - s$, $2 - s$ and $-1 - s$. (c) For period 4 lattice states, the wave vectors of the eigenstates exist on the reciprocal lattice spanned by $\pi/2$. These lattice sites are labeled by the red dashed lines. There are only 4 period 4 eigenstates, with eigenvalues $-s$, $2 - s$, $-s$ and $-2 - s$. $k = \pi$ and $k = -\pi$ are different by a reciprocal lattice translation, so they are a same wave vector and should be only counted once.

2021-09-06 Han Bloch theorem is not very useful to us. Let the (3.79) be the orbit Jacobian matrix that acts on the infinite lattice. The orbit Jacobian matrix \mathcal{J} commute with the translation operator r and the reflection operator σ , so it has the D_∞ symmetry. The translation group of D_∞ is described by a Bravais lattice, which is the integer lattice. So the reciprocal lattice of this Bravais lattice is spanned by the basis vector $b = 2\pi$. The eigenstates of the orbit Jacobian matrix have the form:

$$\psi_k(z) = e^{ikz} u(z),$$

where z is the coordinate on the 1-dimensional direct temporal space, $u(z)$ is a periodic function with period 1 (the periodicity of $u(z)$ is given by the integer lattice), and k is a wave vector in the first Brillouin zone $k \in (-\pi, \pi]$. For our problem the value of the function only exist on the integer lattice site, so function $u(z)$ with period 1 can be seen as a constant. The eigenstates of the orbit Jacobian matrix can always be written as:

$$\psi_k(z) = e^{ikz}$$

with eigenvalue $E_k = 2 \cos k - s$, which does not depend on the period of the eigenstate. Known that the wave vector k is in the first Brillouin zone, we can plot the 'eigenvalue band' of the orbit Jacobian matrix, as shown in figure 18.66.

After we have the 'eigenvalue band', we can find eigenstates that satisfy periodic boundary condition. If the period of the lattice state is n , the

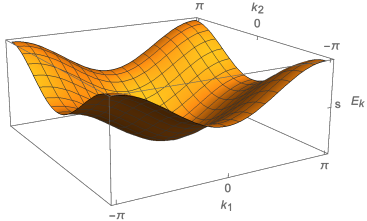


Figure 18.67: The eigenvalue E_k of the orbit Jacobian matrix on the infinite spatiotemporal lattice as a function of the wave vector k . The point group symmetry of the orbit Jacobian matrix is D_4 so the eigenvalue function also has the D_4 symmetry.

wave vector can only exist on a finer lattice in the reciprocal space, the lattice spanned by $2\pi/n$. Then only finite amount of wave vectors can be used as wave vectors of these periodic eigenstates. For example, in figure 18.66 (b) the reciprocal lattice sites of the period 3 lattice states are labeled by red dashed lines. There are only 3 reciprocal lattice sites in the first Brillouin zone. So we find 3 eigenstates, with wave vectors $k = -2\pi/3, 0$ and $2\pi/3$, and eigenvalues $-1 - s, 2 - s$ and $-1 - s$. In figure 18.66 (c) the reciprocal lattice sites of the period 4 lattice states are labeled by red dashed lines. There are only 4 reciprocal lattice sites in the first Brillouin zone. We find 4 eigenstates, with wave vectors $k = -\pi/2, 0, \pi/2$ and π , and eigenvalues $-s, 2 - s, -s$ and $-2 - s$. Note that $k = -\pi$ and $k = \pi$ are a same wave vector as they are different by a reciprocal lattice translation.

The point group symmetry of the orbit Jacobian matrix is also the symmetry of the 'eigenvalue band' in the reciprocal space. For the temporal cat lattice, we only need to know the eigenstates with wave vectors $k \geq 0$ as other eigenstates can be found by a reflection, and the eigenvalues are invariant under the reflection. For the 2-dimensional spatiotemporal cat lattice, as shown in figure 18.67, we only need eigenstates with wave vectors in 1/8 of the first Brillouin zone, the rest of the eigenstates can be found by reflections and rotations from the D_4 group.

The function E_k in the figure 18.66 is $E_k = 2 \cos(k) - s$. We can compute:

$$\exp \int_{-\pi}^{\pi} \ln |E_k| dk = \exp(2\pi \ln \Lambda) = \Lambda^{2\pi},$$

where Λ is the expanding eigenvalue of the cat map. This result is not surprising, because by computing the exponential of trace of the logarithm I'm hoping to find the determinant of the orbit Jacobian matrix on the infinite lattice. And the determinant of this orbit Jacobian matrix is probably the weight of a infinitely long lattice state which should converge to Λ^n as $n \rightarrow \infty$. The 2π is probably introduced by the integral

which can be fixed. But I'm hoping to find a formula that I can compute the determinant or trace of the orbit Jacobian matrix on infinite lattice times variable z plus some other operators and then retrieve, hopefully, the contribution to the dynamical zeta function from a single prime orbit.

2021-09-10 Han I do not have the Hamiltonian, forward-in-time Jacobian matrix J_t for an orbit with time reflection symmetry.

Let $f(\phi_{n-1}, \phi_n) = (\phi_n, \phi_{n+1})$ be the map forward in time. For cat map we have:

$$f(\phi_{n-1}, \phi_n) = (\phi_n, -\phi_{n-1} + s\phi_n) \pmod{1}. \quad (18.384)$$

And let map $t(\phi_{n-1}, \phi_n) = (\phi_n, \phi_{n-1})$ be the time reflection in the state space.

The Hamiltonian forward in time orbit Jacobian matrix is the Jacobian matrix of $(\phi_0, \phi_1) - f^n(\phi_0, \phi_1)$, if the time reversal symmetry is not taken into account. With the time reversal symmetry, a periodic point needs to satisfy a different set of conditions. Consider period-7 lattice state

$$\phi_0 | \overline{\phi_1 \phi_2 \phi_3 \phi_4} | \phi_3 \phi_2 \phi_1|. \quad (18.385)$$

2021-09-11 Predrag I do not like the interloper ϕ_0 in (18.385); notation $\overline{\text{block}}$ means infinite repeat of "block". At $-\infty$ you stick in ϕ_0 ; cannot do that. Also, please follow our convention (3.158) for odd period orbits:

$$|\overline{\phi_0} \phi_1 \phi_2 \phi_3 | \phi_3 \phi_2 \phi_1|. \quad (18.386)$$

2021-09-10 Han If the period-7 lattice state is $\phi_0 | \overline{\phi_1 \phi_2 \phi_3 \phi_4} | \phi_3 \phi_2 \phi_1|$, the two boundaries need to satisfy

$$t(\phi_0, \phi_1) = (\phi_0, \phi_1), \quad (18.387)$$

and

$$t \circ f(\phi_3, \phi_4) = (\phi_3, \phi_4). \quad (18.388)$$

So now we have 3 conditions that need to be satisfied:

$$\begin{aligned} (\phi_0, \phi_1) - t(\phi_0, \phi_1) &= 0, \\ (\phi_3, \phi_4) - t \circ f(\phi_3, \phi_4) &= 0, \\ (\phi_3, \phi_4) - f^3(\phi_0, \phi_1) &= 0. \end{aligned} \quad (18.389)$$

If we compute the determinant of the Jacobian matrix of the first and second conditions, the results are 0, which means that there are a continuous set of points in the state space that satisfy these two conditions. I have tried to use the first two conditions to write ϕ_1 as a function of ϕ_0 , and

ϕ_4 and a function of ϕ_3 , then compute the determinant of the Jacobian matrix:

$$\tilde{\mathcal{J}} = \frac{\partial[(\phi_3, \phi_4(\phi_3)) - f^3(\phi_0, \phi_1(\phi_0))]}{\partial(\phi_0, \phi_3)}, \quad (18.390)$$

but the result is apparently wrong (not an integer for cat map). So we cannot perturb any two field values and get the correct Hill determinant.

Let $F(\phi_0, \phi_1, \phi_3, \phi_4)$ be a function with 4 components. The first two components are given by $(\phi_3, \phi_4) - f^3(\phi_0, \phi_1)$. The third and fourth components are $\phi_0 - \phi_1$ and $2\phi_3 - s\phi_4$ (for cat map), which are equal to 0 if the first two conditions in (18.389) are satisfied. Then the Hill determinant is:

$$\begin{aligned} \text{Det}(\tilde{\mathcal{J}}) &= -s^4 + s^3 + 4s^2 - 3s - 2 \\ &= -\mu^2 (\mu^6 + 7\mu^4 + 14\mu^2 + 7), \end{aligned} \quad (18.391)$$

which is equal to -76 if $s = 3, \mu = 1$, in agreement with table 18.3. I wonder if the coefficients 7 and 14 have something to do with the lattice state period being 7.

2021-09-11 Predrag I get $\text{Det}(\tilde{\mathcal{J}}) = -29$, which is -up to the sign- in agreement with table 18.3.

2021-09-11 Predrag We really have to rethink the definition of orbit Jacobian matrices to avoid this pesky minus signs for odd period Hill determinants.

2021-09-11 Predrag I was expecting vaguely something like

$$\begin{aligned} &\boxed{\phi_0} \phi_1 \phi_2 \phi_3 | \phi_3 \phi_2 \phi_1 \\ J^7(\phi_0) &= \sqrt{J_0} J_1^\top J_2^\top J_3^\top J_3 J_2 J_1 \sqrt{J_0} \\ &= \sigma \tilde{J}_{\tilde{p}} \sigma_1 \tilde{J}_{\tilde{p}} \\ \text{Det}(\tilde{J}_{\tilde{p}}) &= \det(1 - \tilde{J}_{\tilde{p}}), \end{aligned} \quad (18.392)$$

where $J_t = J(\phi_t)$ is the 1-time-step Jacobian matrix evaluated on lattice site ϕ_i ; see example 2.4 for what these 2-dimensional Jacobian matrices products look like.

The square roots are in the spirit of the boundary orbit treatment in Chaos-Book Example 25.9. Reflection symmetric 1-d maps.

2021-09-12 Predrag The above square roots are suspect, they come from my insistence on the reflection border being "shared" by the adjacent tiles. The correct formulation is probably the inclusion-exclusion principle (18.278), (1.91).

2021-09-14 Predrag Some matrix square roots around eq. (15.57). See also the discussion around eq. (18.305).

2021-09-14 Predrag Checked that the orbit Jacobian matrix factorization (4.40), metal temporal lattice condition (4.41) works also for the orbit X dependent case (3.84).

That presumably takes care of the no reflection symmetry case figure 3.157. Symmetric cases (3.158)-(3.160) still require boundary conditions treatment.

As to the time-step case (18.392), I would prefer 1/2 time step $J = \tilde{J}^\top \tilde{J}$ -type factorization to taking a square. It's the right form for time-reversal symmetry, I think.

2021-09-24 Predrag to Han Looking at sect. 3.7.2 *Cyclic groups*, I think there is more to get out of the $s = 2$ Bernoulli example.

On the reciprocal lattice only symmetry subspace is the origin (I think); you can define the fundamental domain as any wedge of angular width $2\pi/n$ (I think) but thinking ahead to the D_n case, it's natural to take real axis as the border included in the fundamental domain, and its $2\pi/n$ rotation as the other, open set border, not a part of the fundamental domain.

For a generic dynamical system there is no time reversal symmetry, so no lattice state lies on the real axis. For Bernoulli you can probably show it, as you have all lattice states in the analytic form (1.83).

Here is my question:

We know all [ChaosBook binary-labelled](#) Bernoulli orbits and their [ChaosBook numbers](#) for $s = 2, 3, 4$. My current understanding that each *orbit* visits the fundamental domain only once, with all irrep points rotated into the fundamental domain, different rotation for each wavenumber k . Is that correct?

2021-09-24 Predrag to everybody A deep but important question for reformulating all of "dynamics" as (lattice) field theory:

One important advantage of the reformulation is that we find all computations (determining lattice states, Hill determinants) more effective and natural on the reciprocal lattice.

How does pruning work in the global, lattice formulation? Can we see it on the reciprocal lattice? In the fundamental domain, where we only see orbits, not the range of lattice states of which perhaps only one strays into the inadmissible territory?

Fundamental (to me) is the pruning theory, the criteria for inadmissible orbits, see [ChaosBook sect. 14.5 Kneading theory](#) and [ChaosBook sect. 15.4 Prune Danish](#).

Is there a pruning criterion on the reciprocal lattice?

I would start by the reciprocal kneading value lattice state for a tent map or Bernoulli map (maybe that one first?), color all pruned orbits a different color, and see whether there is a 'pruning front' in the fundamental domain?

2021-10-18 Predrag to Han You might enjoy the discussion of “fundamental domains” in

 *Knots in hyperbolic space.*

now in CB

2021-10-31 Predrag to Han Does not mention ‘Burnside’, but seems like [Matt Macauley](#) ([homepage](#)) on visualizing group actions is a possible path to understanding Burnside marks...

The course is [here](#), and it, as well as Dana Ernst’s online [An inquiry-based approach to abstract algebra](#) are inspired by

Nathan Carter’s [Visual Group Theory](#), (read it online through [GaTech-Library](#)) seems very good.

Now, none of the above has “Burnside” in their index. The next one does:

Also available online: Tom Judson’s online [Abstract Algebra: Theory and Applications](#).

Obviously, I’ve fallen into a major rabbit hole, better stop now:)

2021-10-31 Predrag to Han I have mentioned that you have to derive trace formula / spectral determinant only for a single unstable lattice state. Once you have that, you simply put the infinity of them together. That is explained in [ChaosBook Appendix A39 Semiclassical quantization, with corrections](#), see [ChaosBook eq. \(39.11\)](#).

You would do Vattay a favor if you drew [ChaosBook Figure A39.1](#), he was too excited with the implications of this chapter to actually do himself such a lowly thing.

2021-11-18 Predrag to Han Have a look at [ChaosBook Append. A33 Statistical mechanics recycled](#). Might be not useful for what you are thinking about now, but the original intention was along the lines we are exploring now: connecting dynamics approaches to the traditional statistical mechanics. Ronnie also wrote a series of articles on this approach [[43–48](#)], and there might be more.

2021-11-16 Han In Lind [[38](#)] and Kim *et al.* [[35](#)] the maps of a dynamical system are related to group operations. For a system with time reversal symmetry, there are two maps. $f : \mathcal{M} \rightarrow \mathcal{M}$ is the map forward in time and $t : \mathcal{M} \rightarrow \mathcal{M}$ is the flip in the state space. These two maps satisfy:

$$t \circ t = 1, \quad t \circ f \circ t = f^{-1}. \quad (18.393)$$

The kernels of the Perron-Frobenius operators of these two maps are

$$\mathcal{L}_f(x, y) = \delta(x - f(y)), \quad \mathcal{L}_t(x, y) = \delta(x - t(y)). \quad (18.394)$$

The Perron-Frobenius operators satisfy the same relation as the group

operation:

$$\begin{aligned}
 (\mathcal{L}_t \circ \mathcal{L}_f \circ \mathcal{L}_t \rho)(x) &= \int_{\mathcal{M}} dy dz dw \delta(x - t(y)) \delta(y - f(z)) \delta(z - t(w)) \rho(w) \\
 &= \int_{\mathcal{M}} dz dw \delta(x - t \circ f(z)) \delta(z - t(w)) \rho(w) \\
 &= \int_{\mathcal{M}} dw \delta(x - t \circ f \circ t(w)) \rho(w) \\
 &= \int_{\mathcal{M}} dw \delta(x - f^{-1}(w)) \rho(w) \\
 &= (\mathcal{L}_{f^{-1}} \rho)(x)
 \end{aligned} \tag{18.395}$$

$$\begin{aligned}
 (\mathcal{L}_t \circ \mathcal{L}_t \rho)(x) &= \int_{\mathcal{M}} dy dz \delta(x - t(y)) \delta(y - t(z)) \rho(z) \\
 &= \int_{\mathcal{M}} dz \delta(x - z) \rho(z) \\
 &= \rho(x).
 \end{aligned} \tag{18.396}$$

So we have:

$$\mathcal{L}_t \circ \mathcal{L}_f \circ \mathcal{L}_t = \mathcal{L}_{f^{-1}}, \quad \mathcal{L}_t \circ \mathcal{L}_t = 1. \tag{18.397}$$

So the Perron-Frobenius operators are linear representations of the D_∞ group. Then the leading eigenvalue of \mathcal{L}_f is 1, which is incorrect because it implies that the system is bounded.

2021-10-29 Han A lattice state is a set of lattice site field values $\mathbf{X} = \{\phi_z\}$ that satisfies the defining equation at every lattice site. The defining equation can be rewritten as a fixed point condition $F[\mathbf{X}] = 0$. The fixed point condition satisfied by a periodic lattice state with period n is $F_n[\mathbf{X}_n] = 0$, where $F_n[\mathbf{X}_n]$ and \mathbf{X}_n are n -dimensional vectors.

The weight of lattice states are computed from:

$$\int \delta(F_n[\mathbf{X}_n]) e^{\beta A(\mathbf{X})} d\mathbf{X}_n = \sum_{\{\mathbf{X}_i : F_n[\mathbf{X}_i] = 0\}} \frac{e^{\beta A(\mathbf{X}_i)}}{|\det \mathcal{J}_i|} \tag{18.398}$$

where

$$\mathcal{J}_i = \frac{\partial F_n[\mathbf{X}_i]}{\partial \mathbf{X}_i}$$

is the orbit Jacobian matrix. From the Hill's formula we know that this is equal to the trace of the time evolution operator:

$$\text{tr } \mathcal{L}^n = \int \delta(\phi - f^n(\phi)) e^{\beta A(\phi)} d\phi = \sum_{\phi_i \in \text{Fix } f^n} \frac{e^{\beta A_i}}{|\det(\mathbf{1} - M^n(\phi_i))|} \tag{18.399}$$

2021-10-29 Han The expectation value of an observable can be computed from the expectation value of the time evolution operator:

$$\langle e^{\beta A} \rangle = \frac{1}{|\mathcal{M}|} \int_{\mathcal{M}} dx \int_{\mathcal{M}} dy \delta(y - f^t(x)) e^{\beta A} = \frac{1}{|\mathcal{M}|} \langle \mathcal{L}^t \rangle. \quad (18.400)$$

Set $\beta = 0$. The time evolution operator acts on a density distribution function as:

$$\begin{aligned} [\mathcal{L}^n \psi](\phi_n)|_{\psi(\phi_0)=1} &= \int_{\mathcal{M}} d\phi_0 \delta(\phi_n - f^n(\phi_0)) \\ &= \int_{\mathcal{M}} d\phi_{n-1} d\phi_{n-2} \dots d\phi_2 d\phi_1 d\phi_0 \\ &\quad \delta(\phi_n - f(\phi_{n-1})) \delta(\phi_{n-1} - f(\phi_{n-2})) \\ &\quad \dots \delta(\phi_2 - f(\phi_1)) \delta(\phi_1 - f(\phi_0)). \end{aligned} \quad (18.401)$$

Let X be the lattice state:

$$X = \begin{pmatrix} \phi_0 \\ \phi_1 \\ \phi_2 \\ \vdots \\ \phi_{n-2} \\ \phi_{n-1} \end{pmatrix}. \quad (18.402)$$

And function F be:

$$F(X, \phi_n) = \begin{pmatrix} \phi_1 \\ \phi_2 \\ \phi_3 \\ \vdots \\ \phi_{n-1} \\ \phi_n \end{pmatrix} - \begin{pmatrix} f(\phi_0) \\ f(\phi_1) \\ f(\phi_2) \\ \vdots \\ f(\phi_{n-2}) \\ f(\phi_{n-1}) \end{pmatrix}. \quad (18.403)$$

The product of delta function is a delta function of function F :

$$\prod_{i=0}^{n-1} \delta(\phi_{i+1} - f(\phi_i)) = \delta(F(X, \phi_n)). \quad (18.404)$$

And the time evolution operator can be rewritten as:

$$[\mathcal{L}^n \psi](\phi_n)|_{\psi(\phi_0)=1} = \int dX \delta(F(X, \phi_n)). \quad (18.405)$$

The trace of the time evolution operator is:

$$\begin{aligned} \text{tr } \mathcal{L}^n &= \int d\phi_n d\phi_0 \delta(\phi_n - \phi_0) \mathcal{L}^n(\phi_n, \phi_0) \\ &= \int dX \delta(F(X, \phi_0)). \end{aligned} \quad (18.406)$$

Let

$$F(\phi_0, \phi_1, \dots, \phi_{n-1}, \phi_0) = F_p(\phi_0, \phi_1, \dots, \phi_{n-1}) = F_p(\mathbf{X}). \quad (18.407)$$

$F_p(\mathbf{X}) = 0$ is the fixed point condition of the lattice state. Compute the trace in a small neighborhood around a fix point ϕ_j :

$$\begin{aligned} \int_{\mathcal{M}_j} d\phi \delta(\phi - f^n(\phi)) &= \int_{\mathcal{M}_{\mathbf{X}_j}} d\mathbf{X} \delta(F(\mathbf{X})) \\ \frac{1}{|\det(\mathbb{1} - \mathbb{J}(\phi_j))|} &= \frac{1}{|\text{Det } \mathcal{J}_j|}. \end{aligned} \quad (18.408)$$

$$\mathcal{J}_j = \frac{\partial F(\mathbf{X}_j)}{\partial \mathbf{X}_j}, \quad (18.409)$$

is the Jacobian matrix of function $F(\mathbf{X})$ at \mathbf{X}_j , which is a periodic lattice state that starts with ϕ_j .

In the previous example, the state ϕ generally is a vector. So this relation (Hill's formula) applies to maps with any dimension. If there exists a multiple points recurrence relation, the orbit Jacobian matrix can be written in a more compact way.

Consider a map with a 3-point recurrence relation. Let $\hat{\phi}_i = (\phi_i, \phi_{i+1})$. The map in the 2-dimensional state space has the form:

$$\begin{aligned} \hat{\phi}_i &= \hat{f}(\hat{\phi}_{i-1}) \\ (\phi_i, \phi_{i+1}) &= (\phi_i, f(\phi_{i-1}, \phi_i)). \end{aligned} \quad (18.410)$$

The the time evolution operator satisfies:

$$\begin{aligned} [\mathcal{L}^n \psi](\hat{\phi}_n) \Big|_{\psi(\hat{\phi}_0)=1} &= \int_{\mathcal{M}} d\hat{\phi}_0 \delta(\hat{\phi}_n - \hat{f}^n(\hat{\phi}_0)) \\ &= \int_{\mathcal{M}} d\phi_0 d\phi_1 \delta(\hat{\phi}_n - \hat{f}^n(\hat{\phi}_0)) \\ &= \int_{\mathcal{M}} d\phi'_n d\phi'_{n-1} d\phi_{n-1} d\phi'_{n-2} \dots d\phi_2 d\phi'_1 d\phi_1 d\phi_0 \\ &\quad \delta(\phi_n - \phi'_n) \delta(\phi_{n+1} - f(\phi'_n, \phi'_{n-1})) \\ &\quad \delta(\phi'_{n-1} - \phi_{n-1}) \delta(\phi'_n - f(\phi'_{n-2}, \phi_{n-1})) \\ &\quad \dots \\ &\quad \delta(\phi'_2 - \phi_2) \delta(\phi_3 - f(\phi_1, \phi_2)) \\ &\quad \delta(\phi'_1 - \phi_1) \delta(\phi_2 - f(\phi_0, \phi_1)) \\ &= \left(\prod_{i=0}^{n-1} \int_{\mathcal{M}} d\phi_i \right) \left(\prod_{i=0}^{n-1} \delta(\phi_{i+2} - f(\phi_i, \phi_{i+1})) \right). \end{aligned} \quad (18.411)$$

Let \mathbf{X} be the lattice state:

$$\mathbf{X} = \begin{pmatrix} \phi_0 \\ \phi_1 \\ \phi_2 \\ \vdots \\ \phi_{n-2} \\ \phi_{n-1} \end{pmatrix}. \quad (18.412)$$

And function F be:

$$F(\mathbf{X}, \phi_n, \phi_{n+1}) = \begin{pmatrix} \phi_2 \\ \phi_3 \\ \phi_4 \\ \vdots \\ \phi_n \\ \phi_{n+1} \end{pmatrix} - \begin{pmatrix} f(\phi_0, \phi_1) \\ f(\phi_1, \phi_2) \\ f(\phi_2, \phi_3) \\ \vdots \\ f(\phi_{n-2}, \phi_{n-1}) \\ f(\phi_{n-1}, \phi_n) \end{pmatrix}. \quad (18.413)$$

$$[\mathcal{L}^n \psi](\hat{\phi}_n) \Big|_{\psi(\hat{\phi}_0)=1} = \int d\mathbf{X} \delta(F(\mathbf{X}, \phi_n, \phi_{n+1})). \quad (18.414)$$

The trace of the time evolution operator is:

$$\begin{aligned} \text{tr } \mathcal{L}^n &= \int d\hat{\phi}_n d\hat{\phi}_0 \delta(\hat{\phi}_n - \hat{\phi}_0) \mathcal{L}^n(\hat{\phi}_n, \hat{\phi}_0) \\ &= \int d\phi_{n+1} d\phi_n \dots d\phi_1 d\phi_0 \delta(F(\phi_0, \phi_1, \dots, \phi_n, \phi_{n+1})) \delta(\phi_0 - \phi_n) \delta(\phi_1 - \phi_{n+1}) \\ &= \int d\mathbf{X} \delta(F(\mathbf{X}, \phi_0, \phi_1)). \end{aligned} \quad (18.415)$$

Let

$$F_p(\mathbf{X}) = F(\phi_0, \phi_1, \dots, \phi_{n-2}, \phi_{n-1}, \phi_0, \phi_1). \quad (18.416)$$

$F_p(\mathbf{X}) = 0$ is the fixed point condition. Compute the trace in a small neighborhood around a fix point $\hat{\phi}_j$:

$$\begin{aligned} \int_{\mathcal{M}_j} d\hat{\phi} \delta(\hat{\phi} - \hat{f}^n(\hat{\phi})) &= \int_{\mathcal{M}_{\mathbf{X}_j}} d\mathbf{X} \delta(F(\mathbf{X})) \\ \frac{1}{|\det(\mathbb{1} - \mathbb{J}(\hat{\phi}_j))|} &= \frac{1}{|\text{Det } \mathcal{J}_j|}, \end{aligned} \quad (18.417)$$

where

$$\mathcal{J}_j = \frac{\partial F(\mathbf{X}_j)}{\partial \mathbf{X}_j}, \quad (18.418)$$

is jacobian matrix of $F(\mathbf{X})$ at \mathbf{X}_j , a periodic lattice state that starts with $\hat{\phi}_j$.
The \mathcal{J}_j is a $[n \times n]$ orbit Jacobian matrix.

2021-11-27 Predrag to Han Continuing today's discussion:

The Cvitanović and Vattay unpublished draft *Variational principle for noisy dynamics* explains how the leading noisy $\sqrt{\text{Det } \mathcal{J}}$ becomes the classical $\text{Det } \mathcal{J}$ (I believe that is included into ChaosBook, but I have not checked). So that would be one way to go from noisy dynamics to the deterministic limit, but I hope we can avoid this in the current paper.

Cvitanović, Dettmann, Mainieri and Vattay *Trace formulae for stochastic evolution operators: Weak noise perturbation theory* [21] and *Smooth conjugation method* [22] starts out by expressing the weak noise expansions in terms of Dirac δ and its derivatives. (For now) you are interested in keeping only the leading term, i.e., the Dirac δ that yields $1/\text{Det } \mathcal{J}$. Exponentiated action appears naturally. See sect. 5.9 *Noise is your friend*.

None of the above have orbit Jacobian matrix, they are all formulated as time-stepping. I think we want to emphasize the primacy of the orbit Jacobian matrix, consider time-evolution as one (awkward) way of formally evaluating $\text{Det } \mathcal{J}$, I say "formally" as time evolution stability cannot be implemented in practice due to exponential overflows / underflows in any numerical evaluation.

Field theorists think of euclidean field theory as sum over probabilities $p(\phi) = \exp(-S[\phi])/Z$, see (5.133). The papers cited there might have a reference to a simple derivation of that formula. I derive it in Cvitanović [15] *Field Theory*, but I hope you do not have to go through that, that takes 1/3 of a semester-long course.

The ϵ trick I talked about is the 'Gaussian damping factor', see mu *Field Theory* [15] *sect. 3B Gaussian integrals*, eq. (3.8).

No one ever promised us *A Rose Garden* :)

References

- [1] R. L. Adler and B. Weiss, "Entropy, a complete metric invariant for automorphisms of the torus", Proc. Natl. Acad. Sci. USA **57**, 1573–1576 (1967).
- [2] R. L. Adler and B. Weiss, *Similarity of automorphisms of the torus*, Vol. 98, Memoirs Amer. Math. Soc. (Amer. Math. Soc., Providence RI, 1970).
- [3] V. I. Arnol'd and A. Avez, *Ergodic Problems of Classical Mechanics* (Addison-Wesley, Redwood City, 1989).
- [4] M. Baake, J. Hermisson, and A. B. Pleasants, "The torus parametrization of quasiperiodic LI-classes", J. Phys. A **30**, 3029–3056 (1997).
- [5] M. Baake, N. Neumärker, and J. A. G. Roberts, "Orbit structure and (reversing) symmetries of toral endomorphisms on rational lattices", Discrete Continuous Dyn. Syst. **33**, 527–553 (2013).

- [6] M. Baake, J. A. G. Roberts, and A. Weiss, “Periodic orbits of linear endomorphisms on the 2-torus and its lattices”, *Nonlinearity* **21**, 2427 (2008).
- [7] J.-C. Ban, W.-G. Hu, S.-S. Lin, and Y.-H. Lin, *Zeta Functions for Two-dimensional Shifts of Finite Type*, Vol. 221, Memoirs Amer. Math. Soc. (Amer. Math. Soc., Providence RI, 2013).
- [8] A. Barvinok, *A Course in Convexity* (Amer. Math. Soc., New York, 2002).
- [9] A. Barvinok, *Lattice Points, Polyhedra, and Complexity*, tech. rep. (Univ. of Michigan, Ann Arbor MI, 2004).
- [10] A. Barvinok, *Integer Points in Polyhedra* (European Math. Soc. Pub., Berlin, 2008).
- [11] M. Beck and S. Robins, *Computing the Continuous Discretely* (Springer, New York, 2007).
- [12] N. Bird and F. Vivaldi, “Periodic orbits of the sawtooth maps”, *Physica D* **30**, 164–176 (1988).
- [13] S. V. Bolotin and D. V. Treschev, “Hill’s formula”, *Russ. Math. Surv.* **65**, 191 (2010).
- [14] S. C. Creagh, “Quantum zeta function for perturbed cat maps”, *Chaos* **5**, 477–493 (1995).
- [15] P. Cvitanović, *Field Theory*, Notes prepared by E. Gyldenkerne (Nordita, Copenhagen, 1983).
- [16] P. Cvitanović, *Group Theory: Birdtracks, Lie's and Exceptional Groups* (Princeton Univ. Press, Princeton NJ, 2008).
- [17] P. Cvitanović, “Charting the state space”, in *Chaos: Classical and Quantum*, edited by P. Cvitanović, R. Artuso, R. Mainieri, G. Tanner, and G. Vattay (Niels Bohr Inst., Copenhagen, 2018).
- [18] P. Cvitanović, “Walkabout: Transition graphs”, in *Chaos: Classical and Quantum*, edited by P. Cvitanović, R. Artuso, R. Mainieri, G. Tanner, and G. Vattay (Niels Bohr Inst., Copenhagen, 2018).
- [19] P. Cvitanović, R. Artuso, R. Mainieri, G. Tanner, and G. Vattay, *Chaos: Classical and Quantum* (Niels Bohr Inst., Copenhagen, 2020).
- [20] P. Cvitanović, R. Artuso, L. Rondoni, and E. A. Spiegel, “Transporting densities”, in *Chaos: Classical and Quantum*, edited by P. Cvitanović, R. Artuso, R. Mainieri, G. Tanner, and G. Vattay (Niels Bohr Inst., Copenhagen, 2017).
- [21] P. Cvitanović, C. P. Dettmann, R. Mainieri, and G. Vattay, “Trace formulas for stochastic evolution operators: Weak noise perturbation theory”, *J. Stat. Phys.* **93**, 981–999 (1998).
- [22] P. Cvitanović, C. P. Dettmann, R. Mainieri, and G. Vattay, “Trace formulae for stochastic evolution operators: Smooth conjugation method”, *Nonlinearity* **12**, 939 (1999).

- [23] P. Cvitanović and H. Liang, *Spatiotemporal cat: A chaotic field theory*, In preparation, 2021.
- [24] J. A. De Loera, R. Hemmecke, J. Tauzer, and R. Yoshida, “Effective lattice point counting in rational convex polytopes”, *J. Symbolic Comp.* **38**, 1273–1302 (2004).
- [25] R. L. Devaney, *An Introduction to Chaotic Dynamical systems*, 2nd ed. (Westview Press, Cambridge, Mass, 2008).
- [26] S. Elaydi, *An Introduction to Difference Equations*, 3rd ed. (Springer, Berlin, 2005).
- [27] J. A. C. Gallas, “Counting orbits in conjugacy classes of the Hénon Hamiltonian repeller”, *Phys. Lett. A* **360**, 512–514 (2007).
- [28] I. S. Gradshteyn and I. M. Ryzhik, *Tables of Integrals, Series and Products*, 8th ed. (Elsevier LTD, Oxford, New York, 2014).
- [29] T. Grava, T. Kriecherbauer, G. Mazzuca, and K. D. T-R. McLaughlin, “Correlation functions for a chain of short range oscillators”, *J. Stat. Phys.* **183**, 1 (2021).
- [30] J. Guckenheimer and B. Meloon, “Computing periodic orbits and their bifurcations with automatic differentiation”, *SIAM J. Sci. Comput.* **22**, 951–985 (2000).
- [31] B. Gutkin, L. Han, R. Jafari, A. K. Saremi, and P. Cvitanović, “Linear encoding of the spatiotemporal cat map”, *Nonlinearity* **34**, 2800–2836 (2021).
- [32] B. Gutkin and V. Osipov, “Classical foundations of many-particle quantum chaos”, *Nonlinearity* **29**, 325–356 (2016).
- [33] S. Holmin, Geometry of Numbers, Class Group Statistics and Free Path Lengths, PhD thesis (KTH Royal Inst. Technology, Stockholm, 2015).
- [34] E. V. Ivashkevich, N. S. Izmailian, and C.-K. Hu, “Kronecker’s double series and exact asymptotic expansions for free models of statistical mechanics on torus”, *J. Phys. A* **35**, 5543–5561 (2002).
- [35] Y.-O. Kim, J. Lee, and K. K. Park, “A zeta function for flip systems”, *Pacific J. Math.* **209**, 289–301 (2003).
- [36] D. A. Klain and G.-C. Rota, *Introduction to Geometric Probability* (Cambridge Univ. Press, 2006).
- [37] H.-T. Kook and J. D. Meiss, “Application of Newton’s method to Lagrangian mappings”, *Physica D* **36**, 317–326 (1989).
- [38] D. A. Lind, “A zeta function for Z^d -actions”, in *Ergodic Theory of Z^d Actions*, edited by M. Pollicott and K. Schmidt (Cambridge Univ. Press, 1996), pp. 433–450.
- [39] D. A. Lind and B. Marcus, *An Introduction to Symbolic Dynamics and Coding* (Cambridge Univ. Press, Cambridge, 1995).

- [40] D. Lind and K. Schmidt, “Symbolic and algebraic dynamical systems”, in *Handbook of Dynamical Systems*, Vol. 1, edited by B. Hasselblatt and A. Katok (Elsevier, New York, 2002), pp. 765–812.
- [41] R. S. MacKay, *Renormalisation in Area-preserving Maps* (World Scientific, Singapore, 1993).
- [42] R. S. MacKay and J. D. Meiss, “Linear stability of periodic orbits in Lagrangian systems”, *Phys. Lett. A* **98**, 92–94 (1983).
- [43] R. Mainieri, Thermodynamic zeta functions for Ising models with long-range interactions, PhD thesis (Physics Dept., New York Univ., 1990).
- [44] R. Mainieri, “Thermodynamic zeta functions for Ising models with long-range interactions”, *Phys. Rev. A* **45**, 3580–3591 (1992).
- [45] R. Mainieri, “Zeta-function for the Lyapunov exponent of a product of random matrices”, *Phys. Rev. Lett.* **68**, 1965–1968 (1992).
- [46] R. Mainieri, Can averaged orbits be used to extract scaling functions?, 1993.
- [47] R. Mainieri, “Cycle expansions with pruned orbits have branch points”, *Physica D* **83**, 206–215 (1995).
- [48] R. Mainieri, Geometrization of spin systems using cycle expansions, 1995.
- [49] C. Meyer, *Matrix Analysis and Applied Linear Algebra* (SIAM, Philadelphia, 2000).
- [50] T. Morita, “Useful procedure for computing the lattice Green’s function - square, tetragonal, and bcc lattices”, *J. Math. Phys.* **12**, 1744–1747 (1971).
- [51] I. Percival and F. Vivaldi, “A linear code for the sawtooth and cat maps”, *Physica D* **27**, 373–386 (1987).
- [52] I. Percival and F. Vivaldi, “Arithmetical properties of strongly chaotic motions”, *Physica D* **25**, 105–130 (1987).
- [53] C. Pozrikidis, *An Introduction to Grids, Graphs, and Networks* (Oxford Univ. Press, Oxford , UK, 2014).
- [54] F. Riesz and B. Sz.-Nagy, *Functional Analysis* (Dover Publ., Mineola, NY, 1955).
- [55] R. C. Robinson, *An Introduction to Dynamical Systems: Continuous and Discrete* (Amer. Math. Soc., New York, 2012).
- [56] I. Stewart and D. Gökaydin, “Symmetries of quotient networks for doubly periodic patterns on the square lattice”, *Int. J. Bifur. Chaos* **29**, 1930026 (2019).
- [57] F. Y. Wu, “Theory of resistor networks: the two-point resistance”, *J. Phys. A* **37**, 6653–6673 (2004).

Chapter 19

Frequencies of Cat Map Winding Numbers

Rana Jafari Summer 2016 Report

19.1 Introduction

The linear mapping A on unit 2-torus is defined as follows:

$$A = \begin{pmatrix} a & 1 \\ ab - 1 & b \end{pmatrix}$$
$$\begin{pmatrix} q_{t+1} \\ p_{t+1} \end{pmatrix} = A \begin{pmatrix} q_t \\ p_t \end{pmatrix} \quad \text{mod } 1 \quad (19.1)$$

Such ‘toral automorphisms’ provide very simple examples of chaotic Hamiltonian dynamical system. The unit determinant results in measure preservation, and $|\text{Tr}(A)| > 2$ in hyperbolicity. We shall refer to the $s = 3$ case as the ‘Arnol’d cat map’ (also known as the Arnol’d-Sinai cat map [1, 3]), and to cases where integer $s > 3$ as ‘cat maps’. The integers obtained by taking modulo 1 can be interpreted as winding numbers [6]. Rational and irrational initial coordinates generate periodic and ergodic orbits, respectively. The properties of periodic orbits are studied in detail by Percival and Vivaldi [7]. The initial part of this report focuses on finding the frequencies of winding numbers generated by the iterations of map (19.1) for different integer values of $s = \text{Tr } A$. These frequencies enable us to find the areas of partitions in phase space corresponding to words of symbolic dynamics of Arnol’d cat map. In sect. 19.4 we apply these methods to computation of the frequencies of symbol patterns for spatiotemporal cats.

19.2 Numbers of periodic orbits

The number of period- n periodic points of the $[2 \times 2]$ matrix transformation \mathbf{A} on a unit torus $[0, 1] \times [0, 1]$, is equal to number of fixed points of transformation \mathbf{A}^n .¹ We can find this number by solving:

$$\mathbf{A}^n \mathbf{x}_0 = \mathbf{x}_0 \pmod{1} \quad (19.2)$$

$$\Rightarrow (\mathbf{A}^n - \mathbf{I}) \mathbf{x}_0 = \mathbf{v}$$

where \mathbf{v} is an integer valued column vector. The number of solutions to (19.2) is equal to $|\det(\mathbf{A}^n - \mathbf{I})|$. Since the $(\mathbf{A}^n - \mathbf{I})\mathbf{x}_0$ transforms unit square to parallelogram with area $|\det(\mathbf{A}^n - \mathbf{I})|$, the parallelogram covers the unit square $|\det(\mathbf{A}^n - \mathbf{I})|$ times. By direct calculation, or by the $[2 \times 2]$ matrix identity

$$\det(\mathbf{A} + \mathbf{B}) = \det(\mathbf{A}) + \det(\mathbf{B}) + \text{tr}(\mathbf{A}) \text{tr}(\mathbf{B}) - \text{tr}(\mathbf{AB}),$$

together with $\det(\mathbf{A}^n) = (\det(\mathbf{A}))^n = 1$:

$$\det(\mathbf{A}^n - \mathbf{I}) = \det(\mathbf{A}^n) + 1 + (-2) \text{tr}(\mathbf{A}^n) - \text{tr}(-\mathbf{A}^n)$$

Hence the number of periodic points is

$$N_n = |\text{tr}(\mathbf{A}^n) - 2| = |\Lambda^n + \Lambda^{-n} - 2|. \quad (19.3)$$

where Λ is the larger eigenvalue of \mathbf{A} .

For the Arnol'd cat map

$$\mathbf{A} = \begin{pmatrix} 1 & 1 \\ 1 & 2 \end{pmatrix},$$

the powers of \mathbf{A} are given by the Fibonacci numbers²

$$\mathbf{A}^n = \begin{pmatrix} F_{2n-1} & F_{2n} \\ F_{2n} & F_{2n+1} \end{pmatrix}$$

with seed values $F_1 = 1, F_2 = 1$. Therefore,

$$N_n = F_{2n-1} + F_{2n+1} - 2$$

For example

$$\begin{aligned} N_1 &= F_1 + F_3 - 2 = 1 + 2 - 2 = 1 \\ N_2 &= F_3 + F_5 - 2 = 2 + 5 - 2 = 5, \quad \dots \end{aligned} \quad (19.4)$$

¹Predrag 2016-08-03: refer to where this is proven, or derive this statement here?

²Predrag 2016-05-21: to RS and AKS make this into an exercise, write up the solution

19.2.1 Keating's counting of periodic points

Keating [5] derives the number of periodic points of the cat map as follows:

The (q_j, p_j) periodic point of period n satisfy

$$\begin{pmatrix} q_{fixed} \\ p_{fixed} \end{pmatrix} = (A^n - I)^{-1} \begin{pmatrix} m \\ n \end{pmatrix} \quad (19.5)$$

"where m and n are integers which correspond to the winding numbers of the associated point (q_{fixed}, p_{fixed}) around the torus under the action of the map A . For this point to have coordinates between 0 and 1, m and n must lie within the parallelogram formed by the action of the matrix $(A^n - I)^{-1}$ on the unit square. We call this the fundamental parallelogram associated with A^n . It tessellates the plane in which the (integer) lattice of winding numbers (m, n) lies. Hence the number of fixed points of A^n is given by its area, which is $\det(A^n - I) = \text{tr}(A^n) - 2$. It may be seen from (19.5) that these fixed points form a lattice in phase space."

19.3 Relative frequencies of cat map words

In this section we evaluate the number of times that a symbol appears in the symbolic sequence of an ergodic orbit of a cat map. The Arnol'd cat map alphabet consists of 4 letters $\mathcal{A} = \{\underline{2}, \underline{1}, 0, 1\}$. \mathcal{A} is obtained from the equation of motion:

$$q_{n-1} - 3q_n + q_{n+1} = m_n, \quad m_n \in \mathcal{A} \quad (19.6)$$

For notational convenience, in alphabets we shall denote negative m by underlining them, i.e., $\{\underline{2}, \underline{1}, 0, 1\} = \{-2, -1, 0, 1\}$. To find $p(m)$, the relative frequency of symbol m , a Python program was written in which 100 arbitrary initial points are iterated for $n = 500000$ times. After each iteration, the obtained symbols are stored in an array of length n , and four counter variables are used to find how many times a symbol appears in the sequence. Finally, the average of number of repetitions for each symbol is found. Dividing these averages by n gives the frequency of each symbol. The final result is

$$p(\underline{2}) = 0.16670, \quad p(\underline{1}) = 0.33328, \quad p(0) = 0.33333, \quad p(1) = 0.16669$$

Next, we look for the relative frequency of $-m_i m_{i+1}-$, $p(m_i m_{i+1})$. To find $p(m_i m_{i+1})$, a function is added to the previous program which checks the next symbol of each item of array, and then, increments the corresponding counter. The relative frequencies of the four symbols with 4^2 combinations (for $_s_i s_{i+1}-$) are listed in Table 19.1. Table 19.2 lists N_n , the total number of pruned blocks of length $n = n_a$, and \tilde{N}_n , the number of new pruned blocks of length n_a , with all length n_a blocks that contain shorter pruned blocks already eliminated.

The relative frequencies can be obtained analytically by eliminating two coordinates corresponding to 2-symbol from the equations of motion. Excluding two coordinates from the equations of motion and applying boundary

	<u>2</u>	<u>1</u>	0	1		<u>2</u>	<u>1</u>	0	1
<u>2</u>	0	0.0208	0.0625	0.0833	=	<u>2</u>	0	1/48	1/16
<u>1</u>	0.0209	0.125	0.125	0.0625		<u>1</u>	1/48	1/8	1/8
0	0.0625	0.125	0.125	0.0209		0	1/16	1/8	1/48
1	0.0833	0.0625	0.0209	0		1	1/12	1/16	1/48

Table 19.1: The relative frequencies of 2-symbol words $m_i m_{i+1}$ for the Arnol'd cat map, obtained (left) from a long-time numerical simulation, (right) analytically. Column: m_i . Row: m_{i+1} . There is only one pruning rule: $\underline{11}$ is pruned. By the reflection symmetry, also $\underline{22}$ is pruned. As defined by (19.7), these frequencies are rational numbers, and their sum is 1.

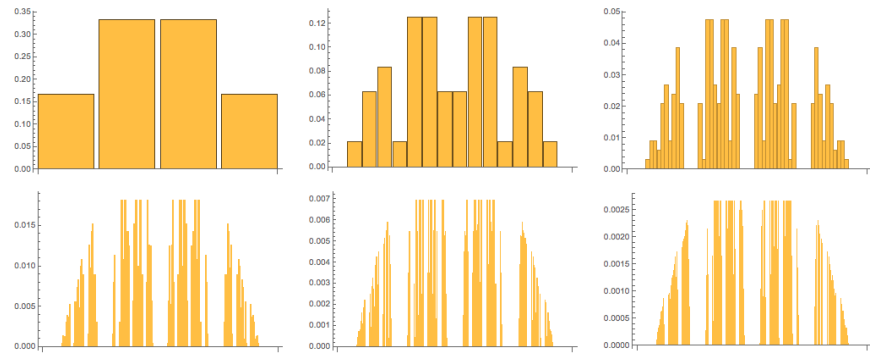


Figure 19.1: Frequencies of words of symbols. (Left to right: sub sequences of length 1, 2, 3, ..., 6.)

conditions ($0 \leq q < 1$) gives the following inequalities for 2-symbol words $-m_i m_{i+1}-$:

$$\begin{aligned} 0 &\leq \frac{1}{8}(-3m_i - m_{i+1} + 3x_1 + x_2) < 1, \\ 0 &\leq \frac{1}{8}(-m_i - 3m_{i+1} + x_1 + 3x_2) < 1. \end{aligned} \quad (19.7)$$

The areas of regions confined by these inequalities represents the relative frequencies corresponding to each 2-symbol word (table 19.1). Figure 19.1 shows the analytically found frequencies of words with lengths 1 to 6.

19.3.1 Numerical computations

To find all the possible periodic lengths of initial sets, $\{q_1, q_2\} = \{\frac{P_1}{N}, \frac{P_2}{N}\}$, we can consider the initial points to be (P_1, P_2) on $[0, N]^2$, and, following ref. [2], after each iteration we take $\mod N$. In this way, we use only integers, and, after each iteration the output is exact, with no floating point round-off errors. The periods that we obtain for the lowest values of N are as follows:

n_a	N_n	\tilde{N}_n	n_a	N_n	\tilde{N}_{n-1}
2	2	2	2	2	0
3	22	8	3	22	2
4	132	2	4	132	8
5	684	30	5	684	2
6	3164	2	6	3164	30
7	13882		7	13894	2
			8	58912	70
(a)			9	244678	16
			10	1002558	198
			11	4073528	2
			12	16460290	528
			13		2
(b)					

Table 19.2: N_n is the total number of pruned blocks of length $n = n_a$ for the Arnol'd cat map, $s = \text{tr}[A] = 3$. \tilde{N}_n is the number of new pruned blocks of length n_a , with all length n_a blocks that contain shorter pruned blocks already accounted for. (a) Computation carried in this report. (b) Numbers obtained by Li Han (unpublished). Note that (empirically) there is a single new pruning rule for each prime-number period (it is listed as 2 rules, but by the reflection symmetry there is only one).

for $\{q_1, q_2\} = \{\frac{P_1}{10}, \frac{P_2}{10}\} : T \in \{1, 2, 3, 6, 10, 30\}$,
 for $\{q_1, q_2\} = \{\frac{P_1}{100}, \frac{P_2}{100}\} : T \in \{1, 2, 3, 6, 10, 30, 50, 150\}$
 for $\{q_1, q_2\} = \{\frac{P_1}{8}, \frac{P_2}{8}\} : T \in \{1, 3, 6\}$
 for $\{q_1, q_2\} = \{\frac{P_1}{17}, \frac{P_2}{17}\} : T \in \{1, 18\}$

19.3.2 Entropy

Given the frequencies $p(a)$ with which a blocks $a = a_1 a_2 \dots a_{n_a}$ occur, the sum

$$\lim_{n_a \rightarrow \infty} -\frac{1}{n_a} \sum_a p(a) \log p(a) = -\log \Lambda, \quad (19.8)$$

where $\Lambda = \frac{3-\sqrt{5}}{2}$ is the eigenvalue of $\mathbf{A} = \begin{pmatrix} 1 & 1 \\ 1 & 2 \end{pmatrix}$.

Evaluating

$$\mathcal{S} = -\frac{1}{n_a} \sum_a p(a) \log p(a) \quad (19.9)$$

for $n_a = 1$ to 10 gives the values listed in table 19.3. Excluding all sequences that contain the external symbols and evaluating \mathcal{S} for the remaining pure $\{1, 0\}$ sequences gives the exact, complete symbolic dynamics expression (B).

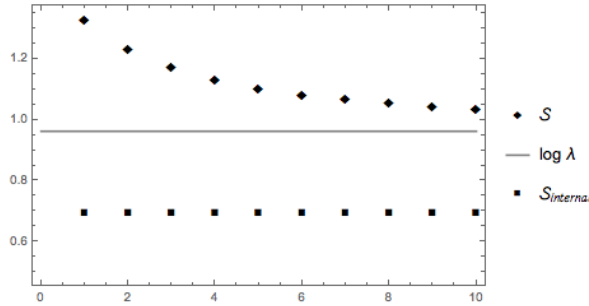


Figure 19.2: Entropies \mathcal{S} and $\mathcal{S}_{internal}$ vs. the length n_a of periodic orbits used to estimate them.

n_a	\mathcal{S}	$\frac{\mathcal{S} - \log \Lambda}{\log \Lambda}$
1	1.3297	%38.1
2	1.2348	%28.3
3	1.1731	% 21.9
4	1.1337	%17.8
5	1.1051	%14.8
6	1.0843	%12.7
7	1.0682	%11.0
8	1.0558	%9.71
9	1.0458	%8.67
10	1.0378	%7.83

Table 19.3: Entropies (19.9) for strings of lengths $n_a = 1$ to 10 , $s = 3$ Arnol'd cat map.

Gutkin, unpublished)

$$\mathcal{S}_{internal} = -\frac{1}{n_a} \log \frac{1}{2^{n_a}} = \log 2,$$

which we verify numerically in figure 19.2.

19.4 Spatiotemporal cat

In the spatiotemporal cat, “particles” (i.e., a cat map at each lattice site) are coupled together by the next-neighbor coupling rules:

$$q_{n,t+1} = p_{n,t} + (s-1)q_{n,t} - q_{n+1,t} - q_{n-1,t} - m_{n,t+1}^q$$

$$p_{n,t+1} = p_{n,t} + (s-2)q_{n,t} - q_{n+1,t} - q_{n-1,t} - m_{n,t+1}^p$$

n	$\underline{3}$	$\underline{2}$	$\underline{1}$	0	1	2	3	N
3	0.04169	0.49896	0.96169	1	0.97298	0.49965	0.04116	4.016
7	0.04062	0.50008	0.95917	1	0.95131	0.50284	0.04054	3.995
10	0.04127	0.50135	0.96255	1	0.96019	0.50066	0.04178	4.007
20	0.04120	0.50256	0.95779	1	0.95871	0.50171	0.04087	4.003

Table 19.4: $s = 4$. Numerically, the relative frequencies of symbols $\underline{1}, 0$ and 1 are close to 1.

The symbols of interest can be found by:

$$m_{n,t} = q_{n,t+1} + q_{n,t-1} + q_{n+1,t} + q_{n-1,t} - s q_{n,t}.$$

The results presented in this section are obtained by simulations. In order to make the computation exact, the denominators and numerators of the coordinates are stored as integers, i.e., only integers are used in all calculations presented here.

19.4.1 Frequencies of symbols

The obtained relative frequencies for different values of parameter b in ³

$$A = -\frac{1}{c} \begin{pmatrix} a & 1 \\ ab - c^2 & b \end{pmatrix}$$

(where $s = \text{tr } A = a + b$) shows the existence of 6 external and $s - 3$ internal symbols from the alphabet $\mathcal{A} = \{-s + 1, -s, \dots, 2, 3\}$. The numerical results were close to the expected values, which are $p(3) = p(-s + 1) = \frac{1}{4!}$, $p(2) = p(-s + 2) = \frac{1}{2}$, and $p(1) = p(-s + 3) = 1 - \frac{1}{4!}$ (the relative frequency of an internal symbols is 1).

The results of Table 19.4 and Table 19.5, suggest that the frequencies are independent of n , the number of particles. Also, the values in Table 19.6 suggest that the normalization factor N is expected to be $1/s$. These values agree with the analytical values derived for the internal and external sequences:

$$\begin{aligned} \frac{1}{N} \left[6 \left(\frac{1}{4!} + \left(1 - \frac{1}{4!}\right) + \frac{1}{2} \right) + (s - 3)(1) \right] &= 1 \\ \Rightarrow N &= s \end{aligned}$$

⁴

³Predrag 2016-11-03: Where did the c come from? Shouldn't it be $c = -1$ by area preservation?
Oh, I see - it has to do with coupling between sites [4].

⁴Predrag 2016-12-20: I do not get $N = s$ from this formula...

<i>n</i>	<u>7</u>	<u>6</u>	<u>5</u>	<u>4</u>	<u>3</u>	<u>2</u>	<u>1</u>	0	1	2	3	<i>N</i>
3	0.0417	0.4996	0.9560	1.	0.9961	0.9993	0.9980	0.9974	0.9535	0.4982	0.0414	7.90
10	0.0414	0.4994	0.9535	0.9942	0.9978	0.9902	0.9938	1.	0.9551	0.49881	0.0411	7.90
20	0.0410	0.5017	0.9442	0.9839	0.9916	0.9837	1	0.9795	0.9576	0.4887	0.0419	7.90

Table 19.5: $s = 8$. Numerically, the relative frequencies of symbols 4, 3, 2, 1, 0 and 1 are close to 1.

<i>s</i>	<i>N</i>
5	5.0004
6	5.9988
7	7.0101
8	8.0014
9	8.9946

Table 19.6: *N*, the normalization factor of relative frequencies.

19.4.2 Frequency of blocks of length two

Next, we look for frequencies of blocks of length 2. These blocks can be formed by two consecutive symbols of one particle (e.g. $m_{n,t}m_{n,t+1}$) or symbols corresponding to two different particles at time t (e.g $m_{n,t}m_{n+1,t}$). Based on the results, there is a symmetry between symbols for a particle (figure 19.3), and symbols at time t for two different particles (figure 19.4) (with the same normalization factor, $N \approx 15$).

The only pruned blocks for both cases are 33 and 33, which is in agreement with the analytical results obtained by simplifying the inequalities of both cases in Mathematica (which implies that the confined area between the hyper planes is zero):

$$0 \leq \frac{1}{15} (-4a_1 - a_2 + 4x_1 + x_2 + x_3 + x_4 + 4x_5 + 4x_6) < 1,$$

$$0 \leq \frac{1}{15} (-a_1 - 4a_2 + x_1 + 4x_2 + 4x_3 + 4x_4 + x_5 + x_6) < 1.$$

According to the simulations, the sum of volumes confined between these planes should be 15.

The normalization factors, *N*, for different values of *s* are shown in Table 19.7. By comparing these values with inequalities obtained by excluding 2 coordinates corresponding to 2 symbols, it is observed that the normalization factors appear in equalities as the biggest common denominator. For example, for $s = 5$ we have the following inequality:

$$0 \leq \frac{1}{35} (-6a_1 - a_2 + 6x_1 + 6x_2 + x_3 + x_4 + x_5 + 6x_6) < 1,$$

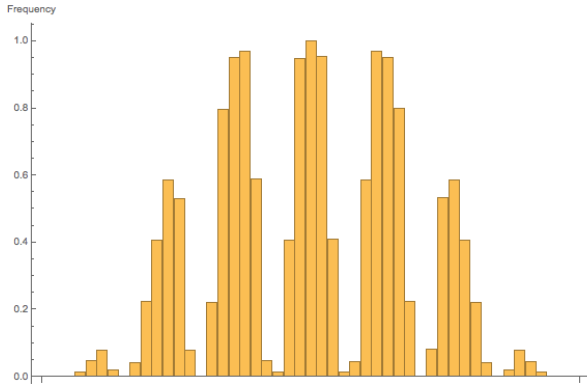


Figure 19.3: Relative frequencies of two symbols for a particle $(m_{n,t} m_{n,t+1})$. $s = 4$.

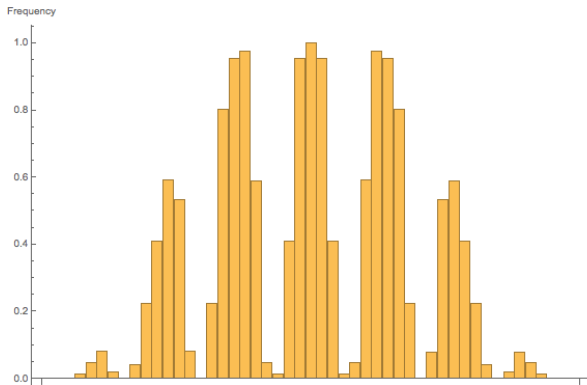


Figure 19.4: Relative frequencies of two symbols at time t for two different particles $(m_{n,t} m_{n+1,t})$. $s = 4$.

s	N
4	14.9168
5	23.8374
6	34.8851
7	48.1024

Table 19.7: Normalization factor, N , for different values of s .

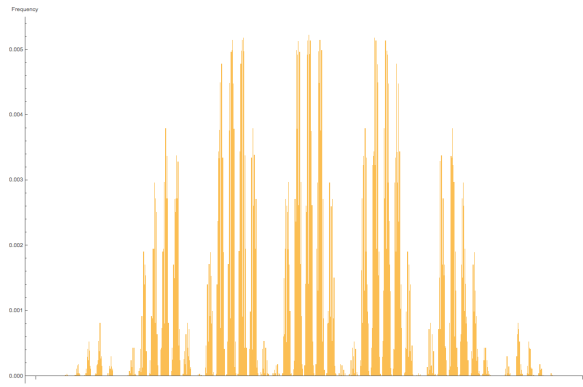


Figure 19.5: $s = 4$. Frequencies of $[2 \times 2]$ spatiotemporal domains.

$$0 \leq \frac{1}{35} (-a_1 - 6a_2 + x_1 + x_2 + 6x_3 + 6x_4 + 6x_5 + x_6) < 1$$

The normalization factor obtained from simulations is approximately 35.

19.4.3 Frequencies of $[2 \times 2]$ spatiotemporal domains

Frequencies of $[2 \times 2]$ spatiotemporal domains of 20 coupled particles for two values of $s = 4$ and $s = 8$ are estimated. The results are presented in figure 19.5 and figure 19.6, respectively. The horizontal axes of graph, represents points starting from $\begin{smallmatrix} -s+1 & -s+1 \\ -s+1 & -s+1 \end{smallmatrix}$ to $\begin{smallmatrix} 3 & 3 \\ 3 & 3 \end{smallmatrix}$.

By arranging elements of the block (square) on a line (due to symmetry, the vertical or horizontal order of arrangement does not matter) as $-s+1 -s+1 -s+1 -s+1$ to $3 3 3 3$ and shifting each element of sequence $m_1 m_2 m_3 m_4$ by $(s-1)$, we can reproduce the symbols as numbers in base $s+3$, and increment them from 0 to $(s+2) s+2 s+2 s+2)_{s+3}$ on the horizontal axes.

By looking at data, the $[2 \times 2]$ spatiotemporal domains with relative frequencies close to 1 do not only consist of internal symbols. For example, for $s = 8$,

$\begin{smallmatrix} 5 & 3 \\ 1 & 0 \end{smallmatrix}$ has a relative frequency equal to 0.995755. The results suggest that if

a column or row of symbols consist of internal symbols, the relative frequency is going to be close to 1.⁵

19.5 Summary

The results obtained by simulations for the frequencies of words are consistent with the unpublished B. Gutkin analytical results. By evaluating analytical

⁵Predrag 2016-08-07: Can you describe Boris' result more precisely? is it 'close to' or 'exactly' 1?

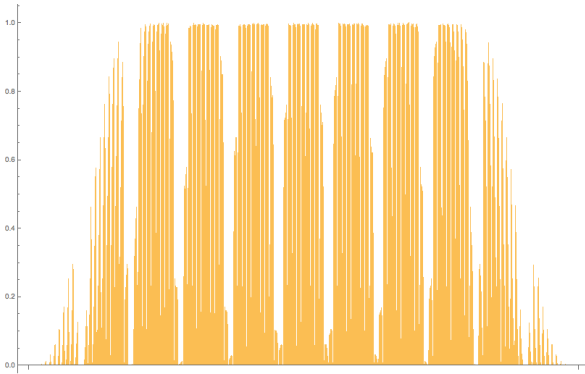


Figure 19.6: $s = 8$. Frequencies of $[2 \times 2]$ spatiotemporal domains.

inequalities and finding the areas corresponding to the frequencies of words of single cat map, we are able to find the inadmissible sequences for words of up to length 6.

While for the spatiotemporal cats the general inequalities can be stated for any rectangular spatiotemporal domain, determining the volumes confined by these inequalities remains an open problem.

References

- [1] V. I. Arnol'd and A. Avez, *Ergodic Problems of Classical Mechanics* (Addison-Wesley, Redwood City, 1989).
- [2] J. Bao and Q. Yang, “Period of the discrete Arnold cat map and general cat map”, *Nonlinear Dyn.* **70**, 1365–1375 (2012).
- [3] R. L. Devaney, *An Introduction to Chaotic Dynamical systems*, 2nd ed. (Westview Press, Cambridge, Mass, 2008).
- [4] B. Gutkin and V. Osipov, “Classical foundations of many-particle quantum chaos”, *Nonlinearity* **29**, 325–356 (2016).
- [5] J. P. Keating, “Asymptotic properties of the periodic orbits of the cat maps”, *Nonlinearity* **4**, 277 (1991).
- [6] J. P. Keating, “The cat maps: quantum mechanics and classical motion”, *Nonlinearity* **4**, 309–341 (1991).
- [7] I. Percival and F. Vivaldi, “Arithmetical properties of strongly chaotic motions”, *Physica D* **25**, 105–130 (1987).

Chapter 20

Symbolic Dynamics for Coupled Cat Maps

Adrien K. Saremi Summer 2016 Report

Abstract

Classical particles are governed by Hamiltonian equations of motion. Instead of continuous function of time, we break down our system's evolution through a series of discrete instants; the generalized coordinates $\{q_{n,t}, p_{n,t}\}$ are then solutions to a system of coupled linear equations, written down in matrix form. Our research consists in studying symbolical dynamics in relation with our N -particle system, through a time evolution of length T by obtaining the nature of our alphabet, by computing the frequencies of appearance of our symbols and by deriving the inadmissible symbolic spatiotemporal domains, through analytic studies and computational models.

20.1 Introduction

Let a system of N particle, evolving through time, over a time lapse of value T . We assume that our system lies in one dimension of space, therefore our generalized coordinates, position and momentum are described as follows:

$$\{q_{n,t}, p_{n,t}\} \text{ where } n \in \{1, \dots, N\} \text{ and } t \in \{1, \dots, T\}$$

Obviously, n is the particle variable and t the time variable. We also refer to n as our space variable. At an instant t , we define our generalized coordinate vector \mathcal{Z}_t :

$$\mathcal{Z}_t = \left\{ \begin{array}{c} q_{n,t} \\ p_{n,t} \end{array} \right\}_{1 \leq n \leq N} = \left\{ \begin{array}{c} q_{1,t} \\ p_{1,t} \\ q_{2,t} \\ p_{2,t} \\ \dots \\ p_{N,t} \\ q_{N,t} \end{array} \right\}$$

Following Gutkin and Osipov [2] *Classical foundations of many-particle quantum chaos*, we write Hamilton's equations for our generalized coordinate vector \mathcal{Z}_t described in this paper's sect. 3.1 *Dynamics*:

$$\mathcal{Z}_{t+1} = \mathcal{B}_N \mathcal{Z}_t$$

with

$$\begin{aligned} \mathcal{B}_N &= \begin{pmatrix} A & B & 0 & \dots & 0 & B \\ B & A & B & \dots & 0 & 0 \\ 0 & B & A & \dots & 0 & 0 \\ \vdots & \vdots & \vdots & \ddots & \vdots & \vdots \\ 0 & 0 & 0 & \dots & A & B \\ B & 0 & 0 & \dots & B & A \end{pmatrix} \\ A &= \frac{1}{c} \begin{pmatrix} a & 1 \\ ab - c^2 & b \end{pmatrix}, \quad B = -\frac{1}{c} \begin{pmatrix} d & 0 \\ db & 0 \end{pmatrix} \end{aligned} \quad (20.1)$$

We start with a system of just $N = 1$ particle. This is usually referred as *Arnol'd cat map*.

20.2 Arnol'd Cat Map

In this section, we introduce the concept of iterative process and compute the time evolution of our system. We fix the parameters of our \mathcal{B}_N matrix:

$$\mathcal{B}_N = \mathcal{B}_1 = A = \begin{pmatrix} 1 & 1 \\ 1 & 2 \end{pmatrix}, \quad \det A = 1.$$

Here we picked the values $a = 1$, $b = 2$ and $c = -1$. The system of equations can be rewritten:

$$\begin{pmatrix} q_{t+1} \\ p_{t+1} \end{pmatrix} = A \begin{pmatrix} q_t \\ p_t \end{pmatrix} \mod 1 \quad (20.2)$$

For the sake of phase space volume conservation, we set the matrix A to have a determinant equal to 1. The underlying difficulty of this problem is that our coordinates must also remain within an interval of length 1. At first we pick this interval to be $[0, 1)$. We will see later that we change this interval

to $[-\frac{1}{2}, \frac{1}{2})$ in order to preserve the symmetry of our coordinates and of our symbolic dynamics with respect to 0.

Our goal is now to find prime periodic orbits p of period $|p|$ and initial points $\{q_{p,1}, p_{p,1}\}$ such that:

$$\begin{pmatrix} q_{p,|p|} \\ p_{p,|p|} \end{pmatrix} = \begin{pmatrix} q_{p,1} \\ p_{p,1} \end{pmatrix} \pmod{1}$$

In what follows, we explain the two approaches in order to reach this goal. For the sake of notational simplicity, we denote our initial set as $\{q_1, p_1\}$, and the final set as $\{q_{|p|}, p_{|p|}\}$. It is understood that we deal with the prime periodic orbit p .

20.2.1 Periodic orbits - first approach

Consider

$$\begin{pmatrix} q_{|p|} \\ p_{|p|} \end{pmatrix} = A^{|p|} \begin{pmatrix} q_1 \\ p_1 \end{pmatrix} \pmod{1}$$

We demand that $\{q_1, p_1\}$ is a periodic point in a prime periodic orbit p on a two-dimensional torus \mathbf{T}^2 , i.e., a relative periodic orbit on \mathbb{Z}^2 , periodic up to a shift by integers $\{m_q, m_p\}$:

$$\begin{pmatrix} q_1 \\ p_1 \end{pmatrix} = A^{|p|} \begin{pmatrix} q_1 \\ p_1 \end{pmatrix} + \begin{pmatrix} m_q \\ m_p \end{pmatrix}$$

Therefore:

$$\begin{pmatrix} q_1 \\ p_1 \end{pmatrix} = (\mathbb{1} - A^{|p|}) \begin{pmatrix} m_q \\ m_p \end{pmatrix}$$

The number of periodic orbits (AKA the number of sets of $\{q_1, p_1\}$) would be then given by:

$$|\det(\mathbb{1} - A^{|p|})| = |(1 - \lambda^{|p|})(1 - \frac{1}{\lambda^{|p|}})|$$

where λ is the largest eigenvalue of A : $\lambda = \frac{3+\sqrt{5}}{2} = 2.6180$ also known as *Floquet multiplier*

Instead of dealing with multiples of the A matrix, and the large number of coordinate vectors Z_t , the second approach includes a larger matrix computation, but allows us to store all coordinates in one single vector.

20.2.2 Periodic orbits - second approach

Here we eliminate $\{p_t\}$ in favor of a 2-step recurrence equation on the position coordinate $\{q_t\}$:

$$p_t = \frac{q_t - q_{t-1}}{\Delta t} = q_t - q_{t-1}$$

Combined with:

$$q_{t+1} = q_t + p_t$$

We obtain:

$$\begin{aligned} q_3 - 3q_2 + q_1 &= m_2 \\ q_4 - 3q_3 + q_2 &= m_3 \\ &\vdots \\ q_{|p|+1} - 3q_{|p|} + q_{|p|-1} &= m_{|p|} \\ q_{|p|+2} - 3q_{|p|+1} + q_{|p|} &= m_{|p|+1} \end{aligned} \tag{20.3}$$

Since we look for periodic orbits, $q_{|p|+1} = q_1$ and $q_{|p|+2} = q_2$. Therefore the last equation reduces to:

$$q_2 - 3q_1 + q_{|p|} = m_1,$$

and the system of equations into the matrix form:

$$\mathcal{D} Q_{|p|} = m_{|p|}$$

with

$$\begin{aligned} Q_{|p|} &= \begin{pmatrix} q_1 \\ q_2 \\ \vdots \\ q_{|p|} \end{pmatrix}, \quad m_{|p|} = \begin{pmatrix} m_1 \\ m_2 \\ \vdots \\ m_{|p|} \end{pmatrix} \\ \mathcal{D} &= \begin{pmatrix} -3 & 1 & 0 & 0 & 0 & \dots & 1 \\ 1 & -3 & 1 & 0 & 0 & \dots & 0 \\ \vdots & & & & & & \\ 1 & 0 & 0 & 0 & \dots & 1 & -3 \end{pmatrix} \end{aligned} \tag{20.4}$$

It then comes down to the nature of our initial set: if the starting set is rational, we will necessarily obtain a periodic system. Indeed, if we assume that the initial momentum and position are rational numbers with some common denominator N , and since the cat map is composed of integers, after t steps, momentum and coordinate have the form $q_t = a_t/N$, $p_t = b_t/N$. And if we travel on the lattice of the size $N \times N$, it will take us a maximum step N to close the loop. Usually, the periodicity is smaller than N , and this is what our MATLAB code computes.

Program evaluation

Using the 2nd approach, sect. 20.2.2, our program computes the position coordinates of our particle for a given initial condition $\{q_1, q_2\}$. The numbers $\{q_t\}$'s and the integers $\{m_t\}$'s are then stored in the matrices Q and m . The program stops if for some iteration t we obtain the same starting set $\{q_{t+1}, q_{t+2}\} = \{q_1, q_2\}$, in which case the period is $|p| = t$.

If it doesn't stop, and it completes all the iteration that the user required, the program then looks for periodic behavior in the m matrix. In other words: does an integer $|p|$ exist such that for all t , $m_{t+|p|} = m_t$. If it's the case, the orbit in question is also periodic, and the program wasn't accurate enough to observe periodicity among the position coordinates (a point that we will discuss later this section).

Results for periodic orbits

We now understand that the rational nature of our initial set $\{q_1, q_2\}$ is determinant for the periodic behavior of our system. We try several sets $\{q_1, q_2\}$ of the form $\{q_1, q_2\} = \{\frac{i}{N}, \frac{j}{N}\}$ where $i, j \in \{0, \dots, N - 1\}$.

- For $\{q_1, q_2\} = \{\frac{i}{10}, \frac{j}{10}\}$, the periodicities found were: $|p| = 1, 2, 3, 6, 10, 30$
- For $\{q_1, q_2\} = \{\frac{i}{100}, \frac{j}{100}\}$, they were: $|p| = 1, 2, 3, 6, 10, 30, 50, 150$
- For $\{q_1, q_2\} = \{\frac{i}{8}, \frac{j}{8}\}$, $|p| = 1, 3, 6$
- And for $\{q_1, q_2\} = \{\frac{i}{17}, \frac{j}{17}\}$ $|p| = 1, 18$
- Nevertheless, for an irrational starting set such as $\{q_1, q_2\} = \{\frac{\pi}{6}, \frac{\pi}{8}\}$ we do not obtain any periodic behaviors, despite running 20 000 iterations.

Before moving to the next part, we briefly discuss the accuracy of our computations, and the limits of our program when it comes to find periodic orbits.

Round-off errors

Our MATLAB calculations often gave us unexpected results, where we could not find periodic orbits through our position coordinates. The advantage of looking at the m sequence instead is that it is made of integers, while the q 's are decimal numbers, and it is possible that after many iteration, the round-off error in computation becomes quite large.

In fact, such errors are directly related to the nature of our system, more precisely the matrix A . The Floquet multiplier λ has an impact on the calculation of the computed value after t iterations, compared to the real value $q_{real,t}$:

$$q_{computed,t} = q_{real,t} + \epsilon \lambda^t, \text{ where } \lambda = \frac{3 + \sqrt{5}}{2} = \text{multiplier}$$

and where ϵ is the round off error of the system. For a 64-bit operating system, $\epsilon = 2^{-53} \approx 10^{-16}$. Now, if we look for a computed value of q within 10^{-4} of its real value, then the maximum number of iteration t_{max} is technically:

$$|\epsilon \lambda^{t_{max}}| \leq 10^{-4}$$

$$\Rightarrow t_{max} \approx \ln(\lambda) \ln\left(\frac{10^{-4}}{\epsilon}\right)$$

$$\Rightarrow t_{max} = 26$$

The exponential growth in error imposes the use of different computation techniques, or to application of the command **digits(n)** which forces n significant digits to any computations.

Through our MATLAB program, we now focus on the nature of the alphabet (m matrix), as well as the frequency of appearance of our symbols. The big stuff....

20.2.3 Symbolic dynamics for 1 particle

Nature of our alphabet

We recall that given our matrix A :

$$q_{i-1} + q_{i+1} = 3q_i + m_i \quad \forall i$$

In fact for a random matrix A (as long as $\det(A) = 1$), if we denote the trace of A by $s = \text{trace}(A)$, then this equation is rewritten as:

$$q_{i-1} + q_{i+1} = s q_i + m_i \quad \forall i$$

Since the nature of m_i only depends on q_{i-1} , q_{i+1} and q_i , consider a sequence of length 3: $\{q_1, q_2, q_3\}$ with the constraint conditions on q_i 's:

$$\begin{aligned} q_1 + q_3 &= s q_2 + m \\ q_i &\in [0, 1] \quad \forall i \end{aligned}$$

Then:

$$\begin{aligned} 0 &\leq q_1 < 1 \\ 0 &\leq q_3 < 1 \\ m &\leq q_1 + q_3 < m + s \end{aligned}$$

The value of s then becomes determinant to why only few symbols are admissible. For example, for $s = 3$ we find that $m_t \in \{-2, -1, 0, 1\}$.

Frequencies of symbols

Using our program, we then compute the frequencies of each symbol for the case $s = 3$. By performing 1 iteration in time to obtain q_3 from q_1 and q_2 and by repeating with several different starting set, we obtain a good probability distribution of symbolic dynamics. We pick starting sets of the form $\{q_1, q_2\} = \{\frac{i}{200}, \frac{j}{200}\}$ where $i, j \in \{0, \dots, 199\}$ and obtain a distribution over 40 000 points:

$$p_{-2} = 0.16583, p_{-1} = 0.33335, p_0 = 0.33310, p_1 = 0.16773$$

In fact, if we plug the different values of m in the system of equation above for $s = 3$, we obtain inequalities on q_1 and q_3 . The admissible area in our

lattice defined by (q_1, q_3) is then the probability of obtaining the symbol p_m . For example for $m = -1$:

$$\begin{aligned} 0 &\leq q_1 < 1 \\ 0 &\leq q_3 < 1 \\ -1 &\leq q_1 + q_3 < 2 \end{aligned}$$

The admissible area is then $\mathcal{A} = 1$, but for $m = -2$:

$$\begin{aligned} 0 &\leq q_1 < 1 \\ 0 &\leq q_3 < 1 \\ -2 &\leq q_1 + q_3 < 1 \end{aligned}$$

And here the admissible area is $\mathcal{A} = \frac{1}{2}$. For $m = 0$ and $m = 1$, we respectively find $\mathcal{A} = 1$ and $\mathcal{A} = \frac{1}{2}$. Therefore our probability distribution matches our numerical calculations and:

$$p_{-2} = \frac{1}{6}, p_{-1} = \frac{1}{3}, p_0 = \frac{1}{3}, p_1 = \frac{1}{6}$$

We observe that the inner symbols -1 and 0 have a higher frequency than the outer ones, a point that will have a major importance when we study many symbols frequencies.

Frequency of sequences of symbols

Another approach to the computation of one or more-than-two sequence of symbols is to analyze the symbolic distribution over an **ergodic** orbit, i.e., a non-periodic orbit. If the sequence of symbols is long enough, one sequence is sufficient to observe a frequency distribution that matches with the theory. This also works for a given sequence of length p , such as $\{m_1 m_2 \dots m_p\}$. We define $N_n(m_1 m_2 \dots m_p)$ as the number of periodic orbits of length n that generate the given sequence. The probability of obtaining the sequence $\{m_1, m_2, \dots, m_p\}$ is then:

$$p(m_1 m_2 \dots m_p) = \lim_{n \rightarrow \infty} \frac{N_n(m_1 m_2 \dots m_p)}{N_n}$$

Figuring out the probability distribution by mathematical analysis (as we did for 1 symbol) can become quite hard as the length of the given sequence increases. We will cover in this section the case of many particles. However, what we can observe is the correlation between disjoint sequence of symbols.

Given a sequence $A = [a_1, \dots, a_u]$ of length u , and a sequence $B = [a_1, \dots, a_v]$ of length v , we now examine the frequency of seeing one repeated a length *space* after the other. Comparing with the product of their distinct frequencies, we then increase the *spacing* and observe how the correlation factor

$$\text{Correl} = p(A, \text{space}, B) - p(A) p(B) \text{ behaves}$$

We obviously limit our study to admissible sequences. For the ergodic orbit $\{q_1, q_2\} = \{\frac{\sqrt{5}}{4}, \frac{\sqrt{2}}{2}\}$ of length $N = 1,000,000$, and the sequences $A = [-1, 1]$ and $B = [-2, 0]$

$$p(A) = 0.1249 \quad p(B) = 0.0623$$

Spacing	$P(A, space, B)$	Correl
1	0.0085	$7.3567 \cdot 10^{-4}$
2	0.0066	-0.0011
3	0.0073	$-4.6733 \cdot 10^{-4}$
4	0.0080	$1.8867 \cdot 10^{-4}$
5	0.0079	$6.8666 \cdot 10^{-5}$
6	0.0078	$4.6655 \cdot 10^{-6}$

For longer sets $A = [-1, -1, -1, -1]$ and $B = [-2, 1, -1, 0]$, and the same orbit, the probabilities are as follow:

$$p(A) = 0.0178 \quad p(B) = 0.0151$$

Spacing	$P(A, space, B)$	Correl
1	$2.9400 \cdot 10^{-4}$	$2.4439 \cdot 10^{-5}$
2	$2.2400 \cdot 10^{-4}$	$-4.5561 \cdot 10^{-5}$
3	$2.4900 \cdot 10^{-4}$	$-2.0561 \cdot 10^{-5}$
4	$2.5100 \cdot 10^{-4}$	$-1.8561 \cdot 10^{-5}$
5	$2.7300 \cdot 10^{-4}$	$3.4392 \cdot 10^{-6}$
6	$2.6900 \cdot 10^{-4}$	$-5.6081 \cdot 10^{-7}$

In both scenarios, the correlation factor diminishes as the separation between the two blocs increases. We notice that for longer sets A and B , the correlation is small enough (but not zero) even for small spacing. It is quite interesting how this correlation, which translates the dependence between future and past symbolic dynamics, vanishes exponentially...

20.3 Coupled Cat Maps

We now extend our study to a many particle system, where N is the number of particles. T will be now known as the period of the orbit, and if it doesn't exist, T will just refer to our ultimate time iteration in the computation of the symbols m 's. Among the objectives of this section, we will explain the impact of the trace of the A matrix ($s = \text{trace}(A)$) on the nature of our alphabet, the length of the periodic orbits, and the admissibility of sequences of symbols.

We will first look at the computation of our periodic orbits, then the nature of our alphabet, and finally the rules that determine whether a sequence of symbols is inadmissible, and if not, what is its frequency of recurrence.

20.3.1 Computation of symbols

As we saw in sect. 20.2, there are two approaches to compute our symbolic dynamics. Here the 1st method that we described in sect. 20.2.1 presents more advantage in the computation of another symbolic dynamics.

Computing the coordinates

Our interval of study is $[-\frac{1}{2}, \frac{1}{2})$, the equation $\mathcal{Z}_{t+1} = \mathcal{B}_N \mathcal{Z}_t \bmod 1$ involves the introduction of *generalized* symbolics $m^{q,p}$ such that:

$$\mathcal{Z}_{t+1} = \mathcal{B}_N \mathcal{Z}_t + m_{t+1}^{q,p}$$

$$\text{where } m_t^{q,p} = \{m_t^q, m_t^p\} = \{m_{1,t}^q, m_{1,t}^p, m_{2,t}^q, m_{2,t}^p, \dots, m_{N,t}^q, m_{N,t}^p\}$$

In fact the MATLAB can now store all the entries of the \mathcal{Z}_t vectors in a larger matrix, where T is the number of columns, and $2N$, which refers to the 2 coordinates or each particle, is the number of rows.

In a effort to keep the time evolution row-wise, and the space evolution column-wise, only the momentum coordinates $\{q_{n,t}\}_{1 \leq n \leq N, 1 \leq t \leq T}^{1 \leq n \leq N}$ are then stored in the Q matrix:

$$Q = \begin{pmatrix} q_{n,1} \\ q_{n,2} \\ \vdots \\ q_{n,T} \end{pmatrix} = \begin{pmatrix} q_{1,t} & q_{2,t} & \dots & q_{N,t} \end{pmatrix} = \begin{pmatrix} q_{1,1} & q_{2,1} & \dots & q_{N,1} \\ q_{1,2} & q_{2,2} & \dots & q_{N,1} \\ \vdots & \vdots & & \vdots \\ q_{1,T} & q_{2,T} & \dots & q_{N,T} \end{pmatrix}$$

Note that in the label $Q = \{q_{n,t}\}$, the column index is n and the row index is t .

Computing the alphabet

What we actually focus on is the symbolic dynamics. The $m^{q,p}$ matrix mentioned above is the *generalized* dynamics, while the one we studied for $N = 1$ was the *Newtonian* dynamics m . There are two ways to compute the later:

- Use our generalized symbolics:

$$m_{n,t} = -b m_{n,t}^q - c m_{n,t+1}^q + m_{n,t}^p$$

- Use the Q coordinates:

$$c (q_{n,t+1} + q_{n,t-1}) + d (q_{n+1,t} + q_{n-1,t}) = -s q_{n,t} + m_{n,t}$$

For computations of admissible sequences, the later method is preferred. And even if our dynamics is not defined at the boundaries, for either $n \in \{1, N\}$ or $t \in \{1, T\}$, the choice of ergodic orbits that run for very large N and T makes irrelevant that a few number of symbols can no longer be computed. For the case of periodic orbits, where T is usually a small number, we will only focus on the generalized coordinates $m^{q,p}$ instead.

Periodic orbits

The absolute criteria to obtain periodic orbits is to start with a rational set \mathcal{Z}_1 , and use integers for the parameters a, b, c and d . Unless specified, we use the following values throughout the rest of our study:

- $c = -1$ such that $\det(A) = 1$
- $d = c$ in order to preserve the symmetry between space and time evolutions
- $b = 1$ and $a = 2$ in order to obtain $s = a + b = \text{trace}(A) = 3$. To observe a hyperbolic evolution, a must remain greater than 2; which is why we will only increase the value of a , and leave b as a fixed parameter, to study the influence of s on our system.

Few periodic orbits were computed, for different number of particles:

- for $N = 3$ and $\mathcal{Z}_1 = \left\{ \frac{31}{100}, \frac{29}{100}, \frac{7}{50}, -\frac{13}{100}, \frac{31}{100}, \frac{3}{100} \right\}$

the periodicity is $T = 60$, and the symbolic dynamics is:

$$\begin{aligned} m^{q,p} &= -2, p_{-2} = 0.011111 \\ m^{q,p} &= -1, p_{-1} = 0.222222 \\ m^{q,p} &= 0, p_0 = 0.536111 \\ m^{q,p} &= 1, p_1 = 0.227778 \\ m^{q,p} &= 2, p_2 = 0.002778 \end{aligned}$$

- for $N = 7$ and

$$\mathcal{Z}_1 = \left\{ \frac{-19}{100}, \frac{21}{50}, \frac{-7}{100}, \frac{-8}{25}, \frac{2}{5}, \frac{47}{100}, \frac{-7}{100}, \frac{-39}{100}, -\frac{1}{4}, -\frac{1}{10}, \frac{9}{100}, \frac{-6}{25}, \frac{1}{10}, \frac{21}{100} \right\}$$

the periodicity is $T = 2790$, and the symbolic dynamics is:

$$\begin{aligned} m^{q,p} &= -2, p_{-2} = 0.012110 \\ m^{q,p} &= -1, p_{-1} = 0.226472 \\ m^{q,p} &= 0, p_0 = 0.526882 \\ m^{q,p} &= 1, p_1 = 0.224014 \\ m^{q,p} &= 2, p_2 = 0.010522 \end{aligned}$$

By always finding periodicity, the program confirms that it evaluates the right coordinates. It also validate that neither the number of particle N , nor the periodicity T have an influence on the nature of our alphabet.

20.3.2 Nature of our alphabet

Through an analytic study, and by confirm with our simulations, we now focus on the impact of the trace of A

Analytically

Given equation $????$ and with $c = d = -1$:

$$s q_{n,t} = q_{n,t+1} + q_{n,t-1} + q_{n+1,t} + q_{n-1,t} + m_{n,t}$$

Since we study the nature of 1 symbol at the time, let's pick the following notations

$$n = 1 \text{ and } t = 1$$

$$q_{1,1} = q_1 \quad m_{1,1} = m_1 \quad q_{1,0} = x_1 \quad q_{2,1} = x_2 \quad q_{1,2} = x_3 \quad q_{0,1} = x_4$$

A system is relabelled as (we will see that this notation is useful for sequence of many symbols)

$$\begin{matrix} & q_{1,0} & & & x_1 \\ q_{0,1} & \mathbf{q}_{1,1} & q_{2,1} & = & x_4 & \mathbf{q}_1 & x_2 \\ & q_{1,2} & & & & & x_3 \end{matrix} .$$

This system we can rewrite as:

$$q_1 = \frac{1}{s} (m_1 + \sum_{i=1}^4 x_i)$$

with the constraints on q_1 and x_i :

$$\begin{cases} -\frac{s}{2} \leq m_1 + \sum_{i=1}^4 x_i < \frac{s}{2} \\ -\frac{1}{2} \leq x_i < \frac{1}{2}, \quad \text{for } i = 1, \dots, 4 \end{cases}$$

For the Arnol'd cat map case $s = 3$, this reduces to

$$\begin{cases} -\frac{3}{2} - m_1 \leq \sum_{i=1}^4 x_i \leq \frac{3}{2} - m_1 \\ -2 \leq \sum_{i=1}^4 x_i \leq 2 \end{cases}$$

This system of inequalities allows us to derive which symbols are admissible. For a given m_1 , the system doesn't admit real solutions for x_i 's (or if the solution is empty), then the symbol is forbidden. For the case $s = 3$, we confirm what we obtained for $N = 1$ and $m \in \{-3, -2, \dots, 2, 3\}$.

Program

Here ergodic orbits run for a large number of particles and over many time iterations T . To speed up the computing process, the program stops looking

for periodic orbits and only focus on the symbolic dynamics, as well as its probability distribution. The simulations are for different values of s , with $N = 5$, $T = 80\,000$, and a random irrational starting set:

$s = 3$	$s = 4$	$s = 5$
$m = -3 \quad p_{-3} = 0.000850$	$m = -3 \quad p_{-3} = 0.010696$	$m = -4 \quad p_{-4} = 0.000592$
$m = -2 \quad p_{-2} = 0.067293$	$m = -2 \quad p_{-2} = 0.126391$	$m = -3 \quad p_{-3} = 0.040080$
$m = -1 \quad p_{-1} = 0.264819$	$m = -1 \quad p_{-1} = 0.236452$	$m = -2 \quad p_{-2} = 0.159941$
$m = 0 \quad p_0 = 0.332571$	$m = 0 \quad p_0 = 0.250635$	$m = -1 \quad p_{-1} = 0.198742$
$m = 1 \quad p_1 = 0.267269$	$m = 1 \quad p_1 = 0.239835$	$m = 0 \quad p_0 = 0.199551$
$m = 2 \quad p_2 = 0.066364$	$m = 2 \quad p_2 = 0.125378$	$m = 1 \quad p_1 = 0.201197$
$m = 3 \quad p_3 = 0.000833$	$m = 3 \quad p_3 = 0.010613$	$m = 2 \quad p_2 = 0.159721$
		$m = 3 \quad p_3 = 0.039697$
		$m = 4 \quad p_4 = 0.000479$

$s = 6$	$s = 7$
$m = -4 \quad p_{-4} = 0.006921$	$m = -5 \quad p_{-5} = 0.000363$
$m = -3 \quad p_{-3} = 0.083823$	$m = -4 \quad p_{-4} = 0.028955$
$m = -2 \quad p_{-2} = 0.159604$	$m = -3 \quad p_{-3} = 0.113895$
$m = -1 \quad p_{-1} = 0.167262$	$m = -2 \quad p_{-2} = 0.141662$
$m = 0 \quad p_0 = 0.165642$	$m = -1 \quad p_{-1} = 0.142537$
$m = 1 \quad p_1 = 0.166942$	$m = 0 \quad p_0 = 0.144154$
$m = 2 \quad p_2 = 0.159625$	$m = 1 \quad p_1 = 0.142207$
$m = 3 \quad p_3 = 0.083206$	$m = 2 \quad p_2 = 0.142849$
$m = 4 \quad p_4 = 0.006975$	$m = 3 \quad p_3 = 0.114120$
	$m = 4 \quad p_4 = 0.028863$
	$m = 5 \quad p_5 = 0.000396$

The resulting alphabet increases in size for larger s . And the more “centered” a symbol is, the more frequently it appears.

For $s \geq 3$, the number of different admissible symbols L is always greater than 7. We define the *external* symbols as the 6 outer symbols in our alphabet (3 on each side) and the *internal* symbols as the remaining ones. Then, for a given s , the probabilities of the internal symbols tend to be the same, an observation we will extend for sequences of many symbols.

20.3.3 Admissibility of sequences of more than 2 symbols

Knowing which symbols are admissible allows us to expand our study to sequences of many symbols, spread over both space and time dimensions. Consider sequence m :

$$\begin{bmatrix} m_{1,1} & \dots & m_{j,1} \\ \vdots & & \vdots \\ m_{1,i} & \dots & m_{j,i} \end{bmatrix} \text{ with } i \text{ and } j \geq 2$$

[2×2] spatiotemporal domains

For aesthetic reasons, we redefine our symbols and our coordinates:

$$\begin{array}{ll} q_{1,0} = x_1 & q_{2,0} = x_2 \\ q_{0,1} = x_8 & \mathbf{q}_{1,1} = \mathbf{q}_1 \quad \mathbf{q}_{2,1} = \mathbf{q}_2 \quad q_{3,1} = x_3 \\ q_{0,2} = x_7 & \mathbf{q}_{1,2} = \mathbf{q}_3 \quad \mathbf{q}_{2,2} = \mathbf{q}_4 \quad q_{3,2} = x_4 \\ q_{1,3} = x_6 & q_{2,3} = x_5 \end{array}$$

as well as $m_{1,1} = a_1$, $m_{2,1} = a_1$, $m_{1,2} = a_3$ and $m_{2,2} = a_4$. And using the Newtonian equation ????, the system of inequalities then becomes:

$$\begin{aligned} q_1 &= \frac{1}{s}(a_1 + q_2 + q_3 + x_1 + x_8) \\ q_2 &= \frac{1}{s}(a_2 + q_1 + q_4 + x_2 + x_3) \\ q_3 &= \frac{1}{s}(a_3 + q_1 + q_4 + x_6 + x_7) \\ q_4 &= \frac{1}{s}(a_4 + q_2 + q_3 + x_4 + x_5) \end{aligned},$$

with conditions

$$\begin{aligned} \forall i \in \{1, \dots, 4\}, \quad -\frac{1}{2} &\leq q_i < \frac{1}{2} \\ \forall j \in \{1, \dots, 8\}, \quad -\frac{1}{2} &\leq x_j < \frac{1}{2} \\ \forall k \in \{1, \dots, 4\}, \quad m_k \in \{\text{alphabet}\} \end{aligned}$$

For $s = 3$:

$$\begin{aligned} -\frac{3}{2} - a_1 &\leq q_2 + q_3 + x_1 + x_8 < \frac{3}{2} - a_1 \\ -\frac{3}{2} - a_2 &\leq q_1 + q_4 + x_2 + x_3 < \frac{3}{2} - a_2 \\ -\frac{3}{2} - a_3 &\leq q_1 + q_4 + x_6 + x_7 < \frac{3}{2} - a_3 \\ -\frac{3}{2} - a_4 &\leq q_2 + q_3 + x_4 + x_5 < \frac{3}{2} - a_4 \end{aligned} \quad \text{with } \begin{cases} -\frac{1}{2} \leq q_i < \frac{1}{2} \\ -\frac{1}{2} \leq x_j < \frac{1}{2} \\ m_k \in \{-3, -2, \dots, 2, 3\} \end{cases}$$

For the Arnol'd cat map case $s = 3$, there are a total of $7^4 = 2401$ possible [2×2] spatiotemporal blocks.¹ Running on Mupad, we solve this system of inequalities for different a 's. The number of empty solutions we obtain is 552 which represents a total of 23% inadmissible spatiotemporal domains, which seems too small...

Running many sequences on MATLAB

We now try to confirm this percentage using our MATLAB program. The probabilistic distribution of every [2×2] spatiotemporal domain has the shape shown in figure 20.1.

The difference in results from our analytical study is quite significant since the number of inadmissible sequences is 1,665 out of 2,401 (69.3%). A number that could be blamed on the size of our sample being not large enough.

¹Predrag 2017-09-08 In ref. [1] I wrote that the $d = 1$ Arnol'd cat map $s = 3$ alphabet has 5 letters $\mathcal{A} = \{2, 1, 0, 1, 2\}$. Am I wrong? You mean $d = 2$ spatiotemporal cat $s = 3$ alphabet on $[-\frac{1}{2}, \frac{1}{2}] \times [-\frac{1}{2}, \frac{1}{2}]$ phase space has $s + 4 = 7$ letters? : R

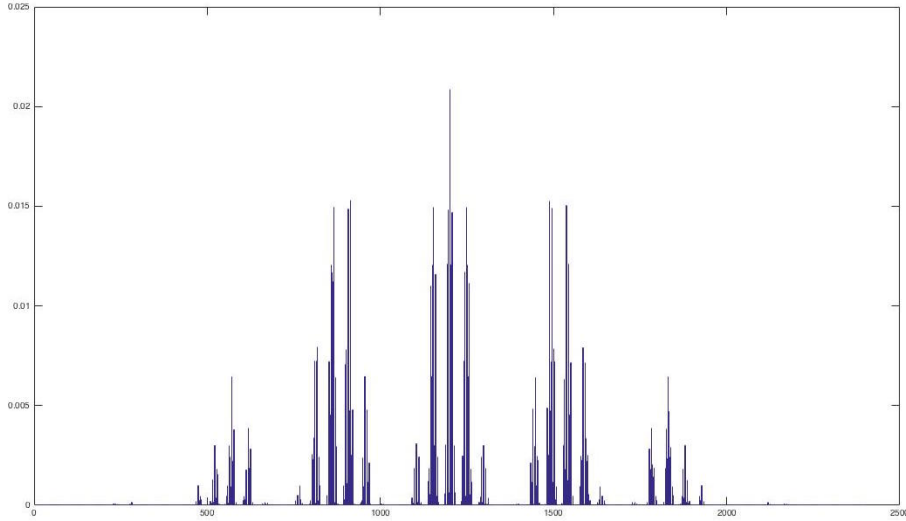


Figure 20.1: Probability distribution for *all* $[2 \times 2]$ spatiotemporal domains.
 $N = 100$ $T = 20\,000$ $s = 3$.

Nevertheless, if our statistical analysis is improved, few other analysis can be accomplished:

- Try spatiotemporal domains of size $[3 \times 3]$. But because the total number $7^9 = 40\,353\,607$, an even larger sample would then be required to appropriately study the probability distribution of those blocks, at least of order of 10^9 .
- Next, look for probing rules for spatiotemporal domains of size $[3 \times 3]$, that are NOT probing rules for $[2 \times 2]$ spatiotemporal domains...

Internal symbols

We close our discussion by focusing on the significance or internal symbols. The frequencies of appearance of all $[2 \times 2]$ and $[3 \times 3]$ internal blocks are analyzed for the case $s = 5$. The internal symbols are then $\{-1, 0, 1\}$ and the simulations are for $N = 30$ and $T = 50\,000$. For this sample, the 81 $[2 \times 2]$ blocks of internal symbols are spread evenly (figure 6.2 a), which confirms that for a given trace s , the internal symbols have a uniform distribution. For the 19683 $[3 \times 3]$ blocks, the same behavior tends to be observed but the ratio *number of sequences to size of the sample* seems once again to "deform" such distribution.

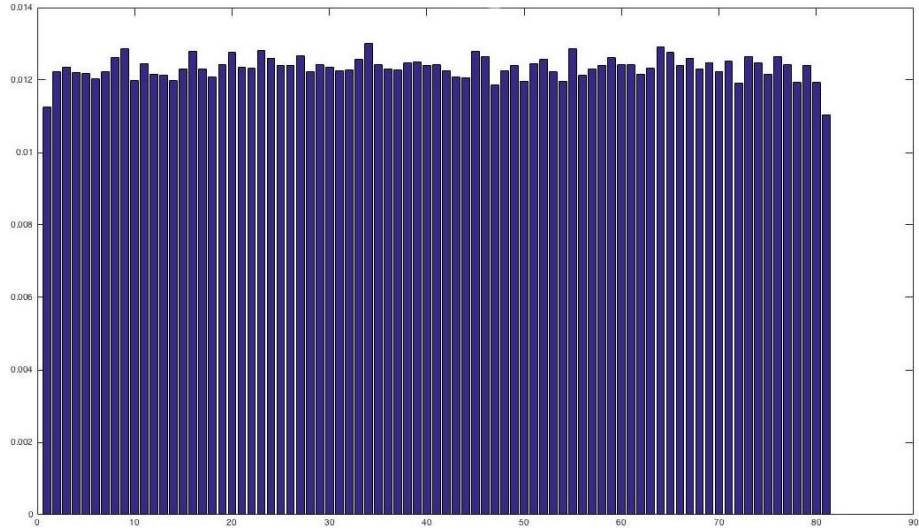


Figure 20.2: (a) $[2 \times 2]$ spatiotemporal domains.

20.4 Future work...

A lot still remains to be done in order to get a complete understanding of Coupled Cat Maps. Among other things, one important factor is the fact that this symbolic dynamics present a symmetry between space and time. In figure 20.3 the probability distribution for spatiotemporal domains of shape $[2 \times 1]$ (evolution in time) and $[1 \times 2]$ (evolution in space) are both drawn. A total of 81 spatiotemporal domains in each case is obtained, and present very similar distributions.²

Other future work also involve the reconstruction of orbits in the phase space based on symbolic sequences. A significant step in the understanding of semi-classical particles in a chaotic regimes...

References

- [1] B. Gutkin, L. Han, R. Jafari, A. K. Saremi, and P. Cvitanović, “[Linear encoding of the spatiotemporal cat map](#)”, *Nonlinearity* **34**, 2800–2836 (2021).
- [2] B. Gutkin and V. Osipov, “[Classical foundations of many-particle quantum chaos](#)”, *Nonlinearity* **29**, 325–356 (2016).

²Predrag 2016-08-02 Rather than ‘similar’, aren’t they supposed to be identically the same? Are there some numerical differences in the columns of the two figures (they cannot be seen in the plots)?:

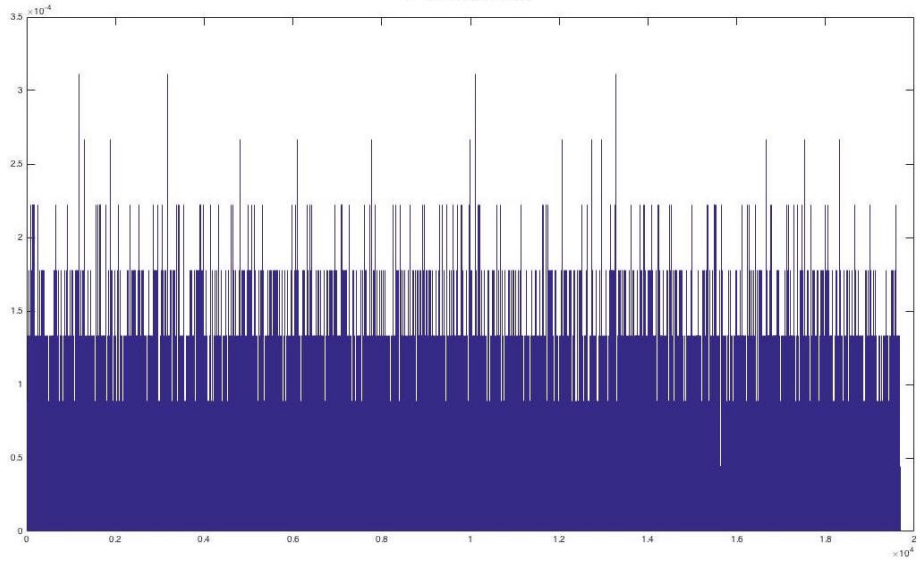


Figure 20.2: (b) $[3 \times 3]$ spatiotemporal domains.
Probability distribution for sequences of internal symbols.
 $N = 30$ $T = 50\,000$ $s = 5$.

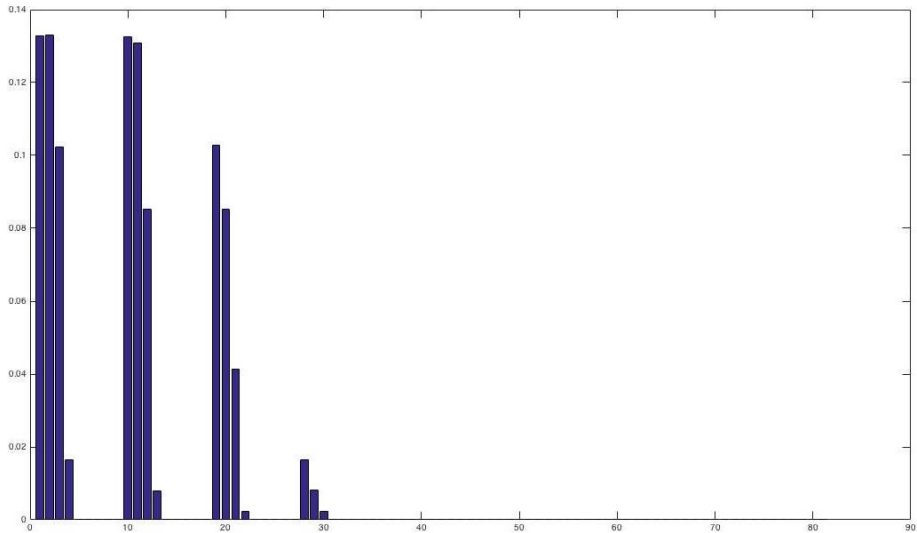


Figure 20.3: (a) $[2 \times 1]$ spatiotemporal domains.

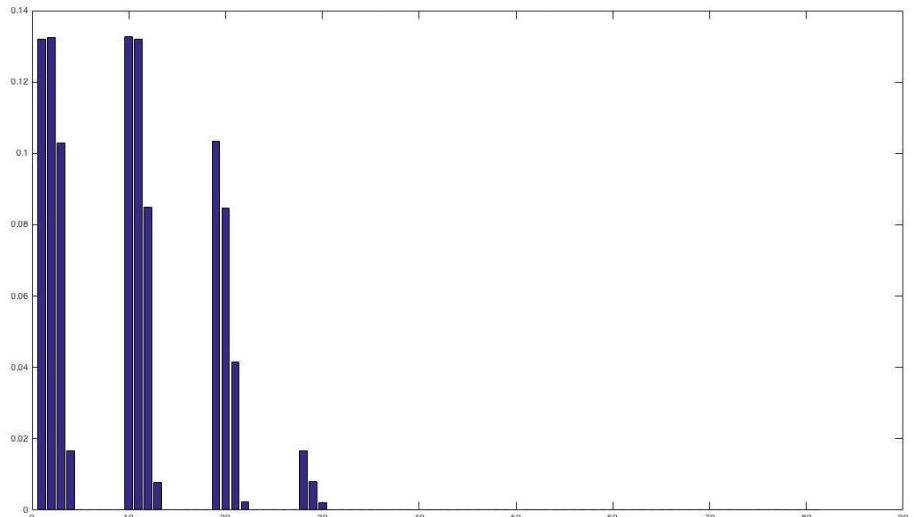


Figure 20.3: (b) $[1 \times 2]$ spatiotemporal domains.
Probability distribution of all $[2 \times 1]$ and $[1 \times 2]$ spatiotemporal domains.
 $N = 30$ $T = 50\,000$ $s = 5$.

Chapter 21

Rana's blog

Rana Jafari <jafari.rana@gmail.com> work blog
The latest entry at the bottom for this blog

2016-01-19 Rana Here is an example of [text edit by me](#), and here one of a footnote by me¹.

2015-11-20 Rana (Discussion with Predrag, Kuramoto-Sivashinsky equilibria and relative equilibria project Spring 2016:

- blog the project progress [here](#)
- blog whatever I'm reading and learning about dynamical systems [here](#)

2016-01-19 Rana I've been working on reading the ChaosBook materials and doing the online Course 1.

2016-06-05 to 06-11 Rana Read Chapters 14, 17, part of 18, and 19 of Chaosbook. Did homework of Weeks 9 and 10. Read 1st chapter of Hao and Zheng [1] *Applied Symbolic Dynamics and Chaos*, and started reading 2nd chapter.

2016-06-13 Predrag Try not to get further into Hao and Zheng [1] than necessary. You want to return to symbolic dynamics for cat map as fast as possible, and then understand Gutkin and Osipov coupled lattice generalization.

2016-07-08 Predrag to Rana: Do you agree with Li Han table 1.1 on the numbers of pruned blocks?

2016-07-10 Rana Li's and my results are in agreement.

¹Rana 2016-01-19: Rana test footnote

2016-07-11 Predrag to Rana: Can you complete table 1.1? Li Han did not write what the numbers of new pruned blocks are.

2016-07-11 Predrag to Rana: I can already see that several of my posts has not been recovered after you erased my edits (by mitting to *svn up* before starting your edits). For example, all my instructions about how to add figures are gone (but there is a copy at the end of Adrien's blog. You have to add *RJfrequencies.png* (or *RJfrequencies.pdf*) to *siminos/figs/*, then *svn add Jfrequencies.png*.

Can you quickly recheck your blog, make sure I have not introduced new errors while trying to recover my edits?

2016-07-12 Rana Li and I checked our the results at the meeting, and we had the same results for $|a|$ up to 5 . I saw table 1.1 today, the number of inadmissible sequences that I found for $|a| = 7$ differs from Li's. I wrote my results in table 19.2.

2016-07-12 Predrag You might have *svn add RJfrequencies.png* (or *RJfrequencies.pdf*) to *siminos/figs/*, but it has not been added to the repository yet (you can see that from the commit emails). Wonder why? Perhaps this:

Remember, always, before *svn up* and *svn ci -m "added entropy figures"* you have to go to the root directory, *cd [...]siminos*. Otherwise you are not refreshing bibtex, figures and other files in the repository.

2016-07-12 Predrag to Rana:

On *zero.physics.gatech.edu*, or Matt's *light.physics.gatech.edu*, or Xiong's *hard.physics.gatech.edu*, or Boris' *love.physics.gatech.edu*, or any other CNS linux workstation your userid is

rjafari7 (the same passwd as for svn - please change it once you log in)

Do not do calculations on the server *zero.physics.gatech.edu* - from any machine (including your laptop)

ssh rjafari7@light.physics.gatech.edu

save all data on the local hard disk */usr/local/home/rjafari7/*. I have made a link in your CNS home directory:

cd homeLight

Help for CNS system is on

www.cns.gatech.edu/CNS-only cnsuser cnsweb

but current crop of grad students, as a matter of principle, never look at any info, or add to these homepages.

Good luck - Xiong knows linux best, also Chris Marcotte and Burak Budanur (via Skype) know a lot. All our documentation is on

References

- [1] B.-L. Hao and W.-M. Zheng, *Applied Symbolic Dynamics and Chaos*, 2nd ed.
(World Scientific, Singapore, 2018).

Chapter 22

Adrien's blog

Adrien K. Saremi <adriensaremi@gmail.com> work blog
[The latest entry at the bottom for this blog](#)

22.1 Introduction

Following Gutkin and Osipov [3] *Classical foundations of many-particle quantum chaos*, we write Hamilton's equations for a set of N particles with generalized coordinates $\{q_n, p_n\}$ described in the section 3.1 *Dynamics*. Let

$$\mathcal{Z}_t = \begin{Bmatrix} q_t \\ p_t \end{Bmatrix} = \begin{Bmatrix} q_{1,t} \\ p_{1,t} \\ \dots \\ p_{N,t} \\ q_{N,t} \end{Bmatrix}.$$

The equations of motion are represented in the matrix form:

$$\mathcal{Z}_{t+1} = \mathcal{B}_N \mathcal{Z}_t$$

with

$$\begin{aligned} \mathcal{B}_N &= \begin{pmatrix} A & B & 0 & \dots & 0 & B \\ B & A & B & \dots & 0 & 0 \\ 0 & B & A & \dots & 0 & 0 \\ \vdots & \vdots & \vdots & \ddots & \vdots & \vdots \\ 0 & 0 & 0 & \dots & A & B \\ B & 0 & 0 & \dots & B & A \end{pmatrix} \\ A &= \frac{1}{c} \begin{pmatrix} a & 1 \\ ab - c^2 & b \end{pmatrix}, \quad B = -\frac{1}{c} \begin{pmatrix} d & 0 \\ db & 0 \end{pmatrix} \end{aligned} \quad (22.1)$$

22.2 Arnol'd cat map

To start our project, Boris advised us to start with just one particle $N = 1$ and pick the values $a = 1, b = 2$ and $c = -1$ (Arnol'd cat map) such that

$$\mathcal{B}_N = \mathcal{B}_1 = A = \begin{pmatrix} 1 & 1 \\ 1 & 2 \end{pmatrix}, \quad \det A = 1.$$

This system can be written as:

$$\begin{pmatrix} q_{t+1} \\ p_{t+1} \end{pmatrix} = A \begin{pmatrix} q_t \\ p_t \end{pmatrix} \mod 1 \quad (22.2)$$

The goal is now to find prime periodic orbits p of period T_p and initial points $(q_{p,1}, p_{p,1})$ such that:

$$\begin{pmatrix} q_{p,T_p} \\ p_{p,T_p} \end{pmatrix} = \begin{pmatrix} q_{p,1} \\ p_{p,1} \end{pmatrix} \mod 1$$

22.2.1 First approach

Consider

$$\begin{pmatrix} q_{||} \\ p_{||} \end{pmatrix} = A^{||} \begin{pmatrix} q_0 \\ p_0 \end{pmatrix} \mod 1$$

Now demand that (q_0, p_0) is periodic point in a prime periodic orbit p on \mathbf{T}^2 (two-dimensional torus), i.e., a relative periodic orbit on \mathbb{Z}^2 , periodic up to a shift by integers (m_q, m_p) :

$$\begin{pmatrix} q_0 \\ p_0 \end{pmatrix} = A^{||} \begin{pmatrix} q_0 \\ p_0 \end{pmatrix} + \begin{pmatrix} m_q \\ m_p \end{pmatrix}$$

Therefore:

$$\begin{pmatrix} q_0 \\ p_0 \end{pmatrix} = (\mathbb{1} - A^{||})^{-1} \begin{pmatrix} m_q \\ m_p \end{pmatrix}$$

Boris suggested that we take two random points (M_q, M_p) apply the inverse of $\mathbb{1} - A^{||}$, and remove the integer part (modulo 1) to find (q_0, p_0) . Unfortunately it is hard to find the number $||\dots||$. The number of periodic orbits (AKA the number of sets of (q_0, p_0)) would be then given by:

$$|\det(\mathbb{1} - A^{||})| = |(1 - \lambda^{||})(1 - \frac{1}{\lambda^{||}})|$$

where λ is the largest eigenvalue of A : $\lambda = \frac{3+\sqrt{5}}{2} = 2.6180 \dots$

We also tried two random initial points $q_0 = 0.5$ and $p_0 = 0.4$, and applied the A matrix several times in hope that the iteration would return to the initial points, but this was unsuccessful (as expected)

22.2.2 2nd approach

Here we eliminate $\{p_t\}$ in favor of a 2-step recurrence equation for $\{q_t\}$ only. Boris gave us a different set of equations of motion, but I believe that we can obtain equations only on $\{q_t\}$ the following way:

$$p_t = \frac{q_t - q_{t-1}}{\Delta t} = q_t - q_{t-1}$$

Combined with:

$$q_{t+1} = q_t + p_t$$

We obtain:

$$q_3 - 3q_2 + q_1 = m_2$$

$$q_4 - 3q_3 + q_2 = m_3$$

⋮

$$q_{||+1} - 3q_{||} + q_{||-1} = m_{||}$$

$$q_{||+2} - 3q_{||+1} + q_{||} = m_{||+1} \quad (22.3)$$

Given that we are looking for periodic orbits, and that $q_{||+1} = q_1$ and $q_{||+2} = q_2$, the last equation reduces to:

$$q_2 - 3q_1 + q_{||} = m_1$$

This set of equations reduces to the following matrix form:

$$\mathcal{D}Q = m$$

With $Q = \begin{pmatrix} q_1 \\ q_2 \\ \vdots \\ q_{||} \end{pmatrix}$, $m = \begin{pmatrix} m_1 \\ m_2 \\ \vdots \\ m_{||} \end{pmatrix}$, and $\mathcal{D} = \begin{pmatrix} -3 & 1 & 0 & 0 & 0 & \dots & 1 \\ 1 & -3 & 1 & 0 & 0 & \dots & 0 \\ \vdots & & & & & & \\ 1 & 0 & 0 & 0 & \dots & 1 & -3 \end{pmatrix}$

Boris suggested to pick a random set of integers $(M_1, M_2, \dots, M_{||-1})^T$ apply the \mathcal{B} matrix, and take the modulo.

BUT AGAIN: how are we supposed to get the size of the matrix?!?!

22.2.3 Computing periodic orbits

2016-06-01 Adrien Since our web meeting of Friday, May 27th, Boris suggested to run simulations on Matlab as follows:

1. use the 2nd approach, sect. 22.2.2, and start with random q_1 and q_2
2. compute q_3 and m_1 using (22.3)
3. q_3 is the decimal part of the equation, while m_1 is the integer part
4. repeat for a large number of iterations

5. if we come back on our feet, AKA $q_{n+1} = q_1$ and $q_{n+2} = q_2$, we have a periodic orbit of period n

I did those simulations, and obtain, as Li Han, values of $m_j \in \{-1, 0, 1, 2\}$. What I also found was that, depending on the few starting point of form $\{q_1, q_2\} = \{\frac{P_1}{10}, \frac{P_2}{10}\}$ that I tried, the period n is either 1, 6, 7, 10, 30 or does not converge to a periodic orbit, computing in Matlab, double precision.

2016-06-17 Predrag You are sure the periods were “ 1, 6, 7, 10, 30”, or is there a typo in this list? ¹

2016-06-09 Adrien Explaining the results:

This program allows us to start with many different sets of points q_1, q_2 . For example, the program will first run the set of points $\{q_1, q_2\} = \{0.0, 0.0\}$, do the computations of $N = 100$ points, and "pray" to find periodicity. What I observed so far was that the largest periodicity for a given starting set would be $n = 30$, otherwise, the orbit would not be periodic.

The next part of the program is to do the same computations for a different starting set, following this method:

$$q_1 = q_1 + \Delta_1 \quad q_2 = q_2 + \Delta_2$$

such that the starting points remain in the unit interval $[0, 1]$.

For $\Delta_1 = \Delta_2 = 0.1$, we obtain orbits for 100 starting sets:

$$\{q_1, q_2\} \in \{\{0.0, 0.0\}, \{0.0, 0.1\} \dots \{0.0, 0.9\}, \{1.0, 0.0\}, \{1.0, 0.1\} \dots \{0.9, 0.9\}\}$$

These starting sets are rational numbers P/Q , $1 \leq P < Q$ of form $P/10$. I have observed that for several different starting sets, the frequency of repetition of symbols $\{-1, 0, 1, 2\}$ has some similarities. For example:

- For $\{q_1, q_2\} = \{0.2, 0.0\}$ the probabilities I obtain are:

$$p_{-1} = 0.204, p_0 = 0.398, p_1 = 0.194, p_2 = 0.204$$

- For $\{q_1, q_2\} = \{0.3, 0.6\}$ we get:

$$p_{-1} = 0.204, p_0 = 0.327, p_1 = 0.265, p_2 = 0.204$$

- And for $\{q_1, q_2\} = \{0.8, 0.3\}$ we get:

$$p_{-1} = 0.204, p_0 = 0.337, p_1 = 0.255, p_2 = 0.204$$

Observations:

¹Predrag : the correct list is (22.4)

1. For those sets, the outer symbols repeat with the same frequency, the inner ones change. Something to look into...
2. There are many frequencies that keep reappearing over for different starting sets. Some even have the same p_{-1}, p_0, p_1, p_2 but different m_j sequences...
3. I still happen to find that some orbits, even though all starting sets are rationals, are not periodic. Pretty sure I still have to work on precision and removing error, because I should obtain periodic orbits, or should I??

2016-06-12 Predrag Don't you think that if you get more statistics (you put no error brackets on your numbers) $p_2 = 0.204$ will become $p_2 = 1/5$, for example?

2016-06-13 Boris If your starting points q_1, q_2 are rational, the resulting orbit is always periodic by the following reason. Assume the initial momentum and coordinate are rational numbers with some common denominator N . Since cat map is composed of integers, after n steps momentum and coordinate have the form $q_n = a_n/N, p_n = b_n/N$ i.e., have the same denominator N . So you travel on the lattice of the size $N \times N$ and sooner or later must close the loop. The reason why sometimes you do not find periodic orbits is due to round-off errors. Another point - the frequency of a symbol appearances in periodic orbits (generated by picking "random" rational initial conditions) might be quite different from one for a generic non-periodic orbit.

2016-06-15 Adrien Explaining results, follow up...:

If I run the program for $N = 1000$, I find the following probabilities:

- For $\{q_1, q_2\} = \{0.2, 0.0\}$:

$$p_{-1} = \frac{1}{5}, p_0 = \frac{2}{5}, p_1 = \frac{1}{5}, p_2 = \frac{1}{5}$$

- For $\{q_1, q_2\} = \{0.3, 0.6\}$:

$$p_{-1} = \frac{1}{5}, p_0 = \frac{1}{3}, p_1 = \frac{4}{15}, p_2 = \frac{1}{5}$$

- For $\{q_1, q_2\} = \{0.8, 0.3\}$:

$$p_{-1} = \frac{1}{5}, p_0 = \frac{1}{3}, p_1 = \frac{4}{15}, p_2 = \frac{1}{5}$$

In some rational starting sets, there were also cases where I could not "come back" to the starting set $\{q_1, q_2\}$. For those starting sets, the program now looks for periodicity in the m_j sequence. And for all starting sets that I described above, even with $\Delta_1 = \Delta_2 = 0.01$, all m_j vectors exhibit a periodic behavior. The most frequent and highest periodicity I found was $n = 30$ for all those starting sets. The periodicities I found were

$$1, 2, 3, 6, 10, 30. \quad (22.4)$$

The second important observation was that for irrational starting points, such as $\{q_1, q_2\} = \{\frac{\pi}{6}, \frac{\pi}{8}\}$, even if $N = 20\,000$, the program found no periodicity, neither in the q_j 's, nor the m_j sequences. That confirms what Boris mentioned in his previous remark.

Should I try with other numbers? More rational? More irrational?

I guess that the next step is what Boris told Rana in their meeting today: looking for frequencies of sequences of 2 symbols, then sequences of 3 symbols, ...

2016-06-17 Predrag : I assume that you stop your program once a periodic orbit is found, not always go all the way to $N = 1000$?

- [] Explain your result for $\{q_1, q_2\} = \{1/5, 0\}$
- [] Explain why your results above, for $\{q_1, q_2\} = \{3/10, 3/5\}$ and $\{q_1, q_2\} = \{4/5, 3/10\}$, are wrong for these initial points (but not for their irrational approximations).
- [] Derive the $\{p_{-1}, p_0, p_1, p_2\} = \{1/5, 1/3, 4/15, 1/5\}$. Hint: derive the $\{m_j\}$ partition of the unit square that Li Han had shown you.

2016-06-17 Predrag : Determine the possible periodic point denominators, periods for

- [] $\{q_1, q_2\} = \{\frac{P_1}{10}, \frac{P_2}{10}\}$
- [] $\{q_1, q_2\} = \{\frac{P_1}{100}, \frac{P_2}{100}\}$
- [] $\{q_1, q_2\} = \{\frac{P_1}{8}, \frac{P_2}{8}\}$
- [] $\{q_1, q_2\} = \{\frac{P_1}{17}, \frac{P_2}{17}\}$

How many decimal digits of accuracy you need to be sure that all periodic orbits close with accuracy of 10^{-4} for

- [] $\{q_1, q_2\} = \{\frac{P_1}{10}, \frac{P_2}{10}\}$?
- [] $\{q_1, q_2\} = \{\frac{P_1}{100}, \frac{P_2}{100}\}$?
- [] $\{q_1, q_2\} = \{\frac{P_1}{8}, \frac{P_2}{8}\}$?
- [] $\{q_1, q_2\} = \{\frac{P_1}{7}, \frac{P_2}{7}\}$?

- [] If the program is computing with double precision accuracy, what is the longest period that can be determined by mindless computation?

Hint: you know Floquet multipliers for all cat map orbits.

2016-06-17 Predrag : Don't let Matlab prevent you from thinking. You know that periodic points are rationals of form $\{q_j, q_{j+1}\} = \{P_j/Q, P_{j+1}/Q\}$, so at every iterate of your trajectory you can correct the 1-step error by replacing your decimal number by the nearest correct rational. This way you can compute any periodic orbit, of any period, as this eliminates the exponential accumulation of errors. Write a program that beats Li Han's zillion digits accuracy :)

- [] If the computation is done by thinking (+ a computer program), estimate the longest period that can be determined by thoughtful computation.

Of course, all this is a magic of rationals and number theory - the moment the maps go nonlinear, none of this trickery works. Still, it might be useful in tracking the symbolic dynamics for nonlinear maps as well, in the way in which the ChaosBook dike map captures the correct symbolic dynamics of any nonlinear unimodal map. For example, slightly deformed cat map still has the same symbolic dynamics as the (piecewise linear) Arnol'd cat map [1].

2016-06-21: Boris' lecture of today - Adrien We're explaining how the symbolic dynamics, in other words the array of m , relate to the trajectory in the phase space.

For the Arnol'd cat map we know that:

$$\mathcal{D}_n Q_n = m_n,$$

with $Q_n = \begin{pmatrix} q_1 \\ q_2 \\ \vdots \\ q_{||} \end{pmatrix}$, $m_n = \begin{pmatrix} m_1 \\ m_2 \\ \vdots \\ m_{||} \end{pmatrix}$ and

$$\mathcal{D}_n = \begin{pmatrix} -3 & 1 & 0 & 0 & 0 & \dots & 1 \\ 1 & -3 & 1 & 0 & 0 & \dots & 0 \\ \vdots & & & & & & \\ 1 & 0 & 0 & 0 & \dots & 1 & -3 \end{pmatrix}$$

For a given n , we define N_n as the total number of orbits with length n . It is pretty clear that $N_n = |\det(\mathcal{D}_n)|$, which also corresponds to $N_n = |\det(1 - A^n)|$ if we follow the first method.

For a given sequence of length p , such as $\{m_1 m_2 \dots m_p\}$, we also define $N_n(m_1 m_2, \dots, m_p)$ as the number of periodic orbits of length n that generate the given sequence. The probability of obtaining the sequence $\{m_1, m_2, \dots, m_p\}$ is then:

$$p(m_1 m_2 \dots m_p) = \lim_{n \rightarrow \infty} \frac{N_n(m_1 m_2 \dots m_p)}{N_n}$$

1. Let's now do the case $p = 1$, where $m_k = a$ and a is a given symbol.
The equations of motion can be rewritten as:

$$\begin{cases} q_{i-1} + q_{i+1} = 3q_i + m_i & \forall i \neq k \\ q_{k-1} + q_{k+1} = 3q_k + a \end{cases}$$

$$\begin{cases} q_{i-1} + q_{i+1} = 3q_i + m_i & \forall i \neq k, k-1, k+1 \\ q_{k-2} + \frac{1}{3}q_{k+1} = \frac{8}{3}q_{k-1} + \frac{a}{3} + m_{k-1} \\ q_{k+2} + \frac{1}{3}q_{k-1} = \frac{8}{3}q_{k+1} + \frac{a}{3} + m_{k+1} \end{cases}$$

This system we can write in the matrix form

$$\mathcal{D}_{n-1} Q_{n-1} = m_{n-1} + \frac{a}{3} J$$

where \mathcal{D}_{n-1} , Q_{n-1} , and m_{n-1} are the same as the \mathcal{D}_n , Q_n , and m_n , with the k^{th} row removed, and with:

$$J^\top = \left(0, 0, \ddots, 1, 1, 0, \dots, 0, \right).$$

The three inequalities we "collect" from all this mess are then:

$$\begin{aligned} 0 &\leq q_{k-1} < 1 \\ 0 &\leq q_{k+1} < 1 \\ a &\leq q_{k-1} + q_{k+1} < a + 3 \end{aligned}$$

For $a \in \{-2, -1, 0, 1\}$, it is pretty clear how to derive the regions admissible in the plane defined by q_{k-1} and q_{k+1}

2. For $p = 2$ and $n = 4$, we specify $m_2 = a$ and $m_3 = b$ and we limit our study to orbits of length 4. Indeed, only the outer points of the given sequence (here q_1 and q_4) span the lattice on which we can derive the admissible regions. For such system, the 4 inequalities that help us doing so are:

$$\begin{aligned} 0 &\leq q_1 < 1 \\ 0 &\leq q_4 < 1 \\ 0 &\leq \frac{1}{8}(3q_1 + q_4 - 3a + b) < 1 \\ 0 &\leq \frac{1}{8}(3q_4 - q_1 - 3b - a) < 1 \end{aligned}$$

2016-06-21 Answering Pedrag's questions - Adrien First of all, I modified my m_j vector such that it is made of the symbols $\{-2, -1, 0, 1\}$. Now answering the questions:

1. For $\{q_1, q_2\} = \{\frac{1}{5}, 0\} = \{0.2, 0\}$ (the decimal or rational notation doesn't make a difference), my program actually computes 1000 iteration since it does not find periodicity through the Q matrix. Nevertheless, it observes a repetition of symbol in the m_j vector as follow:

$$m = \begin{pmatrix} -2 \\ 0 \\ 0 \\ -2 \\ 1 \\ 0 \\ -1 \\ -1 \\ 0 \\ 1 \end{pmatrix}$$

It is then easy to figure that:

$$p_{-2} = \frac{1}{5}, p_{-1} = \frac{1}{5}, p_0 = \frac{2}{5}, p_1 = \frac{1}{5}$$

2. For $\{q_1, q_2\} = \{\frac{3}{10}, \frac{3}{5}\}$ the m_j vector is:

$$m^T = (0, 0, -2, 1, -1, -2, 1, 0, 0, -2, 1, -1, 0, -1, -1, 0, -1, 1, -2, 0, 0, 1, 2, -1, 1, -2, 0, -1, 0, 0)$$

and for $\{q_1, q_2\} = \{\frac{4}{5}, \frac{3}{10}\}$

$$m^T = (0, 0, 1, -2, -1, 1, -2, 0, -1, 0, 0, -1, 0, -2, 1, -1, -2, 1, 0, 0, -2, 1, -1, 0, -1, -1, 0, -1, 1, 0)$$

For both cases, the periodicity is $n = 30$.

By counting the frequencies of $-2, -1, 0, 1$, I confirm the probabilities are different than the ones I wrote earlier. I might have wrongly interpreted the fractions given the decimal approximation of Matlab. For $\{q_1, q_2\} = \{0.3, 0.6\}$:

$$p_{-2} = \frac{1}{5}, p_{-1} = \frac{7}{30}, p_0 = \frac{11}{30}, p_1 = \frac{1}{5}$$

However, for $\{q_1, q_2\} = \{0.8, 0.3\}$, the result is identical:

$$p_{-2} = \frac{1}{5}, p_{-1} = \frac{4}{15}, p_0 = \frac{1}{3}, p_1 = \frac{1}{5}$$

3. I am not so sure about this question. We know now that the following distribution $p_{-2} = \frac{1}{5}, p_{-1} = \frac{4}{15}, p_0 = \frac{1}{3}, p_1 = \frac{1}{5}$ can be generated from the starting set $\{q_1, q_2\} = \{0.8, 0.3\}$. But we obtain such frequencies after 30 iterations, since it's the length of this periodic orbit. If we refer to what Li Han presented over last week, we actually look at 1 iteration but for a GREAT number of starting sets spread over the unit square.

For $\{q_1, q_2\} = \{i\Delta_1, j\Delta_2\}$ with $\Delta_1 = \Delta_2 = \frac{1}{200}$ and $i, j = 0, 1, 2, \dots, 199$, we obtain data for m_1 over 40,000 points spread over the unit square:

$$p_{-2} = 0.16583, p_{-1} = 0.33335, p_0 = 0.33310, p_1 = 0.16773$$

Which should fit with the theoretical values that we get from "Boris inequalities" that lead to admissible areas in the unit square spanned by $\{q_0, q_2\}$:

$$p_{-2} = \frac{1}{6}, p_{-1} = \frac{1}{3}, p_0 = \frac{1}{3}, p_1 = \frac{1}{6}$$

4. For "starting sets" of the form $\{\frac{i}{N}, \frac{j}{N}\}$, we obtain the following periodicities:

- For $\{q_1, q_2\} = \{\frac{i}{10}, \frac{j}{10}\}$, the periodicities found were: $n = 1, 2, 3, 6, 10, 30$
- For $\{q_1, q_2\} = \{\frac{i}{100}, \frac{j}{100}\}$, they were: $n = 1, 2, 3, 6, 10, 30, 50, 150$
- For $\{q_1, q_2\} = \{\frac{i}{8}, \frac{j}{8}\}$, $n = 1, 3, 6$
- And for $\{q_1, q_2\} = \{\frac{i}{17}, \frac{j}{17}\}$ $n = 1, 18$

Now if I understand your question carefully, we try to make sure than the final computed value of q_N , or q_n for periodic orbits, is within 10^{-4} from the actual $q_{n,real}$, in the worst case scenario. Let n_{max} the highest periodicity, and ϵ the error; then:

$$q_{n,comp} = q_{n,real} + \epsilon \lambda^{n_{max}}, \text{ where } \lambda = \frac{3 + \sqrt{5}}{2} = \text{multiplier}$$

So we want:

$$|\epsilon \lambda^{n_{max}}| \leq 10^{-4} \Rightarrow \epsilon \leq 10^{-4} \lambda^{-n_{max}}$$

- For $\{q_1, q_2\} = \{\frac{i}{10}, \frac{j}{10}\}$, $\epsilon \approx 10^{-18}$
- For $\{q_1, q_2\} = \{\frac{i}{100}, \frac{j}{100}\}$, $\epsilon \approx 10^{-68}$
- For $\{q_1, q_2\} = \{\frac{i}{8}, \frac{j}{8}\}$, $\epsilon \approx 10^{-8}$
- And for $\{q_1, q_2\} = \{\frac{i}{17}, \frac{j}{17}\}$ $\epsilon \approx 10^{-12}$

5. If we use double digit accuracy, aka 64 bits but 53 bits for accuracy, it means the error $\epsilon = 2^{-53}$. Following the same logic:

$$|\epsilon \lambda^{n_{max}}| \leq 10^{-4}$$

$$\Rightarrow n_{max} \approx \ln(\lambda) \ln\left(\frac{10^{-4}}{\epsilon}\right)$$

$$\Rightarrow n_{max} = 26$$

6. Coming soon...

2016-07-10 Adrien One more thing to add regarding the single Cat Map: the correlation of frequencies. I found interesting how the correlation between future and past symbolic dynamics vanish exponentially.

I pretty much did what Rana had done before, computing frequency of a given sequence $A = [a_1, \dots, a_u]$ of length u , another one $B = [a_1, \dots, a_v]$ of length v , as well as the frequency of seeing one repeated a length *space* (for example *space* = 3) after the other. We then increase the *spacing* and observe how the correlation factor:

$$\text{Correl} = p(A, \text{space}, B) - p(A)p(B) \quad \text{behaves}$$

For the ergodic orbit $\{q_1, q_2\} = \{\frac{\sqrt{5}}{4}, \frac{\sqrt{2}}{2}\}$, $A = [-1, 1]$, and $B = [-2, 0]$ and of length $N = 1,000,000$, we obtain the following:

$$p(A) = 0.1249 \quad p(B) = 0.0623$$

Spacing	$P(A, \text{space}, B)$	Correl
1	0.0085	$7.3567 \cdot 10^{-4}$
2	0.0066	-0.0011
3	0.0073	$-4.6733 \cdot 10^{-4}$
4	0.0080	$1.8867 \cdot 10^{-4}$
5	0.0079	$6.8666 \cdot 10^{-5}$
6	0.0078	$4.6655 \cdot 10^{-6}$

For longer sets $A = [-1, -1, -1, -1]$ and $B = [-2, 1, -1, 0]$, and the same orbit, the probabilities are as follow:

$$p(A) = 0.0178 \quad p(B) = 0.0151$$

Spacing	$P(A, \text{space}, B)$	Correl
1	$2.9400 \cdot 10^{-4}$	$2.4439 \cdot 10^{-5}$
2	$2.2400 \cdot 10^{-4}$	$-4.5561 \cdot 10^{-5}$
3	$2.4900 \cdot 10^{-4}$	$-2.0561 \cdot 10^{-5}$
4	$2.5100 \cdot 10^{-4}$	$-1.8561 \cdot 10^{-5}$
5	$2.7300 \cdot 10^{-4}$	$3.4392 \cdot 10^{-6}$
6	$2.6900 \cdot 10^{-4}$	$-5.6081 \cdot 10^{-7}$

Conclusion: We clearly see that in both scenarios, the Correlation factor diminishes as the separation between the two blocs increases. We also notice that for longer sets A and B , the correlation is small enough (but not zero) even for small spacing...

22.3 Coupled Cat Maps

We now get to more complicated systems by increasing the number of particle N . T will be now known as the period of the orbit, and if it doesn't exist, T will just refer to latest time iteration in the computation of the symbols m 's. Another objective of this study is to explain the impact of certain factors such as the trace of the A matrix (that we refer as $s = \text{trace}(A)$) on the nature of our alphabet, the frequencies of symbols repetition, the length of periodic orbits. and the admissibility of particular sequences of symbols.

22.3.1 Periodic orbits

We first verify the accuracy of our calculations by checking that rational sets $\{q_{1,1}, p_{1,1}, q_{2,1}, p_{2,1}, \dots, q_{N,1}, p_{N,1}\}$ belong to periodic orbits. To do so, we perform the iteration:

$$\mathcal{Z}_{t+1} = \mathcal{B}_N \mathcal{Z}_t$$

over and over, until we obtain:

$$\mathcal{Z}_{T+1} = \mathcal{B}_N \mathcal{Z}_1$$

in which case, the periodicity is T . We first tried with a number of 3 particles ($N = 3$), and picked the same trace $s = 3$ that we used in part 7.2. The initial coordinates of \mathcal{Z}_1 are multiples of hundredth, chosen randomly, but above all are **between** $[-\frac{1}{2}, \frac{1}{2}]$. Therefore, our symbolic dynamic $m = \{m^q, m^p\}$ should be symmetric with respect to 0 (which is the case) and our matrix \mathcal{B}_3 is:

$$\mathcal{B}_3 = \begin{pmatrix} 2 & 1 & -1 & 0 & -1 & 0 \\ 1 & 1 & -1 & 0 & -1 & 0 \\ -1 & 0 & 2 & 1 & -1 & 0 \\ -1 & 0 & 1 & 1 & -1 & 0 \\ -1 & 0 & -1 & 0 & 2 & 1 \\ -1 & 0 & -1 & 0 & 1 & 1 \end{pmatrix}$$

- for $\mathcal{Z}_1 = \left\{ \frac{31}{100}, \frac{29}{100}, \frac{7}{50}, -\frac{13}{100}, \frac{31}{100}, \frac{3}{100} \right\}$

the periodicity is $T = 60$, and the symbolic dynamics is:

$$\begin{aligned} m &= -2, p_{-2} = 0.011111 \\ m &= -1, p_{-1} = 0.222222 \\ m &= 0, p_0 = 0.536111 \\ m &= 1, p_1 = 0.227778 \\ m &= 2, p_2 = 0.002778 \end{aligned}$$

- for $\mathcal{Z}_1 = \left\{ -\frac{3}{20}, \frac{43}{100}, \frac{37}{100}, \frac{1}{20}, \frac{3}{25}, \frac{2}{25} \right\}$

the periodicity is $T = 60$, and the symbolic dynamics is:

$$\begin{aligned} m &= -2, p_{-2} = 0.016667 \\ m &= -1, p_{-1} = 0.222222 \\ m &= 0, p_0 = 0.511111 \\ m &= 1, p_1 = 0.244444 \\ m &= 2, p_2 = 0.005556 \end{aligned}$$

- for $N = 5$ and $\mathcal{Z}_1 = \left\{ -\frac{3}{10}, -\frac{1}{5}, -\frac{3}{100}, -\frac{27}{100}, \frac{17}{50}, -\frac{31}{100}, -\frac{7}{25}, -\frac{33}{100}, -\frac{7}{25}, -\frac{7}{100} \right\}$

the periodicity is $T = 60$, and the symbolic dynamics is:

$$\begin{aligned} m &= -2, p_{-2} = 0.007333 \\ m &= -1, p_{-1} = 0.222667 \\ m &= 0, p_0 = 0.540667 \\ m &= 1, p_1 = 0.221333 \\ m &= 2, p_2 = 0.008000 \end{aligned}$$

- And for $N = 7$ and

$$\mathcal{Z}_1 = \left\{ -\frac{19}{100}, \frac{21}{50}, -\frac{7}{100}, -\frac{8}{25}, \frac{2}{5}, \frac{47}{100}, -\frac{7}{100}, -\frac{39}{100}, -\frac{1}{4}, -\frac{1}{10}, \frac{9}{100}, -\frac{6}{25}, \frac{1}{10}, \frac{21}{100} \right\}$$

the periodicity is $T = 2790$, and the symbolic dynamics is:

$$\begin{aligned} m &= -2, p_{-2} = 0.012110 \\ m &= -1, p_{-1} = 0.226472 \\ m &= 0, p_0 = 0.526882 \\ m &= 1, p_1 = 0.224014 \\ m &= 2, p_2 = 0.010522 \end{aligned}$$

22.3.2 Ergodic orbits

We now focus on the nature of our symbolic dynamics, by choosing ergodic orbits, running for a very very long time $T = 80,000$. To do so, we start with an irrational set \mathcal{Z}_1 but $N = 5$ particles. The trace of the A matrix increases from 3 to 7 in order to obtain a larger alphabet of symbols. Remember that the trace $s = a + b$, so we just set $b = 1$ and $a \in \{2, \dots, 7\}$ such that $s \in \{3, \dots, 8\}$. Our initial set is:

$$\mathcal{Z}_1 = \left\{ \frac{\sqrt{5}}{6}, 0, -\frac{\sqrt{3}}{6}, \frac{\sqrt{2}}{8}, \frac{\sqrt{3}}{14}, -\frac{\sqrt{5}}{12}, -\frac{\sqrt{6}}{20}, \frac{1}{17}, \frac{3}{10}, \frac{\sqrt{2}}{10} \right\}$$

Observations:

1. The first thing we observe is that the orbit is not periodic. We obviously compute the frequencies of symbol that only appear in our dynamics. The number of particles $N = 5$ clearly has an impact on the nature of our

symbols.

We also compute the frequencies of the *Newtonian* dynamics, defined as:

$$c(q_{n,t+1} + q_{m,t-1}) + d(q_{n+1,t} + q_{n-1,t}) = -(a+b)q_{n,t} + m_{n,t}$$

The code computes our $\{m_{n,t}^q, m_{n,t}^p\}$ by only referring to the equation $\mathcal{Z}_{t+1} = \mathcal{B}_N \mathcal{Z}_t$ and by "capturing" the integer parts of the coordinates q 's and p 's (similarly to the Single Cat Map code I wrote). Once the orbit has been computed, the Newtonian symbolics $m_{n,t}$ (no upper index) can be derived from the position coordinates $q_{n,t}$.

Let's look at the frequencies of every of those symbols, as a function of the trace s .

- For $s = 3$, the frequencies obtained are:

$$\begin{aligned} m^{q,p} &= -2, p_{-2} = 0.011450 \\ m^{q,p} &= -1, p_{-1} = 0.224397 \\ m^{q,p} &= 0, p_0 = 0.529401 \\ m^{q,p} &= 1, p_1 = 0.223045 \\ m^{q,p} &= 2, p_2 = 0.011706 \end{aligned}$$

And:

$$\begin{aligned} m &= -3, p_{-3} = 0.000850 \\ m &= -2, p_{-2} = 0.067293 \\ m &= -1, p_{-1} = 0.264819 \\ m &= 0, p_0 = 0.332571 \\ m &= 1, p_1 = 0.267269 \\ m &= 2, p_2 = 0.066364 \\ m &= 3, p_3 = 0.000833 \end{aligned}$$

- For $s = 4$, the frequencies obtained are:

$$\begin{aligned} m^{q,p} &= -3, p_{-3} = 0.000444 \\ m^{q,p} &= -2, p_{-2} = 0.044169 \\ m^{q,p} &= -1, p_{-1} = 0.258639 \\ m^{q,p} &= 0, p_0 = 0.394029 \\ m^{q,p} &= 1, p_1 = 0.257650 \\ m^{q,p} &= 2, p_2 = 0.044615 \\ m^{q,p} &= 3, p_3 = 0.000455 \end{aligned}$$

And:

$$\begin{aligned} m &= -3, p_{-3} = 0.010696 \\ m &= -2, p_{-2} = 0.126391 \\ m &= -1, p_{-1} = 0.236452 \\ m &= 0, p_0 = 0.250635 \\ m &= 1, p_1 = 0.239835 \\ m &= 2, p_2 = 0.125378 \\ m &= 3, p_3 = 0.010613 \end{aligned}$$

- For $s = 5$, the frequencies obtained are:

$$\begin{aligned}
 m^{q,p} = -3, p_{-3} &= 0.005604 \\
 m^{q,p} = -2, p_{-2} &= 0.095479 \\
 m^{q,p} = -1, p_{-1} &= 0.254543 \\
 m^{q,p} = 0, p_0 &= 0.290261 \\
 m^{q,p} = 1, p_1 &= 0.252449 \\
 m^{q,p} = 2, p_2 &= 0.095980 \\
 m^{q,p} = 3, p_3 &= 0.005685
 \end{aligned}$$

And:

$$\begin{aligned}
 m = -4, p_{-4} &= 0.000592 \\
 m = -3, p_{-3} &= 0.040080 \\
 m = -2, p_{-2} &= 0.159941 \\
 m = -1, p_{-1} &= 0.198742 \\
 m = 0, p_0 &= 0.199551 \\
 m = 1, p_1 &= 0.201197 \\
 m = 2, p_2 &= 0.159721 \\
 m = 3, p_3 &= 0.039697 \\
 m = 4, p_4 &= 0.000479
 \end{aligned}$$

- For $s = 6$, the frequencies obtained are:

$$\begin{aligned}
 m^{q,p} = -4, p_{-4} &= 0.000255 \\
 m^{q,p} = -3, p_{-3} &= 0.025382 \\
 m^{q,p} = -2, p_{-2} &= 0.142405 \\
 m^{q,p} = -1, p_{-1} &= 0.220257 \\
 m^{q,p} = 0, p_0 &= 0.224046 \\
 m^{q,p} = 1, p_1 &= 0.218919 \\
 m^{q,p} = 2, p_2 &= 0.143320 \\
 m^{q,p} = 3, p_3 &= 0.025151 \\
 m^{q,p} = 4, p_4 &= 0.000264
 \end{aligned}$$

And:

$$\begin{aligned}
 m = -4, p_{-4} &= 0.006921 \\
 m = -3, p_{-3} &= 0.083823 \\
 m = -2, p_{-2} &= 0.159604 \\
 m = -1, p_{-1} &= 0.167262 \\
 m = 0, p_0 &= 0.165642 \\
 m = 1, p_1 &= 0.166942 \\
 m = 2, p_2 &= 0.159625 \\
 m = 3, p_3 &= 0.083206 \\
 m = 4, p_4 &= 0.006975
 \end{aligned}$$

- For $s = 7$, the frequencies obtained are:

$$\begin{aligned}
 m^{q,p} = -4, p_{-4} &= 0.003830 \\
 m^{q,p} = -3, p_{-3} &= 0.061620 \\
 m^{q,p} = -2, p_{-2} &= 0.160081 \\
 m^{q,p} = -1, p_{-1} &= 0.182371 \\
 m^{q,p} = 0, p_0 &= 0.184342 \\
 m^{q,p} = 1, p_1 &= 0.182932 \\
 m^{q,p} = 2, p_2 &= 0.159601 \\
 m^{q,p} = 3, p_3 &= 0.061515 \\
 m^{q,p} = 4, p_4 &= 0.003706
 \end{aligned}$$

And:

$$\begin{aligned}
 m = -5, p_{-5} &= 0.000363 \\
 m = -4, p_{-4} &= 0.028955 \\
 m = -3, p_{-3} &= 0.113895 \\
 m = -2, p_{-2} &= 0.141662 \\
 m = -1, p_{-1} &= 0.142537 \\
 m = 0, p_0 &= 0.144154 \\
 m = 1, p_1 &= 0.142207 \\
 m = 2, p_2 &= 0.142849 \\
 m = 3, p_3 &= 0.114120 \\
 m = 4, p_4 &= 0.028863 \\
 m = 5, p_5 &= 0.000396
 \end{aligned}$$

=> One thing that Boris emphasized on during our last meeting, is how the frequency of the internal Newtonian symbols (*difference internal/external coming soon...*) should be the same for a given $s = \text{trace}(A)$. According to Boris, in all the cases, the external symbols are the 6 outer ones in our alphabet. As you can see, the frequencies of the inner symbols tend to be the same for a particular s , but still differ by the $\frac{1}{1000}$. I'm going to run longer simulations ($T = 500,000$) but just for one particular trace $s = 5$ and the same initial conditions. Hopefully, the frequencies will even be closer...

2. The next part is to derive analytically the frequencies for just 1 symbol, by exposing the equations that govern our symbolic dynamics. The number of inequalities we obtain then depends on the system: the number of particle N , the trace of A s and the symbol itself m_0 (that Boris calls a as well). This is something Rana, Li Han and I will discuss in details tomorrow (Tuesday), before our Wednesday meeting.
3. Looking for symmetry between time and space evolution T and N .

22.4 Adrien's blog

2016-01-19 Adrien Here is an example of [text edit by me](#), and here one of a footnote by me².

2015-11-20 Adrien (Discussion with Predrag, Kuramoto-Sivashinsky equilibria and relative equilibria project Spring 2016:

- blog the project progress here
- blog whatever I'm reading and learning about dynamical systems here

2016-01-19 Adrien I've been working on reading the ChaosBook materials and doing the online Course 1.

2016-05-13 Report Adrien I am going to upload the tex. version of what I accomplished with Rana and Boris. The code can be copy/paste on Latex to be easily read. Sorry for taking so long, getting used to Latex is kind of a pain..

2016-05-16 Predrag I feel no guilt at all, only pride: you cannot be a physicist and write in Micro\$h!t Word. What does not kill you will make you stronger :). I'll help with LaTeX - but please, do diff the edited files (Xiong or I can show you how) so I do not have to do the same edits over and over again.

2016-05-26 Predrag My suggestion is in the blog, but you might have not read it: "**2016-05-21 Predrag** Adrien and Rana wondered why are (22.2) and (22.3) the same equation. Have a look at the two forms of the [Hénon equation](#) in the ChaosBook Example 3.6. Or see (??) (eq. (2.2) in Percival and Vivaldi [4]). Does that help in understanding the relation? Once you do, write it up in your reports."

In any case, looks like you have done that, in deriving (22.3).

2016-06-01 Xiong Equation just above (22.2) may have a typo because there is a factor $1/c$ in the definition of A .

2016-06-02 Predrag : At the start of sect. 22.2 Adrien sets $c = -1$, so I think the rest is correct?

2016-06-06 Adrien : List of things to work through:

1. 14.1 Qualitative dynamics
2. 14.3 Temporal ordering: Itineraries
3. 14.4
4. 14.6 Symbolic dynamics, basic notions

²Adrien 2018-01-19: Adrien test footnote

Figure 22.1: Spatiotemporal plots of the ???. (a) this; (b) that. The initial ?? is given by ???.

5. Examples 14.2, 14.3, 14.6, 14.7 and 14.8
6. skip Chapter 15 "Stretch, fold, prune" for now
7. 17 Walkabout: Transition graphs (skip 17.3.1 "Converting pruning blocks into transition graphs" for now)
8. Example 17.1 Full binary shift; 17.2 Complete N-ary dynamics; 17.4 Pruning rules for a 3-disk alphabet; 17.4 Pruning rules for a 3-disk alphabet; 17.7 Complete binary topological dynamics; 17.8 ?Golden mean? pruning;

2016-06-22 Predrag Save your plots in *siminos/figs/* as *AKSmy1stFig.png* and *AKSmy2ndFig.png* (or *AKS*.pdf*), by the names referred to in the (currently commented) parts of figure 22.1.

You can rename the graphical files whatever you find natural, just prefix them by *AKS* and do not use spaces and too many special characters in their names - that might confuse Linux.

Make graphical files modest in size, $\approx 10\text{ KB}$, rather than $\approx 100\text{ KB}$, otherwise the whole repository grows to big and unwieldy. If do not know how to produce small graphical files, ask Xiong for help.

For an example of a table, see table 19.1.

2016-07-11 Adrien :

- Thanks for the heads up to include graphs in our blog. For now though, I have no graph, just results in forms of tables mostly (frequencies for example).
- I will complete the rest of my report on coupled maps once I obtain results for long (very long) computations. Probably will run those through the night...

2016-08-02 Adrien I would like to know how can we mention our references (for me, it will just Gutkin and Osipov [3]) given that we constantly use them? I mentioned his paper at the beginning of my report, but it wasn't more than that. Do you want us to repeatedly mention his publication, or can we mention it just once during the introduction, and make it clear for the rest of the document?

2016-08-02 Predrag Well, if you have not read anything else but the single Gutkin and Osipov [3] paper, I guess there is not much else to refer to.

But they did not invent cat maps, coupled lattices, cat map symbolic dynamics, linear coding, etc., so if you define the project and explain what is

already known (in order to explain what is new in your work) you might need more than one citation. My cat map chapter 1 and spatial lattice chapter 12 have about 30 or so citations, and the common blog chapter ?? has 57. You can see what some of the other student's projects have looked like [here](#).

2017-09-06 Predrag Rana and Adrian reports are in this blog, in `siminos/spatiotemp/chapter/blogCats.tex` (check rev. 5445 message).

2017-09-06 Adrien I am not sure if you guys want me to change the symbol representation in the current figure 8 (current page 30)? I think I could add the numbers in question on top of the colored squares for better visual... but this may become overly 'dense.'

2017-09-06 Predrag I like your colorful figure 8, with the thin and thick square borders around the interior regions, and using both colored tiles and numbered tiles representations, current figures 10 and 12, just to illustrate the two possibilities. Boris and Li Han prefer that all three figures use the number representation. If that is the majority decision, I'm fine with it. We have the old figure 8 numbered tiles in `siminos/figs/AKSs7BlockBorderM1*.tex`, can restore them.

2017-09-06 Adrien What do you mean by "integer $s > 4$ " is not the correct condition, for $d = 2$ $s = 4$ is already hyperbolic. Give the correct condition on s , explain it."

I believe that we choose $s > 4$ to keep our system hyperbolic and to have a sufficiently large number of internal symbols in our alphabet \mathcal{A} . Would that be the reason you're looking for?

2017-09-06 Predrag A cat map is a fully chaotic Hamiltonian dynamical system if its stability multipliers (Λ , Λ^{-1}), where

$$\Lambda = (s + \sqrt{(s-2)(s+2)})/2, \quad \Lambda = e^\lambda, \quad (22.5)$$

are real, with a positive stability exponent $\lambda > 0$. The eigenvalues are functions of a single parameter $s = \text{tr } A$, and the map is chaotic if and only if $|s| > 2$. Otherwise Λ is on the unit circle in the complex plane, and the map is elliptic.

What is the equivalent statement for the *spatiotemporal cat*?

I do not know if it is only a coincidence, but $\mathcal{R} = [2 \times 2]$ measure inequalities are bounded by $P(s) = s(s-2)(s+2)$.

In your report you look at the linear code for $s = 3$ and numerically compute the block measures (relative frequencies) for that case, figure 20.1, so why are we demanding that $s = 5$ or larger?

2017-09-07 Adrien

- Glad as well than the former figures with numbers weren't deleted, meaning I technically won't have to re-run them unless for my following point.

- From what I see in my Mathematica notebooks, we set our system with $c = d = -1$ and $a + b = s$ and $q_{n,t}, p_{n,t}$ falling in the unit interval $[0,1]$ so that our alphabet $\mathcal{A} = \{0, \dots, s - 2d\} = \{0, \dots, s - 4\}$. Since Boris had requested that the switching of 'blocks' in array of symbols $m_{n,t}$ would be done on admissible sequences, and given that internal symbols simply satisfy this condition, we would need to pick an alphabet \mathcal{A} with at least 2 internal symbols; otherwise it's no fun. $s = 5$ has no internal symbols; $s = 7$ has two internal symbols (1 and 2) -> which is why we pick $s \geq 7$ for all these 'switching' experiments.
- In my summer report however, I believe I was using a different set of conditions for the cat map itself:

$$a = 2 \quad b = 1 \rightarrow s = 3 \quad c = d = -1 \text{ but } -1/2 \leq q_{n,t}, p_{n,t} \leq 1/2$$

We picked the unit interval $[-1/2, 1/2]$ for symmetry reasons, but once the summer was over, Boris made it clear that we would now focus on $[0,1]$.

With such $q_{n,t}, p_{n,t}$ falling in $[-1/2, 1/2]$, the list of admissible symbols was different. I tried to tackle this in my summer report, see sect. 20.3.2.

2017-09-08 Predrag

I always prefer the unit interval $[-1/2, 1/2]$ (but not for this paper - that ship is long gone). Asymmetric choice makes both the alphabet and its symmetry under time reversal unnecessarily awkward. You use unit interval, though, in your sect. 20.2.3.

In ref. [2] I write that the $d = 1$ Arnol'd cat map $s = 3$ alphabet has 5 letters $\mathcal{A} = \{2, \underline{1}, 0, 1, 2\}$.

I think you meant $d = 2$ spatiotemporal cat $s = 3$ alphabet on $[-\frac{1}{2}, \frac{1}{2}] \times [-\frac{1}{2}, \frac{1}{2}]$ phase space has $s + 4 = 7$ letters? I assume that is what we see in figure 20.1, except that the two exterior letters $\{-3, 3\}$ seem almost totally pruned. Are they, or the little histogram glitches are real? You do not explain how the histogram is ordered, I assume that is as explained in ref. [2].

References

- [1] S. C. Creagh, "Quantum zeta function for perturbed cat maps", *Chaos* **5**, 477–493 (1995).
- [2] B. Gutkin, L. Han, R. Jafari, A. K. Saremi, and P. Cvitanović, "Linear encoding of the spatiotemporal cat map", *Nonlinearity* **34**, 2800–2836 (2021).

- [3] B. Gutkin and V. Osipov, “Classical foundations of many-particle quantum chaos”, *Nonlinearity* **29**, 325–356 (2016).
- [4] I. Percival and F. Vivaldi, “A linear code for the sawtooth and cat maps”, *Physica D* **27**, 373–386 (1987).

Chapter 23

Spatiotemporal cat, blogged

I'm a space and time continuum
— Red Wanting Blue

The latest entry at the bottom for this blog

2016-01-12 PC Literature related to Klaus Richter - Engl *et al.* [18] *Coherent backscattering in Fock space: A signature of quantum many-body interference in interacting bosonic systems*; Engl *et al.* [19] *Boson sampling as canonical transformation: A semiclassical approach in Fock space*

Some of the stuff might already be in Richter [48] book *Semiclassical Theory of Mesoscopic Quantum Systems*.

2016-05-16 Predrag I am putting all stuff about cat maps known to us into sect. 12.1.

2016-05-17 Predrag I have added for the time being chapter 12 *Statistical mechanics applications* from ChaosBook to this blog. Note that there are yet more references to read in the Commentary to the chapter 12.

2016-05-17 Boris There has been some progress in the cat maps direction. Li did a simple simulation for single cat map which has confirmed my guesses so far. General question is about 2D symbolic dynamics which we used in our paper with Vladimir [27]. We encoded trajectories by winding numbers so the alphabet is small. This radically differs from standard symbolic dynamics - Markov partitions, etc. which you normally find in the literature.

Question: Given rectangular domain of symbols - what is the probability to find it within a generic N-particle spatiotemporal cat trajectory of duration T (N and T are large)? To my surprise an answer for this question might be within reach (at least for most of the sequences, small rectangles, etc.) This symbolic dynamics is much nicer then what I thought it

would be. If true, this will be a nice project for students. I am writing some notes, will send this crude staff at night today - hopefully it will be digestible.

2016-05-18 Boris To speed up everything I send my notes ([click here](#)) on recent progress on cat map symbolic dynamics. Very crude, limited edition (probably barely digestible :). This what I managed to put in latex tonight. More staff and explanations will come on Friday . So far only few things (and only for single cat) were checked numerically.

2016-05-21 Boris The current version of my notes: ([click here](#)), with more staff, more or less the same level of disorder. The main news - this symbolic dynamics (for single cat) was investigated a time ago by Percival and Vivaldi [42]. At least some of their results are of relevance for us and maybe overlap with my results. Need some time to digest their paper.

2016-05-21 Predrag For simple linear maps with integer coefficient it might be possible to write explicitly all period points in terms of rational numbers. See [ChaosBook](#) example 14.10 *Periodic points of the full tent map*.

2016-06-01 Predrag The downside the Percival-Vivaldi [42] 'linear code' is that the Markov/generating partition is infinite, meaning that for longer and longer orbits there are more and more new pruning (inadmissible blocks) rules, ad infinitum.

As far as I can tell, for N coupled maps this gets harder to describe, as in general there is an coupling strength parameter. Perhaps for rational values of it some miracles might happen.

2016-07-10 Boris The current ver. 5020 of my notes: ([click here](#)),

Main attractions:

1. Single cat: Frequencies of sequences which are composed of internal symbols eq. (2.23) - analytic answer.
2. Infinity of cats, pp. 9-11: Results for single symbol frequency. Some results for $[2 \times 2]$ squares - Rana eqs, internal symbols, forbidden sequences. Looks like extendable to general rectangles (Future looks bright [gotta wear shades](#)).

To Rana, Adrien and Li - we Skype Wednesday 5pm.

2016-08-15 Predrag : Before I start sounding critical: Rana, Adrien and Li are all good students / postdoc, and the work and what people learned this summer is very good. Now, to my first impressions (Boris still has to chime in, and we should all meet soon to discuss).

Boris was the primary advisor for Adrien and Rana, and he did not push them to write; European style, more hands off than is the American custom. Rana has written too little, not covering all the work that she did

(which was good, but only Boris knows what it was). Adrien also has some work to do before the report can be read by anyone other than the members of this team.

For me, what lacks in Rana, Adrien and Li's work is that they did not (on their own initiative) read the literature, or if they did, they never summarized what they learned in their blogs, or cited the original sources in their reports (if it is not recorded, I assume it did not happen). I did an exhaustive literature search for them (for coupled maps, see above in this blog, chapter 23; for cat maps see sect. ?? and sect. 12), but they did not pick it up, so I'll have to do that work myself.

2016-10-03 Predrag Not quick or easy to explain, but I have a hunch that the spatiotemporal zeta function should be something like the 2D Ising model zeta function described by Aizenman, see chapter 13.

2016-11-06 Predrag Early references on the spatiotemporal invariants and invariant measures:

Grassberger [24] *Information content and predictability of lumped and distributed dynamical systems* "... we point out the difference between difficulty and possibility of forecasting, illustrating it with quadratic maps. Next, we ask ourselves how this should be generalized to distributed, spatially extended and homogeneous systems. We point out that even the basic concepts of how information is processed by such systems are unknown. Finally, we discuss some intermittency-like effects in coupled maps and cellular automata.

Most interesting systems are spatially extended ("distributed") and have thus, in the infinite-volume limit, an infinite number of degrees of freedom. Nevertheless, concepts developed for dynamical system with few degrees of freedom can be applied.

Let us first consider a system located in a finite space volume V with fixed boundary conditions. For the moment we assume that the field variables (local observables) are continuous, while space and time are discrete.

It is very plausible that the number of excited degrees of freedom in such a system is proportional to the volume, at least in typical situations. More precisely, we expect that both the metric entropy h and the dimension D are extensive quantities. This is supported by overwhelming theoretical [20, 41, 50] and numerical evidence that the Lyapunov exponents (ordered such that 2_i decreases with i) scale as

$$\lambda_i \approx f(i/V) \quad (23.1)$$

[...] The limit $\eta = \lim_{V \rightarrow \infty} (h/V)$ is called density of metric entropy. [...] more interesting is the information needed to describe a finite part of an infinite system than that needed to describe the system as a whole."

2016-11-06 Boris Papers to read:

Bardet and Keller [8] *Phase transitions in a piecewise expanding coupled map lattice with linear nearest neighbour coupling* write: " We construct a mixing continuous piecewise linear map on [-1,1] with the property that a two-dimensional lattice made of these maps with a linear north and east nearest neighbour coupling admits a phase transition. We also provide a modification of this construction where the local map is an expanding analytic circle map. The basic strategy is borrowed from Gielis and MacKay (2000 Nonlinearity 13 867-88); namely, we compare the dynamics of the CML with those of a probabilistic cellular automaton of Toom's type; see MacKay (2005) *Dynamics of coupled map lattices and of related spatially extended systems* (Lecture Notes in Physics vol 671) ed J-R Chazottes and B Fernandez (Berlin: Springer) pp 65-94) for a detailed discussion. "

de Maere [36] *Phase transition and correlation decay in coupled map lattices* writes: " For a Coupled Map Lattice with a specific strong coupling emulating Stavskaya's probabilistic cellular automata, we prove the existence of a phase transition using a Peierls argument, and exponential convergence to the invariant measures for a wide class of initial states using a technique of decoupling originally developed for weak coupling. This implies the exponential decay, in space and in time, of the correlation functions of the invariant measures. "

Schmitt [54] *Spectral theory for nonanalytic coupled map lattices* write: " We consider weakly coupled strong mixing interval maps on the infinite lattice with finite range couplings. We construct Banach spaces defined by bounded variation conditions such that the transfer operator associated with the full infinite system has a simple eigenvalue 1 (corresponding to a unique natural invariant probability measure) and a spectral gap. "

2016-11-11 Predrag Bountis and Helleman [11] On the stability of periodic orbits of two-dimensional mappings: " We apply our criterion and derive a sufficient stability condition for a large class of periodic orbits of the widely studied "standard mapping" describing a periodically 'kicked' free rotator. "

I find this paper quite interesting, because the computation of Floquet multipliers, i.e., linearization of periodically 'kicked' free rotor, is full of matrices that look like Laplacians + a diagonal term which varies along the periodic orbit. For cat maps this term is constant, essentially the stretching factor s . This might help with interpreting coupled 'kicked' rotor lattices.

This is presumably related to the block circulant stability matrices [4, 21] for spatially and temporally periodic orbits in coupled map lattices.

2017-02-13 Predrag Consider admissible Lagrangian trajectories in the $[x_0, x_{\ell+1}]$ plane. The 1-step Lagrangian map is

$$x_2 = (s x_1 - m_1) - x_0. \quad (23.2)$$

For $s = 3$ have $m_j \in \{-1, 0, 1, 2\}$, and the partition borders are slope -1 lines defined by $x_1 = 0$ or 1.

$$-m_1 - x_0 \leq x_2 \leq s - m_1 - x_0. \quad (23.3)$$

Anything outside $0 \leq x_2 \leq 1$ is not a constraint.

$$1 - x_0 \leq x_2^{(-1)} \leq 4 - x_0. \quad (23.4)$$

$$-x_0 \leq x_2^{(0)} \leq 3 - x_0. \quad (23.5)$$

$$-1 - x_0 \leq x_2^{(1)} \leq 2 - x_0. \quad (23.6)$$

$$-2 - x_0 \leq x_2^{(2)} \leq 1 - x_0. \quad (23.7)$$

So, there is no pruning for $x_2^{(0)}$ and $x_2^{(1)}$; the only pruning constraints are

$$1 - x_0 \leq x_2^{(-1)}, \quad (23.8)$$

$$x_2^{(2)} \leq 1 - x_0. \quad (23.9)$$

2-step Lagrangian map

$$x_3 = (s - 1)(x_2 + x_1) - x_0 - m_2 - m_1, \quad (23.10)$$

Eliminate x_2 by (23.2)

$$x_2 + x_1 = ((s + 1)x_1 - m_1) - x_0. \quad (23.11)$$

$$x_3 = (s^2 - 1)x_1 - s x_0 - m_2 - s m_1, \quad (23.12)$$

2016-09-28 Predrag Learned much more from [Rafael de la Llave](#) that I can possibly remember.

He says that fancy Smilians, like Pugh and Shub, who studied dynamical systems with ‘multiple times’. The results are expressed in terms of ‘Weyl chambers’. They are particularly simple if symmetries commute. They call that the ‘Abelian case’.

2016-09-28 Predrag Volevich [57] *Kinetics of coupled map lattices* writes: “ A simple example of coupled map lattices generated by expanding maps of the unit interval with some kind of diffusion coupling is considered. The author proves that probability measures from some natural class weakly converge to the unique invariant mixing measure under the actions of dynamics. The main idea of the proof is the symbolic representation of his system by two-dimensional lattice model of statistical mechanics. ”

2016-09-28 Predrag Giberti and Vernia [13, 22] *Normally attracting manifolds and periodic behavior in one-dimensional and two-dimensional coupled map lattices* study weakly coupled logistic maps in one- and two-dimensional lattices. They show numerically for some classes of coupled map lattices that the stability of a spatial structure is determined by the stability of its pattern with the minimal (spatial) scale, i.e. by the tiniest detail of this structure. Continued in Livi, Martínez-Mekler and Ruffo [7, 14, 33] *Periodic orbits and long transients in coupled map lattices*.

Hopefully something we can ignore as long as we are interested into the “high-temperature” phase.

2016-10-03 Predrag In 1986 Zimmer outlined a general program directed at understanding smooth actions of lattices in semisimple Lie groups on compact manifolds. So hopefully this has nothing to do with CLMs.

de la Llave and Mireles James [34] *Connecting orbits for compact infinite dimensional maps: Computer assisted proofs of existence* is indigestible from get go.

2016-11-11 Predrag Boris A. Khesin [course notes](#) might be helpful if we ever get to Hamiltonian PDEs :)

2016-11-11 Predrag Belykh and Mosekilde [9] *One-dimensional map lattices: Synchronization, bifurcations, and chaotic structures* study

$$\begin{aligned} x_{n,t+1} &= f(x_{n,t}) + \epsilon[x_{n+1,t} - (1 + \gamma)x_{n,t} + \gamma x_{n-1,t}] \\ &= f(x_{n,t}) + (1 - \gamma)\epsilon(x_{n,t} - x_{n-1,t}) + 2\epsilon \square x_{n,t}, \end{aligned} \quad (23.13)$$

asymmetrically drifting due to coupling by $(1 - \gamma)$. With $g(x) = f(x) - x$, and rescaling the nonlinearity, this is a discretization of a dynamics of extended, non-equilibrium media PDE

$$\frac{\partial x}{\partial t} = g(x) + (1 - \gamma) \frac{\partial x}{\partial s} + \frac{\partial^2 x}{\partial s^2}. \quad (23.14)$$

Consider the diffusively coupled maps (23.13) for $\gamma = 1$ and $N = 2m$ and assume periodic boundary conditions ($m \rightarrow \infty$ when the array is unbounded). As this has a spatial Laplacian (the dynamics is now reflection-symmetry invariant) they construct a pair of new variables $x_{n,t}, y_{n,t}$ from x_n with odd or even n , and obtain a 2D lattice symmetric under $(x, y) \leftrightarrow (y, x)$. Then the symmetric and asymmetric spaces behave differently. In particular, the second period-doubling bifurcation can be changed into a torus bifurcation [47].

2016-11-11 Predrag Belykh and Mosekilde [9] is a descendent of the system previously studied by Reick and Mosekilde [47] in *Emergence of quasiperiodicity in symmetrically coupled, identical period-doubling systems*: “When two identical period-doubling systems are coupled symmetrically, the

period-doubling transition to chaos may be replaced by a quasiperiodic transition. The reason for this is that at an early stage of the period-doubling cascade, a Hopf bifurcation instead of a period-doubling bifurcation occurs. Our main result is that the emergence of this Hopf bifurcation is a generic phenomenon in symmetrically coupled, identical period-doubling systems. The whole phenomenon is stable against small nonsymmetric perturbations. Our results cover maps and differential equations of arbitrary dimension. As a consequence the Feigenbaum transition to chaos in these coupled systems - which exists, but tends to be unstable - is accompanied by an infinity of Hopf bifurcations."

The seemingly first remark on this splitting is due to Ruelle [49]. He noted that the symmetry of the coupling results in a splitting into a symmetric solution and a nonsymmetric solution, where for the latter the two subsystems are 180° out of phase. Later Neu [39, 40] specialized the problem to linear coupling and analyzed the stability of the symmetric and nonsymmetric solutions by singular perturbation methods.

All of these might be of importance for Burak's torus birth and destruction [12].

As for the cats crowd, these seem to suggest that spacetime interchange symmetry $t \leftrightarrow n$ of the spatiotemporal cat [26] should lead to different dynamics (and symbolic dynamics! only positive (n, t) are needed after the decomposition) in symmetrized and anti-symmetrized lattices, with a possible flow-invariant subspace currently invisible. In Gibson, Halcrow and Cvitanović [23] *Visualizing the geometry of state-space in plane Couette flow* we also had a $D_1 \times D_1$ symmetry, with important consequences on types of solutions, and invariant subspaces.

2016-11-23 Predrag Having a variational principle (action (7.73) in case at hand) and a continuous symmetry means that the **Noether's theorem** applies

"To every one-parameter, continuous group of symmetries of a Lagrangian dynamical system there corresponds a scalar, real-valued conserved quantity."

Is there is a version of it for discrete translations? What is the conserved quantity for a single cat map? What is it for the lattice? Internet says many contradictory things:

"The fact that a Lagrangian is unchanged by a discrete transformation is of no significance. There is no conserved quantity associated with the transformation."

"For infinite symmetries like lattice translations the conserved quantity is continuous, albeit a periodic one. So in such case momentum is conserved modulo vectors in the reciprocal lattice. The conservation is local just as in the case of continuous symmetries."

Read about it [here](#).

Mansfield [37] in [proceedings](#) and in her [talk](#) defines *total difference* and says “Just as an integral of a total divergence depends only on the boundary data, so does the sum over lattice domain of a total difference.”

She states the discrete Noether’s Theorem, and in Example 1.3.7 she shows that for a discretization of a standard mechanical Lagrangian, time invariance³ yields “energy” as a the conserved quantity.

Hydon and Mansfield [28].

Capobianco and Toffoli [16] [Can anything from Noether’s Theorem be salvaged for discrete dynamical systems?](#) is fun to read (but ultimately unsatisfactory):

“ we take the Ising spin model with both ferromagnetic and antiferromagnetic bonds. We show that-and why- energy not only acts as a generator of the dynamics for this family of systems, but is also conserved when the dynamics is time-invariant.”

The *microcanonical Ising model* is strictly deterministic and invertible: on a given step, a spin will flip (that is, reverse its orientation) if and only if doing so will leave the sum of the potential energies of the four surrounding bonds unchanged. The Ising dynamics is a second-order recurrence relation. They define “energy” as the length of the boundary between ‘up’ and ‘down’ domains. While the magnetization-number of spins up minus number of spins down-may change with time, that length, and thus the energy, remains constant. The total energy of a system may be defined as

1. A real-valued function of the system’s state,
2. that is additive,
3. and is a generator of the dynamics.

In a discrete Hamiltonian dynamics, a state is no longer a “position/momentum” pair $\langle q, p \rangle$ as in the continuous case, but an ordered pair of configurations $\langle q_0, q_1 \rangle$.

A second-order dynamical system has an evolution rule of the form

$$x_{t+1} = g(x_t, x_{t-1}).$$

2016-12-10 Predrag Read Akila *et al.* [3] *Semiclassical identification of periodic orbits in a quantum many-body system*

2016-12-12 Predrag Spatiotemporal cat claim retracted:

On the second thought, spatiotemporal cat is not radically different from the previous examples of $(D+1)$ -dimensional spatiotemporal symbolic dynamics cited by Boris (Pesin and Sinai [43], Bunimovich and Sinai [15],

Pethel, Corron and Bollt [44, 45]). In all coupled maps literature, the starting point is time evolution of a non-interacting particle at each site, with its 1-dimensional temporal symbolic dynamics, with spatial coupling to D spatial neighbors subsequently tacked on. While the *coordinate* of site is $(D+1)$ -dimensional, its symbolic dynamics is 1-dimensional. In all models the I am aware of, with the exception of zeta functions in $d = 2$, the field being discretized (“particles” at sites) is *scalar*, and so is the spatiotemporal cat field (I was wrong when I claimed in a conversation with Boris that is a *vector* field). In d spatiotemporal dimensions it is d -dimensional, but its symbolic dynamics alphabet at each site is 1-dimensional set.

The zeta functions in $d = 2$, reviewed in chapter 6, are not based on any dynamics, and have problems of their own. In nutshell, for such zeta functions grammars are awkward, while in the spatiotemporal cat the grammar rules are automatically obeyed by any simulation, and can be explicitly computed as a finite set of rules for any given invariant 2-torus.

2018-12-05 Predrag Liverani’s paper Keller and Liverani [31] *Uniqueness of the SRB measure for piecewise expanding weakly coupled map lattices in any dimension* is an example of rigorous work on ergodicity of weakly couple chaotic maps. Cite, emphasize weak-coupling is NOT what we do. Also, our Euclidian metric leads to hyperbolicity, no attracting subsets and phase transitions in the evolution.

2016-12-17 Predrag Read Qin [46] *Bifurcations of steady states in a class of lattices of nonlinear discrete Klein-Gordon type with double-quadratic on-site potential*

2017-02-17 Predrag For a single cat map linear code is simply awkward

1. depends on choice of x_t origin: 4 letters for Boris, 5 for (symmetric) Vivaldi
2. linear code partition areas have no relation to periodic orbit weights
3. linear code pruning rules undercount periodic orbit pruning rules
4. periodic orbits are intrinsic to the flow, so makes more sense to use AW Markov partition

Boris 2017-02-17 Mostly agree, but linear code has its own charm: internal part of the code has trivial grammar rules, it is very homogeneous, i.e., admissible sequences of finite length have volumes either close to zero or close to max (volumes of internal sequences).

Boris 2017-02-17 For p iterations of the map situation rapidly improves - number of internal symbols grows exponentially with p , number of external symbols is fixed (kind of renormalization).

Predrag 2017-03-04 That’s just a cheat. For a piecewise linear expanding map of mod 1 variety, it is always the orbit of the outermost critical point (in your language, exterior alphabet) that defines the grammar, in

the spirit of the kneading theory, with no grammar rules for the interior alphabet, see ChaosBook chapter *Deterministic diffusion*. If one looks at iterates of the map, of course the number of interior alphabet sequences grows exponentially, but that does not mean that they dominate the topological entropy - that ones is what it is, an irrational number larger than $\ln N_{A_0}$, the same number for the original map or any of its iterates.

2017-04-29 Predrag Tourigny [56] *Networks of planar Hamiltonian systems* writes things we probably disagree with:

"Hamiltonian systems famously do not admit attractors, but rather families of periodic orbits parameterised by level sets of the Hamiltonian. There have been surprisingly few attempts to study complex networks consisting of coupled Hamiltonian systems. Consequently, in this paper we initiate the study of complex networks whose autonomous units are planar Hamiltonian systems. We choose to focus on planar Hamiltonian systems because already there exists a rich theory that may be identified with the geometry of planar algebraic curves."

Define a weighted graph \mathcal{G} by assigning a vertex to each $i \in V$ and an edge with "weight" $W_{ij} = W(i, j)$ joining vertex i to j . We assume this graph \mathcal{G} is *undirected* (i.e., $W_{ij} = W_{ji}$) and *connected* meaning that there always exists a path from any vertex i to any other vertex j . The network is then defined to be the dynamical system on $\mathbb{R}^{m \times n}$ whose time evolution is governed by the equations

$$\dot{z}_i = F_i(z_i) + \sum_{j=1}^n W_{ij} U(z_i, z_j).$$

We will actually only be concerned with networks where the autonomous units are planar ($m = 2$) and the coupling function is *diffusive*, implying $U(z_i, z_j) = U(z_i - z_j)$. We say that a network is an *oscillator network* if each of the underlying systems $\dot{z}_i = F_i(z_i)$ admits at least one periodic solution."

This work is inspired by Winfree, Kuramoto and Turing (rather than coupled maps lattices). If the dynamics on a node is the same everywhere, the network (graph) is "homogenous", otherwise it is "heterogenous." The diffusive coupling $W_{ij} = W_{ji}$ couples all nodes, in his model with the same strength, but the nodes are assumed heterogenous. After further reading it seems that the networks are not Hamiltonian (coupling destroys that, and that we can safely avoid this literature).

Rest in pacem.

2017-10-10 Boris Our recent [1] *Semiclassical prediction of large spectral fluctuations in interacting kicked spin chains*, arXiv:1709.03601, hides a feline creature in the form of (23.15):

“Integrable Case: For $b^x = 0$ all rotations are around the z -axis and therefore commute with the Hamiltonian making the system integrable. As a result the dynamics of the kicked system for arbitrary times is equivalent to one at fixed time, e.g. $T = 1$ with rescaled system parameters $J \rightarrow JT$ and $b^z \rightarrow b^z T$. Moreover, the flow induced by the Hamiltonian $\hat{H}_I + \hat{H}_K$ for time T is identical to the evolution of the kicked system for T time steps with the same parameters.

For the classical trajectories $p_n = \text{const.}$ holds for each n and periodic orbits form L dimensional manifolds. To close a trajectory in phase-space after T iterations it is sufficient that the total change in angles Δq_n is a multiple of 2π ,

$$\Delta q_n = 4T(J(p_{n-1} + p_{n+1}) + 2Vp_n) + 2b^z T = 2\pi\hat{m}_n. \quad (23.15)$$

The $\hat{m}_n \in \mathbb{Z}$ is a local winding number for spin n . Since the momenta are bounded, $|p_n| \leq 1$, $\chi_n = p_{n-1} + p_{n+1}$ resides within the interval $[-2, +2]$. Therefore, this equation has no solution if, for instance, $b^z > 4(J + V)$ and $4(J + V) + b^z < \pi/T$. In such cases the system does not possess any classical periodic orbits of period T or shorter. If all parameters (times T) are sufficiently small, the first accessible winding number is necessarily zero. With increasing time T the number of possible \hat{m}_n grows linearly, and with it the number of possible distinct periodic orbits grows algebraically. With respect to L the number of periodic orbits is determined by all admissible combinations of the winding numbers. If there is more than one allowed m_n the growth is thus exponential in L . This exponential growth also holds for non-integrable parameter choices. ”

Boris continues: This is the (dual) equation for “spatially” periodic orbits of an integrable spin chain. For $4JT = 2\pi$ it is the cat map

$$p_{n+1} - s p_n + p_{n-1} = -m_n, \quad (23.16)$$

with the cat map “stretching” parameter $s = -2TV/\pi$, and the winding number $m_n = b^z T / \pi - \hat{m}_n \in \mathbb{Z}$. For other times T , the map is non-symplectic but still linear. The equation says, loudly, that temporally integrable system can be “spatially” chaotic (e.g., number of spatial periodic orbits grows exponentially with the spatial period L (in case at hand, the number of “particles”).

On the quantum side the corresponding “dual” evolution is exactly the quantum cat map.

2017-10-10 Predrag Thanks for pointing it out, I would have never noticed that the very feline (23.16) is hiding within (23.15). So, whenever one has the nearest neighbor couplings, spatially, spatial translation invariance, a spatial reflection symmetry, and a linear dynamics on the site, one gets a spatial cat map. Your $T = 1$ example is the discrete time analog of the Michelson [38] $T = 0$ study of equilibria on the kneading sequence

spatial $L \rightarrow \pm\infty$ (described in the parallel `blog.tex`, in this subversion repo directory). This system is not integrable, but, needless to say, the number of equilibria does not grow with increasing T (it is constant).

This continues with **2020-01-11 Predrag** post below.

2017-10-10 Predrag Currently open ends:

1. Finish the Pythagorean tiling of figure ?? in terms of two rectangles. In these coordinates the cat map should again have a linear encoding, but with no pruning rules (the two rectangles are a generating partition).
2. Do the same for $d > 1$.
3. Redo everything with doubly-periodic boundary conditions, where all Green's functions trivial.
4. I have started writing up the spatiotemporal Jacobian and the $\det(1 - J)$ for d -tori in what is currently called Sect. 1.3.2 *Spatiotemporal stability* in the parallel `blog.tex`. In the discrete spacetime case, that should agree with the determinants that Boris has computed.

2018-01-20 Predrag Akila, Waltner, Gutkin, Braun and Guhr [2] *Collectivity and periodic orbits in a chain of interacting, kicked spins* is presumably closely related to ref. [1] *Semiclassical prediction of large spectral fluctuations in interacting kicked spin chains*, see **2017-10-10 Boris** post above.

2018-01-20 Predrag Catnipping is taking a delirious turn. Axenides, Floratos and Nicolis [5] *The quantum cat map on the modular discretization of extremal black hole horizons* write: " We present a toy model for the chaotic unitary evolution of infalling black hole horizon single particle wave packets. We construct explicitly the eigenstates and eigenvalues for the single particle dynamics for an observer falling into the BH horizon, with time evolution operator the quantum Arnol'd cat map (QACM). Using these results we investigate the validity of the eigenstate thermalization hypothesis (ETH), as well as that of the fast scrambling time bound (STB). We find that the QACM, while possessing a linear spectrum, has eigenstates which are random and satisfy the assumptions of the ETH. We also find that the thermalization of infalling wave packets in this particular model is exponentially fast, thereby saturating the STB, under the constraint that the finite dimension of the single-particle Hilbert space takes values in the set of Fibonacci integers. "

2018-03-28 Predrag Plasma physicists Xiao *et al.* [58] *A lattice Maxwell system with discrete space-time symmetry and local energy-momentum conservation*, [arXiv:1709.09593](https://arxiv.org/abs/1709.09593) might of interest to us. By 'Maxwell' they mean EM on a discrete spacetime lattice. Their system has gauge symmetry, symplectic structure and discrete space-time symmetry. They generalized Noether's theorem to discrete symmetries for the lattice Maxwell system,

and the system is shown to admit a discrete local energy-momentum conservation law corresponding to the discrete space-time symmetry. These conservation laws make the discrete system an effective algorithm for numerically solving the governing differential equations on continuous space-time.

There is also Stern *et al.* [55] *Geometric computational electrodynamics with variational integrators and discrete differential forms*, They write: “ We develop a structure-preserving discretization of the Lagrangian framework for electrodynamics, combining the techniques of variational integrators and discrete differential forms. This leads to a general family of variational, multisymplectic numerical methods for solving Maxwell’s equations that automatically preserve key symmetries and invariants. We generalize the Yee scheme to unstructured meshes in 4-dimensional space-time, which relaxes the need to take uniform time steps or even to have a preferred time coordinate. We introduce a new asynchronous variational integrator (AVI) for solving Maxwell’s equations. These results are illustrated with some prototype simulations that show excellent numerical behavior and absence of spurious modes. ”

2018-04-05 Boris You show that your Adler-Weiss (Markov) partition can be used to get position of the points in the phase space by linear transformation. So your partition is good on both fronts = simple grammar rules + easy walk from phase space to symbolic representation and back (as opposed to the linear code of Percival-Vivaldi, where only the second part is true).

Q: Was it known already (I mean simple connection between phase space and symbolic dynamics for Adler-Weiss partitions)?

2018-04-08 Predrag The generating partition of figure 18.4 is new.

Newer still is the generating partition of figure 18.17(a) which incorporates the invariance of the cat map dynamics (1.118) under spatial reflection flip across the $x_1 = -x_0$ anti-diagonal, together with $s_n \rightarrow -s_n$ time reversal symmetry, so the full symmetry is $D_1 \times D_1$. This should lead to very simple symbolic dynamics, but sect. 18.4 *Reduction to the fundamental domain* has still to be completed.

2018-04-05 Boris Start from e.g., 5 letter alphabet, then translate admissible sequences (from the transition graph) into tree letter (-1,0,1) LINEAR alphabet (1.9), and use Green’s function to get to the phase space points. Right?

2018-04-08 Predrag As explained in ChaosBook.org, in symmetry reduction the *links* of such graphs are not labelled arbitrarily, they have a precise group-theoretic meaning.

Figure 18.4 (d) indeed has 5 links (I prefer not use an arbitrary ‘alphabet’ to label them), but the important thing is that the links correspond to the

symmetry group elements; they enable you to reconstruct from a walk on the torus the corresponding walk in the space tiled by the copies of the torus. In the symmetry reduction of dynamical systems we call that “reconstruction equations”. It is these group elements (18.18), (18.21), etc., that are the *alphabet*, as explained in [ChaosBook.orgpaper.shtml#diffusion](#) diffusion chapter, and the preceding chapters that deal with discrete symmetry reduction (like the 3-disk billiard).

To repeat: we are reducing translational symmetry. Hence the alphabet are the group elements that reduce global motions to the elementary cell, in this case our 2-rectangle partition.

2018-04-05 Boris If linear refers to linear connection between symbol sequences and phase space points (my definition) then your three letter code is indeed linear, but (probably) not the original 5-letter one.

2018-04-08 Predrag What code? There is no “original 5-letter” code... Maybe you mean link labels in the (18.17) calculation? That just looks like clumsy notation to me. Writing down a transition graph with 5 nodes corresponding to such ‘alphabet’ would be a mess, I did not do it.

2018-04-05 Boris I would say that under any Adler-Weiss looms a linear code

2018-04-08 Predrag I think so too. While the canonical Thom-Arnol’d cat map (1.1) and the Percival-Vivaldi [42] two-configuration representation (1.5) are related by the anti-symplectic transformation (5.191), the Thom-Arnol’d cat map seems clumsier, as it seems to require 2D translations in figure 1.1 to return subpartitions back into the 2-rectangle partition (have not bothered to work that out). Still a linear code.

2018-04-05 Boris Adler-Weiss code is not linear on its own. Agree?

2018-04-08 Predrag I agree - I have never seen it recast in the group-theoretic symbolic dynamics. Percival-Vivaldi [42] do discuss Adler-Weiss, and do write down the 1D (damped) screened Poisson equation and 1D Green’s functions, but they never saw that Adler-Weiss could be combined with their linear code. Would sure have saved a ton of needless work in the subsequent literature.

2018-04-05 Boris The biggest question to me what are you doing/going to do in $d = 2$ case. For me, Adler-Weiss partitions can be (probably) turned to 1D linear code (with a huge alphabet), but not to the 2D linear code. Right, Wrong?

2018-04-08 Predrag Wrong. Why would one turn $d = 2$ Adler-Weiss into 1D linear code? For finite spatial periodicity L that would be stupid, and for $L \rightarrow \infty$ (the subject of these papers) impossible. No, for $d = 2$ one has to partition the 4D invariant 2-torus partition hypercube. I’m optimistic about us being able to accomplish that. Symmetries should help.

The stupid Percival-Vivaldi [42] hypercube is already working (see Han's examples (18.65), etc.), now we have to find a generating partition.

Just get cracking :)

2017-12-18 Predrag More seriously, what is wrong with the argument so far?

I used the Hamiltonian, evolution-in-time thinking to generate the $d = 1$ generating partition. That will not work in higher dimensions, so the above argument has to be recast in the Lagrangian form.

In principle, it is just a discrete Legendre transform, see sect. 8.2 *Generating functions; action*, but I do not see it yet...

2018-04-12 Boris By the "original 5-letter" code I mean the one which appears in (18.10). You can use it to label paths on the transition graph = all admissible sequences/trajactories. The grammar rules for this encoding/labeling (call it whatever) are local - you just say which pairs of symbols are admissible. In other words if I give you an arbitrary sequence of symbols (from this five letter alphabet) you can easily say me whether it admissible or not. Right?

2018-04-19 Predrag If by "local" you mean "full shift", i.e., transition graph of memory 1, wrong. They are walks on the transition graph (18.8)(e), so 2 cannot be followed by 1 or 3, 5 cannot be followed by 4, etc. But any transition graph of *finite* memory encodes a finite grammar (subshift of finite type)- no need to recode it as a memory 1 code.

2018-04-12 Boris But what about your 3 letter code (18.13)? Given a sequence of symbols from this 3-letter alphabet, can you say easily whether it admissible or not (without going to the phase space)? In other words, whether the grammar rules are local here?

2018-04-19 Predrag Don't you see how brilliant our solution is?

1. Any walk M on the transition graph figure 18.4 (d) is admissible
2. By linearity of the (damped) screened Poisson equation, to each admissible block M corresponds a unique admissible state X .

Done.

2018-05-14 Predrag There is some **excitement** about new regularities of Bragg peaks in diffraction patterns of 1-dimensional aperiodic crystal composed of primes. I find the limit periodic structures, such as the spatial period-doubling [6] particularly intriguing (see Fig. 6.1 in Torquato, Zhang and De Courcy-Ireland, [arXiv:1804.06279](#)).

2018-10-06 Predrag Ruelle [51] *Zeros of graph-counting polynomials*, and Ruelle [52] *Graph-counting polynomials for oriented graphs* deal with things like counting subgraphs, motivated by studies of zeros of the grand partition function, such the circle theorem of Lee and Yang. I truly do not understand why this is done... I am not alone, as very few people cite these articles.

2018-11-05 Predrag **Mark Paul** and Jonathan Barbish are testing their covariant vector codes on the diffusive coupled map lattices (CML) (5.1) of Kaneko [29, 30] type on finite spatial periodic lattice of periodi L ,

$$u_{j+1}^n = f(u_j^n) + [f(u_j^{n-1}) - 2f(u_j^n) + f(u_j^{n+1})] = (1 + \epsilon \square)f(u_t^n), \quad (23.17)$$

where the individual site dynamical system $f(x)$ is the 1D quadratic map

$$f(x) = ax + bz(1 - z), z = x \bmod 1, \quad (23.18)$$

studied in Grigoriev and Cross [25] *Dynamics of coupled maps with a conservation law*.

A differential or discrete equation of this form represents the competition between: generation of chaotic perturbations by $f(x)$ and their dissipation the diffusive coupling induced by the spatial Laplacian.

For map (23.17) the space average of the ‘velocity field’ u

$$\langle u \rangle = \frac{1}{L} \sum_j u_j^n \quad (23.19)$$

is conserved (Galilean invariance), so the system has, in addition to the two parameters a and b of the local map f , as the additional control parameter the conserved quantity $\langle u \rangle$, which can be defined by the initial condition. The give plots of possible phases in the $[a, u]$ and $[b, u]$ parameter planes.

Their objectives is to determine the effect of this conservation law on the dynamics of the extended chaotic system; it leads to the singularity in Lyapunov spectrum at $\lambda_j = 0$, shown in their fig. 10(b). They break the conservation law in their eq. (70). In Kuramoto-Sivashinsky we do not seem to get anything much out of it, as far as I remember, but they comment on that in their eq. (18).

In their eqs. (10) and (13) they give analytically the two 2-cycles. As is the case for parabola, it might be possible to give 3-cycles analytically, but nothing beyond.

They state that there are non-linear waves (we call these relative equilibria or travelling waves), propagating trough the laminar background with unit velocity, their fig. (3): “All defects move with a constant velocity, but while the majority of defects is moving with the maximal speed $v = \pm 1$, the rest have a smaller speed.” They neither derive nor prove existence of relative equilibria (travelling defects) with $|v| \leq 1$, nor do they study their stability.

If I were Jonathan, I would first look for equilibria $u^n = u^{n+1}$ for small L , then for relative equilibria $u^n = u^{n+q} + p$. Show that phase velocity is maximal for $v = 1$, ($q = p$). Determine their linear stability – perhaps $v = 1$ is the least unstable, that’s why you see it all the time. The go on finding unstable periodic and relative equilibria for small (L, T) tori (periodic tilings).

2019-09-28 Predrag Boris gets a [prestigious grant](#).

2019-11-18 Boris There are some exciting developments during the last two years regarding quantum dual models, mostly by the group of Tomáš Prosen, see Bertini, Kos, and Prosen [10] *Exact correlation functions for dual-unitary lattice models in 1+1 dimensions*, [arXiv:1904.02140](https://arxiv.org/abs/1904.02140).

Although they go by some funny names - dual-unitary spin chains, dual local quantum circuits etc., behind each of these model sits a (quantized) spatiotemporal cat. Amazingly, we know how to calculate correlations between local operators in such models resp. in quantum spatiotemporal cat (even in perturbed one).

This generates some funny questions regarding classical cats as well. One should be able to do it also for the classical model as well. In short, if you look for an interesting problem – calculating classical correlators in spatiotemporal cats might be the hit.

In a week I will be able to send you a Duisburg preprint (with setting closer to cats).

2020-01-11 Predrag This continues the conversation that includes (23.15) above, but I do not understand the details - some of the quantum notation obscures them for me.

No further peep from Boris, but this is presumably the Duisburg preprint: Boris Gutkin, Petr Braun, Maram Akila, Daniel Waltner and Thomas Guhr, *Local correlations in dual-unitary kicked chains*, [arXiv:2001.01298](https://arxiv.org/abs/2001.01298).

Turns out Boris knows how to upload to arXiv, but was too busy to do it with our preprint :)

2020-12-16 Predrag My 2000 *Chaotic Field Theory: A sketch* [17] gets cited every so often. Most citations seems useless, with the exception of these two:

Stam Nicolis *Supersymmetry and Deterministic Chaos* (2020): We show that the fluctuations of the periodic orbits of deterministically chaotic systems can be captured by supersymmetry, in the sense that they are repackaged in the contribution of the absolute value of the determinant of the noise fields, defined by the equations of motion.

[...] In a chaotic phase there are infinitely many periodic orbits and there have been attempts to use them to construct the measure they define, using perturbative field theoretic techniques [17] (that's me). [... He] discusses another way to address this issue, that does not rely on perturbation theory, following the approach of his earlier papers, he writes a *lattice action* and computes the identities that the correlation functions that the noise fields would be expected to satisfy, were the system consistently closed.

Bernd Mümken *A Dynamical Zeta Function for Pseudo Riemannian Foliations* (2006): "We investigate a generalization of geodesic random walks to pseudo Riemannian foliations. The main application we have in mind

is to consider the logarithm of the associated zeta function as grand canonical partition function in a theory unifying aspects of general relativity, quantum mechanics and dynamical systems."

It looks familiar in glimpses, but the math is killing me...

2CB

2020-01-13 Predrag MacKay, Johnson and Sansom [35] *How directed is a directed network?,* ([click here](#)):

We consider directed networks (also known as directed graphs or digraphs) with set N of nodes (also known as vertices) and set E of directed edges (also known as links). We suppose that there is at most one edge from a node m to a node n , and denote the edge by mn . There can also be an edge from n to m . Each edge carries a weight $w_{mn} > 0$. This can represent the strength of the edge. We write $w_{mn} = 0$ if there is no edge from m to n and we assemble the w_{mn} into a matrix W . The edge weights could be set to 1, as is common in the literature, and the array W is then called the adjacency matrix A of the network, but the ability to represent the strength of the edge is a useful extension. If there were multiple edges from m to n then we would amalgamate them into a single edge by adding the weights. Self-edges mm (also called loops) are permitted.

The *weight* of the node n is

$$u_n = w_n^{in} + w_n^{out}$$

and the *imbalance* for node n by

$$v_n = w_n^{in} - w_n^{out}$$

In matrix form the (weighted) graph-Laplacian operator Λ on functions $h : N \rightarrow \mathbb{R}$ is defined by

$$\Lambda = \text{diag}(u) - W - W^\top$$

They seek the solution h of the linear system of equations

$$\Lambda h = v$$

This always has a solution but it is non-unique, because one can add an arbitrary constant in each connected component of the network. Etc.

They seek levels to minimise the *trophic confusion* :)

A directed network is said to be normal if its weight matrix W commutes with its transpose W^\top :

$$WW^\top = W^\top W$$

Note that W^\top represents the same weighted network but with all the edges reversed. The term "normal" came from people who spent their lives with self-adjoint operators and unitary operators, both of which are

2CB

normal, but people working in stability of ordinary differential equations are fully cognizant that most matrices are not normal.

For the unweighted case of an adjacency matrix A , normality implies the imbalance vector $v = 0$. This is because $(A^\top A)_{mn}$ is the number of sources in common to nodes m and n , and $(AA^\top)_{mn}$ is the number of sinks in common. In particular, $(A^\top A)_{nn} = w_n^{in}$ and $(AA^\top)_{nn} = w_n^{out}$, so $A^\top A = AA^\top$ implies that $w^{in} = w^{out}$ and $v = 0$. When $v = 0$ we say a network is balanced.

Another special case of normality is symmetric networks $W^\top = W$.

Normality of W is equivalent to existence of a unitary matrix U such that $U^\dagger W U$ is diagonal.

A cycle in a directed network is a closed walk in it. We allow repeated edges and repeated nodes. In particular, we allow a cycle to be a periodic repetition of a shorter cycle. The weight w of a cycle is the product of the weights along its edges. The total weight of cycles of length p is given by the trace of the p th power of W : $\text{tr } W^p$.

2CB

The orbits are those which are not repetitions of a shorter cycle. We consider two orbits to be the same if they differ only by a cyclic permutation. We denote by \mathcal{P} the set of orbits,

$$1/\zeta_{\text{top}}(z) = \prod_p (1 - z^{|p|} w_p)$$

This can be reduced to one in terms of “elementary cycles”, those which do not repeat a node before closing. They are prime and for a finite network there are only finitely many of them. The formula is

$$1/\zeta_{\text{top}}(z) = 1 + \sum_C \prod_{p \in C} (-z^{|p|} w_p)$$

where the sum is over non-empty collections C of disjoint elementary cycles. Might want to study MacKay’s proof to see if it is better than what is in ChaosBook.

2020-06-30 Moshe Rozali *Effective Field Theory for Chaotic CFTs* “ Relations between chaos and hydrodynamics are one of the unique feature of holographic CFTs. The early time Lyapunov regime can described by an effective field theory of a single mode, which for maximally chaotic systems is an hydrodynamic mode. We describe that effective field theory for conformal field theories, both in two dimensions and in higher dimensions, and show how it captures maximal chaos and pole skipping. We discuss the relation of the theory to other formulations of CFTs and show how it captures interesting objects such as conformal blocks and partial waves. We speculate on what is needed to extend the discussion to non maximal chaos.”



[arXiv:1712.04963](#); [arXiv:1808.02898](#); [arXiv:1909.05847](#)

[arXiv:1612.06330](#); [arXiv:1811.09641](#); [arXiv:1812.10073](#);

G.J. Turiaci [arXiv:1901.04360](#); [arXiv:1912.02810](#)

2020-07-02 Ruairí Brett *From two to three-body systems in lattice QCD*

Problem: finite box has no continuous spectrum, scattering. [arXiv:1911.09047](#)

2-body scattering: quantization condition is given by the Lüscher formula, stated as a determinant. [arXiv:1707.05817](#) implements is with group theory, octahedral O_h crystallographic irreps for a cubic box which mix some the continuous limit $O(4)$. They also compute on elongated boxes, with different discrete symmetry. These (elongated in the z , not the temporal t direction) yields many more states.

[arXiv:1901.00483](#)

relation to relativistic formulation [arXiv:1905.12007](#)

[arXiv:1709.08222](#) 2-body scattering is a sub-calculation in the 3-body scattering.

“Wrap-around effects” arise from finite temporal size of the lattice.

The cleanest example is $\pi^+\pi^+\pi^+$ elastic scattering. Lattice simulation data are surprisingly sharp. They are close to 3 non-interacting pions. The agreement with the determinant zeros (infinite volume limit) using only 2-body scattering date, no fit are very sharp. So the 3-body contact term will be small (they are working on that now)

The latest 3-pion formalism: [arXiv:2003.10974](#)

2020-11-22 Uzy To dig out the “Levit-Smilansky theorem” you had to be a real archaeologist. A more profound representation is in the subsequent paper, about the phase space representation of the path integral, Levit and Smilansky [32] *The Hamiltonian path integrals and the uniform semiclassical approximations for the propagator*, (1977); cited over 50 times. The stability operator turns out to be a Dirac like (and not Schrödinger like) operator, with spectrum which covers the entire line. Yet, we wrote a similar expression for its regularized determinant and the Maslov index turns out to be the excess of negative eigenvalues. The phase space representation is of dimension (1+1) (not in your sense) but still it might be related by some miracle/good reason???

2020-11-22 Predrag Scher, Smith and Baranger [53] *Numerical calculations in elementary quantum mechanics using Feynman path integrals* (1980): “ We show that it is possible to do numerical calculations in elementary quantum mechanics using Feynman path integrals. Our method involves discretizing both time and space, and summing paths through matrix multiplication. We give numerical results for various one-dimensional potentials. The calculations of energy levels and wave functions take approximately 100 times longer than with standard methods, but there are other problems for which such an approach should be more efficient. ”

CHAPTER 23. SPATIOTEMPORAL CAT, BLOGGED

2020-11-23 Predrag Could it be that in the large $[L \times T]$ limit we should be looking at Floquet of ‘Brillouin’ bands?

2020-11-23 Predrag Temporal cat satisfies 1-d Klein-Gordon equation. Does it mean there is a Gaussian solution on it? Probably not, as the usual situation has a Gaussian spreading in time, but here time is taken to ∞ ...

2020-12-16 Predrag Not exactly ‘Gaussian’, but maybe the outgoing Klein–Gordon Green’s function (5.12) or the ‘Yukawa potential’ (5.17) maybe answer the above random thought.

2017-09-16 Predrag We know the exact, Adler-Weiss answer, in terms of a golden mean - state it. The half-baked linear encoding is an arbitrary, infinite sequence of approximations to the exact answer.

2021-02-01 Predrag *Gabriel Peyré*: The Fiedler vector of a graph is the second eigenvector of the Laplacian. It is the lowest Fourier mode and is useful to order the nodes (clustering, dimensionality reduction, etc).

[Wiki](#).

2021-09-23 Martin Richter <martin.richter@nottingham.ac.uk>

Can you give a presentation here in Nottingham? The subject of Fritz Haake talk would be great. However, I would like to hear the second half in only 1/2-Tomaž-Prosen speed :-)

2021-10-11 Predrag A half? That would kill you, my talk was at 1.0 deciProsen. You are pleading for milliProsens, I assume. I make no promises in that spatiotemporal direction.

I would like to give a technical talk, because you guys have a lot of experience with Laplacians, and I’m puzzled.

My schedule is pretty flexible, and I do not mind getting up at 1:30am (for the pleasure of being slapped around by Tomaž Prosen, to give a random example. Or Bogomolny).

For the people who would rather just be entertained, I would suggest listening to one of the talks on [overheads/Spatiotemporal](#). Thanks to my graduate students (yet another level of paper-writing reluctant) there are no papers to read :-(

2021-09-23 Martin A question: Is there an intuitive reason why the Klein-Gordon equation shows up? Why not something first order, for example? Either like the eikonal equation or better something linear like Dirac? There is probably a very simple answer to this but I was just wondering. Is there a geometrical reason, for example? Nothing of urgency, otherwise I would have shouted earlier.

2021-10-11 Predrag That will precisely be the technical part: Klein-Gordon shows up because of the nearest neighbor coupling, and it has to be second order because of the reflection symmetry, so Laplacian. So far, we have only looked at the Euclidean version, to keep things as simple as possible. Yes, we can take the "square root" of Laplacian and get two 1st order, time-asymmetric equations and a factorized Hill determinant, but I am not sure what to make of it. So far the field theory is only a scalar, single field component per site. I'm very reluctant to get into Dirac spin-1/2 fields at this time, because of lattice no-go-theorems, and the usual fermion nonsense in lattice formulations...

2020-02-02 Predrag Cata at work. Can we weave this into our presentations?

2017-09-30 Predrag Cats rule.

References

- [1] M. Akila, B. Gutkin, P. Braun, D. Waltner, and T. Guhr, “Semiclassical prediction of large spectral fluctuations in interacting kicked spin chains”, *Ann. Phys.* **389**, 250–282 (2018).
- [2] M. Akila, D. Waltner, B. Gutkin, P. Braun, and T. Guhr, “Collectivity and periodic orbits in a chain of interacting, kicked spins”, *Acta Phys. Pol. A* **132**, 1661–1665 (2017).
- [3] M. Akila, D. Waltner, B. Gutkin, P. Braun, and T. Guhr, “Semiclassical identification of periodic orbits in a quantum many-body system”, *Phys. Rev. Lett.* **118**, 164101 (2017).
- [4] R. E. Amritkar, P. M. Gade, A. D. Gangal, and V. M. Nandkumaran, “Stability of periodic orbits of coupled-map lattices”, *Phys. Rev. A* **44**, R3407–R3410 (1991).
- [5] M. Axenides, E. Floratos, and S. Nicolis, The quantum cat map on the modular discretization of extremal black hole horizons, 2017.
- [6] M. Baake and U. Grimm, “Diffraction of limit periodic point sets”, *Philos. Mag.* **91**, 2661–2670 (2011).
- [7] F. Bagnoli, S. Isola, R. Livi, G. Martínez-Mekler, and S. Ruffo, Periodic orbits in a coupled map lattice model, in *Cellular Automata and Modeling of Complex Physical Systems: Proceedings of the Winter School, Les Houches 1989*, edited by P. Manneville, N. Boccara, G. Y. Vichniac, and R. Bidaux (Springer, Berlin, 1989), pp. 282–290.
- [8] J.-B. Bardet and G. Keller, “Phase transitions in a piecewise expanding coupled map lattice with linear nearest neighbour coupling”, *Nonlinearity* **19**, 2193 (2006).
- [9] V. N. Belykh and E. Mosekilde, “One-dimensional map lattices: Synchronization, bifurcations, and chaotic structures”, *Phys. Rev. E* **54**, 3196–3203 (1996).

- [10] B. Bertini, P. Kos, and T. Prosen, “Exact correlation functions for dual-unitary lattice models in 1+1 dimensions”, *Phys. Rev. Lett.* **123**, 210601 (2019).
- [11] T. Bountis and R. H. G. Helleman, “On the stability of periodic orbits of two-dimensional mappings”, *J. Math. Phys.* **22**, 1867–1877 (1981).
- [12] N. B. Budanur and P. Cvitanović, “Unstable manifolds of relative periodic orbits in the symmetry-reduced state space of the Kuramoto-Sivashinsky system”, *J. Stat. Phys.* **167**, 636–655 (2015).
- [13] L. A. Bunimovich, V. Franceschini, C. Giberti, and C. Vernia, “On stability of structures and patterns in extended systems”, *Physica D* **103**, 412–418 (1997).
- [14] L. A. Bunimovich, R. Livi, G. Martínez-Mekler, and S. Ruffo, “Coupled trivial maps”, *Chaos* **2**, 283–291 (1992).
- [15] L. A. Bunimovich and Y. G. Sinai, “Spacetime chaos in coupled map lattices”, *Nonlinearity* **1**, 491 (1988).
- [16] S. Capobianco and T. Toffoli, “Can anything from Noether’s theorem be salvaged for discrete dynamical systems?”, in *Unconventional Computation: 10th Intern. Conf., UC 2011, Turku, Finland*, edited by C. S. Calude, J. Kari, I. Petre, and G. Rozenberg (Springer, Berlin, Heidelberg, 2011), pp. 77–88.
- [17] P. Cvitanović, “Chaotic Field Theory: A sketch”, *Physica A* **288**, 61–80 (2000).
- [18] T. Engl, J. Dujardin, A. Argüelles, P. Schlagheck, K. Richter, and J. D. Urbina, “Coherent backscattering in Fock space: A signature of quantum many-body interference in interacting bosonic systems”, *Phys. Rev. Lett.* **112**, 140403 (2014).
- [19] T. Engl, J. D. Urbina, Q. Hummel, and K. Richter, “Complex scattering as canonical transformation: A semiclassical approach in Fock space”, *Ann. Phys.* **527**, 737–747 (2015).
- [20] C. Foias, O. Manley, R. Temam, and Y. Treve, “Asymptotic analysis of the Navier-Stokes equations”, *Physica D* **9**, 157–188 (1983).
- [21] P. M. Gade and R. E. Amritkar, “Spatially periodic orbits in coupled-map lattices”, *Phys. Rev. E* **47**, 143–154 (1993).
- [22] C. Giberti and C. Vernia, “Normally attracting manifolds and periodic behavior in one-dimensional and two-dimensional coupled map lattices”, *Chaos* **4**, 651–663 (1994).
- [23] J. F. Gibson, J. Halcrow, and P. Cvitanović, “Visualizing the geometry of state-space in plane Couette flow”, *J. Fluid Mech.* **611**, 107–130 (2008).
- [24] P. Grassberger, “Information content and predictability of lumped and distributed dynamical systems”, *Phys. Scr.* **40**, 346 (1989).

- [25] R. O. Grigoriev and M. C. Cross, “Dynamics of coupled maps with a conservation law”, *Chaos* **7**, 311–330 (1997).
- [26] B. Gutkin, L. Han, R. Jafari, A. K. Saremi, and P. Cvitanović, “Linear encoding of the spatiotemporal cat map”, *Nonlinearity* **34**, 2800–2836 (2021).
- [27] B. Gutkin and V. Osipov, “Classical foundations of many-particle quantum chaos”, *Nonlinearity* **29**, 325–356 (2016).
- [28] P. E. Hydon and E. L. Mansfield, “Extensions of Noether’s Second Theorem: from continuous to discrete systems”, *Proc. R. Soc. London A* **467**, 3206–3221 (2011).
- [29] K. Kaneko, “Transition from torus to chaos accompanied by frequency lockings with symmetry breaking: In connection with the coupled-logistic map”, *Prog. Theor. Phys.* **69**, 1427–1442 (1983).
- [30] K. Kaneko, “Period-doubling of kink-antikink patterns, quasiperiodicity in antiferro-like structures and spatial intermittency in coupled logistic lattice: Towards a prelude of a “field theory of chaos””, *Prog. Theor. Phys.* **72**, 480–486 (1984).
- [31] G. Keller and C. Liverani, “Uniqueness of the SRB measure for piecewise expanding weakly coupled map lattices in any dimension”, *Commun. Math. Phys.* **262**, 33–50 (2006).
- [32] S. Levit and U. Smilansky, “The Hamiltonian path integrals and the uniform semiclassical approximations for the propagator”, *Ann. Phys.* **108**, 165–197 (1977).
- [33] R. Livi, G. Martínez-Mekler, and S. Ruffo, “Periodic orbits and long transients in coupled map lattices”, *Physica D* **45**, 452–460 (1990).
- [34] R. de la Llave and J. D. Mireles James, “Connecting orbits for compact infinite dimensional maps: Computer assisted proofs of existence”, *SIAM J. Appl. Dyn. Sys.* **15**, 1268–1323 (2016).
- [35] R. S. MacKay, S. Johnson, and B. Sansom, “How directed is a directed network?”, *Proc. Natl. Acad. Sci. USA* **117** (2020).
- [36] A. de Maere, “Phase transition and correlation decay in coupled map lattices”, *Commun. Math. Phys.* **297**, 229–264 (2010).
- [37] E. L. Mansfield, Noether’s theorem for smooth, difference and finite element schemes, in *Foundations of computational mathematics, san-tander 2005*, Vol. 331, London Math. Soc. Lect. Notes (2006), pp. 230–254.
- [38] D. Michelson, “Steady solutions of the Kuramoto-Sivashinsky equation”, *Physica D* **19**, 89–111 (1986).
- [39] J. C. Neu, “Coupled chemical oscillators”, *SIAM J. Appl. Math.* **37**, 307–315 (1979).

- [40] J. C. Neu, “Chemical waves and the diffusive coupling of limit cycle oscillators”, SIAM J. Appl. Math. **36**, 509–515 (1979).
- [41] B. Nicolaenko, “Some mathematical aspects of flame chaos and flame multiplicity”, Physica D **20**, 109–121 (1986).
- [42] I. Percival and F. Vivaldi, “A linear code for the sawtooth and cat maps”, Physica D **27**, 373–386 (1987).
- [43] Y. B. Pesin and Y. G. Sinai, “Space-time chaos in the system of weakly interacting hyperbolic systems”, J. Geom. Phys. **5**, 483–492 (1988).
- [44] S. D. Pethel, N. J. Corron, and E. Bollt, “Symbolic dynamics of coupled map lattices”, Phys. Rev. Lett. **96**, 034105 (2006).
- [45] S. D. Pethel, N. J. Corron, and E. Bollt, “Deconstructing spatiotemporal chaos using local symbolic dynamics”, Phys. Rev. Lett. **99**, 214101 (2007).
- [46] W.-X. Qin, “Bifurcations of steady states in a class of lattices of nonlinear discrete Klein-Gordon type with double-quadratic on-site potential”, J. Phys. A **36**, 9865–9873 (2003).
- [47] C. Reick and E. Mosekilde, “Emergence of quasiperiodicity in symmetrically coupled, identical period-doubling systems”, Phys. Rev. E **52**, 1418–1435 (1995).
- [48] K. Richter, *Semiclassical theory of mesoscopic quantum systems* (Springer, Berlin, 2000).
- [49] D. Ruelle, “Some comments on chemical oscillations”, Trans. N. Y. Acad. Sci. **35**, 66–71 (1973).
- [50] D. Ruelle, “Large volume limit of the distribution of characteristic exponents in turbulence”, Commun. Math. Phys. **87**, 287–302 (1982).
- [51] D. Ruelle, “Zeros of graph-counting polynomials”, Commun. Math. Phys. **200**, 43–56 (1999).
- [52] D. Ruelle, “Graph-counting polynomials for oriented graphs”, J. Stat. Phys. **173**, 243–248 (2018).
- [53] G. Scher, M. Smith, and M. Baranger, “Numerical calculations in elementary quantum mechanics using Feynman path integrals”, Ann. Phys. **130**, 290–306 (1980).
- [54] M. Schmitt, “Spectral theory for nonanalytic coupled map lattices”, Nonlinearity **17**, 671 (2004).
- [55] A. Stern, Y. Tong, M. Desbrun, and J. E. Marsden, Geometric computational electrodynamics with variational integrators and discrete differential forms, in *Geometry, Mechanics, and Dynamics: The Legacy of Jerry Marsden*, edited by D. E. Chang, D. D. Holm, G. Patrick, and T. Ratiu (Springer, New York, 2015), pp. 437–475.
- [56] D. S. Tourigny, “Networks of planar Hamiltonian systems”, Commun. Nonlinear Sci. Numer. Simul. **53**, 263–277 (2017).

- [57] V. L. Volevich, “Kinetics of coupled map lattices”, *Nonlinearity* **4**, 37–48 (1991).
- [58] J. Xiao, H. Qin, Y. Shi, J. Liu, and R. Zhang, “A lattice Maxwell system with discrete space-time symmetry and local energy-momentum conservation”, *Phys. Lett. A* **383**, 808–812 (2019).

Chapter 24

Pow Wows

Scribes Sidney, Han and Matt.

The latest entry at the bottom for this chapter

24.1 Pow wow 2020-12-08

Scribe Predrag

One must distinguish *coordinate system* symmetries (the floor cat dances on) from *dynamical* symmetries (the cat reflected through its bisection plane).

24.1.1 Hereby resolved:

Task 1 Define temporal cat phase space fundamental domain for the *dynamical* $D_1 = \{e, \sigma\}$ symmetry
Predrag 2020-12-XX: Done! See XXX

Task 2 Define temporal cat phase space fundamental domain symbolic dynamics.
XXX 2020-12-XX: Done! See XXX

Task 3 Factorize temporal cat zeta using the *dynamical* $D_1 = \{e, \sigma\}$ symmetry on the traces (lattice states count), then exponentiating.
XXX 2020-12-XX: Done! See XXX

Suggestion Check the above guess factorization for the Bernoulli first. It is more instructive to assume that the s branch map is not piecewise linear, and work out weights t_p factorization, write down cycle expansions in terms of orbits.

XXX 2020-12-XX: Done! See XXX

24.2 Pow wow 2020-12-28

Scribe Predrag

2020-12-28 Han (See the post above including (18.283).) The fundamental domain should be $\{\hat{\phi}_{t-1}, \hat{\phi}_t\} \in [0, 1]^2 / D_1$, i.e., $1/2$ of the phase space unit square area, not the quarter of the area $[0, 1/2]^2$. Any codimension-1 hyperplane going through the center of mass $\hat{\phi}_t = 1/2$, all $t \in \mathbb{Z}$ point can serve as a boundary of the fundamental domain.

2020-12-XX Predrag done!: The natural fundamental domain is given by XXX

24.2.1 Hereby resolved:

Task 1 Sidney Define Hénon [ChaosBook \(15.20\)](#) phase space fundamental domain for the *coordinate* time reversal $D_1 = \{e, \sigma\}$ symmetry. To Predrag, the [ChaosBook fig. 15.5](#) and Gutkin *et al.* [5] cat map [figure 2](#) suggest that the fundamental domain border is the diagonal, but Predrag is usually wrong.

Sidney 2021-01-XX: Done! See refeqXXX.

Task 2 Sidney Define Hénon phase space fundamental domain symbolic dynamics. Predrag expects it to be like what is described in [ChaosBook sect. 25.5 \$D_1\$ factorization](#).

Sidney 2021-01-XX: Done! See XXX

Task 3 Sidney Factorize Hénon zeta using the *dynamical* $D_1 = \{e, \sigma\}$ symmetry. Predrag expects it to be like what is described in [ChaosBook sect. 25.5 \$D_n\$ factorization](#).

Sidney 2021-01-XX: Done! See XXX

24.3 Pow wow 2021-01-08

Scribe Predrag

2021-01-08 Predrag Try to understand irreps of D_n : For worked out D_2 , D_4 and D_n examples, see the text following (4.188).

24.3.1 Hereby resolved:

Task 1 Han Derive temporal cat factorization (4.183) and (4.181) into $1/\zeta'(t)$'s, either from the dynamical D_1 symmetry, or from the lattice coordinate time-reversal D_1 symmetry.

Han 2021-01-XX: Done! The D_1 irrep decomposition of the temporal cat orbit Jacobian matrix \mathcal{J} is given by XXX

Task 1 Predrag Incorporate into ChaosBook the D_2 , D_4 and D_n examples from the text following (4.188).

Predrag 2021-01-XX: Done!

24.4 Pow wow 2021-03-22

Scribe Predrag

Homework: verify whether

1. Hamiltonian (4.69) equations lead to the golden (Fibonacci [2]) cat map (4.179)?
2. is this consistent with the Yukawa massive field mass μ relation (5.27) to the spatiotemporal cat stretching parameter s by $\mu^2 = d(s - 2)$. Note that Grava *et al.* [4] sect. 4.3.1 is full of such square roots relations for parameters, such as $\tau_0 = -\sqrt{\kappa_1}$.
3. is what they call " m -physical vector and half- m -physical vector" the same as our $\sqrt{\dots}$ or half-unit spacing lattice?
4. this leads to factorization (4.183), (4.177)?
5. this works (or not) for nonlinear systems? I believe we have to verify it for the orbit Jacobian matrix \mathcal{J}_\pm , for each solution, not on the lattice states themselves. Sidney's Hénon (2.12) first, than
6. this works any nonlinear map?

The above is a failed attempt again, it seems...

24.5 Pow wow 2021-04-02

Scribe Predrag

1. Predrag believes that Han's approach - for example (18.328) and thereabouts is the right way to go about it.
2. Sidney and Predrag should understand Gallas [3] *Counting orbits in conjugacy classes of the Hénon Hamiltonian repeller*, see (2.18)
3. Han should derive temporal cat formulas corresponding to Gallas Hénon $C_{||}, D_{||}, N_{||}$.
4. Han will presumably do it only for $s = 3$, but Predrag would be happier to see this done for arbitrary integer μ ...
5. Then figure out what this has to do with $D_{||}$

6. Added

- (a) example 2.5 Hamiltonian Hénon map, reversibility
- (b) example 2.6 Symmetry lines of the standard map
- (c) remark 1.5 Symmetries of the symbol square
- (d) sect. 2.4 Symmetries of the symbol square
- (e) See eq. (2.16)

24.6 Pow wow 2021-04-09

Scribe Predrag

- (a) Han knows how to count the three types of time-reversal self-dual orbits, and has explicit trigonometric products expressions for their Hill determinants.
- (b) **2021-03-10 Predrag** The discussion reminds me of Baake *et al.* 1997 paper [1] *The torus parametrization of quasiperiodic LI-classes* ([click here](#)) (enter what you learn from that paper into sect. 4.3.3: is the only paper we found that associates a 1/2-shift unit length lattice with time reversal). But under my reading the paper does not seem to be applicable to our 1D lattice with time-inversion problem. Here is what we can adopt:
- (c) An infinite lattice state can be self-dual under time-inversion about an integer lattice point (with a single field ϕ_0 invariant under inversion), or about 1/2 midway point between two integer lattice sites, with all lattice fields paired as $\phi_i = \phi_{-i}$, with no invariant field. For a finite period \parallel lattice state, there are four pairs of time-inversion points for self-dual lattice states

$$(0, 0) \ (1/2, 0) \ (0, 1/2) \ (1/2, 1/2) , \quad (24.1)$$

that form $D_1 \times D_1$ the discrete subgroup of ‘two-reflection points’ of \mathbb{Z}/\parallel . A lattice state starts at a reflection points, marches to the other reflection point, and then it marches back, so any self-dual lattice state has two reflections points, no more and no less. As reflection destroys cyclic invariance, all self-dual lattice states are prime, they cannot be tiled by repeats of a shorter segment (??).

$(1/2, 0)$ and $(0, 1/2)$ are the same by a half-period rotation, so there are three kinds of self-dual cycles illustrated in figure 2.1 (a,b,c). (compare with (2.16): Han has two diagonal classes instead of Gallas one)

- i. Both time-inversion invariant fields on the integer lattice (18.336) (Gallas [3] class ? D_1 ?)

- ii. One time-inversion point on the integer lattice, the other on the 1/2-integer lattice (18.335) (class ? D_2 ?)
- iii. Both time-inversion points on the 1/2-integer lattice (18.334) (class ? N ?)
- (d) MacKay had the logistic map counts listed already in Table 1.2.3.5.1 of his 1982 PhD thesis [6] ([click here](#)). Should be the same as Gallas Table. 1, but I do not see the correspondence for all columns - you might want to check MacKay's construction, it is very clearly explained.
- (e) MacKay says that for self-dual cycles of odd period there is precisely one periodic point on the symmetry line; or two or none for even period cycles, so he correctly separates the two kinds of 'diagonal' cycles that Gallas lumps into one.
- (f) MacKay might be the first to note (p. 46) that period-6 is the smallest period for which there are non-symmetric periodic orbits.
- (g) The (2.16) hunch for time-reversal quotiented zeta function: in the numerator all cycles appear in pairs, but that overcounts the boundary cycles, which thus contribute ($D_1 D_2 N$) to the denominator???

2CB

24.7 Pow wow 2021-04-27

Scribe, for some inscrutable reason, always Predrag

2021-04-27 Predrag in progress:

example 2.2 *Temporal Hénon*

example 2.4 *Temporal Hénon stability*

Note the rescaled definition of the field $\phi = a \phi$

24.7.1 Hereby resolved:

Task 1 Sidney compute the orbit Jacobian matrix \mathcal{J}_p for a set of shortest periods lattice states p

Task 2 Sidney compute the lattice states p orbit Jacobian matrix eigen-values, -vectors.

Task 3 Sidney Interpret these eigen-values, -vectors.

Task 1 Sidney & Han compute analytically the orbit Jacobian matrix $\det \mathcal{J}_p$ for fixed points, period-2 and periods-3.

Task 2 Sidney & Han verify Hill's formula for each

Task 1 Han time-symmetry reduce the orbit Jacobian matrix $\det \mathcal{J}_p$ for fixed points, period-2 and periods-3.

Task 1 Sidney & Han verify the time-symmetry factorization of the Hill's formula for each

24.8 Pow wow 2021-05-04

Scribe, for some inscrutable reason, always Predrag

2021-05-04 Predrag in progress:

example 2.4 *Temporal Hénon stability*

24.8.1 Hereby resolved:

Task 1 Han Figure out how to piece together period $r||$ repeats of period-|| orbit Jacobian matrix \mathcal{J}_p . (4.77) and (4.78) are failed attempts.

Task 2 Han Figure out how to piece together period $\tilde{\mathcal{J}}_p$ with its time-reversed copy $\tilde{\mathcal{J}}_p^\top$ by pulling out a matrix representation of the group element (in this case, a pair of the two types of reflections).

Dream 1 Han Replace the forward-in-time Perron-Frobenius operator by including the time-reversal into the operator definition. Perhaps by complexifying it, as in ChaosBook (28.10) and ChaosBook (29.17)? By replacing the monomial x^k eigenvectors ChaosBook (28.18), with exponential multipliers, with a time-reversal invariant combination of eigenvalues, something like \tanh ?

24.9 Pow wow 2021-05-07

Scribes Han, Predrag

1. Using the reflection operator in the space of lattice state, the orbit Jacobian matrix can be projected into symmetric and antisymmetric subspace of time reflection. Han used the symmetric eigenvectors of the orbit Jacobian matrix to project the orbit Jacobian matrix into symmetric subspace. A better way is to use the time reflection operator to find the projection operators as in (4.60–4.61).
2. There are two kinds of reflection points, corresponding to two kinds of reflection operators, denoted by a bar or a box, as in (18.334), and 3 (or 4) kinds of time-reversal self-dual orbits (2.32), (2.33) and (2.36), or (18.336), (18.335), and (18.334).
3. The eigenvalues of the antisymmetric eigenvectors *probably* count the number of antisymmetric lattice states: $\{X \in \mathbb{T}^{\mathbb{Z}} | RX \bmod 1\}$.

4. However, mod 1 does not allow for $\phi_t < 1$. Perhaps we should replace the mod 1 condition by the $\phi_t \in [-1/2, 1/2]$ condition. In that case, the antisymmetric eigenspace might be taking care of what we call the ‘dynamical’, site-wise symmetry under $\phi_t \leftrightarrow -\phi_t D_1$, specific to temporal cat.
5. We still don’t know how to piece together orbit Jacobian matrices, other than by doing the multiplication along temporal evolution, and then using the Hill’s formula. The orbit Jacobian matrices for repeats of orbits do not multiply, as their determinants do not multiply.
6. The $\sum 1/|\text{Det } \mathcal{J}_j|$ always satisfies the flow conservation sum rule [Chaos-Book \(23.18\)](#). Except that for Hénon we are working with [ChaosBook sect. 20.3 Open systems](#), so the sum is related to the escape rate.

24.10 Pow wow 2021-05-14

Scribe Predrag

2021-05-14 Han There is no proposal for time-reversal quotiented topological zeta function, dynamical zeta function or spectral determinant.

2021-05-14 Predrag We have: the topological zeta function for metal cat maps (4.45); the $\mu = 1$ golden (Fibonacci [2]) cat zeta function (4.181); the time-reflection factorized (?) $1/\tilde{\zeta}(t)$ (4.177); the Hamiltonian factorized (4.80), (4.88), (1.125), (1.126); the unique Euler product (4.118); the D_1 dynamical zeta function factorization (4.268); something like (2.16) computed on the fundamental domain; spatiotemporal cat Z-transform (discrete Laplace transform) ζ function (6.8); Ihara zeta functions (13.55), (13.60). The last I looked.

2021-05-14 Han I’m 99% sure that the metal (4.45); tand the golden cat (4.181) factorization have nothing to do with time-reversal.

2021-05-14 Predrag NOTHING to do with time-reversal? You are willing to bet \$100 to \$1 that they have NOTHING to do with time-reversal?

24.10.1 Hereby resolved:

Task 1 Han Think some more.

References

- [1] M. Baake, J. Hermisson, and A. B. Pleasants, “The torus parametrization of quasiperiodic LI-classes”, *J. Phys. A* **30**, 3029–3056 (1997).

- [2] M. Baake, N. Neumärker, and J. A. G. Roberts, “Orbit structure and (reversing) symmetries of toral endomorphisms on rational lattices”, *Discrete Continuous Dyn. Syst.* **33**, 527–553 (2013).
- [3] J. A. C. Gallas, “Counting orbits in conjugacy classes of the Hénon Hamiltonian repeller”, *Phys. Lett. A* **360**, 512–514 (2007).
- [4] T. Grava, T. Kriecherbauer, G. Mazzuca, and K. D. T.-R. McLaughlin, “Correlation functions for a chain of short range oscillators”, *J. Stat. Phys.* **183**, 1 (2021).
- [5] B. Gutkin, L. Han, R. Jafari, A. K. Saremi, and P. Cvitanović, “Linear encoding of the spatiotemporal cat map”, *Nonlinearity* **34**, 2800–2836 (2021).
- [6] R. S. MacKay, *Renormalisation in Area-preserving Maps* (World Scientific, Singapore, 1993).